UFS 3-220-20
26 March 2026

UNIFIED FACILITIES SUPPLEMENT (UFS)

FOUNDATIONS AND EARTH STRUCTURES (DM 7.2)

APPROVED FOR PUBLIC RELEASE; DISTRIBUTION UNLIMITED

FOREWORD

Unified Facilities Supplements (UFS) provide non-mandatory, supplemental information in support of Unified Facilities Criteria (UFC). Only UFC establish enforceable criteria. UFS are For Information Only (FIO) and exist to help users understand and apply UFC requirements.

The purpose of UFS is to offer procedural guidance, best practices, lessons learned, examples, and explanatory materials that clarify how to meet UFC criteria. They may include step-by-step procedures, checklists, illustrations, or decision aids, but they do not create new requirements or modify UFC content.

UFS are developed by Discipline Working Groups (DWGs) and published by the Military Services under MIL-STD-3007. Because they are not criteria, they do not require Coordinating Panel (CP) or Engineering Senior Executive Panel (ESEP) approval.

UFS content may be referenced or incorporated into project documents at the discretion of project delivery teams but are not binding unless explicitly included in contract requirements. For Service-specific supplemental guidance, refer to Facilities Supplements (FS).

UNIFIED FACILITIES SUPPLEMENT (UFS)

FOUNDATIONS AND EARTH STRUCTURES (DM 7.2)

TABLE OF CONTENTS

PROLOGUE P. SHEAR STRENGTH FOR GEOTECHNICAL DESIGN 1
P-1 SCOPE. 1
P-2 STRENGTH ENVELOPES. 1
P-2.1 Mohr-Coulomb Failure Criteria. 1
P-2.2 Nonlinear Envelopes. 3
P-3 SELECTION OF SHEAR STRENGTH PARAMETERS. 8
P-3.1 *In situ* Deposit of Coarse-Grained Soil (Sand to Gravel). 8
P-3.2 Engineered Deposit of Coarse-Grained Soil (Sand to Gravel). 9
P-3.3 *In situ* Deposit of Fine-Grained Soil. 10
P-3.4 Engineered Deposit of Fine-Grained Soil. 16
P-4 NOTATION. 18
CHAPTER 1. GEOTECHNICAL DESIGN IN PROBLEM SOILS AND SPECIALTY CONSTRUCTION METHODS 21
1-1 INTRODUCTION. 21
1-2 TYPES OF PROBLEM SOILS. 21
1-2.1 Stiff Fissured Clays. 22
1-2.2 Stiff Desiccated Clays. 22
1-2.3 Loess. 23
1-2.4 Sensitive or Quick Clays. 23
1-2.5 Residual Silts and Clays. 24
1-2.6 Laterites. 24
1-2.7 Talus. 24
1-2.8 Loose Sands. 24
1-2.9 Soft Clays. 25

1-2.10 Glacial Till. 25
1-2.11 Organic Soils. 25
1-2.12 Expansive Soils. 27
1-2.13 Expansive Shale. 28
1-2.14 Collapsible Soils. 28
1-2.15 Dispersive Soils. 29
1-2.16 Dredged Soils. 29
1-2.17 Low Plasticity and Nonplastic Silts. 31
1-2.18 Municipal Solid Waste. 32
1-3 SPECIALTY GEOTECHNICAL CONSTRUCTION METHODS. 33
1-3.1 GeoTechTools Website Interactive Selection System. 36
1-3.2 Geotechnical Site Technology Examples. 38
1-4 NOTATION. 54
CHAPTER 2. EXCAVATIONS 55
2-1 INTRODUCTION. 55
2-2 OPEN CUT EXCAVATIONS 55
2-2.1 Sloped Excavations. 55
2-2.2 Vertical Excavations. 56
2-2.3 Other Design Considerations for Open Cut Excavations. 56
2-3 TRENCHING. 57
2-3.1 Site Exploration. 57
2-3.2 Trench Stability. 57
2-3.3 Support Systems. 59
2-4 DEEP EXCAVATION SYSTEMS 66
2-4.1 Types of Wall and Support Systems. 66
2-4.2 Site Considerations for Deep Excavations. 70
2-4.3 Wall and Excavation Stability 72
2-4.4 Ground Movements Adjacent to Deep Excavations. 76
2-4.5 Construction Considerations 89
2-5 ROCK EXCAVATIONS 91
2-5.1 Preliminary Considerations. 91
2-5.2 Assessment of Rock Excavation Methods. 92

2-5.3 Blasting. 94
2-6 GROUNDWATER CONTROL. 97
2-6.1 Preliminary Considerations. 97
2-6.2 Permeability of Sheet Piling. 98
2-6.3 Methods of Controlling Groundwater. 99
2-7 PROBLEM SOILS AND EXCAVATIONS. 103
2-8 NOTATION. 104
2-9 SUGGESTED READING. 106
CHAPTER 3. EARTHWORK, HYDRAULIC, AND UNDERWATER FILLS 107
3-1 INTRODUCTION. 107
3-1.1 Scope. 107
3-1.2 Earthwork Process and Purpose of Compaction. 107
3-1.3 Types of Fills and Applications. 108
3-2 COMPACTION THEORY. 108
3-2.1 Process of Compaction. 109
3-2.2 Characterizing Compaction. 109
3-2.3 Influence of Compaction on Engineering Parameters. 113
3-3 FILL MATERIALS. 118
3-3.1 Borrow Exploration. 119
3-3.2 Preliminary Selection based on Classification. 119
3-3.3 Laboratory Characterization of Fill Materials. 123
3-3.4 Alternative Fill Materials. 127
3-4 CONSTRUCTION OF COMPACTED FILLS. 130
3-4.1 Drainage. 130
3-4.2 Subgrade Preparation. 131
3-4.3 Excavation, Transport, and Placement. 133
3-4.4 Compaction. 136
3-4.5 Special Construction Conditions. 140
3-5 CONTROL OF COMPACTED FILLS. 142
3-5.1 Compaction Requirements. 142
3-5.2 Field Test Sections. 145
3-5.3 Compaction Control Tests. 147

3-5.4 Analysis of Compaction Control Test Data. 151
3-5.5 Compaction Control of Rock Fill. 154
3-5.6 Intelligent Compaction Systems. 154
3-5.7 Indirect Evaluation of Deep Fills. 155
3-6 DESIGN OF EMBANKMENTS. 156
3-6.1 Primary Design Conditions. 156
3-6.2 Embankments on Stable Foundations. 158
3-6.3 Embankments on Weak Foundations. 158
3-6.4 Reinforced Embankments. 158
3-6.5 Deep and/or Valley Fills. 160
3-6.6 Earth Dam Embankments. 161
3-6.7 Side Hill Fills. 164
3-7 HYDRAULIC AND UNDERWATER FILLS. 165
3-7.1 Purpose and Use of Hydraulic Fill. 165
3-7.2 Placement of Hydraulic Fill. 166
3-7.3 Performance of Hydraulic Fills. 166
3-7.4 Consolidation of Hydraulic Fills. 167
3-7.5 Underwater Fill. 168
3-8 PROBLEM SOILS AND EARTHWORK. 169
3-9 NOTATION. 171
3-10 SUGGESTED READING. 173
CHAPTER 4. ANALYSIS OF WALLS AND RETAINING STRUCTURES 175
4-1 INTRODUCTION. 175
4-2 DEVELOPMENT OF EARTH PRESSURES AND LOADS. 175
4-2.1 At-Rest Earth Pressure. 176
4-2.2 Rankine Active and Passive Earth Pressures. 177
4-2.3 Movement Required to Develop Active and Passive States. 179
4-2.4 Earth Pressure Distributions and Loads. 179
4-2.5 Rankine Method Examples. 182
4-2.6 Wall/Soil Interface Friction Angle. 184
4-3 ACTIVE AND PASSIVE EARTH PRESSURE FROM OTHER METHODS 185

4-3.1 Coulomb Wedge Method. 186
4-3.2 Log Spiral Method. 190
4-3.3 Presumptive Earth Pressure Coefficients and Equivalent Fluid Pressures. 194
4-3.4 Earth Pressure Examples for Complex Geometries. 196
4-3.5 Use of Slope Stability Software for Earth Pressures..... 199
4-4 EARTH PRESSURES FROM OTHER SOURCES..... 199
4-4.1 Water Pressure Effects..... 199
4-4.2 Surface Loads Behind Retaining Structures. 203
4-4.3 Earth Pressures Due to Compaction. 208
4-4.4 Seismic Earth Pressures on Retaining Structures. 214
4-5 RIGID GRAVITY RETAINING STRUCTURES. 218
4-5.1 Design Calculations for Rigid Retaining Walls..... 219
4-5.2 Drainage Behind Rigid Walls. 225
4-6 ALTERNATIVE GRAVITY RETAINING STRUCTURES. 228
4-6.1 Mechanical Stabilized Earth (MSE) Retaining Structures... 228
4-6.2 Gabion Walls. 228
4-6.3 Earth-Filled Crib Walls and Bin Walls. 230
4-7 FLEXIBLE RETAINING STRUCTURES. 231
4-7.1 Factored Passive Resistance. 231
4-7.2 Anchored Bulkheads. 232
4-7.3 Anchor Design. 238
4-7.4 Cantilever Flexible Walls. 241
4-7.5 Soldier Pile Walls..... 248
4-7.6 Secant Pile Walls and Tangent Pile Walls. 249
4-7.7 Soil Nail Walls..... 250
4-8 EXCAVATION SUPPORT. 252
4-8.1 Apparent Earth Pressure Diagrams. 253
4-8.2 Stability of Base of Excavations..... 254
4-8.3 Internal Support (Excavation Bracing). 254
4-8.4 External Support (Tied Back Walls). 260
4-9 CELLULAR COFFERDAM DESIGN..... 261
4-9.1 Cell Deformations. 267

4-9.2 Cell Fill. 267
4-9.3 Cofferdam Drainage. 267
4-10 PROBLEM SOILS AND RETAINING WALLS. 267
4-11 NOTATION. 268
4-12 SUGGESTED READING 271
CHAPTER 5. SHALLOW FOUNDATIONS 273
5-1 INTRODUCTION. 273
5-1.1 Scope. 273
5-1.2 Applications. 274
5-1.3 Design Philosophy. 274
5-2 SHALLOW FOUNDATION DESIGN CONSIDERATIONS. 275
5-2.1 Foundation Depth. 275
5-2.2 Gross and Net Bearing Pressure. 275
5-2.3 Eccentricity. 276
5-2.4 Allowable Bearing Pressure 278
5-2.5 Presumptive Allowable Bearing Pressure. 280
5-3 BEARING CAPACITY OF SOIL AND ROCK 283
5-3.1 Bearing Capacity Theory. 283
5-3.2 Groundwater Correction. 291
5-3.3 Methods to Account for Complicating Effects. 292
5-3.4 Foundations Near the Top of Slopes. 296
5-3.5 Bearing Capacity Examples. 301
5-3.6 Nonuniform Soil and Layered Stratigraphy. 306
5-3.7 Bearing Capacity of Rock. 316
5-4 GEOTECHNICAL DESIGN OF COMBINED AND MAT FOUNDATIONS. 318
5-4.1 Definitions and Applications 319
5-4.2 Rigid Foundations 319
5-4.3 Flexible Foundation Criteria. 321
5-4.4 Required Input for Analysis of Continuous and Mat Foundations. 322
5-4.5 Modulus of Subgrade Reaction. 323
5-4.6 Iterative Process in Design. 330

5-4.7 Node Coupling of Soil Effects. 330
5-4.8 Indirect Method to Allowing Coupling. 332
5-4.9 Floating Mat Foundation. 334
5-4.10 Two- or Three-Dimensional Problems. 335
5-5 DESIGN FOR SPECIAL LOADING CONDITIONS. 335
5-5.1 Pressure Resistant and Relieved Foundation Slabs and Walls. 335
5-5.2 Uplift Resistance. 339
5-6 DESIGN FOR SPECIAL SOIL CONDITIONS. 350
5-6.1 Shallow Foundations on Engineered Fill. 350
5-6.2 Foundations on Expansive Soil and Rock. 351
5-6.3 Foundations on Collapsible Soils. 355
5-6.4 Other Problem Soils. 359
5-7 NOTATION. 360
5-8 SUGGESTED READING. 363
CHAPTER 6. DEEP FOUNDATIONS 364
6-1 INTRODUCTION. 364
6-1.1 Scope. 364
6-1.2 Organization 364
6-1.3 Applications. 364
6-1.4 General Considerations. 365
6-2 DESIGN ASPECTS AND CONSIDERATIONS. 366
6-2.1 Design Aspects. 366
6-2.2 Site and Project Considerations. 369
6-2.3 Subsurface Characterization Considerations. 375
6-2.4 Construction Considerations. 376
6-3 FOUNDATION TYPES. 377
6-3.1 Overview. 377
6-3.2 Summaries of Common Deep Foundation Types. 379
6-3.3 Summary of Material Properties. 384
6-4 CONSTRUCTION. 384
6-4.1 Driven Piles. 384
6-4.2 Drilled Shafts. 393

6-4.3 Continuous-Flight Auger Piles. 397
6-4.4 Drilled Displacement Piles. 398
6-4.5 Aggregate Columns. 398
6-4.6 Micropiles. 399
6-4.7 Helical Piles. 402
6-5 GEOTECHNICAL STATIC AXIAL CAPACITY AND SETTLEMENT. 402
6-5.1 Introduction. 402
6-5.2 Limit States. 403
6-5.3 Load Transfer. 403
6-5.4 Static Axial Capacity in Compression for Single Elements. 409
6-5.5 Static Axial Capacity in Compression for Groups of Elements. 431
6-5.6 Uplift Capacity. 433
6-5.7 Negative Skin Friction. 437
6-5.8 Settlement. 438
6-6 GEOTECHNICAL LATERAL CAPACITY. 450
6-6.1 Introduction. 450
6-6.2 Lateral Loading and Foundation Response. 451
6-6.3 Lateral Analysis of Batter Piles. 454
6-6.4 Lateral Analysis of Single Vertical Piles. 455
6-6.5 Groups of Vertical Piles. 465
6-7 STRUCTURAL CAPACITY 468
6-7.1 Allowable Stresses. 469
6-7.2 Buckling. 473
6-7.3 Considerations for Pile Caps. 475
6-7.4 Design for Drag Force. 476
6-8 STATIC LOAD TESTING. 478
6-8.1 Introduction. 478
6-8.2 Axial Load Tests. 479
6-8.3 Interpretation of Axial Compressive Load Tests. 483
6-9 DYNAMIC METHODS OF ANALYSIS AND TESTING 485
6-9.1 Introduction. 485
6-9.2 Wave Mechanics Basics. 487

6-9.3 Wave Equation Analysis of Pile Driving. 492
6-9.4 High-Strain Dynamic Measurements. 492
6-9.5 Case Method. 495
6-9.6 Signal Matching. 495
6-9.7 Rapid Load Tests. 496
6-10 INTEGRITY TESTING. 498
6-10.1 High-strain Dynamic Measurements. 498
6-10.2 Low-strain Dynamic Measurements. 498
6-10.3 Cross Hole Sonic Logging. 499
6-10.4 Thermal Integrity Profiling. 499
6-10.5 Gamma-Gamma Logging. 500
6-11 PROBLEM SOILS AND dEEP FOUNDATIONS. 500
6-12 NOTATION. 502
6-13 SUGGESTED READING. 507
CHAPTER 7. PROBABILITY AND RELIABILITY IN GEOTECHNICAL ENGINEERING 508
7-1 INTRODUCTION. 508
7-1.1 Scope and Purpose. 508
7-2 PRINCIPLES OF STATISTICS AND PROBABILITY. 508
7-2.1 Statistics. 509
7-2.2 Methods of Plotting Data. 509
7-2.3 Probability. 512
7-3 UNCERTAINTY IN GEOTECHNICAL ENGINEERING. 519
7-3.1 Sources of Uncertainty. 519
7-3.2 Effects of Correlation on Uncertainty. 527
7-3.3 Designing for Uncertainty. 528
7-4 APPLICATIONS. 528
7-4.1 Evaluation of Field and Laboratory Data. 529
7-4.2 Reliability Analysis. 530
7-4.3 Risk Assessment. 544
7-4.4 Hazard Analysis and Return Periods. 546
7-4.5 Load and Resistance Factor Design (LRFD). 549
7-5 NOTATION. 555

7-6 SUGGESTED READING. 557
APPENDIX A. REFERENCES 558
APPENDIX B. VERIFICATION EXAMPLES 596
B-1 EXAMPLE 1 – CANTILEVER CUT WALL. 596
B-1.1 Description of the Problem. 596
B-1.2 Goals and Limitations of the Analysis. 596
B-1.3 Evaluation of Forces and Moments. 599
B-1.4 Overturning. 600
B-1.5 Sliding 601
B-1.6 Bearing capacity 602
B-1.7 Conclusions from the Analysis 604
B-1.8 Additional Comments on Overturning Factor of Safety 605
B-2 EXAMPLE 2 – ANCHORED CUT WALL. 606
B-2.1 Description of the Problem. 606
B-2.2 Goals and Limitations of the Analysis. 607
B-2.3 Calculation of Lateral Pressures and Forces. 608
B-2.4 Embedment of Sheet Pile and Tie Rod Force. 610
B-2.5 Selection of Sheet Pile Section 611
B-2.6 Location of Maximum Moment 612
B-2.7 Design of Continuous Anchor. 614
B-2.8 Conclusions from the Analysis 617
B-3 EXAMPLE 3 – BEARING CAPACITY OF SHALLOW FOUNDATIONS. 618
B-3.1 Description of the Problem. 618
B-3.2 Goals and Limitations of the Analysis. 618
B-3.3 Bearing Capacity Equations. 619
B-3.4 Footing 1 – Located Far from the Top of the Slope. 621
B-3.5 Footing 2 – Located Close to the Top of the Slope 623
B-3.6 Footing 3 – Located on the Slope. 625
B-3.7 Conclusions from the Analysis 626
B-4 EXAMPLE 4 – MAT FOUNDATION DESIGN. 627
B-4.1 Description of the Problem. 627
B-4.2 Goals and Limitations of the Analysis. 628

B-4.3 Immediate Settlement. 628
B-4.4 Primary Consolidation. 631
B-4.5 Modulus of Subgrade Reaction. 633
B-4.6 Conclusions from the Analysis. 633
B-5 EXAMPLE 5 – PILE GROUP CAPACITY AND SETTLEMENT. 633
B-5.1 Description of the Problem. 633
B-5.2 Goals and Limitations of the Analysis. 635
B-5.3 Trial Dimensions. 635
B-5.4 Geotechnical Strength Limit State Analysis. 636
B-5.5 Neutral Plane Analysis. 638
B-5.6 Structural Strength Limit State Analysis. 640
B-5.7 Settlement Analysis. 641
B-5.8 Conclusions from Analysis. 643
B-6 EXAMPLE 6 – LATERAL LOAD ANALYSIS. 644
B-6.1 Description of the Problem. 644
B-6.2 Goals and Limitations of the Analysis. 645
B-6.3 Characteristic Load Method Analysis 645
B-6.4 Conclusions from the Analysis. 651
B-7 EXAMPLE 7 – RELIABILITY ANALYSIS OF A RETAINING WALL. 651
B-7.1 Description of the Problem. 651
B-7.2 Overturning. 652
B-7.3 Sliding. 653
B-7.4 Bearing Capacity. 655
B-7.5 Conclusions from Analysis. 659
APPENDIX C. GLOSSARY 660

LIST OF FIGURES

Figure P-1 Mohr-Coulomb Failure Envelopes for Effective and Total Stress Conditions 2
Figure P-2 Example Use of a Linear Envelope to Represent a Nonlinear Strength Envelope for a Specific Range of Stress. 3
Figure P-3 Other Types of Power Function – (a) Undrained Shear Strength and (b) Three-Parameter 4
Figure P-4 Determining Equivalent Mohr-Coulomb Parameters from Power Function Parameters 6
Figure P-5 Example Conversion between Normalized Parameters and Parameters with Units 7
Figure P-6 Undrained Strength Distribution Example 11
Figure P-7 Drained Envelopes for Saturated Fine-Grained Soils (after Castellanos and Brandon 2014) 13
Figure P-8 Drained Strength Envelopes for Fine-Grained Soils in the Normally Consolidated and Overconsolidated Conditions for Different Values of Preconsolidation Stress (after Duncan et al. 2014) 14
Figure 1-1 Interactive Selection Categories for GeoTechTools Website 37
Figure 1-2 Summary of Key Elements of Aggregate Columns 39
Figure 1-3 Summary of Key Elements of Bulk Infill Grouting 40
Figure 1-4 Summary of Key Elements of Blast Densification 41
Figure 1-5 Summary of Key Elements of Chemical Grouting 42
Figure 1-6 Summary of Key Elements of Column Supported Embankments 43
Figure 1-7 Summary of Key Elements of Compaction Grouting 44
Figure 1-8 Summary of Key Elements of Dynamic Compaction 45
Figure 1-9 Summary of Key Elements of the Deep Mixing Method 46
Figure 1-10 Summary of Key Elements of the Mass Mixing Method 47
Figure 1-11 Summary of Key Elements of Pre-Fabricated Vertical Drains 48
Figure 1-12 Summary of Key Elements of Sand Compaction Piles 49
Figure 1-13 Summary of Key Elements of Soil Nail Walls 50
Figure 1-14 Summary of Key Elements of Vacuum Preloading 51
Figure 1-15 Summary of Key Elements of Vibro-Compaction 52
Figure 1-16 Summary of Key Elements of Vibro-Concrete Columns 53

Figure 2-1 Trench Shield; a) Typical Trench Shield, b) Maximum Slopes for Various Soil Types Defined by OSHA (after OSHA Technical Manual) 60

Figure 2-2 Hydraulic Shoring - a) Spot Bracing, b) Plywood, c) Stacked, and d) Waler System (after OSHA Technical Manual 2020) 63

Figure 2-3 Timber Shoring: a) Skeleton; b) Close (tight); c) Box; d) Telescoping (after OSHA Technical Manual 2020) 64

Figure 2-4 Typical Profiles of Movement for Braced and Tieback Anchor Walls (after Clough and O'Rourke 1990) 67

Figure 2-5 Examples of Combined Sheet Piling Cross Sections (after DeepEX Combined Sheet Pile Walls Software 2021) 67

Figure 2-6 Examples of Support Systems (after USACE 1983b and FHWA 2015) 69

Figure 2-7 Methods for Calculating Factor of Safety Against Basal Instability or Heave (after Wong and Goh 2002) 75

Figure 2-8 Zones of Soil Settlement Behind Excavation Walls (after Peck 1969) 77

Figure 2-9 Observed Maximum Movements for Stiff Clays, Residual Soils and Sands: (a) Vertical and (b) Horizontal (after Clough and O'Rourke 1990) 79

Figure 2-10 Movements Adjacent to Excavations in Stiff to Very Stiff Clays – (a) Measured Settlement, (b) Measured Horizontal Movement, and (c) Recommended Movement Profile (after Clough and O'Rourke 1990) 80

Figure 2-11 Movements Adjacent to Excavations in Sand – (a) Measured Settlement and (b) Recommended Dimensionless Movement Profiles (after Clough and O'Rourke 1990) 81

Figure 2-12 Settlement Adjacent to Excavations in Soft to Medium Clays – (a) Measured Settlement and (b) Normalized Settlements with Recommended Settlement Profile (after Clough and O'Rourke 1990) 82

Figure 2-13 Maximum Horizontal Wall Deflection for Soft to Medium Clays (after Clough et al. 1989 and Clough and O'Rourke 1990) 83

Figure 2-14 Range of Deformations Typical of Excavations in Various Soils Relative to Building Damage Potential (after Clough and O'Rourke 1990) 86

Figure 2-15 Estimation of Movements and Evaluation of Underpinning Requirements Adjacent to an Excavation Supported by a Deep Excavation Support System - Stiff to Hard Clay 88

Figure 2-16 Estimation of Movements and Evaluation of Underpinning Requirements Adjacent to an Excavation Supported by a Deep Excavation Support System - Soft to Medium Clay 89

Figure 2-17 Excavatability of Rock Masses: a) $I_{s(50)}$ < 31 tsf (3 MPa) and b) $I_{s(50)}$ > 31 tsf (3 MPa) (after Tsiambaos and Saroglou 2010) 93

Figure 2-18 Ripper Performance: a) Medium Tractor, b) Heavy-Duty Tractor, and c) Very Heavy Tractors (after Caterpillar 2000) 95

Figure 2-19 Blast Effects Scale (after Konya and Walter 2006) 96

Figure 2-20 Human Response to Vibrations (after Konya and Walter 2006) 97

Figure 2-21 Limits of Dewatering Methods Applicable to different Soils (after Keller Moretrench American Corporation 1954) 98

Figure 2-22 Example Problem for Flow into an Excavation Through Sheet Piling .. 99

Figure 2-23 Methods of Construction Dewatering a) Details of Wellpoint System and b) Details of Deep Well with Submersible Pump (after Mazurkiewicz 1980) 101

Figure 2-24 Methods of Construction Dewatering a) Two Stage Well Point System (after Mazurkiewicz 1980) and b) Combined Well Point and Deep Well System (after USACE 1983a) 102

Figure 3-1 Earthwork Objectives and Methodology 107

Figure 3-2 Changes in Weight-Volume Relationships from Compaction and Changes in Water Content 110

Figure 3-3 Effects of Compactive Effort and Water Content on Compacted Soil Properties 111

Figure 3-4 Effect of Compaction on (a) Shear Strength and (b) Hydraulic Conductivity of Coarse-Grained Soils 114

Figure 3-5 15-Point Method for Determining Engineering Parameters of Compacted Soil 115

Figure 3-6 Engineering behavior of compacted clay – (a) consolidation, (b) stress-strain, (c) total stress cohesion, and (d) total stress friction angle (after DiBernardo and Lovell 1979, Seed et al. 1960, and Kulhawy et al. 1969) 117

Figure 3-7 Variation in consolidated undrained shear strength ratio with as-compacted degree of saturation (after VandenBerge et al. 2015) 118

Figure 3-8 Saturated hydraulic conductivity of laboratory compacted clay – (a) typical variation (based on Mitchell et al. 1965, Garcia-Bengochea 1978) and (b) variation with initial saturation (after Benson and Trast 1995) 118

Figure 3-9 Typical Subgrade Modulus and California Bearing Ratio by USCS (after Porter 1943, USACE 1960, PCA 1992) 120

Figure 3-10 Vertical Compression of Compacted Fill by USCS (after Gould 1954) 121
Figure 3-11 Typical Drained Shear Strength Parameters of Compacted Fill – μ Indicates Mean Value and σ Indicates Standard Deviation (after USBR 1998) 121
Figure 3-12 Oversize Correction Example Calculations 124
Figure 3-13 Borrow Excavation Example 136
Figure 3-14 Schematic of Field Test Section Process 146
Figure 3-15 Typical Soil Compaction for Field Verification – (a) One-Point Method (after ODOT 2010) and (b) Typical Range of Compaction Curve Peak (after ASTM D5080) 150
Figure 3-16 Graphical Analysis of Control Test Data 152
Figure 3-17 Two-Step Interpretation of Control Test Results (after Hilf 1991) 153
Figure 3-18 Compaction Control Guided by Intelligent Compaction (after NCHRP 2010) 155
Figure 3-19. Schematics of Typical Embankment Design Sections (not to scale) . 157
Figure 3-20 Methods to Address Foundation Instability (after TRB 1990 and Holtz 1989) 159
Figure 3-21 Concentrated Leak Erosion and Cracking Resistance of Fill Materials (after Sherard 1953, Wan and Fell 2004) 163
Figure 3-22 Hydraulic Fill Illustration (after Sowers 1979) 165
Figure 4-1 Influence of Movement on Active and Passive Earth Pressure Zones 175
Figure 4-2 Mohr Circles for At-Rest, Rankine Active, and Rankine Passive Stress States 177
Figure 4-3 Active and Passive Earth Pressure – (a) Mobilization with respect to Wall Movement, (b) Active Earth Pressure Distribution and Load, (c) Passive Earth Pressure Distribution and Load, and (d) Required Magnitude of Wall Rotation for Various Soil Types (after Kim et al. 1991) 180
Figure 4-4 Earth Pressure Distributions for Active and Passive Rankine Cases 182
Figure 4-5 Rankine Active Earth Pressure Calculation for No Wall Friction and Uneven Water Elevations 183
Figure 4-6 Rankine Passive Earth Pressure Calculation for No Wall Friction and Uneven Water Elevations 183

Figure 4-7 Gravity Retaining Wall with Sloping Backfill, Sloping Wall, and Interface Friction Angle 185

Figure 4-8 Free Body Diagrams and Force Polygons for Coulomb Method for Various Wall and Backfill Geometries 187

Figure 4-9 Values of K_A and K_P for the Coulomb Method for Vertical Walls with No Wall Friction 188

Figure 4-10 Inclination of the Failure Plane for the Coulomb Method for Vertical Walls with No Wall Friction 189

Figure 4-11 “Actual” and Linear Failure Planes for Active and Passive Earth Pressure Cases for $\phi' = \delta = 30°$ (after Perloff and Baron 1976) 191

Figure 4-12 Values of K_A and K_P for the Log Spiral Method for a Sloping Wall with a Horizontal Backfill (after Kerisel and Absi 1990) 192

Figure 4-13 Values of K_A and K_P for the Log Spiral Method for a Vertical Wall with a Sloping Backfill (after Kerisel and Absi 1990) 193

Figure 4-14 Coulomb Method Applied to a Complex Active Earth Pressure Case 197

Figure 4-15 Passive Earth Pressure Calculations Similar to the Log-Spiral Method with a Circular Arc Replacing the Log Spiral Portion of the Failure Surface 198

Figure 4-16 Effects of the Presence of Water on the Loads Applied to Walls for Cases of (a) Static Water Pressure, (b) Extreme Rainfall Events on Walls with Drainage Elements, and (c) Seepage Beneath a Cantilever Wall 202

Figure 4-17 Lateral Pressure on an Unyielding Wall at the Corner of a Uniform Rectangular Surface Load 205

Figure 4-18 Horizontal Pressure and Resultant Force for a Single Point Load Applied at the Surface of the Backfill 206

Figure 4-19 Horizontal Pressure and Resultant Force for Line Load Applied at the Surface of the Backfill Parallel to the Retaining Structure 207

Figure 4-20 Horizontal Pressure from a Line Load Perpendicular to the Retaining Structure 208

Figure 4-21 Distribution of Horizontal Pressure from a Line Load Perpendicular to the Retaining Structure for Varying Load Geometries and Depths 210

Figure 4-22 Earth Pressures Due to Compaction from Rollers (after Duncan et al. 1991) 211

Figure 4-23 Earth Pressures due to Compaction by Vibratory Plates (after Duncan et al. 1991) 212

Figure 4-24 Earth Pressures due to Compaction by Rammer Plates (after Duncan et al. 1991)..... 213
Figure 4-25 Application of the Simplified M-O Procedure for a Vertical Gravity Retaining Wall with a Horizontal Backfill..... 215
Figure 4-26 Example of M-O Method for a Retaining Wall Having a Sloping Face and a Sloping Backfill..... 216
Figure 4-27 Analysis Methods for Stability Assessment of Gravity Retaining Walls 220
Figure 4-28 Pressure Distributions at the Base of Rigid Retaining Walls (after Kim et al. 1991)..... 222
Figure 4-29 Analysis Method for Gravity Retaining Wall Base with a Key..... 224
Figure 4-30 Low (<12 ft Tall) Retaining Walls – (a) Geometry and Forces and (b) Equivalent Fluid Unit Weights by Soil Type..... 226
Figure 4-31 Drainage Systems Used for Rigid Retaining Structures (after Kim et al. 1991)..... 227
Figure 4-32 Design Notes for Gabion Retaining Walls..... 229
Figure 4-33 Design Elements of Crib Walls and Bin Walls..... 230
Figure 4-34 Total Regular Pressure Diagram and Net Pressure Diagram..... 233
Figure 4-35 Failure Modes for Anchored Bulkheads (after USACE EM 1110-2-2504 1994)..... 234
Figure 4-36 Rowe's Moment Reduction Factors for Flexible Walls..... 236
Figure 4-37 Anchored Bulkhead Design Scenarios..... 237
Figure 4-38 Types of Anchoring Systems for Bulkheads (after USACE EM 1110-2-2504)..... 239
Figure 4-39 (a) Effect of Anchor Position Relative to Wall, and (b) Wall Anchor Capacity Equations..... 240
Figure 4-40 Effect of Depth and Spacing of Anchor Blocks..... 241
Figure 4-41 Calculation Procedure for Cantilever Retaining Structures..... 242
Figure 4-42 Chart for Determining Penetration Depth and Maximum Moment in a Cantilever Flexible Wall in Sand..... 243
Figure 4-43 Example for a Cantilever Wall in Sand..... 245
Figure 4-44 Chart for Determining Penetration Depth and Maximum Moment in a Cantilever Flexible Wall in Sand Overlying Clay..... 246
Figure 4-45 Example for Cantilever Sheet Pile in Sand Underlain by Clay..... 247

Figure 4-46 Soldier Pile and Lagging Walls – (a) Section View, (b) Elevation and Plan View, (c) Passive Pressure Assumptions, and (d) Example Calculation 248
Figure 4-47 Plan View of Secant Pile Wall 250
Figure 4-48 Plan View of Tangent Pile Wall 250
Figure 4-49 Cross Section of a Typical Soil Nail Wall (after FHWA 2015) 251
Figure 4-50 Potential Failure Modes of Soil Nail Walls (after FHWA 2015) 253
Figure 4-51 Apparent Pressure Diagrams for Sands for Internally and Externally Supported Retaining Structures (Wolosick and Scott 2012; FHWA 1999). 255
Figure 4-52 Apparent Pressure Diagrams for Soft to Medium Clay for Internally- and Externally-Supported Structures (Wolosick and Scott 2012; FHWA 1999) 255
Figure 4-53 Apparent Pressure Diagrams for Stiff Clay for Internally and Externally Supported Structures (Wolosick and Scott 2012; FWHA 1999) 256
Figure 4-54 Design Steps for Internally-Supported, Flexible Walls Used for a Narrow Excavation 257
Figure 4-55 Example of Excavation Bracing Analysis Procedure for a Narrow Cut in Fine-Grained Soil 258
Figure 4-56 Design Steps for Flexible Wall Supported by Raking Braces (Rakers) 259
Figure 4-57 Geometry and Design Parameters for Cellular Cofferdams 262
Figure 5-1 Eccentricity for (a) Rectangular Footing and (b) Circular Footing (after Bowles 1996) 278
Figure 5-2 Presumptive Bearing Pressure for Weaker Layer Underlying Bearing Stratum 283
Figure 5-3 Bearing Capacity Failure Modes – (a) General Shear, (b) Local Shear, (c) Load-Settlement Behavior, and (d) Effect of Relative Density on Failure Mode (after Das 2022, Terzaghi 1943, Vesic 1973) 284
Figure 5-4 Assumptions for Bearing Capacity of a Continuous Footing - a) Terzaghi, Brinch Hansen, and Vesic Methods and b) Meyerhof Method 287
Figure 5-5 Bearing Capacity Factors (after Terzaghi 1943, Meyerhof 1951, Brinch Hansen 1970, Coduto et al. 2016) 290
Figure 5-6 Effects of Groundwater Table on Bearing Capacity Calculations 292

Figure 5-7 Shallow Foundation with Inclined Load, Base, and Ground (after Brinch Hansen 1970) 293

Figure 5-8 Foundations Near the Top of Slopes (After Meyerhof 1957, Leshchinsky and Xie 2017) 297

Figure 5-9 Bearing Capacity Factors for Strip Footing for c' = 0 Conditions – a) No Embedment and b) $D_f / B = 1$ (after Meyerhof 1957) 300

Figure 5-10 Example Calculations Illustrating the Terzaghi Method with the Meyerhof Method Used as a Check 302

Figure 5-11 Example Calculations Illustrating the Meyerhof Method 303

Figure 5-12 Example Calculations Illustrating the Brinch Hansen Method 304

Figure 5-13 Eccentricity Calculations – Meyerhof and Brinch Hansen Methods ... 305

Figure 5-14 Non-uniform and Stratified Soils Conditions – (a) Case 1 and (b) Cases 2 to 4 306

Figure 5-15 Variation of N_c for Clay with Increasing s_u with Depth (after Chi and Lin 2020) 307

Figure 5-16 Bearing Capacity Example – Increasing Strength with Depth (Case 1) 308

Figure 5-17 Displacement Vectors for a) Soft Over Stiff Clay and b) Stiff Over Soft Clay (after Griffiths 1999) 309

Figure 5-18 Modified Bearing Capacity Factors for Two-Layer Clay Stratigraphy for a) Strip and b) Circular Footings (after Brown and Meyerhof 1969) .. 310

Figure 5-19 Bearing Capacity Example – Layered, Undrained Clay (Case 2) 311

Figure 5-20 Bearing Capacity Example – Mixed Soil Layers (Case 3) 312

Figure 5-21 Bearing Capacity of Sand Over Relatively Weak Clay (after Meyerhof 1974) 313

Figure 5-22 Coefficients K_s and $s{\cdot}K_s$ for Punching Shearing Resistance (after Meyerhof 1974, Meyerhof and Hanna 1978) 314

Figure 5-23 Bearing Capacity Example – Sand Layer Over Clay (Case 4) 315

Figure 5-24 Modified Factors for – (a) Bearing Capacity and (b) Shape for Circular Footings (after Meyerhof 1974) 316

Figure 5-25 Example Calculations for Bearing Capacity of Rock 318

Figure 5-26 Idealized Distribution of Contact Pressure and Settlement Under a Uniformly Distributed Load for a Rigid Foundation - a) Coarse-grained (c' = 0 psf) and b) Fine-grained (ϕ = 0°) (after Das 2022) 320

Figure 5-27 Idealized Distribution of Contact Pressure and Settlement Under a Uniformly Distributed Loading for a Flexible Foundation – a) Fine-grained Soil, (ϕ = 0 deg) and b) Coarse-grained Soil (c' = 0) (after Das 2022) 321

Figure 5-28 Subgrade Pressure versus Settlement Curve Defining k_s (after Bowles 1996) 323

Figure 5-29 Elastic Influence Factors - (a) μ_I with ν = 0.5, (b) μ_I with ν = 0.3, and (c) μ_0 with ν = 0.25 and 0.5 (after Giroud 1972 and Burland 1970)..... 326

Figure 5-30 Undrained Modulus Correlation for Clay Soils with OCR and PI (after Duncan and Buchignani 1976) 329

Figure 5-31 Computation of Uncoupled Winkler-type Soil Node Springs (after ACI 2002) 331

Figure 5-32 Coupled and Uncoupled Springs (after ACI 2002)..... 331

Figure 5-33 Example Mat Foundation Indirect Coupling Problem..... 333

Figure 5-34 Schematic of a Pressure Slab and Wall System..... 336

Figure 5-35 Schematic of a Relieved Slab and Wall System 337

Figure 5-36 Schematic of a Cutoff Foundation Wall to a Low Permeability Stratum 337

Figure 5-37 Schematic of Ground Anchor Components 340

Figure 5-38 Ground Anchor Design Requirements – (a) Mass Breakout, (b) Grout-Rock or Grout-Soil Shear, (c) Grout-Tendon Shear, and (d) Tendon Capacity (after FHWA 1999)..... 342

Figure 5-39 Example Problem for Single Rock Anchors 344

Figure 5-40 Resisting Hydrostatic Uplift with Ground Anchors (after FHWA 1999) 346

Figure 5-41 Resistance to Transient Uplift Loads on Footings, Piers, and Posts . 348

Figure 5-42 Design Guidance for Uplift Resistance by Concrete Deadman 349

Figure 5-43 Geometric Limits for Structural Fill Beneath Footings..... 351

Figure 5-44 Construction Details for Swelling Soils 353

Figure 5-45 Potential Sulfidic Rock Heave (after Bryant et al. 2003) 354

Figure 5-46 Loess Distribution – (a) United States, (b) South America, (c) Europe, and (d) Asia (after Muhs 2013)..... 356

Figure 5-47 Criteria for Evaluation of Collapsing Soils (after USBR 1992) 357

Figure 6-1 Major Elements of the Process to Design Deep Foundations 366

Figure 6-2 Configurations of Deep Foundation Elements 369
Figure 6-3 Erosion Categories for Soils and Rock Based on Velocity (after Briaud 2008) 371
Figure 6-4 Annual Loss of Metal Thickness Versus Exposure Time in Non-Marine Environments (after Decker et al. 2008) 375
Figure 6-5 Typical Crane-Mounted Pile Driver 385
Figure 6-6 Pile Driving Hammers 386
Figure 6-7 Estimated Vibration Level Due to Pile Driving (after Bay 2003) 390
Figure 6-8 Typical Effects of Disturbance During Driving of Piles (after Broms 1966) 391
Figure 6-9 Dry and Wet Methods of Drilled Shaft Construction 394
Figure 6-10 Micropiles – (a) Construction Sequence and (b) Connection Detail 400
Figure 6-11 Load Transfer Concepts 405
Figure 6-12 Geometry for SCA of Deep Foundations – (a) Length and Diameter and (b) Base Area 407
Figure 6-13 Ratio of K/K_0 for Non-Displacement and Full-Displacement Columns (after Salgado 2008) 413
Figure 6-14 Variation of α with Normalized Undrained Shear Strength for Different Deep Foundation Types and Embedments 417
Figure 6-15 Group Geometry 432
Figure 6-16 Uplift Resistance of Column-Soil Block for Groups of Columns – (a) Coarse-Grained and (b) Fine-Grained Soils 436
Figure 6-17 Load-displacement Curve for Drilled Shafts (after Chen and Kulhawy 2002) 443
Figure 6-18 Locating the Equivalent Footing 446
Figure 6-19 Schematic of the Neutral Plane Method for Estimating Settlement 450
Figure 6-20 Axial Capacity of Batter Pile 455
Figure 6-21 Earth Pressure, Shear, and Moment Diagrams for Broms Method in Undrained Soil Conditions (after Brown et al. 2010) 457
Figure 6-22 Earth Pressure, Shear, and Moment Diagrams for Broms Method in Drained Soil Conditions (adapted from Brown et al. 2010) 458
Figure 6-23 *p-y* Relationships 460
Figure 6-24 Nonlinear Superposition Process to Estimate Deflection 464

Figure 6-25 Geometry for a Group of Foundation Elements Subjected to Lateral Load 466
Figure 6-26 Locating the Neutral Plane 478
Figure 6-27 Schematics of Top-Down and Bi-Directional Axial Load Tests (after ASTM D1143, ASTM D3689, ASTM D8169) 481
Figure 6-28 Interpretation of Failure Load from Static Load Tests 484
Figure 6-29 Definition Sketch for Wave Mechanics Basics 489
Figure 6-30 Forces in Pile Due to Downward and Upward-Traveling Waves 491
Figure 6-31 Typical Force and Velocity Records for Different Resistance Conditions 494
Figure 7-1 Example Statistical Plots Illustrating Important Definitions. 511
Figure 7-2 Sample Space, Events, and Probability Calculations. 514
Figure 7-3 Use of Random Variables to Relate Sample Space to the Real Line 515
Figure 7-4 Common Types of Distribution 516
Figure 7-5 Uncertainty in Characterization of Actual Field Conditions (after Phoon and Kulhawy 1999a) 520
Figure 7-6 Typical Inherent Variability (after Phoon and Kulhawy 1999a, Guan et al. 2021) 521
Figure 7-7 Typical Measurement COV (after Phoon and Kulhawy 1999a, ASTM D1586, ASTM D2216, ASTM D4318) 522
Figure 7-8 Model Uncertainty Examples 524
Figure 7-9 Combined Effects of Uncertainty on Geotechnical Design 525
Figure 7-10 Parameter Selection Using Probabilistic Concepts 531
Figure 7-11 Example Distributions for (a) Load and Resistance and (b) Safety Margin and Factor of Safety Formulations 532
Figure 7-12 Point Estimate Method for Two Random Variables (after Baecher and Christian 2003) 536
Figure 7-13 Guides for Application of the Point Estimate Method (after Harr 1987) 537
Figure 7-14 Hasofer-Lind Reliability Index Concept for Two Random Variables .. 539
Figure 7-15 Convergence of Monte Carlo Simulation with Increasing Trials 540
Figure 7-16 Monte Carlo Simulation Trial Number Requirements 542
Figure 7-17 Example of Correlation Effects on Geotechnical Analysis 543

Figure 7-18 Example F-N Chart 545
Figure 7-19 Example Event Tree (after USACE 2020) 546
Figure 7-20 Example Decision Tree (after Baecher and Christian 2003) 547
Figure 7-21 Example Hazards for an Eastern US Site – (a) to (c) Hazard Curves and (d) to (f) Probability of Exceedance Curves 548
Figure 7-22 LRFD Concept (after FHWA 2001) 551
Figure 7-23 LRFD Pile Design Example 554
Figure B-1 Rationale for Assumption of No Vertical Earth Force 594
Figure B-2 Geometry of the Proposed Cantilever Retaining Wall 595
Figure B-3 Forces for Wall Stability Analysis 597
Figure B-4 Graphical Implicit Solution for Footing with Desired F_{BC} 601
Figure B-5 Retaining Wall Conditions with F_{OT} = 1 602
Figure B-6 Proposed Anchored Bulkhead in Sand 604
Figure B-7 Distribution of Earth and Water Pressures on the Sheetpile 606
Figure B-8 Sum of Moments versus Trial Values of Sheet Pile Embedment 608
Figure B-9 Integration of Pressure Distribution to Locate Elevation of Zero Shear Force 609
Figure B-10 Shear Force Versus Height Above the Dredge Line 609
Figure B-11 Location of the Continuous Anchor 612
Figure B-12 Net Anchor Resistance to Counteract Tierod Force 613
Figure B-13. Three Rows of Footings – Example 3 615
Figure B-14 Plan and Profile of Site 624
Figure B-15 Intepretation of Influence Factors for Elastic Settlement 627
Figure B-16 Proposed Pile Group in Soft and Stiff Clay 631
Figure B-17 Interpretation of Alpha Factor 634
Figure B-18 Load and Resistance Curves 636
Figure B-19 Laterally Loaded Pile Group in Soft and Stiff Clay 641
Figure B-20 Development of Active and Passive Pressures on Pile Cap 644
Figure B-21. Load-Deflection Relationship with Strength Limit State Check 646
Figure B-22. Load-Deflection Relationship with Service Limit State Check 646
Figure B-23 Proposed Cantilever Retaining Wall 648

Figure B-24 Distribution of the Factor of Safety from a Subset of the Monte Carlo Analysis of Bearing Capacity 655

LIST OF TABLES

Table P-1 Effective Stress and Total Stress Shear Strength Parameters and Associated Equation for Calculating Shear Strength on the Failure Plane 2
Table P-2 Shear Strength Methods for *In situ* Coarse-Grained Soil 9
Table P-3 Shear Strength Methods for Engineered Coarse-Grained Soil 10
Table P-4 Undrained Shear Strength Methods for *In situ* Fine-Grained Soil 12
Table P-5 Drained Shear Strength Methods for *In situ* Fine-Grained Soil 15
Table P-6 Strength Methods for *In situ* Nonplastic and Low Plasticity Silt 16
Table P-7 Undrained Shear Strength Methods for Engineered Fine-Grained Soil 17
Table P-8 Drained Shear Strength Methods for Engineered Fine-Grained Soil ... 17
Table 1-1 Sensitivity categories (after Rosenqvist 1953) 23
Table 1-2 List of Technologies Included in GeoTechTools and GEC 13. 34
Table 1-3 Technologies Used to Address Basic Goals of Soil Improvement (after FHWA 2017) 35
Table 1-4 Soil Types and Foundation Conditions for Different Technologies (after FHWA 2017). 36
Table 2-1 Soil Types (after OSHA CFR Part 1926, Subpart P, Appendix A) 60
Table 2-2 Aluminum Hydraulic Shoring - Soil Types A and B, No Walers (after OSHA 2020 Appendix D, Tables D-1.1 and D-1.2) 61
Table 2-3 Aluminum Hydraulic Shoring – Soil Types B and C with Wales (after OSHA 2020 Appendix D, Tables D-1.3 and D-1.4) 62
Table 2-4 Minimum Requirements for Timber Trench Shoring (after OSHA 2020) 65
Table 2-5 Types of Walls and Factors Involved with Selection 68
Table 2-6 Factors Influencing the Selection of Support Systems 70
Table 2-7 Influence of Soil Conditions on Selection of Deep Excavation Wall and Support Systems 71
Table 2-8 Typical Settlement and Horizontal Movement Relative to Height (after Clough and O'Rourke 1990) 78
Table 2-9 Some Common Methods of Underpinning 87
Table 2-10 Construction Considerations for Deep Excavation Support Systems .. 90
Table 2-11 Methods of Groundwater Control 100

Table 2-12 Problem Soil Considerations for Sloped Open Cut Excavations (after Clough and Davidson 1977) 103
Table 2-13 Problem Soil Considerations for Deep, Supported Excavations 104
Table 3-1 Typical Compaction Properties and Hydraulic Conductivity based on USCS (after USACE 1960) 120
Table 3-2 Relative Desirability of Soils for Compacted Fill based on USCS Classification (after USBR 1998) 122
Table 3-3 Applicability of Testing Methods by USCS Classification 125
Table 3-4 Stress and Particle Effects on the Shear Strength of Rock Fill 127
Table 3-5 Typical Properties of Common Recycled Fill Materials (after Soleimanbeigi et al. 2014, Soleimanbeigi and Edil 2015, DiGioia and Nuzzo 1972, Masad et al. 1996). 128
Table 3-6 Common Lightweight Fill Materials (after FHWA 2017, Arulrajah et al. 2015) 129
Table 3-7 Fill Transport Methods and Haul Distances (after Coduto et al. 2011) 134
Table 3-8 Equipment Type Summary 139
Table 3-9 Applicability of Compaction Equipment to Different Soil Types 140
Table 3-10 Simple Compaction Control Methods for Field Engineers (after TRB 1990, USACE 1995a) 143
Table 3-11 Typical Compaction Specifications for Soil with Appreciable Fines ... 144
Table 3-12 Compaction Control Criteria for Compacted Earth Dams (after USBR 1987) 145
Table 3-13 Comparison of Common Compaction Control Test Methods 148
Table 3-14 Control Testing Requirements for Different Types of Fill (after Hilf 1991, USBR 1998, USACE 1995a, Sowers 1979) 149
Table 3-15 Statistical Approach to the Selection of Mean Relative Compaction Requirements 154
Table 3-16 Erosion Resistance Categories (after USBR and USACE 2019) 162
Table 3-17 Dispersive Tendency from Double Hydrometer, Pinhole and Crumb Tests (after ASTM D4221, D4647, D 6572) 164
Table 3-18 Methods of Underwater Fill Placement (after Johnson et al. 1972) ... 169
Table 3-19 Problem Soil Considerations for Earthwork 170

Table 4-1 Interface Friction Angles and Adhesion Values for Wall/Soil Interfaces 184
Table 4-2 Comparison of K_A and K_P Values for Earth Pressure Methods (β=θ=0°) 194
Table 4-3 Equivalent Fluid Unit Weights for At-Rest and Active Conditions for Horizontal and Sloping Backfills (after Kim et al. 1991) 195
Table 4-4 Adjustment Factors for Earth Pressures Induced by Compaction with Rollers (after Duncan et al. 1991) 211
Table 4-5 Adjustment Factors for Earth Pressures Induced by Compaction with Vibratory Plates 212
Table 4-6 Adjustment Factors for Earth Pressures Induced by Compaction with Rammer Plates (after Duncan et al. 1991) 213
Table 4-7 Modes of Failure and Design Details for Sheet Pile Cofferdams 264
Table 4-8 Problem Soil Considerations for Retaining Structures 268
Table 5-1 Presumptive Allowable Bearing Pressures (B > 3 ft) (after NRCS 2022, Das 2022) 282
Table 5-2 Bearing Capacity Factors, N_c, N_q, and N_γ 289
Table 5-3 Suitability of Terzaghi, Meyerhof, and Brinch Hansen Methods to Calculate q_{ult} (after Bowles 1996) 291
Table 5-4 Bearing Capacity Methods for Local Shear 291
Table 5-5 Shape Factors for the Terzaghi Upper Bound Method 294
Table 5-6 Bearing and Correction Factors for the Meyerhof (1963) Method 294
Table 5-7 Bearing and Correction Factors for the Brinch Hansen (1970) Method – ϕ = 0 295
Table 5-8 Bearing and Correction Factors for the Brinch Hansen (1970) Method – ϕ' > 0 296
Table 5-9 Bearing Capacity Reduction Coefficients for Foundations Near Slopes in Undrained Conditions (after Leshchinsky and Xie 2017) 298
Table 5-10 Bearing Capacity Reduction Coefficients for Foundations Near Slopes in Saturated Drained Conditions (after Leshchinsky and Xie 2017) 299
Table 5-11 Values of Bearing Capacity Factor, N_{ms}, for Strip Footings (after Brown and Meyerhof 1969, Meyerhof and Hanna 1978, Merifield et al. 1999, and Zhu 2004) 310
Table 5-12 Range of Properties for Rock Types (after Wyllie and Norrish 1996 and Bowles 1996) 317

Table 5-13 Typical Modulus of Subgrade Reaction Values (after Bowles 1996) . 324
Table 5-14 Typical Soil Moduli (after Bowles 1996) 327
Table 5-15 Correlations for the Drained Modulus of Coarse-Grained Soils with SPT and CPT (after FHWA 2002a, Duncan and Bursey 2007, Coduto 2015, McGregor and Duncan 1998) 328
Table 5-16 Typical Values of Poisson's Ratio (after Bowles 1996) 329
Table 5-17 Vertical Pressure Profiles for Selected Points Beneath a Foundation Mat (after ACI 2002) 334
Table 5-18 Methods of Foundation Dampproofing and Waterproofing 339
Table 5-19 Presumptive Average Ultimate Bond Stress for Anchor Grout/Rock Interfaces with Gravity Grouting (After PTI 1996, in FHWA 1999) 343
Table 5-20 Presumptive Average Ultimate Bond Stress for Anchor Grout/Soil Interfaces with Gravity Grouting (After PTI 1996 in FHWA 1999) 345
Table 5-21 Classification of Collapse (after ASTM D 5333, Jennings and Knight 1975) 358
Table 5-22 Problem Soil Considerations for Shallow Foundations 359
Table 6-1 Organization of Chapter 6 365
Table 6-2 Site and Project Considerations for Deep Foundations 370
Table 6-3 Conditions that Pose a Heightened Risk of Foundation Deterioration (after AASHTO 2020) 374
Table 6-4 Guidance for Minimum Center-to-Center Spacing 377
Table 6-5 Deep Foundation Construction Tolerances 377
Table 6-6 Summary of Timber Piles and Steel H-Piles 380
Table 6-7 Summary of Steel Pipe Piles and Concrete Piles 381
Table 6-8 Summary of Drilled Shafts and Continuous Flight Auger Columns 382
Table 6-9 Summary of Drilled Displacement Columns and Helical Piles 383
Table 6-10 Summary of Material Properties of Foundation Materials 384
Table 6-11 Recommended Strength Limit State Resistance Factors for Axial Compressive Resistance Evaluated by SCA (AASHTO 2020) 410
Table 6-12 Recommended Minimum Factors of Safety for Compressive Loading 411
Table 6-13 Ratio of Shaft Friction Earth Pressure Coefficient to At-Rest Earth Pressure Coefficient 412

Table 6-14 Interface Friction Angle Ratios for Evaluating Shaft Friction 412
Table 6-15 Guidance for Estimating β 414
Table 6-16 Influence of Clay Consistency on α for Driven Piles (Tomlinson 1994) 416
Table 6-17 Base Resistance Factors for Drained Conditions based on Soil Type and Friction Angle (after Fellenius 2021, Cheng 2004) 421
Table 6-18 Factors for Approximating Volumetric Strain 423
Table 6-19 Correlations Between SPT N Values and Nominal Shaft Resistance 426
Table 6-20 Correlations Between SPT N values and Nominal Base Resistance. 426
Table 6-21 Side Resistance Factor (after Bustamante and Gianeselli 1982) 427
Table 6-22 Maximum Unit Side Resistance (after Bustamante and Gianeselli 1982) 427
Table 6-23 Base Bearing Factor (after Bustamante and Gianeselli 1982)..... 427
Table 6-24 Typical Nominal Unit Grout-to-Ground Bond Strengths (FHWA 2005) 428
Table 6-25 Joint Modification Factors, α_E, for Unstable Rock (after FHWA 1999)430
Table 6-26 Group Efficiency Factor for Groups of Elements 432
Table 6-27 Recommended Strength Limit State Resistance Factors for Block Failure (AASHTO 2020) 433
Table 6-28 Recommended Strength Limit State Uplift Resistance Factors (AASHTO 2020) 434
Table 6-29 Recommended Minimum Factors of Safety for Tension Loading 435
Table 6-30 Guidance for Consideration of Down Drag 437
Table 6-31 Relationships for Normalized Drilled Shaft Settlement vs Normalized Loading..... 444
Table 6-32 Guidance for Locating the Equivalent Footing..... 447
Table 6-33 Recommended Factors for Lateral Geotechnical Resistance (after FHWA 2018b)..... 454
Table 6-34 Equations for Characteristic Parameters (Clarke and Duncan 2002) 461
Table 6-35 R_I Values for Circular Reinforced Concrete Section..... 462
Table 6-36 Constants for Load and Moment Deflection Equations (after Brettmann and Duncan 1996)..... 462
Table 6-37 Coefficients for Estimating the Maximum Moment..... 464

Table 6-38 p-Multipliers to Account for Group Effects in Design (after AASHTO 2020, Mokwa 1999) 466
Table 6-39 AASHTO (2020) Resistance Factors During Pile Driving 469
Table 6-40 Yield Stress and Driving Stress Limit for Common Steel Piles 470
Table 6-41 Allowable Stresses Parallel to the Grain for Treated Timber Graded in Accordance with ASTM D25 (AWPI 2002) 471
Table 6-42 Resistance Factors for Structural Strength Limit State (AASHTO 2020) 472
Table 6-43 Recommended Allowable Stresses for Typical Foundation Materials (ICC 2015) 473
Table 6-44 Rate (n_h) of Increase in Subgrade Modulus with Depth for Sands (AASHTO 2020) 475
Table 6-45 Recommended Strength Limit State Resistance Factors for Axial Loading based on Static and Dynamic Testing 480
Table 6-46 Interpretation of Failure Load from Static Load Tests 484
Table 6-47 Common Dynamic Methods Based on Wave Mechanics 486
Table 6-48 Strength Limit State Resistance Factors for Axial Loading based on Rapid Load Testing (after McVay et al. 2013, FHWA 2018a) 497
Table 6-49 Problem Soil Considerations for Deep Foundations 501
Table 7-1 Common Statistics 510
Table 7-2 Probabilistic Terminology (after Ayyub and McCuen 2016, Baecher and Christian 2003) 513
Table 7-3 Properties of Random Variables 517
Table 7-4 Typical Combined COV for Common Geotechnical Parameters (after Phoon and Kulhawy 1999a,b; Sleep and Duncan 2014, FHWA 2001, Guan et al. 2001) 526
Table 7-5 Reliability Analysis Methods 534
Table 7-6 Comparison of Ultimate Limit State Design Methodologies (after Kulhawy 2017) 550
Table 7-7 Resistance Factors based on Fitting Directly to ASD rather than Reliability Theory (after FHWA 2001) 552
Table B-1 Forces and Moments for Wall Stability Analysis 598
Table B-2 Implicit Solution for Footing Width with Desired FBC 600

Table B-3 Summary of Minimum Footing Widths Meeting Stability Requirements 601
Table B-4 Summary of Stability Checks for Example 1 602
Table B-5 Earth Pressure Coefficients Used in the Design 605
Table B-6 Summary of Lateral Pressure and Force Calculations 606
Table B-7 Summary of Moment Calculations 607
Table B-8 Calculation of the Maximum Bending Moment in the Sheet Pile 610
Table B-9 Properties of the PZ-22 Hot Rolled Steel Sheet Pile 610
Table B-10 Calculation of Net Allowable Anchor Resistance 613
Table B-11 Summary of Anchor Design 614
Table B-12 Calculation of the Elevation of the Resultant Force 614
Table B-13 Summary of Anchored Bulkhead Design Example 614
Table B-14 Design Properties of Overconsolidated Clay 615
Table B-15 Bearing Capacity Factors for the Example 3 616
Table B-16. Meyerhof Corrections for Footing Shape and Depth 618
Table B-17. Brinch Hansen Corrections for Footing Shape and Depth 619
Table B-18 Interpolation of Bearing Capacity Factors for Sloping Conditions 621
Table B-19 Corrections for Footing Shape, Depth, and Ground Inclination (Brinch Hansen 1970) 622
Table B-20 Iterative Sizing of Footing 3 623
Table B-21 Summary of Bearing Capacity Analyses – Example 3 623
Table B-22 Subsurface Profile 624
Table B-23 Calculated Vertical Stresses, OCR, and Modulus at Layer Midpoints 627
Table B-24 Evaluation of Initial Stresses Prior to Construction 629
Table B-25 Evaluation of Preconsolidation Stress and Stress Changes 629
Table B-26 Strain and Compression Calculations 629
Table B-27 Summary of Estimated Settlements and Subgrade Reaction Moduli 630
Table B-28 Key Values for Load and Resistance Curves 637
Table B 29 Delineation of Compressible Soil Profile and Initial Vertical Stress ... 638
Table B-30 Consolidation Settlement Calculations 639
Table B-31 Estimated Elastic Compression of the Piles above the Neutral Plane 640

Table B-32 Calculation of Weighted p-Multiplier 643
Table B-33 Pile Cap Pressure Calculations 644
Table B-34 Deflection, Lateral Pile Load, and Maximum Moment due to Unfactored Loading 647
Table B-35 Probabilistic Material Properties for Wall Design 649
Table B-36 FOSM Approximation for Retaining Wall Example 650
Table B-37 Summary of Probabilities of Unsatisfactory Overturning Resistance 650
Table B-38 Summary of Probabilities of Unsatisfactory Sliding Resistance 652
Table B-39 Approximate FOSM Analysis of Bearing Capacity 653
Table B-40 Point Estimate Analysis of Bearing Capacity 654
Table B-41 Monte Carlo Analysis of Bearing Capacity 655
Table B-42 Summary of Probabilistic Stability Checks for Wall Design 656

PROLOGUE P. SHEAR STRENGTH FOR GEOTECHNICAL DESIGN

P-1 SCOPE.

The design methods presented in this manual require shear strength parameters for the soil materials encountered. However, the correct methods to measure or estimate the shear strength parameters are not explained in detail in the forthcoming chapters. The purpose of this prologue is to provide the designer with suggestions on how to arrive at the parameters necessary for successful design and analysis.

The procedures included in this prologue are accepted in mainstream geotechnical engineering practice. There are more advanced theories of soil behavior that are reported in various geotechnical publications, but those are more appropriately applied to designs that are more advanced than those presented in this manual.

This prologue divides soils generally into coarse-grained or granular soils, often called *cohesionless* materials; and fine-grained or *cohesive* materials. These distinctions are useful in that coarse-grained soils do not develop significant pore pressures during normal construction loading, while fine-grained soils can show increases in pore pressures for compressive loads and decreases in pore pressures during reductions in loads or excavations.

This prologue is organized by first addressing factors that apply to both fine-grained and coarse-grained soils, and then specifically outlining the methods of arriving at design shear strength parameters.

P-2 STRENGTH ENVELOPES.

P-2.1 Mohr-Coulomb Failure Criteria.

The limit equilibrium procedures described in this manual, such as pile capacity, bearing capacity of shallow foundations, and stability of retaining structures, require shear strength parameters that are defined by Mohr-Coulomb failure criteria. In short, the Mohr-Coulomb theory relates the shear strength of the soil to the normal stress on the failure plane. For the case of drained or effective stress strengths, the shear strength is related to the effective normal stress on the failure plane. For the case of undrained or total stress strengths, the shear strength is related to the total normal stress on the failure plane. For saturated soils, there exists a special case whereby the undrained strength is independent of the stress of the failure plane ($\phi = 0$ case). Examples of these three failure envelopes, with the simplifying assumption of a linear envelope, are shown in Figure P-1.

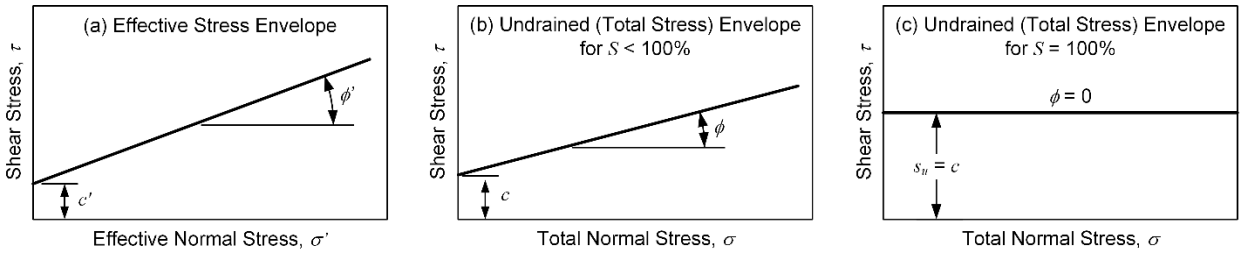

Figure P-1 Mohr-Coulomb Failure Envelopes for Effective and Total Stress Conditions

Shown in Table P-1 are the basic shear strength parameters for these three envelopes and the general equation used to calculate shear strength (s) as a function of the normal stress. In geotechnical engineering practice, the prime symbol (′) is used to denote effective stress or drained parameters. In some older references and manuals, a bar above the parameter is used instead of the prime symbol (e.g., $\overline{\phi}$ and $\overline{c}$). Unfortunately, many papers, manuals, and textbooks are not consistent in clearly indicating drained or effective stress parameters. The prime symbol is often omitted even though the shear strength parameters refer to effective stress or drained parameters, and the reader should be aware of this issue.

The strength equations shown in Table P-1 are simple equations for a line, with the σ and σ' parameters denoting the total and effective stress normal to the failure plane. For the limit equilibrium analyses presented in this manual, the use of these equations is often embedded into the derivation of the equilibrium equation and is not readily apparent.

Table P-1 Effective Stress and Total Stress Shear Strength Parameters and Associated Equation for Calculating Shear Strength on the Failure Plane

Case (S = degree of saturation)	**Parameters[A]**	**Strength Equation**
Drained ($0 \le S \le 100\%$)[B]	ϕ' = effective stress friction angle c' = effective stress friction angle	$s = c' + \sigma' \tan \phi'$
Undrained ($S < 100\%$)	ϕ = total stress friction angle c = total stress cohesion	$s = c + \sigma \tan \phi$
Undrained ($S = 100\%$)	$\phi = 0$ = total stress friction angle c = total stress cohesion	$s_u = c$

[A] "Drained" is often used synonymously for "effective stress." "Undrained" is often used synonymously for "total stress."

[B] Effective stress or drained parameters can be used for any degree of saturation, but in conventional practice, these are used for zero or positive pore water pressures.

P-2.2 Nonlinear Envelopes.

The envelopes in Figure P-1 are linear, and the equations used to calculate the shear strength use the intercept (c' or c) and the slope ($\tan \phi'$ or $\tan \phi$) to calculate the shear strength.[1] Although strength envelopes for soils are commonly nonlinear, a single value of intercept and slope may be accurate enough to represent the strength of a soil over a specific pressure range. Figure P-2 shows a curved envelope, and a linear representation for the pressure range indicated. For the range of normal stresses shown, the resulting shear strength calculated from the values of c' and ϕ' would be sufficiently accurate for design analyses. However, for normal stresses less than or greater than the range of stresses shown, the linear envelope would overpredict the shear strength. This should be kept in mind when using a design procedure or formula that requires single values of ϕ' and c' (or ϕ and c). There are many ways to accommodate nonlinear failure envelopes. Examples of four different methods are outlined in Duncan et al. (2014).

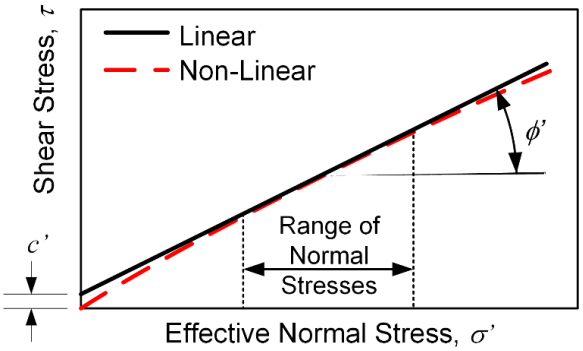

Figure P-2 Example Use of a Linear Envelope to Represent a Nonlinear Strength Envelope for a Specific Range of Stress

P-2.2.1 Two-Parameter Power Function.

The use of a two-parameter power function to model the envelope is one method available in some limit equilibrium slope stability programs, which are useful for checking global stability for retaining walls and other structures. Instead of the usual shear strength parameters of ϕ' and c', the alternative parameters a and b can be used in the equation below:

[1] The $\phi = 0$ envelope experimentally determined for saturated clays using the unconsolidated-undrained triaxial test may be slightly nonlinear for a large range of cell pressures, but should always be interpreted as a horizontal linear envelope for saturated fine-grained soils.

$$s = aP_a\left(\frac{\sigma'}{P_a}\right)^b \tag{P-1}$$

where:
a and b = power function strength parameters and
P_a = atmospheric pressure.

Although less common, the two-parameter power function can also be used to represent undrained shear strengths. For example, as shown in Figure P-3(a), undrained strength can be related to the effective consolidation stress as:

$$s_u = a_u P_a\left(\frac{\sigma'_{1,con}}{P_a}\right)^{b_u} \tag{P-2}$$

where:
s_u = undrained shear strength,
a_u and b_u = power function strength parameters.

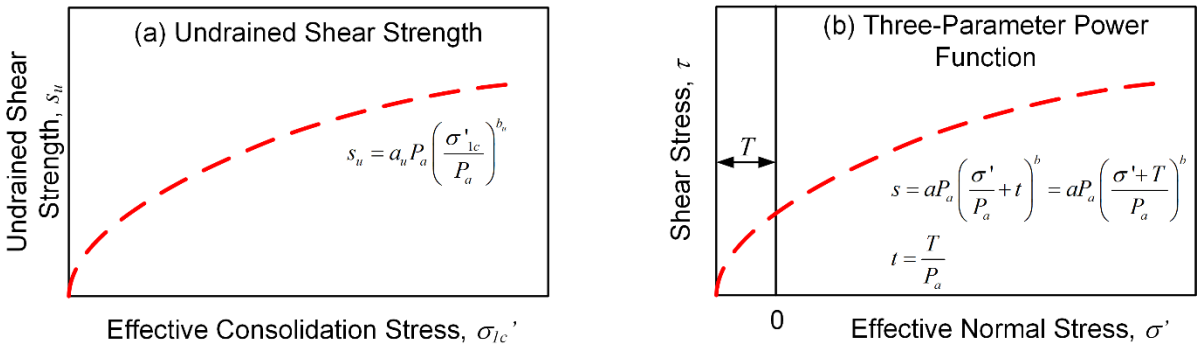

Figure P-3 Other Types of Power Function – (a) Undrained Shear Strength and (b) Three-Parameter

P-2.2.2 Three-Parameter Power Function.

Equation A-1 cannot model a shear strength intercept. A three-parameter function is required for cases where an intercept is warranted. Jiang et al. (2003) suggested the following form which is plotted in Figure P-3(b):

$$s = aP_a\left(\frac{\sigma'}{P_a}+t\right)^b \tag{A-3}$$

where:
t = tensile intercept (T) normalized by atmospheric pressure.

An alternate method with a normalized cohesion intercept outside the parentheses was given by McGuire and VandenBerge (2017). For practical purposes, the two forms give equivalent results. A useful summary of nonlinear failure envelopes is found in VandenBerge et al. (2018).

P-2.2.3 Application of Power Functions in Geotechnical Analysis.

To use a power function in analysis, the computer software must be programmed to accept the a and b parameters and correctly calculate the shear strength. Further details for using the power function can be found in VandenBerge et al. (2018).

If the parameters a and b are available, it is possible to estimate ϕ' and c' for a range of pressures, as shown in Figure P-2 for a curved envelope. Figure P-4 shows an example for calculating the ϕ' and c' shear strength parameters for the normal effective stress range of 2000 to 4000 psf.

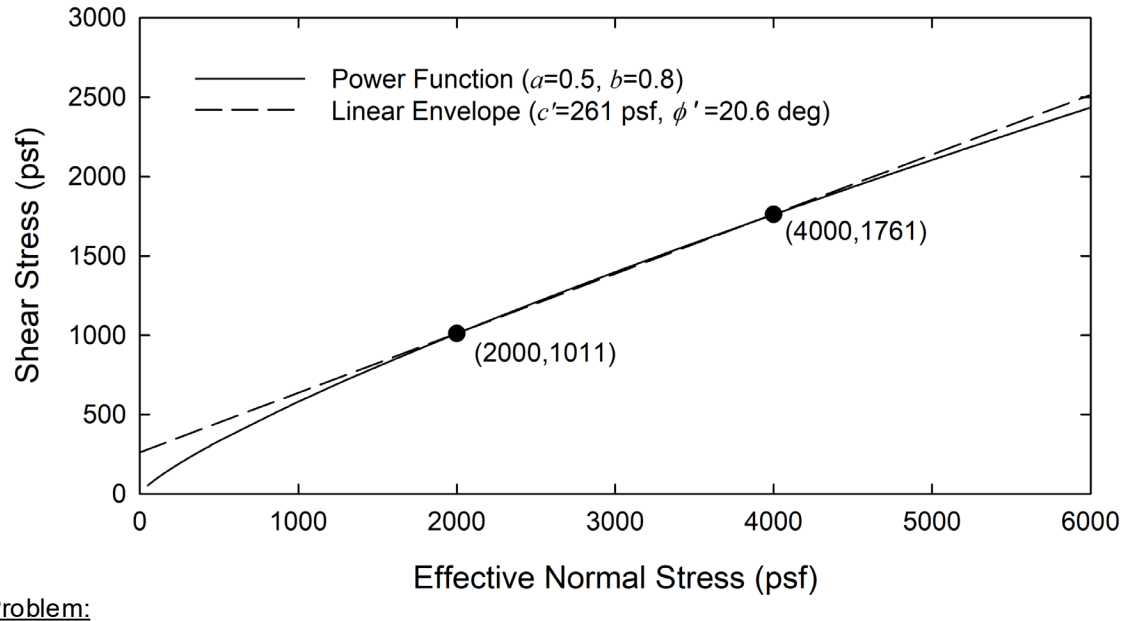

Problem:

Given a nonlinear failure enveloped presented by a power function with a = 0.5 and b = 0.8, Find an equivalent linear envelope for σ' between 2000 and 4000 PSF.

Solution:

Shear Strength at 2000 psf: $$s = (0.5)(2116\,psf)\left(\frac{2000\,psf}{2116\,psf}\right)^{0.8} = 1011\,psf$$

Shear Strength at 4000 psf: $$s = (0.5)(2116\,psf)\left(\frac{4000\,psf}{2116\,psf}\right)^{0.8} = 1761\,psf$$

Equivalent Friction Angle: $$\phi'_{EQ} = \tan^{-1}\left(\frac{1761-1011}{4000-2000}\right) = 20.6^{\circ}$$

Equivalent Cohesion Intercept: $$c' = 1011 - (2000-0)\left(\frac{1761-1011}{4000-2000}\right) = 261\,psf$$

Figure P-4 Determining Equivalent Mohr-Coulomb Parameters from Power Function Parameters

Some analysis methods or software that accommodate power functions may use parameters with units rather than the normalized parameters presented in Eqn. P-1 and P-2. The equivalent parameters can be determined by setting the two equations equal to each other and solving. An example is provided in Figure P-5.

A. Give a nonlinear failure envelope represented by a power function with a = 0.5 and b = 0.8, find equivalent parameters with units for the equation:

$$s = A\left(\sigma'\right)^{B}$$

1) Equate the two forms of the power function:

$$aP_a\left(\frac{\sigma'}{P_a}\right)^{b} = aP_a^{1-b}\left(\sigma'\right)^{b} = A\left(\sigma'\right)^{B}$$

2) It is evident that normalization does not change the exponent:

$$B = b$$

3) Canceling the effective normal stress terms:

$$A = aP_a^{1-b}$$

4) For this particular example:

$$A = \left(0.5\right)\left(2116\,psf\right)^{1-0.8} = 2.312\,psf^{0.2}$$

$$B = 0.8$$

B. Given a nonlinear failure envelope represented by a three-parameter power function with a = 0.6, b = 0.9, and t = 0.4, find equivalent parameters with units for the equation:

$$s = A\left(\sigma'+T\right)^{B}$$

1) Equate the two forms of the power function:

$$aP_a\left(\frac{\sigma'}{P_a}+t\right)^{b} = aP_a^{1-b}\left(\sigma'+tP_a\right)^{b} = A\left(\sigma'+T\right)^{B}$$

2) Solving for the various parameters results in:

$$T = tP_a \qquad B = b \qquad A = aP_a^{1-b}$$

3) For this particular example:

$$T = \left(0.4\right)\left(2116\,psf\right) = 846\,psf \qquad B = 0.9 \qquad A = \left(0.6\right)\left(2116\right)^{1-0.9} = 1.29\,psf^{0.1}$$

Figure P-5 Example Conversion between Normalized Parameters and Parameters with Units

P-3 SELECTION OF SHEAR STRENGTH PARAMETERS.

The shear strength parameters for different soil types may be measured or estimated using one or more of the following:

1. Laboratory tests on disturbed, reconstituted, or compacted test specimens
2. Laboratory tests on “undisturbed” or intact test specimens
3. *In situ* or field tests
4. Correlations

Details regarding these methods can be found in DM-7.1. The selection of shear strength parameters will be discussed for two general types of deposits:

(1) *In situ* undisturbed soils. These normally would be natural soils, but also can include existing fill soils.

(2) Engineered and un-engineered fill materials. The category would include embankments, dams and levees, retaining wall backfills, dredge materials, etc.

P-3.1 *In situ* Deposit of Coarse-Grained Soil (Sand to Gravel).

The most common shear strength parameter used for coarse-grained soil is the drained or effective stress friction angle (ϕ'). Although these materials can have nonlinear failure envelopes, particularly over a wide range of stresses, a single value of the friction angle normally is required at a specific depth for design.

The methods for arriving at an effective stress friction angle for *in situ* deposits of coarse-grained soils are discussed based on the four methods listed earlier.

Table P-2 Shear Strength Methods for *In situ* Coarse-Grained Soil

Method	Guidance
Laboratory tests on disturbed, reconstituted, or compacted test specimens	**Rarely Appropriate** For *in situ* deposits of sands and gravel, laboratory tests on reconstituted test specimens are rarely useful. Many important field effects, such as aging, cementation, and OCR, cannot be modeled in laboratory specimens.
Laboratory tests on "undisturbed" or intact test specimens	**Rarely Appropriate** Intact samples of coarse-grained soils cannot usually be obtained. Although there are some elaborate methods, such as ground freezing, that can be used, these methods are rare in practice.
In situ or field tests	**Very Appropriate** *In situ* and field tests are the best approach for determining the *in situ* friction angle of coarse-grained soils. These tests include the Standard Penetration Test (SPT), Cone Penetration Test (CPT), and Becker Hammer Test (BPT). Equations for calculating ϕ' from the SPT blow count and q_c from the CPT can be found in Chapter 8 of DM 7-1. Both the SPT and CPT can have testing issues for materials much coarser than sands. The BPT has been successful in testing material in very coarse granular soils (Harder and Seed 1986).
Correlations	**Often Appropriate** There are many correlations to determine the drained friction angle based on a variety of parameters, such as classification, gradation, particle shape, etc. A large collection of these is found in Chapter 8 of DM-7.1. The correlation developed by Mike Duncan (Duncan et al. 2014) is particularly well-documented and useful. The input parameters are soil type (SP, SW, or GP), normal stress on the failure plane, and relative density. This correlation has an advantage in that the curvature of the strength envelope is considered. A key to applying this correlation to *in situ* soils is the estimate of the relative density. The relative density can be estimated using the SPT or CPT.

P-3.2 Engineered Deposit of Coarse-Grained Soil (Sand to Gravel).

Again, the most common shear strength parameter used for engineered deposits is the drained or effective stress friction angle (ϕ'). When it is necessary to provide a total stress friction angle (ϕ) for an analysis, the effective stress friction angle is commonly used since these are drained materials. The methods for determining the shear strength of engineered coarse-grained soils are summarized in Table P-3.

Table P-3 Shear Strength Methods for Engineered Coarse-Grained Soil

Method	Guidance
Laboratory tests on disturbed, reconstituted, or compacted test specimens	**Very Appropriate** Laboratory tests are appropriate for engineered coarse grained soils, provided that the test specimen has a maximum particle size within the limits set by the ASTM standards. Examples of triaxial test results conducted on common gravel gradations can be found in Duncan et al. (2007). Some direct shear test apparatuses are large enough to test gravel-sized material. Laboratory test specimens should be compacted to the appropriate dry unit weight expected for the field compaction or placement method. Unless the soil has a significant amount of fines (> 15%), the compaction water content for the laboratory specimens is not critical as long as long as the specified dry unit weight is achieved. The test specimens should be saturated, and either drained or undrained tests (with pore pressure measurements) can be conducted. Laboratory tests should be conducted at a range of stresses similar to those expected during the operation of the structure. The stresses on the failure planes of the laboratory specimens should bracket those calculated or estimated for field conditions.
Laboratory tests on "undisturbed" or intact test specimens	**Rarely Appropriate** Not applicable for new fills. Existing fills have the same sampling difficulties as natural coarse-grained soils.
In situ or field tests	**Marginally Appropriate** Not applicable for fills, except as used for QA/QC tests on fills. The Dynamic Cone Penetration Test (DCP) can be used for indicating the density of a fill, but no reliable correlations exist for the DCP and the effective stress friction angle. If the fill has been in place for a considerable time, then the methods outlined for *in situ* deposits can be followed (see Table).
Correlations	**Often Appropriate** Table and Chapter 8 of DM-7.1 discuss correlations to determine the drained friction angle. Duncan's correlation (Duncan et al. 2014) is also useful for compacted granular soils. It is especially useful for coarse soils that have maximum particle sizes too large for normal laboratory test apparatuses. The relative density required for this correlation can be determined from the compaction specifications or the compaction control testing.

P-3.3 *In situ* Deposit of Fine-Grained Soil.

For *in situ* deposits of saturated fine-grained soils, the methods used depend on whether drained or undrained strengths are appropriate. Undrained strengths are generally important when the stability for short term conditions is required, particular if the project loading increases the pore water pressure.

For partially saturated fine-grained soils, undrained strengths are often necessary for locations above the phreatic surface. The appropriate undrained strength characterization is a c-ϕ envelope.[2] Often in engineering practice, the soil is

[2] Ideally, these parameters should be obtained from Unconsolidated-Undrained triaxial tests on intact test specimens.

characterized with an s_u for an assumed $\phi = 0$ condition. This is not ideal, but as long as the value of s_u is interpreted using a conservative method, it should suffice.

Drained strength parameters are appropriate for long-term conditions where the pore water pressures can be measured, calculated, or estimated with reasonable accuracy. An example of this would be when increases or decreases in pore water pressure caused by the project loading have dissipated, and the pore water pressures have returned to hydrostatic conditions. A second example would be when a steady-state seepage condition has been achieved, and pore water pressures can be calculated. Drained strength parameters are often assigned to partially-saturated soils above the phreatic surface.

The next two sections discuss methods to determine undrained shear strengths and drained shear strength of fine-grained soils, particularly those which behave in a clay-like manner and classify as lean clay, fat clay, or elastic silt. Nonplastic and low plasticity silts behave differently and are discussed in the third section.

P-3.3.1 Undrained Shear Strength - *In situ* Deposit of Fine-Grained Soil.

The design procedures in this manual may require the distribution of undrained strength versus depth for saturated, fine-grained deposits. This strength is associated with a $\phi = 0$ strength model. Figure P-6 shows an example stratigraphy and shear strength distribution. The goal is often to have enough data points to represent the strength distribution with accuracy. The methods to determine the value of undrained strength versus depth are summarized in Table P-4.

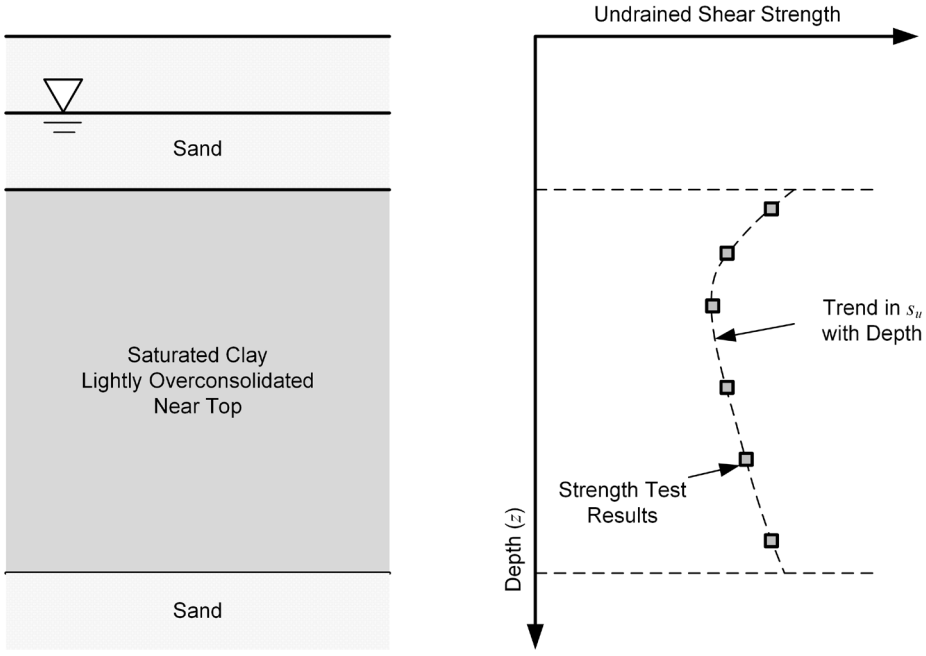

Figure P-6 Undrained Strength Distribution Example

Table P-4 Undrained Shear Strength Methods for *In situ* Fine-Grained Soil

Method	Guidance
Laboratory tests on disturbed, reconstituted, or compacted test specimens	**Marginally Appropriate** The only value of testing disturbed specimens is to determine the undrained strength for normally consolidated conditions. The soil can be remolded, and the undrained strength can be measured with a variety of tests. These include the miniature vane shear test, the fall cone test, UU triaxial tests, and the direct simple shear test. Details of these tests are provided in Chapter 3 of DM-7.1. These tests, conducted on carefully remolded samples, could provide a lower bound undrained strength. However, the resulting strengths do not allow the undrained strength versus depth relationship to be accurately determined for in situ conditions.
Laboratory tests on "undisturbed" or intact test specimens	**Very Appropriate** Laboratory tests on intact test specimens is a common method to acquire undrained strengths for design. The applicable tests are discussed individually below, and discussed in greater detail in Chapter 3 of DM-7.1. *Laboratory miniature vane shear test (LMVT)* – The LMVT can be performed directly on undisturbed test specimens. The results are most applicable for saturated fine-grained soils that have undrained strengths less than about 1400 psf. The test is well suited for measuring the strength of soft soils (s_u < 500 psf) where other test methods may have difficulty. *Fall cone tests (FC)* – There is not an ASTM specification for a fall cone test, but there are standards developed in Norway, Germany, and other countries. This test works best on soft clays. *Unconsolidated-Undrained (UU) triaxial test* – UU triaxial tests are probably the most common test method for determining values of s_u for intact test specimens. A range of confining pressures should be used, and these pressures should bracket the minor total stress at the sample location. Provided the test specimens are saturated, a horizontal envelope should be interpreted from the data. Other triaxial tests, such as the Consolidated-Undrained (CU) triaxial test, have been used in the past, but the resulting values of undrained strength are too high. *Direct Simple Shear Test (DSS)* – The DSS test can be used in a variety of ways for determining s_u. The Bjerrum Method (Bjerrum 1973) is perhaps the most straight forward, in that the intact test specimens are consolidated to the vertical effective stress (at the time of sampling). Each test produces one value of undrained shear strength. A more complicated method to use the DSS test is described by Ladd and DeGroot (2003). This method, referred to as the SHANSEP method, requires consolidation test results to define the preconsolidation pressure profile. A relationship between the undrained strength ratio and the overconsolidation ratio is developed, and used in conjunction with the preconsolidation pressure profile to plot the undrained strength versus depth.
In situ or field tests	**Very Appropriate** Field tests are very useful in determining the undrained strength versus depth relationship. For deposits that have undrained strengths less than about 2000 psf, the Vane Shear Test is probably the best overall test method. The test data should be corrected for strain-rate effects as indicated in the ASTM specification. The CPT test is often used to determine undrained strength distributions. A variety of methods are available to determine the undrained strengths from various CPT parameters, and these are presented in Chapter 2 and Chapter 8 of DM-7.1. The methods that rely on the tip resistance (q_c or q_t) are the most reliable. The SPT has been used in the past, but it is considered unreliable. Other *in situ* test methods are reported in geotechnical literature, but these are not as useful as the VST and CPT.
Correlations	**Sometimes Appropriate** Correlations have limited usefulness for determining the undrained strength distribution vs. depth. Several correlations are available to determine the undrained strength or undrained strength ratio for remolded clays or clays in a normally consolidated state, but these have limited value in practice. Other correlations are available that rely on the preconsolidation pressure profile, if those data are available. Some methods of interpreting laboratory or field test data are in essence site-specific correlations. Examples include SHANSEP and the various methods (N_c, N_k, and N_{kt}) for relating CPT data to undrained shear strength.

P-3.3.2 Drained Strength - *In situ* Deposit of Fine-Grained Soil.

Three sets of drained strength parameters can be measured for fine-grained soils. These are shown for direct shear test results in Figure P-7. If the soil is initially overconsolidated *in situ*, then an envelope results from plotting the peak strengths. This is shown as the upper envelope in Figure P-7, with the indicated shear strength parameters c'_p and ϕ'_p.[3] A second strength envelope can be determined if the test specimens are remolded, loaded to normally consolidated conditions, and then sheared. This results in the fully softened envelope shown with a friction angle defined as ϕ'_{FS} in Figure P-7. The effective stress cohesion for the fully softened condition is normally equal to zero, or the fully softened envelope is nonlinear and passes through the origin. The third envelope is obtained by shearing undisturbed or remolded test specimens to very high displacements, and this produces the residual strength envelope, with a drained friction angle of ϕ'_r. The residual strength envelope is expected to pass through the origin.

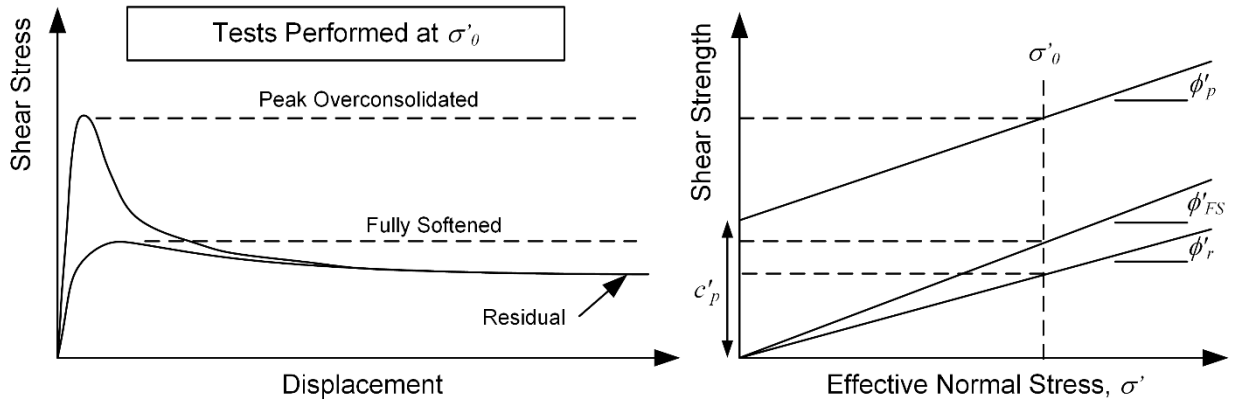

Figure P-7 Drained Envelopes for Saturated Fine-Grained Soils (after Castellanos and Brandon 2014)

Different types of projects require one of the three different failure envelopes. The peak strength envelope is often used for fine-grained soils having a $PI < 20$ and $LL < 40$ that are relatively free of fissures. The peak shear strength parameters depend on the preconsolidation pressure of the test specimens. Figure P-8 shows that one envelope is appropriate for a fine-grained soil in the normally consolidated condition, but the ϕ' and c' of the envelopes for the overconsolidated condition depend on the preconsolidation pressure.

[3] Although the figure shows the stress-displacement relationship for only one test, at least three tests, at different normal stresses, are required to define any of the three envelopes shown.

The fully softened strength envelope is used for soils that do contain fissures and have a $PI > 20$ and $LL > 40$ (Castellanos et al. 2016). This envelope is particularly appropriate for stability assessment of *in situ* fine-grained soils where the stresses have been reduced due to excavation. The fully softened envelope is also used for clays that are essentially normally consolidated *in situ*. The residual strength envelope is used when there has been large displacement due to a shear failure, and the residual condition has been achieved.

Table P-5 summarizes methods for determining the drained shear strength of *in situ* fine-grained soil deposits.

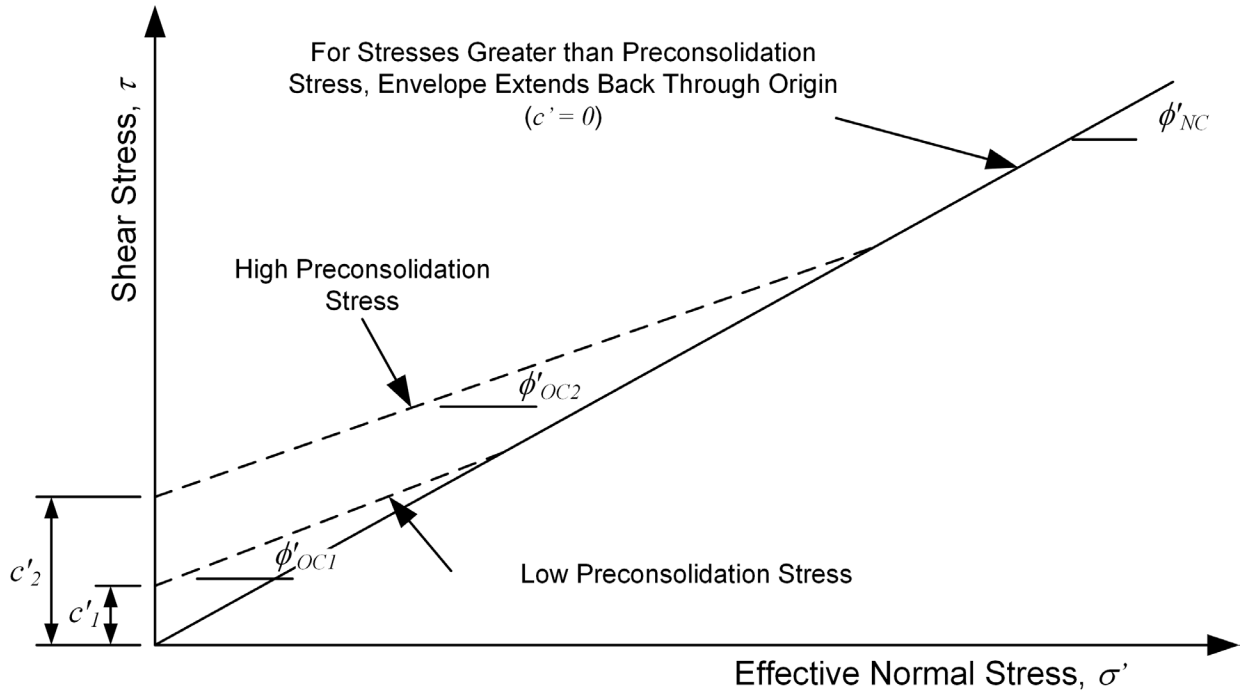

Figure P-8 Drained Strength Envelopes for Fine-Grained Soils in the Normally Consolidated and Overconsolidated Conditions for Different Values of Preconsolidation Stress (after Duncan et al. 2014)

Table P-5 Drained Shear Strength Methods for *In situ* Fine-Grained Soil

Method	Guidance
Laboratory tests on disturbed, reconstituted, or compacted test specimens	**Often Appropriate** Test specimens prepared in the laboratory are useful for determining fully softened and residual shear strengths of fine-grained soils. The best test methods for fully softened strengths are the direct shear test and the consolidated-undrained (CU) triaxial compression test. The best test method for residual shear strength is the ring shear test. In both cases, specimens are prepared to a water content at or above the liquid limit and consolidated to the desired test stresses prior to shearing.
Laboratory tests on "undisturbed" or intact test specimens	**Often Appropriate** Intact specimens are required to measure peak drained shear strength of fine-grained soil. The best test methods are the direct shear test and the consolidated-undrained (CU) triaxial compression test. Test specimens should be consolidated to a range of test stresses, such that the range of effective normal stresses on the failure plane at failure brackets the range of normal stresses anticipated in the analysis.
In situ or field tests	**Rarely Appropriate** Field tests are not useful for drained strength of fine-grained soils. Accurate measurement of drained strength requires knowledge of pore pressure during shearing, which cannot be determined accurately by *in situ* test methods.
Correlations	**Sometimes Appropriate** Correlations are not useful for peak drained shear strength of fine-grained soil because of the dependence of the shear strength on the preconsolidation stress. Chapter 8 of DM-7.1 presents many correlations between index properties (e.g., LL, PI, clay fraction) the fully softened and residual shear strength. These correlations are useful for preliminary analysis, for checking laboratory test results, and for limited design for conditions with limited consequences of failure.

P-3.3.3 *In situ* Deposit of Nonplastic or Low Plasticity Silt.

Silt deposits with low plasticity (i.e., $PI < 10$ and $LL < 50$) require different types of characterization than clayey fine-grained soils. These silts are very dilatant and easily disturbed, which makes them extremely hard to sample and test in the laboratory. Compared to clays with similar liquid limit, the silts tend to be stronger and much less compressible (Brandon et al. 2006). Consolidation tests on low plasticity silts are difficult to interpret and show little effect of preconsolidation, likely due to sampling disturbance.

If it can be determined, the coefficient of consolidation can be used to determine how the silt will behave when loaded. Silts with lower c_v (1 to 10 ft^2/day) will retain excess pore pressures for significant time periods and behave in an undrained manner. Silts with higher values of c_v (greater than 100 ft^2/day) will dissipate excess pore pressures quickly and will behave mostly in a drained manner. Low plasticity silts typically have effective stress friction angles in the range of 35 to 40 degrees with little to no cohesion intercept (Duncan et al. 2014). This indicates that low plasticity silts are relatively competent soils, provided confining stress is maintained. Guidance for determining appropriate shear strength parameters for low plasticity silt is provided in Table P-6.

Table P-6 Strength Methods for *In situ* Nonplastic and Low Plasticity Silt

Method	Guidance
Laboratory tests on disturbed, reconstituted, or compacted test specimens	**Often Appropriate** *Undrained* - Undrained strengths can be measured using CU triaxial compression tests. Dilative tendency during shear can create large negative excess pore pressures. In order to prevent cavitation, back pressures must be significantly higher than required for saturation. The failure criterion will have a large effect on the undrained shear strength. The point where excess pore pressure is zero (i.e., $\bar{A}_f = 0$) is recommended. *Drained* – Drained strengths can be measured using CU triaxial compression tests. The effects of disturbance are less pronounced on the drained strength. In addition, the failure criterion has less impact on the measured ϕ'.
Laboratory tests on "undisturbed" or intact test specimens	**Marginally Appropriate** While such tests can be performed in theory, high-quality, undisturbed specimens of low plasticity silt are extremely difficult to obtain. UU triaxial compression tests are not advised because disturbance creates substantial scatter. See the previous row for further guidance.
In situ or field tests	**Rarely Appropriate** Because of their intermediate values of c_v, it is difficult to determine whether low plasticity silts behave in a drained, undrained, or intermediate state during *in situ* testing. This makes the field test results difficult to interpret with respect to shear strength. Correlations developed for sand and clay have been shown to be unreliable for low plasticity silt.
Correlations	**Marginally Appropriate** Published correlations are not available for low plasticity silts. However, typical values of undrained ratio ($USR = s_u / \sigma'_{vc}$) can sometimes be used to estimate the undrained shear strength. Assuming zero excess pore pressure at failure and $c' = 0$, the USR for various failure modes can be calculated as: • ICU triaxial compression: $USR = \sin \phi' / (1 - \sin \phi')$ • ACU triaxial compression: $USR = \sin \phi'$ • DSS: $USR = \sin \phi' - 0.5 \sin^2 \phi'$

P-3.4 Engineered Deposit of Fine-Grained Soil.

Fine-grained soils are used as engineered fill in many different scenarios, including embankments, dams and levees, and seepage barriers. In many ways, the considerations for shear strength are similar to those for *in situ* deposits of fine-grained soil. The primary cases where undrained shear strength is required for fine-grained engineered fill are end-of-construction (EOC), rapid drawdown (RDD), and seismic analysis. Drained shear strengths are used for long-term conditions with peak strengths being appropriate for compacted fine-grained soils with $PI < 20$ and $LL < 40$. For soils with higher LL or PI, fully softened shear strengths should be considered for compacted slopes (Kayyal and Wright 1991) and retaining walls (Wright 2005). Methods for determining both undrained and drained shear strength of fine-grained engineered deposits are summarized in Table P-7 and Table P-8.

Table P-7 Undrained Shear Strength Methods for Engineered Fine-Grained Soil

Method	Guidance
Laboratory tests on disturbed, reconstituted, or compacted test specimens	**Very Appropriate** Undrained shear strength can be measured on specimens compacted to match the field compaction conditions. Alternatively, the 15-point method (see Chapter 2) can be used to evaluate the variation in shear strength parameters across the compaction plane. *End-of-Construction* - At least three UU triaxial compression tests should be performed for each combination of water content and compacted dry unit weight. The results can be interpreted as c–ϕ envelopes for each compaction state. The variation in c and ϕ can be plotted with the Proctor curves to evaluate appropriate compaction specifications. *RDD and Seismic* – These design scenarios require undrained strength of compacted soils after consolidation to a long-term condition. For this reason, these undrained strengths are measured using CU triaxial compression tests. Test specimens must be saturated prior to consolidation. The amount of swelling allowed during saturation has a substantial impact on the measured undrained strength. Interpretation of the test data for such conditions is specific to the analysis method.
Laboratory tests on “undisturbed” or intact test specimens	**Often Appropriate** Although relatively uncommon in practice, intact specimens may be obtained from a fine-grained engineered fill during or after construction. These specimens can be tested using the test methods described in Table P-4 especially the UU triaxial compression test, to determine EOC shear strength parameters.
In situ or field tests	**Rarely Appropriate** Not applicable except possibly as QA/QC during construction of the fill.
Correlations	**Marginally Appropriate** Published correlations are not useful for compacted fine-grained fill. It may be possible to develop regional or soil-specific correlations between undrained strength and relative compaction. The 15-point is an example of a material specific correlation. Other correlations may be useful for non-engineered fine-grained fills, especially those placed in a normally consolidated state, such as some types of dredge spoils or mine tailings.

Table P-8 Drained Shear Strength Methods for Engineered Fine-Grained Soil

Method	Guidance
Laboratory tests on disturbed, reconstituted, or compacted test specimens	**Very Appropriate** Compacted specimens can be tested to determine the peak drained shear strength. The direct shear test and CU triaxial compression test are best suited for this purpose. Test specimens must be saturated and allowed to reach equilibrium at a range of consolidation stresses. The drained shear strength parameters for compacted fine-grained soils tend to be relatively insensitive to the compaction state. If needed, the fully softened and residual strength of compacted fine-grained soil can be determined as described in Table P-5.
Laboratory tests on “undisturbed” or intact test specimens	**Often Appropriate** Although relatively uncommon in practice, intact specimens may be obtained from a fine-grained engineered fill during or after construction. These specimens can be tested using direct shear or CU triaxial compression tests to determine drained shear strength parameters.
In situ or field tests	**Rarely Appropriate** Not applicable for compacted fine-grained soils.
Correlations	**Sometimes Appropriate** Correlations are not useful for the peak drained shear strength of compacted fine-grained soil. As noted in Table P-5, correlations can be used in some situations to estimate the fully softened and residual shear strength parameters.

P-4 NOTATION.

Variable	Definition
a	Power function strength parameter defining the steepness of the curve
A	Power function strength parameter for three-parameter function
$\bar{A}_f$	Skempton's pore pressure parameter at failure
a_u	Power function strength parameter
b	Power function strength parameter defining the amount of curvature
B	Power function strength parameter for three-parameter function
b_u	Power function strength parameter
c	Total stress or undrained cohesion intercept
c'	Drained or effective stress cohesion intercept
$\overline{c}$	Effective stress or drained cohesion intercept
c'_p	Peak drained or effective stress cohesion intercept
c_v	Coefficient of consolidation
N_c, N_k, N_{kt}	Bearing capacity factors for cone penetration interpretation of undrained strength
q_c	Cone penetrometer tip resistance
s	Shear strength
S	Degree of saturation
s_u	Undrained shear strength for ϕ = 0 envelope
t	Tensile intercept normalized by atmospheric pressure
T	Tensile strength or attraction
USR	Undrained strength ratio
ϕ	Total stress or undrained friction angle
ϕ'	Effective stress or drained friction angle
$\overline{\phi}$	Effective stress or drained friction angle
ϕ'_{EQ}	Equivalent friction angle
ϕ'_{FS}	Fully softened friction angle
ϕ'_{OC}	Drained or effective stress friction angle for portion of strength envelope where the specimen is overconsolidated at failure

Variable	Definition
ϕ'_p	Peak drained or effective stress friction angle
ϕ'_R	Residual friction angle
σ	Total normal stress
σ'	Effective normal stress
σ'_0	Vertical consolidation stress
$\sigma'_{1,con}$	Major effective consolidation stress

This Page Intentionally Left Blank

CHAPTER 1.GEOTECHNICAL DESIGN IN PROBLEM SOILS AND SPECIALTY CONSTRUCTION METHODS

1-1 INTRODUCTION.

Most of the design techniques that will be described in the next six chapters will generically characterize soils as sand or coarse-grained (often called “cohesionless”) or as clay or fine-grained (often called “cohesive”). This is a useful expedient in that the two soil groups represent the endpoints of common soil behavior. Sands are most often drained under normal types of loading, and the strength parameters can be represented as a linear envelope with a slope equal to the effective stress friction angle, ϕ' (with c' = 0), or a curved or non-linear envelope represented by a power function or other equation. Clays[4] can be undrained in the short term and drained in the long term; therefore, both types of strength parameters (drained and undrained) are needed for the various types of design methods presented. Sands are often considered to be relatively incompressible and/or the compression occurs quickly. Clays are considered to be much more compressible, and the compression occurs more slowly for an extended time period.

Separating the soils into two major groups, sands and clays, is very useful since these are the recognized endpoints for both drained vs. undrained behavior as well as relatively incompressible vs. compressible behavior. However, there are soils that fit within these two groups that can exhibit special problems. In addition, there are other soils with specific names, such as *loess*, that can be problematic for the design methods presented.

This section is organized by listing the different soils that are identified as being problematic in the upcoming chapters and, in general, geotechnical engineering practice.

1-2 TYPES OF PROBLEM SOILS.

The following sections describe problematic soil conditions that can affect the design of excavations, earthwork, retaining walls, and foundations. Tables are included at the conclusions of Chapters 2 through 6, which map some of these problem soil conditions to the particular contents of each chapter. For example, the tables in Section 2-7 describe how problem soil conditions relate to sloped and supported excavations.

[4] In geotechnical engineering nomenclature, *clay* normally refers to *inorganic* or *mineral* clays. Clays with an appreciable organic content are referred to specifically as *organic clays*.

1-2.1 Stiff Fissured Clays.

Stiff fissured clay is both a general and specific term. Specifically, stiff fissured clays have an unconfined compressive strength greater than or equal to 2000 psf and contain fissures that are often attributed to unloading from very high stresses. According to ASTM D2488 (ASTM 2023), the criterion for fissures is "breaks along definite planes of fracture with little resistance to fracturing." Generally, the term *stiff fissured clays* most often refers to heavily overconsolidated clays that contain fissures, with examples being London brown clay (U.K.), Beaumont clay (Texas), and Pierre shale (North Dakota and South Dakota). According to Skempton (1964), stiff fissured clays often have a liquidity index near zero. The problematic soils generally often have liquid limit values greater than 40 and plasticity indices greater than 20 (Castellanos and Brandon 2016).

The main issue with stiff fissured clays is that the long-term mobilized shear strength in the field is often less than the peak shear strength measured using laboratory tests. This reduction in strength or softening results from unloading, weathering, and water ingress through the fissures. Softening is likely an artifact of progressive failure, whereby the peak shear strength is not fully mobilized on the failure surface at the same point in time. These mechanisms take time to occur, and failures in stiff-fissured clays can occur many years after a cut, excavation, or unloading has taken place. Because of these factors, the fully softened shear strength is normally used for drained or effective stress analyses for long-term conditions.

The fully softened shear strength is appropriate for drained or effective stress analyses of long-term conditions in stiff fissured clays where the strength is expected to decrease over time (Skempton 1970). The fully softened strength is empirically equal to the normally consolidated peak strength measured for remolded test specimens. Detailed information about measuring the fully softened strength and other engineering aspects of stiff fissured clays can be found in Castellanos et al. (2016) and Castellanos and Brandon (2017).

1-2.2 Stiff Desiccated Clays.

Stiff desiccated clays exhibit many of the same characteristics as stiff fissured clays. These are often fat clays (CH) that are normally located near the ground surface, and contain cracks or fissures that can be several feet deep. Aubeny and Lytton (2003) recorded desiccation cracks up to 8 feet deep, but these cracks are typically 3 to 4 ft deep. These soils are often heavily overconsolidated due to the negative pore water pressures caused by desiccation. The cracks or fissures can allow water to seep into the soil and can cause softening. Fissures also can be problematic for excavations.

Fully softened shear strengths are normally appropriate for these soils for long-term conditions if they classify as CH soils. For stiff desiccated clays having $LL < 40$ and $PI < 20$ (CL soils), the peak strength may be applicable for long-term conditions.

1-2.3 Loess.

Loess is a fine-grained soil deposited by wind. These soils are often silt-sized and have little to no plasticity. They often may be slightly cemented by calcium carbonate. Cycles of deposition and plant growth result in vertical root casts, and these features impact the behavior of these soils. Loess soils can be very erodible in slopes that are non-vertical, but vertical slopes can often be stable for many years. Another issue with loess deposits is that they can be very collapsible when inundated. Large irreversible settlements can occur when these soils are flooded. More information on loess can be found in Section 5-6.3.

1-2.4 Sensitive or Quick Clays.

Sensitivity (S_t) is defined as the peak undrained shear strength divided by the remolded undrained shear strength. The remolded shear strength is best measured using field or laboratory vane shear tests, or laboratory fall cone tests. For soils with low values of sensitivity, soil samples can be remolded by hand kneading and formed into cylindrical specimens. The resulting specimens can be tested to determine the remolded undrained shear strength. Sensitivity values as high as 1000 have been measured (Terzaghi et al. 1996). Soils that have sensitivity values greater than 4 are considered to be *very sensitive soils*. Soils with sensitivities greater than 16 are considered to be *quick clays*. Quick clays are found in Scandinavia and parts of Canada and are formed by fresh water leaching of salt within the clays' structure. Sensitive soils can be formed by other means, such as clays formed from volcanic ash as the parent material, or other depositional or post-depositional factors that create a metastable structure. Sensitive soils are most often fine-grained materials. Table 1-1 shows general sensitivity categories. Chapter 1 of DM 7.1 contains an additional discussion of sensitive clays.

Table 1-1 Sensitivity categories (after Rosenqvist 1953)

Sensitivity Category	Sensitivity, S_t
Insensitive	~1.0
Slightly Sensitive	1-2
Medium Sensitive	2-4
Very Sensitive	4-8
Slightly Quick	8-16
Medium Quick	16-32
Very Quick	32-64
Extra Quick	>64

Some sensitive clays may be overconsolidated, and these can be especially problematic. These deposits can have a high undisturbed strength and can support imposed loads without significant settlement due to their preconsolidation. Loss of strength can occur on disturbance, but it will be less dramatic than with quick clays.

These soils will exhibit unrealistically low Standard Penetration Test (SPT) N values due to the sensitivity of the clay.

1-2.5 Residual Silts and Clays.

Residual soils are formed by physical and chemical weathering of parent rocks in-place or from weathering of volcanic ash deposits. Residual soils can be found in many different areas, such as the piedmont regions of Virginia, North Carolina, South Carolina, and Georgia; and in wet tropical environments. The term *residual soil* covers a wide range of materials, ranging from clay-sized soils to sandy soils. Soils containing the relic features of the parent rock, often called *saprolites*, can have even larger particle sizes. An excellent reference on residual soils is *Geotechnical Engineering in Residual Soils* by L. Wesley (2010).

Residual soils are more heterogeneous than alluvial soils and other soils that have been formed by sedimentary processes. Therefore, stress history does not have the same impact on strength and compressibility (Wesley 2010). One of the main problems regarding geotechnical engineering in residual soils is that correlations developed for sedimentary soils, which are commonplace in engineering practice, do not necessarily apply to residual soils. Considerable engineering judgment is required for efficient design in residual soils.

1-2.6 Laterites.

Laterites are a category of residual soils formed by weathering of igneous parent materials, often in tropical climates. In many cases, laterites can be strongly cemented or can contain aggregates of clay ranging in size from sand to gravel. In geotechnical engineering nomenclature, the term *laterite* is not strictly defined, and it has been applied to a range of soils, both strongly cemented and not cemented (Wesley 2010). Laterites may be poor materials for the support of foundations or embankments, particularly if loaded cyclically or exposed to flowing groundwater (McCarthy 2007).

1-2.7 Talus.

Talus is a loose deposit of rock debris located at the base of a cliff. Talus is a colluvial material deposited by gravity. Depending on the location with respect to the cliff and the slope of the deposit, the global stability of a talus deposit may be low.

1-2.8 Loose Sands.

Sand, in general, is not considered to be a problematic soil. However, *loose sands* can exhibit significant compression when loaded and can liquefy in the event of seismic loading. Fine loose sands are also prone to erosion or scour. Loose sands can be defined as sand-sized soils having a relative density less than 40% and an SPT blow count less than 10 blows/ft (Duncan et al. 2014).

Blast vibrations and equipment loading may cause settlement of loose sands. Settlement and global stability of loose sands may be evaluated using the methods of Chapters 5 and 7 of DM 7.1 for static loading conditions.

One behavioral condition that is unique to loose sands and non-plastic silts is *static liquefaction*. This can occur when excavations are made in loose contractive sand deposits that were formed by sluicing, such as for tailings or dams. An increase in stress by application of additional load can also cause static liquefaction. Saturated loose sands can fail catastrophically by liquefying under undrained loading if the *in situ* stress exceeds the yield shear strength as deformation occurs (Olson 2002). The yield shear strength is typically reached at very low strains, often less than 1%.

1-2.9 Soft Clays.

Soft clays have undrained strengths in the range of 500 psf to 1000 psf. Clays with undrained strengths less than 500 psf are termed *very soft*. Soft clays are most often normally consolidated or slightly overconsolidated. Soft clays often have liquidity indices near one.

1-2.10 Glacial Till.

Glacial tills can contain a range of particle sizes from clay size (0.002 mm) to boulders. In most cases, glacial tills are an excellent construction material. However, tills that contain large amounts of silt-sized and sand-sized materials can be prone to erosion, particularly if they are not protected by a graded filter.

1-2.11 Organic Soils.

Organic soils have been the bane of conventional geotechnical engineering practice for many years. Specifications for earth fills often state that 0% organics are allowed. This strict specification is neither practical nor enforceable. There are a variety of types of organic soils, and these differ in the amount and type of problems they can cause in geotechnical projects.

Organic clays, as defined by ASTM D2487, are fine-grained soils with Atterberg limits plotting above the A-line and having a ratio of the oven-dried liquid limit to the not-dried liquid limit less than or equal to 0.75. These have the group symbol of OH if the liquid limit (not-dried) is greater than 50, and they have the group name of *organic clay*. OH soils are considered to have “sufficient organic content to influence the soil properties.” If the liquid limit is less than 50, the group symbol is OL, but the group name remains *organic clay*.

Organic silts are defined similarly, but the Atterberg limits plot below the A-line. The same criterion regarding the ratio of the oven-dried to not-dried liquid limit also applies. An organic silt has the same group symbol of OH as an organic clay if the not-dried

liquid limit is greater than 50. Organic silts that have a liquid limit less than 50 have a group symbol of OL, and the group name is still *organic silt*.

Peats, represented by the group symbol PT, are described in ASTM D2487 as "primarily organic matter, dark in color, and organic odor." This classification is not based on Atterberg limits, and peats are described as having a texture from fibrous to amorphous. *Muskeg* is a peat soil that is found in parts of Alaska and Western Canada (Sowers 1989).

Peats are further classified based on the measured organic content, as described in ASTM D4427 (Standard Classification of Peat Samples by Laboratory Testing). Peats have an ash content less than 25%, as determined by ASTM D2974, which means true peats have at least 75% organic material.[5] Peats are also differentiated by the fiber content, acidity, and absorbency. More information about the classification and engineering behavior of organic soils can be found in VandenBerge et al. (2017) and Sleep et al. (2009).

One of the main issues with organic soils, and particularly with peats, is that they are very compressible. Organic soils can have very high *in situ* moisture contents – sometimes in excess of 1000% for peats. This results in very low unit weights and correspondingly low *in situ* effective stresses. A peat can be normally consolidated, and since the effective stresses are very low, the equilibrium void ratio can be very high – often greater than 4. If the effective stress is increased due to a geotechnical project loading, large settlements can occur. Preloading a site can help to alleviate extreme settlement magnitudes.

Organic soils can also decompose over time. If organics are incorporated into a fill material, the decomposition of the organics may result in settlement over time; however, there is some debate regarding the amount of decomposition possible in an anaerobic environment. Even so, there are strict limits normally placed on the organic content of structural fills, with a limit of 0% to 10% often being specified.

Although peats are very compressible, research conducted on fibrous peats show that other engineering parameters are often within the range of other soil deposits (Edil and Wang 2000; Landva and La Rochelle 1983; and Landva et al. 1983). Listed below are general facts about fibrous peats:

- Peats have a high strain to failure for both drained and undrained loading.
- Peats develop high pore pressures during undrained loading, with $\bar{A}$ values at failure greater than 0.5 and often equal to 1.0.

[5] Other groups and organizations have their own definitions of peat, which often differ from ASTM D4427 in the required ash content.

- K_0 values of fibrous peats are around 0.3.
- Peats normally have a c' close to zero and a high value of ϕ'. Values reported in the literature for ϕ' range from about 40 degrees to 65 degrees.
- Peats are not weak *per se*. The undrained strength ratios of peats reported in the literature range from about 0.4 to 1.5, with Edil and Wang (2000) reporting an average value of 0.59. The reason that peats are often considered to be weak is that, owing to the very low unit weight, the effective stresses within peat deposits are very low. If a peat deposit is overlain by a mineral soil, the undrained shear strength can be much higher than that of a normally consolidated clay.
- Peats have a high permeability (10^{-3} cm/sec) in a normally consolidated condition at low effective stresses. If a peat is consolidated by placing a fill on top of it, the permeability drastically decreases during consolidation.
- Vane shear tests have often been used to measure the undrained shear strength of peat.
- The shear strength of peat is highly anisotropic since the fibers are usually horizontally oriented.

1-2.12 Expansive Soils.

Certain types of fine-grained soils can expand when given access to water. The pressure developed from expansion can be large enough to cause significant damage to geotechnical structures. There are five related factors that influence the swell potential of fine-grained soils (Bursey et al. 2006):

1) Clays at low initial degrees of saturation expand more than clays at higher degrees of saturation.
2) The swell potential increases with increasing soil unit weight.
3) Clays with very active soil minerals (smectite and montmorillonite) expand more than soils with less active clay minerals (kaolinite and illite).
4) Soils with higher plasticity expand more than soils with lower plasticity.
5) Clays with a flocculated structure swell more than clays with a dispersed structure.

The International Building Code (IBC) provides threshold guidelines to determine if a soil has a potential swelling problem. Soils are deemed *not expansive* if the plasticity index is less than 15, less than 10% passes the No. 200 mesh sieve, or less than 5% of the soil is finer than 0.005 mm. If a soil is considered to be potentially expansive, two ASTM test procedures are available to assess the swell potential:

1) ASTM D4546 “Standard Test Methods for One-dimensional Swell or Settlement Potential of Cohesive Soil” and
2) ASTM D4829 “Standard Test Method for Expansion Index of Soil.”

In addition, the conventional one-dimensional consolidation test (ASTM D2435) can be used to measure the swell pressure of soils. The *swell pressure* is the applied stress that prevents volume change when the test specimen is inundated. Also, many correlations are available to estimate the swell potential of soils, and these can be found in Chapter 8 of DM 7.1.

Expansive soils can be a problem because the volume change characteristics can be reversible. Soils that expand significantly when wetted can also shrink considerably when dried. Shrink-swell issues in fine-grained soils often occur over the range of depth corresponding to seasonal moisture content variation.

1-2.13 Expansive Shale.

Many types of shales can also expand when provided with access to water. Since shale usually contains clay minerals, the same basic factors that influence the swell potential of soils apply to shales, particularly if the shale is excavated and used for a structural fill.

Pyritic shales pose a particularly severe problem if they are exposed during excavation. The problems can be more severe than just ground heave since the byproducts of oxidation of pyritic shales (gypsum and sulfuric acid) can cause degradation of steel and concrete. Issues with pyritic shales are documented in the southeastern and mid-Atlantic states as well as in Canada, the United Kingdom, and many other countries. Bryant et al. (2003) summarize many case histories of issues with pyritic shales.

Engineers developing sites which have Devonian age shales in the stratigraphy should be aware of the problems with pyritic shales. Problematic shales are normally dark gray to black (Bryant et al. 2003), and certain types of fossils are prevalent in these shales, which can serve to identify their age. Pyrite crystals may be visible in pyritic shales. Chemical tests can be conducted to identify the total sulfur present in shales to identify ones that are of concern.

1-2.14 Collapsible Soils.

Some soils can exhibit large compressive volume changes upon wetting. Types of soils that can exhibit this behavior are loess, alluvial flood plain deposits, colluvial deposits, residual soils, volcanic tuff, and lean clays and silts compacted dry of optimum (Brandon et al. 1990, Xanthakos et al. 1994).

Geotechnical laboratory tests are available to determine the amount of compression due to wetting (*hydrocompression* or *hydrocompaction*). Basic test procedures are outlined in Brandon et al. (1990). The test procedure given in ASTM D4546 (Standard Test Method for One-Dimensional Swell or Collapse of Soil) can be used for measuring the collapse potential of compacted soils.

The collapse potential of compacted soils can sometimes be controlled by careful selection of the compaction specifications. The collapse potential can be reduced by compacting the soils wet of optimum at modest values of relative compaction. However, there are trade-offs in controlling collapse with compaction specifications, because other properties, such as strength and stiffness, might be compromised.

The collapse potential of natural *in situ* soils can be difficult to address. In some cases, berms have been constructed around portions of the site, and the site is flooded so that the soil is forced to collapse prior to development. In other cases, soil improvement methods, such as dynamic compaction, can be used to densify the soil and to reduce the amount of future collapse. Further discussion of collapse in the context of shallow foundations is provided in Section 5-6.3.

1-2.15 Dispersive Soils.

Some fine-grained soils are prone to *dispersion* or *deflocculation* when subjected to flowing water having a particular chemistry. These types of soils are termed *dispersive soils* and are normally clay or silt soils. Dispersive soils can erode quickly due to separation of the particles, and some dam failures have been attributed to erosion of dispersive soils (Sherard 1986).

Owing to the engineering importance of dispersive soils in earth dams and canals, several tests have been developed to identify these soils:

1) ASTM D4221 “Standard Test Method for Dispersive Characteristics of Clay Soil by Double Hydrometer,”
2) ASTM D4647 “Standard Test Methods for Identification and Classification of Dispersive Clay Soils by the Pinhole Test,”
3) ASTM D6572 “Standard Test Methods for Determining Dispersive Characteristics of Clayey Soils by the Crumb Test,” and
4) ASTM D4542 “Standard Test Method for Pore Water Extraction and Determination of the Soluble Salt Content of Soils by Refractometer.”

Interpreting the results of these tests requires engineering judgment. The results of the tests are very general, in that soils can be considered dispersive, slightly dispersive, or non-dispersive (ASTM D4647). As an example, if twenty specimens are tested at a site, and two are considered to be dispersive, judgment is required to determine if dispersion is a problem or not. Dispersive soils are also discussed in Section 3-6.6.

1-2.16 Dredged Soils.

Dredged soils are excavated or pumped materials that are obtained from below a water surface. A main source of dredged soils comes from the maintenance of navigable waterways and harbors. The US Army Corps of Engineers maintains over 25,000 miles

of waterways and over 400 ports, and they are responsible for the excavation of the bulk of dredged materials in the US (ERDC 2001). Environmental dredging is another category of dredging, and it is used to remove contaminated sediments from waterways and harbors. The US Navy and Coast Guard also direct dredging projects as well as local, state, and other federal government organizations.

In some cases, dredged materials can be used for engineering projects, such as land reclamation, or if properly sorted, construction materials. Dredging can also be used for excavation around infrastructure projects, such as bridge abutments and pier locations. There are many different types of dredges including mechanical, hydraulic, and pneumatic dredges. In many cases, the dredged soils are mixed with water so that they can be pumped to the location of disposal.

The dredged soils can be deposited at onshore placement facilities (confined disposal facilities) or in nearshore or open water areas. For onshore deposition, the dredged materials need to be dewatered to transition from a slurried consistency to a semi-solid soil consistency. The slurried dredge materials are normally deposited within an area surrounded by containment dikes. Over time, the soil particles settle out and the supernatant is drained from the surface. The remaining soil materials are remolded and have very high water contents, very low densities, and very low shear strengths. The character of the dredged materials depends on the source, and the grain sizes can vary considerably from clay to gravel size. Shear strengths of dredged soils can be increased by the installation of wick drains and preloading the site.

Owing to their experience with dredging and dredged soils, the US Army Corps of Engineers has an impressive research portfolio on many aspects of dredging. They have investigated factors that influence the dredgeability of soils, construction of containment dikes, and properties of dredged soils.

Conventional geotechnical laboratory and field test equipment can be used with dredged soils; however, the very low shear strengths mean that test interpretation is at the lower end of normal calibrations. CPTs can be used in dredged soils, but it is necessary to maximize the sensitivity of the cone tip by using a low-capacity cone or cones having larger tip areas. Special penetrometers have been developed for very soft soils. Vane shear tests have also been used with good results in fine-grained dredged deposits.

It is difficult to sample dredged soils, but successful sampling is possible with fixed-piston samplers. When samples are obtained, trimming triaxial test specimens may be challenging owing to the very low shear strengths. Laboratory miniature vane shear tests (ASTM D4648) or fall cone tests might be better alternatives for measuring undrained shear strengths. For drained strength parameters, trimming direct shear test specimens is often easier than triaxial specimens.

1-2.17 Low Plasticity and Nonplastic Silts.

Silts can be characterized by their Atterberg limits or by their size. Soils that plot under the A-line with $LL > 50$ have the group symbol MH and the group name *elastic silt*[6]. These soils are ordinarily not problematic and can be treated in the same manner as clay. Soils that plot under the A-line, with an $LL < 50$ and a $PI < 4$, have the group symbol ML and a group name of *silt*. Soils that have a grain size ranging from 0.002 mm to 0.075 mm are considered to be *silt-sized*.

Problematic silts are those that have very low plasticity ($PI < 4$ and $LL < 25$), particularly silts that are *nonplastic*. According to ASTM D4318, a soil is considered to be nonplastic, if it is not possible (1) to roll out a plastic limit thread or (2) to maintain the cut groove in the liquid limit test for more than 25 blows. Low plasticity and nonplastic silts can be difficult to deal with in engineering projects because of the following issues (Brandon et al. 2006):

1) Unconsolidated-Undrained (UU) triaxial tests conducted on saturated silts often exhibit substantial scatter.
2) Correlations developed for clay soils (CL and CH) may not apply to silts. These include correlations for interpreting the results of *in situ* tests.
3) The consolidation compression curve often does not exhibit a clear preconsolidation pressure.

Many of the problems with these silts may be due to the fact that their grain size, and corresponding permeability, give them behavioral characteristics that are unlike clays and sands. Whereas many *in situ* tests in clays are considered to be undrained, these tests might be partially drained in silt. Silts may cavitate during undrained loading owing to their dilative tendencies (Skempton and Golder 1948). Also, the lack of significant plasticity may prevent their behavior from being greatly influenced by the preconsolidation pressure.

Most of the problems with low plasticity and nonplastic silts occur when trying to characterize the undrained strength. If the undrained strength is characterized using Consolidated-Undrained triaxial tests, the issue with scatter in UU triaxial tests can be avoided. The undrained strength can also be estimated based on drained shear strength parameters combined with an assumed pore pressure at failure that is greater than or equal to zero to avoid relying on negative pore water pressures for undrained strength (Duncan et al. 2014).

---

[6] While these soils are called *elastic silts*, there is nothing indicative in their behavior which provides the expectation that these soils behave elastically in a classic sense (e.g., no volume change under application of shear stress or significant recoverable strain).

1-2.18 Municipal Solid Waste.

Municipal solid waste (MSW) is generated in huge quantities throughout the US. Research into the geotechnical properties began in earnest in the early 1990s in response to new EPA regulations. Knowledge of the properties is important for several reasons:

1) The engineering properties of the MSW can factor into the design of the landfill, particularly the stability of landfill interior slopes and cover system.

2) After landfills are closed, light site development is often planned for the site. Facilities such as public parks and golf courses have been constructed on top of closed landfills.

3) MSW deposits exist in unengineered landfills that predate current regulations. Development at old landfill sites can occur both with and without initial knowledge of the presence of the existing MSW.

It is not possible to definitively state the properties of MSW since the engineering properties depend on a wide array of factors. The composition of the waste stream can vary for different geographical areas as well as for different seasons of the year. In addition, as the MSW decomposes, the properties change over time (Reddy et al. 2011); therefore, it is only possible to give ranges of properties.

Measuring the shear strength of MSW is difficult since the size of the material is larger than can be accommodated by most shear testing apparatuses that were designed for soils. Also, obtaining a representative sample of material that is so heterogeneous is very difficult. Some researchers have resorted to manufacturing “synthetic” test specimens of MSW to obtain repeatable test specimens for property measurement (Dixon et al. 2008; Reddy et al. 2009; Reddy et al. 2011). Other research programs have tried to back-calculate the strength parameters from failed slopes in landfills (Eid et al. 2000; Bray et al. 2008).

The use of *in situ* tests to characterize MSW is not recommended since penetration of the landfill material can be difficult, and no reliable correlations exist regarding interpretation of the tests. These factors are compounded with the fact that the pore fluid may be leachate with unknown properties instead of water.

Bray et al. (2009) suggested using an effective stress cohesion intercept of 300 psf and a drained friction angle of 36 degrees at a normal stress of 2000 psf with the friction angle decreasing by 5 degrees for each tenfold increase in normal stress. Other references cite strength parameters considerably smaller (Reddy et al. 2009). Pandey and Tiwari (2015) report published values of c' ranging from 0 to 1000 psf and friction angles (ϕ') ranging from 27 to 41 degrees for MSW.

It is an easier task to measure the compressibility of MSW. One-dimensional consolidometers can be constructed to test large specimens of MSW. Although it isn't possible to test "undisturbed" specimens, reconstituted specimens can be formed that are within the range of densities found in landfills. Pandy and Tiwari (2015) summarize the results of consolidation tests for specimen diameters up to 20 inches, and strain-based compression ratios ($C_{\varepsilon c}$) from 0.16 to 0.35 were measured, with most results falling between 0.25 and 0.30.

In summary, MSW can be a very difficult material to deal with using conventional geotechnical engineering tools. It is very heterogeneous, and it isn't practically possible to take undisturbed samples. Disturbed samples can be taken, normally by excavation as opposed to rotary borings, but it can be hazardous owing to the constituents in the waste. Conventional laboratory test apparatuses are ill-suited for testing MSW, and *in situ* tests are of little value. Accurate and reliable correlations are not available for MSW; therefore, a great deal of engineering judgment is required when dealing with this material.

1-3 SPECIALTY GEOTECHNICAL CONSTRUCTION METHODS.

Geotechnical construction methods are constantly being updated, refined, and newly developed. Many innovative specialty contractors are engaged in geotechnical construction, and new and inventive construction methods are introduced every year. Some of the specialty construction methods make use of existing equipment while others employ complex custom equipment.

There are many valuable resources available that provide important details about specialty geotechnical construction methods. In November 2012, *GeoTechTools* was launched and now can be accessed through the ASCE Geo-Institute web page (https://www.geoinstitute.org/geotechtools/). GeoTechTools was created with funding from the Strategic Highway Research Project 2 (SHRP2), administered by the Transportation Research Board in conjunction with the Federal Highway Administration (FHWA) and the American Association of State Transportation and Highway Officials (AASHTO). Details can be found in the *Ground Modifications Methods Reference Manual - Volumes 1 and 2* (FHWA 2017). These references are commonly referred to as the FHWA Geotechnical Engineering Circular No. 13 (GEC 13).

The website provides detailed information about many geotechnical technologies. Some of these have been incorporated into civil engineering construction for many years, such as *excavation and replacement* and *conventional compaction*. Others are less common in typical construction, such as intelligent compaction, or are current topics of research, such as *bio-treatment* of soils. Table 1-2 lists the various technologies that are addressed. Although the development of the manuals and website was focused on transportation projects, the technologies described have direct applications to the topics covered in this manual.

Table 1-2 List of Technologies Included in GeoTechTools and GEC 13.

Aggregate Columns	Beneficial Reuse of Waste Materials
Bio-Treatment for Subgrade Stabilization	Blast Densification
Bulk-Infill Grouting	Chemical Grouting/Injection Systems
Chemical Stabilization of Subgrades and Bases	Column-Supported Embankments
Combined Soil Stabilization with Vertical Columns	Compaction Grouting
Continuous Flight Auger Piles	Dynamic Compaction
Deep Mixing Methods	Drilled/Grouted and Hollow Bar Soil Nailing
Electro-Osmosis	Excavation and Replacement
Fiber Reinforcement in Pavement Systems	Geocell Confinement in Pavement Systems
Geosynthetic Reinforced Construction Platforms	Geosynthetic Reinforced Embankments
Geosynthetic Reinforcement in Pavement Systems	Geosynthetic Separation in Pavement Systems
Geosynthetics in Pavement Drainage	Geotextile Encased Columns
High-Energy Impact Rollers	Hydraulic Fill with Geocomposite and Vacuum Consolidation
Injected Lightweight Foam Fill	Intelligent Compaction
Jet Grouting	Lightweight Fill
Mass Mixing Methods	Mechanical Stabilization of Subgrades and Bases
Mechanically Stabilized Earth Wall System	Micropiles
Onsite Use of Recycled Pavement Materials	Partial Encapsulation
Prefabricated Vertical Drains and Fill Preloading	Rapid Impact Compaction
Reinforced Soil Slopes	Sand Compaction Piles
Screw-in Soil Nailing	Shoot-in Soil Nailing
Shored Mechanically Stabilized Earth Wall System	Traditional Compaction
Vacuum Preloading with and without Prefabricated Vertical Drains (PVDs)	Vibro-Concrete Columns
Vibrocompaction	

Many of these technologies can be broadly classified as ground modification techniques. The basic goals of applying these techniques is to (1) increase the soil shear strength and bearing capacity, (2) increase the soil dry unit weight, (3) increase or decrease soil permeability and/or drainage, (4) increase soil stiffness or control volume

change, (5) accelerate consolidation of fine-grained soils, (6) decrease loads applied to structures, (7) increase earthquake stability of soils, and (8) transfer stresses from less competent layers to more competent layers (FHWA 2017). Table 1-3 shows the types of technologies associated with the different improvement goals.

Table 1-3 Technologies Used to Address Basic Goals of Soil Improvement (after FHWA 2017)

Function	Technologies
Increase shear strength and bearing capacity	Vibro-Compaction Dynamic Compaction Compaction Grouting Mixing Methods PVDs Stone Columns Rammed Aggregate Piers Chemical Stabilization Mechanical Stabilization
Increase soil dry unit weight	Vibro-Compaction Dynamic Compaction Blasting Compaction Compaction Grouting Mixing Methods PVDs
Decrease permeability	Bulk-infill Grouting Chemical Grouting Jet Grouting Deep Mixing Methods
Control deformations (settlement, heave, distortions)	Column Supported Embankments Reinforced Load Transfer Platforms Non-Compressible Columns Mixing Methods Vibro-Compaction Dynamic Compaction Stone Columns Rammed Aggregate Piers Chemical Stabilization Mechanical Stabilization Encapsulation
Increase drainage	PVDs Aggregate Columns Geotextile Encased Columns Electro-Osmosis Geosynthetic Drains
Accelerate consolidation	PVDs Aggregate Columns Geotextile Encased Columns
Decrease imposed loads	Granular Fills (Wood Fiber; Blast Furnace Slag; Fly Ash; Boiler Slag; Expanded Shale, Clay, and Slate; Tire Shreds) Compressive Strength Fills (Geofoam, Foamed Concrete) Geosynthetic Reinforcement
Increase resistance to liquefaction	Aggregate Columns Dynamic Compaction Deep Mixing Jet Grouting Vibro-compaction
Transfer embankment loads to more competent layers	Column Supported Embankments Reinforced Soil Load Transfer Platforms Compressible and Non-Compressible Columns

Certain technologies are applicable to a broad range of soil types while others are best suited for specific soil types. Table 1-4 presents various soil types and ground conditions paired with the general types of technologies that apply.

Table 1-4 Soil Types and Foundation Conditions for Different Technologies (after FHWA 2017).

	Soil Types and Foundation Conditions	Applicable Technologies
General	All soil types, in particular weak soils that cannot support surface loads	Non-compressible columns
	All soil types, except very soft soils; low undrained shear strength	Compressible columns
	Clays, silts, loose silty sands, and uncompacted fill	Aggregate columns
	Broad applicability; no geologic or geometric limitations	Lightweight fills: geofoam, foamed concrete, wood fiber, blast furnace slag, fly ash, boiler slag, expanded shale, tire shreds
	Wide range of soil types, including weakly cemented rock-fill materials	Chemical (permeation) grouting
	Coarse-grained soils, collapsible soils, and unsaturated fine-grained soils (may be used to fill voids in sinkholes or abandoned mine shafts and can arrest settlement under a structure and lift foundations that have settled).	Compaction grouting
	Suitable in large range of soils, particularly those that can be stabilized with cement, lime, slag, or other binders	Deep soil mixing
	Wide range of soil types and groundwater conditions	Jet grouting
Clay	Compressible saturated clays	Prefabricated vertical drains, with and without preloading for accelerated consolidation
	Soft soil foundations, with no limitation on depth of soft soils	Reinforced embankments
	Soft compressible clay, peats, and organic soils where settlement and global stability are concerns	Column supported embankments and reinforced soil load transfer platform
	Peat, soft clay, dredged soil, soft silt, sludges, and contaminated soils	Mass soil mixing
Sands	Loose pervious and semi-pervious soils with fines contents less than 15%; materials containing large voids, spoils, and waste areas	Dynamic compaction (DC)
	Coarse-grained soils; clean sands with less than 15% silts and/or less than 2% clay	Vibro-compaction
Strong Soil / Rock	Steep-sided terrain, soils subject to instability, and poor foundation conditions	Reinforced soil walls
	Firm foundation soils	Reinforced soil slopes
	Fractured rock	Rock fissure grouting
	Dense to very dense granular soils with apparent cohesion, weathered rock, stiff to hard fine-grained soils, engineered fill, residual soils, and glacial till	Soil nail walls

1-3.1 GeoTechTools Website Interactive Selection System.

The GeoTechTools website allows a user to interactively select between various technologies for four basic screening categories. The application categories are (1) construction over unstable soils, (2) construction over stable or stabilized soils, (3)

geotechnical pavement components, and (4) working platforms. These four categories are shown graphically in Figure 1-1.

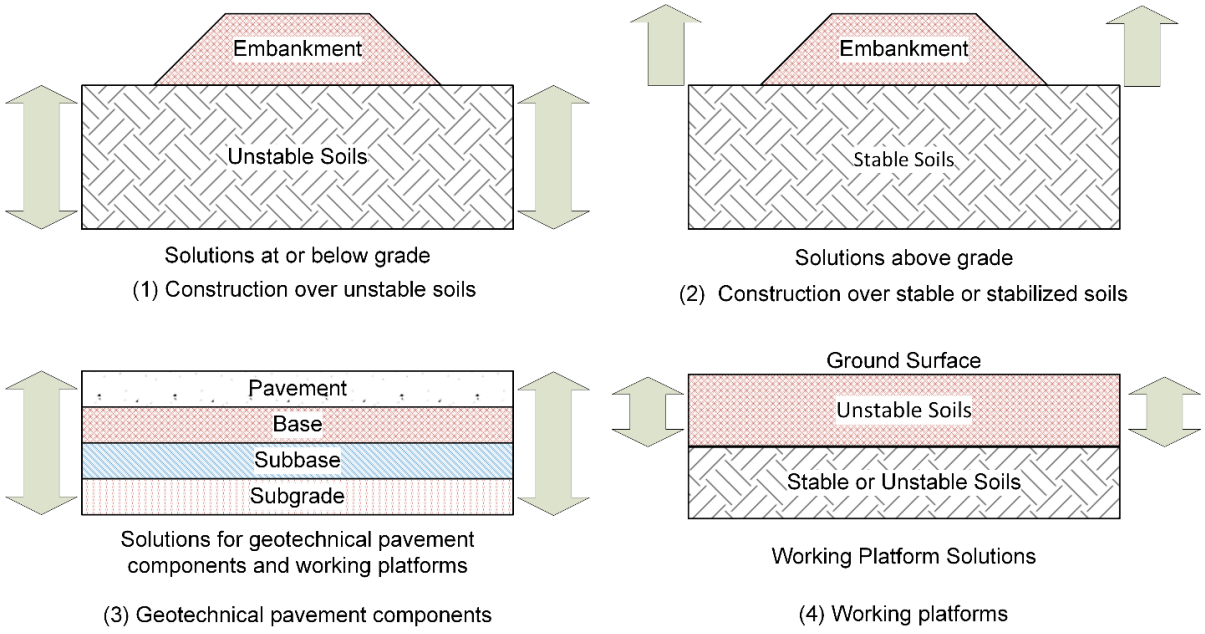

Figure 1-1 Interactive Selection Categories for GeoTechTools Website

All of these categories have applications to the design elements presented in this manual. If category No. 1 is selected, the user has a choice of various unstable ground conditions, such as (a) wet and weak fine-grained soils, (b) unsaturated loose granular soils, (c) saturated loose granular soils, (d) voids – sinkholes and abandoned mines, and (e) problem soils and sites. If (a) wet and weak fine-grained soils are selected, the user is prompted to indicate the depth below the ground surface where treatment is required, and various treatment options are suggested based on the depth selection. For this example, if a treatment depth of 10 to 30 ft is selected, the following treatment technologies are offered:

- Aggregate columns
- Column-supported embankments
- Combined soil stabilization with vertical columns
- Continuous flight auger piles
- Deep mixing methods
- Electro-osmosis
- Geosynthetic reinforced embankments
- Geotextile encased columns
- Jet grouting
- Lightweight fill
- Mass mixing methods
- Micropiles
- Prefabricated vertical drains and fill
- Sand compaction piles
- Vacuum preloading
- Vibrocompaction

Selecting one of the suggested technologies connects the user with both general and detailed information about the choice. There is a brief overview, a fact sheet, photographs of the technology, case histories, design guidance, QA/QC information, cost information, example specifications, and references for further study are provided.

1-3.2 Geotechnical Site Technology Examples.

In the following pages, examples of several popular geotechnical site technologies are presented. Figure 1-2 through Figure 1-16 summarize the benefits of the procedure and the basic construction process. Advantages and disadvantages are presented, along with the site conditions that are most favorable for the specific technology. The key design parameters are listed, and other alternative technologies are included. More information on most of the technologies can be found in FHWA (2017) or in the other references provided in each figure.

Aggregate Columns

Controlling Engineering Principles

Aggregate columns:

- Create a pier element by using compacted aggregate,
- Increase bearing capacity,
- Increase the soil shear strength,
- Increase the consolidation rate,
- Increase liquefaction resistance, and
- Reduce settlement.

Basic Construction Process

Aggregate Columns can be installed by vibro-replacement, vibro-displacement, or the replacement method. The installation includes:

- Form holes in the soil either by excavation or vibratory method,
- Backfill with gravel or crushed rock, and
- Compact the backfill either by ramming or vibratory methods.

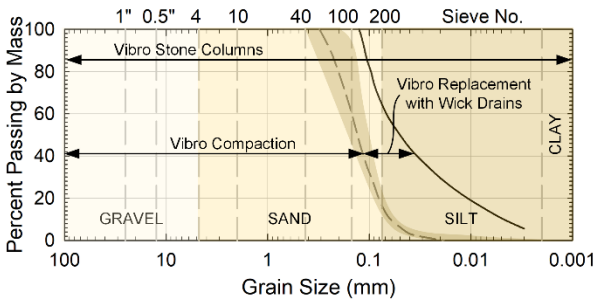

Typical application and failure modes

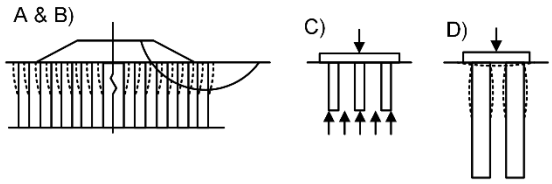

A) Lateral spreading – wide embankment load
B) General circular failure
C) Punch failure of short columns - homogeneous soft soils
D) Bulging failure – small group

(after FHWA 2017)

COMPARATIVE INFORMATION

Advantages

- Potentially economical alternative to deep foundations
- Can be quicker than site pre-loading on time-critical projects
- Can reduce dynamic settlement to an acceptable level in seismic areas

Disadvantages

- Not a solution for all soft soil problems
- Dense overburden, boulders, cobbles, or other obstructions may require pre-drilling
- Cost can be high when compared to other methods

Preferred Applications

- Soft organic clays, loose silt and sand
- Embankments over highly compressible soil
- Bridge approach fills
- Bridge abutment and foundation support
- Liquefaction mitigation

KEY DESIGN PARAMETERS	DESIGN GUIDANCE	COULD ALSO CONSIDER
• Soil shear strength and compressibility • Aggregate column friction angle and modulus	• FHWA (2017) – Chapter 5 • DM 7.1 – Chapter 5	• Sand compaction piles • Prefabricated vertical drains • Deep and mass mixing • Jetted grout columns

Figure 1-2 Summary of Key Elements of Aggregate Columns

Bulk Infill Grouting

Controlling Engineering Principles

Bulk infill grouting:

- Uses a large quantity of cement-based grout to fill subsurface voids and
- Provides remediation for sinkholes.

Basic Construction Process

The process of bulk infill grouting includes

- Identifying subsurface voids such as mines, karst topography, etc.,
- Boring a hole from ground surface to the floor of the void,
- Adding a grout bag and starting to inject grout into the void,
- Leaving a sodium silicate blanket over the grout, and
- Removing the grout bag.

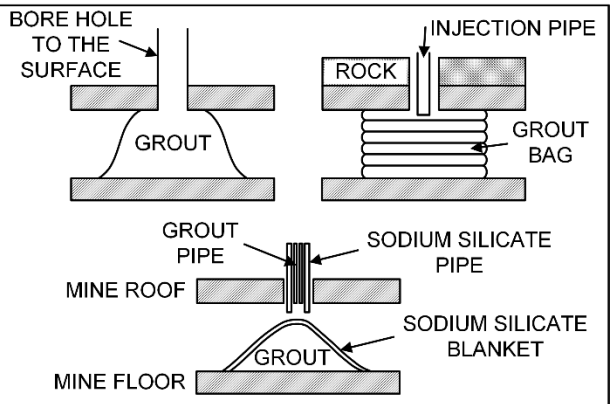

(after FHWA 2017)

Typical application and construction process

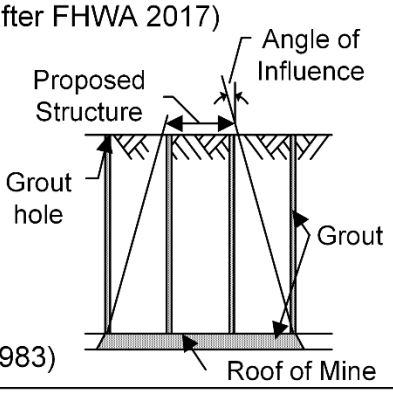

(after Ryan 1983)

COMPARATIVE INFORMATION

Advantages

- Low cost per unit volume when using cheap fillers
- Minimum disturbance
- Strength of grout can be fit to the *in situ* condition
- Essentially yields full roof contact
- Grout can penetrate all voids with low risk of grout flowing, washing away, or settling

Disadvantages

- Little control where the grout goes
- Difficult to obtain sufficient knowledge of the voids position, shape, and infilling
- Cannot provide consistent reliable support in common karst conditions

Preferred Applications

- Can be used in karst topography, chalk deposits, and salt deposits
- Embankments over unstable soils
- Abandoned or old mines
- Repairing of scour problems under bridges

KEY DESIGN PARAMETERS	DESIGN GUIDANCE	COULD ALSO CONSIDER:
• Grout mix proportions • Knowledge of subsurface voids	• FHWA (2017) – Chapter 8	• Drilled shafts • Other forms of grouting • Deep dynamic compaction • Excavation and replacement

Figure 1-3 Summary of Key Elements of Bulk Infill Grouting

Blast Densification

Controlling Engineering Principles

Blast densification:

- Uses a detonation to induce liquefaction,
- Consolidates the soil to a denser and more stable configuration,
- Reduces long-term settlement, and
- Improves the foundation soil strength.

Basic Construction Process

Blast densification can be successfully done by using either pre-drilled or jetted holes. The process includes:

- Placing charges in a grid pattern of holes and
- Detonating charges with delays to enhance cyclic loading while also minimizing peak acceleration.

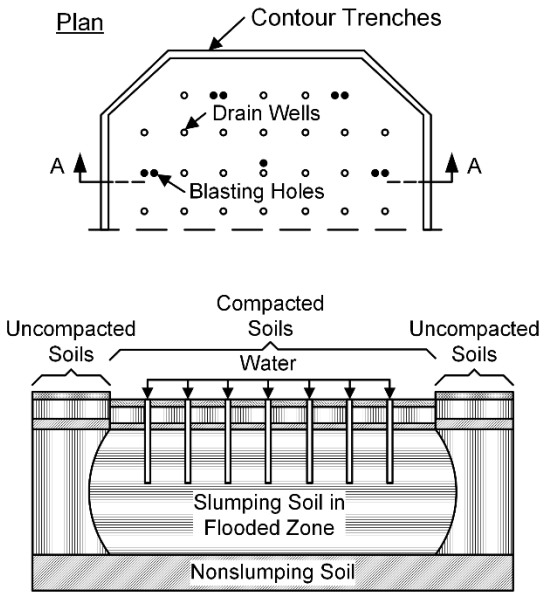

(after Mitchell 1981)

Typical application and construction process

COMPARATIVE INFORMATION

Advantages

- Ability to treat deep soils
- Rapid
- Inexpensive
- Successful under a variety of climate and environmental extremes

Disadvantages

- Lack of validated theoretical design
- Improvement may be time dependent
- Limits on how much densification can occur
- Difficult to place large charges at great depths
- Oversized charges may cause cratering, slope failure, or vibration-related damages

Preferred Applications

- Best suited for clean sands and silty sands with relative densities less than 50% to 60% and maximum clay content of 5% to 10%
- Embankment foundations
- Liquefaction mitigation

KEY DESIGN PARAMETERS	DESIGN GUIDANCE	COULD ALSO CONSIDER:
• Layer depth • Charge spacing • Relative density of soil • Clay content	• FHWA (2017) – Chapter 4 • Narin and Mitchell (1994, 1995)	• Dynamic compaction • Vibro-compaction

Figure 1-4 Summary of Key Elements of Blast Densification

Chemical Grouting

<u>Controlling Engineering Principles</u>

Chemical grouting:

- Uses grouts with no suspended particles,
- Bonds soil particles together and fills voids,
- Can increase soil strength for construction, and
- Can create a seal to limit water intrusion into a subsurface area.

<u>Basic Construction Process</u>

Chemical grouting can be accomplished by:

- Injecting the grout through a manchette or packing system and
- Filling discrete flow paths with an expansive and/or flexible material using simple drill and injection principles.

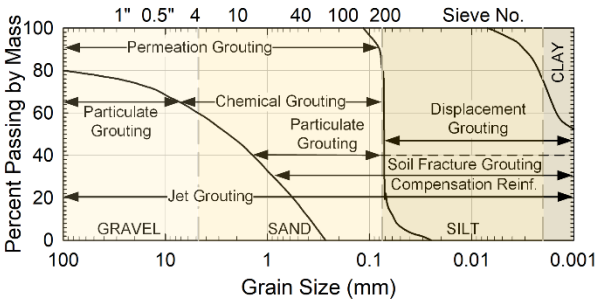

Typical application and construction process

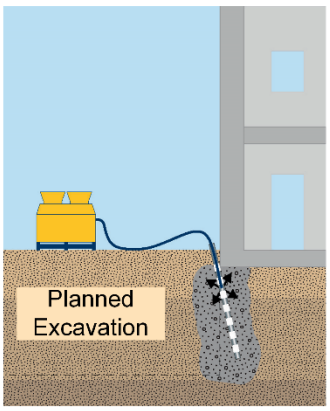

(Courtesy of Keller)

COMPARATIVE INFORMATION

<u>Advantages</u>

- Chemical grouts can be used in soils with finer pores than particulate grouts
- Computer monitoring of grouting shows real-time analysis of construction process

<u>Disadvantages</u>

- Experienced contractors are needed
- Time-consuming process
- Some chemical grouts break down over time, reducing capacity to improve the soil and releasing toxic material into the soil
- Expensive

<u>Preferred Applications</u>

- Soils with permeability as low as 10^{-4} cm/s and fines contents less than about 20%
- Embankment over unstable soils
- Stabilization of pavement working platforms

KEY DESIGN PARAMETERS	DESIGN GUIDANCE	COULD ALSO CONSIDER:
• Fines content and permeability of soil • Grout proportions	• FHWA (2017) – Chapter 8 • USACE (1997)	• Jet grouting

Figure 1-5 Summary of Key Elements of Chemical Grouting

Column Supported Embankments

Controlling Engineering Principles

Column supported embankments:

- Use vertical columns to transfer the load of the embankment through a soft compressible layer down to a firm foundation layer and
- Can use a load transfer platform to transfer the load to the columns and maintain acceptable deformation.

Basic Construction Process

Column supported embankments can use a variety of column types and installation methods. General installation includes:

- Construction of columns,
- Placement of load transfer platform and geosynthetic reinforcement, and
- Construction of embankment.

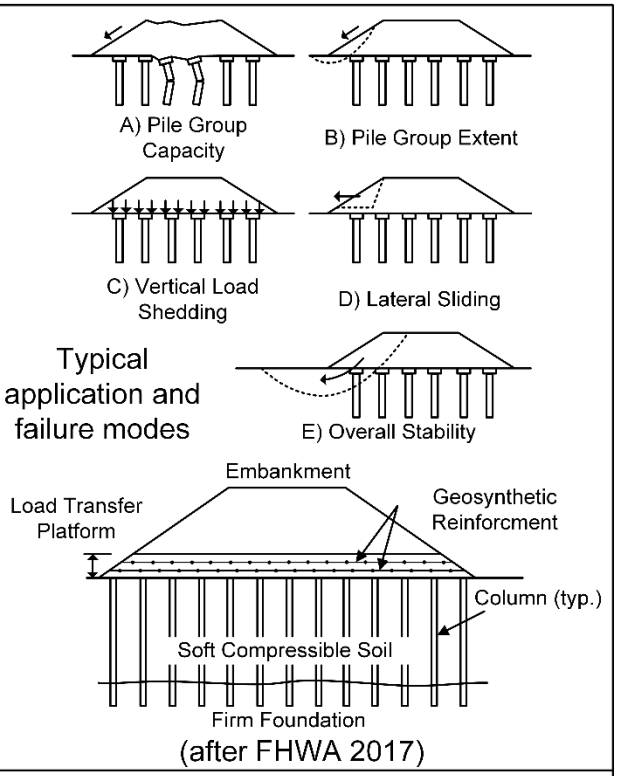

(after FHWA 2017)

COMPARATIVE INFORMATION

Advantages

- Accelerates construction compared to conventional methods
- Reduces total and differential settlement
- Protects adjacent facilities from distress
- Can use a wide variety of columns to accommodate different site conditions

Disadvantages

- Can have a higher cost than other technologies
- Lack of standard design procedures
- Lack of knowledge about technology benefits, design procedures, and construction techniques

Preferred Applications

- Soft soil underlain by stiffer soil or bedrock
- Embankment stabilization
- Roadway widening
- Bridge approach fill stabilization
- Bridge abutment and other foundation support

KEY DESIGN PARAMETERS	DESIGN GUIDANCE	COULD ALSO CONSIDER:
• Embankment height • Allowable settlement • Geosynthetic strength • Foundation soil strength and compressibility	• FHWA (2017) – Chapter 6	• Prefabricated vertical drains • Lightweight fill • Staged construction • Excavation and replacement

Figure 1-6 Summary of Key Elements of Column Supported Embankments

Compaction Grouting

Typical application and construction process

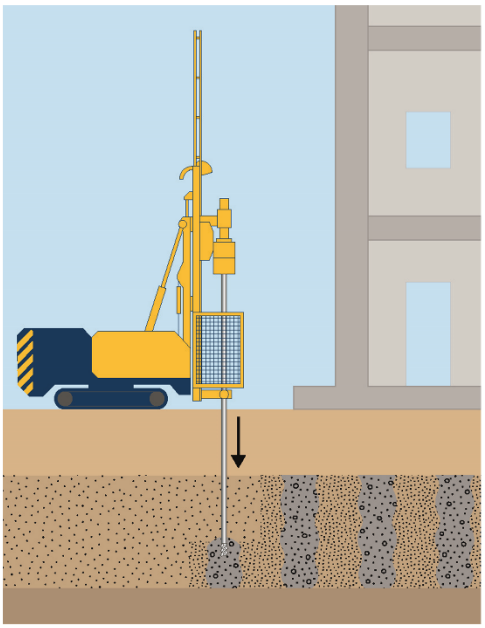

(Courtesy of Keller)

Controlling Engineering Principles

Compaction grouting:

- Displaces soil with low mobility grout,
- Compacts surrounding soil, and
- Strengthens and stiffens soil by densification of the soil itself rather than through the strength of the grout.

Basic Construction Process

Compaction grouting is accomplished by:

- Driving or drilling the grout casing to the desired depth and location,
- Pumping the grout until the design termination criteria have been reached, and
- Forming grout bulbs every 1 to 3 feet depending on the application of the project.

COMPARATIVE INFORMATION

Advantages

- Effectiveness has been well-proven in practice
- Can be implemented in areas of restricted vertical room
- Directly treats the area that needs improvement
- Can be installed under existing structures

Disadvantages

- Grout rheology requires further investigation
- Can cause a build-up of excess pore pressure in fine-grained soil
- QA/QC procedures need further development
- Design methodology is not well defined

Preferred Applications

- Silts and well-graded sands have greater success than clays and poorly-graded sands and gravels
- Embankment foundations
- Working platforms
- Correction of differential settlement
- Settlement controls over tunnels or sinkholes

KEY DESIGN PARAMETERS	DESIGN GUIDANCE	COULD ALSO CONSIDER:
• Depth and area of soil to be modified • Grout mix proportions	• FHWA (2017) – Chapter 8	• Jet grouting • Deep mixing • Deep dynamic compaction • Micropiles

Figure 1-7 Summary of Key Elements of Compaction Grouting

Dynamic Compaction

Typical application and construction process

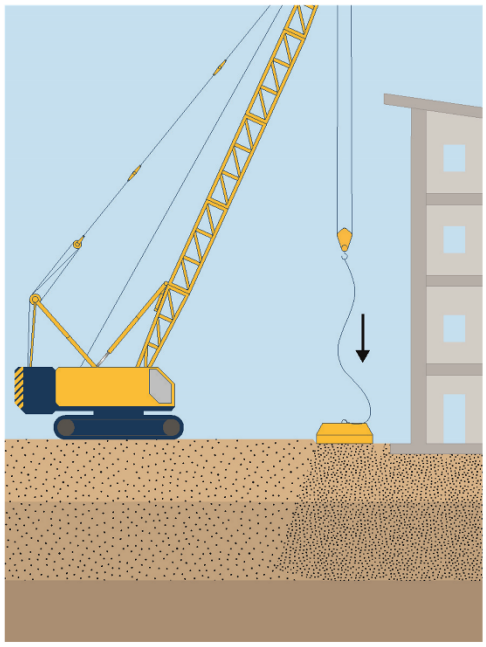

(Courtesy of Keller)

Controlling Engineering Principles

Dynamic compaction:

- Uses cranes to drop tampers onto the soil which compact the soil,
- Increases the soil's resistance to liquefaction,
- Increases bearing capacity, and
- Reduces settlement.

Basic Construction Process

Dynamic compaction can be accomplished by:

- Dropping a tamper by a crane in a systematic pattern,
- Using a first phase with high-energy to improve the deeper soil, and
- Following with a second phase of lower-energy to improve the upper layers of soil.

COMPARATIVE INFORMATION

Advantages

- Suitable for many types of soils
- Low cost for large area improvement
- Ability to measure improvement
- Non-specialty contractors
- Simple equipment
- Produces relatively uniform compressibility
- Not weather dependent

Disadvantages

- Vibrations can travel far
- Lateral ground displacement can occur
- Mobilization costs
- Limited effective treatment depth
- Some safety concerns
- Ineffective in fine-grained soils

Preferred Applications

- Loose pervious and semi-pervious soils with fines contents less than 15%
- Densification of loose deposits
- Collapse of large voids and collapse-susceptible soils
- Embankments over compressible coarse-grained soils

KEY DESIGN PARAMETERS	DESIGN GUIDANCE	COULD ALSO CONSIDER:
• Soil type • Required depth of compaction	• FHWA (2017) – Chapter 4	• Deep foundation systems • Sand compaction columns • Vibrocompaction • Blast densification

Figure 1-8 Summary of Key Elements of Dynamic Compaction

Deep Mixing Method

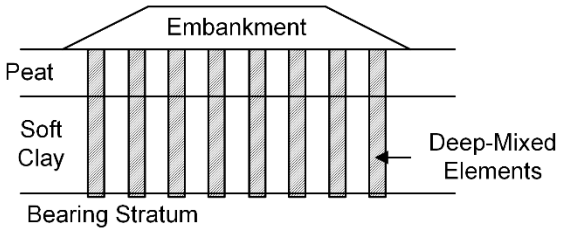

(after FHWA 2017)

Controlling Engineering Principles

The deep mixing method:

- Creates soil-cement zones that have the improved properties,
- Increases strength, and
- Decreases compressibility.

Basic Construction Process

Deep mixing can be completed using either water-binder slurry or dry power binder, which is based on the type of soil that exists on the site. The process includes:

- Inserting the soil mixing equipment (either vertical axis, horizontal axis, or chainsaw-like),
- Delivering the binder, and
- Mixing of soil and binder.

Typical application and construction process

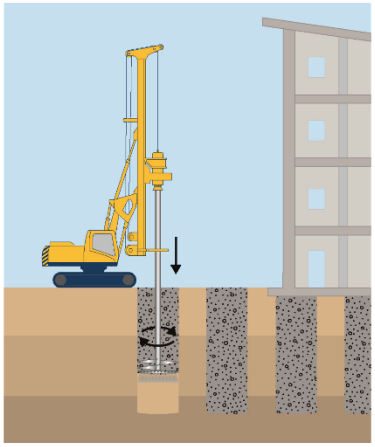

(Courtesy of Keller)

COMPARATIVE INFORMATION

Advantages	Disadvantages	Preferred Applications
• Economical on large projects • Less noise and vibrations compared to other technologies • High production capacity • Relatively easy installation procedures	• Mobilization and unit cost may be higher than other technologies • Obstructions can interfere with penetration of mixing equipment • The wet method requires heavy equipment that may be too heavy for softer soils • Can be slower than other methods	• Wide range of applicable soils • Can be used above water or below water • Embankments • Retaining walls • Abutments • Bridge piers

KEY DESIGN PARAMETERS	DESIGN GUIDANCE	COULD ALSO CONSIDER:
• Soil-cement shear strength and modulus	• FHWA (2017) – Chapter 7	• Prefabricated vertical drains • Dynamic compaction • Piles, aggregate columns, or vibro-concrete columns

Figure 1-9 Summary of Key Elements of the Deep Mixing Method

Mass Mixing Method

<u>Controlling Engineering Principles</u>

The mass mixing method:

- Creates soil-cement zones that have improved properties,
- Increases shear strength, and
- Limits settlement.

<u>Basic Construction Process</u>

Mass mixing can be completed using either water-binder slurry or dry power binder mixed with the existing soil. The process includes:

- Dividing the treatment area into overlapping blocks prior to treatment,
- Mixing the soil and binder using an excavator-mounting mixing tool, and
- Topping the soil-cement with a preload after mixing to induce consolidation of the treated soil while curing occurs.

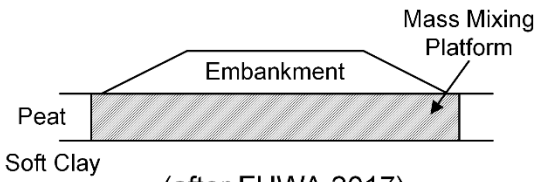

(after FHWA 2017)

Typical application and construction process

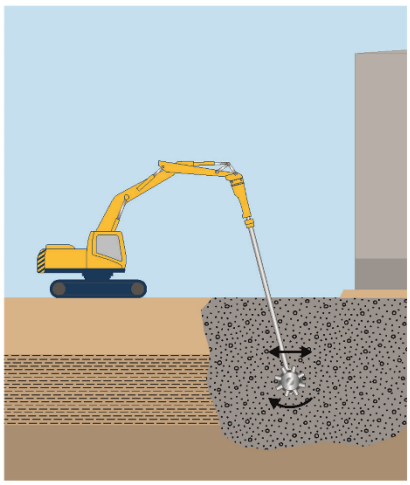

(Courtesy of Keller)

COMPARATIVE INFORMATION

<u>Advantages</u>

- Can be done rapidly
- Can stabilize peat and other soft soils, and can treat contaminated soils
- Less expensive than deep mixing on a unit volume basis
- Can stabilize large blocks of soil
- Lower environmental impacts compared to other technologies

<u>Disadvantages</u>

- Limited treatment depth
- Cannot easily penetrate dense or stiff soils
- Cost-effectiveness is dependent on accuracy of the measurement of binder quality
- Organic soils may require higher binder content or specific binder types

<u>Preferred Applications</u>

- Soft clay, dredged soil, sludges, contaminated soils, and soft silts
- Embankments over highly compressible soil
- Tanks
- Stabilizing excavations
- Land reclamation
- Contaminant fixation

KEY DESIGN PARAMETERS	DESIGN GUIDANCE	COULD ALSO CONSIDER:
• Soil-cement shear strength and modulus • Organic content	• FHWA (2017) – Chapter 7	• Prefabricated vertical drains • Column-supported embankments • Deep mixing methods

Figure 1-10 Summary of Key Elements of the Mass Mixing Method

Pre-Fabricated Vertical Drains

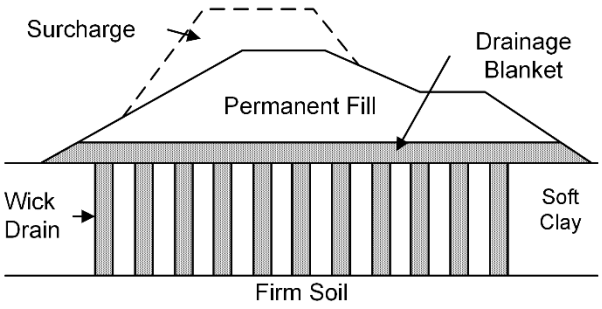

(after FHWA 2017)

Controlling Engineering Principles

Pre-fabricated vertical drains (PVDs):

- Create a shorter drainage path for consolidation,
- Increase the consolidation rate,
- Increase rate of strength gain, and
- Can be combined with surcharging or preloading.

Basic Construction Process

PVDs can be installed by static, vibratory, jetting, or combined methods. PVD installation includes:

- Threading PVD material into mandrel,
- Attaching an anchor to bottom of mandrel,
- Inserting the mandrel and PVD into the ground,
- Withdrawing the mandrel, and
- Cutting off and anchoring the PVD.

Typical application and construction process

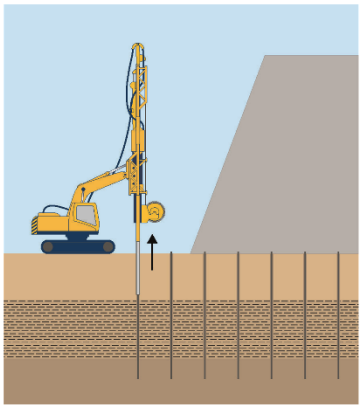

(Courtesy of Keller)

COMPARATIVE INFORMATION

Advantages

- Economical method
- Very fast installation
- Permanent drainage path
- Minimal soil removal or displacement
- Simple QA/QC
- Adaptable equipment
- Water typically not required (unless jetted)

Disadvantages

- Equipment must be taller than PVD depth
- PVD material degrades in sunlight
- Soil improvement limited by size of added load or surcharge
- Less appropriate for soils with significant secondary compression
- Can weaken stiff clays

Preferred Applications

- Saturated normally consolidated or lightly overconsolidated silt
- Embankments over highly compressible soil
- Tank foundations
- Reduction of pile negative skin friction
- Liquefaction mitigation
- Land reclamation

KEY DESIGN PARAMETERS	DESIGN GUIDANCE	COULD ALSO CONSIDER:
• Compressible layer thickness • Coefficients of consolidation, c_v and c_h	• FHWA (2017) – Chapter 2 • DM 7.1 – Chapter 5	• Aggregate columns • Geotextile encased columns

Figure 1-11 Summary of Key Elements of Pre-Fabricated Vertical Drains

Sand Compaction Piles

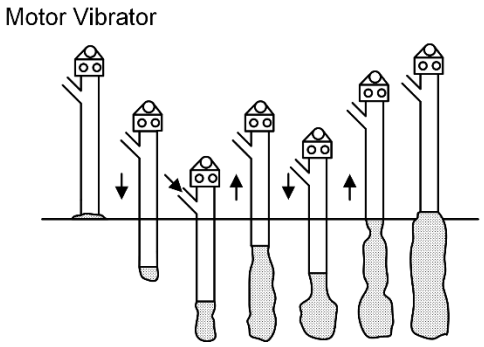

After Tanimoto (1973)

Typical application
and construction process

Controlling Engineering Principles

Sand compaction piles:

- Create a drainage pathway for clay soils,
- Increase the bearing capacity,
- Prevent stability failures,
- Reduce settlement,
- Accelerate consolidation, and
- Increase liquefaction resistance.

Basic Construction Process

Sand compaction piles are installed either in loose sand or soft clay. Installation of sand compaction piles includes:

- Driving pipe through soil using vibratory or nonvibratory means,
- Backfilling the pipe with sand, and
- Densifying the surrounding soil by repeated penetration and extraction of the pipe.

COMPARATIVE INFORMATION

Advantages

- Rapid construction, less risk of intrusion of soil into the pile compared to stone columns
- Fully-supported hole during construction prevents collapse
- Liquefaction prevention
- Settlement reduction

Disadvantages

- Not commonly used in the United States
- Smearing effects when constructed in clay
- Greater replacement ratios are necessary compared to other columns
- Vibration and noise during construction
- Sand can be costly and availability limited

Preferred Applications

- Wide range of soils, from soft clays to sandy soils
- Embankments over unstable soils

KEY DESIGN PARAMETERS	DESIGN GUIDANCE	COULD ALSO CONSIDER:
• Type of soil • Sand backfill properties	• Aboshi, H. (1991) • Barksdale, R.D. (1987) • Kitazume, M. (2005)	• Vibrocompaction • Stone columns • Aggregate piers • Vibroconcrete columns

Figure 1-12 Summary of Key Elements of Sand Compaction Piles

Soil Nail Walls

Typical application and construction process

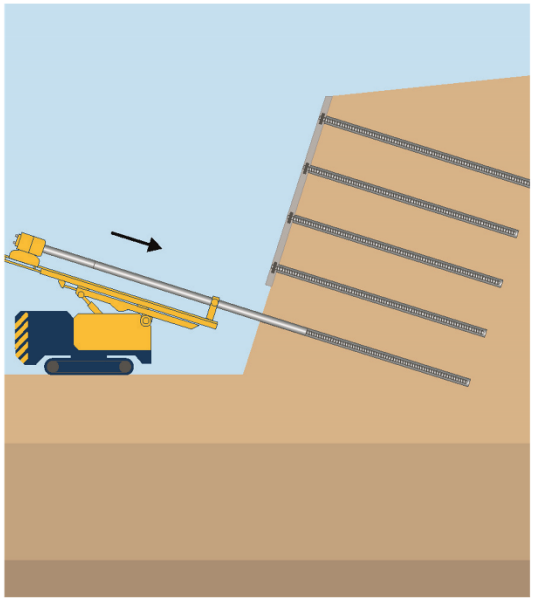

(Courtesy of Keller)

Controlling Engineering Principles

Soil nail walls:

- Reinforce existing soil,
- Provide tensile resistance, and
- Require temporary stability during installation.

Basic Construction Process

The soil nail wall is a top-down constructed retaining system. Installation includes:

- Excavating an initial lift,
- Drilling a nail hole,
- Installing and grouting the nail,
- Repeating for additional nails,
- Placing initial facing,
- Installing drainage,
- Constructing subsequent levels, and
- Placing final facing.

COMPARATIVE INFORMATION

Advantages

- Relatively fast installation
- Good for temporary walls
- More cost effective in remote locations due to availability of smaller equipment
- Perform well during seismic events
- Can withstand large deformations
- Easily monitored and tested

Disadvantages

- Not well-suited in areas with large amounts of groundwater seeping into the excavation
- Permanent soil nail walls require permanent underground easements
- If projects have strict wall movement criteria, additional measures may be required

Preferred Applications

- Soil that can stand unsupported temporarily
- Ground conditions that remain stable without collapse until grouted
- Tunnel portals
- Roadway cuts
- Shored Mechanically Stabilized Earth (SMSE) walls
- Basement walls

KEY DESIGN PARAMETERS	DESIGN GUIDANCE	COULD ALSO CONSIDER:
• Soil strength • Ground water table	• FHWA (2017) – Chapter 5	• Cantilever wall • Gravity wall • MSE wall • Counterfort concrete wall

Figure 1-13 Summary of Key Elements of Soil Nail Walls

Vacuum Preloading

Controlling Engineering Principles

Vacuum preloading:

- Increases effective stress in foundation soils through reduction in pore pressures,
- Improves saturated soils by consolidation, and
- Can be combined with prefabricated vertical drains.

Basic Construction Process

The steps for vacuum preloading include:

- Covering soil site with an airtight membrane,
- Using dual venturi and vacuum pumps to create a vacuum over the site which will create and maintain the loads, and
- Maintaining the water table at the base of the granular platform through a combination of dewatering and vacuum action.

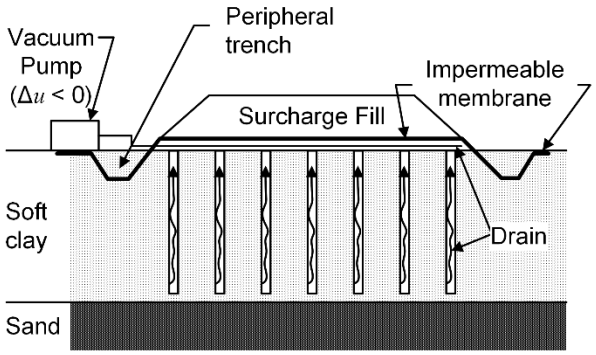

(after Fernandes, 2020)

Typical application
and construction process

COMPARATIVE INFORMATION

Advantages

- Fill not required
- Staged loading is not required
- No heavy equipment
- Environmentally friendly
- Established design methods and QC/QA requirements
- Cheaper and faster compared to surcharge loading

Disadvantages

- Maintenance of vacuum pressure is difficult
- May cause cracks in surrounding soils
- Vacuum pressure is limited to 1 atm
- Inward lateral movements from vacuum preloading can cause damage to adjacent structures

Preferred Applications

- Compressible soft, uniform clays
- Sites with shallow ground water table
- Embankment over unstable soil
- Stabilization of working platforms

KEY DESIGN PARAMETERS	DESIGN GUIDANCE	COULD ALSO CONSIDER:
• Compressible layer thickness • Coefficients of consolidation, c_v and c_h	• FHWA (2017) – Chapter 2	• Deep foundation elements • Prefabricated vertical drains • Stone columns • Grouting

Figure 1-14 Summary of Key Elements of Vacuum Preloading

Vibro-Compaction

Typical application and construction process

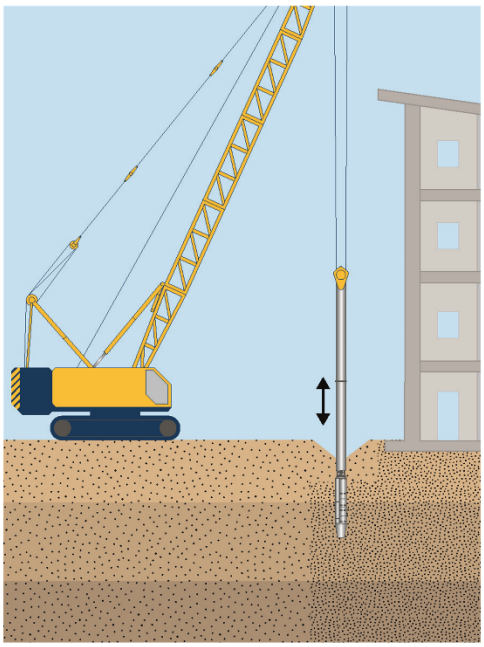

(Courtesy of Keller)

Controlling Engineering Principles

Vibro-compaction:

- Uses a probe and vibrator to densify the surrounding soil,
- Increases the soil's resistance to liquefaction,
- Increases bearing capacity, and
- Increases shear strength.

Basic Construction Process

Vibro-compaction can be accomplished by:

- Using a vibrator and probe to rearrange the soil particles into a denser state following the grid layout,
- Inserting the probe in phase one using a high frequency, and
- Densifying the soil in phase two using a low frequency.

COMPARATIVE INFORMATION

Advantages	Disadvantages	Preferred Applications
• Economical and fast method for deep foundations • Effective above and below the water table • Many case histories in United States	• Only effective for coarse-grained (cohesionless) soils • Maximum depth is about 165 feet • Noise and vibrations • Contractor experience is critical • Quality control should be monitored carefully	• Coarse-grained cohesionless soils • Embankment foundations • Underwater embankments • Tunnels • Liquefaction mitigation • Compaction of potential cavities • Foundation soils beneath proposed structures

KEY DESIGN PARAMETERS	DESIGN GUIDANCE	COULD ALSO CONSIDER:
• Initial and final relative density • Grain size distribution	• FHWA (2017) – Chapter 4	• Sand compaction piles • Deep dynamic compaction • Aggregate columns • Vibro-concrete columns

Figure 1-15 Summary of Key Elements of Vibro-Compaction

Vibro-Concrete Columns

Typical application and construction process

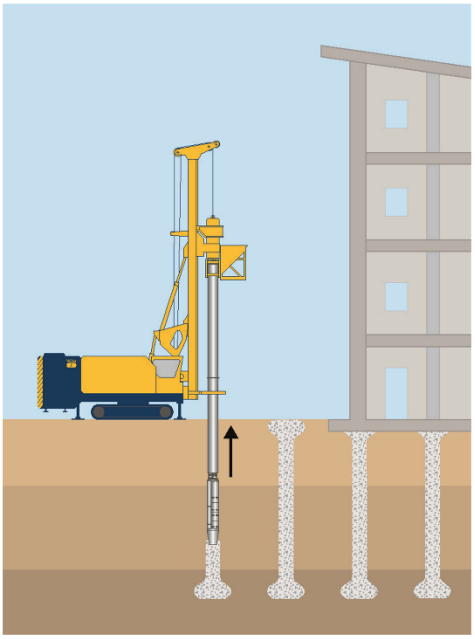

(Courtesy of Keller)

Controlling Engineering Principles

Vibro-concrete columns:

- Create columns similar to aggregate columns with concrete in place of aggregate,
- Increase the bearing capacity, and
- Can be combined with column-supported embankments to reduce total and differential settlement.

Basic Construction Process

The vibro-concrete column installation includes:

- Using a vibrator to penetrate soil to specified depth,
- Pumping concrete to fill the void while the vibrator is being extracted, and
- Repenetrating with the vibrator during extraction to create bulbs at top and bottom of the columns.

COMPARATIVE INFORMATION

Advantages

- Reduces total, differential, and seismic settlements
- Greater column stiffness compared to aggregate columns
- Quick construction
- Environmentally friendly (no spoils)

Disadvantages

- Lack of well-established design procedure
- More expensive than aggregate columns

Preferred Applications

- Best used in soft clays or peat with low undrained shear strength
- Embankments over unstable soils

KEY DESIGN PARAMETERS	DESIGN GUIDANCE	COULD ALSO CONSIDER:
• Compressible layer thickness • Strength of bearing layer	• FHWA (2017) – Chapter 5	• Aggregate columns • Prefabricated vertical drains • Driven piles • Vibrocompaction

Figure 1-16 Summary of Key Elements of Vibro-Concrete Columns

1-4 NOTATION.

Variable	Definition
$\bar{A}$	Skempton's pore pressure parameter for change in shear stress
c'	Drained or effective stress cohesion intercept
$C_{\varepsilon c}$	Modified compression index (in terms of strain)
c_h	Coefficient of consolidation in the horizontal direction
c_v	Coefficient of consolidation in the vertical direction
K_0	Lateral earth pressure coefficient for at-rest conditions
LL	Liquid limit
N	Standard penetration test blow count (uncorrected)
PI	Plasticity index
S_t	Sensitivity
ϕ'	Drained or effective stress friction angle

CHAPTER 2.EXCAVATIONS

2-1 INTRODUCTION.

This chapter covers the methods of evaluating the stability of shallow and deep excavations. There are two basic types of excavations: 1) *open cut excavations* where stability is achieved by providing stable side slopes and 2) *braced excavations* where vertical or sloped sides are supported laterally by internal or external structural elements. The topics in this chapter include:

- Open cut excavations,
- Trenching,
- Deep excavation systems,
- Rock excavation, and
- Groundwater control.

The primary site conditions controlling the selection and design of an excavation system include soil and rock type and stratigraphy, soil and rock strength and consolidation parameters, and groundwater conditions. These can be identified using methods described in Chapters 2 and 3 of DM 7.1 and FHWA (2017) Additional considerations include the required excavation depth, side and bottom stability, construction procedures, excavation support system stability, and vertical and lateral movements of adjacent areas and existing structures.

2-2 OPEN CUT EXCAVATIONS.

2-2.1 Sloped Excavations.

The methods described in Chapter 7 of DM 7.1 may be used to evaluate the stability of sloped excavations in soils and rocks. In clay soils, instability typically involves side slopes but may also include soils below the base of the excavation. Clay soils that increase in shear strength with depth typically exhibit failures that occur on the side slopes. For clay soils that exhibit relatively constant shear strength with depth, the failure may extend into the base of the excavation. In coarse-grained soils, instability usually does not extend significantly below the base of the excavation, provided seepage is controlled. In rock, stability is often controlled by adversely orientated planes of weaknesses such as joints, foliation planes, or faults.

In some problem soils, and in rocks with adversely orientated geologic planes of weaknesses, special considerations are needed when evaluating stability of open cut excavations as discussed in Section 2-7. In any soil, the stability of excavated slopes may decrease with time, saturation, and disturbance. Some soils may not conform to common shear strength correlations used in design. For example, the properties of residual soil, which cover about half of Earth’s land mass, are difficult to relate to stress

history. Local knowledge may be helpful when determining the analysis approach in these problem soils.

Slope stability can be improved by reducing the driving forces that cause instability. The top of a slope can be lowered, or the slope angle can be reduced, if an adequate factor of safety against instability is not achieved. Surcharge loading from equipment and/or stockpiles should be kept away from the top of an excavation when these negatively impact stability.

2-2.2 Vertical Excavations.

2-2.2.1 Clay Soils.

Many cuts in clays will stand with vertical slopes for a period of time before failure occurs. The maximum depth of a vertical cut in clay, or *critical depth*, (H_{crit}) is defined as:

$$H_{crit} = \frac{4s_u}{\gamma_t} \tag{2-1}$$

where:
s_u = undrained shear strength and
γ_t = total or moist unit weight of the clay.

However, changes in the shear strength of the clay with time and stress release resulting from the excavation can lead to progressive deterioration in stability. The Occupational Safety and Health Administration (OSHA) requires all excavations be sloped and trenches supported if greater than 5 ft in depth (OSHA 2020).

2-2.2.2 Rock.

Excavations in rock can be made vertical without support (rock bolts or tieback anchors) depending on the rock quality, lack of adversely oriented joints and faults, and sufficient mobilized shear strength along structural features to provide a stable condition. The stability of rock slopes is also covered in Chapter 7 of DM 7.1.

2-2.3 Other Design Considerations for Open Cut Excavations.

Dewatering may be required to allow construction without water in the excavation.[7] Dewatering increases effective stress and can cause settlement under nearby structures. It may be necessary to consider installation of a low permeability cutoff trench, filled with soil-bentonite or soil-cement-bentonite mixtures, between the

[7] Sometimes referred to as “in the dry.”

excavation and nearby structures. Dewatering in an area of carbonate rocks may cause sinkhole development. Additional discussion about dewatering can be found in Section 2-6 and Unified Facilities Criteria (UFC) UFS 3-220-05 (DoD 2004). Perimeter drains should be used around an excavation to prevent surface water from flowing into the excavation and causing erosion.

The excavation and surrounding area should be monitored during excavation. Bottom heave, slope movement, and settlement of areas beyond the slope should be carefully observed and monitored. Monitoring can be accomplished by conventional survey techniques, heave points, and piezometers (see DM 7.1, Chapter 2). Piezometers can be used to investigate excess pore pressures below an excavation and the potential for piping or heaving.

Structures near excavated slopes may need to be underpinned. Underpinning (Section 2-4.4) should be considered when the bearing elevation of the foundations is higher than the bottom of the excavation and influenced by critical failure surfaces for the slope.

The effect of vibrations from blasting, pile driving, and heavy equipment movements on settlement or damage to adjacent structures should also be considered. Prior to any activity that may cause damage due to vibrations, a preconstruction survey with photographs should be performed. In addition, a test blast program should be required before any blasting. During construction, vibration monitoring is critical. The impact of vibrations on rock with adversely oriented rock structure should also be evaluated. See Section 2-5.3 for additional discussion of blasting.

2-3 TRENCHING.

2-3.1 Site Exploration.

Individual trenching projects frequently extend over long distances. An exploration program should be performed to define the soil and groundwater conditions over the full extent of the project so that the design of the shoring system can be adjusted to accommodate varying subsurface conditions.

2-3.2 Trench Stability.

Excavation support for trenches is regulated by OSHA (2020). Principal factors influencing trench stability are the lateral earth pressures (see Chapter 4) on the wall support system, bottom heave, and the pressure and erosive effects of infiltrating groundwater (see Chapter 6 of DM 7.1). Additional external factors which influence trench stability include:

- Surface surcharge loads,
- Vibration loads,

- Groundwater seepage, and
- Surface water flow.

2-3.2.1 Surface Surcharge Loads.

Surface loads may be present adjacent to a trench and cause loading on the trench support system. The effects of surface loads should be considered if the load is between the edge of the excavation and the intersection of the ground surface with the possible failure plane. Section 4-4.2 provides additional guidance on earth pressures caused by surface loading.

2-3.2.2 Vibration Loads.

The effects of vibrating machinery, blasting, other dynamic loads, and earthquakes in the vicinity of the excavation must be considered. The effects of vibrations are cumulative over periods of time and can be particularly dangerous in soft clays which amplify vibrations. In addition, vibrations from earthquakes or blasting can cause loose contractive sands and silts to fail as brittle materials at low strains. Once disturbed, these materials flow, which can result in catastrophic damage. Excavations in these types of soil are very problematic. While dense coarse-grained soils are also brittle and fail at low strains, they do not flow and are not problematic for excavations. If blasting is required in a trench, the size of the charge should be as small as possible, and the effect of vibrations on settlement of or damage to adjacent structures must be considered.

2-3.2.3 Groundwater Seepage.

Groundwater seepage at the bottom of an excavation can result in bottom heave. *Bottom heave* refers to upward movement of the base of the excavation caused by a high upward gradient that exceeds the critical gradient of the soil. This is also referred to as a *quick* condition. Heaving or quick soils lose all or most of their shear strength because the effective stress approaches zero. Bottom heave can occur in coarse-grained soils that are improperly dewatered.

In addition to heave, seepage can result in *internal erosion*, which is the movement of soil particles from within the soil structure. Fine sands and silts are most susceptible to internal erosion. Prediction methods and design for internal erosion are discussed in Chapter 6 of DM 7.1.

2-3.2.4 Surface Water Flow.

Uncontrolled surface water can enter the retained soil, increase the water content, and potentially result in saturation. Saturation greatly increases loads on the wall support system and may reduce the shear strength of the soil. Site drainage should be designed to divert surface water away from trenches. This is especially important for

the zone between the edge of the excavation and the intersection of a possible failure plane with the ground surface.

2-3.3 Support Systems.

OSHA (2020) requires protective measures for any trench greater than 5 feet deep, except in stable rock. Protective measures are also required for some excavations at any point less than 5 feet deep where there is evidence of a potential cave-in as determined by a *competent person*. OSHA (2020) describes a competent person as someone capable of identifying hazards or unsafe working conditions who possesses authority to take corrective measures.[8]

Shoring and sheeting plans should be certified by a registered professional engineer. For trenches greater than 20 feet deep, a licensed professional engineer must approve the design (OSHA 2020).

The commonly used excavation support systems discussed in the following sections include trench shields, hydraulic shoring, timber shoring, and steel shoring. Cross braces or trench jacks shall be placed in true horizontal position; spaced vertically; and secured to prevent sliding, falling, or kickouts.

2-3.3.1 OSHA Soil Types.

OSHA (2020) defines Soil Types A, B, and C for the design of trenches as summarized in Table 2-1. Appendix A of the OSHA manual provides definitions of terms used in defining these soil types. OSHA's definitions do not conform to the Unified Soil Classification System (ASTM D2487).

2-3.3.2 Trench Shield.

A *trench shield* is a rigid prefabricated steel support system used in lieu of other types of shoring, which extends from the bottom of the excavation to the ground surface. The trench shield is placed within a wider excavation with vertical walls and protects the enclosed space from trench collapse. Piping systems or other structures are constructed within the shield, which is pulled ahead, as trenching and construction proceed. Figure 2-1(a) illustrates a trench shield. This system is useful in most soils with the exception of very dense or hard soils. The trench shield must extend to the ground surface of vertical excavations. Where part of the excavation is sloped, the trench shield extends 18 inches above the toe of the slope as shown in Figure 2-1(b).

[8] See OSHA (2020) Paragraph 652(a)(1)(ii) for the legal definition of competent person.

The trench shield must be designed for the full height of the excavation including the sloped portion above the trench shield.

Table 2-1 Soil Types (after OSHA CFR Part 1926, Subpart P, Appendix A)

Soil Type	Soil Description	Unconfined Compressive Strength (tsf)	Estimated Soil Classification (USCS) (ASTM D2487)	Exclusions or Inclusions
A	Cohesive[A]	>1.5	CH, CL, MH, SC, GC, OH, including cemented soils	Type A cannot be: • Fissured, • Previously disturbed, • Dipping into excavation at a slope > 4H:1V • Subject to vibration from traffic
B	Cohesive	>0.5 to < 1.5	CH, CL, SC, GC, OH	Include soil that categorizes as Type A but is fissured, previously disturbed, or subject to vibrations. Exclude soils from Type B that have layers that dip into the excavation at a slope > 4H:1V.
	Granular cohesionless[B]	--	ML, OL, SM, SW, SP, GM, GW, GP	
C	Cohesive	<0.5	CH, CL, SC, GC, OH	Include soil that categorizes as Type A or B but has layers that dip into excavation at a slope > 4H:1V
	Granular cohesionless	--	ML, OL, SM, SW, SP, GM, GW, GP	

OSHA Defintions:

[A] "Cohesive soil means clay (fine grained soil), or soil with a high clay content, which has cohesive strength. Cohesive soil does not crumble, can be excavated with vertical side slopes, and is plastic when moist. Cohesive soil is hard to break up when dry, and exhibits significant cohesion when submerged. Cohesive soils include clayey silt, sandy clay, silty clay, clay and organic clay."

[B] "Granular soil means gravel, sand, or silt (coarse grained soil) with little or no clay content. Granular soil has no cohesive strength. Some moist granular soils exhibit apparent cohesion. Granular soil cannot be molded when moist and crumble easily when dry."

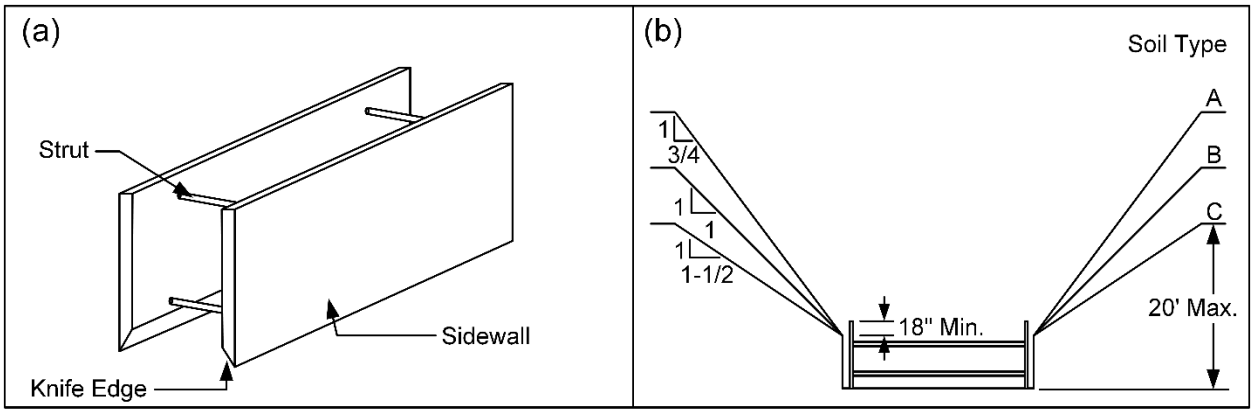

Figure 2-1 Trench Shield; a) Typical Trench Shield, b) Maximum Slopes for Various Soil Types Defined by OSHA (after OSHA Technical Manual)

Excavation depths of up to 20 feet are permitted by OSHA (2020) using manufactured trench shields designed in accordance with OSHA standards. These shields should be used in accordance with the manufacturer's specifications, recommendations, tabulated data, and limitations. Shield systems must not be subjected to loads exceeding those which the system was designed to withstand.

Excavations up to 2 feet below the shield are permitted when the shield is designed to resist the forces for the full depth of the trench. This type of excavation is only permitted when there is no indication of loss of soil from behind or below the bottom of the shield. When designing for an excavation below the bottom of the shield, consideration must be given to the potential for internal erosion or heaving. During use, the excavation should be observed for evidence of these problem conditions. Surcharge loading, vibrations, or loads from adjacent structures also must be considered.

2-3.3.3 Hydraulic Shoring.

Hydraulic shoring consists of aluminum hydraulic cylinder braces and heavy plywood (Finform) sheets. It has gained popularity over timber shoring, because it is less costly and does not require workers to enter a trench to construct the shoring. Table 2-2 and Table 2-3 provide hydraulic shoring requirements from OSHA (2020). Figure 2-2 illustrates typical applications of hydraulic shoring (OSHA 2020).

Hydraulic shoring can typically be used to a depth of about 25 feet with trench widths up to 12 feet. The trench width can be increased with cylinder extensions referred to as *steel tube oversleeves*. Hydraulic shoring design guidelines are found in OSHA (2020) Appendix D, Item (g).

Table 2-2 Aluminum Hydraulic Shoring - Soil Types A and B, No Walers (after OSHA 2020 Appendix D, Tables D-1.1 and D-1.2)

OSHA Soil Type	Depth of Trench, H (ft)[A]	Hydraulic Cylinder Spacing and Diameter				
		Maximum Horizontal Spacing, (ft)	Maximum Vertical Spacing (ft)	Cylinder Diameter for Trench Width, B (ft)		
				B < 8	8 ≤ B < 12	12 ≤ B < 15
A	5 ≤ H < 10	8	4	2 in.	2 in.[B]	3 in.
	10 ≤ H < 15	8	4			
	15 ≤ H < 20	7	4			
B	5 ≤ H < 10	8	4	2 in.	2 in.[B]	3 in.
	10 ≤ H < 15	6.5	4			
	15 ≤ H < 20	5.5	4			

Notes:
[A] Design trench with depths greater than 20 feet using manufacturers' tabulated data, and refer to Code of Federal Regulations (CFR) Part 1926, Subpart P 652(c)(2) and 652(c)(3).
[B] At this width, 2-inch diameter cylinders shall have structural steel tube oversleeves (3.5x3.5x0.1875 in), or structural oversleeves of manufacturers' specification, extending the full, collapsed length.

Table 2-3 Aluminum Hydraulic Shoring – Soil Types B and C with Wales (after OSHA 2020 Appendix D, Tables D-1.3 and D-1.4)

OSHA Soil Type	Depth of Trench, H (ft)[A]	Wales		Hydraulic Cylinder Spacing and Diameter for Trench Width, B (ft)						Timber Uprights (in. x. in.)		
				B < 8		8 ≤ B < 12		12 ≤ B < 15				
		Vertical Spacing (ft)	Section Modulus (in.^{3})	Horizontal Spacing (ft)	Cylinder Diameter (in.)	Horizontal Spacing (ft)	Cylinder Diameter (in.)	Horizontal Spacing (ft)	Cylinder Diameter (in.)	Solid Sheet	2 ft Horizontal Spacing (O.C.)[C]	3 ft Horizontal Spacing (O.C.)
B	5 to <10	4	3.5	8.0	2	8	2[B]	8	3	--	--	3x12
			7.0	9.0	2	9	2[B]	9	3			
			14.0	12.0	3	12	3	12	3			
	10 to <15	4	3.5	6.0	2	6	2[B]	6	3	--	3x12	--
			7.0	8.0	3	8	3	8	3			
			14.0	10.0	3	10	3	10	3			
	15 to <20	4	3.5	5.5	2	5.5	2[B]	5.5	3	3x12	--	--
			7.0	6.0	3	6	3	6	3			
			14.0	9.0	3	9	3	9	3			
C	5 to <10	4	3.5	6.0	2	6.0	2[B]	6.0	3	3x12	--	--
			7.0	6.5	2	6.5	2[B]	6.5	3			
			14.0	10.0	3	10.0	3	10.0	3			
	10 to <15	4	3.5	4.0	2	4.0	2[B]	4.0	3	3x12	--	--
			7.0	5.5	3	5.5	3	5.5	3			
			14.0	8.0	3	8.0	3	8.0	3			
	15 to <20	4	3.5	3.5	2	3.5	2[B]	3.5	3	3x12	--	--
			7.0	5.0	3	5.0	3	5.0	3			
			14.0	6.0	3	6.0	3	6.0	3			

Notes:
[A] Design trench with depths greater than 20 feet using manufacturers' tabulated data, and refer to CFR Part 1926, Subpart P 652(c)(2) and 652(c)(3).
[B] At this width, 2-inch diameter cylinders shall have structural steel tube oversleeves (3.5x3.5x0.1875) or structural oversleeves of manufacturers' specification, extending the full, collapsed length.
[C] O.C. stands for on center spacing.

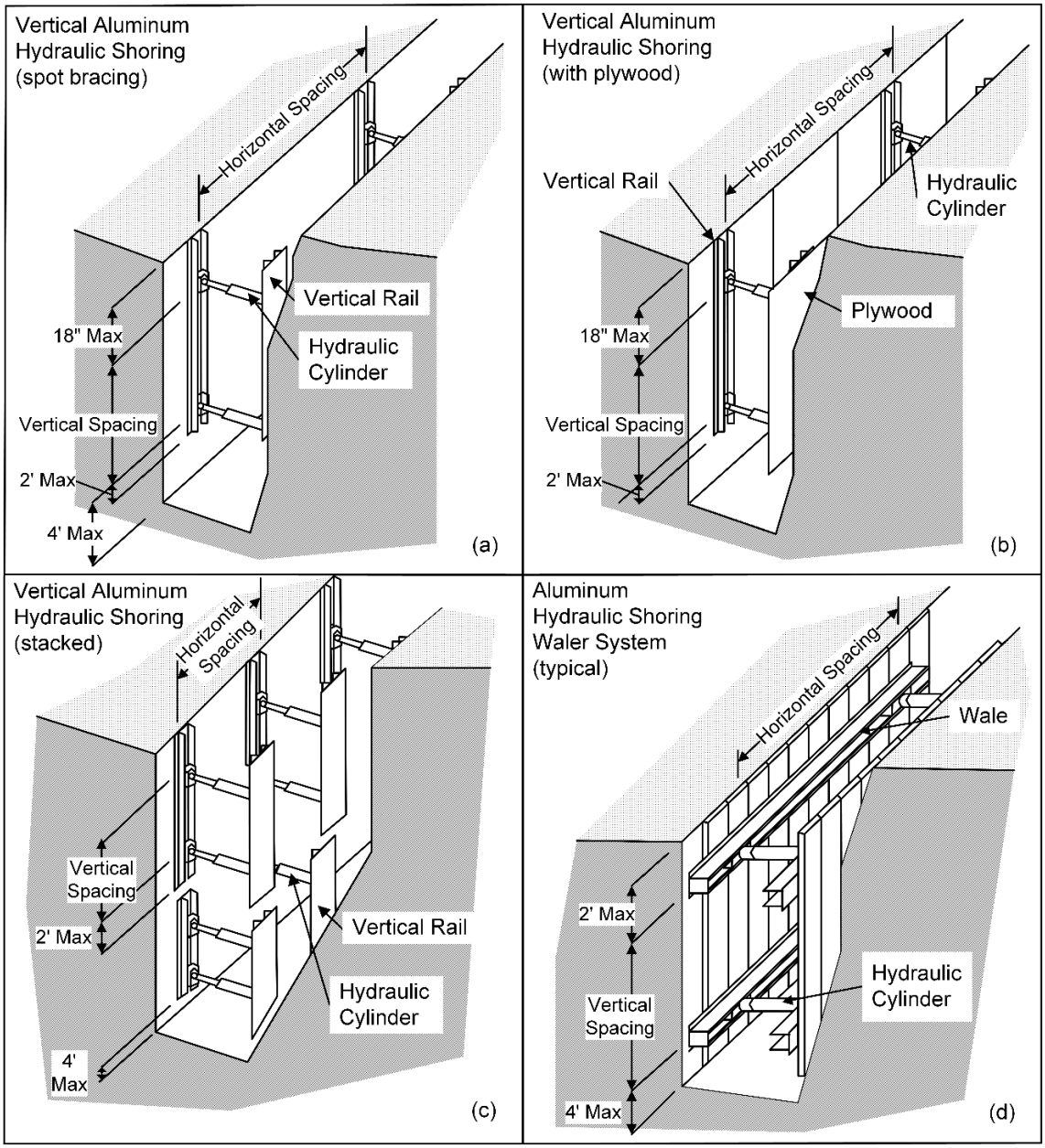

Figure 2-2 Hydraulic Shoring - a) Spot Bracing, b) Plywood, c) Stacked, and d) Waler System (after OSHA Technical Manual 2020)

2-3.3.4 Timber Shoring.

Timber shoring uses a temporary structure made of wood to support a trench. The four types of timber shoring are illustrated in Figure 2-3. The systems use vertical uprights or horizontal timbers against the soil, which are supported by a system of wales and cross-braces. *Skeleton shoring* does not use continuous upright members and is

applicable when running soils[9] are not expected. It can be used to depths up to 20 feet. *Close (tight) shoring* uses continuous upright timbers to support the soil and is useful where seepage and cave-ins are expected. *Box shoring* uses horizontal timbers to support the soil. Box shoring is applicable to trenching in any soil and is only limited in depth by the structural strength and size of the timber. *Telescopic shoring* is used for very deep trenches and consists of nested trenches that decrease in width as the trench depth increases.

Timbers used for shoring must be sound and free from large or loose knots. Timber shoring must be designed and installed to the bottom of the excavation. Braces and uprights for timber shoring must be installed at the same time as the excavation. Braces and diagonal shores of timber should not be subjected to compressive stresses in excess of the allowable compressive stress. The allowable compressive stress will vary by species of wood. Additional information on the structural properties of timber can be found in Section 6-7.1.1.3 as well as the *Wood Handbook* (USDA 2010). The allowable compressive stress will decrease as the slenderness of the shoring member increases. The ratio of length to least width is typically limited to 50 or less.

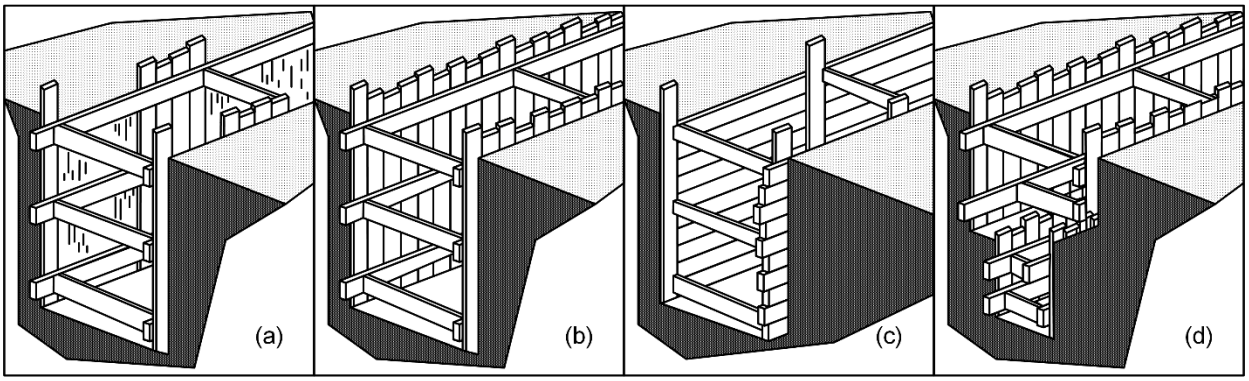

Figure 2-3 Timber Shoring: a) Skeleton; b) Close (tight); c) Box; d) Telescoping (after OSHA Technical Manual 2020)

Table 2-4 summarizes the OSHA (2020) minimum requirements for trench shoring. The data in the table are for nominal size timber with spacing measured center to center. A maximum of two feet of soil surcharge adjacent to the trench and a maximum equipment surcharge of 20,000 lb are assumed in the design. The region adjacent to the trench is defined as a horizontal distance on each side of the trench equal to its depth. OSHA (2020) indicates that tight sheeting, such as tongue and groove timber at least three inches thick or steel sheet piling, must be used when submerged conditions are encountered to resist the lateral water pressure and to reduce loss of fines behind

[9] Running soils have no ability to hold a vertical face and will flow or cave into the excavation if unsupported. Clean, dry coarse-grained soils are an example. Seepage can also result in running soil.

the sheeting. Table 2-4 does not cover the case of submerged conditions. A licensed professional engineer must approve the design for trenches greater than 20 ft deep, submerged conditions, and other conditions as noted in Table 2-4.

Table 2-4 Minimum Requirements for Timber Trench Shoring (after OSHA 2020)

OSHA Soil Type	Trench Depth, H (ft)	Size (Nominal) and Spacing of Members[B,C,D]									
		Cross Brace Spacing and Size							Wales		Upright Size (in x in) @ Maximum Allowable Horizontal Spacing, (ft) (0 = OSHA Close Spacing)
		Brace Spacing (ft)		Size of Members (in x in) for Specified Trench Width:							
		Horizontal	Vertical	≤ 4 ft	≤6 ft	≤9 ft	≤12 ft	≤15 ft	Size (in x in)	Vertical Spacing (ft)	
A	5 to 10	≤ 6	4	4x4	4x4	4x4	4x4	4x6	None	-	4x6@6
		≤ 8					4x6				4x8@8
		≤ 10		4x6	4x6	4x6	6x6	6x6	8x8	4	4x6@5
		≤ 12[A]									4x6@6
	10 to 15	≤ 6	4	4x4	4x4	4x4	6x6	6x6	None	-	4x10@6
		≤ 8		4x6	4x6	4x6			6x8	4	4x6@4
		≤ 10[A]		6x6	6x6	6x6			8x8		4x8@5
		≤ 12[A]							8x10		4x6@4,4x10@6
	15 to 20	≤ 6	4	6x6	6x6	6x6	6x6	6x6	6x8	4	3x6@0
		≤ 8[A]							8x8		3x6@0, 4x12@4
		≤ 10[A]						6x8	8x10		3x6@0
		≤ 12[A]					6x8		8x12		3x6@0, 4x12@4
B	5 to 10	≤ 6	5	4x6	4x6	4x6	6x6	6x6	6x8	5	3x12 @3, 4x12@5
		≤ 8				6x6			8x8		3x8@2, 4x8@4
		≤ 10						6x8	8x10		4x8@3
	10 to 15	≤ 6	5	6x6	6x6	6x6	6x8	6x8	8x8	5	3x6@0, 4x10@2
		≤ 8		6x8	6x8	6x8	8x8	8x8	8x10		
		≤ 10[A]				8x8			10x12		
	15 to 20	≤ 6	5	6x8	6x8	6x8	6x8	8x8	8x10	5	4x6@0
		≤ 8[A]					8x8		10x12		
		≤ 10[A]		8x8	8x8	8x8			12x12		
C	5 to 10	≤ 6	5	6x6	6x6	6x6	6x6	8x8	8x8	5	3x6@0
		≤ 8					8x8		10x10		
		≤ 10				8x8			10x12		
	10 to 15	≤ 6	5	6x8	6x8	6x8	8x8	8x8	10x10	5	4x6@0
		≤ 8		8x8	8x8	8x8			12x12		
	15 to 20	≤ 6	5	8x8	8x8	8x8	8x10	8x10	10x12	5	4x6@0

Refer to OSHA (2020) Appendix C, Tables C-2.1 through C-2.3 for more information. Notes:

[A] A licensed professional engineer must approve the design in accordance with CFR Part 1926 Subpart P Excavations Paragraph 926.652(c) for combinations of depth, soil type, and spacing not listed.

[B] Member sizing considers effective horizontal stress calculated as follows where H = depth of trench: Soil Type A: σ'_h = (25×H)+72 psf; Soil Type B: σ'_h = (45×H)+72 psf; and Soil Type C: σ'_h = (80×H)+72 psf. An assumed 2 ft surcharge is accounted for by the added 72 psf.

[C] Timber is Douglas fir or equivalent with a bending strength ≥ 1,500 psi.

[D] Manufactured members of equivalent strength may be substituted for wood.

2-3.3.5 Steel Shoring.

Steel sheeting and bracing can be used in lieu of hydraulic or timber shoring. Structural members should be designed to safely withstand water and lateral earth pressures. Steel sheeting with timber wales and struts have also been used.

2-4 DEEP EXCAVATION SYSTEMS.

The discussion of deep excavation support systems includes consideration of the factors that influence wall design and selection, design against basal heave, prediction of the movement of walls and the adjacent soil and structures, and construction. Further information can be found in FHWA (2008) and Clough and O'Rourke (1990). Detailed discussion of earth pressures is included in Chapter 4.

2-4.1 Types of Wall and Support Systems.

Deep excavation support systems are sometimes required to facilitate the construction of structures below ground. Design of these support systems must consider how much they will move during construction and how this movement will impact surrounding structures and the project to be built within the excavation. Movements of deep excavation walls are a function of many variables including:

- Soil type, strength, compressibility, permeability, and earth pressures;
- Groundwater level and changes in the groundwater level during construction;
- Depth and shape of excavation;
- Type and stiffness of wall;
- Type and stiffness of support system;
- Method of construction of the wall;
- Adjacent building and surcharge loads; and
- Length of time the deep excavation support system is in place.

Experience with deep excavations indicates three major types of movement during construction of braced and tied-back deep excavation walls (Clough and O'Rourke 1990). The first stage of movement occurs when the wall is unsupported or in the cantilever condition as shown in Figure 2-4(a). In this first stage, the largest movements occur near the top of the wall. As the excavation moves downward, the upper part of the wall is supported, reducing further movement. However, additional lateral and vertical movement can occur as the resistance of the support system is mobilized. Movement can also occur before the additional supports are installed, and basal movement can occur as shown in Figure 2-4(b). Clough and O'Rourke described this movement as *deep inward movement*. The cumulative movement is shown in Figure 2-4(c).

Variation occurs in the magnitude of movement because of differences in wall stiffness, depth of excavation without support installation, and soil conditions. Clough and

O'Rourke note that in sands and stiff to hard clays, cantilever movement typically dominates, and settlement behind the wall has a triangular distribution. In soft to medium clays, deep inward movement dominates, and settlement behind the wall takes on a trapezoidal distribution.

The major types of deep excavation wall systems include sheet piling, combined sheet piling with H-piles or pipe piles (See Figure 2-5), soldier piles (H-piles) and lagging, concrete diaphragms, secant and tangent pile walls, and deep soil mixing. The factors involved in the selection of a wall type are summarized in Table 2-5.

Support systems, shown in Figure 2-6, may be internal to the excavation, such as rakers, cross lot struts, or braces. External support systems include prestressed tieback anchors and soil nails. Berms can be added to any support system to help reinforce the toe of the wall. Berms used for temporary support must consider the movement required to achieve passive resistance. A berm constructed from stiff or dense soil is more effective compared to a loose berm because passive pressure is developed with less movement. A low factor of safety against basal heave may allow the berm to move with the soil and provide minimal passive resistance. Table 2-6 summarizes project conditions that influence the selection of a support system.

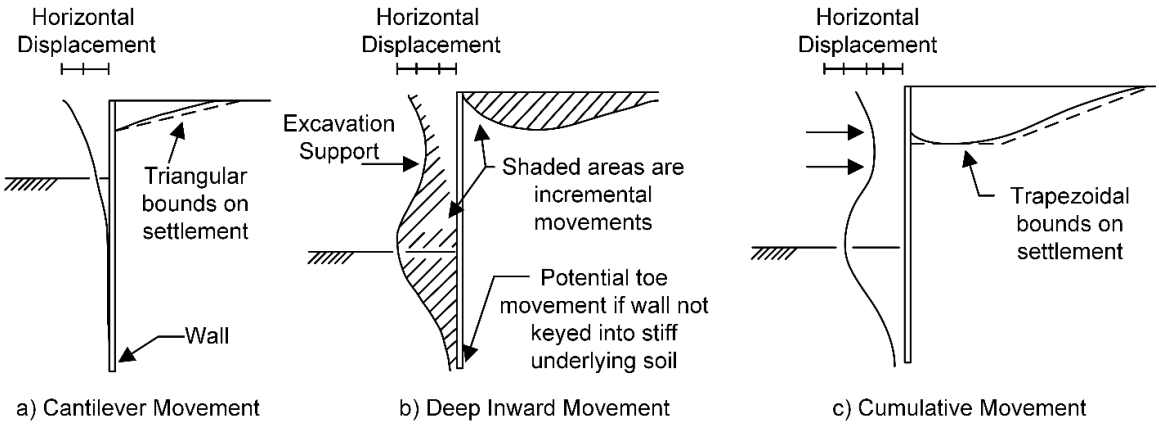

Figure 2-4 Typical Profiles of Movement for Braced and Tieback Anchor Walls (after Clough and O'Rourke 1990)

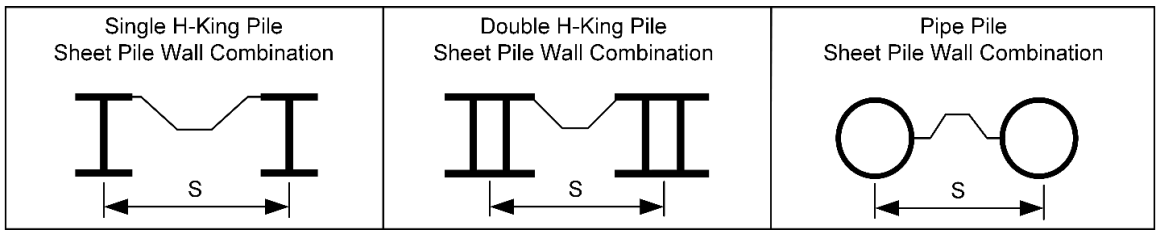

Figure 2-5 Examples of Combined Sheet Piling Cross Sections (after DeepEX Combined Sheet Pile Walls Software 2021)

Table 2-5 Types of Walls and Factors Involved with Selection

Wall Type	Relative Stiffness and Cost	Factors Involved with Selection
Steel Sheet Piling	Flexible Low Cost	• Simple, rapid construction. • Essentially impervious but leakage may occur if interlocks separate. • Materials are easily handled and can be reused. • Easy to modify length by welding. • Interlocks may separate during hard driving. • Use of vibratory hammers may cause settlement. • Every fourth or fifth sheet may be driven deeper to achieve improved bearing and passive resistance. • Basal heave factor of safety, F_{BH} , greater than 2 required in soft to medium clay.
Soldier Pile (H-pile) and Lagging	Flexible Low Cost	• Simple, rapid construction. • Permits drainage of groundwater. • Piles can be driven, or preaugered and backfilled with lean concrete. • Lean concrete compressive strength of 300 psi is usually adequate. • Lagging is usually wood although precast concrete is used for permanent installations. • Backfilling behind lagging helps transfer soil load to H-piles and prevents loss of soil.

Combined Sheet Piling	Inter-mediate Flexibility and Cost	• Types of Combined Sheet Piling (See Figure 2-5) include:
		  ○ Single king pile (H-pile) with sheet piling,
		  ○ Double king pile (H-pile) with sheet piling, and
		  ○ Pipe pile with sheet piling.
		• Essentially impervious but leakage may occur if interlocks separate.
		• King piles can be driven or drilled deeper than sheet piling to achieve bearing or greater passive resistance.
		• Use of vibratory hammers may cause settlement.
		• Complicated construction techniques required.
		• Can reduce potential for basal heave.

Secant Pile	Stiff Inter-mediate Cost	• Surface guide required to properly align piles. • Drilled piles constructed with about 3 inches of overlap. • Essentially impervious, but leakage may occur at overlap of piles if out of alignment. • Piles may be constructed from lean concrete with compressive strength of about 300 psi or structural concrete if foundation bearing unit. • Secondary, unreinforced piles constructed first. • Primary, reinforced piles constructed second. • Vertical tolerances may be difficult to achieve for deep piles • Lean concrete can be shaped to provide anchor bearing with H-pile reinforcement. • Requires significant area for equipment. • Can reduce potential for basal heave.
Tangent Pile		• Piles constructed adjacent to each other without overlap. • Groundwater leakage likely between piles. • See Secant Piles for other factors.
Deep Soil Mix	Stiff Inter-mediate Cost	• Consist of overlapped soil cement columns. • Essentially impervious. • Soil-cement compressive strength of 100 to 150 psi is usually adequate. *In situ* strengths usually less than laboratory strengths of soil-grout mixture. • Reinforcing (H-piles or cages) installed in alternating columns before slurry sets. • Soil cement can be shaved off in excavation if needed to provide anchor or brace bearing with H-pile reinforement. • Not compatible in soils with cobbles and boulders. • Requires significant area for equipment. • Reduces potential for basal heave.
Concrete Diaphragm	Very Stiff High Cost	• Impervious - use when part of permanent structure and when dewatering of adjacent soils must be avoided. • Constructed in panels with reinforcing cages. • Requires significant area for equipment. • Reduces potential for basal heave.

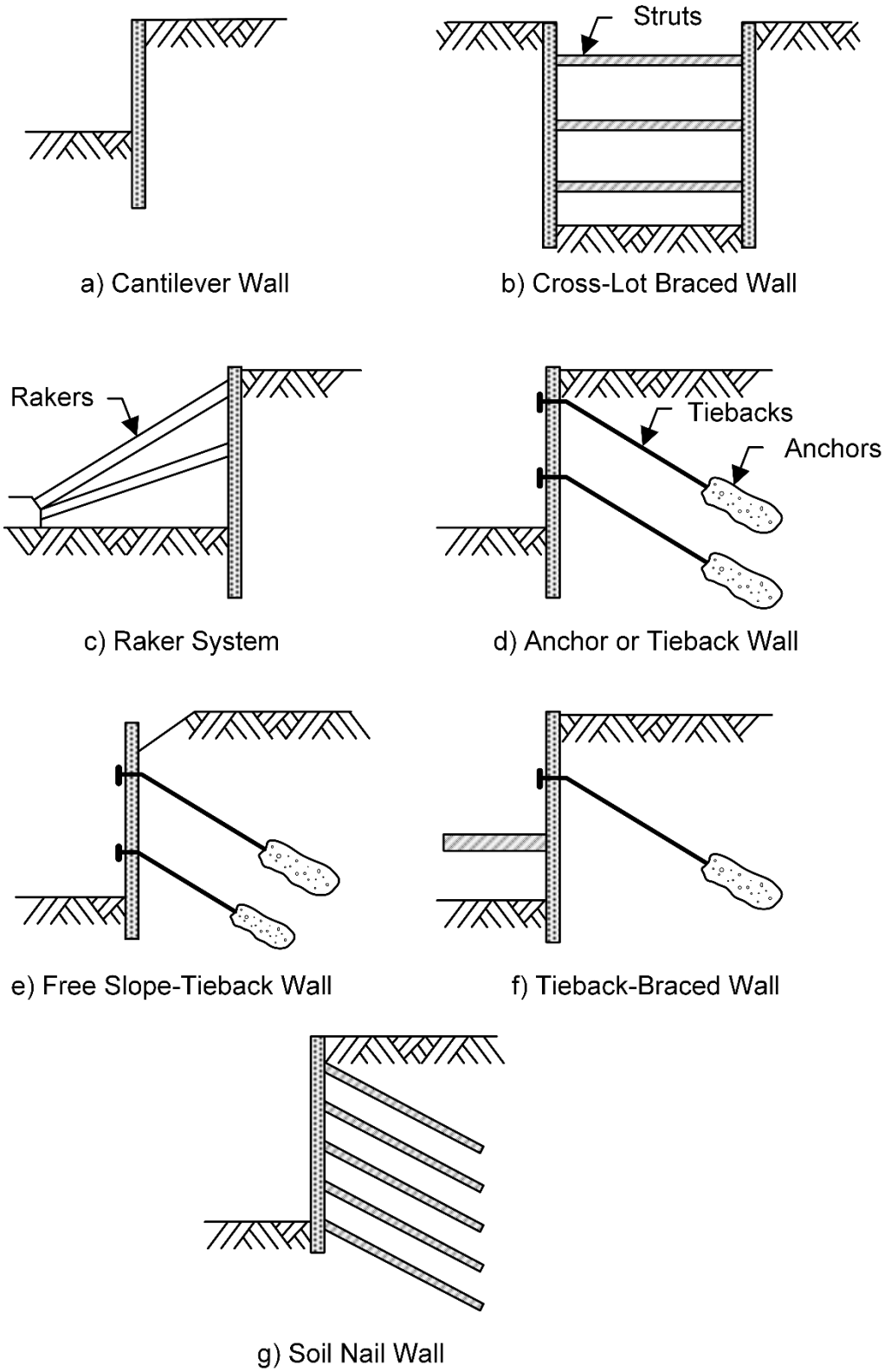

Figure 2-6 Examples of Support Systems (after USACE 1983b and FHWA 2015)

Table 2-6 Factors Influencing the Selection of Support Systems

Requirement	Lends Itself to Use of:	Comments
Low Cost	• Soil slopes combine with soldier pile (H-pile) and lagging or sheet pile wall. • Rakers. • Soil nails.	• Tieback anchors may be required to eliminate internal interference with construction. • Tieback anchors costlier than rakers. • Soil nails are not prestressed.
Avoid Dewatering	• Concrete diaphragm walls are impervious. • Sheet piling, combined sheet piling, secant, and soil mixing walls are essentially impervious.	• Soldier pile and lagging walls are pervious.
Minimize movement	• High prestress on tieback anchors, struts, or rakers.	• Analyze for basal heave.
Wide Excavation ≥ 65 ft	• Tieback anchors or rakers.	• Tieback anchors preferred but costlier than rakers.
Narrow Excavation < 65 ft	• Cross lot bracing.	• Tieback anchors may be required for better interior access.

2-4.2 Site Considerations for Deep Excavations.

2-4.2.1 Influence of Soil Type.

The type of soil supported by a deep excavation will influence the selection of an appropriate type of wall and support system. Table 2-7 provides a guide for this selection process based on soil type.

The soil type will also control the earth pressures and forces on deep excavation systems, which are discussed in detail in Chapter 4. Earth pressures depend on wall movement relative to the soil. When little to no movement occurs, the earth pressure condition is referred to as at-rest. The stress state in the soil approaches an active condition at locations where the wall moves away from the soil. This occurs behind the wall system above the base of the excavation. The stress state in the soil approaches a passive condition at locations where the wall moves toward the soil. This occurs on an embedded portion of the wall system below the base of the excavation. Different amounts of wall movement must occur to fully mobilize active and passive pressures. The movement required to mobilize active pressure is much lower than that required for passive pressure. Restricting wall movement in the passive case greatly reduces the mobilized passive earth pressure, but this is necessary in most design cases due to movement limitations.

Actual earth pressures depend on wall deformation, and this in turn depends on several factors including stiffness of wall and support system, stability of the base of the excavation, and depth of excavation. These factors are discussed in more detail in Sections 2-4.3 and 2-4.4.

Table 2-7 Influence of Soil Conditions on Selection of Deep Excavation Wall and Support Systems

Soil Type	Wall Stiffness Critical to Design	Appropriate Wall and Support Type								Comments
		Sheet Pile	Soldier Pile and Lagging	Combined Sheet Pile	Secant & Tangent Pile	Deep Soil Mix	Concrete Diaphragm	Internal Support	External Support	
Deep Soft to Medium Clays	✓	✓	✓	✓	✓	✓	✓	✓		• High wall stiffness (concrete diaphragm) preferred to reduce movements and basal heave. • Tieback anchors may not be suitable due to low strength of clay. • Soil nails not suitable due to lack of prestressing.
Stiff to Hard Clays and Sands		✓	✓	✓	✓	✓	✓	✓	✓	• Soil nails may not be suitable in sands. • Increased soil stiffness reduces lateral movements. • Higher at-rest earth pressure coefficient, K_0, has potential to increase earth pressure at excavation and cause increased lateral movements.
Dense Sands, Gravels, and Clayey Sands			✓		✓	✓	✓	✓	✓	• Sheet piling and combined sheet piling difficult to drive and interlocks may separate. • Soil nails may not be suitable in sands. • Increased soil stiffness reduces lateral movements.
Soils with Boulders/ Residual Floaters			✓		✓		✓	✓	✓	• Chisels or hydromills may be needed to excavate for concrete diaphragm wall. • Soldier (H-pile) and lagging, secant and tangent piles but may require rock coring. • Vertical alignment of piles may be difficult

2-4.2.2 Influence of Groundwater.

Groundwater conditions must be evaluated during the selection and design of a deep excavation. Some walls are impervious and prevent seepage through the wall. Where water is retained, water pressures on the wall may be greater than earth pressure. Excess pore pressures at the base of an excavation can result in heave, loss of passive resistance, seepage, and internal erosion. Particle erosion can also occur between open pile interlocks, lagging, and gaps in tangent pile walls.

In some cases, the soil adjacent to and below an excavation can be dewatered to improve stability and reduce wall loads. Some walls are not watertight and will allow water to seep into the excavation. The adjacent water level will drop provided the water is removed from the excavation. Dewatering will tend to cause settlement that may be

detrimental to adjacent infrastructure. Water levels adjacent to excavations should be monitored before and during construction to confirm design assumptions. The selected wall type must be compatible with the observed groundwater conditions.

2-4.3 Wall and Excavation Stability.

The deep excavation wall and supports must be designed to carry the forces from the earth and water pressures. Chapter 4 provides detail on the methods used to determine these forces so that the structural design of the wall can be completed. Those designs should also include the effects of thermal expansion and contraction on internal bracing, as well as the effects of frost penetration on tiebacks and struts. In addition, wall settlement, global stability, and basal heave must be considered.

2-4.3.1 Wall Settlement.

Earth pressure forces and inclined support system forces have vertical components that can cause settlement of deep excavation wall systems. Wall settlement can cause destressing of tiebacks and stressing of internal bracing systems. Wall settlement must be considered and controlled, because wall design methods typically assume no vertical movement or settlement of the wall.

With the exception of sheet piling or combined sheet piling, the wall system should be driven, drilled, or excavated to a suitable bearing layer to avoid excessive wall settlement. For sheet piling or combined sheet piling, settlement can be reduced by driving or drilling sufficient sheet piles (e.g., every 5th pile) to a suitable bearing stratum. If a bearing stratum is not present, estimates of wall movement should be made using the methods of Chapter 6, and efforts should be made to reduce the vertical component of the support system forces.

2-4.3.2 Global Stability.

Deep excavation design should consider the possibility of deep seated stability below the wall and behind any ground anchors. The stability analyses should consider surface loads from surcharges or adjacent buildings. If there are any berms or slopes in the system, these must also be considered. The stability analyses should be performed using the methods described in Chapter 7 of DM 7.1.

Excavations in rock below the wall may require rock bolting at the toe if bedding or adversely oriented joints dip into excavation or the rock surface slopes into excavation.

2-4.3.3 Basal Instability or Heave.

Basal heave is the tendency of the bottom of an excavation to move upward because of the weight of the soil adjacent to the excavation. Basal heave in deep excavations is

usually only an issue where the width of excavation (B) is greater than depth (H). It is primarily a concern for soft to medium clays that extend to significant depth.

A method for calculating basal instability of braced excavations in coarse-grained soils is provided in Figure 2-7(a). Basal instability is less common in coarse-grained soils than clays.

For clays, the method used to calculate the factor of safety against basal heave (F_{BH}) depends on the relative wall flexibility. Flexible walls (e.g., sheet piling) will deform with the soil, and the portion of the wall that penetrates below the base of the excavation is ignored. Stiff walls (e.g., concrete diaphragm) prevent the soil from deflecting toward the base of the excavation. The soil must flow beneath the wall and up towards the base of the excavation for heave to occur. Thus, for stiff walls, the wall penetration below the base is considered. A factor of safety of at least 1.5 should be used against basal heave failure as discussed by Mana and Clough (1981). The normalized wall stiffness, K_{wall}, as defined by Mana and Clough (1981) can be found as:

$$K_{wall} = \frac{EI}{\gamma_t h^4} \tag{2-2}$$

where:
E = Young's modulus of wall,
I = second moment of the area of the wall section ($I = t^3 / 12$ for wall thickness t),
γ_t = total unit weight of the retained soil, and
h = vertical spacing of the support system braces or anchors.

The normalized wall stiffness is greatly influenced by the spacing of the support system, because this variable is raised to the fourth power. A secondary consideration is the movement required to mobilize the support system. Ground anchors and internal bracing can be prestressed to reduce mobilization movement. In contrast, soil nails require movement to develop support forces.

The calculation of basal heave for clays is shown in Figure 2-7(b) and (c). For flexible walls, the driving force is the weight of the soil extending a distance, B_1, beyond the excavation plus the surcharge loading. The resisting force is developed along the sides of the block of soil defined by B_1 and in the soil below the excavation.[10]

[10] This definition of F_{BH} differs from that proposed by Terzaghi (1943) and used by Mana and Clough (1981). The two definitions give similar results for F_{BH} < 1.5. Terzaghi (1943) subtracted the strength above the base from the net driving force, which can lead to unreasonably high factors of safety for narrow excavations.

For very stiff walls, the shear resistance in the clay along the inside of the wall may be included. An adhesion factor (α) between the wall and clay is multiplied by the undrained strength of the clay in this layer. Very stiff walls are much more effective at reducing lateral movement and basal heave than flexible walls, producing the higher factors of safety against basal heave.

(a) Cut in Cohesionless Soil

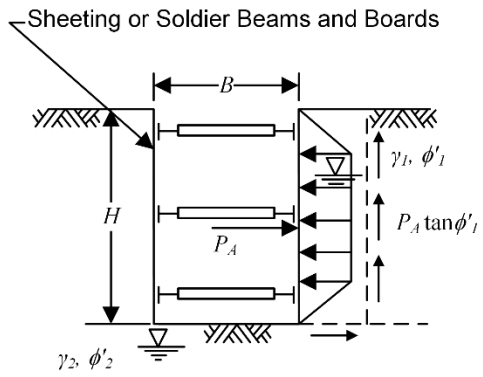

Stability is independent of H and B, but varies with γ, ϕ' and seepage condition.

Factor of Safety: $F_{BH} = 2N_\gamma \left(\frac{\gamma_2}{\gamma_1}\right) K_A \tan\phi'_1$

N_γ = bearing capacity factor for soil below excavation (Chap. 5)

K_A = active earth pressure coefficient (see Chap. 4)

Groundwater conditions:

If groundwater is at a depth of (B) or more below base of cut:
γ_1 and γ_2 are moist unit weights

If groundwater is static at base of cut:
γ_1 = moist unit weight, γ_2 = submerged unit weight.

If seepage is moving upward to base of cut:
γ_2 = saturated unit weight – uplift pressure / unit length

(b) Cut in Clay – Flexible Wall

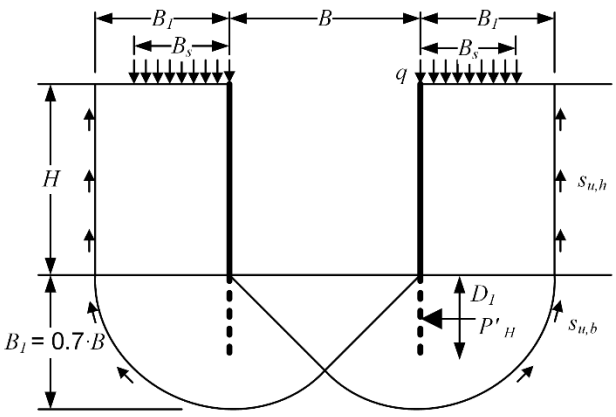

Ignore sheeting below base of cut.

Factor of Safety: $F_{BH} = \frac{5.7 s_{u,b} B_1 + s_{u,h} H}{\gamma_t H \cdot B_1 + q \cdot B_s}$

$s_{u,b}$ = average s_u below the base of the excavation

$s_{u,h}$ = average s_u above the base of the excavation

q = Surface surcharge

If the base is unstable, a force, P'_H, acts on the buried length:

$D_1 > 0.47B$: $P'_H = 0.7\left(H\left(\gamma_t \cdot B - 1.4 \cdot s_u\right) - \pi \cdot s_u \cdot B\right)$

$D_1 < 0.47B$: $P'_H = 1.5 D_1 \left(H\left(\gamma_t - \frac{1.4}{B} \cdot s_u\right) - \pi \cdot s_u\right)$

(c) Cut in Clay – Very Stiff Wall

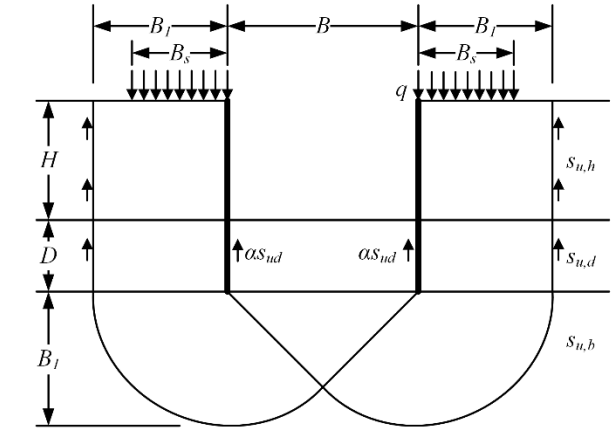

Include adhesion on inside of the wall.

Factor of Safety: $F_{BH} = \frac{5.7 s_{u,b} B_1 + s_{u,h} H + (1+\alpha) s_{u,d} D}{\gamma_t H \cdot B_1 + q \cdot B_s}$

$s_{u,h}$ = average s_u above the base of the excavation

$s_{u,d}$ = average s_u along embedded section of the wall

$s_{u,b}$ = average s_u below the base of the excavation

α = adhesion between the clay and the wall

Figure 2-7 Methods for Calculating Factor of Safety Against Basal Instability or Heave (after Wong and Goh 2002)

Flexible walls, such as sheet piling, tend to have normalized wall stiffness in the range of K_{wall} = 10 to 50. Stiffer concrete diaphragm walls often have normalized wall stiffness greater than 100. Soldier piles and wood lagging walls are stiffer than sheet piling walls but are likely to deflect similar to a sheet piling wall. Secant piles, tangent piles, deep soil mix and combined sheet piling walls are not as stiff as concrete diaphragm walls below the base of an excavation. These walls may deflect more than a concrete diaphragm wall but the soil must move around them and up to the excavation. The actual factor of safety against basal heave for walls of intermediate stiffness may lie between the values calculated using the equations found in Figure 2-7(b) and (c), and judgment is required to select the appropriate method to calculate F_{BH}.

2-4.4 Ground Movements Adjacent to Deep Excavations.

Prediction of wall movement is an important part of the design of deep excavation systems. This section presents procedures to estimate (1) the anticipated maximum horizontal or lateral movements and the maximum settlement immediately behind the excavation support wall, (2) the profile of movement with distance from the wall, and (3) methods to predict damage to structures adjacent to excavations.

Observations of settlement behind sheet piling walls and soldier pile (H-pile) and lagging walls in the mid-20th century suggested the trends shown in Figure 2-8 (Peck 1969). The settlement (δ_V) and distance from the wall (d) are both normalized by the depth of excavation (H). The movements shown in Figure 2-8 were state of the practice in the late 1960s and can occur today with poor construction workmanship or by lowering the groundwater during construction, which may increase the load on the wall. Peck separated typical movements into three zones of interest based on soil type and basal stability:[11]

- Zone I – Sand and hard clays (limited soft clay): $F_{BH} > 2$,
- Zone II – Soft clays below excavation: $1 < F_{BH} < 2$, and
- Zone III – Soft clays to significant depth below excavation: $F_{BH} \approx 1$.

[11] Peck (1969) used the stability number. Factor of safety is used here for consistency.

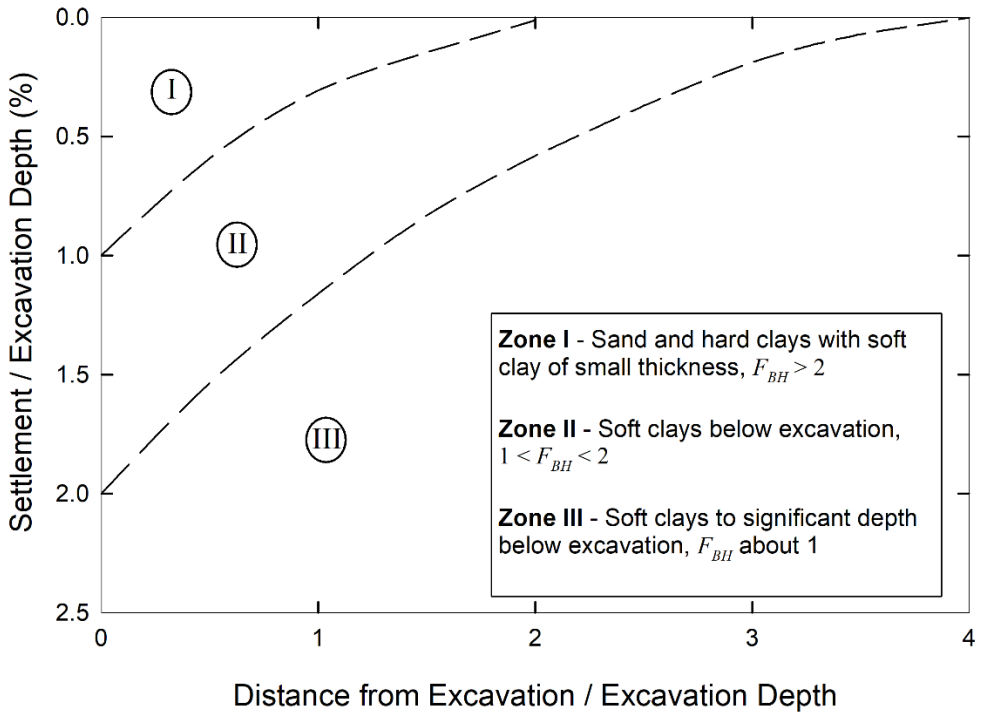

Figure 2-8 Zones of Soil Settlement Behind Excavation Walls (after Peck 1969)

Control of movements has improved in deep excavations. New methods of support and new walls have been introduced since Peck developed Figure 2-8. Clough and O'Rourke (1990) updated Peck's approach and attempted to screen projects to remove movements that were not primarily related to the excavation support processes (O'Rourke 1981, Mana and Clough 1981, Clough et al. 1989). This section presents the subject in the following categories:

- Maximum movements of excavation support walls in stiff clays, sands and residual[12] soils;
- Profiles of movements beyond excavation support walls in stiff to hard clays and sands; and
- Maximum movements of excavation support walls and profiles of movements beyond excavation support walls in soft to medium clays.

Typical values of settlement and horizontal movement at the wall are summarized in Table 2-8. The values are presented as a percentage of the excavation depth (H). The lateral extent of movement is also summarized as a ratio compared to H. More detailed discussion of each soil category is provided in the following sections.

[12] In this context, the term residual soils refer to Piedmont and Blue Ridge Physiographic Province soils derived from weathering of underlying rock which typically are silty to clayey sand and sandy silt.

Table 2-8 Typical Settlement and Horizontal Movement Relative to Height (after Clough and O'Rourke 1990)

Soil Category	Calculated Factor of Safety Against Basal Heave	Settlement, δ_{Vm} / H	Horizontal, δ_{Hm} / H		Lateral Extent of Movement, d / H
			Stiff K_{wall} > 200	Flexible K_{wall} < 50	
Stiff to Hard Clays	High	0.15% average 0.3% max.	0.2%		3
Sand	High	0.15% average 0.3% max.	0.2%		3
Soft to Medium Clay	About 1	2%	1%	> 3%	1.5 to 2
	About 1.5		0.3% to 0.5%	0.8% to 1.7%	
	Greater than 2	1%	0.2%	0.8%	

2-4.4.1 Movements in Stiff Clays, Sands, and Residual Soils.

Based on case histories of walls in these soils, the maximum horizontal (lateral) movement (δ_{Hm}) and the maximum settlement (δ_{Vm}) vary approximately linearly with excavation depth as shown in Figure 2-9 (Clough and O'Rourke 1990). This suggests that the retained soil masses behave approximately as an elastic material. The maximum settlement is presented in Figure 2-9(a) and indicates that the average δ_{Vm} was about $0.15\% \cdot H$ and ranged up to about $0.5\% \cdot H$. Figure 2-9(b) presents the maximum lateral movement and indicates that the average δ_{Hm} was about $0.2\% \cdot H$ and also ranged up to about $0.5\% \cdot H$.

The points with very large movements likely relate to factors other than the support system, such as lowered groundwater or poor construction practices. Some of these points would plot in Zones II and III of Figure 2-8 at $d/H = 0$. The ground movements below the $0.5\% H$ lines can be attributed to movement of the support system and not extraneous factors.

Two important concepts are illustrated in Figure 2-9. The horizontal movement data is more scattered than the settlement data. In addition, there are no significant differences in the data for different types of wall construction (e.g., sheet piling, soldier pile (H-pile) and lagging, diaphragm, drilled piers, deep soil mix).

Clough and O'Rourke (1990) used finite element analyses to confirm the the $\delta_{Hm} = 0.2\% \cdot H$ trend line indicated by the data in Figure 2-9(b). The effects of soil modulus (E_s), normalized wall stiffness (K_{wall}), support spacing (h), and coefficient of lateral earth pressure (K_0) on wall movements were also studied. K_0 accounts for the higher horizonal earth pressures found in overconsolidated soils. The finite element analyses, which considered the elastic nature of these relatively stiff soils, found that:

- E_s and K_0 generally had a greater impact on wall δ_{Hm} than wall stiffness,
- Higher E_s and lower K_0, yielded lower δ_{Hm}, and

- Lower E_s and higher K_0, yielded higher δ_{Hm}.

In these cases, the soil was stiff enough to minimize the influence of wall stiffness. Figure 2-9 can be used to estimate δ_{Hm} and δ_{Vm} of new excavation support systems in stiff clays, sands, and residual soils.

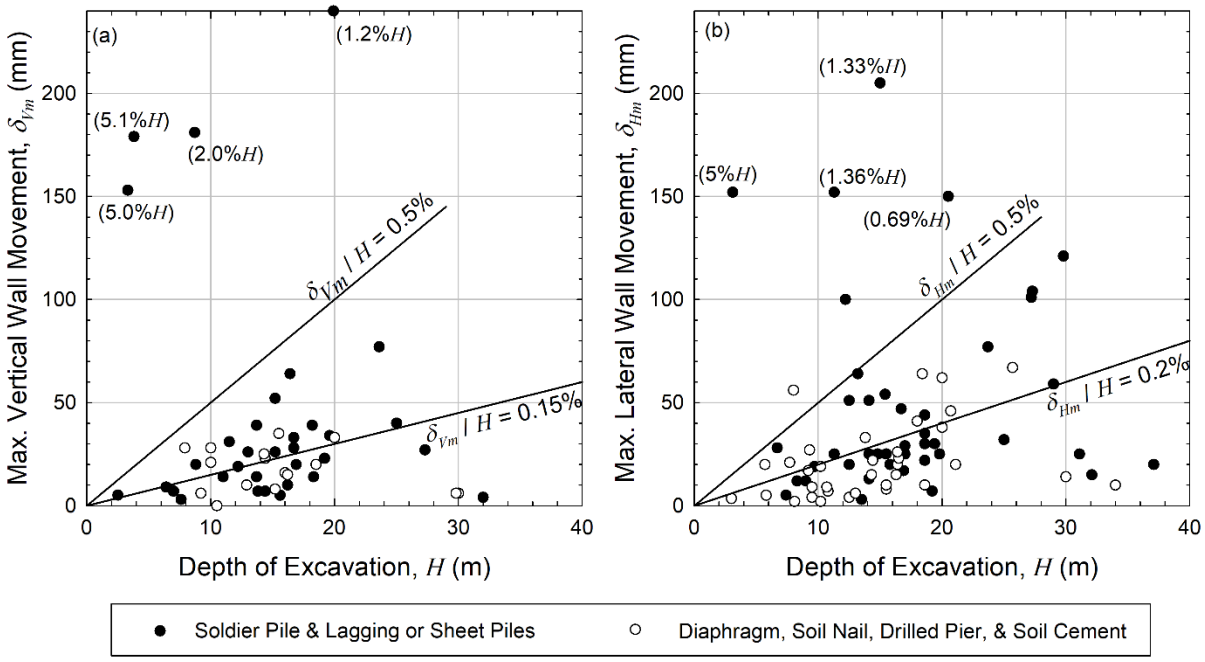

Figure 2-9 Observed Maximum Movements for Stiff Clays, Residual Soils and Sands: (a) Vertical and (b) Horizontal (after Clough and O'Rourke 1990)

Clough and O'Rourke (1990) separated the case history data for stiff and hard clay soils from the sands and residual soils and analyzed the profiles for settlement and horizontal movement of these soils. The next two sections present the profiles of settlement and horizontal movement extending various distances behind the excavation support walls for stiff to hard clays and for sands.

2-4.4.1.1 Profiles of Movement in Stiff to Hard Clays

Figure 2-10 summarizes case histories for stiff to hard clays. The wall and bracing systems include soldier piles and lagging with tieback anchors, concrete diaphragm walls with tieback anchors, concrete diaphragm walls with cross lot struts, drilled shaft walls and tieback anchors, and walls with with internal raker braces. For more information on specific data points, see Clough and O'Rourke (1990).

Settlements: Figure 2-10 indicates that δ_{Vm} ranged from 0% to $0.3\% \cdot H$ and averaged about $0.15\% \cdot H$. This average maximum settlement is consistent with Figure 2-9(a). The

settlement decreased from the wall to negligible values at $d/H = 3.0$ where d is the distance from the face of the excavation support wall. A few of the cases experienced heave due to stress relief experienced by the stiff to very hard clays surrounding the deep excavations. The dimensionless settlement profile (Figure 2-10(c)) may be used to estimate the vertical movement pattern adjacent to an excavation in stiff to hard clay.

Horizontal Movements: Two categories of horizontal movement are shown in Figure 2-10(b). Support system with high horizontal stiffness reduce movement, resulting in a δ_{Hm} of about $0.3\% \cdot H$. An average value of $\delta_{Hm} = 0.2\% \cdot H$ is appropriate for most estimates, which similar to the typical trend shown in Figure 2-9(b). Support systems with low horizontal stiffness allow increased movement, and the maximum lateral movement is up to $0.8\% \cdot H$. Similar to the settlement profile, a triangular horizontal movement profile can be used to estimate the horizontal movement with δ_H decreasing to a negligible value at $d/H = 3.0$.

Very stiff to hard clays and shales may have high *in situ* K_0 in the range of 2 to 3. The value of K_0 can be estimated from the overconsolidation ratio and friction angle (see Equation 4-2). Excavations in these materials may induce lateral stress relief and large lateral movement. Anchors in these materials may move with the soil if not installed beyond the zone of movement, which can conservatively be assumed to extend up from the base of the excavation at an angle of 45° from horizontal.

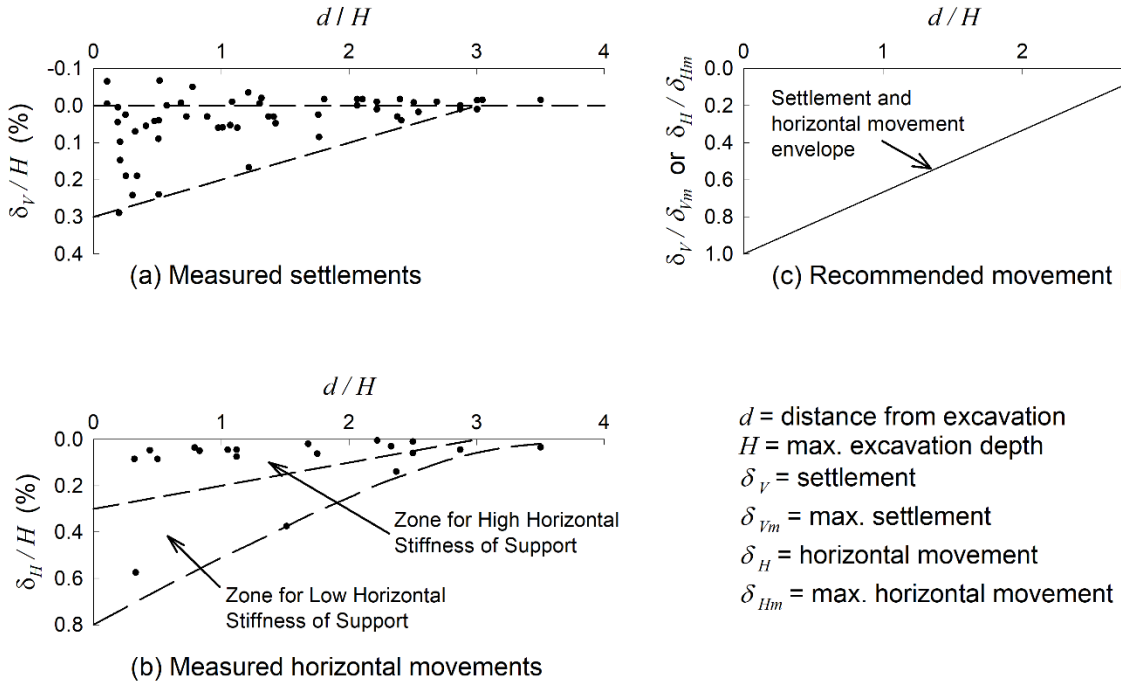

Figure 2-10 Movements Adjacent to Excavations in Stiff to Very Stiff Clays – (a) Measured Settlement, (b) Measured Horizontal Movement, and (c) Recommended Movement Profile (after Clough and O'Rourke 1990)

2-4.4.1.2 Profiles of Movement in Sands

Figure 2-11 summarizes case histories for subsurface profiles consisting of sand or sand and gravel with limited clay layers (Clough and O'Rourke 1990). Groundwater was either lowered, or recharged to reduce settlement, but did not vary during construction. The wall systems include both flexible and stiff walls, including soldier piles and lagging with cross lot struts or tieback anchors, sheet piling with tieback anchors, and concrete diaphragm walls with cross lot struts.

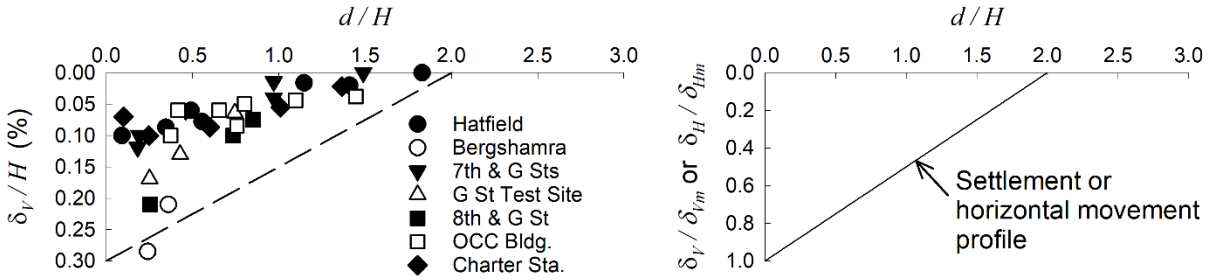

(a) Measured settlements (b) Recommended profile

Notation:
δ_V = Settlement, δ_{Vm} = Max. Settlement, δ_H = Horizontal Movement, δ_{Hm} = Max. Horiz. Movement
H = Max. Excavation Depth, d = Distance from excavation

Figure 2-11 Movements Adjacent to Excavations in Sand – (a) Measured Settlement and (b) Recommended Dimensionless Movement Profiles (after Clough and O'Rourke 1990)

Settlements: The maximum settlement tends to be less than $0.3\% \cdot H$ in sand and decreases to a negligible value at $d/H = 2.0$. In the majority of cases, the range of δ_{Vm} was about $0.1\% \cdot H$ to $0.2\% \cdot H$ and averaged about $0.15\% H$, which may be used to estimate the maximum settlement. The dimensionless settlement profile in Figure 2-11(b) may be used to estimate the vertical movement pattern adjacent to an excavation in sand.

Horizontal Movements: Clough and O'Rourke (1990) do not give specific recommendations for horizontal movement in excavations made in sand. For sand, the average value of $\delta_{Hm} = 0.2\% \cdot H$ can be used from Figure 2-9(b). Horizontal movements are expected to decrease to negligible values at $d/H = 2.0$ with a horizontal movement profile similar to the settlement profile in Figure 2-11(b).

2-4.4.2 Movements in Soft to Medium Clays.

Figure 2-12 summarizes case histories of wall movements in soft to medium clays (Mana and Clough 1981, Clough et al. 1989, Clough and O'Rourke 1990). The types of

wall and bracing systems were sheet piling with cross lot struts, soldier piles and lagging with cross lot struts, and concrete diaphragm walls with cross lot struts. On some projects, berms and rakers were used as full or supplemental support. The Peck (1969) zones are included on Figure 2-12(a) for reference.

Settlements: The maximum settlements are limited to about $2\%{\cdot}H$ and have a trapezoidal profile behind the wall as shown in Figure 2-12(a). The trapezoidal profile extends at δ_{Vm} = $2\%{\cdot}H$ from the wall to $d/H = 0.75$ and then slopes up to δ_V = 0.0 at d/H = 1.5 where settlements decreased to negligible values. In most cases, the settlement was less than $1\%{\cdot}H$. When reasonable care is used during constuction and the factor of safety against basal heave is about 2, δ_{Vm} = $1\%{\cdot}H$ may be assumed. This is true for either flexible or stiff excavation support walls, provided large cantilever movements are limited. When excavation support walls are flexible and the factor of safety against basal heave is less than 1.5, δ_{Vm} = $2\%{\cdot}H$ is a reasonable assumption.

The settlements are normalized by δ_{Vm} in Figure 2-12(b). The settlements fall within a trapezoidal region that extends to zero at d/H of about 1.5 or can conservatively be extended to $d/H = 2$ as proposed by Clough and O'Rourke.

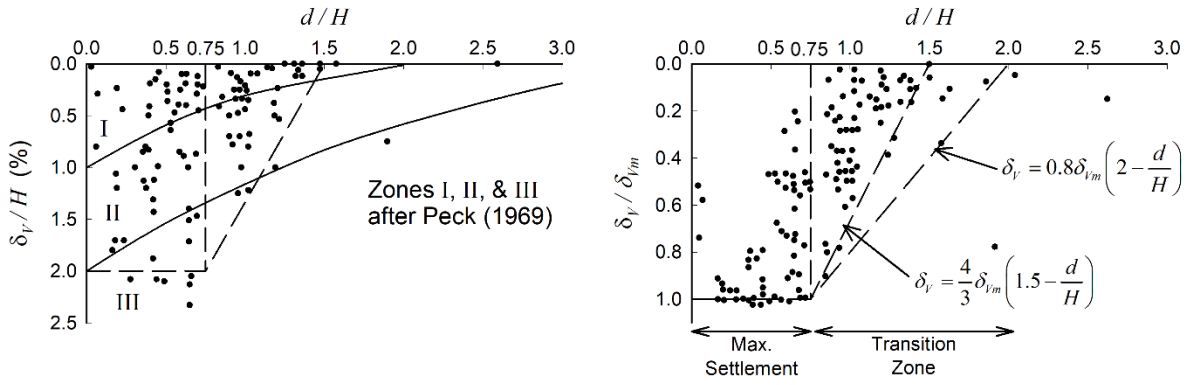

(a) Measured settlements

(b) Normalized settlements

Figure 2-12 Settlement Adjacent to Excavations in Soft to Medium Clays – (a) Measured Settlement and (b) Normalized Settlements with Recommended Settlement Profile (after Clough and O'Rourke 1990)

Horizontal Movements: The case history data of δ_{Hm} / H for soft to medium clays are plotted against normalized wall stiffness in Figure 2-13 for sheet piling and slurry concrete diaphragm walls. The overall wall stability increased as the basal factor of safety is increased as shown in Figure 2-13. For soft to medium clays, horizontal movements are highly dependent on the factor of safety against basal heave. The stiff diaphragm walls generally had a factor of safety greater than 2. The more flexible sheet

piling walls had a factor of safety generally less than 1.5 except where the subsurface conditions were favorable to a stable base.

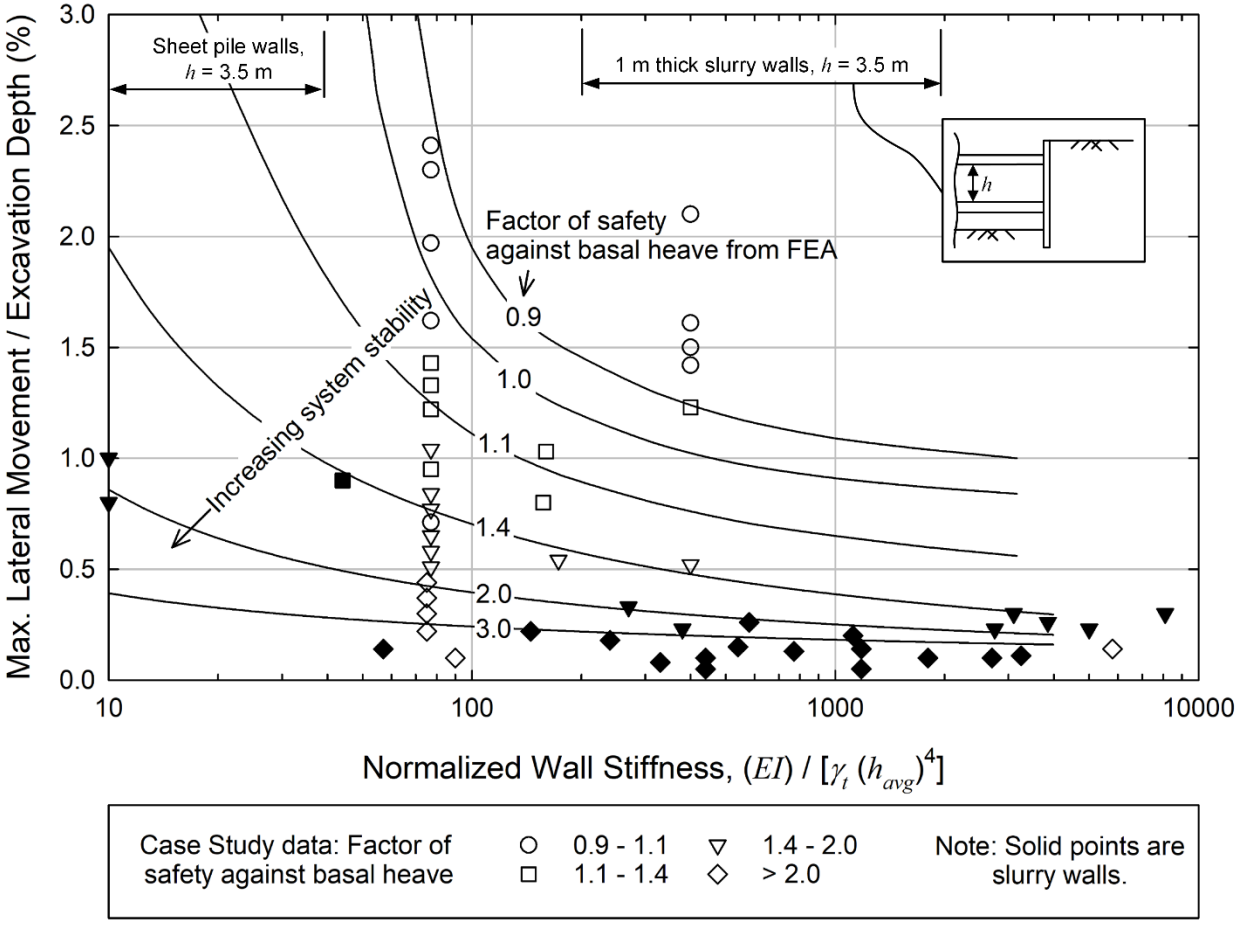

Figure 2-13 Maximum Horizontal Wall Deflection for Soft to Medium Clays (after Clough et al. 1989 and Clough and O'Rourke 1990)

Figure 2-13 also presents the results of finite element analyses by Clough and O'Rourke (1990), which match the case history data well. The finite element curves can be used to select δ_{Hm} / H based on normalized wall stiffness and factor of safety against basal heave for excavations in soft to medium clays. Note that the normalized wall stiffness is greatly influenced by spacing of the bracing or anchors (h). The range of normalized wall stiffness used in the finite element analyses are shown at the top of the Figure 2-13 where the bracing was set at h = 3.5 m or about 12 feet, which is a typical design spacing.

The profile of horizontal movements for soft clays is likely similar to that observed for settlements. Thus, a dimensionless horizontal movement profile similar to that shown in Figure 2-12 for settlement may be assumed for soft to medium clays.

2-4.4.3 Prediction of Damage to Adjacent Structures.

The movements of braced or anchored deep excavation support systems should be evaluated to determine if adjacent structures supported by shallow foundations require underpinning. The distance of existing structures from the excavation support system should be compared to the movement profiles in Figure 2-10 to Figure 2-12. Tolerance of structures to movement is discussed in Chapter 5 of DM 7.1. Other factors that influence the need for underpinning include:

- Lowering groundwater by dewatering may cause soil consolidation and settlement.
- Soldier piles and lagging, sheet piling, and tangent piles all leak to various degrees, and this will lower groundwater.
- Leaks in the excavation support system can also cause loss of fines, piping, and settlement if not properly filtered.

The predicted angular distortion, β, and the horizontal strain, ε_h, across the building can be used to assess damage potential. Angular distortion is the differential vertical movement between two points divided by distance separating the points:

$$\beta = \frac{\delta_{Vi} - \delta_{Vj}}{d_b} \tag{2-3}$$

where:
δ_{Vi}, δ_{Vj} = estimated settlements at two points, i and j, on the building and
d_b = distance separating the points (likely the width of the building).

Similary, the horizontal strain (ε_h) between two points is:

$$\varepsilon_b = \frac{\delta_{Hi} - \delta_{Hj}}{d_b} \tag{2-4}$$

where:
δ_{Hi}, δ_{Hj} = estimated settlements at two points on the building and
d_b = distance separating the points (likely the width of the building).

In most cases, β and ε_h will be measured across the whole building width. In this case, the movements would be estimated at the front and back of the building (compared to the excavation), and d_b would equal the building width. The movements may be estimated from δ_{Vm}, δ_{Hm}, and the movement profile behind the wall, which are found using the methods in Sections 2-4.4.1 and 2-4.4.2.

For stiff to hard clays and sands, the movements can be estimated as:

$$\delta_i = \delta_m \left(\frac{d_0 - d_i}{d_0} \right) \tag{2-5}$$

where:
δ_i = desired horizontal (δ_{Hi}) or vertical (δ_{Vi}) movement at the point of interest,
δ_m = maximum horizontal (δ_{Hm}) or vertical movement (δ_{Vm}) at the wall,
d_i = distance from wall to a point of interest and
d_0 = $3H$ for stiff to hard clays, and $2H$ for sand.

For soft to medium clays, movements can be estimated as:

$$\delta_i = \begin{cases} \delta_m \text{ for } 0 \le d_i \le 0.75H \\ \delta_m \left(\dfrac{1.5H - d_i}{0.75H} \right) \text{ for } 0.75H \le d_i \le 1.5H \end{cases} \quad \text{(2-6)},$$

A method to evaluate the severity of damage from excavations to adjacent structures based on β and ε_h is presented in Figure 2-14 (Clough and O'Rourke 1990). Figure 2-14 maps damage categories for masonry load-bearing wall structures to predicted values of horizontal strain and angular distortion (Boscardin and Cording 1989). The damage categories are negligible, very slight, slight, moderate to severe, and severe to very severe. This damage mapping is based on theoretical structural response to deformation, field observations of building damage, and measurement of building horizontal and vertical displacements. When $\beta \approx 0$, the boundaries for the categories are nearly horizontal and represent horizontal tensile strains that equal the critical tensile strains. When $\varepsilon_h \approx 0$, the boundaries are inclined at about 45° and represent diagonal tensile strains that equal the critical tensile strains.

The estimated ratio of horizontal to vertical movements at the edge of the excavation may be estimated from δ_{Hm} and δ_{Vm}. These ratios are expected to be uniform from the wall to a distance of $d = 0.5\ H$. Ratios of δ_{Hm} / δ_{Vm} are superimposed for stiff soil types in Figure 2-14(a) and for soft to medium clays in Figure 2-14(b) (Clough and O'Rourke 1990, O'Rourke 1981). The ratios are based on the data analyzed in Figure 2-10 to Figure 2-13. In sands and stiff to hard clays, damage typically is bounded by the moderate to severe level, and construction controls can diminish the severity of movement. In soft to medium clays, damage typically is bounded by severe to very severe level, and insufficiently stiff bracing can result in additional movement.

If estimated movements are too large as indicated by Figure 2-14 for the existing structure to tolerate, underpinning will be required. Underpinning methods are described in FHWA (1978). Since underpinning may be required for adjacent buildings when considering deep excavation support systems, underpinning methods are discussed in Table 2-9. Example problems considering the topic of deep excavation support systems are presented in Figure 2-15 for stiff to hard clay and in Figure 2-16 for soft to medium clay.

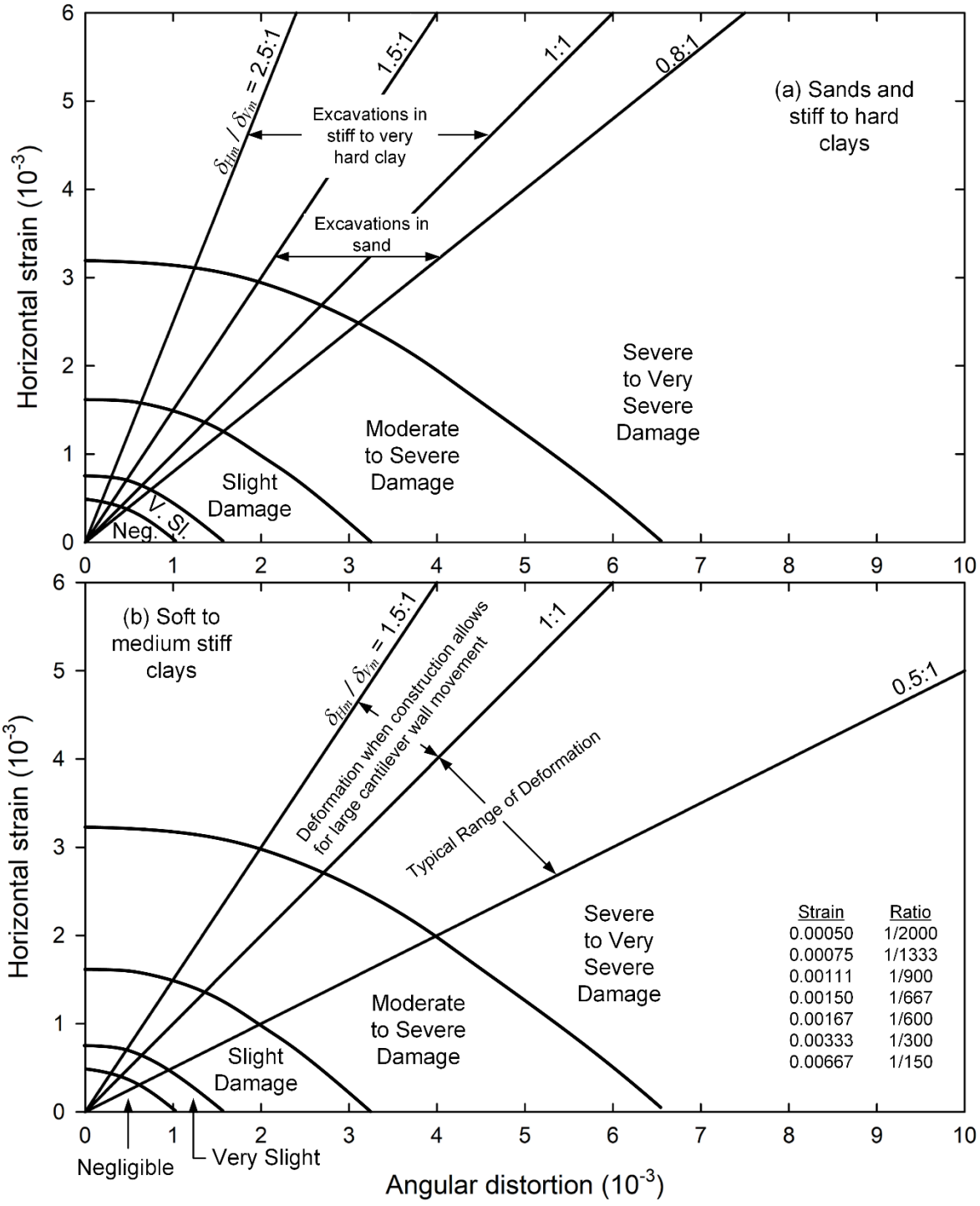

Figure 2-14 Range of Deformations Typical of Excavations in Various Soils Relative to Building Damage Potential (after Clough and O'Rourke 1990)

Table 2-9 Some Common Methods of Underpinning

Type of Underpinning	Comments
Micropiles	• Micropiles are often the method of choice. • Small diameter (3- to 10-inch) piles installed through footings. • Connection to footing is made by high strength grout.
Piles (H-piles, open-ended pipe piles)	• Piles are jacked into position in sections within a shored pit using footing as reaction. • When in final position, wedges are installed, jacks removed, and head of pile encased in concrete. • Piles may be driven on both sides of footing with beams placed across piles and a plate added under footing. • Space between footing and plate is then dry packed. • A footing bracket can be welded to piles if access is available only on one side of footing. • Piles can also be placed in an auger hole and moved into position under footing. • Piles are load tested to greater than anticipated load.
Helical Piers	• Elements are screwed into position. • A bracket is placed under footing and connected to pier.
Underpinning Pits	• Pits are an old and effective procedure, may be expensive if depth is too great. • Concrete is placed in pit, and a dry pack sand and cement mixture is used to assure contact with base of footing.

PROBLEM STATEMENT

- Tolerable angular distortion is 0.005 for existing 3-story building
- Excavation support will be H-piles with wood lagging and prestressed anchors with stiffness = 70
- Factor of safety against basal heave is found to be greater than 2
- Good construction practices are anticipated
- Groundwater is deeper than the excavation

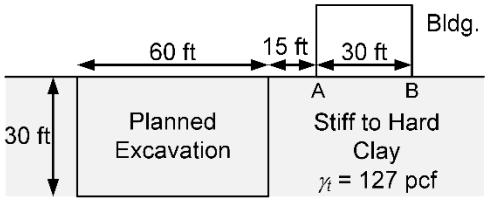

(1) Estimate horizontal and vertical movements at front and back of building.
(2) Determine if underpinning is required.

Horizontal and Vertical Movements

- From Fig. 2-10: δ_{Hm} = 0.2%H and δ_{Vm} = 0.15%H

$$\delta_{Hm} = 0.002(30\ ft) = 0.06\ ft = 0.72\ in$$
$$\delta_{Vm} = 0.0015(30\ ft) = 0.045\ ft = 0.54\ in$$

- Settlement and horizontal movement at front (A): (d/H = 15/30 = 0.5)
  From Fig. 2-10: $\delta_V / \delta_{Vm} = \delta_H / \delta_{Hm}$ = 0.83

$$\delta_{HA} = 0.83 \cdot \delta_{Hm} = 0.83(0.72\ in) = 0.60\ in$$
$$\delta_{HB} = 0.50 \cdot \delta_{Hm} = 0.50(0.72\ in) = 0.36\ in$$

- Settlement and horizontal movement at back (B): (d/H = 45/30 = 1.5)
  From Fig. 2-10: $\delta_V / \delta_{Vm} = \delta_H / \delta_{Hm}$ = 0.50

$$\delta_{VA} = 0.83 \cdot \delta_{Vm} = 0.83(0.54\ in) = 0.45\ in$$
$$\delta_{VB} = 0.50 \cdot \delta_{Vm} = 0.50(0.54\ in) = 0.27\ in$$

Is Underpinning Required?

- Estimate Angular Distortion, β

$$\beta_b = \frac{\delta_{VA} - \delta_{VB}}{d_b} = \frac{0.45 - 0.27\ in}{(30\ ft)(12\ in/ft)} = 0.0005$$

- Estimate Horizontal Strain, ε_h

$$\varepsilon_h = \frac{\delta_{HA} - \delta_{HB}}{d_b} = \frac{0.60 - 0.36\ in}{360\ in} = 0.0007$$

Conclusion: Plotting ε_B and β on Fig. 2-14 indicates that the damage potential is **Very Slight**. The ratio of horizontal to vertical deflection is 1.33, which places the deflection within the stiff to hard clay zone on Fig. 2-14(a). Underpinning is not required because of the predicted damage, and the angular distortion is less than the tolerable level.

Figure 2-15 Estimation of Movements and Evaluation of Underpinning Requirements Adjacent to an Excavation Supported by a Deep Excavation Support System - Stiff to Hard Clay

Problem Statement

- Tolerable angular distortion is 0.005 for existing 3-story building
- Support will be H-piles with wood lagging and prestressed anchors with wall stiffness of 70
- Good construction practices are anticipated
- Groundwater is deeper than the excavation

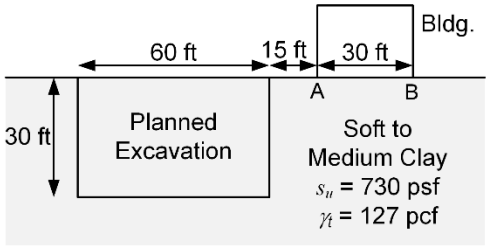

1) Estimate factor of safety against basal heave
2) Estimate horizontal and vertical movements at front and back of building.
3) Determine if underpinning is required.

Factor of Safety Against Basal Heave

- No surcharge and adhesion of 0.6
  - Use approach in Figure 2-7
  - B_1 = 0.7B = 42 ft, d = 15 ft
  - Use F = 1.2

$$F = \frac{5.7(730\ psf)(42\ ft)+(730\ psf)(30\ ft)}{(127\ pcf)(30\ ft)(42\ ft)} = \frac{196700}{160000} = 1.2$$

Horizontal and Vertical Movements

- From Fig. 2-12, use δ_{Vm} = 2%H for Zone II (1 < F < 2)

$$\delta_{Vm} = 0.02(30\ ft) = 0.6\ ft$$

- From Fig. 2-13, use δ_{Hm} = 1.1%H for F = 1.2 and wall stiffness of 70.

$$\delta_{Hm} = 0.011(30\ ft) = 0.33\ ft$$

- Vertical and horizontal movement at front (A) (d/H = 15/30 = 0.5): From Fig. 2-12: $\delta_V/\delta_{Vm} = \delta_H/\delta_{Hm}$ = 1.0

$$\delta_{VA} = 1.0\delta_{Vm} = 1.0(0.6\ ft) = 0.6\ ft$$
$$\delta_{VB} = 0.0\delta_{Vm} = 0.0(0.6\ ft) = 0\ ft$$

- Vertical and horizontal movement at back (B) (d/H = 45/30 = 1.5): From Fig. 2-12: $\delta_V/\delta_{Vm} = \delta_H/\delta_{Hm}$ = 0.0

$$\delta_{HA} = 1.0\delta_{Hm} = 1.0(0.33\ ft) = 0.33\ ft$$
$$\delta_{HB} = 0.0\delta_{Hm} = 0.0(0.33\ ft) = 0\ ft$$

Is Underpinning Required?

- Estimate Angular Distortion, β

$$\beta_b = \frac{\delta_{VA}-\delta_{VB}}{d_b} = \frac{0.6-0.0\ ft}{30\ ft} = 0.02 \quad > \text{limit of } 0.005$$

- Estimate Horizontal Strain, ε_h

$$\varepsilon_h = \frac{\delta_{HA}-\delta_{HB}}{d_b} = \frac{0.22\ ft}{30\ ft} = 0.0073$$

Conclusion: If ε_h and β are plotted on Fig. 2-14, the damage potential is **Severe to Very Severe**. Underpinning is required because of the predicted damage and because the angular distortion exceeds the tolerable level.

Figure 2-16 Estimation of Movements and Evaluation of Underpinning Requirements Adjacent to an Excavation Supported by a Deep Excavation Support System - Soft to Medium Clay

2-4.5 Construction Considerations.

Construction procedures can have an impact on deep excavation support system movements. Table 2-10 lists many of the construction considerations for various wall and support system features. FHWA (2008) provides additional guidance.

Table 2-10 Construction Considerations for Deep Excavation Support Systems

Wall or Support System Element	Construction Considerations and Comments
Sheet Pile	• The ball end of the sheets should lead when driving to reduce interlock separation. • Hard driving can be overcome by using spud piles, preaugering, or using a different type of wall. • Interlock separation is the greatest cause of seepage and piping of soil. • Lowering the groundwater by pumping or seepage through the sheeting can cause settlement. • When sheets are removed, care must be used to not remove soil which could cause settlement. Coat sheets in bitumen in plastic clays. • Vibratory hammers can cause settlement in loose to medium sands.
Soldier Piles (H-Piles) and Lagging	• Driven piles can cause: o Noise and vibration. o Settlement behind wall - consider single acting hammers. o Alignment concerns due to obstructions - use heavy section and pile points for hard driving. o Piles should only be removed if soil remains in place. • Predrilled holes for piles: o Reduce noise and vibration. o Use percussion or rotary drill to fracture boulders and rock. o Provide for precise location of piles. o Backfill with lean concrete so that it can be shaved for tiebacks or internal bracing. • Lagging: o Most of earth pressure arches to soldier piles. o Usually placed behind front flange of soldier pile. o Over-excavation should be backfilled with soil for intimate contact. o Lagging is typically 3 inches thick, unless a very deep excavation. o Soft clay or loose sand below water table can exert stress on lagging. o Straw or geotextile is used between lagging to prevent ground loss from drainage of groundwater. o Lowering the groundwater by pumping or seepage through lagging can cause settlement. o Lagging should be removed after construction if above the water table.
Combined Sheet Pile	• Special interlocks required between sheet piles and king piles can cause problems if not properly aligned. • Vertical alignment of piles is critical. • Comments on sheet piling and soldier piles placed in predrilled holes are also applicable.
Secant and Tangent Piles	• A reinforced concrete guide wall (3 to 5 ft deep) is required for proper wall alignment and to provide stability at the top of the trench. • Concrete piles are constructed using slurry, continuous hollow stem augers, or open hole. o Concrete should have a slump of 7 to 8 inches. o For slurry and open holes, concrete is tremied to bottom of pile under positive concrete head (8 to 10 ft). o For hollow stem augers, concrete is pumped to the bottom in the auger as the auger is withdrawn. o Open holes require test piles to verify holes will remain open at desired diameter. • Reinforcing cages or H-beams installed in primary piles for reinforcement. • Alternating piles constructed to avoid damaging fresh concrete. • Secant pile wall requires unreinforced piles to be constructed with lean concrete so that alternating piles can be cut into concrete. • Vertical tolerances can be an issue when hard drilling or cobbles or boulders are present. • Tangent piles are drilled adjacent and have the potential for more leakage of groundwater. • Grouting may be required between tangent piles to prevent leaks if vertical alignment cannot be maintained.
Deep Soil Mixing	• Wall relies on use of *in situ* soil as a construction material thus cobbles, boulders, and obstructions must be removed and replaced with suitable soil. • Monitoring of equipment and operational procedures required. o Revolutions of mixing paddles per unit volume of *in situ* soil. o Grout injection rate varies with soil type encountered. • Test columns are required. • Extraneous material (water, debris, or spoil material) is not allowed to enter production columns.

Wall or Support System Element	Construction Considerations and Comments

Concrete Diaphragm	• A reinforced concrete guide wall (3 to 5 ft deep) is required for proper wall alignment and to provide stability at the top of the trench.
	• Alternating panels are constructed to avoid damaging concrete.
	• Excavation is typically made in three steps (a.k.a., bites): left, right, and middle.
	• Trench stability during excavation is maintained by a bentonite-water slurry and arching to the end points of each panel.
	• The slurry should be:
	  o Kept above the groundwater level and perhaps part way up the guide wall.
	  o Checked for design properties (new and returned slurry).
	• Hard soils or boulders can be broken by chisels or percussion tools.
	• A hydromill, or similar device, should be used to remove rock.
	• Potential problem soils are:
	  o Clean sands and gravels – consider higher bentonite concentration and fine sand to plug pore space.
	  o Very soft clays (s_u < 500 psf) – squeezing and surface settlement can occur. Test panels required to evaluate.
	  o Stiff fissured clays – overbreak and collapse can occur. Test panels required to evaluate.
	• Stop ends should be placed to define the ends of the panel.
	• The trench must be checked for verticality and required dimensions before lowering the reinforcing cage.
	• Concrete should:
	  o Have a slump of 7 to 8 inches.
	  o Placed by tremie to the bottom of the trench with a positive head of concrete (8 to 10 ft).

Internal Bracing	• Prestress to about 50% of the anticipated load to avoid overstressing if load increases. • Temperature changes can cause strain, and stresses in bracing should be monitored. • Movement of deep excavation walls should be monitored throughout construction. • Excavation below support level should not be allowed. • Slow construction can allow clays to creep.
Tieback Anchors	• Stiff to hard clays and medium to dense granular soils and rock are preferred. • Soft clays may not suitable, and loose coarse-grained soils may be a concern. • Inclined anchors cause a vertical component of load on the wall. Significant vertical movement will cause a reduction in anchor stress and wall movement. • Each anchor should be tested to beyond its anchor load (usually 115% to 125% and then locked off at 75% to 100% of design load). • Slow construction can allow clays to creep.

2-5 ROCK EXCAVATIONS.

2-5.1 Preliminary Considerations.

Rock excavation planning and design must be based on detailed field investigations including: 1) review of available data for the site, 2) geological mapping of any exposed rock, and 3) test borings sufficient to define the stratigraphy. To the extent possible, infrastructure constructed in rock should be oriented favorably with the geological structure. For example, tunnels should be aligned with axis perpendicular to the strike of faults or major fracture zones. Downslope dip of discontinuities into open excavations should be avoided.

In general, factors that must be considered in planning, designing, and constructing a rock excavation are as follows:

- Presence and orientation of faults, folds, fractures, and previous sliding surfaces;
- *In situ* stresses;
- Groundwater conditions;
- Nature of material filling joints;
- Depth and slope of cut surfaces;
- Direction of potential sliding surfaces;
- Dynamic loading;
- Design life of cut as compared to weathering or deterioration rate of rock face;
- Rippability and/or the need for blasting; and
- Effect of excavation and/or blasting on adjacent structures.

The influence of most of these factors on excavations in rock is similar to that of excavations in soil.

More information on the description, classification, and testing of rock can be found in Chapters 1 to 3 of DM 7.1. In addition, DM 7.1 contains pertinent discussion of stress distributions (Chapter 4), seepage and drainage (Chapter 6), and rock slope stability (Chapter 7).

2-5.2 Assessment of Rock Excavation Methods.

Rock excavation can be accomplished by excavators, rippers, hoe rams, and blasting. The following paragraphs discuss how to evaluate which of these methods are most appropriate.

2-5.2.1 Rock Excavatability Based on Rock Test Sections.

The field observation of a rock test section is helpful during the design phase of a project. Various types of equipment, such as excavators, rippers, and hoe rams, can be tested to evaluate which type of equipment would be most effective during construction. The size and shape of the area to be excavated is a significant factor in estimating the ability to rip rock. This exploration technique will provide valuable data on the depth that can be ripped or excavated with each type of equipment and will also define where and at what depth blasting will be required.

2-5.2.2 Rock Excavatability Based on Correlations with GSI.

The excavatability of rock by various methods can be related to Geologic Strength Index (GSI) (Hoek et al. 1992, Marinos and Hoek 2000). The GSI is assigned based on the rock mass structure and the surface condition as shown by the numbered contours in Figure 2-17. Tsiambaos and Saroglou (2010) split sedimentary and metamorphic rock masses ranging from blocky to disintegrated into two groups by point load strength index ($I_{s(50)}$). The region corresponding to the rock's structure and surface conditions

can be determined. The shaded areas indicate different levels of excavatability. Digging means the rock can be excavated with power excavators. Ripping indicates excavation with D8 and D9 type tractors. Hammer (and blasting) means that breaking with a hoe or hydraulic ram will likely be required. Blasting indicates the need for blasting.

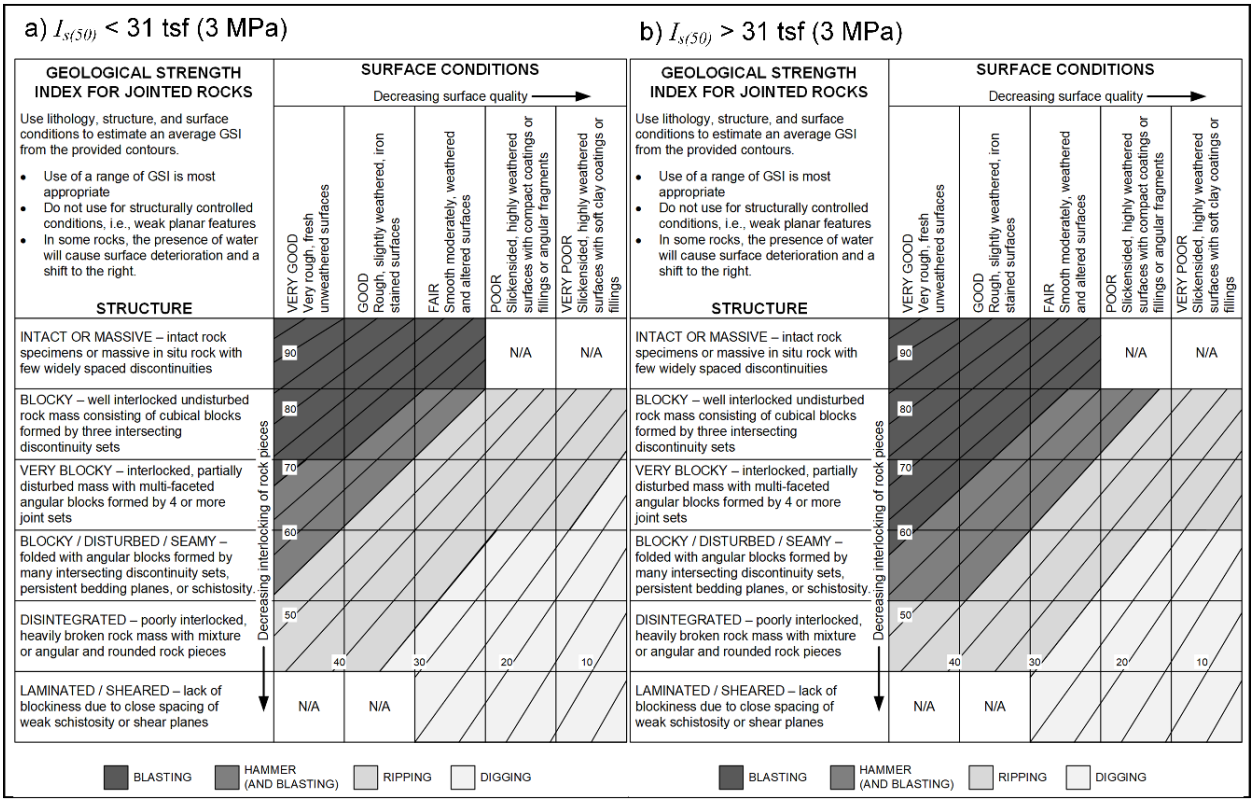

Figure 2-17 Excavatability of Rock Masses: a) $I_{s(50)}$ < 31 tsf (3 MPa) and b) $I_{s(50)}$ > 31 tsf (3 MPa) (after Tsiambaos and Saroglou 2010)

2-5.2.3 Rippability Based on Correlations with Compression Wave Velocity.

Ripping of rock materials is governed by many factors: 1) rock mass lithology including strata, fracture condition, and orientation; 2) rock weathering; 3) rock strength; and 4) rock ripper equipment size and condition. Rock rippability can be assessed from field observation and correlations with the GSI as discussed above or by using correlations with seismic wave velocity.

The most common rock rippability correlation is based on compression wave velocity, or P-wave velocity, obtained from seismic refraction studies. The velocity is based on the fracture condition of the rock. Figure 2-18 illustrates example charts for the performance of rippers mounted on medium (Caterpillar D-8 tractor), heavy (D-9 tractor), and very heavy-duty (D-11 tractor) tractors related to seismic compression

wave velocity of various rock materials (Caterpillar 2000). These types of charts are available from equipment manufacturers.

2-5.3 Blasting.

Once it has been determined that blasting is required, a pre-blasting survey should be performed. As a minimum, this should include: 1) examination of the site, 2) detailed examination and a photographic record of adjacent structures, and 3) establishment of horizontal and vertical survey control points.

2-5.3.1 Blasting Design.

Design of blasting for a project can be estimated by considering the maximum particle velocity. The *peak* (or *maximum*) *particle velocity* (PPV) is the longitudinal velocity of a particle in the direction of the wave that is generated by blasting. The major concern in blasting is the influence of the blasting on adjacent structures. PPV is an accepted criterion for evaluating the potential for structural damage induced by blasting vibration. The critical level of the particle velocity depends on the rock properties, the nature of the overburden, the frequency characteristics of the structure, and the capability of the structure to withstand dynamic stresses.

The effects of a blast on a structure can be evaluated by the scaled distance (USBM 1971, Oriard 1987). The *scaled distance* (SD) is the true distance from the charge to the structure corrected by the weight of the charge and can be calculated as:

$$SD = \frac{D}{W^{\beta}} \tag{2-7}$$

where:
D = true distance from charge to structure (ft),
W = weight of charge (lb), and
β = 0.33 for near field structures (i.e., <20 ft from charge) or 0.5 further from charge.

The scaled distance is not correct dimensionally and requires use of the indicated units.

Using SD, the PPV can be estimated using:

$$PPV = K \cdot SD^{-1.6} \tag{2-8}$$

where:
K = confinement factor (lower bound = 20, upper bound = 242, average = 150).

The values of K are empirical and require the use of the indicated units. K may be calculated from blast data as follows:

$$K = \frac{PPV}{SD^{-1.6}} \tag{2-9}$$

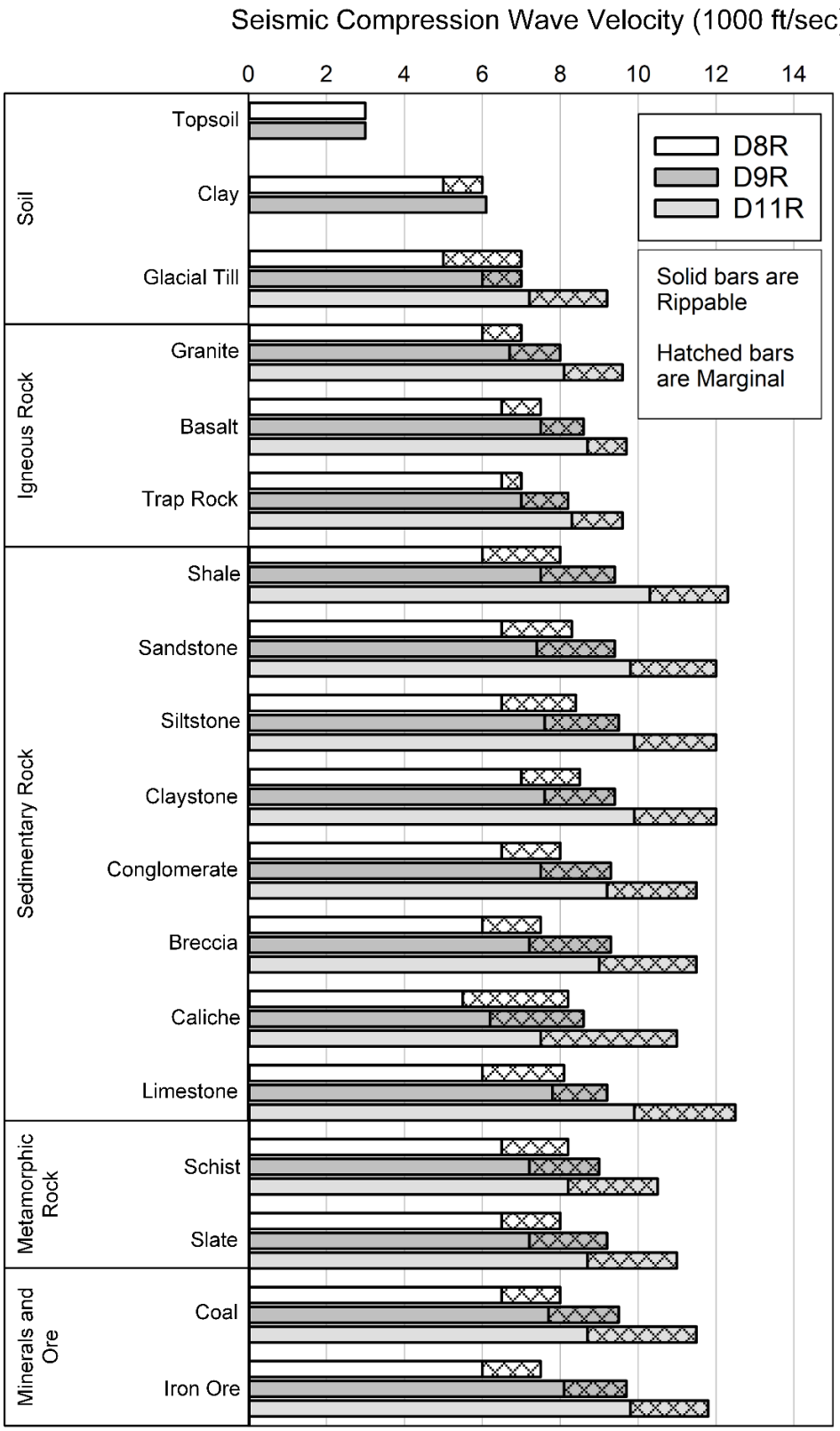

Figure 2-18 Ripper Performance: a) Medium Tractor, b) Heavy-Duty Tractor, and c) Very Heavy Tractors (after Caterpillar 2000)

Figure 2-19 can then be used to estimate potential damage to structures based on the estimated PPV. Human response to vibrations is given in Figure 2-20.

2-5.3.2 Monitoring Blasting.

During construction, vibration monitoring stations should be established, and monitoring should be performed. Detailed records should be kept of charge weight, location of blast point, distance from blast point to existing structures, delays, and response as indicated by vibration monitoring. For safety, small charges should be used initially to establish a site-specific relationship between charge weight, distance, and peak particle velocity along with the associated structural response.

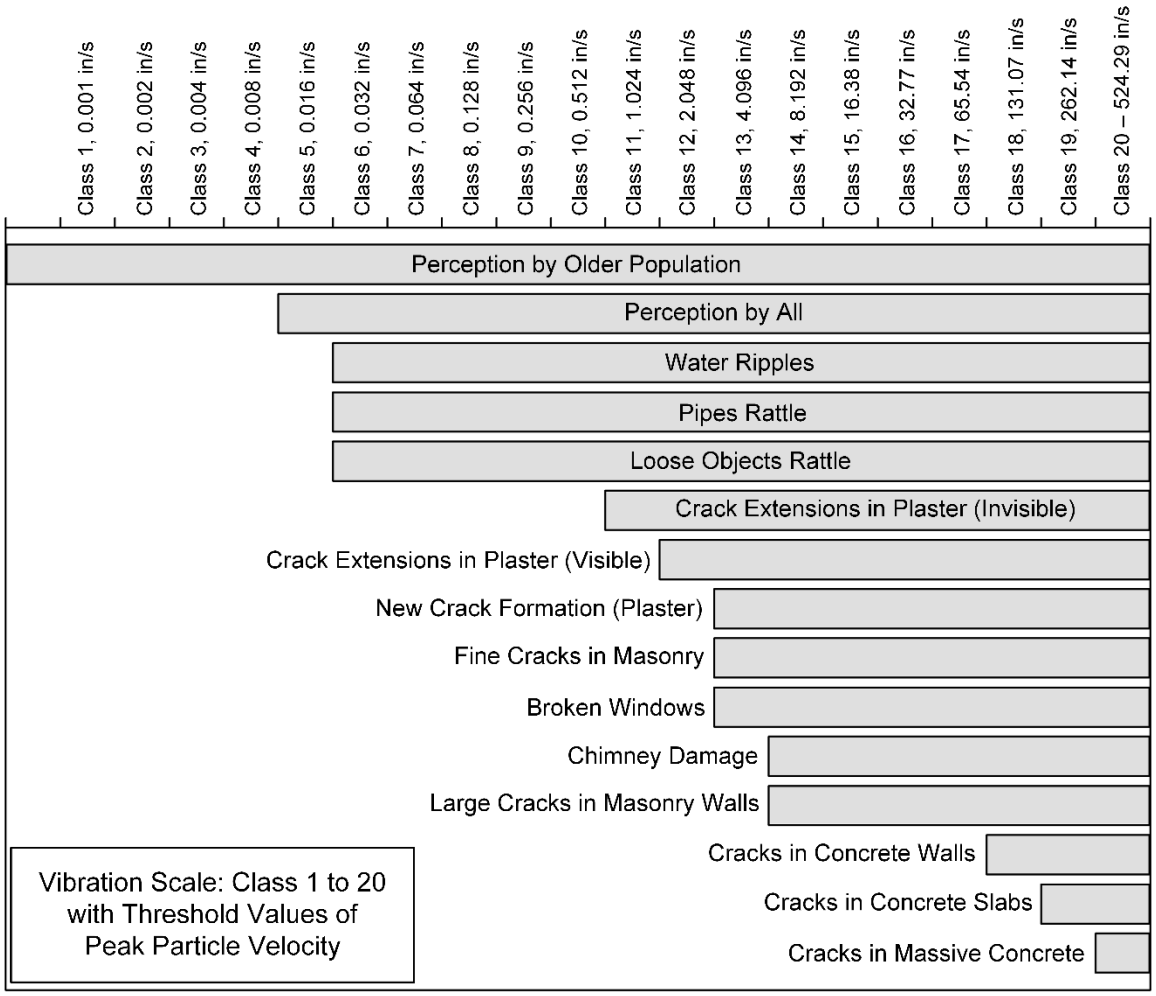

Figure 2-19 Blast Effects Scale (after Konya and Walter 2006)

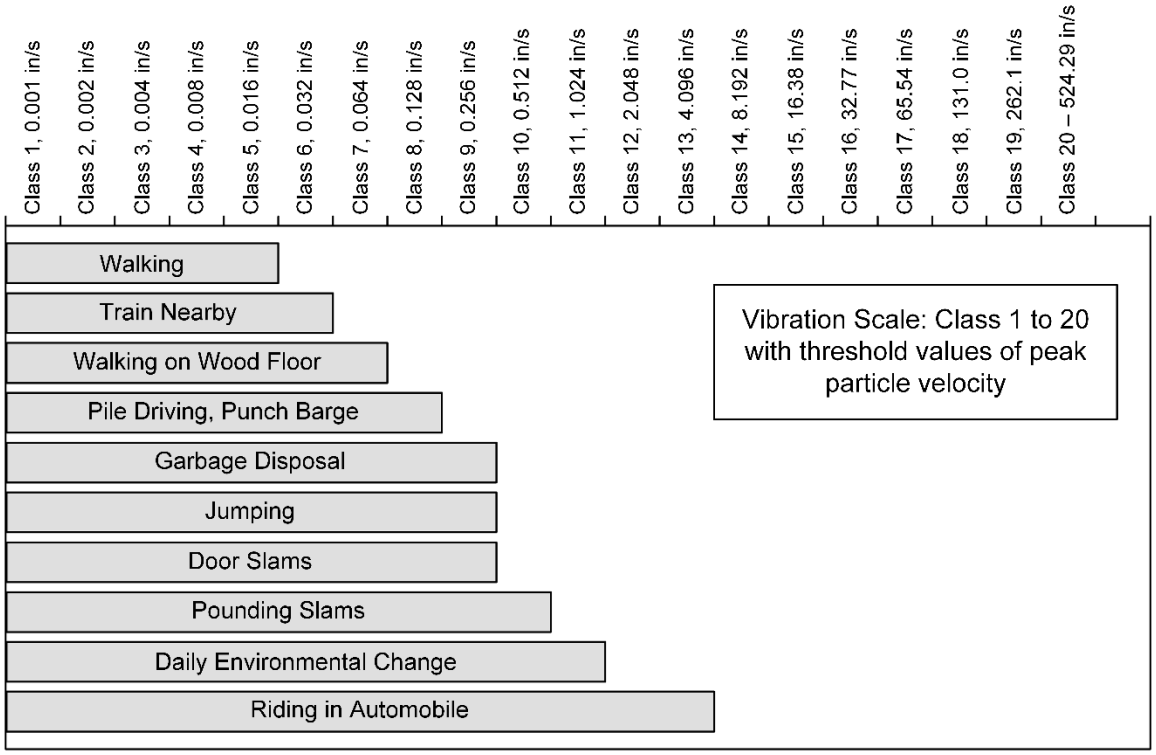

Figure 2-20 Human Response to Vibrations (after Konya and Walter 2006)

2-6 GROUNDWATER CONTROL.

2-6.1 Preliminary Considerations.

Excavations below the groundwater table require groundwater control. This typically consists of controlling seepage into the excavation and controlling excess pore water pressures below the bottom of the excavation. Sumps, wellpoints, and deep wells are most commonly used to lower groundwater in excavations. Figure 2-21 illustrates applicable limits of these dewatering methods for different soil gradations.

Slurry cutoff walls (soil-bentonite or cement-soil-bentonite), concrete diaphragm walls, secant pile walls, and deep soil mix walls are the most effective walls for reducing seepage into an excavation. Concrete diaphragm walls may become part of the final structure. Sheet piling is often considered impervious but seepage occurs through the interlocks. If interlocks split due to hard driving, the rate of seepage can increase greatly. Special waterstops are available.

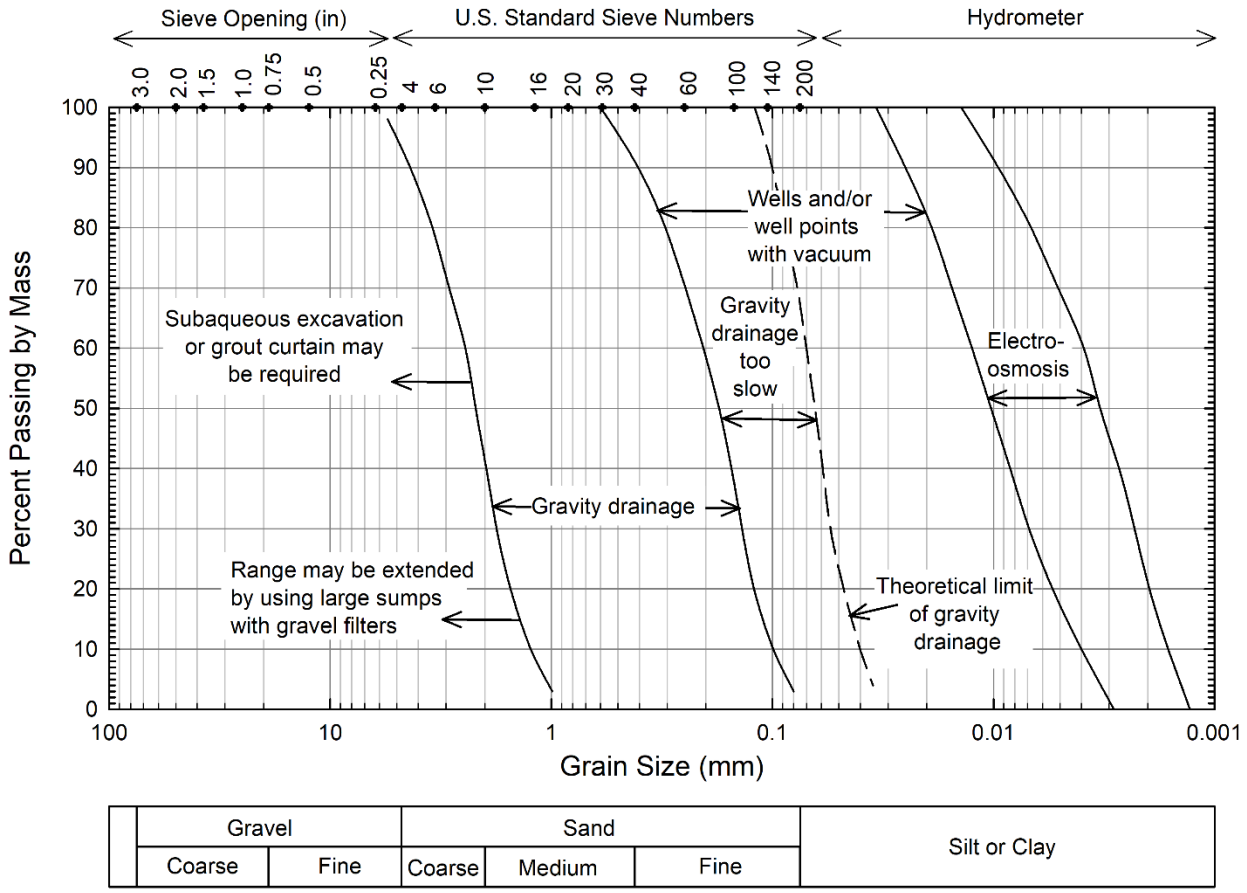

Figure 2-21 Limits of Dewatering Methods Applicable to different Soils (after Keller Moretrench American Corporation 1954)

2-6.2 Permeability of Sheet Piling.

The permeability of sheet pile walls, which occurs only through the interlocks, is usually expressed in terms of the inverse specific resistance, ρ, explained in European Standard EN 12063 (1999) which is defined as follows:

$$\rho = \frac{q\gamma_w}{\Delta p} \tag{2-10}$$

where:
q = discharge or flow rate per unit height along the interlock,
γ_w = unit weight of water, and
Δp = differential pressure.

Seepage can be reduced by maintaining tension in the interlocks and/or by sealing the joints. Test sections have been performed on sheet piling sealed with various bitumen and swelling fillers (Sellmeijer et al. 1995). These tests indicate that ρ ranges from

about 10^{-3} cm/sec for unsealed joints to about 10^{-9} cm/sec for sealed joints without tension in the joint. Bitumen sealants are slightly less effective than swelling sealants. Tests on vinyl sheet piling indicate ρ ranging from 10^{-5} cm/sec for unsealed joints in tension to about 10^{-10} cm/sec for sealed joints.

If ρ is known or assumed, Equation 2-10 can be rearranged to calculate the flow rate per unit length of interlock. This allows the flow rate through a section of sheet piling to be calculated. An example problem for leakage through sheet piling is shown in Figure 2-22.

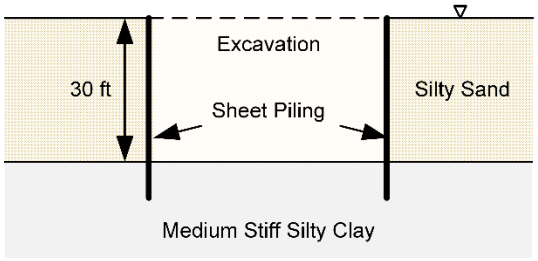

Cross-Section of Excavation

Problem Requirements

- Perimeter of Excavation = 800 ft
- Estimated Specific Resistance of Untreated Sheet Pile Joints, ρ = 1x10^{-3} cm/s = 2x10^{-3} ft/min
- Estimated Specific Resistance of Joints Treated with Bitumen sealant, ρ = 1x10^{-7} cm/s = 2x10^{-7} ft/min
- Width of Sheet Piling is 1.8 ft
- Maximum Allowable inflow is 20 gal/min

Find leakage into the excavation with and without sealant. Is the sealant required?

- Calculate the number of interlocks, N, around the perimeter of the excavation

$$N = \frac{800\,ft}{1.8\,ft\,/\,pile} = 444 \text{ piles}$$

- Average pressure difference (at midheight)

$$\Delta p = (15\,ft)(62.4\,psf) = 936 \text{ psf}$$

Solution Without Interlock Sealant

- Calculate discharge per unit height along the interlock

$$q = \frac{\rho \cdot \Delta p}{\gamma_w} = 2\times10^{-3}\,\frac{ft}{\min}\left(\frac{936\,psf}{62.4\,pcf}\right) = 0.03\,\frac{ft^3}{\min\cdot ft}$$

- Calculate the total flow into the excavation

$$Q = q \cdot H \cdot N = \left(0.03\,\frac{ft^3}{\min\cdot ft}\right)(30\,ft)(444) = 400\,\frac{ft^3}{\min} = 3000\,\frac{gal}{\min}$$

Solution with Interlock Sealant

- Calculate discharge per interlock per unit length of wall

$$q = \frac{\rho \cdot \Delta p}{\gamma_w} = 2\times10^{-7}\,\frac{ft}{\min}\left(\frac{936\,psf}{62.4\,pcf}\right) = 3\times10^{-6}\,\frac{ft^3}{\min\cdot ft}$$

- Calculate the total flow into the excavation

$$Q = q \cdot H \cdot N = \left(3\times10^{-6}\,\frac{ft^3}{\min\cdot ft}\right)(30\,ft)(444) = 0.04\,\frac{ft^3}{\min} = 0.3\,\frac{gal}{\min}$$

Conclusion: Without the sealant, the inflow is too high. Sealant is required.

Figure 2-22 Example Problem for Flow into an Excavation Through Sheet Piling

2-6.3 Methods of Controlling Groundwater.

Table 2-11 lists methods of controlling groundwater, their applicability, and limitations. The methods represent groundwater lowering techniques including sumps, wellpoints, deep wells, and jet-eductor wells. Cutoff walls include sheet piling, slurry walls, concrete diaphragm walls, secant pile walls, and mix-in-place walls.

Table 2-11 Methods of Groundwater Control

Method	Suitable Soils	Use	Comments
Sumps	Sands and gravels	Shallow localized dewatering	• Pumping from perforated drum or casing. • Geotextile should be used to prevent movement of fines.
Wellpoint Systems with Suction Pumps	Sands, silty sands, and silts	Open excavations including pipe trenches	• Easy to install. • Limited to about 18 ft lift. • Multi-stage wells at 15 ft vertical intervals required to dewater greater depth.
Deep Wells with Submersible Pumps	Sands, silty sands, and silts; fractured rock	Deep excavations	• No limitation of depth of drawdown. • Design of screen openings and filter pack required. • Can be sited clear of excavation area.
Jet-eductor Wells	Sands, silty sands, and silts	In limited space and when well point systems not possible	• No limitation of depth of drawdown. • Design complex. • Low efficiency.
Sheet Pile Cutoff Walls	All soils except dense sand and gravel, glacial till, and boulder soils	Unrestricted use except for hard driving conditions; can be permanent	• Hard driving and boulders can cause interlock failure. • Can be recovered. • Hot rolled sheets have lower permeability. • Decrease interlock leakage with bitumen, water swelling filler, or bentonite. • Sealable joint sheet piling is available. • With proper sealing of interlocks, can be as effective as slurry trench, concrete diaphragm, secant piles, and deep soil mix.
Slurry Trench Cutoff Walls	Silt, sand, gravel and cobbles, and boulders	Unrestricted	• Needs to be keyed into less permeable stratum to reduce seepage. • Can be keyed into rock.
Concrete Diaphragm Cutoff and Foundation Wall	Silt, sand, gravel, cobbles, and boulders	Basement, excavation support, and shafts	• Needs to be keyed into less permeable stratum to reduce seepage. • Can be keyed into rock. • Consider bearing and settlement.
Secant and Tangent Pile Cutoff and Foundation Walls	Silt, sand, gravel and cobbles	Basement, excavation support, and shafts	• Needs to be keyed into less permeable stratum to reduce seepage. • Can be keyed into soft rock. • Consider bearing and settlement. • Tangent piles leak more because piles do not overlap.
Mix-In-Place Walls	Sands, silty sands, and silts	Excavation support and shafts	• Needs to be keyed into less permeable stratum to reduce seepage. • Consider bearing and settlement.
Freezing: Ammonium/ brine refrigerant	All types of saturated soils and rock	Formation of ice in voids prevents water movement	• Better for large areas of long duration. • Takes long time to develop.
Freezing: Liquid nitrogen refrigerant			• Better for small areas of short duration where quick freezing is required. • Expensive and requires strict site controls. • Some ground heave will occur.

Figure 2-23 shows details of a wellpoint system and a deep well with a submersible pump. Figure 2-24 illustrates an example of a two stage well point system and a dewatering system using deep wells.

Design procedures related to seepage analysis and dewatering control are included in Chapter 6 of DM 7.1. Other good references include Mansur and Kaufman (1961) and Cedergren (1997).

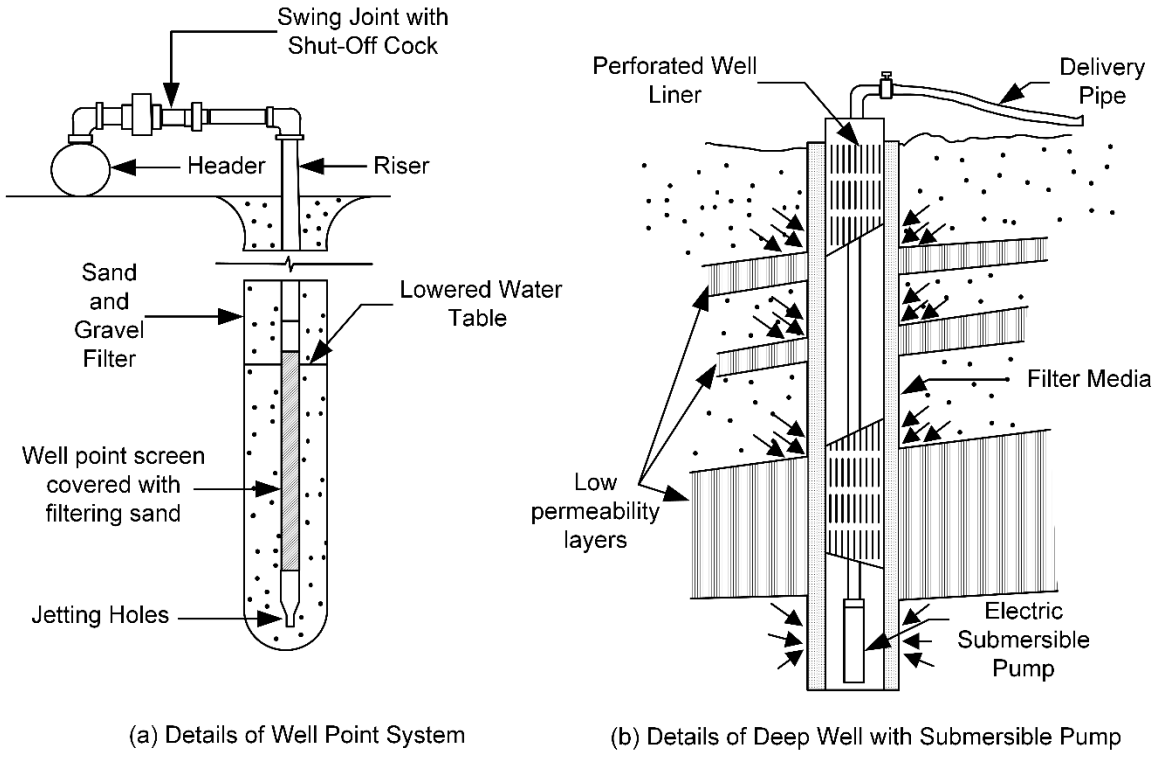

Figure 2-23 Methods of Construction Dewatering a) Details of Wellpoint System and b) Details of Deep Well with Submersible Pump (after Mazurkiewicz 1980)

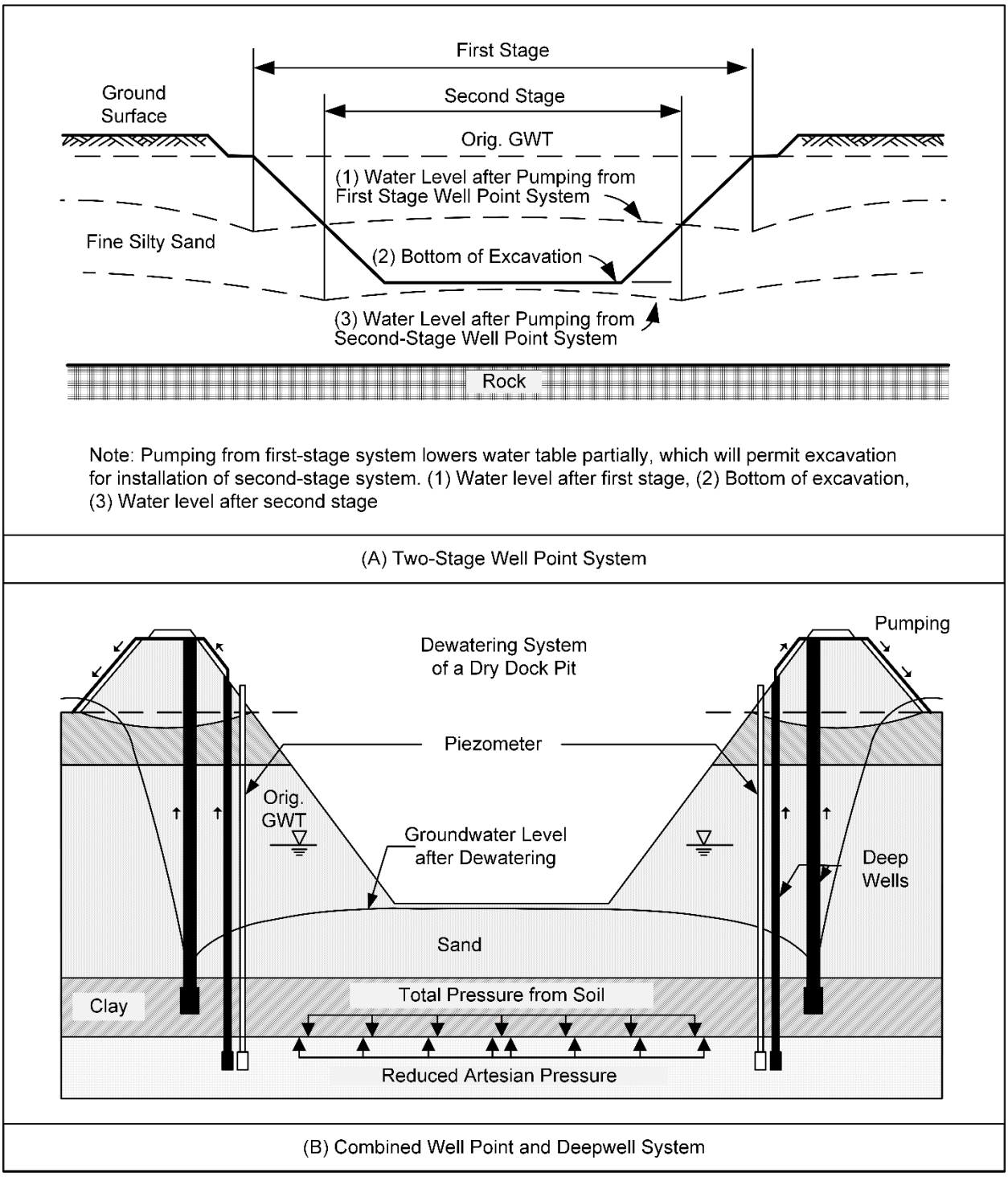

Figure 2-24 Methods of Construction Dewatering a) Two Stage Well Point System (after Mazurkiewicz 1980) and b) Combined Well Point and Deep Well System (after USACE 1983a)

2-7 PROBLEM SOILS AND EXCAVATIONS.

Chapter 1 provides a summary of many types of problem soil conditions that can affect the design of foundations and earth structures. Table 2-12 and Table 2-13 summarize important conditions for the design of excavations in problem soils.

Table 2-12 Problem Soil Considerations for Sloped Open Cut Excavations (after Clough and Davidson 1977)

Soil Type	Primary Considerations for Slope Design

Fissured Stiff Highly Plastic Clays and Soft Shales	• Field shear resistance may be less than laboratory tests.
	• First time slope failures may occur progressively due to:
	  o Stress relief,
	  o An increase in void ratio,
	  o Softening due to surface water seeping into fissures, and
	  o Variation of displacements along the failure surface.
	• Fully softened drained shear strength should be used for analysis of first-time slides. See Chapter 3 of DM 7.1 for testing procedures.
	• Residual shear strength should be used when previous failure surfaces are present.
	• Residual friction angles of shale may be as low as 7 to 12 degrees.

Stiff Desiccated Highly Plastic Clays	• Depth of softening and reduced strength is related to the depth of desiccation cracking. • Desiccation cracks have been reported up to 8 ft deep. • Fully softened drained strengths should be used to analyze the stability of these soils which typically have shallow failure surfaces.

Loess and Other Collapsible Soils	• Potential for collapse/erosion of relatively dry material upon wetting.
	• Loess slopes are more stable when cut near vertical.
	  o To prevent infiltration, and
	  o Benches may be used for high slopes.
	• See Chapter 1 of DM 7.1.

Sensitive Clays	• Considerable loss of strength can occur upon remolding. • Estimate sensitivity from unconfined compression tests, or alternatively, field or laboratory vane tests. • Marine clays can have a high sensitivity because of structure (flocculated) and leaching of salts by freshwater (clay deposits uplifted or sea level lowering during past geologic history). • A Liquidity Index > 1 ($w > LL$) is an indication of a sensitive clay. • See Section 1-2.4 for further description of sensitive clays.
Residual Soils	• Significant local variations in properties should be expected. • Variation occurs due to the weathering profile which is developed from parent rock. • The properties of these soils are unrelated to stress history. • Few reliable correlations are available.
Talus	• Talus is characterized by a loose aggregation of rock that accumulates at the base of rock cliffs. • Stable slopes are commonly 1-1/4 to 1-3/4 horizontal to 1 vertical. • Instability is associated with abundance of water.
Loose Sands	• May settle under blasting vibration. • When saturated under earthquake loading, may liquify and lose strength. • Static liquefaction is also possible in loose contractive sands. • Prone to erosion and piping.
Rock with Weak Planes	• Planar or wedge failures on discontinuities dippin toward excavation and daylighting on the slope. • Toppling of slabs of rock that dip steeply into the excavation face

Table 2-13 Problem Soil Considerations for Deep, Supported Excavations

Soil Type	Primary Considerations for Deep, Supported Excavation Design
Soft Clays	• Basal heave • Large wall movements • High apparent earth pressures
Fissured Stiff Highly Plastic Clays and Soft Shales	• May need to consider the effects of softening for permanent or semi-permanent structures • High earth pressures should be anticipated depending on the K_0 value before excavation. • Water should be diverted away from the soil retained by thet support system.
Loess and Other Collapsible Soils	• Metastable structure of the soil can collapse under loading, especially wetting. • Lower earth pressures should be expected because of the structure of the soil.
Sensitive Clays	• Areas susceptible to vibration may cause sensitive clays to lose strength. • Sensitivity above 4 should be given special consideration. • Impervious walls are suggested. • Keep shear stresses below the peak undrained shear strength throughout the sensitive soil. Use high F_{BH} or consider numerical analysis.
Residual and Lateritic Soils	• Most of these soils will behave similar to stiff clays. • Lateritic soils may have higher permeability.
Loose Sands	• May require extensive dewatering system if saturated. • Internal erosion of particles through the wall or at the base may be a concern.
Glacial Till	• Boulders may complicate some types of excavation and wall systems.
Organic Soils, Peat, and Muskeg	• Low undrained shear strength may be present. • Passive resistance will be low because of low unit weight. • Wall settlement may be a concern.

2-8 NOTATION.

Variable	Definition
B	Excavation or trench width
B_1	Width of zone adjacent to excavation in clay that contributes to basal instability
B_s	Width of surcharge adjacent to excavation
D	Embedded depth of wall below base of excavation
d, d_i	Distance from excavation to a point of interest
d_0	Typical distance from excavation at which no movement occurs
d_b	Distance separating two points on a structure for calculation of distortion or strain
E	Young's modulus
E_s	Elastic modulus of soil
F_{BH}	Factor of safety against basal heave

Variable	Definition
GSI	Geological strength index
h, h_{avg}	Vertical spacing of support system braces or anchors
H	Excavation depth
H_{crit}	Critical vertical excavation depth in clay for undrained conditions
I	Second moment of inertia
$I_{s(50)}$	Point load strength index of rock
K	Confinement factor for blasting calculations
K_A	Lateral earth pressure coefficient for active conditions
K_0	Lateral earth pressure coefficient for at-rest conditions
K_{wall}	Normalized wall stiffness
N	Number of interlocks in a sheet pile retaining wall
$N\gamma$	Bearing capacity factor
P_A	Active earth pressure force
P'_H	Unbalanced earth force on embedded section of excavation retaining wall
PPV	Peak particle velocity
q	Discharge or flow rate of water per unit height along a sheet pile interlock
Q	Total water flow into an excavation
S	Spacing of structural elements for combined sheet pile walls
SD	Scaled distance for blasting calculations
s_u	Undrained shear strength
$s_{u,b}$	Undrained shear strength below base of excavation
$s_{u,d}$	Undrained shear strength along embedded section of wall
$s_{u,h}$	Undrained shear strength above base of excavation
W	Weight of blasting charge
w	Gravimetric water content
α	Adhesion factor between fine-grained soil and retaining structure
β	Angular distortion of a structure caused by differential movement
δ_H, δ_{Hi}, δ_{Hm}	Horizontal movement of the ground adjacent to an excavation; m indicates maximum

Variable	Definition
Δp	Differential water pressure between the excavation and retained soil for sheet pile seepage
δv, δv_i, δv_m	Vertical movement of the ground adjacent to an excavation; m indicates maximum
ε_b	Horizontal strain of a structure caused by differential movement
γ, γ_t	Moist or total unit weight
γ_w	Unit weight of water
ϕ'	Drained or effective stress friction angle
ρ	Specific resistance of sheet pile interlocks to seepage
σ'_h	Effective horizontal stress

2-9 SUGGESTED READING.

Topic	Reference
Excavation Safety and Shoring	Occupational Safety and Health Administration (OSHA). 2020. CFR Part 1926, Subpart P, Excavations, with Appendices A - F. https://www.osha.gov/laws-regs/regulations/standardnumber/1926/1926SubpartP.
Deep Excavations	FHWA. 2008. *Earth Retaining Structures, FHWA NHI-07-071*. U.S. Department of Transportation, Federal Highway Administration, Washington, DC.
	Clough, G. W., and O'Rourke, T. D. 1990. "Construction Induced Movements of *In situ* Walls." *Proc. of Conf. on Design and Performance of Earth Retaining Structures. ASCE Geotechnical Special Publication No. 25.*
Dry Docks and Groundwater Control	Mazurkiewicz, B.K. 1980. *Design and Construction of Dry Docks*. Trans Tech Publications, Rockport, MA.
	USACE. 1983. *Dewatering and Groundwater Control, TM 5/818-5/AFM 88-5*. Department of the Army, Washington, DC.
Dewatering	Mansur, C. and Kaufman, R. 1961. "Dewatering." *Foundation Engineering*, Ed. Leonards, McGraw Hill, 514 pp.
	Cedergren, H. 1997. *Seepage, Drainage, and Flow Nets*, 3rd Ed., Wiley-Interscience, 496 pp.

CHAPTER 3.EARTHWORK, HYDRAULIC, AND UNDERWATER FILLS

3-1 INTRODUCTION.

3-1.1 Scope.

This chapter summarizes the design and construction of compacted earth, hydraulic fill, and underwater fill. It explains the theory of compaction and the engineering behavior of fill materials. Guidelines for the construction process and control of compacted fills are provided, along with compaction requirements for various applications and equipment. General requirements for the design of various types of embankments are included. The construction and control of hydraulic fills, both on land and underwater, are discussed.

3-1.2 Earthwork Process and Purpose of Compaction.

Earthwork is the process of changing the topography to accommodate construction and to provide drainage. As illustrated in Figure 3-1, earthwork is a manufacturing process using soil or rock, and includes excavation, transport, placement, and amendment. The final step of the process is c*ompaction*, which refers to the removal of air from the soil by the temporary application of a mechanical load, such as rolling, tamping, or vibration.

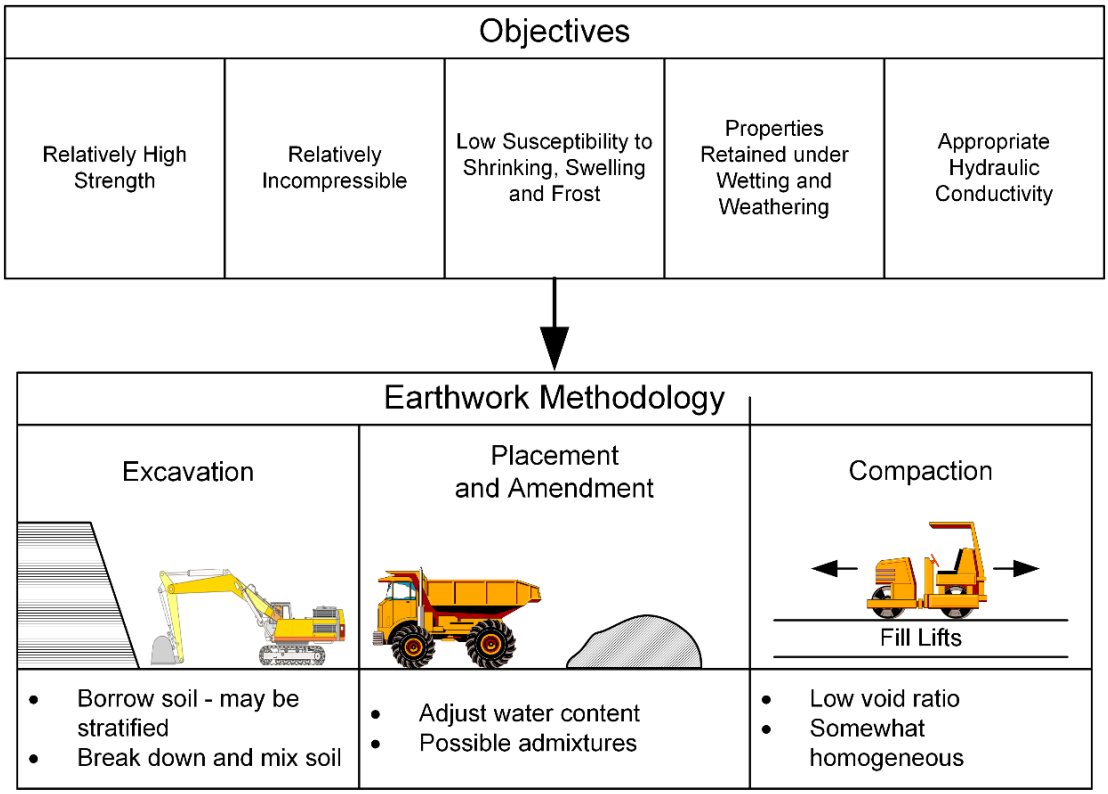

Figure 3-1 Earthwork Objectives and Methodology

As noted by Sowers (1979), the engineer has more control over some aspects of the earthwork process than others. For example, the water content of a fill can be controlled during but not after construction. Similarly, sources of suitable fill material typically depend on local availability, but careful excavation or processing can be used to create select soil or rock materials.

3-1.3 Types of Fills and Applications.

Fills can be grouped into three major categories based on the method of placement. *Controlled compacted fill* is created using a process similar to that shown in Figure 3-1. This process creates compacted fill that is more rigid and uniform than most natural soils. Properly compacted fill also tends to have higher shear strength and lower compressibility. *Hydraulic fill* is placed using flowing water and cannot be compacted during placement. For this reason, the type of soil used for hydraulic fill must be selected carefully. Hydraulic fills tend to be weaker and more compressible than compacted fills. *Uncontrolled fills* consist of soil, rock, or other materials that are placed without control of one or any of the factors discussed in this chapter, including material type, lift thickness, and compaction energy. Uncontrolled fills may contain industrial and domestic wastes, ash, slag, chemical wastes, building rubble, and refuse. An important distinction should be made between uncontrolled fills and fills that intentionally use recycled or waste materials in a controlled manner. The use of ash, slag, and chemical waste is regulated, and current Environmental Protection Agency (EPA) and other appropriate regulations must be considered.

The principal uses of controlled compacted fill include support of structures or pavements, embankments for water retention or for lining reservoirs and canals, and backfill surrounding structures or buried utilities. Hydraulic fill was historically used in dam and levee construction where large quantities of fill were transported long distances. While now less common, hydraulic fill is still used in select cases for the creation of dam and levee structures. Both controlled and hydraulic fills should be created in a such a manner as to maintain slope stability. Uncontrolled fills should not be created or used for engineering purposes without modification.

3-2 COMPACTION THEORY.

This section summarizes the weight volume relationships involved in the process of compaction and how those relationships are represented graphically. Methods for characterizing the level of compaction are discussed for soils both with and without appreciable amounts of fines. Finally, this section explores the effect of compaction on the engineering properties of soil.

3-2.1 Process of Compaction.

Compaction focuses on changing the dry unit weight (γ_d) of soil (and rock) which is defined as:

$$\gamma_d = \frac{W_s}{V_t} = \frac{\gamma_t}{\left(1 + {}^{w}\!/_{100}\right)} \tag{3-1}$$

where:
W_s = weight of solids,
V_t = total volume,
γ_t = total unit weight, and
w = water content (percentage).

The degree of saturation (S), which is the percentage of the void space filled with water, is also important to understanding the behavior and construction of controlled fill. The dry unit weight is related to S by:

$$\gamma_d = \frac{\gamma_w S}{\left(\frac{w}{100} + \frac{S}{G_s}\right)} \tag{3-2}$$

where:
γ_w = unit weight of water = 62.4 pcf,
w = water content (percentage), and
G_s = specific gravity of solids.

To illustrate the compaction process, phase diagrams are shown in Figure 3-2 for different points on the *compaction plane*, which plots dry unit weight against water content. Moving from left to right on the compaction plane (A→C→E), the dry unit weight stays constant but the amount of water in the voids increases with the water content. In other words, the degree of saturation (S) increases. In order to compact the soil, a compactive effort must be applied to the soil to remove void space in the form of air, following paths similar to A→B or C→D. Further compaction of the soil at Points D or E is not possible unless water is removed, and the water content is decreased.

3-2.2 Characterizing Compaction.

3-2.2.1 Soils with Appreciable Fines.

For soils with more than about 5% to 15% fines (i.e., particles passing the #200 sieve), compacted soil behavior is often idealized using the concave-down *compaction curves* shown in Figure 3-3. These curves were first explained by Proctor (1933) in an effort to improve the quality of fill for earth dam construction. A compaction curve is obtained

when soil is compacted using a constant *compactive effort*, which is the amount of work performed on the soil per unit volume during compaction. Hogentogler (1936) further explained compaction in terms of lubrication and particle hydration and noted that air becomes trapped at water contents higher than optimum. Barden and Sides (1970) later confirmed that the peak in the compaction curve occurs at the degree of saturation where air is no longer able to flow freely from the soil during compaction. The compaction process has also been explained in terms of the effective stresses that develop during compaction (Olson 1963) and capillary pressures in the unsaturated state (Hilf 1956).

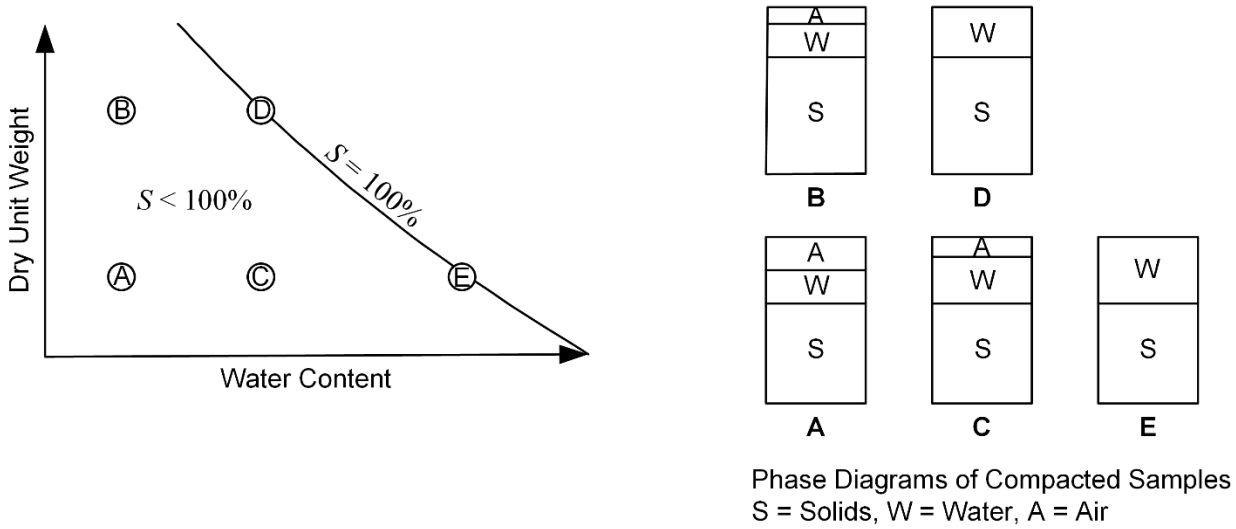

Figure 3-2 Changes in Weight-Volume Relationships from Compaction and Changes in Water Content

All of these theories provide valuable insight into the behavior of compacted soil. As the water content increases, less compactive effort is required to break up the lumps of soil. However, once air can no longer easily leave the soil, additional water simply takes up space and prevents higher levels of compaction. This creates a peak in the compaction curve. The dry unit weight at the peak of a particular compaction curve is referred to as the *maximum dry unit weight* ($\gamma_{d,max}$) for the corresponding compactive effort. The water content corresponding to the peak of a compaction curve is called the *optimum water content* (w_{opt}). If the compaction energy is increased, the compaction curve shifts toward lower water contents and higher dry unit weights. The relationship between the change in compactive effort and the shift of compaction curve is highly nonlinear.

The two most common levels of compactive effort are standard Proctor (ASTM D698) and modified Proctor (ASTM D1557). Standard Proctor is more often used as the reference energy for compaction control. The compactive effort for standard Proctor is 12,400 lbf-ft/ft^3. Modified Proctor was originally developed for compaction of airfield pavement subgrades. The compactive effort for modified Proctor is 56,000 lbf-ft/ft^3.

Modified Proctor is sometimes used as the reference standard for compaction of the upper few feet of a heavily loaded fill.

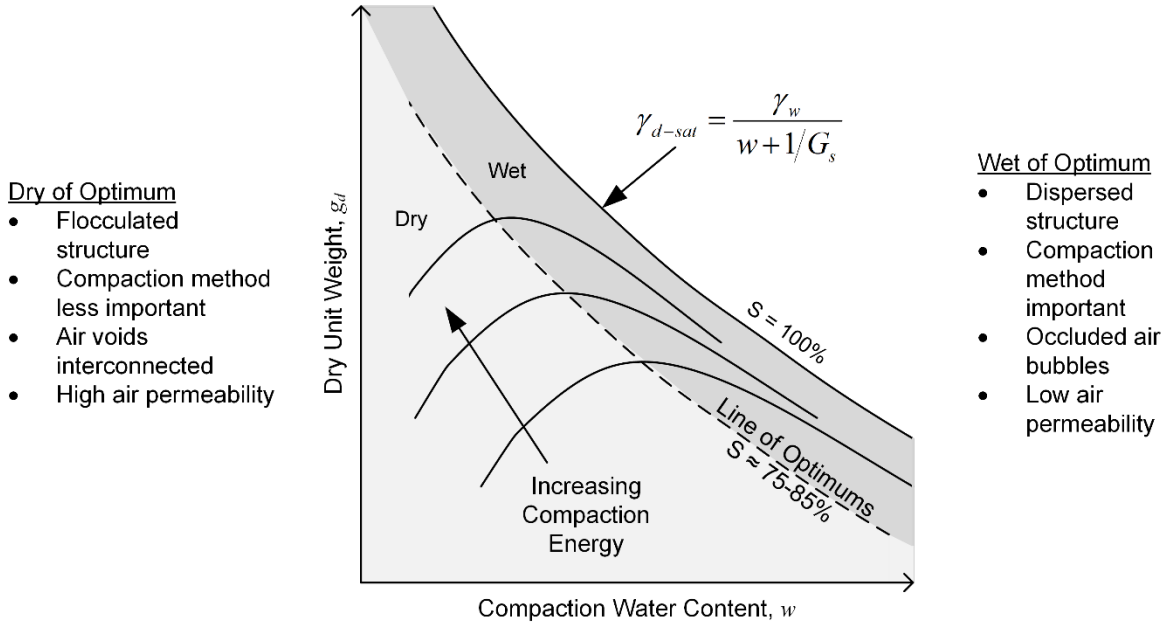

Figure 3-3 Effects of Compactive Effort and Water Content on Compacted Soil Properties

The peaks of a series of compaction curves can be connected to form a *line of optimums*, which often corresponds to S in the range of 75 to 85%. Compaction to a state to the left of this curve is referred to as *dry of optimum* while compaction states to the right are termed *wet of optimum*. All possible compaction states for a particular soil are bounded on the right side by the $S = 100\%$ curve (a.k.a., *zero air voids curve*). Properties typically associated with “dry” and “wet” compaction are summarized in Figure 3-3.

The dry unit weight and water content of a compacted soil can be compared to the conditions at the peak of a compaction curve for the same soil. *Relative compaction* ($R.C.$) is used for soils with appreciable fines and is defined as:

$$R.C. = \frac{\gamma_{d,field}}{\gamma_{d,\max}} \times 100\% \tag{3-3}$$

where:
$\gamma_{d,field}$ = dry unit weight of compacted fill and
$\gamma_{d,max}$ = maximum dry unit weight for a specified compactive effort.

The *relative water content* (Δw) of the compacted fill is:

$$\Delta w = w_{opt} - w_{field} \quad (3\text{-}4)$$

where:
w_{field} = water content of the compacted fill.

The position and shape of the compaction curve can be affected by variables other than compactive effort. For example, different methods of applying the compactive effort, such as kneading compaction, impact compaction, and static compaction, result in different soil structure and change the compaction curves. Similarly, different types of field compaction equipment result in different compaction behavior.

Some soils and rocks undergo irreversible changes during drying and compaction, and they may exhibit drastically different compaction curves in the field compared to those created in the laboratory unless special care is taken. These materials include clays containing halloysite or allophane minerals, which are chemically altered when dried (Hilf 1991). Some weak rocks may degrade differently during field and laboratory compaction. Very dense glacial till clays can have field compacted dry unit weights much higher than the laboratory $\gamma_{d,max}$ because of the extensive loosening required to perform the laboratory compaction tests.

3-2.2.2 Compaction of Soils with Little Fines.

For soils without an appreciable fines content (i.e., $F < 5$ to 15%), compaction behavior is much less sensitive to water content. In some cases, the compaction curve is poorly defined below optimum (Sowers 1979). In other soils, a minimum value of γ_d may be reached at a midrange water content because the bulking of sand or gravel grains inhibits compaction (Hilf 1991).

For these materials, characterization in terms of void ratio can be more appropriate. The loosest state that the soil can sustain with a regular structure is referred to as the *maximum void ratio* (e_{max}) and can be found using ASTM D4254. The densest configuration of the soil is called the *minimum void ratio* (e_{min}) and can be found using a vibratory table as described in ASTM D4253. The value of e_{min} depends on particle shape and size. Some compaction methods and levels of compactive effort may break particles, which can lower e_{min} (Sowers 1979). Corresponding values of minimum dry unit weight ($\gamma_{d,min}$) and maximum dry unit weight ($\gamma_{d,max}$) can be calculated. The value of e_{min} determined by ASTM D4253 corresponds to approximately 100% of $\gamma_{d,max}$ determined by ASTM D698 or 95% of $\gamma_{d,max}$ determined by ASTM D1557.

For coarse-grained soils without appreciable fines, *relative density* (D_r) is sometimes used for determining the level of compaction and assessing the influence of compaction on the engineering properties. Relative density is defined as:

$$D_r = \frac{e_{\max} - e}{e_{\max} - e_{\min}} \times 100\% = \frac{\gamma_{d,field} - \gamma_{d,\min}}{\gamma_{d,\max} - \gamma_{d,\min}} \left(\frac{\gamma_{d,\max}}{\gamma_{d,field}} \right) \times 100\% \quad (3\text{-}5)$$

where:
e = compacted void ratio ($\gamma_{d,field}$ = corresponding dry unit weight),
e_{max} = maximum void ratio ($\gamma_{d,min}$ = corrsponding dry unit weight), and
e_{min} = minimum void ratio ($\gamma_{d,max}$ = corrsponding dry unit weight).

3-2.3 Influence of Compaction on Engineering Parameters.

Compaction produces an engineered fill with relatively high dry unit weight or low void ratio. Compaction changes the strength, compressibility, and hydraulic conductivity of the fill, fulfilling three of the objectives in Figure 3-1.

3-2.3.1 Engineering Parameters of Compacted Coarse-Grained Soils.

Coarse-grained soils, especially those with little fines, are often characterized in terms of relative density (D_r). Coarse-grained soils will have a low relative density (0 to 20%) when placed loosely. Satisfactory compaction will tend to increase D_r to the range of 75 to 100%. The trends described in this section can be used to set appropriate compaction control requirements.

The shear strength of compacted coarse-grained soils is typically quantified in terms of an effective stress friction angle (ϕ'), which increases as D_r increases. As D_r increases from 0% to 100%, the friction angle increases by about 8 to 12 degrees (Hilf 1991, Duncan et al. 2014) as shown in Figure 3-4(a). This increase is also reflected in correlations between ϕ' and D_r presented in Duncan et al. (2014) and Chapter 8 of DM 7.1 (NAVFAC 2021). The compaction water content tends to have a minor effect on the shear strength of coarse-grained soils and should usually be as high as possible.

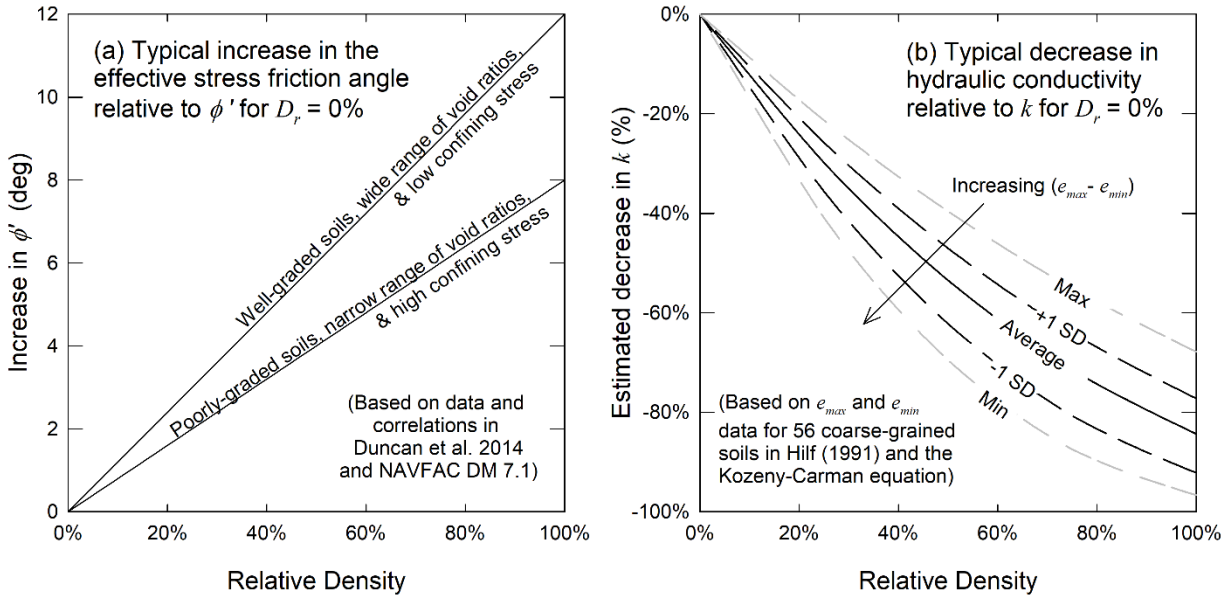

Figure 3-4 Effect of Compaction on (a) Shear Strength and (b) Hydraulic Conductivity of Coarse-Grained Soils

As soil is compacted and D_r increases, coarse-grained soils become stiffer or less compressible. Based on typical values of the elastic modulus, sands and gravels become about four times stiffer when D_r is increased from 0% to 100%.

The hydraulic conductivity (k_{sat}) of coarse-grained soils is inversely related to void ratio and will decrease as D_r increases. In Figure 3-4(b), the approximate percent decrease in k_{sat} is estimated using the Kozeny-Carman equation. A greater reduction in k_{sat} occurs when the soil has a wide range of possible void ratios (i.e., e_{max} - e_{min} is larger).

3-2.3.2 Engineering Parameters of Compacted Fine-Grained Soils.

The engineering parameters of compacted fine-grained soil, particularly clay, depend on the initial compaction conditions, the stress history following compaction, and the time of the design condition with respect to compaction. In particular, the effects of volume change caused by collapse or swelling must be considered. Clays which become saturated after compaction will tend to swell unless subjected to confining pressure. Swelling reduces the dry unit weight of the compacted clay and may reduce shear strength and increase compressibility. Laboratory tests used to measure the parameters of compacted clays should match field conditions to the extent possible.

As illustrated in Figure 3-3, both the water content and the compacted unit weight will affect the structure of the clay. In order to comprehensively determine the effect of compaction on fine-grained soil parameters, the 15-point method can be used as illustrated in Figure 3-5. In this method, three levels of compaction energy are selected, and five specimens are compacted at each energy, resulting in 15 combinations of

compacted water content and dry unit weight. The appropriate test (shear strength, compressibility, hydraulic conductivity, etc.) is conducted on each specimen, which allows the variation in this parameter to be assessed across the compaction plane.

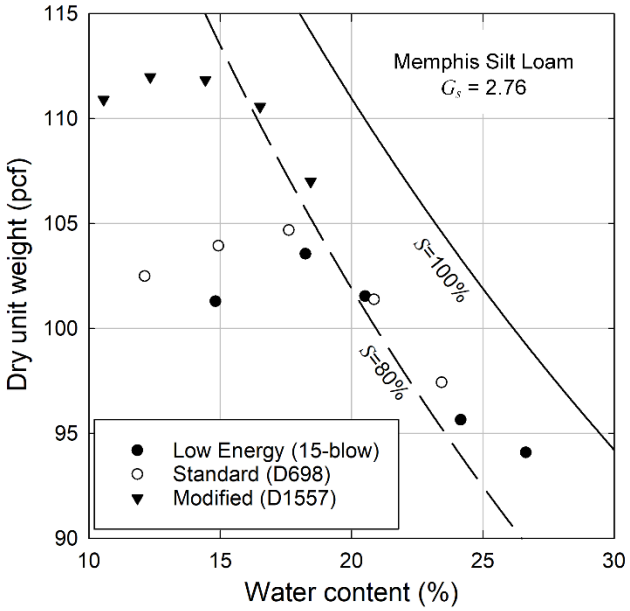

15-Point Method

1) Split soil sample into three sub-samples.
2) Mix specimens from each sub-sample to five water contents.
3) Compact specimens using a constant compaction energy for each sub-sample.
4) Plot compaction curves as shown in the example to the left.
5) Perform engineering property test(s), such as shear strength or hydraulic conductivity, at each compaction condition.
6) Plot results from Step 5 on the compaction plane. For example, see Figure 3-6.

Figure 3-5 15-Point Method for Determining Engineering Parameters of Compacted Soil

The 15-point method is appropriate mostly for large projects or research efforts. For smaller projects, it is often necessary to pick a particular $R.C.$ and water content at which to perform tests to determine engineering parameters. If this approach is taken, care must be used to choose a conservative compaction state. VandenBerge et al. (2017) provide guidance on the selection of compaction conditions for shear strength tests on compacted clays.

Within practical levels of compaction, compacted clays are heavily overconsolidated. For both consolidation and axial compression, compaction dry of optimum tends to produce a more brittle response. Compaction wet of optimum tends to produce ductile soil behavior. Clays compacted dry of optimum will exhibit an apparent yield stress as shown in Figure 3-6(a). In contrast, a more gradual stress-strain behavior is observed in clays compacted wet of optimum. Under low stress levels, dry compaction will usually result in less strain or settlement. At higher stress levels, the strains tend to become similar regardless of the initial compaction state. Compression indices for compacted soil can be measured in one-dimensional consolidation tests provided the initial saturation condition in the laboratory appropriately matches the field conditions. The behavior of saturated specimens of compacted clay tested in consolidated-undrained (CU) triaxial compression is shown in Figure 3-6(b). Compaction dry of optimum will tend to create a stiffer initial response. The strength of compacted clay is

about equal at high axial strain, regardless of the compaction condition. These observations apply to specimens with the same dry unit weight after consolidation.

The effective stress shear strength of compacted clay is not substantially affected by the compaction state (Johnson and Lovell 1979, VandenBerge et al. 2015). However, the pore pressure response of compacted clay varies widely by compaction state, which in turn impacts the undrained shear strength. Trends in behavior for as-compacted (UU) conditions are illustrated in Figure 3-6(c) and (d). Total stress cohesion increases with increasing compaction, while the total stress friction angle decreases with increasing water content or degree of saturation. For saturated, consolidated undrained conditions, VandenBerge et al. (2015) found that the undrained strength ratio is approximately constant up to about 70% saturation, as shown in Figure 3-7, and increases for clay compacted to higher degrees of saturation. Consolidated undrained strengths are heavily influenced by the amount of swelling that occurs during saturation.

The saturated hydraulic conductivity (k_{sat}) of laboratory specimens of compacted clay is affected by the initial compaction state. As shown in Figure 3-8(a), k_{sat} can vary three or four orders of magnitude within the range of typical compaction. Benson and Trast (1995) studied the hydraulic conductivity of 13 compacted clays and found an inverse relationship between k_{sat} and initial saturation (Figure 3-8(b)). Daniel (1994) stressed the importance of field-scale considerations, such as cracking and defects, on the acting hydraulic conductivity of compacted clay liners. Tinjum et al. (1997) discusses the unsaturated properties of compacted clays.

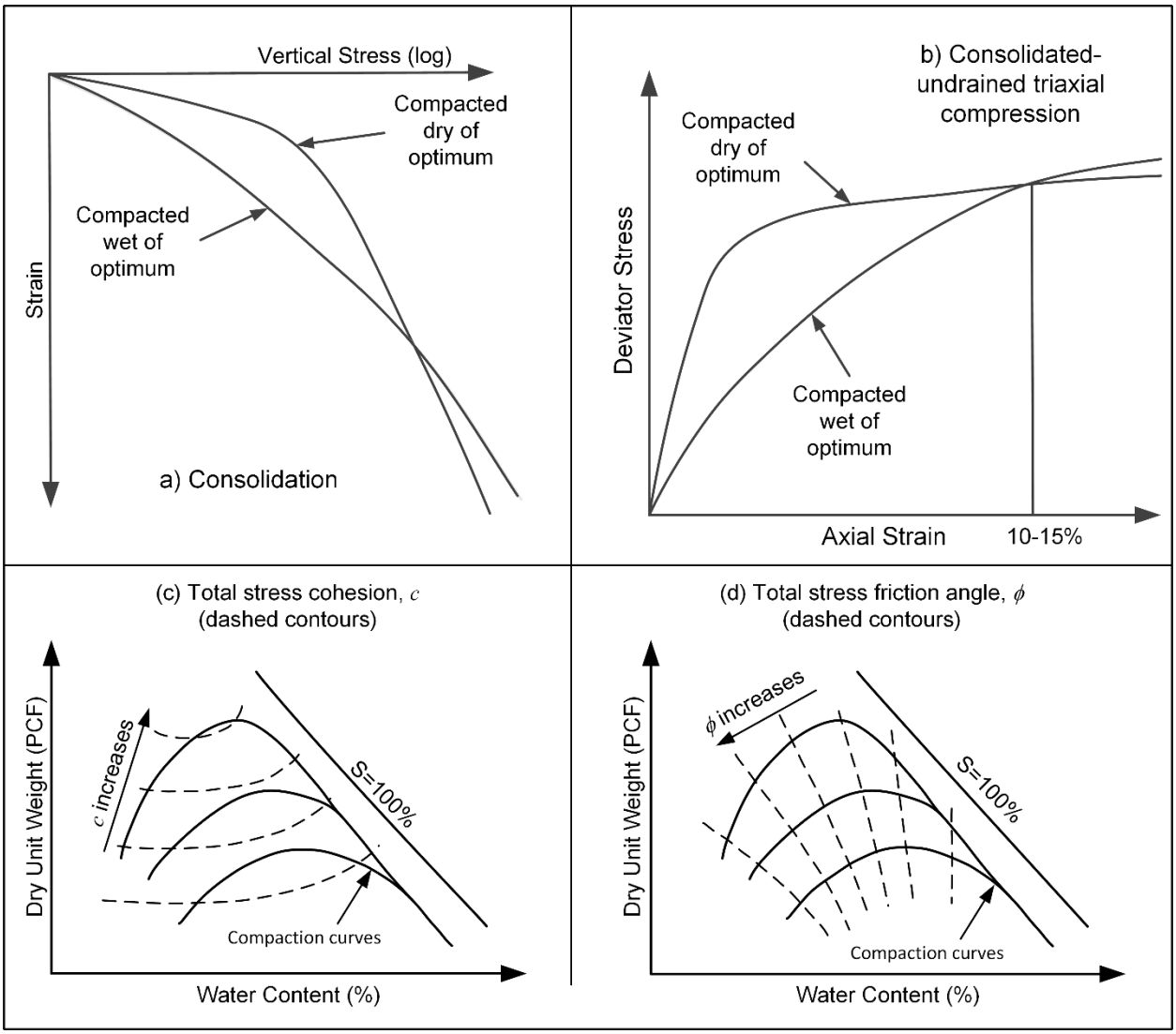

Figure 3-6 Engineering behavior of compacted clay – (a) consolidation, (b) stress-strain, (c) total stress cohesion, and (d) total stress friction angle (after DiBernardo and Lovell 1979, Seed et al. 1960, and Kulhawy et al. 1969)

In most cases, specimens of candidate fill materials should be compacted and tested in the laboratory to directly measure the desired engineering parameters. The trends presented in this section can help to guide the laboratory testing program. For example, clay soils will tend to have the lowest unconsolidated, undrained shear strength at high water content and low relative compaction. Thus, UU tests should be conducted at the highest water content allowed by the specification and lowest specified R.C. Similarly, k_{sat} is highest for low initial saturation. For this reason, laboratory specimens should use the lowest specified water content to obtain a conservative measure of k_{sat}, provided low k_{sat} is desired.

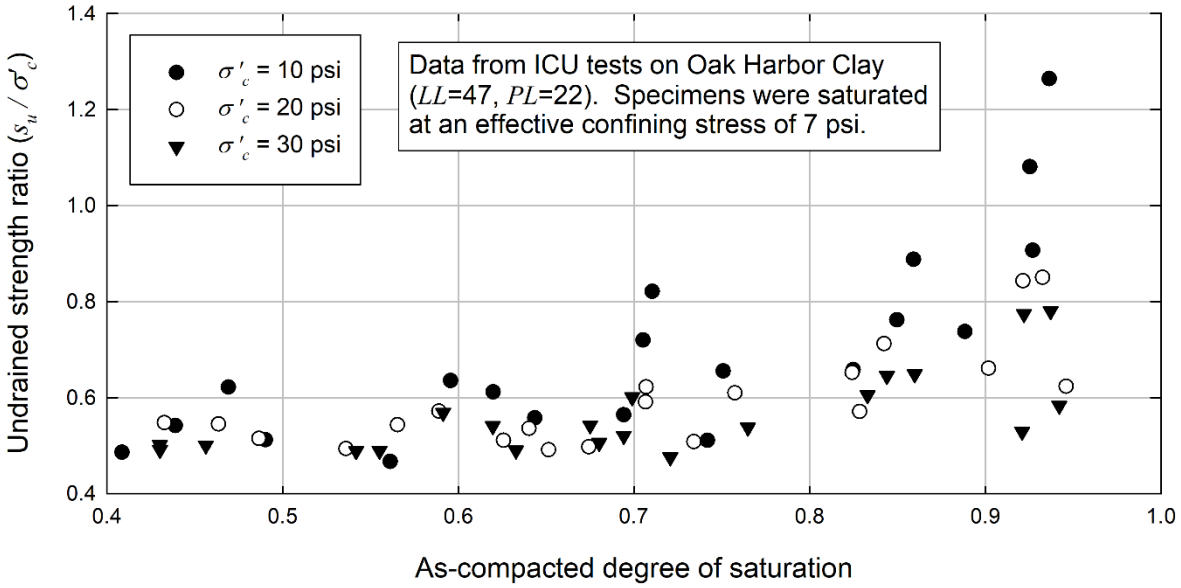

Figure 3-7 Variation in consolidated undrained shear strength ratio with as-compacted degree of saturation (after VandenBerge et al. 2015)

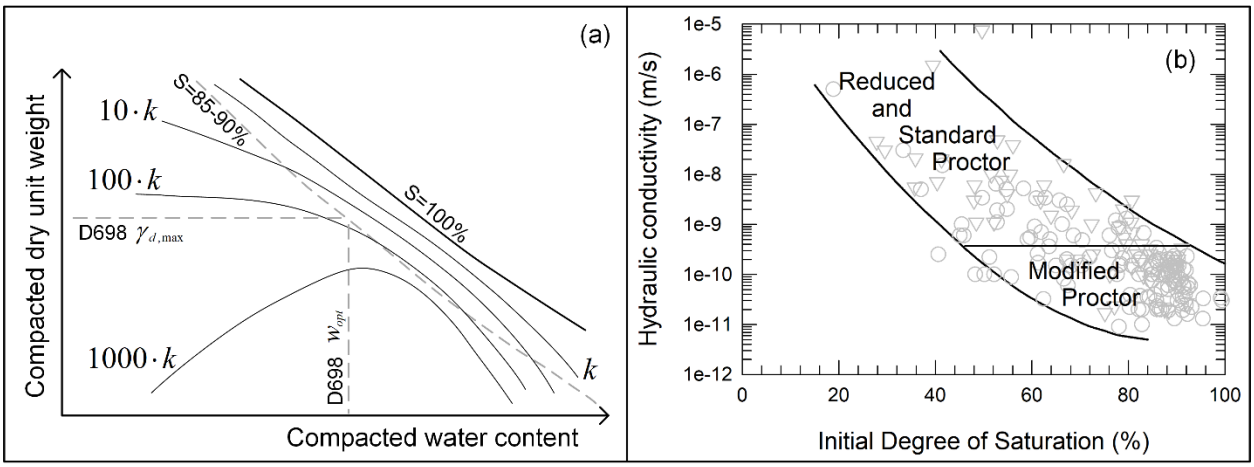

Figure 3-8 Saturated hydraulic conductivity of laboratory compacted clay – (a) typical variation (based on Mitchell et al. 1965, Garcia-Bengochea 1978) and (b) variation with initial saturation (after Benson and Trast 1995)

3-3 FILL MATERIALS.

The selection of fill material for a particular engineering application must consider both the purpose and the availability of fill materials. The selection process may include the following steps: (1) gather samples of all the available and viable fill sources, (2) perform classification tests (i.e., Atterberg limits and grain-size analysis), (3) use soil classification to determine typical properties of the available fill materials based on Table 3-1, Figure 3-9, Figure 3-10, and Figure 3-11, (4) select a small number of soils to obtain larger samples, (5) perform tests to determine appropriate engineering

parameters at representative compaction levels (i.e., compaction, strength, shrink/swell, hydraulic conductivity), and (6) select an appropriate soil for the application (Sowers 1979). This type of selection process may be appropriate on large projects. However, on many smaller projects, the engineer specifies the type of material, and the contractor submits particular materials for the engineer's approval, limiting this type of detailed involvement in the selection process.

3-3.1 Borrow Exploration.

The source of the fill material is referred to as the *borrow*. Sufficient borings or test pits should be performed to determine the approximate quantity and quality of construction materials within an economical haul distance from the project. For mass earthwork, initial exploration should be on a 200-foot grid. If variable conditions are found during the initial exploration, intermediate borings or test pits should be completed.

One purpose of the borrow exploration is to determine a reasonably accurate subsurface profile to the anticipated depth of excavation, including the groundwater level. The approximate volume and engineering parameters should be determined for each material considered for use as fill. The other purpose of the borrow exploration is to obtain samples that can be used for classification testing as well as to ascertain the presence of salts, gypsums, or undesirable minerals, and the extent of organic or contaminated soils, if encountered.

3-3.2 Preliminary Selection based on Classification.

Typical properties of compacted soils are summarized by USCS classification in Table 3-1, Figure 3-9, Figure 3-10, and Figure 3-11, which may be used for preliminary selection and analysis. For final analysis, tests should be completed on compacted soil samples to determine engineering parameters.

The ranges of hydraulic conductivity provided for clay soils in Table 3-1 correspond to laboratory compacted specimens. However, a compacted clay mass will contain cracks and discontinuities. For this reason, the mass value of k is typically about two orders of magnitude higher than the laboratory value (Daniel 1984).

Table 3-2 summarizes the relative desirability of various soil types in earth fill dams, canals, roadways, and foundations. Practically any inorganic, insoluble soil may be incorporated in an embankment when modern compaction equipment and control standards are employed. However, some soils may be difficult to use economically. For some embankment zones, fine-grained soils may have insufficient shear strength or excessive compressibility. Clays of medium to high plasticity ($PI > 20$ and/or $LL > 40$) tend to expand if placed at low water content and exposed to low confining pressures for long periods of time. Identification of soils susceptible to volume expansion is discussed in Chapter 1 of DM 7.1. High plasticity soils with high natural moisture are

difficult to process for proper moisture for compaction. Stratified soils may require extensive mixing in order to produce a homogeneous fill.

Table 3-1 Typical Compaction Properties and Hydraulic Conductivity based on USCS (after USACE 1960)

USCS Group Symbol	Soil Type	ASTM D698		Typical Hydraulic Conductivity, k (ft/s)[A]
		Maximum Dry Unit Weight (pcf)	Optimum Moisture, Percent	
GW	Well graded clean gravels, gravel-sand mixture	125 to 135	11 to 8	10^{-3} to 10^{-5}
GP	Poorly graded clean gravels, gravel-sand mix	115 to 125	14 to 11	10^{-2} to 10^{-4}
GM	Silty gravels, poorly graded gravel-sand-silt	120 to 135	12 to 8	10^{-5} to 10^{-7}
GC	Clayey gravels, poorly graded gravel-sand-clay	115 to 130	14 to 9	< 10^{-8}
SW	Well graded clean sands, gravelly-sands	110 to 130	16 to 9	10^{-3} to 10^{-5}
SP	Poorly graded clean sands, sand-gravel mix	100 to 120	21 to 12	10^{-2} to 10^{-4}
SM	Silty sands, poorly graded sand-silt mix	110 to 125	16 to 11	10^{-5} to 10^{-7}
SM-SC	Sand-Silt clay mix with slightly plastic fines	110 to 130	15 to 11	10^{-7} to 10^{-9}
SC	Clayey sands, poorly graded sand-clay-mix	105 to 125	19 to 11	< 10^{-8}
ML	Inorganic silts and clayey silts	95 to 120	24 to 12	10^{-7} to 10^{-9}
CL-ML	Mixture of inorganic silt and clay	100 to 120	22 to 12	< 10^{-9}
CL	Inorganic clays of low to medium plasticity	95 to120	24 to 12	< 10^{-9}
OL	Organic silts and silt-clays, low plasticity	80 to 100	33 to 21	< 10^{-9}
MH	Inorganic clayey silts, elastic silts	70 to 95	40 to 24	< 10^{-10}
CH	Inorganic clays of high plasticity	75 to105	36 to 19	< 10^{-10}
OH	Organic clays and silty clays	65 to 100	45 to 12	< 10^{-10}

[A] Hydraulic conductivity ranges for clay soils are typical of laboratory compacted specimens. The hydraulic conductivity of a compacted clay mass is typically about two orders of magnitude higher than the laboratory value.

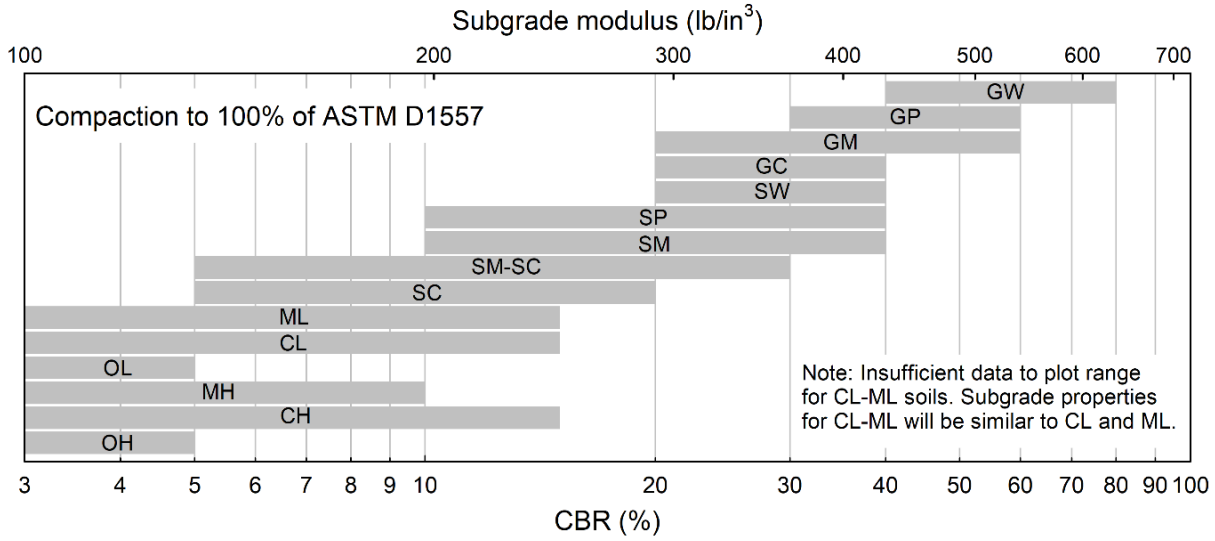

Figure 3-9 Typical Subgrade Modulus and California Bearing Ratio by USCS (after Porter 1943, USACE 1960, PCA 1992)

Fill Compression Parameters by USCS		
Classification Group	a_Δ	b_Δ
1: GM-GP, GM, GM/SM	0.30 - 0.41	0.64
2: SM	0.32 – 0.58	0.80 – 0.58
3: ML	0.28 – 0.53	0.76 – 0.72
4: SC/GC, SC-SM	0.43 – 0.51	0.81 – 0.75
5: SC	0.54 – 1.00	0.66 – 0.61
6: CL-ML, CL/SC, CL/GC	0.33 – 1.35	1.08 – 0.60
7: CL (PI = 8 – 15)	0.28 – 0.92	1.17 – 0.66
8: CL (PI = 10 – 21)	0.22 – 0.68	1.15 – 0.94
Parameters for estimating fill compression based on data from 25 USBR dams. Higher values of a_Δ tend to correspond to lower values of b_Δ.		

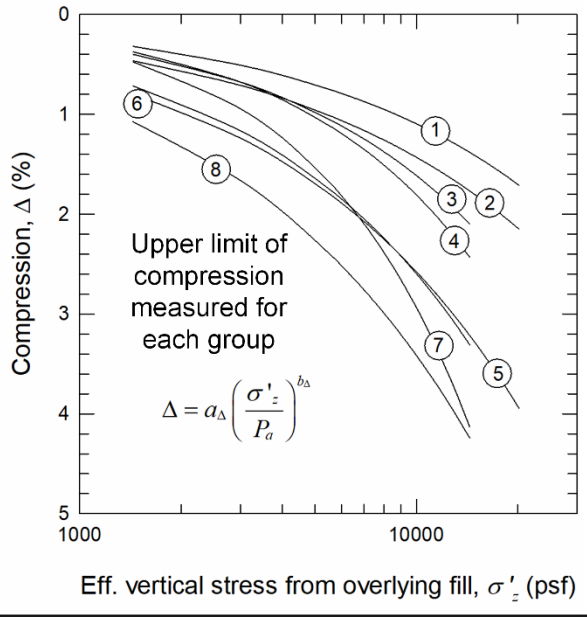

Figure 3-10 Vertical Compression of Compacted Fill by USCS (after Gould 1954)

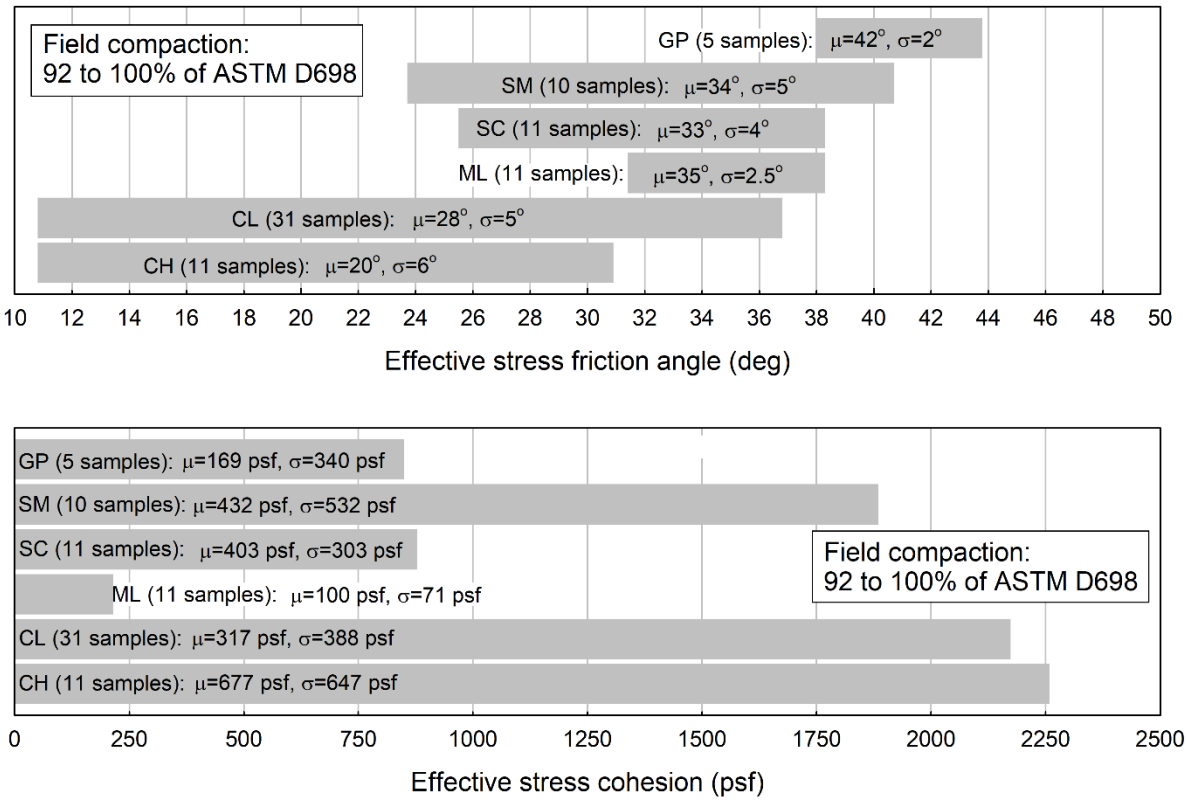

Figure 3-11 Typical Drained Shear Strength Parameters of Compacted Fill – μ Indicates Mean Value and σ Indicates Standard Deviation (after USBR 1998)

Table 3-2 Relative Desirability of Soils for Compacted Fill based on USCS Classification (after USBR 1998)

USCS Group Symbol	Soil Type	Relative Desirability for Various Uses (1 = very suitable, 2 = suitable, 3 = somewhat suitable, 4 = marginally suitable, 5 = unsuitable)									
		Earth Fill Dams			Canal Sections		Foundation		Roadway		
									Fill		
		Homogeneous Embankment	Core	Shell	Erosion Resistance	Compacted Earth Lining	Seepage Important	Seepage Not Important	Frost Heave Not Possible	Frost Heave Possible	Surfacing
GW	Well graded gravels, gravel-sand mixtures, little or no fines	5	5	1	1	5	5	1	1	1	2
GP	Poorly graded gravels, gravel-sand mixtures, little or no fines	5	5	2	1	5	5	2	2	1	5
GM	Silty gravels, poorly graded gravel-sand-silt mixtures	1	2	5	2	2	1	2	2	3	3
GC	Clayey gravels, poorly graded gravel-sand-clay mixtures	1	1	5	2	1	1	2	2	2	1
SW	Well graded sands, gravelly-sands, little or no fines	5	5	3[A]	3	5	5	1	1	1	2
SP	Poorly graded sands, gravelly sands, little or no fines	5	5	3[A]	3[A]	5	5	2	2	2	5
SM	Silty sands, poorly graded sand-silt mixtures	2	3	5	3[A]	3[B]	2	3	3	3	3
SC	Clayey sands, poorly graded sand-clay mixtures	2	1	5	2	1	2	3	3	2	1
ML	Inorganic silts and very fine sands, rock flour, silty or clayey fine sands with slight plasticity	3	3	5	5	3[B]	3	3	3	3	5
CL	Inorganic clays of low to medium plasticity, gravelly clays, sandy clays, silty clays, lean clays	2	2	5	4	2	2	3	3	2	4
OL[D]	Organic silts and silt-clays, low plasticity	4	4	5	5	3[B]	3	4	4	4	5
MH	Inorganic silts, micaceous or diatomaceous fine sandy or silty soils, elastic silts	4	4	5	5	5	3	4	4	4	5
CH	Inorganic clays of high plasticity, fat clays	3	3	5	4	4[C]	4	4	4	4	5
OH[D]	Organic clays of medium high plasticity	4	4	5	5	5	4	4	4	4	5

[A] Suitable if gravelly
[B] Consideration of erosion is critical
[C] Consideration of volume change is critical
[D] USACE experience has shown that organic soils can be incorporated in embankments if necessary. See Chapter 1 for more information.

For normal embankment construction, the maximum particle sizes should not exceed 3 inches (i.e., gravel-sized or smaller) or 50 percent of the compacted layer thickness. Where economic borrow sources contain larger particles, compaction trials should be performed before approval.

3-3.3 Laboratory Characterization of Fill Materials.

3-3.3.1 Reference Compaction Tests.

In order to guide both fill placement and the selection of engineering parameters for compacted fill, tests must be completed to define compaction behavior under a specified compactive effort. For soils containing appreciable fines, the standard Proctor (ASTM D698) and modified Proctor (ASTM D1557) tests are used. These tests are described in more detail in Chapter 3 of DM 7.1. The compactibility of clean soil and rock may alternatively be characterized using e_{min} and e_{max} (ASTM D4253 and D4254). When multiple different soils will be used as fill, a family of compaction curves should be obtained to represent the typical fill materials for the project.

Many soils contain some percentage of particles that are larger than the maximum size allowed using a given compaction mold (e.g., larger than 4.75 mm for 4-inch mold or ¾-inch for 6-inch mold). These particles are referred to as *oversize* and interfere with compaction of the finer soil fraction in the mold. However, in the field, these particles will be present in the field compacted fill and will influence the compacted dry unit weight.

For soils with more than 5% oversize particles, corrections can be made to the water content and dry unit weight measured on the soil without the oversize particles.[13] The corrected water content is found as:

$$w_T = P_C w_C + P_F w_F \tag{3-6}$$

where:
w_T = combined water content of the finer and oversize fractions (decimal),
P_C = percent oversize fraction (decimal),
w_C = water content of the oversize fraction (decimal),
P_F = percent finer fraction (decimal), and
w_F = water content of the finer fraction (decimal).

[13] These corrections are typically limited to 40% oversize for 4.75 mm particles and 30% oversize for ¾-inch particles.

The corrected dry unit weight is found as:

$$\gamma_{dT} = \frac{\gamma_{dF} G_{sC} \gamma_w}{\gamma_{dF} P_C + G_{sC} \gamma_w P_F} \tag{3-7}$$

where:
γ_{dT} = combined dry unit weight of the finer and oversize fractions,
γ_{dF} = dry unit weight of the finer fraction,
G_{sC} = specific gravity of solids of the oversize fraction, and
γ_w = unit weight of water (62.4 pcf, 9.81 kN/m^3).

In addition to correcting laboratory results for oversize as in the previous equations, ASTM D4718 allows the influence of the oversize fraction to be corrected out of the field results by solving Equations 3-6 and 3-7 for w_F and γ_{dF}. An example of the two types of oversize correction is provided in Figure 3-12. The two methods do not give, exactly, the same results, and the method desired for each project should be clearly specified.

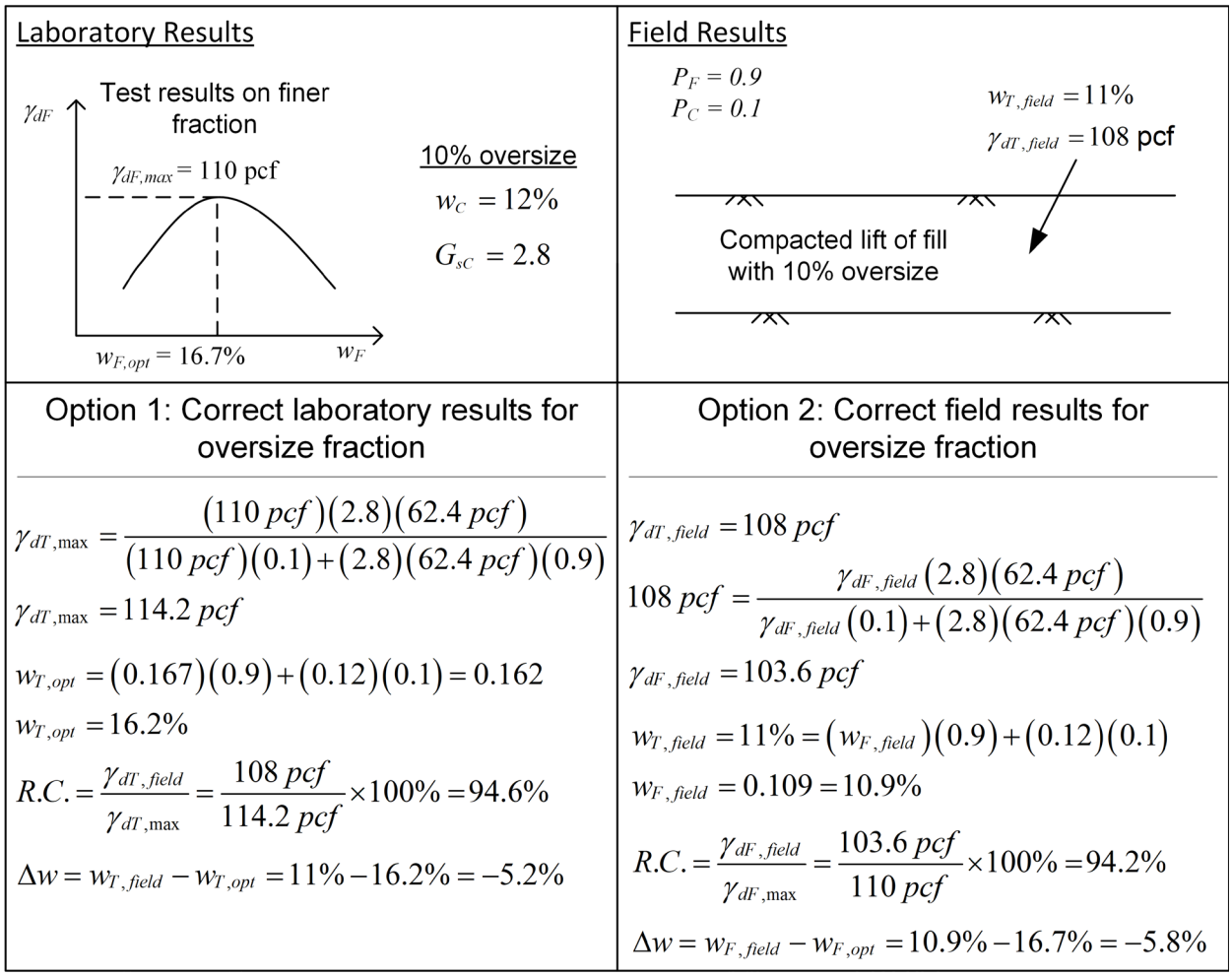

Figure 3-12 Oversize Correction Example Calculations

3-3.3.2 Engineering Parameter Testing.

In addition to reference compaction tests, engineered fill materials are often tested to verify adherence to material specifications and to determine soil-specific values of shear strength, compressibility, and hydraulic conductivity. While project conditions will dictate the specific types of information that are required, the applicable test methods for various fill materials are summarized in Table 3-3. Further description of these test methods can be found in Chapter 3 of DM 7.1 (NAVFAC 2021).

Table 3-3 Applicability of Testing Methods by USCS Classification

USCS Group Symbol	Test Methods (ASTM method)												
	Atterberg Limits (D4318)	Grain size distribution (D6913, D7928)	Moisture-Unit Weight (Proctor) (D698, D1557)	Maximum and Minimum Index Density (D4253, D4254)	California Bearing Ratio (D1883)	Direct shear (D3080)	Unconsolidated Undrained Triaxial Compression (D2850)	Consolidated Undrained Triaxial Compression (D4767)	Consolidated Drained Triaxial Compression (D7181)	Torsional Ring Shear (Residual Shear Strength) (D6467)	Hydraulic Conductivity (D5084)	One-Dimensional consolidation (D2435)	One Dimensional Swell or Collapse (D4546)
GW		A	A	A	A	S		A	A		A		
GP		A		A	A	S			A				
GM	A	A	A		A	S		A	A		A		
GC	A	A	A		A	S	M	A	M		A		A
SW		A	A	A	A	A		A	A		A		
SP		A		A	A	A			A				
SM	A	A	A		A	A	A	A	A		A	A	A
SC	A	A	A		A	A	A	A	M		A	A	A
ML	A	A	A		A	A	A	A			A	A	A
CL	A	A	A		A	A	A	A		A	A	A	A
MH	A	A	A		A	A	A	A		A	A	A	A
CH	A	A	A		A	A	A	A		A	A	A	A

A = test is applicable, M = test is marginally applicable, S = test is applicable with specialized equipment
Note: D3080 was officially withdrawn by ASTM in 2020 but remains an applicable method for testing many soils.

3-3.3.3 Rock Fill.

Rock fill can be defined as containing at least 30% clean rock with a grain size greater than ¾-inch and containing less than 15% fines (Breitenbach 1993). Rock fill is often placed with the major objective of creating a free-draining fill with rock-to-rock contacts throughout.

As discussed for the oversize portion of compaction test, laboratory characterization of rock fill materials is challenging because of the constraints on particle size imposed by laboratory testing equipment and standards. For example, the maximum particle size is limited to one-tenth of the specimen height for direct shear tests and one-sixth of the specimen diameter for triaxial tests. These constraints effectively limit laboratory shear strength testing to materials with particles no larger than 1 inch diameter, even for the most well-equipped commercial geotechnical laboratories. Most rock fills have a substantial fraction larger than 1 inch. Specialized large scale testing devices have been developed but are not commonly available.

The two primary alternatives for shear strength testing of rock fill with large particles are scalping and parallel gradations (Marachi et al. 1972). A *scalped* gradation refers to the complete removal of all particles larger than a particular grain size. The grain size distribution coefficients, C_c and C_u, of the scalped gradation will be lower than those of the parent rock fill. The scalped gradation is more poorly-graded than the rock fill. A *parallel* gradation is created by shifting the grain-size distribution to have 100% passing the largest allowable particle size but maintaining the shape of the distribution and the values of C_c and C_u. Creation of a parallel distribution requires a substantially larger initial soil sample and causes a more drastic change in the overall classification of the soil. Because of the level of effort and the size of the sample required, scalped gradations are typically preferred.

The shear strength of rock fill is affected by the stress level, roughness, and size of the particles as summarized in Table 3-4. Leps (1970) and others have described nonlinearity in the shear strength or friction angle of rock fill using a variety of equations. Larger particles are more likely to have defects and tend to break more easily. This effect can be considered through the parameters S or m described in Table 3-4. Marachi et al. (1972) found that increasing the particle size by a factor of four (i.e., $D_B/D_A = 4$) produced a 2 to 3.5 degrees decrease in ϕ', while the reduction in ϕ' was in the range of 3 to 5 degrees for $D_B/D_A = 12$. The Frossard et al. (2012) approach predicts similar reduction in ϕ'. The effect of particle size is most pronounced for rock fill with a wide range of particle strength or low m. The value of m for a rock fill can be measured using a large number of laboratory crushing tests (Marsal 1967, Lee 1992).

Two additional factors must be considered for rock fill but are difficult to quantify: (1) changes in the rock fill gradation during excavation and placement and (2) deterioration after placement (Sowers 1979). The first can be evaluated using a test embankment section and grain size analysis of samples of the fill following compaction. Potential for deterioration is especially important for shales, or sedimentary rocks composed primarily of clay and silt. These rocks have a wide range of hardness and can degrade substantially through wetting and drying, which is referred to as *slaking*. The most problematic shales for use as engineered fill are those which are initially hard but do not retain their properties after excavation and placement.

Where fill materials will contain shale, an appropriate system must be selected to determine the durability of the shale as well as its susceptibility to chemical degradation. Huber (1997) reviewed the available systems for classifying shale durability and recommended those proposed by FHWA (1978), Franklin (1981), and Wiles (1988). These systems use the jar slake test (Deo 1972), the slake durability test (ASTM D4644), the point load strength test (ASTM D5731), and Atterberg limits (ASTM D4318). The FHWA (1978) system divides shales into two major categories: soil-like and rock-like. The former require compaction similar to soil, while the latter are durable and can be treated as rock fill. Franklin's (1981) system provides a shale rating that has been correlated to various shale fill parameters. Wiles (1988) devised a durability rating system based on the loss of shear strength caused by wetting in triaxial tests. Susceptibility to chemical weathering is indicated by a pH less than 6 in the slake durability water as well as dark gray, green, or black color.

Table 3-4 Stress and Particle Effects on the Shear Strength of Rock Fill

Effect	Description	Applicable Equations	References
Nonlinearity	The shear strength envelope for rock fill is distinctly curved. The friction angle decreases with increasing effective normal stress.	$\phi' = \phi'_0 - \Delta\phi' \log\left(\frac{\sigma'_f}{P_a}\right)$ $\tau_f = a \cdot P_a \left(\frac{\sigma'_f}{P_a}\right)^b$	Leps (1970) Charles and Soares (1984) Lade (2010) Duncan et al. (2014) VandenBerge et al. (2018)
Particle strength and roughness	Frictional resistance is affected by rock fill roughness (related to relative density, origin, roundness, and smoothness) and particle strength, which tends to decrease with particle size.	$\phi' = R \cdot \log\left(\frac{S}{\sigma'_f}\right) + \phi'_b$	Barton and Kjaernsli (1981)
Particle diameter	As particle size increases, the likelihood of breakage increases. This can be described by a material parameter, m, which for rock fill varies from 4 for a wide range of particle strength to about 15 for uniform particle strength.	$a_B = a_A \left(\frac{D_B}{D_A}\right)^{\frac{-3\cdot(1-b_A)}{m}}$	Marsal (1967) Marachi et al. (1972) Frossard et al. (2012)

Notation: ϕ'_0 and $\Delta\phi'$ = parameters describing the change in friction angle with normal stress , P_a = atmospheric pressure (used for normalization), σ'_f = effective normal stress at failure (plane or orientation depends on usage), a and b = power function parameters describing nonlinearity (also a_A, a_B, b_A, and b_B), R = roughness factor, S = particle compressive strength, ϕ'_b = base friction angle, D_B/D_A = ratio of sizes between two parallel gradations, and m = Weibull distribution parameter for particle strength (mean value of 6 in data by Marsal 1967).

3-3.4 Alternative Fill Materials.

Materials other than natural soil can be used as fill. These materials include recycled products from construction or other industry as well as lightweight products manufactured for use as fill. Motivations for the use of alternative fill include concerns about sustainability, economics, lack of availability of appropriate natural materials, and efforts to reduce vertical or horizontal earth pressures.

Selection of alternative fill materials should consider multiple costs, including basic material cost, transportation cost, and placement costs. The quantity of required fill, availability of the alternative material, and local experience with construction methods also must be considered. Finally, special concerns, such as fill durability requirements, environmental concerns, and fill thermal parameters, must be addressed. Some of the intangible benefits of alternative materials may be reduced installation time leading to accelerated construction, lower weather sensitivity compared to natural soil, and reduced requirements for field quality control (FHWA 2017, Arellano 2019).

3-3.4.1 Recycled Fill Materials.

Typical properties of recycled fill materials are summarized in Table 3-5. Recycled fill materials are used as a replacement for natural soil in order to reduce disposal impacts and prevent disturbance of natural ground to obtain fill. In many cases, the recycled materials have more favorable engineering properties than natural soils.

Table 3-5 Typical Properties of Common Recycled Fill Materials (after Soleimanbeigi et al. 2014, Soleimanbeigi and Edil 2015, DiGioia and Nuzzo 1972, Masad et al. 1996).

Material	Typical properties or ranges					
	USCS	G_s	w_{opt} (%)	$\gamma_{d,max}$ (pcf)	k (cm/s)	ϕ' (deg)
Recycled asphalt pavement	SP, GW	2.45	5 to 10	120 to 125	10^{-3} to 10^{-2}	42
Recycled concrete aggregate	GW	2.7	5 to 10	120 to 125	10^{-4} to 10^{-3}	46
Recycled pavement material	GW	2.39	< 5	120 to 125	10^{-4} to 10^{-3}	44
Bottom ash	SP	2.67	< 5	95 to 100	10^{-3} to 10^{-2}	44
Recycled asphalt shingles	SW	1.74	5 to 10	70 to 75	10^{-4} to 10^{-3}	33
Foundry sand	SW	2.36	< 5	70 to 75	10^{-3} to 10^{-2}	36
Fly ash	ML	2.39	15 to 20	50 to 80	10^{-9} to 10^{-6}	33 to 40
Tire derived aggregate	SP and GP sized	1.07	NA	25 to 30	10^{-4} to 10^{-3}	NA

An important environmental consideration for recycled materials is that the fill does not contaminate groundwater or surface water through leaching or runoff. It is also important to note that the use of recycled materials does not necessarily lead to a more sustainable project. For example, long transportation can offset the benefits of using a recycled material. The most beneficial recycled materials are those which are available locally, improve the engineering properties of the fill, and are environmentally benign (VandenBerge et al. 2015).

3-3.4.2 Lightweight Fill Materials.

Engineered fill increases the stresses in the underlying ground. This can cause settlement, an increase in the stress on existing structures or walls, and a decrease in the stability of slopes. Lightweight fill materials, such as those listed in Table 3-6, can substantially reduce the stresses applied by a fill or embankment. Lightweight fill is commonly used for soft ground conditions and is often combined with ground improvement methods such as prefabricated vertical drains, deep mixing, and column-supported embankments (FHWA 2017).

Table 3-6 Common Lightweight Fill Materials (after FHWA 2017, Arulrajah et al. 2015)

Material	Unit weight (pcf)	k (cm/s)	Lateral earth pressure, K	Shear strength	Comments
Geofoam	0.7 to 3	10^{-6} to 10^{-2}	0.1	6 to 14 psi	Manufactured from expanded polystyrene (EPS) or extruded polystyrene (XPS), typically installed in large blocks, stability analyses must consider interface properties with soil and between blocks, unit weight increases with time when saturated, provides thermal insulation
Foamed glass aggregate (FGA)	15 to 20	High	Use ϕ' to estimate	ϕ' = 36 to 54°	Synthetic aggregate produced by heating recycled glass, closed and open cell available, provides thermal insulation, used in drainage blankets and green roofs, higher CBR than most lightweight materials
Cellular concrete	20 to 80	10^{-1}	Negligible for self-weight or vertical loads	10 to 300 psi	Manufactured, preformed foam mixed with cement slurry, pumped into place, can be permeable, generates negligible lateral earth pressure
Tire shreds or tire derived aggregate	30 to 73	0.5 to 60	0.25 to 0.47	ϕ' = 19 to 30°	Tires shredded into chips, can be bound together into bales, can be mixed with natural soil, more guidance can be found in ASTM D6270
Expanded clay shale (ECS)	40 to 65 (dry)	High	Use ϕ' to estimate	ϕ' = 35 to 45°	Synthetic, vitrified aggregate produced by heating clay or claystones, often used as aggregate in lightweight concrete, can degrade under steel-tracked equipment
Wood chips, fiber, and sawdust	45 to 60	≈10^{-5}	Use ϕ' to estimate	ϕ' = 25 to 49°	Friction angle increases as size of the particles increases, volume reduction of 40% on compaction, commonly used in low-volume roads
Blast furnace slag	70 to 94 (total)	10^{-3} to 1	Use ϕ' to estimate	ϕ' = 35 to 40°	By-product of iron production, air-cooled slag solidified under atmospheric conditions and is angular and vesicular, expanded slag is solidified using water which increases cellular nature, granulated slag is chilled quickly forming a glassy product, expanded and granulated slags are lighter but more expensive, pH in range of 8 to 12

Design of lightweight fill should determine which stresses must be reduced to make the design functional in terms of both stability and settlement (Arellano 2019). Once the required amount of stress reduction has been determined, appropriate lightweight fill materials can be considered based on the unit weight, availability, and costs. Lightweight mineral materials achieve low unit weight through a porous particle structure. For this reason, the crush resistance and durability of these materials should be considered (TRB 1990).

3-4 CONSTRUCTION OF COMPACTED FILLS.

Compacted fills are constructed to meet some, or all, of the objectives shown in Figure 3-1 for a particular purpose. In order to create a fill that meets these objectives, the construction process starts with establishing suitable drainage and preparing the fill subgrade. The selected fill material(s) are then excavated, transported, placed, and compacted at the site. Throughout the fill construction process, the engineer has the responsibility of protecting both the project owner and the broader environment. This includes confirming that appropriate materials are used, implementing compaction specifications, and enforcing contractor procedures for the control of runoff and the protection of adjacent bodies of water (TRB 1990).

3-4.1 Drainage.

According to Sowers (1979), drainage is a critical, but often overlooked, component of high quality fill construction. Establishing good drainage may have a high initial cost but tends to save money over the course of most projects. In general, soil becomes weaker and more difficult to compact as its water content increases. Inadequate drainage leads to construction delays and unstable subgrade or fill soils. Where possible, surface water should be kept dispersed rather than concentrated to reduce erosion potential. As needed, surface water should be intercepted by ditches or drains and directed away from the fill area. Prior to excavation, including at borrow areas, slope ditches should be installed near the crest and at midslope to keep water out of the excavation and to keep the fill dry.

Subsurface water should also be considered by observing the site topography and knowledge of groundwater sources. The groundwater control methods described in Chapters 1 and 6 of DM 7.1 (NAVFAC 2021) can be used to lower groundwater below fill areas or in excavations. Surface and subsurface drainage is especially important where the embankment soils are susceptible to deterioration when exposed to water, including high plasticity clays and shale fills.

3-4.2 Subgrade Preparation.

3-4.2.1 Ground Preparation.

After drainage has been established, the subgrade must be prepared for evaluation prior to the placement and compaction of the initial lift of fill. *Clearing*, which refers to removal of vegetation, trash, debris, and topsoil from the ground surface, should be completed within the bounds indicated on the plans. Topsoil is often stockpiled onsite for future use. *Grubbing* refers to deeper removal of stumps, heavy root mats, and buried objects. The extent of grubbing required must be specified. Deeper fills and those with less critical support requirements may not require grubbing (TRB 1990). Subsurface structures or debris that will interfere with compaction or the future construction should be removed. The sides of holes created by grubbing should be flattened, scarified, and compacted to similar unit weight as the foundation soil (USACE 1995a).

Unsuitable subgrade materials should be identified by subsurface exploration and observation after clearing and grubbing. Organically contaminated soils (Pt, OH, and OL) are generally not suitable for embankment support. Because of the detrimental effects of differential frost action, special attention should be given to removing near-surface frost susceptible soils and to limiting the availability of water to backfill.

Sites containing old fill, waste, ashes, sludge, slag, and mining spoils often require special preparation with specifics guided by the composition and past compaction of the old fill. For example, construction on poor quality existing fill will likely require ground improvement using methods described in Chapter 1. When dealing with mine waste, variable conditions can be present, including loose dumped materials as well as slurry and tailings deposits.

Special ground preparation is required for fills placed adjacent to existing slopes. If the slope is steeper than 3H:1V, the ground should be benched. Each *bench* consists of a horizontal cut followed by vertical step, typically not more than 4 feet high. The stair-stepped bench pattern prevents a weak zone from being created at the interface between the fill and the existing slope. In addition, slope protection in the form of riprap or drainage blankets may be needed to handle seepage from the fill or existing slope. The slope protection will help to prevent erosion and surficial slope failure (TRB 1990).

Finally, special preparation is required at the transitions between (1) cut and fill and (2) rock cut and soil cut in order to gradually accommodate the change between the differing subgrade support conditions. Material in these transition zones should be uniform without large (diameter greater than 6 inches) particles (TRB 1990). Where water may seep from the cut rock or soil, the transition fill may be used to provide drainage and prevent saturation and instability of the fill.

3-4.2.2 Proof Rolling and Subgrade Stability.

After clearing, grubbing, and other preparation, the relative stability of the fill subgrade is evaluated, often by *proof rolling*. Proof rolling refers to systematic trafficking of the subgrade surface by a loaded dump truck or roller. The purpose of proof rolling is to find instability and inconsistency in the subgrade or fill but not to induce widespread failure. A gross weight of 30 tons with 40 psi tire pressure is typically suitable for proof rolling of cut subgrades (TRB 1990). Once an acceptable proof rolling weight is determined, the proof roller should make two complete coverages of the subgrade and deflecting zones should be highlighted. In road construction, proof rolling can also be completed at the completion of the general earth fill and prior to placement of subbase.

The fill subgrade should be scarified and brought to optimum moisture content with special attention given to deflecting zones identified during proof rolling. The subgrade is then compacted and may be subjected to compaction control tests or further proof rolling prior to the placement of new fill.

3-4.2.3 Methods to Mitigate Subgrade Instability.

Where proof rolling indicates extensive instability or cannot be completed, soft subgrade conditions are present, and an initial thick stabilizing or bridging layer of sand, gravel, or crushed rock is required. Biaxial geogrid can be used below the layer to reduce the thickness of the bridging lift, and separation geotextile may be needed to prevent soft subgrade from pushing into the bridging lift. Gravity drainage should be provided to prevent water from collecting in the bridging lift. Vibrating construction equipment can exacerbate instability and should be limited until a stable working platform is achieved.

Chemical stabilization of the existing soil can also be used to improve subgrade stability. Stabilization is achieved by mixing a drying and/or cementing admixture, such as cement, fly ash, lime, or cement kiln dust, into the unstable soil. Shallow mixing can be accomplished by discing while deeper (up to 24 inches) treatment can be achieved using a specialized soil stabilizing mill. The appropriate percentage of the chemical admixture can be selected based on experience or a formal mix design that uses laboratory testing. Guidance for the selection of admixtures can be found in FHWA (2017).

Unstable soils may present concerns of long-term consolidation or low shear strength below the fill. In this case, vertical drains and/or preloading may be required to accelerate or induce consolidation (see Section 5.7.4 of DM 7.1, NAVFAC 2021) and increase the shear strength. The unstable material may also be improved using ground improvement methods described in Chapter 1.

3-4.3 Excavation, Transport, and Placement.

3-4.3.1 Methods.

Excavation is an important part of the process of manufacturing a quality fill and should be supervised by the engineer. Adequate drainage should be provided in the borrow area in order to maintain the appropriate water content of the fill material for efficient excavation and compaction. In addition, material processing may be required at the borrow, such as scalping oversize or mixing strata to create a homogenous fill.

Selection of appropriate and efficient excavation equipment is typically the decision of the contractor. Excavation methods can include hand tools, excavators, scrapers, graders, and draglines. In some cases, ripping and blasting may be required prior to excavation. More guidance on these can be found in Section 2-5 and FHWA (1991). Because the excavation method can affect the degree of mixing at the borrow, the engineer should be consulted. Blasting also requires consultation with the owner and engineer to determine vibration limitations, inspection requirements, and requirements for the final condition of the borrow area (TRB 1990).

Special care is required where the borrow source contains both durable rock fill and either soil or nondurable rock, such as degradable shale. Mixtures of these two materials should be avoided, because they are very difficult to adequately compact. In particular, nondurable shale should not be mixed with more durable sandstone or limestone in rock fill (FHWA 1978). Where borrow contains both, the durable rock should be separated for use as drainage fill and the outer shell of slopes, while the nondurable rock can be compacted separately as general fill.

An appropriate method must be selected to transport the fill. A variety of transport methods and economical haul distances are summarized in Table 3-7. The transportation and placement of fill can promote either segregation or mixing. If material separation is required, transportation methods should be carefully considered. As fill is dumped and spread, attention should be given to breaking large lumps of soil and removal of deleterious materials. Additional mixing of the fill can be performed at the fill location, if needed.

Table 3-7 Fill Transport Methods and Haul Distances (after Coduto et al. 2011)

Transport Method	Transport Details	Economical Haul Distance (ft)
Bulldozer	Fill pushed over ground surface, off-road only	< 300
Wheel loader	Fill carried in loader bucket (up to about 15 C.Y.), off-road only	150 to 500
Scraper	Fill excavated, hauled, and placed with one machine, about 25 to 35 C.Y. capacity, off-road only	1000 to 8000
Dump truck	Fill loaded into truck, hauled, and end-dumped at site, capacity ranges from 15-25 ton (on-road) to 42 ton (off-road articulating) up to 400 ton (mining)	1100 to 21,000 (4 miles)
Conveyor belt	Move large quantities over rough terrain, can be used with automated processing facilities	100 to 36,000 (7 miles)
Semi-Tractor Wagon	Fill end, side, or bottom-dumped at site, can be towed on or off-road, up to 120 ton capacity	> 10,000 (2 miles)

In many cases, the water content of the fill must be adjusted to meet the compaction specifications. Depending on the soil type as well as the method and distance of transport, this may be accomplished at the borrow area or at the fill. Coarse-grained soils with little fines often require additional water for compaction, and water trucks or hoses are used to increase the water content immediately prior to or during compaction. While water can be added and mixed into fine-grained soils, it is more common that the water content of these materials is too high. Drying can be accomplished by evaporation over time and accelerated by mixing the soil with a disk, harrow, or tiller. Chemical admixtures, such as cement, fly ash, lime, or cement kiln dust, are also drying agents and can be used when weather or time do not allow air drying.

3-4.3.2 Borrow and Fill Quantities.

Calculation of fill volumes at the borrow site, during transportation, and after compaction is an important aspect of earthwork planning. In the borrow, the soil has an average dry unit weight ($\gamma_{d,B}$). As the soil or rock is excavated for transport, *bulking*[14] will occur, which is a decrease in dry unit weight caused by an increase in the overall volume. Coarse-grained soils tend to bulk about 10% when excavated while fine-grained soils may bulk 30% to 40% (Coduto et al. 2011). Once the soil is placed and compacted, the dry unit weight of the fill ($\gamma_{d,F}$) may be either greater or less than $\gamma_{d,B}$. An average value of $\gamma_{d,F}$ can be estimated using the laboratory compaction curve and assuming an average relative compaction about 2% higher than the minimum specified value (Coduto et al. 2011).

Some fill material will be lost in the earthwork process, which is referred to as *waste*. Waste can be intentional, such as the removal of oversize material, or unintentional.

[14] This increase in volume is also referred to as *swelling*. However, bulking will be used in this manual to distinguish from the volume expansion that occurs when clay minerals are hydrated.

For example, a borrow with a large percentage of cobbles (diameter > 3 inches) may have a large amount of waste if the cobbles are excluded from the fill.

Comparison of total borrow and fill volumes must consider both changes in unit weight and waste. *Shrinkage* occurs when the earthwork process causes a reduction of volume. Bulking can occur overall if $\gamma_{d,F}$ is less than $\gamma_{d,B}$ and the amount of waste is low. The total weight of solids remains constant through the calculations even though the total volume changes.

If the fill volume (V_F) is known and the total waste (W_L) can be estimated, the total borrow volume can be calculated as:

$$V_B = V_F \frac{\gamma_{d,F}}{\gamma_{d,B}} + \frac{W_L}{\gamma_{d,B}} \tag{3-8}$$

where:
V_B = total borrow volume required,
$\gamma_{d,F}$ = average dry unit weight of the fill,
$\gamma_{d,B}$ = average dry unit weight of the borrow, and
W_L = total weight of waste.

In some cases, the waste must be estimated as loss percentage (X_L) and the total borrow volume is:

$$V_B = V_F \frac{\gamma_{d,F}}{\gamma_{d,B}}\left(1 + X_L\right) \tag{3-9}.$$

The overall *shrinkage factor* can be defined as:

$$\frac{\Delta V}{V_F} = \frac{\gamma_{d,F}}{\gamma_{d,B}}\left(1 + X_L\right) - 1 \tag{3-10}$$

where:
ΔV = change in total volume = V_B - V_F.

If more detailed unit weight information is not available, a shrinkage factor of 10% to 15% of V_F can be used for estimating purposes. If required, transportation volumes can also be calculated by replacing $\gamma_{d,B}$ in the preceding equations with the dry unit weight during transport, ($\gamma_{d,trans}$). An example of borrow and fill calculations is provided in Figure 3-13.

Embankment Borrow Calculations

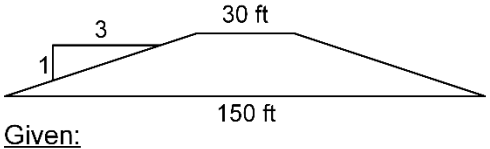

Cross-Sectional Area: $A = \frac{150\,ft + 30\,ft}{2} \cdot 20\,ft = 1800\,ft^2$

Volume of Fill (per foot): $V_F = 1800\,ft^3$

Given:

Soil Properties: G_s = 2.7, $\gamma_{d,max}$ = 115 pcf, w_{opt} = 14% (ASTM D698), and $\gamma_{d,borrow}$ = 102 pcf

Compaction: Average $R.C.$ = 98% at w = 14%,

Assume:

Void ratio in truck e_{truck} = 1 and Loss Factor = 2% by dry weight

Find (Per Foot of Embankment):

- Trucking Volume
- Volume of Borrow
- Waste

Fill Volume

$$\gamma_d = \frac{\gamma_w G_s}{1 + e_{truck}} = \frac{(62.4\,pcf) \cdot 2.7}{1+1} = 84.2\,pcf \qquad \gamma_{d,f} = \frac{RC}{100} \cdot \gamma_{\max} = \frac{98\%}{100} \cdot 115\,pcf = 112.7\,pcf$$

$$V_{truck} = V_F \cdot \left(\frac{\gamma_{d,f}}{\gamma_{\gamma,truck}} \right) = 1800\,ft^3 \cdot \left(\frac{112.7\,pcf}{84.2\,pcf} \right) = 2409 \frac{ft^3}{ft} = 89 \frac{CY}{ft}$$

Volume of Borrow

$$V_{borrow} = V_F \cdot \frac{\gamma_{d,f}}{\gamma_{\gamma,truck}} (1 + X_c) = 1800\,ft^3 \cdot \left(\frac{112.7\,pcf}{102\,pcf} \right) (1 + 0.02) = 2029 \frac{ft^3}{ft} = 75 \frac{CY}{ft}$$

Waste

$$W_L = V_F \cdot \gamma_{d,f} \cdot X_c = (1800\,ft^2)(112.7\,pcf)(2\%) = 4057 \frac{lb}{ft} = 2 \frac{tons}{ft}$$

Figure 3-13 Borrow Excavation Example

Because of its dense state *in situ*, rock fill will experience bulking from the borrow to the fill state. Maximum bulking will tend to occur for borrow consisting of dense, hard rock with fine fracture systems that breaks into uniform sizes. In this case, the shrinkage factor may be -50% (i.e., unit volume in the borrow will produce approximately 1.5 volumes in the fill). A minimum bulking (a.k.a., minimum expansion) condition occurs in porous, friable rock that breaks into broadly-graded pieces with numerous spalls and fines. In this case, the shrinkage factor may be as low as -10%.

3-4.4 Compaction.

After soil is transported to the project site, it is spread and compacted in layers or lifts of relatively uniform thickness by consistent coverage of the compaction equipment. This

aspect of earthwork involves control of the major factors that influence soil compaction behavior (Section 3-2), including soil type, water content, compactive effort, and type of compaction. Efforts should also be made to route equipment, such as dozers and dump trucks, uniformly across the surface of the fill. This will provide some compactive effort and will minimize the effort required from other equipment. In addition, it will reduce the potential for rutting and overloading the fill.

3-4.4.1 Influence of Soil Type and Water Content.

Most soils used as fill are at least somewhat sensitive to the water content during compaction. For example, silts and some silty sands have steep compaction curves, and field moisture must be controlled within narrow limits for effective compaction. Clays are sensitive to moisture. If they are too wet, they are difficult to dry to optimum moisture, and if they are dry, it is difficult to mix the water in uniformly. An extreme example is sensitive clays, which do not respond to compaction because they lose strength upon remolding or manipulation. Soils in this category tend to compact more effectively using impact, static, and kneading compaction.

Coarse-grained soils with less than 5% to 15% fines are relatively insensitive to the compaction water content. The lower limit applies to well-graded soils while poorly-graded soils can contain more fines and still be insensitive to compaction moisture. These soils tend to have a hydraulic conductivity greater than 0.001 cm/s. These materials can be placed at the highest practical moisture content, preferably close to 100% saturation. Vibratory compaction generally is the most effective procedure. In these materials, a relative density of 70 to 75 percent can be obtained with proper compaction procedure, and relative density should be used for compaction control.

Gravel, cobbles, and boulders are also insensitive to compaction moisture. Compaction with smooth wheel vibrating rollers is the most effective procedure.

3-4.4.2 Types of Equipment.

The four major methods of compaction are (1) pressure; (2) impact; (3) vibration; and (4) manipulation, kneading, or shearing. With the exception of small equipment, most compaction equipment possesses significant weight. However, the contact pressure can vary widely from high pressures under tamping foot (a.k.a., sheepsfoot) rollers[15] to low pressures under smooth-drum rollers. While impact compaction is the primary method of laboratory compaction, it is primarily used in the field by power tampers and some operation modes of tamping and grid rollers. Vibration applies dynamic forces to soil particles that promote compaction and is used by vibratory tamping foot and

[15] While the term *sheepsfoot* is commonly used, rollers which use true sheepsfoot tines are rare in current earthwork practice.

smooth-drum rollers, vibratory base plate compactors, and grid compactors. Kneading compaction manipulates and shears the soil and is applied by tamping foot and rubber-tired rollers.

Table 3-8 lists commonly used compaction equipment with typical sizes and weights. In general, the compaction equipment should exert the highest contact pressure that does not result in rutting (i.e., bearing capacity failure) or failure to *walk out* of the fill (Sowers 1979). Walking out refers to the ability of tamping foot rollers to penetrate less and less into the fill as the fill becomes well-compacted.

The appropriate lift thickness will depend on the combination of the soil type, equipment, and fill purpose. Table 3-9 provides guidance on the applicability of different equipment to various soil conditions along with typical compacted lift thickness and number of passes. In general, the thicknesses in Table 3-9 are a satisfactory starting point. Thicker lifts may be appropriate for general purpose fills, if adequate compaction is still achieved. For water retaining fills, thinner lifts may be required to produce the desired hydraulic conductivity throughout the fill.

Selection of appropriate compaction equipment continues through the earthwork process by observation of the fill performance. When fill that is wet of optimum is compacted excessively, it deforms and deflects in an elastic manner, which is referred to as *weaving* or *pumping*. In this state, the fill is nearly saturated, and application of compactive effort is ineffective at removing further air from the fill. Further compaction can lower the dry unit weight. When the compaction equipment is too heavy for the fill or the fill is too wet, the equipment will sink into the fill causing *rutting*, which is a bearing capacity failure that must be fixed before earthwork can continue (TRB 1990).

Table 3-8 Equipment Type Summary

Equipment	Dimensions and Weight			Possible Variations in Equipment
Tamping Foot Roller	Soil Type	Contact area	Foot contact pressure	For earth dam, highway and airfield work, articulated self-propelled rollers are commonly used. For smaller projects, towed 40 to 60 inch drums are used. Foot contact pressure should be regulated to avoid shearing the soil on the third or fourth pass. Tamping foot rollers must penetrate a loose lift (too light otherwise) and should walk out as compaction proceeds (too heavy otherwise or soil too wet).
	Fine, PI > 30	5 to 12 ft^2	250-500 psi	
	Fine, PI < 30	7 to 14 ft^2	200-400 psi	
	Coarse	10 to 14 ft^2	150-250 psi	
	Efficient compaction wet of optimum requires less contact pressure than that required for the same soil at lower moisture contents.			
Rubber Tire Roller	Tire inflation pressures of 35 to 130 psi for clean granular material of base course and subgrade compaction. Wheel load of 18,000 to 25,000 lbs.			A wide variety of rubber tire compaction equipment is available. For fine-grained soils, light-wheel loads, such as provided by wobble-wheel equipment, may be substituted for heavy-wheel load if lift thickness is decreased. For granular soils, large-size tires are desirable to avoid shear and rutting. In general, higher tire pressure is more effective than higher wheel load. Increased tire size with same pressure results in deeper compaction.
	Tire inflation pressures in excess of 65 psi, for fine-grained soils of high plasticity. For uniform clean sands or silty fine sands, use large size tires with pressures of 40 to 50 psi.			
Smooth Wheel Rollers	Tandem type rollers for base course or subgrade compaction; 10 to 15-ton weight or 300 to 500 lb per inch of rear roller width.			Three-wheel rollers are obtainable in wide range of sizes. Two-wheel tandem rollers are available in the weight range of 1 to 20 tons. Three-axle tandem rollers are generally used in the weight range of 10 to 20 tons.
	Three-wheel roller for compaction of fine-grained soil; weights from 5 to 6 tons for materials of low plasticity to 10 tons for materials of high plasticity.			
Vibrating Tamping Foot Rollers	1 to 20-ton ballasted weight. Dynamic force up to 20 tons.			May have either fixed or variable cyclic frequency.
Vibrating Smooth Drum Rollers	1 to 20-ton ballasted weight. Dynamic force up to 20 tons.			May have either fixed or variable cyclic frequency. Heavy roller with low frequency for rockfill and clays. Lighter and high frequency for sand. Best performance for soil at, or slightly above, optimum.
Vibrating Baseplate Compactors	Single pads or plates should weigh no less than 200 lb. May be used in tandem where working space is available. For clean coarse-grained soil, vibration frequency should be no less than 1,600 cycles per minute.			Vibrating pads or plates are available, hand-propelled, single or in gangs, with width of coverage from 1.5 to 15 ft. Various types of vibrating-drum equipment should be considered for compaction in large areas.
Grid Pattern Roller	Towed by a tractor or dozer. Contact pressure between 200 and 900 psi with 50% coverage.			Generates vibration, crushing, and impact when towed at high speeds.
Crawler Tractor or Dozer	Vehicle with standard tracks having contact pressure not less than 10 psi.			Tractor weight up to 85 tons.
Power Tamper or Rammer	30-lb minimum weight. Considerable range is tolerable, depending on materials and conditions.			Weights up to 250 lb, foot diameter 4 to 10 in.

Table 3-9 Applicability of Compaction Equipment to Different Soil Types

Type of Fill Material		Typical compacted lift thickness (inches) for different compaction equipment (compaction method indicated in parentheses)									# of passes or coverages
		Tamping foot (kneading)	Pneumatic / rubber tired (kneading)	Smooth wheel (static only)	Vibrating tamping foot (kneading, vibration)	Vibrating smooth drum (vibration)	Vibratory baseplate compactor (vibration)	Grid (vibration, impact)	Crawler tractor	Power tamper or rammer (impact)	
Fine-grained	General fine-grained	6 to 12	6 to 8	6 to 8							4 to 8
	Water retaining fills	6 to 12	6 to 8								4 to 6
Coarse-grained	General coarse-grained	6 to 12	6 to 8	6 to 8	8 to 12	6 to 12	8 to 10	6 to 12	6 to 10		3 to 5
	Dirty, $P_{\#200}$ > 8%	6 to 12	6 to 8	6 to 8	8 to 12	6 to 12		6 to 12			6 to 8
	GW base or subbase			8 to 12		6 to 12		6 to 12			4
	Clean, $P_{\#200}$ =4-8%		10	8 to 12		6 to 12	8 to 10	6 to 12	6 to 10		3 to 5
	Gravel			8 to 12		6 to 12		6 to 12			3 to 5
	Durable rock fill					up to 36					4 to 6
All soils, difficult access such as trench backfill										4 to 6	2

3-4.5 Special Construction Conditions.

3-4.5.1 Rock Fill.

Rock fill should be placed and compacted to a dense state without large voids so that overlying material will not settle or migrate into the rock fill. Rock fill can be placed in compacted lifts up to 3 feet thick. In general, the compacted lift thickness should be at least 1.5 times the largest particle diameter (TRB 1990). Dozers can be used to crush oversized particles or rake them from the fill. Compaction should be performed with 10 to 20-ton vibratory rollers operating at about 20 to 25 Hz. Appropriate compaction is typically achieved with about four to six roller passes, while additional passes pulverize

the surface without increasing compaction. The rock fill fraction smaller than ¾-inch diameter should be near its optimum moisture content for best compaction (Breitenbach 1993).

Special attention should be given to the durability of rock fill as discussed in Section 3-3.3.3. Nondurable rock should be treated similar to soil when used as fill. It should be broken down during compaction such that the large voids are filled and particle migration will be prevented if slaking occurs. This can be difficult if the shale is hard but nondurable. Problematic shales often require use of a tamping foot roller to break the particles followed by a large rubber-tired roller to compact the fill. Experience has shown that good compaction with a lift thickness of 8 inches will result in no major problems and few minor problems, regardless of the durability of the fill (FHWA 1978).

3-4.5.2 Retaining Wall Backfill.

As described in TRB (1990), lateral earth pressures on fill-type retaining walls depend heavily on the type of soil used as backfill, the placement conditions, and compaction methods. Prediction of these pressures is discussed in more detail in Chapter 4. If possible, clean, free-draining soil should be used as retaining wall backfill. Material substitutions should not be allowed for retaining wall backfill without approval of the engineer. Frozen material should not be used as backfill.

Retaining wall backfill should be spread evenly in lifts of 6 to 8 inches or less, depending on the size of the compaction equipment. The water content should be controlled closely and kept near optimum to minimize the required compactive effort and loading on the wall.

3-4.5.3 Cold Weather Considerations.

Experience and research have shown that adequate compaction of moist soil is very difficult in freezing temperatures. The water in the soil has higher viscosity at low temperature. Even coarse-grained soils require much higher compactive effort when compacted near or below freezing. For example, Modified effort at 30° Fahrenheit produces a lower dry unit weight than Standard effort at 74 deg Fahrenheit (TRB 1990). In addition to difficulty compacting the soil, frozen soil may contain substantial moisture in the form of ice. When this ice eventually thaws, the fill may be softened by the additional moisture, leading to poor performance.

3-4.5.4 Trench Backfill.

Backfill within trenches (depth greater than width and width less than about 15 feet) must be adequately compacted, even when poorly graded gravel, such as a #57 gradation, is used. Compaction in trenches can be difficult and requires special and/or small equipment. In addition, OSHA safety considerations apply as described in

Chapter 2. While sometimes it may be necessary to jet sand backfill into place around utility pipes (Coduto et al. 2011), flooding of fill into trenches is not recommended (Holtz et al. 2011). In trenches less than 3 to 4 feet wide, the backfill should be a clean sand or gravel that can be easily placed in 6 to 12-inch thick compacted lifts at a high water content. USACE (1995b) provides guidance on compaction in confined areas for water retaining structures.

3-5 CONTROL OF COMPACTED FILLS.

Compaction improves all or most of the engineering parameters of a soil or rock fill (see Figure 3-1) but is expensive both economically and environmentally. Thus, the decision whether an adequate level of compaction has been achieved is a critical step in the earthwork process (Coduto et al. 2011). This decision-making process is referred to as *quality assurance* (QA) when completed by an entity other than the contractor and *quality control* (QC) when completed by the contractor. *Compaction control* refers to the QA process coupled with in-depth regulation of the earthwork process appropriate to an owner's representative.

Most of this section focuses on the quantitative aspects of field testing for compaction control. However, the visual observations and simple measurements summarized in Table 3-10 are just as critical to good compaction control. Field engineers monitoring earthwork using these methods will stay active throughout the earthwork process regardless of the number of compaction control tests performed.

3-5.1 Compaction Requirements.

The target level of compaction is typically defined using either end-result or method specifications. The number and size of QA tests performed on an earthwork project is always small with respect to the size of the fill (USBR 1987). For this reason, a well-defined compaction procedure is required for adequate compaction control, regardless of the type of specification used.

End-result specifications require that the fill be compacted to a minimum and/or average dry unit weight and may include a limitation on the compaction water content. End-result specifications may include a maximum lift thickness but allow the contractor freedom in the selection of compaction methods and equipment. Because of soil variability and the uncertainties in the construction process, the specified dry unit weight is typically stated in terms of relative compaction or relative density as compared to an applicable standard. Most often, compaction specifications use relative compaction (Equation 3-3), which is applicable to soils with appreciable fines. For these soil types, an acceptable range of relative water content (Equation 3-4) may also be specified.

Relative density (Equation 3-5) is sometimes used to determine the compaction of clean coarse-grained soils. However, D_r ranges from 0% to 100% over approximately the

range of dry unit weights corresponding to $R.C.$ of 80% to 100%. For this reason, D_r is much more sensitive to small changes in the field dry unit weight, and more variation should be expected in the compaction control tests, if D_r is used. A useful alternative for clean coarse-grained soils is to use the relative compaction concept along with ASTM D4253 as means of determining the maximum dry unit weight rather than the Proctor compaction test.

Table 3-10 Simple Compaction Control Methods for Field Engineers (after TRB 1990, USACE 1995a)

Compaction Variable to Monitor	Simple Control Method
Compaction method	Record equipment used to place and compact the soil, including equipment model or weight.
Compactive effort	Count and record number of passes of compactor.
Compacted lift thickness	Elevation of each test via global positioning system (GPS), conventional surveying, or hand level and benchmark.
Soil type	Regularly record visual soil description and classification (ASTM D2488). If possible, have the field engineer help with laboratory characterization of fill materials (i.e., Atterberg limits and Proctor tests).
Soil moisture (soil with appreciable fines)	Use Visual-Manual tests to assess proximity to Plastic Limit and optimum water content (typically $w_{opt} = PL$ - 2%±).
	Excessively wet soil: Rubber-tired equipment will sink up to 50% of tire width. Fill surface weaves or pumps in response to compaction equipment. Fill remains stuck to the roller.
	Appropriate moisture: Rollers track in 3 to 4 inches on first pass but progressively penetrates less deeply with each pass (i.e., *walks out*). Feet of tamping foot rollers become clean after a few passes.
	Excessively dry soil: Fill surface becomes hard and dry after a few passes. Fill shows little or no response to weight of compaction equipment.
Soil response to hauling and compaction equipment	Soil with appreciable fines: Weaving and rutting indicates excessively wet soil or excessively heavy compaction equipment. Some springing or deformation immediately under the equipment is expected.
	Clean coarse-grained soils: Vibratory rollers should only push a small amount of soil in front of the roller, otherwise the vibration frequency is incorrect, or the material has too high of a fines percentage.
Penetration resistance	Soil with appreciable fines: Use T-Probe, Proctor needle, or pocket penetrometer to obtain a semi-quantitative assessment of compacted fill. The feel of the probe or measured values provide a site-specific correlation to level of compaction.
	Clean coarse-grained soils: Press a boot heel into the compacted soil. The heel will create a rotational general shear type of bearing capacity failure in well-compacted soil. The heel will simply sink into poorly compacted soil.

Table 3-11 summarizes typical end-result compaction specifications in terms of relative compaction for various purposes. These specifications can be modified to meet site-specific conditions and materials. USBR (1987) requirements for earth dams are summarized in Table 3-12 in terms of both relative compaction and relative density.

Table 3-11 Typical Compaction Specifications for Soil with Appreciable Fines

Fill Used for:	Typical Min. *R.C.*	Δw^A	Compacted Lift Thick.	Special Requirements
Structural Support	100% (D698) 95% (D1557)	-2% to +2%	Up to 12 inches	Fill should be uniform. Blending or processing of borrow may be required. For plastic clays, investigate expansion induced by saturation for various compaction moisture and densities at loads equal to those applied by structure, to determine condition to minimize expansion. Clays that show expansive tendencies generally should be compacted at or above optimum moisture to a unit weight consistent with strength and low compressibility required of the fill.
Lining for canal or small reservoir	95% (D698) 90% (D1557)	-2% to +2%	Up to 6 inches	For thick linings, GW-GC, GC, and SC are preferable for stability and to resist erosive forces. Single size silty sands with PI less than five generally are not suitable. Remove fragments larger than 6 inches before compaction.
Support of pavements	100% (D698) 95% (D1557)	-2% to +2%	---	Place coarsest borrow materials at top of fill. Investigate expansion of plastic clays placed near pavement subgrade to determine compaction moisture and unit weight that will minimize expansion and provide required soaked CBR values.
Backfill surrounding structure	95% (D698) 90% (D1557)	-2% to +2%	Up to 8 inches	Where backfill is to be drained, provide pervious coarse-grained soils. For low walls, do not permit heavy rolling compaction equipment to operate closer to the wall than a distance equal to about two-thirds of the unbalanced height of fill at any time. For highwalls or walls of special design, evaluate the surcharge produced by heavy compaction equipment by the methods of Chapter 4 and specify safe distances back of the wall for its operations.
Backfill in pipe or utility trenches	95% (D698) 90% (D1557)	-2% to +2%	Up to 8 inches for general sitework; 12 inches or more for pipelines	Material excavated from the trench generally is suitable for general trench backfill if it does not contain organic matter or refuse. The excavated material is typically unsuitable for pipe bedding. Instead bedding material is typically coarse-grained soil or controlled low-strength material (flowable fill). Where free draining sand and gravel is utilized, the trench bottom may be finished flat and the granular material placed saturated under and around the pipe and compacted by vibration. More stringent compaction requirements may be appropriate in the upper foot of trenches, especially in pavement areas. Special backfilling procedures may be required in seismic zones.
Drainage blanket or filter	95% (D698) 90% (D1557)	Wet	Up 8 inches	Ordinarily, vibratory compaction equipment is utilized. Blending of materials may be required for homogeneity. Segregation must be prevented in placing and compaction. For compaction adjacent to and above drainage pipe, use hand tamping or light travelling vibrators.
Structure subgrade excavation	100% (D698) 95% (D1557)	-2 to +2	---	For uniform bearing or to break up pockets of frost susceptible material, scarify the upper 8 to 12 inches of the subgrade, dry or moisten as necessary and recompact. Certain materials, such as heavily preconsolidated clays, which will not benefit by compaction, or saturated silts and silty fine sands that become quick during compaction, should be blanketed with a working mat of lean concrete or coarse-grained material to prevent disturbance or softening. Depending on foundation conditions revealed in exploration, a substantial thickness of loose soils may have to be removed below subgrade and recompacted, or compacted in place by vibration, or pile driving.
Water retaining structures	See Table 2-12		Up to 12 inches	Core material and other impervious zones should be placed and compacted to create a homogeneous fill without horizontal stratification. The compacted surface of each lift should be heavily scarified prior to the placement of the next lift.

[A] Relative water content, $\Delta w = w_{field} - w_{opt}$

Table 3-12 Compaction Control Criteria for Compacted Earth Dams (after USBR 1987)

Material	Fraction of soil passing #4 sieve ($P_{\#4}$)	Compaction Control Criteria (based on $P_{\#4}$ fraction)					
		Height less than 50 ft			Height greater than 50 ft		
		Minimum	Average	Δw[A]	Minimum	Average	Δw[A]
Soil with appreciable fines	$P_{\#4}$ > 75%	$R.C. \geq 95\%$	$R.C. \geq 98\%$	-2% to +2%	$R.C. \geq 98\%$	$R.C. \geq 100\%$	-2% to 0%
	$P_{\#4}$ = 75% to 50%	$R.C. \geq 93\%$	$R.C. \geq 95\%$		$R.C. \geq 95\%$	$R.C. \geq 98\%$	
	$P_{\#4}$ < 50%	$R.C. \geq 90\%$	$R.C. \geq 93\%$		$R.C. \geq 93\%$	$R.C. \geq 95\%$	
Soil without appreciable fines	Fine sand, $P_{\#4}$ > 75%	$D_r \geq 75\%$	$D_r \geq 90\%$	Soil should be very wet	$D_r \geq 75\%$	$D_r \geq 90\%$	Soil should be very wet
	Medium sand $P_{\#4}$ > 75%	$D_r \geq 70\%$	$D_r \geq 85\%$		$D_r \geq 70\%$	$D_r \geq 85\%$	
	Coarse sand and gravel	$D_r \geq 65\%$	$D_r \geq 80\%$		$D_r \geq 65\%$	$D_r \geq 80\%$	

[A] Relative water content, $\Delta w = w_{field} - w_{opt}$

Method specifications require the contractor to use a particular earthwork process (i.e., placement, lift thickness, equipment type, water content, number of passes, etc.) that is known to produce the desired result in the compacted fill. Method specifications are most common for large projects and for locations or materials where the determination of $\gamma_{d,field}$ is difficult, such as confined spaces or rock fills. The earthwork process in a method specification is typically determined using a field test section, which is a smaller scale embankment compacted using a variety of means and methods (see Section 3-5.2). In some cases, special equipment can be specified based on experience with local conditions and available fill materials.

3-5.2 Field Test Sections.

A field test section can be used to define a definite and appropriate compaction procedure for a particular combination of site conditions and fill material. In some cases, the field test section is used to develop a method specification. In other cases, a test section may be used to refine the compaction procedure. An example of the field test section process is shown in Figure 3-14. Combinations of the compaction variables, such as water content, compaction equipment, lift thickness, and equipment passes, are varied systematically. The results are typically plotted in terms of dry unit weight and number of passes.

Test sections provide an opportunity for field-scale testing of the engineering parameters of the fill material. Shelby tubes or block samples can be obtained from the

compacted fill for laboratory shear strength, compressibility, or hydraulic conductivity testing. Any differences in the field compacted parameters can be used to refine the project design. Large double-ring infiltrometer tests (ASTM D3385) can be performed to evaluate the field hydraulic conductivity of compacted fine-grained soils used as seepage barriers. The results from these field tests can be used to select the appropriate compaction procedure or can be correlated to laboratory tests, which can be more easily performed.

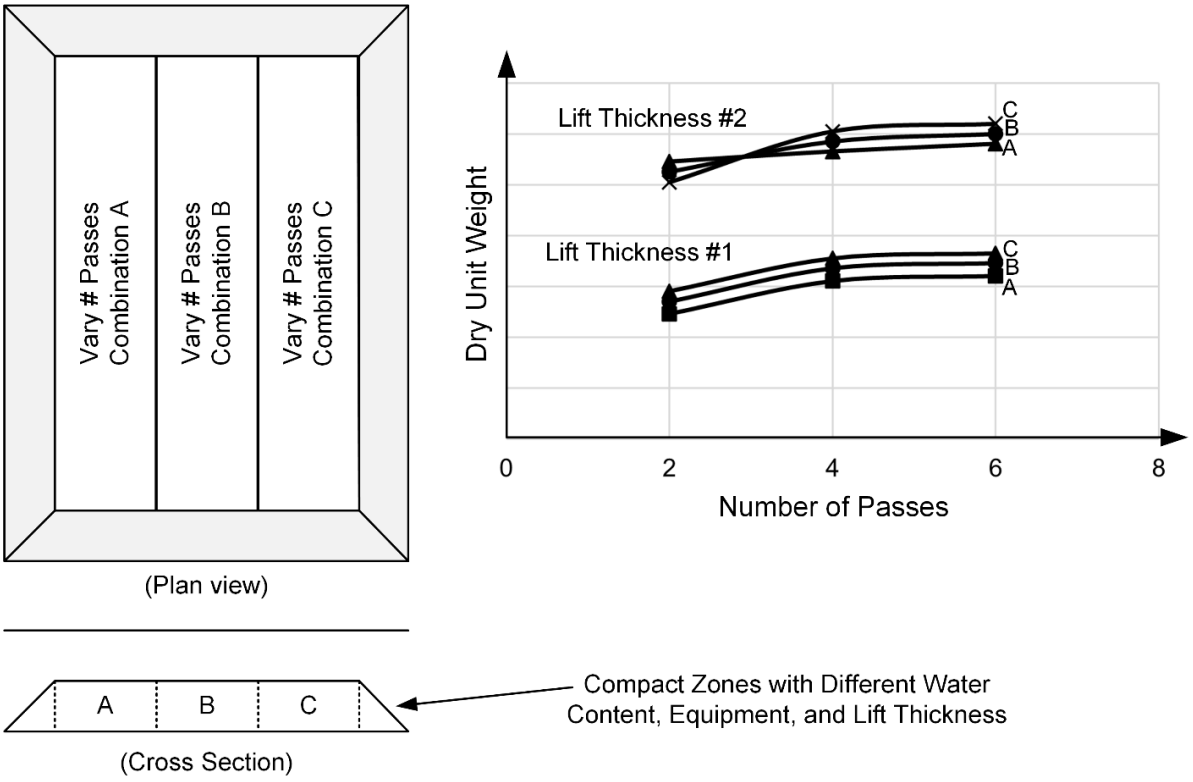

Figure 3-14 Schematic of Field Test Section Process

Field test sections are particularly important for rock fills (USACE 1994b), especially those constructed with nondurable rock, such as shale. The compacted dry unit weight of rock fill is time-consuming and expensive to determine and is often impractical to regularly measure during earthwork. In addition, the engineering parameters of rock fill are difficult to measure in the laboratory without altering the grain-size distribution. A field test section allows some parameters, such as compacted hydraulic conductivity, to be measured directly. It is not feasible to determine reference unit weights or void ratios in the laboratory. The test section provides a quantitative basis for proper compaction procedures in rock fill. While gradation tests are sometimes required before and after compaction of a rock test fill to evaluate particle breakage (USACE 1994b), a field test section combined with a performance specification may eliminate the need for this testing.

Detailed guidance and examples of field test sections are provided in USACE (1994b). The field test section should preferably be located near the quarry or borrow area for economic reasons and should have a similar foundation as the planned fill. An effort should be made to use similar means and methods to those anticipated in construction. For example, fill material should only be temporarily stockpiled for the test section if such stockpiling will occur during production. The geometry of the test section should be carefully planned to include sufficient space for the various combinations of compaction equipment, layer thickness, and water content. Space for traffic lanes and side slopes must also be considered. Multiple side-by-side test sections have been used successfully to reduce side slope requirements. At a minimum, settlement measurements should be obtained using surveying after each roller pass. For rock fill test sections, the dry unit weight of the fill may be measured occasionally. For soil test sections, a combination of conventional field dry unit weight tests and intact samples can be used to evaluate the compaction process and the properties of the compacted fill.

3-5.3 Compaction Control Tests.

Compaction control tests are used directly with end-result specifications. In general, a field measurement is made of the compacted dry unit weight ($\gamma_{d,field}$) and water content (w_{field}) of the fill. The available methods for determining these values are discussed in Chapter 2 of DM 7.1 (NAVFAC 2021). Some of the common methods are compared in Table 3-13, especially focusing on the typical variability of each method. In all of the studies used to collect this data, it is difficult to separate the effects of variability in the compacted fill itself from variability in the measurement of $\gamma_{d,field}$ and w_{field}.

3-5.3.1 Control Test Methods.

The common methods for determining field dry unit weight or relative compaction tend to have standard deviations of 1 to 2 pcf or 1% to 2%, respectively. This indicates that the range in measured γ_d may be as high as 5 to 10 pcf, simply due to measurement error. As noted in DM 7.1, the sand cone test is still regarded as the most accurate method, provided the sand is new, dry, and well-calibrated and the technician is experienced. However, McCook and Shanklin (2000) found that under field conditions the sand cone has similar variability as the nuclear gauge, which was attributed to the difficulty of calibrating the sand cone properly.

The time required to complete a compaction control test (summarized in Table 3-13) is an important consideration in the selection of a method. The nuclear gauge is the quickest method, being about six times faster than the sand cone. Because of its relative speed, a larger number of nuclear gauge control tests can be performed in a reasonable time period. Assuming the nuclear gauge is correctly calibrated, the use of multiple nuclear gauge tests will substantially reduce the uncertainty in the measured values of $\gamma_{d,field}$ and w_{field} that results from either actual fill variability or the variability of

the test method. Unfortunately, this perspective is not always appreciated, and the speed of the test is simply used to permit faster construction.

Table 3-13 Comparison of Common Compaction Control Test Methods

Method (ASTM)	Comments	Time Required per Test	Variability in Measurement	
			Unit Weight or $R.C.$	Water Content
Sand cone (D1556)	Noorany et al. (2000) found this method to be more accurate than drive cylinder or nuclear gauge but still with an $R.C.$ range of 5%±. McCook and Shanklin (2000) found the method to be more variable and to require more careful calibration.	30 to 45 minutes	Reported variability differs by study. Noorany et al.): $SD(R.C.)$=1.5 to 2% McCook and Shanklin: $SD(\gamma_d)$=1.4 to 5.8 pcf	These methods use oven drying (ASTM D2216) of field samples. Reported variability differs by study. Noorany et al.: $SD(w)$=0.1 to 0.5% McCook and Shanklin: $SD(w)$=1.3 to 3.6%
Rubber balloon (D2167)	Tends to compress soft soils (may not be an issue in well-compacted fill) leading to low unit weight.	15 to 30 minutes	ASTM 2167 indicates that two tests by same operator shouldn't vary by more than 1 pcf.	
Drive cylinder (D2937)	Tends to be less accurate than sand cone or nuclear density gauge. Some soils may loosen during driving while others may compress.	10 to 15 minutes	ASTM 2937: $SD(\gamma_d)$=2 pcf Noorany et al.: $SD(R.C.)$=1.5 to 2.5% McCook and Shanklin: $SD(\gamma_d)$=1.6 to 2.1 pcf	
Nuclear gauge (D6938)	Direct transmission method is more accurate than backscatter mode. Noorany et al. (2000) found higher variability and up to 10% difference in $R.C.$ compared to the as-compacted value. McCook and Shanklin (2000) found the method to be just as or more accurate than the sand cone, provided a water content correction is performed. Can have good repeatability but lack accuracy because of incorrect calibration.	5 to 10 minutes	Reported variability differs by study. Noorany et al.: $SD(R.C.)$=1 to 3% ASTM D6938: $SD(\gamma_t)$=0.3 to 1.2 pcf for direct transmission $SD(\gamma_t)$ = 2 pcf for backscatter McCook and Shanklin: $SD(\gamma_d)$=0.5 to 3.9 pcf	$SD(w)$=0.3 to 1.0% Higher values may be observed if soil is variable. Variability between two gauges and operators is about twice as large as variability between tests for the same operator and equipment.
Calcium Carbide (a.k.a. Speedy) (D4944)	Commonly used as an alternative to oven-drying with displacement methods or as a field check to the nuclear gauge.	5 to 10 minutes	NA	McCook and Shanklin: $SD(w)$=1.6 to 2.1% Sotelo et al. (2014): $COV(w)$ = 5%
eGauge (D8167)	License exempt nuclear device. Measures moisture content using an electronic probe, which is less accurate than the nuclear gauge. No backscatter option. Requires site-specific background radiation calibration. Bursey et al. (2016) found good relationship between unit weights measured by the eGauge and nuclear gauge.	5 to 10 minutes	Troxler (2019) $SD(\gamma_t)$=0.3 pcf	Variability data not available. Accuracy is greatly improved through use of soil-specific calibration or moisture offset.

Notes: $SD(\bullet)$ indicates the standard deviation of the variable, $COV(\bullet)$ indicates the coefficient of variation of the variable

3-5.3.2 Control Test Frequency.

Minimum testing frequencies for different types of fill are summarized in Table 3-14. Where the earthwork operation is large and employs a consistent procedure, the testing frequency is low. In contrast, more frequent testing is required for small areas where the compaction procedure is less regular. Multiple lifts should not be placed without control testing. More frequent testing is also required at the beginning of the project as the compaction procedure is becoming established (USACE 1995a). Some agencies also require that *record samples* be obtained on a less frequent basis than the routine control tests. Record samples are block or other intact samples of the fill that can be used for laboratory shear strength or consolidation testing. For example, USACE (1995a) requires record samples every 30,000 to 50,000 C.Y.

Table 3-14 Control Testing Requirements for Different Types of Fill (after Hilf 1991, USBR 1998, USACE 1995a, Sowers 1979)

Type of Compacted Fill	Minimum Testing Frequency
Mass earthwork / embankment	1 test / 2000 C.Y.
Relatively thin sections, canals, and reservoir linings	1 test / 1000 C.Y.
Pervious materials	1 test / 1000 C.Y.
Large fill areas	1 test / lift / 10,000 to 20,000 ft^2
Trench backfill and around structures	1 test / 200 C.Y. to 1 test / 500 C.Y.
Small fill areas	2 to 3 tests / lift / area
Minimum for mass earthwork	1 test / shift
Areas of doubtful quality	1 test / area
Instrumentation locations	1 test / instrument

Compaction control tests should be made at regions of doubtful quality, including transitions between materials, areas where rollers turn, lifts that may be too thick, lifts with improper water content, lifts compacted with insufficient roller passes or too light of rollers, fill compacted with clogged rollers, fill containing oversize rock or minor frost, and fill that is different from the average material. Such tests should be distinctly labeled as different from the routine spot tests. Proof rolling can also be used to identify doubtful regions but may be practical only for the final lift of an earthwork project or below pavements.

3-5.3.3 Control Test Comparison to Reference Values.

The results of field spot tests are compared to reference values of $\gamma_{d,max}$ and w_{opt}, or minimum and maximum void ratios. The reference values can come from laboratory compaction tests on the same soil or field test sections. More details on laboratory compaction testing procedures are found in Chapter 3 of DM 7.1. It is common to perform a series of these tests on the soils that are planned for use as fill, forming a set of standard compaction curves for the project. An appropriate compaction curve is

selected for each lift of fill by the field engineer based on visual classification and either the relative compaction or relative density is calculated. During construction, additional laboratory compaction tests should be performed on samples of the fill, depending on the variability of materials.

Laboratory compaction tests can be supplemented by rapid, one-point compaction tests that are performed in the field. A variety of procedures have been proposed (e.g., Hilf 1991, AASHTO T272). As shown in Figure 3-15, the compaction curves for a range of soils tend to fall along a line of optimums for a particular compactive effort.

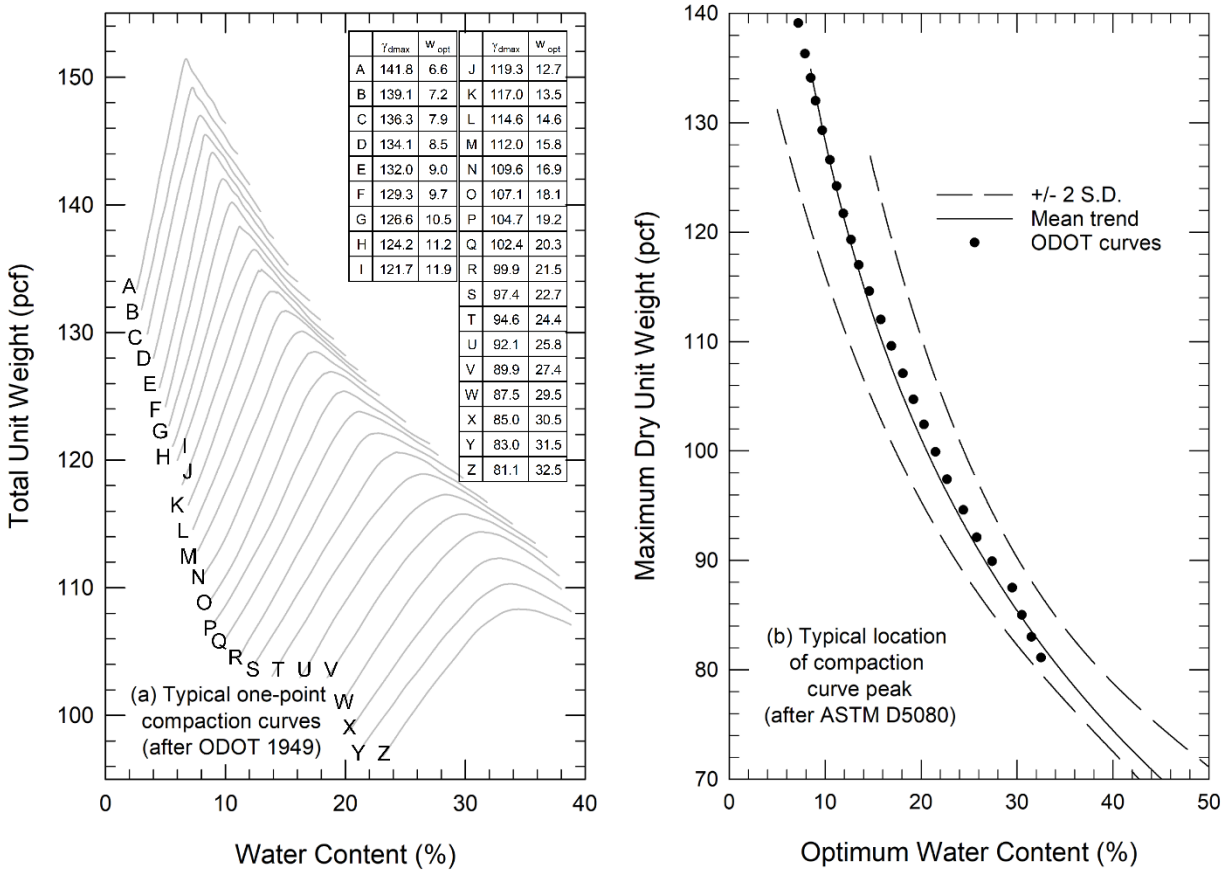

	γ_{dmax}	w_{opt}
A	141.8	6.6
B	139.1	7.2
C	136.3	7.9
D	134.1	8.5
E	132.0	9.0
F	129.3	9.7
G	126.6	10.5
H	124.2	11.2
I	121.7	11.9
J	119.3	12.7
K	117.0	13.5
L	114.6	14.6
M	112.0	15.8
N	109.6	16.9
O	107.1	18.1
P	104.7	19.2
Q	102.4	20.3
R	99.9	21.5
S	97.4	22.7
T	94.6	24.4
U	92.1	25.8
V	89.9	27.4
W	87.5	29.5
X	85.0	30.5
Y	83.0	31.5
Z	81.1	32.5

Figure 3-15 Typical Soil Compaction for Field Verification – (a) One-Point Method (after ODOT 2010) and (b) Typical Range of Compaction Curve Peak (after ASTM D5080)

After performing a field compaction control test, the field engineer excavates soil from the field test location. The excavated soil is compacted in accordance with the appropriate test procedure (e.g., ASTM D698 or ASTM D1557), which results in a total unit weight and water content. The γ_t and w point is plotted on a family of typical compaction curves (e.g., Figure 3-15a). The nearest typical curve is selected, or a similarly shaped compaction curve can be interpolated. The values of $\gamma_{d,max}$ and w_{opt} are

provided for the typical curves because these values do not correspond directly to the peaks of the total unit weight curves. In order for the rapid compaction method to work, the soil must be dry of optimum because the compaction curves merge together at water contents above optimum. If it is necessary to provide clarity, a second specimen can be compacted by wetting or drying another sample of the soil. Because compaction characteristics depend on local geology and mineralogy, the families of typical compaction curves are best obtained from the local experience of geotechnical laboratories or from regional agencies, such as state departments of transportation. The typical range of compaction curve peak values is provided in Figure 3-15b. When using reference compaction values, field engineers must be careful to avoid choosing a reference curve on the basis of allowing the field control test to pass.

In some cases, field determination of the minimum and maximum void ratios may be required for evaluation of relative density. USACE (1995a) indicates that correlations have successfully been developed based on the percent passing the #16 sieve.

3-5.4 Analysis of Compaction Control Test Data.

A regular, consistent procedure should be selected to report the results of compaction control tests. At a minimum, the soil description, reference compaction curve, test location and elevation, $R.C.$ (or D_r), and Δw should be reported along with the test results. Each test result should be evaluated with respect to the project end-result specification. Where a minimum average $R.C.$ is specified, average values should also be calculated for the interval specified or requested by the project engineer.

In addition to the evaluation of individual test results, analysis of the entire compaction control data set will reveal general trends in compaction and may suggest the need to alter compaction methods. Two simple methods can be used by the field or project engineer: (1) plot the test results on the compaction plane with the reference compaction curve and (2) tabulate the frequency of γ_d and w (or $R.C.$ and Δw). An example of how these two methods can be combined is provided in Figure 3-16. The results can be plotted in this manner either by hand or electronically.

Control tests plotted on the compaction plane should also include the $S = 100\%$ curve and the specification limits. Test points that are grouped near the edge of the limits indicate a need to adjust either the water content, the compactive effort, or both. If test results are grouped near the $S = 100\%$ curve, the fill may be overcompacted and have lower shear strength, even if the $R.C.$ and water content meet the specification. This is of particular concern for high embankments and earth dams (Turnbull and Foster 1956). Test results that plot above the $S = 100\%$ curve are theoretically impossible and indicate uncertainty in the control testing method, error in the compaction control test, or a change in soil type and G_s value used to plot the $S = 100\%$ curve. Control tests with calculated $S > 100\%$ should not be discarded categorically but should be evaluated carefully (Schmertmann 1989).

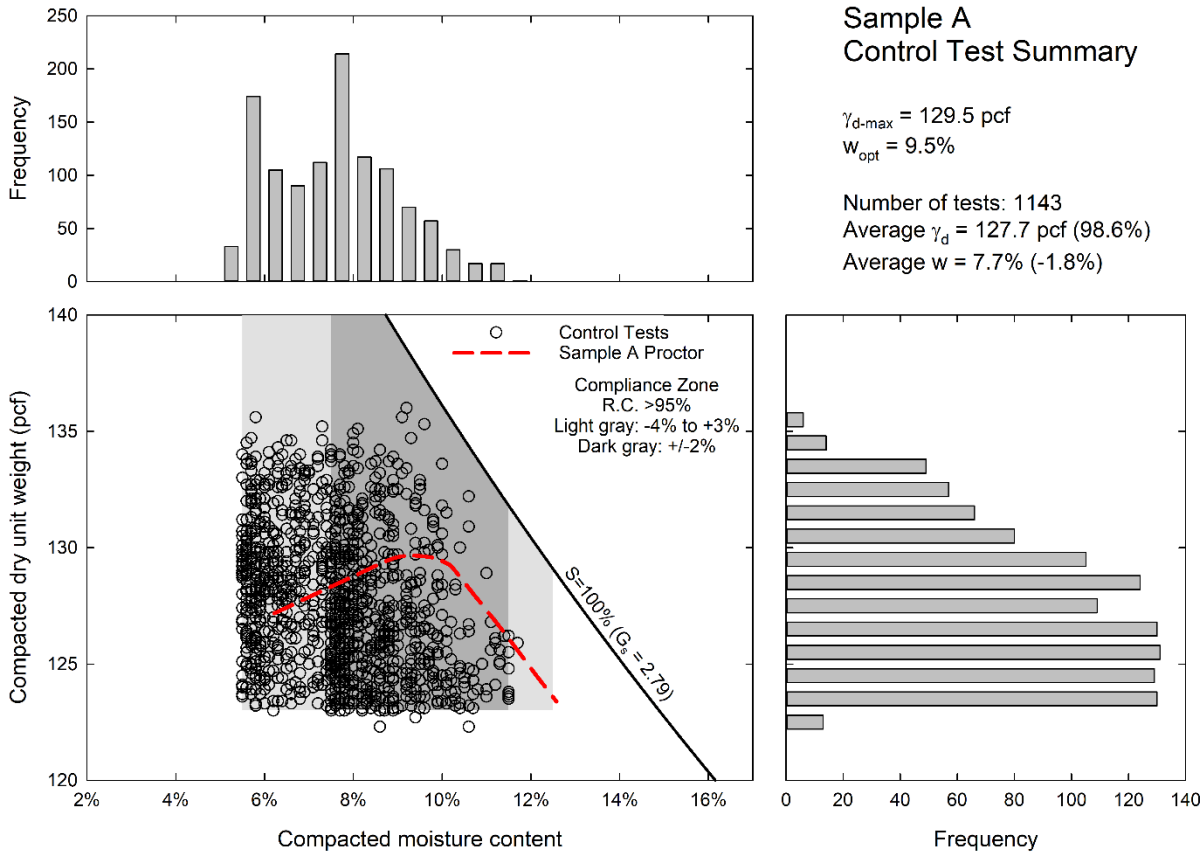

Figure 3-16 Graphical Analysis of Control Test Data

Tables or histograms of the frequency of γ_d and w can be used to understand the distribution of the compacted properties. Once an adequate number of test results is available (40 or more), the mean and standard deviation of γ_d and w (or $R.C.$ and Δw) can begin to be estimated from these distributions (see Chapter 7 for calculations). Simple tabulation methods provided in Davis (1953) and USBR (1998) can be used to create field histograms and cumulative distribution plots similar to those in Figure 3-16. The standard deviation can be estimated knowing that about two-thirds of the data falls within one standard deviation of the mean and 95% of the data falls within two standard deviations of the mean (for a normal distribution).

The mean and standard deviation of $R.C.$ help to evaluate the compactive effort being used. Because a compacted fill will have variable compacted dry unit weight, the mean or average $R.C.$ must be above the minimum specified $R.C.$ in order for all of the fill to meet the specification. Standard deviations of $R.C.$ for well-controlled compaction are typically less than about 3%. Higher standard deviation indicates insufficient or erratic compaction and improvement is required in the uniformity of moisture control, compaction equipment weights and pressures, or level of equipment coverage.

The mean and standard deviation of Δw help to evaluate moisture control. The mean Δw should be close to the midpoint of the specified range of water contents. A standard deviation of Δw of 1.5% or less is evidence of good moisture control. If the standard deviation of Δw is more than 3%, the moisture control is erratic, and the borrow materials may need to be better blended and moisture conditioned.

Variation in the $\gamma_{d,max}$ and w_{opt} of the borrow may also lead to apparent variation in the $R.C.$ and Δw. For example, Hilf (1991) considers two soils with similar mean properties, a uniform aeolian soil and a more variable alluvial soil. The standard deviation of $\gamma_{d,max}$ was 1.5 pcf for the aeolian soil and about 2.8 pcf for the alluvial soil. If this variation in the reference compaction curve is ignored, the reported $R.C.$ may have a larger standard deviation than is actually present in the fill. This further emphasizes the importance of obtaining regular samples for laboratory compaction testing and checking with rapid compaction tests.

Some portion of the compaction control results will fall outside the specification limits. Hilf (1991) presents a decision-making approach for determining if such tests indicate an unacceptable compacted lift, which depends on the specification limits. An example set of compaction specifications is plotted in Figure 3-17. In Hilf's approach, the first control test is compared to the outer bounds of the specification. Tests are accepted if the γ_d and w are both in the specified range and rejected if both γ_d and w are insufficient. In regions with tests that indicate insufficient water content or γ_d, a retest is performed. The retest may be compared to a tighter specification because the two control tests provide a stronger statistical case for acceptance or rejection.

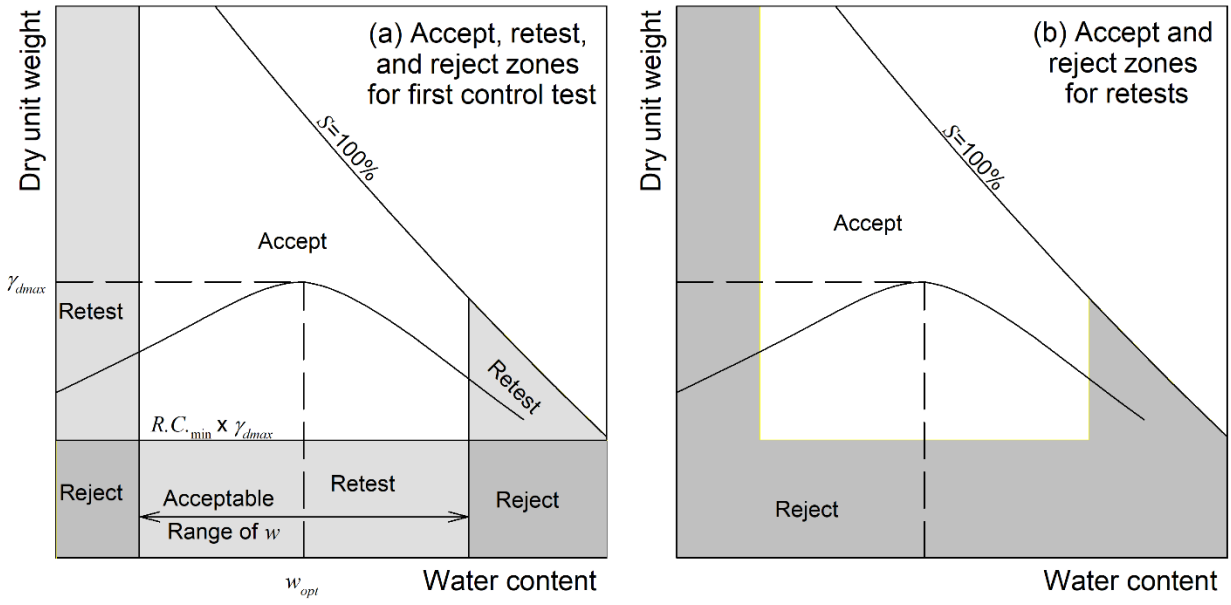

Figure 3-17 Two-Step Interpretation of Control Test Results (after Hilf 1991)

In some cases, compaction control specifications include a mean relative compaction that must be met or exceeded. This approach recognizes that some variability will always exist within the compacted fill. It may be desirable to specify the mean $R.C.$ such that only a certain percentage of the fill will have a $R.C.$ below a lower threshold. In Table 3-15, the lower threshold is referred to as $R.C._{10}$ for which only 10% of the $R.C.$ values will be lower. Based on the selected value of $R.C._{10}$ and the estimated variability of the fill, a mean relative compaction can be selected. For example, if it is desired to have only 10% of the fill with $R.C.$ less than 95%, the mean $R.C.$ should be 100% for a fill with medium variability.

Table 3-15 Statistical Approach to the Selection of Mean Relative Compaction Requirements

Fill Variability	Required Mean $R.C.$ to Achieve Indicated Value of $R.C._{10}$			
	$R.C._{10}$ = 90%	$R.C._{10}$ = 93%	$R.C._{10}$ = 95%	$R.C._{10}$ = 98%
Low $COV(R.C.)$ = 2%	92%	95%	97%	101%
Medium $COV(R.C.)$ = 4%	95%	98%	100%	103%
High $COV(R.C.)$ = 6%	97%	101%	103%	106%
Notes: $R.C._{10}$ = relative compaction for which only 10% of the values are lower. A sufficient number of compaction control tests must be performed to adequately determine the mean $R.C.$ A normal distribution has been assumed for $R.C.$ $COV(R.C.)$ = coefficient of variation of relative compaction (see Chapter 7).				

3-5.5 Compaction Control of Rock Fill.

In most cases, field test sections and method specifications should be used for the primary control of rock fill (Breitenbach 1993). The test section establishes the number of passes and particular equipment required to achieve suitable compaction of the rock fill. Large-scale unit weight tests should be performed occasionally to verify the compaction procedure. Such tests require an excavation with a diameter at least four times greater than the maximum particle size and the removal of about 1000 to 2000 pounds of rock fill (Breitenbach 1993, Holtz et al. 2011).

3-5.6 Intelligent Compaction Systems.

Intelligent compaction (IC) systems are those which continuously monitor soil properties from roller vibrations, provide automatic feedback to the roller vibration, and use GPS to map the measurements to a GIS model of the site (NCHRP 2010). The rollers record a measurement value (MV), which is an indicator of compaction to a depth of about 3 to 4 feet. Depending on the system and manufacturer, the MV may indicate soil stiffness, modulus, or roller vibration characteristics.

NCHRP (2010) summarizes the interaction between the MV and soil/subgrade conditions. The response of the soil below the roller is highly nonlinear. The MVs for thin layers are substantially affected by different stiffness of the underlying soil. Many

correlations between MV and soil parameters, such as dry unit weight and plate load test moduli, are available.

Figure 3-18 illustrates the simplest manner in which intelligent compaction can be used to monitor compaction. The MVs are plotted in plan view to identify weak or soft regions in the fill based on low MV. Compaction control tests are performed on those regions. A more advanced approach to IC monitors the change in the MV with subsequent passes of the roller and compares this change to a specified threshold. Other methods correlate the MV to field compaction control tests or laboratory tests in order to determine threshold values of MV.

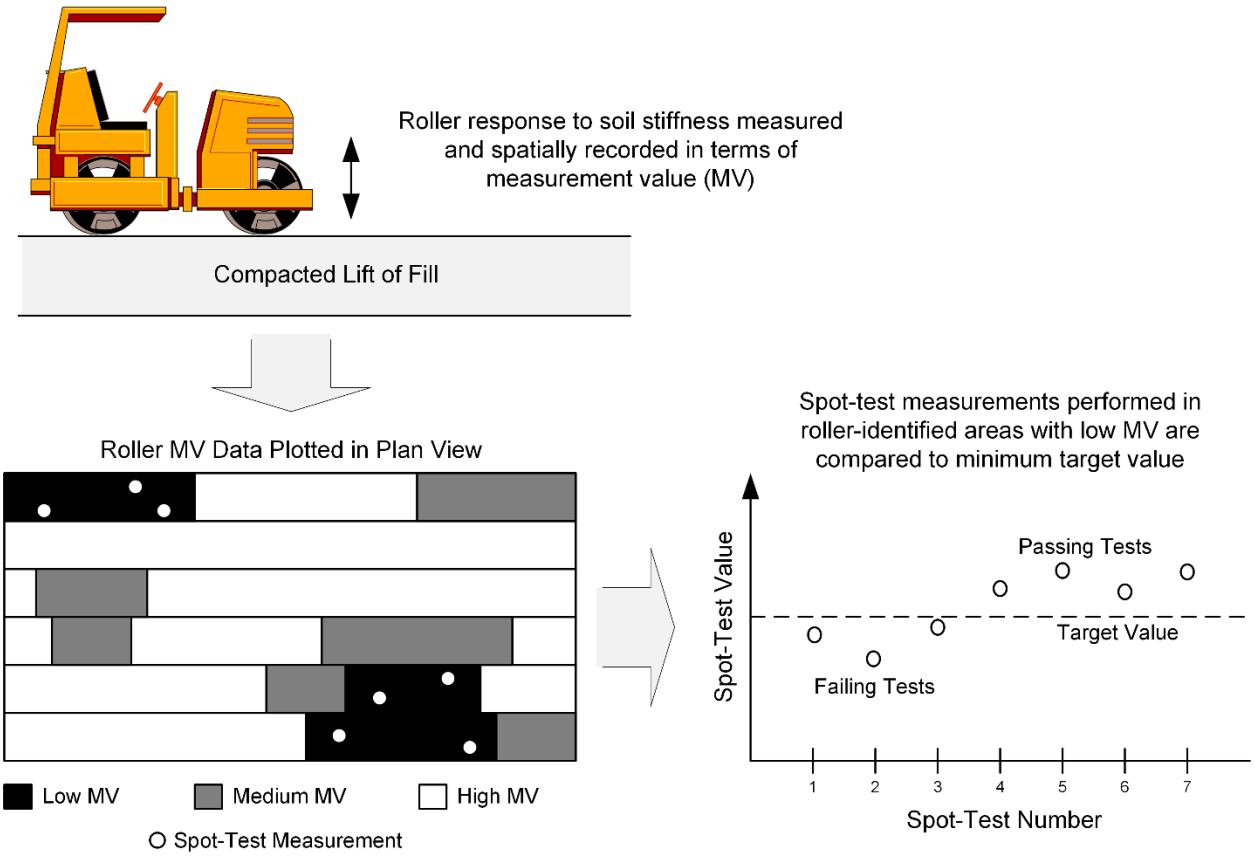

Figure 3-18 Compaction Control Guided by Intelligent Compaction (after NCHRP 2010)

3-5.7 Indirect Evaluation of Deep Fills.

Deep fills can be evaluated using subsurface exploration techniques as discussed in Chapter 2 of DM 7.1 (NAVFAC 2021). In particular, soil borings with SPT, CPT soundings, and geophysical surveys are useful to assess previously placed fills. In fill constructed from fine-grained soil, Shelby tube samples can be obtained to measure the dry unit weight of the fill. The water content of a fill can change after compaction, and

samples obtained a significant time after compaction should be used with caution. A major concern in the evaluation of deep fills is the ability to evaluate the uniformity of compaction using widely spaced *in situ* testing.

Ground improvement can be used to densify deep fill (see Chapter 1 for specific methods). *In situ* testing performed both before and after the ground improvement can be used to measure its effect.

3-6 DESIGN OF EMBANKMENTS.

Proper design and satisfactory performance of embankments depend on a high-quality subsurface exploration and laboratory characterization program. Chapter 2 of DM 7.1 and NCHRP (2018) provide in depth guidance on these topics. The major types of embankments are illustrated in Figure 3-19 and are discussed in the following sections.

3-6.1 Primary Design Conditions.

3-6.1.1 Slope Stability.

The stability of embankment slopes is controlled primarily by the shear strength of the fill and supporting foundation, the groundwater conditions, and the geometry of the slope. Some soils are susceptible to softening from weathering, climatic effects, and progressive failure. Changes in the properties of these soils with time must be considered. Procedures for calculating slope stability can be found in Chapter 7 of DM 7.1. Guidance for the selection of appropriate shear strength parameters can be found in Chapter 1.

3-6.1.2 Settlement.

Settlement of an embankment is caused by foundation consolidation, consolidation of the embankment material itself, and secondary compression in the embankment after its completion. Foundation consolidation occurs as a result of the weight of the embankment fill. Chapter 5 of DM 7.1 summarizes methods to calculate foundation settlement as well as procedures to decrease foundation settlement and/or accelerate consolidation.

The compacted embankment may also experience consolidation. Significant excess pore pressures can develop during construction of fills exceeding about 80 feet in height or for lower fills of clays compacted wet of optimum. As these excess pore pressures dissipate after construction, the embankment will settle. Settlements of about 1% to 2% of the fill height are commonly experienced. Estimates based on past experience can be made using the data in Figure 3-10. For earth dams and other high fills where settlement is critical, construction pore pressures should be monitored by the methods described in Chapter 2 of DM 7.1.

Even for well-compacted embankments, secondary compression and shear strain can cause slight settlements after completion. Normally, this is only of significance in high embankments. This secondary compression typically is between 0.1% and 0.2% of the fill height after three to four years and increases to 0.3% and 0.6% after 15 to 20 years. The larger values are for clay soils.

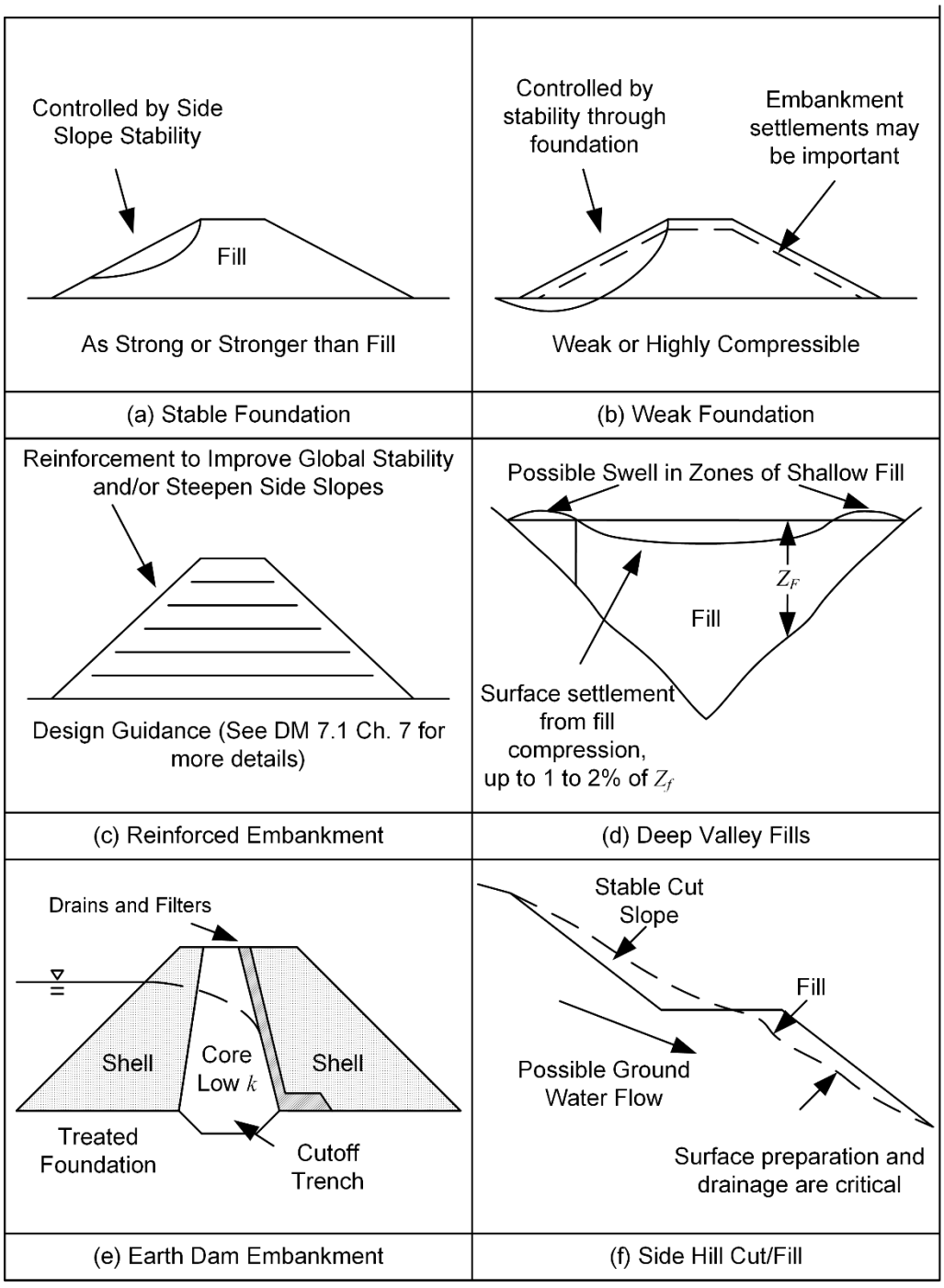

Figure 3-19. Schematics of Typical Embankment Design Sections (not to scale)

3-6.2 Embankments on Stable Foundations.

A stable foundation for an embankment has low compressibility and is as strong or stronger than the planned fill as shown in Figure 3-19(a). In this case, the stability of the side slopes controls the design, which will be affected by the type of soil used to build the fill and the seepage conditions. For slopes without significant seepage forces, the appropriate side slope angle varies between 1.5H:1V and 3H:1V. Steeper slopes are appropriate for compacted coarse-grained soils while flatter slopes may be required for compacted clays. The geometry of slopes and berms is also controlled by requirements for erosion control, maintenance, and mowing.

Special caution is required when constructing embankments from high plasticity clays. These soils experience the detrimental effects of shrink-swell due to weathering and moisture content changes, which leads to progressive failure and the development of fully softened conditions. Appropriate side slope design for these soils depends on selection of applicable fully softened shear strength parameters (Duncan et al. 2011, Castellanos et al. 2015).

3-6.3 Embankments on Weak Foundations.

Embankments built over weak foundations must consider settlement and instability through the foundation soil as indicated in Figure 3-19(b). Weak foundation soils may need to be partially or completely removed or densified *in situ*.

A range of methods for addressing embankment foundation instability is illustrated in Figure 3-20. Some approaches, such as slope reinforcement and flattening of side slopes, will only improve slope stability but will not reduce settlement. Other methods will improve both slope stability and settlement and include reducing the embankment weight using lightweight fill, transferring the load to deeper strata, removing and replacing problem materials, and implementing ground improvement. For cases where settlement is primary concern, preloading methods with surcharges and vertical drains are appropriate. Chapter 1 summarizes methods for addressing problem soils with ground improvement. More comprehensive guidance can be found in FHWA (2017).

3-6.4 Reinforced Embankments.

Reinforced embankments are constructed by incorporating tensile reinforcement horizontally between layers of compacted fill (Figure 3-19(c)). Most often, reinforced soil slopes (RSS) use geosynthetic reinforcement. For embankments on stable foundation, reinforcement improves stability within the embankment and allows steeper side slopes. Over a weak foundation, reinforcement can be used to prevent instability through the embankment and into the foundation soil. The reinforcement requires the RSS embankment to act as a unit and effectively reduces the bearing pressure on the weak foundation. Many column-supported embankments contain partial reinforcement

in the lower lifts to help transfer load to the columns. Chapter 7 of DM 7.1 contains a summary of RSS design, and a comprehensive coverage of the topic is found in FHWA (2009). Where reinforcement is required in fill that is used as seepage barrier (i.e., earth dams), special compaction techniques are required for the layers adjacent to the reinforcement (Gregory 1993)[16]. Fiber admixtures can be used to repair shallow slope failures and reinforce slopes (Gregory 2006, Hatami et al. 2018).

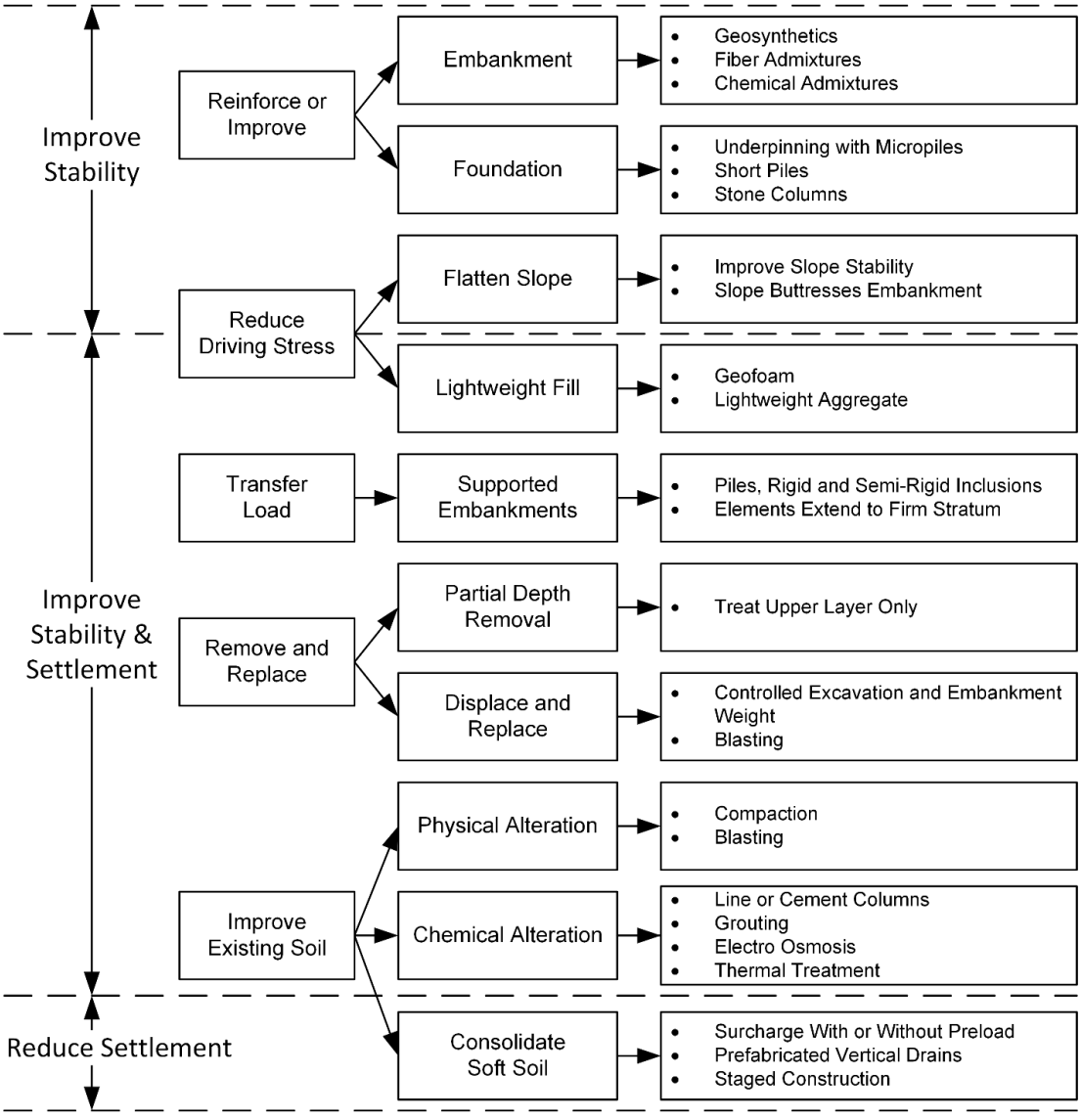

Figure 3-20 Methods to Address Foundation Instability (after TRB 1990 and Holtz 1989)

[16] Local regulations should be checked. Some jurisdictions do not allow reinforcement in earth dams and other seepage barriers.

Suitable performance of RSS depends on the performance of the reinforcement, which in turn is related to the selection of appropriate fill material, installation of the reinforcement, and careful earthwork practice. In general, fill for RSS should be coarse-grained (less than 50% fines), and the fines should have a PI not exceeding 20. Coarse-grained fill provides the relatively high shear strength desired for an RSS and the high level of soil-reinforcement interaction required to develop the reinforcement capacity. In order to prevent damage during earthwork, reinforcement should be installed and fill should be placed according to the manufacturer's specifications, at a minimum. These specifications will include limitations on the types of equipment that can operate on or near the reinforcement as well as appropriate lift thicknesses above the reinforcement. Construction restrictions may also prevent turning and sudden starts or stops of compaction equipment above the reinforcement. The manufacturer's specifications will also provide information about seams or overlap requirements. Special care should be taken to align the reinforcement in the proper direction because the properties are often direction dependent.

3-6.5 Deep and/or Valley Fills.

Relatively deep fills, as illustrated in Figure 3-19(d), experience settlement over time. Settlement can be the result of consolidation of both the foundation and the embankment fill itself. It can also be related to secondary compression over time. This behavior is especially important for dams because the long-term crest elevation is a key design consideration and for valley fills where the depth of the embankment varies greatly through the cross-section. Duncan and Bursey (2006) found that valley fills tend to experience 0.1% to 2% settlement in 50 years. Because the settlement is relative to the thickness of the embankment, valley fills may experience significant differential movement.

Over time, deep fills will experience changes in water content in response to the surrounding climate and human activity such as irrigation. In the case of earth dams, inundation will saturate some portion of the embankment. Shallow layers of compacted fill may swell while deeper layers consolidate or collapse when wetted (Brandon et al. 1990). Thus, swelling behavior can further exacerbate differential movement.

Some amount of compression and differential movement is inevitable in deep fills. Appropriate construction practice is the primary means of design to counteract these effects (Coduto et al. 2011). The lower portions of deep fills should be built with a higher specified relative compaction, which reduces the potential for further consolidation. The compaction water content may also need to be varied with lower water contents being more appropriate near the bottom of the fill. In shallower zones of deep or valley fills, expansive fill should not be used, if at all possible. In all cases, deep fills should be designed for some degree of wetting using methods such as those proposed by Brandon et al. (1990) or Noorany and Stanley (1994).

3-6.6 Earth Dam Embankments.

USACE (2004), USBR (2012), and Chapters 6 and 7 of DM 7.1 provide guidance on the design of earth dams for stability and seepage under a variety of conditions, including end of construction, steady state seepage, rapid drawdown, and seismic loading. Earth dams may be homogeneous or zoned as illustrated in Figure 3-19(e). Considerations of shear strength and hydraulic conductivity will control the both the cross-sectional geometry of an earth dam embankment as well as the parameters required of the engineered fill in each zone of the dam. This section focuses on the general properties required of fill materials used for dams. The shear strength of compacted fill should be characterized using laboratory testing on compacted specimens. The influence of compaction on shear strength of compacted soil and rock is summarized in Section 3-2.3.

With the exception of homogeneous dams, most earth dams have zones of both free-draining soil with very high hydraulic conductivity (k) and nearly impervious soil with very low k. Filter and drain zones with high k are used to intercept seepage through dams and consist of sands and gravels with little fines. These zones should be kept free of contamination with fines or the core soil during construction. Methods to estimate the hydraulic conductivity of different types of soil and to design filters between zones can be found in Chapter 6 of DM 7.1. In contrast, compacted fine-grained soils with low k are used to retain water. Compacted fill for a dam core should be free of lenses, pockets, or layers of pervious material, and successive lifts should be well bonded to each other. If a borrow source contains more than 1% oversize by mass, it should be removed prior to arrival on the earth dam embankment.

The soils selected for the zones of an earth dam must not erode under the seepage forces to which they are subjected. This includes both external erosion at the surface of the compacted fill as well as internal erosion of particles. The critical location for seepage-induced external erosion is the downstream face of a homogenous embankment. Internal erosion occurs as finer particles move into larger void spaces and can be subdivided into scour, backward erosion piping (BEP), internal migration, and internal instability (USBR and USACE 2019).

In the context of earth dams, *scour* refers to movement of soil particles by water flowing along an unprotected interface, most often by concentrated leak erosion (CLE). Concentrated leaks can occur through cracks or defects in fill and along unprotected discontinuities, such as conduits through the fill and foundation defects or joints. Selection of fill to resist CLE can be guided by the categories in Table 3-16. Figure 3-21(a) presents the typical gradation ranges of soils in the more resistant categories. Soils that are susceptible to CLE include gap-graded soils and soils with a well-graded flat tail, as shown Figure 3-21(b). Because CLE can occur at cracks within the fill itself, the cracking resistance of fill should be considered for earth dams. Figure 3-21(c) can be used to evaluate the likelihood of cracking.

Table 3-16 Erosion Resistance Categories (after USBR and USACE 2019)

Erosion Resistance Category	Applicable Soil Types
1 (best)	CL, CH, and well-graded SC with $PI > 15$, any compaction level
2	Well-graded with clay binder, $15 > PI > 6$, any compaction level
	Well-graded, coarse-grained, $PI < 6$, well compacted
3 (worst)	Well-graded, coarse-grained, $PI < 6$, poorly compacted
	Very uniform, fine sands, $PI < 6$, any compaction level
	Gap-graded soils, any compaction level

The mechanics of BEP and internal instability are discussed in detail in Chapter 6 of DM 7.1 along with guidance on the selection of fill materials for filters. In addition, the diagonal lines shown on Figure 3-21 can be used as a preliminary assessment for internal instability. If the grain size distribution curve of a soil has sections flatter than the diagonal lines, the soil may be internally unstable. A summary of other methods for evaluating the internal instability potential of soils can be found in USBR and USACE (2019).

Dispersive clays are clay minerals that contain a high percentage of dissolved sodium in the pore water and are very susceptible to erosion. Water flowing through holes and cracks will quickly erode these clays. Dispersive clays can be identified using laboratory methods, such as the double hydrometer (ASTM D4221), the analysis of pore water extract (ASTM D4542), the pinhole test (ASTM D4647), or the crumb test (ASTM D6572). Dispersive clays should not be used as fill in dam embankments because they are very susceptible to internal erosion. Categories of dispersive tendency and associated laboratory test procedures are summarized in Table 3-17.

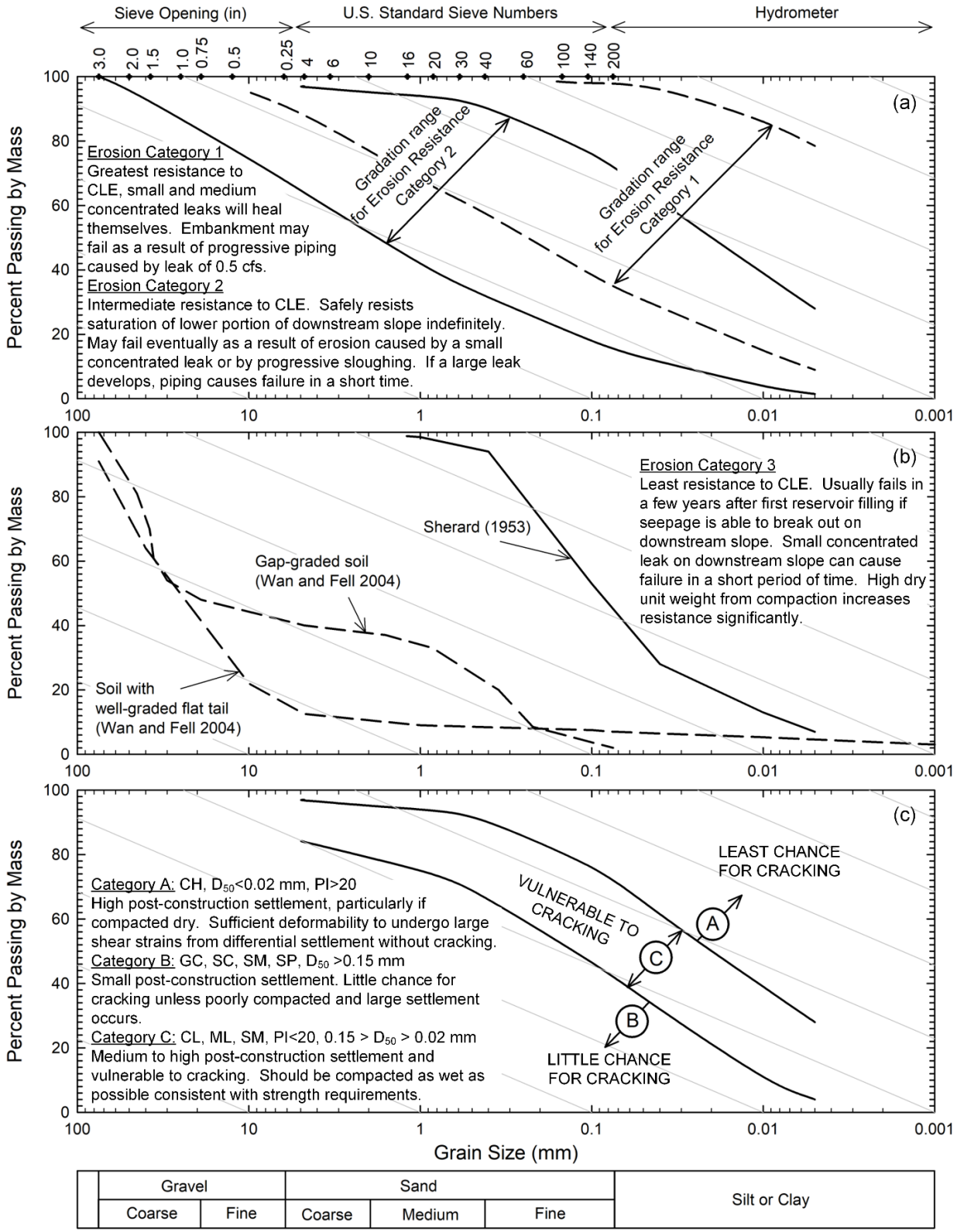

Figure 3-21 Concentrated Leak Erosion and Cracking Resistance of Fill Materials (after Sherard 1953, Wan and Fell 2004)

Table 3-17 Dispersive Tendency from Double Hydrometer, Pinhole and Crumb Tests (after ASTM D4221, D4647, D 6572)

Dispersive Tendency	Percent Dispersion by Double Hydrometer (ASTM D4221, 2018)	Dispersive Classification by Pinhole Test (ASTM D4647 Method B)				Dispersive Grade by Crumb Test (ASTM D6572)
		Class	Applied Head (mm)	Cloudiness from side	Hole size after test (mm)	
Dispersive	$\frac{P_{2\mu m,nd}}{P_{2\mu m,d}} > 50\%$	D	50	Dark to slightly dark	≥ 1.5	Grade 4 – dense cloud of colloids appears in water
						Grade 3 – visible cloud of colloids appears in water
Moderate to slightly dispersive	$30\% \le \frac{P_{2\mu m,nd}}{P_{2\mu m,d}} \le 50\%$	SD	180 to 380	Barely visible	≥ 1.5	Grade 2 – faint cloud of colloids appears around soil in water
Nondispersive	$\frac{P_{2\mu m,nd}}{P_{2\mu m,d}} < 30\%$	ND	380	Clear	< 1.5	Grade 1 – no reaction to water, soil may slake or crumble, but no turbidity

$P_{2\mu m,nd}$ = percent passing 2 μm in soil-water suspension with no dispersant and minimal agitation.
$P_{2\mu m,d}$ = percent passing 2 μm in soil-water suspension with dispersant in regular hydrometer

Note: Dispersive tendency was previously measured using the 5-micron particle size. The engineer should take care comparing test results using the newer standard to historical guidelines and experience.

3-6.7 Side Hill Fills.

In areas with hilly or mountainous terrain, side hill fills are a commonly used method to create level space for roads and structures. As shown in Figure 3-19(f), a *side hill fill* is created by compacting fill on an existing slope with some of the fill material often coming from an adjacent cut. Side hill fills are often prone to instability even when the fill is appropriately compacted, leading to regular or seasonal slippage. While many of these landslides are a maintenance nuisance, some cause serious damage or loss of life. Conditions in the natural slope that typically lead to these problems include high or fluctuating groundwater and relatively weak foundation materials, such as colluvial or residual soils or degradable rock.

Although side hill fills can be problematic, they are often unavoidable, and appropriate design guidelines are required. The typical problems suggest the primary design considerations, and the side hill fill should be treated as a transition zone (TRB 1990). First, groundwater control is essential. Drainage systems should be designed to intercept groundwater seeping from the natural slope and to route surface water off the fill (see Chapter 6 of DM 7.1). The drainage should prevent both the fill and the natural soil below the fill from becoming saturated. Conservative groundwater levels, including seasonal fluctuations, should be used in slope stability calculations. Second, the interface between the compacted fill and natural slopes steeper than 3H:1V should be benched prior to compaction. Benching allows all fill to be placed horizontally. More importantly, the inclined interface between the new fill and the natural slope is removed,

which reduces the potential for the fill to simply slide down the slope. This is especially important for slopes where a thin layer of weak soil is present at the surface.

3-7 HYDRAULIC AND UNDERWATER FILLS.

3-7.1 Purpose and Use of Hydraulic Fill.

Since the advent of modern methods of excavation, transportation, and compaction in the 1930s, hydraulic fill is used mostly in particular situations, such as underwater fill and land reclamation. However, understanding the hydraulic fill process may prove helpful for interpreting the behavior of existing structures, particularly old dams, built with this method.

Hydraulic fill is a method of earthwork that uses water to excavate, transport, and place fill. Soil can be excavated hydraulically with jets, dredging, or cutter heads. The soil-water slurry is then pumped by pipe from the excavation site to the fill. Where ample water is available and large fill quantities are required, the ability to economically transport soil long distances is the main advantage of hydraulic fill. The slurry is discharged from the transport pipe as illustrated in Figure 3-22, and the soil is deposited at the hydraulic fill site, creating a fan with significant segregation and difference in the slope of the fill (Sowers 1979). Removal or placement of soil by hydraulic methods must conform to applicable water pollution control regulations. Fills that are excavated conventionally and placed using water, such as puddled clay cores or sluiced rock fill, can be classified as semi-hydraulic fill (USBR 1998).

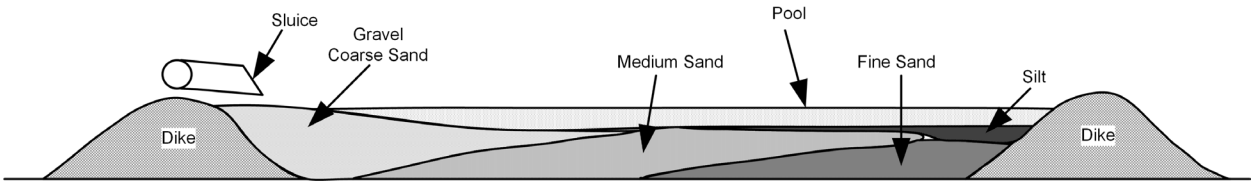

(a) Stage I – Low Dikes and Initial Pool

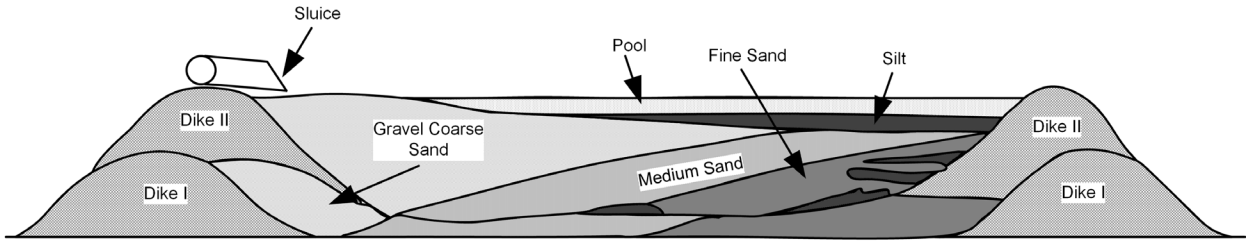

(b) Stage II – Dikes Built up from Stage I Filling, Followed by More Fill

Figure 3-22 Hydraulic Fill Illustration (after Sowers 1979)

3-7.2 Placement of Hydraulic Fill.

Hydraulic fill can be placed either on land or underwater. When used, hydraulic fill should be placed in a manner that produces the required usable area while minimizing environmental impact.

On land, hydraulic fills are commonly placed by pipeline but can also be created using clam shells or draglines. When hydraulic fill is discharged from a pipe, it creates a fan as the soil-water slurry spreads. The particles will segregate by size with the largest particle settling first. The fill will be wide with slopes ranging from 5H:1V to 40H:1V. Similar to underwater, dikes are required to create steeper slopes. The rate of flow can be used to control the gradation of the fill. The fine particles will remain in suspension for longer periods of time and can be removed if short sedimentation times are used (Sowers 1979).

Hydraulic fill with steeper side slopes requires the use of a mixed sand and gravel fill material or a control method during placement. Underwater slopes as steep as 3H:1V or 2.75H:1V may be achieved by careful placement of fill containing about equal amounts of sand and gravel. Berms or dikes of the coarse fill or large rock can be created around the perimeter of the fill to confine it laterally. The voids in rock placed underwater are filled with sand by sluicing to reduce compressibility and possible loss of hydraulic fill into the rock.

3-7.3 Performance of Hydraulic Fills.

Coarse-grained soils with less than 15% non-plastic fines or less than 10% plastic fines create the most satisfactory hydraulic fills. They cause the least turbidity during placement, drain faster, and are more suitable for structural support than fine-grained material. Relative densities of 50% to 60% can be obtained without compaction with a coefficient of variation of about 25%. Allowable bearing pressures are in the range of 500 to 2000 psf depending on the level of permissible settlement. Coarse-grained hydraulic fill may be variable and may contain zones of low permeability that develop high pore water pressures under seismic loading (USBR 1998). Relative density, allowable bearing pressure, and resistance to seismic liquefaction may be increased substantially by the ground improvement methods described in Chapter 1.

Hydraulic fills constructed from soft fine-grained soils, such as bottom silts and clays produced by maintenance dredging, will initially be placed at very high-water contents. Depending on measures taken to induce surface drainage, it will take approximately 2 years before a crust sufficient to support light equipment is formed and the water content of the underlying materials approaches the liquid limit. In order to allow more rapid use, a 1 to 3 feet thick layer of coarse-grained fill can be spread above the fine-grained hydraulic fill. This layer will improve the surface conditions rapidly so that they can support surcharge fills, with or without vertical drains to accelerate consolidation.

Care must be exercised in applying the surcharge so that the shear strength of the soil is not exceeded.

Experience has been gained on existing hydraulic fill dams via field tests. At one dam which was constructed by discharging slurry from pipes along the sides of the dam, the resulting hydraulic fill consisted of a free-draining coarse-grained shell of gravelly silty sand with a core of silty sand and sandy non-plastic silt.[17] The shell was generally loose to medium dense ($N_{1,60}$ of 5 to 30 with mean of 17) with isolated zones of $N_{1,60}$ below 5. Effective stress friction angles were determined to be in the range of 31° to 34°. The loose zones in the shell were determined to have undrained steady state shear strengths in the range of 150 to 500 psf. The hydraulic fill core was very loose to loose ($N_{1,60}$ below 5 with mean of 3), and the effective stress friction angle was estimated and measured in the range of 29° to 32°. For undrained conditions, the core behaved as a normally consolidated, fine-grained soil. Shear wave velocities from seismic CPT mostly ranged from 400 ft/s to 800 ft/s and increased with depth (i.e., increased effective vertical stress). Based on these observations, new or existing hydraulic fill can be evaluated using conventional *in situ* testing techniques provided the engineer anticipates the spatial distribution of soil composition and relative density that results from hydraulic fill placement.

3-7.4 Consolidation of Hydraulic Fills.

Coarse-grained hydraulic fills with high permeability and high coefficient of consolidation will consolidate quickly and will gain shear strength as excess pore pressures dissipate. Reasonable estimates of shear strength can be made based on estimated relative density. Hydraulic fills with k < 0.001 cm/s (fine sands and fine-grained soils) will take a long time to consolidate, and prediction of the behavior of the completed fill will be difficult. Settlement and pore pressure monitoring can be used to assess the state of consolidation of the hydraulic fill under its own weight and that of any surcharge. Settlement plates can be placed both on top of the underlying soil and within the hydraulic fill to observe settlement rates and amounts.

After self-weight consolidation, a hydraulic fill will be normally consolidated and further consolidation may be desirable. As noted by Sowers (1979), this compression can be completed by various ground improvement methods. For coarse-grained soils, vibro-compaction, pile driving, and blast densification can be used to increase relative density. Vibration at the surface of the fill can be effective to depths of about 10 feet. Silty hydraulic fills can be consolidated using well points.

[17] Confidential location (personal communication)

The consolidation of fine-grained hydraulic fills will depend on the properties of the borrow material. Those derived from stiff clays will have a structure consisting of hard clumps in a matrix of soft clay, making laboratory tests inapplicable. Hydraulic fills derived from soft clays can be evaluated using one-dimensional consolidation tests. The coefficient of compressibility (m_v) of fine-grained hydraulic fills ranges from 3×10^{-6} to 5×10^{-5} 1/psf. In both cases, preloading of fine-grained hydraulic fills is effective to reduce settlements. Pore pressure dissipation rates of hydraulic fills range from hours to years depending on the sand content and cannot be estimated from laboratory tests (Whitman 1970).

3-7.5 Underwater Fill.

Some projects require fill to be placed underwater, which poses unique challenges. In most cases, experience with underwater fill placement has been limited to depths of about 100 feet or less. Pollution control, including the use of turbidity curtains, is critical during underwater fill construction.

Dredging is an important part of the underwater fill placement process similar to subgrade preparation for conventional fill. Dredging can be used to remove unsuitable soil, cut slopes in existing submerged materials, and clean the fill area. At a minimum, the latter is required to remove settled fine-grained material resulting from the construction activity (Johnson et al. 1972).

The primary methods of placing fill underwater are summarized in Table 3-18. The placement method will be governed by the available equipment, the depth of water, and the required side slopes. Fill quantities are tracked by bathymetric methods. The effects of settlement during construction on the measured fill quantities should be considered.

Control of underwater fill is typically completed using *in situ* testing techniques, such as SPT or CPT. Testing should be completed as placement of the fill progresses, particularly to check for unsuitable materials trapped below or within the fill. Samplers can be used, if necessary, to obtain physical samples of the underwater fill. Experience has shown that large, rugged sampling techniques are more effective than refined, sophisticated ones (Bazett and Foxall 1972).

The relative density of underwater fill is typically up to 50% to 60% and is highly variable. Zones of low relative density may be a concern for settlement under moderate to heavy loads and for liquefaction. Vibro-compaction is the primary method used to densify hydraulic and underwater fills after placement. Examples include dry docks (Zola and Boothe 1960), dams (Hassouna and Shenouda 1970), and man-made islands.

Table 3-18 Methods of Underwater Fill Placement (after Johnson et al. 1972)

Method	Characteristics	Schematic
Bottom-dump scows	• Quick • Relatively flat slopes unless retained by dikes or sheet piles, slope angle flattens as water depth increases • Boat drafts limit to minimum depth of about 15 ft • Discharge of fill entraps air and limits segregation	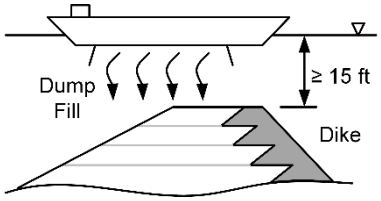
Deck scows	• Slower • Fill pushed from deck by dozer, placed by clamshell, or jetted from deck • Steeper sides achievable, slope angle flattens as water depth increase	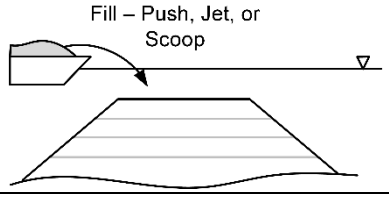
Hydraulic fill	• Segregation between coarse and fine materials occurs • Fines may collect in low areas, requiring removal • May cause shear failures in soft foundation soils • More difficult to inspect	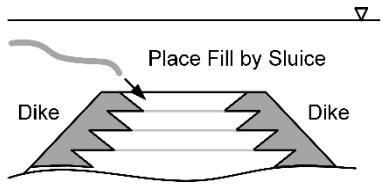
Dump fill on land and push into the water	• Advance the central part of the fill first so that softer bottom materials can be displaced • Bulldozer blades can be used in shallow water to displace soft materials • Fines in fill placed below the water accumulate in front of the advancing fill	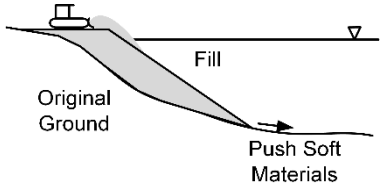

3-8 PROBLEM SOILS AND EARTHWORK.

Chapter 1 provides a summary of many types of problem soil conditions that can affect the design of foundations and earth structures. Table 3-19 summarizes important conditions for the design of earthwork in problem soils.

Table 3-19 Problem Soil Considerations for Earthwork

Soil Type	Primary Considerations for Earthwork Design

Soft Clays	• Soft clays do not provide a stable platform for the compaction of fill. Solutions may include:
	  ○ Mechanical stabilization with crushed stone, possibly reinforced with geogrid, or
	  ○ Chemical stabilization of upper layer.
	• Staged construction may be required to allow strength gain resulting from consolidation.

Highly Plastic Expansive Clays and Shales	• Compacted clay embankment soils may shrink and swell due to seasonal moisture changes, leading to progressive failure. • Slope design should be based on fully-softened shear strength parameters.
Collapsible Soils	• Earthwork loading can cause compression of natural collapsible soils, such as loess, especially if the earthwork is combined with changes in moisture content. • Compacted clays may have a collapsible structure if compacted dry of optimum, which can be reduced by compacting wet of optimum. This consideration is especially important for deep fills.
Sensitive Clays	• Earthwork loading of sensitive clays can cause deformations leading to remolding and catastrophic failure. • Design should maintain a high factor of safety, such that imposed shear stresses remain below the peak shear strength at all points in the sensitive clay.
Residual and Colluvial Soils	• Residual and/or colluvial soils are often problematic if left in place below side hill fills. • May have lower shear strength compared to the compacted fill, creating a weak layer. • Residual materials may have adverse planes of weakness, which can be addressed by proper benching procedures.
Laterites	• Provide poor support for embankments if loaded cyclically or exposed to flowing groundwater
Talus	• Global stability should be considered for design of earthwork over talus deposits
Loose Sands	• Loose sands may not provide a stable platform for compacted fill, particularly if saturated (see soft clays above). • Significant compression should be anticipated due to embankment loading. • In seismic zones, loose sands may present a liquefaction hazard for embankments. • Where fine, loose sands are present in foundation or embankments, erosion potential should be considered.
Glacial Till	• Problematic erosion may occur in sand and silt-sized glacial tills.
Organic Soils, Peat, and Muskeg	• Organic soils do not provide a stable platform for the compaction off fill (see soft clays above). • Organic soils are highly compressible and may experience substantial primary consolidation and secondary compression from earthwork loading. • Organic content of structural fills is often strictly controlled by specifications.
Dispersive Soils	• Dispersive soils are susceptible to internal erosion by flowing water, particularly when used as seepage barriers in earth dams or levees. • Use of dispersive clays in dams should be avoided, because they are very difficult to protect even with well-designed filters.
Dredged Soils	• Most dredged soil deposits will be loose or soft and earthwork construction will require considerations discussed above for soft clays or loose sands. • Dredged material typically has a high water content, which would need to be lowered prior to use as fill.
Low Plasticity Silts and Clays	• Silts can be extremely unstable, both as a working platform for earthwork and within a fill. • Some low plasticity lean clays (PI in range of 9 to 15) have a high percentage (60 to 80%) of silt-sized particles. Fill or subgrades constructed from these soils experience substantial strength loss when wetted and lose ability to support pavements.
Municipal Solid Waste	• Earthwork performed above MSW or in conjunction with landfills must consider the shear strength and compressibility of the waste. Some correlations are available. • Consideration should be given to changes in MSW properties with time.

3-9 NOTATION.

Variable	Definition
a	Power function strength parameter defining the steepness of the curve
b	Power function strength parameter defining the amount of curvature
a_Δ	Fill compression parameter controlling magnitude of compression with vertical effective stress
b_Δ	Fill compression parameter controlling nonlinearity of compression with vertical effective stress
c	Total stress or undrained cohesion intercept
C_c	Coefficient of curvature from grain size analysis, a.k.a, coefficient of gradation
C_u	Coefficient of uniformity
D_r	Relative density
e_{max}	Maximum void ratio
e_{min}	Minimum void ratio
G_s	Specific gravity of solids
G_{sC}	Specific gravity of oversize fraction (particle size implied by *oversize* depends on the test method)
k	Hydraulic conductivity
k_{sat}	Hydraulic conductivity for saturated conditions
LL	Liquid limit
m	Weibull distribution parameter used for the effects of particle size on shear strength
m_v	Coefficient of compressibility
$N_{1,60}$	Standard Penetration Test blow count corrected for overburden stress and efficiency
P_a	Atmopheric pressure
P_C	Percent oversize fraction (particle size implied by *oversize* depends on the test method)
P_F	Percent finer fraction (particle size implied by *finer* depends on the test method)
pH	Quantitative measure of acidity
PI	Plasticity index
PL	Plastic limit
R	Roughness factor used for operational strength of rockfill
$R.C.$	Relative compaction
S	Degree of saturation

Variable	Definition
s_u/σ'_c	Undrained strength ratio
V_t	Total volume
w	Water content
w_C	Water content of oversize fraction (particle size implied by *oversize* depends on the test method)
w_F	Water content of finer fraction (particle size implied by *finer* depends on the test method)
$w_{F,opt}$	Optimum water content of finer fraction
w_{field}	Water content of field compacted soil
w_{opt}	Optimum water content associated with a particular compactive effort
W_s	Weight of solids
w_T	Water content of the combined finer and oversize fractions
$\Delta\phi'$	Parameter describing the change in effective friction angle with confinings
$\Delta V/V_F$	Overall shrinkage factor
Δw	Relative water content
γ	Total or moist unit weight
$\gamma_{d,B}$	Average dry unit weight of borrow material
$\gamma_{d,F}$	Dry unit weight of finer fraction (particle size implied by *finer* depends on the test method)
$\gamma_{d,field}$	Dry unit weight of field compacted soil
$\gamma_{d,max}$	Maximum dry unit weight associated with minimum void ratio
$\gamma_{d,min}$	Minimum dry unit weight associated with maximum void ratio
γ_{dT}	Dry unit weight of the combined finer and oversize fractions
$\gamma_{dT,field}$	Dry unit weight of the combined finer and oversize fractions as compacted in the field
γ_w	Unit weight of water
ϕ	Total stress friction angle
ϕ'	Effective stress or drained friction angle
ϕ'_0	Effective stress friction at reference stress (typically one atmosphere)
μ	Mean value
σ'_c	Effective consolidation stress
σ'_f	Effective normal stress at failure

Variable	Definition
σ	Standard deviation
σ'_z	Effective vertical stress

3-10 SUGGESTED READING.

Topic	Reference
General Earthwork	TRB 1990. *Guide to Earthwork Construction, State of the Art Report 8*, National Research Council, Washington, D.C.
	Hilf, J. W. 1991. "Compacted fill." *Foundation Engineering Handbook*, 2nd Edition, Ed. H.-Y. Fang, Springer Nature, 249-316.
Earth Dam Construction	USACE, 2004. *General Design and Construction Considerations for Earth and Rock-Fill Dams, EM 1110-2-2300*, Department of the Army, Washington, D.C.
	USBR, 2012. "Chapter 10: Embankment Construction." *Design Standards No. 13 Embankment Dams*, Technical Service Center, United States Bureau of Reclamation.
Rock Fill	Breitenbach, A. J. 1993. "Rockfill placement and compaction guidelines." *Geotechnical Testing Journal*, 16(1), 76-84.
Underwater Fill	*Underwater Soil Sampling, Testing, and Construction Control, ASTM Special Technical Publication 501*, ASTM International.

This Page Intentionally Left Blank

CHAPTER 4. ANALYSIS OF WALLS AND RETAINING STRUCTURES

4-1 INTRODUCTION.

Earth retaining structures are among the oldest built structures in the history of civilization. They are necessary to accommodate a change in grade or ground surface elevation over a short distance. Earth retaining structures are also necessary in harbors, shores, and riverbanks to allow easy access to water. Some of the first technical papers in geotechnical engineering concerned theories for calculating earth pressures for retaining structures (Coulomb 1776; Rankine 1857).

Although a myriad of types of earth retaining structures are part of 21st century civil engineering construction, the basic earth pressure theories and major design elements of these structures share common links.

This chapter presents the basic theories and principles behind the calculation of earth pressure. The application of these theories and principles is illustrated for a variety of retaining structures encountered in civil engineering construction.

4-2 DEVELOPMENT OF EARTH PRESSURES AND LOADS.

The earth pressures acting on buried structures, such as retaining walls, basement walls, ground anchors, etc., are dependent on the relative movement between the structure and the surrounding soil. In the simplest form, this is often shown as a buried plate within a soil mass (Figure 4-1). If the plate or structure does not move, then the pressures on the right side and left side of the structure are equal, and this is called an *at-rest earth pressure* condition.[18] In the at-rest earth pressure condition, the soil *is not* in a condition of failure.

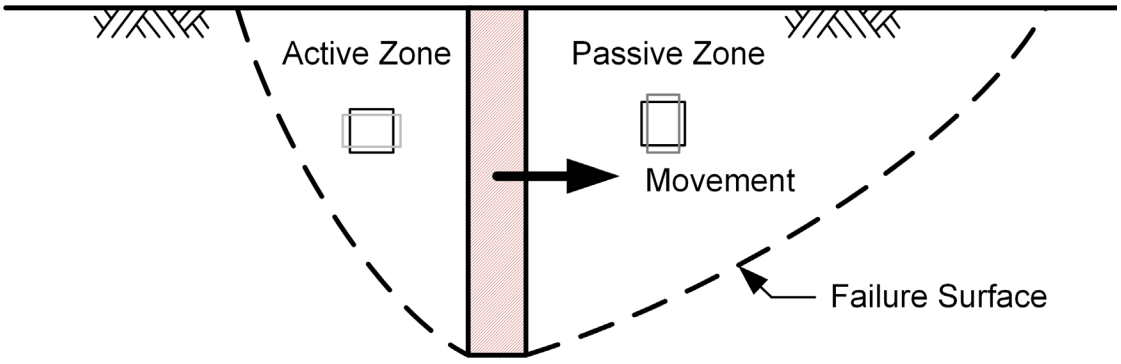

Figure 4-1 Influence of Movement on Active and Passive Earth Pressure Zones

[18] This is also called a K_o condition or *zero lateral strain* condition.

If a load is applied to the plate to move it toward the right, the soil to the right of the structure is compressed horizontally, and the shear resistance of the soil is mobilized. A *passive earth pressure* condition develops on the right side. On the left side of the structure, the horizontal stress is decreased, and the soil is extended or stretched until the shear resistance of the soil is mobilized. This is called an *active earth pressure* condition. The figure also shows how a square element of soil would deform for each of the cases. In the passive zone, the square element is compressed laterally, and in the active zone, the square element is extended laterally. Provided the active and passive conditions are fully developed, the soil is in a condition of failure in both the active and passive zones.

A common parameter used in earth pressure calculations is the *earth pressure coefficient*, K. The earth pressure coefficient is normally defined as the ratio of the horizontal *effective* stress to the vertical *effective* stress at a point within the soil mass. The earth pressure coefficient is occasionally assumed to be the ratio of the horizontal total stress to the vertical total stress.[19] In this chapter, K is defined as the ratio of the effective stresses unless specifically stated otherwise.

4-2.1 At-Rest Earth Pressure.

For at-rest conditions, the earth pressure coefficient is defined as:

$$K_0 = \frac{\sigma'_h}{\sigma'_z} \tag{4-1}$$

where:
K_0 = at-rest earth pressure coefficient,
σ'_h = horizontal effective stress, and
σ'_z = vertical effective stress.

For this equation to be valid, the soil mass must be in a state of zero lateral strain. Within a soil mass, at-rest conditions normally require a horizontal ground surface and the absence of surface loads of limited areal extent. At-rest conditions can exist when there is a rigid boundary, such as a basement wall, that will satisfy the condition of zero lateral or horizontal strain. For most applications, the horizontal and vertical stresses are the major and minor principal stresses with the relative directions depending on the value of K_0 (i.e., $\sigma'_h = \sigma'_1$ if $K_0 > 1$ and $\sigma'_h = \sigma'_3$ if $K_0 < 1$).

Standardized laboratory tests are not available to measure the value of K_0. Some special tests apparatuses have been developed to measure K_0 (Filz 1992; Sehn 1990),

[19] Total stress earth pressure coefficients can be useful for specifying earth pressures in numerical analyses concerned only with total stresses.

but these are not used in conventional engineering practice. The Menard pressuremeter, the self-boring pressuremeter, and the Marchetti dilatometer have been used to obtain an *in situ* measurement of K_0, but these devices are not in common use for the design of earth retaining structures.

The most common method used to determine K_0 is based on a correlation presented by Mayne and Kulhawy (1982):

$$K_0 = (1 - \sin\phi') \cdot OCR^{\sin\phi'} \quad (4\text{-}2)$$

where:
K_0 = at-rest earth pressure coefficient,
ϕ' = effective stress friction angle for normally consolidated conditions, and
OCR = overconsolidation ratio.

K_0 values are less than one for normally consolidated soils, and can range from about 0.3 to 0.8. For simple calculations, K_0 is often assumed to be equal to 0.5. In overconsolidated soils, it is common for the value of K_0 to be greater than one, indicating that the horizontal effective stress is greater than the vertical effective stress.

4-2.2 Rankine Active and Passive Earth Pressures.

Both the active and passive earth pressure coefficients represent the effective stress ratio for a failure condition in the soil. The earth pressure coefficients K_A and K_P are best explained using Rankine's (1857) earth pressure theory. Mohr circles representing at-rest, active, and passive conditions are shown in Figure 4-2.

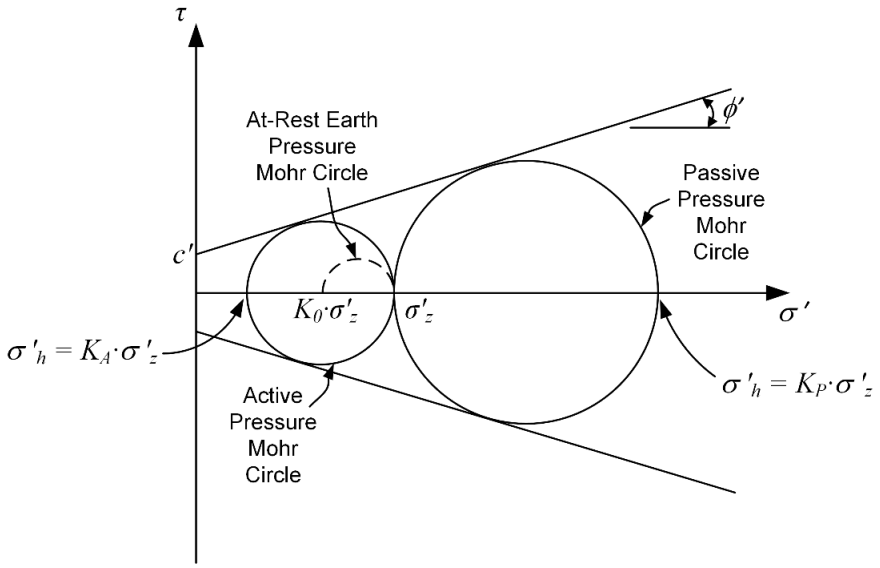

Figure 4-2 Mohr Circles for At-Rest, Rankine Active, and Rankine Passive Stress States

For the at-rest conditions, the Mohr circle is not tangent to the envelope; therefore, it does not represent a condition of failure. The circle representing an active failure shows that the horizontal stress is equal to K_A multiplied by the vertical stress, and the Mohr circle is tangent to the envelope. The circle representing the passive failure condition shows that the horizontal stress is equal to K_P multiplied by the vertical stress. In the active condition, the major principal stress (σ'_1) is vertical and the minor principal stress (σ'_3) is horizontal. For the passive condition, the major principal stress (σ'_1) is horizontal and the minor principal stress (σ'_3) is vertical. For both of these cases, the horizontal stress is the earth pressure.

Rankine's theory and the geometry of the Mohr circles shown in Figure 4-2 result in the following equations for the active and passive earth pressure coefficients:

$$\textit{Active: } K_A = \frac{1-\sin\phi'}{1+\sin\phi'} = \tan^2(45-\frac{\phi'}{2}) \quad (4\text{-}3),$$

$$\textit{Passive: } K_P = \frac{1+\sin\phi'}{1-\sin\phi'} = \tan^2(45+\frac{\phi'}{2}) \quad (4\text{-}4),$$

and

$$K_A = \frac{1}{K_P} \quad (4\text{-}5)$$

where:
K_A = coefficient of active earth pressure,
K_P = coefficient of passive earth pressure, and
ϕ' = effective stress friction angle.

The Mohr circles in Figure 4-2 allow the horizontal effective stress to be predicted for both active and passive conditions for the stresses at any point within the failure zone. The horizontal pressures are calculated as:

$$\textit{Active: } \sigma'_h = K_A \cdot \sigma'_z - 2 \cdot c' \cdot \sqrt{K_A} \quad (4\text{-}6)$$

and

$$\textit{Passive: } \sigma'_h = K_P \cdot \sigma'_z + 2 \cdot c' \cdot \sqrt{K_P} \quad (4\text{-}7)$$

where:
K_A = coefficient of active earth pressure,
K_P = coefficient of passive earth pressure,
σ'_h = horizontal effective stress (earth pressure),
σ'_z = vertical effective stress, and
c' = effective stress cohesion intercept.

From Equations 4-6 and 4-7, the effective cohesion intercept theoretically decreases the active earth pressure and increases the passive earth pressure. The value of c' is usually assumed to be zero for coarse-grained soils. Fine-grained soils that are represented by a linear failure envelope may have a value of c', which is associated with overconsolidation or compaction. These soils creep, shrink, and swell with time, and the operating value of c' can decrease or reach zero. For this reason, the changes to the earth pressures caused by c' are usually neglected for fine-grained soils.

4-2.3 Movement Required to Develop Active and Passive States.

An important consideration in earth pressure theory is the amount of movement required to develop the active and passive earth pressure conditions. Much more movement or displacement is required to develop the passive condition than the active condition. This is particularly important in the design of earth retention structures or soil anchors since both active and passive pressures affect the performance of the structure. However, the amount of displacement of the structure might not be an explicit parameter in the calculations.

Figure 4-3(a) illustrates the importance of wall movement on the development of active and passive earth pressures. For active and passive pressures to fully develop, the wall must translate laterally or tilt (rotate). The figure shows general trends developed from experimental data linking the magnitude of the earth pressure coefficient to wall rotation, expressed as the ratio of horizontal displacement (Y) to the wall height (H). Typical magnitudes for different soil types are summarized in Figure 4-3(d). About five to ten times more displacement is required to develop passive pressures than active pressures.

The amount of displacement required to mobilize active and passive states also depends on the soil type and compaction. Dense sands require less displacement than loose sands. Compacted clays require five to ten times more movement than dense sands.[20] As noted in Figure 4-3(d), theoretical values of K_A and K_P can only be sustained for short time periods by clay soils because of creep.

4-2.4 Earth Pressure Distributions and Loads.

Figure 4-3(b) and (c) illustrate the active and passive pressure distributions acting on a retaining wall. The earth pressure is calculated over the depth of the backfill (H). The cases shown have horizontal backfill, no effective stress cohesion, and no friction between the wall and backfill. The active and passive earth pressures result in triangular pressure distributions.

[20] The Rankine method for calculating earth pressures is more applicable to coarse-grained soils than fine-grained soils. Other methods are recommended for calculating earth pressures of fine-grained soils.

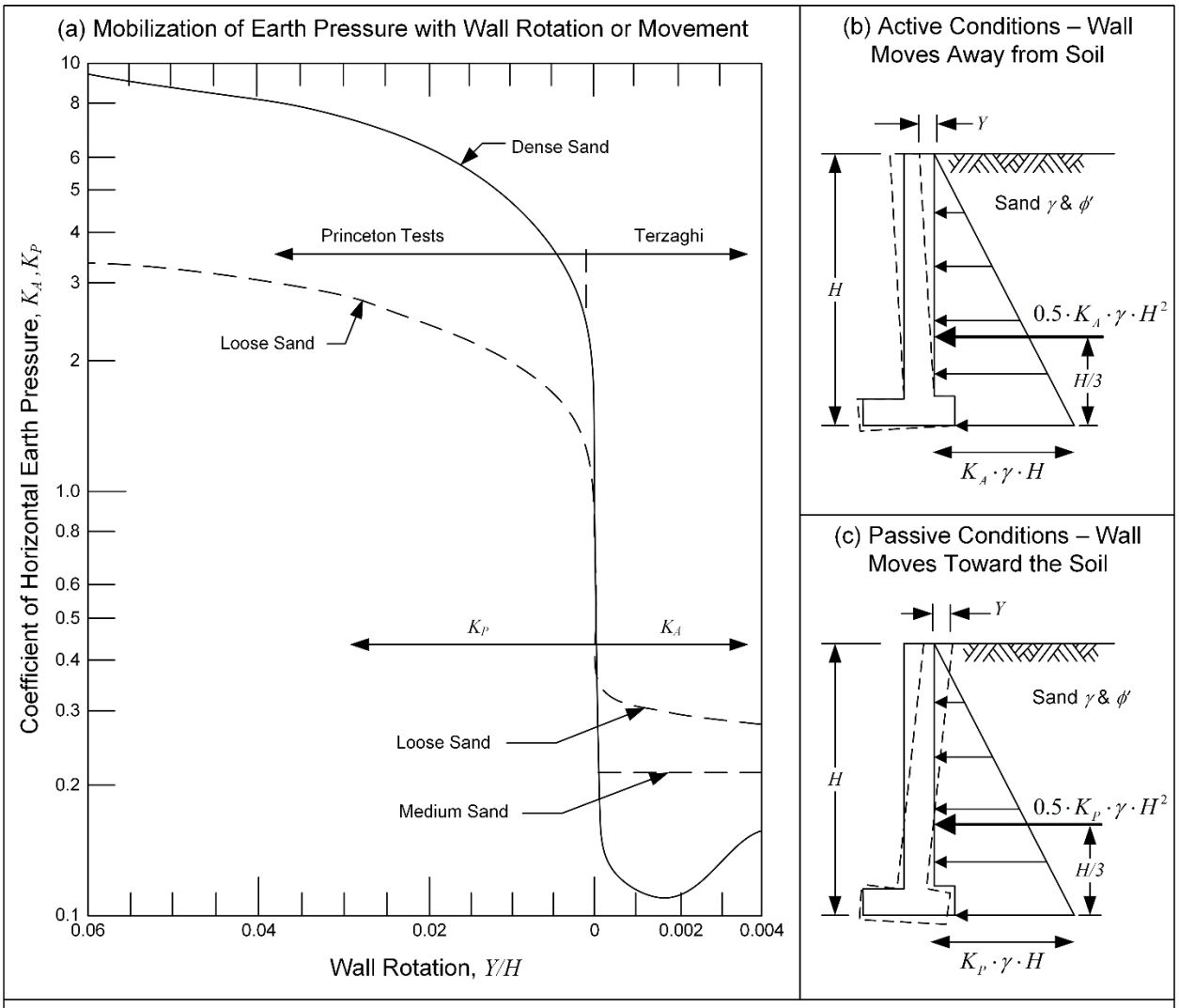

(d) Magnitudes of Wall Rotation to Fully Mobilize Earth Pressure by Soil Type

Soil Type and Condition	Rotation Y/H	
	Active	Passive
Dense Sand	0.001	0.01
Medium Dense Sand	0.002	0.02
Loose Sand	0.004	0.04
Compacted Silt	0.002	0.02
Compacted Lean Clay**	0.01	0.05
Compacted Fat Clay**	0.01	0.05

Y = Horizontal Displacement and H = Height of the Wall

** Under stress conditions close to the minimum active or maximum passive pressure, clay soils will creep continually. These levels of movement will only temporarily produce active or passive pressure. With time, the active pressure will approach the at-rest value, and the passive pressure will approach about 40% of the passive value.

Figure 4-3 Active and Passive Earth Pressure – (a) Mobilization with respect to Wall Movement, (b) Active Earth Pressure Distribution and Load, (c) Passive Earth Pressure Distribution and Load, and (d) Required Magnitude of Wall Rotation for Various Soil Types (after Kim et al. 1991)

The resultant force of the triangular pressure distribution is determined for the active and passive cases as:

$$\textit{Active: } P_A = K_A \cdot \frac{\gamma \cdot H^2}{2} \tag{4-8}$$

and

$$\textit{Passive: } P_P = K_P \cdot \frac{\gamma \cdot H^2}{2} \tag{4-9}$$

where:
P_A = active earth pressure resultant force,
P_P = passive earth pressure resultant force,
γ = unit weight of backfill soil, and
H = height of wall.

The equations shown above are for effective stress or drained analyses. The same equations can be expressed for undrained or total stress analyses. For this case, total stress strength parameters (c, ϕ, or s_u) are used in the equations, and the calculated earth pressure is the total horizontal stress (σ_h). There are some important issues regarding the application of the Rankine method to undrained or total stress conditions, which are discussed in Section 4-3.3.

Figure 4-4 shows earth pressure distributions for active and passive cases using the Rankine theory. The application of the Rankine theory is generally limited to cases where there is not any friction between the retaining wall and the soil (i.e., smooth wall) and the backfill is horizontal although there are published techniques that can accommodate inclined backfills.

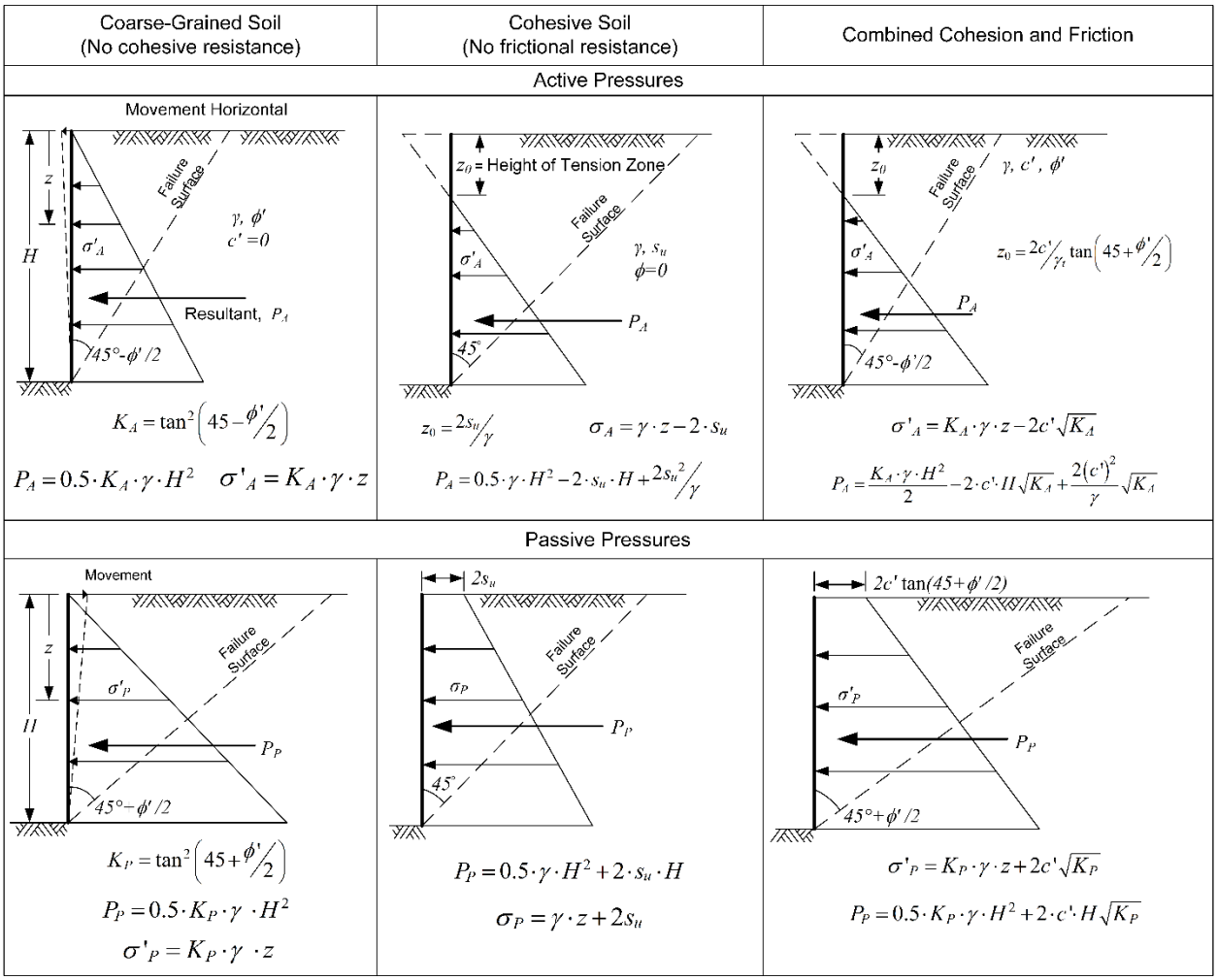

Figure 4-4 Earth Pressure Distributions for Active and Passive Rankine Cases

4-2.5 Rankine Method Examples.

Figure 4-5 shows an example for active pressure determination using the Rankine method for the following conditions:

- horizontal backfill,
- uniform surcharge load (q),
- no wall friction,
- horizonal water surfaces on both sides of the wall, and
- homogeneous soil conditions with strength characterized by c' and ϕ'.

For this example, moist unit weights are used above the water table and buoyant unit weights are used below the water table in order to calculate the correct vertical effective stress. In this example, the earth pressure caused by the surcharge is greater than the reduction in earth pressure due to the effects of cohesion, so the earth pressure at the

ground surface is greater than zero. It is common to ignore the contribution of the cohesion term in earth pressure calculations for additional conservatism.

Figure 4-6 has the same cross section as Figure 4-5, but the equations for passive earth pressure are shown. The calculations are very similar to the active earth pressure example (Figure 4-5).

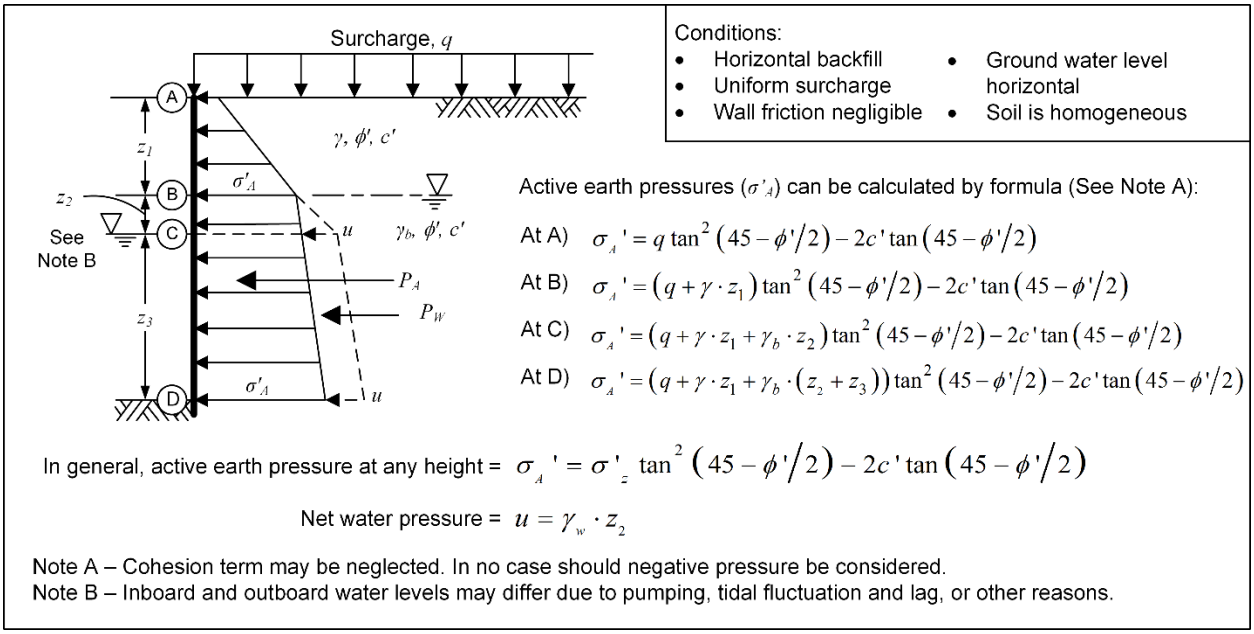

Figure 4-5 Rankine Active Earth Pressure Calculation for No Wall Friction and Uneven Water Elevations

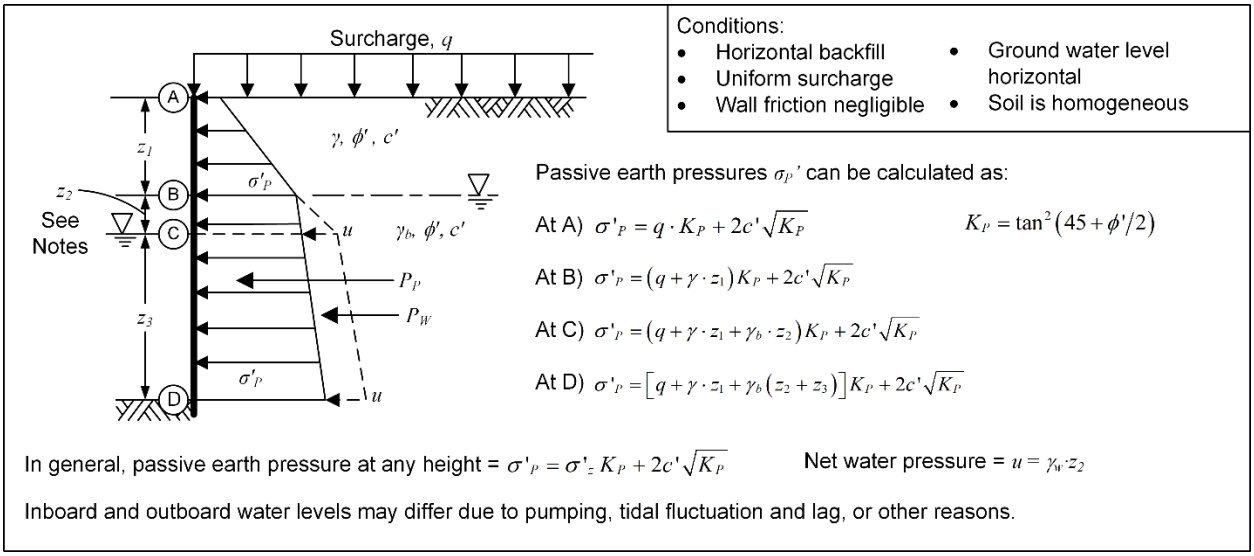

Figure 4-6 Rankine Passive Earth Pressure Calculation for No Wall Friction and Uneven Water Elevations

4-2.6 Wall/Soil Interface Friction Angle.

The interface friction angle (δ) between the wall and soil backfill can be an important parameter in retaining wall analysis. The angle is equal to that obtained in a direct shear apparatus when the bottom half of the shear box is the wall material (normally concrete or steel) and the top half is soil. Tests can be conducted at pressures in the same range as the earth pressures, and a linear envelope is fit through the data. In geotechnical practice, these special direct shear tests are not often conducted, and the value of δ is most often obtained from published data, such as that presented in Table 4-1. Typical δ values for various combinations of wall materials and soil types are provided. For clayey soils located at an interface, such as the bottom of a wall or adjacent to a sheet pile, the resistance is termed the *adhesion*, C_a.

Table 4-1 Interface Friction Angles and Adhesion Values for Wall/Soil Interfaces

Frictional Interface between Various Materials	Interface friction angle, δ (deg)	Friction Factor (tan δ)
Mass concrete or masonry on the following foundation materials		
Clean sound rock	35	0.7
Clean gravel, gravel-sand mixtures, coarse sand	29 - 31	0.55 – 0.60
Clean fine to medium sand, silty medium to coarse sand, silty or clayey gravel	24 - 29	0.45 – 0.55
Clean fine sand, silty or clayey fine to medium sand	19 - 24	0.35 – 0.45
Fine sandy silt, nonplastic silt	17 - 19	0.30 – 0.35
Very stiff and hard residual or overconsolidated clay	22 - 26	0.40 - 0.50
Medium stiff and stiff clay and silty clay	17 - 19	0.30 - 0.35
Steel sheet piles against the following soils		
Clean gravel, gravel-sand mixtures, well-graded rock fill with spalls	22	0.40
Clean sand, silty sand-gravel mixture, single size hard rock fill	17	0.30
Silty sand, gravel or sand mixed with silt or clay	14	0.25
Fine sandy silt, nonplastic silt	11	0.20
Formed concrete or concrete sheet piling against the following soils		
Clean gravel, gravel-sand mixture, well-graded rock fill with spalls	22 - 26	0.40 – 0.50
Clean sand, silty sand-gravel mixture, single size hard rock fill	17 - 22	0.30 – 0.40
Silty sand, gravel or sand mixed with silt or clay	17	0.30
Fine sandy silt, nonplastic silt	14	0.25
Various structural materials		
Masonry on masonry, igneous and metamorphic rocks		
Cleaned and scaled soft rock on cleaned and scaled soft rock	35	0.70
Cleaned and scaled hard rock on cleaned and scaled soft rock	33	0.65
Cleaned and scaled hard rock on cleaned and scaled hard rock	29	0.55
Masonry on wood (cross grain)	26	0.50
Steel on steel at sheet pile interlocks	17	0.30
Interface with Clayey Soils (Undrained shear strength)	**Adhesion C_a (psf)**	
Very soft fine-grained soil (0 - 250 psf)	0 – 250	
Soft fine-grained soil (250 - 500 psf)	250 – 500	
Medium stiff fine-grained soil (500 - 1000 psf)	500 – 750	
Stiff fine-grained soil (1000 - 2000 psf)	750 – 950	
Very stiff fine-grained soil (2000 - 4000 psf)	950 - 1300	

4-3 ACTIVE AND PASSIVE EARTH PRESSURE FROM OTHER METHODS.

The values of K_A and K_P for the Rankine method, as presented in Equations 4-3 and 4-4, are solely a function of the drained friction angle, ϕ'. Other methods of calculating earth pressure coefficients, such as the trial wedge method developed by Coulomb (1776) and the log spiral method summarized by Caquot and Kerisel (1948), are available. With the trial wedge and log spiral methods, the effects of other factors, such as sloping backfills and wall friction, can be accommodated, and these effects are reflected in the values of the earth pressure coefficients. A gravity retaining wall with a sloping backfill (β) and wall (θ) is shown in Figure 4-7 for a case where the wall/soil interface friction angle (δ) is considered.

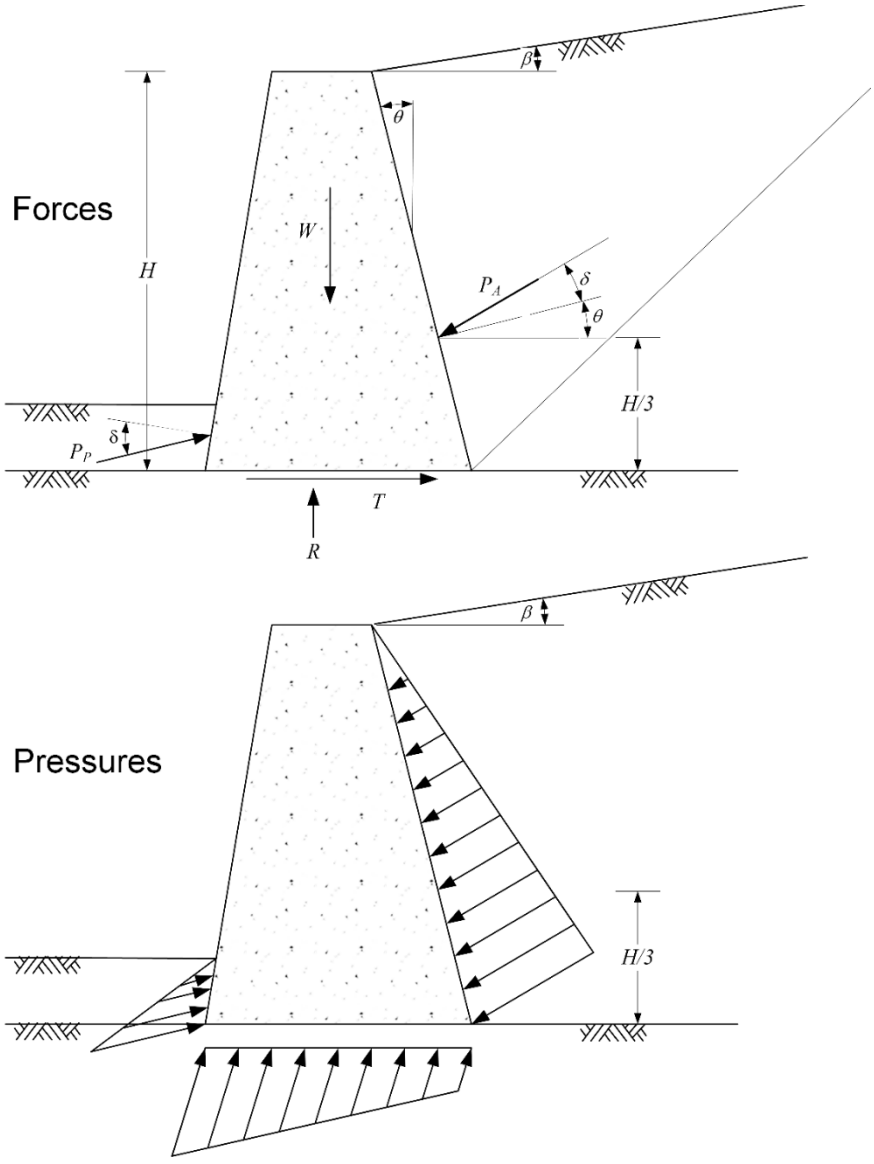

Figure 4-7 Gravity Retaining Wall with Sloping Backfill, Sloping Wall, and Interface Friction Angle

4-3.1 Coulomb Wedge Method.

Coulomb (1776) developed a limit equilibrium method for calculating the force applied to a wall or anchor for the active and passive earth pressure conditions. This method, along with other modifications of the method, analyzes the forces acting on an active or passive failure wedge defined by a linear failure surface. The main differences between the active and passive cases are the angle at which the resultant force acts on the wall and the direction of the shear forces acting on the failure plane, owing to the difference in the direction of movement of the wedge.

The Coulomb method has advantages over the Rankine method in that it can accommodate:

- irregular ground surfaces,
- sloping wall faces,
- irregular surcharge loads on the ground surface, and
- interface friction between the wall and the soil backfill.

A Coulomb analysis can be performed as a graphical solution, chart solution, or equations can be developed for direct calculations. Different failure surfaces are analyzed until the maximum active force or minimum passive force is obtained. The free body diagrams and force polygons for the active and passive conditions for cases with and without wall friction are shown in Figure 4-8.

For the conditions given in Figure 4-8(a), Figure 4-9 provides values of K_A and K_P for different friction angles and backfill slopes, assuming c' = 0. Once the earth pressure coefficient has been determined, then a resultant force (P_A or P_P) can be calculated using the same procedure as used for the Rankine method (Equations 4-8 and 4-9). Figure 4-10 allows the determination of the slope of the linear failure surface measured from vertical (α).

The active earth pressure load can be directly calculated for the more complex case of a sloping wall face (θ), sloping backfill (β), and interface friction angle (δ) as:

$$P_A = \frac{1}{2} \cdot \gamma \cdot H^2 \cdot \frac{\cos^2(\phi' - \theta)}{\cos^2\theta \cdot \cos(\theta + \delta)\left[1 + \sqrt{\frac{\sin(\phi' + \delta)\sin(\phi' - \beta)}{\cos(\theta + \delta)\cos(\theta - \beta)}}\right]^2} \quad (4\text{-}10)$$

where:
P_A = active earth pressure force,
γ = unit weight of backfill soil,
H = wall height,
ϕ' = effective stress or drained friction angle,
θ = slope angle of the wall face,
δ = interface friction angle between wall and soil, and
β = slope of backfill surface.

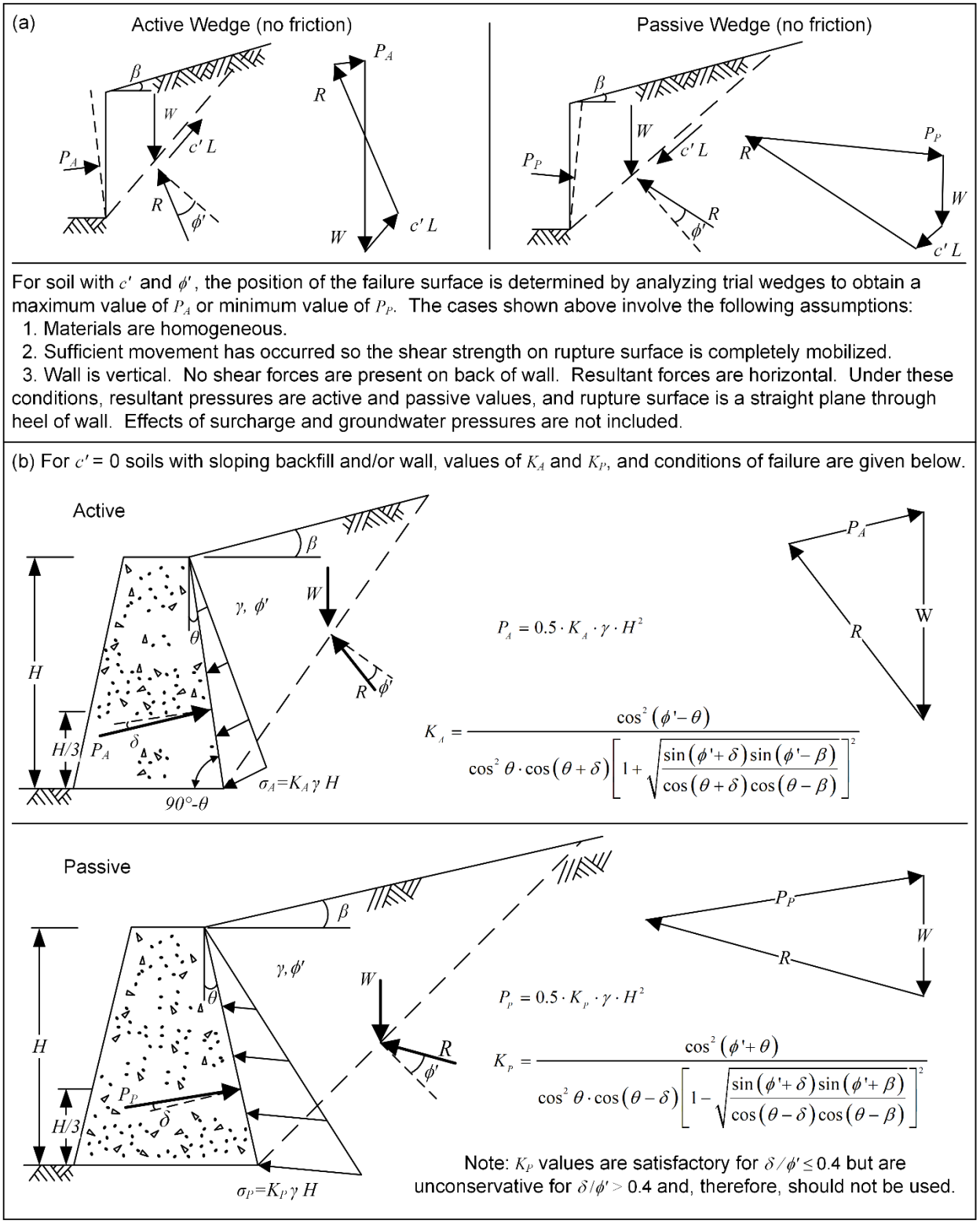

Figure 4-8 Free Body Diagrams and Force Polygons for Coulomb Method for Various Wall and Backfill Geometries

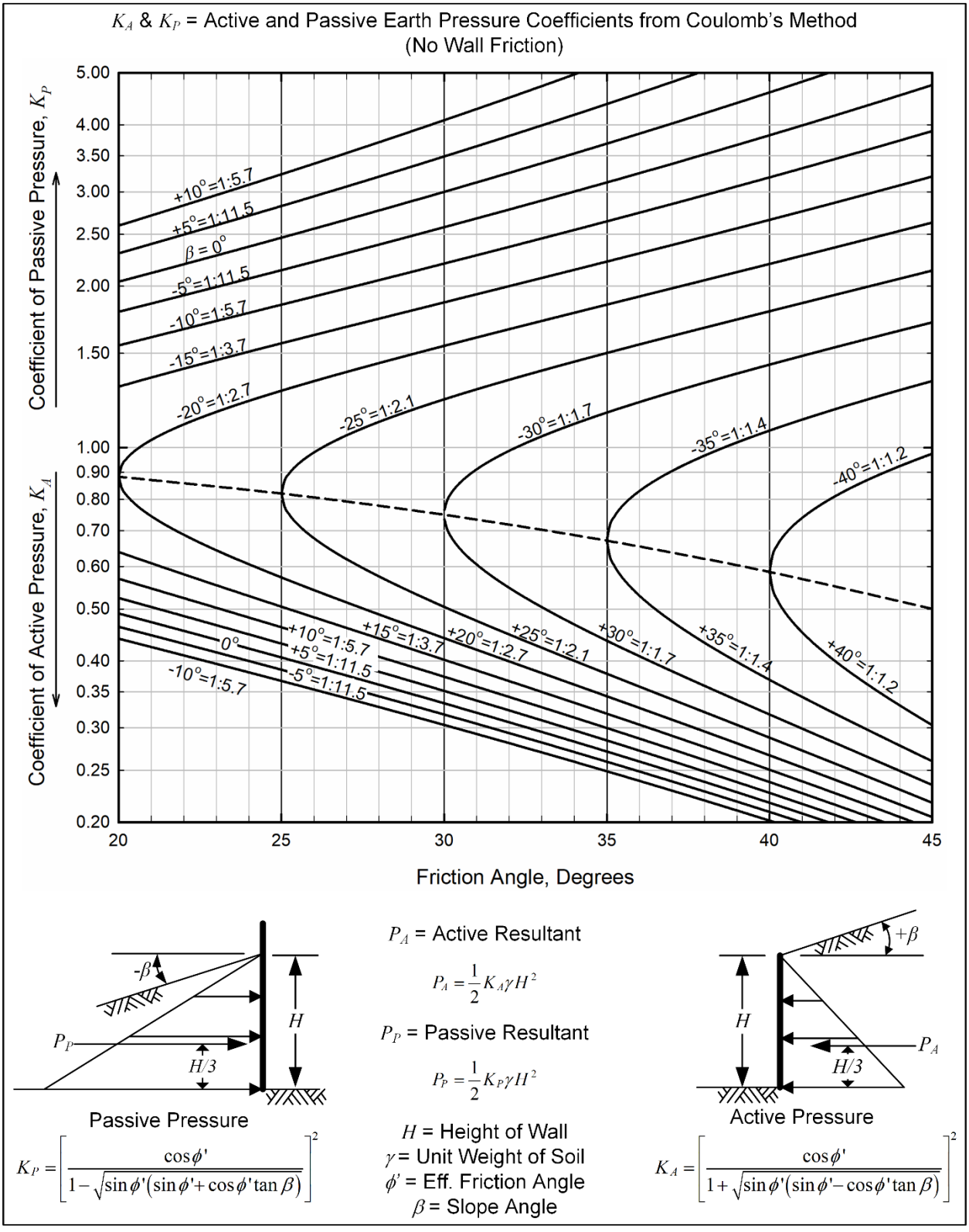

Figure 4-9 Values of K_A and K_P for the Coulomb Method for Vertical Walls with No Wall Friction

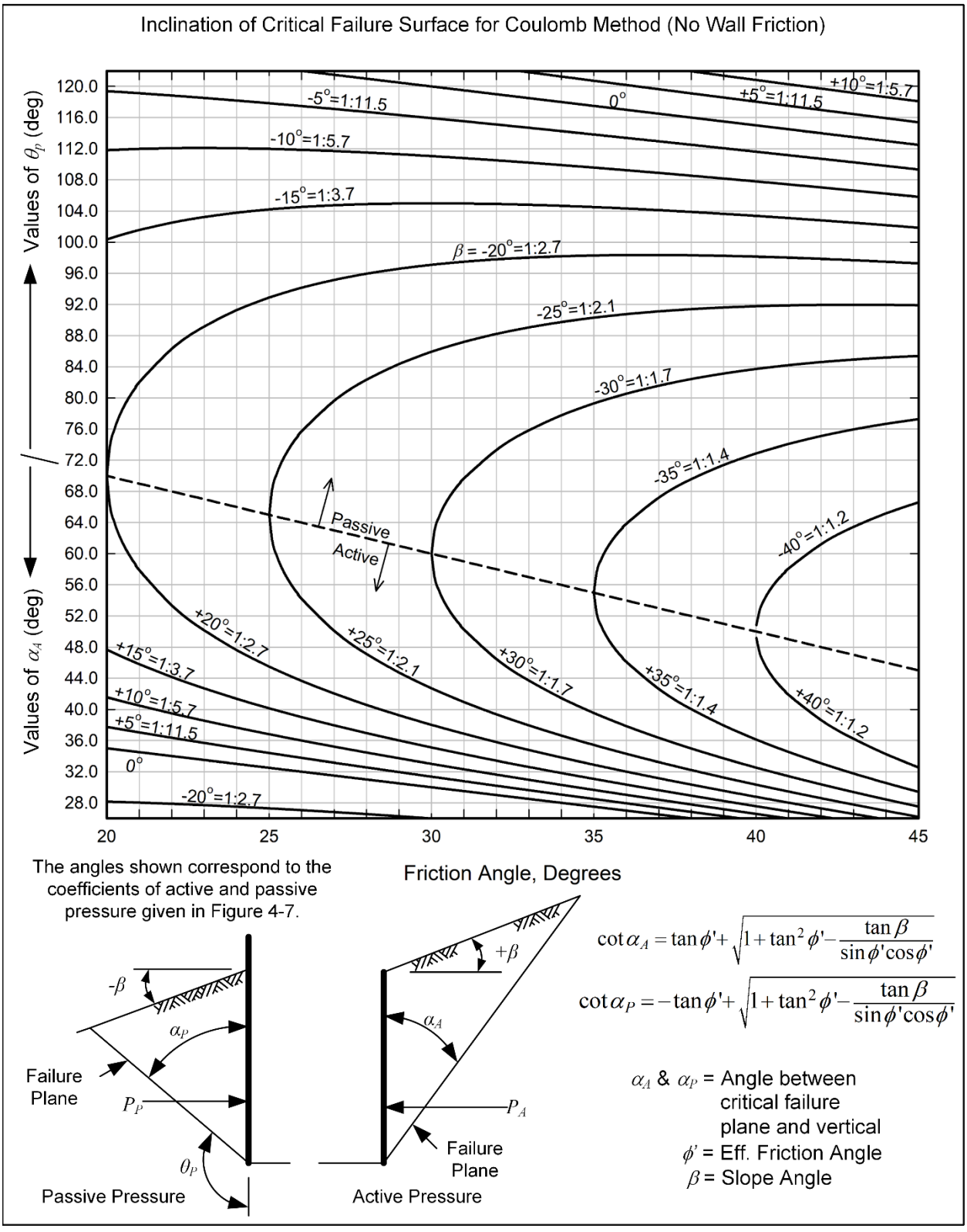

Figure 4-10 Inclination of the Failure Plane for the Coulomb Method for Vertical Walls with No Wall Friction

The passive earth pressure load can be calculated as:

$$P_P = \frac{1}{2} \cdot \gamma \cdot H^2 \cdot \frac{\cos^2(\phi' + \theta)}{\cos^2\theta \cdot \cos(\theta - \delta)\left[1 - \sqrt{\frac{\sin(\phi' + \delta)\sin(\phi' + \beta)}{\cos(\theta - \delta)\cos(\theta - \beta)}}\right]^2} \quad (4\text{-}11)$$

where:
K_P = passive earth pressure force.

For cases with surcharge loads, irregular backfill slopes, line loads, etc., the individual forces in the free body diagram (FBD) should be calculated, and force equilibrium should be used to find the values of P_A and P_P for trial failure surfaces. In addition, for active earth pressure cases where the wall is expected to settle a significant amount, it may be necessary to reverse the direction of the shear force on the wall in the FBD. This is called a *negative δ case*, and the reversal of the direction of the shear force is detrimental to wall stability.

4-3.2 Log Spiral Method.

One simplification of the Rankine and Coulomb methods is the assumption of a linear failure plane. Experimental and numerical analysis have shown that the true failure surface is curved instead of linear. The surface closely approximates a logarithmic spiral. The linear and log spiral failure surfaces for the active and passive earth pressure cases are shown in Figure 4-11. The difference in the failure planes is not substantial for the active earth pressure case, but there is a considerable difference in the passive case. If the Coulomb method is used to calculate the passive resistance of an earth anchor, the resistance will be greatly overestimated compared to results using the log spiral method. Much less soil is engaged by the true, log spiral surface compared to the linear Coulomb surface. This is especially true as the interface friction angle approaches the friction angle of the soil (i.e., $\delta/\phi' > 0.4$). Therefore, passive pressure should be calculated using the log spiral method and not the Coulomb method.

Unfortunately, the calculations for the log spiral method are not as simple as for the Coulomb method. Caquot and Kerisel (1948) provide tables of values of K_A and K_P for different wall geometries and interface friction angles. Alqarawi et al. (2021) provide the equations for using a spreadsheet to perform log spiral analysis calculations. Alternatively, charts can be used to determine values of K_A and K_P for log spiral solutions.

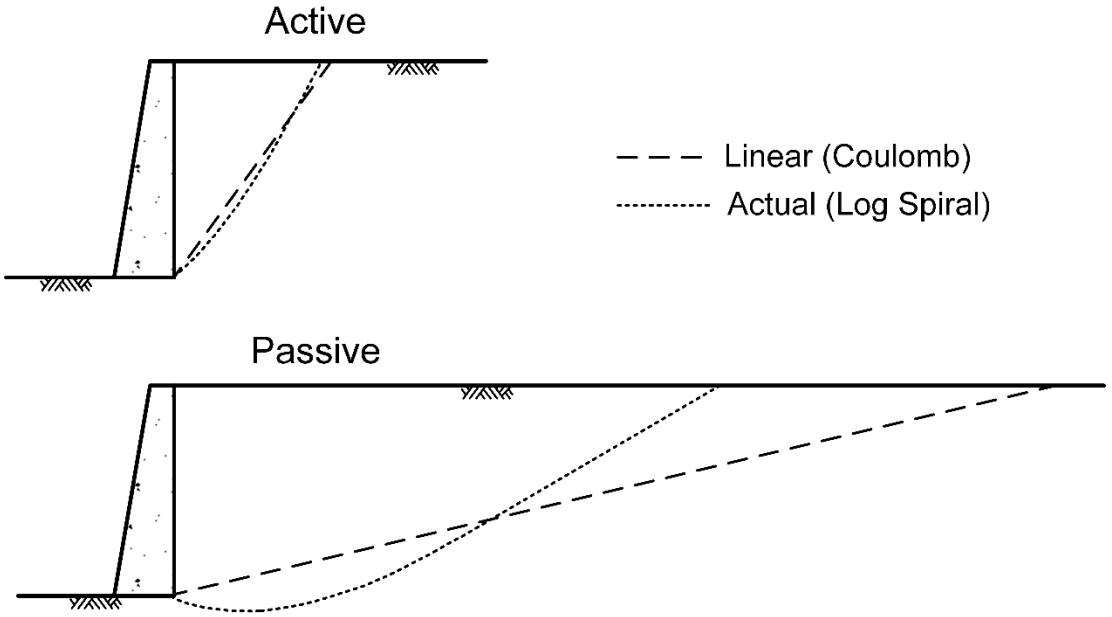

Figure 4-11 "Actual" and Linear Failure Planes for Active and Passive Earth Pressure Cases for $\phi' = \delta = 30°$ (after Perloff and Baron 1976)

Figure 4-12 shows values of K_A and K_P for the log spiral method for walls with a sloping face and $\delta/\phi' = 0.66$ based on the published data of Kerisel and Absi (1990). Figure 4-13 is a similar chart for vertical-faced walls having a sloping backfill. [21]

The log spiral method is commonly used for cut walls, such as sheet pile or soldier pile and lagging, where both K_A and K_P are required. These walls are vertical and often have no backslope. While $\delta/\phi' = 0.66$ is a common assumption, this type of design may require K_p for a different value of wall friction. For conditions with $\theta = 0$ deg and $\beta = 0$ deg, the value of K_p can be approximated as:

$$\ln\left(K_p\right) = \ln\left(\frac{1+\sin\left(\phi'\right)}{1-\sin\left(\phi'\right)}\right)\left[1.443\left(\frac{\delta}{\phi'}\right)\sin\phi'+1\right] \qquad (4\text{-}12)$$

where:
K_p = log spiral passive earth pressure coefficient for $\theta = 0$ deg and $\beta = 0$ deg,
ϕ' = effective stress friction angle, and
δ = wall-soil interface friction angle.

[21] It is important to note that Figure 4-12 and Figure 4-13 differ significantly from the charts provided in the 1982 version of DM 7.2. Those charts used $\delta/\phi' = 1$ along with reduction ratios for other values of friction angle and δ/ϕ'. The reduction ratios were averages that introduced substantial inaccuracy for some cases. For this reason, a single value of δ/ϕ' was selected to reproduce the charts.

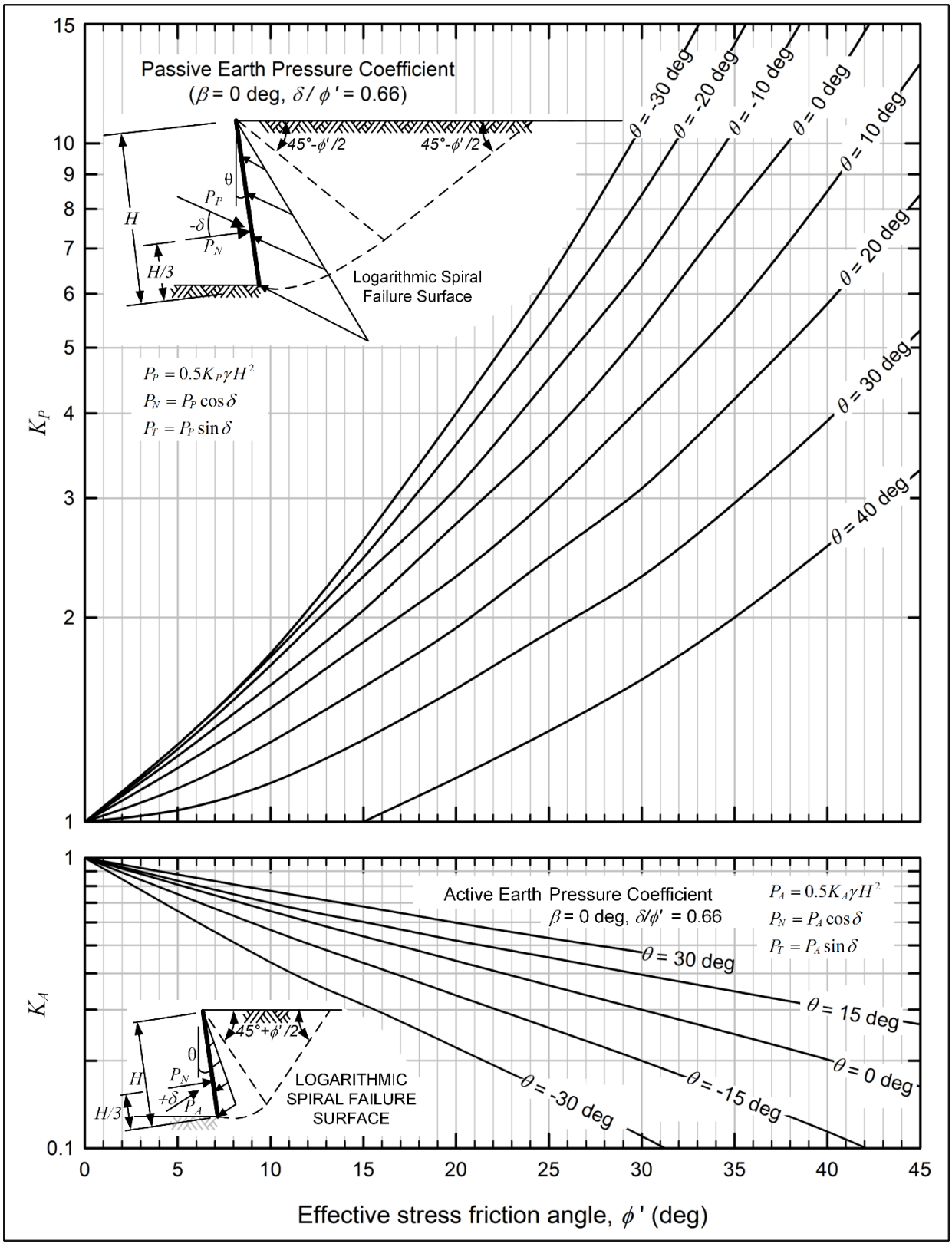

Figure 4-12 Values of K_A and K_P for the Log Spiral Method for a Sloping Wall with a Horizontal Backfill (after Kerisel and Absi 1990)

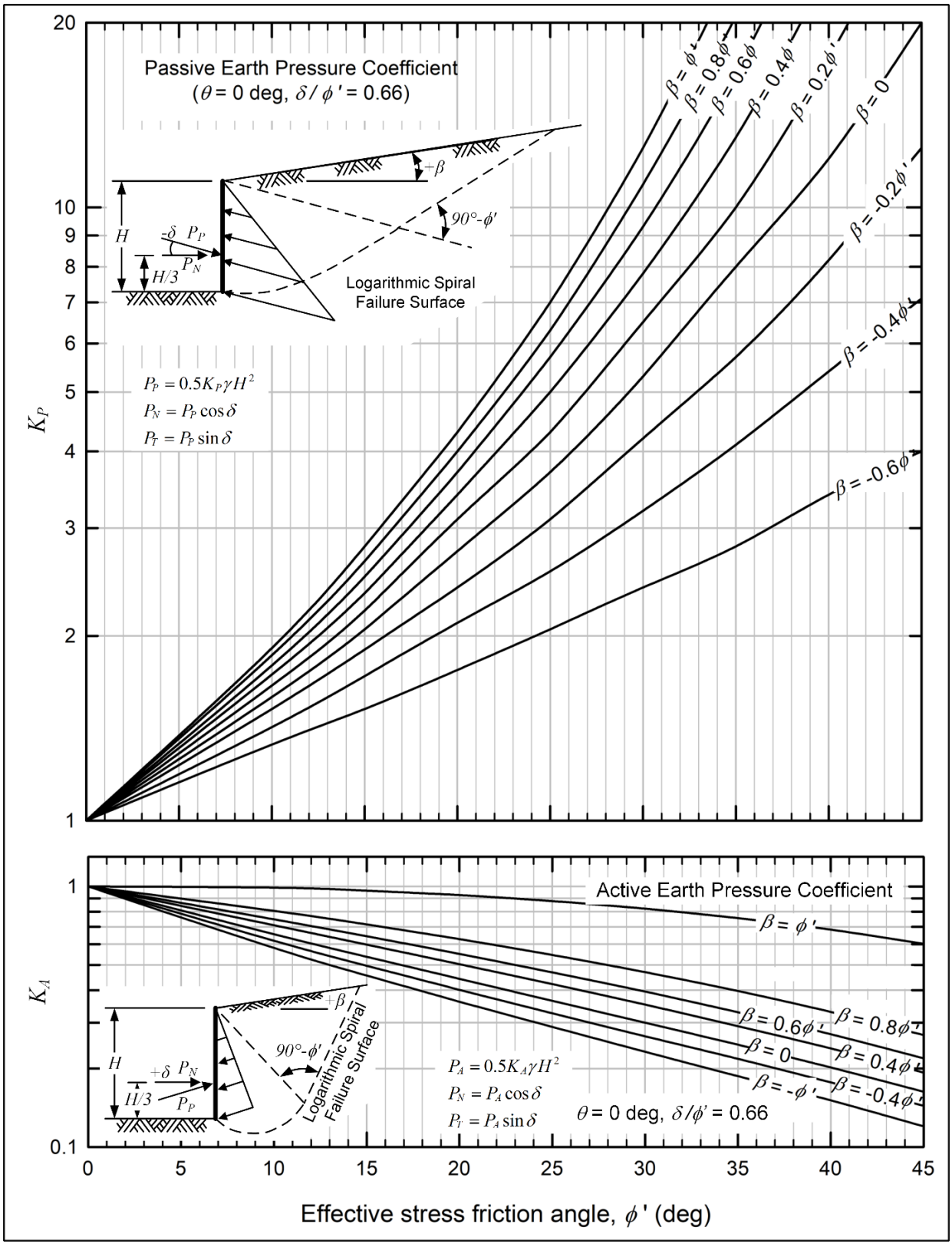

Figure 4-13 Values of K_A and K_P for the Log Spiral Method for a Vertical Wall with a Sloping Backfill (after Kerisel and Absi 1990)

As expected, Equation 4-12 results in the Rankine value of K_p if wall friction is neglected.

Table 4-2 compares K_A and K_P values calculated by the Rankine, Coulomb, and Log Spiral methods for a range of friction angles and δ / ϕ' values. Examining the active case, the method and wall friction have little effect on the predicted K_A. In most cases, the Rankine method is appropriate for active condtions without sloping wall or backfill. For the passive case, the earth pressure theory and wall friction have a large impact on the magnitude of the predicted K_P. The log spiral K_P can be in the range of two to five times higher than the Rankine value. This is especially important for the design of cut-type retaining walls, such as sheet pile and soldier pile, that rely on passive earth pressures for stability.

Table 4-2 Comparison of K_A and K_P Values for Earth Pressure Methods (β=θ=0°)

Friction Angle (deg)	δ / ϕ'	Active			Passive		
		Rankine	Coulomb	Log Spiral	Rankine	Coulomb	Log Spiral
30	0	0.33	0.33	0.33	3.00	3.0	3.0
	0.5	NA	0.30	0.3	NA	(6.1)	5.3
	1	NA	0.30	0.31	NA	(10)	6.5
35	0	0.27	0.27	0.27	3.69	3.7	3.7
	0.5	NA	0.24	0.25	NA	(9.8)	8.0
	1	NA	0.25	0.26	NA	(23)	10.5
40	0	0.22	0.22	0.22	4.60	4.6	4.6
	0.5	NA	0.20	0.2	NA	(18)	12
	1	NA	0.21	0.22	NA	(92)	18
45	0	0.17	0.17	0.17	5.83	5.8	5.8
	0.5	NA	0.16	0.16	NA	(44)	20
	1	NA	0.18	0.19	NA	(∞)	35

Note: Values in parentheses are unconservative applications of Coulomb theory and should not be used.

4-3.3 Presumptive Earth Pressure Coefficients and Equivalent Fluid Pressures.

The earth pressures theories presented within this section are based on the shear strength of the backfill material. Pressures imparted by water and other loads applied to the backfill will be discussed in Section 4-4. A few additional factors that may impact the loads applied to retaining structures are discussed below.

In particular, fine-grained soils can *creep*. There are many definitions for creep in the geotechnical literature, but the term usually refers to a time-dependent deformation of a soil at a constant effective stress. For structures constructed to retain fine-grained soils, the active earth loads applied to the structure can increase over time to values that significantly exceed the loads calculated by earth pressure theory. Similarly, passive earth loads may decrease over time in fine-grained soils. For this reason, presumptive earth pressure coefficients that empirically incorporate the effects of creep are often an appropriate alternative to values based on earth pressure theory.

In addition, the typical design and construction sequence imposes another practical constraint on the calculation of earth pressures and loads. Gravity retaining walls are often designed prior to the selection of a specific backfill material with well-defined properties (e.g., ϕ' and γ). In this case, presumptive earth pressure coefficients will be just as accurate as design based on assumed values of ϕ' and γ.

Presumptive values based on relative density and soil type are provided in Table 4-3 for both at-rest and yielding wall conditions. These values can be used to account for the effects of creep as well as the constraints of the design and construction process.

Table 4-3 Equivalent Fluid Unit Weights for At-Rest and Active Conditions for Horizontal and Sloping Backfills (after Kim et al. 1991)

Type of Soil	Level Backfill				Sloping Backfill (2H:1V)			
	At-Rest		Rotation Y/H = 1/240		At-Rest		Rotation Y/H = 1/240	
	γ_{eq} (pcf)	K_0	γ_{eq} (pcf)	K_A	γ_{eq} (pcf)	K_0	γ_{eq} (pcf)	K_A
Loose sand or gravel	55	0.45	40	0.35	65	0.55	50	0.45
Medium dense sand or gravel	50	0.40	35	0.25	60	0.50	45	0.35
Dense sand or gravel	45	0.35	30	0.20	55	0.45	40	0.30
Compacted silt (ML)	60	0.50	40	0.35	70	0.60	50	0.45
Compacted lean clay (CL)	70	0.60	45	0.40	80	0.70	55	0.50
Compacted fat clay (CH)	80	0.65	55	0.50	90	0.75	65	0.60

For the case of no backfill surcharge, the earth pressure applied to retaining structures has a triangular pressure distribution. For this reason, it is often convenient to use the *equivalent fluid unit weight*, γ_{eq}, to calculate earth pressures using the same methodology as for hydrostatic fluids. The equivalent fluid unit weight is found as:

$$\gamma_{eq} = \gamma \cdot K \tag{4-13}$$

where:
γ = the unit weight of the backfill and
K = an appropriate earth pressure coefficient (at-rest or active).

Table 4-3 shows values of γ_{eq} for horizontal and sloped backfills for different backfill soil types. The effects of creep are reflected in the γ_{eq} values for the clay backfill materials. The choice of the value of the equivalent fluid unit weight should consider wall movement and the potential of the backfill soil to creep over time. Since equivalent fluid pressures are only an approximate method to calculate earth pressures, their use should be limited to walls that are less than 20 feet tall.

A uniform surface surcharge (discussed in more detail in Section 4-4.2) can also be considered using presumptive earth pressures. Using the appropriate values listed in

Table 4-3, the horizontal earth pressure at the bottom of the wall, σ_h, can be calculated as:

$$\sigma_h = \gamma_{eq} \cdot z + K \cdot q \tag{4-14}$$

where:
γ_{eq} = equivalent fluid unit weight,
z = depth below ground surface,
K = horizontal earth pressure coefficient, and
q = uniform surcharge pressure.

4-3.4 Earth Pressure Examples for Complex Geometries.

A more complex active pressure problem is shown in Figure 4-14. In this case, the surface of the backfill is uneven, and an irregular surcharge is present. Two different soil types are present, and the contact between these soils is not horizontal. The ground water table is not horizontal, which means it is a hydrodynamic case (e.g. water is flowing). Friction between the wall and backfill will be considered.

The type of problem shown in Figure 4-14 is too complicated for the Rankine method, and the Coulomb method must be used. In addition, the problem is too complex for the Coulomb charts (Figure 4-9 and Figure 4-10), and different trial failure surfaces must be analyzed by hand. The figure shows the FBDs and force polygons for two trial surfaces.

In this example, the moist unit weight should be used above the water table and the saturated unit weight should be used below the water table when calculating the weight of the wedge. The water pressure force, acting normal to the failure surface, must be calculated. Since two soil types are present, the active wedge is subdivided into two free bodies, with the vertical boundary between the free bodies defined by the location where the layer interface crosses the failure plane. The forces acting on the vertical boundary are assumed to be horizontal.

Figure 4-15 shows a passive pressure example with a cross-section very similar to Figure 4-14. Since wall friction is considered in this example, it would be unconservative to use the linear failure surface assumed by the Coulomb method. Ideally, the log spiral method would be used to solve this problem. However, in this example, a simpler procedure is adopted where the portion of the failure surface that would normally be represented by a log spiral has been replaced with a circular arc. Three free bodies are used in the example solution separated by two vertical boundaries. One boundary between the free bodies has been defined where the circular failure surface transitions into the linear failure surface. The second boundary is located where the interface between the two layers intersects the linear failure surface. The passive earth force for this example is determined by resolving the forces for the

three force polygons. To determine the vertical location of the passive force on the wall, moments should be summed about the toe of the wall.

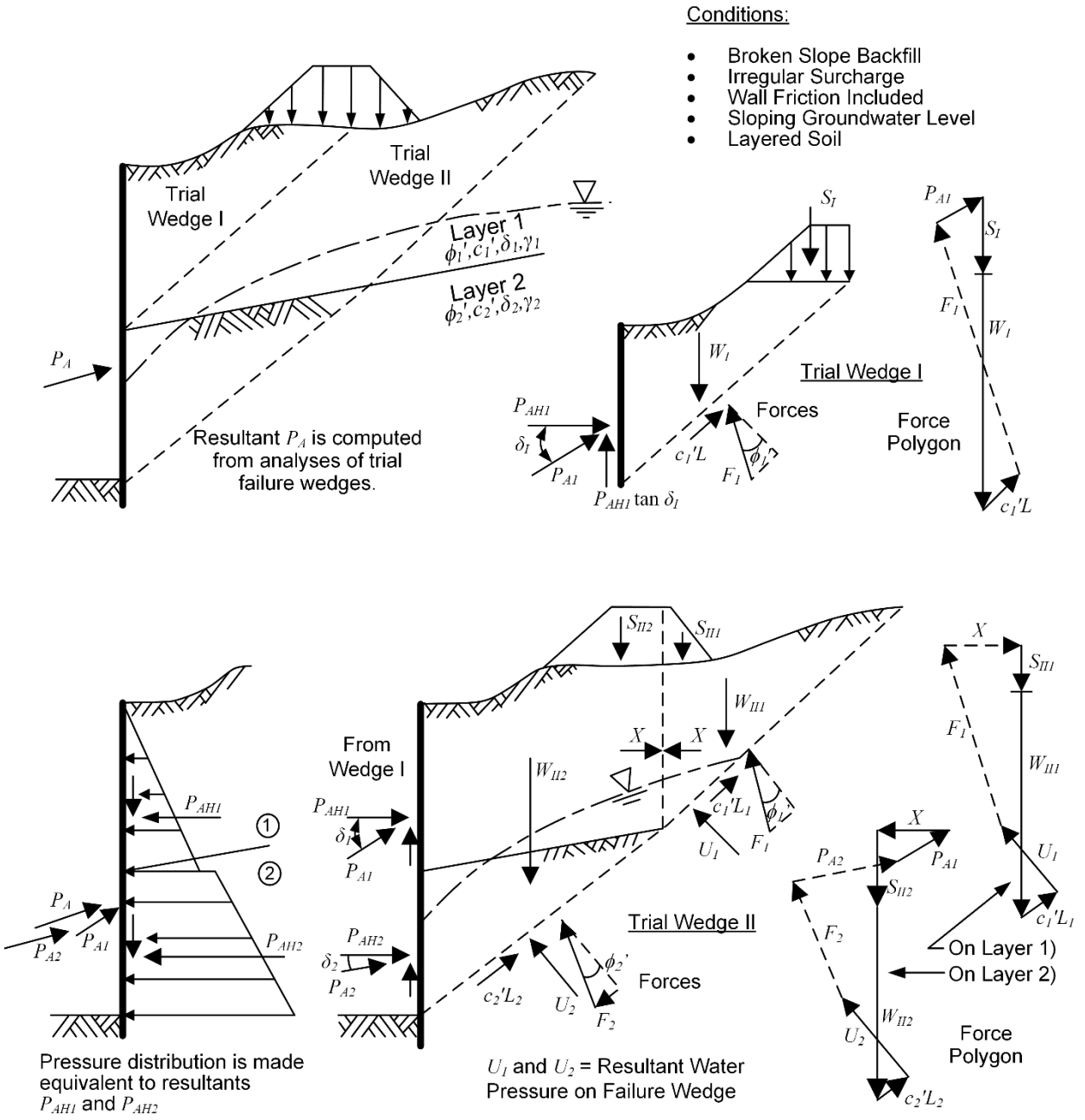

Figure 4-14 Coulomb Method Applied to a Complex Active Earth Pressure Case

For earth pressure problems that exhibit complex cross-sections, such as those in Figure 4-14 and Figure 4-15, other methods can be used to determine the passive earth pressure. Some limit equilibrium slope stability software can be employed to solve earth pressure problems, and these programs can easily accommodate different soil layering and nonhorizontal contact surfaces. However, the results from these programs

should be carefully checked against hand calculations for simpler cross-sections to verify that the user is correctly using the computer software. Also, finite element and finite difference soil structure interaction software can be used to solve these types of problems, but considerable skill is required to obtain meaningful results.

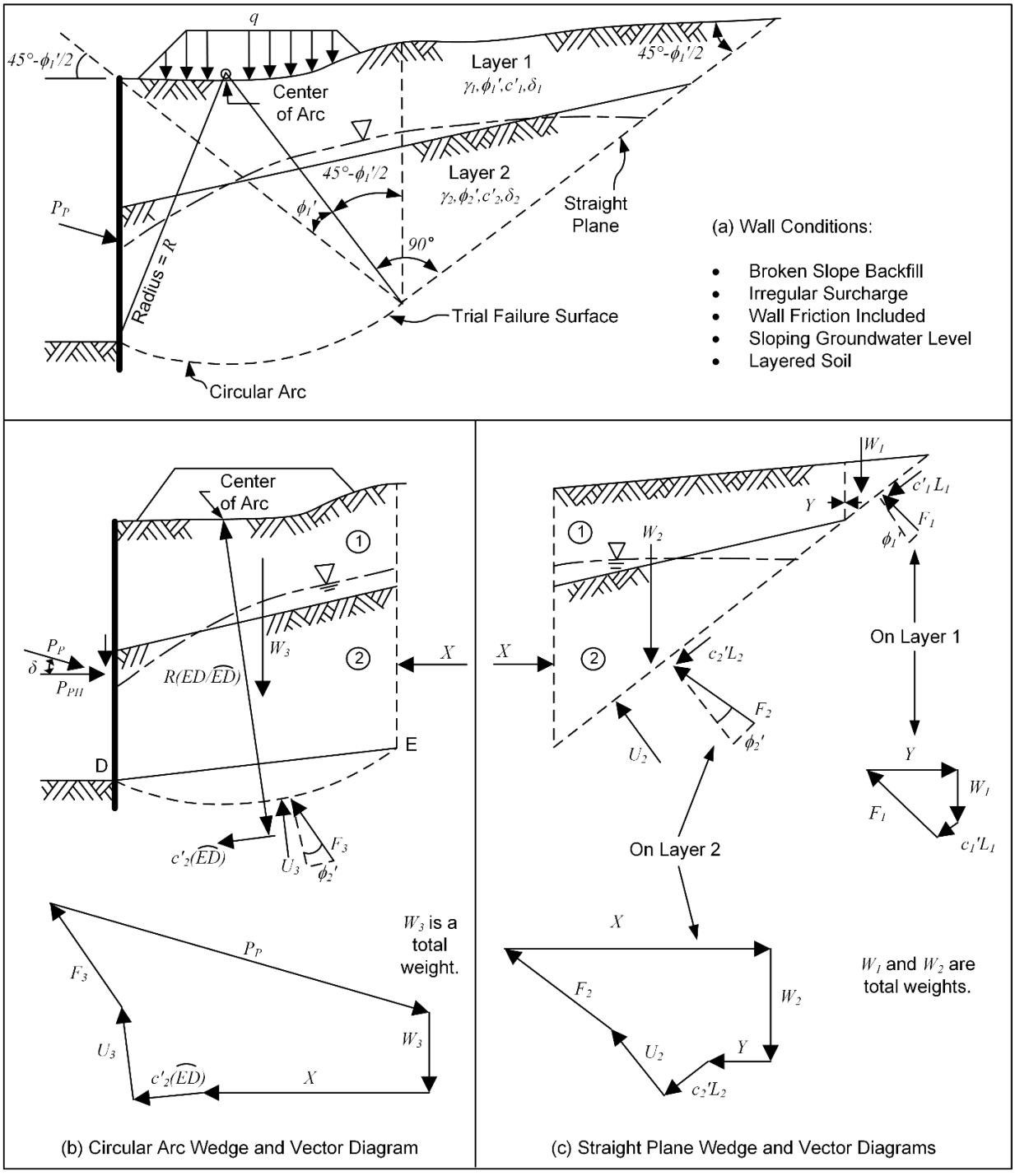

Figure 4-15 Passive Earth Pressure Calculations Similar to the Log-Spiral Method with a Circular Arc Replacing the Log Spiral Portion of the Failure Surface

4-3.5 Use of Slope Stability Software for Earth Pressures.

Many of the procedures outlined thus far in this manual use the limit equilibrium procedure to determine the forces acting on retaining structures. This is the same basic analysis technique used by most slope stability software. In the hands of an engineer skilled in its use, slope stability software can be used to find the earth forces acting on a retaining structure for complex site conditions. This approach can accommodate more scenarios than the equations and chart solutions normally used in engineering practice. Situations where slope stability software can be particularly useful are:

1) The shear strength of the backfill soil is more accurately represented by a nonlinear strength envelope as opposed to a linear failure envelope,

2) Hydrodynamic groundwater conditions (as opposed to hydrostatic conditions),

3) Layered soil stratigraphy,

4) Nonlinear failure surfaces in the backfill, and

5) Presence of tension cracks.

Slope stability software can be used for retaining wall analysis by applying the earth pressure force as a line load on the structure at the approximate vertical location. The trial slip surface can be forced to intersect a point at the heel of the wall. Next, the earth pressure force is varied until a factor of safety of unity is achieved. The slope stability method should solve all conditions of equilibrium, such as Spencer's method or the Morgenstern and Price method.

Although the software manual may include examples of retaining wall analysis, the user should be confident in their abilities to do this sort of analysis prior to attempting a design. The results of simple example problems using log-spiral solutions should be compared to computer solutions before more complicated strength models and geometries are analyzed.

4-4 EARTH PRESSURES FROM OTHER SOURCES

4-4.1 Water Pressure Effects.

Water ponded on the interior of a retaining structure can apply substantial forces to the structure. Water applies a triangular pressure distribution equivalent to a soil with a unit weight of 62.4 pcf and an earth pressure coefficient of unity. The examples given in Figure 4-5 and Figure 4-6 show the net water pressure distribution when there are unequal water elevations on the front and back of the structure.

Because of the large pressures that water can apply to walls, significant efforts are required to prevent water from collecting behind retaining structures. Wall drainage systems are presented in Section 4-5.2. Although water behind a wall creates additional loading, there are many design cases where water loads on walls are unavoidable. Many walls used in waterfront structures have an elevated water level on the ground side compared to the water side. This is also often the case for lock structures on navigable rivers. Sometimes, the drainage system behind a wall can be overwhelmed by significant rainfall events, and the wall may experience potentially damaging, albeit temporary, water loads. Clogging of drainage systems can also lead to damaging water loads.

When the soil behind a wall becomes saturated, the pressure on the wall is controlled by two factors. First, the earth pressure is reduced since the effective stress is decreased. Instead of the total unit weight (γ), the buoyant or effective unit weight (γ_b) is used in the earth pressure equations for soils below the water table. The second effect is that an additional load, supplied by the water pressure, is applied to the wall. Figure 4-16(a) shows combined influence of these two effects. The consequence of an increasing water level is expressed as a ratio of the height of water (H_w) to the height of the wall (H). When $H_w = H$, the water level is at the ground surface. The relative increase in the pressure applied to the wall is quantified in the upper right inset as the ratio of the sum of the earth pressure and water pressure force divided by the earth pressure force for $H_w = H$. As the friction angle increases, this ratio increases.

Figure 4-16(b) shows an analysis case demonstrating the effects of a large rainfall event on the stability of a retaining wall that contains a drainage layer next to the wall. Even with the drainage system installed, a large rainfall event can still increase the pore pressure in the backfill. The flow net shows the head loss as a function of depth. For a potential failure plane, oriented at the angle α_A (measured from vertical), the pore pressure distribution can be calculated, and the resulting pore pressure force, U, can be determined. The middle inset shows the ratio of the pore pressure force to the force that would be applied for hydrostatic conditions for different failure plane angles. As the angle of the failure plane increases, the relative water pressure force also increases. The right inset shows the increase in the force applied to the wall, expressed as a ratio of the force calculated from both soil and water for the rainfall event to the active earth pressure force for the case of no water pressures. As the friction angle of the soil increases, this ratio also increases.

For waterfront and riverfront earth retaining structures, active seepage can be occurring, and this can compromise stability. Figure 4-16(c) shows a cantilever sheet pile wall installed in a coarse-grained soil. The water levels are higher on the landside of the wall than on the riverside; therefore, water flow is occurring from right to left. As shown on the figure, the active and passive earth and water pressures should first be calculated assuming conditions of “no flow.” Next, corrections to the active and passive

pressures can be made to account for the seepage conditions. The correction factors depend on the ratio of the length of the sheeting ($H+D$) to the depth of embedment and the earth pressure coefficient. The development of the passive pressure occurs at a much greater wall displacement than the active pressure. For cantilever walls, which must include passive pressure, this can be accommodated by a reduction in the value of K_P used in the analysis. Cantilever sheet pile design is covered in more detail in Section 4-7.4.

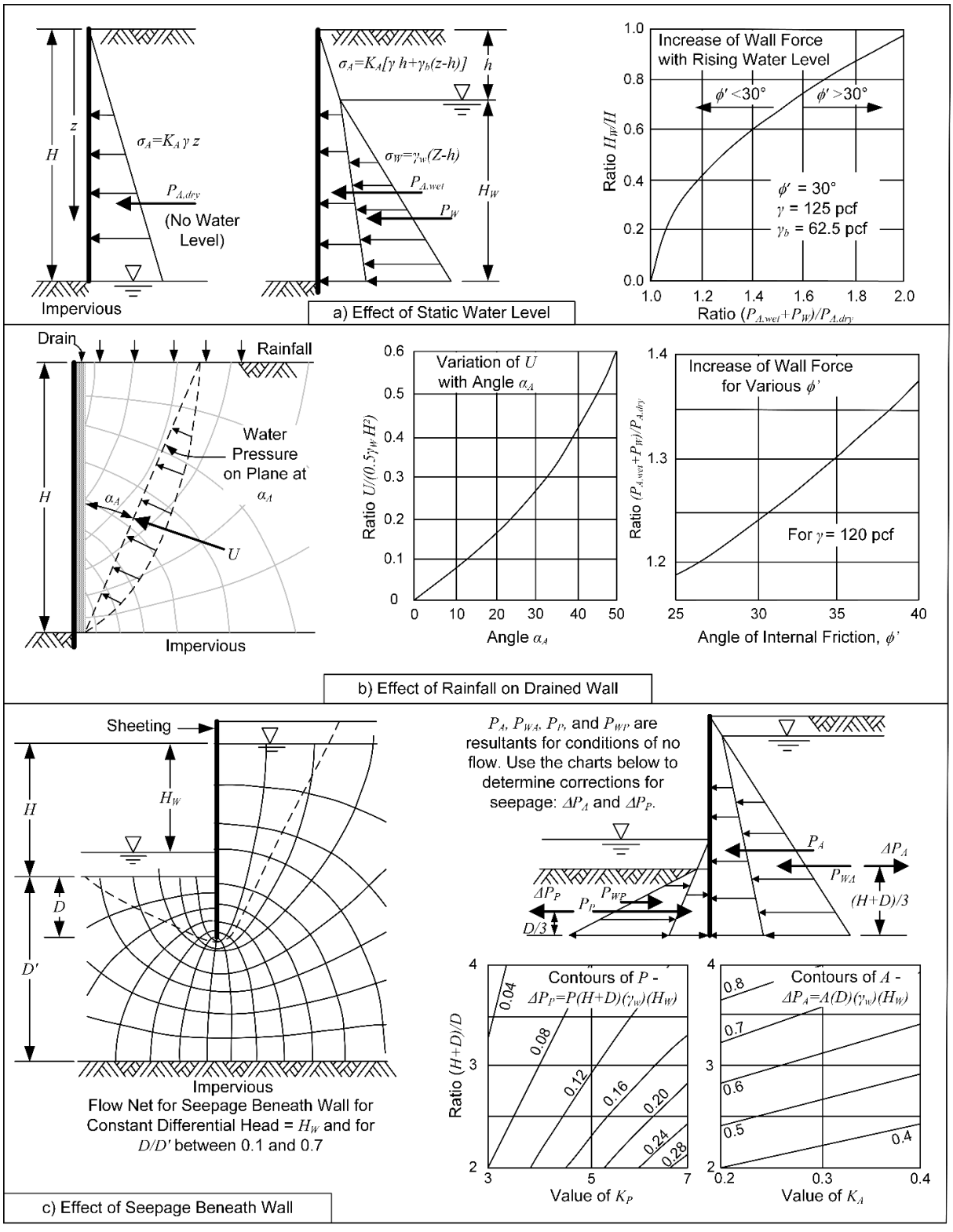

Figure 4-16 Effects of the Presence of Water on the Loads Applied to Walls for Cases of (a) Static Water Pressure, (b) Extreme Rainfall Events on Walls with Drainage Elements, and (c) Seepage Beneath a Cantilever Wall

In some analysis methods, the seepage forces exerted on the soils on both sides of the wall are accommodated. This is particularly an issue if hydrostatic water pressure conditions are assumed to exist when calculating the earth pressures. A simple means to do this involves modifying the unit weight of water based on the hydraulic gradient. On the side of the wall with the highest phreatic surface, the water flow is downward, and the unit weight of water is decreased resulting in higher earth pressures. On the opposite side of the wall, the unit weight of water is increased, resulting in lower earth pressures.

Water pressures can add an uplift force on the base of retaining walls which can be detrimental to the wall stability. These are discussed in the section on overall wall stability (Section 4-5).

4-4.2 Surface Loads Behind Retaining Structures.

Loads applied to the ground surface behind a retaining structure can impose a pressure distribution to the wall. The types of loads considered here are:

1) Surcharge loading (wide extent compared to wall),

2) Rectangular or surcharge loading over limited area,

3) Point loads,

4) Line loads parallel to wall, and

5) Line loads perpendicular to the wall.

Many of these solutions are based on elastic theory, which require the assumption that the wall is rigid and unyielding. This means that the same load would be applied for the active and passive earth pressure cases. The assumption of an unyielding wall would be conservative for the active earth pressure case but may be unconservative for the passive earth pressure case, depending on the specific application.

If the retaining structure is expected to yield or move sufficiently to develop active conditions, then 75% of the load calculated using the following methods can be used. This value will be approximately halfway between the pressures expected for yielding and unyielding walls, and thus, should still be conservative.

It is prudent to include surface loads on the backfill of retaining structures in urban construction since it may not be possible to determine future loads. Construction materials can sometimes be stockpiled on the ground surface near the top of walls, or loads applied by construction equipment may be present. Sometimes, building codes require a specified minimum distributed load be applied to the top of the retaining structure backfill for design calculations.

4-4.2.1 Surcharge Loading.

In many cases, loads behind retaining structures are idealized as a unifom surcharge or uniformly loaded (q) area with large extent compared to the wall size. A surcharge is relatively easy to accommodate in Rankine earth pressure theory because q can directly be added to the vertical effective stress term for all depths. In the Coulomb method, the increase in the weight of the soil wedge can be calculated by multiplying q by the horizontal length of the top boundary of the wedge.

4-4.2.2 Uniform Rectangular Surface Load.

The wall backfill may support a rectangular uniform load that extends a limited distance (L) along the wall and extends a distance (B) perpendicular to the wall. The additional horizontal stress applied to the wall at the corner of this load can be calculated using the influence factors in Figure 4-17. The surcharge load, q, is expressed in units of stress or pressure. The highest horizontal stress will be applied to the wall at the midpoint of the loaded area, corresponding to a load width of $L/2$. Because the chart determines the pressure at the corner of the loaded area, the principle of superposition (NAVFAC DM-7.1 Chapter 4) should be used to determine the horizontal stress at the midpoint.

For design purposes, it is common to consider a distributed surface load surcharge on the order of 300 psf to account for storage of construction materials and equipment. This surcharge is usually applied within a rather limited work area of about 20 feet to 30 feet from the wall and can also be used to account for concentrated loads from heavy equipment (concrete trucks, cranes, etc.) located more than about 20 feet away. If such equipment is anticipated within a few feet of the wall, it must be accounted for separately using the methods described in the following sections.

4-4.2.3 Point Load.

A point load on the backfill of a retaining structure might be the force applied by an outrigger of a crane or other similar condition where a force is applied over a small area. Sometimes, the loads caused by construction traffic are modeled assuming that the tire contact positions are point loads, and the principle of superposition is applied to calculate the load applied by all of the tires.

The modified elastic solution for the pressure distribution and the horizontal resultant force (P_H) from a point load (Q_p) is shown in Figure 4-18. Since a point load is limited in lateral extent, the force applied to the wall is greatest at the minimum perpendicular distance from the point load to the wall.

The individual curves shown on the influence chart are for different values of m, which is the distance to the load divided by the height of the wall. For values of $m \leq 0.4$, the solution is not closely dependent on m, and the same influence curve can be used for all

values of $m \leq 0.4$. For values of $m > 0.4$, the proper influence curve should be used corresponding to the value of m.

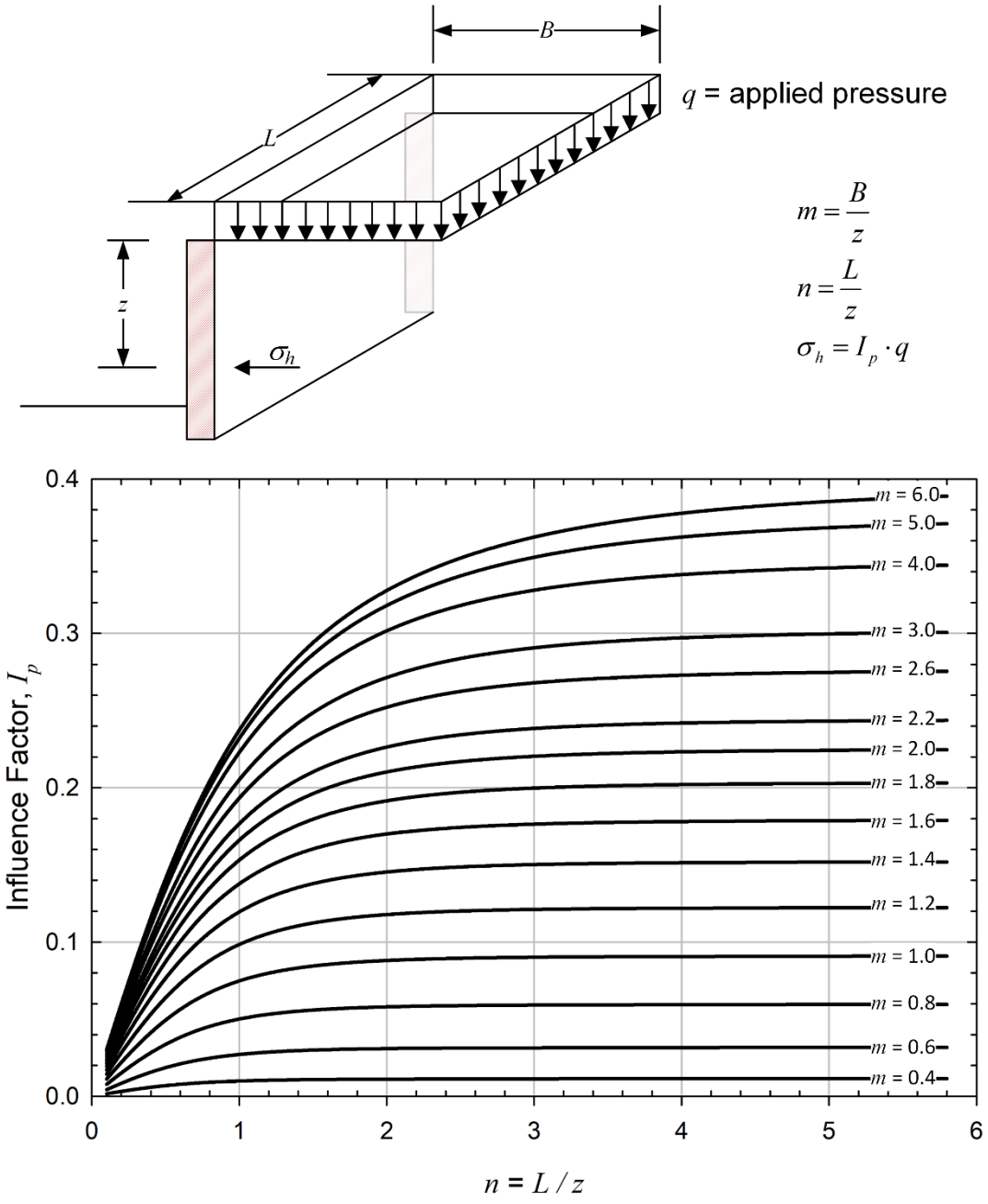

Figure 4-17 Lateral Pressure on an Unyielding Wall at the Corner of a Uniform Rectangular Surface Load

The value of the resultant force (P_H) can be estimated as a function of m from the inset table on the influence chart. The point of application of P_H, located a vertical distance (y) from the ground level on the front of the wall, can be calculated using the table for different values of m. The value of P_H is the maximum force per unit length of wall

caused by Q_P, rather than the total horizontal load for the entire length of wall. Thus, P_H occurs at the point where θ is zero degrees.

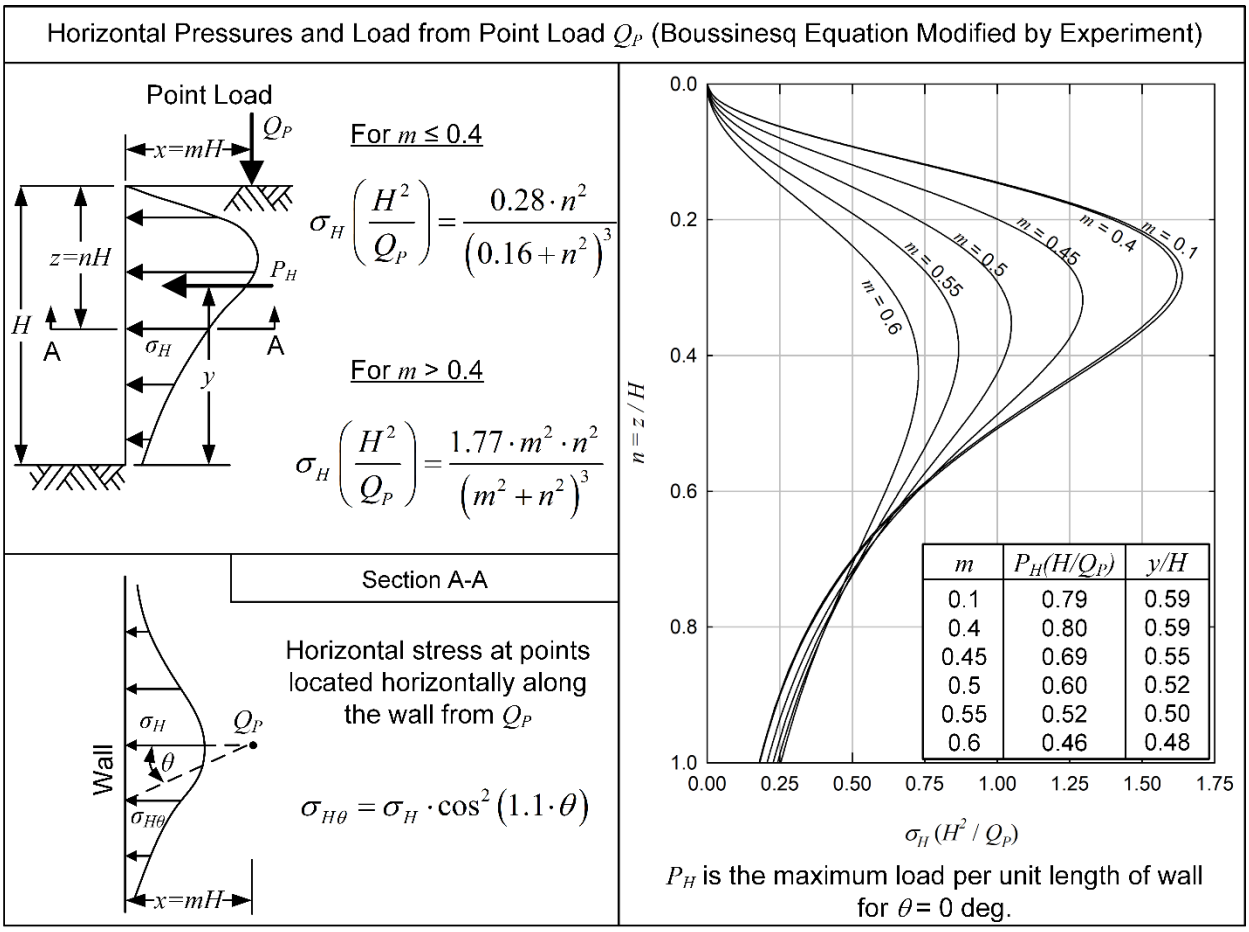

m	$P_H(H/Q_P)$	y/H
0.1	0.79	0.59
0.4	0.80	0.59
0.45	0.69	0.55
0.5	0.60	0.52
0.55	0.52	0.50
0.6	0.46	0.48

Figure 4-18 Horizontal Pressure and Resultant Force for a Single Point Load Applied at the Surface of the Backfill

The horizontal variation of pressure ($\sigma_{H\theta}$) can be calculated from the maximum pressure exerted by the point load (σ_H) for a given depth based on the angle (θ) between a horizontal line drawn from the point load to the wall and a line drawn from the point load to the point on the wall where $\sigma_{H\theta}$ is to be calculated.

4-4.2.4 Line Load Parallel to the Structure.

A line load on the backfill of a retaining structure can be used to represent a strip footing from a structure or other long, narrow loading. Line loads (Q_L) are considered to be as long as the retaining wall, and the loads are expressed as a force per distance. Since line loads are considered numerically to be of infinite length, the calculated pressures do not vary along the length of the retaining structure.

Similar to the equations for a point load, the influence factors do not vary considerably for values of $m \leq 0.4$, and the curve shown for $m = 0.4$ can be used for m values less than 0.4 as well. For values of m > 0.4, the influence value can read off of the chart if the correct value of m is available, or it can be calculated from the formula indicated in Figure 4-19.

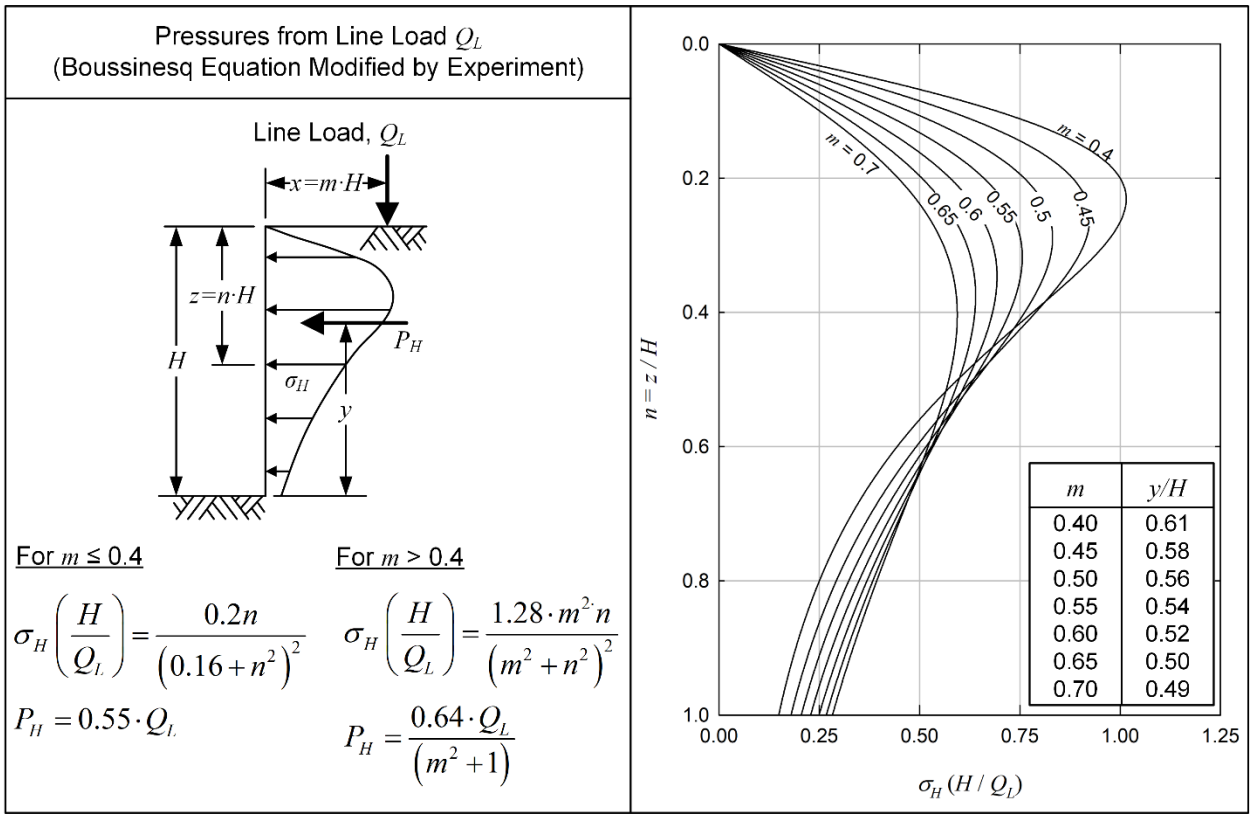

Figure 4-19 Horizontal Pressure and Resultant Force for Line Load Applied at the Surface of the Backfill Parallel to the Retaining Structure

4-4.2.5 Line Load Perpendicular to the Structure.

Figure 4-20 and Figure 4-21 show the geometry for a line load (Q) oriented perpendicular to the structure, expressed as a force per unit length. The maximum pressure is applied to the wall at the perpendicular intersection of the line load and the wall. The pressure decreases along the wall in each direction from this point.

Figure 4-20 shows the general form of the solution for a line load parallel to the wall along with the geometric definitions. Figure 4-21 provides influence factors for specific situations.

4-4.3 Earth Pressures Due to Compaction.

The operation of a compactor near a retaining structure can impose two types of loads on the wall. First, a transient load can be applied due to the weight of the compactor and the force applied at the ground surface. Second, horizontal stress can be "locked-in" due to the compaction process, and this increased pressure can remain after the compactor is removed.

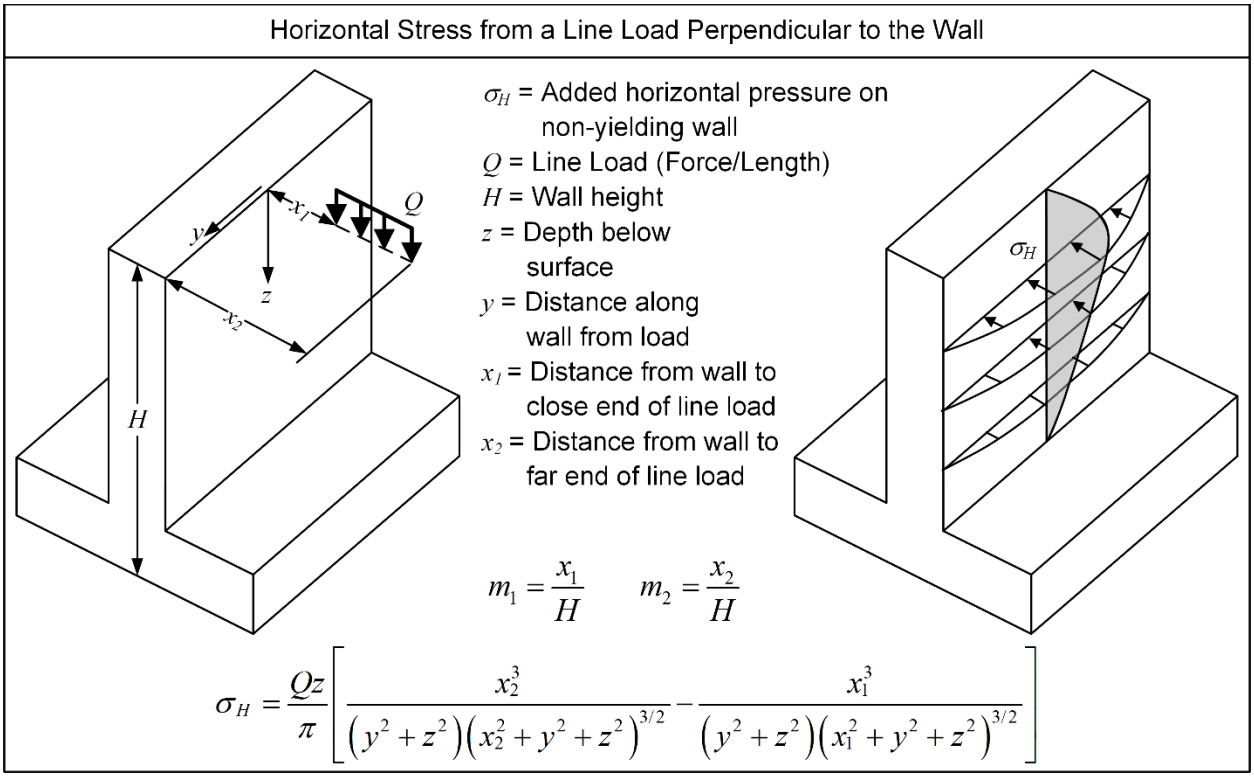

Figure 4-20 Horizontal Pressure from a Line Load Perpendicular to the Retaining Structure

The "locked-in" horizontal pressures from compaction can be calculated using tables and figures from Duncan et al. (1991).[22] In Figure 4-22 to Figure 4-24, the earth pressures due to compaction by rollers are shown by the solid and single-dashed lines. The at-rest earth pressures are shown for comparison using dash-dot lines. The charts were developed from experimental data on rollers, plate compactors, and rammer plates operating 0 to 0.5 feet from the wall. The lift thickness varied from 0.33 to 0.5 feet and the backfill material had a friction angle of 35 degrees. For compaction

[22] The discussions and closure to this paper contain important corrections that are reflected in the figures and tables included here.

conditions that vary from these assumptions, correction factors for the earth pressure are given in Table 4-4 to Table 4-6.

The force imparted by the specific compactor can be found by consulting the manufacturer's information. Duncan et al. (1991) summarized the compactor specifications for many small compactors at the time of publication of the paper. The specifications for current compactors should be checked prior to using these tables and figures.

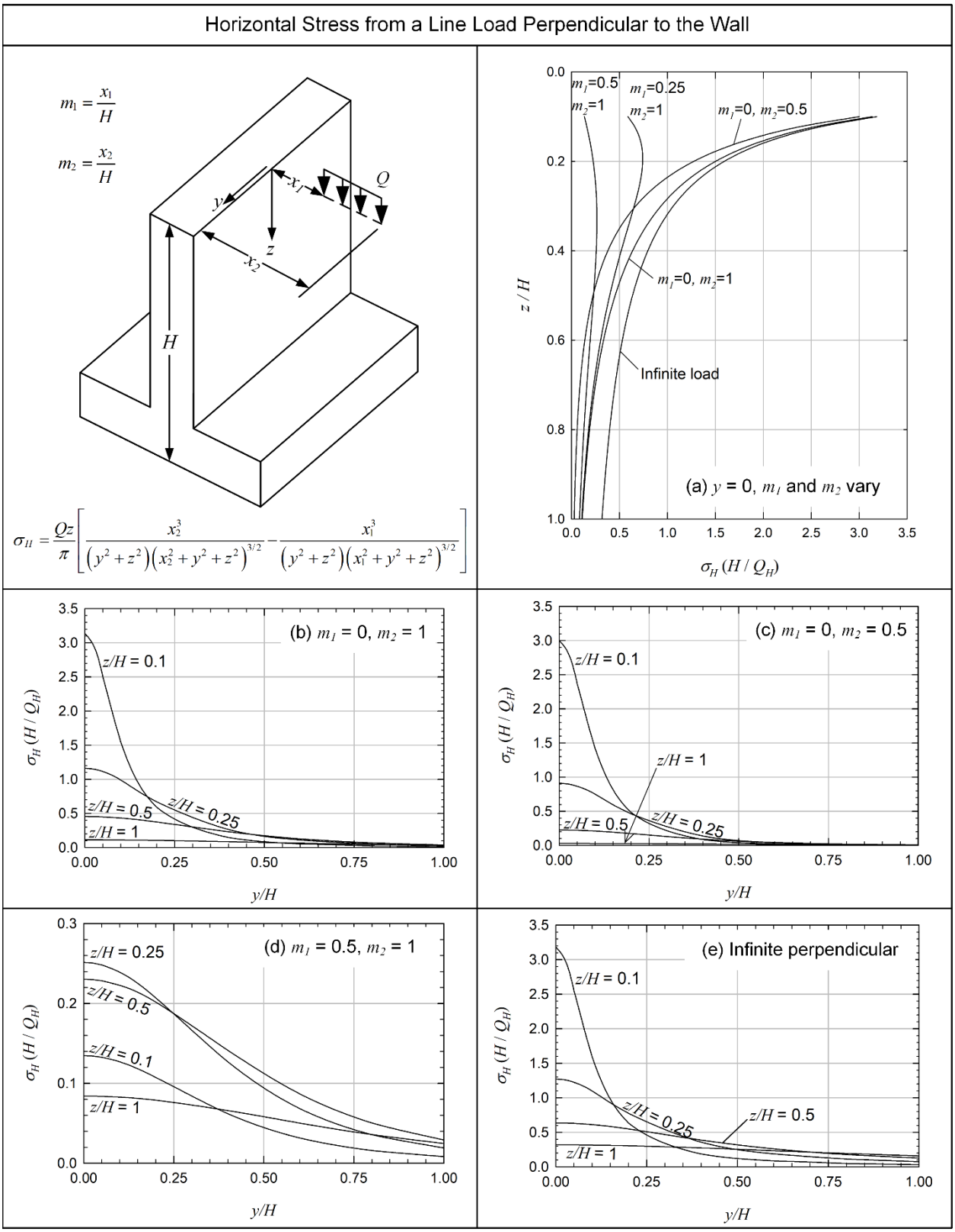

Figure 4-21 Distribution of Horizontal Pressure from a Line Load Perpendicular to the Retaining Structure for Varying Load Geometries and Depths

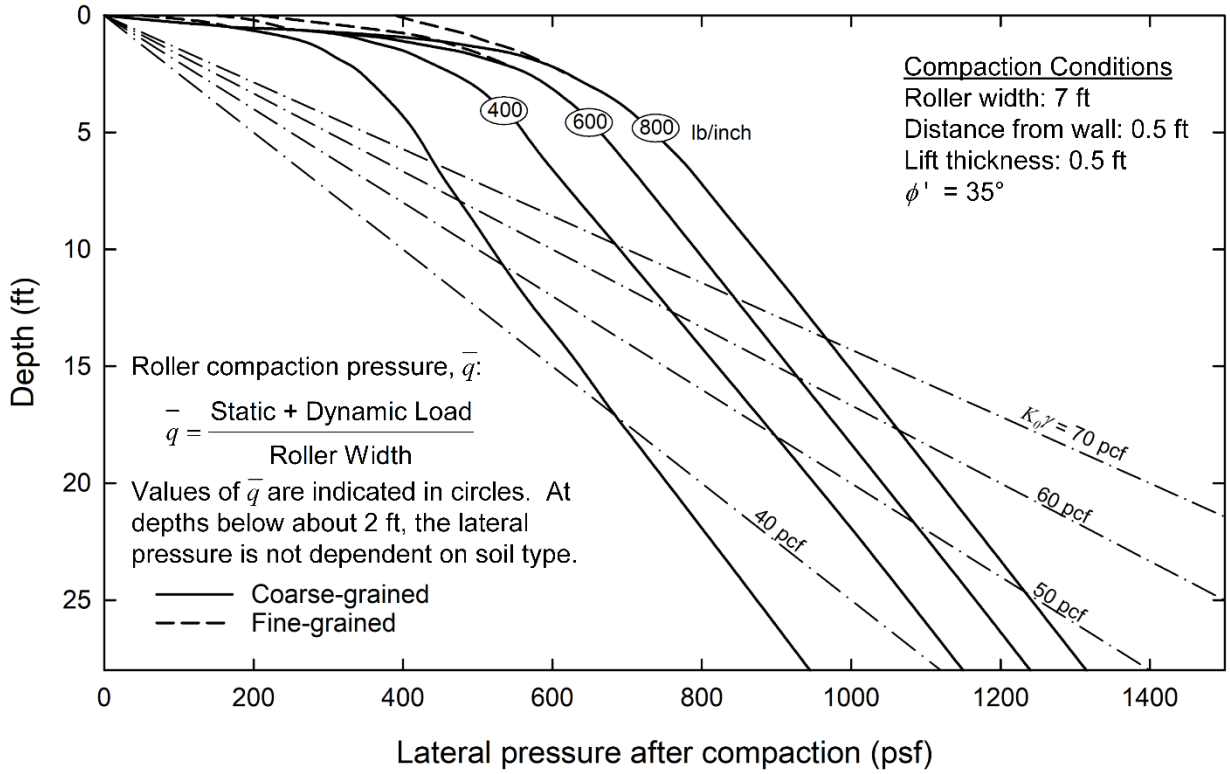

Figure 4-22 Earth Pressures Due to Compaction from Rollers (after Duncan et al. 1991)

Table 4-4 Adjustment Factors for Earth Pressures Induced by Compaction with Rollers (after Duncan et al. 1991)

Variables	Multiplier factors for z =			
	2 ft	4 ft	8 ft	16 ft
(a) Distance from Wall (x) and Lift Thickness (t). Adjustment factors are combined				
x = 0.0 ft, t = 0.5 ft	1.00	1.0	1.0	1.0
x = 0.2 ft, t = 0.5 ft	1.00	1.0	1.0	1.0
x = 0.5 ft, t = 0.5 ft	1.00	1.0	1.0	1.0
x = 1.0 ft, t = 0.5 ft	0.87	0.88	0.89	0.90
x = 0.0 ft, t = 1.0 ft	0.94	0.95	0.95	0.96
x = 0.2 ft, t = 1.0 ft	0.94	0.95	0.95	0.96
x = 0.5 ft, t = 1.0 ft	0.94	0.95	0.95	0.96
x = 1.0 ft, t = 1.0 ft	0.83	0.84	0.86	0.88
(b) Roller Width (w)				
w = 1.25 ft	0.80	0.80	0.80	0.88
w = 3.50 ft	0.96	0.94	0.94	0.97
w = 7.00 ft	1.00	1.00	1.00	1.00
w = 10.00 ft	1.00	1.01	1.02	1.04
(c) Friction angle (ϕ')				
ϕ' = 25°	0.59	0.70	0.81	0.96
ϕ' = 30°	0.75	0.83	0.89	0.98
ϕ' = 35°	1.00	1.00	1.00	1.00
ϕ' = 40°	1.23	1.16	1.10	1.03

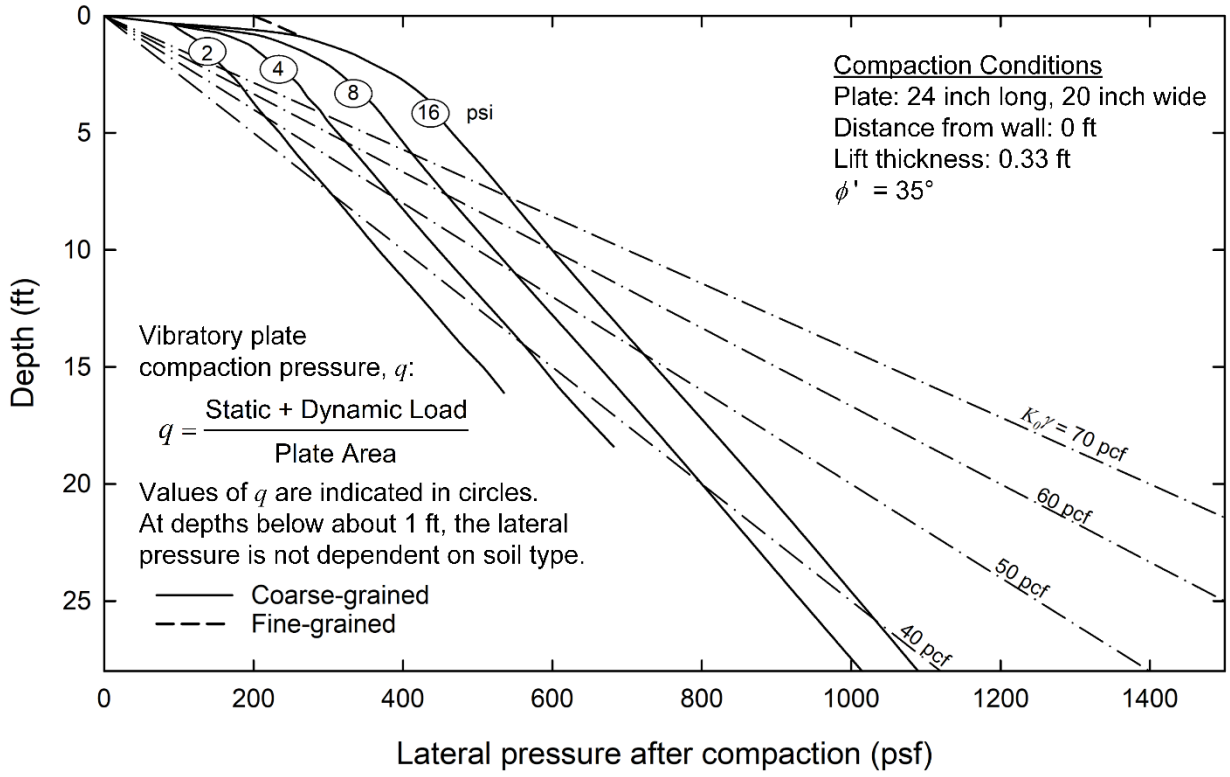

Figure 4-23 Earth Pressures due to Compaction by Vibratory Plates (after Duncan et al. 1991)

Table 4-5 Adjustment Factors for Earth Pressures Induced by Compaction with Vibratory Plates

Variables	Multiplier factors for z =			
	2 ft	4 ft	8 ft	16 ft
(a) Distance from Wall (x) and Lift Thickness (t). Adjustment factors are combined.				
x = 0.0 ft, t = 0.33 ft	1.00	1.00	1.00	1.00
x = 0.5 ft, t = 0.33 ft	0.85	0.88	0.88	0.90
x = 0.0 ft, t = 0.5 ft	0.87	0.88	0.91	0.95
x = 0.5 ft, t = 0.5 ft	0.75	0.75	0.88	0.99
(b) Area of Vibratory Plate				
Area = 240 sq. in.	0.85	0.85	0.90	0.95
Area = 480 sq. in.	1.00	1.00	1.00	1.00
Area = 960 sq. in.	1.12	1.15	1.11	1.07
(c) Friction angle (ϕ')				
ϕ' = 25°	0.70	0.82	0.96	1.00
ϕ' = 30°	0.82	0.89	0.98	1.00
ϕ' = 35°	1.00	1.00	1.00	1.00
ϕ' = 40°	1.15	1.08	1.01	1.00

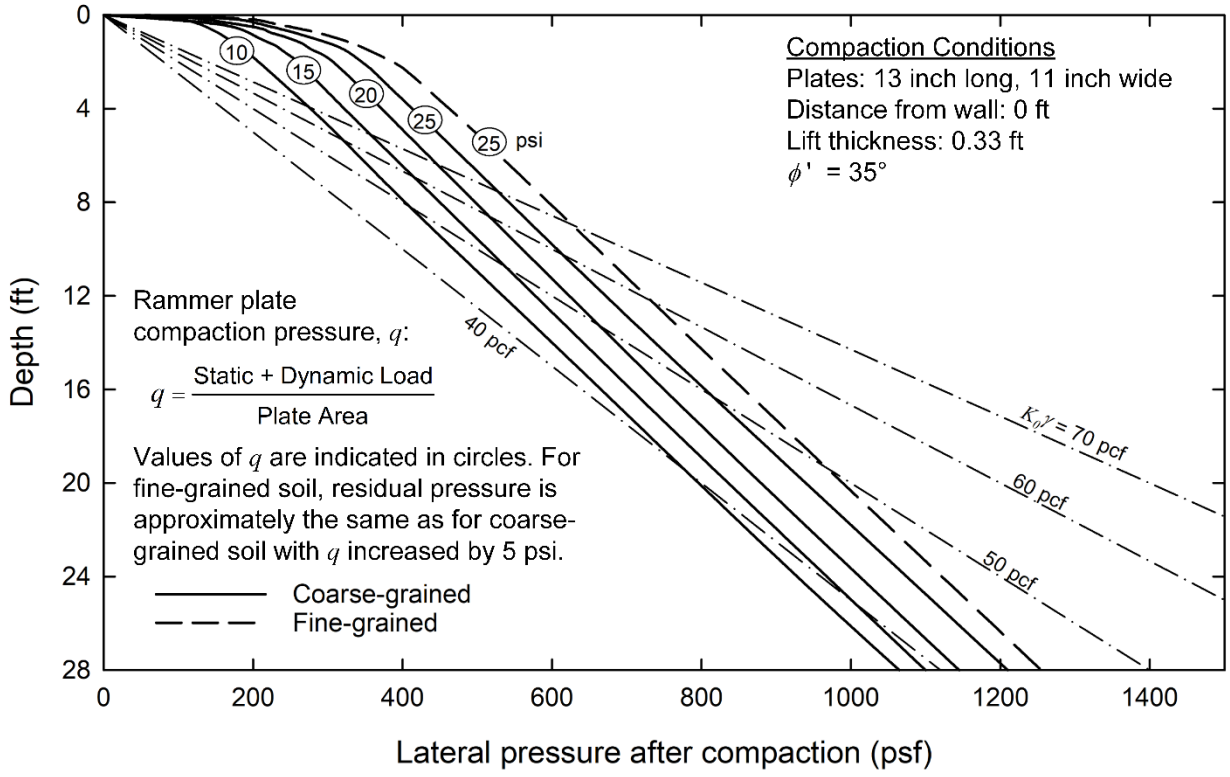

Figure 4-24 Earth Pressures due to Compaction by Rammer Plates (after Duncan et al. 1991)

Table 4-6 Adjustment Factors for Earth Pressures Induced by Compaction with Rammer Plates (after Duncan et al. 1991)

Variables	Multiplier factors for z =			
	2 ft	4 ft	8 ft	16 ft
(a) Distance from Wall (x) and Lift Thickness (t). Adjustment factors are combined.				
x = 0.0 ft, t = 0.33 ft	1.00	1.00	1.00	1.00
x = 0.5 ft, t = 0.33 ft	0.81	0.82	0.82	0.82
x = 0.0 ft, t = 0.5 ft	0.86	0.89	0.93	0.97
x = 0.5 ft, t = 0.5 ft	0.72	0.73	0.82	0.90
(b) Area of Rammer Plate				
Area = 72 sq in	0.82	0.86	0.92	0.98
Area = 144 sq in	1.00	1.00	1.00	1.00
Area = 288 sq in	1.18	1.17	1.10	1.05
(c) Friction angle (ϕ')				
ϕ' = 25°	0.68	0.79	0.92	1.00
ϕ' = 30°	0.79	0.87	0.95	1.00
ϕ' = 35°	1.00	1.00	1.00	1.00
ϕ' = 40°	1.18	1.12	1.05	1.00

4-4.4 Seismic Earth Pressures on Retaining Structures.

Earthquakes can increase the loading on retaining structures. In the past, waterfront structures have performed poorly under earthquake loading (FEMA 2009). The methods for calculating the effects of seismic loading are rapidly evolving. The procedures presented in this section are very basic and are based on the 2009 edition of the NEHRP *Recommended Seismic Provisions* (FEMA 2009). Earthquake assessment of retaining structure is an evolving topic, and the users of this manual are encouraged to seek out the most recent design guidance. Seismic effects are quantified in terms of the vertical ground acceleration (k_v) and horizontal ground acceleration (k_h), both in units of gravity.

Retaining structures are separated into two major categories: (1) yielding walls that are free to rotate or laterally translate, and (2) nonyielding walls, such as basement walls that are restrained on the top and bottom.

4-4.4.1 Yielding Walls.

The assessment of yielding walls is based on the Coulomb earth pressure theory presented earlier in this chapter. The wall movement is assumed to be sufficient to allow an active earth pressure condition to develop. The framework that has been adopted for analysis is the Mononobe-Okabe (M-O) seismic coefficient analysis (Mononobe and Matsuo 1929; Okabe 1924).

The seismic active earth pressure coefficient (K_{AE}) considers the normal factors in a Coulomb analysis (i.e., soil strength, backfill slope, interface friction angle, slope of wall face) and also the horizontal and vertical ground acceleration. K_{AE} can be calculated by:

$$K_{AE} = \frac{\cos^2(\phi' - \theta - \psi)}{\cos\psi \cdot \cos^2\theta \cdot \cos(\delta + \theta + \psi) \cdot \left[1 + \sqrt{\frac{\sin(\phi' + \delta) \cdot \sin(\phi' - \beta - \psi)}{\cos(\delta + \theta + \psi) \cdot \cos(\beta - \theta)}}\right]^2} \quad (4\text{-}15)$$

where:
ϕ' = backfill soil friction angle,
β = slope of backfill,
θ = slope of wall back,
δ = interface friction angle between soil backfill and wall, and
$\psi = \tan^{-1}(k_h / (1 - k_v))$.

The basic equation for calculating the seismic earth pressure assumes that the backfill material is a cohesionless soil and that the phreatic surface is below the base of the wall.

With these assumptions, the seismic earth force is:

$$P_{AE} = \frac{\gamma H^2}{2}(1 - k_v)K_{AE} \tag{4-16}$$

where:
P_{AE} = active earth pressure force including seismic effects,
γ = unit weight of backfill soil,
H = wall height, and
K_{AE} = seismic active earth pressure coefficient.

Seed and Whitman (1970) provide a simplified application of Equation 4-16 by separating the total applied earth pressure force (P_{AE}) into static (P_A) and dynamic (ΔP_{AE}) components. The static component is calculated as described in Section 4-3. For the case of a horizontal backfill, vertical wall face, and no wall friction, the dynamic component is calculated as:

$$\Delta P_{AE} = \frac{3}{8} \cdot k_h \cdot \gamma \cdot H^2 \tag{4-17}$$

where:
ΔP_{AE} = dynamic earth pressure force and
k_h = horizontal ground acceleration assumed equal to the maximum ground acceleration.

The dynamic component of the earth pressure force is assumed to act at $0.6H$ above the wall base. This simplified approach is limited to cases where the backfill is horizontal and the wall height is less than 20 feet. An example for calculating the static and dynamic forces acting on a wall is shown in Figure 4-25.

Example: Vertical Wall with Horizontal Backfill

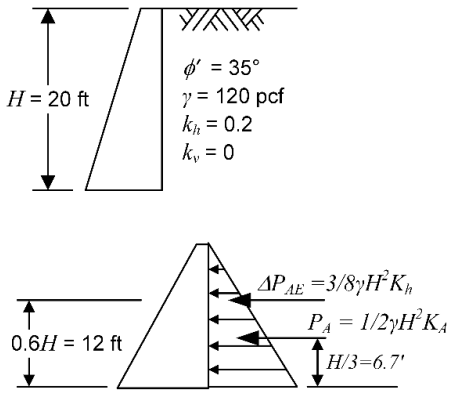

Combined Effect of Static and Dynamic Force.

Force	Equations and Values	Resultant Location above Base of the Wall
P_A (Static)	K_A = 0.27 for ϕ' = 35° $P_A = 1/2\gamma H^2 K_A$ $P_A = 1/2(120)(20)^2(0.27)$ = 6480 lb	$H/3$ = 6.7 ft
ΔP_{AE} (Seismic)	$\Delta P_{AE} = 3/8\gamma H^2 k_h$ $\Delta P_{AE} = 3/8(120)(20)^2(0.2)$=3600 lb	$0.6H$ = 12 ft
P_{AE}	$P_{AE} = P_A + \Delta P_{AE}$ P_{AE} = 6480 + 3600 = 10,800 lb	8 ft
Resultant location of P_{AE} found by summing moments about toe.		

Figure 4-25 Application of the Simplified M-O Procedure for a Vertical Gravity Retaining Wall with a Horizontal Backfill

The M-O procedure can also be applied for conditions where the backfill is not horizontal and the wall has a batter. The combined active earth pressure force can be calculated using Equation 4-16. If separate values of the static and dynamic earth pressure forces are desired, the conventional static active earth pressure force, P_A, can be calculated using K_A determined from the values of β and θ. The dynamic component, ΔP_{AE}, can be calculated by subtracting P_A from P_{AE}.

The resultant force for this method can vary in its location depending on wall movement, ground acceleration, and wall batter. For practical purposes, it may be applied at $0.6H$ above the base of the wall. An example using the M-O method for a wall having a sloping backfill and face is shown in Figure 4-26.

Mononobe-Okabe Method – Sloping wall with sloping backfill

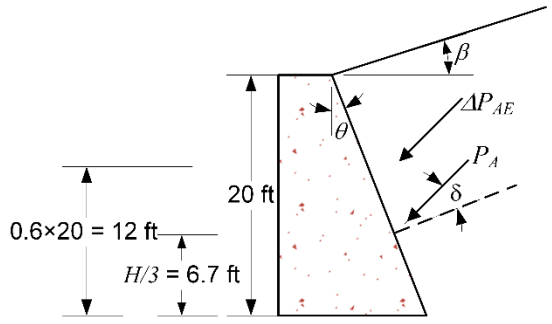

Soil Properties
ϕ' = 35 degrees
γ = 120 pcf
k_h = 0.2
k_v = 0.05

For a wall with θ of 10 degrees and a backslope of 15 degrees, find P_A, P_{AE}, and ΔP_{AE}. Assume the wall is smooth (δ = 0).

Horizontal acceleration angle: $\psi = \tan^{-1}\left(\frac{k_h}{1-k_v}\right) = \tan^{-1}\left(\frac{0.2}{1-0.05}\right) = 12°$

Determine earth pressure coefficient and forces:

Active earth pressure:
K_A from Figure 4-8
K_A = 0.41
K_{AE} from Equation 4-15

$$K_{AE} = \frac{\cos^2(35-10-12)}{\cos(12)\cos^2(10)\cos(22)\left[1+\sqrt{\frac{\sin(35)\sin(35-15-12)}{\cos(10+12)\cos(15-10)}}\right]^2} = 0.64$$

Static earth pressure force: $P_A = 0.5(0.41)(120\ pcf)(20\ ft)^2 = 9840\ lb/ft$

Earth pressure force with seismic effects: $P_{AE} = 0.5 \cdot \gamma \cdot K_{AE}(1-k_v)H^2$

$P_{AE} = 0.5 \cdot (120\ pcf) \cdot (0.64)(1-0.05)(20\ ft)^2 = 14592\ lb/ft$

Dynamic earth pressure force: $\Delta P_{AE} = 14592 - 9840 = 4752\ lb/ft$

Figure 4-26 Example of M-O Method for a Retaining Wall Having a Sloping Face and a Sloping Backfill

The M-O method should not be used for site conditions where there are high ground accelerations and complex soil backfill conditions. For more complex conditions,

evaluation of ground motions is often required, and numerical methods assessing wall displacements are employed.

If the wall does not move or rotate sufficient to develop active pressure, the actual applied pressure can be much greater than the pressure calculated using the M-O method. If there is uncertainty about the ability of the wall to displace sufficiently, more advanced numerical methods are warranted. A simplified approach to calculate seismic pressures on nonyielding walls is presented in the next section.

4-4.4.2 Nonyielding Walls.

Walls that are unable to develop seismic active earth pressures are considered to be *nonyielding walls*. Basement walls are often used as a practical example of a nonyielding wall. Very rigid walls founded on rock can classify as nonyielding walls.

Wood (1973) developed a simplified approach to calculate an increase in the earth pressure force (ΔP_E) for nonyielding walls during seismic events. This force would be added to the existing static pressure to determine the total applied force. The earth pressure force can be calculated by:

$$\Delta P_E = k_h \cdot \gamma \cdot H^2 \quad \text{(4-18).}$$

The point of application of ΔP_E is normally assumed to be at $0.6H$ above the base of the wall. Other solutions for nonyielding walls include inertial effects and kinematic soil-structure interaction effects.

4-4.4.3 Dynamic Water Pressure.

Seismic loading also changes the water pressure applied to walls. The solutions presented below assume that the backfill is saturated. Methods for partially submerged conditions can be found in Kramer (1996) and Matsuzawa et al. (1985). Calculation approaches can be separated by the hydraulic conductivity of the soil.

4-4.4.3.1 High Hydraulic Conductivity Soils.

For soil with hydraulic conductivity greater than about 10^{-3} cm/s, the water in the voids will act independently of the soil and will impart a hydrodynamic water pressure (p_w) that can be calculated as:

$$p_w = 0.875 \cdot k_h \cdot \gamma_w \sqrt{H \cdot z} \quad \text{(4-19)}$$

where:
γ_w = unit weight of water,
z = depth below the phreatic surface, and
H = total depth of water behind the wall.

This equation can also be used to estimate the hydrodynamic pressure acting on a wall from an impounded reservoir.

The resultant force from the hydrodynamic water pressure is found as (Kramer 1996):

$$P_w = \frac{7}{12} k_h \cdot \gamma_w \cdot H^2 \quad \text{(4-20).}$$

If the hydrodynamic water pressure is calculated in this manner, the seismic earth force should be calculated using the buoyant unit weight in Equation 4-16.

4-4.4.3.2 Low Hydraulic Conductivity Soils.

For soil with hydraulic conductivity less than about 10^{-3} cm/s, the water will tend to move with the soil, and a separate hydrodynamic water pressure is not required. However, the effect of increased pore pressures on stability must be considered (Kramer 1996).

The seismic earth pressure coefficient should be calculated using Equation 4-15 with:

$$\psi = \tan^{-1}\left[\frac{\gamma_{sat} k_h}{(\gamma_{sat} - \gamma_w)(1 - r_u)(1 - k_v)}\right] \quad \text{(4-21)}$$

where:
γ_{sat} = saturated total unit weight of soil,
γ_w = unit weight of water,
k_h = horizontal ground acceleration (g),
k_v = vertical ground acceleration (g), and
r_u = pore pressure coefficient.

The seismic earth pressure force can be calculated using Equation 4-16 with an adjusted unit weight to account for seismically induced excess pore pressure is:

$$\gamma = (\gamma_{sat} - \gamma_w)(1 - r_u) \quad \text{(4-22)}$$

where:
γ_{sat} = saturated total unit weight of soil,
γ_w = unit weight of water, and
r_u = pore pressure coefficient.

4-5 RIGID GRAVITY RETAINING STRUCTURES.

The preceding sections provide the theories for calculating earth and water pressures on retaining structures. A key element in the development of earth pressures is the wall movement or displacement. For design, retaining structures are divided into two basic categories: (1) rigid gravity structures and (2) flexible structures. Alternative forms of

gravity structure are presented in Section 4-6. The design of flexible walls is discussed in Section 4-7.

Rigid retaining walls are structures that displace (translation or rotation) monolithically, and for the most part, they develop their lateral resistance from their own weight and the weight of overlying soil. The construction process for rigid walls typically involves construction of the wall followed by the placement of backfill. Examples of rigid retaining structures are concrete gravity walls, concrete cantilever walls, counterfort walls, buttress walls, and gabion walls. The design of rigid retaining structures is discussed in this section.

4-5.1 Design Calculations for Rigid Retaining Walls.

Examples of four rigid retaining walls are shown in Figure 4-27. The pressures acting on the face of rigid walls follow the theory, presented earlier in this chapter, that depends on the displacement or rotation of the wall. Once the earth and water pressures are determined, the forces and pressures acting on the other parts of the wall are assessed so that an entire free-body diagram can be constructed. With a knowledge of the FBD, a variety of modes of failure can be assessed. Figure 4-27 summarizes the calculations for the following modes of failure:

1) Overturning,
2) Sliding,
3) Bearing capacity and settlement, and
4) Global or overall stability.

Passive forces are indicated above the toe of the retaining walls in Figure 4-27. However, the passive pressure on the front of the wall is typically ignored when assessing the stability. As shown in Figure 4-1, there is a marked difference in displacement required for developing passive pressure as compared to active pressure. By the time that full passive pressure has been developed, the wall displacement would be too great for the performance to be considered satisfactory. Also, the soil in front of the wall might be excavated at a later date, so relying on passive pressure often is not warranted.

4-5.1.1 Pressure Distribution at the Base of Walls.

The pressure distribution acting on the base of retaining walls impacts the stability assessment for different failure modes. Using the equations for force equilibrium, the magnitude of the resultant normal force (R) and the shear force (T) can be determined. The location of R can be determined from moment equilibrium about the toe of the wall. The distance that R acts from the centerline or midpoint of the base of the wall is defined as the *eccentricity*, e. Figure 4-27 provides the method for calculating the resultant location and eccentricity.

<table>
<tr><th>Type of Wall</th><th>Load Diagram</th><th>Design Calculations</th></tr>
<tr><td>Gravity</td><td rowspan="3">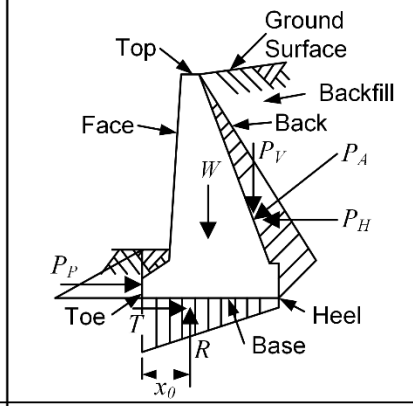
</td><td rowspan="3">Location of Resultant
Moment Arm about Toe:
$x_0 = \left(W \cdot a - P_v \cdot f - P_H \cdot b\right) / \left(W + P_v\right)$
assuming P_P = 0.
Eccentricity can be calculated from x_0 as:
$e = B/2 - x_0$

Overturning
Moment about toe:
$F_{OT} = \left(W \cdot a\right) / \left(P_H \cdot b - P_V \cdot f\right) \geq 1.5$

Design is safe for overturning if R within middle third for soil or middle half for rock. Check R at different horizontal planes for gravity walls.

Resistance Against Sliding
The resisting force at the base of the wall, T, is:
$T = \left(W + P_V\right) \tan \delta + C_a \cdot B_e$
where:
C_a = Adhesion between soil and base
tan δ = friction factor between soil and base
W = weight of wall
Weight includes soil in front of gravity and semigravity walls and includes weight of soil above footing for cantilever and counterfort walls. For coefficients of friction between base and soil see Table 4-1.
The factor of safety against sliding is calculated as:
$F_{SL} = T / P_H \geq 1.5$

If passive pressure is considered:
$F_{SL} = \left(T + P_P\right) / P_H \geq 2.0$

Contact Pressure on Foundation
For allowable bearing pressure for inclined load on strip foundation, see Section 5-3.3.

Settlement and Overall (Global) Stability
For analysis of settlement and overall stability, see Chapters 5 and 7 of DM 7.1.

*Variables defined on diagrams.</td></tr>
<tr><td>Semigravity</td></tr>
<tr><td>Cantilever</td></tr>
<tr><td>Counterfort</td><td>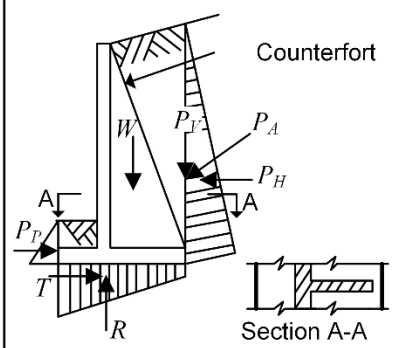
</td></tr>
</table>

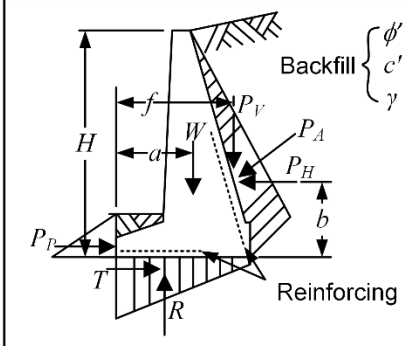

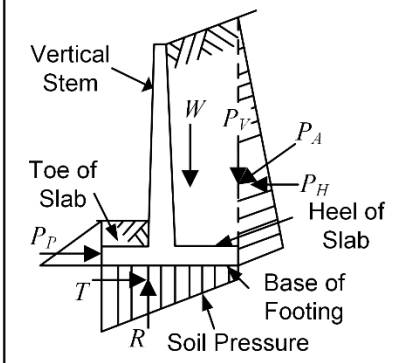

Figure 4-27 Analysis Methods for Stability Assessment of Gravity Retaining Walls

Knowledge of the magnitude and position of R allows the pressure distribution on the bottom of the wall to be calculated. Theoretically, the shape of pressure distribution is either triangular or trapezoidal as shown in Figure 4-28. If the resultant acts precisely at the one-third point of the base, a triangular pressure distribution results, with the full base of the wall under compression. If the resultant acts within the middle third of the base, a trapezoidal distribution results, and the maximum pressure, q_{max}, acting at the toe is:

$$q_{\max} = \frac{R}{B} + \frac{6Re}{B^2} \quad \text{(4-23).}$$

The resultant of the pressure distribution acts at the centroid of the pressure diagram. The minimum pressure, q_{min}, acting on the heel side of the trapezoidal pressure distribution that provides the correct location of the resultant (R) can be calculated by:

$$q_{\min} = \frac{R}{B} - \frac{6Re}{B^2} \quad \text{(4-24).}$$

If the resultant is located outside of the middle third of the base, the maximum stress can be calculated by:

$$q_{\max} = \frac{2R}{3x_0} \quad \text{(4-25)}$$

where:
x_0 = $B/2 - e$ = horizontal distance between R and the toe.

When the resultant is outside of the middle third of the base, only a portion of the base is under compression. The amount of base under compression, B_e, can be calculated by:

$$B_e = 3x_0 \quad \text{(4-26).}$$

As shown at the bottom of Figure 4-28, the pressure distribution can be simplified by assuming that the pressure acts uniformly over a width of $2 \cdot x_0$. If the pressure distribution is assumed to be uniform, its magnitude is:

$$q_{\max} = \frac{R}{2x_0} \quad \text{(4-27).}$$

For the simplified uniform distribution of pressure, the amount of the base that is under compression is:

$$B_e = 2x_0 \qquad \text{(4-28).}$$

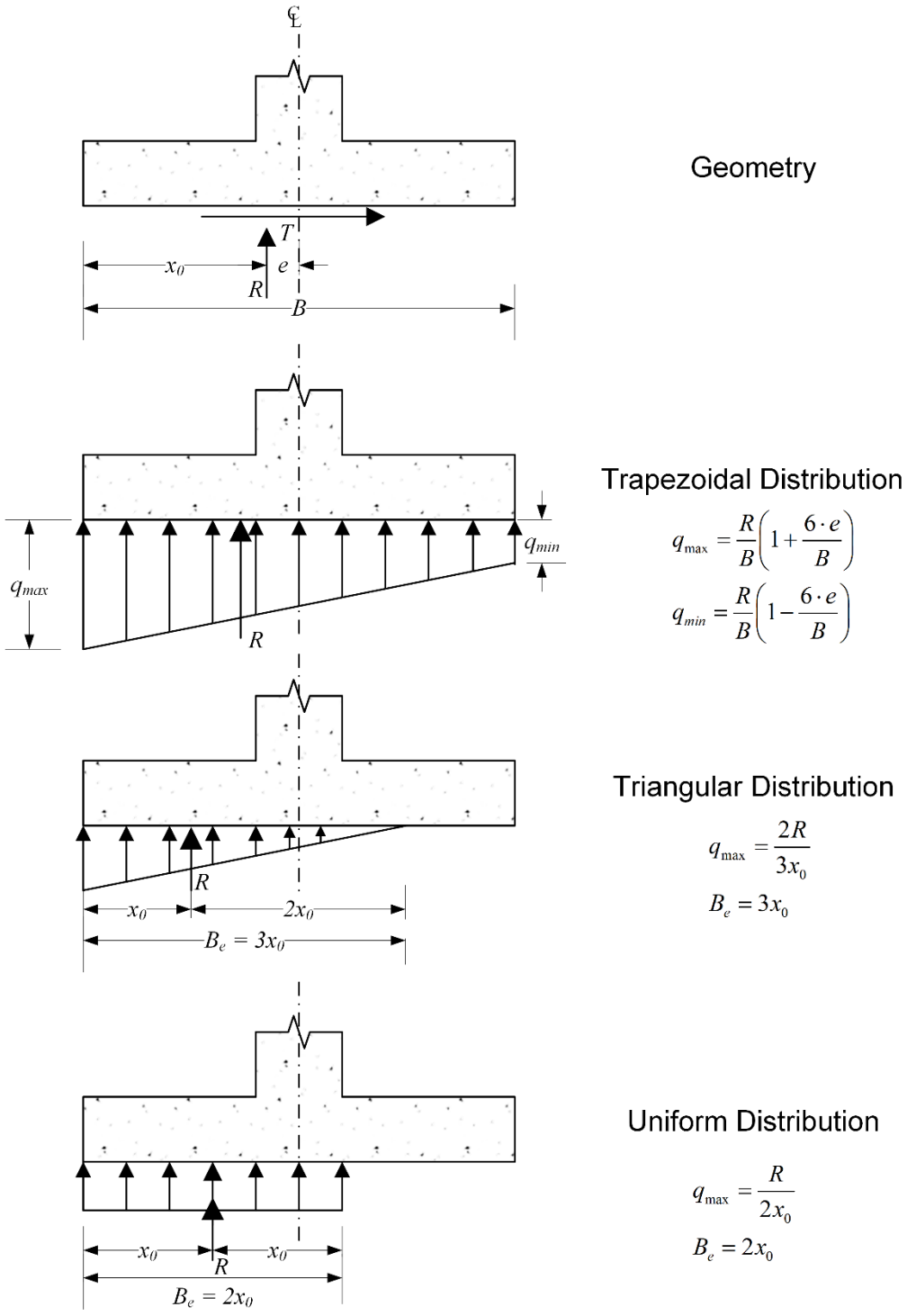

Figure 4-28 Pressure Distributions at the Base of Rigid Retaining Walls (after Kim et al. 1991)

4-5.1.2 Overturning.

The stability of the wall for the failure mode of overturning can be determined by defining a factor of safety equal to the restoring moment divided by the overturning moment. The factor of safety, F_{OT}, should be greater than or equal to 1.5.

An alternative method is to examine the location of the resultant, R, relative to the width of the base of the wall. If R is in the middle one-third of the base for walls founded on soil, the wall is considered safe. For walls founded on rock, R should be located in the middle one-half of the base for the wall to be considered safe.[23]

4-5.1.3 Sliding.

The stability of the wall for the failure mode of sliding is normally determined by using horizontal force equilibrium. The factor of safety against sliding, F_{SL}, is the ratio of the resisting force to the horizontal earth pressure force. The resisting force is a combination of the frictional resistance at the base of the wall and the adhesion between the base of the wall and the soil foundation. For sliding resistance on fine-grained soils, the adhesion should be multiplied by the effective width of the base (B_e) found using the uniform bearing pressure method. The factor of safety should be greater than or equal to 1.5. The parameters used to calculate F_{SL} are shown on Figure 4-27. If passive resistance is included, the minimum F_{SL} should be increased to 2.0. Minimum F_{SL} may also need to be increased when base adhesion is included in the resistance.

In some cases, a layer of coarse-grained soil may be placed below the wall as a bearing material. Sliding should be checked at two locations. The shear resistance, T, should be taken as the lowest of (1) the resistance at the interface between the base of the wall and the bearing material and (2) the resistance within the clay using the full undrained shear strength.

If stability against sliding is an issue, gravity retaining walls can be designed with a *key* to increase the sliding resistance by adding a passive resistance component. Figure 4-29 shows an outline of the analysis method to accommodate a wall base with a key. Note that the passive pressure is applied only along the depth of the key and not along the entire burial depth of the wall. It is also prudent to consider some amount of future excavation in front of the wall that would reduce passive resistance.

[23] If LFRD techniques are used for design, there are wider thresholds for the location of the resultant force if factored loads are used.

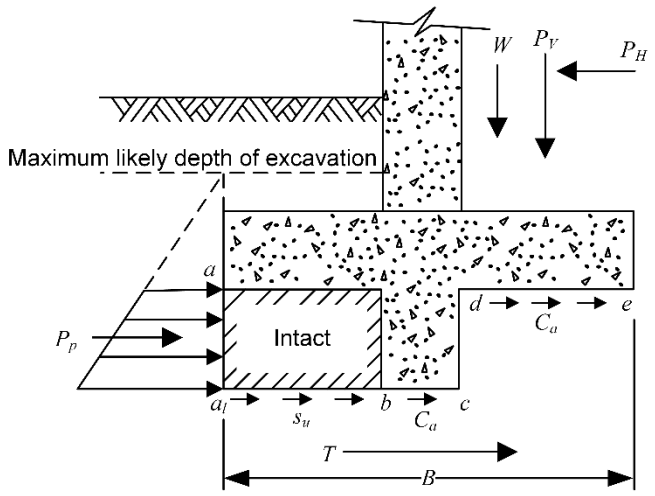

Resistance Against Sliding on Keyed Foundations

Undrained: $T = C_a \cdot \left(B_e - \overline{a_1 b} \right) + s_u \cdot \overline{a_1 b} + P_p$

Drained: $T = \left(W + P_V \right) \tan \delta + P_p$

Factor of Safety Against Sliding, F_{SL}

$$F_{SL} = \frac{T}{P_H}$$

where:
P_p = Passive resistance
P_V = Vertical earth force
P_H = Horizontal earth force
s_u = Undrained shear strength of foundation soil
C_a = Adhesion for cohesive soil and concrete
δ = Interface friction angle for granular soil & concrete
Note: Values of C_a and δ are given in Table 4-1.

Figure 4-29 Analysis Method for Gravity Retaining Wall Base with a Key

4-5.1.4 Bearing Capacity and Settlement.

The bearing capacity of the soil below a retaining wall is calculated by assuming the wall acts as a conventional strip footing with eccentric, inclined loading, which is discussed in Chapter 5. The depth of embedment is equal to the depth on the toe side of the wall.

The bearing capacity should be compared to the maximum bearing pressure calculated as shown in Figure 4-28. A factor of safety of 2.5 to 3 is typically appropriate. A uniform pressure distribution can be used to determine q_{max} if the soil below the wall is relatively ductile. For more brittle materials, such as rock and sensitive clays, the triangular or trapezoidal pressure distribution should be used to find q_{max}. Because load inclination affects bearing capacity, the factor of safety against bearing capacity failure and sliding are often closely related.

Settlement of retaining walls can be an important factor in overall stability. For the examples shown in Figure 4-27, the backfill places a downward pressure on the retaining wall. This pressure increases the contact stress at the base of the wall, thus increasing the sliding resistance. If the wall settles considerably more than the backfill, then the relative movement between the wall and backfill can be reversed, and the vertical pressure can act up instead of down. This is a destabilizing force on the wall since it decreases the resistance to sliding.

Settlement analyses can be performed using the procedures outlined in Chapter 5 of DM 7.1. Settlement should consider net changes in stress by comparing the conditions before and after the wall was constructed.

4-5.1.5 Overall or Global Stability.

Overall or global stability is assessed using the same tools employed for slope stability analysis. This mechanism of failure considers slip surfaces that extend from the back of the wall to the front of the wall, and the slide mass contains the wall and backfill. Slope stability is discussed in Chapter 7 of DM 7.1.

4-5.1.6 Design of Low Walls.

For low retaining walls (less than 12 feet tall), the retaining wall loads can be calculated based on equivalent fluid pressures, provided the consequences of failure are not significant. Figure 4-30 provides a method for determining the loads on low retaining walls for three different soil categories based on the Unified Soil Classification System. This method accommodates a *broken* backslope, in which the backslope levels are relatively close to the wall. The equivalent fluid unit weights can be used to calculate horizontal and vertical forces applied to the wall.

Figure 4-30 is based on equivalent fluid pressures associated with the different soil types listed above, and similar charts are found in several geotechnical textbooks. However, the specific details on how these charts were created are unclear. If these charts are used, it is prudent to check the results using other methods.

4-5.2 Drainage Behind Rigid Walls.

Water should not be allowed to pond behind retaining structures or within the backfill, if at all possible. The presence of a phreatic surface in the wall backfill decreases the effective stress in the soil, so the earth pressure is reduced. However, as discussed in Section 4-4.1, the water itself applies a pressure to the wall, and the net result is that lateral forces on the wall are increased. Many failures of retaining structures are due to unanticipated or unmitigated water pressures.

Drainage systems should be incorporated into the design of retaining structures if there is a potential for water pressures to act on the wall. The drainage system design should satisfy several criteria:

1) An elevated water table should not be present behind the wall, even in the case of large rainfall events.

2) Any water that finds its way to the backfill should be safely conveyed away from the wall. The water should be drained laterally down the wall to a safe exit or through weep holes in the face of the wall.

3) The drainage system should not allow erosion of the backfill materials or migrations of fines within the backfill. This may require the use of a graded filter or geosynthetic filter fabric.

Examples of drainage and filter systems that can be incorporated into rigid wall design are shown in Figure 4-31.

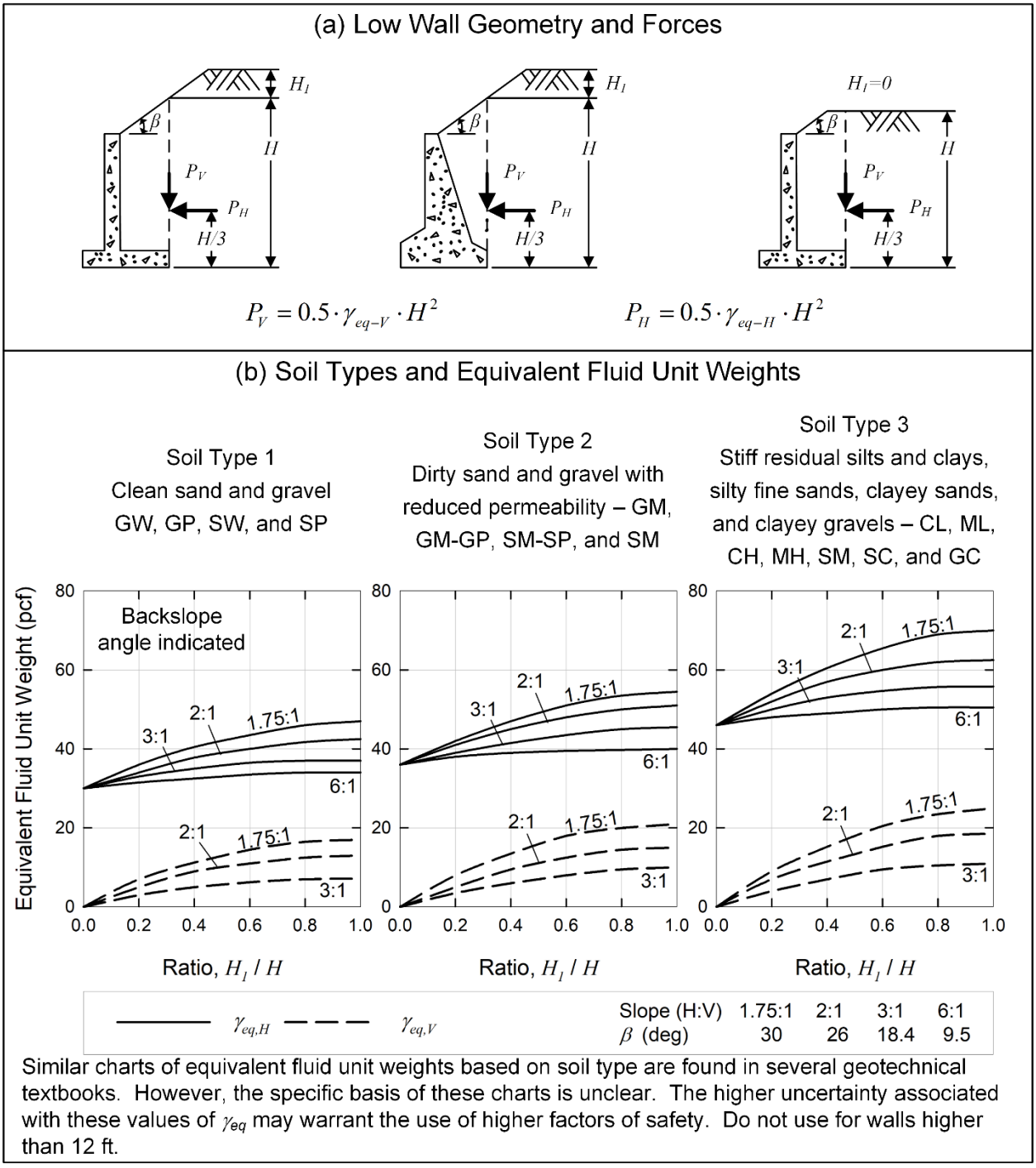

Figure 4-30 Low (<12 ft Tall) Retaining Walls – (a) Geometry and Forces and (b) Equivalent Fluid Unit Weights by Soil Type

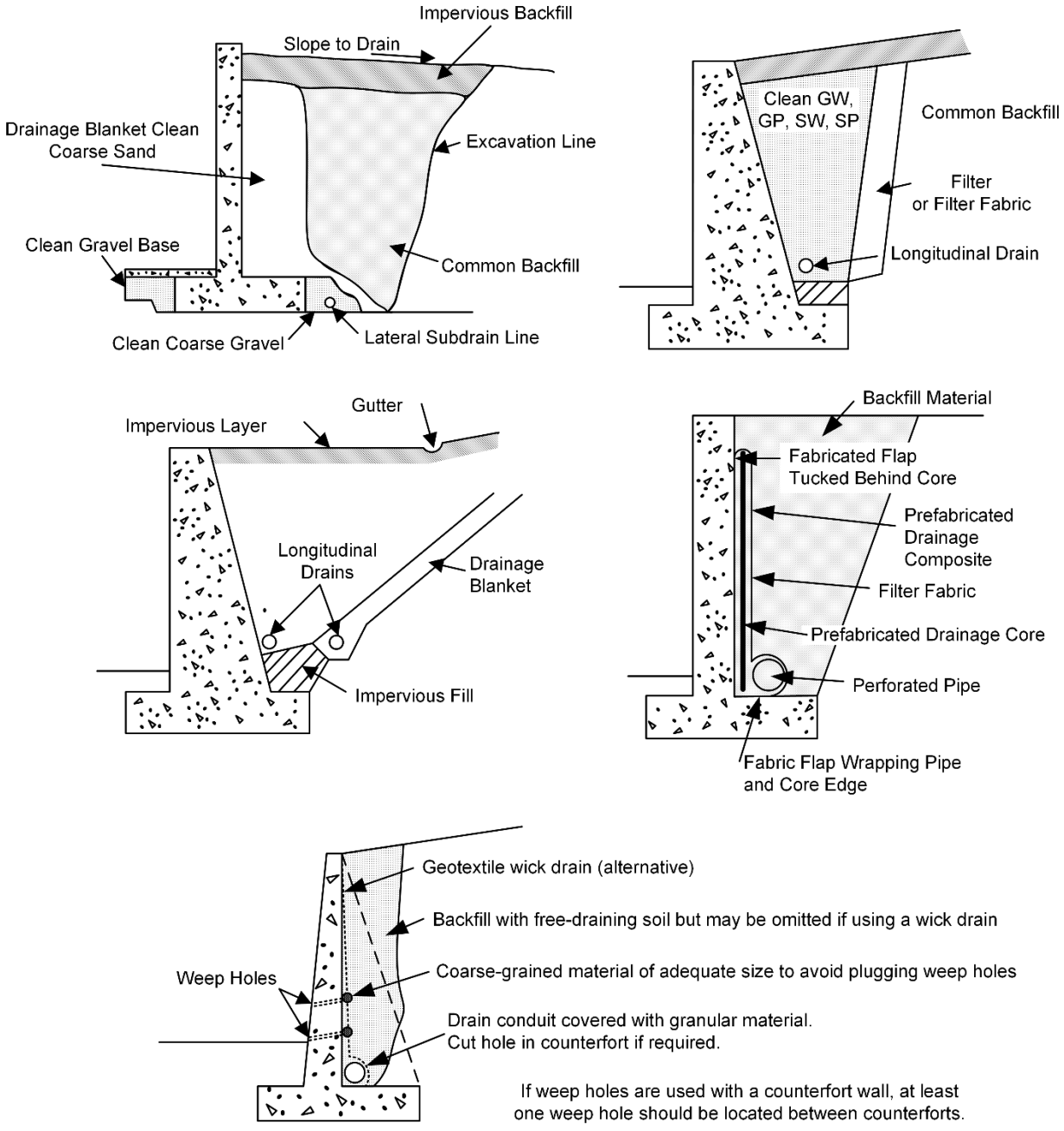

Figure 4-31 Drainage Systems Used for Rigid Retaining Structures (after Kim et al. 1991)

4-6 ALTERNATIVE GRAVITY RETAINING STRUCTURES.

4-6.1 Mechanical Stabilized Earth (MSE) Retaining Structures.

Mechanically stabilized earth (MSE) retaining structures are a popular alternative to rigid retaining structures. The technology and design methods used for MSE walls and slopes are very similar, and they share the same design manuals from the FHWA. If the face angle of the structure is greater than or equal to 70 degrees, then the structure is considered to be a *wall*. If the face angle is less than 70 degrees, then the structure is considered to be a *slope* (FHWA 2009). Walls also have a facing material, while slopes normally do not.

NAVFAC DM-7.1 covers many of the details regarding the internal design of MSE structures in Chapter 7. These details included the backfill materials, reinforcing materials, drainage systems, and the steps for designing MSE structures. These structures must also be designed for overturning, sliding, bearing capacity, settlement, and global stability.

Further discussion of MSE is beyond the scope of this manual. There are several technical reports available from the FHWA that provide design methods for MSE walls and slopes. FHWA (2009) describes Load and Resistance Factor Design (LRFD) for MSE walls. This manual is considered to be an update for the Allowable Stress Design (ASD) manual, FHWA NHI-00-043 (FHWA 2001).

4-6.2 Gabion Walls.

Gabions are compartmented, rectangular containers made of heavily galvanized steel or polyvinylchloride (PVC) coated wire, filled with stone from 4 to 8 inches in size, and are used for control of bank erosion and stabilization as well as earth retaining structures. Design notes for gabion retaining walls are given in Figure 4-32. When the water quality is in doubt (pH > 12 or pH < 6) or where high concentration of organic acid may be present, PVC coated gabions are necessary. At the construction site, the individual gabion units are laced together with wire and filled with stone. Specifications for the gabion baskets are available in the Corps of Engineers CW-02541 (1980).

Gabions are designed as mass gravity structures using the same design procedures as rigid retaining walls that are presented in Figure 4-27. When designing a vertical face wall, it should be battered at an angle of about 6° to keep the resultant force toward the back of the wall. The interface friction angle between the base of a gabion wall and a coarse-grained foundation soil can assumed to be equal to the effective stress friction angle of the foundation. For the back of the wall, the ratio of interface friction to the friction angle of the backfill (δ / ϕ') can be set equal to 0.9. Where the retained material is mostly sand, a geosynthetic filter fabric or granular filter is recommended to prevent any erosion of the backfill soil into the gabions. Along all exposed gabion faces, the

outer layer of stones should be hand placed to ensure proper alignment, and to achieve a neat, compact, square appearance.

A system of gabion counterforts is recommended when designing gabion structures to retain clay slopes. They should be used as headers and should extend from the front of the wall to a point at least one gabion length beyond the critical slip circle of the bank. Counterforts may be spaced from 13 feet (very soft clay) to 30 feet (stiff clay). A filter is also required on the back of the wall so that clay will not clog the free-draining gabions.

Gabion Retaining Wall Configurations

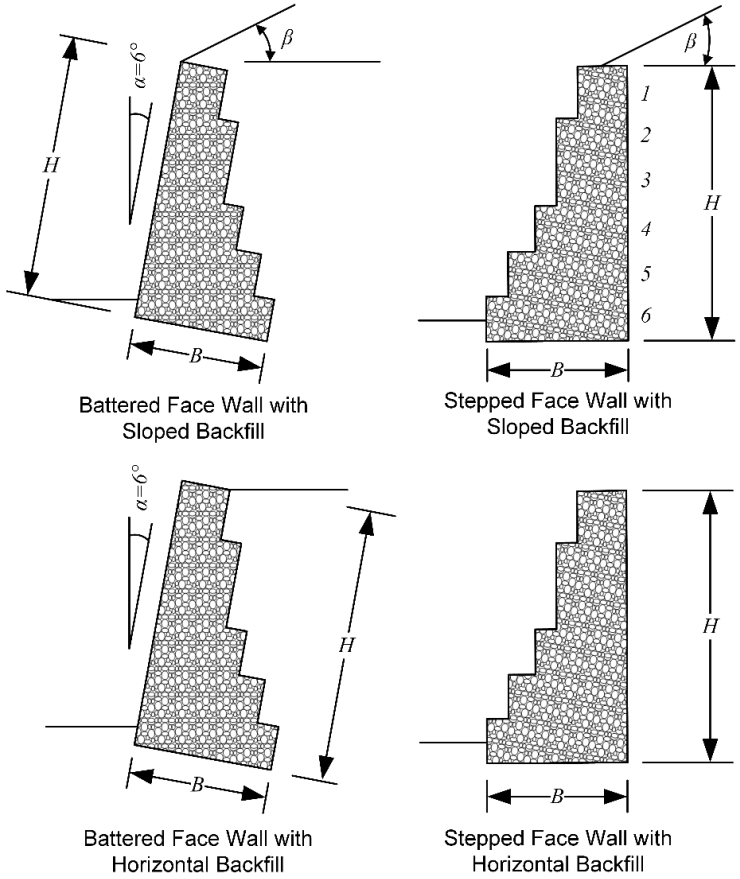

Gabion Retaining Wall
The common gabion wall configurations are shown to the left.

The choice of either battered or stepped face rests with designer. A stepped face is recommended, if the gabion wall is more than 10 feet high.

Gabion Fill
Use hard, durable, clean stone 4 to 8 inches in diameter or other approved size

Typical total unit weight:

γ = (44 pcf)×G_s

For common gabion fill, G_s ranges from 2.2 for some sandstone to 3.0 for basalt.

Gabion Wall Design

Design criteria for gravity walls apply. Wall section must resist overturning and sliding. To increase wall stability, it is recommended to tilt the wall at an angle of 6° (i.e. 1:10). On the base of the wall, use tan δ = tan ϕ' between the gabion wall and coarse-grained soil. At the back of the wall, assume tan δ = 0.9 tan ϕ'. For retaining clay slopes, a system of gabion counterforts is recommended.

Compute active soil pressure behind the wall using the Coulomb wedge theory, and design the mass of the wall to balance the force exerted by that soil wedge. Earth pressures higher than active may be used, depending on compactions conditions and limitations on deformations. Maximum pressure at the base of the gabion wall must be less than the allowable bearing capacity of the soil under the wall.

When water quality is in doubt (pH below 6 or greater than 12) or where high concentration of organic acids may be present, the use of PVC (polyvinvlychloride) coated gabions is recommended.

Figure 4-32 Design Notes for Gabion Retaining Walls

Hesco Bastion Concertainers®, commonly referred to as *Hesco baskets*, are similar to gabions in that they are wire baskets or cages that are filled with cobbles or other granular soils. Hesco baskets are normally lined with a non-woven geotextile. Common sizes for Hesco baskets are 3 ft x 3 ft x 15 ft and 4 ft x 3 ft x 15 ft. Hesco baskets have been used for a variety of functions in the Armed Forces. They can be used in lieu of sandbags for erosion and seepage control purposes, particularly at the crest of levees to increase the functional height of the levee. Hesco baskets can also be used to create walls to protect personnel as a force protection barrier system (MIL-DTL-32488 2014).

4-6.3 Earth-Filled Crib Walls and Bin Walls.

Crib walls and *bin walls* can be used as retaining structures when site access is too difficult to use other earth retaining structures. These also are designed as mass gravity structures using the same design methodology presented in Figure 4-27. Examples of the design elements of crib and bin walls are shown in Figure 4-33. The height of crib and bin walls should generally be less than 30 feet. For taller walls, consideration should be given to other wall types that are generally more robust.

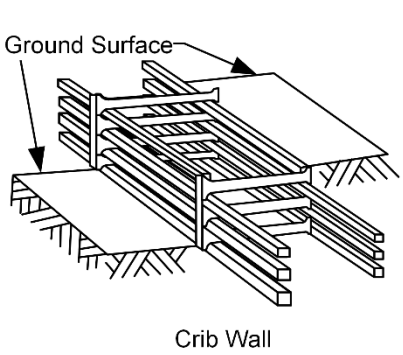

Crib Wall

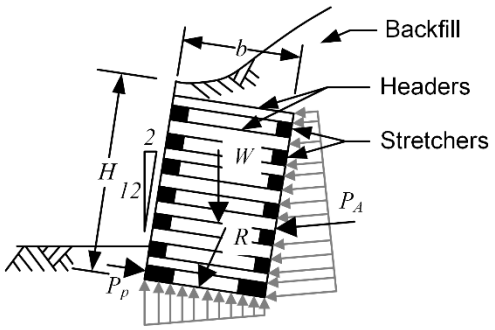

Typical Section

Cribbing Materials – Timber, Concrete, and Metal.

Fill – Crushed stone or other coarse grained material, including rock less than 12 inches in diameter.

Design – Design criteria for gravity wall apply. Wall section resisting overturning is taken as a rectangle with dimensions H and b. Weight of crib is equal to that of material with a plumb face. Higher walls are battered on the face at least 2 inches per foot. For high walls (i.e., 12 ft high and greater), the batter is increased or supplemental cribs are added at the back. Such walls are very sensitive to transverse differential settlements. Walls with a convex back are more desirable for greater height. In open-face cribs, the space between stretchers should not exceed 8 inches so as to properly retain the fill. Expansion joints for concrete and metal cribbing are spaced no more than 90 feet.

Filling – The wall should not be laid up higher than 3 feet above the level of the fill within the crib.

Bin Type Retaining Wall – Composed of metal bins or cells joined to special columnar units at the corners. The design requirements are the same as for crib walls except that suitable drainage behind the walls is needed. Internal stresses are investigated in accordance with criteria for cellular walls.

Figure 4-33 Design Elements of Crib Walls and Bin Walls

Crib walls can be constructed of timber or precast concrete beams. Interlocking precast concrete beams are available for rapid wall construction. Crib walls can be constructed with common earth-moving equipment and manual labor. The walls can accommodate changes in alignment and topography better than other types of walls. Crib walls can be more tolerant to differential settlement than other stiffer wall types.

Bin walls are often made of corrugated steel panels that are bolted together and filled with coarse-grained soils. It is important for the backfill of bin walls to be free-draining, and the high permeability of the backfill should be maintained.

4-7 FLEXIBLE RETAINING STRUCTURES.

Flexible retaining structures consist primarily of vertical structural elements that are inserted prior to excavation. The structures may be braced or anchored. Examples include sheet pile, soldier beam and lagging, and concrete diaphragm walls. Flexible structures can exhibit a range of displacements depending on the fixity of the buried parts of the wall and on the location of supports or anchors.

The embedded portion of a flexible structure develops passive resistance resulting from displacement of the structure toward the soil. In addition, flexible structures are often braced or supported as shown in Figure 2-6 because embedment alone is insufficient. *Internally-supported* systems use structural supports that are internal to the excavation. *Externally-supported* systems use anchors or tiebacks within the soil that are external to the excavation.

A variety of flexible retaining structures are used for waterfront structures, excavation bracing, permanent retaining walls, and other support systems. These walls often appear to be quite rigid, but due to the length of the support elements, they deflect under earth and water loads. As described earlier, earth pressures vary according to wall deflections, and the design of flexible retaining structures can be quite involved. Limit equilibrium analyses have been historically used for the design of these structures, and those are the methods that are described in this manual. Numerical methods, such as finite element and finite difference, are often used in geotechnical engineering practice, especially when limiting wall deflections is important or for deep excavations. However, the use of limit equilibrium methods is still widespread in engineering practice.

4-7.1 Factored Passive Resistance.

As noted above, the stability of many flexible structures depends on the passive resistance at the base of the wall and in front of supporting anchors. In the analysis methods that follow, two different methods may be used to provide an adequate factor of safety. Where passive earth pressure forces are directly calculated, the allowable passive force ($P_{P,allow}$) can be found as:

$$P_{P,allow} = \frac{P_P}{F} \tag{4-29}$$

where:
P_P = passive earth pressure force calculated using the shear strength parameters and
F = factor of safety.

As such, the factor of safety is applied to load, which is similar to the approach used in bearing capacity analysis. In this case, the value of F should be 2 to 3 for coarse-grained soils (effective stress design). A value of F = 1.5 to 2.0 can be used for undrained analysis in fine-grained soils. These factors of safety will provide approximately equivalent factors of safety with respect to shear strength.

Alternatively, the value of K_P can be determined from an allowable effective stress friction angle (ϕ'_{allow}) which is found as:

$$\phi'_{allow} = \tan^{-1}\left(\frac{\tan\phi'}{F}\right) \tag{4-30}$$

where:
ϕ' = effective stress friction angle.

The second method (Eqn. 4-30) provides a factor of safety on shear strength, similar to slope stability. In this case, a factor of safety of 1.5 to 2.0 is appropriate, regardless of the soil types or analysis conditions.

4-7.2 Anchored Bulkheads.

Anchored bulkheads are waterfront structures used to allow a change in elevation for access to the water. These structures are often driven sheet piles that are restrained on the landside by some form of anchoring system. Sheet piles are often steel, but can also be made of concrete, wood, vinyl, and plastic.[24] Excavations are made on the waterside down to the *dredge line* to allow sufficient draft for vessels. The dredge line is the lowest depth to which soil is removed in front of the wall.

Several references are available that provide design guidance and construction details for anchored bulkheads. These include:

- USACE (1995b) Design of Coastal Revetments, Seawalls, and Bulkheads, EM 1110-2-1614, CECW-EH-D.

[24] Plastic and vinyl sheet piles have exceptional corrosion resistance, but the interlock strength is much less than steel sheet piles. Plastic and vinyl sheet piles should not be used for cases where there are significant consequences of failure, especially loss of life.

- USACE (1994a) Design of Sheet Pile Walls, CECW-ED, EM 1110-2-2504.
- US Steel (1984) Steel Sheet Piling Design Manual, Updated and reprinted by the US Department of Transportation/FHWA.

The earth pressure and water pressure distributions on anchored bulkheads can be quite complex. The ground surface elevation is different on the landside and the waterside. The water level on the landside and waterside is often different as well. In addition to soil and water loads, the anchoring system applies a concentrated force on the wall. Anchored bulkheads are often constructed by excavation and dredging in natural soils or unengineered fills; therefore, the soil properties can vary greatly. An important part of the engineering design of these structures is to accurately simplify the cross section and soil parameters into relatively homogeneous layers that can be accommodated by earth pressure theory.

Anchored bulkheads can be designed by determining the appropriate pressures acting on each side of the wall separately. Sometimes, it is more convenient to use *net pressure diagrams*, where the difference in the pressure on each side of the wall is calculated. Examples of a total pressure diagram and a net pressure diagram are shown in Figure 4-34.

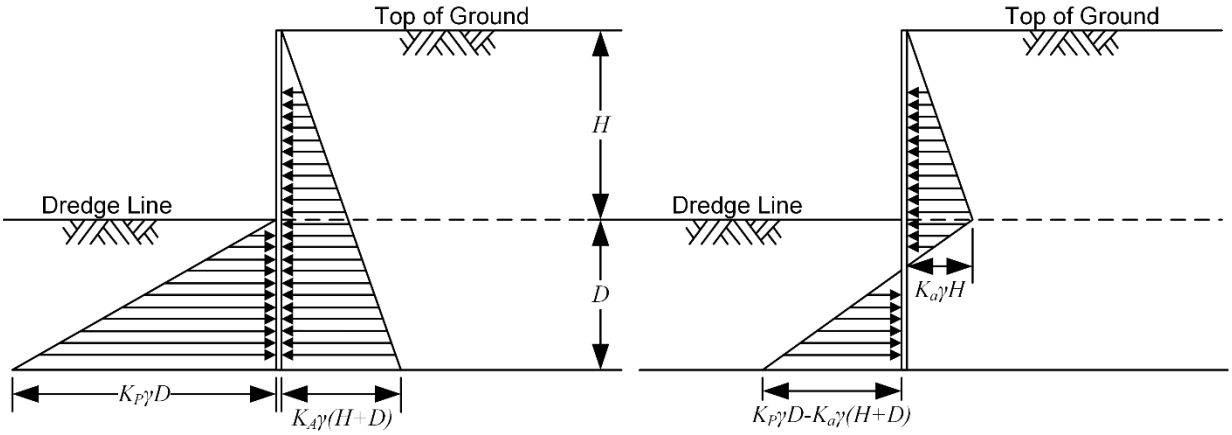

Figure 4-34 Total Regular Pressure Diagram and Net Pressure Diagram

Anchored bulkheads can be designed using limit equilibrium methods. An important element in using limit equilibrium methods is to define the possible modes of failure. Anchored bulkheads can fail in many different ways, as shown in Figure 4-35. A proper design will examine each potential mode of failure of the different anchored bulkhead elements. Interlock failure should also be considered.

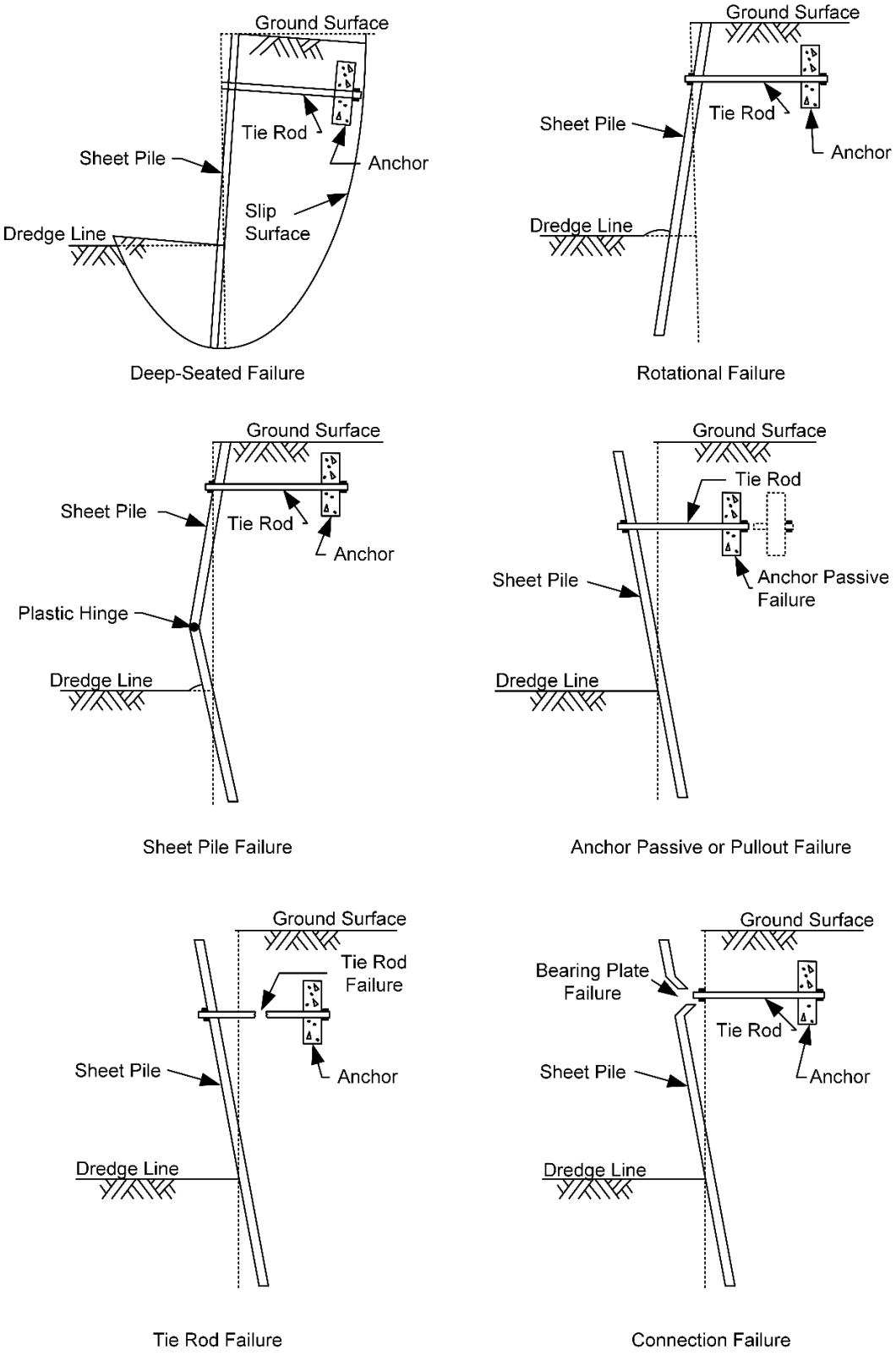

Figure 4-35 Failure Modes for Anchored Bulkheads (after USACE EM 1110-2-2504 1994)

Methods for the analysis of anchored bulkheads are often categorized into *free earth* or *fixed earth* support methods. The difference between these two methods involves the behavior of the wall below the dredge line. In free earth analysis, the passive resistance below the dredge line is not developed to the point that movement of the sheet pile tip is prevented. The tip of the sheet pile can deflect toward the water side. The free earth support system tends to overpredict the bending moments in the sheet pile, and techniques are available to correct the bending moment. In fixed earth analysis, which is less commonly used, the lower end of the wall is essentially fixed so that no movement is allowed.

Experience and scale model testing have shown that the free earth support method overpredicts the bending moment in flexible walls (Rowe 1952). The differences from theory are explained by flexural of the wall but above and below the dredge line. Corrections to the predicted moment, often referred to as *moment reduction*, depend on the relative flexibility (ρ) of the wall, which is defined as:

$$\rho = \frac{\left(H + D\right)^4}{EI} \tag{4-31}$$

where:
H = exposed height of the wall (inches),
D = depth of penetration below the dredge line (inches),
E = Young's modulus of the wall (psi), and
I = moment of inertia of the wall (inch^4/ft).

The relative flexibility is used with Figure 4-36 to determine the ratio of the design moment to the theoretical moment. The moment is reduced for walls that penetrate into medium dense or better sand. The moment is not reduced for penetration into fine-grained soils or loose sands.

Three example scenarios showing the design steps for anchored bulkheads are shown in Figure 4-37. These examples are complex in that they have the following characteristics:

1) Two or more layers of soil,

2) Backfill loaded by point load (Q) and surcharge area (q), and

3) Different interior and exterior water levels. The difference in the water pressures is accommodated by a trapezoidal unbalanced water pressure distribution.

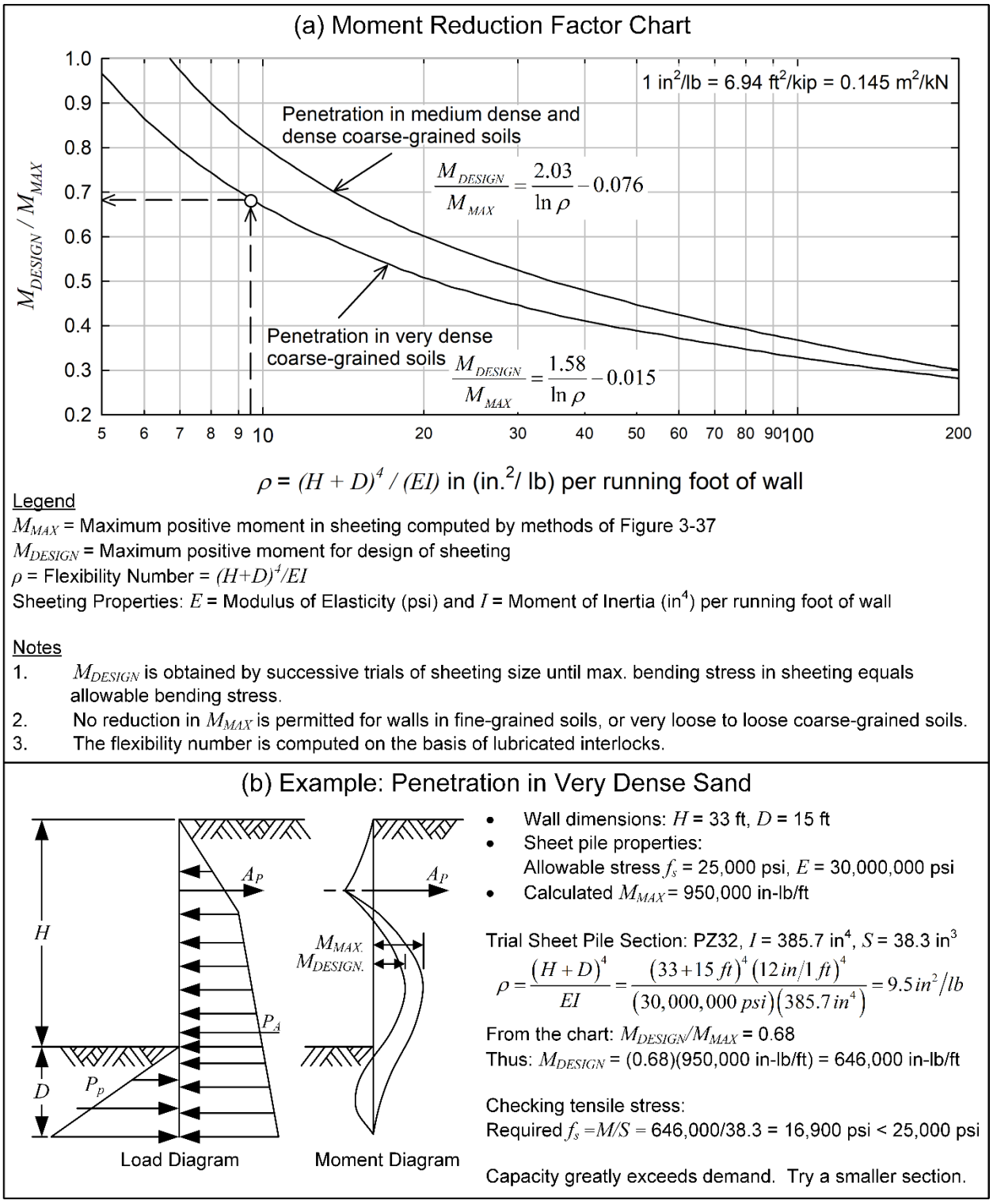

Figure 4-36 Rowe's Moment Reduction Factors for Flexible Walls

Scenario 1: Free Earth Support – General Case

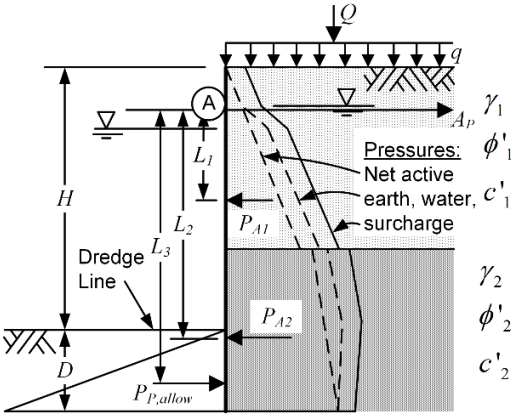

1. Compute pressures by methods of Figures 4-4 to 4-13. Passive pressures for clean coarse grained soils include wall friction (see Table 4-1). For active or passive pressures in all other soil types, ignore wall friction.
2. Determine depth of penetration required by taking moments about Point A and solving for D:

$$P_{A1} \cdot L_1 + P_{A2} \cdot L_2 = P_{P,allow} \cdot L_3$$

3. Calculate anchor pull (A_P) for anchor spacing (d)

$$A_P = \left[P_{A1} - P_{A2} + P_{P,allow} \right] \cdot d$$

4. Compute maximum bending moment (M_{MAX}) in sheeting by the free Earth support method, using P_{A1}, P_{A2}, $P_{P,allow}$, and A_P. for sheeting in sand. Apply moment reduction if appropriate (Figure 4-36).
5. Increase calculated penetration (D) by 20% to allow for dredging, scour, etc.

Note: L_1, L_2, and L_3 are the dimensions from Point A

Scenario 2: Penetration in Compact Coarse-Grained Stratum

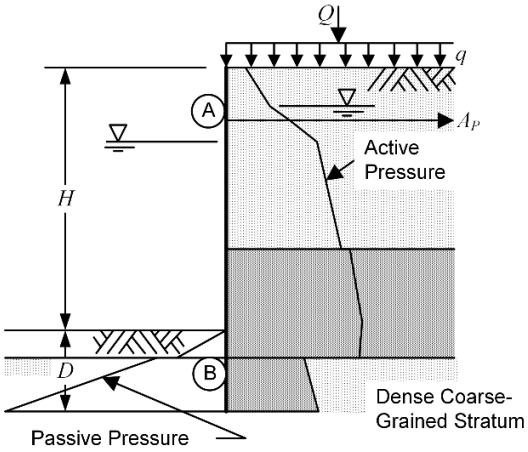

1-3. Use the same Design Steps 1, 2, and 3 as above for Free Earth Support method.

4. Compute maximum bending moment (M_{MAX}) in sheeting by Free Earth Support method, using P_A, $P_{P,allow}$, and A_P.
5. Compute ρ according to Figure 4-36.

   If $\rho \geq 20$, M_{DESIGN} is computed for the span Points A to B assuming simple support at Point B.

   If $\rho < 20$, use the moment reduction for flexibility from Figure 4-36.
6. Increase the calculated penetration (D) by 20% to allow for dredging, scour, etc.

Scenario 3: Penetration to Top of Hard Unyielding Stratum

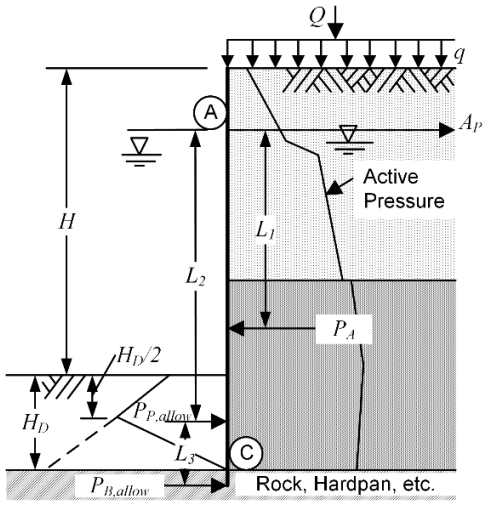

1. Compute pressures as above, except that passive pressure decreases to zero at top of hard stratum.
2. Determine required penetration into hard stratum by taking moments about Point A and solving for $P_{B,allow}$:

$$P_A \cdot L_1 - P_{P,allow} \cdot L_2 = P_{B,allow}(L_2 + L_3)$$

   and estimate if reaction $P_{B,allow}$ can be provided by shallow penetration in hard stratum.
3. Calculate anchor pull:

$$A_P = \left[P_A - P_{P,allow} - P_{B,allow} \right] \cdot d$$

4. Compute maximum bending moment (M_{MAX}) in sheeting, using P_A, $P_{P,allow}$, and A_P to span Points A to C assuming simple support at Point C with no reduction for flexibility.

Note: L_1, L_2, and L_3 are the dimensions from Point A, respectively.

Figure 4-37 Anchored Bulkhead Design Scenarios

Important design details illustrated in the the example scenarios are as follows:

1) The effects of interface friction between the wall and soil are only considered for passive pressure in granular soils. Wall friction is ignored in all other cases.

2) A factor of safety is applied to the passive pressure determination below the dredge line, and for passive pressures calculated for the anchor.

3) The calculated depth of penetration below the dredge line (D) is increased by 20% to allow for scour, additional dredging, etc.

4) The calculated bending moment in the sheet pile is reduced using Figure 4-36.

Scenario 1 is the general case for the free-earth method. The step-by-step method, indicated on Figure 4-37 would be appropriate for coarse-grained soils, with the material below the dredge line being similar to the soil retained by the wall. The soil properties used for the layers would be drained or effective stress parameters (c' and ϕ'). For the calculation of the earth pressures, moist or total unit weights are used above the landside water table elevation, and effective or buoyant unit weights are used below the water table. The net water pressure applied to the landside of the wall decreases from the dredge line elevation to a value of zero at depth, D, to account for seepage effects.

Scenario 2 is similar, but a different method is needed to determine the design moment in the sheet pile. For this example, the sheet pile is driven into a dense granular soil. If the wall system is less flexible as reflected by the value of ρ (Figure 4-36), the moment is calculated assuming that the wall behaves like a simply-supported beam.

Scenario 3 in Figure 4-37 shows a case where the sheet pile is socketed or toed into a very hard material (rock or hardpan). Since no displacement occurs at the tip of the sheet pile, the passive pressure decreases to zero at the surface of the hard foundation. The moment is not reduced using Rowe's diagram (Figure 4-36).

4-7.3 Anchor Design.

Various types of anchors can be used with anchored bulkheads. Examples of different anchor systems are given in Figure 4-38. The *deadman* anchor has been historically popular and its design incorporates earth pressure theory. Deadman anchors can be discrete individual elements, or they can be a continuous reinforced concrete wall parallel to the bulkhead. Anchors are normally constructed to a depth equal to twice the anchor height. The distance between the anchor and the wall is important. In order to maximize the capacity, the anchor needs to be located outside of the potential failure wedge. Figure 4-39(a) provides guidance on the location of a deadman anchor relative to the active wedge.

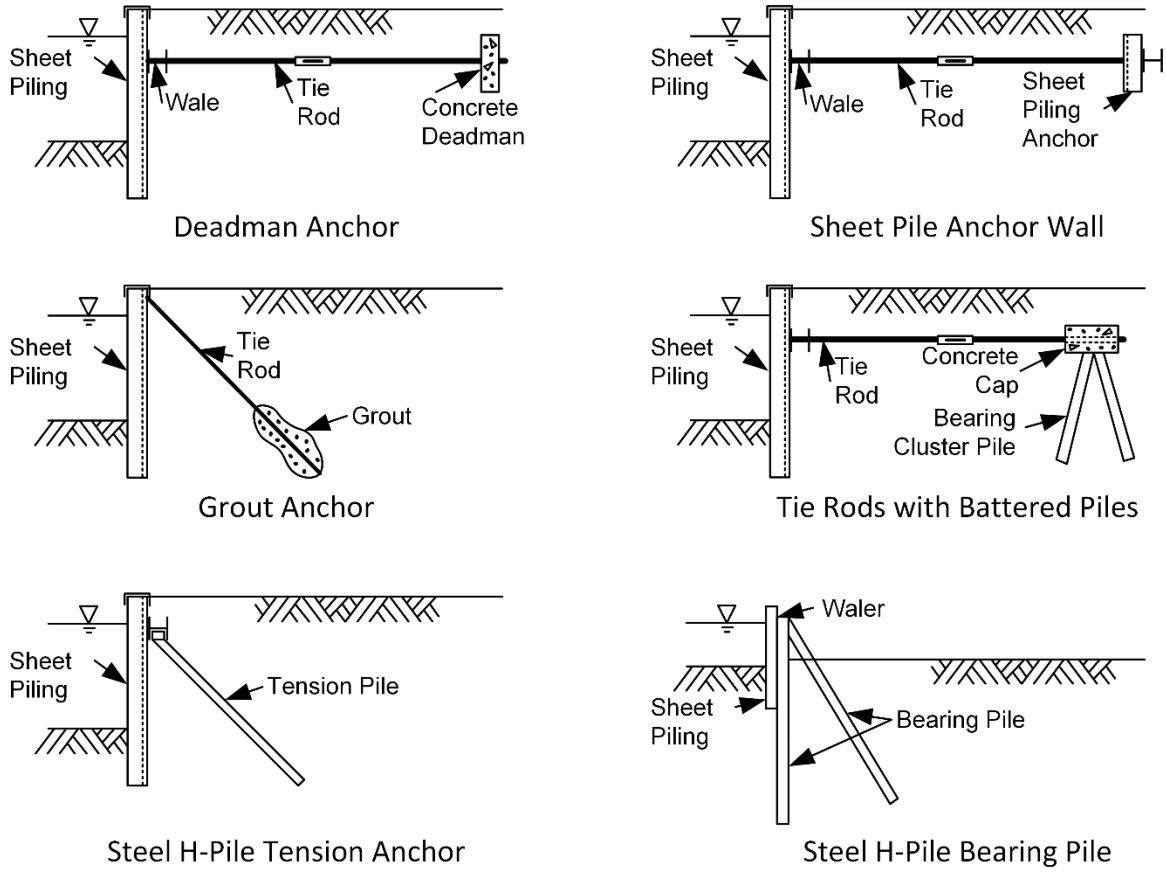

Figure 4-38 Types of Anchoring Systems for Bulkheads (after USACE EM 1110-2-2504)

The equations for calculating the capacity of a continuous wall anchor are shown in Figure 4-39(b). The interface friction angle between the anchor and soil is considered in the determination of the passive earth pressure coefficient. The calculated passive resistance of the anchor is dependent on where the anchor is located. A reduced anchor capacity results for anchors placed close to the active failure wedge. Figure 4-40 shows a section view of the wall anchor in Figure 4-39. The differences in the capacity of wall anchors versus individual anchor blocks are summarized.

The FHWA Geotechnical Engineering Circular No. 4 - *Ground Anchors and Anchored Systems* (FHWA 1999) provides design procedures for many different types of anchors.

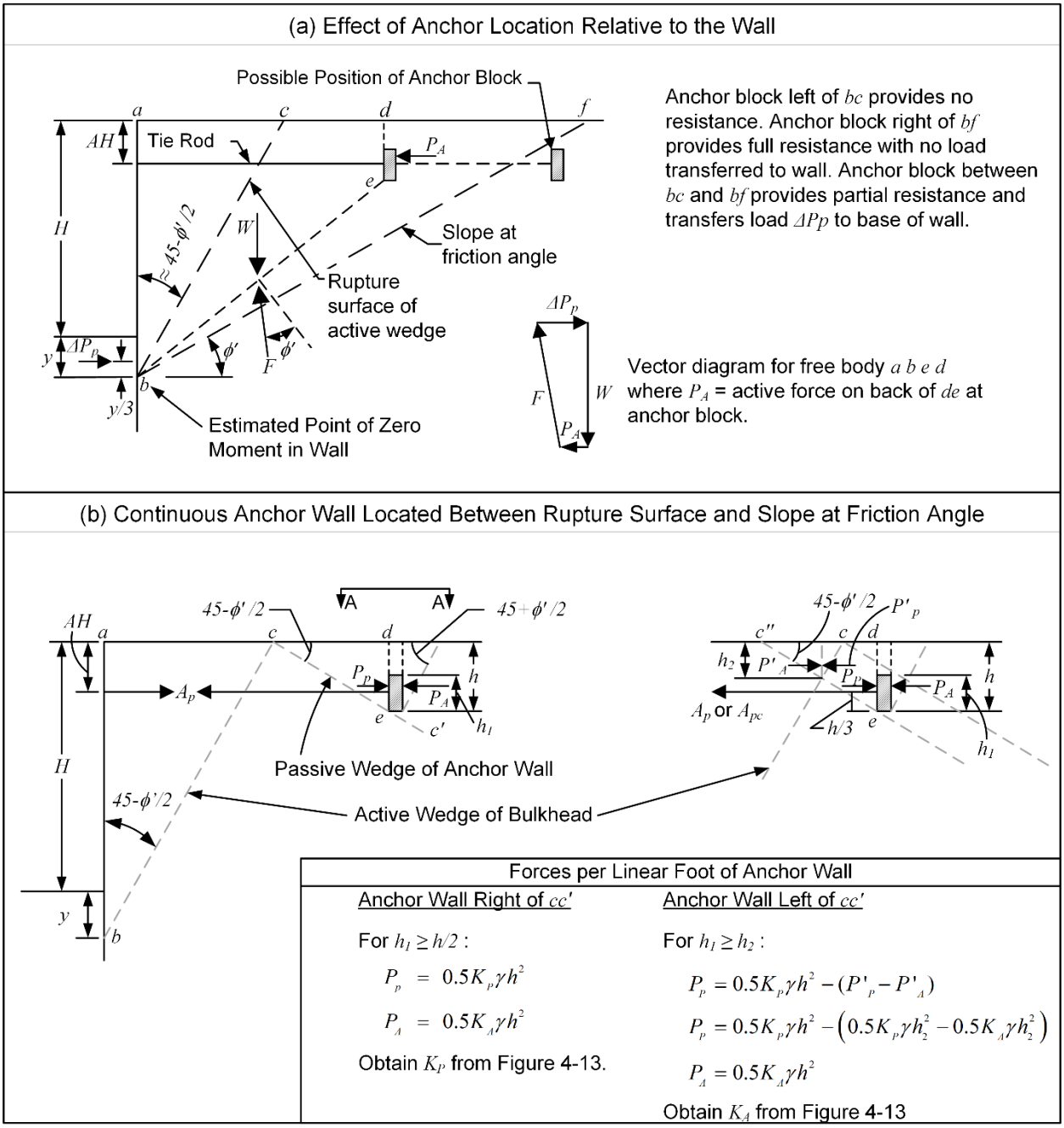

Figure 4-39 (a) Effect of Anchor Position Relative to Wall, and (b) Wall Anchor Capacity Equations

Effect of Depth and Spacing of Anchor Blocks

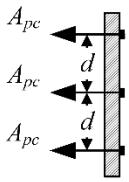

Section A-A
Continuous Wall

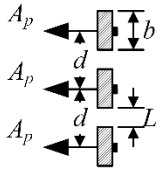

Section A-A
Individual Anchors

Anchor Resistance for $h_1 \geq h/2$

1. Continuous Wall: The ultimate resistance is $A_{pc} / d = P_p - P_A$, where A_{pc} / d is anchor resistance, and P_p and P_A are taken per linear foot of wall.
2. Individual Anchors:
   If $d > (b + h)$, the ultimate resistance is found using the resultant at-rest soil force (P_0) on vertical area cde or $c''de$ as $A_p = b(P_P - P_A) + 2P_0 \tan \phi'$.

   If $d = (h+b)$, the ultimate resistance (A_p/d) is 70% of A_{pc}/d for a continuous wall. L for this condition is L' and $L'=h$.

   If $d < (h+b)$, $L'=h$ and $A_p/d = A_{pc}/d - (L/L')(0.3\ A_{pc} / d)$.

Anchor Resistance for $h_1<h/2$

The ultimate A_p / d OR A_{pc} / d equals the bearing capacity of a strip footing of width, h_1, and surcharge load $\gamma(h - h_1 / 2)$. See Chapter 5. Use friction angle (ϕ^*) such that $\tan \phi^* = 0.6 \tan \phi'$.

(see Figure 4-39 for definition of dimensions and section)

General Requirements:

1. Divide the ultimate value of A_p or A_{pc} by 2 to determine the allowable value with a factor of safety of 2 against failure.
2. Values of K_A and K_P are for cohesionless materials. If backfill has both ϕ' and c' strength parameters, compute active and passive forces according to Figures 4-5 and 4-6 Fine-grained soils of medium to high plasticity should not be used to support the anchor.
3. Soils within passive wedge of anchorage shall be compacted to no less than 90% of maximum dry unit weight (ASTM D698).
4. Tie rod is designed for allowable A_p and A_{pc}. Tie rod connections to wall and anchorage are designed for 1.2 times the allowable A_p or A_{pc}.
5. Tie rod connection to anchorage is made at the location of the resultant earth pressures acting on the vertical face of the anchorage.

Figure 4-40 Effect of Depth and Spacing of Anchor Blocks

4-7.4 Cantilever Flexible Walls.

A *cantilever* flexible wall supports the soil without anchors or bracing. These walls are commonly constructed from sheet piling and can be used as earth retention structures for exposed wall heights less than about 15 feet. Stiffer types of flexible structure may be able to support higher walls. The pattern of deflection of the sheet pile results in complex earth pressures acting on the wall. Figure 4-41 shows the net pressure diagram for cantilever sheet piling. The designer should be aware of cases where there is a difference in the water level on each side of the wall. The figure shows a step-by-step approach to determine the depth of penetration (D) for design of a cantilever flexible wall for effective stress conditions.

Standard Penetration Resistance, N (blows/foot)	Approximate Depth of Penetration
0 - 4	2.0H
5 - 10	1.5H
11 - 30	1.25H
31 - 50	1.0H
+50	0.75H

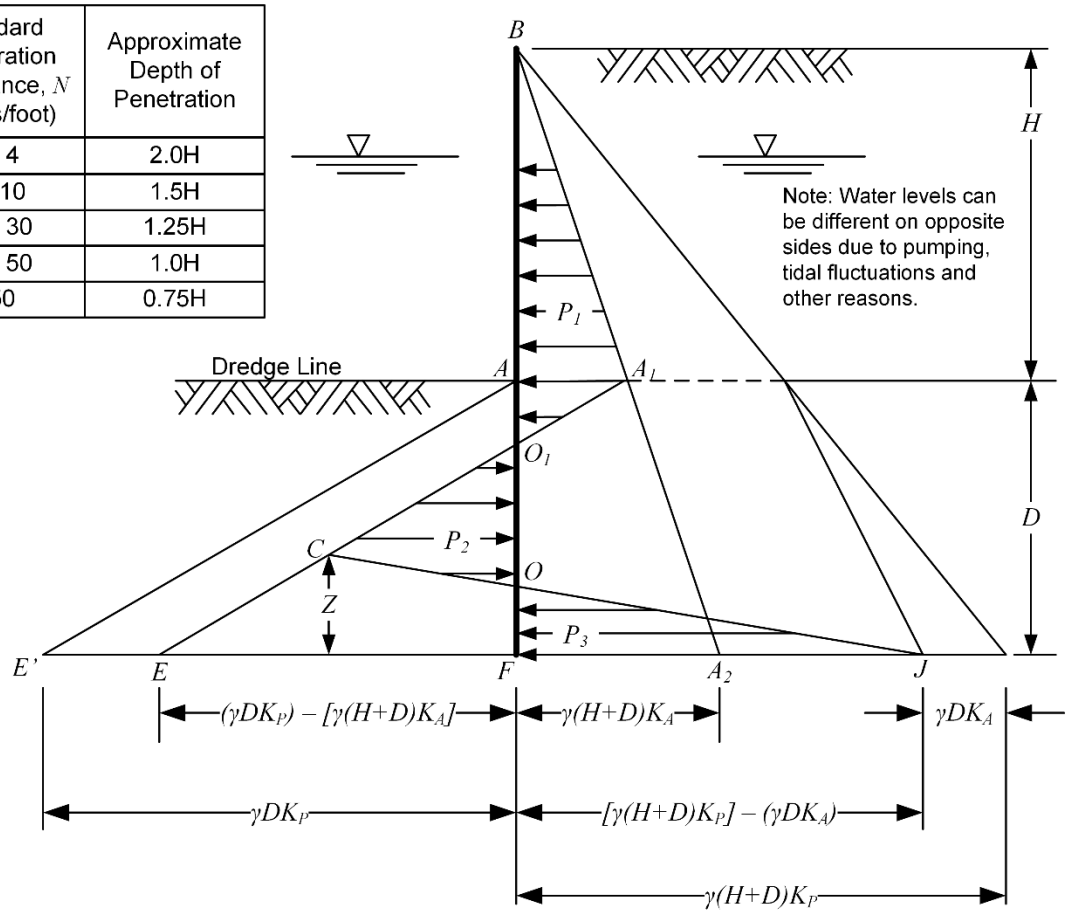

Calculation steps:

1. Assume a trial depth of penetration, D. The SPT penetration resistance can be used with the table above.
2. Determine the active and passive lateral pressure using appropriate coefficients of lateral earth pressure. The passive earth pressure coefficient should be based on ϕ'_{allow} as discussed in Section 4-7.1. Alternatively apply a factor of safety to the value of K_p.
3. Satisfy the requirements of static equilibrium. The sum of the forces in the horizontal direction must be zero, and the sum of the moments about any point must be zero. The sum of the horizontal forces may be written in terms of pressure areas:

$$\Delta\left(EA_1A_2\right) - \Delta\left(FBA_2\right) - \Delta\left(ECJ\right) = 0 \qquad \text{or} \qquad P_1 - P_2 + P_3 = 0$$

Solve the above equation to find distance, Z. For a uniform coarse-grained soil (either fully saturated or no water),

$$Z = \frac{K_P D^2 - K_A\left(H+D\right)^2}{\left(K_P - K_A\right)\left(H+2D\right)}$$

4. Take moments about Point F. If sum of moments is other than zero, adjust D and repeated calculations until sum of moments around Point F is zero.
5. Compute maximum moment at point of zero shear.
6. Increase D by 20% to allow for dredging, scour, etc.

Figure 4-41 Calculation Procedure for Cantilever Retaining Structures

Two charts are available to simplify the cantilever wall calculations for sites with simple stratigraphy. Figure 4-42 allows the penetration depth (D) to be determined for a site consisting of coarse-grained soil that can be characterized by a single value of effective stress friction angle. A phreatic surface can be accommodated assuming that the level is the same on both sides of the sheet pile. There are two families of curves on the chart, with one used for determining the maximum moment in the sheet pile and the other for determining the embedment depth. This chart was developed assuming that the total unit weight of the soil was 124.8 pcf, which is twice the buoyant unit weight. An example of the use of this chart for a cantilever sheet pile wall with a height of 15 ft in a coarse-grained soil is given in Figure 4-43.

The value of K_P used with Figure 4-42 should be factored as described in Section 4-7.1. In addition, the final value of D should be increased by about 20% to design against future dredging or scour.

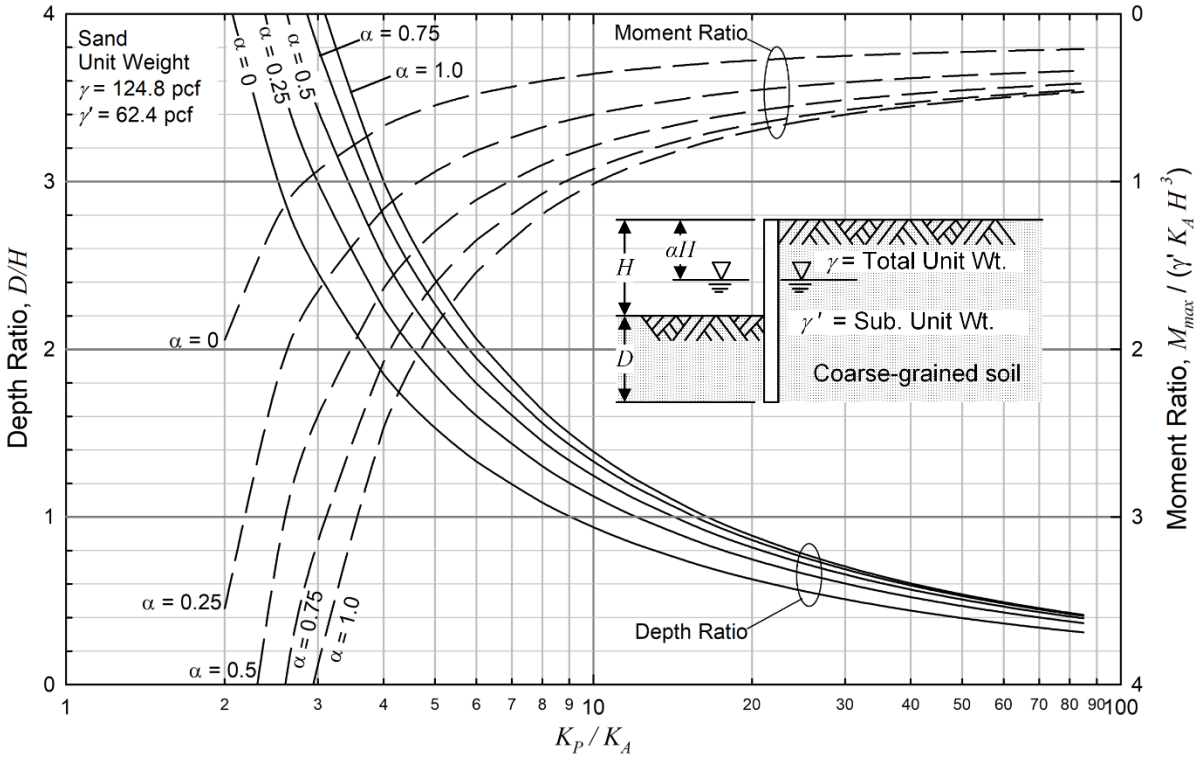

Figure 4-42 Chart for Determining Penetration Depth and Maximum Moment in a Cantilever Flexible Wall in Sand

The second chart (Figure 4-44) was developed for a sand layer overlying a saturated clay layer. The sand layer extends down to the dredge line. The sand layer is characterized by ϕ', and the clay layer is assigned a single undrained strength (s_u). The effective stress at dredge level in the sand layer should be calculated based on the position of the water table using the appropriate unit weights. An example using this chart is shown in Figure 4-45.

A wall designed using Figure 4-44 is supported by passive pressure associated with the undrained shear strength of the clay. The undrained shear strength can be factored as indicated in the figure. The strength is factored only on the passive side of the wall, which leads to the equation provided. This approach allows an explicit consideration of F. Alternatively, if the full undrained shear strength is used, the penetration depth must be increased by 30% to 40% to allow for a factor of safety. The magnitude of F is unknown with the latter approach.

The US Steel (USS) *Sheet Piling Design Manual* (USS 1984) contains more details about the design of cantilever sheet piles in coarse-grained and fine-grained soils and provides additional design examples.

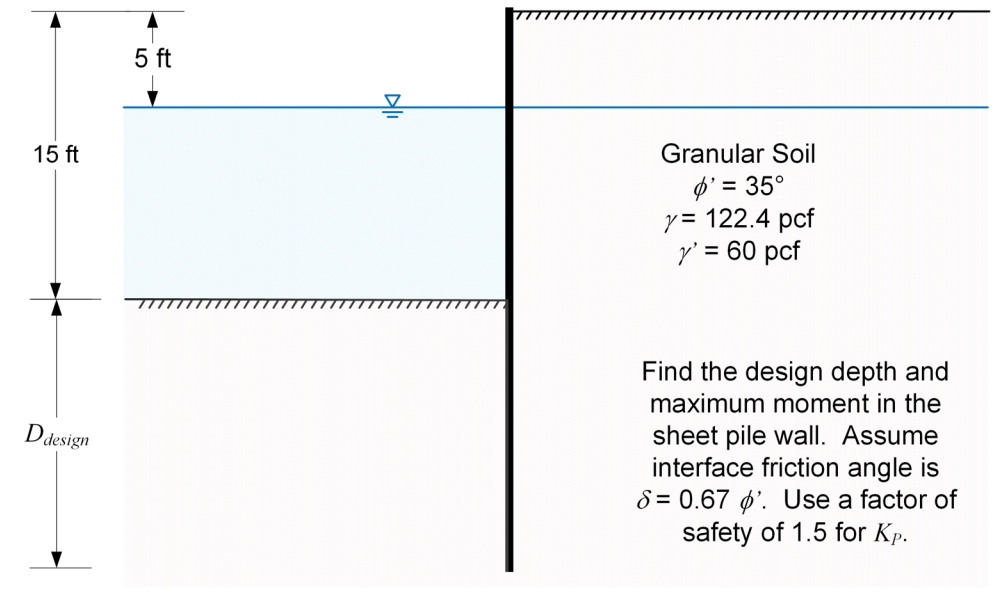

Earth pressure coefficients:

K_A = 0.25 for ϕ ' = 35 deg (from Figure 4-12)

ϕ'_{allow} = $\tan^{-1}$(tan(35 deg)/1.5) = 25 deg

K_P = 3.6 for ϕ'_{allow} = 25 deg (from Figure 4-12)

Inputs for Figure 4-42:

Relative water level: a = (5 ft) / (15 ft) = 0.33

K_P / K_A = 3.6 / 0.25 = 14.4

Depth ratio (from Figure 4-42): D / H = 0.95, D = 0.95 (15 ft) = 14.25 ft

Design depth: D_{design} = 1.2 (14.25 ft) = 17 ft

Moment ratio (from Figure 4-42): $M_{max} / (\gamma' K_A H^3)$ = 0.6

Maximum moment: M_{max} = 0.6 (62.4 pcf)(0.25)(15 ft)^3 = 31,590 ft-lb/ft of wall

Figure 4-43 Example for a Cantilever Wall in Sand

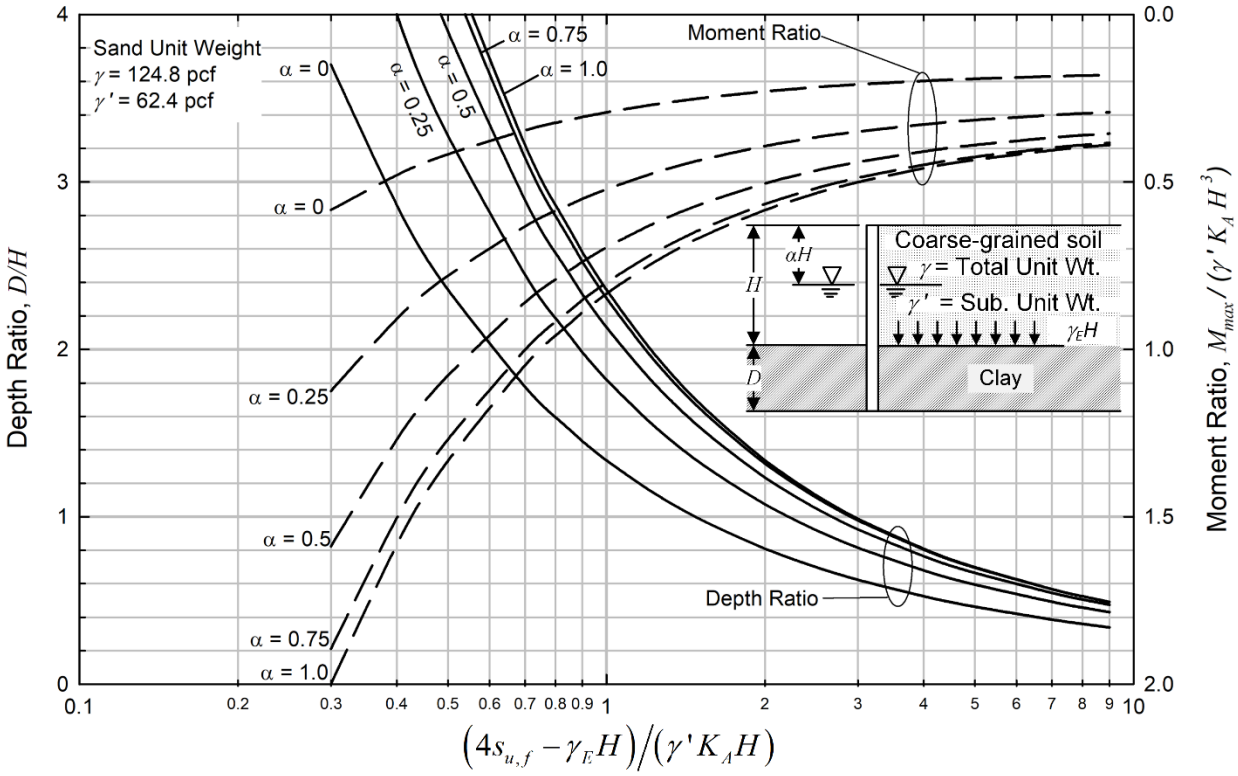

Factored undrained strength of clay ($s_{u,f}$):

$$s_{u,f} = s_u\left(\frac{F+1}{2F}\right)$$

where:

s_u = unfactored undrained strength

F = factor of safety

Vertical Effective Pressure at Top of Clay:

$$\gamma_E H = \alpha H\gamma + (1-\alpha)H\gamma'$$

$$\gamma_E H = \left[\alpha\gamma + (1-\alpha)\gamma'\right]H$$

Figure 4-44 Chart for Determining Penetration Depth and Maximum Moment in a Cantilever Flexible Wall in Sand Overlying Clay

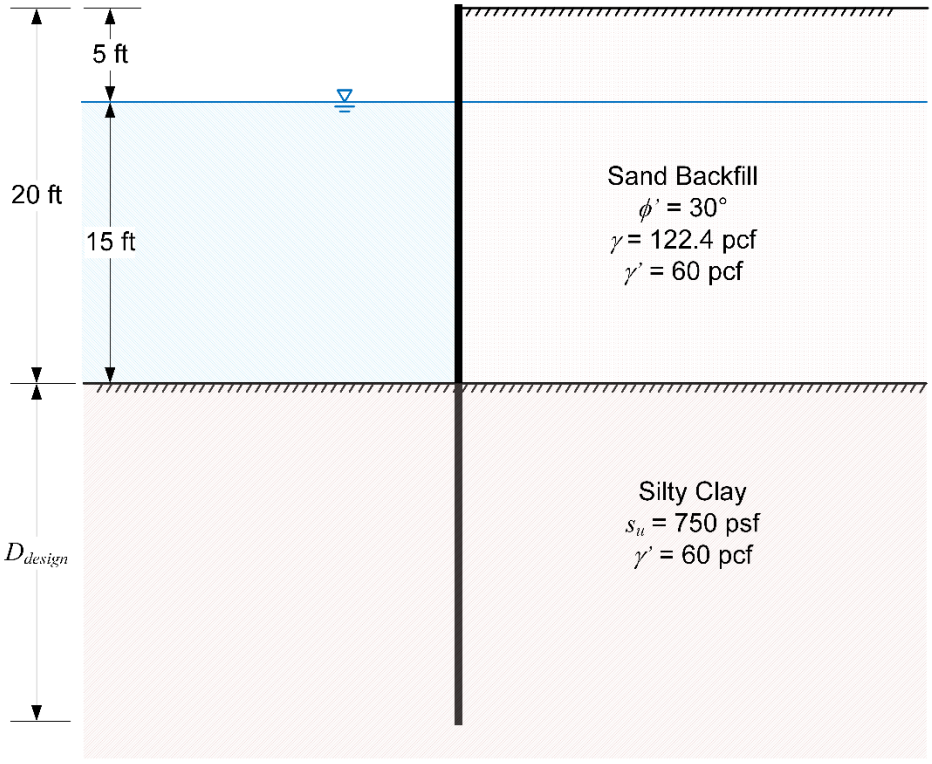

Earth pressure coefficients:

Backfill - K_A = 0.30 for ϕ ' = 30 deg (from Figure 4-12)

Vertical effective pressure at the dredge line:

$\gamma_E H$ = [(0.25)(122.4 pcf) + (1-0.25)(60 pcf)](20 ft) = 1512 psf

Factored undrained shear strength:

$s_{u,f}$ = (750 psf)[(1.5+1)/(2·1.5)] = 625 psf

Determine x-axis value for Figure 4-44:

$(4s_{u,f} - \gamma_E H) / (\gamma' K_A H)$ = [4(625 psf) - 1512 psf] / [(60 pcf)(0.30)(20 ft)] = 2.74

Depth ratio (Figure 4-44): D / H = 0.86; D = 0.86 (20 ft) = 17.2 ft

Design depth: D_{design} = 1.2 (17.2 ft) = 20.6 ft ≈ 21 ft

Moment ratio (Figure 4-44): $M_{max} / (\gamma' K_A H)$ = 0.36

Maximum moment: M_{max} = 0.36 (60 pcf)(0.30)(20 ft)^3 = 51,840 ft-lb/ft

Figure 4-45 Example for Cantilever Sheet Pile in Sand Underlain by Clay

4-7.5 Soldier Pile Walls.

Soldier pile and lagging walls consist of discrete vertical soldier piles (or beams) that support horizontal lagging as shown in Figure 4-46. The lagging transfers earth pressures from the soil to the soldier piles. In the typical construction sequence, the soldier piles are placed in shafts drilled prior to excavation for the wall. Concrete is used to secure the soldier pile in place below the dredge line. Above the dredge line, the shafts are often backfilled with low strength concrete or flowable fill. As excavation proceeds adjacent to the soldier piles, lagging is placed between the piles from the top down. Soldier pile and lagging walls may be supported internally or externally. A cantilever design can be used if strong soil or rock is present at the base of the wall and the soldier piles are sufficiently stiff.

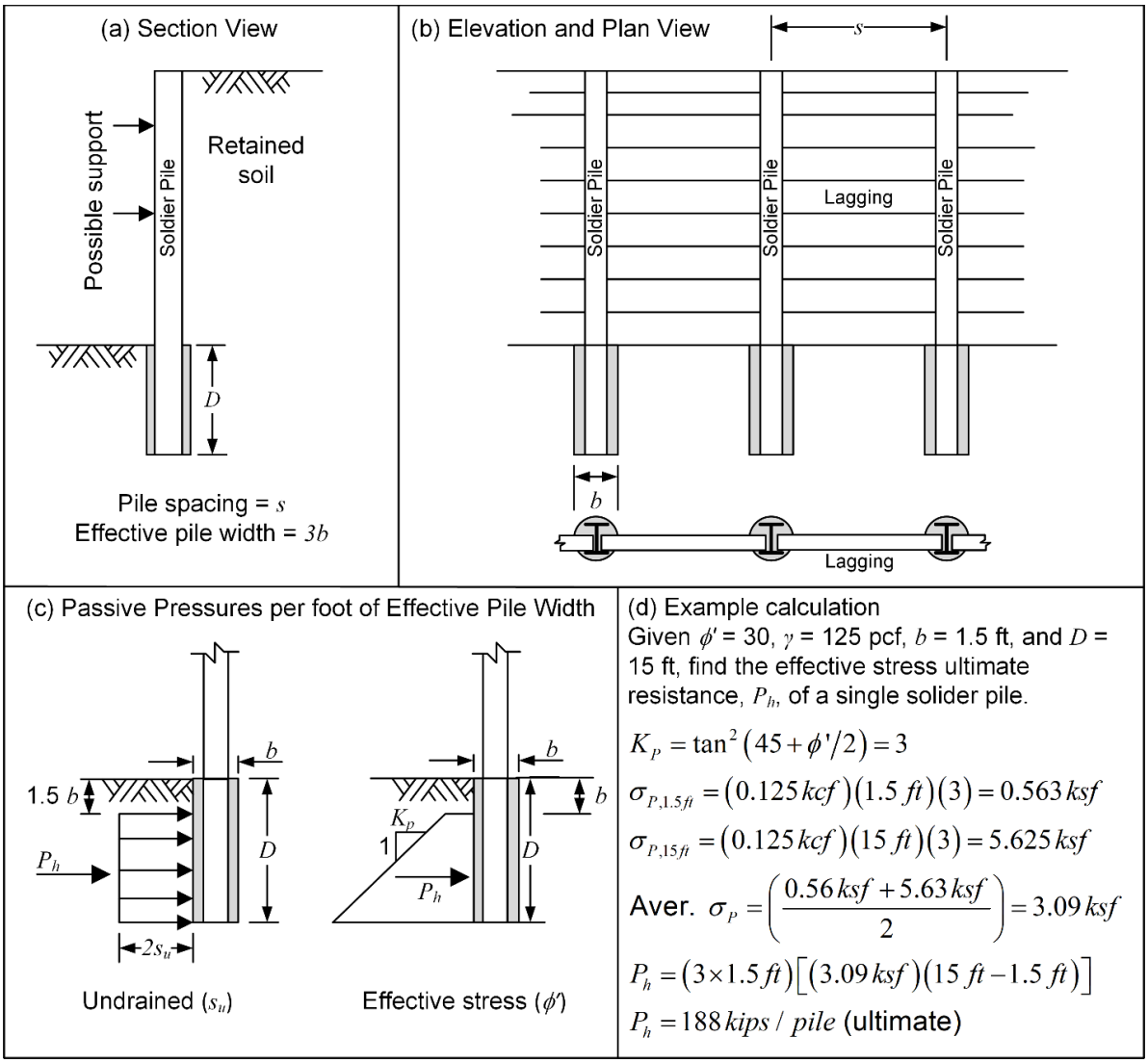

Figure 4-46 Soldier Pile and Lagging Walls – (a) Section View, (b) Elevation and Plan View, (c) Passive Pressure Assumptions, and (d) Example Calculation

The anchored and cantilever design methods can be used for soldier pile walls except that the passive resistance is developed by individual pile elements rather than a continuous wall. The passive earth resistance acting on individual soldier piles may be computed as shown in Figure 4-46. For fine-grained soils, a uniform resistance of $2 \cdot s_u$ can be used, neglecting the soil resistance to a depth of 1.5 times the shaft width, b, from the bottom of the excavation. For coarse-grained soils, the value of K_P should be determined without wall friction. The soil resistance should be ignored to a depth equal to b below the bottom of the excavation. Total resisting force accounts for arching between the piles and is computed by assuming the pile to have an effective width of $3b$ for all types of soils.

4-7.6 Secant Pile Walls and Tangent Pile Walls.

Secant and tangent pile walls are alternatives to sheet pile walls and soldier pile walls where greater lateral stiffness is required. As discussed in Section 2-4, the increased stiffness reduces vertical deformations at the ground surface adjacent to the wall. Neither secant nor tangent pile walls require the time-consuming lagging installation required for soldier pile walls.

Secant pile walls are constructed by installing primary and secondary concrete shafts that overlap (Figure 4-47). First, the primary shafts are drilled,[25] with the position of the shafts aligned by a template and the template controlling the distance between primary shafts. The concrete shafts are constructed without reinforcement. The secondary shafts are drilled between the primary piles such that they intersect the piles on both sides of the alignment. The secondary piles are reinforced with steel rebar cages or with steel beams (W sections). Secant pile walls have an additional benefit over sheet pile walls and soldier pile walls in that well-constructed secant pile walls provide a seepage barrier.

Tangent pile walls are constructed such that there is no overlap between piles (Figure 4-48). Ideally, the shafts are drilled such that they are tangent to the adjacent piles, but there is often a space between shafts. The shafts are reinforced with steel beams (I or W sections) or rebar cages. Tangent pile walls do not have the same seepage resistance as secant pile walls, since gaps are often present between piles. Also, clean sands may ravel or run between the piles in tangent pile walls.

Secant and tangent pile walls are often tied-back, especially when deformations outside of the excavation must be controlled or if the excavations are deep. Since controlling deformations is a key factor in the selection of secant and tangent pile walls, analysis procedures often are based on calculating deformations as opposed to determining

[25] In common geotechnical engineering nomenclature, piles are “driven” and shafts are “drilled.” However, the concrete shafts in tangent and secant pile walls are most often called “piles.”

stress limit states. Methods for estimating horizontal and vertical displacements behind these walls are provided in Section 2-4.4. Numerical methods that allow the use of constitutive models for soils, as well as interface elements to model soil-structure interaction, are frequently used in practice for the design of these types of walls.

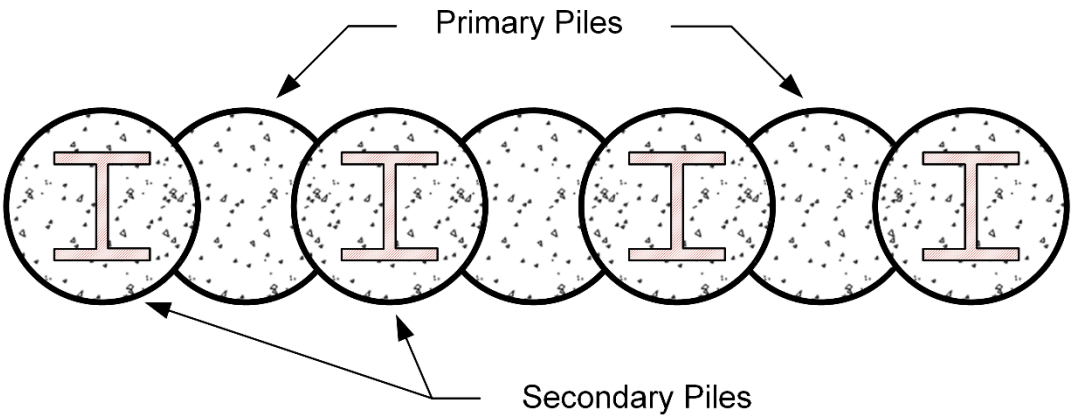

Figure 4-47 Plan View of Secant Pile Wall

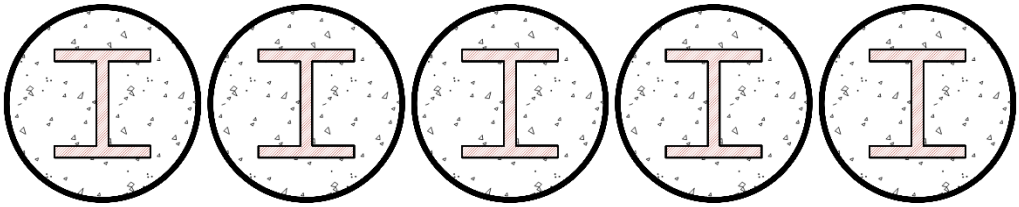

Figure 4-48 Plan View of Tangent Pile Wall

4-7.7 Soil Nail Walls.

Soil nailing is a method to create a reinforced soil mass for the purpose of long-term support of permanent excavations. Detailed design, construction, and inspection procedures for soil nail walls can be found in *Geotechnical Engineering Circular No. 7* (FHWA 2015).

Soil nail walls can be a cost-effective wall system for sites with limited right-of-way or overhead restrictions. The equipment used for constructing these types of walls is commonly available and limited in size, so these walls can be constructed at remote sites. This type of wall system also accommodates curves in the wall alignment better than other wall types.

A *soil nail* is commonly a steel reinforcing bar or steel tendon placed in a grout-filled hole. The reinforcing element acts passively, in that it is not post-tensioned. A soil-nail wall is constructed using a *top down* method where soil nails and shotcrete are installed

as the excavation progresses. The nails are placed on a vertical spacing of 3 to 5 feet and a horizontal spacing of 4 to 6 feet. The soil nails are often oriented at 15 degrees below horizontal. Strip drains are typically installed at regular spacing between the nails to prevent water from collecting behind the facing. After the full depth of excavation is achieved, a final shotcrete or concrete facing is installed. A cross section of a soil nail wall is shown in Figure 4-49. The length of the soil nails is often around 70% of the height of the wall, but specific design cases may require longer or shorter nails.

Soil nail walls are best suited for soil deposits which can sustain vertical cuts of 4 to 6 feet for up to 48 hours to allow for the installation of the nails. In addition, it is desired that the drill holes remain open during the tendon installation and grouting. Soil deposits that have proven appropriate for soil nail wall construction include dense granular soils, weathered rock, stiff fine-grained soils, stiff residual soils, and some glacial tills. Adverse soil conditions include dry, uniform, granular soils, pervious soils with high phreatic surfaces, soils with cobbles and boulders, and soft organic and inorganic fine-grained soil.

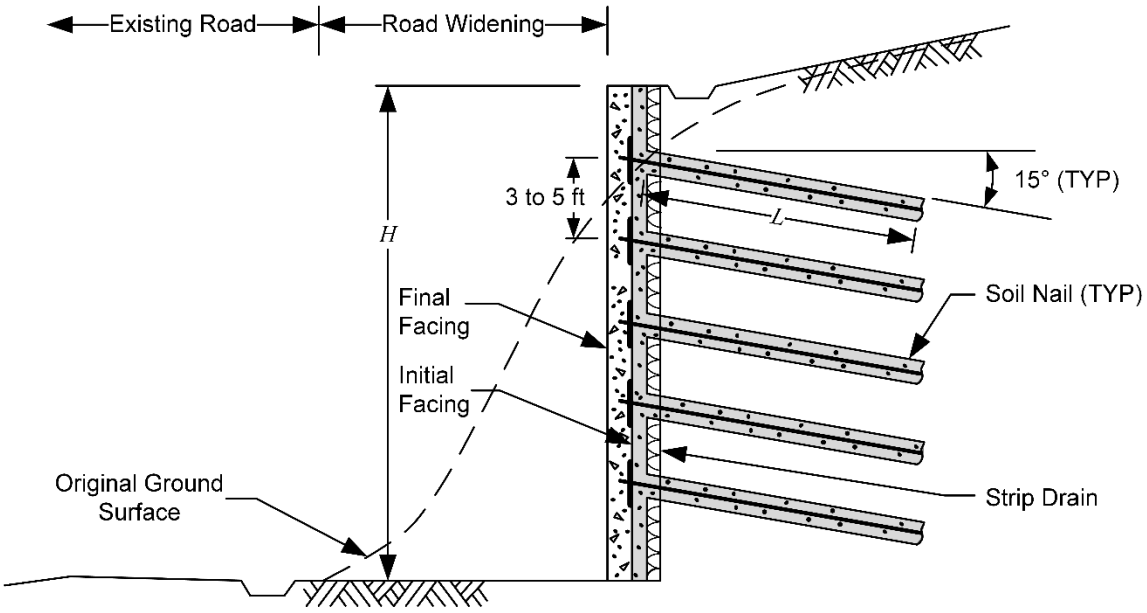

Figure 4-49 Cross Section of a Typical Soil Nail Wall (after FHWA 2015)

Soil nail walls are designed for long-term support; therefore, drained shear strength parameters are normally required for design.[26] For walls constructed to support stiff, overconsolidated soils, fully softened strengths obtained from triaxial or direct shear

[26] For walls constructed in weaker saturated fine-grained soils, it may be prudent to determine undrained strengths to assess if the unsupported slope is stable during excavation for the depth of the excavation stage. Undrained strengths might also be necessary for basal heave calculations (Section 2-4.3.3).

tests would be more appropriate than peak shear strengths. Since soil nail walls are often constructed to support granular soils, the results of *in situ* tests, such as the SPT or CPT, are often used to estimate the drained friction angle.

The design of soil nail walls is quite complex, and computer programs are normally used in practice. There are many potential failure modes, and a summary of these is shown in Figure 4-50. Earth pressures, in a classic sense, are not calculated per se, but stability is assessed based on limit equilibrium procedures, similar to that used in slope stability analyses.[27] Both internal and external stability are assessed. For internal stability assessment, a variety of slip surfaces are examined as the depth of the excavation proceeds. Failure surfaces are analyzed for slip surfaces intersecting the soil nails and for slip surfaces extending past the stabilized zone. Computer programs developed specifically for soil nail walls are available for these types of analyses. External stability is assessed assuming that the failure mass includes the entire area of reinforcement, and conventional slope stability computer software can be used.

Compared to conventional retaining wall analysis, there are many additional parameters necessary to assess the stability of a soil nail wall. These include nail pullout resistance and tendon tensile strength, along with many factors associated with the wall facing failure modes. Detailed examples for the design and analysis of soil nail walls, along with recommended factors of safety, are given in FHWA (2015).

4-8 EXCAVATION SUPPORT.

Flexible retaining structures are an important part of excavation design, which has been discussed in detail in Chapter 2. In many cases, the retaining walls for excavations must supported, either internally or externally. Determining the forces that act on the support system elements is an important part of the excavation design. The interaction between the wall, soil, and support system makes the forces quite complex. The forces depend on the rate of construction, the distance between supports, the installation quality, etc. The earth pressure distributions were based largely on case history measurements from instrumented excavations and are presented in the following section. These pressure distributions are then used to determine the forces that must be resisted by internal or external support.

[27] If basal sliding is deemed a possible failure mechanism, then active earth pressures determined using the Coulomb method can be used along with the conventional analysis of sliding stability of retaining walls (Section 4-5.1.3).

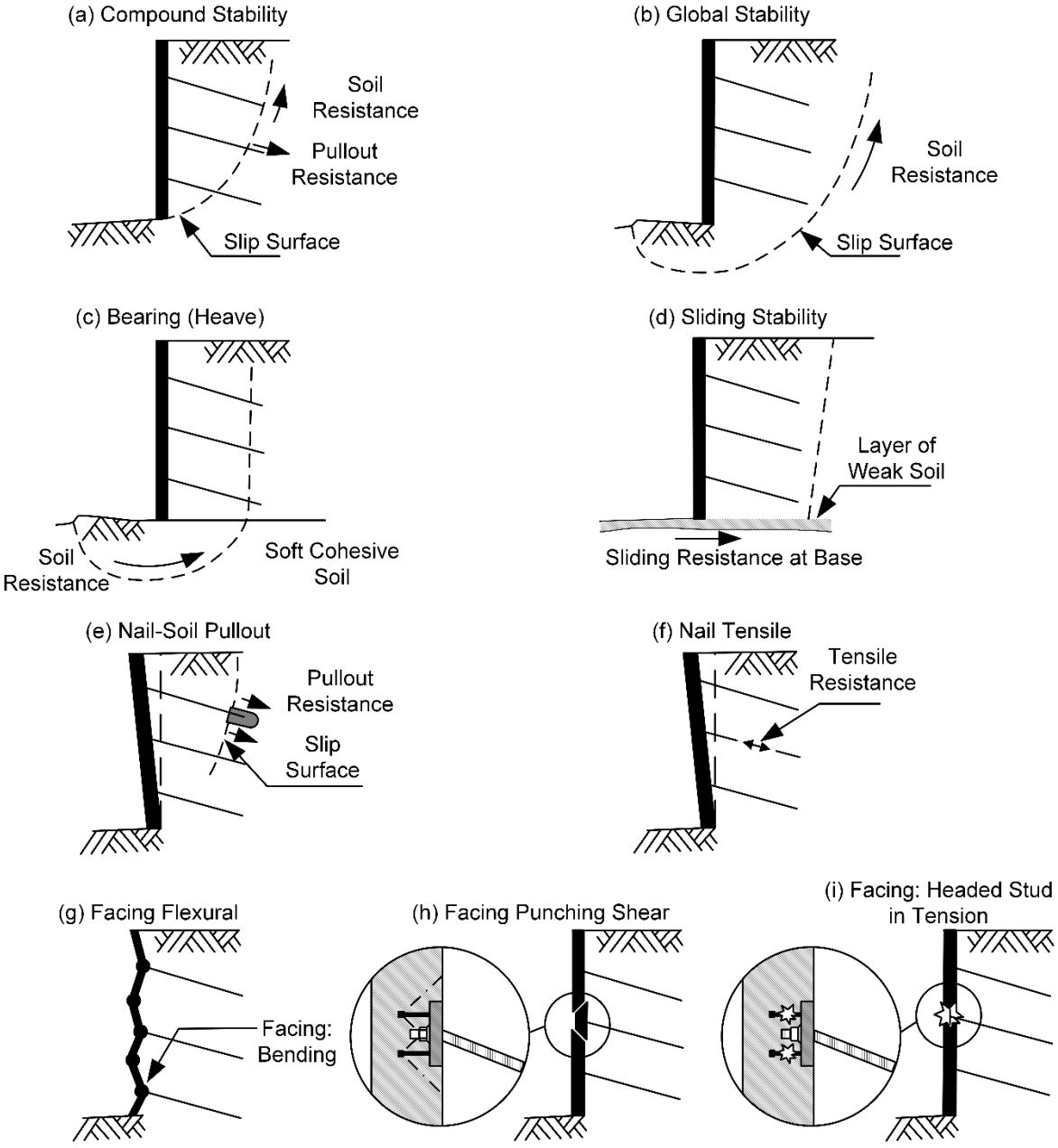

Figure 4-50 Potential Failure Modes of Soil Nail Walls (after FHWA 2015)

4-8.1 Apparent Earth Pressure Diagrams.

Earth pressures for supported flexible retaining structures have been semi-empirically determined based on measured support loads on engineering projects. The pressure diagrams were drawn to encompass the measured earth pressures, and actual pressures are likely lower than those shown. They are referred to as *apparent earth pressure* diagrams because of this semi-empirical basis. However, the diagrams have a basis in earth pressure theory in that the peak pressures are calculated with values of

the active earth pressure coefficient, K_A. The shape of the diagrams depends on the vertical location of support force application (struts or anchors). Apparent pressure diagrams are used for the design of internally- and externally-supported excavations, which will be discussed later in this section.

The apparent earth pressure diagrams are provided in Figure 4-51 through Figure 4-53. The magnitude and shape of the diagrams depend on the soil type. One set of apparent earth pressure diagrams has been historically used for internally braced support systems (Terzaghi and Peck 1967). A different set of pressure diagrams was developed for externally supported systems (FHWA 1999). These diagrams were developed because of differences in when the supports are installed, the amount of displacement that can occur prior to support installation, and the magnitude of the preload applied to the support elements. It is up to the judgement of the design engineer to decide if the FHWA (1999) apparent earth pressure diagrams should be used for both internally- and externally-braced support structures, particularly when the struts are preloaded for excavation bracing.

The horizontal strut force, represented as T on the apparent earth pressure diagrams, is determined by using the earth pressure distribution in one of two different ways: (1) tributary area and (2) hinge method. For the tributary area method, the load on each strut is calculated using the assumption that a strut carries the pressures existing from one-half the vertical distance to the strut above to one-half the vertical distance to the strut below. The hinge method is based on summing moments about strut locations (e.g., “hinges” where moment = 0) to calculate specific strut loads.

In general, the apparent pressure diagrams were developed for fairly deep (> 20 ft) excavations that are relatively wide.

4-8.2 Stability of Base of Excavations.

The stability of the base of excavations is very important in that it is a potential failure mechanism for cuts. In addition, the base stability can also influence the earth pressure applied to the wall. Section 2-4.3 provides information regarding the basal stability of excavations.

4-8.3 Internal Support (Excavation Bracing).

Internal support or excavation bracing refers to support systems that are inside of the excavation, such as cross-lot braces or rakers (Figure 2-6). Once the support loads are predicted, the design of internal support is primarily a structural engineering task.

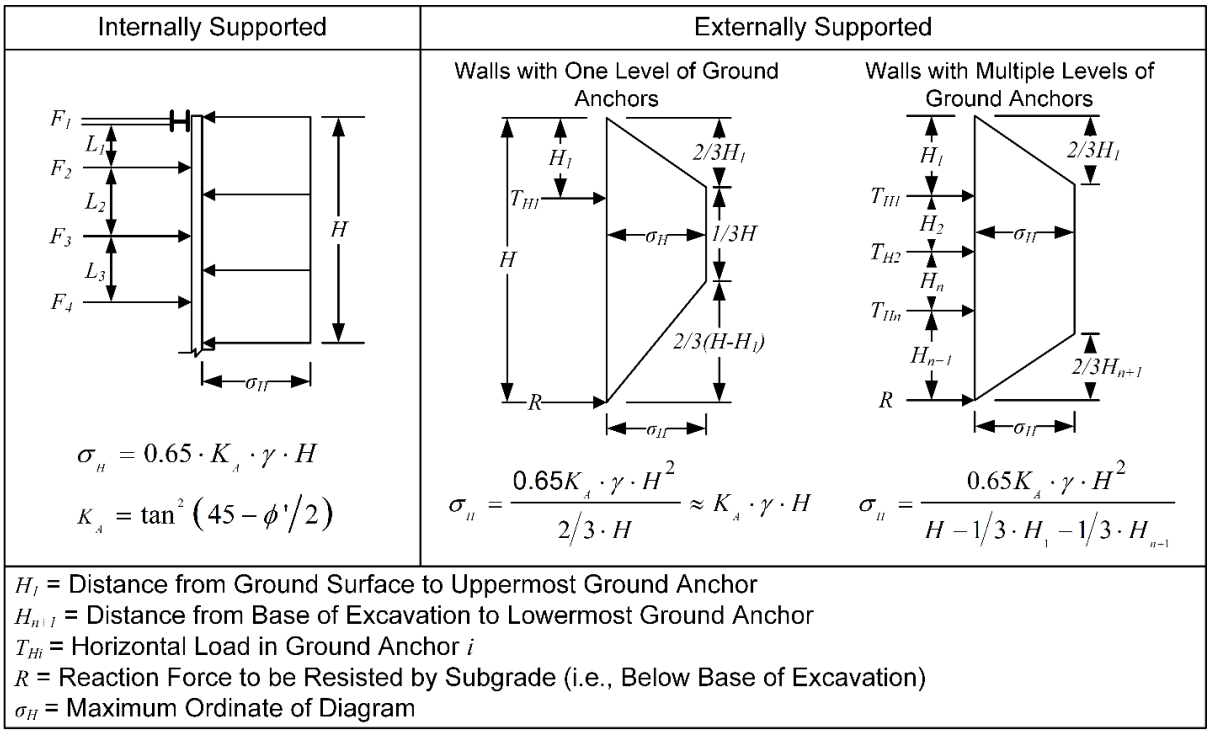

Figure 4-51 Apparent Pressure Diagrams for Sands for Internally and Externally Supported Retaining Structures (Wolosick and Scott 2012; FHWA 1999).

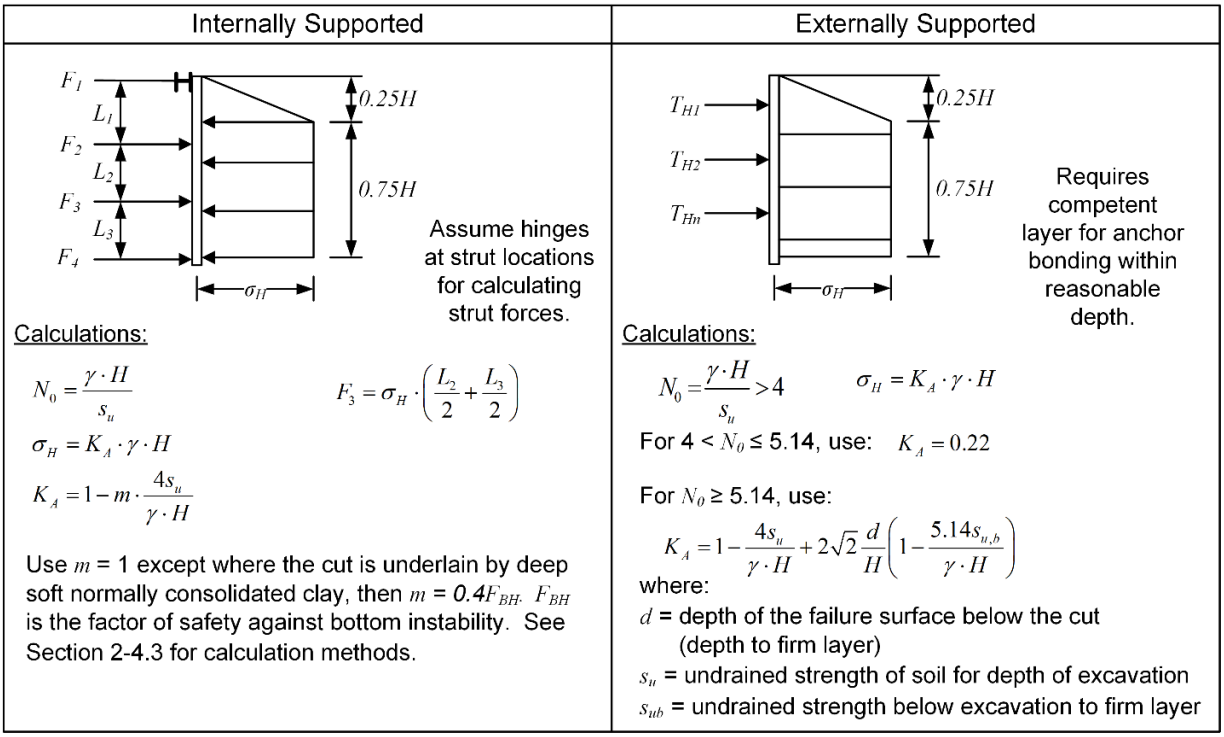

Figure 4-52 Apparent Pressure Diagrams for Soft to Medium Clay for Internally- and Externally-Supported Structures (Wolosick and Scott 2012; FHWA 1999)

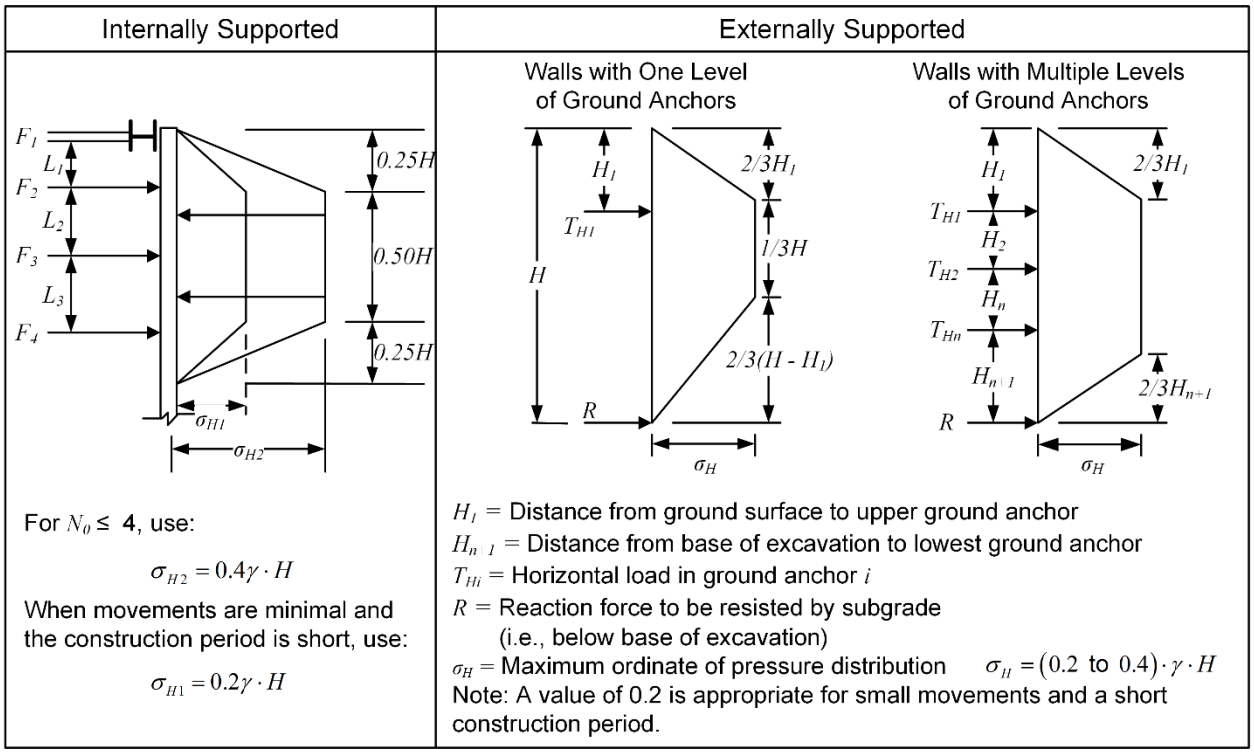

Figure 4-53 Apparent Pressure Diagrams for Stiff Clay for Internally and Externally Supported Structures (Wolosick and Scott 2012; FWHA 1999).

4-8.3.1 Internally-Braced Narrow Excavations.

Special design procedures are applied for narrow braced excavations. The design steps for a narrow cut supported by a flexible wall are shown in Figure 4-54. The appropriate apparent earth pressure diagrams are used to determine the pressure distribution above the excavation depth. The unbalanced water pressures need to be considered if the retained water table is above the base of the excavation. An example for this type of design is presented in Figure 4-55.

The basic procedure for the design of walls for narrow cuts is as follows:

1) Calculate the factor of safety for base stability using the procedures shown in Section 2-4.3.

2) Compute the strut forces as outlined in Figure 4-54.

3) Compute the required section for the wall and wale. In computing the required wall section, arching could be accounted for by reducing the pressures in all but the upper span. A reduction of 80% of the values shown is appropriate.

4) Recompute the strut forces and the required sections of the wall and wales using active earth pressures at each stage instead of the active earth pressure diagrams (similar to Figure 4-56).

5) Compare the strut forces and required sections computed in Step 4 to Step 3, and select the larger force or section for design.

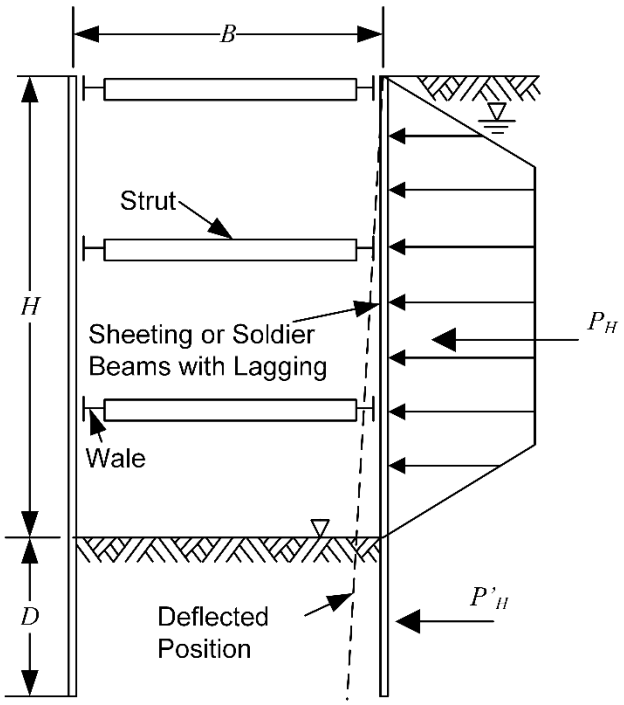

Soil Properties
γ, ϕ', or s_u

Use apparent earth pressure diagrams to determine P_H and strut forces.

Force on buried length, P'_H:

If $D > (\sqrt{2} \cdot B)/3$:

$$P'_H = 0.7\left(\gamma_T \cdot H \cdot B - 1.4 \cdot s_u \cdot H - \pi \cdot s_u \cdot B\right)$$

If $D < (\sqrt{2} \cdot B)/3$,

$$P'_H = 1.5D\left(\gamma_T \cdot H - 1.4 \cdot s_u \cdot \left(H/B\right) - \pi \cdot s_u\right)$$

Design Steps for a Narrow Cut

1. Compute pressures on wall above base of cut by methods of Figures 4-51 to 4-53. For saturated backfill, use $\gamma = \gamma'$ and add pressures for unbalanced water level. For water at base of cut, use total unit weight. Interpolate between these pressure diagrams for an intermediate water level.
2. Determine stability of base of cut by methods of Section 2-4.3.3. If the base is stable, the sheeting should penetrate several feet, and no force acts on the buried length. If the base is unstable (primarily a concern in clays), an unbalanced force, P'_H, acts on the buried length. In any case, penetration may be controlled by requirement for cut-off of underseepage.
3. Moments in sheeting braces are 80% of the simple span moments, except for the upper span where the moment equals the simple span moment. Moments in sheeting at the lowest strut are computed for the cantilever span below the lowest strut, including the unbalanced force P'_H.
4. Reactions at the braces are computed assuming simple span between braces.

Figure 4-54 Design Steps for Internally-Supported, Flexible Walls Used for a Narrow Excavation

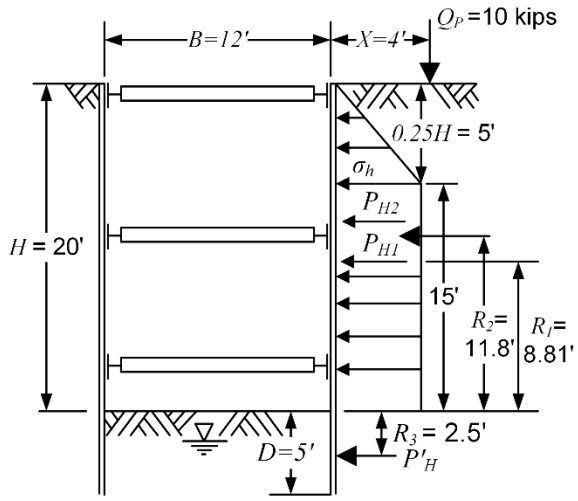

Given Conditions

Excavation in silty clay with deep underlying normally consolidated clay:

$s_u = 400\,\text{psf},\ \phi = 0^\circ,\ \gamma = 120\,\text{pcf}$

Length of Excavation:

$L = 80'$

Determine:

- Stability of Base of Cut,
- Pressures on Wall, and
- Force on Buried Length of Sheeting.

Stability of Base of Cut (See Section 2-4.3.3)

- No uniform surcharge, q = 0
- $B_1 = 0.7\,B$ = 8.4 ft
- F_{SB} < 1.5 so drive sheeting below base of the excavation

$$F_{SB} = \frac{5.7(400\ psf)(8.4\ ft)+(400\ psf)(20\ ft)}{(120\ pcf)(20\ ft)(8.4\ ft)} = 1.35$$

Pressure on Wall from Surrounding Soil

- Use Soft to Medium Clay because N_0 = 6 (Figure 3-52)

$$N_0 = \frac{\gamma H}{s_u} = \frac{(120\ pcf)(20\ ft)}{400\ psf} = 6$$

- Determine m Coefficient

$$m = 0.4F_{SB} = 0.4(1.35) = 0.54$$

- Determine K_A

$$K_A = 1 - m\frac{4s_u}{\gamma H} = 1-(0.54)\left(\frac{4(400\ psf)}{(120\ pcf)(20\ ft)}\right) = 0.64$$

- Calculate Maximum Horizontal Stress

$$\sigma_h = K_A\gamma H = 0.64(0.12\ kcf)(20\ ft) = 1.54\ ksf$$

- Resultant Force, P_{H1}

$$P_{H1} = (15\ ft + 20\ ft)(1.54\ ksf)/2 = 27\ k/ft$$

- Resultant Location, R_1

$$R_1 = \left[(1.54)\left((5/2)(15+5/3)+(15)(15/2)\right)\right]/27 = 8.8\ ft$$

Pressure on Wall from Surcharge Force (See Figure 4-18)

- Relative Distance of Q_P from Wall

$$m = 4\ ft / 20\ ft = 0.2$$

- Resultant Force, P_{H2}

$$P_{H2} = 0.80\,Q_P / H = 0.80(10\ kips/20\ ft) = 0.4\ kips$$

- Resultant Location, R_2

$$R_2 = 0.59H = 0.59(20\ ft) = 11.8\ ft$$

Force on Buried Length of Sheeting (See Figure 4-54)

- Buried Length: $D < \frac{\sqrt{2}}{3}B$

$$P'_H = 1.5D(\gamma_t H - (1.4s_u H)/B - \pi s_u)$$

$$P'_H = 1.5(5)((0.12)(20)-(1.4\cdot 0.4\cdot 20)/12 - \pi\cdot 0.4)$$

- Calculate Resultant Force, P'_H

$$P'_H = 1.6\ kips$$

Note: All computations are per linear foot of wall.

Figure 4-55 Example of Excavation Bracing Analysis Procedure for a Narrow Cut in Fine-Grained Soil

4-8.3.2 Internally-Braced Excavations with Raking Braces.

When a wall is supported by raking braces, considerable displacement of the wall may occur prior to the installation of support elements. Figure 4-56 shows the earth pressure distribution on a flexible wall where wall displacements created an active earth pressure condition. This arrangement would be for temporary support. The unbalanced water load needs to be considered in this cross section.

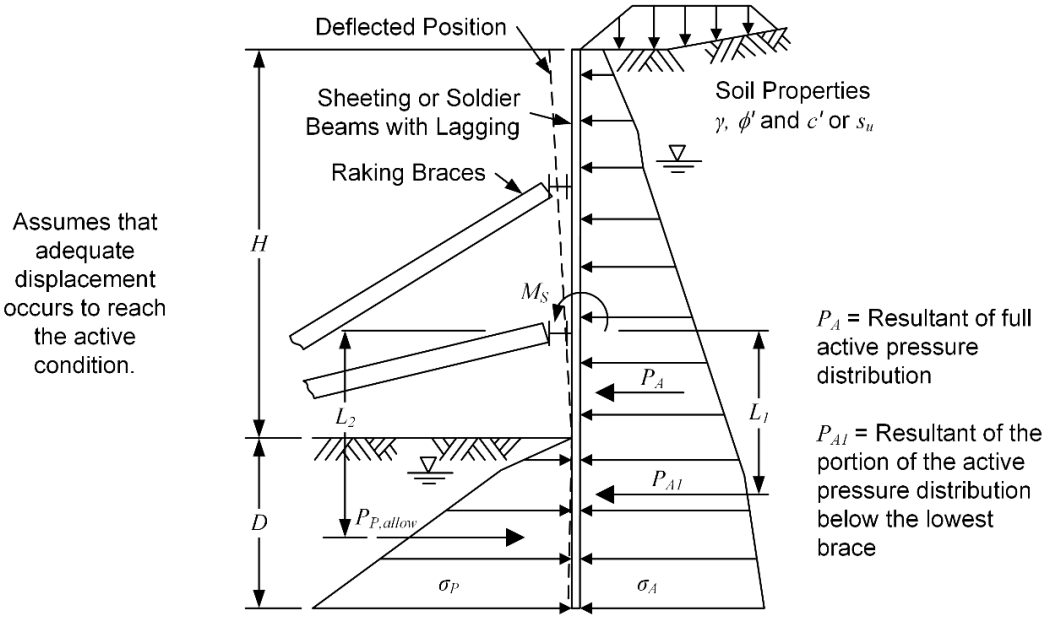

Design Steps for Flexible Wall with Raking Braces

1. Compute active and passive pressures by methods in Sections 4-2 to 4-3. Passive pressures for clean, coarse-grained soils may include wall friction (for values of δ, see Table 4-1). Wall friction should be ignored for passive pressures in other soil types and for active pressures in all soils.
2. Maximum movements in sheeting and maximum loads in braces are usually obtained at the construction stage, when excavation for a brace and wale is complete and just prior to placing the brace. For each successive stage of excavation, compute sheeting moments and braces loads by assuming a simple span between the lowest brace in place and the point of zero net pressure below the excavation.
3. For temporary construction conditions, apply a factor of safety of 1.5 to compute passive pressures. To allow for possible construction surcharge and rigidity of the upper brace point, increase the load on the upper wale and brace by 15% of computed value.
4. Required penetration of sheeting below final subgrade elevation generally is controlled by conditions at completion of excavation. Penetration required is determined by equilibrium of the free ended span below the lowest brace. Assuming fixity at the lowest brace, the allowable moment in the sheeting (M_s) can be calculated as:

$$M_S = P_{A1} \cdot L_1 - P_{P,allow} \cdot L_2$$

5. Check positive moments in the span below the lowest brace for the final loading condition.

Figure 4-56 Design Steps for Flexible Wall Supported by Raking Braces (Rakers)

4-8.4 External Support (Tied Back Walls).

Tied back walls use external support, such as ground anchors, to provide stability and offer distinct advantages compared to internally-braced support systems. For excavation bracing, tied back walls keep the excavation open since the support elements are located outside of the excavation footprint. Tied back walls can be either temporary or permanent structures. The wall elements can be sheet piles, soldier beams and lagging, diaphragm walls, or other wall systems.

The FHWA Geotechnical Engineering Circular No. 4 (FHWA 1999) provides design details that can be applied to internally braced excavations. Many of the basic procedures shown for excavation bracing and anchored bulkheads are used for tied back walls. However, the anchors (tie-backs) can be installed earlier in wall construction. The anchors are preloaded and prevent significant displacement from occurring. For this reason, tied back wall design uses apparent earth pressure diagrams that are different than those used for internally supported excavation bracing. The apparent earth pressure diagrams for externally supported retaining structures are shown on the right side of Figure 4-51 through Figure 4-53.

For sands and stiff clays, the position of the top and bottom support must be known. The reaction force, R, is based on the passive resistance of the soil, and a factor of safety of 1.5 should be applied to this resistance. The depth of penetration, D, is selected to obtain the correct value of the passive resistance. A δ / ϕ' ratio equal to 0.5·to 1.0·can be used in the passive resistance calculation. Table 4-1 should be consulted for the value of δ. K_P should be obtained from Figure 4-12.

The design of tied back walls is complex, and a proper design consists of numerous steps. Compared to internally-braced excavations, externally-braced excavations have many additional elements that are geotechnical (as opposed to structural) in nature. FHWA (1999) outlines the individual steps, and these are given below:

1) Establish project requirements, including all geometry, external loading conditions (temporary and/or permanent, seismic, etc.), performance criteria, and construction constraints.

2) Evaluate site subsurface conditions and relevant properties of *in situ* soil and rock.

3) Evaluate design properties, establish design factors of safety or load and resistance factors, and select level of corrosion protection.

4) Select lateral earth pressure distribution acting on the back of the wall for final wall height. Add appropriate water, surcharge, and seismic pressures, and

evaluate total lateral pressure. A staged construction analysis may be required for walls constructed in marginal soils.

5) Calculate horizontal ground anchor loads and wall bending moments. Adjust vertical anchor locations until an optimum wall bending moment distribution is achieved.

6) Evaluate required anchor inclination based on right-of-way limitations, location of appropriate anchoring strata, and location of underground structures.

7) Resolve each horizontal anchor load into a vertical force component and a force along the anchor.

8) Evaluate horizontal spacing of anchors based on wall type. Calculate individual anchor loads.

9) Select type of ground anchor.

10) Evaluate vertical and lateral capacity of wall below excavation subgrade. Revise wall section if necessary.

11) Evaluate internal and external stability of anchored systems. Revise ground anchor geometry if necessary.

12) Estimate maximum lateral wall movements and ground surface settlements. Revise design if necessary.

13) Select lagging, if required. Design wales, facing drainage systems, and connection devices.

4-9 CELLULAR COFFERDAM DESIGN.

Cellular sheet pile cofferdams are structures constructed from sheet piles driven in a variety of geometries and filled with soil. Cofferdams perform many purposes, such as creating dewatered construction areas, lock walls, retaining structures, mooring structures, and spillway weirs.

Cofferdam geometries include circular cells, semicircular cells, and cloverleaf cells. These different configurations are shown in Figure 4-57(a). For hand calculations, these configurations are transformed into equivalent parallel wall cofferdams of width, B. The strict definition of B is that it is the width of a rectangular section that has a sectional modulus equivalent to that of the actual cofferdam cell. Since this can be a difficult calculation, approximate methods to calculate B for the different cofferdam cell configurations are shown on Figure 4-57(a).

Figure 4-57(b) shows a typical section used for cofferdam design. In some designs, there may be soil against the outboard face, and the berm may not be present on the inboard face.

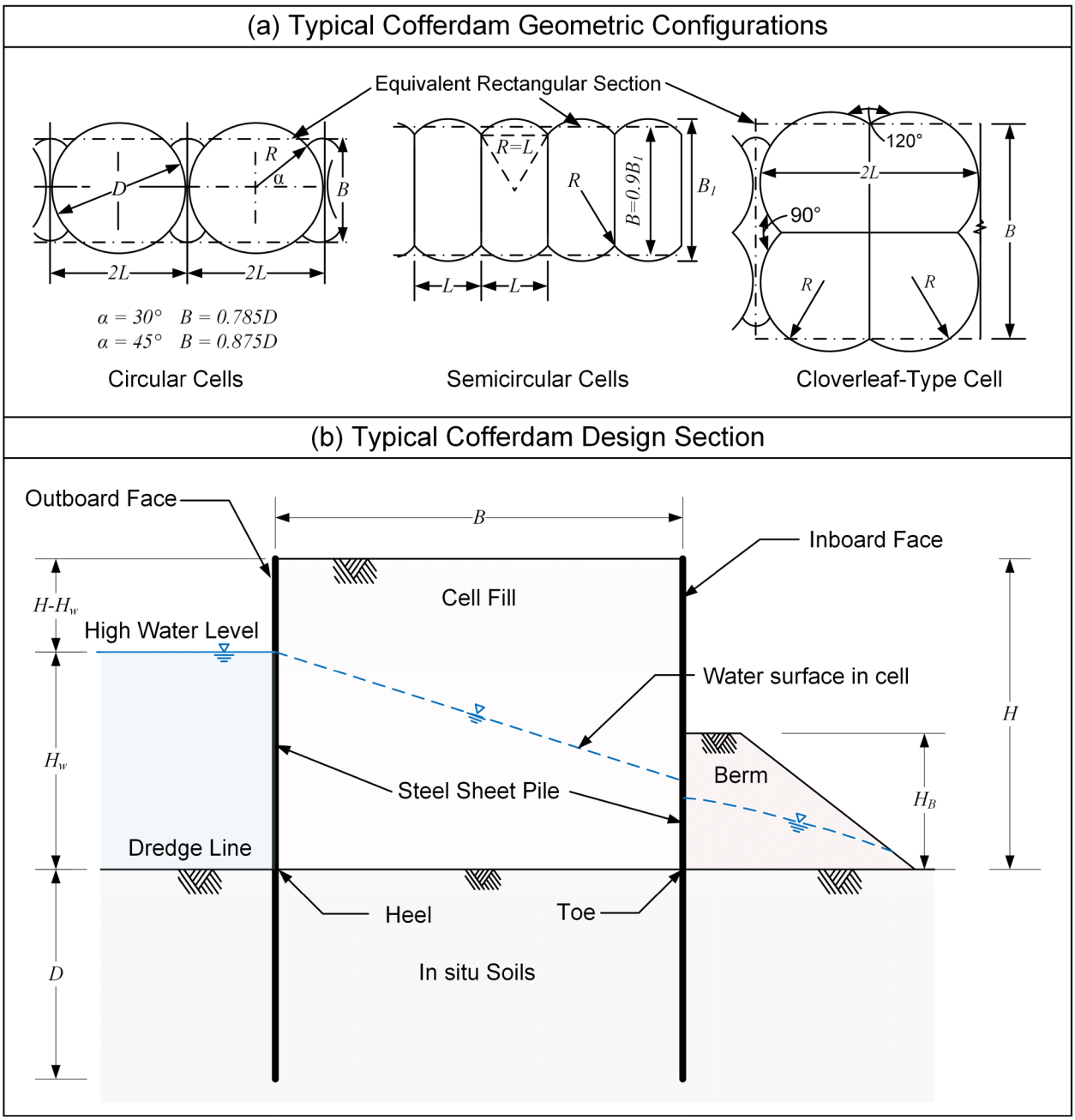

Figure 4-57 Geometry and Design Parameters for Cellular Cofferdams

Many factors must be considered in the design of cellular cofferdams. Because of the complexity involved in cofferdam design, numerical methods modeling soil-structure interaction are often used. The stability of cofferdams depends on ratio of the width to the height, the resistance of an inboard berm, if any, and the type and permeability of

cell fill materials. Usually active and/or passive pressures act on exterior faces of the sheeting. The shear strength of the cofferdam fill material is a very important factor in the overall stability of cofferdams. Equally important is the line of saturation or phreatic surface in the cell fill. The position of the water surface or line of saturation in the cell fill is usually determined by the soil type used. For coarse-grained, free-draining fill, a slope of 1H:1V is assumed. For fine-grained, poorly-draining cell fill, a slope of 3H:1V is often used. In some cases, the line of saturation is assumed to extend from the outboard face of the cofferdam to the top elevation of the berm on the outside of the inboard face. The inboard ground surface or berm also may have an elevated phreatic surface, but the stabilizing effect of the inboard face water pressure is often ignored in design calculations (USS 1984; USACE 1989).

Many different loading cases and failure conditions are used to assess the stability and performance of cofferdams. The main loading conditions are: Case I – maximum pool conditions, Case II – initial filling conditions, and Case III – drawdown conditions (USACE 1989). For each of these loading conditions, the following modes of failure must be assessed:

- Sliding
- Overturning
- Rotation (Hansen method)
- Deep seated sliding
- Bearing capacity
- Settlement
- Seepage
- Interlock tension
- Vertical shear resistance (Terzaghi method)
- Horizontal shear resistance (Cummings method)
- Vertical shear resistance (Schroeder-Maitland method)
- Pullout of outboard sheets
- Penetration of inboard sheets

Some of the analysis methods, such as overturning, are very similar to those used for gravity retaining walls (Section 4-5.1). Other modes of failure are unique to cellular cofferdams and were developed specifically for the various modes of failure. Many of the failure modes employ earth pressure calculations outlined in this chapter, but the earth pressure coefficients, particularly for the cell fill material, lie between the active and passive pressure conditions used for other retaining structures. Table 4-7 outlines several failure modes and specifics of the analysis methods for cofferdams. Details regarding the stability of sheet pile cofferdams, along with solutions to example problems, can be found in the *USS Steel Sheet Piling Design Manual* (USS 1984) and the Corps of Engineers' EM 1100-2-2503 (USACE 1989).

Table 4-7 Modes of Failure and Design Details for Sheet Pile Cofferdams

Failure Mode	Design Guidance
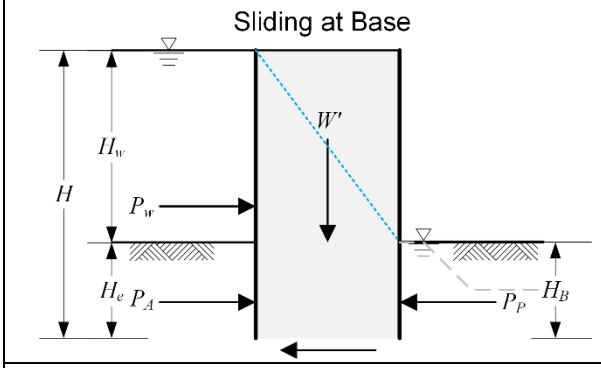	• Use $F \geq 1.25$ for temporary structures • Use $F \geq 1.50$ for permanent structures $$F = \frac{W' \tan\delta + P_P}{P_w + P_A}$$ where: W' = effective weight of backfill P_w = net water pressure force δ = interface friction angle along bottom = 0.5 for smooth rock = ϕ' for soil at base
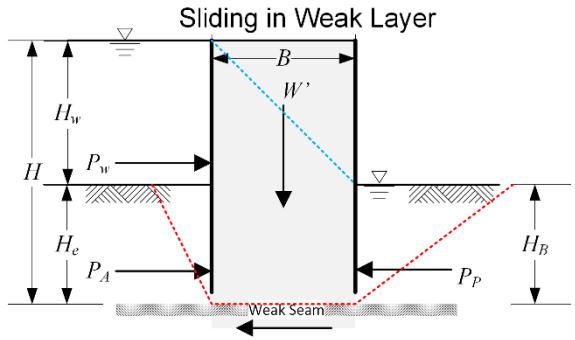	• Location of failure plane must be assumed • Active and passive pressure calculated to top of weak seam • W' includes soil beneath sheet piles to top of weak seam • Use $F \geq 1.25$ for temporary structures • Use $F \geq 1.50$ for permanent structures $$F = \frac{W' \tan\phi' + c'B + P_P}{P_w + P_A}$$ where: ϕ' = effective stress friction angle of weak seam c' = effective stress cohesion of weak seam
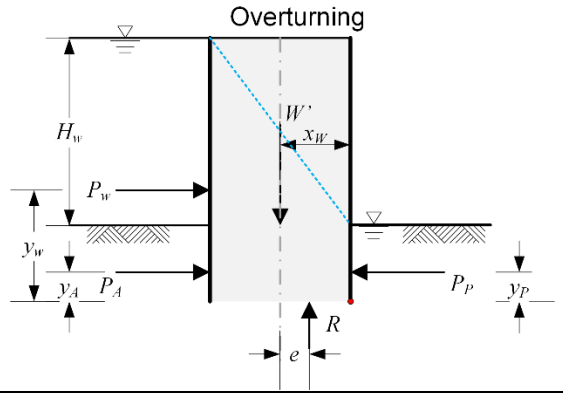	• Resultant force, R, must be located in the middle third of base • Calculate eccentricity as: $$e = \frac{P_w y_w + P_A y_A - P_P y_P}{W'} - x_W + \frac{B}{2}$$ • Maintain $\lvert e \rvert \leq B/6$ • Note: This is not a realistic failure mode owing to the flexibility of the cofferdam structure. Nonetheless, it is customary to still check the overturning mode in cofferdam design.
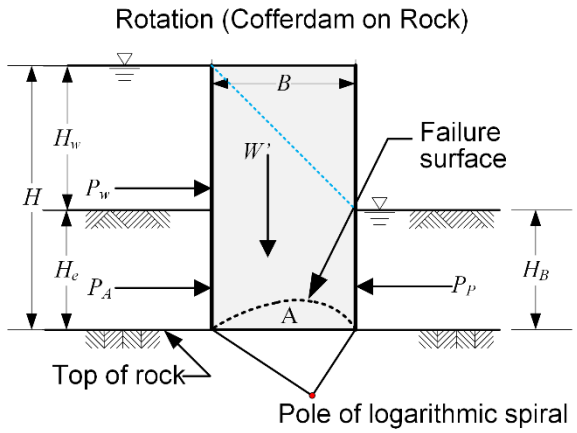	• Failure is assumed to occur on a logarithmic spiral surface. • W' calculated by removing the area (A) below the failure surface. • Critical surface is found by trial and error or by locating the surface using the point of application of the W' and ΣP forces and the locus of poles of the logarithmic spiral function. • Use $F \geq 1.25$ for temporary structures • Use $F \geq 1.50$ for permanent structures $$\sum P = P_W + P_A - P_P \text{ and } F = \frac{M_B}{M_\omega}$$ where: M_B = moment about pole for W' M_ω = moment about pole for ΣP

Failure Mode	Design Guidance
Rotation (Cofferdam on Soil) Failure Plane Outside of Cofferdam 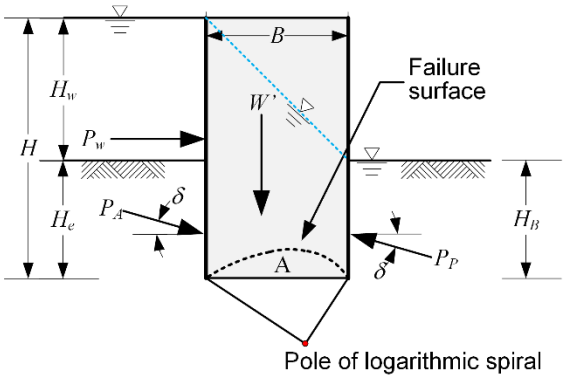 Failure Plane Outside of Cofferdam 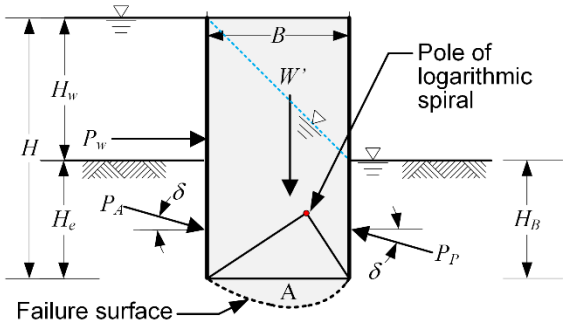 	• Failure is assumed to occur on a logarithmic spiral surface. The surface may be located inside or outside of the cofferdam. • The interface friction angle (δ) between the steel sheet pile and soil is often used in the analysis. Owing to the rotation of the cofferdam, the active and passive earth pressure forces are assumed to act in a reversed direction compared to conventional retaining wall analysis. • Normally, only the horizontal component of the earth pressure force is used in the stability calculations. • W' calculated by either adding or removing the area (A) depending if the pole is above or below the base of the cofferdam. • The critical surface found by trial and error or by locating the surface using the point of application of the W' and ΣP forces and the locus of poles of the logarithmic spiral function. • Use $F \geq 1.25$ for temporary structures. • Use $F \geq 1.50$ for permanent structures. $$\sum P = P_W + P_A - P_P \text{ and } F = \frac{M_B}{M_\omega}$$ where: M_B = moment about pole for W' M_ω = moment about pole for ΣP
Bearing Capacity 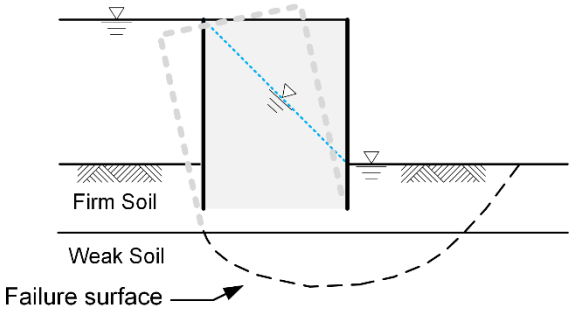 	• Seepage into the cofferdam can affect bearing capacity. • Bearing capacity analysis performed in addition to rotational failure analysis. • Bearing capacity methods presented in Chapter 5 should be applied to cofferdam analysis. • Use $F \geq 2.0$ for cofferdams founded on sand (permanent and temporary). • Use $F \geq 3.0$ for cofferdams founded on clay (permanent and temporary).
Settlement 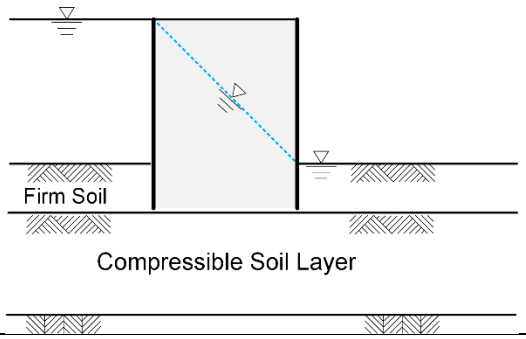 	• Settlement of soil beneath cofferdam can increase tilt, which can increase the moment for overturning. • Stress distribution varies both horizontally and vertically. • Stress distributions can be estimated using elastic theory influence charts (See DM7.1, Chapter 4). • Calculation of consolidation settlement should be performed using procedures presented in DM7.1 (Chapter 5).

Table 4-7 Modes of failure and design details for sheet pile cofferdams (cont.)

Failure Mode	Design Guidance
Sheet Pile Interlock Tension 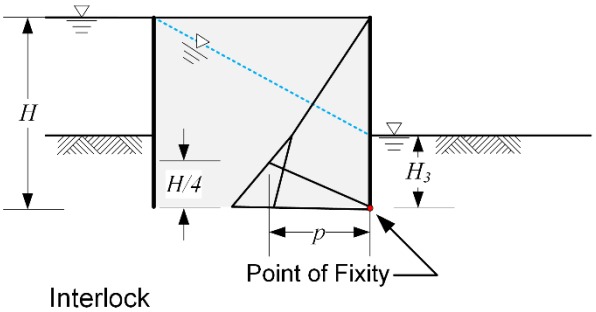 Interlock Stress in Cell 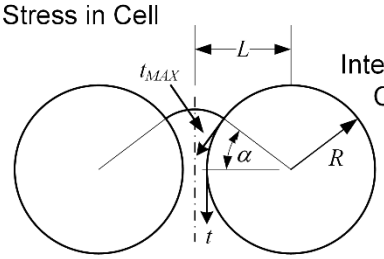 Interlock Stress at Connections	• Pressure caused by cell fill should not cause the allowable sheet pile interlock tension to be exceeded. • Critical horizontal pressure assumed to occur at $H/4$ above the point of fixity. Alternatively, the earth pressure can be calculated at the top elevation of the inboard berm. • Use $F \geq 2$ to 4. $F = \frac{\text{Manufacturer's reported interlock strength}}{\text{Computed interlock tension}}$ • For the main cell, the maximum inboard sheeting pressure (p) and maximum interlock tension (t_{max} in lbs per linear inch) can be found as: $p = K_A\left(\gamma\left(H - H_3\right) + \gamma'\left(H_3 - H/4\right)\right) + \gamma_w\left(H_3 - H/4\right)$ $t = p \cdot R$ where: K_A = 0.4 R = cell radius • For connections between the main cell and connecting arcs: $t_{max} = p \cdot L \cdot \sec\alpha$
Slippage between Sheeting and Cell Fill 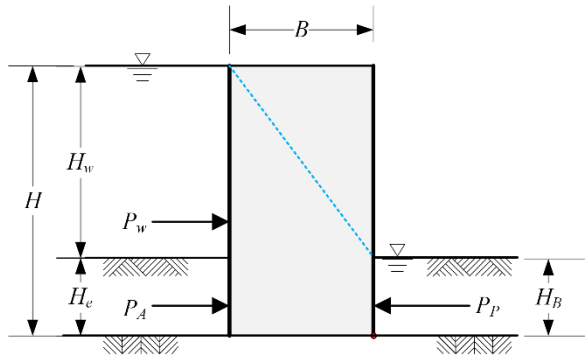 	• Outboard sheet piles can lift out due to applied moment, and cell fill can be lost. • Shear occurs between fill and sheet piles. • F is the resisting moment due to friction on outboard piling divided by the overturning moment due to earth and water pressures. • Use $F \geq 1.5$ for permanent structures. $F = \frac{3B\left(P_W + P_A\right)\tan\delta + P_P H_B}{P_W H + P_A H_e}$
Shear Failure on Centerline of Cell 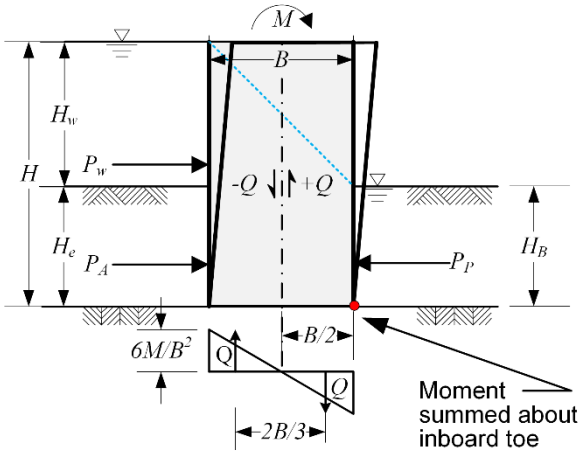 	• Tilting can cause excessive shear on a vertical plane through the centerline of the cofferdam fill. • The shear resistance of the cofferdam cell fill and the frictional resistance of the sheet pile interlocks must exceed the applied shear stress due to the overturning forces. • Use $F \geq 1.5$ for permanent structures. • The earth pressure coefficient used to calculate the shear resistance at the centerline is greater than the active earth pressure coefficient. • The total shear force (Q) is found as: $Q = \frac{3M}{2B}$ where: M = net overturning moment.

4-9.1 Cell Deformations.

The maximum bulging of cells occurs at about one-quarter of the height above the base of the cofferdam. Deflections under the lateral overturning loads are a function of the dimensions, the foundation support, and the properties of the cell fill (Brown 1963).

4-9.2 Cell Fill.

Clean, coarse-grained, free-draining soils are preferred for cell fill. They may be placed hydraulically or dumped through water without compaction or special drainage. Clean granular fill materials should be used in large and critical cells. A thorough study of alternatives should made before accepting fine-grained backfill. Fine-grained soils produce high bursting pressures and minimum cell rigidity. Their use may necessitate interior berms, increased cell width, or possibly consolidation by sand drains or pumping within the cell. All soft material trapped within the cells must be removed before filling.

4-9.3 Cofferdam Drainage.

Weep holes should be installed on inboard sheeting to the cell fill. For critical cells and cells with marginal fill material, supplementary drainage by well points, or wells within cells, have been used to increase cell stability.

4-9.3.1 Cofferdam Retardation of Corrosion.

When cofferdams are used as permanent structures, particularly in brackish water or seawater, severe corrosion occurs from top of the splash zone to a point just below mean low water level. Use protective coatings, corrosion resistant steel, and/or cathodic protection in these areas.

4-10 PROBLEM SOILS AND RETAINING WALLS.

Chapter 1 provides a summary of many types of problem soil conditions that can affect the design of foundations and earth structures. Table 4-8 summarizes important conditions for the design of retaining walls in problem soils.

Table 4-8 Problem Soil Considerations for Retaining Structures

Soil Type	Primary Considerations for Retaining Structures

Soft Clays	• Flexible walls built in soft clays will experience relatively high apparent earth pressures and must consider basal stability.
	• Walls founded in soft clays may experience problematic settlement
	  ○ Consolidation settlement of gravity and MSE structures built over soft clays should be determined using approaches in Chapter 5 of DM 7.1.
	  ○ Flexible walls can settle as a result of the downward components of the lateral pressure and any ground anchor forces. Soldier pile walls are especially susceptible, because the downward forces are concentrated at the soldier piles.

High Plasticity Expansive Clays	• Earth pressures for permanent walls retaining high plasticity soils should be determined using fully softened shear strength parameters.
Loess and Other Collapsible Soils	• In an undisturbed condition, earth pressures from these soils may be very low due to cementation of particles. However, collapse on wetting will increase earth pressures. • Any measured cohesion intercept should be ignored in the calculation of earth pressure.
Sensitive Clays	• Retaining structures in sensitive clays should minimize disturbance. Vibrations may be problematic. • Avoid local concentrations of shear stress from temporary steep slopes or open excavations.
Loose Sands	• Select methods that do not require an open excavation or exposed vertical face, particularly if the groundwater level is high. • Retaining wall construction methods that induce vibrations may cause settlement.
Glacial Till	• Construction of some times of wall can be difficult in glacial till as a result of the presence of cobbles and boulders.
Organic Soils, Peat, and Muskeg	• Low undrained shear strength may be present. • Passive resistance will be low because of low unit weight. • Wall settlement may be a concern.
Dredged Soils	• Similar considerations to soft clays and loose sands, depending on the soil composition.
Low Plasticity and Nonplastic Silts	• May be susceptible to “running” or fluid-like behavior, if below the groundwater level. • Construction methods that require open excavation may be difficult, if saturated.
Municipal Solid Waste	• Earth pressures may be difficult to characterize accurately. • Cut walls that require installation of vertical structural elements may encounter obstruction in the waste.

4-11 NOTATION.

Variable	Definition
c'	Effective stress cohesion intercept
C_a	Adhesion
E	Young’s modulus
F	Factor of safety
F_{OT}	Factor of safety against overturning
F_{SL}	Factor of safety against sliding
I	Moment of inertia
K_{AE}	Seismic active earth pressure coefficient

Variable	Definition
K_0	At-rest earth pressure coefficient
K_A	Active earth pressure coefficient
k_h	Horizontal ground acceleration
K_P	Passive earth pressure coefficient
k_v	Vertical ground acceleration
m	Parameter used to determine influence factors for stresss from applied loads
M_{Design}	Maximum moment used for design of cantilever cut walls
M_{max}	Maximum moment calculated for cantilever cut walls
n	Parameter used to determine influence factors for stresss from applied loads
OCR	Overconsolidation ratio
p	Earth pressure on the inboard side of a cofferdam
P_A	Resultant force from active earth pressure
P_{AE}	Seismic active earth pressure force
P_H	Resultant force from the horizontal component of earth pressure
P_N	Resultant normal force from earth pressure
P_P	Resultant force from passive earth pressure
$P_{P,allow}$	Allowable resultant force from passive earth pressure after applying a factor of safety
P_T	Resultant shear force from earth pressure
P_v	Resultant force from the vertical component of earth pressure
p_w	Hydrodynamic water pressure
P_w	Resultant force from water pressure
P_{wA}	Resultant force from water pressure on the active side of a wall
P_{wP}	Resultant force from water pressure on the passive side of a wall
q	Uniform surcharge pressure behind a retaining structure
q	Compaction pressure of a vibratory plate tamper
q	Compaction pressure of a rammer plate
$\overline{q}$	Compaction pressure from a roller
q_{max}	Maximum pressure below an eccentrically loaded retaining foundation

Variable	Definition
q_{min}	Minimum pressure below an eccentrically loaded retaining foundation
Q_p	Point load
r_u	Pore pressure coefficient
s_u	Undrained shear strength
$s_{u,F}$	Undrained shear strength with applied factor of safety
t_{max}	Maximum interlock tension for sheet piles in cofferdams
u	Water pressure
U	Resultant force from water pressure
Y	Horizontal displacement of wall
z	Depth below ground surface
α_A, α_P	Acute angle between critical Coulomb failure plane and vertical
β	Slope of inclined backfill
δ	Interface friction angle
ΔP_{AE}	Increase in resultant active earth pressure force caused by seismic loading
ΔP_A	Change in resultant active earth pressure force caused by seepage
ΔP_P	Change in resultant passive earth pressure force caused by seepage
ϕ	Total stress friction angle
ϕ'	Effective stress friction angle
ϕ'_{allow}	Allowable effective stress friction angle
γ	Total or moist unit weight
γ_b	Bouyant unit weight
γ_{eq}	Equivalent fluid unit weight
γ_{sat}	Saturated total unit weight
ρ	Flexibility number
σ'_h	Effective horizontal stress
$\sigma'_{H\theta}$	Increase in horizontal stress as a function of the location with respect to an applied load
σ'_z	Effective vertical stress
θ	Angle of the wall face on the retained side

Variable	Definition
θ_P	Obtuse angle between critical Coulomb failure plane and vertical
ψ	Horizontal acceleration angle for seismic loading

4-12 SUGGESTED READING

Topic	Reference
Anchored Bulkheads	United States Steel (USS). 1984. *Steel Sheet Piling Design Manual.*
Apparent Earth Pressures	FHWA. 1999. *Ground Anchors and Anchored Systems. Geotechnical Engineering Circular No. 4. Publication FHWA-IF-99-015*. Federal Highway Administration, Washington, D.C.
Ground Anchors	
Soil Nail Walls	
Mechanically Stabilized Earth Walls	FHWA. 2009. *Design and Construction of Mechanically Stabilized Earth Walls and Reinforced Soil Slopes – Volumes I and II, FHWA-NHI-10-024 and FHWA-NHI-10-025.* Federal Highway Administration, Washington, D.C.
Cofferdams	USACE. 1989. *Design of Sheet Pile Cellular Structures, Cofferdams, and Retaining Structures, EM 1110-2-2503.* Department of the Army, CECW-EP, 186 pp.

This Page Intentionally Left Blank

CHAPTER 5.SHALLOW FOUNDATIONS

5-1 INTRODUCTION.

5-1.1 Scope.

This chapter describes design for shallow foundations, including presumptive and empirical methods, as well as those based on bearing capacity theory for soil and rock. Special loading conditions for shallow foundations are discussed, including the design of foundations and slabs below the groundwater level and resistance of uplift. This chapter also considers special soil conditions, such as foundations on engineered fill, foundations on expansive and collapsing soil and expansive rock, and foundations in other problem soils.

Shallow foundations can be defined as foundations with a depth to width (D/B) ratio less than about 5. *Spread* foundations[28] transfer structural loads to the soil or rock over a relatively wide area and are usually synonymous with shallow foundations. Another type of shallow foundation is a *mat* foundation, in which the weight of the structure is distributed across the entire footprint of the structure. Most shallow foundations are constructed from reinforced, cast-in-place concrete. The interface between the shallow foundation and the soil or rock is referred to as the *bearing surface* and is located at the *foundation bearing elevation*. The *bearing pressure* is the stress imposed on the bearing surface by the foundation.

The primary geotechnical task for shallow foundation design is to select an allowable bearing pressure. This pressure is then used to size the foundations to support the anticipated structural loads. The allowable bearing pressure depends on two factors. First, an adequate factor of safety against ultimate bearing capacity failure must be provided. This is a strength limit state. Second, the settlements caused by changes in stress from the shallow foundations must not exceed the tolerances of the structure. This is a serviceability limit state. For the majority of structures, the design of shallow foundations is controlled by settlement, which is discussed in Chapter 5 of DM 7.1.

This chapter assumes that field investigations have been performed using sufficient *in situ* and laboratory testing to define the soil and/or rock stratigraphy as well as the groundwater conditions. For shallow foundations, the investigation should extend below the depth at which the change in stress imposed by the foundations is negligible (see Chapters 4 and 5 of DM 7.1). The investigation should provide the parameters required for bearing capacity and settlement analysis. Chapter 2 of DM 7.1 provides further information on field exploration while laboratory testing is discussed in Chapter 3 of that volume.

[28] The terms *footer* and *footing* are common synonyms for shallow spread foundations.

5-1.2 Applications.

Shallow foundations may be used at locations where suitable bearing soils are present within a few feet below the structure, provided that the stresses imposed by the foundation do not create unacceptable settlements.

Where suitable bearing soils are underlain by more compressible soils with depth and settlements are unacceptable, either deep foundations (see Chapter 6), ground improvement methods (see Chapter 1), or temporary surcharging (Chapter 5 of DM 7.1) may be required to bypass or modify the compressible soils. In some cases, shallow foundations can still be used if the bearing capacity of the near surface soils can be improved to allow smaller footings with higher bearing pressures. Construction of high quality compacted structural fill may also allow higher bearing pressures. In both cases, smaller footings will reduce stress penetration, which may reduce settlements.

Where a relatively thin layer of unsuitable loose or soft soil is present near the ground surface, it may be possible to deepen spread footings to suitable soils. Alternatively, the unsuitable soils can be excavated and replaced with higher quality compacted structural fill.

Shallow foundations may also be supported on rock. Where both rock and soil are found at bearing grade in different areas of a building, differential settlements may be of concern as discussed in Section 5-2.4.1. Over excavation of rock and replacement with a soil cushion between rock and the foundation may be required to reduce differential settlement.

5-1.3 Design Philosophy.

Two design philosophies are used to prevent bearing capacity failure of shallow foundations. Allowable stress design determines the ultimate bearing capacity of the soil and applies a factor of safety to determine an allowable bearing pressure. Load and resistance factor design (LRFD) uses load factors to account for uncertainties in loading conditions and resistance factors to accommodate uncertainty in resistance. The basis of the LRFD approach is discussed in Section 7-4.5. Settlement analysis is typically performed using unfactored loads, removing any difference between the two approaches.

Allowable stress design, which will be used in this chapter, requires the selection of a factor of safety against bearing capacity failure. The appropriate factor of safety, F_{BC}, depends on the uncertainty of both the loading and the soil conditions, as well as the consequences of failure. Lower values of F_{BC} are appropriate for well-defined conditions and low consequences, while higher F_{BC} should be used for greater uncertainty and consequences. Typical values of F_{BC} are in the range of 2 to 3 when the bearing pressure is calculated using dead load and permanent live load. Mat and

tank foundations may use a factor of safety of 1.7 to 2.5 for cases with sufficient field exploration. The lower factor of safety may be reduced by about one-third for cases with temporary or transient live load, such as earthquake, wind, and snow. UFC 3-220-01 (2021) contains additional information about factors of safety.

5-2 SHALLOW FOUNDATION DESIGN CONSIDERATIONS.

5-2.1 Foundation Depth.

In general, individual footings should be placed below: 1) the depth of frost penetration (see Chapter 1 of DM 7.1 for guidance or the National Oceanic and Atmospheric Adminstration website for site specific data), 2) zones of high volume change due to moisture fluctuations, and 3) scour depths for foundations in or adjacent to rivers and streams. Section 6-2.2.1 provides additional guidance for scour. Footings should extend to bear below organic materials, disturbed upper soils, uncontrolled fills, and zones of collapse-susceptible soils that are present. Alternatively, the unsuitable material should be removed and replaced with compacted structural fill.

Where other constraints do not control, shallow foundations on soil are typically embedded at least 12 to 18 inches. Some building codes specify minimum depth as a function of load.

5-2.2 Gross and Net Bearing Pressure.

The total load applied to the foundation bearing surface is the sum of the structural load (Q_{DL+LL}), the weight of the foundation (W_F), and the weight of any overlying soil (W_S). The *gross bearing pressure* applied to the soil by a shallow foundation is the total load divided by the area (A) of the bearing surface. The gross allowable bearing pressure is found as:

$$q_{gross} = \frac{Q_{DL+LL} + W_F + W_S}{A} \quad (5\text{-}1).$$

The net bearing pressure is sometimes used as a more convenient measure because it does not depend upon the weight of the foundation and overlying soil. The *net bearing pressure* is the gross bearing pressure minus the existing vertical overburden pressure at the foundation bearing elevation or:

$$q_{net} = q_{ult} - \sigma_{zD} \quad (5\text{-}2).$$

The unit weights of the foundation and soil backfill are typically assumed to be the same as the existing soil, which means that:

$$q_{net} = q_{gross} - \sigma_{zD} \approx \frac{Q_{DL+LL} + W_F + W_S}{A} - \frac{W_F + W_S}{A} = \frac{Q_{DL+LL}}{A} \quad \text{(5-3).}$$

Equation 5-3 defines the net bearing pressure only in terms of the structural load and foundation dimensions.

5-2.3 Eccentricity.

Shallow foundations may be eccentrically loaded by moments applied about one or both axes. The applied moments may be the result of either non-concentric vertical loading or directly applied to the foundation by the structure. The resulting eccentricity (e) is defined as the horiztonal distance between the resultant force on the bearing surface and the centerlines of the foundation.

Eccentricity is calculated as:

$$e = \frac{M}{Q} \quad \text{(5-4)}$$

where:
M = applied moment and
Q = gross vertical load on the footing.

For cases where non-concentric vertical loading causes eccentricity, the applied moment can be determined by summing moments about the centerline of the footing. Where the eccentric loading is not aligned with the axes of the foundation, it is convenient to split the eccentricity into two parts and calculate e_B and e_L from the respective moments, M_B and M_L. By convention, the width (B) is the shorter dimension of the foundation, and the length (L) is the longer dimension.

Eccentricity causes an uneven bearing pressure. If the eccentricity is too high, the bearing pressure will no longer be compressive under all of the foundation. In order to prevent this, the eccentricity must be limited for normal loading. For eccentricity in one direction, the resultant must be in the middle one-third of the foundation or:

$$|e_B| \le \frac{B}{6} \text{ or } |e_L| \le \frac{L}{6} \quad \text{(5-5)}$$

For cases with eccentricity in two directions, the resultant must fall within a diamond-shaped area in middle of the rectangular foundation called the *kern* and the following should be satisfied:

$$\frac{6|e_B|}{B} + \frac{6|e_L|}{L} \le 1 \quad \text{(5-6).}$$

If the eccentricity falls within these limits, the bearing pressure at the four corners of the rectangular foundation can be found as:

$$q_{corner} = q_{gross}\left(1 \pm \frac{6|e_B|}{B} \pm \frac{6|e_L|}{L}\right) \quad \text{(5-7).}$$

The maximum value, q_{max}, should be used for comparisons with ultimate bearing capacity for brittle materials such as sensitive soil and rock. For more ductile materials, it is appropriate to approximate the applied bearing pressure using the equivalent footing method (Meyerhof 1953). The *equivalent footing* is the bearing area on which the resultant bearing force is centered. The equivalent width (B') and length (L') are calculated as:

$$B' = B - 2e_B \quad \text{(5-8)}$$

and

$$L' = L - 2e_L \quad \text{(5-9).}$$

The equivalent uniform bearing pressure for a rectangular foundation can be found as:

$$q_{unif} = \frac{Q_{LL+DL} + W_F + W_S}{B' \cdot L'} \quad \text{(5-10).}$$

The conditions for two-way eccentricity for a rectangular foundation are summarized in Figure 5-1(a). The theoretical pressure distributions with solid lines are indicated along the four sides of the foundation. The equivalent dimensions and area are shown by the shaded rectangle. The dashed pressure distribution shows the equivalent uniform bearing pressure.

Circular footings can only have eccentricity in one direction as shown in Figure 5-1(b). The resultant is centered on the lens-shaped area circumscribed by the two arcs labeled *abcd*. The equivalent rectangular area is shaded. If the aspect ratio of the equivalent rectangle is the same as the circumscribed area, then the equivalent dimensions can be calculated as:

$$L' = \overline{a'b'} = \sqrt{\left[2r^2 \cos^{-1}\left(\frac{e_x}{r}\right) - 2e_x\sqrt{r^2 - e_x{}^2}\right]\left(\frac{\sqrt{r^2 - e_x{}^2}}{r - e_x}\right)} \quad \text{(5-11)}$$

and

$$B' = \overline{b'c'} = L'\left(\frac{r - e_x}{\sqrt{r^2 - e_x{}^2}}\right) \tag{5-12}$$

where:
e_x = eccentricity and
r = radius of the foundation.
Note that the inverse cosine term in Eqn. 5-11 must be expressed in radians.

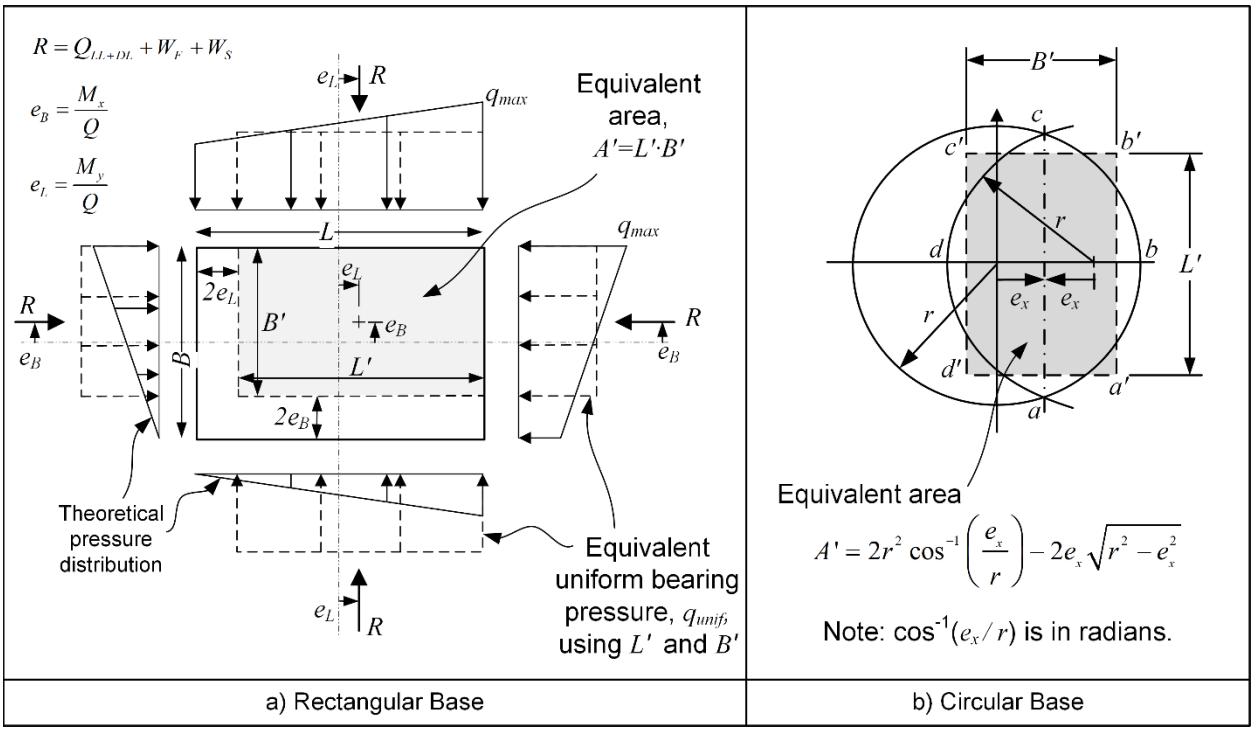

Figure 5-1 Eccentricity for (a) Rectangular Footing and (b) Circular Footing (after Bowles 1996)

5-2.4 Allowable Bearing Pressure.

The *allowable bearing pressure* (q_{all}) is the highest bearing pressure that meets the design requirements for both factored bearing capacity and settlement. In a general sense, the allowable bearing pressure can be determined using the following steps:

1) Calculate the ultimate bearing capacity (q_{ult}) using the methods in Section 5-3.

2) Apply an appropriate factor of safety (F_{BC}) to the ultimate bearing capacity. In some cases, it may be appropriate to start with a presumptive allowable bearing pressure from Section 5-2.5 rather than factoring a calculated bearing capacity.

    a. The gross allowable bearing pressure is found as:

$$q_{all,gross} = \frac{q_{ult}}{F_{BC}} \quad \text{(5-13).}$$

b. The net allowable bearing pressure is found as (Peck et al. 1974):

$$q_{all,net} \leq \frac{q_{ult}}{F_{BC}} - \sigma_{zD} \quad \text{(5-14).}$$

3) Calculate settlement using foundations sized according to $q_{all,net}$.

a. If the total, differential, and distortion settlement criteria are met, then the net allowable bearing pressure from Equation 5-14 can be used and the design is controlled by the bearing capacity.

b. If not, reduce the bearing pressure until the settlement criteria are met. The reduced value is the net allowable bearing pressure that should be used for design. The design is controlled by settlement.

Once an allowable bearing pressure has been determined, it is compared to the calculated bearing pressure. Either net or gross pressures can be used, as appropriate. The foundation dimensions are adjusted to obtain an applied bearing pressure less than, but not greatly exceeding, the allowable value. This process is often iterative.

5-2.4.1 Settlement Considerations.

Settlement constraints govern the design of many shallow foundations and should be carefully considered prior to a comprehensive consideration of bearing capacity. Chapter 5 of DM 7.1 provides detailed instructions for settlement calculations. Some additional considerations specific to shallow foundations are considered in this section.

Some structures have widely varying column or wall loads that have the potential to cause problematic differential settlement. In this case, $q_{all,net}$ can be varied in attempt to equalize settlements. Often this requires using a lower bearing pressure and larger footings to support the heavier column loads. If the settlement prone soils are shallow, it may also be possible to increase the $q_{all,net}$ for the heavily loaded footings by excavating poor soils and replacing with high-quality compacted structural fill along an interior line of columns.

At some sites, the depth to rock varies widely and both rock and soil may be found at the bearing elevation. In this case, differential settlements will be a concern, because of the dissimilar settlement characteristics of soil and rock. The choice of an appropriate solution will be informed by both the extent of the dissimiliar bearing condition and the relative flexibility of the supported structure. One procedure that may be used to reduce

differential settlement is to over excavate the rock where footings are located and backfill with compacted structural fill. The compacted structural fill should be designed to compress such that differential settlements are no longer a concern. Typically, the fill is clay placed with a lower relative compaction criterion, such as to 90 percent of maximum dry density. A thickness of one to two feet of this type of material will usually improve the differential settlement characteristics. The length of the transition zone required to mitigate differential settlement will depend on the flexibility of the structure. Section 5-6.1 further describes procedures for shallow foundations on fill.

Alternatively, a deepened footing can be reinforced as a grade beam that can allow the differential settlement to be distributed over a longer span. In other cases, it may be most economical to use shallow foundations bearing on rock for most of the structure along with deep foundations and grade beams at the locations where the rock is deeper.

5-2.4.2 Alternative Methods of Supporting Shallow Spread Foundations.

For sites with highly compressible soils, very low bearing pressures may be required to meet the settlement criteria. As the size of isolated foundations becomes large, the use of a mat foundation should be considered (see Section 5-4).

Other alternatives to individual shallow foundations are available. If stronger or less compressible soils are present, the foundation depth may be increased to reach suitable bearing soils. Another alternative is to excavate and replace unsuitable soils with compacted structural fill for individual column footings, or in strips along column lines. Turned down edge foundations integral with the floor slab may be used for lightly loaded structures. Many of the site improvement techniques discussed in Chapter 1 are suitable to improve bearing capacity and reduce settlement for shallow foundations. Some of these techniques work by transferring load to a suitable bearing stratum while others densify the soil, reducing settlement potential. Useful techniques for shallow foundations include rigid inclusion piers, aggregate piers, vibro-compaction, dynamic compaction, soil mixing methods, and preloading with or without wick drains to facilitate improved drainage.

5-2.5 Presumptive Allowable Bearing Pressure.

Presumptive bearing pressures are selected without formal calculation of bearing capacity and/or settlement. They are sometimes used to estimate allowable bearing pressures (q_{all}) for: 1) preliminary estimates for any project, 2) design values for lightly loaded structures, or 3) design values for foundations on rock materials where detailed analysis is unnecessary due to the relatively high bearing capacity of the rock. Presumptive bearing pressures should not be used for foundations on normally consolidated clays, organic soils, or uncontrolled fills.

Table 5-1 lists presumptive allowable bearing pressures for a variety of rock and soil types. These presumptive q_{all} values are intended to provide a reasonable safety factor against ultimate failure and to avoid detrimental total and differential settlements of individual footings for footings subjected to vertical loads. The effects of eccentricity on bearing pressure should be considered when using presumptive q_{all}. Presumptive q_{all} values for soils should be used with caution and verified by performance of nearby structures founded on similar density or consistency material. Bearing strata underlain by a weaker material can be considered using presumptive bearing pressures and the method illustrated in Figure 5-2.

When presumptive q_{all} are used in lieu of bearing capacity analysis, it may still be appropriate to check settlement. The zones of induced stresses from adjacent foundations should not overlap within a depth of $2B$ below square footings or $4B$ below continuous footings because of settlement concerns. In order to accomplish this, lines projected downward from adjacent footings at angle of 30° from the vertical should not intersect within these depths.

Table 5-1 Presumptive Allowable Bearing Pressures (B > 3 ft) (after NRCS 2022, Das 2022)

Type of Bearing Material	Rock or Soil Quality, Consistency, or Relative Density (RQD, UCS, or SPT N)	q_{all} (ksf)
Massive crystalline igneous/metamorphic rock: granite, diorite, basalt, gneiss, marble	Very hard, sound rock (RQD ≥ 75%) UCS = 1400 to 5200 ksf	160
Foliated metamorphic rock: slate, schist	Hard, sound rock (RQD ≥ 50%) UCS = 650 to 3600 ksf	70
Sedimentary rock; siltstone, sandstone, limestone without cavities	Moderately hard, sound rock (RQD ≥ 25%) UCS = 240 to 2800 ksf	40
Weathered rock of any kind, except highly argillaceous rock (shale)	Moderately soft, sound rock (RQD ≤ 25%) UCS = 110 to 800 ksf	20
Indurated clay; shale	Soft, unsound rock (RQD = 0% by definition) UCS = 20 to 800 ksf	10
Well graded gravel and sand mixtures with clay: glacial till, hardpan (GW-GC, GC)	Very dense (N > 50) Medium to dense (N = 10 to 50) Compacted ($R.C.$ ≥ 95% of D698)	8 5 5
Sand with gravel (SW-SC, SC)	Very dense (N > 50) Medium to dense (N = 10 to 50) Compacted ($R.C.$ ≥ 95% of D698) Very loose/Loose (N ≤ 10)	7 5 5 3
Sand, silty, or clayey (SW, SM, SC)	Very dense (N > 50) Medium to dense (N = 10 to 50) Compacted ($R.C.$ ≥ 95% of D698) Very loose/Loose (N ≤ 10)	5 4 4 2
Homogeneous inorganic lean or fat clay, sandy or gravelly (CL, CH)	Hard (N > 30) Stiff to very stiff (N = 8 to 30) Compacted ($R.C.$ ≥ 95% of D698) Soft to medium (N = 2 to 8)	6 3 3 1.5
Inorganic silt and elastic silt, sandy (ML, MH)	Very dense (N > 50) Medium to dense (N = 10 to 50) Very loose/Loose (N ≤ 10)	6 3 1.5

Notes:

- Definitions: RQD = Rock quality designation, UCS = Unconfined compressive strength
- Minimum bearing depth is 18 inches for foundations bearing on soil or soft rock.
- For foundations with width (B) < 3 ft, multiply q_{all} by (B / 3) with B in feet.
- Presumptive q_{all} for rock should not exceed 10% of the UCS, if measured.
- For foundations on soft rock or coarse-grained soil, increase presumptive q_{all} by 5% for each foot of depth below 18 inches.
- For foundations on moderately hard or better rock, increase presumptive q_{all} by 10% for each foot of depth below the ground surface.
- Presumptive q_{all} for compacted soil assumes relative compaction ($R.C.$) ≥ 95% based on ASTM D698, moisture content within 2% of optimum, and lift thickness ≤ 8 inches. Higher q_{all} may be appropriate for higher levels of relative compaction.
- Presumptive q_{all} for transient loads from wind or earthquakes.

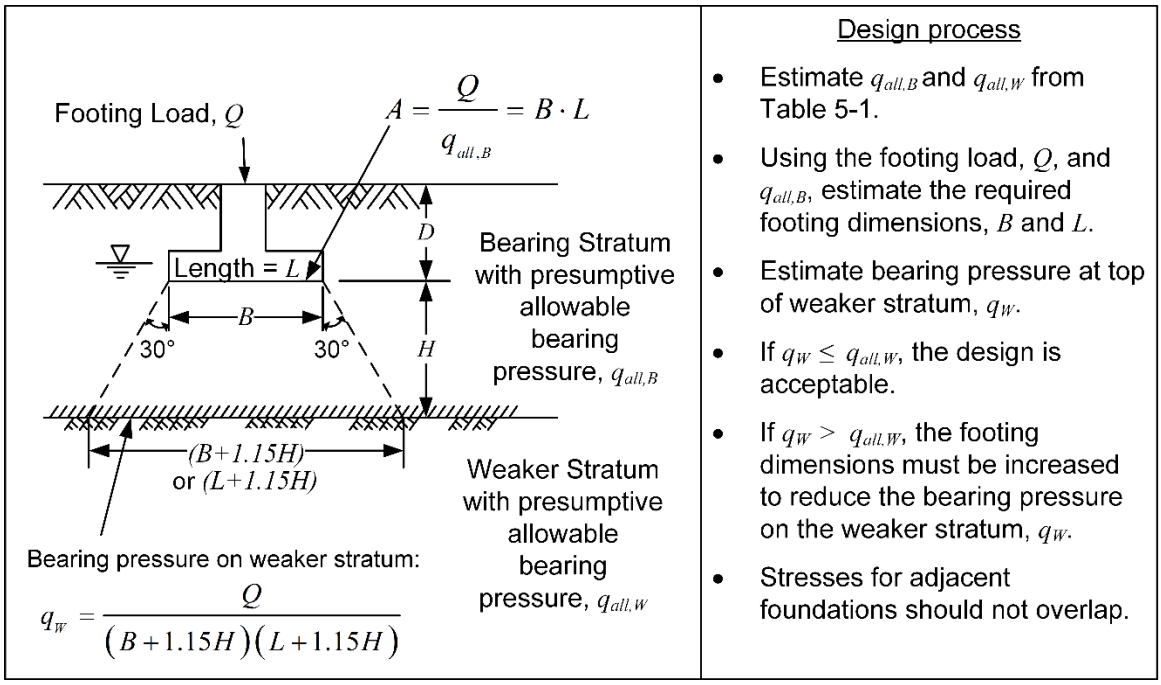

Figure 5-2 Presumptive Bearing Pressure for Weaker Layer Underlying Bearing Stratum

5-3 BEARING CAPACITY OF SOIL AND ROCK.

5-3.1 Bearing Capacity Theory.

The *ultimate bearing capacity* can be defined as the highest applied stress that the soil or rock withstands at the point of plastic failure. As developed by Terzaghi (1943), ultimate bearing capacity considers two types of failure.

General shear failure occurs along a well-defined failure surface below and beyond the edges of a footing as shown in Figure 5-3(a). The triangular Zone I under the footing in Figure 5-3 acts as though it is part of the footing, and the soil remains in an elastic state. For a vertical load, the major principal stress is aligned vertically in Zone I. In Zone III, the soil reaches a state of Rankine passive earth pressure with the major principal stress aligned horizontally. Zone II is known as the zone of radial shear, which allows the stress system to rotate between Zones I and III.

General shear failure normally occurs in a dense coarse-grained or very stiff cohesive soil. At failure, the soil on both sides of the footing bulges and the footing may rotate. A state of plastic equilibrium is reached in Zones II and III in this type of failure. General shear failure can be catastrophic for large mat supported structures although individual footings rarely experience this type of failure. Dense and very stiff soils generally experience relatively low settlements at typical allowable bearing pressures.

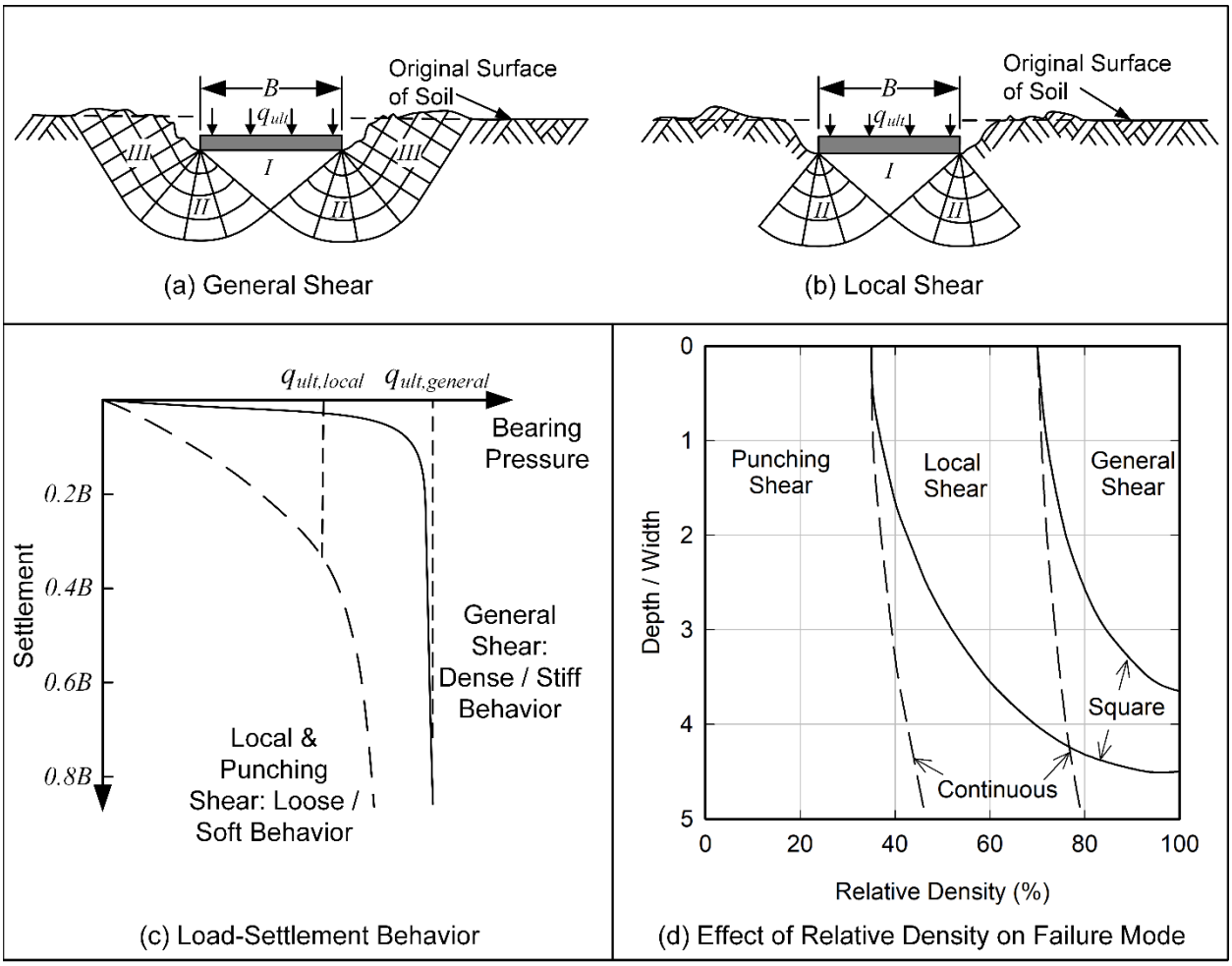

Figure 5-3 Bearing Capacity Failure Modes – (a) General Shear, (b) Local Shear, (c) Load-Settlement Behavior, and (d) Effect of Relative Density on Failure Mode (after Das 2022, Terzaghi 1943, Vesic 1973)

Local shear failure occurs when the soil in Zone II compresses rather than developing a plastic shear state as shown in Figure 5-3(b). For this reason, the soil in Zone III is not engaged in the failure mechanism. Individual shear failure surfaces typically do not reach the ground surface. Failure is not sudden, and tilting does not occur. Settlements are usually substantial, and plastic equilibrium is only partially developed.

As shown in Figure 5-3(c), the dense or stiff soils associated with general shear failure develop q_{ult} at low strain or settlement. The ultimate bearing capacity is well-defined. In constrast, the local shear mechanism in loose or soft soils results in large strains and settlements. Because much of the movement is associated with the compressibility of the soil, the magnitude of q_{ult} is much less distinct.

Punching shear is dominated by compression of the soil below and vertical shear along the sides of the footing (Vesic 1973). Little to no movement occurs in the soil adjacent

to the footing. Considerations of settlement will control when punching shear is the dominant bearing capacity failure mode. The term punching shear is also used by some to refer to the case of a footing punching through a thin layer of stiff consistency or dense soil into a soft consistency or loose soil below. This mechanism is discussed in Section 5-3.6.

As indicated by Figure 5-3(d), the general shear mechanism applies mostly to dense soils at relatively shallow depths. At lower relative densities and greater footing depths, the failure mode transitions through local failure to punching shear. The bearing capacity theories discussed in Section 5-3.1.2 assume a general shear failure mechanism. Methods to account for local shear are discussed in Section 5-3.1.3.

5-3.1.1 Shear Strength for Bearing Capacity Analysis.

Bearing capacity is controlled by the shear strength of the soil. The type of shear strength parameters used in bearing capacity analyses depends on the field loading condition, soil type, and groundwater level. Loads are typically applied to foundations over a period of time, such as when a building or a bridge is under construction. This loading condition may represent drained or undrained loading depending on the type of soil being loaded and the length of time required to apply the load.

In clean sands and gravels, drainage is almost instantaneous and does not practically depend on how long it takes to build the structure. These soils only require effective stress analysis unless dynamic loading is anticipated. If substantial fines are present, the possibility of developing an undrained condition should be considered.

In contrast, substantial time is required for excess pore pressures to dissipate in fine-grained soils after loading. These soils usually require undrained analysis for conditions at the end of loading as well as for any rapid or dynamic loading. In some cases, long-term effective stress conditions should also be checked. For example, the drained bearing capacity of heavily overconsolidated clays often controls the design.

Laboratory and field testing methods to determine shear strength parameters for most soil types are summarized in the Prologue. For bearing capacity analysis, effective strength parameters (ϕ', c') should be used for long-term conditions in all soil types. For saturated fine-grained soils, the use of undrained shear strength (s_u) with $\phi = 0$ is appropriate. Undrained shear strength parameters (ϕ, c) should be used for unsaturated soils with low permeability, including coarse-grained soils with substantial fines.

5-3.1.2 Calculation of Ultimate Bearing Capacity.

Bearing capacity is a complex phenomenon that cannot be modeled exactly. Multiple equations have been developed to estimate the ultimate bearing capacity of soil. These equations are based on the upper and lower bound theorems of plasticity and include

the work of Prandtl (1920), Terzaghi (1943), Meyerhof (1951), Brinch Hansen (1970), and Vesic (1973, 1975). In their basic form, the equations apply to general shear failure below a continuous strip footing of width, B, with soil shear strength governed by the Mohr-Coulomb failure criterion. The basic bearing capacity solutions also assume vertical loading, a horizontal bearing surface, foundation depth less than the width, and a horizontal ground surface. Methods to address other variations of these factors are discussed in Section 5-3.3.

In most methods, the bearing capacity problem is simplified by replacing the soil above the bearing elevation with an equivalent surcharge as shown in Figure 5-4(a). This conservatively neglects the shear strength of the soil above the foundation depth. Alternatively, Meyerhof (1951) assumed that the failure surface continued to the ground surface and replaced the triangular wedge with equivalent stresses, p_0 and s_0. Meyerhof's geometry is shown in Figure 5-4(b). Basic formulations also assume that the groundwater table is deeper than the failure zone.

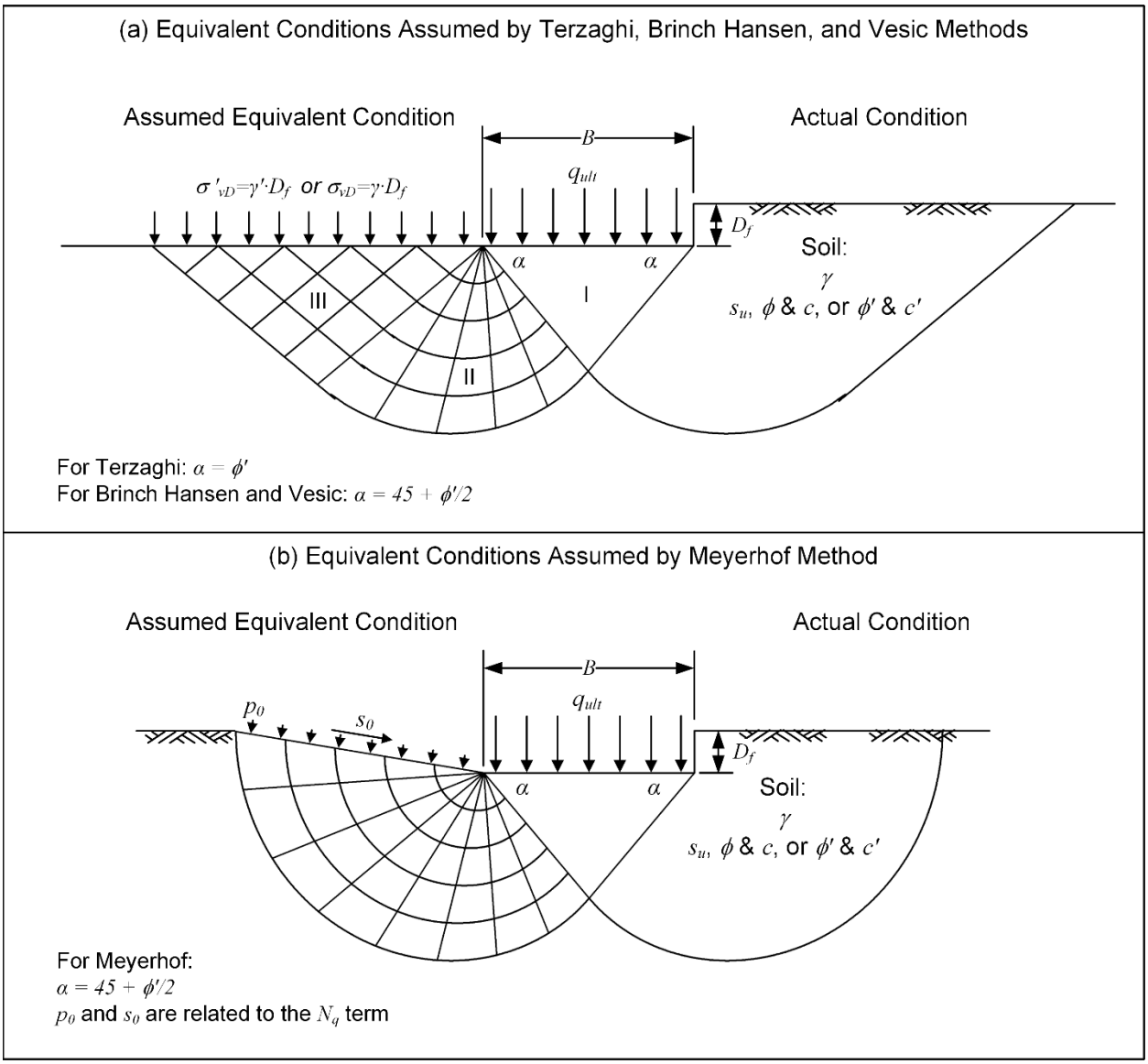

Figure 5-4 Assumptions for Bearing Capacity of a Continuous Footing - a) Terzaghi, Brinch Hansen, and Vesic Methods and b) Meyerhof Method

With these assumptions, the bearing capacity problem can be separated into three distinct terms or superimposed sources of bearing resistance. The first term is connected to the cohesion (or undrained shear strength) along the failure surface and has a bearing capacity factor, N_c. The second term is related to the surcharge and has a bearing capacity factor, N_q. The third term is related to the weight of the soil above the failure surface and has a bearing capacity factor, N_γ.

For effective stress or drained analysis, the ultimate bearing capacity of the soil is:

$$q_{ult} = c' N_c \Psi_c + \sigma'_{zD} N_q \Psi_q + 0.5 \gamma B N_\gamma \Psi_\gamma \quad (5\text{-}15)$$

where:
c' = effective stress cohesion,
ϕ' = effective stress friction angle,
γ = average effective unit weight of soil between D_f and $D_f + B$,
σ'_{zD} = effective vertical stresss at the bearing elevation,
N_c, N_q, N_γ = bearing capacity factors that depend on the effective friction angle, ϕ', and
Ψ_c, Ψ_q, Ψ_γ, = factors used to correct for complicating effects (see Section 5-3.3).

For undrained conditions in unsaturated soils, the ultimate bearing capacity is:

$$q_{ult} = c \cdot N_c \Psi_c + \sigma_{zD} N_q \Psi_q + 0.5 \gamma B N_\gamma \Psi_\gamma \quad (5\text{-}16)$$

where:
c = undrained cohesion,
ϕ = undrained friction angle,
γ = average total unit weight of soil between D_f and $D_f + B$,
σ_{zD} = total vertical stresss at the bearing elevation, and
N_c, N_q, N_γ = bearing capacity factors that depend on the total stress friction angle, ϕ.

For undrained conditions in saturated soils, the ultimate bearing capacity is:

$$q_{ult} = s_u N_c \Psi_c + \sigma_{zD} \Psi_q \quad (5\text{-}17)$$

where:
s_u = undrained cohesion,
σ_{zD} = total vertical stresss at the bearing elevation, and
N_c = bearing capacity factor for $\phi = 0$.

The bearing capacity factors depend on the friction angle of the soil because it controls the shape of the failure surface. Three methods are provided herein to determine the bearing capacity factors. The values are provided in Table 5-2 for the Terzaghi (1943), Meyerhof (1951), and Brinch Hansen (1970) methods. The factors provided by Vesic (1973) are nearly identical to those proposed by Meyerhof and Hansen. The factors can also be determined from the plots or equations provided in Figure 5-5.

Table 5-2 Bearing Capacity Factors, N_c, N_q, and N_γ

ϕ (deg)	N_c		N_q		N_γ		
	Terzaghi	*Meyerhof & Brinch Hansen*	*Terzaghi*	*Meyerhof & Brinch Hansen*	*Terzaghi*	Meyerhof	*Brinch Hansen*
0	5.7	5.14	1.0	1.0	0	0	0.00
2	6.3	5.6	1.2	1.2	0.15	0.01	0.01
4	7.0	6.2	1.5	1.4	0.31	0.04	0.05
6	7.7	6.8	1.8	1.7	0.51	0.11	0.11
8	8.6	7.5	2.2	2.1	0.74	0.21	0.22
10	9.6	8.4	2.7	2.5	1.0	0.37	0.39
12	11	9.3	3.3	3.0	1.4	0.60	0.6
14	12	10.	4.0	3.6	1.9	0.92	1.0
16	14	12	4.9	4.3	2.5	1.4	1.4
18	15	13	6.0	5.3	3.3	2.0	2.1
20	18	15	7.4	6.4	4.4	2.9	2.9
21	19	16	8.3	7.1	5.1	3.4	3.5
22	20	17	9.2	7.8	5.9	4.1	4.1
23	22	18	10.	8.7	6.8	4.8	4.9
24	23	19	11	9.6	7.9	5.7	5.7
25	25	21	13	11	9.2	6.8	6.8
26	27	22	14	12	11	8.0	7.9
27	29	24	17	13	12	9.5	9.3
28	32	26	18	15	15	11	11
29	34	28	20	16	17	13	13
30	37	30.	22	18	20	16	15
31	40	33	25	21	24	19	18
32	44	35	29	23	28	22	21
33	48	39	32	26	33	26	24
34	53	42	37	29	40	31	29
35	58	46	41	33	47	37	34
36	64	51	47	38	57	44	40
37	70	56	54	43	68	53	47
38	78	61	62	49	82	64	56
39	86	68	71	56	100	77	67
40	96	75	81	64	120	94	80
41	110	84	94	74	150	110	95
42	120	94	110	85	180	140	110
43	130	110	130	99	230	170	140
44	160	120	150	120	280	210	170
45	170	130	170	130	350	260	200
46	200	150	200	160	440	330	250
47	220	170	240	190	550	410	300
48	260	200	290	220	700	530	370
49	300	230	350	270	890	670	460
50	350	270	420	320	1150	870	570

Notes:
Terzaghi (1943) only provided N_γ values for 0, 34, and 48 degrees. In addition, the method for determining $K_{P\gamma}$ involves complex graphical procedures. The values provided in this table have been calculated using an approximation by Coduto et al. (2016).
Values for large friction angles have been rounded to limit implied accuracy.

Various studies have compared the bearing capacity methods to full-scale loading test data (e.g. Milovic 1965, Bowles 1996). The comparisons focused on foundations with D_f / B less than one and L / B less than four. Recommendations for the suitability of the various methods are provided in Table 5-3.

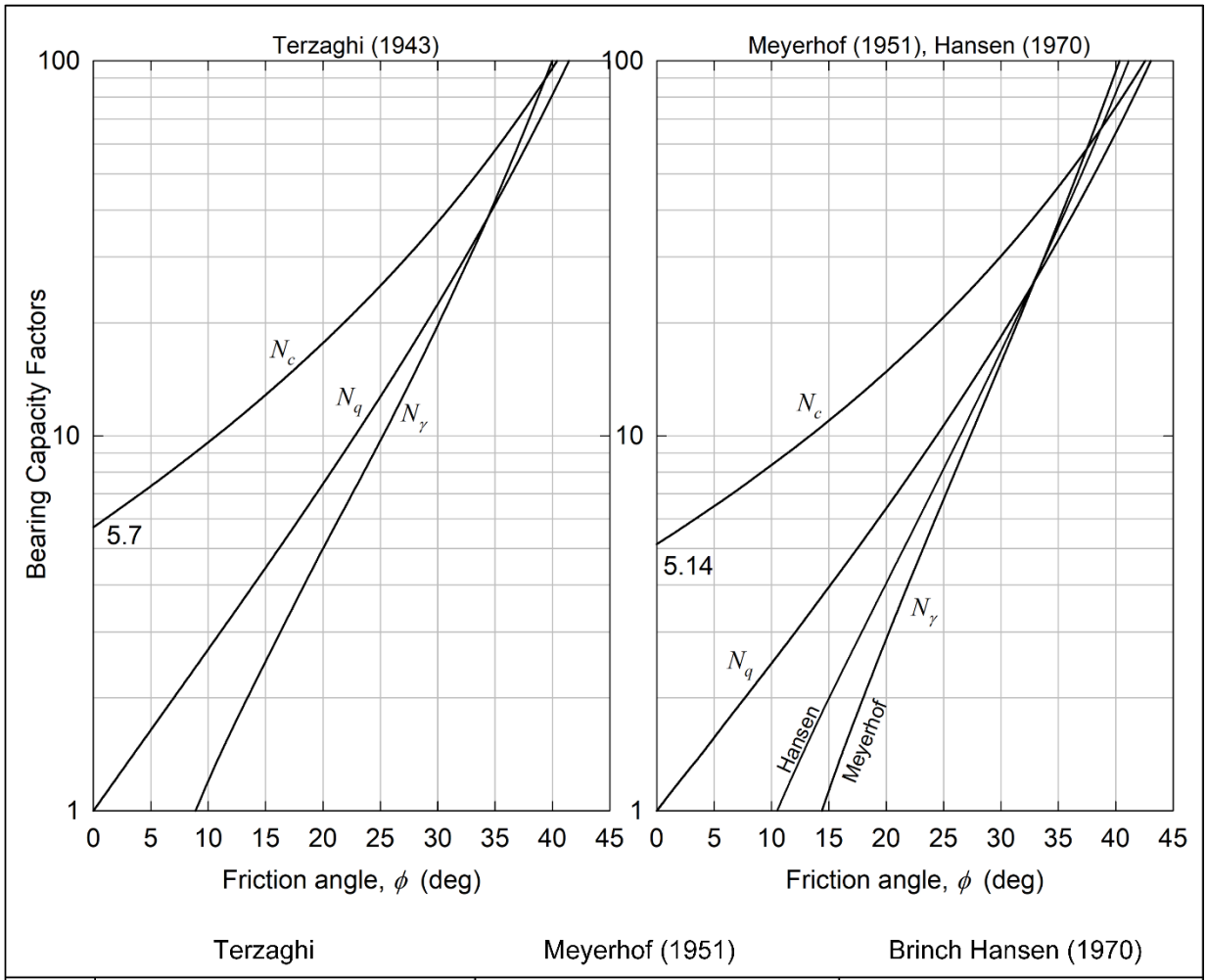

	Terzaghi	Meyerhof (1951)	Brinch Hansen (1970)
N_γ	$N_\gamma = \left(\frac{\tan\phi'}{2}\right)\left(\frac{K_{P\gamma}}{\cos^2\phi'} - 1\right)$	$N_\gamma = \left(N_q - 1\right)\tan\left(1.4\phi'\right)$	$N_\gamma = 1.5\left(N_q - 1\right)\tan\left(\phi'\right)$
N_q	$N_q = \frac{e^{2\pi\left(0.75-\phi'/360\right)\tan\phi'}}{2\cos^2\left(45+\phi'/2\right)}$	$N_q = \tan^2\left(45+\phi'/2\right)e^{\pi\tan\phi'}$	
N_c $\phi = 0$	$N_c = 5.7$	$N_c = 5.14$	
N_c $\phi > 0$	$N_c = \left(N_q - 1\right)\cot\phi'$		

Note: Either ϕ or ϕ' can be used in these equations. Angles should be entered in degrees.
Terzaghi's N_γ value can be approximated as: $N_\gamma \approx [2(N_q+1)\tan\phi'] / [1+0.4\sin(4\phi')]$

Figure 5-5 Bearing Capacity Factors
(after Terzaghi 1943, Meyerhof 1951, Brinch Hansen 1970, Coduto et al. 2016)

Table 5-3 Suitability of Terzaghi, Meyerhof, and Brinch Hansen Methods to Calculate q_{ult} (after Bowles 1996)

Method	Applicability	Comments
Terzaghi	Undrained conditions soils where $D_f / B \leq 1$. Do not use for footings with inclined load, on slopes, or with tilted bases.	Most accurate for soils with shear strength dominated by cohesive parameters (i.e., high s_u or c')
Meyerhof	Any bearing capacity conditions, except footings with a tilted base, including footings with $D_f / B > 1$.	Use with soils with shear strength dominated by frictional parameters (high ϕ'). Also reasonably accurate for soils with higher cohesive shear strength.
Hansen	Any bearing capacity conditions including footings with $D_f / B > 1$.	

5-3.1.3 Bearing Capacity Corrections for Local and Punching Shear.

As noted in the introduction to this section, the bearing capacity theories assume a general shear failure mode, which is only appropriate for dense and/or stiff soils. For most soils, a local or punching shear mechanism is more appropriate. In these cases, settlement considerations will almost always control the allowable bearing pressure and an accurate determination of the ultimate bearing capacity is less important. A variety of methods to approximate local shear have been proposed. A few of the more common approaches are summarized in Table 5-4.

Table 5-4 Bearing Capacity Methods for Local Shear

Local Shear Method	Application	Comments
Constant reduction of shear strength parameters (Terzaghi 1943)	Use c^* and ϕ^* to calculate q_{ult}: $c^* = 0.67\ c'$ $\phi^* = \tan^{-1}(0.67 \tan \phi')$	Probably too conservative for sands. Doesn't account for transitional behavior with D_r. May be unsafe in some cases (Vesic 1973).
Variable reduction of shear strength parameters based on relative density (D_r) (Vesic 1973)	Use c^* and ϕ^* to calculate q_{ult}: $c^* = R \cdot c'$ $\phi^* = \tan^{-1}(R \cdot \tan \phi')$ For $D_r < 0.67$, $R = 0.67 + D_r - 0.75 D_r^2$ For $D_r > 0.67$, $R = 1$	Allows for transitional behavior between local and general shear. Based on limited test results by Vesic (1973).
Compressibility factors based on rigidity index (Vesic 1973)	Calcualte rigidity index based on footing dimensions, soil properties, and stress conditions.	See Vesic (1973) for detailed description.

5-3.2 Groundwater Correction.

Groundwater correction is required when the groundwater table is higher than one footing width below the bearing elevation. Groundwater correction is only required for drained (effective stress) analysis. Groundwater is considered by changing the unit weight used in the bearing capacity calculations. The three possible cases are shown in Figure 5-6. These cases assume hydrostatic conditions (i.e., no seepage forces exist).

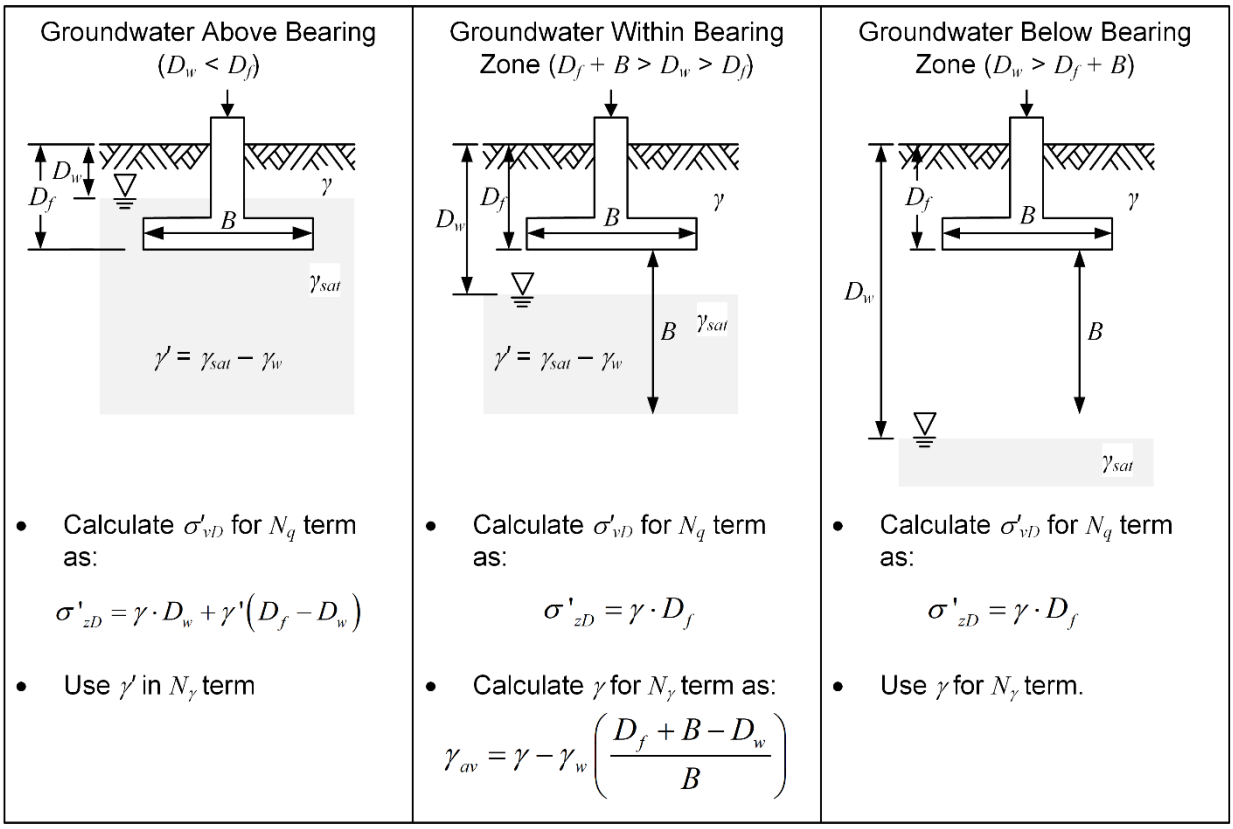

Figure 5-6 Effects of Groundwater Table on Bearing Capacity Calculations

For undrained analysis, total unit weights are used without regard to the position of the groundwater table.

Uplift is present on the base of the foundation when the groundwater table is above the bearing elevation. Its effect on the bearing pressure can be conservatively ignored unless sliding or uplift is a concern.

5-3.3 Methods to Account for Complicating Effects.

Multiple aspects of a foundation design can affect the bearing capacity that are not included in the basic solutions presented in Section 5-3.1.2. These include foundation shape and depth, load inclination, base inclination, and ground inclination. A shallow foundation with all three inclinations is illustrated in Figure 5-7.

The correction methods in the following sections are based on both theoretical considerations and empirical evidence. For this reason, the correction factors cannot usually be applied across methods, i.e., Meyerhof corrections should be used only with the Meyerhof bearing capacity factors. In addition, care should be taken combining many corrections within a given method. If bearing capacity controls a design with

multiple complicating factors, numerical analysis is likely warranted. Limit equilibrium slope stability analysis can be used to analyze strip foundations on slopes.

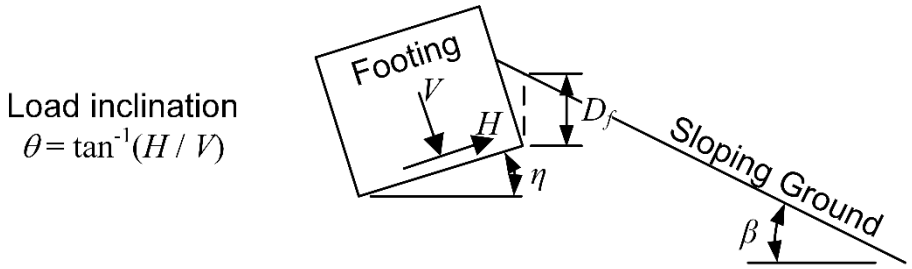

Figure 5-7 Shallow Foundation with Inclined Load, Base, and Ground (after Brinch Hansen 1970)

Lumped correction factors for complicating effects (Ψ_c, Ψ_q, and Ψ_γ) were included in Eqn. 5-15 to 5-17. In most cases, these factors are found by multiplying factors for individual effects, such that:

$$\Psi_c = s_c \cdot d_c \cdot i_c \cdot b_c \cdot g_c \quad (5\text{-}18),$$

$$\Psi_q = s_q \cdot d_q \cdot i_q \cdot b_q \cdot g_q \quad (5\text{-}19),$$

and

$$\Psi_\gamma = s_\gamma \cdot d_\gamma \cdot i_\gamma \cdot b_\gamma \cdot g_\gamma \quad (5\text{-}20),$$

where:
s_c, s_q, s_γ = shape factors,
d_c, d_q, d_γ = depth factors,
i_c, i_q, i_γ = load inclination factors,
b_c, b_q, b_γ = sloping base factors, and
g_c, g_q, g_γ = sloping ground factors.

As discussed in Section 5-2.3, foundations are sometime eccentrically loaded. Eccentricity affects the bearing capacity as well as the bearing pressure. The most common approach is to use the equivalent dimensions, B' and L' (Eqn. 5-8 and 5-9), to determine the shape factors. The B' dimension should also be used in the N_γ term to calculate bearing capacity. Conservatively, the actual dimensions should be used to calculate the depth factors.

5-3.3.1 Terzaghi (1943) Method.

Shape is the only complicating factor considered by the Terzaghi upper bound method. The factors are listed in Table 5-5. In some cases, interpolation can be used between

the shape factors for square and continuous foundations. The other factors should be set equal to 1 in Eqn. 5-18 to 5-20.

Table 5-5 Shape Factors for the Terzaghi Upper Bound Method

Method	Shape	Analysis Condition	Shape Factors		
			s_c	s_q	s_γ
Terzaghi	Continuous	Any	1	1	1
	Square	Any	1.3	1	0.8
	Circular	Any	1.3	1	0.6

5-3.3.2 Meyerhof (1963) Method.

Meyerhof (1963) presents shape, depth, and load inclination factors, which are summarized in Table 5-6. The laboratory experiments used to develop the inclination factors indicated that the shape factors tend toward one under inclined load. In other words, it is safe to assume that $s_c = s_q = s_\gamma = 1$ if load inclination is present.

Meyerhof (1963) did not provide base or inclination factors in this form. Meyerhof developed a separate solution for sloping ground that is discussed briefly in Section 5-3.4.

Table 5-6 Bearing and Correction Factors for the Meyerhof (1963) Method

Factor	Analysis Condition	c Factor	q Factor	γ Factor
Bearing	$\phi = 0°$	$N_c = 5.14$	$N_q = K_P \cdot e^{\pi \cdot \tan(\phi')}$	$N_\gamma = (N_q - 1) \cdot \tan(1.4\phi')$
	$\phi' > 10°$	$N_c = (N_q - 1)\cot(\phi')$		
Shape[A]	$\phi = 0°$	$s_c = 1 + 0.2(B/L) \cdot$	$s_q = 1$	$s_\gamma = 1$
	$\phi' > 10°$	$s_c = 1 + 0.2(B/L) \cdot K_P$	$s_q = 1 + 0.1(B/L) \cdot K_P$	$s_\gamma = 1 + 0.1(B/L) \cdot K_P$
Depth	$\phi = 0°$	$d_c = 1 + 0.2\ k\ (K_P)^{0.5}$	$d_q = 1$	$d_\gamma = 1$
	$\phi' > 10°$		$d_q = 1 + 0.1\ k\ (K_P)^{0.5}$	$d_\gamma = 1 + 0.1\ k\ (K_P)^{0.5}$
Inclined Load[B]	All	$i_c = (1 - 2\theta / \pi)^2$	$i_q = (1 - 2\theta / \pi)^2$	$i_\gamma = (1 - \theta / \phi')^2$

Angles are expressed in radians for consistency.
B = width; L = Length; ϕ' = drained friction angle; ϕ = undrained friction angle; $K_P = \tan^2(\pi/4 + \phi'/2)$, $k = D_f / B$
H = horizontal component of load, V = vertical component of load; $\theta = \tan^{-1}(H / V) < \phi'$ (in radians)

[A] Use B/L = 1 for circle. Do not combine factors for shape and inclined load.

5-3.3.3 Brinch Hansen (1970) Method.

The Brinch Hansen (1970) method allows the most complicating factors to be considered. For this reason, it is more complex than the other methods. Similar to Meyerhof, the shape factors are adjusted for inclined loading.

Brinch Hansen considered conditions for undrained shear strength ($\phi = 0$) separately. The $\phi = 0$ factors are summarized in Table 5-7. An important difference is that the lumped correction factor is additive, yielding:

$$\Psi_{c,BH,\phi=0} = \left(1 + s_c + d_c - i_c - b_c - g_c\right) \tag{5-21}$$

where:
$\Psi_{c,BH,\phi=0}$ = Brinch Hansen correction factor for N_c term for $\phi = 0$ analysis.

Table 5-7 Bearing and Correction Factors for the Brinch Hansen (1970) Method – $\phi = 0$

Brinch Hansen	***c* Factor**	***q* Factor**
Bearing	$N_c = 5.14$	$N_q = 1$
Shape - (vertical load)	$s_c = 0.2(B/L)$	No correction $\Psi_q = 1$
Shape - (inclined load)	$s_{cB} = 0.2 i_{cB} \cdot (B/L)$, $s_{cL} = 0.2 i_{cL} \cdot (L/B)$	
Depth	$d_c = 0.4\,k$	
Inclined Load	$i_c = 0.5 - 0.5[1\text{-}H / (A' \cdot C_a)]^{0.5}$	
Inclined Base	$b_c = \eta / (\pi / 2 + 1)$	
Inclined Ground	$g_c = \beta / (\pi / 2 + 1)$	
Angles are expressed in radians for consistency. For $D_f / B < 1$: $k = D_f / B$. For $D_f / B \geq 1$: $k = \tan^{-1}(D_f / B)$ in radians H = horizontal component of load; C_a = base adhesion; A' = equivalent bearing area		

The Brinch Hansen factors for unsaturated undrained ($\phi > 0$) and drained conditions are summarized in Table 5-8. Brinch Hansen did not provide factors for the N_c term. Three options are available to address this shortcoming:

- Use Brinch Hansen's alternative bearing capacity equation, which is provided in the notes to Table 5-8,
- Ignore the contribution of the N_c term, which is often an appropriately conservative assumption, or
- Use the c factors provided in Table 5-8, which are based on the relationship between N_c and N_q (Hansen 1961, de Beer 1970).

For vertical loading, the bearing capacity of a rectangular foundation is controlled by the narrower dimension (B). However, load inclination may cause the longer dimension to control. The direction of the horizontal loading should be considered when calculating the inclination factors in Table 5-7 and Table 5-8. The direction of the inclination factor

affects the shape factors. Bearing capacity should be checked in both directions for a rectangular foundation with inclined loading.

The development of Brinch Hansen's method does not clearly consider the interaction between inclined ground and the other factors. Caution should be used with the Brinch Hansen g factors for cases with inclined ground steeper than 2H:1V or $D_f / B > 1$.

Table 5-8 Bearing and Correction Factors for the Brinch Hansen (1970) Method – $\phi' > 0$

Factor	c Factor[C]	q Factor	γ Factor
Bearing	$N_c = (N_q - 1)\cot(\phi')$	$N_q = \tan^2(\pi+\phi'/2)e^{\pi\cdot\tan(\phi')}$	$N_\gamma = 1.5\cdot(N_q - 1)\cdot\tan(\phi')$
Shape[A] (vertical load)	$s_c = 1+(B/L)(N_q / N_c)\cos(\phi')$	$s_q = 1 + \sin(\phi')(B/L)\cdot$	$s_\gamma = 1 - 0.4(B/L)$
Shape[A] (inclined load)	$s_c = 1+(B/L)(N_q/N_c)\cos(\phi')i_c$	$s_{qB} = 1 + \sin(\phi')(B/L)\cdot i_{qB}$ $s_{qL} = 1 + \sin(\phi')(L/B)\cdot i_{qL}$	$s_{\gamma B} = 1 - 0.4(B/L)(i_{\gamma B} / i_{\gamma L}) \geq 0.6$ $s_{\gamma L} = 1 - 0.4(L/B)(i_{\gamma L} / i_{\gamma B}) \geq 0.6$
Depth[B]	$d_c = 1+ k\cdot(1-\sin\phi')^2(N_q/N_c)$	$d_q = 1+2\,k\cdot\tan\phi'\cdot(1-\sin\phi')^2$	$d_\gamma = 1$
Inclined Load	$i_c = \dfrac{i_q N_q - 1}{N_q - 1}$	$i_q = \left[1 - \dfrac{0.5H}{V + A'C_a\cot\phi'}\right]^5$	$i_\gamma = \left[1 - \dfrac{\left(0.7 - \eta/2.5\pi\right)H}{V + A'C_a\cot\phi'}\right]^5$
Inclined Base	Not provided.	$b_q = \exp(-2\cdot\eta\cdot\tan\phi')$	$b_\gamma = \exp(-2.7\cdot\eta\cdot\tan\phi')$
Inclined Ground	Not provided.	$g_q = (1 - 0.5\tan\beta)^5$	$g_\gamma = (1 - 0.5\tan\beta)^5$

Angles are expressed in radians for consistency.

B = equivalent width; L = equivalent length; ϕ' = drained friction angle; ϕ = undrained friction angle; H = horizontal component of load; V = vertical component of load; C_a = base adhesion; A' = equivalent bearing area

[A] Use B/L = 1 for circle.

[B] For $D_f / B < 1$: $k = D_f / B$. For $D_f / B \geq 1$: $k = \tan^{-1}(D_f / B)$ in radians

[C] Shape, depth, and factors have been determined based on the q factors using correspondence formula found in Brinch Hansen (1961) and de Beer (1970). This approach is not appropriate for the inclined base and ground factors. Brinch Hansen did not provide c factors for $\phi' > 0$ but presented the following equivalent form of the bearing capacity equation:

$$q_{ult} = \left(\sigma'_{vD} + c'\cot\phi'\right) N_q \Psi_q - c'\cot\phi' + 0.5\gamma B N_\gamma \Psi_\gamma$$

This equation does not require c factors but only applies to conditions with no ground inclination.

5-3.4 Foundations Near the Top of Slopes.

In some cases, foundations must be placed near slopes, which may reduce the bearing capacity of the soil. Many procedures have been proposed with varying levels of complexity. The solutions by Leshchinsky and Xie (2017) and Meyerhof (1957) have been selected for their relative simplicity and general applicability using the geometry summarized in Figure 5-8. These solutions are for strip foundations and can be used as a conservative estimate for rectangular foundations. The shape factors from Section 5-3.3 may be appropriate but have not be fully explored by numerical or laboratory testing.

Saturated undrained conditions and drained conditions are considered separately in this section. The Leshchinsky and Xie (2017) approach ignores the effects of embedment, which is an appropriately conservative assumption if the foundation is relatively close to the slope. The depth factors in Table 5-6 to Table 5-8 do not include slope effects and should not be included. A comprehensive method that incorporates embedment depth can be found in Yang et al. (2019). The Yang et al. method can accommodate any combination of shear strength parameters. Slope stability software can also model foundation loading and can be used to explore this condition in more detail.

<table>
<tr>
<td>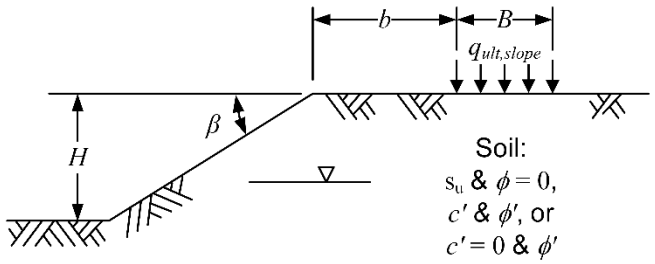
</td>
<td>Saturated, undrained soil:
$q_{ult,slope} = 5.14 \cdot s_u RC_{slope}$
See Table 5-9 for values of RC_{slope}.</td>
</tr>
<tr>
<td>Drained c'-ϕ' or undrained c-ϕ soil:
$q_{ult,slope} = \left[c' N_c + 0.5 \cdot \gamma \cdot B \cdot N_\gamma \right] RC_{slope}$
See Table 5-10 for values of RC_{slope}.
Use Meyerhof / Brinch Hansen value of N_q (Figure 5-5) to calculate $N_\gamma = 2(N_q + 1) \tan \phi'$.
Use average effective unit weight to account for groundwater. See Section 5-3.2.</td>
<td>Drained $c' = 0$ soil (Meyerhof 1957):
$q_{ult,slope} = 0.5 \cdot \gamma \cdot B \cdot N_{\gamma,slope}$
See Figure 5-9 for values of $N_{\gamma,slope}$.
Use average effective unit weight to account for groundwater. See Section 5-3.2.</td>
</tr>
</table>

Figure 5-8 Foundations Near the Top of Slopes (After Meyerhof 1957, Leshchinsky and Xie 2017)

5-3.4.1 Saturated Undrained Conditions.

For saturated undrained conditions (s_u, $\phi = 0$), the effect of the slope tends to be small unless the foundation is close to the slope ($b/B < 2.5$) or the slope is steep ($\beta > 30°$). The influence of the stability of the slope on bearing capacity can be incorporated using a stability number defined as:

$$N_S = \frac{\gamma \cdot H}{s_u} \tag{5-22}$$

where:
γ = total unit weight of the soil,

H = slope height, and
s_u = undrained shear strength of the soil.

The ultimate bearing capacity for foundations near slopes is calculated using a reduction coefficient (RC_{slope}) as indicated in Figure 5-8. Table 5-9 provides values of RC_{slope} based on foundation dimensions (B/H), distance from the slope (b/B), slope angle (β), and slope stability number (N_S) (Leschinsky and Xie 2017). Interpolation should be used to determine RC_{slope} for intermediate conditions. For steeper slopes or larger b/B, Leshchinsky and Xie (2017) should be consulted.

Table 5-9 Bearing Capacity Reduction Coefficients for Foundations Near Slopes in Undrained Conditions (after Leshchinsky and Xie 2017)

B/H	b/B	RC_{slope} for $N_s = \gamma H / s_u = 0$			RC_{slope} for $N_s = \gamma H / s_u = 2$			RC_{slope} for $N_s = \gamma H / s_u = 4$		
		$\beta = 0°$	$\beta = 30°$	$\beta = 60°$	$\beta = 0°$	$\beta = 30°$	$\beta = 60°$	$\beta = 0°$	$\beta = 30°$	$\beta = 60°$
0.2	0	1	0.8	0.59	1	0.78	0.56	1	0.76	0.52
	1.25	1	1	0.85	1	0.97	0.79	1	0.95	0.54
	2.5	1	1	1	1	1	0.92	1	1	0.53
0.4	0	1	0.77	0.57	1	0.73	0.49	1	0.63	0.30
	0.63	1	0.83	0.73	1	0.83	0.59	1	0.66	0.30
	1.25	1	0.94	0.83	1	0.92	0.66	1	0.71	0.33
	1.88	1	1	0.92	1	1	0.72	1	0.75	0.39
	2.5	1	1	1	1	1	0.79	1	0.79	0.46
1	0	1	0.76	0.56	1	0.62	0.37	1	0.40	0.16
	0.25	1	0.80	0.63	1	0.66	0.43	1	0.43	0.20
	0.5	1	0.83	0.69	1	0.70	0.49	1	0.44	0.24
	0.75	1	0.87	0.74	1	0.74	0.55	1	0.46	0.29
	1.0	1	0.90	0.79	1	0.77	0.60	1	0.48	0.32
	1.25	1	0.92	0.83	1	0.81	0.65	1	0.50	0.36
	1.5	1	0.95	0.86	1	0.84	0.70	1	0.53	0.39
	1.75	1	0.97	0.90	1	0.87	0.74	1	0.56	0.42
	2.0	1	0.98	0.93	1	0.90	0.78	1	0.61	0.47
	2.5	1	1	0.96	1	0.95	0.85	1	0.65	0.60

5-3.4.2 Drained Conditions.

For drained conditions, the effect of the slope on bearing capacity can be more significant. The reduction in bearing capacity depends on the effective stress friction angle in addition to similar factors as the undrained case. Table 5-10 summarizes reduction coefficients for common conditions encountered in engineering practice where $c' > 0$. Coefficients for $B/H = 2$ and other slope angles are available in Leshchinsky and Xie (2017). For conditions with $c' = 0$, the Meyerhof (1957) method presented at the end of this section can be used.

For soils modeled using an effective stress cohesion intercept, a stability number is required to incorporate its influence as:

$$N_S = \frac{\gamma \cdot H}{c'} \tag{5-23}$$

where:
γ = unit weight of the soil considering groundwater effects (Section 5-3.2),
H = slope height, and
c' = undrained shear strength of the soil.

Table 5-10 Bearing Capacity Reduction Coefficients for Foundations Near Slopes in Saturated Drained Conditions (after Leshchinsky and Xie 2017)

B/H	b/B	RC_{slope} for $N_s = \gamma H / c' = 0$						RC_{slope} for $N_s = \gamma H / c' = 2$					
		$\phi' = 20°$		$\phi' = 30°$		$\phi' = 40°$		$\phi' = 20°$		$\phi' = 30°$		$\phi' = 40°$	
		β=10°	β=30°	β=10°	β=30°	β=10°	β=30°	β=10°	β=30°	β=10°	β=30°	β=10°	β=30°
0.2	0	0.91	0.62	0.84	0.52	0.77	0.4	0.89	0.58	0.81	0.46	0.71	0.34
	0.5	0.88	0.68	0.83	0.57	0.76	0.43	0.87	0.65	0.81	0.52	0.73	0.38
	1.25	0.92	0.77	0.86	0.63	0.78	0.48	0.92	0.75	0.85	0.6	0.77	0.44
	2.5	0.97	0.88	0.9	0.72	0.81	0.54	0.98	0.89	0.92	0.73	0.83	0.53
	5	1	1	0.99	0.88	0.88	0.65	1	1	1	0.95	0.93	0.72
	10	1	1	1	1	0.99	0.84	1	1	1	1	1	1
	15	1	1	1	1	1	1	1	1	1	1	1	1
0.4	0	0.88	0.64	0.83	0.53	0.76	0.43	0.61	0.61	0.77	0.38	0.77	0.38
	0.5	0.91	0.7	0.85	0.58	0.78	0.47	0.91	0.68	0.81	0.44	0.81	0.44
	1.25	0.93	0.76	0.87	0.63	0.8	0.51	1	0.75	0.82	0.49	0.82	0.49
	2.5	1	0.9	0.93	0.74	0.84	0.59	1	0.94	0.92	0.62	0.92	0.62
	5	1	1	1	0.9	0.91	0.71	1	1	1	0.82	1	0.82
	10	1	1	1	1	1	0.89	1	1	1	1	1	1
	15	1	1	1	1	1	0.96	1	1	1	1	1	1
1.0	0	0.88	0.48	0.83	0.46	0.78	0.58	0.71	0.34	0.77	0.38	0.78	0.48
	0.5	0.91	0.7	0.86	0.64	0.79	0.71	0.73	0.38	0.81	0.44	0.81	0.66
	1.25	0.93	0.76	0.87	0.68	0.8	0.73	0.77	0.44	0.82	0.49	0.84	0.69
	2.5	1	0.9	0.93	0.78	0.86	0.76	0.83	0.53	0.92	0.62	0.92	0.78
	5	1	1	1	0.92	0.93	0.8	0.93	0.72	1	0.82	1	0.9
	10	1	1	1	1	1	0.94	1	1	1	1	1	1
	15	1	1	1	1	1	0.98	1	1	1	1	1	1
Note: $RC_{slope} = 1$ for for conditions without a slope (β = 0°).													

As indicated in Figure 5-8, the reduced bearing capacity is found by multiplying RC_{slope} with q_{ult} for non-sloping conditions with no embedment. The largest reductions in bearing capacity occur for foundations with low b/B ratios and steep slopes.

The reduction coefficients provided in Table 5-10 are for N_S less than 2, which indicates relatively high values of c'. Leshchinsky and Xie also provide coefficients for $N_s = 4$. For these higher stability numbers, the stability of the slope itself is likely controlling, or the situation is dominated by frictional strength and it may be appropriate to ignore the effects of c'.

When c' is absent or ignored, the chart solution provided by Meyerhof (1957) can be used and is provided in Figure 5-9. Meyerhof provided factors ($N_{\gamma,slope}$) for embedment effects for $D_f/B = 1$ and recommended interpolation for intermediate embedment ratios. As indicated in Figure 5-8, the N_q term is not used to calculate bearing capacity because its contribution is included in the values of $N_{\gamma,slope}$.

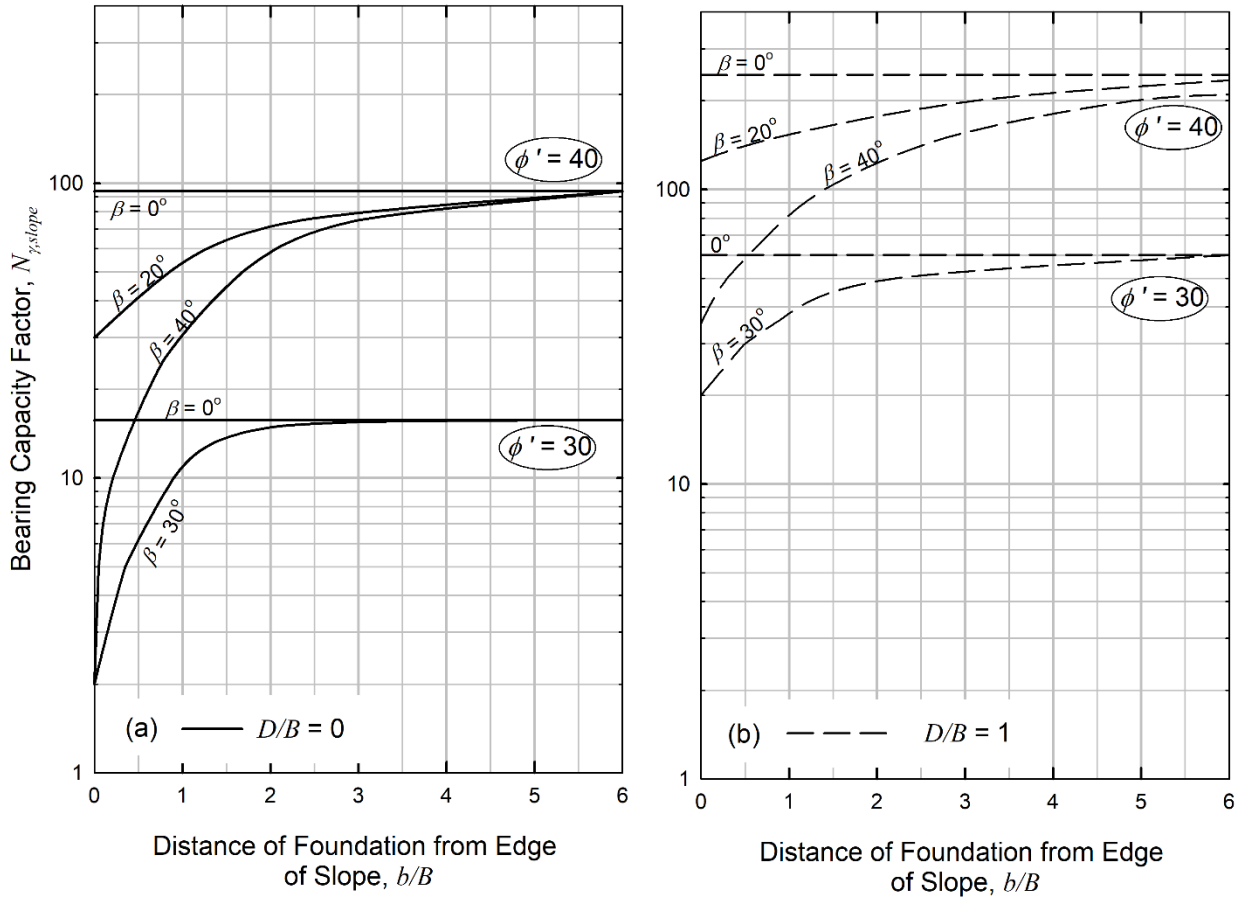

Figure 5-9 Bearing Capacity Factors for Strip Footing for $c' = 0$ Conditions – a) No Embedment and b) $D_f / B = 1$ (after Meyerhof 1957)

5-3.5 Bearing Capacity Examples.

Figure 5-10 to Figure 5-12 provide detailed examples of the application of the Terzaghi, Meyerhof, and Brinch Hansen methods for bearing capacity analysis. They illustrate the use of shape, depth, and inclination factors. Eccentricity calculations using both the Meyerhof and Brinch Hansen approaches are provided in Figure 5-13.

Problem Statement: Estimate the ultimate and allowable bearing pressure using the Terzaghi Method and check with the Meyerhof method

Project and Site Details

Three-story Building
100 ft by 200 ft
Column Q = 180 kips
Estimated q_{all}=5000 psf

Very stiff clay (CH)
s_u = 2000 psf based on five SPT borings (Average N = 20)
γ_t = 130 pcf (assumed)
Groundwater at depth of 3 ft

Trial Foundation Size

$$AREA = \frac{Q}{q_{all}} = \frac{180{,}000\,lb}{5000\,psf} = 36\,ft^2$$

$$B = \sqrt{AREA} = \sqrt{36\,ft^2} = 6\,ft$$

Trial Design

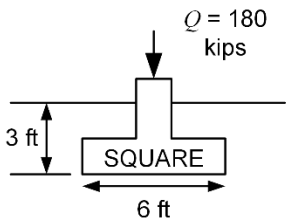

Terzaghi Method

Bearing capacity factors for ϕ = 0 deg:

$$N_c = 5.7,\ N_q = 1,\ N_\gamma = 0$$

Vertical stress at foundation level:

$$\sigma_{zD} = D_f \gamma_t = (3\,ft)(130\,pcf) = 390\,psf$$

Ultimate bearing capacity:

$$q_{ult} = s_c s_u N_c + qN_q + \tfrac{1}{2} s_\gamma \gamma_t B N_\gamma$$
$$= (1.3)(2000\,psf)(5.7) + (390\,psf)(1) + 0$$
$$= 14{,}820 + 390 = 15{,}210\,psf$$

Allowable bearing pressure:
(Use F = 3 because s_u estimated from SPT)

$$q_{all,net} = \frac{15{,}210\,PSF}{3} - 390\,psf = 4680\,psf$$

Meyerhof Method (Check)

Bearing capacity factors for ϕ = 0 deg:

$$N_c = 5.14,\ N_q = 1,\ N_\gamma = 0$$

Shape, depth, and lumped factors:

$$s_c = 1 + 0.2\left(\tan^2(45 + 0/2)\right) = 1.2,\ d_c = 1 + 0.2\left(\frac{3\,ft}{6\,ft}\right) = 1.1$$

$$\Psi_c = (1.2)(1.1) = 1.32$$

$$s_q = 1,\ d_q = 1$$

$$\Psi_q = (1)(1) = 1$$

Ultimate bearing capacity:

$$q_{ult} = s_u N_c \Psi_c + \sigma_{zD} N_q \Psi_q + \tfrac{1}{2} s_\gamma d_\gamma \gamma_t B N_\gamma$$
$$= (2000\,psf)(5.14)(1.32) + (390\,psf)(1) + 0$$
$$= 13{,}570 + 390 = 13{,}960\,psf$$

$$q_{ult,net} = 13{,}960 - 390 = 13{,}570\,psf$$

Check Factor of Safety with q_{all} = 5000 psf:

$$F = \frac{13{,}570\,psf}{5000\,psf} = 2.71$$

The net allowable bearing pressure calculated with the Terzaghi method is lower than 5000 psf. Similarly, the factor of safety found by Meyerhof's method is less than 3. Thus, the proposed foundation dimensions may be slightly small based on the design requirements. Consideration should be given to increasing B or refining the value of s_u based on shear strength testing.

Figure 5-10 Example Calculations Illustrating the Terzaghi Method with the Meyerhof Method Used as a Check

Problem Statement: Estimate the ultimate and allowable bearing pressure using the Meyerhof method for both the vertical and inclined loads

Project and Site Details

One-Story Building - 200 × 600 ft,
Column Loads of 60 kips,
One Inclined with θ = 15 deg

Medium Dense Silty Sand
N_{ave} = 10 based on 21 borings (20 ft deep)
Groundwater at depth of 6 ft
Assumed Parameters: ϕ' = 30 deg, c' = 0 psf
Measured: γ_t = 120 pcf

Trial Designs

Estimated q_{all} = 2000 psf

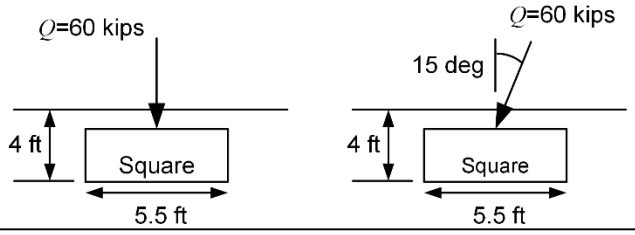

Meyerhof Method – Vertical Load

Bearing Capacity Factors for ϕ' = 30 deg: $N_q = 18.4, N_\gamma = 15.7$

Vertical Stress at Foundation Level: $\sigma_{zD} = D_f \gamma_t = (4\,ft)(120\,pcf) = 480\,psf$

Groundwater within B below bearing
Interpolate to Determine Average Unit Weight: $\gamma_{ave} = 120\,pcf - (62.4)\dfrac{(4+5.5-6\,ft)}{5.5\,ft} = 80.3\,pcf$

Shape and Depth Factors:

$$s_q = s_\gamma = 1 + 0.1\left(\tan^2(45+30/2)\right) = 1.30$$

$$d_q = d_\gamma = 1 + 0.1(4\,ft/5.5\,ft)\left(\tan(45+30/2)\right) = 1.12$$

$$\Psi_q = \Psi_\gamma = (1.3)(1.12) = 1.456$$

Ultimate Bearing Capacity:
(No Cohesion Term)

$$q_{ult} = \sigma_{zD} N_q \Psi_q + 0.5\gamma_{ave} B N_\gamma \Psi_\gamma$$
$$= (480\,psf)(18.4)(1.456) + (0.5)(80.3\,pcf)(5.5\,ft)(15.7)(1.456)$$
$$= 12,859 + 5,048 = 17,907\,psf$$

Net Allowable Bearing Pressure:
(Use F = 3 because ϕ' estimated from SPT)

$$q_{all,net} = \frac{17907\,psf}{3} - 480\,psf = 5,489\,psf > 2,000\,psf$$

Meyerhof Method – Inclined Load

Bearing capacity factors and depth factors are unchanged. Shape factors are not used.

Inclination Factors: $i_q = \left(1 - 15^\circ/90^\circ\right)^2 = 0.69 \qquad i_\gamma = \left(1 - 15^\circ/30^\circ\right)^2 = 0.25$

Lumped Factors: $\Psi_q = (0.69)(1.12) = 0.773 \qquad \Psi_\gamma = (0.25)(1.12) = 0.28$

Ultimate Bearing Capacity:
(No Cohesion Term)

$$q_{ult} = \sigma_{zD} N_q \Psi_q + 0.5\gamma_{ave} B N_\gamma \Psi_\gamma$$
$$= (480\,psf)(18.4)(0.773) + 0.5(80.3\,pcf)(5.5\,ft)(15.7)(0.28)$$
$$= 6,827 + 970 = 7,797\,psf$$

Allowable Bearing Pressure:
(Use F = 3 because ϕ' estimated from SPT)

$$q_{all,net} = \frac{7,797\,psf}{3} - 480 = 2,119\,psf > 2,000\,psf$$

The column foundation design is appropriate because q_{all} exceeds the design bearing pressure.

Figure 5-11 Example Calculations Illustrating the Meyerhof Method

Problem Statement: Estimate the Ultimate and Allowable Bearing Pressure Using the Brinch-Hansen Method for Both the Vertical and Inclined Loads

Project and Site Details

One-Story Building - 200 × 600 ft,
Column Loads of 60 kips,
One Inclined with θ = 15 deg

Medium Dense Silty Sand
N_{ave} = 10 based on 21 borings (20 ft deep)
Groundwater at Depth of 6 ft
Assumed Parameters: ϕ' = 30 deg, c' = 0 psf
Measured: γ_t = 120 pcf

Trial Designs

Estimated q_{all} = 2000 psf

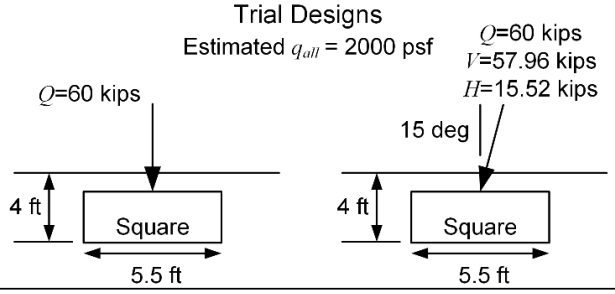

Brinch-Hansen Method – Vertical Load

Bearing Capacity Factors for ϕ' = 30 deg:

$$N_q = 18.4,\ N_\gamma = 15$$

Vertical Stress at Foundation Level:

$$\sigma_{zD} = D_f \gamma_t = (4\,ft)(120\,pcf) = 480\,psf$$

Groundwater within B below Bearing Surface
Interpolate to Determine Average Unit Weight:

$$\gamma_{ave} = 120\,pcf - 62.4\,pcf\left(\frac{(5.5+4-6\,ft)}{5.5\,ft}\right) = 80.3\,pcf$$

Shape and Depth Factors:

$$s_q = 1+\sin(30) = 1.50,\qquad s_\gamma = 0.6$$

$$d_q = 1+2(4\,ft/5.5\,ft)\tan(30)(1-\sin(30))^2 = 1.21,\qquad d_\gamma = 1$$

$$\Psi_q = (1.5)(1.21) = 1.82,\qquad \Psi_\gamma = (0.6)(1) = 0.6$$

Ultimate Bearing Capacity:
(No Cohesion Term)

$$q_{ult} = \sigma_{zD} N_q \Psi_q + 0.5\gamma_{ave} B N_\gamma \Psi_\gamma$$
$$= (480\,psf)(18.4)(1.82) + (0.5)(80.3\,pcf)(5.5\,ft)(15)(0.6)$$
$$= 16,074 + 1,987 = 18,061\,psf$$

Allowable Bearing Pressure:
(Use F = 3 because ϕ' estimated from SPT)

$$q_{all,net} = \frac{18061\,psf}{3} - 480\,psf = 5540\,psf > 2,000\,psf$$

Brinch-Hansen Method – Inclined Load

Bearing capacity factors and depth factors are unchanged.

Inclination and Shape Factors:
(η = 0 deg, c_a = 0)

$$i_q = \left[1-0.5\left(\frac{15.52k}{57.96k}\right)\right]^5 = 0.487 \qquad i_\gamma = \left[1-\left(\left(0.7-\frac{\eta}{450^\circ}\right)\left(\frac{15.52k}{57.96k}\right)\right)\right]^5 = 0.354$$

$$s_q = 1+\sin(30)(5.5/5.5)\cdot 0.487 = 1.24 \qquad s_\gamma = 1-0.4(5.5/5.5) = 0.6$$

$$\Psi_q = (0.487)(1.24)(1.1) = 0.73 \qquad \Psi_\gamma = (0.354)(0.6) = 0.212$$

Ultimate Bearing Capacity:
(No Cohesion Term)

$$q_{ult} = \sigma_{zD} N_q \Psi_q + 0.5\gamma_{ave} B N_\gamma \Psi_\gamma$$
$$= (480\,psf)(18.4)(0.73) + 0.5(80.3\,pcf)(5.5\,ft)(15)(0.212)$$
$$= 6447 + 702 = 7149\,psf$$

Allowable Bearing Pressure:
(Use F = 3 because ϕ' estimated from SPT)

$$q_{all,net} = \frac{7419\,psf}{3} - 480\,psf = 1903\,psf < 1,916\,psf = \frac{57960\,lb}{(5.5\,ft)^2}$$

The column foundation design is appropriate for the vertical load. For the inclined load, the bearing pressure is greater than the net allowable bearing pressure. The size of the footing should be increased for the inclined load.

Figure 5-12 Example Calculations Illustrating the Brinch Hansen Method

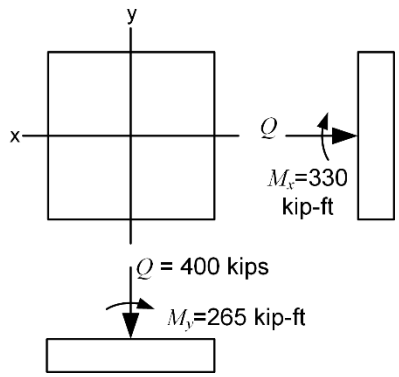

Find eccentricity and allowable bearing pressure using Meyerhof and Brinch Hansen methods

- Square Footing, B = 10 ft
- Silty Sand, γ_t = 120 pcf
- Estimated ϕ' = 30 deg
- Estimated c'=0
- D_f = 6 ft
- Groundwater at 20 ft Depth

Eccentricity

$$e_L = \frac{M_y}{Q} = \frac{265k-ft}{400k} = 0.662\,ft$$

$$e_B = \frac{M_x}{Q} = \frac{330k-ft}{400k} = 0.825\,ft$$

$$\frac{6(0.662\,ft)}{10\,ft} + \frac{6(0.825\,ft)}{10\,ft} = 0.892 < 1$$

$$B' = 10 - 2(.825) = 8.35\,ft$$

$$L' = 10 - 2(0.662) = 8.68\,ft$$

Meyerhof Method

Equivalent Area:

$$A' = B'L' = (8.35\,ft)(8.68\,ft) = 72.48\,ft^2$$

Bearing Capacity Factors for ϕ' = 30 deg:

$$N_q = 18.4,\ N_\gamma = 15.7$$

Vertical Stress at Foundation Level:

$$\sigma_{zD} = D_f\gamma_t = (6\,ft)(120\,pcf) = 720\,psf$$

Shape and Depth Factors:
(Using B' and L')

$$s_q = s_\gamma = 1 + 0.1(8.35/8.68)\left(\tan^2(45+30/2)\right) = 1.29$$

$$d_q = d_\gamma = 1 + 0.1(6\,ft/8.35\,ft)\left(\tan(45+30/2)\right) = 1.12$$

$$\Psi_q = \Psi_\gamma = (1.29)(1.12) = 1.44$$

Ultimate Bearing Capacity:
(No Cohesion Term)
(Using B' for B)

$$q_{ult} = \sigma_{zD}N_q\Psi_q + 0.5\gamma_{ave}BN_\gamma\Psi_\gamma$$
$$= (720\,psf)(18.4)(1.44)$$
$$+ (0.5)(120\,pcf)(8.35\,ft)(15.7)(1.29)$$
$$= 19,077 + 11,326 = 30,403\,psf$$

Allowable Bearing Pressure:
(Use F = 3 because ϕ' estimated from SPT)

$$q_{all,net} = \frac{30,403\,psf}{3} - 720 = 9,414\,psf$$

Applied Bearing Pressure:
(Using Equivalent Area)

$$q_{applied} = \frac{400,000lb}{72.48\,ft^2} = 5,519\,psf < 9,414\,psf$$

Brinch-Hansen Method

Bearing Capacity Factors for ϕ' = 30 deg:

$$N_q = 18.4,\ N_\gamma = 15$$

Shape and Depth Factors:
(Using B' and L')

$$s_q = 1 + \sin(30)(8.35/8.68) = 1.381,\quad s_\gamma = 1 - 0.4(0.962) = 0.615$$

$$d_q = 1 + 2(6\,ft/8.35\,ft)(\tan(30))(1-\sin 30)^2 = 1.21,\quad d_\gamma = 1$$

$$\Psi_q = (1.381)(1.21) = 1.67,\quad \Psi_\gamma = (0.615)(1) = 0.615$$

Ultimate Bearing Capacity:
(No Cohesion Term)
(Using B' for B)

$$q_{ult} = (720\,psf)(18.4)(1.67) + (0.5)(120\,pcf)(8.35\,ft)(15)(0.615)$$
$$= 22,124 + 4,621 = 26,745\,psf$$

Allowable Bearing Pressure:
(Use F = 3 because ϕ' estimated from SPT)

$$q_{all,net} = \frac{26,745\,psf}{3} - 720 = 8,195\,psf > 5,519\,psf$$

The column foundation design is appropriate because $q_{all,net}$ exceeds the applied bearing pressure (either method).

Figure 5-13 Eccentricity Calculations – Meyerhof and Brinch Hansen Methods

5-3.6 Nonuniform Soil and Layered Stratigraphy.

Soil conditions are rarely uniform as assumed by the bearing capacity theories. For example, clays are often modeled using an undrained shear strength that increases with depth. Layered soils may present a problem for bearing capacity analysis when the strength of the two layers differs significantly. Layering must be considered when the top of the lower layer is above the maximum depth of general shear failure. In this case, both layers contribute to the bearing capacity of the footing. Zone II (Figure 5-4) typically extends to a depth of about $0.85B$ to B below the bearing elevation. Conservatively, this depth has been assumed to equal B for these methods. Four cases can be considered for layered soils as follows:

- Case 1: Undrained – increasing s_u with depth,
- Case 2: Undrained – layered clay,
- Case 3: Undrained – mixed unsaturated soils (c-ϕ), and
- Case 4: Sand (drained, $c' = 0$) over clay (undrained, s_u).

Figure 5-14 illustrates the conditions used for these four cases. Each of these cases is discussed in the following paragraphs.

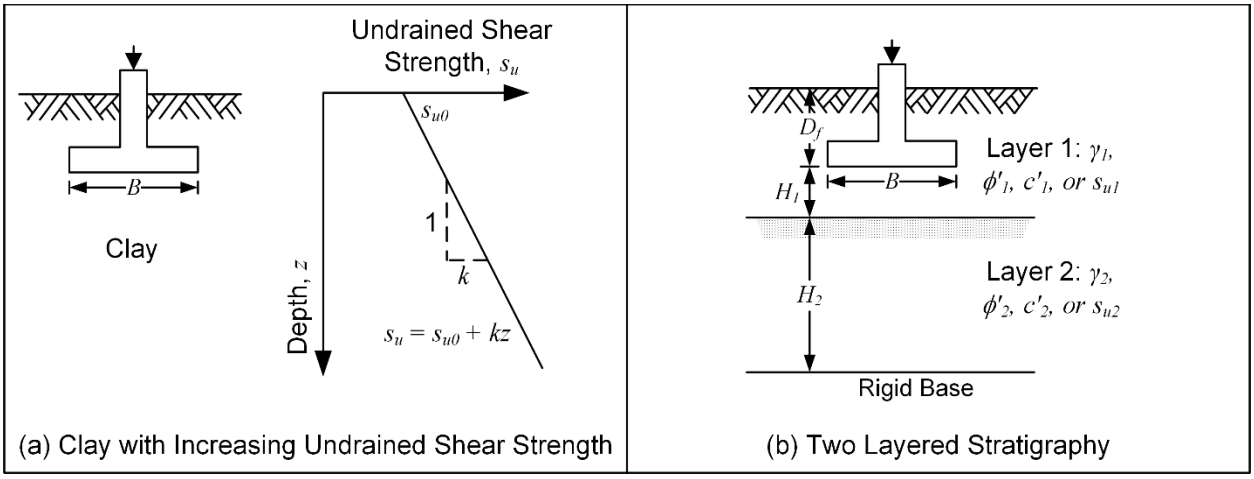

Figure 5-14 Non-uniform and Stratified Soils Conditions – (a) Case 1 and (b) Cases 2 to 4

5-3.6.1 Case 1: Undrained Clay - Increasing s_u with Depth.

Case 1 represents typical strength gain with depth for normally and some overconsolidated clays, as illustrated in Figure 5-14(a). The bearing capacity will increase as a result of increased strength with depth. Davis and Booker (1973) considered this in terms of the undrained strength ratio.

Based on an upper bound plasticity solution, Chi and Lin (2020) suggested that the bearing capacity factor, N_c, for a perfectly smooth strip footing on clay soil with increasing strength with depth can be found as:

$$N_c = 5.14 + \frac{k \cdot B}{s_{u0}} \tag{5-24}$$

where:
s_{u0} = cohesion at surface of clay layer,
B = footing width, and
k = rate of increase in s_u with depth.

Solutions for N_c from Davis and Booker (1973) and Chi and Lin (2020) are plotted in Figure 5-15. Equation 5-22 lies between the solutions for perfectly smooth and perfectly rough footings. Since footings are neither perfectly smooth or perfectly rough, this approach is a good fit for actual footings. Bearing capacity is determined using the calculated value of N_c and s_{u0}. An example is provided in Figure 5-16.

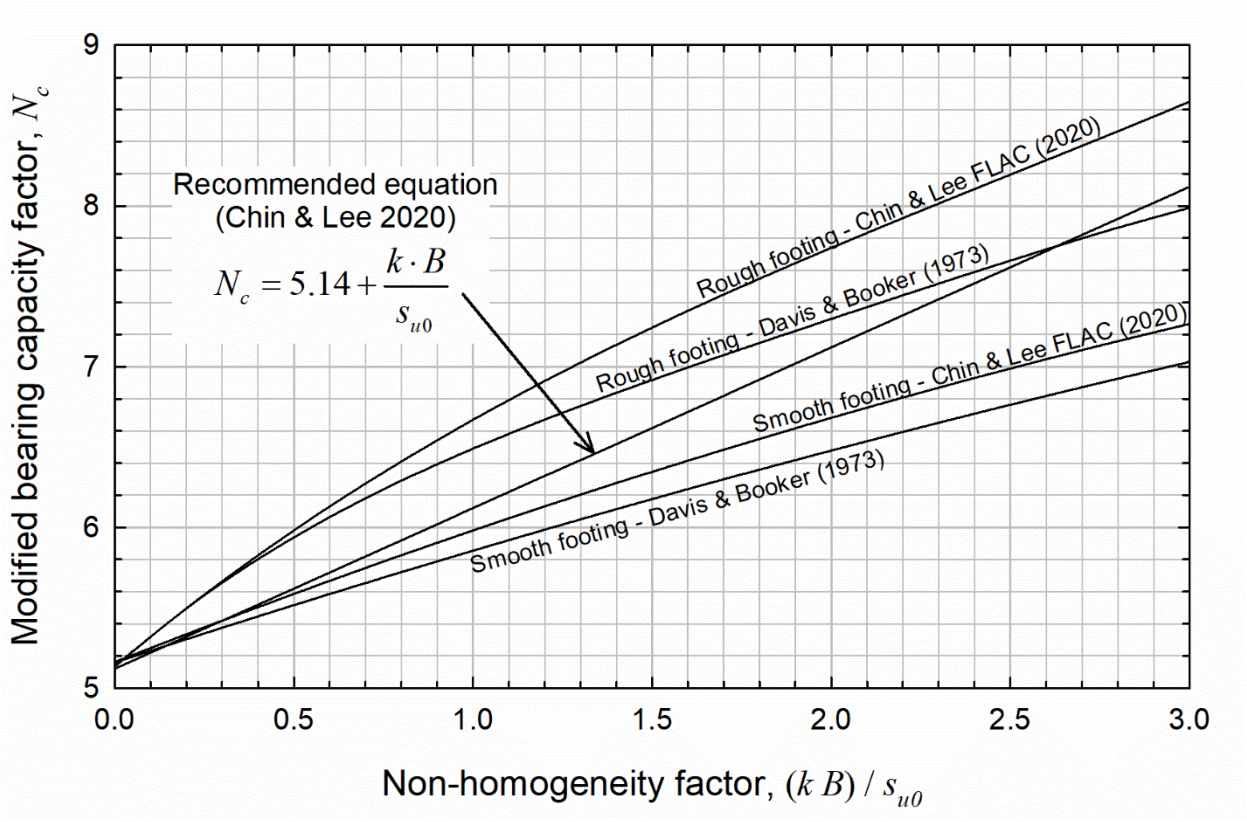

Figure 5-15 Variation of N_c for Clay with Increasing s_u with Depth (after Chi and Lin 2020)

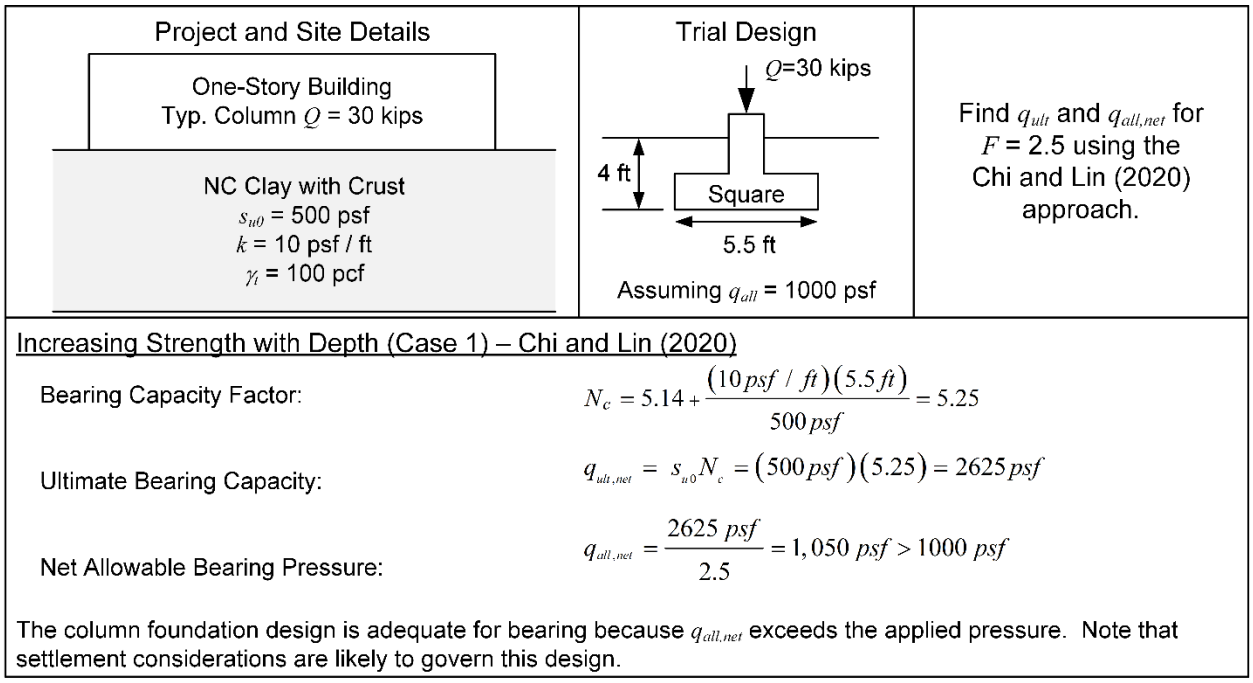

Figure 5-16 Bearing Capacity Example – Increasing Strength with Depth (Case 1)

5-3.6.2 Case 2: Undrained, Layered Clay.

Layered clay stratigraphy occurs often in practice. For example, a younger post-glacial low strength clay may overlay an older stiffer clay. In other cases, a stiffer clay, created by desiccation, may overlay a softer clay. Many researchers have considered this type of layering (e.g., Button 1953, Brown and Meyerhof 1969, Griffiths 1982, Merifield et al. 1999, Zhu 2004, Szypcio and Dołżyk 2006, and Chi and Lin 2020).

When the top layer is softer or weaker than the underlying clay, the failure occurs in the upper soft layer or along the interface of the two layers. This can be illustrated with computer simulations as shown in Figure 5-17(a) (Griffiths 1999). In this case, a classic general shear bearing capacity failure does not occur; rather, a squeezing type failure occurs above or along the boundary. Brown and Meyerhof (1969) presented the relationships shown in Figure 5-18 to estimate modified bearing capacity factors ($N_{c,m,s}$ and $N_{c,m,c}$) for strip and circular footings on two layer clay systems. The right side of the figure is used for conditions where the upper layer is soft. When the top of the strong layer is more than 70% of the foundation width below the bearing elevation ($H/B \geq 0.7$), the bearing capacity is not affected by the presence of the stronger layer. Brown and Meyerhof did not define equations for the right side of Figure 5-18. However, Table 5-11 presents ranges of modified bearing capacity factors for these conditions.

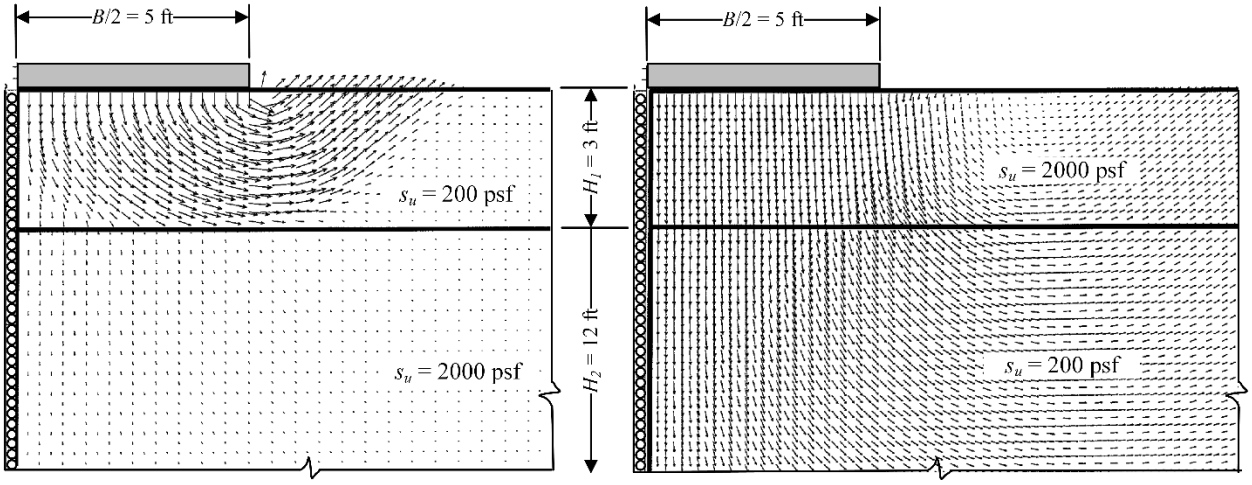

Figure 5-17 Displacement Vectors for a) Soft Over Stiff Clay and b) Stiff Over Soft Clay (after Griffiths 1999)

When the stiffer or stronger layer is on top, the footing tends to punch through the stiff layer into the soft layer developing a general shear failure in the soft clay as shown in Figure 5-17(b). The equations provided in Figure 5-18 can be used when the top layer is stiffer or stronger. The undrained strength of the top layer is used to calculate bearing capacity with these modified bearing capacity factors. When $0.7 < s_{u2}/s_{u1} < 1$, it is prudent to reduce the values of $N_{c,m,s}$ and $N_{c,m,c}$ by 10 percent. When the weak layer is more than three foundation widths below the bearing elevation ($H/B > 3$), the bearing capacity is not affected by the presence of the deeper layer.

For a layered clay soil profile, the modified bearing capacity for a rectangular foundation ($N_{c,m,r}$) can be estimated from the circular and strip factors as:

$$N_{c,m,r} = N_{c,m,c}\left(\frac{B}{L}\right) + N_{c,m,s}\left(1 - \frac{B}{L}\right) \tag{5-25}$$

where:
$N_{c,m,s}$ = modified bearing capacity factor for strip footing - Figure 5-18(a),
$N_{c,m,c}$ = modified bearing capacity factor for circular footing - Figure 5-18(b),
B = rectangular foundation width, and
L = rectangular foundation length.

The effect of overburden (N_q = 1) may be included along with the $N_{c,m}$ factors discussed in this section. Inclined loads were not included in the experiments on which these factors are based. Thus, inclination factors should not be combined with these modified bearing capacity factors. An example is provided in Figure 5-19.

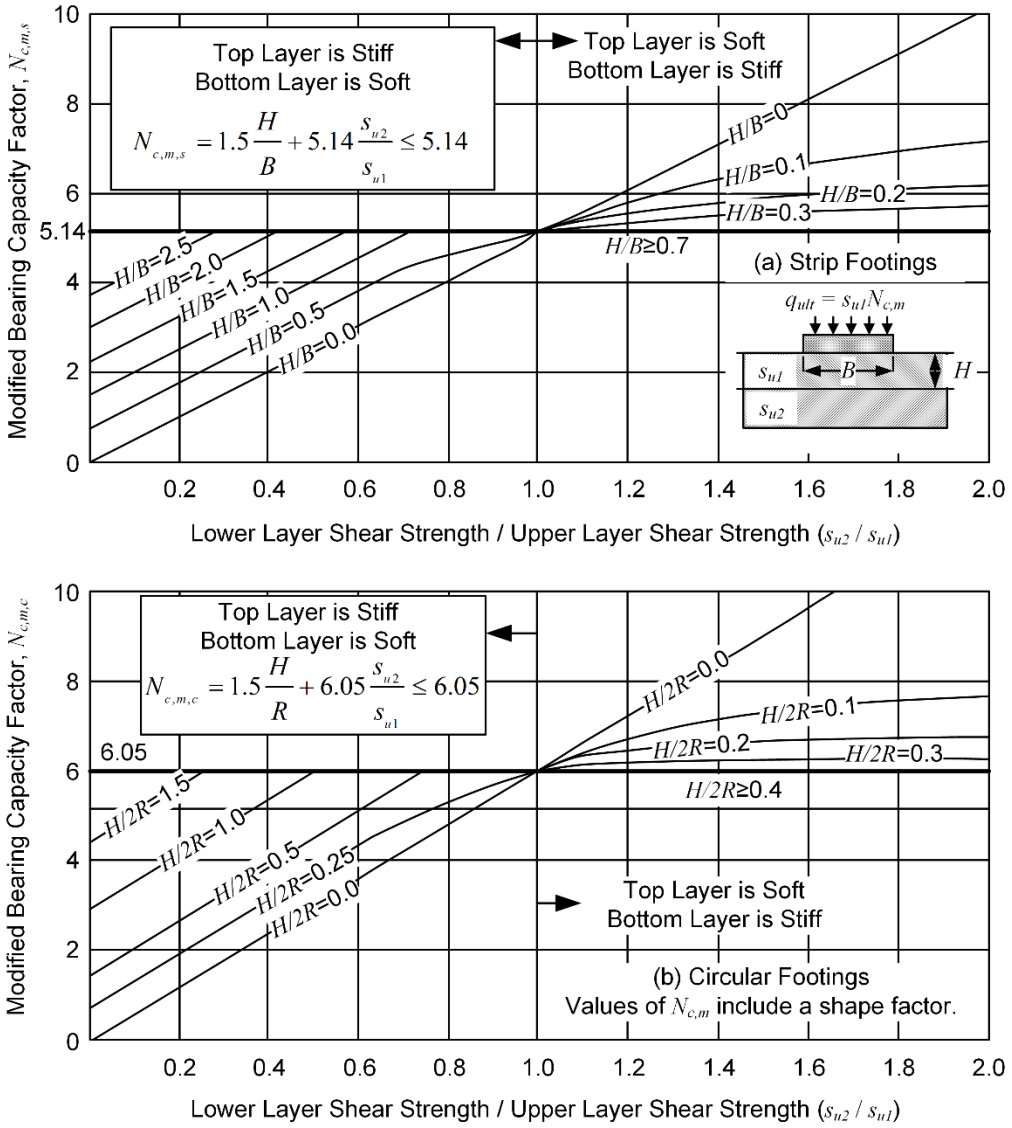

Figure 5-18 Modified Bearing Capacity Factors for Two-Layer Clay Stratigraphy for a) Strip and b) Circular Footings (after Brown and Meyerhof 1969)

Table 5-11 Values of Bearing Capacity Factor, N_{ms}, for Strip Footings (after Brown and Meyerhof 1969, Meyerhof and Hanna 1978, Merifield et al. 1999, and Zhu 2004)

H/B	Values of $N_{c,m,s}$ for Ratios of s_{u2} / s_{u1}						
	0.2	0.5	0.67	1.00	1.5	2.0	5.0
	Stiff over soft			Uniform	Soft over stiff		
0.125	1.2 to 1.4	2.8 to 2.9	3.7 to 3.8	5.14	6.4 to 7.0	6.9 to 8.6	8.2 to 9.4
0.50	1.8 to 2.3	3.5 to 3.7	4.3 to 4.4	5.14	5.2 to 5.3	5.2 to 5.4	5.2 to 5.4
0.75	2.2 to 2.8	4.0 to 4.2	4.6 to 4.9	Little effect of layering			
1.5	3.4 to 4.2	Little effect of layering					

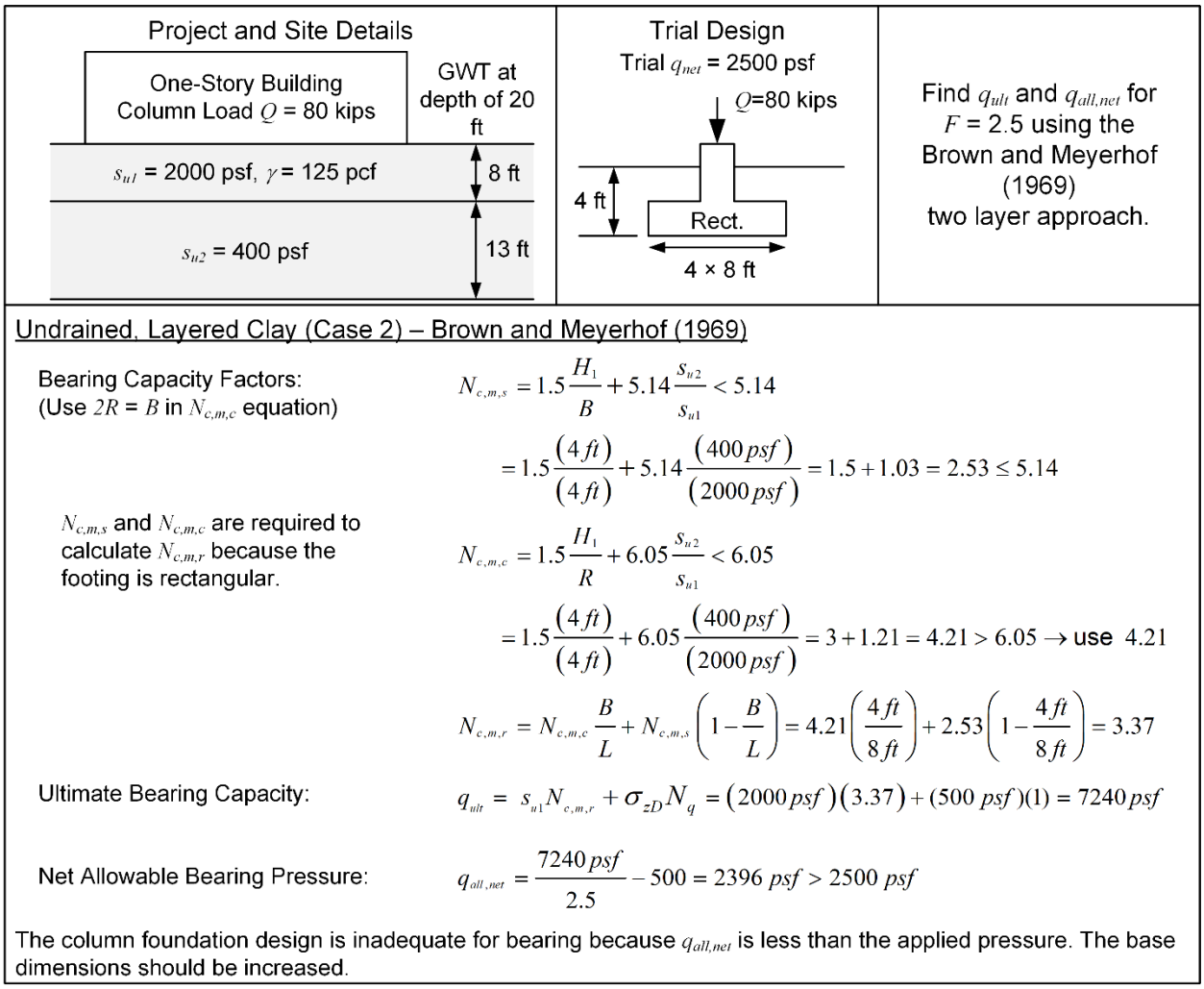

Figure 5-19 Bearing Capacity Example – Layered, Undrained Clay (Case 2)

5-3.6.3 Case 3: Mixed Soil Layers - Unsaturated Undrained.

The bearing capacity of mixed soil profiles of sand and clay can be evaluated using the method by Satyanarayana and Garg (1980). The method was validated using unsaturated, compacted samples and should be considered applicable to unsaturated, undrained conditions characterized by c-ϕ parameters. Unless a rigid boundary is encountered as shown in Figure 5-14(b), the thickness of the second layer is defined as:

$$H_2 = (2B - H_1)\left(\frac{c_1 + \tan\phi_1}{c_2 + \tan\phi_2}\right) \tag{5-26}$$

where:
B = width of strip footing,
H_1 = thickness of top layer below bearing elevation,

c_1, c_2 = undrained cohesion of top and bottom layers, respectively, and
ϕ_1, ϕ_2 = undrained friction angle of top and bottom layers, respectively.

The average shear strength parameters calculated as:

$$c_{ave} = \frac{H_1 c_1 + H_2 c_2}{H_1 + H_2} \tag{5-27}$$

and

$$\phi_{ave} = \tan^{-1}\left[\frac{H_1 \tan\phi_1 + H_2 \tan\phi_2}{H_1 + H_2}\right] \tag{5-28}$$

These parameters should be used with Terzaghi's bearing capacity theory.

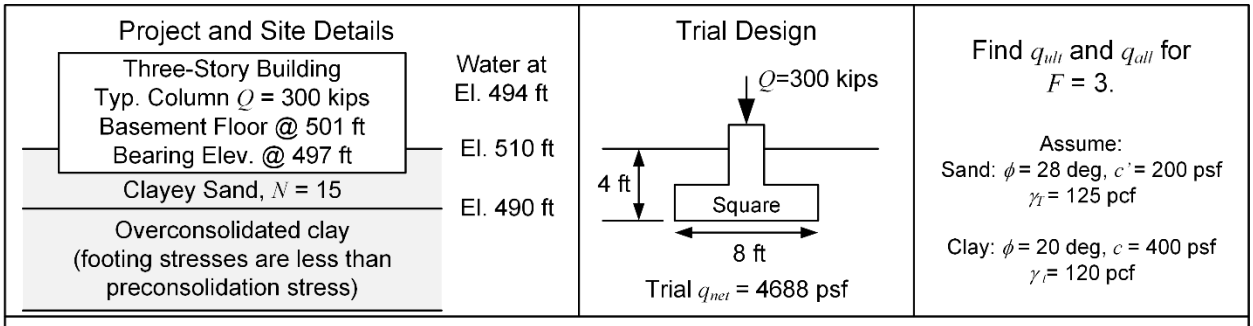

Mixed Soil Layers (Case 3) – Satyanarayana and Garg (1980)

Dimensions:

$$H_1 = 497 - 490 = 7\,ft$$

$$H_2 = (2B - H_1)\left(\frac{c_1 + \tan\phi_1}{c_2 + \tan\phi_2}\right) = (2(8\,ft) - 7\,ft)\left(\frac{200\,psf + \tan(28)}{400\,psf + \tan(20)}\right) = 4.5\,ft$$

Average Strength Parameters:

$$c_{ave} = \frac{(7\,ft)(200\,psf) + (4.5\,ft)(400\,psf)}{7 + 4.5\,ft} = 278\,psf$$

$$\phi_{ave} = \frac{\tan^{-1}((7\,ft)\tan(28) + (4.5\,ft)\tan(20))}{7 + 4.5\,ft} = 25\,\text{deg}$$

Bearing Capacity Factors:
(Use Terzaghi for 25 deg)

$$N_c = 25, N_q = 13, N_\gamma = 9.2$$

Average Unit Weight:

$$\gamma_{ave} = \frac{(125\,pcf)(7\,ft) + (120\,pcf)(4.5\,ft)}{11.5\,ft} = 123\,pcf$$

Ultimate Bearing Capacity:

$$q_{ult} = 1.3(278\,psf)(25) + (4\,ft)(125\,pcf)(13) + 0.4(123\,pcf)(8\,ft)(9.2)$$

$$q_{ult} = 19{,}156\,psf$$

Allowable Bearing Pressure:

$$q_{all,net} = \frac{19{,}156\ psf}{3} - 500\ psf = 5{,}885\ psf > 5000\ psf$$

The column foundation design is adequate for bearing capacity because $q_{all,net}$ exceeds the applied pressure.

Figure 5-20 Bearing Capacity Example – Mixed Soil Layers (Case 3)

5-3.6.4 Case 4: Sand Layer Over Clay.

Meyerhof (1974) investigated shallow foundations on layers of sand and clay. In some cases, surficial layers of sand or coarse-grained soil are underlain by clay. The sand layer may be natural or a layer of engineered fill. Figure 5-21 shows two possibilities. A thin and/or dense layer of sand is depicted on the left, and the bearing capacity failure surface may break through the sand into the clay. A passive force (P_P) develops along the failure surface through the sand, which helps to resist the foundation loading.

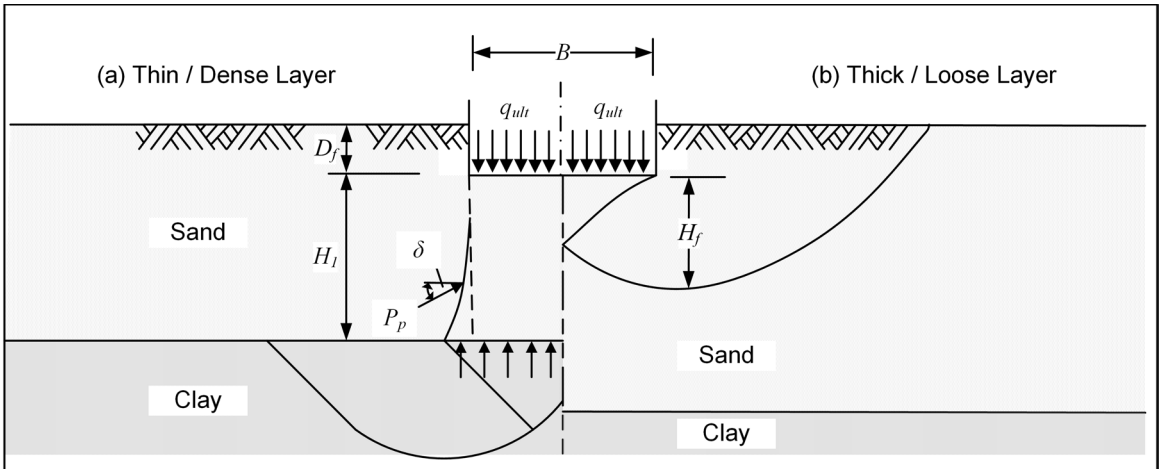

Use the minimum value of the following as q_{ult}:

Strip	$s_u N_c + \gamma H_1^2 \left(1 + \frac{2D_f}{H_1}\right)\left(\frac{K_s \tan\phi'}{B}\right) + \gamma D_f$	$\gamma D_f N_q + 0.5\gamma B N_\gamma$
Circle	$1.2 s_u N_c + 2\gamma H_1^2 \left(1 + \frac{2D_f}{H_1}\right)\left(\frac{s \cdot K_s \tan\phi'}{B}\right) + \gamma D_f$	$\gamma D_f N_q + 0.3\gamma B N_\gamma$

Variables: s_u = undrained strength of the clay, γ = unit weight of sand, ϕ' = sand friction angle, K_s or $s{\cdot}K_s$ = punching shear coefficient, N_c = BC factor for clay, N_q and N_γ = BC factors for sand

Figure 5-21 Bearing Capacity of Sand Over Relatively Weak Clay (after Meyerhof 1974)

When the sand is loose or thick, the bearing capacity failure surface may remain within the sand layer as shown in Figure 5-21(b). The location of the failure depends on the relative density of the sand, the ratio of the footing width to the depth of the sand below the bearing elevation, H_1, and the relative strength of the underlying clay. If both strata have similar individual bearing capacities, the bearing capacity failure surface may extend into the clay.

The coefficients, K_s and $s{\cdot}K_s$, can be estimated using the trends in Figure 5-22. The value of δ/ϕ' is for the inclination of the passive force on the failure surface through the sand as shown in Figure 5-21. Model tests by Meyerhof (1974) and field observations

of full-sized footings indicate that the theoretical trends can be safely used. Meyerhof and Hanna (1978) show that δ/ϕ' increases to 1 as the bearing capacity of the clay approaches the bearing capacity of the sand. An example is provided in Figure 5-23.

If stiff clay or rock lies below the sand, the thin sand layer may squeeze out from under the footing as it fails. The bearing capacity and shape factors applicable to this situation depend on the ratio of H_1 / B, where H_1 is the thickness of the sand layer below the bearing elevation. The modified bearing capacity and shape factors can be found in Figure 5-24 and should be used with Equation 5-15. The bearing capacity calculated using the modified factors should be compared to the bearing capacity of the underlying stiff clay. If the bearing capacity of the clay is lower, it should be used instead.

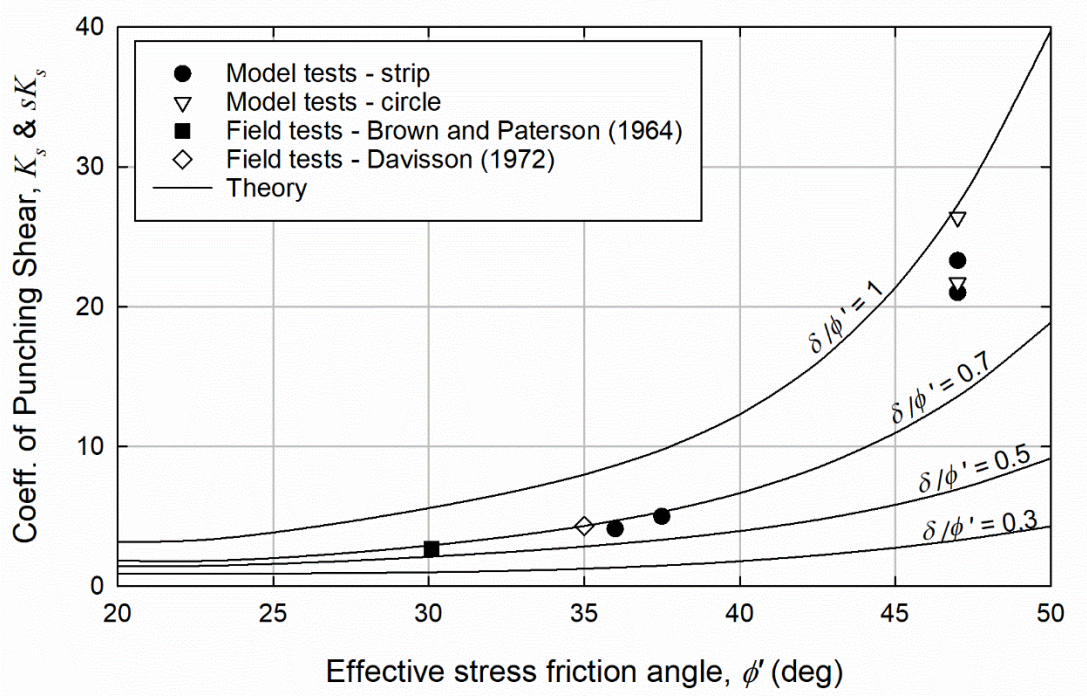

Figure 5-22 Coefficients K_s and $s \cdot K_s$ for Punching Shearing Resistance (after Meyerhof 1974, Meyerhof and Hanna 1978)

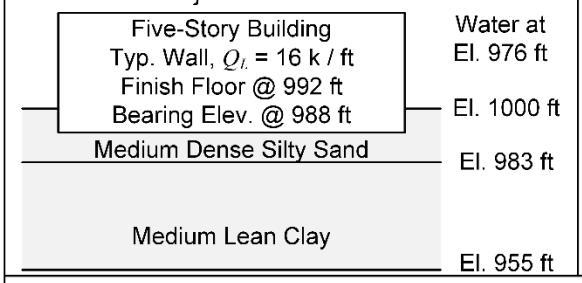

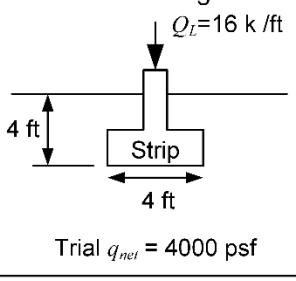

Find q_{ult} and q_{all} for F = 2.5.

Soil Parameters:
Sand: ϕ' = 34 deg, γ_t = 125 pcf

Clay: s_u = 1600 psf, γ_t = 120 pcf

Sand Layer Over Clay (Case 4) – Meyerhof (1974)

Thickness of Sand Layer: $H_1 = 988 - 983 = 5\,ft$

Bearing Capacity Factors: For clay: $N_c = 5.14$ For sand: $N_q = 29,\ N_\gamma = 31$

Coefficient of Punching Shear: Assume δ/ϕ' = 0.7, $K_s \approx 4$ from Figure 5-22

Ultimate Bearing Capacity:

$$q_{ult} = \min\begin{cases} (5.14)(1600\,psf) + (125\,pcf)(5\,ft)^2\left(1+\dfrac{2(4\,ft)}{5\,ft}\right)\left(\dfrac{(4.0)\tan(34)}{4\,ft}\right) + (125\,pcf)(4\,ft) = 14,204\,psf \\ (125\,pcf)(4\,ft)(29) + 0.5(125\,psf)(4\,ft)(31) = 22,250\,psf \end{cases}$$

$$q_{ult} = 14,204\,psf$$

Allowable Bearing Pressure:

$$q_{all,net} = \frac{14,204\ psf}{2.5} - 500\ psf = 5,186\ psf > 5000\ psf$$

The column foundation design is adequate for bearing because $q_{all,net}$ exceeds the applied pressure. The ratio of bearing capacity of the clay to the sand is about 0.6 for K_s = 4. According to Meyerhof and Hanna (1978), a slightly higher value of δ/ϕ' and K_s might be warranted. This would increase the bearing capacity further.

Figure 5-23 Bearing Capacity Example – Sand Layer Over Clay (Case 4)

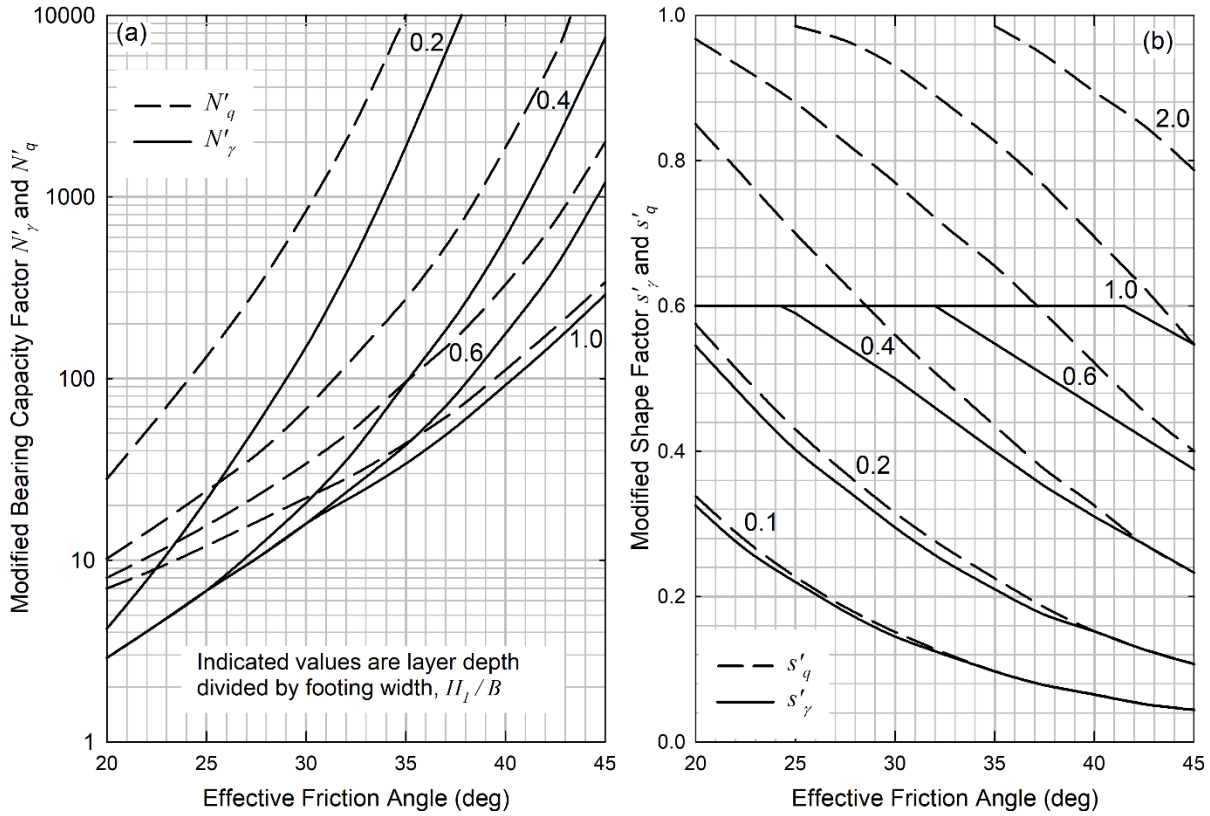

Figure 5-24 Modified Factors for – (a) Bearing Capacity and (b) Shape for Circular Footings (after Meyerhof 1974)

5-3.7 Bearing Capacity of Rock.

Three types of shear strength parameters are used in rock mechanics depending on the rock structure being evaluated: 1) shearing of an intact specimen, 2) shearing along a joint or fracture, or 3) shearing through a fractured rock mass. For bearing capacity, shearing along a rock fracture is the most applicable.

Table 5-12 provides typical ϕ' values for rock fractures and joints. Rock fractures have undulations or irregularities called *asperities*, which add to the frictional resistance of smooth rock fractures (Stagg and Zienkiewicz 1968). The asperity angle (i) usually ranges from 10 to 15°. The design friction angle (ϕ'_{rf}) is found by adding the rock friction angle, such as those in Table 5-12, and the asperity angle.

Table 5-12 Range of Properties for Rock Types (after Wyllie and Norrish 1996 and Bowles 1996)

Rock Type	Unit Weight, γ (pcf)	Average Effective Rock Fracture Shear Strength	
		ϕ' (deg)	c' (psf)
Granite, Basalt, Conglomerate, Limestone	170	37	0
Sandstone, Siltstone, Gneiss, Slate	160	31	0
Schist (high mica content)	165	27	0
Shale	120	24	0

The bearing capacity of rock may be calculated using the Terzaghi method along with the Terzaghi shape factors (Table 5-5). However, the bearing capacity factors are different for rock and are given by Stagg and Zienkiewicz (1968) based on ϕ'_{rf} as:

$$N_c = 5\tan^4\left(45+\phi'_{rf}/2\right) \quad (5\text{-}29),$$

$$N_q = \tan^6\left(45+\phi'_{rf}/2\right) \quad (5\text{-}30),$$

and

$$N_\gamma = N_q + 1 \quad (5\text{-}31),$$

where:
ϕ'_{rf} = rock fracture friction angle including the effect of asperities.

The evaluation of rock bearing capacity should also include some measure of the rock quality, such as Rock Quality Designation (RQD) or Geological Strength Index (GSI). RQD can be incorporated as a reduction to the ultimate bearing capacity as suggested by Bowles (1996):

$$q'_{ult} = q_{ult} \cdot RQD^2 \quad (5\text{-}32)$$

where:
q'_{ult} = reduced ultimate bearing capacity.

For Equation 5-32, the RQD should be evaluated to a depth of B below the footing and should be expressed as a decimal, not a percentage. A factor of safety of 3 to 4 is recommended to calculate $q_{all,net}$ from q'_{ult} for rock foundations. When using RQD, the rock material must meet the hardness and soundness criteria defined by Deere and Deere (1989). In massive rock with few fractures, the RQD will likely be 100 percent (1.0), and the q'_{ult} value will equal q_{ult}.

Some rock is soft and highly weathered to completely weathered, which means that most or all of the minerals have decomposed to soil. Texture becomes indistinct but fabric and structure are preserved (ISRM 1978). Soft rock can be scraped with a knife and indented 1 to 3 mm with a pick (NRCS 2022). In this case, the RQD will be close to zero, and the soft rock material should be evaluated as soil using the bearing capacity factors from Section 5-3.1.2. The undrained shear strength for this calculation may be obtained from a soil pressuremeter or rock pressuremeter (rock dilatometer) depending upon the strength of the material as discussed in Chapter 2 of DM 7.1. Example calculations illustrating rock bearing capacity are provided in Figure 5-25.

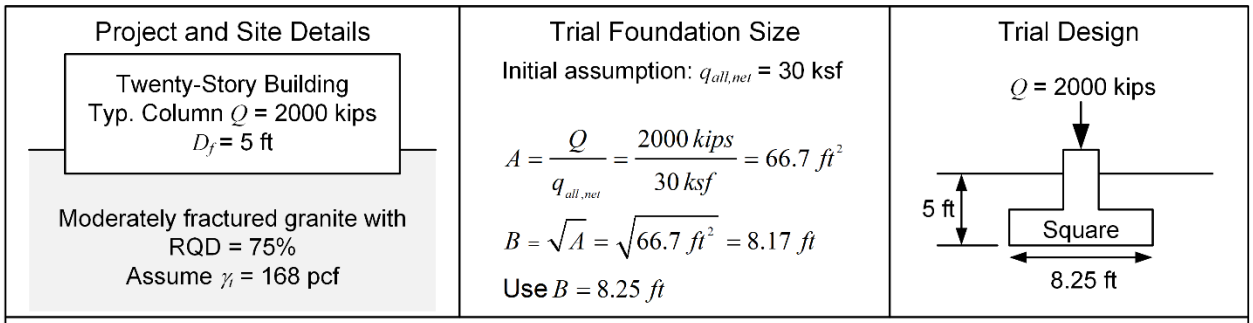

Rock Properties

Rock Fracture Shear Strength (From Table 5-10): ϕ' = 37 deg, Asperity Angle, i = 10 deg, ϕ_{rf} = 47 deg

Ultimate Bearing Capacity

Bearing Capacity Factors:
(Stagg and Zienkiewicz 1968)

$$N_q = \tan^6\left(45 + 42/2\right) = 268$$

$$N_\gamma = 268 + 1 = 269$$

Vertical Stress at Foundation Level:

$$\sigma_{zD} = (5\ ft)(168\ pcf) = 840\ psf$$

Ultimate Bearing Capacity:

$$q_{ult} = \sigma_{zD} N_q + 0.4\gamma_t B N_\gamma$$
$$= (840\,psf)(268) + 0.4(168\,pcf)(8.25\,ft)(269)$$
$$= 225{,}120 + 149{,}134 = 374{,}254\,psf$$

RQD Reduction:

$$q'_{ult} = q_{ult} \cdot RQD^2 = (374\,ksf)(0.75)^2 = 211\,ksf$$

Allowable Bearing Pressure:
(F = 3)

$$q_{all,net} = \frac{210\,ksf}{3} - 0.84\,ksf = 69.2\,ksf > 30\,ksf$$

The design is suitable for bearing because the allowable bearing pressure exceeds the assumed design value.

Figure 5-25 Example Calculations for Bearing Capacity of Rock

5-4 GEOTECHNICAL DESIGN OF COMBINED AND MAT FOUNDATIONS.

Combined footings and mat foundations are designed as described by the American Concrete Institute (ACI) (2002). The following paragraphs describe the required input that geotechnical engineers need to provide to structural engineers before and during

their design of these foundations. An extended example of the necessary field investigation, laboratory testing, and calculations is provided in Appendix B.

5-4.1 Definitions and Applications.

This section considers the design of shallow foundations carrying more than a single column or wall load as defined above. The following definitions are helpful and have been summarized from ACI (2002):

- *Combined footing* – footing supporting more than one column load. Combined footings are used when column loads are closely spaced so that individual footings would overlap and thus the footings are combined to support the loads.
- *Continuous footing* – footing supporting two or more columns in a row. Continuous foundations are used under wall loads and when the distance between columns is sufficiently close that individual footings can be combined.
- *Grid foundation* – a foundation formed by intersecting continuous footings. Grid foundations are a variation on continuous footings.
- *Mat foundation* – a continuous footing supporting columns in several rows in each direction, covering an area of at least 75 percent of the total structure area. Mat foundations are generally appropriate if: 1) the sum of individual footing base areas exceeds about 75% of the total foundation area; 2) the subsurface strata contain cavities or compressible lenses and differential settlements are a concern; 3) the subsurface strata are highly compressible and a reduction in bearing pressures is helpful; or 4) resistance to hydrostatic uplift is required.
- *Rigid foundation* – loads cause differential to total settlement ratios ≤ 0.1.
- *Flexible foundation* – does not meet requirements for rigid foundations.

Design of these foundations, especially mats, is an iterative process between the geotechnical engineer and the structural engineer. The soil response is based on mat contact pressures, which in turn are based on mat loads, flexibility, and modulus. Thus, the computed mat deflections and soil responses must converge. Economic considerations will also have an impact on selection of a combined footing and mat foundation over other alternatives. Slabs-on-grade are excluded from this discussion.

5-4.2 Rigid Foundations.

Rigid foundations are those which, because of their stiffness, will not allow individual columns or walls to settle differentially. Rigid foundations produce uniform settlements if loaded uniformly. The contact pressures, however, are not uniform for ideal coarse-grained soil (c' = 0 psf) or saturated fine-grained soil (ϕ = 0), as shown in Figure 5-26. In design, structural engineers generally assume the contact pressure to be an average of the total load on the foundation divided by the area of the foundation for these rigid foundations. This is an acceptable approach according to ACI (2002) because of conservative load estimates used for calculation of settlement and an ample safety

factor against the ultimate bearing capacity. Many foundations, however, support loads that are not uniform. It is common practice, in these cases, to assume a linear, nonuniform contact pressure, such as under a retaining wall where the toe pressure is maximum and the heel pressure is minimum.

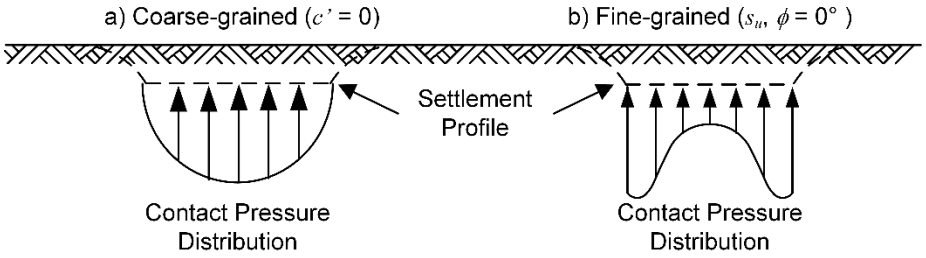

Figure 5-26 Idealized Distribution of Contact Pressure and Settlement Under a Uniformly Distributed Load for a Rigid Foundation - a) Coarse-grained (c' = 0 psf) and b) Fine-grained (ϕ = 0°) (after Das 2022)

5-4.2.1 Rigid Foundation Criteria.

Combined footings and mat foundations may be designed as rigid structures if they meet the relative stiffness factor criteria, K_r, developed by Meyerhof (1953):

$$K_r = \frac{E' \cdot I_b}{E_s \cdot B^3} \tag{5-33}$$

where:
$E' \cdot I_b$ = flexural stiffness of the structure (beyond scope of this document),
E_s = soil modulus, and
B = width of foundation.

Calculation of the relative stiffness is a joint effort of the structural and geotechnical engineers. A preliminary E_s value must be provided by the geotechnical engineer to the structural engineer. An approximate value of stiffness per unit width of building and foundation width is estimated by the structural engineer. Using this information, the structural engineer calculates the relative stiffness, K_r, of a foundation. The structural engineer should indicate to the geotechnical engineer whether the foundation is rigid or flexible, or whether both types of foundations should be considered by the geotechnical engineer. When $K_r \geq 0.5$, the ratio of differential to total settlement is about 0.1 or less and the foundation may be considered rigid.

The spacing of columns can be used to determine if continuous foundations may be considered rigid using a factor (λ) based on soil and foundation stiffness:

$$\lambda = \sqrt[4]{\frac{k_s \cdot B}{4E_c \cdot I}} \quad (5\text{-}34)$$

where:
k_s = modulus of subgrade reaction (see Section 5-4.5),
E_c = modulus of concrete, and
I = moment of inertia of footing.

A foundation can be considered rigid if the average spacing of two adjacent column spans is less than $1.75 / \lambda$, provided adjacent column loads and column spacing do not vary by more than 20 percent. This assessment is typically completed by the structural engineer.

If the foundation meets either of these criteria, it may be designed as a rigid foundation with a linear distribution of soil pressure based on statics. Thus, the assumption for design is that a straight-line relationship exists between maximum and minimum contact pressures below the footing. In this case, the geotechnical engineer is responsible for providing a net allowable soil bearing pressure, $q_{all,net}$, as described in Section 5-2.4. The settlement should be estimated using the methods of Chapter 5 of DM 7.1.

5-4.3 Flexible Foundation Criteria.

If $K_r < 0.5$, the foundation should be designed as a flexible foundation. For example, when $K_r = 0$, the ratio of differential settlement to total settlement is about 0.5 and 0.35 for continuous and square footings, respectively, according to ACI (2002).

If a foundation is considered flexible, it is usually designed by the structural engineer as a beam on elastic foundation. Figure 5-27 illustrates the contact pressure for these foundations when uniformly loaded and supported on ideal coarse-grained soil ($c' = 0$) and fine-grained soil ($\phi = 0$). The contact pressure will be uniform for a uniform load, and the settlement will be greatest at the edges of the foundation for coarse-grained soil and dish shaped (concave up) for a saturated clay with the greatest settlement at the center of the foundation.

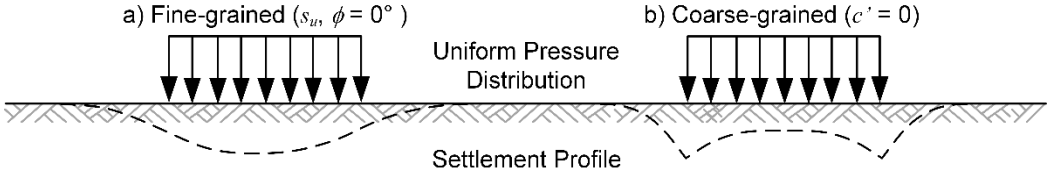

Figure 5-27 Idealized Distribution of Contact Pressure and Settlement Under a Uniformly Distributed Loading for a Flexible Foundation – a) Fine-grained Soil, ($\phi = 0$ deg) and b) Coarse-grained Soil ($c' = 0$) (after Das 2022)

5-4.4 Required Input for Analysis of Continuous and Mat Foundations.

Most structural engineers use software to design continuous and mat foundations. Closed form analytical solutions are available for specific problems (Hetenyi 1948) but not more complex situations. The two procedures often used to evaluate the soil response for continuous footings or mat foundations are the finite element method (FEM) using elastic constants and the finite grid method (FGM) using a Winkler foundation model with elastic springs. The springs can be either coupled or uncoupled. The properties of these springs are estimated using a subgrade modulus (k_s), which is adjusted for footing size or tributary area of a node for a mat. Consideration is also given to the change of subgrade modulus with depth. Uncoupled springs are a simplifying assumption that structural engineers may use in their design.

Flexible foundations present significant soil structure interaction issues that require the geotechnical engineer and structural engineer to work together to find an appropriate solution. When the relative stiffness factor indicates the foundation may be borderline rigid/flexible, the structural engineer may choose to analyze the foundation as both a rigid and flexible structure. The analyses of a foundation as a flexible plate on an elastic foundation may appear to be a more exact approach. However, a number of factors reduce the accuracy of this approach, including:

- Difficulty in estimating and assigning elastic soil parameters: k_s, E_s, and ν,
- Horizontal and vertical variation of soil strata thickness and properties,
- Mat shape,
- Variety of superstructure loads and assumptions in their development, and
- Interaction effects between the superstructure stiffness and stiffness of the continuous footing or mat foundation.

Depending on whether an FEM or FGM approach is being used, the structural engineer may require the following input from geotechnical engineers for flexible foundation design:

- Net allowable soil bearing pressure, $q_{all,net}$,
- Estimated settlement, s,
- Estimated soil modulus, E_s,
- Poison's ratio, ν, and
- Estimated modulus of subgrade reaction, k_s.

Generally, the soil is not homogeneous under a combined footing or mat foundation and the geotechnical engineer must develop soil behavior and properties that represent the stratigraphy, loading condition, and depth of stress penetration. Estimation of the allowable bearing pressure was discussed in Sections 5-2 and 5-3. Methods of calculating the estimated settlement are included in Chapter 5 of DM 7.1. Methods to estimate k_s, E_s, and ν are discussed in the following section.

These input recommendations must also consider time-dependent effects that can result in changes to moments and shear forces within the mat foundation and superstructure. Time-dependent effects occur both during and after construction and include the following:

- Heave and recompression of the subgrade after excavation and
- Long-term consolidation settlement of clays.

The following loadings must be considered: 1) staged loading, 2) dead loading followed by live loading, 3) short-term elastic settlement of sands, and 4) foundation soil shear displacements. Staged loading and dead and live loading will be included in the settlement estimate since the structural loading is used for settlement estimates. Time-dependent elastic settlement of sands can also be included in the settlement estimate by using the Schmertmann et al. (1978) approach. Soil shear displacements should not occur if an adequate bearing capacity factor of safety is used.

5-4.5 Modulus of Subgrade Reaction.

The modulus of subgrade reaction (k_s) is the ratio of the contact pressure divided by the corresponding deformation, or settlement, and has the units of force per cubic length. Other names include the coefficient of subgrade reaction or subgrade reaction. The modulus of subgrade reaction is depicted in Figure 5-28 and can be calculated as:

$$k_s = q/s \tag{5-35}$$

where:
q = contact pressure acting perpendicular to the contact area and
s = soil settlement.

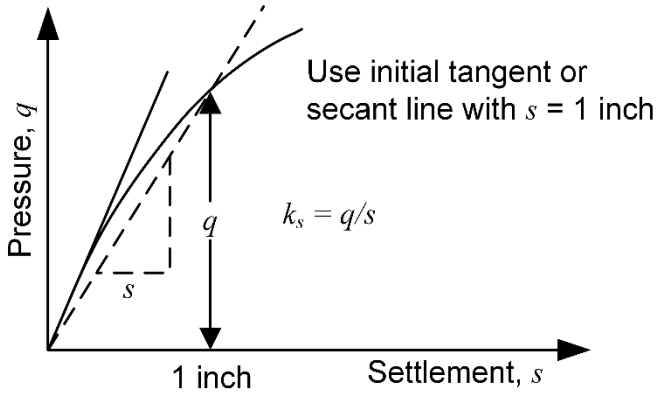

Figure 5-28 Subgrade Pressure versus Settlement Curve Defining k_s (after Bowles 1996)

Typical k_s values are provided in Table 5-13 that can be used as a guide for comparison to measured or calculated values. The table should not be used to calculate an average

value of k_s because of the breadth of the range of values. Two procedures for estimating k_s are discussed below.

Table 5-13 Typical Modulus of Subgrade Reaction Values (after Bowles 1996)

Soil Type		k_s (pci)
Loose sand		20 to 60
Medium dense sand		30 to 300
Dense sand		250 to 500
Clayey medium dense sand		120 to 300
Silty medium dense sand		100 to 200
Clay	q_{all} ≤ 4,000 psf	50 to 100
	q_{all} = 4,000 to 16,000 psf	100 to 200
	q_{all} > 16,000 psf	> 200

5-4.5.1 Estimating k_s from Plate Load Tests.

A plate load test may be used to estimate k_s, which pushes a 1-foot wide square or circular plate into the ground. The pressure and deflection are measured as shown in Figure 5-28. The pressure-deflection relationship is typically nonlinear. The secant modulus through a specific settlement point, for example 1-inch of settlement and the origin, is usually used to define k_s for a plate load test.

The plate load test is of limited value for foundations due to the size of the plate and scale effects. If the combined footing has a width less than or equal to 5 ft with uniform soil conditions within the depth of influence ($2B$ for square footings or $4B$ for continuous footings), the k_s value for design of the footing may be approximated from a plate load test as suggested by Sowers (1977):

$$k_s = k_p \left(B_p / B \right)^n \tag{5-36}$$

where:
k_p = the modulus of subgrade reaction from the plate load test,
B_p = width of plate,
B = width of foundation, and
n = 0.5 to 0.7.

Plate load test results cannot be scaled for larger footings and mats because of the variation of soil properties within the depth of stress penetration.

5-4.5.2 Estimating k_s from Elastic Parameters.

Assuming the soil acts as an elastic medium, settlement can be estimated based on the foundation size and bearing pressure as well as the soil properties, E_s and ν. Influence factors (μ_0 and μ_1) are used to account for depth of embedment, foundation shape and depth to a firm layer. These factors are provided in Figure 5-29.

Using the definition of k_s in Equation 5-32, the elastic settlement equation can be rewritten as:

$$k_s = \frac{q}{s} = \frac{1}{\left(B/E_s\right)\mu_0\mu_1} \tag{5-37}$$

where:
B = width of foundation,
E_s = elastic modulus of the soil within the zone of influence for the foundation,
μ_0 = influence factor related to embedment of the load and ν, and
μ_1 = influence factor related to problem geometry and ν.

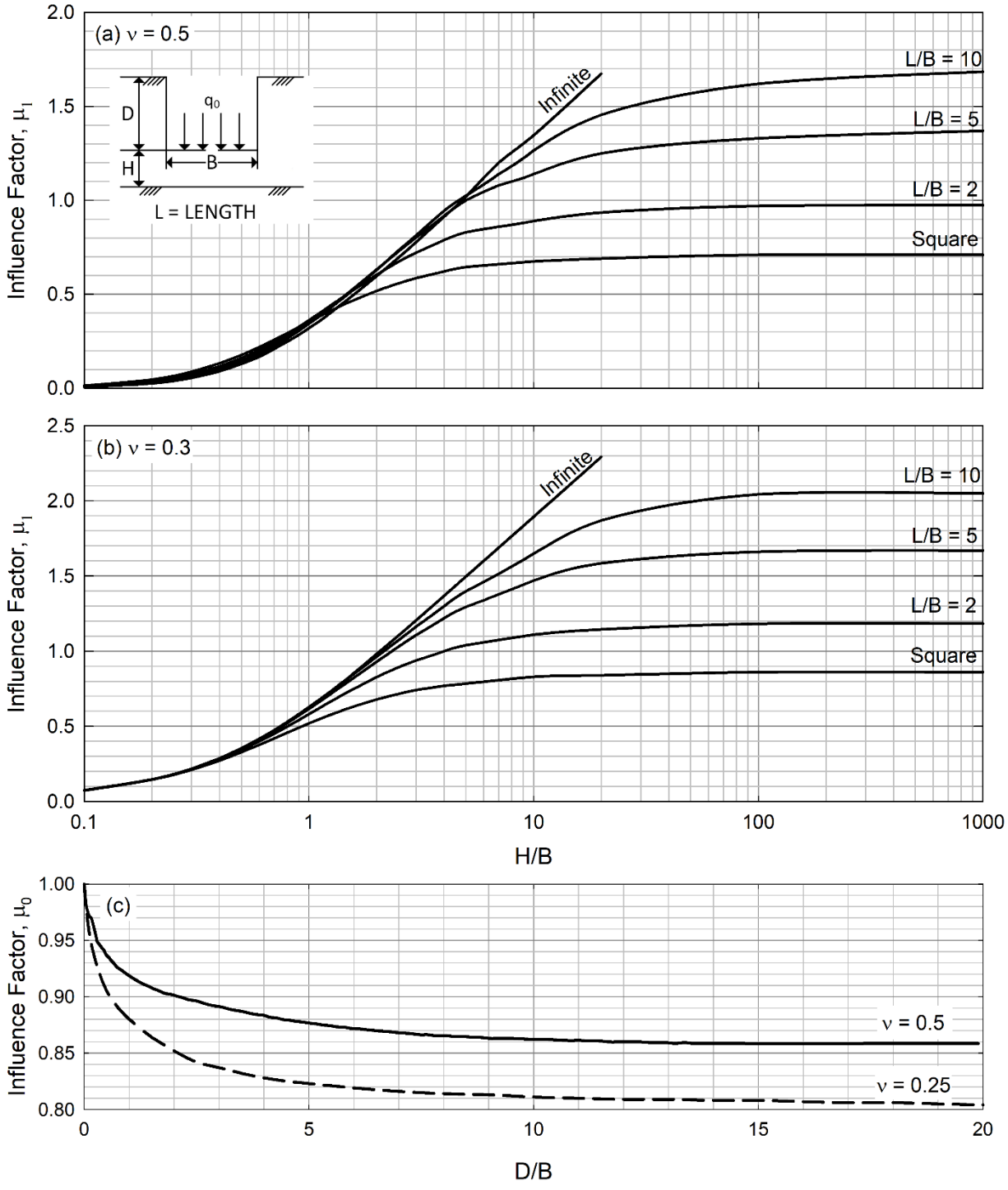

Figure 5-29 Elastic Influence Factors - (a) μ_I with $\nu = 0.5$, (b) μ_I with $\nu = 0.3$, and (c) μ_0 with $\nu = 0.25$ and 0.5 (after Giroud 1972 and Burland 1970)

5-4.5.3 Estimating Elastic Parameters, E_s and ν.

Accurately estimating the value of the soil modulus, E_s, with depth below a combined footing or mat foundation can be challenging. The modulus tends to:

- Increase with increasing overconsolidation ratio (OCR),
- Increase with increasing unit weight,
- Decrease with increasing water content,
- Decrease in the laboratory compared to the field, and
- Decrease due to disturbance.

The soil modulus also depends on the drainage condition with E_s used as general soil modulus, E'_s for drained soil modulus, and E_{us} for undrained soil modulus. These modulus values are much different than a true elastic material. In addition, the method of laboratory testing (confined, unconfined, drained, undrained) has an impact on the value of modulus. The values are typically defined using a secant method based on the stress and strain a particular percentage of the ultimate strength. Typically, drained secant moduli are used for coarse-grained soils, and undrained secant moduli are used for fine-grained soils. Soil modulus values may be obtained from triaxial tests on undisturbed samples or *in situ* tests. The typical soil modulus values for all types of soil that are summarized in Table 5-14 should be used as a guide to check the validity of values from *in situ* or laboratory testing.

Table 5-14 Typical Soil Moduli (after Bowles 1996)

Soil Type	Consistency or Density	E_s (tsf)
Clay	Very soft	20 to 140
	Soft	45 to 235
	Medium	140 to 465
	Hard	465 to 930
Sandy clay	Any	235 to 2,330
Glacial till	Loose	95 to 1,400
	Dense	1,400 to 6,715
	Very dense	4,660 to 13,425
Loess	Any	140 to 560
Sand	Loose	94 to 235
	Dense	465 to 750
Silty sand	Any	45 to 185
Sand and gravel	Loose	465 to 1,400
	Dense	930 to 1,865

In coarse-grained soil, the value of E'_s varies with confinement. Thus, under a flexible mat foundation, the edges of the mat will deflect more than the center because the confinement is less at the edges. Also, the modulus increases with depth due to

increased confining stress and increases during the application of load on the mat. *In situ* tests are preferred for estimating E'_s for granular soils due to disturbance issues with laboratory testing. Table 5-15 provides correlations of drained E'_s with SPT N and CPT q_c values for coarse-grained soils.

Table 5-15 Correlations for the Drained Modulus of Coarse-Grained Soils with SPT and CPT (after FHWA 2002a, Duncan and Bursey 2007, Coduto 2015, McGregor and Duncan 1998)

Soil Type		E'_s (tsf)	E'_s (tsf)
Silts, sandy silts, slightly cohesive mixtures		$4\ (N_1)_{60}$	$(1 \text{ to } 2)\ q_c$
Clean fine to medium sands and slightly silty sands		$7\ (N_1)_{60}$	
Coarse sands and sands with little gravel		$10\ (N_1)_{60}$	
Sandy gravels		$12\ (N_1)_{60}$	
Gravelly sand and gravels	For $N_{60} \le 15$	$6\ (N_{60}+6)$	
	For $N_{60} > 15$	$6\ (N_{60}+6)+20$	
Clayey sands		$3.2\ (N_{60}+15)$	
Silty sands		$3\ (N_{60}+6)$	
OC clean sands (age < 100 years) (SW-SP)		$5\ (N_{60}+15)$ all ages	$(2.5 \text{ to } 3.5)\ q_c$
NC clean sands (age > 100 years) (SW-SP)			$(3.5 \text{ to } 6)\ q_c$
OC clean sands (SW-SP)		$180+7.5\ N_{60}$	$(6 \text{ to } 10)\ q_c$
NC silty or clayey sands (SM-SC)			$1.5\ q_c$
OC silty or clayey sands (SM-SC)			$3\ q_c$
Notes: NC = Normally consolidated, OC = over consolidated, q_c = CPT tip resistance N_{60} = SPT blow count corrected to 60% of the theoretical free-fall hammer energy $(N_1)_{60}$ = SPT blow count corrected to 1 tsf of overburden pressure and 60% of the theoretical free-fall hammer energy			

For fine-grained soils, the undrained modulus usually increases with increasing vertical effective stress and undrained shear strength. The modulus also increases with OCR and lower moisture contents. Figure 5-30 provides a simple correlation between E_{us}, plasticity index (PI), and overconsolidation ratio (OCR). Once an appropriate ratio is selected, the undrained modulus can be estimated based on the undrained shear strength. Either *in situ* or laboratory tests are suitable for estimating E_{us} for fine-grained soils.

When layers with different soil properties underlie the mat, an appropriate weighted average E_s must be determined. Within the depth of influence, the modulus of each layer can be multiplied by the layer thickness and summed. The weighted average is this sum divided by the total thickness. The depth of influence is usually assumed to be $2B$ and $4B$ for square and continuous foundations, respectively.

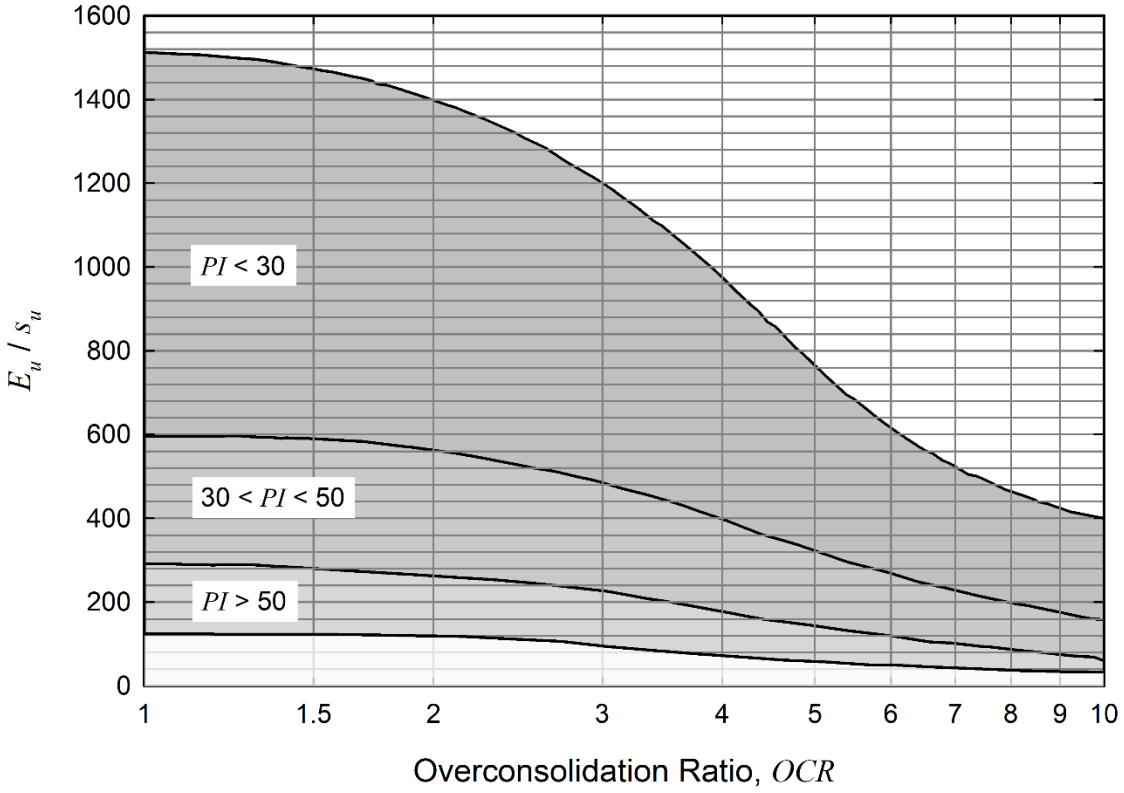

Figure 5-30 Undrained Modulus Correlation for Clay Soils with OCR and PI (after Duncan and Buchignani 1976)

Typical values of Poisson's ratio, which is also required for an elastic analysis, are provided in Table 5-16. Note, ν is 0.5 for undrained conditions (i.e., no volume change $\Delta V = 0$). For drained conditions, ν can be related to the friction angle:

$$\nu = \frac{1 - \sin\phi'}{2 - \sin\phi'} \quad \text{(5-38).}$$

When $\phi' = 20°$ to $55°$, the ν values range from 0.4 to 0.15.

Table 5-16 Typical Values of Poisson's Ratio (after Bowles 1996)

Soil Type	Poisson's Ratio, ν
Clay, saturated	0.45 to 0.5
Clay, unsaturated	0.1 to 0.3
Sandy clay	0.2 to 0.3
Silt	0.3 to 0.35
Medium to dense sand, gravelly sand	0.3 to 0.4
Loose to medium sand	0.2 to 0.35
Loess	0.1 to 0.3
Concrete	0.15

5-4.5.4 Evaluation of k_s for Time-Dependent Settlement.

Time-dependent settlements must be included in the estimate for k_s for a continuous footing or mat foundation when the structure imposes stresses beyond the preconsolidation stress, or when recompression or heave occurs due to excavation for the foundation. Neither of these settlements are included in the k_s values estimated from Equation 5-35. In this case, consolidation settlement (s_c) must be added to the elastic settlement, and the reduced subgrade modulus (k_{sc}) is:

$$k_{sc} = \frac{s \cdot k_s}{s + s_c} = \frac{q}{q\left(B/E_s\right)\mu_0\mu_1 + s_c} \quad (5\text{-}39).$$

5-4.6 Iterative Process in Design.

Although the contact pressures below a flexible mat are uniform for a uniform load, the settlements may vary across the mat because of variable stratigraphy. Also, the mat may not be uniformly loaded, and this will also cause settlements to be varied. Both of these nonuniformities can cause the design of a mat foundation to be an iterative process.

Contact pressures and settlements may be estimated by the structural engineer in the mat analysis, using the initial data provided by the geotechnical engineer including k_{sc}. These should be compared to the contact pressures and settlements estimated by the geotechnical engineer. If they are substantially different, the geotechnical engineer should reevaluate the E_s, ν, and k_s or k_{sc} values and settlements. Revised values should be provided to the structural engineer for the next iteration of modeling. The purpose is to make the settlements and contact pressures developed by the geotechnical engineer match closely with those of the structural engineer. An example mat design has been included in Appendix B.

5-4.7 Node Coupling of Soil Effects.

Mats are commonly designed using software that employs the FEM or FGM (ACI 2002). At the interface between the mat and the soil, the soil response is concentrated at nodes using a concept called a Winkler foundation. The soil is replaced by an equivalent spring with stiffness, K. The value of K for each node is determined by multiplying k_s or k_{sc} by the area (A_{cont}) that contributes to the node:

$$K = k_s \cdot A_{cont} \quad (5\text{-}40).$$

The units of K are force per length. Figure 5-31 illustrates the procedure that is used to estimate K for various mat foundation contributary areas. The k_s value assigned to each area shown in Figure 5-31 is based on the closest boring. A number of areas defined

by the mat nodes may use the same k_s value. This method produces uncoupled spring K values. An indirect method to allow coupling of nodes of Winkler foundations is discussed in the next section.

Uncoupled and coupled springs are illustrated in Figure 5-32. Uncoupling means that the settlement at any spring is unrelated to the settlement at any adjacent spring. The impact of coupling can be significant and can be seen for a uniformly loaded flexible foundation, such as a tank supported on clay. When the nodes are coupled, the deflection is correct and is dish shaped (concave). When uncoupled, the settlement is uniform and incorrect.

Coupling allows the responses at adjacent springs to affect each other. Coupling can also be accomplished when using a finite element computer program with the subgrade defined as an elastic medium, E_s and ν, but this is seldom done because of the difficulty in programing and cost.

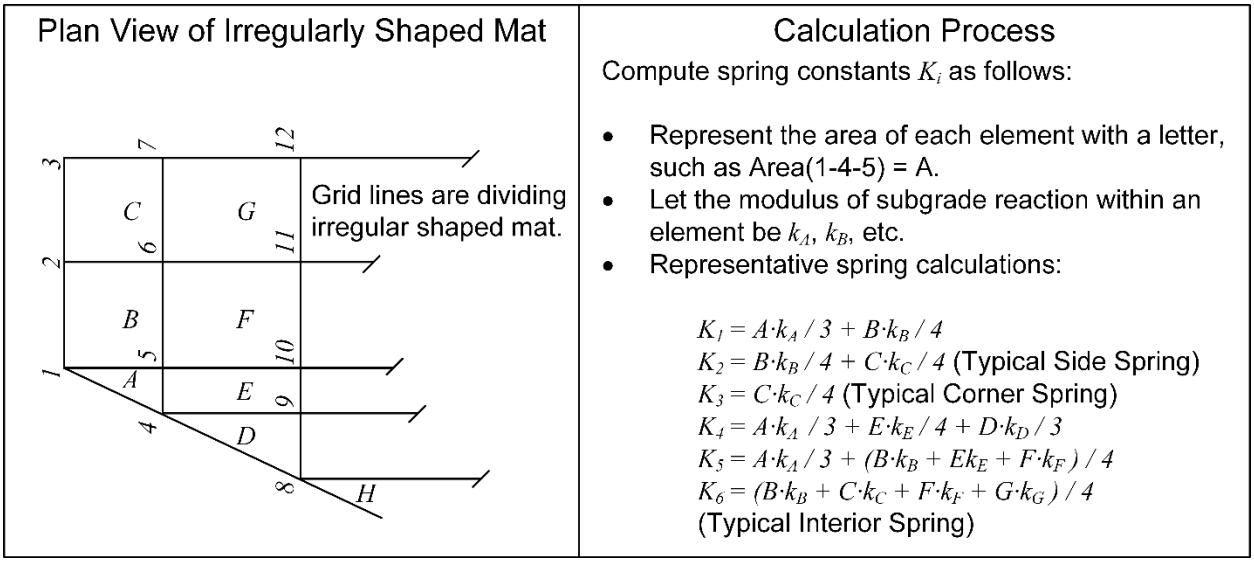

Figure 5-31 Computation of Uncoupled Winkler-type Soil Node Springs (after ACI 2002)

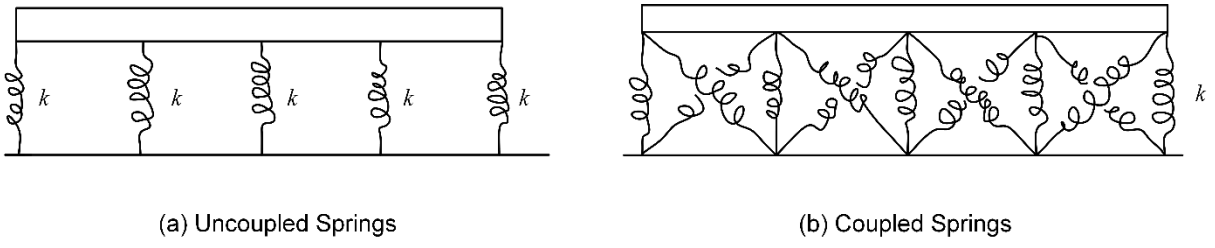

Figure 5-32 Coupled and Uncoupled Springs (after ACI 2002)

5-4.8 Indirect Method to Allowing Coupling.

Bowles (1996) suggested an indirect method for considering coupling in a mat foundation. This a structural consideration but is included herein to illustrate why this concept of coupling is important. The procedure is accomplished by selecting points on the mat plan so that the mat can be zoned with different values of k_s. One point must be on the edge of the mat, and this must be assigned the k_s value calculated for that location. The k_s values on other interior points on the mat foundation are then reduced based on the edge k_s using the procedure described in the following steps (see Figure 5-33):

1) Select sufficient points on the mat plan so that the mat can be zoned with different values of k_s. See Points 1, 2, and 3 for a square mat in Figure 5-33. Point 1 is on the edge of the mat.

2) Select a depth of influence of $4B'$ (B' = the longest side of the mat and is unrelated to the usual depth of influence of $2B$ for square footings).

3) Plot vertical stress profiles for the square mat at points 1, 2, and 3 using the Boussinesq method (Figure 5-33b). For a square mat, $4B' = 4B$ and q_0 is the contact pressure.

4) Numerically integrate stress profiles to obtain the average vertical stress, $\sigma_{z,ave} = (\sigma_z / q_{net}) \cdot q_{net}$. See Table 5-17.

5) These $\sigma_{z,ave}$ are then designated $\sigma_{z,ave(1)}$, $\sigma_{z,ave(2)}$, and $\sigma_{z,ave(3)}$ to correspond to Points 1, 2, and 3.

6) Compute k_s for any point i as follows:

$$k_{s,i} = k_s \left(\frac{\sigma_{z,ave(1)}}{\sigma_{z,ave(i)}} \right) \tag{5-41}$$

where:
$\sigma_{z,ave(i)}$ = average vertical stress at other points (Points 2 and 3 in Figure 5-33).

This procedure assumes an initial uniform k_s value throughout the mat foundation. The example illustrates the difference between contributary areas and zones for the indirect method of allowing coupling. When k_s values vary, as in the example in Figure 5-33 where Areas A, B, and C had different k_s values, k_s in Equation 5-39 varies with location. The procedure will reduce the k_s values, but they will not be based on a uniform k_s value as shown in the example of Figure 5-33. Table 5-17 contains estimated k_{si} values for different B'/L ratios.

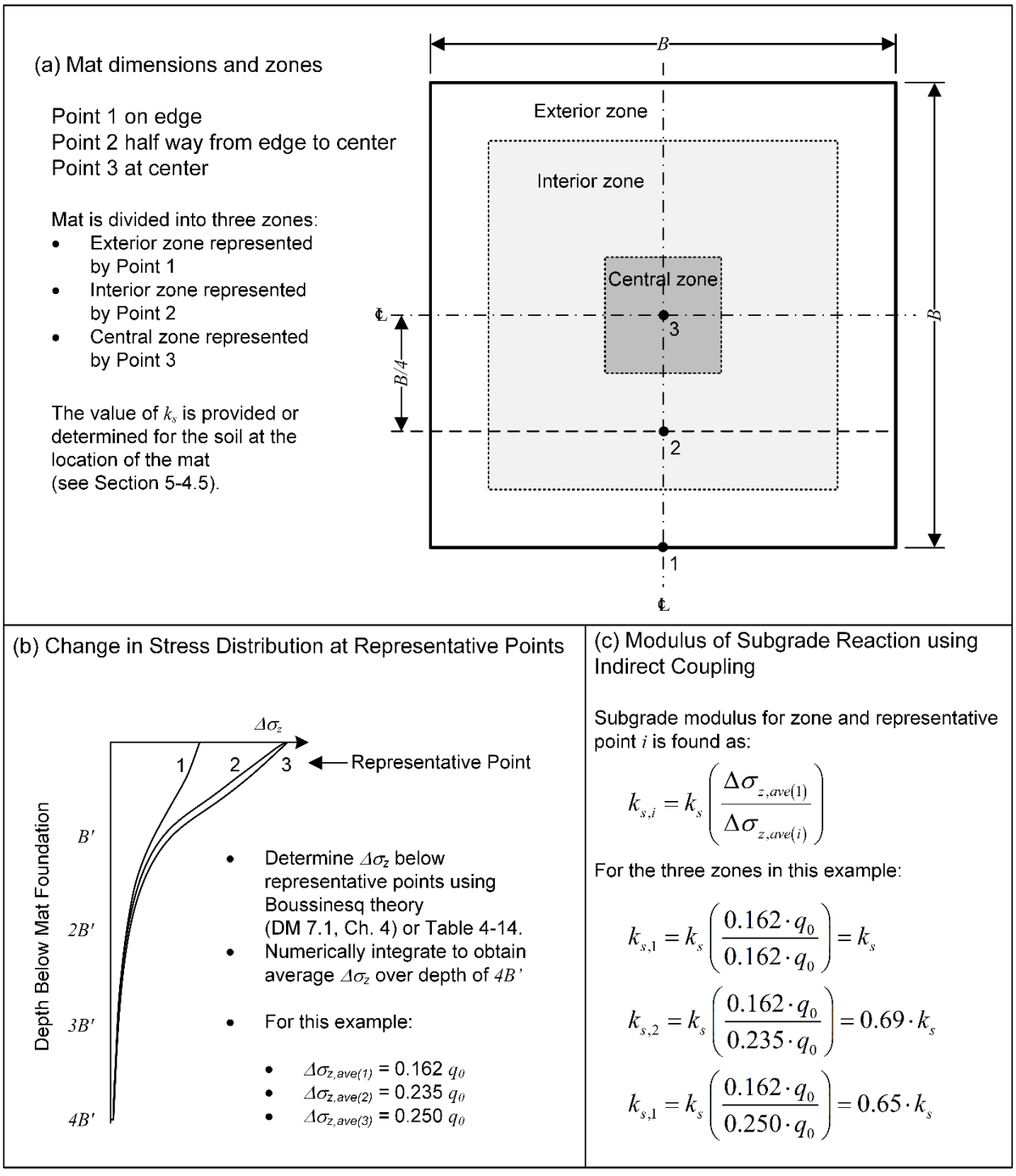

Figure 5-33 Example Mat Foundation Indirect Coupling Problem

Table 5-17 Vertical Pressure Profiles for Selected Points Beneath a Foundation Mat (after ACI 2002)

Mat Aspect Ratio, B/L	Average $\Delta\sigma_z$ / q_0 from 0 to 4B below Points 1 to 10 (see inset)									
	1	2	3	4	5	6	7	8	9	10
1	0.162	0.217	0.235	0.246	0.250	0.153	0.206	0.222	0.232	0.235
2	0.189	0.273	0.304	0.319	0.324	0.180	0.259	0.288	0.302	0.306
3	0.198	0.305	0.340	0.355	0.359	0.189	0.289	0.321	0.336	0.340

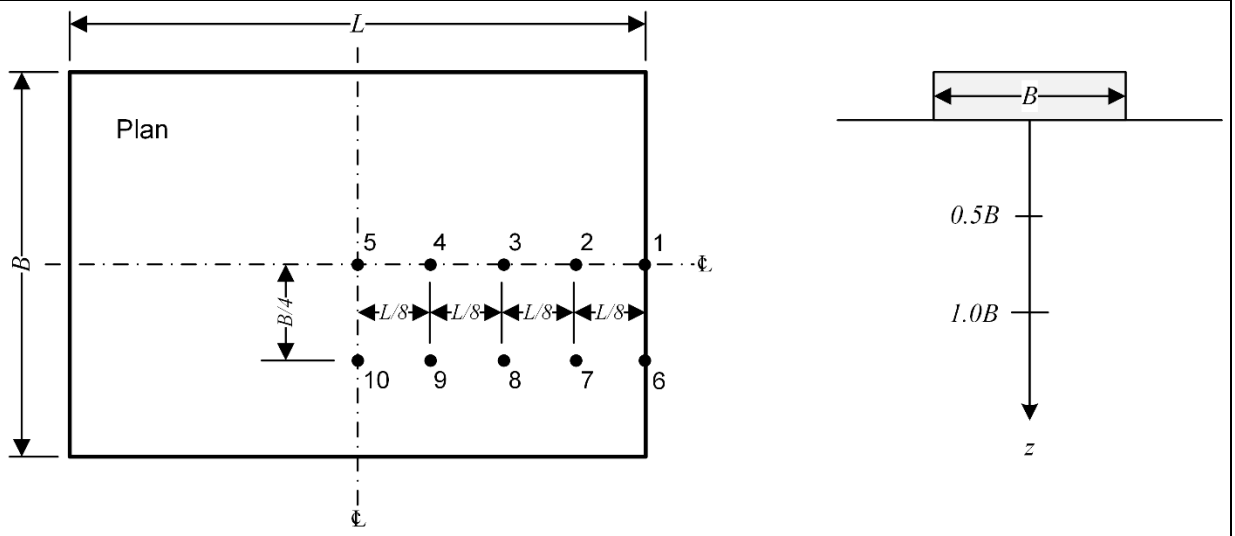

Note: Values of $\Delta\sigma_{z,ave}$ / q_0 found by numerically integrating $\Delta\sigma_z$ over z from 0 to 4B and dividing by 4B.

5-4.9 Floating Mat Foundation.

Depending on the structural geometry, weight, and load distribution on the mat, a mat foundation may *float* the structure in the soil, so that settlement only relates to recompression or heave. Where uniform, the pressure that results in settlement in a mat analysis can be computed as follows:

$$q_{net} = \frac{W_{structure} - W_{excavated}}{A_{mat}} \tag{5-42}$$

where:
$W_{structure}$ = total weight of structure,
$W_{excavated}$ = total weight of excavated soil, and
A_{mat} = area of mat.

5-4.10 Two- or Three-Dimensional Problems.

A two-dimensional analysis is normally defined as a mat designed as a beam on elastic foundation using soil concentrations at the nodes. A three-dimensional analysis involves modeling the soil as a three-dimensional elastic solid. Three-dimensional analyses are very expensive and are not recommended except for very elaborate projects.

5-5 DESIGN FOR SPECIAL LOADING CONDITIONS.

This section discusses the design of shallow foundations for special loading conditions. Design considerations for foundations and slabs to resist high groundwater are presented. Uplift resistance of shallow foundations is also considered.

5-5.1 Pressure Resistant and Relieved Foundation Slabs and Walls.

Hydrostatic pressure resistant and relieved foundation slabs and walls are considered in this section. Guidelines for the selection of appropriate drainage material are presented. Methods of dampproofing and waterproofing are also discussed.

Where the water table is deep, infiltration of surface water may still occur, and basement walls should be dampproofed. A drainage layer should be installed along walls with a foundation drain. A layer of drainage material should be placed under the slab with a vapor barrier.

Where the permanent water table is above the top of the basement slab, two general schemes are employed for basements. A pressure resistant slab and exterior foundation walls, *pressure slab and walls,* can be used. In this case, walls must be waterproofed to the maximum potential level of groundwater. Alternatively, the uplift pressures on the slab and the water pressure on walls can be relieved by a drainage system. This is referred to as a *relieved slab and walls* and requires dampproofing. In some cases, groundwater can be cut off by exterior foundation walls that extend into a low permeability thick clay layer or low permeability rock. In this case, a relieved slab is used and the exterior walls are waterproofed.

In general, the choice between pressure resistant or relieved slabs and walls depends on overall economy, maintenance, layout, and operation. This must be evaluated for each project individually.

5-5.1.1 Hydrostatic Pressure Slabs and Walls.

For basements extending only a small depth below groundwater, a pressure slab to resist maximum probable hydrostatic uplift pressures may be economical. Water-stops should be provided at the construction joints, and a drainage layer should be installed between the pressure slab and floor slab to collect any leakage through the pressure

slab. Drainage material should be as described in Section 5-5.1.3, and a slotted PVC corrugated drainage pipe should be added beneath the slab depending on the anticipated flow. A sump will be required to remove any water from the drainage layer. The exterior walls must be designed to withstand water pressure to the maximum anticipated level of ground water and must be waterproofed below this level. A vapor barrier should be placed over the drainage layer and under the slab to reduce the potential for moisture to migrate to the floor. An illustration of the pressure slab concept is shown in Figure 5-34.

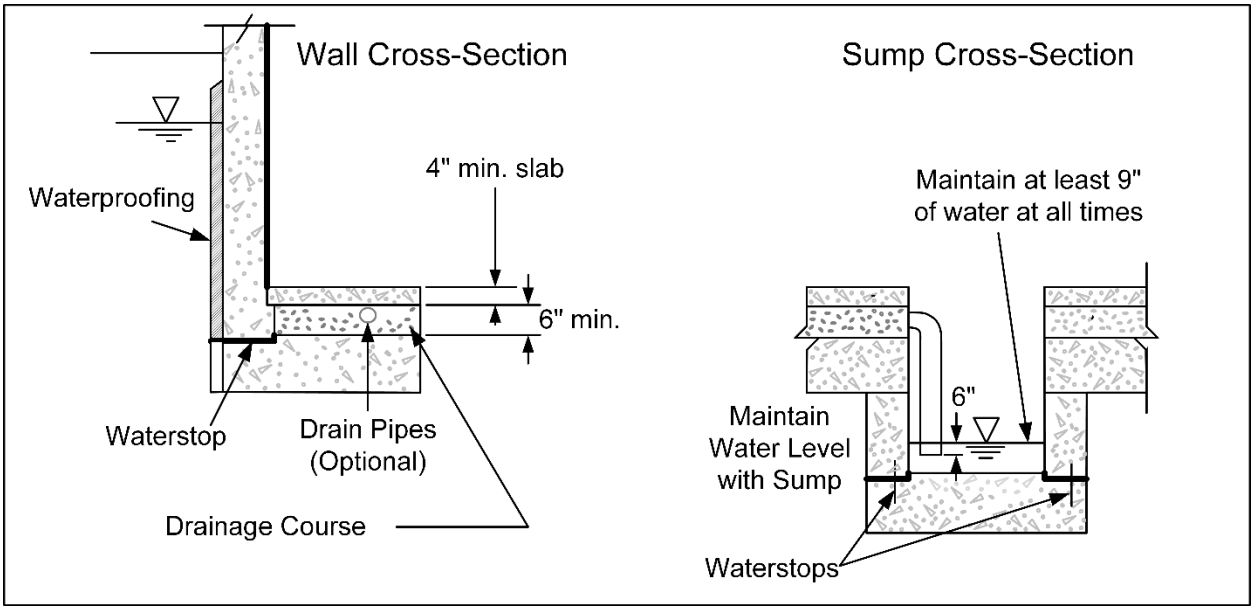

Figure 5-34 Schematic of a Pressure Slab and Wall System

5-5.1.2 Relieved Slabs.

For basements at considerable depth below the groundwater level, it is usually economical to provide pressure relief along the foundation walls and beneath the floor slab. Drainage layers and drains are required at exterior walls and under floors to maintain no hydrostatic pressure on the walls or floor slab. Exterior walls below grade must be dampproofed. Additional dampproofing may be required on the interior of the basement walls depending upon the use. Figure 5-35 provides an example for this type of design.

If a thick, underlying stratum of low permeability clay or rock is relatively shallow, a cutoff foundation wall system may be economical as shown in Figure 5-36. In this case, the foundation walls extend into the low permeability stratum and reduce water flow and pressures under the slab. Exterior walls below grade must be waterproofed, but wall drains may be omitted. Since some seepage may occur under the cutoff foundation walls, a drainage layer is required below the floor slab to maintain no hydrostatic pressure. Drain pipes are likely not needed due to low anticipated flow requirements.

Additional dampproofing may be required on the interior of the basement walls depending upon the use.

Drainage material for relieved slabs should be as described in Section 5-5.1.3, and slotted PVC corrugated drain pipes may be needed beneath slab, depending on the anticipated flow. A sump is required to remove any water from the drainage layers as shown in Figure 5-34. A vapor barrier should be placed over the drainage layer and under the slab to reduce the potential for moisture to migrate to the floor.

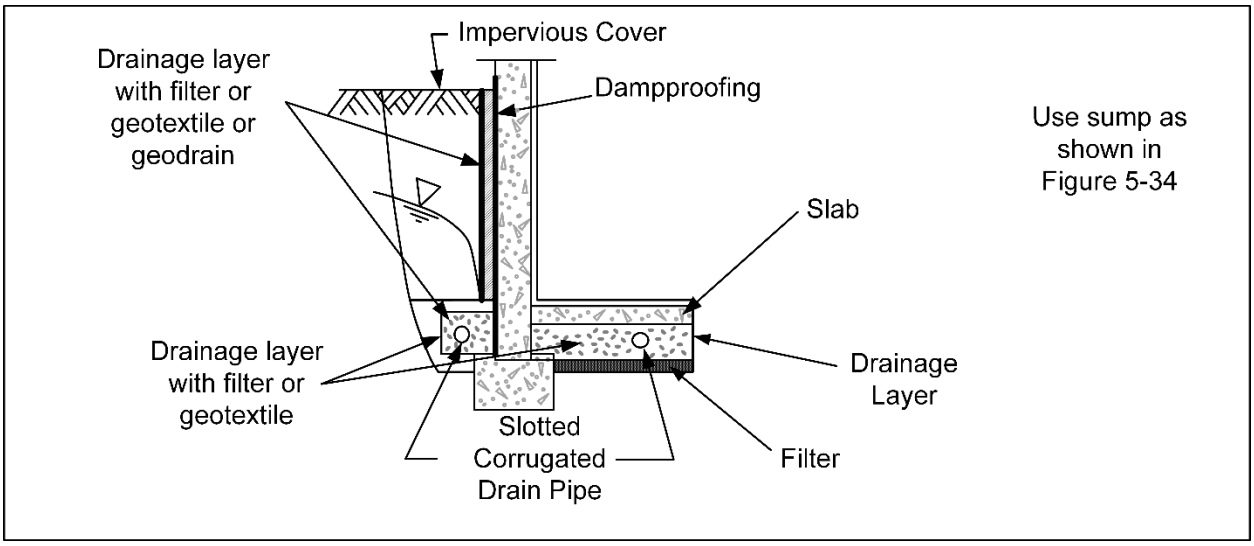

Figure 5-35 Schematic of a Relieved Slab and Wall System

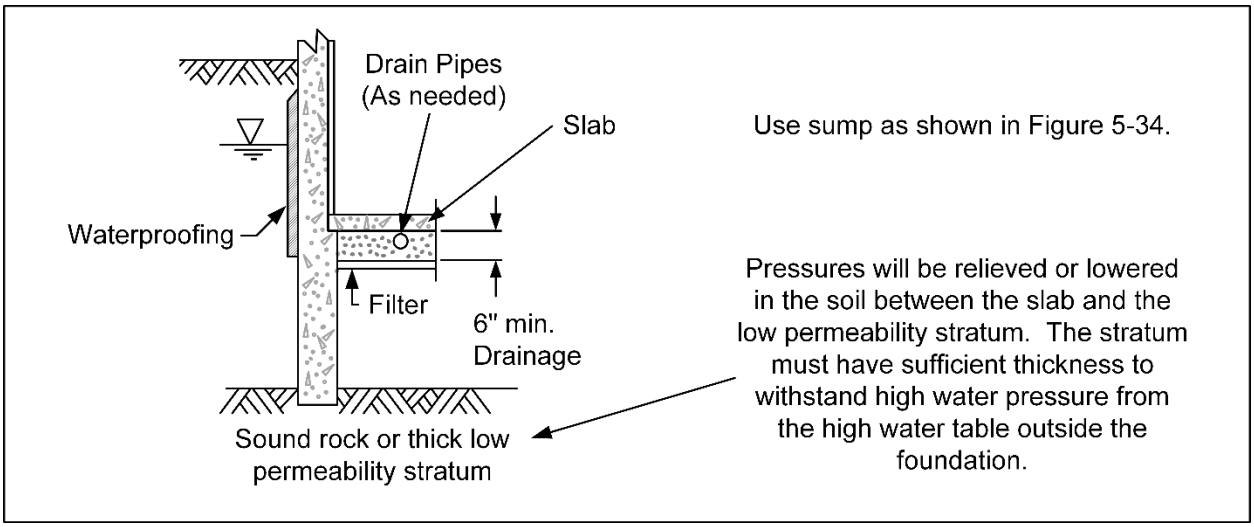

Figure 5-36 Schematic of a Cutoff Foundation Wall to a Low Permeability Stratum

5-5.1.3 Underdrain System.

Drainage material should be sound, clean gravel or crushed stone graded between 3/4 and 2 inches. This material should be densified and leveled with a plate compactor. If needed, slotted PVC corrugated drainage pipes may be added beneath the slab and around the exterior walls. The pipes should be sized to carry the anticipated flow. The drainage material and pipes should flow to the sump for discharge. Drainage layer filter requirements and drain spacing are discussed in Chapter 6 of DM 7.1.

5-5.1.4 Dampproofing and Waterproofing Requirements.

Dampproofing is defined as material that resists the passage of water with no hydrostatic pressure. Dampproofing is intended to keep soil moisture from entering a below grade space. A coating, usually asphalt-based, is either sprayed or hand applied to the outside of the wall. Dampproofing is not used when the groundwater level will be above a below grade space. *Waterproofing* is defined as material that resists the passage of water under hydrostatic pressure. A listing of damp proofing and waterproofing systems is provided in Table 5-18. Before application of damp proofing or waterproofing, all wall surfaces must be clean and dry and any defects corrected.

Table 5-18 Methods of Foundation Dampproofing and Waterproofing

	Type	Material	Application and Workmanship	Remarks
Dampproofing	Surface Treatment	Silicates of sodium or potassium and sulphates of aluminum, zinc, and magnesium	Applied with a brush.	
	Surface Course	Bitumen	Applied with brush, thickness ~ 3 mm	
		Mastic asphalt	Heating asphalt with sand or mineral fillers.	
		Cement mortar	Add small quantity of lime (1:6) and water proofing agents.	
	Integral	Chalk, talc, flutter earth: chemical compounds such as calcium chloride, aluminum sulphate, calcium chloride and waxes, oils, fatty acids, soaps, petroleum compounds	It is advisable to avoid waxes and fats in the tropics because they melt at elevated temperatures.	
Waterproofing	Cementitious	Portland hydraulic cement with acrylic additives and may be fiber reinforced	Can be brushed or sprayed.	Easy to apply but less flexibility.
	Hot-applied bitumen systems	Applied in alternating layers of bitumen (coal, tar, or asphalt) and felt (fiberglass or organic).	Three to five plies of reinforcement provide durability. Fumes and high temperatures (400° F) can create safety and environmental hazards.	Less use than the previous.
	Hot-applied rubberized asphalt	Blend of asphalt and modified rubber polymers containing mineral stabilizers.	High temperatures (400°F) can create safety hazards.	Seamless
	Film or sheet membrane	Bentonite clay imbedded in mesh with protective cover.	Applied in sheets which are mechanically attached or can be spray applied.	Joints critical for success
		High density polyethylene (HDPE) sheet	Usually, self-adhered but also mechanically applied.	
		Ethylene propylene diene monomer (EPDM)	Usually, self-adhered but also mechanically applied.	
		Polyvinyl chloride (PVC)	Usually, self-adhered but also mechanically applied.	

5-5.2 Uplift Resistance.

Ground anchors to resist uplift must be designed for two possible failure mechanisms: 1) failure of an individual anchor to resist the uplift load and 2) failure of a group of anchors in a ground mass where the total uplift load exceeds the capacity of the ground mass. In a group of anchors, the capacity of the group may be less than that of individual anchor times the number of anchors.

5-5.2.1 Applications.

Anchors can be either passive or active. A *passive anchor* is one which is not prestressed and usually has no unbonded or free length. As load is applied, the anchor

must move to engage resistance in the soil or rock. An *active anchor* is prestressed to a specific load and locked off. Active uplift anchor systems are considered herein and include: 1) resistance to transient uplift loads on tower legs, guys, and antennas, 2) sustained uplift loads on structures, and 3) structures impacted by hydrostatic uplift forces. Anchored systems, such as flexible anchored walls and soil nails have been discussed in Chapter 4. Landslide stabilization anchors are not considered. A brief discussion of corrosion protection is included at the end of this section. More detailed guidance for these subjects is found in FHWA (1999).

A ground anchor has multiple components as shown in Figure 5-37. A stressing anchorage and bearing plate connect the anchor to the structure. Anchors usually have an unbonded length that will transfer the load to soil or rock further from the structure. The final section of the anchor is the bond length where the resistance is developed. The load is transferred from the beginning of the anchor bond length and then progresses to the end of the anchor. Only a portion of the bond length is stressed under the allowable load. Ground anchors usually consist of deformed bars grouted in soil or rock. Tendons consisting of steel strand are also acceptable, and FHWA (1999) should be consulted for design. Bond stress may be increased by using washers or splayed bar ends. Spacers are used in angled holes to maintain the centrality of the bar in the anchor hole. The bond length and unbonded length should be grouted in one stage. This will help assure hole stability and provide continuous grout cover.

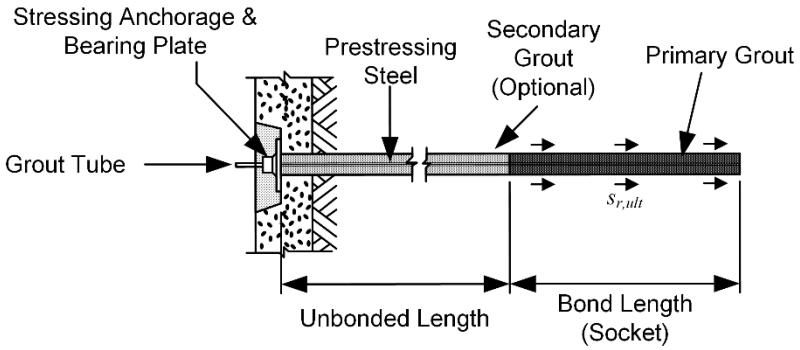

Figure 5-37 Schematic of Ground Anchor Components

5-5.2.2 Rock Anchors.

Anchors are often bonded into rock. In most cases, local experience and knowledge should be relied upon to obtain the best anchor performance. As an alternative, the rock mass breakout theory presented in this section can be applied. It should be recognized that this theory is very conservative and is primarily applicable to weathered, severely fractured rock.

Rock mass breakout is resisted by the weight of the material above the bonded length. Four potential failure modes are considered in rock anchors that are often used to tiedown foundations:

- Failure from to cone breakout of the rock mass
- Failure in shear along the grout/rock interface,
- Failure in shear along the grout/tendon interface, and
- Failure of the tendon in tension.

Design for these four failure modes is summarized in Figure 5-38. The required embedment or unbonded length is calculated based on the volume of the inverted cones above each anchor. The unbonded length (h) must be greater than 10 ft for bar anchors. When the anchor extends through soil before encountering rock, the cone diameter at the surface of rock is projected to the ground surface as a cylinder. The weight of the soil is included in the evaluation of h without considering the shear strength of the soil. Typically, the apex of the cone is placed at the top of the bond length of the anchor. The cone angle is typically assumed to fall between 60 to 90°, as shown in Figure 5-38(a) and is selected based on the quality of rock. As stated above, this approach assumes that the rock is severely fractured and acts as a strong soil, rather than an intact rock mass.

The spacing of rock anchors must consider the interference of cones shown in Figure 5-38(a). In essence, the depth will be greater if the spacing causes the cones to overlap since the volume of the individual cone will be less. This lowers the allowable capacity unless the unbonded length is increase. Spacing can also be constrained by the necessity for closely spaced anchors due to structural stiffness issues and the presence of existing underground structures. If the anchor spacing is flexible, the spacing can be set as $2R$, which causes the cones to touch but not overlap.

The anchor capacity will also be limited by the shear strength of the interface between the grout and the rock. For transient loads, a factor of safety of 2 to 3 is applied to the ultimate bond stress. For sustained loads, F of 3 is appropriate. The required anchor bond length (L) may be determined as shown in Figure 5-38(b). Presumptive ultimate bond stresses for various rock types are shown in Table 5-19. A lower factor of safety may be used for competent rock that is not highly fractured, and a higher factor of safety is required when highly weathered, fractured, or loose rock is engaged.

(a) Rock or Soil Mass Breakout

Use 60°:
For highly weathered, soft rock; highly-fractured rock mass; or fine-grained soils

$R = h \rightarrow V = 1.036h^3$

Use 90°:
For slightly weathered fresh rock mass or coarse-grained soils

$R = 0.5h \rightarrow V = 0.262h^3$

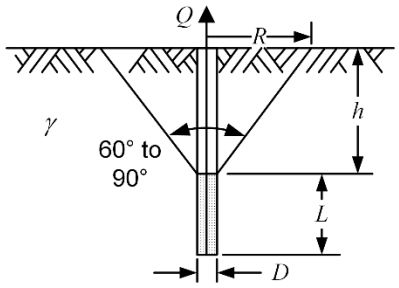

Volume of rock or soil in the cone:

$$V = \frac{\pi}{3} R^2 \cdot h$$

Required unbonded length (consider overlap separately):

$$Q = V \cdot \gamma$$

$$h \geq \frac{3Q}{\pi \cdot R^2 \cdot \gamma}$$

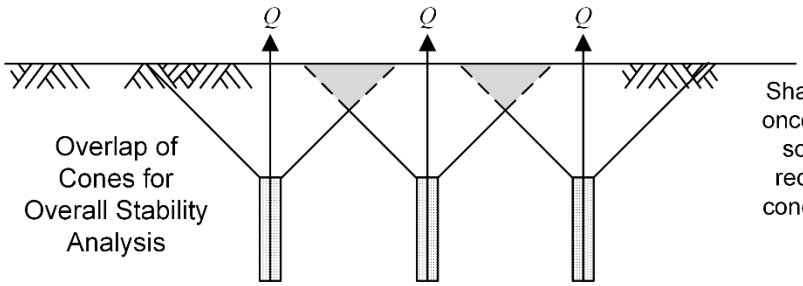

Overlap of Cones for Overall Stability Analysis

Shaded zones can only be counted once in the calculation of volume for soil or rock mass breakout. The reduced volume from overlapping cones will require larger values of h.

(b) Shear Along Grout-Rock or Grout-Soil Interface (Bonded Length)

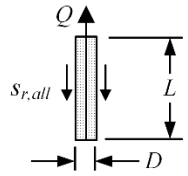

The allowable bond stress ($s_{r,all}$) along the bonded length (L) multiplied by the grouted side area must equal or exceed Q. Allowable bond stress between grout and rock (or soil) is found by dividing the ultimate bond stress ($s_{r,ult}$) by a factor of safety. The values of $s_{r,all}$ and L can be found as:

$$s_{r,all} = \frac{s_{r,ult}}{F}$$

$$L \geq \frac{Q}{\pi \cdot D \cdot s_{r,all}}$$

(c) Shear Along Grout-Tendon Interface (Bonded Length)

The allowable bond stress between the grout and tendon can be assumed as: $s_{g,all} = 0.1\ UCS$, where UCS is the unconfined compressive strength of the grout. The stress applied to grout-tendon interface (s_g) is the load divided by the side area of the tendon with bar diameter, D_b.

$$s_g = \frac{Q}{\pi \cdot D_b \cdot L}$$

$$s_{g,all} \geq s_g$$

(d) Tendon Tensile Capacity

The allowable tensile capacity of the tendon ($s_{s,all}$) must exceed the tensile stress applied to the tendon. An allowable stress of 20 ksi can be assumed. The applied stress is the load divided by the tendon area, A_b.

$$s_{s,all} \geq \frac{Q}{A_b}$$

Figure 5-38 Ground Anchor Design Requirements – (a) Mass Breakout, (b) Grout-Rock or Grout-Soil Shear, (c) Grout-Tendon Shear, and (d) Tendon Capacity (after FHWA 1999)

In weak rocks, such as mudstones and shales, rock anchor capacity is typically limited by the grout-rock interface. In strong, massive rock, the limiting failure mode may be at the grout-tendon interface as described in Figure 5-38(c), depending on the assumptions and construction methods. The allowable bond stress between the grout and tendon is typically assumed to be 10% of the unconfined compressive strength of the grout.

Finally, the tensile capacity of the tendon must be checked as described in Figure 5-38(d). The applied tensile stress should be calculated based on the applied load and the cross-sectional area of the tendon. Example calculations for a rock anchor are included in Figure 5-39.

Table 5-19 Presumptive Average Ultimate Bond Stress for Anchor Grout/Rock Interfaces with Gravity Grouting (After PTI 1996, in FHWA 1999)

Material	Ultimate Grout/Rock Interface Bond Stress, $s_{r,ult}$ (psi)	Comments
Granite and Basalt	250 to 450	The ultimate bond stress at grout/rock interface may be estimated as 10% of the unconfined compressive strength (UCS) of the rock, not exceeding 450 psi.
Dolomitic Limestone	200 to 300	
Soft Limestone	150 to 200	
Slates and Hard Shale	120 to 200	
Soft Shale	30 to 120	
Sandstone	120 to 250	
Concrete	200 to 400	

FHWA (1999) provides guidance on corrosion protection for ground anchors. Three levels of minimum corrosion protection are usually specified in U.S. practice.

- Class I protection – used for permanent anchors:
  - Unbonded length – bar surrounded with grease filled sheath within smooth bond breaker surrounded by grout and casing.
  - Bonded length – bar within grout-filled encapsulation surrounded by grout within soil or rock.
- Class II protection:
  - Unbonded length – bar surrounded with grease filled sheath surrounded with grout and casing.
  - Bonded length – grout surrounding bar within soil or rock.
- No protection for unbonded length and grout in bonded length.

Each ground anchor is load tested past the design load before putting it into service. About 2 percent of anchors are performance tested to 133 percent of the design load in a cycled test where 25, 50, 75, 100, 125, and 133 percent of the load is applied in steps and released. The load is then locked off at 75 to 100 percent of the design load. A

hold is included in the performance test at 133 percent of design load to monitor creep movements. Every anchor that is not performance tested is proof tested to 125 percent of design load. This test is conducted in the same steps noted above, and the load is then locked off at 75 to 100 percent of the design load. FHWA (1999) provides additional guidance.

Rock Anchor Example: Tower Guy Wire Support

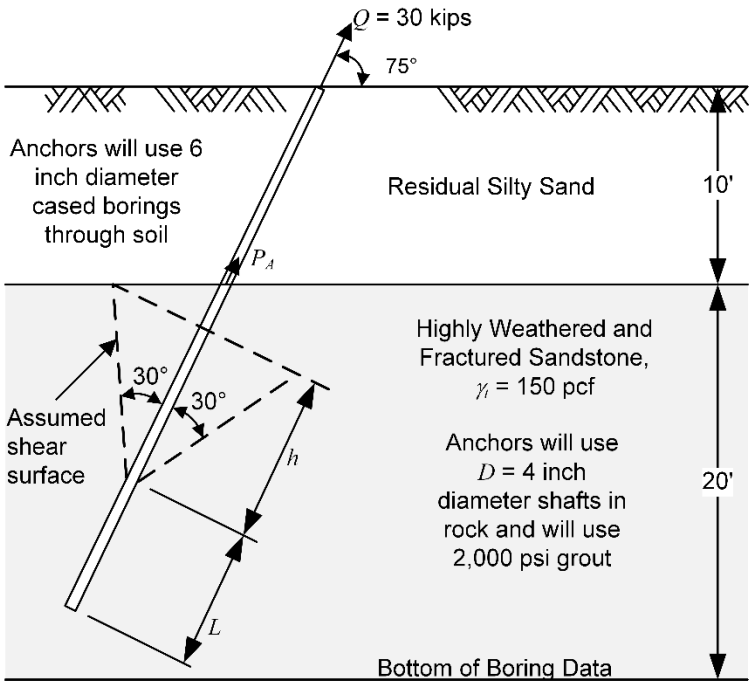

Find Anchor Length (L), Bar Size, and Free Length (h)

Anchor Length

Select an Interface Bond Strength: $s_{r,ult} = 120\,psi$

Allowable Bond Strength (F=3): $s_{r,all} = 40\,psi$

Required Length:

$$L = \frac{Q}{\pi D s_{u,all}} = \frac{30,000\,lb}{\pi\,(4\,inch)\,(40\,psi)}$$

$L = 59.7\,inches$, use $L = 5\,ft$

Bar Size

Determine Required Bar Area: (Use $s_{s,all}$ = 90 ksi)

$$A \geq \frac{Q}{s_{s,all}} = \frac{30\,k}{90\,ksi} = 0.33\,in^2$$

A 1-inch deformed bar with area of 0.85 in^2 will be acceptable.

Free Length

For simplicity, ignore the anchor inclination and soil above the rock.

The cone volume for a 60° angle is: $V = 0.262 \cdot h^3$

The weight of the cone must equal Q; thus: $V = \frac{Q}{\gamma_t} = \frac{30,000\,lb}{150\,pcf} = 200\,ft^3$

Solving for h: $V = 200\,ft^3 = 0.259h^3 \rightarrow h = 9.17\,ft$, use $h = 10\,ft$ (Minimum of 10 ft)

The minimum value for h is 10 ft for a deformed bar. In this case, the additional rock due to the angle of the anchor and 10 ft of soil will more than meet this requirement.

Check Bar Pullout from Grout

Applied Grout-Bar Interface Stress, s_g: $s_g = \frac{Q}{\pi D_b L} = \frac{30,000\,lb}{\pi\,(1\,in)\,(60\,in)} = 159\,psi$

Allowable Grout-Bar Interface Stress: $s_{g,all} = 0.1 \cdot UCS = 0.1\,(2000\,psi) = 200\,psi$ OK

Summary: Anchor Length: L = 5 ft, Bar Size: D_b = 1 inch, Free Length: h = 10 ft

Figure 5-39 Example Problem for Single Rock Anchors

5-5.2.3 Soil Anchors.

Shallow anchors in soil have similar failure mechanisms as in rock: cone breakout and shear along the grout/soil interface. The cone breakout mechanism is typical for shallow anchors. However, if the minimum unbonded length of 10 feet for bars is used, it is generally not necessary to consider cone breakout. Soil anchors tend to be much deeper because the grout/soil interface bond stress is lower. Soil anchors with an uplift load are essentially to micropiles with an uplift load. The minimum spacing between soil anchors should be 5 feet (Caltrans 2020). The appropriate inverted cone angle is in the range of 60 to 90°.

The design requirements shown in Figure 5-38 can also be used for soil anchors. The design should include selection of h, L, and tendon size. Presumptive ultimate bond stresses at the grout/soil interface for various soil types are shown in Table 5-20. Factors of safety of 2 and 3 can be used for transient and sustained loads, respectively, to calculate allowable bond stress. If the soil type changes along the anchor length, the side resistance can be divided into layers to allow the calculation of L.

Table 5-20 Presumptive Average Ultimate Bond Stress for Anchor Grout/Soil Interfaces with Gravity Grouting (After PTI 1996 in FHWA 1999)

Category	Soil Type	Plasticity or Relative Density	$s_{s,ult}$ (psf)
Fine-Grained	Soft lean clay	--	600
	Stiff fat clay	Medium to high	600
	Very stiff fat clay	Medium to high	1,400
	Stiff fat clay	Medium	2,100
	Very stiff fat clay	Medium	2,900
	Very stiff sandy silt	Medium	5,800
Coarse-Grained	Silty sand	--	3,500
	Fine to medium sand	Medium dense to dense	1,700
	Medium to coarse sand with gravel	Medium dense	2,300
	Medium to coarse sand with gravel	Dense to very dense	5,200
	Sandy gravel	Medium dense to dense	4,400
	Sandy gravel	Dense to very dense	5,800
	Glacial till	Dense	6,300

5-5.2.4 Design of Anchors to Resist Hydrostatic Uplift.

Ground anchors may also be used to provide resistance against uplift forces caused by hydrostatic pressures. Two cases can be considered: 1) the structure is founded on rock or relatively stiff soil or 2) the structure is founded on relatively compressible soil with the anchors are secured in deeper soil or rock. When the structure is founded on rock or suitable soil for anchor development, the calculations presented in Section 5-5.2.2 and 5-5.2.3 can be used. When a more compressible soil layer exists between

the structure and the anchors, as shown in Figure 5-40, changes in anchor loads resulting from movement of enclosed compressible ground mass (i.e., groundwater fluctuations, consolidation settlement or heave, or creep deformations) must be considered.

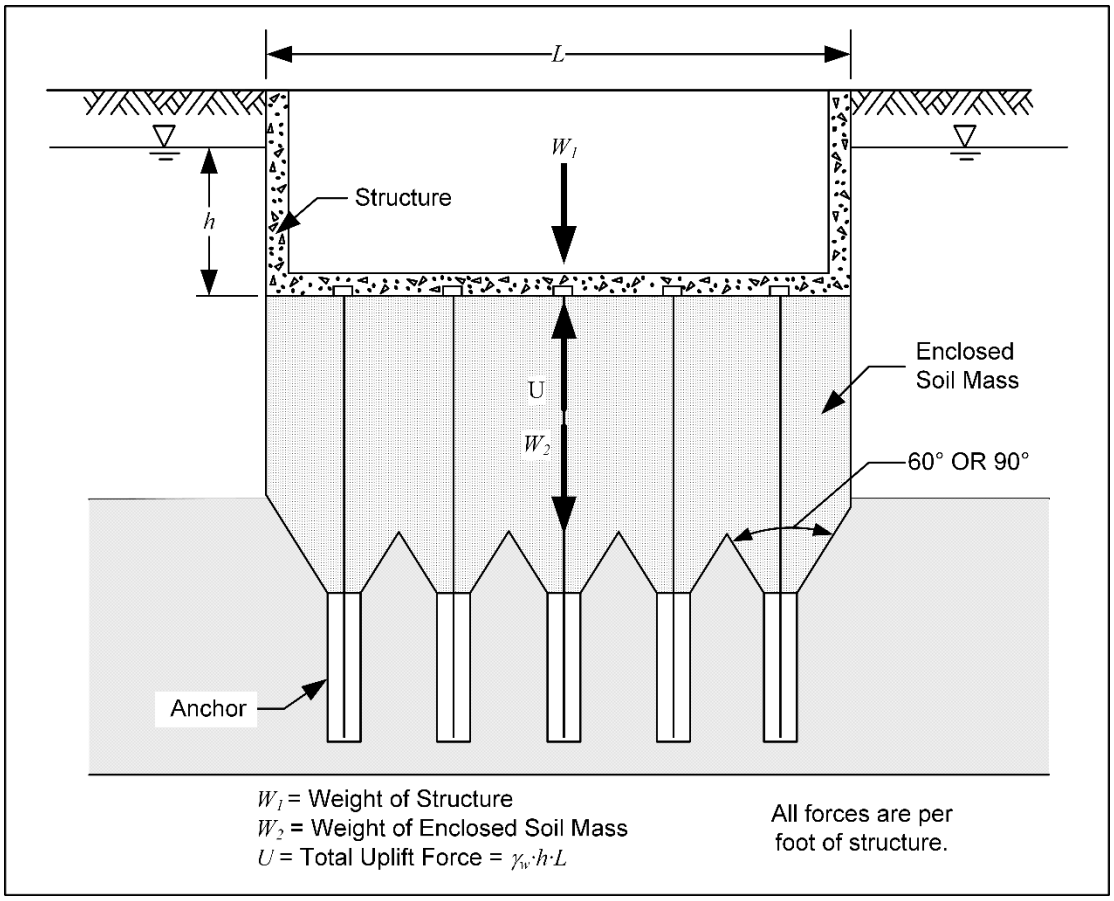

Figure 5-40 Resisting Hydrostatic Uplift with Ground Anchors (after FHWA 1999)

The design should verify that the hydrostatic uplift force (U) can be resisted by the weight of the structure (W_1) plus the weight of the enclosed soil mass (W_2). The uplift force should be calculated based on the maximum elevation of the water table. The buoyant unit weight of soils should be used for soils below the water table. Frictional resistance is neglected between the soil and walls of the structure. Friction is also neglected along the hypothetical vertical plane within the soil between the structure and the top of the bonded zone for the anchor (FHWA 1999).

The anchor loads can change with time. Groundwater fluctuations may cause cyclic changes in the anchor load. Consolidation and creep may result in detensioning. If any of these movements could cause additional tension in the tendons after lock-off, the tendons should be sized accordingly (FHWA 1999).

5-5.2.5 Transient Uplift Loads and Moments on Footings, Piers, and Posts.

Transient uplift and moment loads can be resisted by shallow foundations. Some simple methods to consider these loadings are presented in Figure 5-41. Design for moment loading can use methods for rigid retaining walls in Chapter 4. Uplift and lateral loading of piers, posts, and piles is addressed in more detail in Chapter 6.

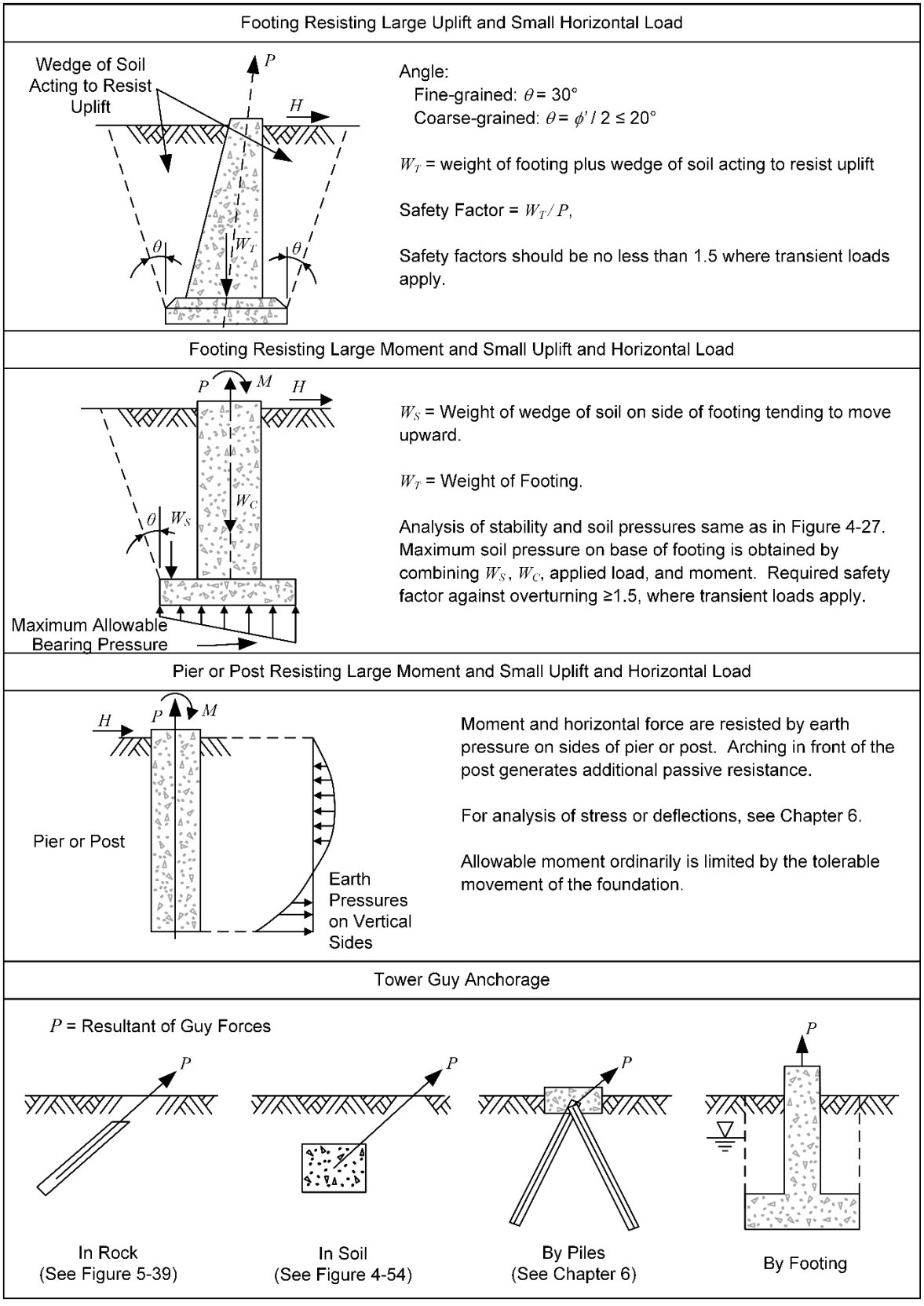

Figure 5-41 Resistance to Transient Uplift Loads on Footings, Piers, and Posts

5-5.2.6 Uplift Resistance Using a Deadman.

Guidance for the use of a concrete deadman for uplift resistance is provided in Figure 5-42. For a deadman in weak soil, it may be feasible to replace a considerable volume of soil with granular backfill and construct the block within the new backfill. If this is done, the passive wedge should be contained entirely within the granular fill, and the stresses on the remaining weak material should be investigated.

Design Guidance

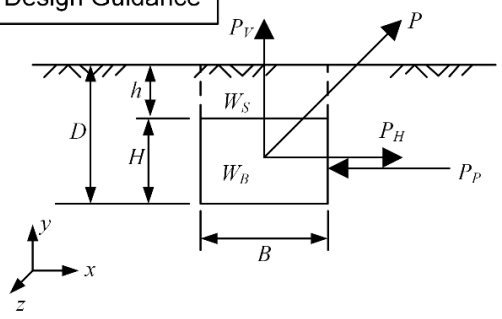

P = Resultant of maximum guy forces
P_H, P_V = Components of P
P_P = Passive earth pressure force (see Section 4-3)
B, H = Block dimensions
L = Block dimension in the z direction
γ = Unit weight of soil
ϕ' = Effective friction angle
W_B = Weight of block
W_S = Weight of soil on block = $B \cdot L \cdot H \cdot \gamma$
W_S = Total weight = $W_B + W_S$

Design Criteria

1. Resistance to Vertical Force

Provide design such that: $\frac{W_T}{P_V} \geq 1.5$ and $\frac{W_B}{P_V} \geq 1.0$

2. Resistance to Horizontal Force

Provide design such that: $\frac{P_P}{P_H} \geq 1.5$

Notes: Passive resistance is calculated only on face of block (Area = $H \cdot L$). Block backfill shall be compacted as described in Chapter 3. Use total unit weights above the water table, and buoyant unit weights below the water table. Keep P_H at 1/2 to 2/3 of block depth.

Example

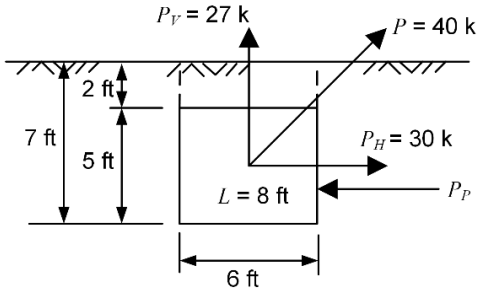

Soil: γ = 110 pcf, γ' = 60 pcf, ϕ' = 30 deg
Groundwater at a depth of 5 ft
Using Rankine: K_P = 3

Weights:
W_S = (6 ft)(8 ft)(2 ft)(110 pcf) = 10,500 lb
W_B = (6 ft)(8 ft)[(3 ft)(150 pcf) + (2 ft)(87.5 pcf)]= 30,000 lb
W_T = 10,500 + 30,000 = 40,500 lb

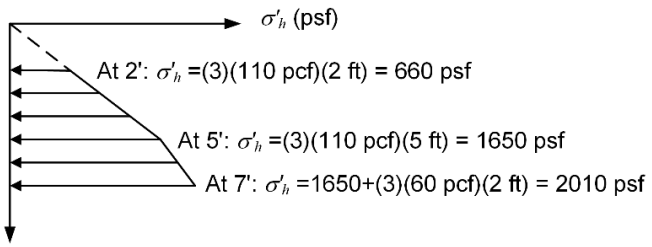

$$P_P = (8\,ft)\left[(3\,ft)\left(\frac{660+1650}{2}\right)+(2\,ft)\left(\frac{1650+2010}{2}\right)\right] = 57{,}000\,lb$$

1. Resistance to Vertical Force

$$\frac{W_T}{P_V} = \frac{40.5k}{27k} = 1.5, \quad \frac{W_B}{P_V} = \frac{30k}{27k} = 1.1 > 1.0 \quad \text{OK}$$

2. Resistance to Horizontal Force

$$\frac{P_P}{P_H} = \frac{57k}{30k} = 1.9 \geq 1.5 \quad \text{OK}$$

Conclusion: The block design will adequately resist the applied loads. A more efficient design may be found by varying the block dimensions and embedment.

Figure 5-42 Design Guidance for Uplift Resistance by Concrete Deadman

5-6 DESIGN FOR SPECIAL SOIL CONDITIONS.

5-6.1 Shallow Foundations on Engineered Fill.

Engineered fill or compacted structural fill can be used to support structures and/or floor slabs. This fill is designed to have specific strength and compressibility properties and, as such, must be controlled in the field by personnel under the direction of a geotechnical engineer. Chapter 3 provides additional detail on fill compaction.

Compacted structural fill is commonly used to raise the general grade for support of a structure. Structural fill may also be used beneath structures to allow for higher bearing pressures and reduce settlements by replacing unsuitable foundation soils and/or providing a relatively stiff mat of soil above less suitable soils.

5-6.1.1 Compacted Structural Fill Requirements.

As noted in Chapter 3, compacted structural fill must be designed and monitored in order to provide adequate foundation support. Design of compacted fill includes selection of appropriate fill type by engineering classification and moisture content limitations. The suitability of subgrade for support of compacted structural fill should be evaluated by the subsurface exploration and field observations. Specifications for fill placement must be selected, including loose lift thickness, minimum relative compaction, and relative moisture content ranges. Section 5-2.5 provided presumptive bearing pressures for compacted fill.

During construction, structural fill should be monitored to determine if the material meets the classification and compaction requirements. Compaction control testing should verify that specifications have been met. Control tests should be checked for errors in testing or interpretation, such as degree of saturation greater than 100%. The fill should be protected against wetting by proper grading and surface drainage. In cold weather, a protective layer should be used to protect the surface from frost penetration.

5-6.1.2 Geometric Limits of Compacted Structural Fill.

Where the general grade is raised for a structure, the entire building pad should be treated as compacted structural fill. The structural fill should extend laterally at least 5 ft outside the edge of the exterior footings or should encompass a zone extending downward at at 1H:2V angle from the footings, whichever is greater. More guidance on deep fills is provided in Section 3-6.5. In some cases, the upper few feet of a structural fill only support floor slabs and will have reduced compaction requirements.

Fill may also be used to replace unsuitable bearing soil. The vertical and lateral limits of the zone of compacted structural fill beneath footings should consider the vertical stresses imposed by the footings as shown in Figure 5-43. Unless adequate bearing soil is reached sooner, the excavation must extend to a depth that adequately reduces

the change in stress from the foundation at the base of the fill. Continuous footings impose stresses to a greater depth than square footings with the same width. With high-quality fill, higher bearing pressures may allow narrower foundations that limit the depth of influence from individual foundations on the underlying soil.

Adequate bearing material may not be present within the depths indicated in Figure 5-43. In that case, the structural fill must be placed over underlying settlement prone material. The bottom of the excavation may require stabilization with geogrid or geotextile to allow fill to be placed and compacted. Alternatively, a bridging layer of gravel or cobble-sized material may be required. Settlement will likely control the net allowable bearing pressure for this situation. Settlement calcuations should consider the increased stress on the underyling soil because of higher unit weight of the fill. Settlement may be caused by individual foundation loading as well as the combined change in stress from all of the building foundations. These should both be evaluated. If settlement cannot be mitigated, either ground improvement or deep foundation will likely be required.

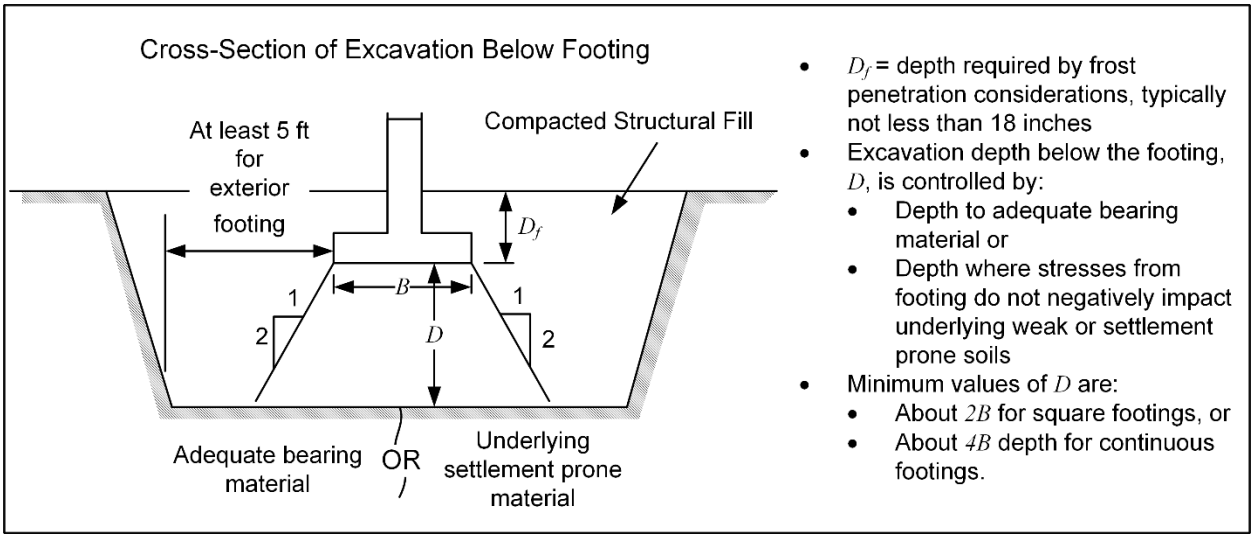

Figure 5-43 Geometric Limits for Structural Fill Beneath Footings

5-6.2 Foundations on Expansive Soil and Rock.

Soils that undergo substantial or problematic volume changes upon wetting and drying are termed expansive or swelling soils. Surficial clays above the water table with a PI greater than about 20 and relatively low natural water content should be considered potentially expansive. These soils are most commonly found where the groundwater table is low in arid climates with a deficiency of rainfall and conditions of over-evaporation. Expansive soils are also found in more temperate climates where clay deposits are present that contain montmorillonite. Mottled, fractured, or slickensided clays, showing evidence of past desiccation, are particularly troublesome. For other

causes of swelling in soils and for the computations of resulting heave see Chapter 5 of DM 7.1. Regional experience is critical for the identification of expansive soils and selection of foundation solutions. Additional information on these soils can be found in Section 1-2.12.

Climate has an important effect on the interaction between expansive soils and foundations. In arid regions, the soils tend to have a relatively low natural water content. Seasonal wetting tends to cause heave around the perimeter of structures and lifting of the edges of exterior foundations and slabs. In contrast, the soils in temperate climates tend to have a relatively high natural water content. Seasonal drying tends to cause shrinkage around the perimeter of structures. In this case, the exterior foundations and slab edges tend to drop or settle within time. These tendencies can affect the selection of appropriate mitigation alternatives for expansive soils.

Foundation design should also consider the potential for sulfide induced heave from soils and rock.

5-6.2.1 Reducing Soil Expansion Potential.

Where economically feasible, remove potentially expansive soils from beneath footings and replace with compacted structural fill of non-expansive materials as shown in Figure 5-44(a). The fill should not allow water to collect or to be introduced to deeper expansive soils. Thus, low plasticity fine-grained soils are preferred. Alternatives to removal and replacement are discussed in the following paragraphs.

In some cases, column loads and floor loads with straight or underreamed drilled shafts founded below the zone of active swelling as illustrated in Figure 5-44(b). The soil along the upper part of the shaft will impart an upward force that must be resisted by the weight of the pier, the dead load, and the underreamed section. At any depth, the tensile force exerted on the shaft equals the shaft adhesion (see Chapter 6) times the difference in side area above and below the point under consideration. The reinforcement must resist these tensile forces and, if used, should extend into the underreamed section of the drilled shaft to allow engagement of the bell to resist uplift. An alternative is to place the shaft in an oversized hole and fill the annular space with a plastic material that can deform without developing adhesion to the shaft. Viscoelastic polymers, such as liquid rubber, are materials that fit this category. Placing the base of the foundation near the water table reduces heave damage because little change in moisture content occurs.

If the structure is sufficiently heavy and the soil is strong, the swell pressures can be resisted by the dead load of the structure. The floor slabs must be structurally supported overlying degradable carboard forms as shown in Figure 5-44(c).

5-6.2.2 Minimizing Expansion Effects.

Where it is not economically feasible to remove expansive materials or to support foundations below depths of possible expansion, the effects can be minimized by the following.

- Place fill with expansion prone plastic fines at moisture contents multiple percentage points above optimum moisture content at dry unit weight no higher than required for strength and compressibility.
- Construct grade beams over degradable carboard.
- Provide impervious blankets or grade surface around structure to drain away from foundations.
- Locate water and drainage lines away from soils supporting foundations.
- Consider stabilization of the foundation soils with lime or cement to reduce the plasticity.

Where heave of the floor slab is not a critical concern, place concrete floor slabs directly on problem soil but provide expansion joints so the floor can move freely from structure.

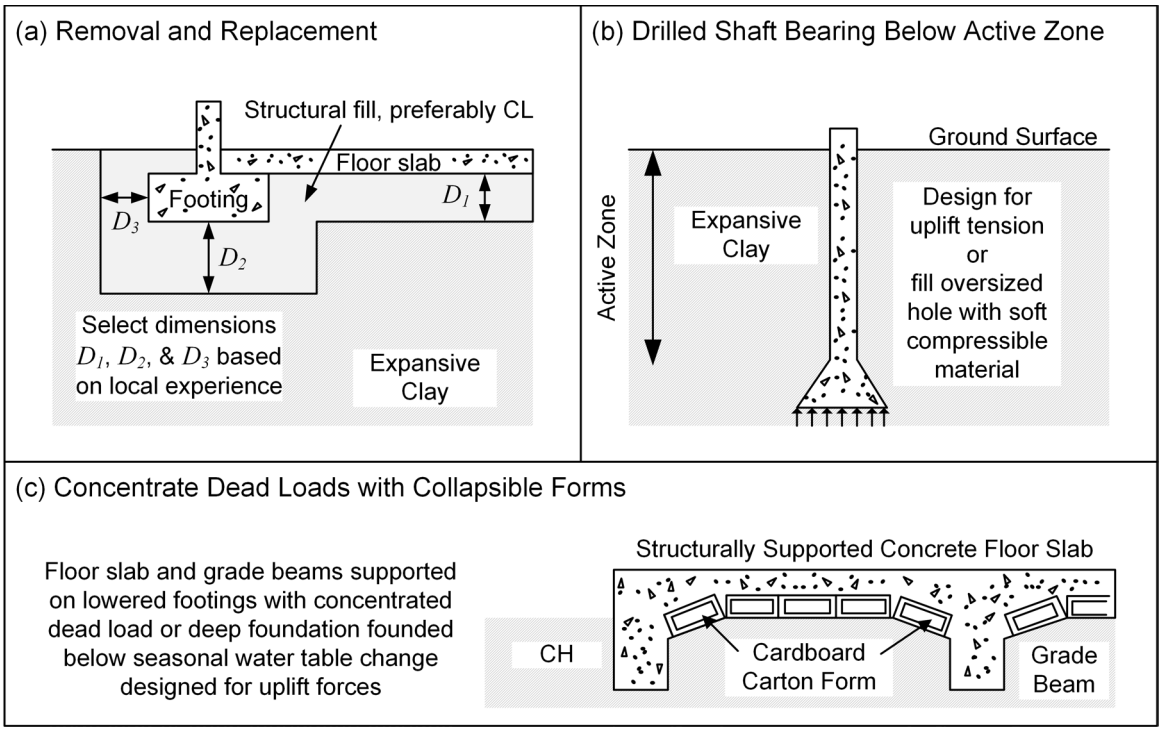

Figure 5-44 Construction Details for Swelling Soils

5-6.2.3 Heave of Sulfide Soils and Rock.

Foundation design should consider the potential for sulfide induced heave and corrosion. Sulfur may be present in sulfidic rock or soils below foundations or within

compacted structural fill constructed of sulfidic rock or soils. The different forms of sulfur consist of (Dubbe 1984):

- Sulfate sulfur - represents a measure of the degree of oxidation and is an indication of the amount of expansion that has taken place before sampling;
- Sulfide (pyritic) sulfur - represents the amount of unoxidized sulfidic material and the potential expansion that can take place in the future; and
- Organic sulfur – represents material that is not believed to be involved in the expansive reaction.

Sulfide soil and rock is typically identified by testing. Samples of rock or soil for chemical testing of total sulfur forms should be wrapped in plastic to prevent any change in moisture content and to reduce oxidation before testing. Bryant et al. (2003) found that sulfide-induced heave can occur in materials containing as little as 0.1% sulfide [pyritic] sulfur. Figure 5-45 illustrates the potential for heave for various concentrations of sulfide [pyritic] sulfur.

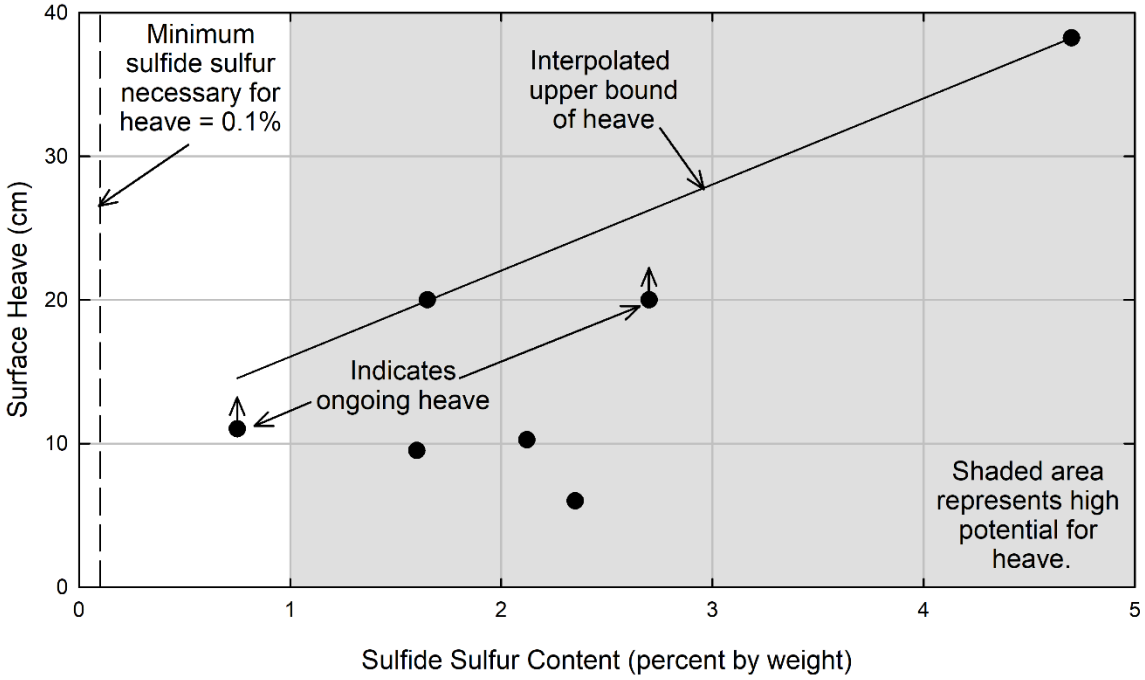

Figure 5-45 Potential Sulfidic Rock Heave (after Bryant et al. 2003)

Ground water should also be tested if it can rise to be in contact with foundations. Sulfide-induced corrosion of concrete can occur if sulfide (pyritic) sulfur exceeds 1200 ppm.

When testing indicates mitigation measures are warranted, the following should be considered:

- For new structures: remove sulfidic soil or rock below floor slab and/or footings unless dead loads are sufficient to prevent heave and use void filler below grade beams and slabs as discussed for expansive soils;
- For protection of concrete subject to sulfidic groundwater use: 1) sulphate resistant cement such as Type V Portland cement, 2) lower water-cement ratio concrete, or 3) coat concrete with bitumen; and
- For existing structures consider partial or complete removal of sulfidic soil or rock below floor slab and/or footings depending upon how heave has impacted the structure.

If testing indicates oxidation is complete and damage has already occurred, the sulfidic soil or rock does not need to be removed. Partial excavation and replacement can be used if necessary but any sulfidic material left in place below the structure should be completely covered with spray mastic to seal the area from air. The excavated areas should be backfilled with structural fill that is below problematic levels for sulfur. Flowable fill has also been used as backfill.

Electrical corrosive properties of soil are important where metal structures such as pipelines, etc. are buried underground. A resistivity survey of the site may be necessary to evaluate the need for cathodic protection.

5-6.3 Foundations on Collapsible Soils.

Collapsible soils are characterized by a metastable structure and undergo an abrupt collapse when they are inundated. Thus, existing deposits are located above the water table in their natural state. Most collapsible soils are either debris flow deposits of low unit weight or wind deposits (loess). Loose fills and decomposed igneous rocks can also be collapsible. They usually consist of silts and sands with a substantial fines content. Additional information on loess is found in Section 1-2.3.

Collapsible soils are located in the Midwest and Southwest United States, parts of Asia, South America, and Southern Africa according to Mitchell and Soga (2005). The geographic location of loess deposits in the United States, South America, Europe, and Asia are shown in Figure 5-46. The depth of collapsible soil deposits can be very great, often up to 100 ft and sometimes over 500 ft (USBR 1992). Because of the substantial thickness, large settlements can result from collapse. USBR (1992) also stated that the amount of collapse is affected by layer thickness, soil mineralogy, initial void ratio, stress history, grain shape, moisture content, pore sizes, any cementing agents, and the amount of added load (hydrostatic or structural).

5-6.3.1 Identification of Collapsible Soils.

The following tasks need to be accomplished when working with collapsing soils (Houston et al. 2001):

- Identification and characterization of collapsible soil sites,
- Estimation of the extent and degree of wetting when collapse occurs,
- Estimation of collapse settlements, and
- Selection of design and mitigation alternatives.

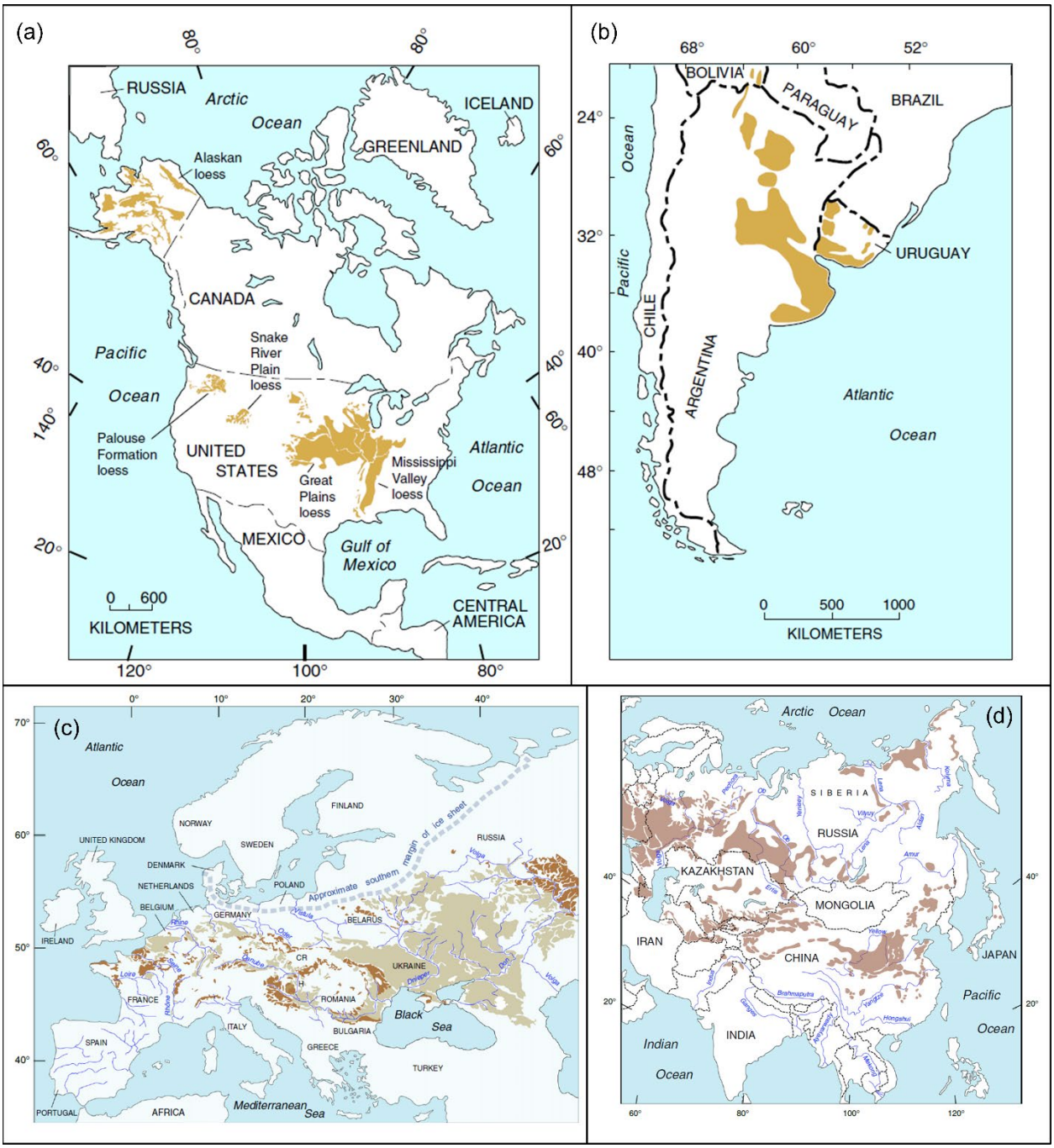

Figure 5-46 Loess Distribution – (a) United States, (b) South America, (c) Europe, and (d) Asia (after Muhs 2013)

Estimation of the extent and degree of wetting required for collapse is the most difficult of these tasks. Rising groundwater is the only method that will ensure 100 percent saturation. Irrigation from the surface will not usually result in 100 percent saturation.

The most danger occurs when these soils are not identified, and a structure is damaged due to soil collapse. As a simple test to identify collapsible soils, the natural dry unit weight of a soil sample can be plotted against the liquid limit on Figure 5-47 (USBR 1992). The curves represent the dry unit weight corresponding to a saturated soil with a water content equal to the liquid limit. If the natural dry unit weight is lower than the saturation line, the soil is potentially collapsible. The most difficult problem with this identification test is obtaining undisturbed samples for testing. Undisturbed sampling of silts and fine sands is difficult, and disturbance will impact the results. Many collapsing soils will slake upon immersion, but this is not a definitive indicator.

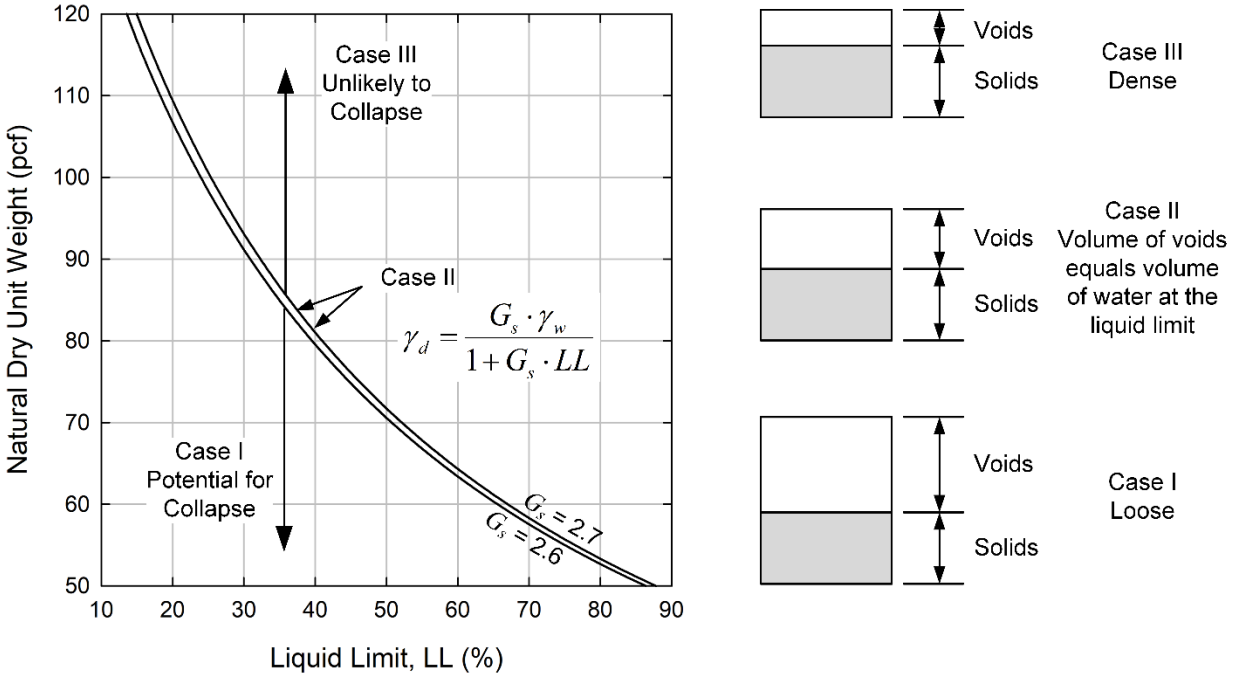

Figure 5-47 Criteria for Evaluation of Collapsing Soils (after USBR 1992)

5-6.3.2 Estimated Degree of Wetting When Collapse Occurs.

Houston et al. (2001) indicate that full collapse only occurs in the field with a rising water table, but partial collapse can occur at moisture contents less required for 100 percent saturation, such as from irrigation. Typical saturation levels achieved during irrigation

are 35 to 60 percent. Full wetting collapse is usually identified in the laboratory using one-dimensional consolidation tests in accordance with ASTM D4546[29].

5-6.3.3 Estimation of Collapse Settlements.

One-dimensional consolidation tests can be used to determine two different qualitative measures of collapse. The *collapse potential* is the strain caused by wetting at any stress level while the *collapse index* is the relative collapse for inundation at a stress of 4000 psf (ASTM D5333, Jennings and Knight 1975). Relative classification of collapse associated with these two measures are summarized in Table 5-21.

Table 5-21 Classification of Collapse (after ASTM D 5333, Jennings and Knight 1975)

Classification of Collapse	Collapse Index (%) (inundation at any stress level)	Collapse Potential (%) (inundation at any 4000 psf)
None	0 to 0.1	0 to 1
Slight	0.1 to 2	1 to 5
Moderate	2.1 to 6	5 to 10
Moderately Severe	6.1 to 10	
Severe	>10	>10

The magnitude of collapse can be estimated using the results of one-dimensional tests on one or more specimens inundated at vertical stress conditions applicable to the project conditions (ASTM D4546). The strain caused by wetting is directly measured for each specimen and used to estimate strain under field conditions. Because close to full saturation is achieved, the strains measured in the laboratory tests tend to be conservative compared to typical field wetting. Boundary conditions and nonuniformity in field conditions can make the laboratory measured rates of collapse unreliable (ASTM D4546).

Settlement caused by collapse can be estimated by multiple the decimal strain by the thickness of the soil layer. If multiple collapse tests are performed at different vertical stresses, the settlement can be predicted for each layer and summed.

In earthquake prone areas, densification and collapse may occur even after mitigation and should be evaluated (Houston et al. 2001). For example, prewetting may only cause partial wetting collapse, and the soil may still be subject to densification by earthquake shaking.

[29] ASTM D5333 and the collapse index have sometimes been used to estimate collapse settlements. However, this standard has been withdrawn from use.

5-6.3.4 Mitigation Alternatives.

Available mitigation alternatives for collapsible soils include:

- Removal and replacement with compacted structural fill,
- Avoidance of wetting,
- Deep dynamic compaction,
- Chemical stabilization or grouting,
- Deep foundations, and
- Prewetting.

The most widely used mitigation method is removal and replacement with compacted structural fill. Often the excavated material is reused as fill. For shallow depths of collapsible material, this is the least costly and best alternative. Avoidance of wetting has also been used where slopes are used to divert water away from the structure. Prewetting is less successful where little additional load is applied during wetting.

5-6.4 Other Problem Soils.

Chapter 1 provides a summary of many types of problem soil conditions that can affect the design of foundations and earth structures. Table 5-22 summarizes important conditions for the design of shallow foundations in problem soils.

Table 5-22 Problem Soil Considerations for Shallow Foundations

Soil Type	Primary Considerations for Shallow Foundations
Soft Clays, Organic Soils, Peat, and Muskeg	• Low shear strength and high compressibility result in very low allowable bearing pressures, which can be uneconomical. • Secondary compression should be included in settlement calculations. • Ground improvement will often improve economic viability. • Deep foundations may also be a more economical solution for foundation support.
Stiff Fissured Expansive Clays and Shales	• Bearing capacity and settlement are typically not a concern, except for very high loads. • Shrink/swell potential of the clay or rock will control foundation design (see DM 7.1, Ch. 5). • Design options include: o Removal and replacement of expansive material within zone of active moisture change, o Deepening of foundations through the active zone, o Chemical modification of the soil to reduce expansive properties, and o Concentration of load to resist swell pressures.
Loess and Other Collapsible Soils	• Metastable structure of the soil can collapse under loading, especially wetting. • Collapse potential increases when the natural dry unit weight is lower than that corresponding to saturation at the liquid limit. • Solutions can vary from controlled wetting to ground improvement to deep foundations.
Sensitive Clays	• The shear stress should not exceed the peak shear strength of the clay at any point below the foundation. • For eccentrically loaded foundations, the factor of safety should be calculated using the maximum bearing pressure caused by the eccentricity.
Residual Soils	• Correlations to engineering properties are less reliable for residual soils and may not be valid. • Settlement calculations may be more accurate using the coefficient of compressibility.
Laterites	• If weakly cemented, laterites may provide poor foundation support, especially for cyclic loads or if exposed to flowing groundwater.
Talus	• Global stability of the talus should be assessed prior to use for the support of shallow foundations.

Loose Sands	• Settlements that exceed the tolerable limits for most shallow foundations can result, even for relatively low bearing pressures. • Settlement should be calculated using an appropriate empirical procedure (see DM 7.1, Chapter 5), preferably selected based on local experience. • In many cases, the CPT provides better characterization of saturated loose sands than SPT.
Dredged Soils	• Dredged soils should be treated as soft or loose for design of shallow foundations (see comments above)

Low Plasticity and Nonplastic Silts	• Difficult construction conditions may occur for shallow foundations resulting from:
	  ○ Wetting of the bearing surfaces or
	  ○ Instability of saturated silts caused by dilatancy.
	• Protection of the bearing surface by a mud mat (thin layer of concrete) may be required to maintain a stable bearing surface during construction.

Municipal Solid Waste	• Shallow foundations will rarely be supported within or above MSW. • Settlement will likely control with special consideration given to differential movement due to the high variability of the MSW. • Ongoing consolidation of MSW under its own weight must also be considered.

5-7 NOTATION.

Variable	Definition
b_c, b_q, b_γ	Bearing capacity factors to account for sloping base conditions
c	Total stress cohesion intercept
c'	Effective stress cohesion intercept
c^*	Reduced cohesion intercept to account for the effects of local and punching shear
d_c, d_q, d_γ	Bearing capacity factors to account for foundation embedment depth
D_r	Relative density
e	Eccentricity
$E'{\cdot}I_b$	Flexural stiffness of a structure
E_c	Young's modulus of concrete
E_s	Elastic modulus of soil
E'_s	Effective or drained modulus of soil
E_{us}	Undrained modulus of soil
F_{BC}	Factor of safety against bearing capacity failure
g_c, g_q, g_γ	Bearing capacity factors to account for sloping ground conditions
G_s	Specific gravity of solids
GSI	Geological Strength Index
h	Depth of structure below groundwater level for design against hydrostatic uplift
H	Horizontal load

Variable	Definition
I	Moment of inertia
i_c, i_q, i_γ	Bearing capacity factors to account for load inclination
K	Equivalent spring stiffness
k_p	Modulus of subgrade reaction from plate load test
Kr	Relative stiffness factor
k_s	Modulus of subgrade reaction
k_{sc}	Modulus of subgrade reaction reduced for time-dependent settlement
K_s	Punching shear coefficient
K_P	Passive earth pressure coefficient
L	Width of structure for design against hydrostatic uplift
LL	Liquid limit
M	Applied moment
N	Standard Penetration Test blow count
$N_{1(60)}$	Standard Penetration Test blow count corrected for overburden and energy
N_{60}	Standard Penetration Test blow count corrected for energy
N_c, N_q, N_γ	Bearing capacity factors
$N_{c,m,s}$, $N_{c,m,c}$	Modified bearing capacity factors for strip and continuous footings
OCR	Overconsolidation ratio
PI	Plasticity index
P_P	Resultant force from passive earth pressure
Q	Gross vertical load
q	Contact pressure
$q_{all,gross}$	Gross allowable bearing pressure
$q_{all,net}$	Net allowable bearing pressure
qc	Cone penetration test tip resistance
Q_{DL+LL}	Structural dead load plus live load
q_{net}	Net bearing pressure
q_{ult}	Ultimate bearing capacity

Variable	Definition
q'_{ult}	Reduced ultimate bearing capacity
q_{unif}	Equivalent uniform bearing pressure
$R.C.$	Relative compaction
RC_{slope}	Reduction coefficient for bearing capacity of foundations near slopes
RQD	Rock quality designation
s	Settlement
s_c	Consolidation settlement
s_g	Stress applied at grout-tendon interface
$s_{g,all}$	Allowable stress for grout-tendon interface
$s_{r,all}$	Allowable bond strength for ground anchors
$s_{r,ult}$	Strength of grout-rock interface
$s_{s,all}$	Allow stress for grout-rock interface
s_c, s_q, s_γ	Bearing capacity factors to account for foundation shape
s_u	Undrained shear strength
U	Hydrostatic uplift force
UCS	Unconfined compressive strength
V	Shear load
W_1	Weight of structure
W_2	Weight of enclosed soil mass
W_f	Weight of foundation
W_s	Weight of soil overlying foundation
α	Bearing capacity failure plane angle
β	Angle of sloping ground
$\Delta\sigma_{z,ave}$	Average change in vertical stress below a mat foundation
γ	Total unit weight
γ'	Bouyant or effective unit weight
γ_d	Dry unit weight
γ_w	Unit weight of water

Variable	Definition
ϕ	Total stress friction angle
ϕ'	Drained or effective stress friction angle
ϕ^*	Reduced friction angle to account for the effects of local and punching shear
ϕ_{rf}	Rock fracture friction angle including the effects of asperities
ν	Poisson's ratio
σ_{vD}	Effective vertical stress at the foundation bearing elevation
$\Psi_c,\ \Psi_q,\ \Psi_\gamma$	Lumped bearing capacity factors used to correct for complicating factors

5-8 SUGGESTED READING.

Topic	Reference
Bearing capacity of soil	Meyerhof, G. G. 1951. "The ultimate bearing capacity of foudations." *Geotechnique*, 2(4), 301-332.
	Vesić, A. S. 1973. "Analysis of ultimate loads of shallow foundations." *Journal of the Soil Mechanics and Foundations Division*, 99(1), 45-73.
	Brinch Hansen, J. 1970. *A Revised and Extended Formula for Bearing Capacity, Bulletin No. 28*. Danish Geotechnical Institute, Copenhagen.
Bearing capacity of rock	Stagg, K. G. and Zienkiewicz, O. C. 1968. *Rock Mechanics in Engineering Practice*. John Wiley & Sons, New York, 442 pp.
Mat foundations	American Concrete Institute (ACI). 2002. *Suggested Analysis and Design Procedures for Combined Footings and Mats, ACI 336.2R-88*, ACI.
Anchors for foundations	FHWA. 1999. *Ground Anchors and Anchored Systems. Geotechnical Engineering Circular No. 4. Publication FHWA-IF-99-015*. Federal Highway Administration, Washington, D.C.
Foundations in expansive soils	Chen, F.H. 1988. *Foundations on Expansive Soils*. 2nd Edition, Elsevier Science Publications, New York, NY.
Foundations in collapsible soils	Houston, S. L., Houston, W. N., Zapata, C. E., and Lawrence, C. 2001. "Geotechnical engineering practice for collapsible soils." *Unsaturated soil concepts and their application in geotechnical practice*, 333-355.

CHAPTER 6. DEEP FOUNDATIONS

6-1 INTRODUCTION.

6-1.1 Scope.

This chapter presents information on the common types of deep foundations, analysis and design procedures, and procedures for installation and quality control. The term *deep foundations*, as used in this chapter, refers to foundations that obtain capacity along their length and/or at their base, generally with a foundation length to width ratio (Z/b) exceeding five. Deep foundations include driven piles and formed-in-place columns, such as drilled shafts, continuous flight auger columns (CFAs), drilled displacement piles (DDPs), aggregate columns, micropiles, and helical piles. This is not an exhaustive list of deep foundation technologies nor is there a consensus on the naming of the technologies.

Since common deep foundation technologies are discussed together in this chapter, generic terminology is used as much as possible to unify the discussion of technical concepts. The terms *column*, *element*, and *pile* are used interchangeably, with the term *driven pile* used to distinguish the specific foundation type. The term *top* is used to refer to the end of the element closest to the ground surface in lieu of alternatives such as *head* and *butt*; the terms *side* and *shaft* are used interchangeably; and the terms *base, tip,* and *toe* are used interchangeably to refer to the end of element that is furthest from the ground surface. This variety of terms is more consistent with source material and disrupts excessive repetition of particular words.

Given the extensive body of knowledge in the area of deep foundations, the scope of this chapter is to provide technical background and present selected design approaches for several popular deep foundation options concisely in one organized location. This chapter is intended to be useful as a standalone resource as well as a primer to the information provided in technology-specific design manuals. Potentially helpful resources that were used in the development of this chapter are provided in Section 6-13.

6-1.2 Organization

Chapter 6 is organized into ten sections. Table 6-1 outlines some key information found in each section as a supplement to the information provided in the Table of Contents for this manual.

6-1.3 Applications.

Deep foundations are used in a variety of applications including:

1) To transmit loads through an upper weak and/or compressible stratum to an underlying competent zone;

2) To provide support in areas where shallow foundations are impractical, such as underwater, in close proximity to existing structures, situations where the magnitude and/or rate of consolidation is intolerable, and on contaminated sites.

3) To provide uplift resistance and/or lateral load capacity.

Deep foundation technologies are also used in ground improvement applications and slope stabilization. These applications are not covered in this chapter.

Table 6-1 Organization of Chapter 6

Section	Key information provided
6-1 Introduction	Scope, applications, and general considerations
6-2 Design aspects and considerations	Overview of design process and considerations related to the project, site, subsurface, and construction
6-3 Foundation types	Overview of deep foundation types and some useful material properties
6-4 Construction	Summary of construction equipment, materials, and processes for common types of deep foundations
6-5 Geotechnical static axial capacity and settlement	Details of practical methods for evaluating geotechnical axial compressive and uplift capacity and settlement for single or a group of deep foundation elements founded in coarse-grained soil, fine-grained soil, or rock.
6-6 Geotechnical lateral capacity	Overview of software and analytical methods for evaluating lateral behavior for single or a group of deep foundation elements founded in coarse-grained or fine-grained soil; details for Broms ultimate load analysis and Characteristic Load Method.
6-7 Structural capacity	Considerations for allowable stresses, buckling, and design of the pile cap
6-8 Static load testing	Overview of axial load tests and details for common methods used to interpret axial compressive load tests
6-9 Dynamic methods of analysis and testing	Summary of basic wave mechanics, use of wave equation, high-strain dynamic measurements, the Case Method, signal matching, and rapid load tests.
6-10 Integrity testing	Overview of common high-strain, low-strain, acoustic, thermal, and nuclear methods to assess foundation integrity

6-1.4 General Considerations.

The decision to use a particular deep foundation type is driven by a variety of technical and non-technical factors. Performance requirements include axial load capacity, durability, response to dynamic and/or lateral loads, and loss of ground support. The latter can occur due to liquefaction, scour, and/or dissolution of carbonate rock, i.e.

karst. Practical considerations for construction include transport, site access, high groundwater, obstructions, noise/vibration, ground deformations, and speed/ease of installation. Some nontechnical factors that influence the selection of a deep foundation include the costs and availability of materials, contractor familiarity, mobilization, available labor, as well as local codes. Navigating the collective technical and nontechnical factors on a particular project requires a careful and diligent evaluation of available options informed by local experience and engineering judgment.

6-2 DESIGN ASPECTS AND CONSIDERATIONS.

6-2.1 Design Aspects.

While the design of deep foundations is specific to the particular technology and application, there are many common elements of the design process. These elements are provided in 15 steps in Figure 6-1 and relevant steps can be applied generally to the design of foundations. The sequential organization of the design steps in Figure 6-1 belies the fact that all designs, especially for complex projects, are iterative and involve communication and coordination among many parties.

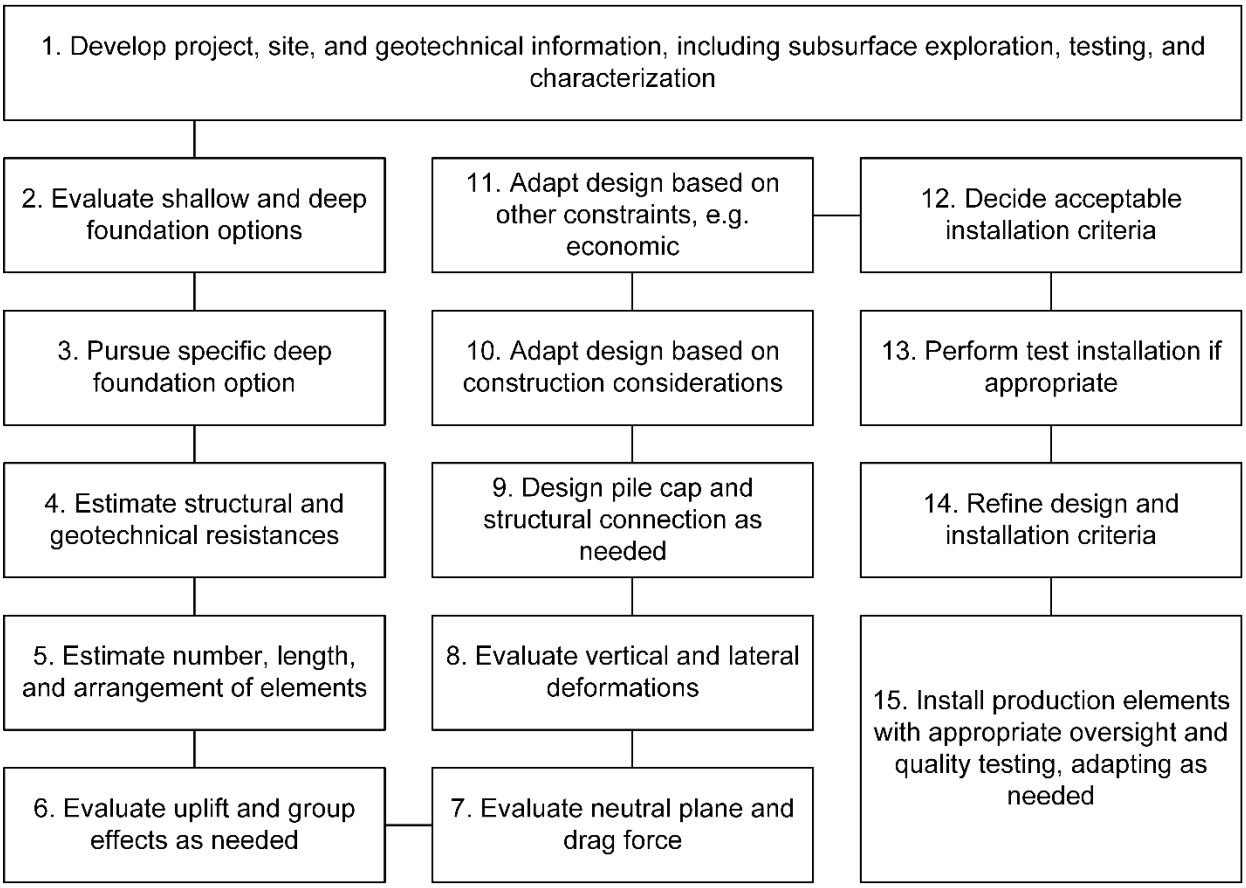

Figure 6-1 Major Elements of the Process to Design Deep Foundations

The following locations in DM 7.1 and 7.2 provide useful information for each step of the deep foundation design process:

1) Develop project, site, and geotechnical information: Project and site considerations are discussed in Section 6-2.2, and subsurface characterization considerations are discussed in Section 6-2.3. Chapters 1, 2, 3, and 8 of DM 7.1 provided detailed information related to the geotechnical characterization of sites and materials.

2) Evaluate shallow and deep foundation options: Refer to Chapter 4 of DM 7.2 for information on shallow foundations and this chapter for information on deep foundations. Ground improvement, discussed in Chapter 1 of DM 7.2, can be employed to increase the suitability of shallow foundations. When suitable, shallow foundations are usually a more economical solution than deep foundations.

3) Pursue specific deep foundation option: After the decision to pursue deep foundations has been made (see Section 6-1.3), refer to guidance in Section 6-3 for selecting a particular technology.

4) Estimate geotechnical and structural resistances: Refer to Section 6-5.4 for guidance related to estimating geotechnical axial resistance in soil and rock and Section 6-7 for guidance related to structural capacity.

5) Estimate the number, length, and arrangement of elements: Figure 6-2 shows typical arrangements of deep foundations. While drilled shafts are often used as single elements without a pile cap, a majority of deep foundation elements are installed in groups that are usually tied together in a pile cap. Driven piles, micropiles, and helical piles can be installed at a batter angle to provide lateral resistance. Batter piles also can be used to avoid obstructions or undesirable subsurface features.

6) Evaluate uplift and group effects as needed: Refer to Section 6-5.5 for group effects on geotechnical axial capacity and Section 6-5.6 for guidance related to uplift (tension loading).

7) Evaluate neutral plane and drag force: In many cases, deep foundation elements are subjected to the effects of settling ground. Ground that settles more than the element imposes a drag force on the sides of the element, while ground that settles less than the element contributes to the settlement of the element in the form of downdrag. These concepts are covered in Sections 6-5.7 and 6-5.8.

8) Evaluate vertical and lateral deformations: Settlement analysis is covered in Section 6-5.8, and evaluation of the lateral deformation of vertical elements is

covered in Section 6-6. Most analysis of lateral loading on vertical elements is performed using commercial software.

9) Design pile cap and structural connection as needed: Comprehensive structural design of deep foundations, pile caps, and other structural connections is not covered in this chapter. Section 6-7 provides some high-level guidance for sizing pile caps. Designers should consult appropriate building code requirements and authorities on reinforced concrete design, e.g., American Concrete Institute (ACI).

10) Adapt design based on construction considerations: Good deep foundation designs consider the constructability of the foundation and the impacts of construction, especially vibration. Section 6-2.4 covers construction considerations, and Section 6-4 provides more detailed information about the construction equipment and processes for popular deep foundation types.

11) Adapt design based on other constraints: Consideration of economic, environmental, and social factors in foundation design and construction is beyond the scope of this chapter. Section 6-2.4 mentions some logistical considerations related to construction, e.g., transport of materials and equipment.

12) Decide acceptable installation criteria: Section 6-4 discusses common installation criteria for popular deep foundation types, such as minimum blow count and/or penetration depth. Installation criteria must be decided to reliably satisfy the performance requirements for the project while considering subsurface conditions and special site considerations, such as obstructions. Static load testing (Section 6-8) and dynamic methods of analysis and testing (Section 6-9) are common approaches to establish installation criteria. Test installations (Step 13) can be an effective way to refine installation procedures and criteria.

13) Perform test installation if appropriate: Test installations or test pile programs allow the observational method to be implemented early enough in the project for the engineers and contractor to make adjustments. Test installations allow the length of driven piles to be tailored for material efficiency (piles not too long) and construction efficiency (number of splices minimized). Test installations allow experimentation with equipment and procedures in advance of the installation of production elements and provide opportunities to perform static and dynamic load testing.

14) Refine design and installation criteria: At this stage, design engineers, construction engineers, and other members of the project team refine the design based on what was learned during the test installation.

15) Install production elements with appropriate oversight and quality testing, adapting as needed: Section 6-2.4 discusses the role of visual inspection, periodic testing, and being prepared for unexpected conditions during construction.

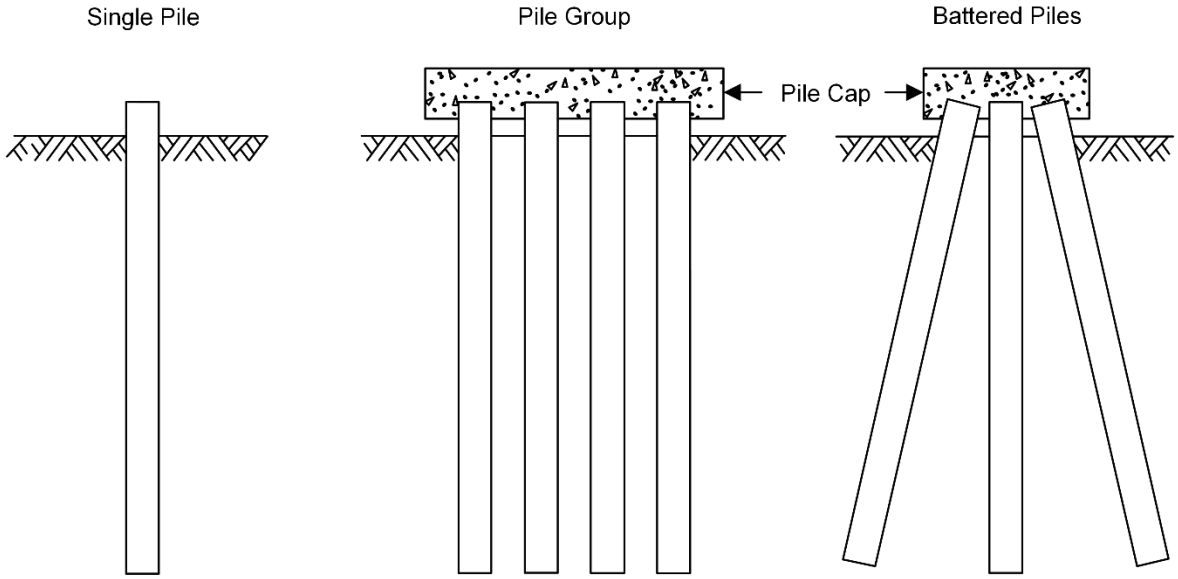

Figure 6-2 Configurations of Deep Foundation Elements

6-2.2 Site and Project Considerations.

The selection of a foundation type, design of the foundation, construction, and long-term maintenance planning require numerous site and project considerations. A non-exhaustive list of these considerations is provided in Table 6-2.

Table 6-2 Site and Project Considerations for Deep Foundations

Category	Site and Project Considerations
Structural and project management	• Structural loading • Deformation tolerances • Service life • Project delivery schedule
Geotechnical	• Qualty and variability of soil and rock • Obstructions • Voids or karst • Groundwater level and fluctuation
Environmental	• Existing contamination • Limits of project disturbance • Protection of aquatic life
Hydraulic and hydrological	• Scour • Debris and ice loading
Seismic	• Seismic loading • Liquefaction potential
Foundation deterioration	• Chemical – corrosion • Mechanical – freeze/thaw, thermal cycling, excessive loading • Biological – insects, marine borers
Site Constraints	• Noise and vibrations • Waterborne sediment and airborne dust • Physical space, including low headroom • Material transportation and staging
Other	• Supply chain disruptions • Natural disruptive events – extreme weather • Human-caused disruptive events

Addressing these considerations requires technical expertise, local experience, and coordination within a multidisciplinary design team and requires project or site specific details. Scour and foundation deterioration can be treated more generally and are discussed in the following sections.

6-2.2.1 Scour.

Scour is the loss of soil by erosion due to the drag force of moving water (Briaud 2008). There are three categories of scour commonly associated with river and stream flows: 1) long-term changes to the stream bed by aggradation and degradation of sediments, 2) contraction of the overall stream channel by the constricting effect of obstacles to flow, and 3) localized scour due to the effect of obstacles on flow path and velocity. Scour is also categorized as either clear water or live bed (FHWA 2012a). *Clear water scour* occurs when the upstream bed material is not being actively transported and deposited. In contrast, *live bed scour* refers to a condition where the upstream bed material is transported and deposited to partially replenish eroded materials. Other sources of scour include wave action and ship propulsion. In the context of bridges and waterfront structures, obstacles to flow include bridge piers, abutments, bulkheads, and pilings for wharves.

Scour occurs whenever hydrodynamic shear stresses acting on the erodible material exceed a threshold critical shear stress (Briaud 2013). While flow velocity and

hydrodynamic shear stress do not adhere to a simple relationship, it is conceptually convenient to express the onset of scour by a critical velocity, v_c. For coarse-grained soils, the critical velocity (in m/s) is correlated to the median particle size, D_{50} (in mm), according to:

$$v_c = 0.35 \cdot \left(D_{50}\right)^{0.45} \quad \text{(6-1).}$$

Note that the units on the constant are m / (s·mm$^{0.45}$)

The critical velocity is not correlated to particle size for fine-grained soils, and Equation 6-1 should not be extrapolated below sand-sized particles. Knowledge about scour of cohesive soils is limited (Hughes 2001). To simplify the assessment of erosion potential, Briaud (2008) categorized soil and rock as shown in Figure 6-3. Six categories are defined based on soil classification, fissuring, and jointing. The zones on the diagram indicate typical ranges of erosion rate for each category based on the water velocity.

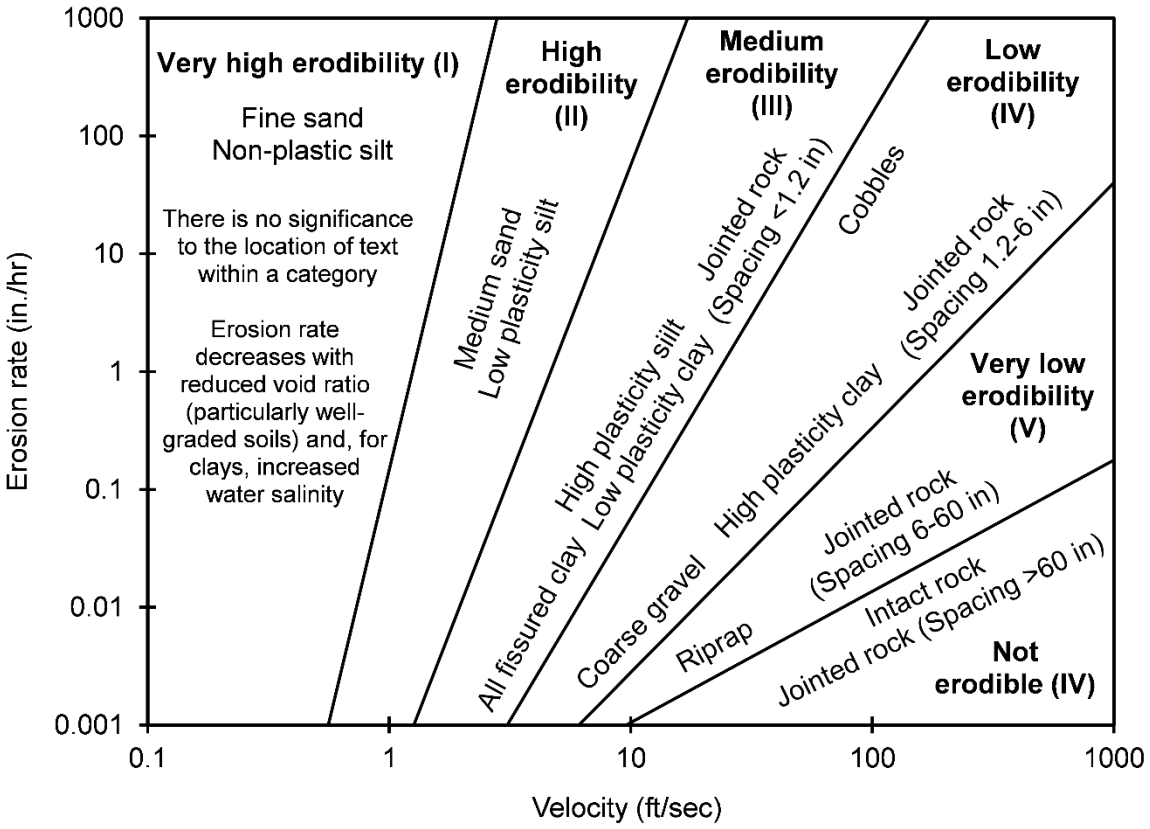

Figure 6-3 Erosion Categories for Soils and Rock Based on Velocity (after Briaud 2008)

The three documents listed below describe the overall process to analyze, evaluate, and remediate scour and stream instability at bridges:

1) Stream Stability and Geomorphic Assessment (HEC-20) (FHWA 2012b): This document describes data collection and analysis procedures to evaluate stream bank and stream bed stability and establishes the level of analysis needed to evaluate scour.

2) Hydrologic, Hydraulic, and Scour Analysis (HEC-18) (FHWA, 2012a): This document describes the hydrologic analysis to evaluate volumetric flow due to water draining from a watershed, the hydraulic analysis to evaluate the depth, velocity, and forces imposed by the flow, and the process to evaluate the components of total scour.

3) Bridge Scour and Stream Instability Countermeasures (HEC-23) (FHWA 2009): This analysis develops an implementation strategy to reduce the likelihood and severity of scour. Countermeasures are often taken for existing foundations in response to scour.

Modeling the fluid dynamics and erosion mechanics of scour problems is a complex undertaking that is typically undertaken by specialists. The U.S. Army Corps of Engineers' Hydrologic Engineering Center (HEC) developed and maintains the River Analysis System software (HEC-RAS) that models flow hydraulics and sediment transport, among other types of analysis.

Scour is typically considered for two flood conditions: 1) the scour design flood and 2) the scour check flood. In the context of roadways and bridges, both flood conditions are usually more severe than the hydraulic design flood for evaluating inundation and overtopping. For example, according to HEC-18 (FHWA 2012b), if the hydraulic design flood is the 100-yr flood (1% annual probability of occurrence), the scour design flood is the 200-yr flood, and scour design check flood is the 500-yr flood. According to AASHTO (2020), the 100-yr flood should be used for the scour design flood and the 500-yr flood should be used for the scour check flood. The scour design flood is considered for all strength and service limits states while the scour design check flood is considered for the extreme event limit state. In some cases, scour depth does not increase with discharge, so the maximum scour depth for the design scour flood and scour check flood should be the worst case for all floods considered. In other words, an overtopping flood with discharge lower than the design scour flood and scour check flood discharges may produce the most severe scour (FHWA 2021).

UFC 4-151-10 (2012) stipulates that all piles should be designed for a minimum of 5 feet of scour and future dredging while Hughes (2001) suggests that a conservative rule of thumb for piles with Z/b greater than 10 is to assume that the maximum scour depth is double the pile diameter.

The total scour depth directly impacts deep foundation design in the following ways:

1) Unbraced length increases by an amount equal to the scour depth

2) Lateral support lost over the scour depth

3) Side resistance lost over the scour depth

4) Additional water load (LRFD load designated WA) applied to the foundation over the scour depth

Additionally, scour reduces the vertical effective stress due in the soil below the depth of scour over a depth interval of approximately 1.5 times the scour depth. Compared to the original stream bed, the vertical stress may decrease to a depth of 2.5 times the scour depth.

In some conditions, scour holes from adjacent bridge piers can overlap and lead to further deepening and/or widening of the local scour.

When static load testing and/or dynamic testing is used to evaluate foundation performance, it is also important to consider that scour will change the ground support conditions from those present at the time of testing.

The scour risk can be reduced in design by 1) lengthening the foundations to account for the scour depth, 2) lengthening the bridge to reduce the impact of the abutments on the stream channel, 3) modifying the size and arrangement of the piers, and 4) deploying scour countermeasures such as riprap, gabions, articulated concrete block mats, and sheet piles. Over the long term, modifications to the design (1-3) are more reliable than using scour countermeasures (4) alone (FHWA 2018a).

6-2.2.2 Deterioration.

Timber, steel, and concrete are vulnerable to one or more modes of deterioration over time. In particular, steel is susceptive to corrosion, concrete is susceptible to attack by acid and sulfate, and timber is susceptible to biological attack. Reinforced concrete is a composite of steel and concrete and, therefore, shares susceptibilities of both materials. Table 6-3 lists ground and water conditions that pose a heightened risk of foundation deterioration. Elevated temperature, stray electrical currents, and access to oxygen can also increase the risk of deterioration. Conditions that are deemed lower risk for deterioration at the time of construction can become higher risk over time, e.g., through the application of deicing salts or changes to groundwater levels by pumping.

Table 6-3 Conditions that Pose a Heightened Risk of Foundation Deterioration (after AASHTO 2020)

Piles on Land	Piles in Water
• pH less than 5.5 • pH between 5.5 and 8.5 in soils with high organic content • Sulfate concentration greater than 1,000 ppm • Resistivity less than 2,000 ohm-cm • Soils subject to mine or industrial drainage • Landfills or cinder soils • Areas with a mixture of high resistivity soils and low resistivity high alkaline soils • Insects (timber piles)	• pH less than 5.5 • High organic content • Sulfate concentration greater than 500 ppm • Chloride concentration greater than 500 ppm • Mine or industrial runoff • Marine borers and other invertebrates (timber piles) • Piles exposed to wet/dry cycles

Deterioration is a process that occurs over time and cannot be avoided entirely. In design, the goal is to reduce the risks of problematic deterioration to acceptable levels over the service life of the foundation. Broadly, measures to mitigate the impacts of deterioration include the following:

- Select or design the foundation material for durability, including:
  - Selection of steel alloy
  - Concrete mix design
  - Selection of wood species
- Protection of the foundation material, including:
  - Coat steel and concrete in various tar and epoxy coatings
  - Galvanize steel
  - Impregnate timber with preservatives such as creosote (oil-borne), Chromated Copper Arsenate (CCA), and Ammoniacal Copper Zinc Arsenate (ACZA) (both waterborne)
  - Cover timber, steel, or concrete in a plastic sleeve, jacket, or wrap, particularly in tidal and splash zones and at the dredge line
- Include sacrificial material and/or add redundancy in the design, such as:
  - Adequate minimum cover depth of concrete between the environment and steel reinforcement, e.g., 3 inches, and
  - Cathodic protection to steel.

The time rate of metal loss due to corrosion is difficult to forecast and influenced by localized electrochemical conditions that are prone to spatial and temporal variability. In the absence of better information, a metal loss of 0.003 inches per year can be conservatively applied in design for unprotected steel in non-marine environments (FHWA 2016). For marine environments, the rate of metal loss can be significantly higher, e.g., 0.007 inches per year (Coduto et al. 2016). The metal loss is the reduction in thickness of the steel, accounting for corrosion on both sides (Romanoff, 1962). For a pipe pile, the thickness is the wall thickness. Decker et al. (2008) found that the

average corrosion rate decreases with time. Figure 6-4 is based on data for non-marine conditions (Decker et al. 2008) and illustrates that an assumed loss rate of 0.003 inches per year is conservative. However, corrosion rates in certain aggressive environments, such as at the splash zone where abrasion can occur, can be higher (FHWA 2016).

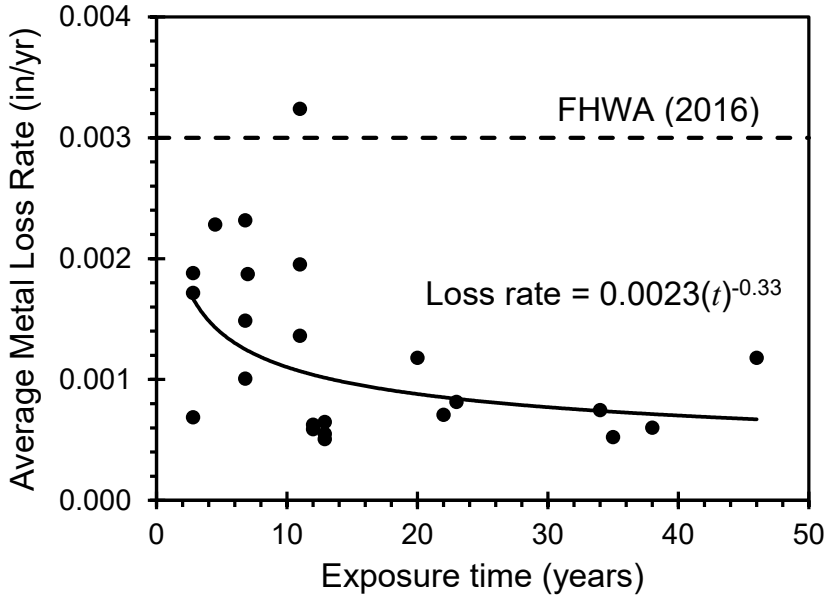

Figure 6-4 Annual Loss of Metal Thickness Versus Exposure Time in Non-Marine Environments (after Decker et al. 2008)

6-2.3 Subsurface Characterization Considerations.

Adequate subsurface exploration must precede the design of a deep foundation. Investigations should include the following:

1) Geological section showing pattern of major strata and presence of possible obstructions, such as boulders and buried manmade objects as well as voids due to karst;
2) Sufficient test data to estimate strength, compressibility, and liquefaction potential of major strata;
3) Determination of probable bearing strata;
4) Evaluation of corrosion potential; and
5) Evaluation of scour potential.

Chapters 2 and 3 of DM 7.1 provide useful guidance for actions performed in the field and in the laboratory to characterize subsurface conditions.

6-2.4 Construction Considerations.

The performance of deep foundations is highly dependent on the installation procedures, quality of workmanship, and installation/design changes made in the field. Thus, inspection of the deep foundation installation by a geotechnical engineer should be required under normal conditions.

This section presents recommendations for minimum spacing between elements and tolerances for placement and alignment.

6-2.4.1 Minimum Spacing.

Guidance for minimum center-to-center spacing between adjacent elements is provided in Table 6-4. Smaller spacing can be impractical from a constructability standpoint due to limitations associated with positioning the equipment, densification of sand that impedes installation, and achievable alignment tolerances as well as group effects on performance (i.e., group efficiency). Minimum spacing guidance is particularly relevant to the discussion of the axial (Section 6-5.5) and lateral (Section 6-6.4) capacity of pile groups.

6-2.4.2 Placement and Alignment Tolerances.

Correct location and alignment of foundation elements is important to minimize the potential for introducing eccentricities not accounted for in design. Eccentricity can introduce additional bending stresses and uneven loading in groups of elements. Additionally, placement and alignment errors can increase the potential for constructability issues and damage to the elements if spacing is too small or if misaligned elements interfere at depth.

The construction tolerances specified by USACE and FHWA for different foundation types are summarized in Table 6-5. The center of each element should be located within the plan location tolerance. The longitudinal alignment refers to the allowable deviation from vertical for most elements or from the planned alignment for batter piles. The pile top elevation should be finished or cut off within the indicated tolerance. The International Building Code requires that deep foundation elements be designed to resist the eccentricity effects of location errors of no less than 3 inches (ICC 2015). The code permits a 10% compressive overload in elements due to location errors.

Table 6-4 Guidance for Minimum Center-to-Center Spacing

Foundation Type	Minimum Spacing Guidance
Driven piles	Minimum spacing is greater of 2.5 ft or s/b = 2.5 (AASHTO 2020) Minimum recommended spacing is greater of 3 ft or s/b = 3.0 (FHWA 2016).
Drilled shafts	Minimum spacing is s/b = 2.5, recommended spacing is at least s/b = 3.0 (FHWA 2018a).
Continuous Flight Auger Piles	Minimum spacing is s/b = 3.0 (FHWA 2007).
Drilled Displacement Piles	Minimum spacing is s/b = 3.0 (FHWA 2007).
Micropiles	Minimum spacing is greater of 2.5 ft or s/b = 3.0 (AASHTO 2020). For micropiles, b is the diameter of the grouted bond zone (FHWA 2005).
Variables: b = element width, s = center-to-center spacing	

Table 6-5 Deep Foundation Construction Tolerances

Foundation Type	Tolerance for:		
	Plan Location	Longitudinal Alignment	Pile Top Elevation
Driven Piles (USACE 1991)	3 to 6 inches	0.25 inches / foot (1H:48V)	Within 1 inch of specified
Vertical Driven Piles (FHWA 2016)	3 inches (bents) 6 inches (capped below grade)	0.25 inches / foot (1H:48V)	Between 1.5 inches above and 4 inches below specified
Batter Driven Piles (FHWA 2016)	3 inches (bents) 6 inches (capped below grade)	0.5 inches / foot (1H:24V)	Between 1.5 inches above and 4 inches below specified
Drilled Shafts (FHWA 2018a)	3 inches for $b \le 2$ ft 4 inches for 2 ft $\le b \le$ 5 ft 6 inches for 5 ft $\le b$	1.5% (1H:67V) in soil 2% (1H:50V) in rock	Between 1 inches above and 3 inches below specified
Micropiles (FHWA 2005)	3 inches for pile 0.75 inches for reinforcement	2% (1H:50V)	Between 1 inches above and 2 inches below specified

6-3 FOUNDATION TYPES.

6-3.1 Overview.

Deep foundation elements are principally comprised of one or more of the following materials: timber, steel, crushed stone, grout, and concrete. Deep foundation technologies are summarized in Table 6-6 through Table 6-9. The selection of a particular foundation technology depends on many factors including the intended application, soil and rock conditions, capacity requirements, installation effects (e.g., noise, vibration, soil displacement), material costs and availability, equipment availability, and contractor experience. In the private sector, the client's comfort with the technology and associated risks may also be a factor.

Broadly speaking, deep foundation technologies can be divided into driven piles and formed-in-place columns. Within each of these categories, deep foundations are distinguished by the amount of soil volume displaced by each element.

Non-displacement elements include the following:

1) Drilled shafts
2) Micropiles

Low- or partial-displacement elements can include the following:

1) Driven piles with a low ratio of cross-sectional area to perimeter, e.g., H-piles and open pipe piles, provided the piles remain unplugged with soil
2) Any pile installed by jetting or pre-boring
3) CFA columns
4) Helical piles
5) Predrilled aggregate piers without ramming or vibration

High- or full-displacement elements include the following:

1) Driven piles with a high ratio of cross-sectional area to perimeter, e.g., timber piles, closed-end pipe piles, tapered piles, and most concrete piles
2) Any driven pile that forms a soil plug and becomes a displacement pile below the depth of plugging
3) Drilled displacement piles (DDP)
4) Aggregate columns – while the installation of aggregate columns often involves drilling, the ramming or vibratory installation methods displace surrounding soil

The effects of soil displacement may be advantageous or detrimental depending on the application, ground conditions, and presence of nearby structures and utilities. The impacts of these effects on shaft and base capacity will be discussed in more detail in Section 6-5, though it suffices to say that soil displacement usually has a positive effect on geotechnical capacity for drained conditions, except for sensitive soils. Soil displacement, particularly associated with driven piles, can also generate positive or negative excess pore pressures. The implications of driving-induced pore pressures are discussed in Section 6-4.1.4.

Soil displacement in the form of heave and/or lateral movement can be damaging to adjacent structures, e.g., below-grade walls, buried utilities, abutments, and other foundation elements. When a group of foundation elements is used, the combined soil displacement may be significantly larger than that caused by a single element.

6-3.2 Summaries of Common Deep Foundation Types.

Table 6-6 through Table 6-9 summarize common deep foundation types. These technologies are also used in ground improvement and slope stabilization applications; however, these applications are not within the scope of this chapter. A summary of the aggregate column technology can be found in Figure 1-2.

Table 6-6 Summary of Timber Piles and Steel H-Piles

Pile type	Timber Piles	Steel H-Piles
Typical lengths	15 to 75 ft for Southern Pine 15 to 120 ft for Douglas Fir	15 to 150 ft
Typical factored resistance	20 to 100 kips	80 to 400 kips
Advantages	• Relatively low initial cost • Easy to deliver and handle • Renewable resource • Sequesters carbon • Permanently-submerged piles are resistant to decay • Not susceptible to corrosion	• Broad range of sizes and lengths • Easy to splice • Can be fitted with hardened driving points for penetrating hard layers and some obstructions • Steel often has high recycled content • High load resistance possible
Disadvantages	• Lengths greater than 60 ft difficult to supply in some locations • Difficult to splice • Vulnerable to damage from hard driving, top and base may need protection • Intermittently-submerged piles are vulnerable to decay unless treated	• Unprotected steel is susceptible to corrosion • Despite being the driven pile with highest potential for survival in hard driving conditions, damage still possible from obstructions and uneven rock, e.g. karst
Remarks	• High displacement timber element • Good option as a friction pile, particularly in cohesionless soils • Equipment and materials may be easier to procure in some remote areas than other deep foundation types	• Low displacement steel element, unless plugged • Good option for end-bearing pile on rock • Relatively low skin friction, particularly in cohesionless soils; not good for shaft resistance, but may be an advantage when downdrag is an issue
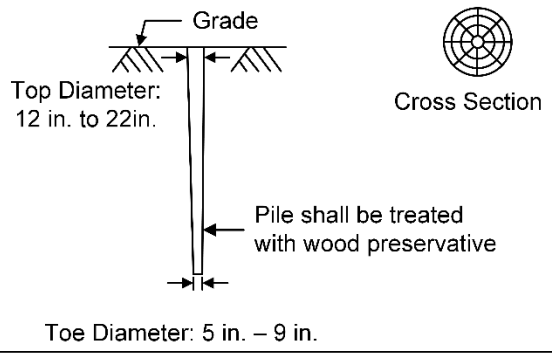		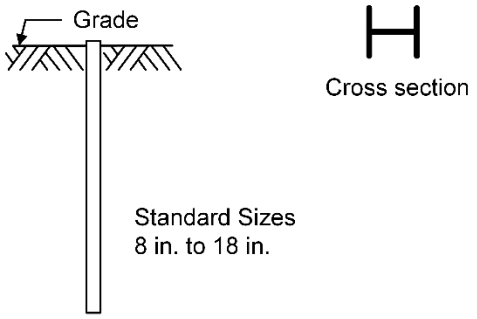

Table 6-7 Summary of Steel Pipe Piles and Concrete Piles

Pile type	Steel Pipe Piles	Precast Prestressed Concrete Piles
Typical lengths	15 to 200 ft	30 to 120 ft
Typical factored resistance	100 to 1,000 kips (unfilled) 100 to 3,000 kips (concrete filled)	100 to 800 kips (square) 200 to 1,200 kips (cylinder)
Advantages	• Like H-piles, broad range of sizes and lengths, easy to splice, steel often has high recycled content, high load resistance possible • Closed-end pipe interior can be inspected after driving • Open-end pipe provides access to clean out base to extend driving • Driving shoes can be used to improve resistance to obstructions	• High corrosion resistance obtainable • High load resistance possible • Rough concrete surface good for frictional resistance • Cylinder piles can provide good bending resistance
Disadvantages	• Unprotected steel is susceptible to corrosion	• Splicing is difficult • Cutting off excess pile is difficult • Handling requires extra care • Damage in hard (compression) and soft driving (tension) possible • Soil displacement can produce unwanted earth movements and pressures
Remarks	• High or low displacement element, sometimes concrete-filled • Provides high bending resistance, including unsupported length • Relatively low skin friction with open end pipe, particularly in coarse-grained soils; not good for shaft resistance, but may be an advantage against downdrag • Closed-end pipe susceptible to buoyancy forces when unfilled.	• High displacement concrete element • Good option for friction piles • Cylinder piles are more common for installations over water • Conventionally-reinforced piles (not prestressed) are rare in North America
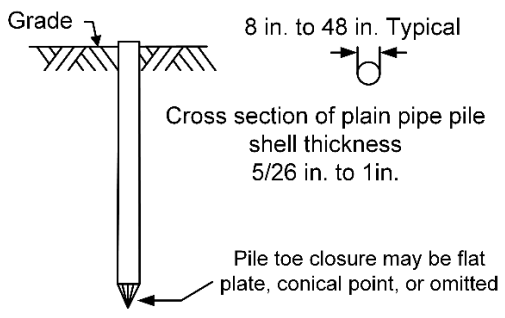		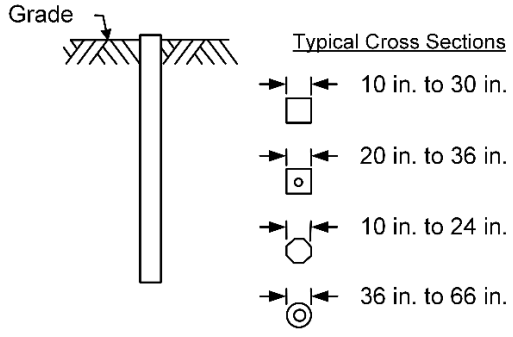

Table 6-8 Summary of Drilled Shafts and Continuous Flight Auger Columns

Pile type	Drilled Shafts	Continuous Flight Auger (CFA)
Typical lengths	20 to 200 ft	30 to 100 ft
Typical factored resistance	300 to 5,000+ kips	100 to 400 kips
Advantages	• High load resistance possible due to rough interface and large base • Possible to inspect cuttings and material at/below base • Installs with low noise and vibration • Simple to modify length during construction • Variety of tooling for excavating through soil and rock • High corrosion resistance obtainable	• Rough interface for good shaft resistance • Installs with low noise and vibration • Simple to modify length during construction • High corrosion resistance obtainable • No open bore hole • Can be installed in low headroom conditions
Disadvantages	• Less redundancy than pile groups • Contractor skill has large influence on quality • Significant mobilization of base resistance may require large settlement, esp. in cohesionless soil • Load tests are difficult and expensive	• Contractor skill has large influence on quality • Augers can overexcavate (mine) loose and/or clean sands and soft soils • Not well suited to hard soil, rock, and obstructions • Not well suited for providing high shear, bending, or uplift resistance
Remarks	• Nondisplacement concrete element • Reinforcement can provide high bending resistance, including unsupported length • Installation may be uncased, cased, or use slurry depending on potential for caving or squeeze • Belling tool can enlarge base area • Barrettes are a special type of shaft with a rectangular base	• Low-displacement concrete or grout element • May or may not include reinforcement • Installation rate can be high • Also known as auger cast-in-place pile

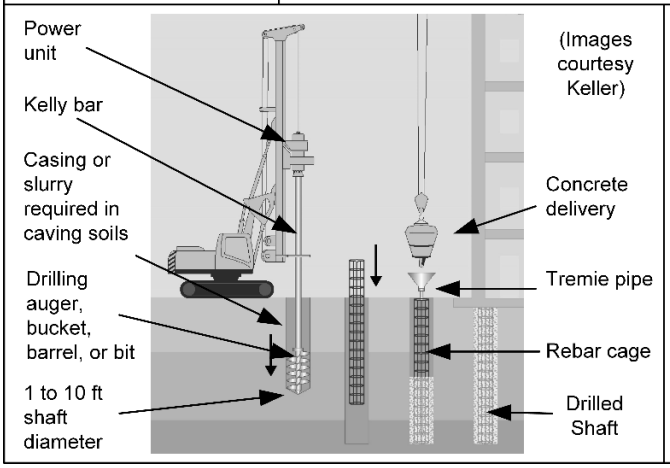

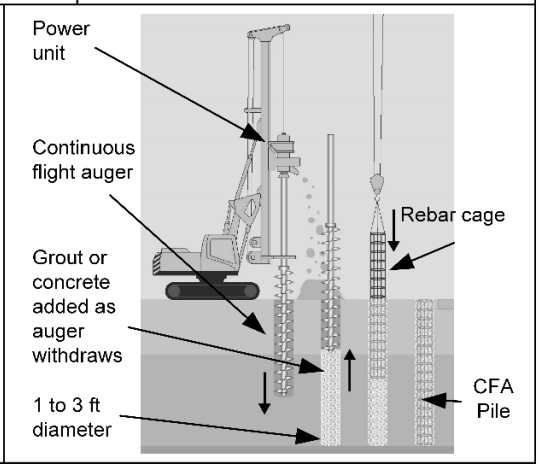

Table 6-9 Summary of Drilled Displacement Columns and Helical Piles

Pile type	Drilled Displacement Columns (DDC)	Helical piles
Typical lengths	20 to 75 ft	10 to 30 ft
Typical factored resistance	75 to 200 kips	20 to 120 kips
Advantages	• Rough interface and soil displacement for good shaft resistance • Installs with low noise and vibration • Simple to modify length during construction • No open bore hole • Fewer issues with overexcavation versus CFA	• Quick installation in any weather and groundwater depth • Can be suitable for compressive and uplift loading • Length adjustable by adding or subtracting prefabricated shaft components • Compact equipment, can be installed in low headroom conditions • Installs with low noise and vibration
Disadvantages	• Not well suited to hard soil, rock, and obstructions • Not well suited for providing high shear, bending, or uplift resistance	• Limited depths • Low bending resistance • Susceptible to corrosion • Not suitable for hard soils, rock, or soil with obstructions • Slenderness poses risk of buckling in soft soils, if liquefaction occurs, and for highly eccentric loadings
Remarks	• High-displacement concrete or grout element • May or may not include reinforcement • Installation rate can be high • Design methods less mature • Also known as rigid inclusions • Several proprietary systems exist, e.g. CMCs	• Low-displacement steel element • Usually six or fewer helices • Good option for underpinning • Installation torque can be monitored to avoid damaging twist of the pile and estimate capacity

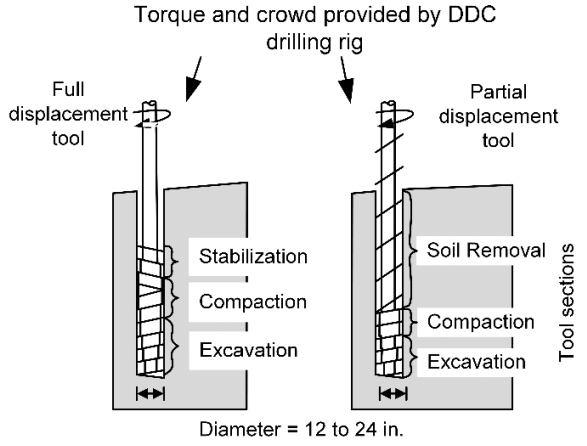

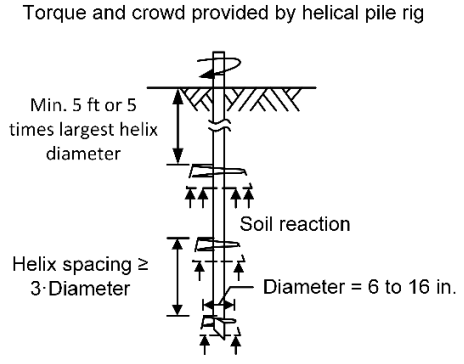

6-3.3 Summary of Material Properties.

Table 6-10 provides the mass density and Young's Modulus for steel, concrete, and timber used in piling. Additionally, Table 6-10 includes applicable material specifications.

Table 6-10 Summary of Material Properties of Foundation Materials

Foundation Material		Unit Weight[1], γ (lbs/ft^3)	Young's Modulus[2], E (ksi)	Specifications
Steel		490	29,000	ASTM A572, A588, or A690 ASTM A252, API 5L or 2B For reinforcing steel, ASTM A82, A615, A722, and A884
Concrete[2,3]		150	$1820\sqrt{f'_c}$	ACI 318
Timber[3]	Southern pine[5]	46 (35)[4]	1,500	AWPA UC4A, UC4B, UC4C, UC5A, UC5B, and UC5C ASTM D25
	Douglas fir[5]	47 (31)[4]	1,500	
	Lodgepole pine	38 (27)[4]	1,000	
	Red oak[5]	50 (39)[4]	1,250	
	Red pine[5]	41 (30)[4]	1,280	

Notes:
1 If required, mass density, ρ (slugs/ft^3), is found by dividing unit weight by gravity, g = 32.17 ft/s^2.
2 Modulus of concrete is estimated based on AASHTO (2020) guidance based on f'_c in ksi. Values for modulus of timber are from AWPI (2002).
3 The properties of concrete and timber are influenced by many factors and may differ significantly from the provided values
4 Numbers without parentheses are for creosote preservative, numbers in parentheses are for CCA and ACZA. Values based on wood at 12% moisture content retaining 12 lbs of creosote (pine and oak), 17 lbs of creosote (fir), or 1 lb of CCA or ACZA preservative per ft^3 (USDA 2010).
5 Southern pine applies to loblolly, longleaf, shortleaf, and slash pines. Douglas fir applies to coastal variety. Red oak applies to northern and southern red oak. Red pine applies to US-grown red pine.

6-4 CONSTRUCTION.

The construction processes for deep foundations vary by technology, site conditions, and contractor. Besides consideration of geotechnical and structural performance, the selection of a deep foundation technology may be heavily influenced by construction considerations such as noise and vibration, spatial constraints (e.g., headroom and staging area size), site access, weather, equipment availability and mobilization, limits on work hours, environmental regulations, and contractor experience. This section provides an overview of the basics of deep foundation construction.

6-4.1 Driven Piles.

6-4.1.1 Equipment.

Pile driving operations traditionally utilize a crane to hoist and suspend the pile, hammer, leads, and other accessories (Figure 6-5). Pile leads guide the hammer and pile. *Fixed leads* are attached to the bottom of the crane boom using a spotter apparatus that holds the leads in place. *Swinging leads* hang from the top of the boom and are allowed to swing. The choice of leads is influenced by alignment needs as well

as the reach required to position the pile. Alternatively, dedicated pile rigs are specialized equipment that use a telescoping mast instead of a lattice boom and allow faster mobilization and on-site set up. For installation of small- to medium-sized piles on land or near shore, tracked excavators are often configured as pile driving rigs with an attached mast and a hydraulic hammer driven by the excavator's hydraulic pump. When suitable, the use of an excavator-mounted pile driver is faster, more maneuverable, and involves lower mobilization costs than those of a crane-mounted rig.

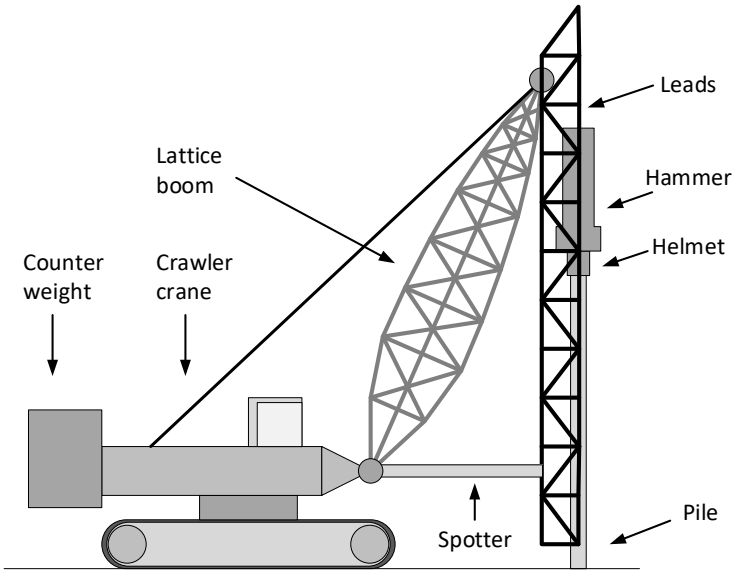

Figure 6-5 Typical Crane-Mounted Pile Driver

Broadly speaking, pile hammers can be classified as either impact or vibratory. The majority of pile driving for deep foundations is performed using an impact hammer. Impact hammers can use compressed air, steam, or pressurized hydraulic fluid to lift and drop a heavy mass to transfer energy to the pile. This energy performs work by advancing the pile deeper into the ground (Figure 6-6a). Single-acting air/steam/hydraulic hammers use a pressurized fluid or gas to lift the ram to the top of the stroke (3 ft is common). A hammer blow is delivered when the ram is allowed to free-fall on the downstroke, strike a steel plate, and transfer energy to the pile as it decelerates. Double-acting and differential hammers also apply pressure on the downstroke of the ram to accelerate the ram beyond gravity alone and allow for higher cycle rates.

Diesel impact hammers deliver energy to the pile through the explosive force from diesel fuel combustion combined with the falling mass of the ram (Figure 6-6b). Similar to a two-stroke internal combustion engine, diesel hammers use the downstroke of a steel ram confined within a cylinder to compress and ignite an air-fuel mixture. The explosion imparts the energy to advance the pile as well as the energy for the upstroke of the ram. Ports in the cylinder allow air to enter on the downstroke and exhaust to exit

on the upstroke. Fuel is injected as a liquid or aerosol on the downstroke. Diesel hammers can be challenging to start or operate efficiently when the ground provides low resistance and/or when air temperatures are cold. Diesel hammers are able to deliver maximum power when the ground provides high resistance. Single-acting (open-end) hammers allow the ram to reach maximum rise on the upstroke while double-acting hammers resist the rise of the ram by compressing air within a bounce chamber to increase the cycle rate.

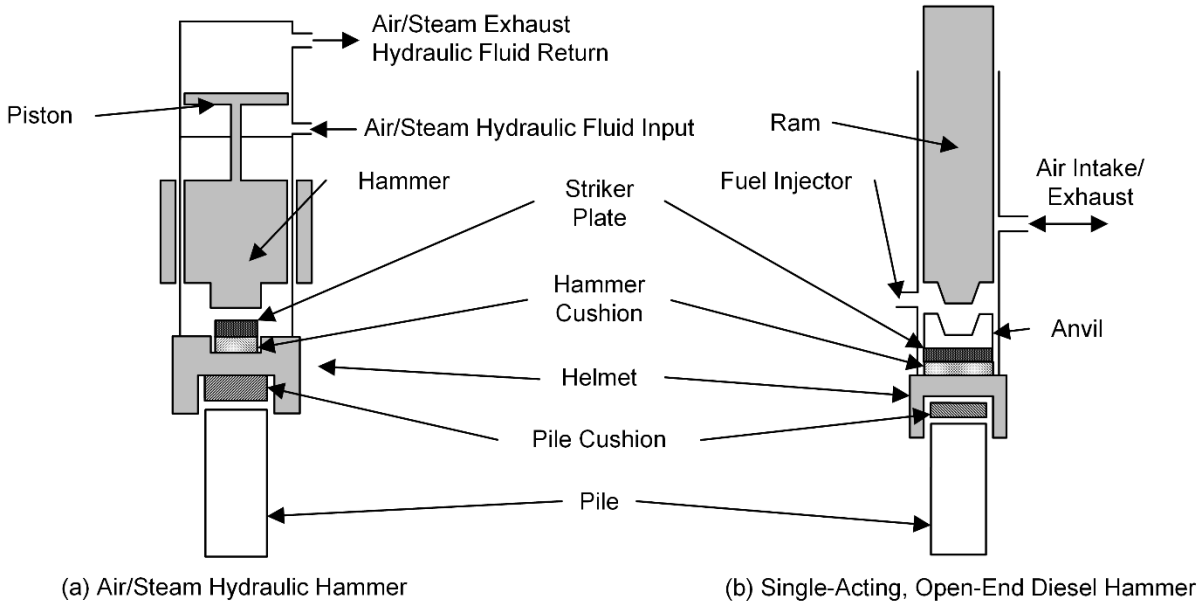

Figure 6-6 Pile Driving Hammers

The drive system is a series of components between the ram and pile that are collectively referred to as appurtenances. These components, listed in order from the ram to the pile, usually include a steel striker plate, hammer cushion (or cap block), and steel helmet (or drive head). Diesel hammers also include a steel anvil between the ram and striker plate as part of the combustion chamber. Modern hammer cushions are typically made from laminates of aluminum, plastic (e.g., nylon), and phenolics (e.g., Micarta) and function to enable efficient energy transfer while mitigating damage to the steel hammer components. The helmet functions to maintain pile alignment within the hammer-pile system and aid in efficient energy transfer. When driving concrete piles, a pile cushion typically made from layers of plywood is used to limit damaging energy transfer between the helmet and pile.

The types and condition of the appurtenances affect the propagation of energy within the hammer-pile system. The pile cushion, in particular, is a rapidly wearing component that has different dynamic properties when it is new (<100 hammer blows) versus when it is at the end of its usable life (often 1,000 to 2,000 hammer blows). This point is

especially important when dynamic testing and/or penetration resistance are used to evaluate pile capacity.

Many factors can contribute to the selection of the type and size of the pile hammer. Some of these factors are related to considerations of drivability and driving stresses as discussed in Sections 6-4.2.1 and 6-9. Manufacturers typically provide an energy rating, E_r, to organize hammers by the relative amount of energy they can deliver. The energy rating should not be interpreted as the actual energy delivered to the pile as no hammer and driving system is 100% efficient. Prior to more rigorous evaluation, such as wave equation analysis, the required hammer energy rating in kip-ft can be preliminarily estimated as 7% of the required nominal pile resistance, R_n, in kips (Coduto et al. 2016).

Piles driven to rock and/or through ground containing cobbles, boulders, and/or other obstructions may be fitted with pile toe attachments. For example, damage potential is reduced using driving shoes for H-piles and conical tips for pipe piles. Toe protection for concrete piles exists but is not commonly used in practice.

Sometimes driving aids are used to reduce the potential for pile damage during driving, speed up the installation process, allow for smaller equipment to be used, mitigate heave, and/or mitigate ground vibration. *Predrilling* is a driving aid in which an auger is used to drill a pilot hole for the pile. Sand and gravel soils can be loosened using *jetting* with a high-pressure water nozzle on a probe. *Spudding* is the practice of driving a heavy pile through an obstruction to make a hole for the production pile. These driving aids reduce the axial and lateral load capacity of the pile, and their effects should be accounted for in the design.

Handling piles refers to the processing of positioning the pile in the leads. Handling requires special lifting equipment or a crane hoist line. Sometimes the ability to handle piles will limit their length. In some cases, the bending stresses experienced by piles during handling are higher than the design loading. Concrete piles, in particular, require care when handling and must be lifted from multiple points. Handling piles becomes more difficult as the ratio of the length to the width increases. As a rule of thumb, a maximum of a 40 ft long square concrete pile having a width of 10 inches can be safely handled. Each additional 5 ft of length requires an additional inch of width to be handled without damage (after Salgado 2008).

6-4.1.2 Drivability and Acceptance Criteria.

Drivability refers to the ability of a hammer and drive system to drive the pile efficiently without damaging the pile. Prior to construction, drivability can be assessed using wave equation analysis (Section 6-9.3). However, the installation of test piles prior to installation of production piles is the best way to confirm drivability. To be drivable, the pile must be sufficiently stiff to transmit driving forces necessary to overcome soil

resistance and sufficiently strong to withstand the driving-induced stresses. Section 6-7.1 discusses structural limits on stress.

Two limiting conditions exist for pile driving. *Soft driving* conditions occur when driving through soft soil prior to reaching a competent bearing layer. In this case, it is possible to produce damaging tensile stresses in the pile, particularly in concrete piles which have relatively low tensile strength. *Hard driving* conditions occur when driving to refusal on rock or penetrating an obstruction. In hard driving, the hammer can produce damaging compressive stresses in the pile. See Section 6-9.2 for more details about how soft and hard driving conditions affect stresses developed in the pile during driving.

A key parameter to assess drivability is the pile's impedance, I, which is:

$$I = \frac{E \cdot A}{c} \tag{6-2}$$

where:
E = elastic modulus of the pile,
A = cross-sectional area of the pile, and
c = material wave speed.

Impedance is further explained in Section 6-9. Piles with higher impedance are able to transmit more force in the same way a heavy masonry nail can penetrate masonry better than a light finishing nail.

The energy delivered by the hammer and the impact velocity are both important factors for matching a hammer to a pile. Heavier hammers with a lower drop height, or stroke, impart energy to the pile with lower particle velocities induced in the pile. For the same energy, lower impact velocity produces lower driving stresses. Heavier hammers with lower impact velocity also have a longer impact time and tend to transmit energy to the pile with fewer losses. They are also more likely to remain in contact with the pile and overcome reflected compression waves that can cause counterproductive upward bouncing of the pile. However, heavier hammers are often harder to mobilize and require larger equipment. Sometimes, higher driving stresses are needed for the pile to penetrate a stiff layer or obstruction. In these cases, a hammer with a lighter ram and longer stroke is preferred provided that the hammer does not produce damaging driving stresses in the pile.

During driving, records are kept of the installed length and number of blows required to drive each pile, typically in terms of blow count or blows per foot. The blow count can be inverted to find the *set*, which is the amount of permanent penetration per blow. *Acceptance criteria* for pile driving generally refers to the point at which pile driving can be terminated. Common acceptance criteria include driving piles to a target blow count or set, driving piles to practical refusal, and/or driving piles to a specified tip elevation.

Practical refusal is often defined as 120 bpf or 10 blows per inch for three consecutive inches of penetration. *Absolute refusal* is often defined as 5 blows per 1/4 inch (240 bpf equivalent). It must be noted that the blow count is relevant only for the particular hammer and drive system used. Driving to a high blow count using a small hammer may only mobilize a portion of the pile resistance while a large hammer may fully mobilize the pile resistance at a modest blow count.

Target blow counts typically fall in the range of 30 to 120 bpf. Blow counts less than 24 bpf are considered soft driving, and the dynamic methods discussed in Section 6-9 can overpredict nominal resistance. The dynamic methods described in Section 6-9 can underpredict nominal resistance when blow counts exceed 120 bpf.

6-4.1.3 Noise and Vibration.

Pile driving is inherently noisy. Noise levels can range from 80 to 135 decibels. Pile driving noise can exceed noise ordinances and challenge relations with neighbors. Noise levels attenuate with distance, and noise suppression devices are available for some hammers. Driving steel piles tends to generate more noise (ringing) as compared to driving timber and concrete piles. Underwater noise generated by driving piles in water can be detrimental to marine life and bubble curtains are sometimes used to mitigate underwater noise.

Pile driving also induces vibration in soil and rock that can cause settlement. Vibrations can be transmitted to, and can potentially damage, nearby structures. The amplitude of vibration is quantified using the peak particle velocity. Local ordinances may include limits on ground vibration levels. Vibrations with peak particle velocities exceeding 0.5 in/sec can damage structures (Wiss 1981); however, settlement and other negative effects can begin to occur at lower intensities (Lacy and Gould 1985). Low intensity vibrations can also be a nuisance to neighbors or affect nearby operations, such as manufacturing. The frequency of vibrations also influences their impacts, but these effects are beyond the scope of this chapter.

The vibrations generated by pile driving depend on the soils and rock at the site, the pile type, the driving system, installation techniques, the penetration depth of the pile, and distance from the pile. While complete attenuation of vibrations may require many hundreds of feet, damaging vibrations are usually limited to a distance approximately equal to the pile penetration depth or 50 ft, whichever is greater (NCHRP 1997b). Figure 6-7 approximates the relationships between vibration and soil type, hammer energy rating, and distance from the pile. These charts do not capture the specific site response to vibrations, e.g., influences of stiff soil crusts, and should only be used in preliminary assessments of vibration impacts.

Condition surveys and vibration monitoring can reduce the likelihood of damage claims and other bad outcomes, particularly in urban areas. Condition surveys document the

condition of nearby facilities before and after construction. Vibration monitoring measures the actual vibrations during pile driving.

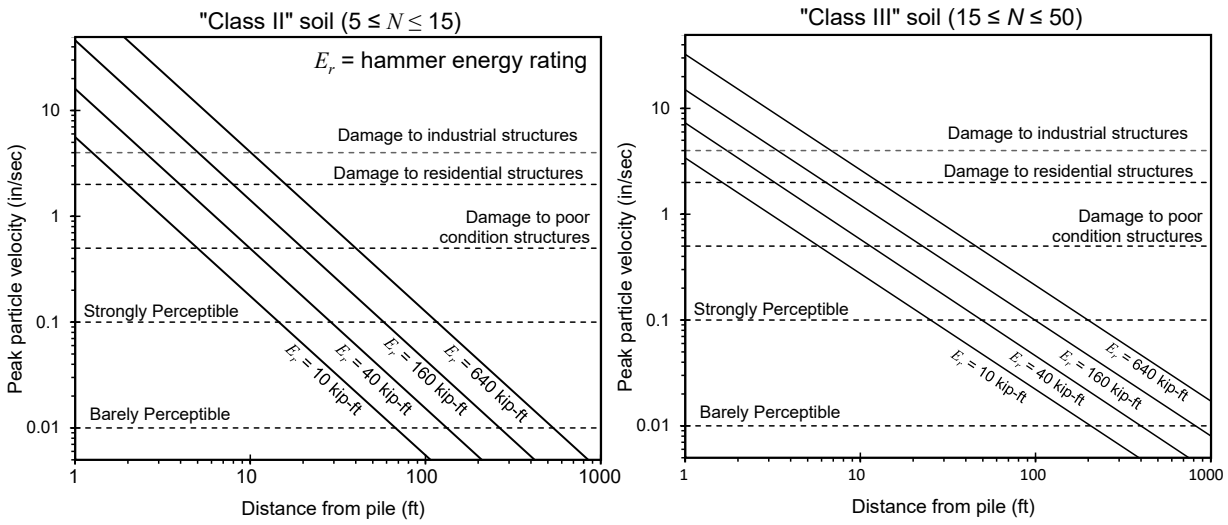

Figure 6-7 Estimated Vibration Level Due to Pile Driving (after Bay 2003)

6-4.1.4 Soil Disturbance and Driving-Induced Pore Pressures.

Pile driving remolds clay soils and can cause volumetric changes and temporary driving-induced pore pressures in all soils. Disturbance effects are more severe as the volume of displaced soil increases. Displacement piles produce greater disturbance than low displacement piles of the same size. The method of installation also influences the severity and spatial reach of disturbance. For example, disturbance can depend on the type of hammer, the use of driving aids, the number of piles, and the pile spacing. As shown in Figure 6-8a, disturbance of clay soils typically produces a zone of heave while disturbance of coarse-grained soils typically produces a zone of settlement (Figure 6-8b).

The initial void ratio of the soil and soil type also influences the impacts of disturbance. Initially, loose to medium dense coarse-grained soils are usually densified by pile driving while dense coarse-grained soils may dilate. Fine-grained soils usually consolidate radially in the vicinity of the pile. The reduction in the soil's volume often does not counter the addition of the pile's volume, particularly in the case of fine-grained soils. Depending on the vertical and lateral boundary conditions, net positive changes in volume can produce heave and/or lateral squeeze of the soil.

Disturbance can impact the soil's shear strength and development of excess pore water pressure. Depending on how quickly the excess pore pressures dissipate, disturbance

that leads to densification and compression may generate temporary positive excess pore pressure while disturbance that leads to dilation may generate temporary negative pore pressure. Chapter 7 in DM 7.1 discusses the effects of excess pore pressure and void ratio changes on shear strength in the context of slope stability analysis.

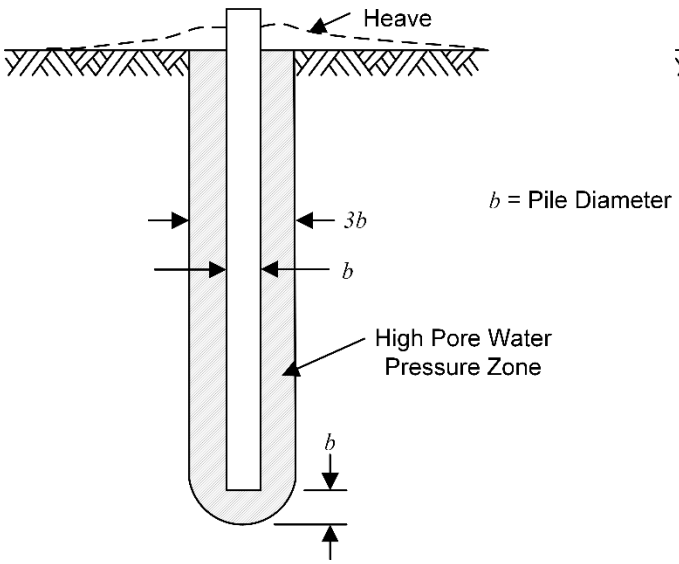

b = Pile Diameter

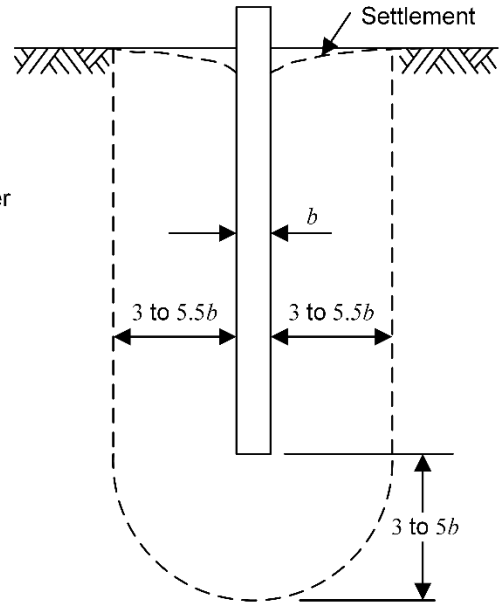

a) Fine-Grained Soils

b) Coarse-Grained Soils

c) Typical Volume and Pore Pressure Changes from Disturbance

Soil Tendency	Short-Term Effects	Long-Term Effects	Typically Occurs in:
Densification / compression	Pore pressure ↑ Undrained shear strength ↓ Pile capacity ↓	Void ratio ↓ Shear strength ↑ Pile capacity ↑	Saturated clay Loose to medium dense silts and fine sands
Dilation / expansion	Pore pressure ↓ Undrained shear strength ↑ Pile capacity ↑	Void ratio ↑ Shear strength ↓ Pile capacity ↓	Dense sands and silts, weak laminated rocks

Figure 6-8 Typical Effects of Disturbance During Driving of Piles (after Broms 1966)

Based on fundamental concepts of effective stress and shear strength, a reduction in void ratio by driving-induced densification will increase long-term shear strength. An increase in void ratio by driving-induced dilation will decrease long-term shear strength. Similarly, a decrease in effective stress from temporary driving-induced positive pore pressures will decrease strength. An increase in effective stress from temporary driving-induced negative pore pressures will temporarily increase shear strength.

While the effects of void ratio changes on shear strength are long lasting, the effects of temporary pore pressure changes on shear strength are temporary. The pile resistance during, and soon after, driving may be different than in the long-term. The term *setup* refers to the increase in pile resistance over time as driving-induced positive pore pressures dissipate. Setup frequently occurs for piles driven in saturated clay and in loose to medium dense silts or fine sands. The term *relaxation* refers to the reduction in pile resistance over time as negative driving-induced pore pressures dissipate. Relaxation can occur for piles driven in dense saturated fine sands, dense silts, and in weak laminated rocks, such as shale.

Setup and relaxation effects usually take a few days to fully manifest. However, effects can sometimes take several weeks. As such, load tests or pile restrikes should be scheduled accordingly to observe the nominal pile resistance without the effects of transient pore pressures.

6-4.1.5 Pile Splicing.

A key decision in pile design is the selection and ordering of piles that are long enough to provide acceptable performance, but not too long to be inefficient. However, sometimes it is not possible or practical to source and/or transport piles at the target length. In other cases, there may be economic advantages to driving shorter piles with smaller equipment and using splices to reach full length. In still other cases, piles can be unexpectedly too short.

Whether planned or unplanned, pile splicing can be used to achieve piles that have necessary length. Steel piles are the easiest to splice and are most often spliced by welding. Preparing the joint surfaces and welding consumes time and requires careful inspection, but when performed correctly, a spliced steel pile can perform as well as an unspliced pile of the same length. Splicing timber piles is difficult and rarely done.

Splicing concrete piles is more difficult and has traditionally been avoided whenever possible because it creates a discontinuity in the prestressed steel and can compromise the capacity and durability of the pile. Furthermore, installing concrete splices is often time consuming, requires specialized equipment and materials, and may be adversely affected by weather and temperature (e.g., epoxy curing). Common concrete splices can be categorized into those that join pile segments with 1) mechanical interlocking end pieces, wedges, or pins, 2) a steel sleeve that fits over the concrete pile segments, and 3) dowels that are secured with epoxy or cement grout. Not discussed here are other niche splicing systems that are usually variants of the three categories listed above. Some splicing options for concrete piles, particularly those with mechanical interlocking pieces, require casting special end pieces into the pile when it is manufactured; therefore, these options are not feasible for unplanned splices.

6-4.2 Drilled Shafts.

Drilled shafts are bored reinforced concrete columns having diameters that typically range from 2.5 to 8 ft and lengths up to 100 ft, though elements up to 12 ft in diameter and 200 ft in length are possible with special equipment. When practical, drilled shafts may be socketed in rock to provide high capacity with small associated settlement. Usually, the diameter of a rock socket is less than or equal to 5 ft, and the length is between 5 and 10 ft, though sockets having larger diameter and length are not uncommon. The diameter of drilled shafts is selected to provide suitable performance. However, shafts may be enlarged to facilitate construction, e.g., to remove rock fragments or match the diameter of the structural column. Compared to driven piles, drilled shafts generally produce fewer disturbance effects, less noise, less vibration and often carry more load per element.

6-4.2.1 Equipment and Methods.

Drilled shafts are constructed using either the dry method or the wet method (Figure 6-9). The *dry method* uses an open shaft without any drilling slurry. The dry method is suitable when the sides and bottom of the open shaft remain stable, and the inflow of water into the shaft is small. Conditions favorable to the dry method include stiff clay and/or rock. Permanent or temporary casing can be used to span problematic zones as discussed below. The dry method is simpler, less expensive, and faster than the wet method.

The *wet method* uses a slurry mixture of water and bentonite or polymer to maintain shaft stability. The wet method is needed when caving along the sides, or heave of the bottom, of an open shaft is possible and/or when the inflow of groundwater is significant and likely to adversely affect the uncured concrete. To provide a stabilizing effect and control water inflow, the head of the slurry inside the shaft is kept higher than the head outside of the shaft. The slurry typically has a viscosity and unit weight greater than water, e.g., bentonite slurry usually has a unit weight of 65 to 70 pcf. The bentonite or polymer additive prevents loss of fluid into the surrounding ground. Bentonite slurry creates a *filter cake* on the sides of the shaft as some of the bentonite is separated from outflowing water. The filter cake is an effective seal but can negatively affect the side resistance of the shaft. Polymer slurry does not create a filter cake. Slurry is usually circulated between the shaft and the holding tank using a pumping system. As the slurry is circulated during drilling it accumulates soil and rock particles that can settle out in the shaft during excavation and create an unsuitable loose layer or become entrapped in the concrete. To avoid these problems, the slurry must be kept clean, or de-sanded, using settling tanks or special de-sanding equipment. When drilling through wet, but otherwise stable ground, the shaft can be simply filled with water to prevent excessive inward seepage. Similar to the dry method, permanent or temporary casing can be used to span problematic zones. If casing can effectively span a

problematic zone and control the inflow of water, it is possible to switch to the dry method of construction.

Permanent or temporary casing is frequently used to span soils prone to caving or squeezing, such as saturated sand and very soft soil. In some situations, casing is advanced below the depth of shaft excavation to create a seal in a more stable stratum. Temporary casing is usually pulled during concrete placement, making sure that the head of concrete is above the head of external water. Pulling temporary casing in very soft soils can be difficult. If casing is pulled too soon, the soft soil can intrude into the concrete. If pulled too late, the concrete sets and bonds to the casing. Permanent casing is often used when constructing drilled shafts in water for bridges or other structures, particularly when working from a barge instead of from within a cofferdam. Permanent casing may also be required to span voids created by karstic features or abandoned mines as well as when drilled shafts are socketed into sound rock and high capacity is desired.

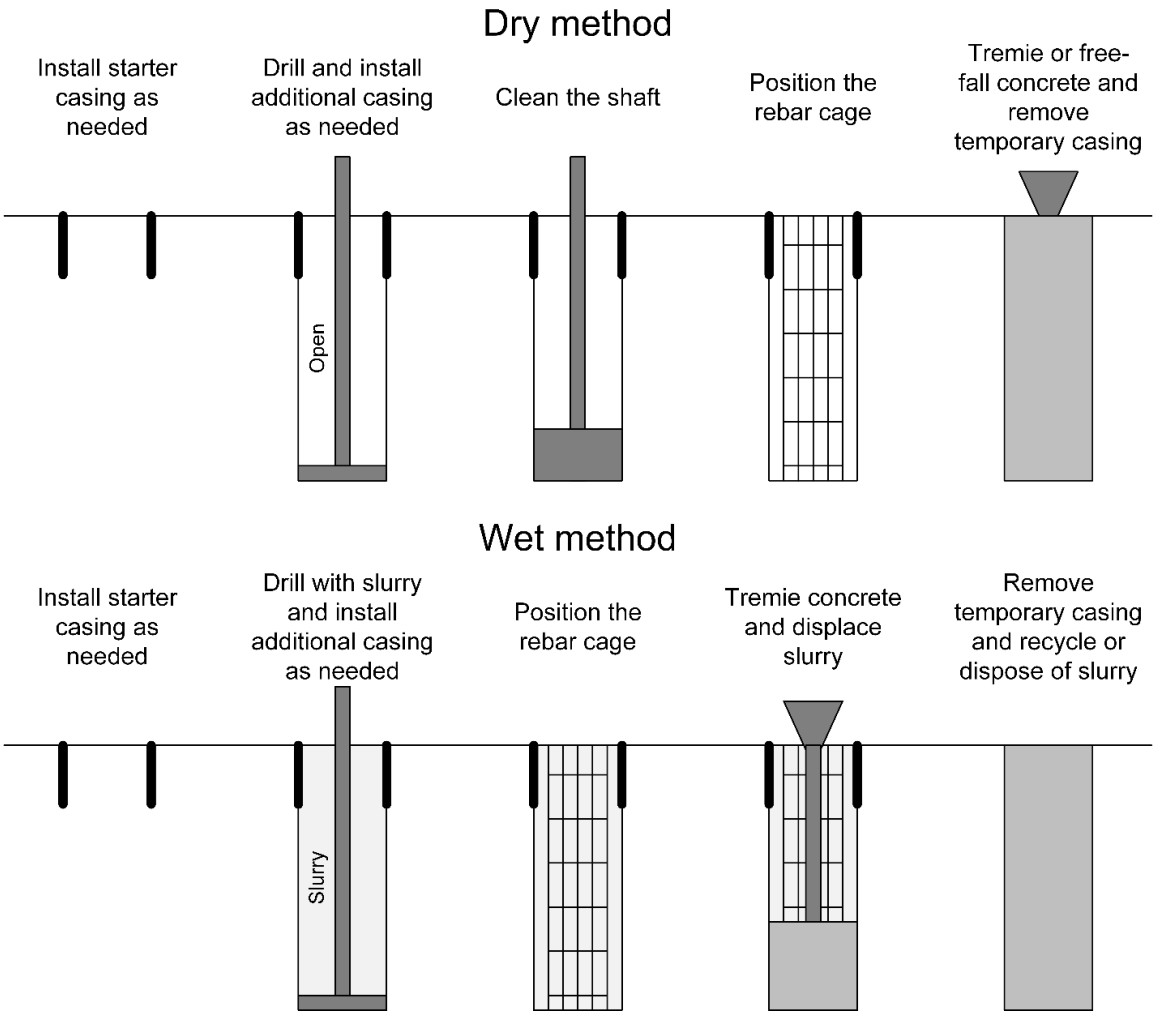

Figure 6-9 Dry and Wet Methods of Drilled Shaft Construction

Most drilled shafts are constructed using hydraulic rotary-drill rigs. The capability of the drill rig is often reported in terms of the maximum torque and downward force, or *crowd*, that can be applied. Drill rigs are usually mounted on a truck or tracked equipment, such as an excavator, crane, or crawler. Some drill rigs, known as top-drive rigs, are mounted directly to casing that is installed prior to drilling. Casing is installed using an impact or vibratory hammer while large diameter casing is sometimes advanced and extracted using oscillator and rotator systems. These machines apply oscillating or continuous torque and crowd to the casing. When this equipment is used, the soil inside the casing is often excavated using a top-drive rig or crane-hoisted buckets.

Rotary drilling tools include augers for soil and rock, drilling buckets for soil, and core barrels for rock. Special rotary tools include an underreamer, or *belling tool*, to enlarge the base of drilled shafts in clay and *muck buckets* for cleaning out the base of the shaft.

Non-rotary drilling tools are also used. Clamshell and grab buckets allow for soil excavation at the base of the shaft. Rock breaker, drop chisel, and impact tools break up rock into fragments that can be lifted by a clamshell or grab bucket. Common impact tools include down-hole hammers, which use one or more pneumatic impact bits, and hammer grabs, which combine the functionality of a rock breaker and clamshell bucket.

A variant of drill shafts, known as barrettes, are diaphragm walls constructed as reinforced deep foundation elements. Barrettes are constructed using non-rotary drilling tools, e.g., hydromill, and the same techniques are used to build diaphragm walls. Unlike conventional drill shafts, barrettes have a rectangular cross section. Barrettes can be constructed using dry or wet methods depending on the ground conditions.

6-4.2.2 Steel Reinforcement and Concrete.

The steel reinforcement used in drilled shafts consists of a fabricated rebar cage formed by concentrically arranged longitudinal bars with transverse reinforcement placed circumferentially around the arrangement of longitudinal bars, often as a hoop or spiral. The cage also includes any centering devices, lifting brackets, and tubing for post grouting and/or nondestructive testing, such as cross-hole sonic logging. The yield strength of the steel is typically between 60 and 100 ksi. The longitudinal reinforcement resists stresses from bending, tension, and compression while the transverse reinforcement resists internal shear and confines the concrete and longitudinal reinforcement. A minimum of six longitudinal bars that are at least No. 5 sized are required by AASHTO (2020). As a rule of thumb, the longitudinal rebar should occupy at least 0.5% of the overall cross-sectional area of the drilled shaft, and the spacing between parallel pieces of longitudinal and transverse rebar should be at least 5 inches or five times the maximum aggregate size in the concrete. Typically, the steel area ratio of longitudinal steel to gross area ranges from 1% to 2%, with 8% being the maximum allowed by AASHTO (2020). Percentages of steel exceeding 4% tend to impede

concrete flow around the rebar cage. A minimum 3 inches of concrete cover is required for rebar according to AASHTO (2020). However, greater depths of cover are recommended for larger diameter shafts, e.g., 6 inches for shaft diameters greater than or equal to 5 ft (FHWA 2018a).

Concrete for drilled shafts must satisfy several basic requirements for strength, durability, stability, and workability, which are addressed by the concrete mix design. Concrete is most often placed down the center of the shaft using a free fall method, tremie pipe, or pumping after the rebar cage has been positioned. Free fall introduces concrete at the rising surface of the concrete, while placement by tremie pipe or pumping introduces concrete from the bottom of a pipe, which is positioned sufficiently below the rising surface of the concrete. Concrete mixes are formulated either for free fall or placement by tremie or pumping to target a 28-day strength of 3,000 to 5,000 psi. Higher strengths are targeted in special cases, such as to satisfy seismic design requirements. The cured concrete must be durable in the groundwater chemistry of the placed environment, which may contain salt and acids. During placement, the concrete must remain stable in terms of bleed, which is separation of water from the mix, and segregation, which is separation of the cement paste from the aggregates. The concrete used in drilled shafts must also be able to self-consolidate and flow through the rebar cage without the assistance of vibration. Therefore, concrete placed by free fall usually has a slump of 6 to 7 inches to provide workability, while avoiding segregation, while concrete placed by tremie or pumping usually has a slump of 7 to 9 inches. The concrete must retain workability often for several hours over the duration of placement and retrieval of the casing.

6-4.2.3 Post Grouting.

Post grouting is used to premobilize and improve the base resistance in drilled shafts using pressurized grout delivered after the concrete has been placed and allowed to gain sufficient strength (>2500 psi). The premobilizing effect is achieved by loading and compressing the soil below the base. This leads to smaller post-construction settlement needed to mobilize the base resistance under service conditions. The ground improving effect is achieved by reducing the void ratio of the soil below the base, permeating grout into the soil, and/or creating an enlarged grout bulb that effectively increases the base area.

Post grouting requires installing grout delivery tubing and a distribution device to the reinforcement cage prior to placing the cage in the shaft. The grout distribution device can be a flat jack design, where grout is pumped from tubing placed between a steel plate and rubber membrane. Alternatively, grout distribution can use a sleeve-port design, where grout is pumped through multiple U-shaped circuits that contain perforations which are sealed with rubber sleeves. Grout exits the delivery and distribution system when the internal grout pressure exceeds the confinement provided by the rubber sleeve/membrane and pressure from the earth and groundwater. The

grout mix is usually a neat cement with a water-cement ratio of 0.4 to 0.55. As the grout is pumped, it applies an upward-acting force on the drilled shaft and a downward-acting force to the soil below the base. An approximately proportional rise in grout pressure with grout volume is desired as this signifies that the soil below the base is being loaded and compressed. Some upward movement of the shaft, e.g., ½ inch, during post grouting is expected. Significant deviations in the proportionality between grout volume and pressure often indicate a problem, such as a blockage in the grouting system, excessive shaft movement, or hydraulic fracturing of the soil. The achievable grout pressure typically ranges from 100 to 900 psi and is limited by the shaft resistance and weight, overburden pressure at the base, and capabilities of the pumping system.

Methods to incorporate the effects of post grouting into the design of drilled shaft include applying multipliers to the nominal resistance of an equivalent ungrouted shaft or using load transfer *t-z* methods. Since routine use of post grouting is still relatively recent, design methods that account for post grouting are still evolving. As such, load tests of grouted shafts are particularly valuable to observe the effects of post grouting.

6-4.3 Continuous-Flight Auger Piles.

Continuous-flight auger (CFA) piles, or auger cast-in-place piles, are similar to drilled shafts in that they are bored piles. However, there are a number of significant differences. First, the hole is drilled in one continuous operation and is always supported by augers, which eliminates need for slurry and/or casing. Second, grout or concrete is pumped under pressure through the augers as they are withdrawn. Third, steel reinforcement is pushed into the uncured grout or concrete pile after the augers are withdrawn. The reinforcement commonly extends through only the upper portion of the pile that is subjected to bending.

CFAs are installed with rotary drill rigs typically to depths up to 100 ft using augers that have a diameter ranging from 12 to 36 inches. With the proper equipment, CFAs can be constructed in low headroom conditions and at a batter angle. CFAs can be installed in soil and some weak/weathered rock but cannot be used in hard rock like drilled shafts. CFAs are also not recommended in geologic formations containing voids. A key to good construction quality is balancing the rotation and penetration rate of the augers so that the augers do not excessively rotate and mine soil from beyond the intended limits of the pile. During drilling, the excavated cuttings should ideally be limited to the volume occupied by the auger plus some accommodation for bulking of the disturbed material. This objective can be difficult to achieve in soft clays that tend to squeeze inward and loose clean sands and gravels prone to caving.

After drilling, grout or concrete is pumped at pressure that exceeds the overburden pressure at the bottom of the auger. As grout is pumped, the auger is withdrawn at a rate that compensates for the volume of grout delivered. As the augers are withdrawn, they are either not rotated or rotated slowly in the direction of drilling. These techniques

are intended to preserve a seal for grout pumping, retrieve the soil between the auger flights, and prevent the augers from getting stuck in the hole.

The decision to use grout or concrete varies by location, e.g., the US favors grout while the EU favors concrete, and the needs for workability, stability, and durability. Grout tends to retain workability longer than concrete and is more fluid than concrete, which facilitates installation of the reinforcing steel. The mix designs for concrete and grout used in CFAs are similar to that of tremie concrete used for drilled shafts (see Section 6-4.2.2), except that the grout omits the coarse aggregate.

6-4.4 Drilled Displacement Piles.

Drilled displacement piles (DDPs) are similar to CFAs in that a continuous operation is used to drill on the downstroke and pump grout or concrete on the upstroke. Instead of the conventional continuous flight augers used by CFAs, DDPs use special augers that displace soil laterally during drilling. Many variants of the augers, e.g., DeWaal and Omega, can be used to drill DDPs, some of which are proprietary. The primary differences among the augers are the amount of displacement (full or partial), the ability to install reinforcement through a hollow stem prior to grouting, and the shaping of the sides of the hole, e.g., smooth or screw-shaped, as the auger is withdrawn during grouting. Some augers use a sacrificial tip that is left in the hole as the grout or concrete is placed when the auger is withdrawn. In some cases, a process known as amelioration, in which sand or gravel is added to the top of the drill hole, is performed to increase shaft resistance.

One advantage of DDPs over CFAs includes the possibility of greater lateral stress between the pile and the soil under certain ground conditions. The side resistances approach those of driven displacement piles. From the standpoint of constructability, DDPs require less finesse by the operator to balance the rate of rotation and the rate of penetration compared to CFAs. DDPs require greater torque to turn the soil-displacing bit, which is a disadvantage compared to CFAs. They also have greater potential for ground heave and/or lateral squeeze of soft soils due to the volume displaced by the pile.

6-4.5 Aggregate Columns.

Aggregate columns include rammed aggregate piers and stone columns (see Figure 1-2). Aggregate columns are not usually structurally-connected to the superstructure, but they often provide the function of a foundation and meet the definition of a deep foundation ($Z/b \geq 5$) adopted herein. Stone columns up to 100 ft in length can be formed using either vibro-replacement or vibro-displacement.

Vibro-replacement columns, a.k.a wet stone columns, are constructed using a down-hole vibrator and water jet to penetrate the ground. The hole is filled with stone dumped

from the top of the hole. A key feature of vibro-replacement is the removal of a portion of the soil as the column is formed. A muddy effluent is created that requires containment, removal, and disposal.

Vibro-displacement columns, a.k.a. dry stone columns, are also constructed using a vibrator except without water jetting, and the soil is displaced by the vibrator rather than removed. Sometimes air jetting or predrilling are required for the dry method. Stone is introduced either from the top, similar to vibro-replacement, or from the bottom using a stone tremie tube attached to the side of the vibrator.

The equipment used to construct vibro-replacement and vibro-displacement stone columns is typically handled and operated using tracked equipment or occasionally a crane. The down-hole vibrators typically have a diameter of 12 to 16 inches and are either electrically or hydraulically powered. Special variants of the vibro-displacement method replace the down-hole vibrator with a vibratory pile hammer, and certain technologies introduce grout with the stone or substitute concrete for the stone.

Rammed aggregate piers are constructed by first drilling a hole with a diameter ranging from 18 to 36 inches and a depth typically ranging from 7 to 35 ft. The pier is formed by introducing lifts of stone into the hole, usually by dumping, and compacting each lift using the ramming action of a special tamper. In addition to compacting the stone, the ramming action of the tamper usually forces some of the stone beyond the drill diameter and below the base of the hole. Special variants of rammed aggregate piers can achieve depths greater than 40 ft. Tracked excavator equipment is most often used to install aggregate columns.

Aggregate piers are most suitable in soils that are not too soft or sensitive and not too stiff or dense. Soft or sensitive soils are prone to excessive volumes of aggregate being required, loss of strength due to the application vibration or ramming, and inward squeezing in the case of the drilled rammed aggregate piers. Stiff or dense soils may be difficult to penetrate with the vibrator. The drilling stage of rammed aggregate pier construction may require temporary casing in soils prone to caving or squeezing.

6-4.6 Micropiles.

Micropiles are bored with a small diameter (<12 inches) and grouted with foundation elements that can be installed in soil and rock to depths up to 200 ft. Greater depths can be achieved with special equipment. Micropiles are very adaptable to drilling in low headroom conditions, hard to access sites, challenging ground conditions, and in close proximity to existing facilities. Micropiles can also readily be installed at a batter angle. Figure 6-10 shows one example of a micropile construction sequence. However, there are many variations to the construction process particularly related to the drilling technique, casing, drilling fluid, grout delivery technique, and number of grouting phases.

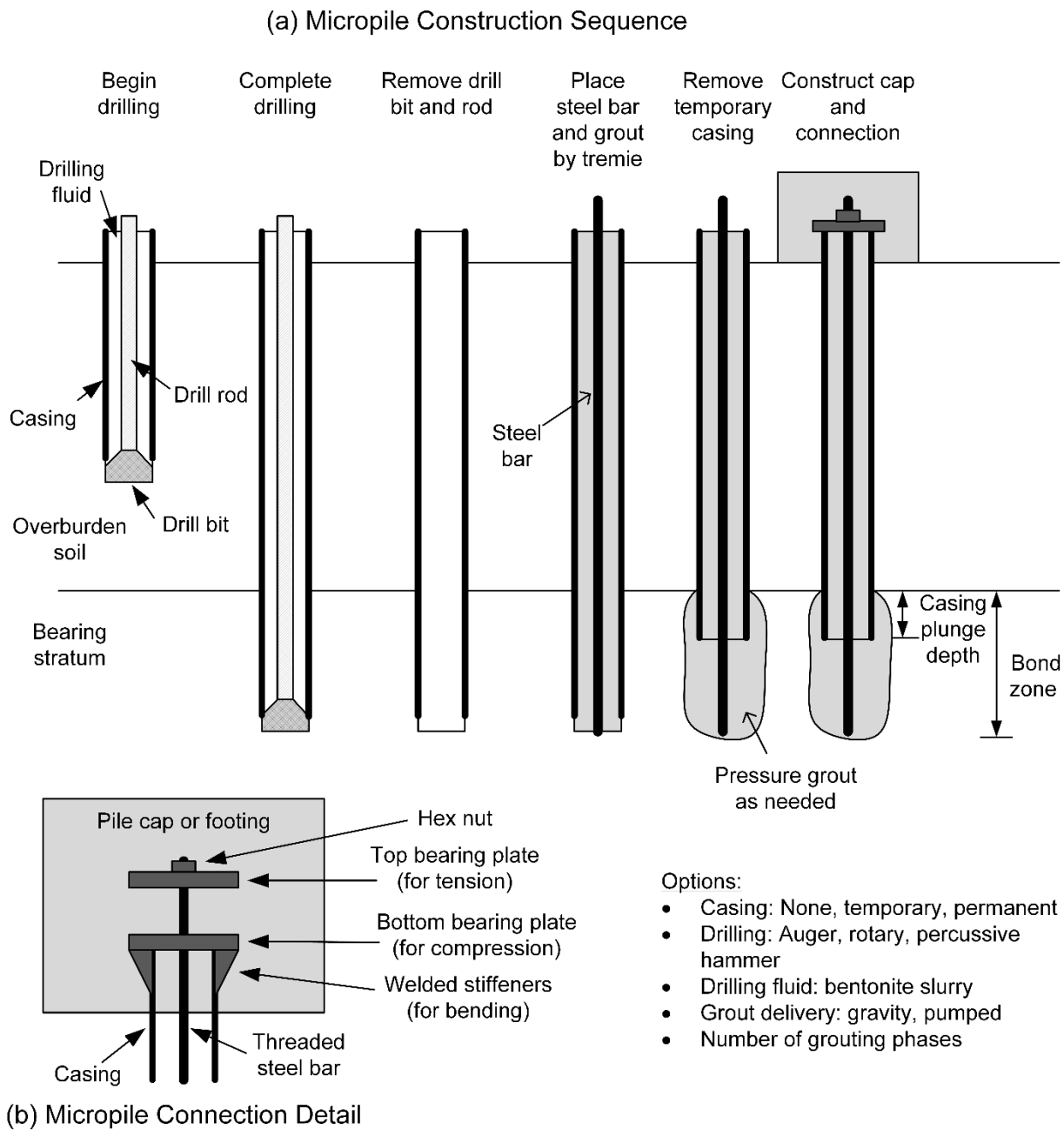

Figure 6-10 Micropiles – (a) Construction Sequence and (b) Connection Detail

Micropile drill rigs are usually mounted on trucks or tracked equipment. Drill rigs usually incorporate a hydraulic power unit to rotate the casing and/or drill rod in the same or opposite directions. Drilling tools are selected to be compatible with the ground conditions and include roller bits, casing with cutter teeth, rock bits, augers, and percussive hammers. Percussive tools, primarily used for rock drilling, may be powered by the rig's hydraulic power unit or a separate air compressor. Percussive force is applied using either a top-drive hammer or down-the-hole hammer. Sonic drilling

advances the hole by vibrating the casing and drill rod. The drill hole is usually flushed by water or slurry to remove cuttings, stabilize the hole when casing is not used, and cool drill bits. Compressed air can also be used to flush the hole but should not be used below the groundwater table, especially in sands. Drilling fluids present the need to supply and circulate the fluid as well as manage spoils.

Micropiles are grouted to create a bond zone with the surrounding soil or rock. Bond zone lengths of 5 to 10 ft are common in rock while longer bond lengths are routinely used in soil. The diameter of the bond zone is influenced by the inside diameter of casing that is used, the use of an underreaming bit to enlarge the drill hole below the casing, and the method of grouting. The grout used for micropile construction is most often a neat cement prepared using a water cement ratio of about 0.40-0.50 by weight to achieve typical target compressive strengths of 4,000 to 5,000 psi. As defined by FHWA (2005), Type A micropiles are grouted under gravity only, while Type B micropiles are first gravity grouted and additional grout is added under pressure as the casing is withdrawn. Type C micropiles are first gravity grouted then post grouted under pressure prior to hardening of the initial grout. Type D micropiles are first gravity grouted and then post grouted under pressure one or more times after hardening of the initial grout. The post grouting for Type C and D micropiles does not occur concurrently with removal of casing. Generally, Type A micropiles are used when the bond zone is in stiff clay or rock while Type B, C, and D micropiles are used in soils.

Micropiles are typically reinforced by a steel pipe and/or a centralized steel rebar that carries at least 40% of the load in the element. The casing is often an 80 ksi steel oil field casing (API N-80)[30] with an outside diameter of 5.5, 7.0, or 9.625 inches and approximately a half-inch wall thickness. The rebar is often a large diameter thread bar, e.g., #18 or #20, made from 75 or 80 ksi steel.

Micropiles are commonly installed in groups and tied together within a pile cap. There are a variety of options available for establishing the connection between the micropile and the pile cap that depend on whether the pile cap (or footing) is new or existing and how heavily the pile is loaded in compression, tension, and bending. For example, the inset in Figure 6-10 shows a pile to cap connection for a pile subjected to significant loads in compression, tension, and bending. One or both of the bearing plates and stiffeners may be omitted if not needed.

[30]Typically mill secondary pipe is used because prime pipe is very expensive. Use of mill secondary pipe requires the implementation of coupon tests, typically two per truckload of pipe, because mill certifications are not available for this material.

6-4.7 Helical Piles.

Helical piles, or screw piles, consist of one or more circular steel bearing plates that are formed into a helix shape with a uniform pitch and welded to a central round or square steel shaft. The pitch of the helix is shaped so that the shaft advances the pitch distance in one revolution without excessive soil disturbance. When properly installed, helical piles are low-displacement elements. Typical helix diameters range from 6 to 36 inches, and completed helical piles lengths are mostly 10 to 30 ft; however, greater depths are routinely obtained using larger piles and equipment. Helical piles are usually installed in segments that are connected using bolted couplings. Since helical piles usually involve steel in direct contact with the ground, the components are galvanized to resist corrosion. Many specifications require a minimum embedment depth of five or more times the largest helix diameter between the ground surface and the upper-most helix. Generally, there are no more than 6 helices per pile. Helical piles are not suitable for ground conditions that may damage the shaft or helices, such as hard soils or soils with large gravel or cobbles. Specialty helical piles are grouted along the shaft to increase the strength and stiffness of the pile as well as increase resistance to buckling and corrosion.

Helical piles are installed using hydraulically-power rotary drills that are often small enough to be mounted on a light tracked loader/excavator or a truck. Helical piles are very adaptable to installation in low headroom conditions, hard to access sites, and in close proximity to existing facilities. Helical piles can readily be installed at a batter angle with proper equipment and can be used for resisting tension loads as well as compressive loads. The installation torque is an important parameter to evaluate capacity and is often measured in the field using a variety of qualitative or quantitative torque indicators. These methods include 1) observing the amount of twist in the shaft over some shaft length (qualitative), 2) using torque-limiting shear pins (quantitative at points of pin failure), 3) digital torque indicators (continuous quantitative readings using strain measurements), and 4) differential pressure torque indicators (continuous quantitative readings using the pressure drop through the hydraulic drill).

6-5 GEOTECHNICAL STATIC AXIAL CAPACITY AND SETTLEMENT.

6-5.1 Introduction.

This section presents selected analysis methods for evaluating static axial capacity and settlement of deep foundations. Section 6-8 describes static load testing, and Section 6-9 describes dynamic methods, which provide important refinements to the initial estimates of the anticipated performance of the deep foundations.

6-5.2 Limit States.

6-5.2.1 Strength Limit State.

Static capacity analyses are performed to estimate the nominal resistance (LRFD) or the ultimate capacity (ASD) of a foundation element subjected to compressive or uplift loading. The nominal resistance or ultimate capacity of a foundation element is evaluated by considering the geotechnical strength of the geomaterials and the structural strength of the material(s) that comprise the foundation element. The strength limit state is defined by the extent to which the nominal resistance may be mobilized under the expected conditions over the service life of the foundation. In the LRFD framework, the nominal resistance is reduced by application of resistance factors. In the ASD framework, an allowable (working) value is determined using a factor of safety. In some cases, different factors are applied to the resistances provided by shaft and base. For example, drilled shafts require greater vertical deformation to mobilize base resistance and have greater uncertainty associated with bearing capacity predictions. Thus, the base resistance is assigned a lower resistance factor.

Often, the criteria defining nominal resistance used to develop static capacity analysis methods are not well documented (Fellenius 2021). While this shortcoming may not be significant in routine design, it is worth referring to original sources, particularly on projects with small allowances for settlement. As discussed in Section 6-8, methods such as the Davisson (1972) failure criterion can be applied to interpret load test results to define nominal resistance in a consistent way.

AASHTO (2020) also defines the Extreme Event Limit State, which is a special case of the strength limit state in which survivability rather than satisfactory performance is the intent of the design checks. Examples of extreme events include loads from collisions, blasts, and earthquakes as well as the impacts of scour from severe flooding and liquefaction. Generally, not all extreme event scenarios are assumed to occur simultaneously in design. Consideration of extreme events is outside the scope of this manual.

6-5.2.2 Service Limit State.

The service limit state is defined by the acceptable limits on deformation, e.g., settlement and lateral deflection, over the service life of the foundation. Section 6-5.8 describes some typical limits for settlement and Section 6-6.2 for lateral deflection.

6-5.3 Load Transfer.

The nominal axial resistance in a deep foundation element, R, is developed from shaft resistance, R_s, and/or base resistance, R_b. The contribution of each source of resistance depends upon the mobilization of shear strength at the soil-shaft or rock-shaft interface and the soil or rock at the base. The peak and post-peak strength is influenced by the

usual compositional and environmental factors that govern soil behavior with respect to strength. Of particular note is the differential shear movement between the soil and shaft as well as the movement of the base required to mobilize shaft and base resistances. Normally, full mobilization of shaft resistance occurs within a ½ inch of column top settlement (FHWA 2018a); however, mobilization of the base typically requires larger column settlements. Full base mobilization in fine-grained soils may require column settlement of about 4% to 5% of the base, width, or diameter while settlements of about 10% of the base, width, or diameter may be required for columns in coarse-grained soils (FHWA 2018a). Full mobilization of shaft and base resistance usually do not occur simultaneously. For large elements, such as drilled shafts, the settlements required to fully mobilize the base may exceed the service limit state criteria. Post-grouting of drilled shafts, described in Section 6-4.2.3, can be implemented to reduce the settlement needed to mobilize the base resistance. A useful rule of thumb to evaluate the nominal base resistance of drilled shafts without post grouting that considers the displacement required for mobilization of resistance at working loads is to reduce the nominal base resistance by 80%, i.e., use a nominal base resistance equal to 20% of the full value as evaluated by static capacity analysis or load testing (Gregory 2023).[31] Application of this rule of thumb still requires that a factor of safety or LRFD resistance factor be applied to the reduced nominal base resistance. This rule was developed for shafts bearing in sedimentary rock and hard clays, but is considered to be generally applicable to shafts bearing on rock as well as competent clays, sands, and gravels.

Figure 6-11 illustrates the basic concepts of load transfer. Inset (a) shows the case of an end bearing pile where the soil along the shaft is too weak to consider in design, or the bearing stratum is so stiff that the expected displacements are insufficient to mobilize shaft resistance. Inset (b) shows a case that could represent a friction pile in uniform clay that provides uniform unit shaft resistance in the short term with a small contribution of base resistance, i.e., the ratio of R_b/R is small. Inset (c) shows a case that could represent a pile in uniform, coarse-grained soil that provides unit shaft resistance that is proportional to the effective vertical stress and a large contribution of base resistance, i.e., the ratio of R_b/R is large.

Figure 6-11 also shows two hypothetical relationships between axial load applied to the top of the pile and the resulting settlement. When R_b/R is small, the resistance is primarily from the shaft, which mobilizes at small displacements. The condition of plunge is associated with a significant increase in the rate of settlement with respect to additional loading. This results in a large increase in the slope of the curve when load is

[31] Personal communication. Gregory developed this rule based on extensive design experience, field testing, and synthesis of the guidance provided by Wyllie (1999) and the findings of Rowe and Armitage (1987a,b).

applied to a pile where shaft resistance is already fully mobilized. When R_b/R is large, the resistance is primarily from the base, which mobilizes at larger displacements. While the rate of settlement with respect to additional loading may increase as the full mobilization of base resistance approaches, plunge usually does not occur if the bearing stratum is coarse-grained soil, stiff clay, or rock. Therefore, as mentioned in Section 6-5.4, the interpretation of the nominal resistance is not always straightforward. In particular, the nominal base resistance is usually estimated by analytical methods developed from load test data where failure requires interpretation by the Davisson or other failure criterion.

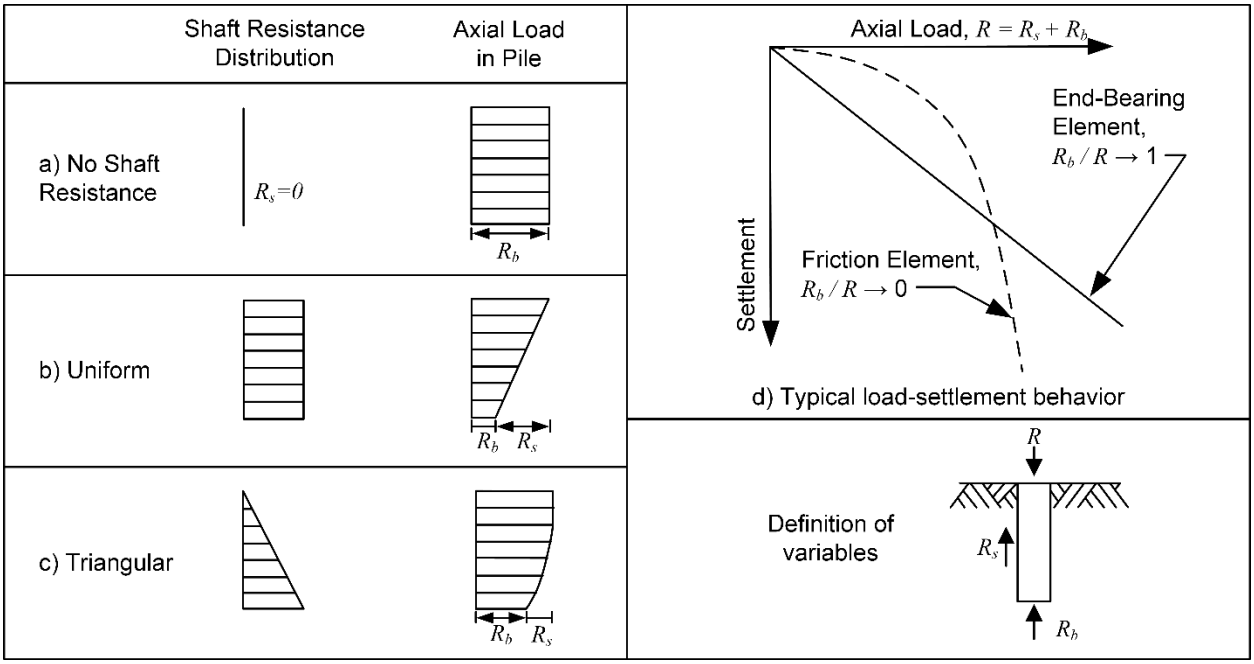

Figure 6-11 Load Transfer Concepts

It is also important to consider that the direction of the displacement of the foundation relative to the soil or rock determines whether load is transferred to or from the element to the soil or rock. Base resistance requires that the foundation element moves downward relative to the bearing stratum. Shaft resistance, i.e., load transferred from the element to the bearing stratum, in compression requires that the foundation element moves downward relative to the surrounding material. Mobilization of uplift resistance along the element shaft requires upward movement of the element relative to the surrounding material (see Section 6-5.6). Relative upward movement of the base does not contribute to uplift resistance by mobilizing shear strength. However, short term resistance can be generated by a suction effect if the rate at which the element moves produces negative excess pore water pressures by exceeding the rate of drainage (Bowles 1996). This suction effect is transient and should not be relied upon in design unless the element is specifically designed to utilize it, as with suction caissons used in offshore applications. A condition known as *negative skin friction*, where load is

transferred from the soil to the element, occurs when the soil moves down relative to the element, for example, from consolidation, secondary compression, or vibration-induced densification. Negative skin friction is discussed in Section 6-5.7.

The nominal resistance, R, is the sum of the nominal shaft resistance, R_s, and base resistance, R_b:

$$R = R_s + R_b \tag{6-3}$$

The nominal shaft resistance is computed by multiplying the unit shaft resistance by the surface area. For heterogenous ground conditions, the shaft can be discretized into multiple segments (i) in which each can be represented by a constant unit shaft resistance and the nominal shaft resistance is:

$$R_s = \sum \left(f_{s,i} A_{s,i} \right) \tag{6-4}$$

where:
$f_{s,i}$ = unit shaft resistance for segment i and
$A_{s,i}$ = surface area for segment i.

Figure 6-12(a) shows important dimensions for deep foundation elements in sand and clay profiles. In cases where the base of the element is enlarged, it is important to distinguish the diameter used to evaluate the surface area of the shaft, B', versus the diameter used to evaluate the area of the base, B. Figure 6-12 also shows that it is common practice to exclude the upper 5 ft of side resistance, or to the depth of seasonal moisture change or frost depth. This exclusion accounts for the potential for softening and/or gapping of the ground leading to a loss or unexpected reduction of shaft resistance (FHWA 2018a). The potential of softening and/or gaps developing from low confining stress and/or volumetric changes in the soil due to changes in temperature or moisture should be evaluated based on local experience and engineering judgment.

The nominal base resistance is computed by multiplying the unit base resistance, q_b, by the appropriate surface area of the base, A_b, as:

$$R_b = q_b A_b \tag{6-5}$$

For formed-in-place columns and driven high-displacement piles, the appropriate base area is the full cross-sectional area as illustrated in Figure 6-12(b). For driven low-displacement piles, the appropriate base area is the area of the pile material. In some situations where a soil plug forms, the decision of how to calculate base area may not be obvious.

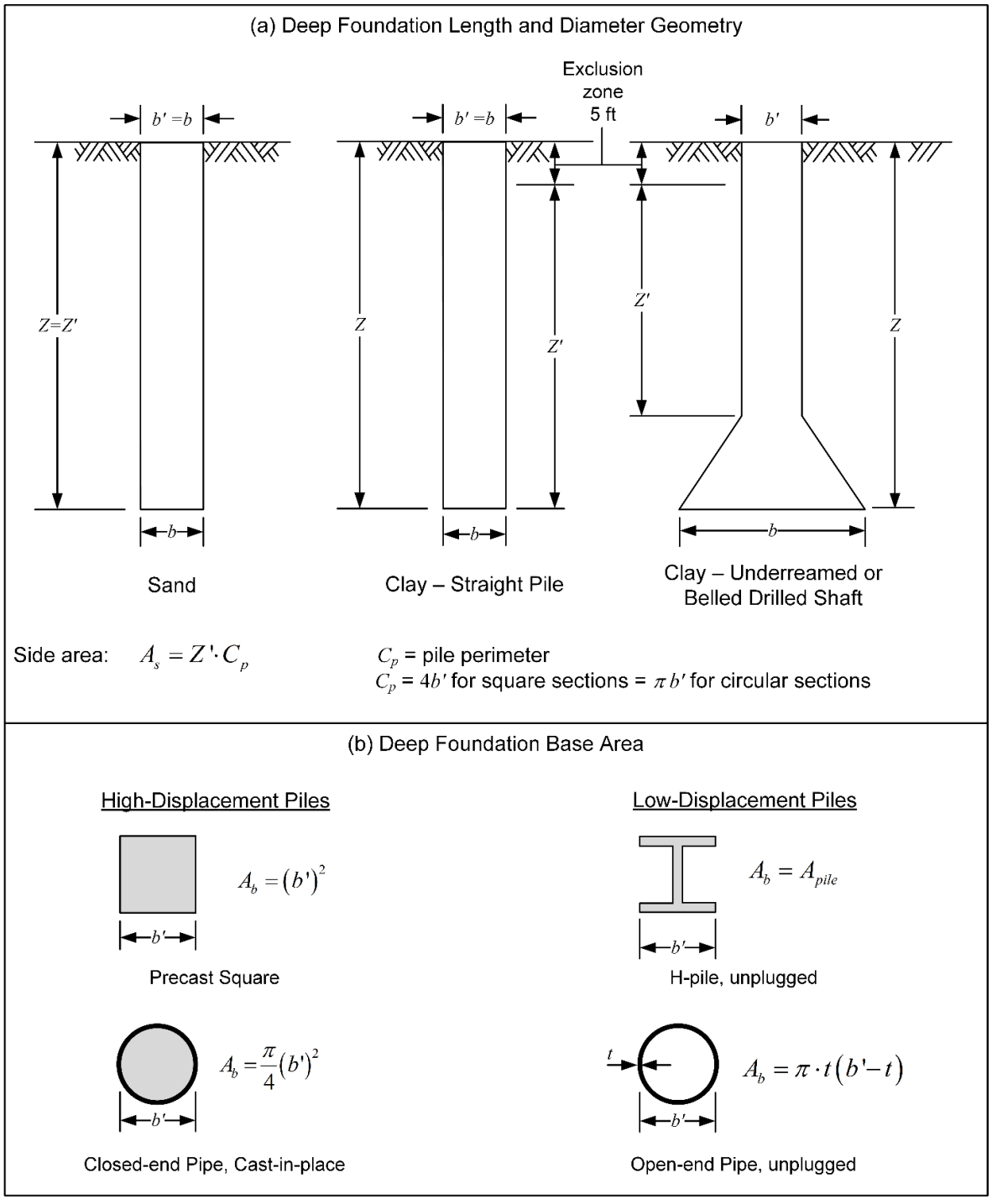

Figure 6-12 Geometry for SCA of Deep Foundations – (a) Length and Diameter and (b) Base Area

The factoring of the nominal shaft and base resistances to reduced (LRFD) or allowable values (ASD) of shaft resistance and base resistance is often dictated by agency practices or code requirements but may be additionally influenced by:

- Consideration of uncertainty in material properties,
  - Variable deposits
  - Weak soils such as soft clay and organics
- Events that have the potential to occur during the service life of the foundation,
  - Scour
  - Seasonal shrink/swell
  - Volume change from temperature changes
  - Volume change from geothermal energy foundations
  - Formation of voids in karst
  - Vibration from natural or manmade sources
  - Liquefaction
  - Impacts of future construction, excavation, or loading
- Costs of a more conservative design, and
- Consequences of unsatisfactory performance.

In some cases, the consequences of uncertain conditions and/or events can be modeled by analytical or numerical analysis, or observed by testing during construction using load testing. However, the actual consequences cannot be precisely known. Therefore, the tools of foundation design have embedded conservatism that, along with engineering judgement, are intended to produce reliable designs. Designers can take efforts to reduce uncertainty through a more robust geotechnical exploration and testing program, performance testing foundation elements via load tests, and working with the entire design team to better estimate the loads applied to the foundation that are expected under normal conditions and possible for abnormal conditions.

6-5.3.1 Limits on Unit Resistances.

Static capacity analysis methods that are at least partially based on empirical observations from load tests may include limits on unit base and shaft resistances. These limits prevent extrapolation of relationships between unit capacity and the input(s) beyond those originally observed by the developers. Such limits may be revised based on site-specific information and engineering judgment.

For coarse-grained soils, some design guidance defines a *critical depth* (USACE 1991) beyond which the unit shaft and base resistances of foundations no longer increase with additional penetration. Other guidance caps the maximum unit resistance based on soil type and relative density (API 2011). The concepts of critical depth and maximum unit resistance are disputed (Fellenius 2021). USACE (1991) recommends limiting unit shaft and base resistances to the value at a depth of $10 \cdot b$ for loose sands and $20 \cdot b$ for dense sands. API (2011) recommends limiting unit shaft and base resistances as the

relative density of the soil decreases and/or the silt content increases. For medium dense sand-silt soils, nominal shaft resistance is limited to 1.4 ksf, and nominal base resistance is limited to 60 ksf. For very dense sand soils, nominal shaft resistance is limited to 2.4 ksf, and nominal base resistance is limited to 250 ksf (API 2011).

6-5.4 Static Axial Capacity in Compression for Single Elements.

As stated in Section 6-5.2.1, the factored axial resistance of a deep foundation element is determined by the lesser of the factored structural resistance and the factored resistance provided by the soil and/or rock, which is often referred to as the factored geotechnical resistance. Usually, the geotechnical resistance controls design. Common methods used in practice to evaluate the geotechnical resistance are:

1) Static Capacity Analysis (SCA),
2) Numerical analysis,
3) Dynamic methods, e.g., Wave Equation (WE), dynamic measurements, signal matching, and
4) Trial installation and load testing, e.g., test piles.

As described in Section 6-2.1, the normal process of deep foundation design follows a path of making initial estimates of performance using simple analytical models that are iteratively refined using more sophisticated analyses. In many cases, test pile programs are used to calibrate the analytical models. Load testing and dynamic methods, such as signal matching, are often used to update the design, which is an application of the observational method that is the hallmark of sound decision making in geotechnical engineering.

The Static Capacity Analysis (SCA) methods presented herein should be viewed as a step toward a complete foundation design. In addition to providing an estimate of capacity with relatively little effort and no specialty equipment or software, these simple methods provide a rational means to provide inputs for more sophisticated analyses to estimate capacity and/or assess driveability. In general, the predictive accuracy of SCA methods is low (Jardine et al 2001), and it is usually not clear what criteria was used to define the nominal axial capacity (Fellenius 2021).

While there are many SCA methods for driven piles and formed-in-place columns, only the Beta method for effective stress analysis of capacity and the Alpha method for total stress analysis of capacity are presented here. These methods were selected because there is widespread familiarity with these methods in US practice. In addition, there are versions for both driven pile and formed-in-place columns, and the methods are easy to implement. For continuity with historical tradition, the Beta method is categorized as being applicable to coarse-grained soils while the Alpha method is categorized as being applicable to fine-grained soils. In addition to coarse-grained soils, the Beta method is

applicable to any soil in a drained condition, e.g., long-term analysis of capacity in clay soils. The Alpha method is targeted at clay soils and some silts that are routinely represented by the undrained condition in the short term. The Beta and Alpha methods are semi-empirical, meaning that they have been calibrated to load test results. For this reason, the guidance presented herein does not encompass all possible ground conditions.

Drilled displacement piles have not yet reached a state of maturity where specific versions of the Beta and Alpha method are available; however, guidance using results from the SPT and CPT are presented in Section 6-5.4.4. According to Coduto et al. (2016), full-displacement DDPs will have shaft resistance that is at least as high as driven piles and base resistance that is on par with CFAs. Therefore, guidance for estimating the shaft resistance of concrete driven piles and the base resistance of CFAs can be used for full-displacement DDPs. For partial-displacement DDPs that generate some spoils, the shaft resistance is between full-displacement DDPs and CFAs (Coduto et al. 2016).

The design methods for aggregate columns and helical piles are significantly different from driven piles and drilled columns. Design guidance for aggregate columns can be found in FHWA (2017), and guidance for helical piles is provided in Perko (2009).

When using an LRFD framework, AASHTO (2020) recommends the resistance factors provided in Table 6-11. Note that resistance factors have not yet been calibrated by AASHTO for certain analysis methods, e.g., Beta Method for driven piles and deep foundation technologies other than driven piles, drilled shafts, and micropiles. For the extreme limit state, a resistance factor equal to 1.0 can be used for compressive axial loading.

Table 6-11 Recommended Strength Limit State Resistance Factors for Axial Compressive Resistance Evaluated by SCA (AASHTO 2020)

Foundation Technology	Recommended Resistance Factor for Axial Compressive Loading[A]
Driven Piles	0.30 – coarse-grained (cohesionless) soil, Meyerhof SPT method, side and base 0.35 – saturated, undrained (cohesive) soil, Alpha method, side and base
Drilled shafts	0.55 – coarse-grained (cohesionless) soil, Beta method, side 0.50 – coarse-grained (cohesionless) soil, Reese and O'Neill (1989) guidance in Table 6-20, base 0.45 – saturated, undrained (cohesive) soil, Alpha method, side 0.40 – saturated, undrained (cohesive) soil, Equation 6-27, base 0.50 – rock, Equation 6-35, side 0.50 – rock, Equation 6-36, base
Micropiles	0.55 – side resistance using presumptive values 0.50 – rock, Equation 6-36, base
[A] AASHTO (2020) states that resistance factors should be reduced by 20% for single drilled shafts, small pile groups (<5 piles) to account for lack of redundancy, and micropiles in marginal ground conditions.	

Table 6-12 provides recommended minimum factors of safety for loading in compression when allowable stress design is used.

Table 6-12 Recommended Minimum Factors of Safety for Compressive Loading

Foundation Technology	Guidance Source	Recommended Minimum Factor of Safety
Driven Piles	USACE (1991)[A]	2.0 – with load tests 2.5 – with dynamic testing 3.0 – other
	UFC (2022)[B]	2.0 – with load tests 2.25 – with dynamic testing and signal matching 3.0 – piles anchored in rock
Drilled shafts	UFC (2022)[B]	2.5 to 4 – drilled shafts anchored in rock
	Coduto et al. (2016)[C]	2.5 – with load tests 3.5 – other
Micropiles	FHWA (2005)[D]	2.0 – with load tests

[A] Values are for "usual" loading; for unusual loading, such as floods, factors of safety may be decreased by factor of 0.75; for extreme loading, such as rare natural disasters, factors of safety may be decreased by factor of 0.57.
[B] Use FS > 3 to limit total and differential settlements to small values. Generally, use FS ≥ 2.5. FS for drilled shafts depends on uncertainties in loading, stratification, and verification testing.
[C] Without load testing, the FS may be reduced by 0.5 for each of the following: uniform ground conditions and extensive site characterization (reduction of 1.0 possible). With load testing, the FS may be reduced by 0.5 for uniform ground conditions and extensive site characterization with an additional reduction of 0.3 possible if the load testing program is very extensive in uniform ground conditions with extensive site characterization.
[D] Load tests should be performed before and during production pile installation, i.e., verification and proof testing. FS should be increased to 2.5 in marginal ground conditions.

6-5.4.1 Shaft Resistance in Drained Conditions – Beta Method.

The Beta method, sometimes referred to as the effective stress method, can be applied to estimate the axial capacity of deep foundations in coarse-grained soils in the short and long term as well as fine-grained soils in long-term, drained conditions. Variants of the Beta method are presented for driven piles (USACE 1991, Fellenius 2021), drilled shafts (Chen and Kulhawy 2002, FHWA 2018a), and other drilled columns (FHWA 2007, Coduto et al. 2016). Other effective stress methods, such as the Nordlund method (Nordlund 1963, 1979), can be adapted to the format of the Beta method.

The Beta method uses the coefficient, β, to relate the effective vertical stress to the unit shaft resistance. The β coefficient is found as:

$$\beta = K \tan(\delta) \tag{6-6}$$

where:
K = earth pressure coefficient and
δ = interface friction angle between the pile and the soil.

The representative unit shaft resistance (f_s) is evaluated over the shaft or each segment of the shaft by:

$$f_s = \beta \sigma'_z \tag{6-7}$$

where:
σ'_z = average effective vertical stress over the shaft or shaft segment.

The process to find K and δ to determine β consists of evaluating 1) the at-rest earth pressure coefficient according to Jaky (1944) without adjustment for overconsolidation, based on conditions before construction, 2) the ratio of the earth pressure coefficient for the column-soil interface to the at-rest earth pressure coefficient, K/K_0, 3) the effective internal friction angle, and 4) the ratio of the interface friction angle to the internal friction angle, δ/ϕ'. Table 6-13 provides guidance for evaluating K/K_0, and Table 6-14 provides guidance for evaluating δ/ϕ'. The value of ϕ' used in the analysis can be determined from laboratory testing or using empirical correlations, such as those found in Chapter 8 of DM 7.1.

Table 6-13 Ratio of Shaft Friction Earth Pressure Coefficient to At-Rest Earth Pressure Coefficient

Source	K/K_0[A]	Applicability
Salgado (2008)	See Figure 6-13 (dashed lines)	Nondisplacement columns – drilled shafts[B]
	See Figure 6-13 (solid lines)	Displacement columns – driven concrete piles, closed-end pipe piles, H-piles, and open pipe piles that are plugged[B]
FHWA (2018a)	$OCR^{\sin(\phi')}$	Drilled shafts[C]
Coduto et al. (2016)	0.50 to 0.70	Driven pile installed by jetting
	Similar to driven displacement pile	DDPs

[A] This guidance assumes that $K_0 = 1 - \sin(\phi')$
[B] For partial displacement columns (e.g., CFAs, H-piles, and unplugged open pipe piles), apply judgment to interpolate between the solid and dashed lines in Figure 6-13.
[C] OCR can be found from lab or field tests or estimated using empirical correlations, e.g., with N_{60}. The shaft friction within 7.5 ft of the ground surface should be evaluated using β determined at a depth of 7.5 ft.

Table 6-14 Interface Friction Angle Ratios for Evaluating Shaft Friction

Source	δ / ϕ'	Applicability
Salgado (2008)	0.95	Concrete driven piles
	0.85	Steel driven piles
	1.00	Concrete formed-in-place columns, e.g., drilled shafts CFAs
USACE (1991)	0.90 to 1.00	Concrete driven piles
	0.67 to 0.83	Steel driven piles
	0.80 to 1.00	Timber driven piles
Chen and Kulhawy (2002)	1.00	Drilled shafts
Coduto et al. (2016)	1.00	DDPs

The lateral earth pressure coefficient is influenced by a number of factors related to installation, such as soil displacement and disturbance from predrilling or jetting. Unless explicitly stated, the guidance provided herein does not apply to piles that are jetted, predrilled, or vibrated into place. When a pile is tapered, the perimeter changes along its length. The perimeter change can be handled directly (Nordlund 1963, 1979) or using a series of equivalent uniform segments, each having a different diameter (Fellenius 2021). Unless pile taper is handled directly (Nordlund 1963, Nordlund 1979), the value of K used should not exceed the Rankine passive earth pressure coefficient.

As an alternative to finding K and δ, the coefficient β can be evaluated directly using the empirical guidance provided in Table 6-15 or back calculated from load test results.

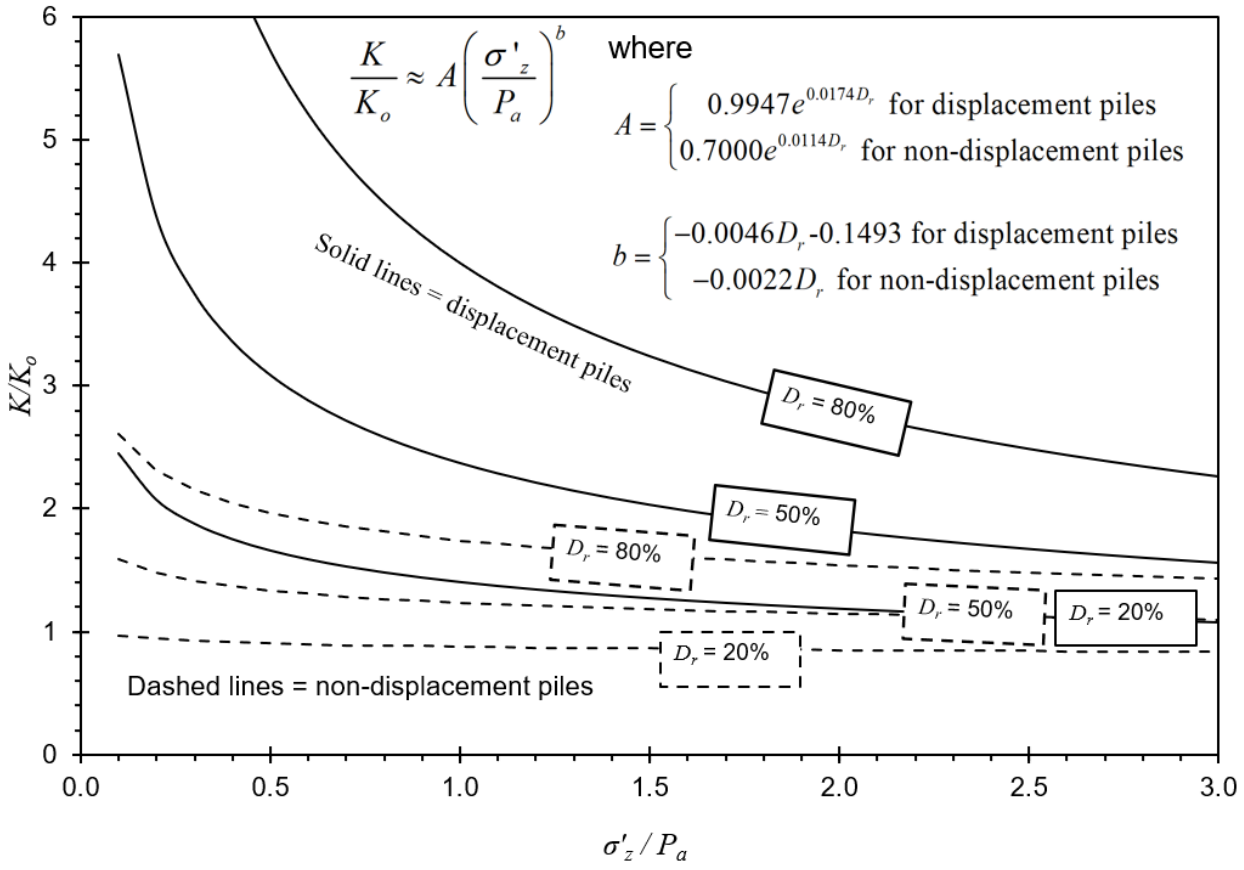

Figure 6-13 Ratio of K/K_0 for Non-Displacement and Full-Displacement Columns (after Salgado 2008)

Table 6-15 Guidance for Estimating β

Source	β	Applicability
Fellenius (2021)	$\beta = 0.15$ for $\phi' = 25°$ $\beta = 0.35$ for $\phi' = 30°$	Driven piles in clay[A]
	$\beta = 0.25$ for $\phi' = 28°$ $\beta = 0.50$ for $\phi' = 34°$	Driven piles in silt[A]
	$\beta = 0.30$ for $\phi' = 32°$ $\beta = 0.90$ for $\phi' = 40°$	Driven piles in sand[A]
	$\beta = 0.35$ for $\phi' = 35°$ $\beta = 0.80$ for $\phi' = 45°$	Driven piles in gravel[A]
FHWA (2007,1999)	$\beta = 1.5 - 0.135 \cdot z^{0.5}$	Drilled shafts[B,C,D], CFAs[C,D]
Rollins et al. (2005)	$\beta = 2.0 - 0.062 \cdot z^{0.75}$	Drilled shafts in gravelly sand[C,E]
	$\beta = 3.4e^{-0.26 \cdot z}$	Drilled shafts in gravel[C,F]
Coleman and Arcement (2002)	$\beta = 5.03 \cdot z^{-0.67}$	CFAs in silts[C,G]
	$\beta = 50.2 \cdot z^{-1.3}$	CFAs in sands[C,G]
Zelada and Stephenson (2000)	$\beta = 1.2 - 0.108 \cdot z^{0.5}$	CFAs in clean sand[C,H]

[A] Guidance based on piles in inorganic alluvium
[B] This version of the Beta Method for drilled shafts has been replaced by the version in FHWA (2018a).
[C] z is the depth in feet below the ground surface to the center of the shaft or subdivided shaft segment.
[D] β limited to $0.25 \le \beta \le 1.2$; for soils having an N_{60} value less than 15 bpf, scale β by $N/15$.
[E] β limited to $0.25 \le \beta \le 1.8$
[F] β limited to $0.25 \le \beta \le 3.0$; e is the base of the natural logarithm = 2.718.
[G] β limited to $0.20 \le \beta \le 2.5$
[H] β limited to $0.20 \le \beta \le 0.96$

6-5.4.2 Shaft Resistance for Saturated, Undrained Soils – Alpha Method.

The Alpha method is based on an undrained characterization of shear strength and is named for the adhesion factor, α. The unit shaft resistance is also referred to as the adhesion, C_α, between the column surface and the soil. Analogous to the interface friction angle, the adhesion is related to the undrained strength by:

$$f_s = C_a = \alpha S_u \tag{6-8}$$

where:
f_s = unit shaft resistance and
s_u = undrained shear strength.

Many authors have presented versions of the Alpha Method for driven piles (Tomlinson 1994, API 1993, Randolph and Murphy 1985, FHWA 2016[32]) and for bored columns (Chen et al. 2011, Salgado 2008). In all forms of the Alpha Method, the values of α are based on empirical observations from load tests that capture installation effects and the properties of the soil-column interface. Depending on the version used, estimates of α may be sensitive to the magnitude of undrained strength, overconsolidation, normalized embedment (Z/b), pile material, installation method, and penetration of overlying soil layers. In general, disturbance of stiff clays by installation lowers adhesion and this effect becomes more pronounced as the undrained strength of the soil increases, meaning that α decreases as s_u increases. The value of α should be limited to values between zero and 1.0.

The effects of embedment length on α are more complex and are addressed in different ways, or ignored altogether, in different versions of the Alpha Method. For example, Tomlinson (1994) recommends reducing α due to the formation of a gap between the shaft and stiff clay near the ground surface. This effect has a more pronounced consequence for shorter piles and discretized pile segments near the ground surface, and thus, the value of α is reduced more at lower ratios of normalized embedment (Z/b). Normalized embedment is defined here as the distance from the ground surface to the bottom of the clay layer, sublayer, or pile, whichever comes first, divided by the pile width or diameter. Doherty and Gavin (2011) describe several versions of the Alpha method that reduce α at greater normalized depths to account for progressive mobilization of shear resistance along the pile length. The length effects described by Tomlinson (1994) are presented here; however, engineering judgment should be exercised for how to consider length effects.

FHWA (2016) provides separate relationships between undrained strength and adhesion for smooth and rough-textured piles, where rough piles exhibit higher adhesion at the same undrained strength. While Tomlinson (1957) observed some influence of pile texture on adhesion, Tomlinson later concluded using additional load test data that pile texture has no discernable effect (Tomlinson, 1970).

The evaluation of unit shaft resistance for driven piles in clay depends in part on the consistency of the clay as described by Tomlinson (1994) and presented in Table 6-16. For piles driven into soft clay, dissipation of driving-induced pore pressures and accompanying consolidation results in adhesion that is at least as high as the undisturbed undrained strength (Tomlinson 1994), corresponding to a value of α equal to 1.0. However, in some situations where the shaft resistance provided by the soft clay

[32] The Alpha Method credited to “Tomlinson (1979)” in FHWA manuals first appeared in FHWA (1982) and is based on published guidance by Tomlinson. To the authors’ knowledge, the source “Tomlinson (1979)” does not exist.

is trivial and/or unreliable, the designer may opt to ignore the soft clay's contribution, corresponding to a value of f_s equal to zero.

Table 6-16 Influence of Clay Consistency on α for Driven Piles (Tomlinson 1994)

Clay Consistency	s_u Range (psf)	s_u/P_a Range	Determination of α and f_s
Soft	< 800	<0.38	$\alpha = 1 \rightarrow f_s = s_u$, or $s_u \approx 0 \rightarrow f_s = 0$
Firm (~Medium Stiff)	800 – 1500	0.38 – 0.71	Use curves A and B in Figure 6-14 to determine α.
Stiff	1500 – 3000	0.71 – 1.42	
Very Stiff	3000 – 6000	1.42 – 2.83	

For driven piles in firm to very stiff clay, the relationships between α and normalized undrained strength for the Tomlinson Alpha method (Tomlinson 1994) are depicted in Figure 6-14 as Curves A and B for normalized embedments (Z/b) of 40 and 10, respectively. The pile shaft can be discretized as needed to capture stratigraphic changes and/or shear strength trends with depth (FHWA 2016). For steel H-piles, FHWA (2016) recommends evaluating the shaft area using the outer "box[33]" perimeter rather than the actual perimeter of the flanges and web.

Tomlinson (1994) also presents guidance to estimate α in stiff clay for special cases where the pile penetrates soft clay or sand/gravel before penetrating the stiff clay. The overlying soft clay tends to coat the pile and reduce α while the sand or gravel is pushed into the stiff clay and tends to increase α. These effects are more pronounced near the interface of the stiff clay and the overlying material. The graphical guidance provided by Tomlinson (1994) for overlying soil layers does not compare logically to the case without an overlying layer and is, therefore, not presented herein. A simple approach to account for the effects of soft clay overlying stiff clay based on Tomlinson (1994) is to define a transition zone from the top of the stiff clay along the upper length of pile in the stiff clay equal to 10 times the pile width or diameter. The value of α within this zone can be estimated by

$$\alpha = 0.28\left(\frac{s_u}{P_a}\right)^{-0.44} \tag{6-9}$$

where:
s_u = undrained shear strength of the stiff clay layer and
P_a = atmospheric pressure in same units as s_u.

[33] The box perimeter is the smallest rectangular shape that encompasses the H-pile cross section.

If the calculated value of f_s is lower for the transition zone than in the soft clay, the unit shaft resistance from the soft clay layer should be used for the transition zone.

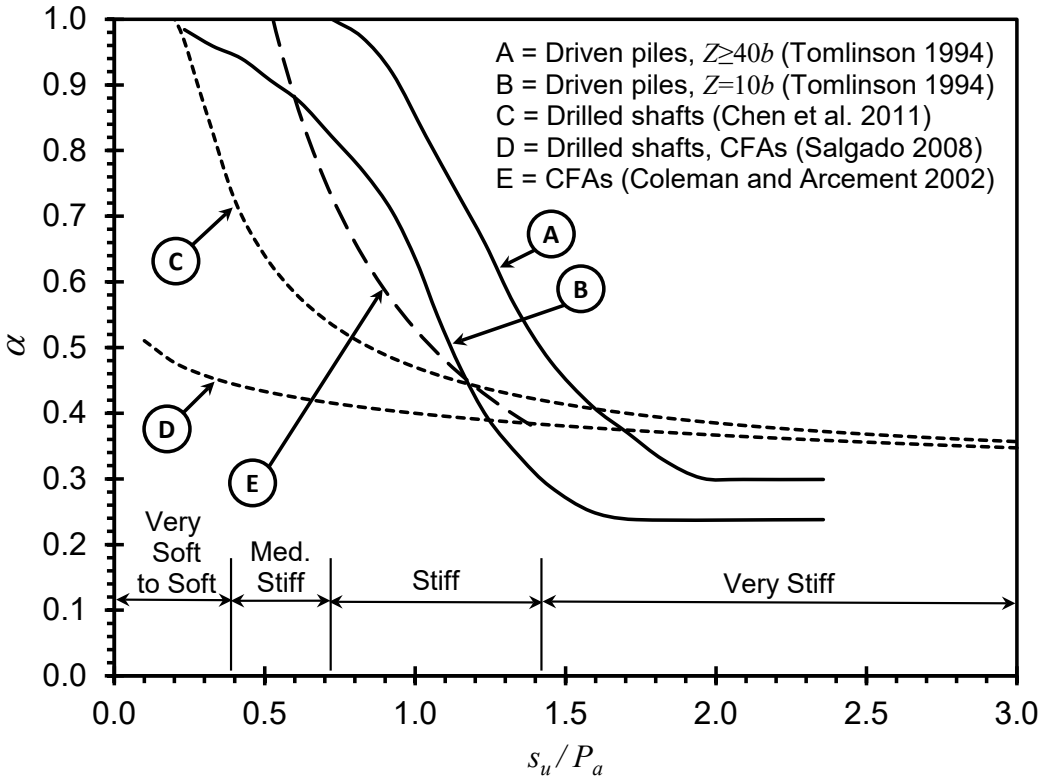

Figure 6-14 Variation of α with Normalized Undrained Shear Strength for Different Deep Foundation Types and Embedments

Equation 6-9 was developed by fitting a power function to the curve proposed by Tomlinson (1994) for penetration of a pile 10 times the width or diameter into stiff clay that underlies soft clay as digitized by FHWA (1993)[34].

Similarly, a simple approach to account for the effects of sand or gravel overlying stiff clay based on Tomlinson (1980) is to define a transition zone from the top of the stiff clay along the upper length of pile in the stiff clay equal to 10 times the pile width or diameter. The value of α within this zone can be assumed to equal to 1.0.

In the cases of overlying soft clay or sand/gravel, values of α below the transition zone are determined as normal using Figure 6-14. Tomlinson (1994) does not give explicit guidance for the cases of soft clay or sand/gravel overlying firm clay; therefore, judgment should be applied to select an appropriate value of α.

[34] The Alpha method presented in Tomlinson (1994) also appears in previous publications by Tomlinson, at least as early as 1975.

For drilled shafts, Chen et al. (2011) recommends estimating α as:

$$\alpha = 0.3 + 0.17\frac{P_a}{s_{u,ICU}} \leq 1 \quad \text{(6-10)}$$

where:
$s_{u,ICU}$ = undrained strength evaluated using an ICU triaxial test and
P_a = atmospheric pressure.

The relationship between α and normalized undrained strength proposed by Chen et al. (2011) is depicted as Curve C in Figure 6-14. Based on guidance provided by Chen and Kulhawy (1993) and Mayne (1985), values of undrained strength evaluated using UC, UU, or DSS tests can reasonably be scaled for the purpose of estimating α as[35]:

$$s_{u,ICU} \approx 1.74 \cdot s_{u,UC} \cdot OCR^{-0.25} \quad \text{(6-11)},$$

$$s_{u,ICU} \approx 1.68 \cdot s_{u,UU} \cdot OCR^{-0.25} \quad \text{(6-12)},$$

and

$$s_{u,ICU} \approx 1.43 \cdot s_{u,DSS} \quad \text{(6-13)}$$

where:
$s_{u,UC}$ = undrained strength evaluated using an unconfined compression test,
$s_{u,UU}$ = undrained strength evaluated using an unconsolidated undrained triaxial test,
$s_{u,DSS}$ = undrained strength evaluated using a direct simple shear test, and
OCR = overconsolidation ratio.

For drilled shafts and CFAs, Salgado (2008) recommends estimating α for soils with a clay fraction of at least 50% and an OCR between 3 and 5 as:

$$\alpha = 0.4\left[1 - 0.12 \cdot \ln\left(\frac{s_u}{P_a}\right)\right] \quad \text{(6-14)}.$$

For lower values of OCR, Equation 6-14 is expected to produce conservative values. Salgado (2006) indicates that s_u is evaluated using a triaxial test, though the specific type is unspecified. The relationship between α and normalized undrained shear strength proposed by Salgado (2008) is depicted as Curve D in Figure 6-14.

[35] Undrained strength ratio calculated using Eqn. 8-20 in DM 7.1 (Jamiolkowski et al. 1985) assuming the fitting parameter, m = 0.8.

Coleman and Arcement (2002) load tested CFAs in mixed alluvial and loessial sand and clay deposits. They found a relationship between α and undrained strength. The relationship (Curve E in Figure 6-14) between α and normalized undrained strength is valid for normalized strengths in the range of 0.24 to 1.42 and is calculated as:

$$\alpha = 0.53\left(\frac{s_u}{P_a}\right) \quad \text{(6-15).}$$

Comparison of Curves A and B for driven piles and Curves C and D for drilled shafts in Figure 6-14 illustrates the effects of soil displacement and disturbance from pile driving. For medium stiff to stiff clays, remolding and consolidation by pile driving generally produce higher values of α compared to drilled shafts. For stiff to very stiff clays, clay cracking and gap development due to pile driving generally produce lower values of α compared to drilled shafts.

The P2A Method described by the American Petroleum Institute (API) (1993) is a modified version of the Alpha Method by Randolph and Murphy (1985) in which α is calculated as:

$$\alpha = 0.5\left(\frac{s_u}{\sigma'_z}\right)^{-0.5} \quad \text{for } \frac{s_u}{\sigma'_z} \le 1 \quad \text{(6-16)}$$

and

$$\alpha = 0.5\left(\frac{s_u}{\sigma'_z}\right)^{-0.25} \quad \text{for } \frac{s_u}{\sigma'_z} > 1 \quad \text{(6-17)}$$

where:
s_u / σ'_z = undrained strength ratio with respect to effective vertical stress.

When the undrained strength ratio is less than 0.25, the value of α should be capped at 1.0. As noted by NCHRP (2015), the P2A method was developed using information from large diameter (i.e. ≥ 36 inches) open-end steel pipe piles installed in an offshore environment. Despite the difference in diameter, the API method should also be helpful for designing concrete cylinder piles (Rausche and Webster, 2007).

The API guidance can also be expressed in terms of OCR as:[36]

[36] Undrained strength ratio calculated using Eqn. 8-20 in DM 7.1 (Jamiolkowski et al. 1985) assuming the fitting parameter, m = 0.8.

$$\alpha = 1.07\left(OCR\right)^{-0.4} \text{ for } OCR \le 4.5 \quad (6\text{-}18)$$

and

$$\alpha = 0.73\left(OCR\right)^{-0.2} \text{ for } OCR > 4.5 \quad (6\text{-}19).$$

When the OCR is less than 1.2, the value of α should be capped at 1.0. Coduto et al. (2016) recommend evaluating the side resistance of full-displacement DDPs in the same way as used for driven concrete displacement piles of the same nominal diameter. For partial displacement DDPs, Coduto et al. (2016) recommend interpolating side resistance somewhere between a driven concrete displacement pile and CFA pile.

6-5.4.3 Base Resistance.

Given sufficient displacement for mobilization, unit base resistance, q_b, is usually significantly larger for drained conditions in coarse-grained soils compared to undrained conditions in fine-grained soils. Special considerations need to be accepted and/or addressed to apply bearing capacity theory to deep foundations. These considerations include:

1) Local, or plunging, mode of failure is often more representative of bearing failure of deep foundations rather than the general shear considered by bearing capacity theory (Coduto et al. 2016).
2) The point of bearing capacity failure is usually difficult to define from the relationship of base settlement and load (Fellenius 2021).
3) Bearing capacity theory does not capture the effects of stress release and disturbance of soils below the base, particularly in drilled shafts (FHWA 2018a).
4) Bearing capacity theory does not capture the effects of adjacent elements, e.g. closely-spaced piles in the group.
5) Inputs to bearing capacity theory, e.g. friction angle, tend to have nonlinear effects on bearing capacity. Thus, small changes to inputs may have large impacts on the bearing resistance considered in design.

Due to the limitations of bearing capacity theory, Vesic (1977) states that “in most situations it may be preferable to determine pile point and skin resistances directly from field tests, such as the static (Dutch) cone test, standard penetration test, and the pressuremeter test.” The SPT and CPT-based methods described in Section 6-5.4.4 are often a good alternative, particularly for coarse-grained soils.

Since the ratio of the base width to the depth below the ground surface is usually small, the N_γ term of the general bearing capacity equation is typically eliminated unless an enlarged base is used. For analysis of deep foundations in drained conditions, only the

N_q term is retained. Only the N_c term is retained for short-term analysis of fine-grained soils.

6-5.4.3.1 Base Resistance for Drained Conditions – Semi-Empirical.

Estimates of the N_q factor based on the soil type and friction angle are provided in Table 6-17. The unit base resistance for deep foundation elements ($Z/b \geq 5$) in drained conditions is found by:

$$q_b = N_q \cdot \sigma'_{zD} \quad \text{(6-20).}$$

where:
σ'_{zD} = vertical effective stress at the base elevation.

Table 6-17 Base Resistance Factors for Drained Conditions based on Soil Type and Friction Angle (after Fellenius 2021, Cheng 2004)

Soil Type	Friction Angle, ϕ' (deg)	Bearing Capacity Factor, N_q			
		Fellenius (2021)	Based on Cheng (2004)		
			Z/b = 10	Z/b = 20	Z/b = 40
Clay	25 to 30	3 to 30	12 to 26	10 to 22	8 to 19
Silt	28 to 34	20 to 40	19 to 52	16 to 46	14 to 40
Sand	32 to 40	30 to 150	37 to 168	32 to 152	27 to 139
Gravel	35 to 45	60 to 300	---	---	---

Values for other friction angles and embedment depths can be determined after Cheng (2004) as:

$$N_q \approx 1.2\left(\frac{Z}{b}\right)^{-0.437} \exp\left[6.34\left(\frac{Z}{b}\right)^{0.0486} \tan\phi'\right] \leq 200$$ unless supported by project-specific information

The equation provided in Table 6-17 is based on Cheng's (2004) correction of theory by Berezantev et al. (1961). The latter was also the basis of Nordlund's (1963, 1979) estimates of base resistance.

6-5.4.3.2 Base Resistance for Drained Conditions – Vesic.

Vesic's (1977) bearing capacity theory for driven pile foundations is based on cavity expansion theory. Application to other deep foundation types is up to the designer's judgment. Given the tendency for local shearing, the compressibility of the soil is accounted for using modified bearing capacity factors, N^*_c and N^*_q. The unit base resistance for deep foundation elements ($Z/b \geq 5$) in drained conditions is found by:

$$q_b = N^*_q \cdot \sigma'_m \quad \text{(6-21).}$$

where
σ'_m = mean effective stress at $b/2$ below the pile base elevation.

Assuming K_0 conditions, the mean effective stress is:

$$\sigma'_m = \left(1 - \frac{2}{3}\sin\phi'\right)\sigma'_{zD+b/2} \tag{6-22}$$

where:
$\sigma'_{zD+b/2}$ = effective vertical stress at $b/2$ below the base prior to pile installation and
ϕ' = peak effective friction within proximity of the base.

Vesic's method uses a reduced rigidity index (I_{rr}) and estimates N^*_q by:

$$N^*_q = \left(\frac{3}{3-\sin\phi'}\right)e^{\left(\frac{\pi}{2}-\phi'\right)\tan\phi'}\tan^2\left(\frac{\pi}{4}+\frac{\phi'}{2}\right)I_{rr}^{\left(\frac{4\sin\phi'}{3(1+\sin\phi')}\right)} \tag{6-23}$$

where:
e = base of the natural logarithm and
ϕ' = peak friction angle in radians within proximity of the base.

The impact of compressibility is assessed using the reduced rigidity index, I_{rr}. The tendency for local shear failure increases as the rigidity index decreases. Characterization of the soil within 1 to 2 pile widths of the base is most important for evaluating base resistance by Vesic's bearing capacity theory. These are the soils mobilized to provide resistance to shearing.

For coarse-grained soils, the rigidity index according to Vesic (1977) is equal to:

$$I_r = \frac{E}{(1+2\nu)\sigma'_m\tan(\phi')} \tag{6-24}$$

where:
E = Young's Modulus and
ν = Poisson's Ratio.

To account for the volume change required to mobilize shear strength, the rigidity index should be reduced to (Vesic 1977):

$$I_{rr} = \frac{I_r}{1+I_r\varepsilon_v} \tag{6-25}$$

where:
ε_v = volumetric strain from the foundation loading.

For piles bearing in soil, the reduced rigidity index normally ranges from 10 to 500. Assuming one-dimensional elastic compression below the pile, the volumetric strain can be estimated by (Bowles 1996):

$$\varepsilon_v = \frac{(1+\nu)(1-2\nu)\Delta\sigma_{zD+b/2}}{E_s(1-\nu)} \approx F_v \frac{q_{b,app}}{E_s} \tag{6-26}$$

where:
$\Delta\sigma_{zD+b/2}$ = change in vertical stress at a depth of $b/2$ below the base,
$q_{b,app}$ = estimated applied bearing pressure at the base of the pile, and
F_v = strain factor based on Boussinesq theory and Poisson's ratio (see Table 6-18).

Table 6-18 Factors for Approximating Volumetric Strain

Pile Shape	Strain Factor, F_v						
	$\nu = 0.2$	$\nu = 0.25$	$\nu = 0.3$	$\nu = 0.35$	$\nu = 0.4$	$\nu = 0.45$	$\nu = 0.5$
Square	0.59	0.54	0.48	0.41	0.30	0.17	0
Circular	0.63	0.58	0.52	0.44	0.33	0.18	0

6-5.4.3.3 Undrained Base Resistance.

The N^*_c factor is required for short-term analysis of fine-grained soils. For undrained conditions, the unit base resistance for deep foundations is:

$$q_b = N^*_c \cdot s_u \tag{6-27}$$

where:
s_u = undrained strength within proximity of the base.

Using Vesic's (1977) approach, the value of N^*_c is found by:

$$N^*_c = \frac{4}{3}(\ln I_{rr} + 1) + \frac{\pi}{2} + 1 \tag{6-28}$$

For undrained conditions, the rigidity index is found by:

$$I_{rr} = I_r = \frac{E_u}{3 \cdot s_u} \tag{6-29}$$

where:
E_u = Young's modulus for undrained conditions and
s_u = undrained strength within proximity of the base.

The volume correction is not needed for undrained conditions, which involves no volume change by definition, i.e. $I_{rr} = I_r$.

Methods other than Vesic (1977) are more commonly used to obtain N^*_c for use in Equation 6-22. According to Brinch Hansen (1957), N^*_c is equal to 9 based on bearing capacity theory for typical deep foundations with Z/b of at least 2.5. An exception exists for formed-in-place columns bearing on fine-grained soil having a representative undrained shear strength less than 2 ksf. In this case, interpreting the guidance by FHWA (1999) suggests that N^*_c is a function of I_r:

$$N_c^* = 1.33\left[\ln\left(I_r\right)+1\right] \le 9 \tag{6-30}$$

or a function of normalized undrained shear strength:

$$N_c^* = 10.2 - 12.4\left(\frac{0.1}{0.1+{s_u}/{P_a}}\right) \le 9 \tag{6-31}.$$

Unlike piles bearing in coarse-grained soils, bearing resistance in clay is often not the dominant contributor to the total nominal axial resistance.

6-5.4.4 SPT and CPT-based SCA Methods.

Many published methods empirically relate shaft and base resistance to the resistances measured by the SPT and CPT (Poulos 1989, Fellenius 2021). In many instances, SPT and CPT-based estimates of base resistance are used in conjunction with estimates of shaft resistance by the Beta and/or Alpha methods. Additionally, certain foundation technologies, such as DDPs, have not yet reached a state of maturity where specific versions of the Beta and Alpha method are available, and presently, designers must rely on SPT and CPT-based SCA methods.

Other *in situ* tests, such as the dilatometer or pressuremeter, can also be used to evaluate axial capacity (Fellenius 2021, Briaud 2013). Presentation of pressuremeter and dilatometer-based methods are beyond the scope of this chapter.

Table 6-19 lists selected methods for estimating shaft friction using SPT blow count, and Table 6-20 lists selected methods for estimating base resistance.

CPT results can also be used to estimate the static axial capacity of deep foundations, e.g., FHWA (1978) or Elsami and Fellenius (1997). The empirical approach developed

by the Laboratoire Central des Points et Chausses (LCPC) (Bustamante and Gianesselli,1982) is presented here due to its simplicity and adaptability to a range of deep foundation technologies.

Nominal unit side resistance and unit base resistance are estimated according to the LCPC method as:

$$f_s = \frac{P_a}{k_s}\left(\frac{q_c}{P_a}\right) \le P_a\left(\frac{f_p}{P_a}\right) \tag{6-32}$$

and

$$q_b = P_a k_t \left(\frac{q_{c,a}}{P_a}\right) \tag{6-33}$$

where:
q_c/P_a = cone tip resistance normalized by atmospheric pressure,
$q_{c,a}/P_a$ = average normalized cone tip resistance in the vicinity of the base (see below),
k_s = side resistance factor (see Table 6-21),
f_p = maximum unit side resistance (see Table 6-22), and
k_t = base bearing factor (see Table 6-23).

The average cone tip resistance in the vicinity of the base is found by averaging resistance values over $1.5 \cdot b$ above and below the base. Values above the base should be discarded until all values fall within 70% to 130% of the average value. Likewise, values below the base should be discarded until all values do not exceed 130% of the average value.

Values of k_s, f_p, and k_t are found using Table 6-21, Table 6-22, and Table 6-23, respectively, based on the categorization of the foundation type and soil conditions. Foundations falling under Group I-A include drilled shafts without permanent casing, CFAs, gravity-grouted micropiles, and barrettes. Group I-B foundations include drilled shafts with permanent casing. Group II-A foundations include driven and jacked concrete piles. Group II-B foundations include driven and jacked steel piles.

Table 6-19 Correlations Between SPT N Values and Nominal Shaft Resistance

Source	f_s (ksf)	Applicability
Meyerhof (1976)[A]	$N_{1,60} / 50 \leq 2$ ksf	Driven non-displacement piles in sand
	$N_{1,60} / 25 \leq 2$ ksf	Driven displacement piles in sand
Brown (2001)[B]	$0.555+(N_{60}) / 25$	Driven piles in sand and clay.
Briaud (2013)	$0.104(N_{60})^{0.7}$	Driven piles in sand and gravel
NeSmith (2002)[C]	$0.1(N) \leq 3.4$ ksf	DDPs in rounded, poorly graded coarse-grained soil with up to 40% fines
	$0.1(N)$ +1 ksf ≤ 4.4 ksf	DDPs in angular, well-graded coarse-grained soil with up to 10% fines

[A] For Meyerhof methods, calculate the overburden-corrected blow count as:

$$N_{1,60} = \left[0.77 \cdot \log\left(40 / \sigma'_z \right) \right] N_{60}$$ where σ′z is the effective vertical stress in ksf

[B] Correlation provided for compressive resistance for pile driven with impact hammer and $3 \leq N_{60} \leq 50$. See original source for other soil, loading, and installation conditions, keeping in mind that SPT N values generally have low reliability in gravelly soils.

[C] N = the uncorrected SPT blow count. Apply judgement to evaluate f_s for intermediate soil conditions.

Table 6-20 Correlations Between SPT N values and Nominal Base Resistance

Source	q_b (ksf)	Applicability
Meyerhof (1976)[A]	$0.8(Z_b/b)(N_{1,60}) \leq 6(N_{1,60})$	Reasonably uniform, non-plastic silt
	$0.8(Z_b/b)(N_{1,60}) \leq 8(N_{1,60})$	Reasonably uniform sand
Brown (2001)[B]	$3.55(N_{60})(1+F_pA_p / A_b)$	Driven piles with soil plug
Briaud (2013)[C]	$20.9(N_{60})^{0.5}$	Driven piles in sand and gravel
Reese and O'Neill (1989)[D]	$1.2N_{60} \leq 60$ ksf	Drilled shafts in coarse-grained soil
Zelada and Stephenson (2000)	$3.4N_{60} \leq 150$ ksf	CFA columns in coarse-grained soil
NeSmith (2002)[E]	$3.8(N) \leq 150$ ksf	DDPs in rounded, poorly graded coarse-grained soil with up to 40% fines
	$3.8(N)$ +28 ksf ≤ 178 ksf	DDPs in angular, well-graded coarse-grained soil with up to 10% fines

[A] Z_b/b = normalized embedment into bearing stratum. Average $N_{1,60}$ over 3 pile widths below base. When embedment for full base resistance is not achieved, linearly interpolate $N_{1,60}$ with overlying weaker stratum or ground surface. Calculate the overburden-corrected blow count as:

$$N_{1,60} = \left[0.77 \cdot \log\left(40 / \sigma'_z \right) \right] N_{60}$$ where σ'_z is the effective vertical stress in ksf

[B] A_p = area of soil plug for open sections; A_b = base area of pile material; F_p = 0.42 for open pipe sections; and F_p = 0.67 for H-piles. To evaluate R_b, apply resulting q_b to A_b.

[C] Average N_{60} over 4 piles widths above and below the base (Briaud and Tucker 1984).

[D] Average N_{60} within two diameters below base.

[E] N = the uncorrected SPT blow count averaged over 4 pile diameters above and below the base. Apply judgment to evaluate q_b for intermediate soil conditions.

Table 6-21 Side Resistance Factor (after Bustamante and Gianeselli 1982)

Soil type	q_c / P_a	k_s			
		Group I		Group II	
		A	B	A	B
Soft clay and mud	<10	30	30	30	30
Moderately compact clay	10 to 50	40	80	40	80
Silt and loose sand	≤ 50	60	150	60	120
Compact to stiff clay and compact silt	> 50	60	120	60	120
Soft chalk	≤ 50	100	120	100	120
Moderately compact sand and gravel	50 to 120	100	200	100	200
Weathered to fragmented chalk	> 50	60	80	60	80
Compact to very compact sand and gravel	> 120	150	300	150	200

Table 6-22 Maximum Unit Side Resistance (after Bustamante and Gianeselli 1982)

Soil type	q_c / P_a	f_p / P_a			
		Group I		Group II	
		A	B	A	B
Soft clay and mud	<10	0.15	0.15	0.15	0.15
Moderately compact clay	10 to 50	0.35 (0.8)	0.35 (0.8)	0.35 (0.8)	0.35
Silt and loose sand	≤ 50	0.35	0.35	0.35	0.35
Compact to stiff clay and compact silt	> 50	0.35 (0.8)	0.35 (0.8)	0.35 (0.8)	0.35
Soft chalk	≤ 50	0.35	0.35	0.35	0.35
Moderately compact sand and gravel	50 to 120	0.8 (1.2)	0.35 (0.8)	0.8 (1.2)	0.8
Weathered to fragmented chalk	> 50	1.2 (1.5)	0.8 (1.2)	1.2 (1.5)	1.2
Compact to very compact sand and gravel	> 120	1.2 (1.5)	0.8 (1.2)	1.2 (1.5)	1.2
Note: Values in parentheses reflect careful construction.					

Table 6-23 Base Bearing Factor (after Bustamante and Gianeselli 1982)

Soil type	q_{ca} / P_a	k_t	
		Group I-A&B	Group II-A&B
Soft clay and mud	<10	0.4	0.5
Moderately compact clay	10 to 50	0.35	0.45
Silt and loose sand	≤ 50	0.4	0.5
Compact to stiff clay and compact silt	> 50	0.45	0.55
Soft chalk	≤ 50	0.2	0.3
Moderately compact sand and gravel	50 to 120	0.4	0.5
Weathered to fragmented chalk	> 50	0.2	0.4
Compact to very compact sand and gravel	> 120	0.3	0.4

6-5.4.5 Micropiles.

Guidance for micropiles used in direct load support applications is provided in FHWA (2005). Due to their small diameter, micropiles develop axial capacity primarily through side resistance developed between the grout and the soil and/or rock in the bond zone. Base resistance is usually neglected; however, for micropiles terminating within hard rock, the procedures for evaluating the base resistance of rock-socketed drilled shafts, described in Section 6-5.4.6.2, can be applied. Given the possibility of high grout-to-ground bond strength, structural capacity often limits micropile capacity.

The nominal side resistance of a micropile bonded in soil or rock can be estimated using:

$$R_s = \alpha_{bond} \left(\pi \cdot b \cdot Z_b \right) \tag{6-34}$$

where:
α_{bond} = nominal unit grout-to-ground bond strength,
b = diameter of the bond zone, and
Z_b = length of the bond zone.

Table 6-24 can be used to make preliminary estimates of α_{bond}, which is sensitive to the grout mix, grout delivery method, and soil/rock properties. Load testing and local experience is most often used to evaluate nominal unit side resistance.

Table 6-24 Typical Nominal Unit Grout-to-Ground Bond Strengths (FHWA 2005)

Soil/Rock Description	Nominal Grout-to-Ground Nond Strength, α_{bond} (psi)			
	Type A	Type B	Type C	Type D
Soft silt and clay	5 to 10	5 to 14	5 to 17.5	5 to 21
Stiff silt and clay	5 to 17.5	10 to 27.5	14 to 27.5	14 to 27.5
Loose to medium dense sand	10 to 21	10 to 27.5	14 to 27.5	14 to 35
Medium to very dense sand	14 to 31	17.5 to 52	21 to 52	21 to 56
Medium to very dense gravel	14 to 38.5	17.5 to 52	21 to 52	21 to 56
Medium to very dense cemented glacial till	14 to 27.5	14 to 45	17.5 to 45	17.5 to 48.5
Soft shale[A]	30 to 80	Types B, C, and D generally not used in rock		
Slates and hard shale[A]	75 to 200			
Limestone[A]	150 to 300			
Sandstone[A]	75.5 to 250			
Granite and basalt[A]	200 to 609			
[A] Rock mass is unweathered with little to moderate fracturing.				

Micropiles are a preferred deep foundation type in karst; however, discontinuities in the rock can cause issues. A conservative option is to drill until a continuous length of competent rock equal to the target length of the bond zone is encountered. A more cost-effective option is to allow for some discontinuous rock to be included within a cumulative length of competent rock equal to the target length of the bond zone. The project specifications should be explicit about the acceptable number and length of any discontinuities allowed within the bond zone.

6-5.4.6 Driven Piles and Drilled Shafts in Rock.

Usually, intact rock provides an excellent material for providing high axial shaft and base resistance with small associated settlement. Due to the high nominal unit resistances relative to soil, the axial capacity of foundations bearing on or in rock may be controlled by the structural capacity of the element (Section 6-7), particularly when the rock is at least moderately strong. While there is not a universal definition of rock strength or hardness used in deep foundation design, Section 1-4 of DM 7.1 presents common ways to describe rock strength, and Section 3-3 of DM 7.1 provides useful information regarding the evaluation of rock strength in the laboratory. The most commonly used measure of rock strength is the unconfined compressive strength test.

Weathered rock and hard soils with N > 50 are sometimes referred to as *intermediate geo-materials* (IGM). The capacity of such materials may be better evaluated using methods for soils rather than methods intended for rock. Moreover, existing rock joints, discontinuities, voids, and installation-induced fractures can partially or completely invalidate conventional capacity analyses. In these cases, base and/or shaft resistance may be reduced or neglected entirely depending on the uncertainty of ground conditions, the potential for more discontinuities to develop over the service life, and the consequences of the loss of capacity. When the strength and quality of the rock is variable, careful observations during construction and evaluation of capacity by static load testing and/or dynamic methods become especially important.

6-5.4.6.1 Driven Piles.

According to AASHTO (2020), driven piles bearing on weak rock can be designed using procedures for soil. For driven piles bearing on hard rock, the axial capacity is usually governed by the structural capacity of the element (USACE 1991). Piles driven to rock typically require steel toe protection (Section 6-4.1.2), and it is important to monitor driving stresses using dynamic methods (Section 6-9.4).

6-5.4.6.2 Drilled Shafts.

Drilled shafts socketed in rock can provide high unit shaft and base resistances. However, in karstic conditions, only the shaft resistance may be included in the design.

As described by Kulhawy et al. (2005), the most common model to evaluate the nominal side resistance of a rock socket is:

$$f_s = C \cdot P_a \left(\frac{q_u}{P_a} \right)^n \quad (6\text{-}35)$$

where:
q_u = lesser of the representative unconfined compressive strength of the rock and the compressive strength of the drilled shaft concrete,
C = fitting parameter, and
n = fitting exponent.

For sockets in "normal rock,"[37] Kulhawy et al. (2005) recommend a value of C = 1 and n = 0.5. For rock that is unstable and prone to caving during drilling, FHWA (1999) recommend a value of $C = 0.65\alpha_E$ and n = 0.5, where α_E is the joint modification factor that is found in Table 6-25 based on RQD and whether the joints are closed. Special tooling can be used to groove and roughen the sides of the socket to increase side resistance. In these cases, load testing and local experience should be applied to evaluate the appropriate values of C and n for use in Equation 6-35.

Table 6-25 Joint Modification Factors, α_E, for Unstable Rock (after FHWA 1999)

RQD	Closed joints		Open or filled joints	
	α_E	*C*	α_E	*C*
100	1.00	0.65	0.85	0.55
70	0.85	0.55	0.55	0.36
50	0.60	0.39	0.55	0.36
30	0.50	0.32	0.50	0.32
20	0.45	0.22	0.45	0.22

The evaluation of base resistance in rock is complicated by the rock mass condition as compared to the measured strength of an intact rock sample. Using an empirical bearing capacity factor (N^*_{cr}), the unit base resistance is evaluated as:

$$q_b = N^*_{cr} \cdot q_u \quad (6\text{-}36).$$

FHWA (2018a) recommends a value of N^*_{cr} = 2.5 if three conditions are met: 1) the shaft bears on a massive or closed jointed rock extending at least one diameter below the base, 2) there are no voids below the base, and 3) the base can be adequately

[37] Normal rock is defined here as relatively massive, unjointed rock, having at least moderate strength.

cleaned prior to placing concrete. If any of these conditions are not met, N^*_{cr} should be evaluated through testing and local experience and application of more sophisticated constitutive models such as the Hoek-Brown failure criterion (Hoek et al. 2002) within numerical analysis, or base resistance should be neglected. Similarly, testing, local experience, and/or numerical analysis may be applied to justify values of N^*_{cr} higher than 2.5. The factored unit base resistance should not exceed the compressive strength of the concrete used for the drilled shaft.

6-5.5 Static Axial Capacity in Compression for Groups of Elements.

Deep foundations are often installed in groups to share the load carrying requirements and provide redundancy. The group behavior of vertically oriented driven piles, drilled shafts, CFAs, DDPs, and micropiles is featured here. Compared to the other foundation technologies, drilled shafts are less commonly installed in groups though adjacent drilled shafts may influence each other.

The minimum recommended center-to-center spacing (s) is three column widths or diameters, which is a consideration for constructability as well as soil-column-soil interaction. Each column has a zone of influence, which is the volume of ground that experiences a change in stress due to installation effects and subsequent load transfer between the column and the ground. When columns are close together, the zones of influence of adjacent columns can overlap. Overlapping zones of influence can have positive or detrimental effects depending on the ground conditions.

The factored axial capacity of the group of foundation elements, $R_{r,g}$, is determined as:

$$R_{r,g} = \min \begin{cases} n \cdot \eta_g \cdot R_r \\ R_{r,gblock} \end{cases} \tag{6-37}$$

where:
n = number of columns,
η_g = group efficiency factor,
R_r = factored single column capacity, and
$R_{r,gblock}$ = factored resistance to block failure.

While single element capacity considers the surface area of the column shaft and base, *block failure* considers the shearing resistance of the area along the sides of the group and the base resistance of the projected base area (soil and columns) of the group, as shown in Figure 6-15 where the base dimension, B, is less than or equal to the base dimension, Z. The effect of the group on the capacity of individual columns is captured by the group efficiency factor, η_g. In practice, this factor is usually taken as equal to unity except as noted in Table 6-26. Interpolation can be applied to evaluate η_g for intermediate spacings.

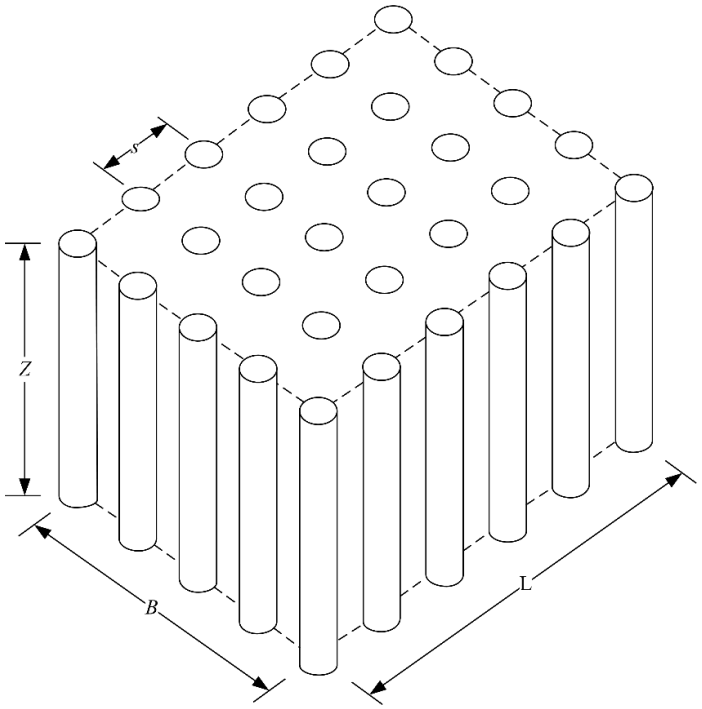

Figure 6-15 Group Geometry

Table 6-26 Group Efficiency Factor for Groups of Elements

Soil Type and Pile Cap Condition	Group efficiency factor, η_g				
	Driven Piles[A]	Drilled Shafts[B]	CFAs[C]	DDPs[D]	Micropiles[E]
Coarse-grained soil and pile cap not in contact with the ground	1.0	0.65 for s/b=2.5 0.80 for s/b=3 1.0 for s/b=4	0.65 for s/b=2.5 1.0 for s/b=6	1.0	1.0
Coarse-grained soil and pile cap in contact with the ground	1.0	1.0	0.65 for s/b=2.5 1.0 for s/b=6	1.0	1.0
Fine-grained soil, s_u< 2 ksf, and pile cap not in contact with the ground	0.65 for s/b=2.5 1.0 for s/b=6	1.0	1.0	0.7 for s/b=3.0 1.0 for s/b=6	0.65 for s/b=2.5 0.70 for s/b=3 1.0 for s/b=6
Fine-grained soil, s_u < 2 ksf, and pile cap in contact with the ground	1.0	1.0	1.0	1.0	1.0
Fine-grained soil, s_u ≥ 2 ksf	1.0	1.0	1.0	1.0	1.0

[A] Minimum spacing is greater of 2.5 ft and s/b = 2.5 (AASHTO 2020); minimum recommended spacing is greater of 3 ft and s/b = 3.0 (FHWA 2016).

[B] Minimum spacing is s/b = 2.5; minimum recommended spacing is greater of s/b = 3.0. If the stability of the shaft is maintained, e.g., by advancing casing ahead of drilled shaft excavation, reductions in coarse-grained soils need not be made (FHWA 2018a).

[C] Minimum spacing is s/b = 3.0. The reductions in coarse-grained soils are likely quite conservative (FHWA 2007).

[D] Minimum spacing is s/b = 3.0 (FHWA 2007).

[E] Minimum spacing is greater of 2.5 ft and s/b = 3.0 (AASHTO 2020). For micropiles, b is the diameter of the grouted bond zone (FHWA 2005).

Block failure should be checked for groups in fine-grained soil and when closely-spaced columns in coarse-grained soils are underlain by weak soil. The nominal resistance to block failure can be estimated as:

$$R_{n,gblock} = 2Z \cdot (B + L) f_{s,1} + B \cdot L \cdot s_{u,2} \cdot N_c \quad (6\text{-}38)$$

where:
L, B, and Z = dimensions as defined in Figure 6-15,
$f_{s,1}$ = weighted average unit shaft resistance over the depth of column embedment, and
$s_{u,2}$ = average undrained strength from the base to a depth of $2B$ to $3B$ below the base.

When the sides of the pile group are in fine-grained soil, $f_{s,1}$ should be set equal to the average undrained shear strength. When the sides of the pile group are in coarse-grained soils, $f_{s,1}$ equals the average unit shaft resistance as evaluated using an SCA method. In the second term, the depth used to average $s_{u,2}$ should be the value that produces the lower estimate of strength. For pile groups in coarse-grained soils underlain by a weak layer, $s_{u,2}$ equals the undrained strength of the weak layer. The bearing capacity factor, N_c, should be evaluated as (Brinch-Hansen 1957):

$$N_c = 5\left(1 + \frac{0.2B}{L}\right)\left(1 + \frac{0.2Z}{B}\right) \leq 9 \quad (6\text{-}39).$$

When using an LRFD framework, AASHTO (2020) recommends the resistance factors provided in Table 6-27 for group block failure. For the combined resistance of the single columns, the appropriate resistance factors provided in Table 6-11 should be used.

Table 6-27 Recommended Strength Limit State Resistance Factors for Block Failure (AASHTO 2020)

Foundation Technology	Recommended Resistance Factor
Driven piles	0.60 – fine-grained (cohesive) soil below group
Drilled shafts	0.55 – fine-grained (cohesive) soil below group
Micropiles[A]	0.60 – fine-grained (cohesive) soil below group
[A] AASHTO (2020) states that resistance factors should be reduced by 20% for micropiles in marginal ground conditions.	

6-5.6 Uplift Capacity.

Uplift capacity is needed to resist tensile loads from the superstructure, such as from wind and earthquake loading. Uplift can also result from bending moment that is resisted through a force couple provided by multiple elements.

There are five important concepts to consider when evaluating the uplift capacity of deep foundations: 1) failure in uplift can be abrupt and result in unrestrained movement,

2) the self-weight of the foundation reduces the net uplift force, 3) the base of the foundation does not provide long-term resistance to uplift, 4) the unit shaft resistance in uplift is usually taken to equal the unit shaft resistance in compression even though this may not strictly be true, particularly for cyclic loading, and 5) in pile groups, uplift resistance is limited by the lesser of the combined uplift resistances of the individual elements and the uplift resistance of a block or wedge of soil surrounding the pile group. An important exception to the third point is suction caissons that are explicitly designed to consider suction at the base.

When using an LRFD framework, AASHTO (2020) recommends application of the resistance factors in Table 6-28 to the nominal side resistance found using an appropriate SCA method. For the extreme limit state, a resistance factor equal to 0.8 can be used for uplift loading for all geomaterials.

Table 6-29 provides recommended minimum factors of safety for uplift when using an allowable stress design framework.

Table 6-28 Recommended Strength Limit State Uplift Resistance Factors (AASHTO 2020)

Foundation Technology	Recommended Uplift Resistance Factor[A]
Driven piles	0.20 – coarse-grained (cohesionless) soil, Beta method 0.25 – fine-grained (cohesive) soil, Alpha method 0.50 – group block uplift, all soils
Drilled shafts	0.45 – coarse-grained (cohesionless) soil, Beta method 0.35 – fine-grained (cohesive) soil, Alpha method 0.40 – rock, Equation 6-38 0.45 – group block uplift, all soils
Micropiles	0.55 – presumptive values 0.50 – group block uplift, all soils
[A] AASHTO (2020) states that resistance factors should be reduced by 20% for single drilled shafts and small pile groups (<5 piles) to account for lack of redundancy and micropiles in marginal ground conditions.	

For the uplift resistance of a single element, the effective weight of the individual column, $W_{r,e}$, is factored using a minimum dead load factor equal to 0.9 (AASHTO 2020). This approach is less conservative than factoring the effective weight by the resistance factor but is usually acceptable since the weight of the element is usually more certain than the side resistance. When evaluating the weight of the element, the effective material unit weight should be used to account for buoyancy effects regardless of whether a total or effective stress analysis is used. When closed-end pipe piles are driven unfilled below the water table, buoyancy should be checked considering the actual weight of the empty pile. This check confirms constructability for piles subsequently filled with concrete or evaluates the long-term reduction in uplift force if the pile is left unfilled over its service life.

Table 6-29 Recommended Minimum Factors of Safety for Tension Loading

Foundation Technology	Guidance Source	Recommended Minimum Factor of Safety
Driven Piles	USACE (1991)	2.0 – with load tests[A] 3.0 – with dynamic testing[A] 3.0[A]
	UFC (2022)	2.0 – with load tests[B] 3.0 – with dynamic testing and signal matching[B] 3.0 – piles anchored in rock[B]
Drilled shafts	UFC (2022)	2.5 to 4 – drilled shafts anchored in rock[B]
	Coduto et al. (2016)	6.0[C] 4.0 – with load tests[C]
Micropiles	FHWA (2005)	2.0 – with load tests[D]

[A] Values are for "usual" loading; for unusual loading, such as floods, factors of safety may be decreased by factor of 0.75; for extreme loading, such as rare natural disasters, factors of safety may be decreased by factor of 0.57.
[B] Use FS > 3 to limit total and differential settlements to small values. Generally, use FS ≥ 2.5. FS for drilled shafts depends on uncertainties in loading, stratification, and verification testing.
[C] Without load testing, the FS may be reduced by 1.0 for uniform ground conditions and extensive site characterization. With load testing, the FS may be reduced by 1.0 for uniform ground conditions and extensive site characterization, with an additional reduction of 0.5 possible if the load testing program is very extensive in uniform ground conditions with extensive site characterization.
[D] Load tests should be performed before and during production pile installation, i.e., verification and proof testing. FS should be increased to 2.5 in marginal ground conditions.

The combined factored uplift capacity of n individual columns, $R_{r,gu,}$ is:

$$R_{r,gu} = \min\begin{cases} n\left(R_{r,s} + W_{r,e}\right) + W_{r,e,cap} \\ R_{r,ublock} \end{cases} \quad (6\text{-}40)$$

where:
$R_{r,s}$ = factored capacity of a single column,
$W_{r,e}$ = factored effective weight of a single column,
$W_{r,e,cap}$ = factored effective weight of the cap, and
$R_{r,ublock}$ = factored uplift capacity of the columns and block calculated as follows.

A practical, conservative method to estimate the uplift capacity of the soil block, $R_{r,ublock}$, associated with the group of columns uses the dimensions and assumed shape shown in Figure 6-16 (Tomlinson 1994, FHWA 2016). The uplift resistance of the block is comprised of the effective weight of the block, $W_{e,g}$, and, in the case of undrained conditions, the contribution of shear strength along the sides of the block. The weight of the foundation and soil between elements are calculated using effective unit weights, regardless of whether a total or effective stress strength analysis is used, to account for buoyancy effects for materials below the water table. Usually, the difference between the unit weight of the foundation material and the soil may be neglected by treating all materials as having the unit weight of soil. The effective weight of the pile cap, W_{cap}, also should account for any expected buoyancy and is included in the weight of the block. The effective weights of the soil block and cap should be left unfactored since

the group block resistance factors provided in Table 6-28 are applied to the effective weight and the side resistance for undrained conditions.

For pile groups in coarse-grained soils, the block resistance is the weight of the truncated prism having a rectangular base, shown in Figure 6-16(a), plus the weight of the cap. For a uniform soil profile (with water table at the ground surface or below the block), the volume of the block, V_{block}, is calculated as:

$$V_{block} = B \cdot L \cdot Z + \frac{Z^2}{4}(B + L) + \frac{Z^3}{12} \quad \text{(6-41).}$$

For layered soil profiles and/or when the groundwater table is located within the block, the block can be divided into layers. The thickness of each layer should replace Z in Equation 6-41. The plan dimensions B and L should be replaced by the dimensions of the block at the bottom of each layer, calculated using the 4V:1H slope.

For deep foundations in undrained conditions, the effective weight of the block is based on the block geometry shown in Figure 6-16(b) and calculated as:

$$W_{e,g} = B \cdot L \cdot (Z_1 \cdot \gamma_m + Z_2 \cdot \gamma_b) + W_{cap} \quad \text{(6-42)}$$

where:
Z_1 = depth of the column group above the water table,
Z_2 = depth of the pile group below the water table,
γ_m= moist unit weight of the soil, and
γ_b = buoyant unit weight of the soil.

The block uplift capacity includes the undrained shear resistance on the sides of the block plus the effective weight of the block and pile cap:

$$R_{n,block} = 2Z \cdot (B + L) \cdot s_{u,avg} + W_{e,g} \quad \text{(6-43).}$$

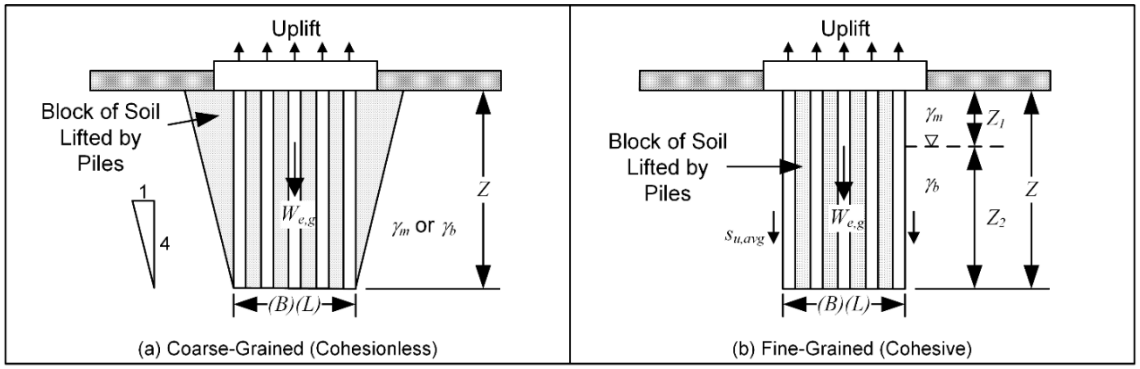

Figure 6-16 Uplift Resistance of Column-Soil Block for Groups of Columns – (a) Coarse-Grained and (b) Fine-Grained Soils

6-5.7 Negative Skin Friction.

Negative skin friction refers to vertical load transfer from the soil to the deep foundation element that occurs when the soil moves down relative to the shaft of the element. The resulting component of the total axial load is called the *drag force*. Negative skin friction requires the reversal of the shaft resistance and is caused by any mechanism that produces settlement in soil, such as consolidation, secondary compression, and vibration-induced densification. Consolidation may be induced by changes in groundwater elevation from dewatering or ground loading during the service life of the foundation. These sources of loading are easy to overlook and are often difficult to predict.

NCHRP (1997a) list conditions that are likely to produce negative skin friction: 1) total ground settlement exceeds 4 inches, 2) post-construction settlement exceeds 0.4 inches, 3) new fill is placed on the ground having a thickness that exceeds 6 ft, 4) the thickness of the compressible soil exceeds 30 ft, and 5) the groundwater table is lowered more than 12 ft.[38] FHWA (2016) states that the stiffness contrast between the piles and the surrounding ground alone is enough to create some amount of drag force; therefore, all designs should consider the possibility of negative skin friction.

When negative skin friction and the resulting drag force occur, the soil moves downward relative to the element until the neutral plane is reached. The *neutral plane* is the elevation along the element at which no relative displacement occurs between the element and the soil. The maximum compressive load in the element occurs at the neutral plane. The position of the neutral plane depends on several factors that are discussed in more detail below and may change over the service life of the foundation. Below the neutral plane, the foundation element moves down relative to the soil, and upward (positive) shaft resistance is developed.

Table 6-30 summarizes the limit states where the the drag force should be included in design. Service limit state calculations are discussed in Section 6-5.8. Inclusion of the drag force in the strength limit state is presented in Section 6-7.4.

Table 6-30 Guidance for Consideration of Down Drag

Design Consideration	Consider Negative Skin Friction and Drag Force?	
	Strength Limit State	Service Limit State
Geotechnical	No (FHWA 2016, 2018a)	Yes, negative skin friction and drag force may increase settlement
Structural	Yes, but it rarely influences the required structural capacity	Yes – location of the neutral plane influences elastic compression

[38] It is important to note that negative skin friction can occur even when none of the conditions are met.

In pile groups, the piles located along the perimeter of the group are exposed to downward movement of the settling ground and associated drag force. In contrast, interior piles are often shielded from drag force since the soil between the piles tends to move with the piles, except near the pile toe (Fellenius 2021). The shielding of interior piles from drag force is more apparent when ground settlement is caused by applied load rather than lowering of the ground water table. Larger pile groups tied together by a stiff cap or raft may experience less settlement due to downdrag than small pile groups and single piles due to support provided to the perimeter piles by the shielded interior piles (Fellenius 2021). The settlement due to downdrag can be nonuniform and lead to structural damage due to differential settlement (Coduto et al. 2016). Methods to mitigate downdrag and drag force are discussed in Section 6-5.8.

As Fellenius (2021) points out, drag force and downdrag settlement are inversely related. An end bearing pile penetrating consolidating ground may experience a large drag force and small downdrag settlement because the neutral plane is located near the base of the column. Conversely, a column floating in consolidating ground may experience a small drag force and large downdrag settlement due to the neutral plane being located further away from the base.

As indicated in Table 6-30, the drag force does not need to be considered for the geotechnical strength limit state. If the axial load approaches the strength limit state, the element will move down relative to the soil, which will fully mobilize positive side resistance along the entire length of the element, removing the effects of the drag force. In other words, the potential for negative skin friction does not reduce the nominal geotechnical axial capacity (Siegel et al. 2014). However, when the ground surrounding the foundation element is settling, the settlement required to mobilize the required geotechnical resistance for service conditions may be intolerably large. While there has historically been debate about whether the drag force should be subtracted from the geotechnical capacity, current FHWA guidance excludes the drag force from geotechnical capacity analysis (FHWA 2018a, 2016).

6-5.8 Settlement.

Settlements are evaluated for the service limit condition. Limits on settlement should be established considering the amount of total and differential settlement that can be tolerated by the structure supported by the foundation. Settlement will also be limited by the operation of the facility, e.g., utility connections, stormwater drainage, and ride quality. The total settlement at the top of the foundation, δ, is equal to:

$$\delta = \delta_e + \delta_s \tag{6-44}$$

where:
δ_e = settlement due to elastic compression of the element and
δ_s = settlement due to compression of the soils supporting the element.

If excessive settlements are estimated, some options include 1) refining the settlement analysis using load tests, 2) resizing the length and/or width of the element(s), 3) exploring other foundation options, 4) increasing the size of the pile group by adding more elements, 5) excluding base resistance and designing only for side resistance, and 6) improving the stiffness of the ground, e.g., by postgrouting drilled shafts.

A few important points about evaluating settlement of deep foundations include the following:

1) Settlements that occur after installation of settlement-sensitive features, e.g., building façade and pavements, are usually more consequential than settlements that occur prior to the installation of sensitive features.

2) Angular distortion is defined as the magnitude of differential settlement divided by the plan-view distance, or span length, over which the settlement occurs. Angular distortion is a useful metric for evaluating whether settlement is likely to be detrimental. Chapter 5 of DM 7.1, NCHRP (1991), and Duncan and Buchignani (1987) list limits on angular distortion for various types of structures. For example, a flexible steel frame structure might be able to tolerate an angular distortion of 0.008 without distress while a concrete block structure might only tolerate an angular distortion 20 times lower, i.e., 0.0004. For multi-span bridges, angular distortion should be limited to 0.004 (FHWA 2016).

3) Estimating the difference in settlement for two foundations is difficult due to the inaccuracies associated with each estimate. When better information is not available, Duncan and Buchignani (1987) recommend estimating differential settlement between two foundations as 75% of the higher estimated settlement for the individual foundations. Later guidance involving Duncan recommends estimating differential settlement between two foundations as 100% of the higher estimated settlement for the individual foundations (NCHRP 1991). Settlements tend to be more erratic for sites with sand, compacted fills, and/or stiff clay profiles.

4) Compression of high coarse-grained permeability soils occurs almost concurrently with applied loading. Compression of low permeability fine-grained soils occurs slowly over time. Since silts and clays also tend to be more compressible than sands and gravels and more susceptible to secondary compression, sites with silt and clay profiles pose greater potential for larger post-construction settlement.

5) The loads included in settlement calculations may depend on the type of settlement being considered. Analyses of immediate settlement and settlement due to compression of coarse-grained soils should consider both permanent and transient loads (Fox 2003). Analyses of consolidation and secondary

compression should consider permanent loads and some reasonable fraction of transient live loads. AASHTO (2020) recommends analyzing settlement of fine-grained soils using the Service I loading condition, excluding transient loads.

6) The settlement at the top of a deep foundation includes elastic compression of the element itself and compression of the soil supporting the element. If the recommended neutral plane concept (Section 6-5.7) is applied, elastic compression of the element that contributes to settlement (δ_e) is above the neutral plane. Likewise, only compression of the soil and rock below the neutral plane should be included in δ_s as contributing to the settlement at the top of the element. For foundations bearing on or in rock, the compression of the rock is usually small enough to ignore.

7) Settlement of single elements can be estimated by developing load-displacement relationships for mobilization of the side and base of the element, evaluating the distribution of axial load in the element, and applying the load-displacement relationships along with consideration of elastic compression of the element itself to estimate movement at the top of the element. Typically, side friction (positive or negative) is mobilized at small displacements, often 0.1 to 0.4 inches, while base resistance mobilizes over larger displacement, often 4% to 10% of the width of the element. Methods to estimate the load transfer movements of single piles include the $t-z$ method (Kraft et al. 1981), which is described succinctly by Coduto et al. (2016), and typically implemented using computer software, and various methods based on elastic theory, as described by Briaud (2013) and Salgado (2008). These methods can be challenging to implement since some of the inputs, particularly those used to evaluate the linear or nonlinear spring stiffness representing mobilization of the base, i.e., the $q-z$ curve, can be difficult to estimate with confidence (Salgado 2008), particularly when relevant load test data is unavailable. Furthermore, the displacement at the top of the element estimated from load transfer relationships does not explicitly include settlement from downdrag. Section 6-5.8.3 describes an empirical load-displacement curve method for estimating settlement of individual drilled shafts.

8) A group of loaded elements should be expected to settle more than a single element carrying the same load as the individual elements in the group (FHWA 2016). This is due to net outcome of group effects. Some effects, such as the stiffening of the soil between the piles, reduces the compression of these soils. However, the dominant effect is the overlapping zones of influence of the individual piles, which results in significant stress change at greater depths.

9) The flexural stiffness of the pile cap ties the elements together and causes all elements to settle uniformly.

6-5.8.1 Elastic Compression of the Foundation Element.

The elastic compression, or elongation, of a foundation element, δ_e, can be found using:

$$\delta_e = \frac{\Delta Q Z}{A_p E_p} \tag{6-45}$$

where:
ΔQ = average change in load in the element over its length including drag load,
Z = length of the element,
A_p = cross-sectional area of the pile material, and
E_p = Young's Modulus of the pile material.

A more refined estimate of elastic compression can be obtained by discretizing the pile into segments, evaluating the average load for each segment, computing the compression of each segment, and summing the compression of the individual segments. If the neutral plane concept is applied, elastic compression above the neutral plane directly contributes to the settlement of the top of the foundation element while elastic compression below the neutral plane does not directly contribute to the settlement. Elastic compression occurs simultaneously with loading, so only loads applied after construction contribute to post-construction settlement.

For typical service loading conditions, the elastic compression of a concrete and/or steel element is generally small and can sometimes be ignored, particularly when all elements are relatively short and similarly loaded. Elastic compression cannot be ignored when the length and/or loading of the foundation elements varies significantly, particularly over short distances, since potentially damaging differential settlement can occur.

6-5.8.2 Empirical Method for Pile Group Settlement in Coarse-Grained Soil.

The settlement of a pile group in coarse-grained soil will largely occur at the rate of loading. This means that post-construction settlement will be limited to that caused by service loads, unless the site is densified or liquefied by an event, such as an earthquake. Therefore, the settlement of deep foundations in coarse-grained soils is often not a controlling factor and can be appropriately checked using simple methods to see if a more detailed numerical analysis is warranted.

The Meyerhof (1976) method is a simple empirical method that correlates overburden-corrected SPT N values to elastic compressibility. The method applies to pile groups in sand that are not underlain by a more compressible stratum. The method does not explicitly include elastic compression of the piles.

The settlement at the top of the pile group can be estimated by:

$$\delta_s = \frac{\left(\frac{Q_d}{B \cdot L}\right)\sqrt{B}}{\overline{N}_{1,60}} I_f \quad (6\text{-}46)$$

where:
δ_s = estimated settlement (in inches) at the top of the pile group,
Q_d = unfactored group design load (in kips) for the service limit state,
B and L = pile group dimensions (in feet) as defined in Figure 6-15, and
$\overline{N}_{1,60}$ = average overburden corrected N value within B below the base (Table 6-19).

The influence factor is computed as:

$$I_f = \max\begin{cases} 1 - Z/(12B) \\ 0.5 \end{cases} \quad (6\text{-}47).$$

where:
Z = length (in same dimensions as B) of the group

For pile groups in silty sand, the settlement estimate from Equation 6-46 should be doubled.

6-5.8.3 Empirical Method for Drilled Shaft Settlement.

The load-displacement curves proposed by Chen and Kulhawy (2002), provided in Figure 6-17, are based on observations from many load tests performed on drilled shafts. This method is intended for preliminary analyses to determine whether settlement will govern the design and a more detailed analysis, such as numerical analysis using computer software, is warranted.

The load-displacement curves are appropriate for drilled shafts in either coarse-grained or fine-grained soil profiles having a diameter between 1 and 6.5 ft, a depth between 16 and 200 ft, and a depth to diameter ratio between 6 and 56. The curves incorporate the composite mobilization of side and base resistances as well as elastic compression of the concrete shaft. The vertical axis of Figure 6-17 is the axial compressive force normalized by the failure threshold. The axial compressive force (ACF) equals the sum of the unfactored applied load and the effective weight of the shaft. Guidance for evaluating the effective weight is provided in Section 6-5.6. The failure threshold (FT) is the axial compressive force corresponding to a displacement normalized by shaft diameter, δ/b, equal to 4%. This force is found by adding the nominal shaft resistance and the nominal base resistance at δ/b equal to 4%, R'_b.

For this method, the nominal shaft resistance should be found by the Alpha Method according to Equation 6-8 for fine-grained soils and by the Beta Method for coarse-grained soils with K/K_0 evaluated according to FHWA (2018a) as provided in Table 6-13.

The nominal base resistance, R_b, should be found according to Equation 6-27 for fine-grained soils and according to Reese and O'Neill (1989) as provided in Table 6-20 for cohesionless soils. The nominal base resistance at δ/b equal to 4% should be found as:

$$R'_b = \begin{cases} R_b \text{ for fine-grained(cohesive) soils} \\ 0.71R_b \text{ for coarse-grained (cohesionless) soils} \end{cases} \quad \text{(6-48).}$$

The equations provided in Table 6-31 approximate the load-displacement curves proposed by Chen and Kulhawy (2002). To estimate settlement, follow these steps:

1) Estimate ACF for the service limit state condition using unfactored loads and the effective weight of the shaft.
2) Apply either the Alpha or Beta method to estimate FT as the sum of R_s and R'_b, as defined above.
3) Compute the ratio ACF / FT.
4) Solve for the value of δ/b using Figure 6-17 or the equations in Table 6-31. Multiply by the shaft diameter, b, to estimate settlement, δ.

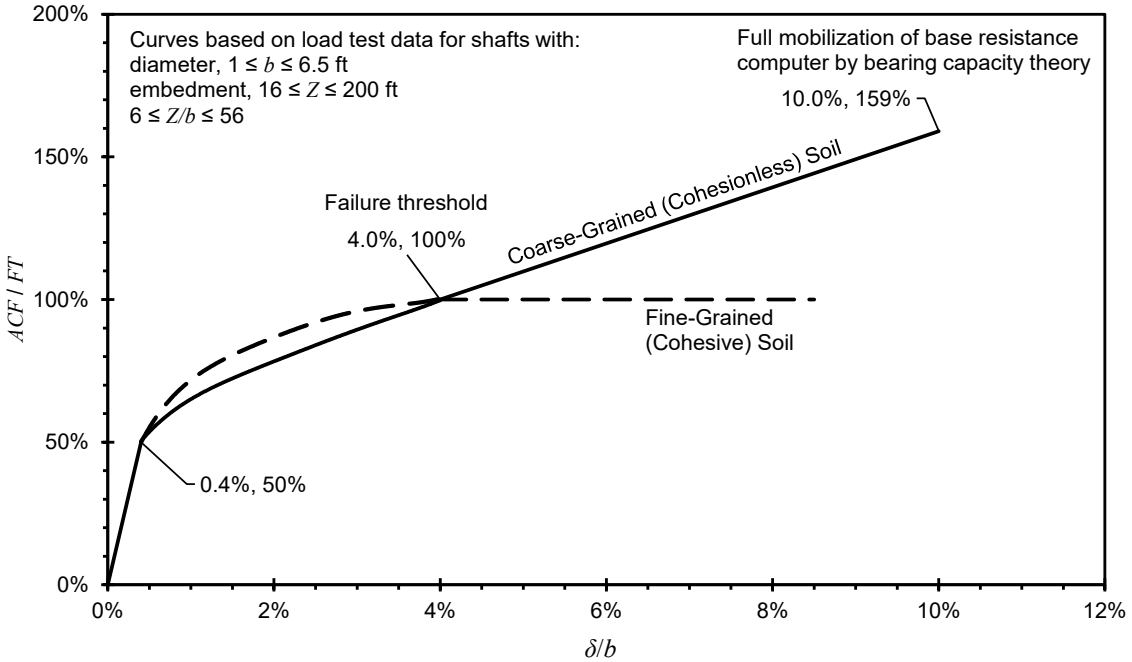

Figure 6-17 Load-displacement Curve for Drilled Shafts (after Chen and Kulhawy 2002)

Table 6-31 Relationships for Normalized Drilled Shaft Settlement vs Normalized Loading

ACF/FT (%)	Approximate δ/b (%)	
	Fine-Grained (Cohesive) Soil[A]	Coarse-Grained (Cohesionless) Soil[B]
0 to 50%	$0.008\left(ACF/FT\right)$	
>50% to 90%	$0.4\% + \dfrac{\left(ACF/FT - 50\%\right)}{50\% - 0.72\left(ACF/FT - 50\%\right)}$	$0.4\% + \dfrac{\left(ACF/FT - 50\%\right)}{27\% - 0.33\left(ACF/FT - 50\%\right)}$
>90% to <100%		$0.102\left(ACF/FT\right) - 6.2\%$
100% to 159%	Large settlements are anticipated	
≥159%	Large settlements are anticipated	Large settlements are anticipated

[A] The fit for fine-grained soils is within ±0.1% of the curve.
[B] The fit for coarse-grained soils is within ±0.1% of the curve, except for $89\% < ACF/FT < 93\%$ where the fit is within ±0.2% of the curve.

6-5.8.4 Equivalent Footing Method.

Equivalent footing methods use the concept of load spread to estimate settlement of pile groups (Fellenius 1988, FHWA 2016) as well as single piles (Greenfield and Filz 2009). These methods can be applied to a variety of foundation types not bearing on or in rock including driven piles, micropiles, CFAs, DDPs, and groups of drilled shafts. Equivalent footing methods have the following common features:

1) Determine an elevation along the element(s) below which shedding of the applied load from the element(s) will compress the underlying soils,

2) Estimate the change in vertical effective stress using an assumed method of spreading of the applied foundation load, e.g., 2V:1H spread, within the zone of influence defined by the lateral boundaries of load spread, and

3) Estimate soil compression or settlement transferred to the foundation using conventional one-dimensional methods for clay and sand soils.

For the service limit state, the applied foundation load is the unfactored permanent load. For the neutral plane method, drag loads are not added to the permanent load and spread below the elevation of load shedding as discussed in Section 6-5.8.4.2 (Fellenius 1988).

In the basic forms presented here, load spread methods ignore the beneficial stiffening and stress shielding effects that groups of foundation elements usually have on the compressibility of the soils within the group. Procedures to account for these effects can be found in Fellenius (2021) and Greenfield and Filz (2009).

6-5.8.4.1 Empirical Selection of Equivalent Footing.

The depth and dimensions of the equivalent footing with plan-view dimensions of B and L can be selected using the guidance provided in Figure 6-18 and Table 6-32. Some spreading of the load above the equivalent footing depth is considered in some cases. The depth (z_s) represents the depth to the bearing layer(s), Z_b is the depth of embedment in the bearing layer(s), z_1 is the depth below the base of the pile cap to the assumed start of load spreading, and z_2 is the depth interval where load spreading is assumed to occur at 4V:1H. The depth to the equivalent footing is the sum of z_1 and z_2, and load spreading is assumed to occur at 2V:1H below the equivalent footing.

The width, B', and length, L', of the equivalent footing are determined from the dimensions of the group of elements (Figure 6-15), B and L, according to the following equations:

$$B' = B + \frac{z_2}{2} \tag{6-49}$$

and

$$L' = L + \frac{z_2}{2} \tag{6-50}.$$

FHWA (2016) provides guidance for sizing the equivalent footing for groups that include battered elements. For batter pile groups supported primarily by side resistance, the dimensions B' and L' should be based on the dimensions of the group at a depth equal to the sum of z_s and $2/3 \cdot Z_b$, including the plan area increase due to the batter angle. For battered groups supported primarily by base resistance, the dimensions B' and L' should be based on the dimensions of the group at a depth equal to the sum of z_b and Z_b, including the plan area increase due to the batter angle.

The change in total vertical stress due to the applied load, Q, at a particular depth, z, is estimated by 2V:1H spreading:

$$\Delta\sigma_z = \frac{Q}{\left(B' + z'\right)\left(L' + z'\right)} \tag{6-51}$$

where:
z' = depth below the equivalent footing = $z - z_1 - z_2$.

Other sources of stress change leading to settlement of the foundations should be investigated and incorporated into the calculations if needed. Potential sources of additional stress change include lowering the groundwater table, placement of fill, and overlap of the zones of influence from adjacent foundations. The neutral plane method

described in the next section is the preferred approach for incorporating other sources of stress change.

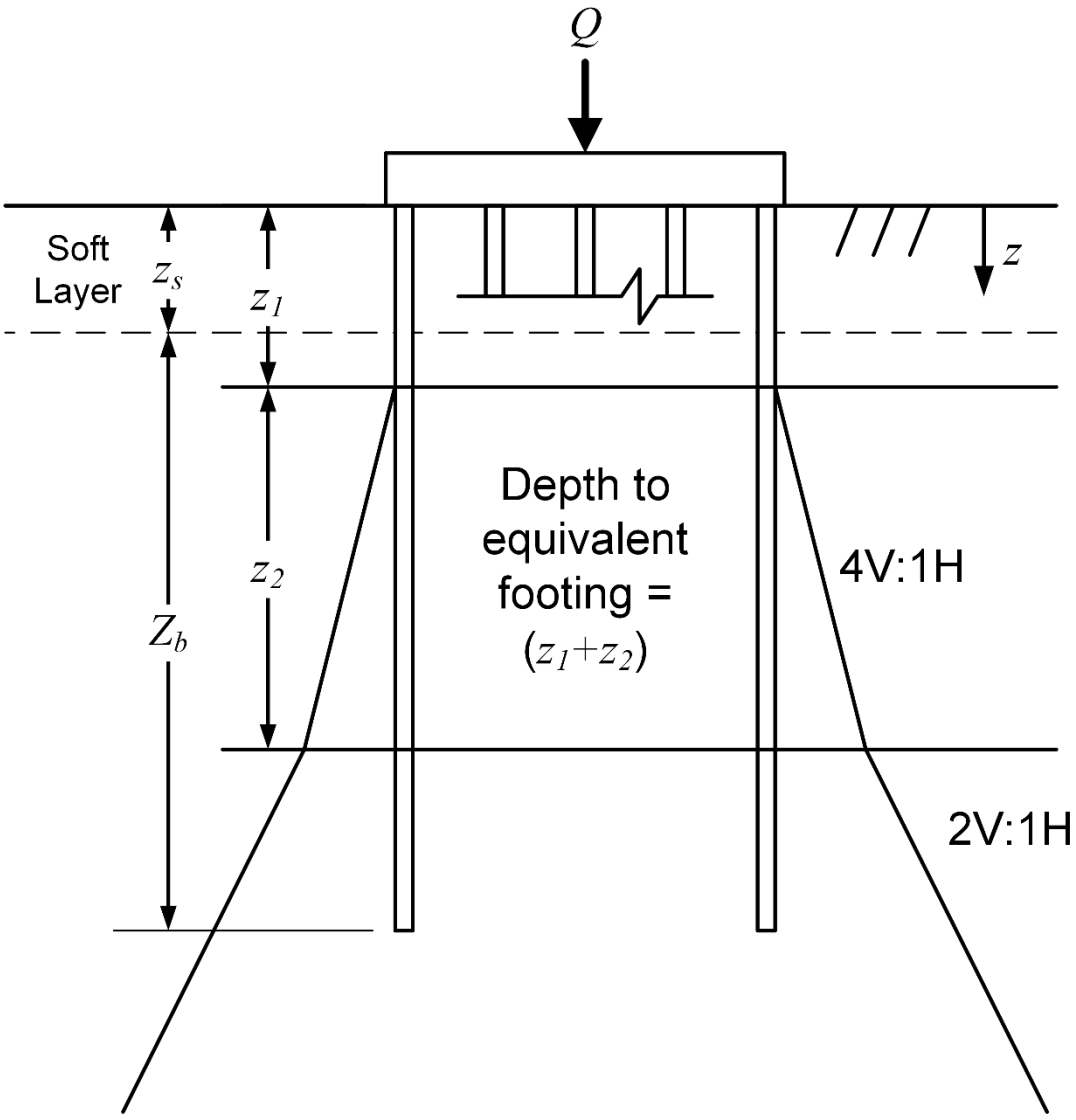

Figure 6-18 Locating the Equivalent Footing

Table 6-32 Guidance for Locating the Equivalent Footing

Columns installed in…	z_1	z_2	Source
Sand or clay, $z_s = 0$	$2Z_b/3$	0	Terzaghi and Peck (1967)
Soft clay over firm clay, z_s = depth to firm clay	$z_s+2Z_b/3$	0	Duncan and Buchignani (1987)
Soft clay over hard clay or sand underlain by soft clay, z_s = depth to hard clay or sand	z_s	0	FHWA (2000)
Clay, $z_s = 0$	0	$2Z_b/3$	
Sand over clay, $z_s = 0$	$2Z_b/3$	$2Z_b/9$	
Layered sand and/or clay, $z_s = 0$	0	$2Z_b/3$	

6-5.8.4.2 Neutral Plane Method.

The neutral plane method described in this section is generally a better approach for locating the equivalent footing since it directly uses the specific loading applied to the element, the side friction, and mobilized base resistance to locate the elevation where load shedding occurs. The neutral plane method can be applied to all cases, not just those where significant drag forces are anticipated.

The neutral plane method rationally considers the applied load, positive and negative skin friction, and the mobilized base resistance to locate the elevation along the element(s) where load shedding leading to foundation settlement begins. The neutral plane method can be applied to a single element as well as groups of elements.

The neutral plane is located using the first five steps of the process described in Section 6-5.7 to evaluate the drag force. For soil profiles that are uniform or become less compressible with depth, the estimated foundation settlement increases as the neutral plane is positioned higher along the element. The assumption of full mobilization of base resistance used to evaluate the drag load for the structural strength limit state is not conservative for settlement calculations.

The more refined estimate of the percentage of base resistance mobilization should be made. Siegel et al. (2013) describe a simpler option and recommend analyzing the problem with a range of different assumed mobilizations of the base, e.g., 0%, 50%, and 100% mobilization. If the conclusion regarding the settlement estimates is not sensitive to the lowest and highest reasonable estimates of base resistance, additional efforts to estimate base mobilization are unlikely to be needed. If the conclusion depends on the assumed base mobilization, calculations can be refined using load transfer-displacement relationships, i.e., t-z and q-z curves, to evaluate the mobilization of the base.

Once the neutral plane has been located, an equivalent footing is positioned at the elevation of the neutral plane, and the settlement analysis can proceed using the equations for one-dimensional compression described in Section 6-5.8.4.3. For a group

of elements, the dimension of the equivalent footing is usually taken to equal the dimensions of the group, i.e., $B' = B$ and $L' = L$. For a single element, the dimensions of the footing are equal to the width of the element.

The change in total vertical stress at a particular depth, z, due to the applied load, Q, and any other sources of stress change, $\Delta\sigma_{z,other}$, is estimated by:

$$\Delta\sigma_z = \frac{Q}{\left(B'+z'\right)\left(L'+z'\right)} + \Delta\sigma_{z,other} \tag{6-52}$$

where:
z' = depth below the equivalent footing to the depth z.

The additional settlement due to $\Delta\sigma_{z,other}$ is the downdrag component of foundation settlement. The magnitude of $\Delta\sigma_{z,other}$ can be found using conventional methods for estimating stress changes at depth, e.g., load spread, Boussinesq, etc.

6-5.8.4.3 Settlement Estimates using the Equivalent Footing.

Once $\Delta\sigma_z$ has been estimated as a function of depth below the equivalent footing, conventional one-dimensional methods can be applied to estimate the compression resulting from the change in stress. For the fully drained condition, the change in effective stress, $\Delta\sigma'_z$, equals the change in total stress $\Delta\sigma_z$. This condition is expected at the time of loading and beyond for high permeability sands and gravels under normal rates of loading. For low permeability materials, the fully drained condition is reached over time. Time rate of consolidation analysis, described in Chapter 5 of DM 7.1 is used to evaluate settlements for partially drained conditions.

For clays and some silts, the compression due to a change in vertical effective stress is found by:

$$\delta_s = H_0\left[C_{\varepsilon r}\log\left(\frac{\min\left(\sigma'_{z0}+\Delta\sigma'_z,\sigma'_p\right)}{\sigma'_{z0}}\right)+C_{\varepsilon c}\log\left(\frac{\max\left(\sigma'_{z0}+\Delta\sigma'_z,\sigma'_p\right)}{\sigma'_p}\right)\right] \tag{6-53}$$

where:
H_0 = initial thickness of the consolidating layer
$C_{\varepsilon r}$ = modified recompression index
$C_{\varepsilon c}$ = modified compression index,
σ'_{z0} = initial effective vertical stress, and
σ'_p = preconsolidation stress.

Elastic compression of coarse-grained soil can be approximated using basic one-dimensional elastic theory according to the following equation:

$$\delta_s = H_0 \left[\frac{(1+\nu_s)(1-2\nu_s)\Delta\sigma'_z}{E_s(1-\nu_s)} \right] \quad (6\text{-}54)$$

where:
ν_S = Poisson's ratio for the soil,
E_S = Young's Modulus for the soil, and
$\Delta\sigma'_z$ = average change in effective vertical stress over the thickness of the sand, H_0.

As described in FHWA (2016), the compression of sand can also be estimated using the nonlinear method proposed by Hough (1959) and later refined by FHWA (2002).

A more refined estimate of the soil settlement can be obtained by discretizing the compressible layer(s) into sublayers, evaluating the average stresses for each sublayer, computing the compression of each sublayer, and summing the compression of the individual sublayers.

Highly compressible deposits may extend a significant depth below the base of the foundation elements. At some depth, the change in vertical stress caused by the applied load becomes sufficiently small to ignore the soil compression. This depth is typically selected where the change in stress is less than 10% of the bearing stress of the equivalent footing.

Figure 6-19 shows that the settlement of the pile and the soil are equal at the neutral plane. The additional pile settlement above the neutral plane is due to elastic shortening of the pile while the additional soil settlement above the neutral plane is the free field settlement due to sources of stress change other than the applied foundation load. Below the neutral plane, the soil settlement is due to the stress changes from the applied foundation load and stress changes from other sources. The difference between the soil and pile settlement at the toe elevation is the pile penetration in the soil. If a q-z curve is defined, an iterative process can be applied, as described by Fellenius (2021), so that the mobilized toe resistance used to locate the neutral plane is compatible with the pile toe penetration.

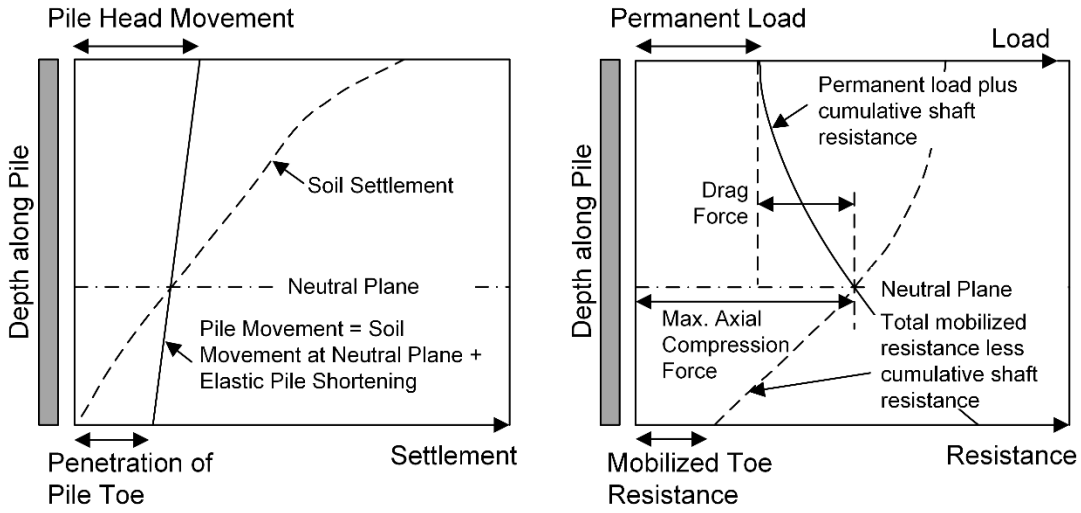

Figure 6-19 Schematic of the Neutral Plane Method for Estimating Settlement

6-5.8.5 Mitigation of Downdrag.

Several measures exist for reducing downdrag and drag force. One approach is to reduce the settlement of the ground that occurs once the columns are installed. This can be accomplished by reducing the total settlement using lightweight fill or ground improvement. Alternatively, consolidation can be accelerated using wick drains, so that a majority of the settlement is complete by the time the columns are installed. Another approach is to intentionally reduce the interface shear strength between the column shaft and soil over some, or all, of the length above the neutral plane. There are many ways to accomplish this. For example, a smooth steel pile can be used instead of a rough concrete column. Columns can be coated in bitumen or epoxy to reduce friction. Columns can also be isolated from the surrounding ground using a slurry or casing.

6-6 GEOTECHNICAL LATERAL CAPACITY.

6-6.1 Introduction.

This section provides guidance for evaluating the lateral capacity of batter and vertical single columns as well as groups of columns. Mainstream contemporary practice has largely migrated to using nonlinear *p-y* analysis software for evaluating lateral capacity; however, analyses that that can be performed by hand remain valuable as checks of software output and in situations where software is unavailable.

The previous version of this manual contained chart solutions for a linear subgrade reaction analysis of laterally loaded piles originally proposed by Reese and Matlock (1956). The effects of nonlinearity in the lateral load-displacement relationship often have significant effect on the outcome of the analysis (Reese et al. 2004); therefore, the nonlinear Characteristic Load Method (CLM) (Evans and Duncan 1982) is presented in

lieu of the linear subgrade reaction charts. As explained below, the CLM method was calibrated to the results of *p-y* analyses. Since *p-y* analyses are not fully applicable to short piles that tend to experience base rotation at the strength limit state, the Broms method (1964a,b, 1965), for short free-head piles that are assumed to be rigid, is also presented.

There are a significant number of software offerings available to perform lateral load analysis, including general purpose finite element and finite difference software. LPILE (Ensoft) and RSPile (Rocscience) are popular software options for performing *p-y* analyses in US practice. Software documentation should be consulted for the details of specific pile-soil models and software usage.

6-6.2 Lateral Loading and Foundation Response.

Sources of lateral loads on foundations include loads transferred by the superstructure from wind, ice, vehicle impacts, ship mooring, moving water, thermal expansion/contraction, earthquakes, and dynamic forces from traffic braking loads and machinery. Additional lateral loads can be directly applied to the foundation from ground displacements due to surface loading, excavation, earthquakes, lateral spreading, landslides, creep, and consolidation in the case of batter piles.

Lateral loading can be static or cyclic. Static loading can be of short duration (uncommon) or sustained. Sustained static loading, e.g., from earth pressures, can cause creep and three-dimensional consolidation of the ground; however, these effects are often not considered for clean sands, overconsolidated clays, and rock. Creep and consolidation due to sustained loading has the effect of softening the relationship between lateral load and deflection. Cyclic loading also softens the load-deflection relationship, particularly in cases where free water is available above a pile in clay. In this case, the cyclic movement of the pile pumps water in and out of the space between the pile and the soil. This effect can lead to significant remolding and erosion of the soil. The selection of input parameters for lateral capacity analysis, e.g., *p-y* curves, should reflect the nature of the loading for the particular pile and soil conditions (Reese et al. 2004). The discussion herein is limited to relatively simple cases of lateral load and/or moment applied to the top of a column installed in level ground.

Laterally loaded piles fall into two major categories. Relatively s*hort piles* behave as approximately rigid elements that will experience rotation and/or translation of the base at the strength limit state for laterally loaded conditions, which is usually controlled by the geotechnical capacity. Short piles include drilled shafts with a low ratio of length to width, foundations for lighting or sign masts, foundations for communications towers, and foundations bearing on shallow rock. In contrast, relatively *long piles* are slender enough to behave as a flexible member having an essentially fixed base, i.e., no rotation or translation. These include most driven pile, CFA, micropile, and DDP elements. Some drilled shafts can also be considered long piles. The strength limit

state for lateral loading of long piles is usually controlled by the structural capacity rather than the geotechnical capacity.

Broms (1965) and Davisson (1970) distinguish between short and long piles based on the ratio of the total length of the element, Z, divided by the *depth to fixity*, Z_f. The definition and methods to calculate the depth to fixity are presented in Section 6-7.2 in the context of buckling.

When Z/Z_f is less than a certain value, the element can be considered a short pile. The response to lateral loading is sensitive to the pile length, but not the stiffness, i.e. the pile can be treated as being infinitely stiff. For elements in undrained fine-grained soil, Broms (1965) characterizes short piles as Z/Z_f less than 2.25 while Davisson (1970) characterizes short piles as Z/Z_f less than $\sqrt{2}$. For elements in coarse-grained soil, Broms (1965) and Davisson (1970) characterize short piles as Z/Z_f less than 1.11.

When the ratio of Z/Z_f is greater than a certain value, the element can be considered a long pile. The response to lateral loading is sensitive to the pile stiffness, but not the length, i.e. the pile can be treated as being infinitely long. For elements in undrained fine-grained soil, Broms (1965) characterizes long piles as Z/Z_f greater than 2.25 while Davisson (1970) characterizes long piles as Z/Z_f greater than $2\sqrt{2}$. For elements in coarse-grained soil, Broms (1965) and Davisson (1970) characterize long piles as Z/Z_f greater than 2.22.

Ratios of Z/Z_f that fall between the criteria for short and long piles are considered intermediate piles, that respond somewhere between a short and long pile. The strength limit state for lateral loading of intermediate piles may be controlled by structural or geotechnical capacity.

6-6.2.1 Limit States for Lateral Capacity Analyses.

Deep foundations that are used to resist lateral loads must consider the strength, service, and extreme event limit states, which are defined in Section 6-5.2. The strength and extreme limit states include consideration of the geotechnical and structural lateral load capacities. The service limit state considers the lateral deflections under service loading conditions. When the modeling capability is available, e.g. LPILE and RSPile, axial loads should be included in the analysis since they influence the maximum flexural capacity as well as lateral deflection. The strength and serviceability limit states should consider the effects of the scour design flood as defined in Section 6-2.2.1.

The preferred way to evaluate the geotechnical strength limit state for vertical piles and drilled shafts is to perform a pushover analysis using the p-y method that reach a state of failure. *Pushover analysis* applies specific combinations of lateral load and/or moment to the top of the pile and predicts the resulting lateral displacement. Pushover

analyses that fail to converge or estimate excessive deformations constitute failure. For example, FHWA (2018a) defines deformations that exceed 10% of the width or diameter of the element as failure. Pushover analyses are frequently performed for incrementally increasing magnitudes of applied load and moment up to, and sometimes beyond, the factored values for the strength limit state. This approach is useful to visualize the load-deflection relationship and identify if nonlinear behavior occurs that may indicate the onset of large displacements with additional loading. For example, FHWA (2018a) recommends that the piles be loaded to an amount equal to the factored loads multiplied by the inverse of the resistance factor. For short piles and other conditions that are not well addressed by p-y analysis (FHWA 2018b), other methods, such as the Strain Wedge Model (SWM) (Norris 1986, Ashour et al. 1998), may be applied using computer software. The Broms Method for short free-head elements provides a hand solution that is widely used for preliminary analysis. A simple method for evaluating the strength limit state of batter piles is presented in Section 6-6.2.

The structural strength limit state is checked to ensure that factored axial, shear, and moment resistances exceed the factored axial loads, shear loads, and bending moments. The p-y method is the preferred analysis method. The nonlinear structural properties of the foundation element, i.e. nonconstant bending stiffness, including the potential for cracking of concrete elements, should be incorporated into the analysis when the software capability is available. The combinations of unfactored axial load (P) and moment (M) that govern the structural strength of the element are depicted on a P-M interaction diagram. A factored interaction diagram is produced by applying a single structural resistance factor that is appropriate for the type of element and design specifications. The combinations of factored loads and moments for each application limit state are plotted on the factored interaction diagram to check whether the combination falls within the acceptable zone defined by the factored diagram. Since axial load can increase moment resistance, both minimum and maximum factored axial loads should be checked. For reinforced and prestressed concrete elements, this step in the design process is used to confirm that the steel area ratio is sufficient and reasonable.

The service limit state is evaluated by ensuring that lateral deflection under service loading conditions is tolerable. The p-y method is the preferred analysis method, though the SWM can also be used. The nonlinear structural properties of the foundation element, including the potential for cracking of concrete elements, should be incorporated into the analysis when the capability is available. Limits on lateral deflection depend upon the project requirements but are usually smaller than the tolerable limit of settlement. Lateral deflection limits are often in the range of ¼ to ½ of an inch.

The extreme limit state is evaluated in a similar fashion as the strength limit state using different applied loading and different resistance factors. The Extreme Event II limit

state (AASHTO 2020) also includes the effects of the scour check flood as described in Section 6-2.2.1.

Table 6-33 provides recommended lateral resistance factors for driven piles and drilled shafts as presented in FHWA (2018b). These factors are appropriate for all geomaterials and are intended to ensure that the shaft remains ductile beyond the factored design load and provides adequate reserve strength. AASHTO (2020) recommends using appropriately-factored loads with resistance factors equal to 1.0 for driven piles and drilled shafts for all lateral load limit states.

Table 6-33 Recommended Factors for Lateral Geotechnical Resistance (after FHWA 2018b)

Limit State	Resistance Factor
Strength: Pushover of individual deep foundation or single row of elements; top is free to rotate	0.67
Strength: Pushover of multiple-row group; tops are restrained by moment connection to cap	0.8
Service	1.0
Extreme event	0.8

6-6.2.2 Fixity.

Embedment of the pile in a pile cap provides rotational restraint at the top of the pile, which affects the response to lateral loads and displacements. A pile top with zero fixity, or *free head* condition, is allowed to rotate and develops zero moment at the top. In this case, the maximum bending moment usually occurs within 8 to 10 pile diameters of the top. A pile top with full fixity, or *fixed head* condition, is not allowed to rotate and develops maximum moment at the top. The degree of fixity is influenced by whether the pile is tied into a cap as part of a group (increases restraint) and the embedment within the cap (deeper embedment increases restraint).

Commonly, the degree of fixity is unknown. It may be prudent to perform lateral analyses twice, once assuming a free head condition and again assuming a fixed head condition. For a given applied load, the free head condition analysis will estimate larger lateral displacement while the fixed head analysis will estimate larger bending moment.

6-6.3 Lateral Analysis of Batter Piles.

Batter piles are installed at a batter angle measured from vertical that is usually less than 45 degrees (1H:1V). Typical batter angles fall between 1H:12V and 1H:3V (FHWA 2018b). Batter piles usually consist of driven piles or micropiles. Pile batter angle can be considered in p-y analyses.

Lateral capacity can be conservatively approximated by assuming that the piles only carry axial load as depicted in Figure 6-20. This assumption combined with practical

limitations on batter angle regulates the lateral capacity of a particular pile. Normally, a pile with a battered alignment is much stiffer laterally compared to the same pile with a vertical orientation. This means that for the same earthquake or blast-induced lateral deflection, batter piles transmit much greater load and moment to the structure compared to the same number and type of vertical piles. Batter piles should also be used cautiously in cases where consolidating ground exerts a drag force on the pile (USACE 2012). Unlike a vertical pile where the drag load from 1D settlement is axial to the pile, a batter pile will experience bending moment due to the drag force.

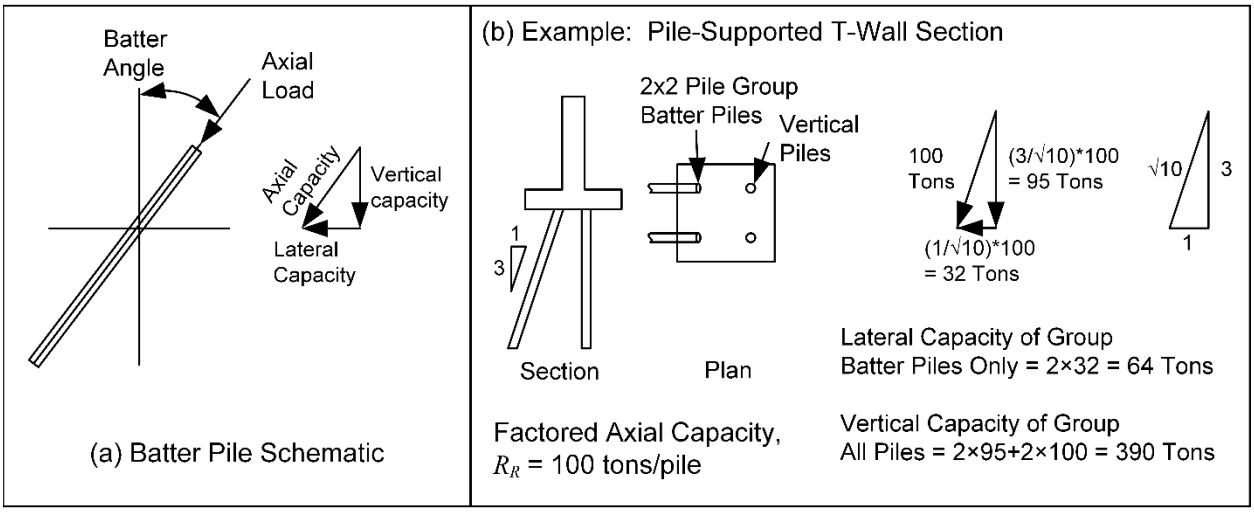

Figure 6-20 Axial Capacity of Batter Pile

6-6.4 Lateral Analysis of Single Vertical Piles.

Lateral loads and moments applied to vertical piles are resisted by the flexural stiffness of the pile and mobilization of resistance in the surrounding soil as the pile deflects. For long piles, consideration of the flexibility of the pile is very important for proper modeling of the soil and pile response. For short piles, pile flexure is small enough to be ignored and a rigid pile can be assumed.

6-6.4.1 Broms' Analysis of Rigid Short Free-Head Piles.

The ultimate geotechnical lateral capacity of short piles can be estimated using ultimate load solutions, such as the one proposed by Broms (1964a,b, 1965). Broms' analysis treats the pile as a rigid body and ignores the axial load in the pile. Separate analyses are provided for uniform undrained and drained soil profiles. There is currently no guidance for applying the Broms Method within an LRFD framework. Broms (1965) recommends scaling the lateral dead load applied to the top of the pile, $P_{t,dead}$, by a factor of 1.5 and the applied lateral live load, $P_{t,live}$, by a factor of 2.0. Since the moment applied at the top of the pile can equivalently be expressed as the product of the applied load and a height of the line of action above the ground line, the same factors apply to

the moment. Therefore, the ultimate load, $P_{t,ult}$, and moment, $M_{t,ult}$, applied to the top of the pile can be found by:

$$P_{t.ult} = 1.5P_{t,dead} + 2.0P_{t,live} \tag{6-55}$$

and

$$M_{t.ult} = 1.5M_{t,dead} + 2.0M_{t,live} \tag{6-56}$$

where:
$M_{t,dead}$ = applied moment from dead load and
$M_{t,live}$ = applied moment from live load.

Broms (1965) recommends factoring the shear strength parameters used in the analyses as follows:

$$s_u^* = 0.75 s_u \tag{6-57}$$

and

$$\phi'^* = \tan^{-1}\left(0.75 \tan \phi'\right) \tag{6-58}$$

where:
s_u = undrained shear strength and
ϕ' = effective stress friction angle.

The pile capacity is checked by comparing the actual pile length to the minimum length calculated from the analysis. If the actual length equals or exceeds the minimum length, the applied load and/or moment to the top of the element should not exceed the geotechnical lateral capacity. If the minimum length exceeds the actual length, the applied load and/or moment should be reduced, and/or the pile should be lengthened.

6-6.4.1.1 Short Pile in Undrained Soil Conditions.

For an element in undrained soil conditions, application of the ultimate load and moment to the top of the pile produces the simplified earth pressure, shear, and moment diagrams shown in Figure 6-21. The minimum length of the pile (Z_{min}) includes an exclusion zone of $1.5 \cdot b$ at the top of the pile, a length (f) that resists the applied load, and a length (g) that creates a couple to resist the applied and induced moment. The length of pile required to resist the lateral load:

$$f = \frac{P_{t,ult}}{9 \cdot s_u^* \cdot b} \tag{6-59}$$

where:
b = width or diameter of the pile.

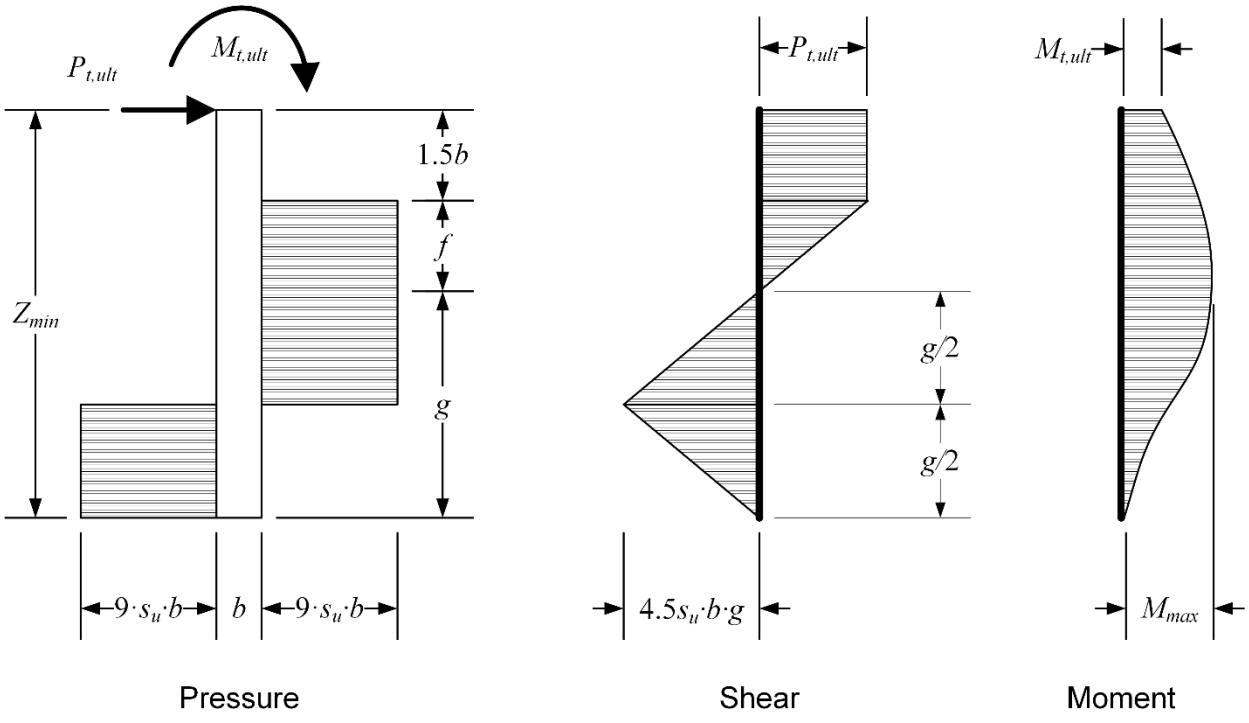

Figure 6-21 Earth Pressure, Shear, and Moment Diagrams for Broms Method in Undrained Soil Conditions (after FHWA 2010)

Once f has been determined, an expression for g can be derived by summing moments:

$$g = \sqrt{\frac{M_{t,ult} + P_{t,ult}\left(1.5 \cdot b + 0.5 \cdot f\right)}{2.25 \cdot b \cdot s_u^*}} \quad \text{(6-60)}.$$

The minimum length is then calculated as:

$$Z_{min} = 1.5 \cdot b + f + g \quad \text{(6-61)}.$$

6-6.4.1.2 Short Pile in Drained Soil Conditions.

For an element in drained soil conditions, application of the ultimate load and moment to the top of the pile produces the earth pressure, shear, and moment diagrams shown in Figure 6-22. The passive soil resistance, P_P, from Rankine theory is assumed to be developed along the entire pile length. This is multiplied by an empirical factor equal to three to account for three-dimensional effects and earth pressures acting on the nonpassive side, resulting in:

$$P_P = \frac{3}{2} b \cdot \gamma' \cdot K_P \cdot Z_{min}^2 \quad \text{(6-62)}$$

where:
γ' = effective unit weight of the soil, and
K_P = Rankine passive earth pressure coefficient determined using ϕ'*.

As shown in Figure 6-22, Broms approximates the lateral reaction force on the toe as a concentrated load. For the applied ultimate load and moment, a minimum pile length is required to develop the countering resistance. The minimum required pile length is found by summing moments about the toe and rearranging to:

$$Z_{min} = \left[\frac{2\left(P_{t,ult} \cdot Z_{min} + M_{t,ult}\right)}{b \cdot \gamma' \cdot K_P} \right]^{1/3} \quad \text{(6-63).}$$

Because Z_{min} is on both sides of the equation, an iterative process is required when both $P_{t,ult}$ and $M_{t,ult}$ are nonzero, a.k.a flagpole loading. An initial value must be assumed for Z_{min} and adjusted until the solution converges.

The maximum moment for the ultimate condition occurs at a depth, f, below the pile top where the shear force is zero, which can be determined by:

$$f = \sqrt{\frac{2P_{t,ult}}{3 \cdot b \cdot \gamma' \cdot K_P}} \quad \text{(6-64).}$$

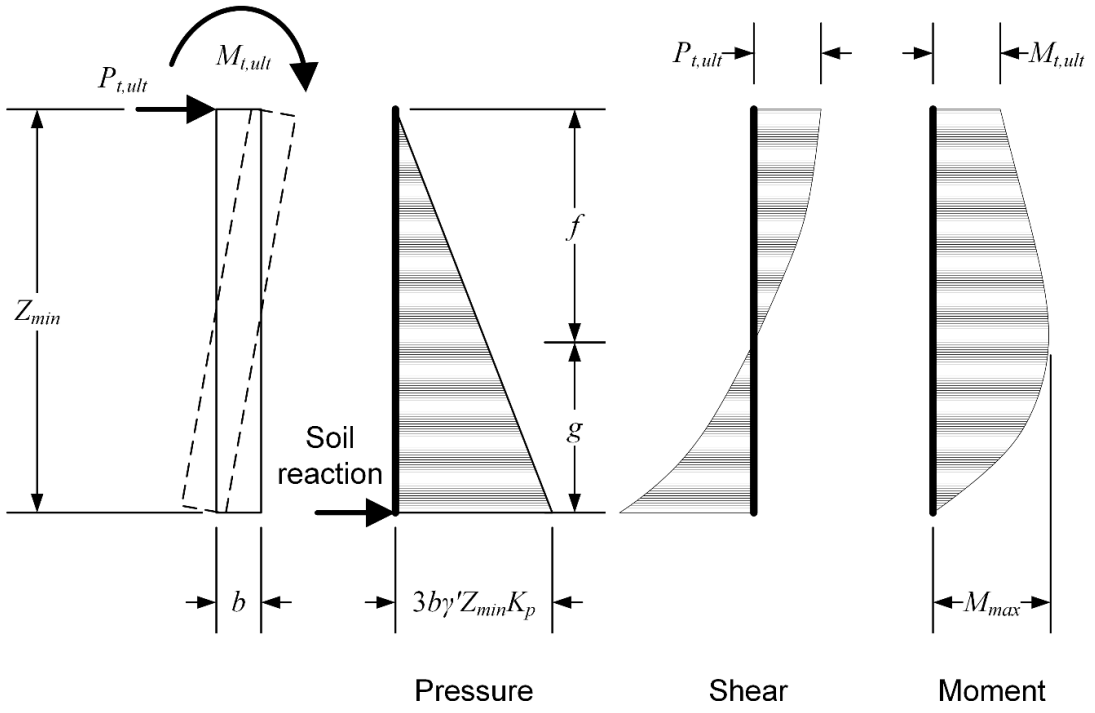

Figure 6-22 Earth Pressure, Shear, and Moment Diagrams for Broms Method in Drained Soil Conditions (adapted from FHWA 2010)

The maximum moment is found by summing moments about the location of zero shear, as:

$$M_{max,ult} = M_{t,ult} + P_{t,ult} \cdot f - \left(\frac{b \cdot \gamma' \cdot f^3 \cdot K_P}{2} \right) \quad \text{(6-65)}.$$

The dimension g is equal to Z_{min} minus the dimension f.

6-6.4.2 *p-y* Analyses.

Numerical p-y analyses (FHWA 1984, 1986) relate load (p) and deflection (y) by discretizing the pile into elements that are connected to the surrounding ground by springs and sliders, as shown in Figure 6-23. Common procedures to define p-y relationships are semiempirical and calibrated based on load test data, e.g., p-y relationships for piles in soft clay proposed by Matlock (1970). The stiffness of the pile elements in bending, the stiffness of the springs, and load required for displacement of the sliders interact to produce the load-deflection and load-moment response of the model.

Contemporary pile-soil spring models are generally nonlinear; however, it is possible to specify linear springs, if desired, to compare to the results from a linear subgrade reaction analysis. The stiffness of a linear pile-soil spring does not depend on how much it is compressed whereas the stiffness of a nonlinear spring does depend on how much it is compressed. If a slider is present, then plastic yield in the soil can be considered. These analyses are performed almost exclusively using commercial software such as LPILE and RSPile. The appendix to FHWA (2018b) provides a good summary of the commonly used p-y models.

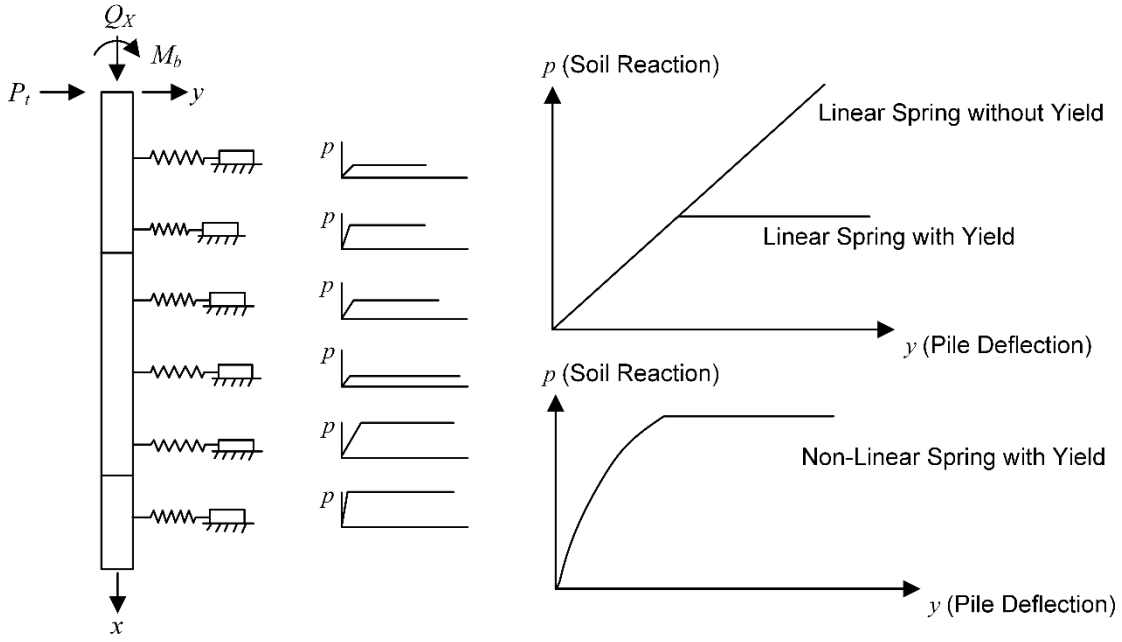

Figure 6-23 *p-y* Relationships

6-6.4.3 Characteristic Load Method.

Duncan et al. (1994) described parametric studies using LPILE and expressed the results in terms of "characteristic load" and "characteristic moment."[39] The resulting Characteristic Load Method (CLM) is simpler than p-y analyses and does not require special software. This approach can be used as a standalone option when computer software is not available or as a check of computer analyses. The CLM can be applied to single elements as described in this section and groups of elements as described in Section 6-6.4. The CLM is directly applicable to long piles in uniform ground conditions. For pile lengths less than $18b$ in clay and $14b$ in sand, consult Duncan et al. (1994) to confirm that the CLM is a suitable approach. Since the upper length of pile is the most important for the lateral response, the CLM is expected to perform acceptably well in nonuniform ground conditions that can be approximated as uniform within 8 to 10 pile widths of the pile top (Duncan et al. 1994).

The CLM estimates the lateral deflection at the top of an element due to an applied ground line load, P_t, and/or moment, M_t. The CLM does not consider the effects of applied axial load on the response of the foundation element to P_t and/or M_t. The characteristic load, P_c, and moment, M_c, are the basis for the dimensionless relationships used in the CLM and are found by applying the appropriate equations

[39] In this context, an applied load or moment equal to the characteristic load or moment will generate a normalized pile deflection equal to a constant value for a particular soil type and fixity.

provided in Table 6-34. The pile is assumed to have constant linear bending stiffness, i.e. nonlinear effects from concrete cracking are not considered. If high bending moments are anticipated, the moment of inertia of the pile (I_p), may be reduced by a factor of 0.4 to 0.5 as an allowance for cracking in concrete elements (Duncan et al. 1994). The bending moment estimated by a CLM analysis considering an uncracked section can provide insight into whether the moments are sufficiently close to the cracking moment of the section to warrant the reduction.

Table 6-34 Equations for Characteristic Parameters (Clarke and Duncan 2002)

Soil	Characteristic Parameter	Equation
Clay	P_c	$P_c = 7.34b^2\left(E_pR_I\right)\left(\frac{s_u \cdot p_{m,avg}}{E_pR_I}\right)^{0.68}$
	M_c	$M_c = 3.86 \cdot b^3\left(E_pR_I\right)\left(\frac{s_u \cdot p_{m,avg}}{E_pR_I}\right)^{0.46}$
Sand	P_c	$P_c = 1.57b^2\left(E_pR_I\right)\left(\frac{\gamma' b \cdot \phi' K_p p_{m,avg}}{E_pR_I}\right)^{0.57}$
	M_c	$P_c = 1.33b^3\left(E_pR_I\right)\left(\frac{\gamma' b \cdot \phi' K_p p_{m,avg}}{E_pR_I}\right)^{0.40}$

b = diameter or width of the element, E_p = Young's Modulus of the element, ϕ' = friction angle (in degrees), $K_P = \tan^2(45 + \phi'/2)$

$p_{m,avg}$ = weighted average p-multiplier when CLM is applied to pile groups as described in Section 6-6.5. Use Mokwa (1999) equations in Table 6-38. For single piles, use $p_{m,avg}$ =1.

R_I = the ratio of the moment of inertia of the pile section, I_p, to the moment of inertia of a solid circular section, I_{circ}. R_I is calculated as:

$$R_I = \frac{I_p}{I_{circ}} = \left(\frac{64}{\pi \cdot b^4}\right) I_p$$

NCHRP (1991) presents a method for evaluating R_I for composite sections of concrete and reinforcing steel. Table 6-35 summarizes values of R_I for a circular concrete section having a Young's modulus equal to 3,500 ksi, reinforced with steel having an Young's modulus of 29,000 ksi, and a combined cross-sectional area of 1% to 8% of the gross area of the section. The reinforcing steel is assumed to have 3 inches of concrete cover. If the values of R_I from Table 6-35 are used, the Young's modulus for the concrete should be used to calculate P_c and M_c.

The shear strength parameter values and Rankine passive earth pressure coefficient, K_P, used to calculate P_c and M_c should be based on representative values over a depth of $8 \cdot b$ because the soils near the top of the element are most important for lateral resistance.

Table 6-35 R_I Values for Circular Reinforced Concrete Section

Steel Area Ratio	R_I values for Reinforced Concrete Sections with Various Diameters			
	b = 18 in.	b = 24 in.	b = 30 in.	b = 36 in.
1%	1.06	1.07	1.09	1.09
2%	1.11	1.14	1.16	1.18
4%	1.21	1.27	1.31	1.34
8%	1.38	1.50	1.58	1.63
Assumptions: E_{steel} = 29,000 ksi, E_{conc} = 3500 ksi, 3 inches cover				

The applied load and moment are normalized by the characteristic load and moment, respectively, and the lateral deflection at the top of the element, y_t, is normalized by the element width. The dimensionless parameter values are related by power functions having values for the constant, a, and exponent, n, given in Table 6-36 and are calculated as:

$$\frac{y_t}{b} = a\left(\frac{P_t}{P_c}\right)^n \quad \text{(6-66)},$$

$$\frac{P_t}{P_c} = \left(\frac{1}{a}\frac{y_t}{b}\right)^{\frac{1}{n}} \quad \text{(6-67)},$$

$$\frac{y_t}{b} = a\left(\frac{M_t}{M_c}\right)^n \quad \text{(6-68)},$$

and

$$\frac{M_t}{M_c} = \left(\frac{1}{a}\frac{y_t}{b}\right)^{\frac{1}{n}} \quad \text{(6-69)}.$$

Table 6-36 Constants for Load and Moment Deflection Equations (after Brettmann and Duncan 1996)

Soil Type	Ratio	Fixity	a	n
Clay	P_t/P_c	Free	50.0	1.822
		Fixed	14.0	1.846
	M_t/M_c	N/A	21.0	1.412
Sand	P_t/P_c	Free	119.0	1.523
		Fixed	28.8	1.500
	M_t/M_c	N/A	36.0	1.308

When P_t or M_t equals zero, straightforward application of Equations 6-66 through 6-69 enable the deflection at the top of the element to be estimated. When both P_t and M_t are nonzero, a process of nonlinear superposition must be followed, as described below and illustrated in Figure 6-24. In this process, the deflection due to applied load, y_{tp}, is distinguished from the deflection due to applied moment, y_{tm}.

The nonlinear superposition involves seven steps:

1) Estimate y_{tp} due to P_t using Equation 6-66.

2) Estimate y_{tm} due to M_t using Equation 6-68.

3) Estimate the equivalent load (P_m) that produces y_{tm}. Substitute P_m for P_t in Equation 6-67.

4) Estimate the equivalent moment (M_p) that produces y_{tp}. Substitute M_p for M_t in Equation 6-69.

5) Combine P_t and P_m to estimate the deflection due to load and moment, y_{tpm}, using Equation 6-66.

6) Combine M_t and M_p to estimate the deflection due to moment and load, y_{tmp}, using Equation 6-68.

7) Average the deflection estimates.

The maximum moment in the element occurs at the top of the element for 100% fixity and a depth below the top for 0% fixity. Using the appropriate coefficients provided in Table 6-37, the maximum moment due to the application of P_t can be estimated as:

$$\frac{M_{\max}}{M_c} \approx a\left(\frac{P_t}{P_c}\right)^n \qquad \text{(6-70)}.$$

Refer to Duncan et al. (1994) for the procedure to estimate the maximum bending moment when P_t and M_t are both nonzero.

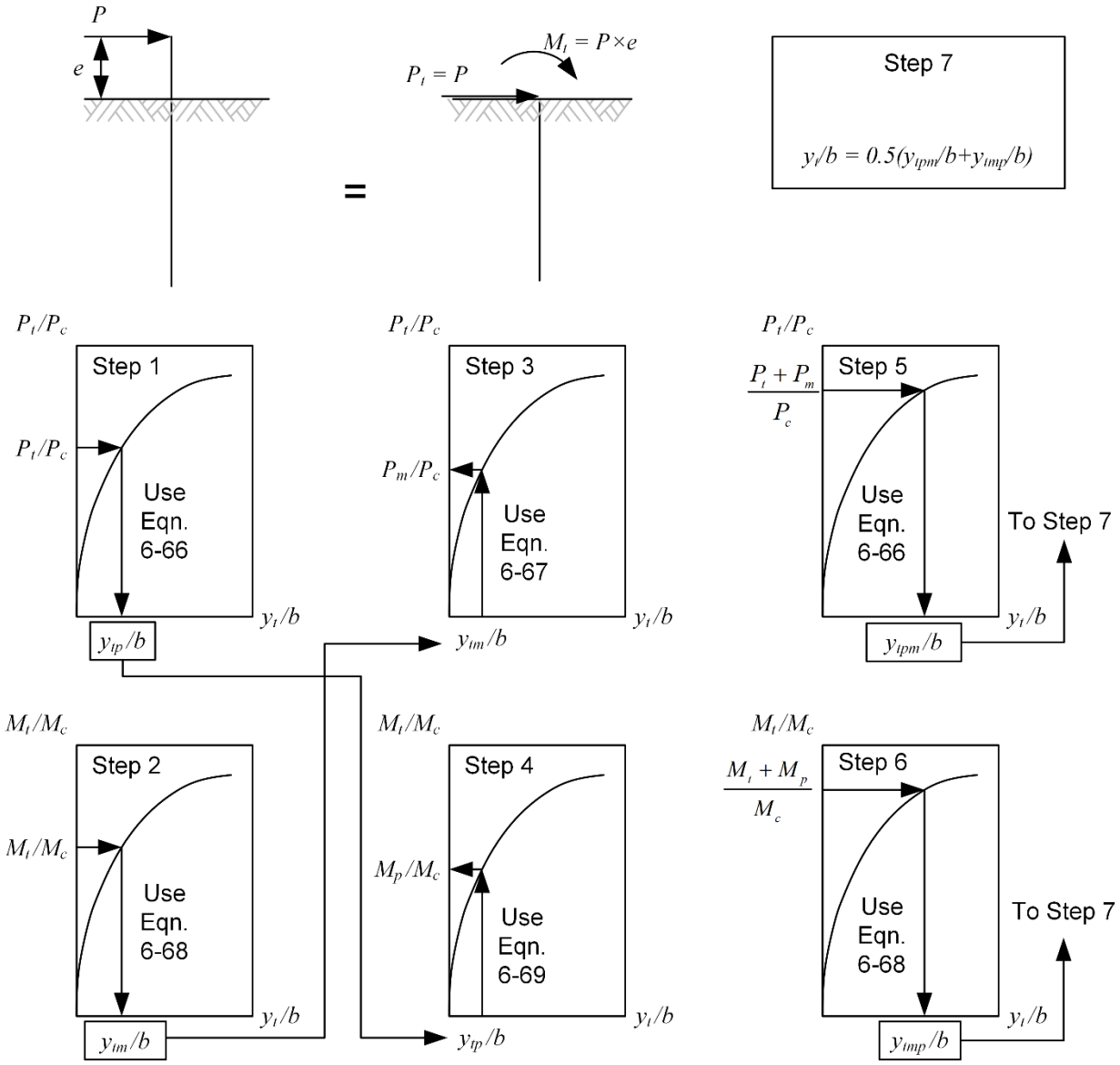

Figure 6-24 Nonlinear Superposition Process to Estimate Deflection

Table 6-37 Coefficients for Estimating the Maximum Moment

Soil	Fixity	*a*	*n*
Clay	Free	0.855	1.288
	Fixed	0.782	1.249
Sand	Free	4.28	1.384
	Fixed	2.64	1.300

Duncan et al. (1994) do not provide guidance for factoring loads and resistances for evaluating the strength limit state. An approach similar to the one proposed by Broms (1965), described in Section 6-6.4.1, to factor up applied loads and moments and factor down shear strength can be used for this purpose. The lateral deformation criterion of 10% of the element width or diameter (FHWA 2018a) can be used to define failure.

6-6.5 Groups of Vertical Piles.

Three important issues govern considerations of the lateral capacity of a pile group:

1) Pile-soil-pile interaction – At the same load per pile, lateral deflections and moments in groups are larger than for single piles because of interaction with adjacent piles through the soil in between. Piles in the corner of a group tend to carry more lateral load than piles in the center of a group, and trailing rows of piles, as defined in Figure 6-25, have significantly less lateral resistance than the lead row.

2) Interaction between the piles and the cap – The stiffness of the pile affects the distribution of loads and moments from the pile cap to individual elements. For elements with some fixity, lateral displacement will cause the cap to rotate and change the loads and moments in the elements.

3) Lateral capacity of the pile cap – If the pile cap is embedded in the ground and is protected from scour and other factors that weaken or remove the surrounding ground, there can be significant passive resistance developed between the cap and the ground to counteract lateral loads (Duncan and Mokwa 2001a).

Items 1 and 2 are group effects that are typically addressed by considering the fixity of the pile group in the cap and through the use of p-multipliers to reduce the force, p, at a particular deflection, y, in the p-y curves. A significant body of experimental and analytical work described in FHWA (2018b) explores appropriate p-multipliers to use for design. For the pile spacing parallel to the direction of loading, pile-soil-pile interaction becomes insignificant at and beyond a center-to-center pile spacing of $6 \cdot b$ (Mokwa 1999). For a single row of piles spaced perpendicular to the direction of loading, pile-soil-pile interaction becomes insignificant at and beyond a center-to-center pile spacing of $5 \cdot b$ (FHWA 2018b). Since it is not advisable to install elements closer than $3 \cdot b$, the primary focus is on values for p-multipliers, p_m, for spacing between $3 \cdot b$ and $6 \cdot b$.

AASHTO (2020) guidance, extrapolated to a pile spacing of $6 \cdot b$, is provided in Table 6-38. Separate p-multipliers exist to account for liquefied soil. The terminology for rows of elements used by AASHTO (2020) is graphically defined in Figure 6-25. Be aware that different sources may use different terminology. Only small sensitivity of p-multipliers to soil type and rate of loading have been observed, and these effects are

usually ignored (FHWA 2018a). Alternatiavely, equations for p-multipliers proposed by Mokwa (1999) are also provided in Table 6-38.

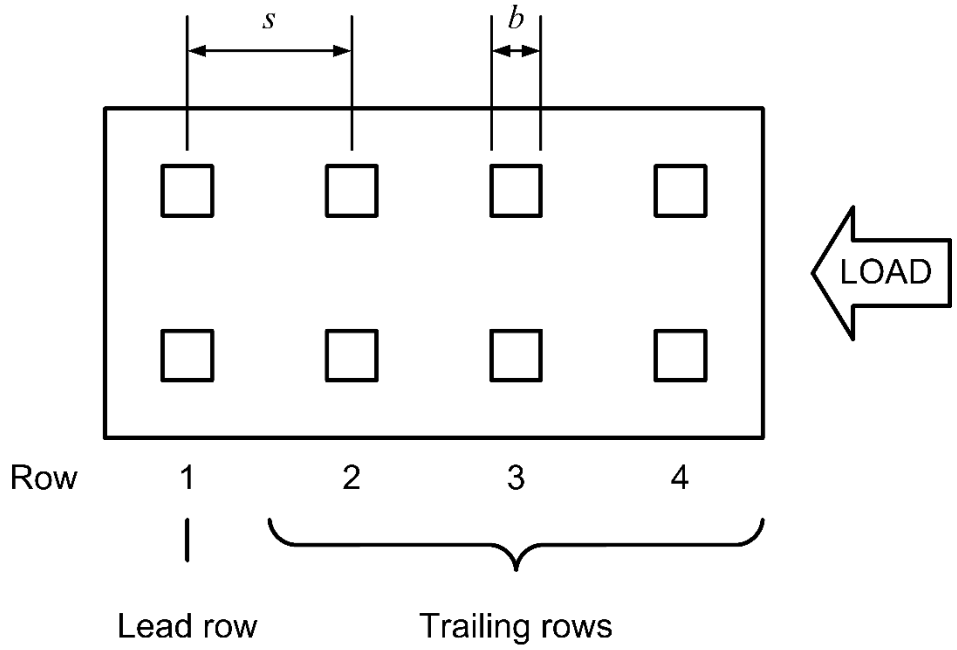

Figure 6-25 Geometry for a Group of Foundation Elements Subjected to Lateral Load

Table 6-38 p-Multipliers to Account for Group Effects in Design (after AASHTO 2020, Mokwa 1999)

Row	AASHTO (2020) p-multiplier, p_m			Mokwa (1999) p_m Equations
	s/b = 3	s/b = 5	s/b > 6	
1	0.80	1.00	1.00	$p_m = 0.06(s/b) + 0.64 \le 1$
2	0.40	0.85	1.00	$p_m = 0.11(s/b) + 0.34 \le 1$
3	0.30	0.70	1.00	$p_m = 0.14(s/b) + 0.16 \le 1$
4 and higher	0.30	0.70	1.00	$p_m = 0.16(s/b) + 0.04 \le 1$

The lateral resistance of the pile cap can be addressed through application of earth pressure theory and a load-displacement relationship for mobilization of passive resistance. Passive resistance can be neglected or reduced in design due to the potential for loss of soil around the cap due to factors such as scour and future excavation. Shearing resistance on the sides and base of the pile cap are typically neglected, and the passive resistance is partially offset by active pressure acting on the trailing side of the cap (Coduto et al. 2016). Passive resistance is most accurately

estimated using log spiral earth pressure theory with correction for 3D effects (Duncan and Mokwa 2001, Mokwa 1999); however, Rankine theory provides a conservative estimate that may be reasonable in some cases. Mokwa (1999) and Duncan and Mokwa (2001) present a hyperbolic load-displacement relationship for mobilization of passive resistance. Assuming that full passive resistance is mobilized at a lateral displacement equal to 4% of the height of the pile cap (Mokwa 1999) and the failure ratio is equal to 0.85 (Duncan and Mokwa 2001), the mobilized passive resistance can be estimated as:

$$\frac{P_{P,mob}}{P_{P,ult}} = \left(\frac{y}{0.85y + 0.006H_{cap}} \right) \leq 1 \tag{6-71}$$

where:
$P_{P,mob}$ = mobilized passive resistance,
$P_{P,ult}$ = fully-mobilized passive resistance,
y = average lateral movement of the pile cap, and
H_{cap} = height of the pile cap in the same length units as the lateral deflection.

Lateral analyses for groups of foundation elements can be performed in a number of ways:

1) Commercial software, e.g., LPILE, developed for single elements with p-multipliers applied to the p-y relationships. This approach empirically accounts for pile-soil-pile effects but does not address interactions between the piles and the cap and lateral resistance provided by an embedded cap. One option is to perform analyses for each row of elements with different p-multiplier values (Brown and Bollmann 1993). A simpler option is to use a weighted average value of p-multiplier, $p_{m,avg}$, for all rows, which implicitly assumes that all piles carry the same lateral load. This is not actually the case since the p-y relationship of each pile, or at least each row, is different and the lateral deflection at the top of all of the piles is approximately the same. A solution is to scale the average maximum calculated moment by a factor to account for the peak value in the group, e.g., for elements at the corners in the lead row. The moment scaling factors recommended by Brown et al. (2001) are 1.20 for s/b equal to 3, 1.15 for s/b equal to 4, 1.05 for s/b equal to 5, and 1.00 for s/b equal to 6.

2) Purpose-built commercial software developed for groups of elements, e.g., GROUP and RSPile. This approach empirically accounts for pile-soil-pile effects, interactions between the piles and the cap, and lateral resistance provided by an embedded cap.

3) General finite element or finite difference codes, e.g., ABAQUS and PLAXIS.

4) Clarke and Duncan (2002) proposed an adapted version of the CLM described in Section 6-6.4.3 that empirically accounts for pile-soil-pile effects and lateral resistance provided by an embedded cap. The adapted CLM for pile groups uses a weighted average of the p-multipliers proposed by Mokwa (1999) for the number of rows in the pile group. The weighted average p-multiplier is applied to the characteristic load and moment applied to the top of the pile as shown in Table 6-38. The spreadsheet PileGroup2 (Robinette and Duncan 2005) applies the CLM for pile groups for the case of loads applied to the pile cap. The case where both lateral load and moment are applied to the pile cap is not able to be modeled using the CLM as currently formulated.

All of the approaches listed above are capable of analyzing simple problems to a reasonable degree of accuracy where a lateral load is applied to a group of elements that is either fixed or pinned within a pile cap. In cases where complex loads and/or moments are applied to pile caps, the problem should be approached using either purpose-built commercial software or numerical modeling software.

6-7 STRUCTURAL CAPACITY.

This section introduces structural design concepts that are useful for the geotechnical design engineer. Readers seeking detailed aspects of structural design should consult design manuals that are specific to the type of foundation, relevant codes (e.g., IBC), and specifications (e.g., ASTM, ACI, AASHTO).

At the most basic level, structural design of a foundation within an LRFD framework includes the following:

1) Determining factored loads for the limit state under consideration,

2) Assigning trial foundation dimensions and properties,

3) Checking axial resistance in compression and tension,

4) Checking shear and moment resistance,

5) Checking resistance for combined axial and loads and moments,

6) Designing to meet demands for steps 3, 4, and 5 as well as constructability and efficiency, and

7) Designing splices, connections, joints, and pile caps.

6-7.1 Allowable Stresses.

Stresses in the foundation element must remain sufficiently below levels that will cause structural damage over the life cycle of the foundation. For all types of foundations, this includes the stresses that the element may experience during normal conditions and during extreme events. For driven piles, stresses during handling and driving are also important. Timber and steel piles are generally tolerant of stresses that arise during typical handling and lifting by a crane; however, concrete piles are susceptible to damage by improper handling, such as using an insufficient number or spacing of pickup points.

6-7.1.1 Driving Stresses.

Driving stresses are estimated during design using a wave equation analysis, which is discussed in Section 6-9.3, and are monitored during construction using high-strain dynamic measurements, as discussed in Section 6-9.4. The high strain rate and short duration of driving-induced stresses allow limits to be set closer to the strength limit state as compared to static design. AASHTO (2020) LRFD resistance factors for driving stresses are provided in Table 6-39. Limiting values for driving stresses, σ_{dr}, are presented in the following sections for steel, concrete, and timber piles. Excessive dynamic stresses during driving can be mitigated through careful selection of the hammer, hammer settings, and pile cushion in the case of concrete piles.

Table 6-39 AASHTO (2020) Resistance Factors During Pile Driving

Pile type	Resistance Factor for Pile Driving, φ_{da}
Steel piles	1.0
Concrete piles	1.0
Timber piles	1.15

6-7.1.1.1 Steel Piles.

Driving stresses for steel piles are limited by the yield strength, f_y. The yield stress for common steel pipe piles and H-piles is provided in Table 6-40. Tensile driving stresses are generally below levels that approach the yield strength. AASHTO (2020) specifications limit compressive stresses to:

$$\sigma_{dr} \le \varphi_{da}\left(0.9 f_y\right) \tag{6-72}$$

Table 6-40 Yield Stress and Driving Stress Limit for Common Steel Piles

Steel Pile Type	Designation or Grade	Yield Stress, f_y (ksi)	Maximum σ_{dr} (ksi)
Pipe piles	ASTM A-252 Grade 2	35	31.5
	ASTM A-252 Grade 3	45	40.5
	ASTM A-252 Grade 3 (Mod)	50 to 80	45 to 72
H-piles	A-36	36	32.4
	ASTM A-572-50	50	45
	ASTM A-572-60	60	54

6-7.1.1.2 Concrete Piles.

Concrete piles are susceptible to damage by compressive and tensile stresses developed during driving. The compressive stresses are assumed to be carried by the concrete, which has a design strength in compression, f_c', typically between 3 and 8 ksi. In current practice, nearly all concrete piles are prestressed in compression to some amount, f_{pe}, typically 0.5 to 1.0 ksi, that is always substantially below f_c'. The longitudinal steel reinforcement is assumed to be responsible for resisting most, but not all, tensile stresses.

AASHTO (2020) specifications limit maximum compressive driving stresses to:

$$\sigma_{dr,comp} \le \varphi_{da}\left(0.85 f_c' - f_{pe}\right) \quad (6\text{-}73).$$

AASHTO (2020) specifications limit maximum tensile driving stresses to:

$$\sigma_{dr,tensile} \le \varphi_{da}\left(0.095\sqrt{f_c'} + f_{pe}\right) \quad \text{(ksi)} \quad (6\text{-}74).$$

6-7.1.1.3 Timber Piles.

For timber piles, AASHTO (2020) specifications limit maximum compressive and tensile stresses to the limit found by:

$$\sigma_{dr} \le \varphi_{da}\left(2.6 f_{cto}\right) \quad (6\text{-}75)$$

where:
f_{cto} = reference value for compressive strength parallel to the wood grain.

Engineering properties for timber can be found in the *Wood Handbook* (USDA 2010). Values of f_{cto} for typical woods used for timber piles are listed in Table 6-41.

Table 6-41 Allowable Stresses Parallel to the Grain for Treated Timber Graded in Accordance with ASTM D25 (AWPI 2002)

Species	f_{cto} (ksi)	Maximum σ_{dr} (ksi)
Southern pine	1.20	3.59
Douglas fir	1.25	3.74
Lodgepole pine	1.15	3.44
Red oak	1.10	3.29
Red pine	0.90	2.69
Southern pine applies to loblolly, longleaf, shortleaf, and slash pines. Douglas fir applies to coastal variety. Red oak applies to northern and southern red oak. Red pine applies to US-grown red pine.		

6-7.1.2 Structural Resistance for Static Design.

When structural capacity of driven piles and drilled shafts is evaluated within an LRFD framework, AASHTO (2020) recommends the LRFD resistance factors provided in Table 6-42. Factored resistances in axial compression (P_r), flexure (M_r), and shear (V_r), must exceed the factored applied axial load (P_u), moment (M_u), and shear load (V_u). Combined axial loading and flexure is handled using interaction equations and/or diagrams to check that stresses and strain from combined loading are sufficiently below the strength limit. The details of the required design checks can be found in design manuals for specific foundation types.

When structural capacity of driven piles and drilled shafts is evaluated within an ASD framework, Table 6-43 provides allowable stresses for materials used in deep foundations as recommended by IBC (ICC 2015).

Table 6-42 Resistance Factors for Structural Strength Limit State (AASHTO 2020)

Foundation Material	Condition	Pile Type	Resistance Factor[A]
Steel (driven piles)	Axial compression – Good driving conditions	H-piles Pipe piles	0.60 0.70
	Axial compression – Potentially damaging driving conditions	H-piles Pipe piles	0.50 0.60
	Combined axial and flexural for undamaged piles	Axial – H-piles Axial – Pipe piles Flexure – Both types Shear – Both types	0.70 0.80 1.00 1.00
Concrete/grout and steel (micropiles)	Compression -	Cased & uncased	0.75
	Tension	Cased & uncased	0.80
Concrete and steel (driven piles and drilled shafts)	Tension controlled[B,C]	Reinforced concrete Prestressed concrete	0.90 1.00
	Compression controlled[B]	Reinforced concrete Prestressed concrete	0.75 0.75
	Shear	Any type	0.90
Timber	Compression parallel to grain Tension parallel to grain Flexure Shear	Any type	0.90 0.80 0.85 0.75

[A] AASHTO (2020) states that resistance factors should be reduced by 20% for single drilled shafts, small pile groups (<5 piles) to account for lack of redundancy, and micropiles in marginal ground conditions.
[B] Refer to AASHTO (2020) for guidance to interpolate between tension and compression-controlled sections based on strain limits for combined axial and flexure loading.
[C] Tension is assumed to be resisted by the reinforcing steel only.

Table 6-43 Recommended Allowable Stresses for Typical Foundation Materials (ICC 2015)

Material	Condition	Maximum Allowable Stress
Concrete or grout in compression	Cast-in-place with permanent casing that is mandrel driven and not included in design resistance	$0.40f'_c$
	Cast-in-place in a pipe, tube, other permanent casing, or rock	$0.33f'_c$
	Cast-in-place without a permanent casing	$0.30f'_c$
	Precast nonprestressed	$0.33f'_c$
	Precast prestressed	$0.33f'_c$ to $0.27f_{pe}$
Nonprestressed reinforcement	Compression	$0.40f_y \leq$ 30ksi
Steel in compression	Cores within concrete-filled pipes or tubes	$0.50f_y \leq$ 32 ksi
	Pipes, tubes, or H-piles with justification[A]	$0.50f_y \leq$ 32 ksi
	Pipes and tubes for micropiles	$0.40f_y \leq$ 32 ksi
	Other pipes, tubes, or H-piles	$0.35f_y \leq$ 16 ksi
	Helical piles	$0.60f_y \leq 0.50\ f_u$
Nonprestressed reinforcement in tension	Within micropiles	$0.60f_y$
	Other conditions	$0.5f_y \leq$ 24 ksi
Steel in tension	Pipes, tubes, or H-piles with justification[A]	$0.50f_y \leq$ 32 ksi
	Other pipes, tubes, or H-piles	$0.35f_y \leq$ 16 ksi
	Helical piles	$0.60f_y \leq 0.50\ f_u$
Timber	In accordance with ANSI/AWC NDS	

Variables: f'_c = compressive strength of concrete or grout, f_{pe} = effective prestress, f_y = yield strength of steel, f_u = tensile strength of steel

[A] With substantiating data to justify higher allowable stresses, e.g., geotechnical investigation and load tests.

6-7.2 Buckling.

Foundation elements act as structural columns and are theoretically vulnerable to buckling. A basic Euler-type analysis of buckling due to axial load considers an unbraced column with pinned end supports. When the end conditions are not both pinned, an effective length factor is used to scale the actual unbraced column length up or down to an equivalent effective length with pinned conditions on both ends. Guidance for the effective length factor is provided by FHWA (2016) and UFC 4-151-10 (UFC 2012) since the restraint provided by the ground and the pile cap do not translate to theoretical end conditions in a straightforward way. From these sources, the smallest recommended effective length factor is equal to 0.65 for the case where pile embedment and the top connection provide significant rotational and translational restraint. The largest value is equal to 2.0 for the case where the ground and top connection provide little restraint against rotation and the top provides little restraint against translation. Buckling is primarily a concern for unbraced piles in air, water, and/or liquefied soil.

In addition to the unbraced length in liquids, the lateral support provided by the ground may be insufficient to brace the element for some depth into the ground. The embedded length of the element that contributes to the total unbraced length is known as the depth to fixity, Z_f (Davisson and Robinson 1965). This length can be found for elements in uniform undrained soil conditions by:

$$Z_f = \sqrt{2}\left(\frac{E_p I_p}{b \cdot k_h}\right)^{0.25} - \quad (6\text{-}76)$$

where:
E_p = elastic modulus of the pile (F/L^2),
I_p = moment of inertia of the pile (L^4),
b = pile width (L), and
k_h = coefficient of horizontal subgrade reaction (F/L^3).[40]

The moment of inertia should be for the weak axis (FHWA 2018b), unless bending is only expected in the strong direction. For undrained conditions modeled by constant k_h, the product of pile width, b, and k_h, is assumed to equal the elastic modulus of the soil, E_s, (AASHTO 2020) and can be estimated as a function of undrained strength:

$$E_s = b \cdot k_h = C \cdot s_u \quad (6\text{-}77)$$

where
C = constant depends on overconsolidation and soil mineralogy.

Davisson (1970) recommends C of 67, which is very low and may underestimate the support provided by the soil. The value of C can also be determined by correlations, such as the one presented in Figure 5-30.

For groups of piles, the value of E_s is affected by neighboring piles when the normalized spacing, s/b, is less than 8. For s/b equal to 3, E_s should be reduced to 25 percent of the value for a single pile (AASHTO 2020). Interpolation should be applied for s/b between 3 and 8.

Coarse-grained soils become stiffer with depth. The horizontal subgrade modulus ($b \cdot k_h$) can be modeled as increasing at a rate, n_h. The parameter n_h can be estimated using Table 6-44 from AASHTO (2020). For elements in coarse-grained soils, the depth to fixity can be estimated as:

[40] Dimensions are provided for this equation for clarity: F = force and L = length.

$$Z_f = 1.8\left(\frac{E_p I_p}{n_h}\right)^{0.2} \quad (6\text{-}78)$$

Table 6-44 Rate (n_h) of Increase in Subgrade Modulus with Depth for Sands (AASHTO 2020)

Density	n_h (ksi/ft)	
	Dry or moist	Submerged
Loose	0.417	0.208
Medium	1.110	0.556
Dense	2.780	1.390
Note the mixed units for n_h.		

UFC 4-151-10 (UFC 2012) provides guidance for the depth to fixity for piling used for waterfront construction. For soft fine-grained soils and loose sands, the depth to fixity can be assumed to range from 8 to 12 ft, with the upper end of the range applying to elements in soft clay having a flexural rigidity (EI) greater than 1010 lbs-in^2. For other ground conditions, the depth to fixity can be assumed to equal 5 ft.

When p-y analysis is applied (Section 6-6.4.2), soil-pile interaction is evaluated directly, and the depth to fixity concept is not needed. Coduto et al. (2016) criticizes the depth to fixity concept for ignoring the soil resistance above the fixity point.

Despite the theoretical possibility of buckling, there is little to no evidence of deep foundation buckling occurring under realistic field conditions (FHWA 2016, Coduto et al. 2016). According to Section 1810.2.1 of IBC (ICC 2015), “Any soil other than fluid soil shall be deemed to afford sufficient lateral support to prevent buckling of deep foundation elements and to permit the design of the elements in accordance with accepted engineering practice and the applicable provisions of this code.” During driving, there is some potential for buckling, which can be mitigated by managing hammer energy during initial driving and/or by providing temporary lateral support (Coduto et al. 2016).

6-7.3 Considerations for Pile Caps.

FHWA (2016) describes background information needed to develop a preliminary size of a pile cap and directs readers to a manual published by the Concrete Reinforcing Steel Institute (Mays 2015) for detailed design guidance according to ACI (2014).

The minimum pile cap width can be established based on the width and length of the pile group at the top of the piles (Figure 6-15) plus twice the minimum distance between the edge of the pile and the edge of the cap. For driven piles and micropiles, AASHTO (2020) stipulates a minimum edge of pile to edge of cap distance of 9 inches. Minimum spacing between elements is provided in Table 6-4 for different foundation types.

The minimum thickness of the pile cap can be established based on the minimum embedment of the piles into the cap plus the structural depth, which includes a minimum 3-inch clear space between the top of the pile and the reinforcement. For driven piles and micropiles, AASHTO (2020) requires that the undamaged top of piles extend a minimum of 12 inches into the cap or 6 inches if the pile is attached to the cap by embedded bars or strands. FHWA (2016) recommends using Equation 5-81 to make an initial estimate of the cap thickness:

$$t_{cap} = \frac{P_{ui}}{12} + 30 \tag{6-79}$$

where:
t_{cap} = estimate of cap thickness (in inches) and
P_{ui} = factored maximum single pile axial load (in kips).

Structural analysis checks should be performed to confirm adequate resistance for several modes of failure in the cap including two-way punching shear, one-way beam shear, and bending.

6-7.4 Design for Drag Force.

The concepts of negative skin friction and the associated drag force are discussed in Section 6-5.7. In most cases, the drag force is insufficient to exceed the structural capacity of the element, especially considering the high stresses that occur during pile driving. In fact, the drag force can act to prestress the column which reduces the elastic compression due to live loads (Fellenius 2021).

However, as indicated in Table 6-30, it is prudent to include the drag force in the structural strength limit state. The drag force is evaluated by the following six steps:

1) Select the foundation element type, width, and length for the analysis.

2) Characterize the nominal side and base resistances using an appropriate SCA method. Keep in mind that lower unit side friction from lower α and β is conservative for resistance, while higher unit side friction from higher α and β is conservative for negative skin friction. When side friction is evaluated using an effective stress method, such as the Beta method, Seigel et al. (2013) demonstrate analytically that unit side friction increases due to the increases in vertical stress. Nominal side and base resistances should be evaluated considering the vertical effective stress profile that includes stress change(s) producing settlement.

3) Characterize the axial displacement required to mobilize side and base resistances. Typically, only small relative movements, e.g., 0.1 inch, between

the column and ground are needed to fully mobilize side resistance. Larger movements are usually needed, e.g., 4% to 10% of the column width, to fully mobilize the base. A conservative approach for evaluating the drag force is to assume that enough relative displacement occurs to fully mobilize side friction and base resistance. A more sophisticated approach is to use static analysis software that accounts for the relationships between axial displacement and side friction, known as t-z curves, and the relationship between axial displacement and base resistance, known as a q-z curve.

4) Develop a diagram similar to Figure 6-26 that shows the axial load and resistance versus depth along the element. The resistance curve (Curve A in Figure 6-26) is created by plotting the mobilized base resistance from Step 3 at the base elevation and adding the cumulative positive skin friction (side resistance) as a function of depth along the length of the element. If side and base resistances are assumed to be fully mobilized, the resistance curve will pass through the nominal geotechnical resistance at the elevation of the top of the element. The load curve (Curve B in Figure 6-26) is created by plotting the unfactored permanent load on the element at the top of the element and adding the cumulative negative skin resistance (drag load) as a function of depth along the length of the element.

   Transient loads are not included at the top of the pile since these loads are assumed to temporarily compress the pile and reverse the skin friction. For the short interval of time that the transient load acts on the pile, positive skin friction is mobilized below the top of the pile over a length that develops enough shaft resistance to counter the transient load. When the transient load is not acting on the pile, the pile rebounds and the skin friction again becomes negative. Therefore, when the transient load is applied to the pile, the drag force is reduced by an equal amount.

5) Locate the neutral plane and the estimated maximum load in the pile, Q_{np}, at the intersection of the load and resistance curves. Note that increasing the permanent load applied to the top of the pile causes the neutral plane to occur at a higher elevation, with the limiting case being where the applied load equals the nominal geotechnical resistance and there is no neutral plane. Conversely, the neutral plane will be located near the interface of the column and the bearing layer for an end-bearing column bearing in a stratum that is much stiffer than the compressible soil.

6) Check the structural limit state by comparing the factored axial structural capacity, P_r, to the factored permanent load and the drag force. The applied permanent load, Q_d, excluding live load, should be factored by the appropriate load factor, γ_p, equal to 1.25 according to AASHTO (2020). The drag force (DF)

is equal to the difference between the maximum load identified in Step 5 and Q_d. FHWA (2016) reports that at least one state transportation agency uses a load factor equal to 1.10 for the drag force, as shown in:

$$1.25 \cdot Q_d + 1.10\left(Q_{np} - Q_d\right) \le P_r \quad \text{(6-80)}.$$

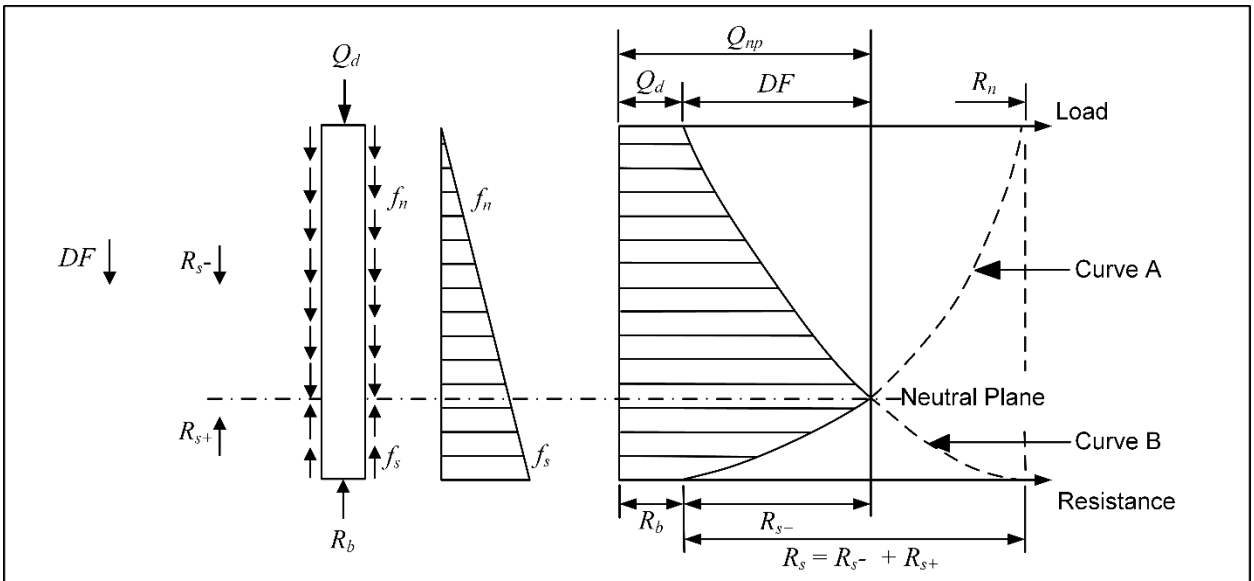

Constructing the Neutral Plane

Q_d = Unfactored Permanent Load	R_s = Shaft Resistance	R_b = Base Resistance
DF = Drag Force at Neutral Plane	R_s- = Negative Shaft Resistance	f_n = Unit Negative Shaft Resistance
R_n = Nominal Resistance	R_s+ = Positive Shaft Resistance	f_s = Unit Positive Shaft Resistance

Figure 6-26 Locating the Neutral Plane

6-8 STATIC LOAD TESTING.

6-8.1 Introduction.

Static load testing provides the most direct way to assess the performance of deep foundations. As discussed in Section 6-8.2, different types of load tests can assess performance in axial compression, axial tension, and lateral loading. The loading used in load tests can be applied incrementally (most common) or to achieve a constant rate of deflection, and some tests are designed to apply cyclic loading. Load testing performed as part of a test pile program prior to construction guides the selection of installation criteria and element length and provides an opportunity to refine the design for constructability and economic efficiency. Load testing performed on production elements during construction provides proof that the tested foundation is adequate, i.e., "proof test," and, in some cases, allows for additional refinements to element lengths and installation criteria.

Procedures for axial compressive load tests are described in ASTM D1143, procedures for axial tensile load tests are described in ASTM D3689, and procedures for lateral load tests are described in ASTM D3966. Section 6-8 focuses on conventional axial load testing where load is applied to the top of the element. The interpretation of conventional axial compressive load tests is described in Section 6-8.3.

Static load tests require engineering oversight as well as personnel and equipment time to mobilize/demobilize the loading testing equipment and to set up and perform the test. The return on the investment of performing load tests is an increase in confidence in the expected foundation performance that is reflected in higher resistance factors or lower factors of safety. Table 6-45 provides recommended resistance factors when static load testing is applied as part of the design and/or construction phases of the project, which may also include dynamic testing and/or wave equation analysis (Section 6-9). Additionally, load tests may reveal ground conditions that are better, or worse, than what was considered in design.

6-8.2 Axial Load Tests.

Conventional axial load tests, sometimes referred to as top-down tests, apply compressive or tensile loads to the top of the element, or a group of elements, using a hydraulic jack and measure the axial displacement at the top of the element. Testing a single element is more common than simultaneously testing a group of elements. To apply the load, the hydraulic jack requires a stiff reaction beam or load frame as illustrated in Figure 6-27(a). Movement of the reaction beam is typically resisted by two or more reaction elements installed around the test element at a sufficient distance away to mitigate pile-soil-pile interaction. ASTM D1143 requires a clear distance of at least 5 times the largest pile width or 8 ft, whichever is greater. In a compression test, the reaction elements resist movement of the reaction beam by uplift resistance. In a tension test, however, the reaction elements are put into compression. A kentledge load test uses a weighted platform instead of reaction elements for compression testing; however, this type of test is limited by the amount of weight that can safely be positioned over the test element.

Table 6-45 Recommended Strength Limit State Resistance Factors for Axial Loading based on Static and Dynamic Testing

Foundation Technology	Recommended Resistance Factor for Axial Loading[A,B]
Driven Piles in compression (FHWA 2016)	0.80 – at least one load test along with dynamic testing[C] of at least 2% of production piles or two piles, whichever is greater 0.75 – at least one load test without dynamic testing 0.75 – dynamic testing[C] of 100% of production piles 0.65 –dynamic testing[C] of at least 2% of production piles or two piles, whichever is greater 0.50 – Wave equation analysis
Driven Piles in tension (FHWA 2016)	0.60 – at least one load test 0.50 – dynamic testing[C]
Drilled shafts in compression (FHWA 2018a)	0.70 – at least one load test
Drilled shafts in tension (FHWA 2018a)	0.60 – at least one load test
Micropiles in compression (AASHTO 2020)	Same as driven piles, but limited to 0.70
Micropiles in compression (AASHTO 2020)	Same as driven piles, but limited to 0.70

[A] AASHTO (2020) states that resistance factors for single drill shafts and small pile groups (<5 piles) should be reduced by 20% to account for lack of redundancy
[B] Minimum number of tests is on a per site condition basis.
[C] Dynamic testing is evaluated for restrike conditions and includes signal matching analysis.

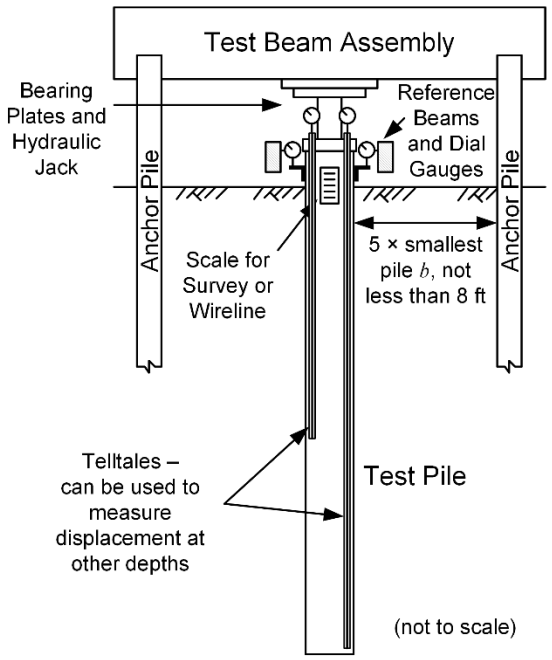

Test Procedure Details for Compressive Loading (ASTM D1143) and Tensile Loading (ASTM D3689)

	Quick Test Procedure A	Maintained Load Test Procedure B
Test Increments	5% of Failure Load (FL) up to FL	25% of FL up to 200% of FL (150% for group)
Time per Increment	4 to 15 min	2 hr or displacement rate < 0.01 in./hr
Readings	At end of increment	At end of increment
Failure Load Hold	Hold FL longer to check creep behavior	Hold at least 12 hr & up to 24 hr. If fails, then hold until displacement equals 0.15b
Unload	5 to 10 decrements, equal duration	Decrements at 25% of max load, hold 1 hr each
Total Time	2 to 6 hr	About 2 days

(a) Schematic of Top-Down Axial Load Tests and Test Procedure Details

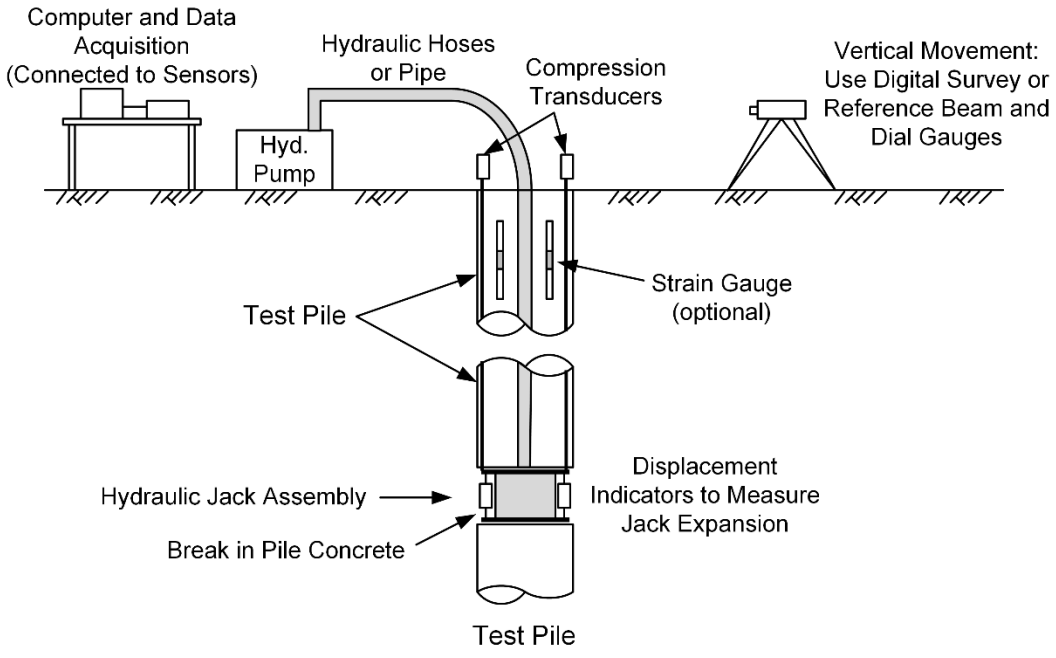

(b) Schematic of Bi-Directional Axial Load Test

Figure 6-27 Schematics of Top-Down and Bi-Directional Axial Load Tests (after ASTM D1143, ASTM D3689, ASTM D8169)

Displacement at the top of the tested element is measured using dial gauges and/or linear variable displacement transducers (LVDTs). Displacements are measured relative to one or more reference beams that are supported independently of the load frame and not significantly affected by ground movements. Redundant measurement methods, such as a scale, mirror, and wire system, and/or optical survey methods, are included as good practice to provide a backup or to confirm the function of the primary measurement devices. The shape of the resulting load-displacement relationship at the top of the element can infer the distribution load along the shaft and base of the test element. As shown in Figure 6-11, an element that develops axial capacity primarily from side resistance tends to mobilize resistance at smaller displacement and plunge more distinctly as compared to an element with large base resistance. In some cases, telltales and/or strain gauges are installed on the test element prior to testing to provide additional measurements of displacement or strain. These additional measurements are needed to make a good estimate of the transfer of load between the element and the ground through shaft and base resistance.

Standard procedures for compressive loading (ASTM D1143) and tensile loading (ASTM D3689) are summarized in Figure 6-27(a). Variations of the Maintained Load Test described in ASTM D1143 reload the test element to failure (Procedure C) or load/unload the element using a shorter 1-hour duration for each load level (Procedure D).

Bi-directional load testing is an alternative used when a conventional load frame and reaction elements are impractical due to high anticipated element capacity and/or challenging site conditions, e.g., foundations in deep water. Standardized procedures for performing a bi-directional load test are described in ASTM D8169. This type of testing is primarily applied to test drilled shafts; though, it is also occasionally applied to CFAs and large diameter steel pipe piles. As shown in Figure 6-27(b), the loading equipment for bi-directional testing consists of one or more expendable hydraulic pancake jacks, e.g., an Osterberg Cell, positioned at or near the bottom of the test element. The jacks are supplied with pressurized hydraulic fluid through lines extending to the top of the element. Once the concrete in the test element has gained sufficient strength, the test can be performed by gradually expanding the jack and separating the test element into upper and lower sections.

In a bi-directional test, each section of the element provides the reaction for the other. The displacement of the jack moves the upper section upward and the lower section downward. Movement of the upper section is resisted by the buoyant weight of the element, the side resistance along the upper section, and any additional surface loading placed on top of the element to assist with the mobilization of base resistance. Movement of the lower section is resisted by the side resistance along the lower section and base resistance. The jack is located in the element at the location where the anticipated resistances to the upward and downward movement of the test element are

equal. The load applied to the upper and lower sections of the test element is typically measured using pressure applied to the jack. Displacements are measured using expendable LVDTs and telltales. Strain gauges are sometimes embedded in the test element to estimate load transfer. Once the test is completed, the jack is filled with grout, and the element can be included in the foundation.

6-8.3 Interpretation of Axial Compressive Load Tests.

Interpretation of proof tests not taken to failure are generally limited to confirming that the magnitude and time rate of settlement do not exceed specified limits, e.g., 0.01 inches per hour. For load tests taken to failure, the interpretation of the load at failure, P_n, can be difficult.

Many methods to interpret load tests have been proposed, and three methods are permitted by the International Building Code, with additional methods permitted by approval of the building official (ICC 2015). This section describes two of the methods permitted by the IBC: the Davisson Offset Limit Method (Davisson 1972) and the Brinch Hansen 90% Criterion (Brinch Hansen 1963). Two additional methods, the Brinch Hansen 80% Criterion (Brinch Hansen 1963) and Corps of Engineers Method (USACE 1991), are also described. For driven piles and micropiles, AASHTO (2020) specifies the Davisson method for elements having a width of 24 inches or less and a modified version of the Davisson method for larger elements. For drilled shafts, AASHTO (2020) defines failure as plunging of the test shaft or displacement of the top of the shaft equal to 5% of the diameter. The failure loads interpreted by different methods should not be expected to agree.

Table 6-46 provides the equations and requirements for interpretation of the failure load from static load test data. Figure 6-28 illustrates the usage of each method for a hypothetical load test with a “true” failure load of 400 kips at a corresponding settlement of 1.2 inches. The curve shown perfectly follows a Chin-Kondner hyperbolic relationship (Chin 1978) in which the failure loads interpreted using the Brinch Hansen 80% and 90% criteria are approximately the same. The pile considered in the example is an 80-ft long, 24-inch diameter steel pipe with a 0.5-inch wall thickness.

The Brinch Hansen criteria usually produces a higher, and arguably more realistic, interpretation of the failure load as compared to the Davisson method (Coduto et al. 2016). Fellenius (2021) asserts that the Brinch Hansen 80% criterion is often close to the “true” ultimate resistance.

Table 6-46 Interpretation of Failure Load from Static Load Tests

Criterion	Interpretation of data	Interpreted P_n (Figure 6-28)
Davisson Offset Limit (Davisson 1972)[A]	P_n equals the intersection of data and $\delta = \frac{PZ}{A_p E_p} + 0.15\,in. + \frac{b}{120\,in.}$	Point A
Brinch Hansen 80% Criterion (Brinch Hansen 1963)[B]	P_n and δ_n satisfy $\frac{\delta \text{ at } P = 0.8P_n}{\delta_n \text{ at } P = P_n} = 0.25$	Point B
Brinch Hansen 90% Criterion (Brinch Hansen 1963)[B]	P_n and δ_n satisfy $\frac{\delta \text{ at } P = 0.9P_n}{\delta_n \text{ at } P = P_n} = 0.50$	Point C
USACE (1991)	P_n is the average of three estimates: 1: P = the intersection of data and δ_n = 0.25 in. 2: P = the intersection of tangents from early and late portions of data 3: P = point on data where the instantaneous slope equals 0.005 in./kip	Point D Point E Point F

[A] All length units must be consistent; inches are presented here.

[B] The hyperbolic relationship that approximately satisfies both the Brinch Hansen 80% and 90% criteria is provided below. The synthetic load test data in Figure 6-28 was generated using the hyperbolic relationship with P_n = 400 kips and δ_n =1.2 inches.

Chin-Kondner hyperbolic relationship for the example: $\frac{P}{P_n} = \frac{\delta/\delta_n}{0.91 \cdot \delta/\delta_n + 0.09}$

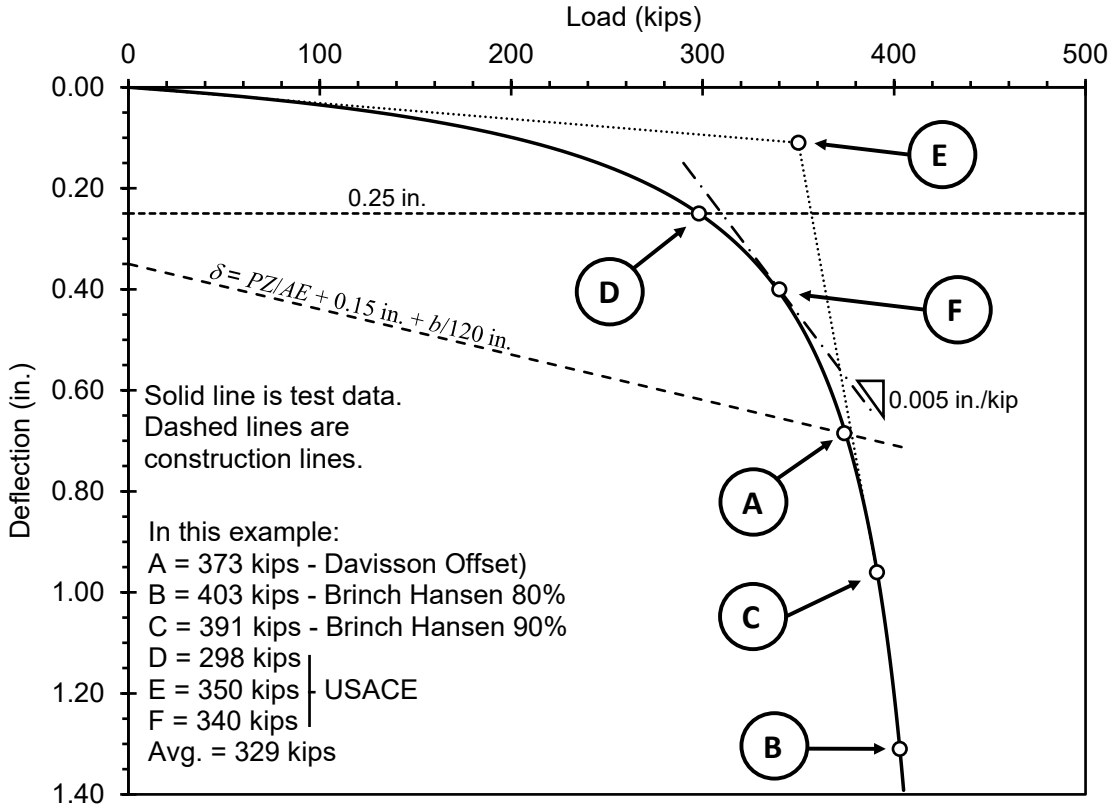

Figure 6-28 Interpretation of Failure Load from Static Load Tests

6-9 DYNAMIC METHODS OF ANALYSIS AND TESTING.

6-9.1 Introduction.

This section is focused on the use of actual or modeled hammer impacts applied to the top of a foundation element to evaluate a variety of aspects that are important to foundation design and construction. Dynamic methods are primarily associated with driven piles; however, some dynamic methods can also be applied to bored piles. While most of the attention in this section is given to methods for driven piles, some of the methods that can be applied to bored piles are also briefly discussed.

Counting the number of hammer blows for a particular pile penetration, e.g., blows per foot (bpf) or blows per inch (bpi), is the most simple and fundamental dynamic method to inform engineering and construction decision-making related to pile foundations. The inverse of the blow count is the set per blow. In the late 19th century, the relationship between set and pile resistance was formalized in the first popular dynamic formula known as the Engineering News Formula. This semi-empirical formula estimates nominal resistance by dividing the theoretical potential energy of the hammer (the product of hammer weight and drop height) by the observed permanent set plus an empirical value to account for factors, such as elastic rebound. As use of the Engineering News Formula and other dynamic formulas became widespread in the 20th century, their inadequacies became well documented. These inadequacies include treating the pile as a rigid body that transfers energy without losses, ignoring inefficiencies in the hammer and drive system components, and errors in isolating the static resistance from the observed resistance, which includes a dynamic component.

Furthermore, dynamic formulas do not provide a means to assess potentially damaging driving stresses and are not well suited to evaluating setup or relaxation effects, which are best observed within the first few hammer blows of a restrike. Due to these shortcomings, dynamic formulas are not recommended as a primary means of evaluating pile resistance. In situations where no other options are available or to provide an approximate check of other methods, dynamic formulas can be useful when applied with appropriate factors of safety or resistance factors, particularly when the analyst has knowledge that is specific to a particular combination of site, pile, and driving system.

The advent of dynamic methods based on wave mechanics provided a rational way to evaluate the nominal static resistance of the pile, driving stresses, and performance of the hammer and driving system. Table 6-47 summarizes dynamic methods commonly used in driven pile design and construction, including whether the methods are primarily applied during design or during installation of the piles. Implementation of these methods requires specialized software and/or hardware in addition to prerequisite knowledge and training. Presentation of the background knowledge and usage of the software and hardware is beyond the scope of this manual; however, a brief overview of

wave mechanics is provided in Section 6-9.2, and key information about the methods referenced in Table 6-47 is provided in the Sections 6-9.3 through 6-9.6.

As discussed in Section 6-8.1, frequent use of dynamic methods during construction, e.g., testing 2% or more of all production piles, often permits higher LRFD resistance factors to be used in design. This can especially be true when dynamic methods are used together with static load testing and/or rapid load tests. While testing adds cost and time to the construction process, the ability to reduce uncertainty, and design less conservatively, often yields overall savings in cost and/or time.

Dynamic methods are more likely to overpredict nominal resistance when the blow count is less than 24 bpf and underpredict nominal resistance when blow count exceeds 120 bpf. Observing the nominal capacity requires a hammer that delivers sufficient energy to mobilize the resistance along the sides and base of the pile.

Table 6-47 Common Dynamic Methods Based on Wave Mechanics

Method	Primarily used… during design	during test installation[B]	during production installation[C]	Used to evaluate…	Comments
Wave equation analysis of pile driving (WEAP) See Section 6-9.3	x			Nominal resistance as related to pile penetration	• Theoretical behavior based on inputs for the hammer, drive system, pile, and soil
	x			Driveability[D]	
	x	x	x	Preferred hammer and cushion design[E]	
Case Method[A] See Section 6-9.5		x	x	Nominal resistance	• Output evaluated in real time for every hammer blow
		x	x	Hammer and driving system performance	
		x	x	Driving stresses and pile integrity	
Signal matching[A] See Section 6-9.6		x	x	Nominal resistance	• Involves additional computation based on dynamic measurements • Performed on selected hammer blows for a particular time and penetration • More refined than Case Method
		x	x	Hammer and driving system performance	
		x	x	Driving stresses and pile integrity	

[A] Uses dynamic force and velocity measurements from PDA or similar device
[B] Commonly, a high percentage of test piles are tested during initial driving and restrike
[C] Commonly, a specified subset of production piles is tested, restrikes are performed as needed to address changes and/or concerns
[D] Driveability includes evaluating hammer energy and driving stresses
[E] The selection of a hammer and cushion is often refined as the project progresses from design to construction

6-9.2 Wave Mechanics Basics.

A hammer impact on the top of a pile generates a time-dependent force that propagates down the pile at the wave speed of the pile material. The wave equation is the governing differential equation that describes such one-dimensional wave propagation. The basics of wave mechanics are defined and presented in Figure 6-29. The impact force generates normal stresses in the pile that are proportional to the axial strain for an elastic material. The local axial strain is equal to the change in local displacement of the pile material with respect to position along the pile. Thus, shortening or lengthening the pile produces strain while uniformly moving the pile does not produce strain. The total resistance to local displacement is comprised of the inertial force and the static and dynamic components of the resistance provided by the material (soil) surrounding the pile. The resistances can be modeled using linear springs and dashpots, as shown in Figure 6-29, or nonlinear springs and dashpots that are available in commercial software.

To apply wave mechanics to estimate the nominal geotechnical static resistance, the inertial force and dynamic resistance must be removed. Usually, there is less uncertainty associated with removing the inertial forces from the pile-soil model as compared to removing the dynamic soil resistance.

The inputs to the hammer-pile-soil model depend on which implementation of wave mechanics is being used, i.e., wave equation analysis, Case Method, or signal matching. The specifics of the driving system, pile, and ground conditions also affect the inputs. The Case Method and signal matching utilize measurements of force and velocity near the top of the pile, as discussed in Section 6-9.4, while wave equation analysis does not. Guidance for selection of parameters used to define the behavior of the hammer and driving system, e.g., cushion, are available in textbooks, design manuals, and software user manuals. Guidance for selecting values for the wave speed, damping, and quake values is shown in Figure 6-29 and as follows:

- Wave speed – The wave speed of a steel pile is approximately 16,800 ft/sec while the wave speed of a concrete pile typically increases with the compressive strength and is typically in the range of 10,000 to 13,000 ft/sec. The wave speed is many times faster than the particle velocity.
- Quake – *Quake* is defined as the displacement where the soil starts to yield plastically. Values are required for the side and base of the pile. A typical value for side quake is 0.1 inches. The typical range is 0.04 to 0.4 for base quake (lower end for rock).
- Damping – Typical values for the Smith damping factor range from 0.05 to 0.2 s/ft for side resistance (lower end for sands, higher end for clays) and 0.15 s/ft for base resistance. The Smith damping model computes dynamic resistance as the product of the damping factor, pile velocity, and mobilized static resistance. The Smith viscous damping model uses the fully-mobilized static resistance in place

of the mobilized static resistance. The dynamic side resistance is proportional to the pile velocity in the Smith viscous damping model while it follows a nonlinear relationship in the Smith damping model. The Case Method uses a different approach to evaluate the dynamic side resistance that involves a dimensionless damping coefficient having a typical range of 0.1 to 1.0 (lower end for sands, higher end for clays).

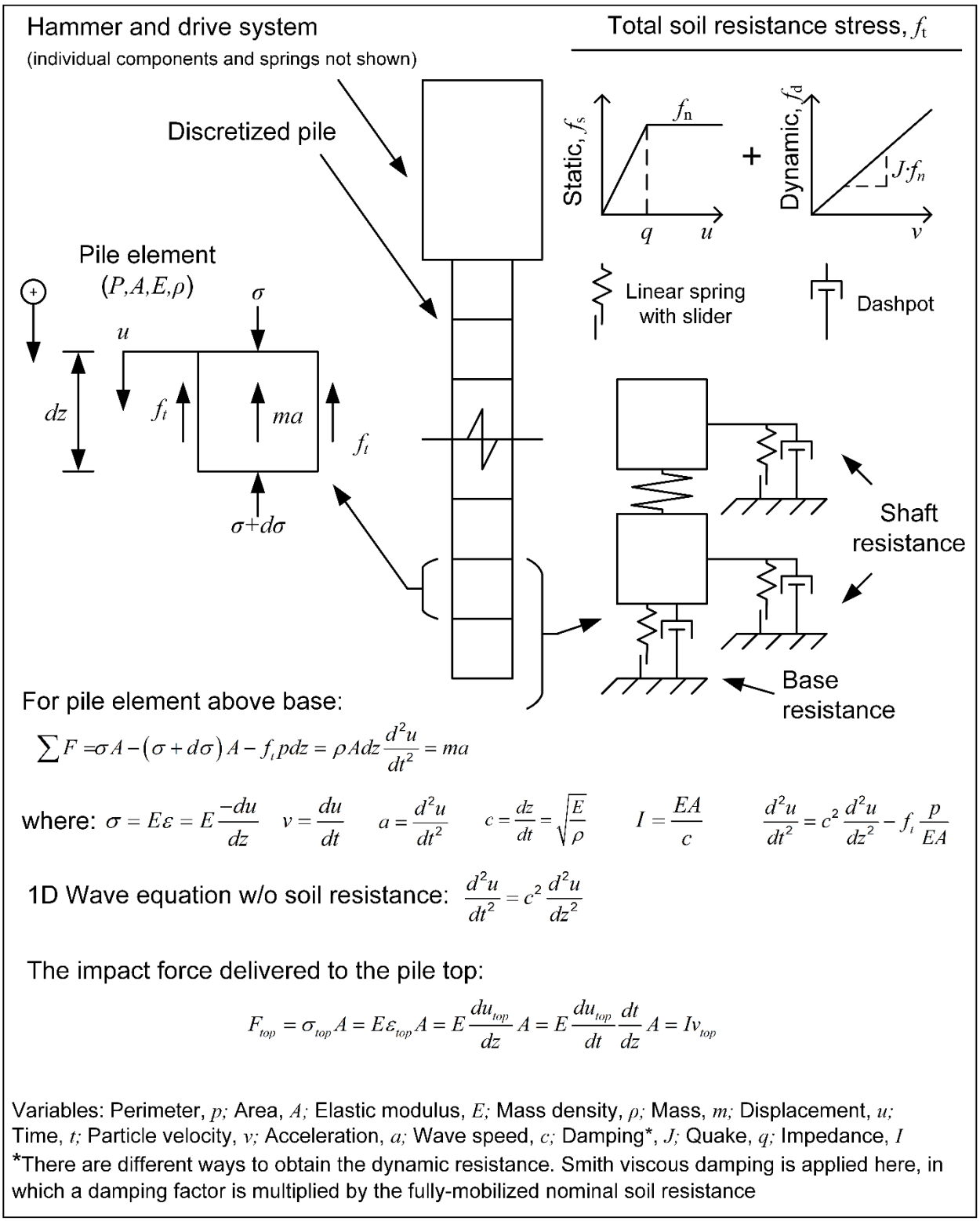

Figure 6-29 Definition Sketch for Wave Mechanics Basics

For a single wave traveling through an infinitely-long uniform pile without side resistance, the force in the pile and the particle velocity are proportional according to the impedance, as defined in Figure 6-29. Increasing the pile cross section area, elastic modulus, and/or mass density increases the impedance. Piles with higher impedance transmit impact force with lower associated particle velocity and driving stresses. Resistance along the sides and base of the pile from the soil reflect some of the wave force. Impedance changes, including the end of the pile itself, also reflect some of the wave force. The creation of multiple waves traveling in the pile by reflections disrupts the proportionality between the force in the pile and the particle velocity.

Figure 6-30 illustrates cases of a pile without side resistance having one of two extreme end conditions. The free-end case, which approximates a pile in very soft ground, illustrates the potential for damaging tensile stresses in the pile. This is particularly important for concrete piles because the tensile strength of concrete is lower than the compressive strength. The fixed-end case, which approximates an end-bearing pile installed through very soft ground, illustrates the potential for damaging compressive stresses in the pile.

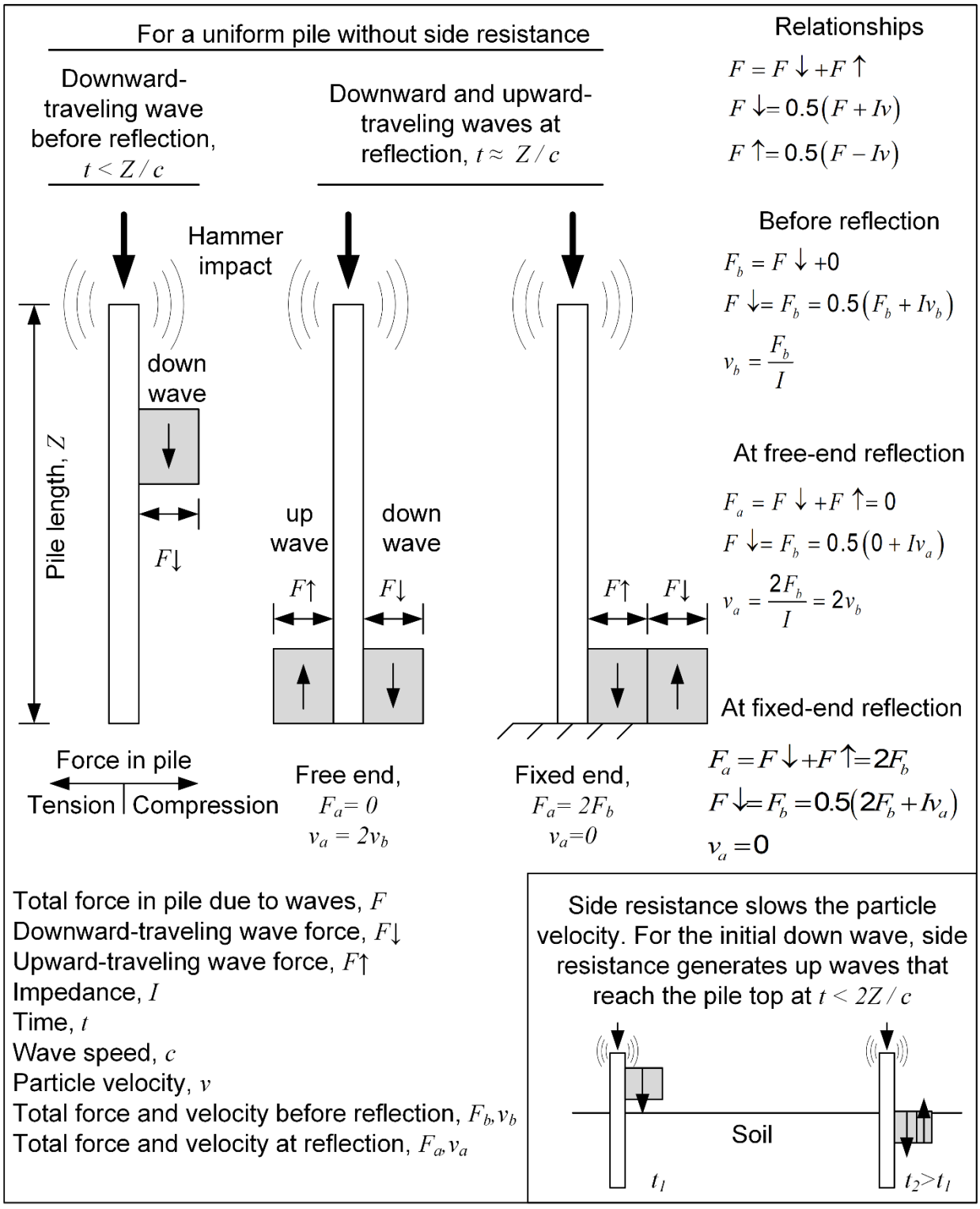

Figure 6-30 Forces in Pile Due to Downward and Upward-Traveling Waves

6-9.3 Wave Equation Analysis of Pile Driving.

Wave equation analysis of pile driving (WEAP) (Smith 1960) is performed using software, such as GRLWEAP, to model the hammer-pile-soil system. The analysis applies the finite difference method to solve for the velocity, acceleration, and forces along the pile at any moment in time. Table 6-47 lists typical uses of WEAP and at what points during the project analyses are typically performed.

A primary use of WEAP is to develop a relationship between the blow count or set and the nominal pile resistance. By itself, an estimate of a pile's nominal resistance made by static capacity analysis does not indicate the type of hammer system that will be suitable nor what driving criteria will be necessary to achieve a target resistance. Inputs to WEAP software include the type and length of pile, the components of the hammer and drive system, the nominal axial resistance, the distribution of resistance along the shaft and base of the pile, and values of damping and quake. Inputs for the hammer and drive system as well as values of quake and damping are usually assigned with guidance from the software. The WEAP analysis computes nominal resistance versus the required blow count or set for the specified parameters. The graphical output of this type of analysis is a called a *bearing graph*. For analyses that include a variable stroke hammer, such as an open-end diesel hammer, the WEAP analysis shows the combination of stroke and blow count that corresponds to the resistance. An inspector's chart analysis plots blow count versus stroke for a particular resistance. A lower stroke requires more blows to reach the target resistance than the same hammer with a higher stroke.

A second primary use of WEAP is to perform a driveability analysis in which the goal is to select a hammer system and pile that can efficiently drive the pile without causing damage to the pile. The key feature of a driveability analysis is the iterative application of WEAP to evaluate blow count, capacity, stresses, and hammer performance over a range of pile penetration depths. The output of a drivability analysis includes plots of the calculated blow count versus depth. Driveability analyses are commonly repeated once the actual driving equipment has been selected by the contractor to refine the plan for hammer settings (e.g., fuel delivery or stroke) and cushion selection.

It is important to emphasize that the outputs of a WEAP analysis, e.g., bearing graph, are only valid for the specific hammer-pile-soil model. Changing any component of the driving system, e.g., cushion, or hammer setting requires a new analysis to be performed.

6-9.4 High-Strain Dynamic Measurements.

Observations of the actual hammer-pile-soil system in action allow designers to overcome some of the limitations of wave equation analysis associated with model uncertainty, such as dynamic soil properties and hammer system performance. These

observations typically include using a pair of strain transducers and a pair of accelerometers mounted in a diametrically opposed manner near the top of the pile. Using a pair of instruments mitigates some of the effects of uneven application hammer energy to the pile. The strain transducers are used along with the pile's area and modulus to measure force in the pile. Single integration of the accelerometer output with respect to time provides the velocity of the pile while double integration provides displacement.

Equipment is required for sensor excitation, data acquisition, data logging, and data processing. One commercially available product is the Pile Driving Analyzer (PDA). The sensors are connected to the PDA by a cable or transmitted wirelessly.

Wave traces are plots of measured force and velocity versus time over the duration of the hammer impact. Typically, velocity is multiplied by the pile impedance to match force since force is proportional to velocity for a single wave traveling along the pile (see Section 6-9.2). The time required for the wave to travel from the instrumentation to the base and back is equal to $2Z'/c$ as indicated in Figure 6-31. As shown, the wave traces can be interpreted to infer the resistance provided along the sides and base of the pile. Wave traces can also be interpreted to assess pile integrity. Bending or cracking of the pile introduces impedance changes that create wave reflections that appear in the wave traces.

Records of force and velocity versus time obtained for each hammer blow initial driving and/or restrike are processed in real time within the PDA using the Case method (Section 6-9.5) to estimate nominal static resistance. Force and velocity records are also able to be processed in real time within the PDA to compute energy transfer, driving stresses, factors related to pile integrity, and hammer stroke. Selected force and velocity records from hammer blows at the end of initial driving or restrike are further processed using signal matching analysis (Section 6-9.6).

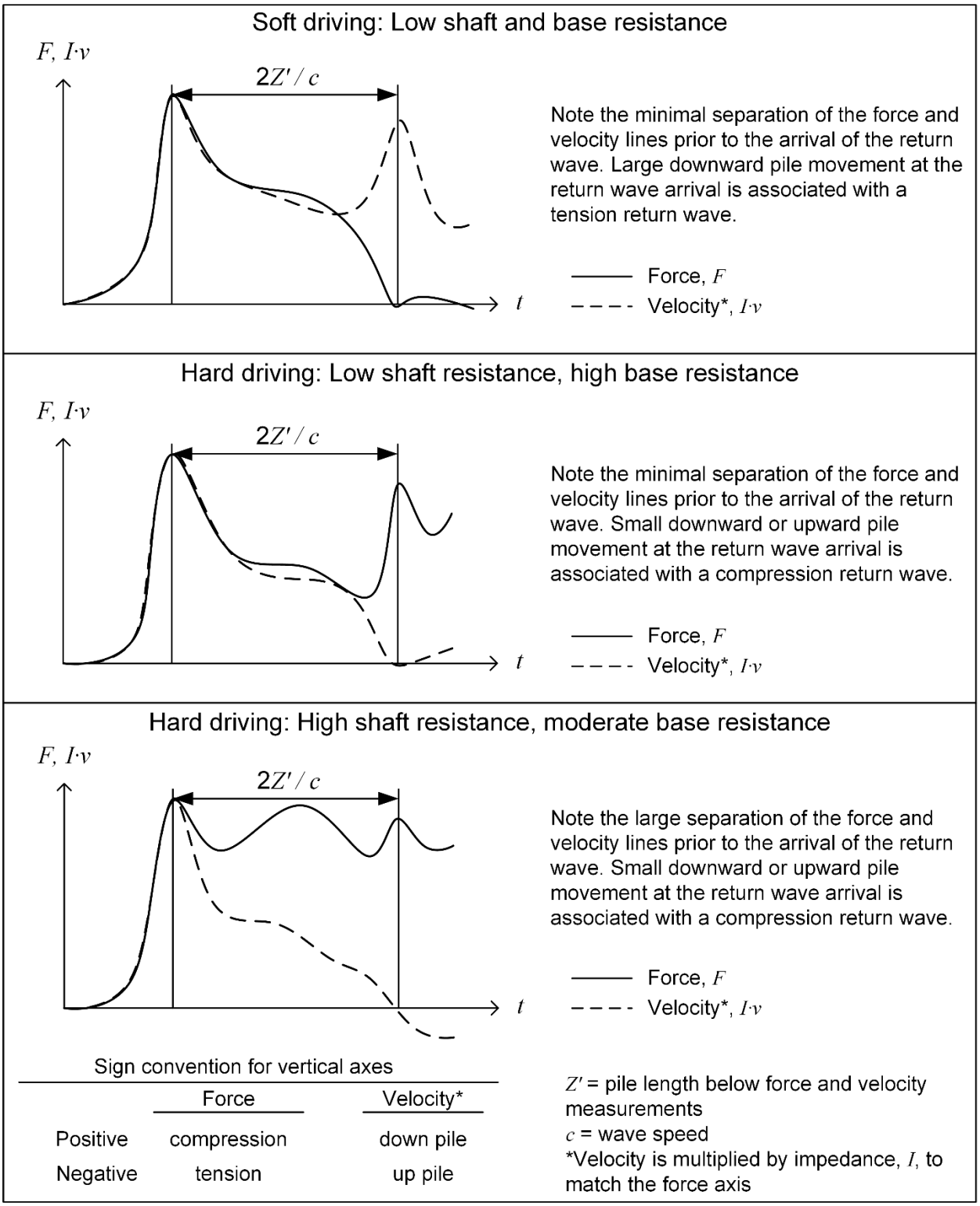

Figure 6-31 Typical Force and Velocity Records for Different Resistance Conditions

6-9.5 Case Method.

High-strain dynamic measurements of force and velocity versus time for each hammer blow (Section 6-8) are interpreted in real-time onboard the PDA using the Case Method to assess static nominal resistance. The Case Method uses a closed-form solution for wave propagation. The Case Method estimates the total pile resistance using measurements of force and velocity when the peak of the initial downward-traveling hammer impact wave reaches the instruments ($t = 0$) and when the reflected impact wave returns to the instruments as an upward-traveling wave ($t = 2Z'/c$). Z' is the distance between the instruments and the end of the pile. A single Case damping coefficient, which is different than the Smith damping factor, is multiplied by the interpreted velocity of the pile base and impedance to remove the dynamic component of the resistance and isolate the static resistance.

There are several variants of the Case Method applied within the PDA, e.g., RMX and RSP. The engineer must be familiarized with these methods to decide which method is most appropriate. FHWA (2016) provides additional description of these methods.

6-9.6 Signal Matching.

High-strain dynamic measurements of force and velocity versus time for a selected hammer blow (Section 6-8) can be processed using special software, such as CAPWAP, to assess static nominal resistance. Often, analysis of a hammer blow at the end of initial driving is compared to an analysis of a hammer blow at the beginning of restrike to evaluate set-up or relaxation effects. Signal matching uses the same application of wave mechanics as WEAP and is thus more rigorous than the Case Method. The measured force record for the downward-traveling impact wave (down wave) is used in the signal matching software in place of the hammer model used in WEAP. The wave equation is applied in the signal matching software with the down wave force record using reasonable estimates of the side and base resistance distribution, quakes, and damping factors to compute the force record at the instrument location due to the upward-traveling reflected impact wave (up wave). The software compares the computed up wave force record for the up wave to the measured up wave force record and adjusts the side and base resistance distribution, quakes, and damping factors until the match quality cannot be improved.

CAPWAP assesses match quality using the match quality parameter, MQ, that increases with greater deviation between the computed and measured up wave force assessed at multiple points in time in the hammer blow record. MQ also increases with greater deviation between the measured and computed blow count (GRL 2013). The final match achieves the lowest value of MQ. Analyses performed using different initial trial parameter values may produce a different final match; however, careful application of signal matching has a proven track record of producing good estimates of static capacity and back-calculated model parameter values. The back-calculated model

parameter values can be used to refine WEAP and the Case Method for site-specific conditions.

6-9.7 Rapid Load Tests.

The rapid load test, also known as force pulse load test, is another type of field test that is primarily used to evaluate nominal geotechnical axial compressive resistance. However, variations of the test have been applied to evaluate the lateral load response of single elements and groups of elements. Rapid load tests are used on a variety of deep foundation types. Unlike static load tests, rapid load tests do not require reaction elements or large reaction weights to apply large forces to the test element. Instead, rapid load tests use a comparatively smaller reaction mass that is often accelerated upward by ignition of a solid propellant. The mass can also be dropped onto cushioning material or a spring positioned between the mass and the test element. For the test that uses an upward accelerated mass, such as a Statnamic test, the combustion gas pressure generated by the propellant to overcome the inertial force of the reaction mass applies a force to the test element. In both test types, the force is imparted to the test element for a longer duration than high-strain dynamic testing described in Section 6-9.4 but for a far shorter duration than static load testing described in Section 6-8. The duration of the force pulse is many times longer than the time required for the stress wave to pass through the test element. Consequently, the effects of wave propagation on the forces in the element are small. However, the applied load is dynamic, and inertial and damping effects are important.

ASTM D7383 describes standardized procedures for rapid load tests. The test element is instrumented with a load cell to measure the force pulse over time. Usually, the element is also instrumented with accelerometers and strain gauges in a similar manner as with high-strain dynamic testing. Additional instrumentation is sometimes used including displacement transducers at the top of the test element and one or more expendable accelerometers located along the length of the test element.

The Unloading Point method (UP) (Middendorp, 1992) is the most common method to analyze static axial resistance from the results of a rapid load test. This method models the test element as a rigid mass, i.e., wave propagation effects are ignored, that is connected to the soil by a non-linear soil spring and a viscous damper. The specifics of this method can be found in the original source and FHWA (2016).

In some cases, the assumption that the test element behaves as a rigid mass is not valid. One case is when the test element has high base resistance and the acceleration, velocity and displacement at the top of the element are significantly different than at the base. Another case applies to long slender piles where wave propagation effects become significant. Both of these cases are addressed using modifications to the Unloading Point method. To address the influence of high base resistance, the Modified Unloading Point method (MUP) (Justason 1997) is applied in which

accelerometers are included at the top and bottom of the test element and the response of the pile is modeled as a rigid mass using the average of the measured accelerations. To address the problems with long slender piles, the Segmental Unloading Point method (SUP) is applied in which a number of accelerometers are positioned along the test element (Mullins et al. 2002). The response of the pile is modeled as a series of rigid segments using the measured acceleration corresponding to each segment. Other methods, such as the Sheffield method (Holscher et al. 2012), are used to address loading rate effects for elements in fine-grained soils.

Due to the faster rate of loading in rapid load tests as compared to static load tests, NCHRP (2006) recommends reduction factors for axial capacities estimated using the UP, MUP, and SUP methods applied to the results of Statnamic tests. The loading rate reduction factors for elements in rock, sand, silt, and clay are equal to 0.96, 0.91, 0.69, and 0.65, respectively. Studies by Weaver and Rollins (2010) and Brown and Powell (2013) propose lower reduction factors for elements in fine-grained soil. Weighed loading rate reduction factors can be determined and applied in mixed soil profiles based on the percentage of nominal resistance provided by each layer (FHWA 2016). FHWA (2016) suggests that reduction factors similar to those applied to Statnamic tests are applicable to rapid load tests performed using cushioned drop weight systems. Note that the loading rate reduction factor is applied in addition to the LRFD resistance factor or ASD factor of safety.

AASHTO (2020) does not provide strength limit state resistance factors for geotechnical resistance based on rapid load tests. FHWA (2016) cites a study by McVay et al. (2003), which is summarized in Table 6-48.

Table 6-48 Strength Limit State Resistance Factors for Axial Loading based on Rapid Load Testing (after McVay et al. 2013, FHWA 2018a)

Pile	Bearing Conditions	Recommended Resistance Factor
Redundant driven piles	Rock and coarse-grained soil	0.70
	Mixed layers of sand, clay, and/or rock[A]	0.60
Nonredundant driven piles	Rock and coarse-grained soil	0.60
	Mixed layers of sand, clay, and/or rock[A]	0.50
Redundant drilled piers[B]	Relatively uniform ground conditions	0.65

[A] Rapid load tests not recommended in fine-grained soils without calibration to a static load test.
[B] FHWA (2018a) recommends lowering resistance factors for non-redundant shafts, sites with high variability, and/or when uncalibrated rapid load tests.

The primary benefit of a rapid load test is the ability to apply a large load with a less expensive and less complicated loading system than a static load test. The cost and time saving benefits often increase on projects with multiple tests. Additionally, unlike bi-directional load tests, rapid load tests can be performed on existing elements.

The main drawbacks of rapid load tests include 1) uncertainty associated with accounting for loading rate effects, particularly in fine-grained soils and/or using cushioned drop weight systems, 2) less accumulated knowledge and experience with rapid load tests as compared with static load tests, 3) the applied force pulse must overcome the static and dynamic ground resistance which can overstress the element, 4) insufficient displacement of the top of the element, i.e., less than 3% of element width, can result in overprediction of capacity (FHWA 2016), 5) conventional interpretation of rapid load tests only determine the total nominal resistance and not the distribution of shaft and base resistance (Coduto et al. 2016), and 6) the availability and mobilization of rapid load test equipment may be challenging in some locations.

6-10 INTEGRITY TESTING.

Integrity testing is used to detect and evaluate damage and/or defects in a deep foundation element. Most integrity tests are nondestructive, with drilling and coring as notable exceptions. Some nondestructive tests require advanced planning and preparation to provide access to the necessary portion(s) of the element. Additionally, integrity tests require specialized equipment and training to perform, and integrity testing using high-strain dynamic measurements requires mobilization of a pile hammer. This section provides a brief overview of some of the most common methods used to perform integrity testing.

Integrity testing using high-strain dynamic measurements is primarily used for driven piles while crosshole sonic logging, thermal integrity profiling, and gamma-gamma testing are primarily applied to drilled shafts.

6-10.1 High-strain Dynamic Measurements.

The Case Method can be applied using high-strain dynamic measurement to evaluate pile integrity. The Beta Method developed by Rausche and Goble (1979) interprets the force and velocity measurements to detect changes in impedance that indicate changes in the cross-sectional area along the element. The pile integrity factor, Beta, abbreviated as BTA, is reported by the PDA to quantify the severity of damage. A BTA equal to 1.0 indicates no damage while a BTA less than 0.8 indicates damage. As the BTA value decreases, the severity of the damage increases.

6-10.2 Low-strain Dynamic Measurements.

The sonic echo and impulse response methods are the most common of several low-strain dynamic measurement methods used to assess foundation element integrity. These methods do not require access tubes in the tested element and can therefore be used without prior preparation of the element. The sonic echo test involves striking the element with a hand-held hammer and recording the initial downward-traveling compression wave and return upward-traveling compression or tension waves using a

geophone that is temporarily glued to the top of the element. Concrete defects or anomalies in cross-sectional area, i.e., necking or bulging, create impedance changes that will cause early reflection of the wave energy, i.e., $t < 2L'/c$. Additionally, the type of impedance change infers the type of anomaly. For example, an increase in cross-sectional area due to a bulge will increase impedance that will create a reflected compression wave. A decrease in cross-sectional area due to necking will decrease impedance that will create a reflected tension wave. The impulse response method is similar to the sonic echo method except that results are analyzed in the frequency domain instead of the time domain.

A limitation of the low-strain dynamic measurement methods is that the strength of the return waves is sometimes too weak to be properly interpreted, particularly when the element is long relative to its width and/or when the element is bearing in rock. Additionally, the resolution of the method is often insufficient to detect small anomalies, particularly near the base of the element.

6-10.3 Cross Hole Sonic Logging.

Cross hole sonic logging requires at least two embedded access tubes installed in the tested element. An acoustic source is lowered down one tube while a receiver is simultaneously lowered down another tube to the same depth as the source. The distance between the source and receiver divided by the time between emission and detection of the acoustic signal gives the compression wave speed of the concrete. Reduced compression wave velocity below a baseline value indicates reduced concrete quality. Standardized procedures for cross hole sonic logging are provided in ASTM D6760. Cross hole tomography is a variation of cross hole sonic logging that includes placing the source and receiver at different depths to obtain a three-dimensional representation of the tested element. A primary limitation of cross hole sonic logging is that only the portions of the element between access tubes can be tested.

6-10.4 Thermal Integrity Profiling.

Thermal integrity testing uses embedded temperature-sensing cables, or multiple access tubes, and a thermal probe to monitor the temperature of the curing concrete. The temperature profile can be interpreted to infer the geometry and concrete quality of the tested element in the following ways: 1) localized low temperature zones indicate the potential for defective concrete, 2) comparisons of local temperature at a particular elevation to the overall average temperature are used to infer the radius and concrete cover at the elevation, and 3) comparison of temperature at diametrically opposite measurement locations are used to infer the cage alignment. Standardized procedures for thermal integrity profiling are provided in ASTM D7949. A primary limitation of thermal integrity profiling is that it can only be performed while the exothermic chemical reaction of cement hydration is still occurring at a significant rate.

6-10.5 Gamma-Gamma Logging.

Gamma-gamma logging requires one access tube installed in the tested element. During the test, a single probe with a gamma ray source and detector is lowered down the access tube. A portion of the gamma rays emitted by the source is reflected back to the probe, i.e., backscatter, and are encountered by the detector. An approximately linear correlation exists between the time rate of gamma ray detection (counts per second) and the density of concrete. A primary limitation of gamma-gamma logging is the security and logistics required to transport, handle, and store the radioactive source. Additionally, the test can only detect anomalies within a radius of several inches of the access tube.

6-11 PROBLEM SOILS AND DEEP FOUNDATIONS.

Chapter 1 provides a summary of many types of problem soil conditions that can affect the design of foundations and earth structures. Table 6-49 summarizes important conditions for the design of deep foundations in problem soils.

Table 6-49 Problem Soil Considerations for Deep Foundations

Soil Type	Primary Considerations for Deep Foundations
Soft Clays, Organic Soils, Peat, and Muskeg	• These soils generally provide poor shaft and end bearing resistance • Settlement of these soils from other loading, such as embankments, and/or lowering of the water table can cause a drag load and downdrag settlement of deep foundations. • Aggregate piers may be unsuitable because of a tendency for excessive lateral compression. • Drilled shafts may require temporary casing to prevent squeezing of the shaft during drilling. • CFA piles may experience inward squeezing, resulting in inconsistent pile diameter. • Displacement piles (driven or drilled) can cause heave and/or lateral soil displacement from the additional volume of the piles added to the ground.
Fissured Stiff Highly Plastic Clays and Soft Shales	• Clay fissures and cracks can reduce deep foundation skin friction. Foundation installation methods, e.g. pile driving, can produce cracks in stiff clays. • Stiff near surface clays are prone to having poor contact with deep foundations, and thus low skin friction, due to the formation of gaps during installation, shrink/swell, and freeze/thaw. • Driven piles in soft shales are susceptible to a loss in geotechnical resistance after driving known as relaxation.
Loess and Other Collapsible Soils	• Inundation settlement of collapsible soil can introduce a drag force and downdrag settlement.
Sensitive Clays	• Cyclic softening reduces geotechnical resistance, particularly lateral resistance.
Loose Sands	• Drilled shafts will likely require temporary casing to prevent collapse of the shaft during drilling. • CFA piles may experience caving, resulting in inconsistent pile diameter. • Aggregate piers may require temporary casing during the drilling stage. • Post-construction densification of loose sand can introduce a drag force and downdrag settlement. • Liquefaction of loose sand increased the unbraced length of deep foundations, may introduce high lateral forces, and temporarily eliminates the geotechnical resistance within the liquefied zones. • Excessive foundation settlement may be required to mobilize base resistance in loose sand

Glacial Till	• Gravel, cobble, and boulder content of the till is the major consideration for deep foundations.
	  ○ These can obstruct pile driving and/or cause misalignment of piles. Pile toe attachments can help prevent damage.
	  ○ Drilled shafts can have difficulty drilling through large boulders, particularly when encountered partially in the alignment of the shaft. Special tooling may be required in tills containing large boulders.

Expansive Soils and Rock	• Low skin friction is possible over the depth of soil that is susceptible to shrink/swell.
Dredged Soils	• Dredged soils should be considered as soft or loose for design of deep foundations (see comments above)
Low Plasticity and Nonplastic Silts	• Squeezing and caving can also occur in these silty soils, especially when saturated. Temporary casing will likely be required for drilled foundations.
Municipal Solid Waste	• The electro-chemical properties of the waste may lead to deterioration of deep foundations, e.g. corrosion of steel piles. Elevated temperatures within the waste accelerate deterioration. • Obstructions within the waste may damage or deflect foundations during installation • Decomposition of waste can introduce a drag force and downdrag settlement

6-12 NOTATION.

Variable	Definition
a	Acceleration in wave mechanics calculations
A	Total or “gross” cross-sectional area of a pile
A_b	Area of pile base
A_p	Cross-sectional area of the pile material
$A_{s,i}$	Shaft area for a pile segment
b	Pile diameter
b'	Enlarged pile base diameter
B	Width of pile group (smaller plan dimension)
B'	Width of equivalent footing (smaller plan dimension)
c	Wave speed in a pile material
C	Fitting paramer for shaft resistance of drilled shafts
C_α	Adhesion
$C_{\varepsilon c}$	Modified compression index
$C_{\varepsilon r}$	Modified recompression index
D_{50}	Median particle size
D_r	Relative density
E	Young’s modulus
E_p	Young’s modulus of pile material
E_r	Energy rating of a pile driving hammer
E_u	Young’s modulus of soil for undrained conditions
F	Force in pile in wave mechanics calculations
F_a	Force in pile after reflection
F_b	Force in pile before reflection
f'_c	Compressive strength of concrete or grout
f_n	Unit negative shaft resistance
f_p	Maximum unit wide resistance
f_{pe}	Effective prestress

Variable	Definition
$f_{s,i}$	Unit shaft resistance for a segment
f_u	Ultimate tensile strength of steel
f_y	Yield strength of steel
FS	Factor of safety
g	Acceleration due to gravity
I	Pile impedance
If	Influence factor
I_p	Moment of inertia of pile
I_r	Rigidity index
I_{rr}	Reduced rigidity index
J	Damping in wave mechanics calculations
K	Earth pressure coefficient
K_0	Coefficient of at-rest earth pressure
k_h	Coefficient of horizontal subgrade reaction
K_P	Coefficient of passive earth pressure
k_s	Side resistance factor
k_t	Base bearing factor
L	Length of pile group (larger plan dimension)
L'	Length of equivalent footing (larger plan dimension)
M_c	Characteristic moment
$M_{t,dead}$	Applied moment from dead load
$M_{t,live}$	Applied moment from live load
M_{ult}	Ultimate moment
n	Fitting parameter for shaft resistance of drilled shafts
N	Standard Penetration Test blow count – uncorrected
$N_{1(60)}$	Standard Penetration Test blow count corrected for overburden and efficiency
N_{60}	Standard Penetration Test blow count corrected for efficiency
N_c, N_q	Bearing capacity factors

Variable	Definition
n_g	Group efficiency factor
N^*_c, N^*_q	Bearing capacity factors modified to account for compressibility and local shear
N^*_{cr}	Bearing capacity factor for unit base resistance of rock
OCR	Overconsolidation ratio
p	Pile perimeter in wave mechanics calculations
P_c	Characteristic load
P_n	Load at failure in
$P_{P,mob}$	Resultant force from mobilized passive resistance
$P_{P,ult}$	Resultant force from fully mobilized passive resistance
P_r	Factored axial structural capacity
$P_{t,dead}$	Applied dead load
$P_{t,live}$	Applied live load
$P_{t,ult}$	Ultimate load
P_{ui}	Factored maximum single pile axial load
P_a	Atmospheric pressure
q	Quake in wave mechanics calculations
q_b	Unit base resistance
q_c / P_a	Cone tip resistance normalized by atmospheric pressure
$q_{c,a} / P_a$	Average cone tip resistance normalized by atmospheric pressure
Q_d	Applied permanent axial load
Q_{np}	Maximum axial load in pile at neutral plane
q_u	Unconfined compressive strength
R, R_n	Nominal axial pile resistance
R_b, R'_b	Base resistance
$R_{n,block}$	Block uplift capacity
$R_{r,g}$	Factored axial capacity of pile group
$R_{r,gblock}$	Factored resistance to block failure
$R_{r,gu}$	Combined factored group uplift capacity

Variable	Definition
$R_{r,s}$	Factored single column capacity
$R_{r,ublock}$	Factored uplift capacity of piles and block
R_s	Shaft resistance
R_{s-}	Negative shaft resistance
R_{s+}	Positive shaft resistance
s_u	Undrained shear strength
$s_{u,UC}$	Undrained shear strength evaluated using the unconfined compression test
$s_{u,DSS}$	Undrained shear strength evaluated using the direct simple shear test
$s_{u,ICU}$	Undrained shear strength evaluated using the isotropically consolidated undrained triaxial test
$s_{u,UU}$	Undrained shear strength evaluated using the unconsolidated undrained triaxial test
s^*_u	Factored undrained shear strength
t	Time in wave mechanics calculations
t_{cap}	Pile cap thickness
u	Pile displacement in wave mechanics calculations
v	Particle velocity in wave mechanics calculations
v_a	Particle velocity at reflection
v_b	Particle velocity before reflection
v_c	Critical velocity for scour
V_{block}	Volume of frustum
$W_{e,g}$	Effective weight of pile group block
W_{re}	Factored effective weight of a single column
y	Lateral deflection of pile or pile cap
y_{tm}	Deflection of pile top due to applied moment
y_{tp}	Deflection of pile top due to applied load
z_s	Depth to bearing layer
z_1	Depth below the base of the pile cap to the assumed start of load spreading
z_2	Depth interval where load spreading is assumed to occur
z'	Depth below the equivalent footing

Variable	Definition
Z	Pile length
Z'	Pile length below strain and acceleration measurements
Z_f	Depth to fixity
α	Adhesion factor
α_{bond}	Nominal unit grout to ground bond strength
α_E	Joint modification factor
β	Beta method coefficient to account for shaft friction and lateral earth pressure
δ	Interface friction angle
δ	Total settlement
δ_e	Elastic settlement of pile
ΔQ	Average change in load in an element over its length
δ_s	Settlement due to compression of soil supporting a pile
γ	Total unit weight
γ', γ_b	Bouyant or effective unit weight of soil
γ_m	Moist unit weight of soil
ε_v	Volumetric strain from foundation loading
ϕ'	Effective stress friction angle
$\phi'*$	Factored effective stress friction angle
φ_{da}	Resistance factor for pile driving
ν	Poisson's ratio, s subscript indicates soil
ρ	Mass density
σ'_m	Mean effective stress at b/2 below the pile base elevation
σ'_p	Preconsolidation stress
σ_{zD}	Vertical stress at the base elevation (total or effective depending on the case)
σ'_z	Average vertical effective stress

6-13 SUGGESTED READING.

Topic	Reference
Driven piles	FHWA. 2016. *Design and Construction of Driven Pile Foundations. Geotechnical Engineering Circular No. 12, FHWA-NHI-16-009*, U.S. Department of Transportation, Federal Highway Administration, Washington, DC.
Drilled shafts	FHWA. 2018. *Drilled Shafts: Construction Procedures and Design Methods, Geotechnical Engineering Circular No. 10, FHWA-NHI-18-024*, U.S. Department of Transportation, Federal Highway Administration, Washington, DC.
Continuous flight auger (CFA) columns	FHWA. 2007. *Design and Construction of Continuous Flight Auger Piles, Geotechnical Engineering Circular No. 8, FHWA-HIF-07-03*, U.S. Department of Transportation, Federal Highway Administration, Washington, DC.
Micropiles	FHWA. 2005. *Micropile Design and Construction. Reference Manual for NHI Course 132078: FHWA-NHI-05-039*. U.S. Department of Transportation, Federal Highway Administration, Washington, DC
Drilled displacement piles (DDP)	FHWA. 2007. *Design and Construction of Continuous Flight Auger Piles, Geotechnical Engineering Circular No. 8, FHWA-HIF-07-03*, U.S. Department of Transportation, Federal Highway Administration, Washington, DC.
Helical piles	Perko, H. A. 2009. *Helical Piles: A Practical Guide to Design and Installation*. Wiley, Hoboken, NJ.
Aggregate columns	FHWA. 2017. *Ground Modification Methods Reference Manual – Volumes I and II, Geotechnical Engineering Circular No. 13, FHWA-NHI-16-009*, U.S. Department of Transportation, Federal Highway Administration, Washington, DC.

CHAPTER 7.PROBABILITY AND RELIABILITY IN GEOTECHNICAL ENGINEERING

7-1 INTRODUCTION.

7-1.1 Scope and Purpose.

This chapter introduces the basic principles of statistics and probability required to understand and begin to use these concepts in geotechnical engineering. Sources of uncertainty in geotechnical design and methods for quantifying that uncertainty are discussed. Applications of probabilistic principles are presented, including use of probability to understand and interpret laboratory and field-testing data, methods to calculate reliability indices, a review of common risk assessment procedures, and discussion of hazard analyses. In many sectors, LRFD is used to design retaining walls and foundations. The probabilistic basis of LRFD is explained to help engineers connect this approach to other design procedures. A primary purpose of this chapter is to familiarize the engineer with common applications of probability in geotechnical engineering. In many cases, additional study would be required to implement these applications fully.

7-2 PRINCIPLES OF STATISTICS AND PROBABILITY.

This section reviews basic principles of statistics and probability to provide a foundational understanding for discussions of uncertainty, reliability, and risk assessment. Deeper treatment of statistics and probability in the context of civil engineering can be found in textbooks, such as Ang and Tang (1975) and Benjamin and Cornell (1970).

The methods presented in this chapter are based on sets of observations or measurements, which are referred to as a *sample*. Every sample comes from a *population*, which is the set of all outcomes for the property being measured for a particular experiment or situation. This terminology can be confusing because geotechnical engineering also uses sampling terminology in field and laboratory testing. The common geotechnical use of the term sample is related to the more rigorous statistical definition. The distinction between the sample and population depends on how the population is defined as illustrated in the following examples. The scope of the population differs in each example.

- The liquid limit below a particular shallow foundation is required for a forensic case. The corresponding population might be defined as the liquid limit at all locations within a Shelby tube of the soil from below the foundation. In this case, the sample might be a set of ten liquid limit tests on soil taken from different locations in the Shelby tube. In reality, the Shelby tube is itself a sample of the soil below the foundation.

- The undrained shear strength of a clay layer at a particular site must be characterized for a foundation design. The population is the undrained shear strength at all locations within the clay layer. The sample might be a set of 30 UU triaxial compression tests on individual Shelby tube specimens of the clay.
- A researcher desires to develop a general relationship for the adhesion of piles in clay using the α method (see Section 6-5.4.2). As a general relationship, the population may be defined as all piles installed in clay or could be restricted to a particular type of pile or stratigraphy. The sample used to develop the relationship might be adhesion measurements from 200 load tests on piles installed in clay.

7-2.1 Statistics.

For a given sample of measured data, any function of the sample data is referred to as a statistic. The most common statistics provide measures of either the central tendency or the spread (a.k.a., dispersion) of the data (Baecher and Christian 2003). Common statistics used to describe a data set and the equations for these statistics are summarized in Table 7 1. It is common to use different symbols to distinguish between statistics from the population and those obtained from a sample. For example, the population mean (average) and variance (mean-squared deviation from the mean) are commonly represented by μ and σ^2 while the sample mean and variance are $\bar{x}$ and s^2.

The definitions of statistical terms used in this chapter are provided in Table 7 1. The reader may need to refer back to this table when these terms are used later in the chapter.

7-2.2 Methods of Plotting Data.

In order to be interpreted usefully, sample observations are usually plotted. While many types of plots can be used (e.g., scatter plots, pie charts, area plots, etc.), the most common means of graphically representing sample data are box and whisker plots, histograms, and cumulative distribution plots. These are readily available in most spreadsheet applications and statistical software tools.

7-2.2.1 Box and Whisker Plots.

A *box and whisker* plot is a depiction of the mean, median, specified percentiles, and extreme values. Two examples are provided at the bottom of Figure 7-1(a) and (b). The box portion is bounded by a lower and upper percentile, usually $x_{0.25}$ and $x_{0.75}$, with a line indicating the median or $x_{0.5}$. A marker or line is plotted at the mean value. The

whiskers are lines that extend out to bars at specified percentiles or at the maximum and minimum values,[41] indicating the meaningful range of the data.

Table 7-1 Common Statistics

Statistic	Symbol	Definition	Equation or comments
Sample Mean	$\bar{x}$	Arithmetic average of n items in a sample from a population	$\bar{x} = \frac{1}{n}\sum_{i=1}^{n} x_i$
Population Mean	μ	Arithmetic average of all N items in the population, or expected value, $\mathrm{E}(X)$, of the variable.	$\mu = \frac{1}{N}\sum_{i=1}^{N} x_i$
Median	$x_{0.5}$	Value for which half of the data are smaller and half larger	Cumulative distribution at the median, $F_X(x_{0.5}) = 0.5$
Mode	NA	Most frequent value in the data	
Maximum	x_{max}	Highest observed value	
Minimum	x_{min}	Lowest observed value	
Range	r_X	Difference between the highest and lowest values	$r_x = \lvert x_{max} - x_{min} \rvert$
Percentile	x_P	Value for which a fraction, P, of the data are smaller	Cumulative distribution at the median, $F_X(x_P) = P$
Sample Variance	$\mathrm{Var}_X = S_X^2$	Second moment of the sample data about the mean	$Var_X = \frac{1}{n-1}\sum_{i=1}^{n}\left(x_i - \bar{x}\right)^2$
Sample Standard Deviation	S_X	Root-mean-square value of the difference between the sample data and the mean, or square root of the variance	$S_X = \sqrt{Var_X} = \sqrt{\frac{1}{n-1}\sum_{i=1}^{n}\left(x_i - \bar{x}\right)^2}$
Sample Covariance	$\mathrm{cov}(x, y)$	Measure of the tendency of two variables (x, y) to vary together	$\mathrm{cov}\left(x, y\right) = \frac{1}{n}\sum_{i=1}^{n}\left(x_i - \bar{x}\right)\left(y_i - \bar{y}\right)$
Sample Correlation Coefficient	r_{xy}	Covariance normalized by the standard deviations of the variables, such that $-1 \le r_{xy} \le 1$.	$r_{xy} = \frac{\mathrm{cov}\left(x, y\right)}{S_x \cdot S_y}$
Population Variance	$(\sigma_X)^2$	Second moment of the population about the mean	$\sigma_X^2 = E\left[\left(X - \mu\right)^2\right] = E\left(X^2\right) - \mu_X^2$
Population Standard Deviation	σ_X	Root-mean-square value of the difference between the sample data and the mean, or square root of the variance	$\sigma_X = \sqrt{\sigma_X^2} = \sqrt{\frac{1}{n}\sum_{i=1}^{n}\left(x_i - \mu\right)^2}$
Coefficient of Variation	COV_X	Standard deviation divided by the mean. Relative measure of dispersion commonly used in geotechnical engineering	$COV_x = \frac{S_x}{\bar{x}}$ or $COV_X = \frac{\sigma_X}{\mu_X}$

Notes:
Expected value is the sum of all possibilities of a variable multiplied by the probability of that value.
For discrete variables, $\mathrm{E}(X) = \Sigma x \cdot \mathrm{P}(x)$. For continuous variables or functions, see Table 7-3.
$(n - 1)$ is used in the equations for variance and standard deviation to produce an unbiased estimate.

[41] In some cases, outliers may be identified using appropriate statistical methods. Such observations are plotted individually beyond the bounds of the whiskers.

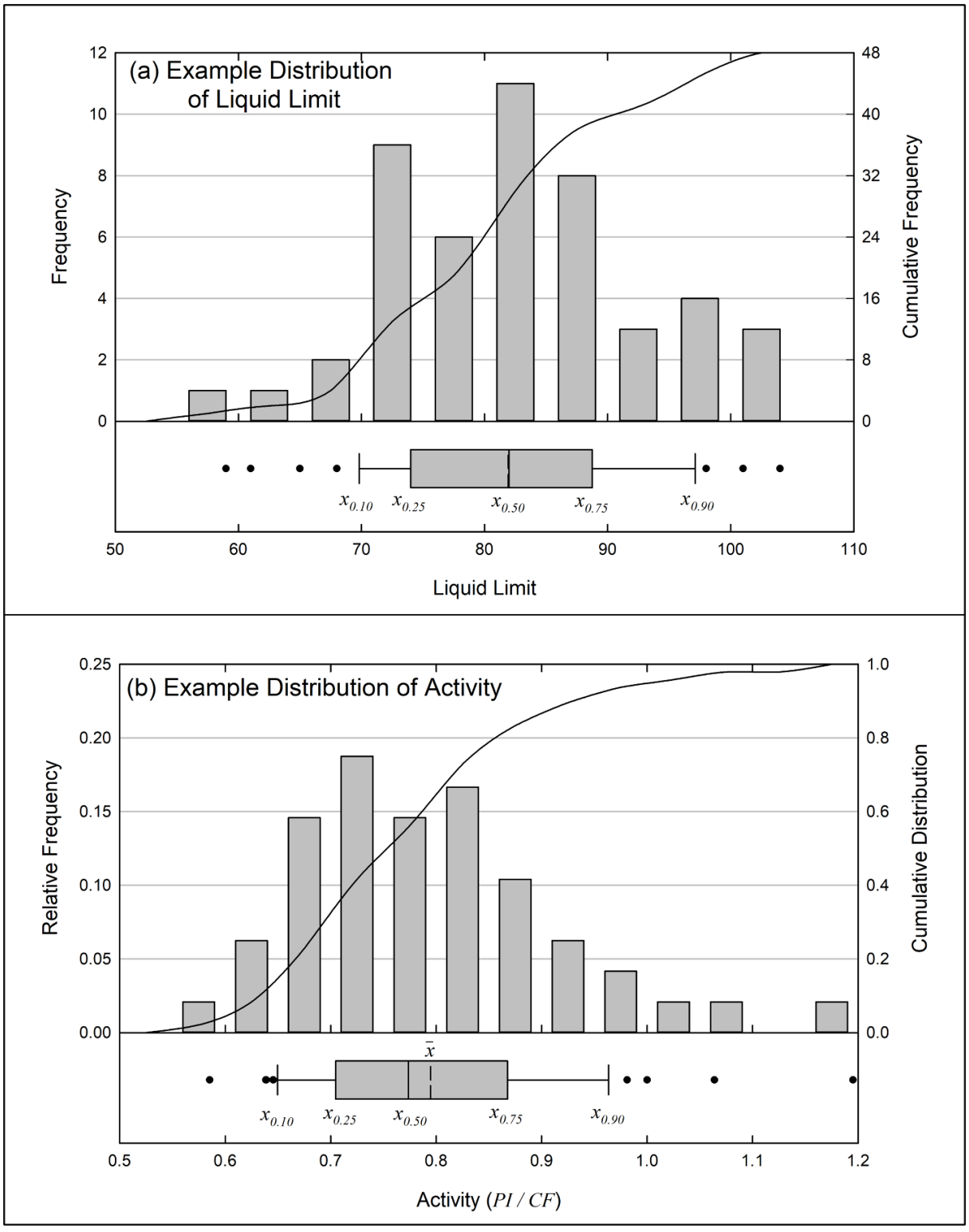

Figure 7-1 Example Statistical Plots Illustrating Important Definitions.

7-2.2.2 Histograms.

The range of a property can be divided into equal intervals or bins, and the number of observations from a sample within each interval can be counted. A *histogram* is a bar graph with the intervals on one axis (typically the x-axis). The frequency or number of observations for each interval is represented by a bar of the appropriate height. The total height of the bars is equal to the number of observations in the sample. If the frequency for each interval is divided by the number of observations in the sample, the histogram plots relative frequency and the sum of the heights of the bars is equal to 1.0. The histograms in Figure 7-1 provide examples of both types of plots.

Histograms are useful for visual interpretation of the statistics of a sample. In Figure 7-1(a), the mean and median liquid limit are both 82 while the mode also corresponds to the interval of 80 to 85. This indicates that the distribution is relatively symmetric about the mean. In contrast, the example of clay activity in Figure 7-1(b) is *skewed*, meaning that the peak or mode of the sample is not at the middle of the range of observations. In this case, the mode is lower than the median while the mean is higher than the median. The observations have a long upper tail, which is referred to as positive skew.

7-2.2.3 Cumulative Distributions.

The *cumulative distribution* shows the number of observations that are less than or equal to a particular value (or interval). The cumulative values are found by progressively summing the number of observations from each interval starting at the lower end of the data. Examples of cumulative distributions are shown by the monotonically increasing curves in Figure 7-1.

7-2.3 Probability.

As discussed at length by Baecher and Christian (2003), the term *probability* can have many definitions. In one sense, probability refers to the relative frequency of an event. Thus, the probability of an event can be thought of as the number of times an event occurs divided by the total number of trials, usually for a large number of trials. This frequentist approach cannot be used for (1) unique occurrences, (2) conditions that cannot be statistically sampled, or (3) direct inference to probabilities on states of nature (Baecher and Christian 2003). In the other sense, probability refers to the degree of belief that an event will occur. This definition of probability can apply to unique occurrences but may be subjective. Further philosophical discussion of the meaning of probability is beyond the scope of this manual.

7-2.3.1 Concepts and Terminology.

In order to understand applications of probability to geotechnical engineering, it is necessary to understand the language of probability. Table 7-2 lists common terminology and provides a general description of the meaning of the terms.

Table 7-2 Probabilistic Terminology (after Ayyub and McCuen 2016, Baecher and Christian 2003)

Terminology	Description
Set	Collection of outcomes. May be discrete or continuous. May be finite or infinite in number.
Subset	Collection of outcomes within a set.
Sample space, S (a.k.a. outcome space)	Set of all possible outcomes for a particular experiment or situation.
Sample points	Individual outcomes within the sample space.
Null set, Ø	Set containing no outcomes.
Event	Subset of the sample space. An event containing no sample points is the null set. An event containing all the sample points is a certain event.
Union, ∪	Subset of outcomes in either A or B (for events A and B).
Intersection, ∩	Subset of outcomes in both A and B (for events A and B).
Complement, $\bar{A}$	Subset of outcomes not in event A.
Overlapping events	Events which intersect. Events A and B are overlapping if $A \cap B \neq \text{Ø}$.
Mutually exclusive events	Events which are completely separate. Events A and B are mutually exclusive if $A \cap B = \text{Ø}$.
Collectively exhaustive events	A set of events that completely comprise the sample space. Events A and B are collectively exhaustive if $A \cup B$.
Partition	A set of collectively exhaustive and mutually exclusive events. The sum of the probabilities of the events in a partition must equal 1.0.
Probability of event, $\mathrm{P}(A)$	Probability that event A occurs with $0 \leq \mathrm{P}(A) \leq 1$.
Conditional probability, $\mathrm{P}(A\|B)$	Probability that event A occurs given the fact that event B occurs.
Independent events	Events for which the probability of one event is not changed by knowing that the other event occurs. For independent events A and B, $\mathrm{P}(A\|B) = \mathrm{P}(A)$ and $\mathrm{P}(B\|A) = \mathrm{P}(B)$.
Dependent events	Events for which the probability of one event is changed by knowing that the other event occurs. For dependent events A and B, $\mathrm{P}(A\|B) \neq \mathrm{P}(A)$ and $\mathrm{P}(B\|A) \neq \mathrm{P}(B)$.
Permutation, $P_{r\|n}$	Number of outcomes possible by picking r items from n possibilities where the order of the items matters (i.e., HTH is different from HHT). $P_{r\|n} = n! \,/\, (n-r)!$
Combination, $C_{r\|n}$	Number of outcomes possible by picking r items from n possibility where the order of the items does not matter (i.e., HTH is the same as HHT). $C_{r\|n} = n! \,/\, [n!\,(n-r)!]$
Binomial coefficient	Alternate notation for combination: $\binom{n}{r} = C_{r\|n} = \frac{n!}{r!(n-r)!}$
Note: The descriptions are intended to be correct but not necessarily rigorous definitions of each term.	

Figure 7-2 illustrates some of these probabilistic concepts in the context of bridge foundation loading. The sample space represents a range of loading conditions for a bridge foundation. Events A, B, and C are extreme loading conditions while Event D represents all other loading conditions. The possibility of combined high traffic, high wind, and flood loading is represented by the overlap of A, B, and C (i.e., $A \cap B \cap C$) and is illustrated by the dark shaded area. Representative probability calculations are also summarized in Figure 7-2. Event D is seen to be the complement of the extreme loadings for the Figure 7-2 example. The probability of the complement of an event is equal to unity minus the probability of the event. Thus, the probability of all other loading conditions is equal to unity minus the probability of the union of A, B, and C.

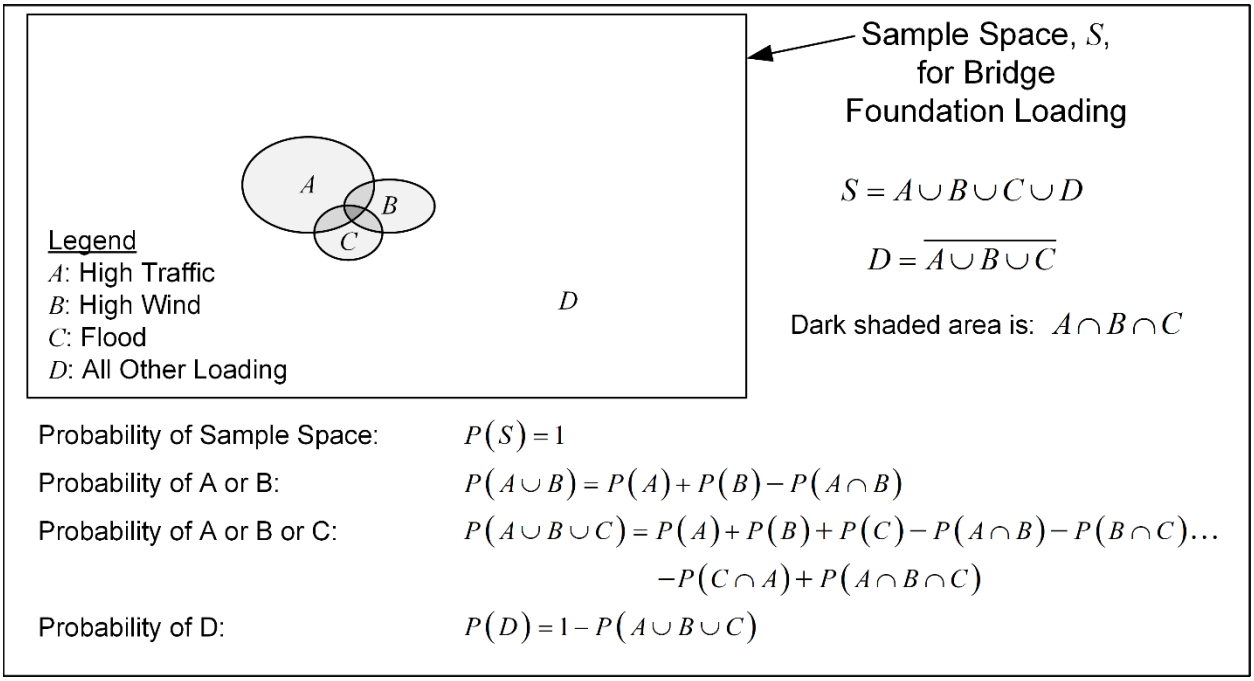

Figure 7-2 Sample Space, Events, and Probability Calculations.

7-2.3.2 Random Variables.

Engineering applications most often are concerned with outcomes that are real numerical values. In this case, a *random variable* (RV) can be used to map every outcome in the sample space to the real line as depicted in Figure 7-3. The mapping may be one-to-one or one-to-many but maintains the probability rules for complements, unions, and intersections. Random variables may be either discrete or continuous. A discrete RV can only take on particular values, usually integers. An example of a discrete RV might be the number of floods larger than a given size at a location in one year. For continuous RV, any value within the range of possible outcomes is valid.

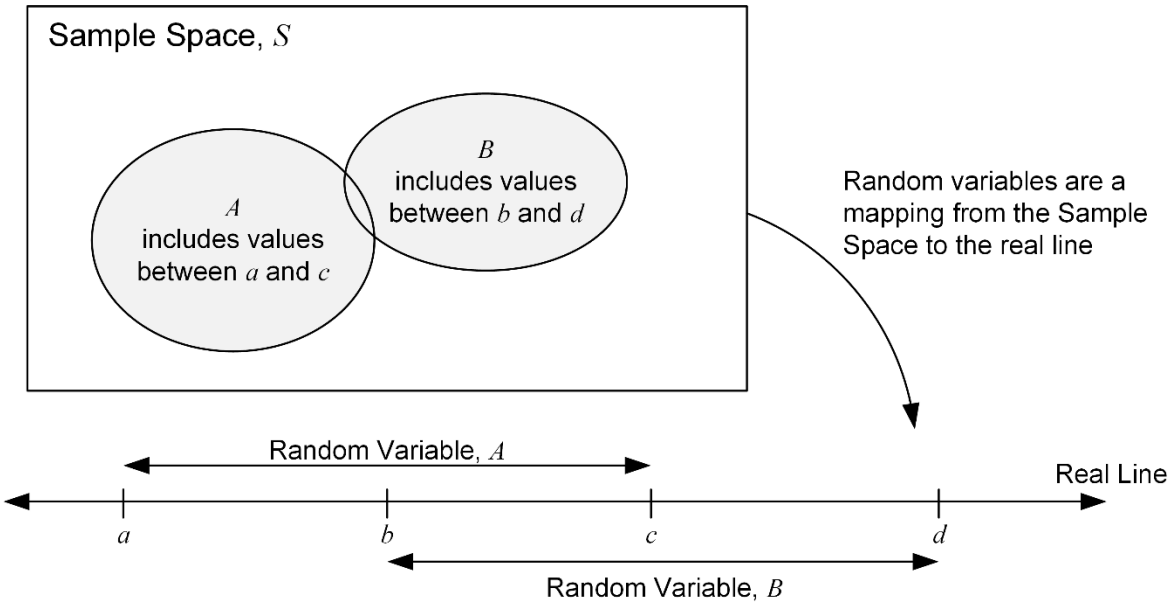

Figure 7-3 Use of Random Variables to Relate Sample Space to the Real Line

7-2.3.3 Probability and Cumulative Distributions.

For discrete RV, probabilities are represented by a *probability mass function* (PMF), which relates probability, $P_X(x_i)$, to particular values of x_i. For each x_i, the PMF provides the probability that the random variable X takes on the value x_i. The *cumulative mass function* (CMF) is defined as the probability that X is less than or equal to x_i or:

$$F_X\left(x_i\right) = P_X\left(X \le x_i\right) = \sum_{j=1}^{i} P_X\left(x_i\right) \qquad (7\text{-}1).$$

Other important properties of discrete random variables are summarized in Table 7-3. Examples are found in Figure 7-4(a) and (c). The left bars of each histogram represent the PMF while the right bars represent the CMF. The CMF bar for each x_i is equal to the previous value of the CMF plus the current value of the PMF. In other words, the PMF is the difference between the CMF for the current and previous values of x_i.

For continuous RV, the probability functions use the term density rather than mass. The *cumulative density function* (CDF) is the probability that X is less than or equal to x_0, which is calculated as:

$$F_X\left(x_0\right) = P\left(X \le x_0\right) = \int_{-\infty}^{x_0} f_X\left(x\right) dx \qquad (7\text{-}2).$$

The integral in the CDF is analogous to the summation for the CMF. The CMF and CDF are both non-decreasing functions as the RV increases.

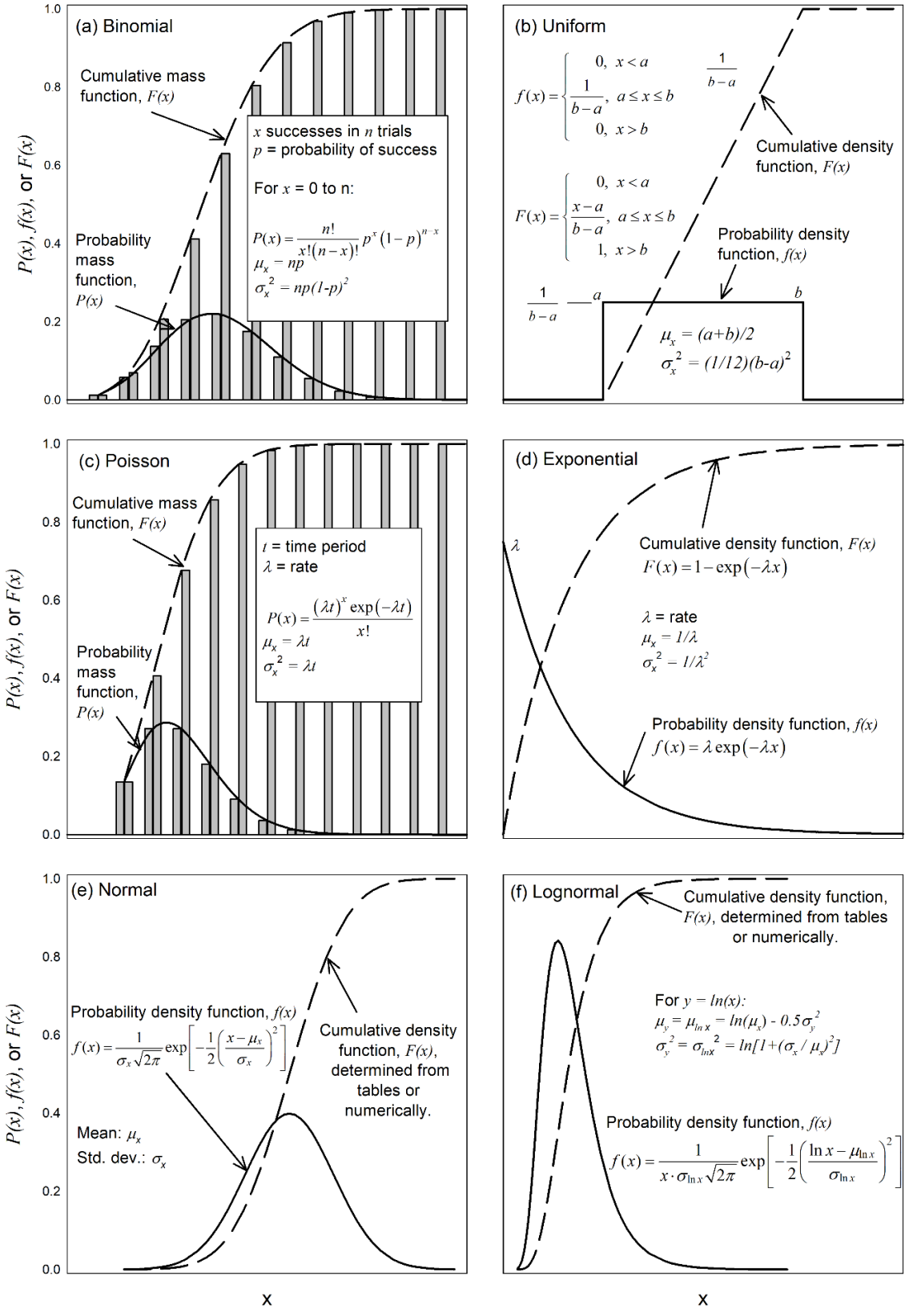

Figure 7-4 Common Types of Distribution

Probabilities of continuous RV are represented by a *probability density function* (PDF), $f_X(x)$. Similar to the PMF, the PDF is the rate of change of the CDF, or its first derivative, such that:

$$f_X(x) = \frac{d}{dx} F_X(x) \tag{7-3}$$

This is illustrated by the uniform distribution in Figure 7-4(b). The uniform CDF increases linearly from 0 to 1 over the interval $[a, b]$. The value of $f_X(x)$ is equal to the slope or derivative of the CDF. For continuous RV, probabilities are defined only over an interval:

$$P(x_1 \le X \le x_2) = \int_{x_1}^{x_2} f_X(x)\,dx \tag{7-4}$$

While the PDF has a value at particular values of X, the probability of a particular value of X is zero.[42] Properties of continuous random variables are summarized in Table 7-3.

Table 7-3 Properties of Random Variables

Distribution Properties	Type of Distribution	
	Discrete	**Continuous**
Total probability and cumulative values at extremes	$0 \le P_X(x_i) \le 1$, $\sum_{i=1}^{n} P_X(x_i) = 1$ $F_X(x_i) = 0$ for $x < x_1$ $F_X(x_i) = 1$ for $x > x_n$	$P(-\infty \le X \le \infty) = 1$ $F_X(-\infty) = 0$ $F_X(\infty) = 1$
First moment about the origin (mean)	$\mu_X = \sum_{i=1}^{n} x_i P_X(x_i)$	$\mu_X = \int_{-\infty}^{\infty} x \cdot f_X(x)\,dx$
Second moment about the mean (variance)	$\sigma_X^2 = \sum_{i=1}^{n} (x_i - \mu_X)^2 P_X(x_i)$	$\sigma_X^2 = \int_{-\infty}^{\infty} (x - \mu_X)^2 \cdot f_X(x)\,dx$
k[th] moment about the mean	$M_k = \sum_{i=1}^{n} (x_i - \mu_X)^k P_X(x_i)$	$M_k = \int_{-\infty}^{\infty} (x - \mu_X)^k \cdot f_X(x)\,dx$
Expected value, E	$E[g(x_i)] = \sum_{i=1}^{n} g(x_i) P_X(x_i)$	$E[g(x)] = \int_{-\infty}^{\infty} g(x) \cdot f_X(x)\,dx$
Notes: The standard deviation is the square root of the variance (σ_X) The population mean (μ_X) can be replaced by the sample mean ($\bar{x}$) for calculations based on a sample rather than the entire population.		

[42] A physical object with a known density must have thickness in order to have a mass. The interval is the thickness required to have mass in probabilistic terms.

The probability functions (PMF or PDF) are often described by their moments about the origin or about the mean, which are analogous to area moments from mechanics. The mean is first moment about the origin, analogous to the center of gravity. The variance is the second moment about the mean, analogous to the moment of inertia. The third and fourth moments about the mean are referred to as the skew and kurtosis, respectively. These moments can be calculated from the PMF or PDF using the equations provided in Table 7-3.

Table 7-3 also defines the *expected value* ($\mathrm{E}[\cdot]$), which is found by multiplying any function by the PMF or PDF over the full range of the random variable. The expected value is a linear operator and can be distributed algebraically through expressions. The expected value of a constant is the constant. The mean is the expected value of x or $\mathrm{E}[x]$, which can be found by substituting x for $g(x)$.

Any function may serve as a PMF or PDF provided that the properties in Table 7-3 are satisfied. Six common distributions are plotted in Figure 7-4 along with equations for the PMF and CMF or PDF and CDF, if available. More information on each of these distributions follows:

- Binomial – discrete distribution that results from repeated experiments with each being a Bernoulli trial (i.e., two outcomes – success or failure) with constant probability, p, for each trial. The binomial distribution uses the binomial coefficient and is useful for modeling the probability of a specified number of events (e.g., floods, earthquakes, etc.) in a certain time period.
- Uniform – continuous RV with equal probability over the specified range and zero probability outside of the interval $[a, b]$.
- Poisson – discrete distribution commonly used to model the occurrence of a random event in a continuous dimension of time or space as a limiting case of the binomial distribution. The three stochastic processes represented by the Poisson distribution are (1) the number of events in a time interval, (2) the intensity of an event, and (3) the separation of the events in time or space. The second and third processes can be continuous rather than discrete.
- Exponential – continuous distribution related to the third Poisson process of time between events. The exponential function is described by a single parameter, λ, which is related to the rate and is the value of the PDF at $x = 0$. The mean of the exponential function is also referred to as the recurrence or return period.
- Normal (a.k.a., Gaussian) – symmetric, bell-shaped, continuous distribution that fits well to the distribution of many naturally occurring properties. The mean and standard deviation are conveniently the parameters of the PDF. The notation $\mathrm{N}(\mu_X, \sigma_X)$ is often used as shorthand for the normal distribution. The CDF cannot be expressed in a closed form equation and must be read from tables or determined numerically. Modern spreadsheets and statistics packages can easily provide the normal CDF. The addition of more than one normally distributed RV

results in another normally distributed RV. When RV with any type of distribution are added together, the resulting distribution will tend to be normal as the number of RV increases. This explains the wide natural occurrence of the normal distribution.

- Lognormal – skewed continuous distribution related to the normal distribution via a transformation ($y = \ln x$), which can be used to determine CDF values. The lognormal distribution does not allow negative values, which is convenient for many engineering properties. Lognormal distributions result from the multiplication of many RV with any type of underlying distribution.

7-3 UNCERTAINTY IN GEOTECHNICAL ENGINEERING.

Uncertainty refers to a condition that is completely or partially unknown, indefinite, indeterminate, or unverified (Baecher and Christian 2003). In the context of geotechnical engineering, soil and rock properties are uncertain because of natural variation in space, and possibly time, and because measurements and interpretations are required to determine these properties. Calculated values, such as settlement, bearing capacity, and lateral earth pressure, may be uncertain because of the uncertainty of both input parameters and the analytical or numerical models used.

7-3.1 Sources of Uncertainty.

Uncertainty in geotechnical engineering occurs mostly within two groups, which sometimes overlap. *Natural variability* (a.k.a., *aleatory* or *external* uncertainty) occurs from physical randomness and describes variability at various locations at the same time, or variations in both time and space. On the other hand, *knowledge uncertainty* (a.k.a., *epistemic* or *internal* uncertainty) occurs from a lack of knowledge, such as data, information, or understanding. As pointed out by Baecher and Christian (2003), the latter manifests most prominently in geotechnical engineering in site characterization, determination of soil and rock parameters, and selection of appropriate engineering models. Geotechnical engineering must also interact with social and economic factors, which may add uncertainties related to operations and decision-making. These are outside the scope of this chapter.

7-3.1.1 Inherent Soil and Rock Variability.

Soil and rock inherently exhibit natural variability as a result of the complex natural processes by which these materials have reached their current location and condition. Inherent variability can apply to both stratigraphy and soil properties within a particular stratum as illustrated in Figure 7-5. The thickness of every soil layer varies spatially, and the soil properties, such as composition, packing, and stress state, vary within each layer. Characterization of these variations is necessarily limited, which, in reality, produces knowledge uncertainty. However, from a practical standpoint, inherent,

natural variability is usually considered *stochastic*, which simply refers to a random variation in time or space.

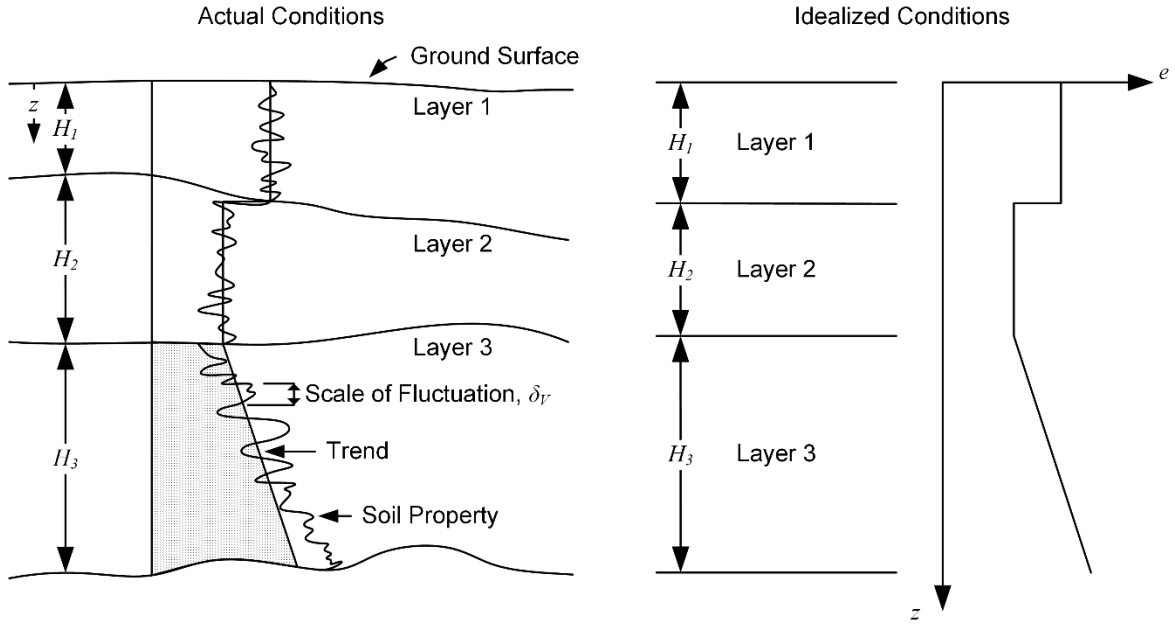

Figure 7-5 Uncertainty in Characterization of Actual Field Conditions (after Phoon and Kulhawy 1999a)

The degree of inherent variability depends heavily on the geologic and environmental history. For example, coarse-grained alluvial deposits have high spatial variability as a result of the rapid changes that occur in stream morphology. In contrast, varved fine-grained lacustrine deposits have low variability in the horizontal direction and high, but predictable, variability vertically across the varves.

Figure 7-6 summarizes the available data for the inherent variability of various soil and rock properties and parameters. The gray bars and dots indicate the range and mean of reported COV, respectively, for each property. The COV normalizes the standard deviation with respect to the mean. Wide gray bars indicate a wide variation in the level of uncertainty for the particular property. The range of mean values of each geotechnical property is provided. For soils with properties outside these ranges, the COVs may differ.

While care was taken to isolate inherent variability from measurement error as much as possible, these values likely contain some uncertainty caused by the measurement technique. Because of the complexity of separating sources of uncertainty, there is a bias towards higher values of COV. The engineer should be aware that the true inherent variability may be lower than as represented by the data in Figure 7-6.

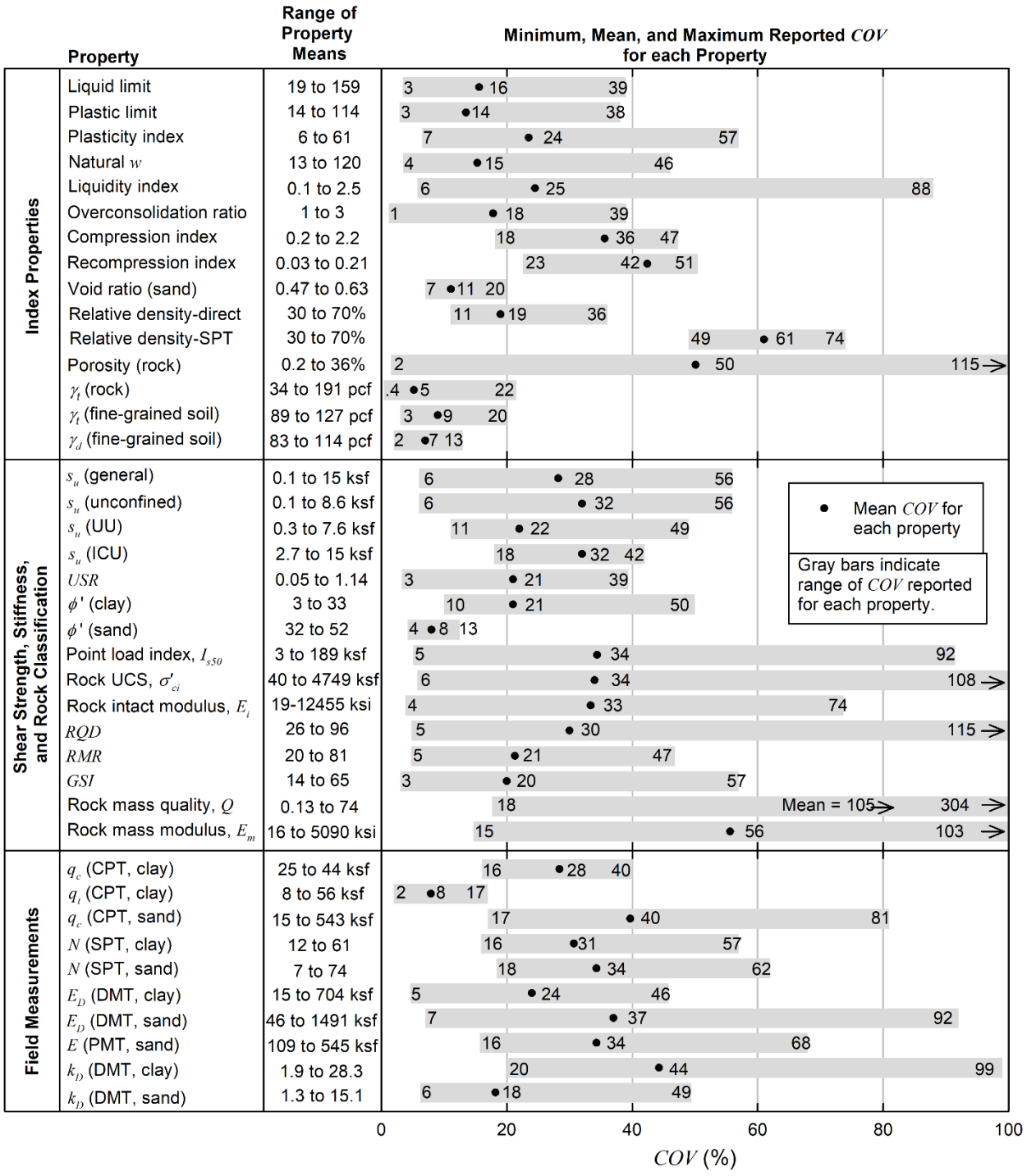

Figure 7-6 Typical Inherent Variability
(after Phoon and Kulhawy 1999a, Guan et al. 2021)

7-3.1.2 Measurement Error.

According to Phoon and Kulhawy (1999a), measurement error can be attributed to equipment effects, operator or procedural problems, and random testing effects. In general, these components of measurement cannot be separated. VandenBerge et al. (2020) used simulation to show that well-calibrated equipment should result in $COV(\phi')$ less than 1%. It appears likely that most laboratory testing error results from operator and procedural testing error, including soil disturbance.

Determination of laboratory measurement errors requires cross-laboratory testing of the same soil, which has been performed by a few studies and by ASTM for a small number of test methods. Field measurement errors have been studied for various types of equipment by Kulhawy and Trautmann (1996). The available data on laboratory and field measurement errors are summarized in Figure 7-7. In general, the measurement uncertainty is lower than the inherent variability. Some of the highest measurement variability occurs for the SPT and the plasticity index.

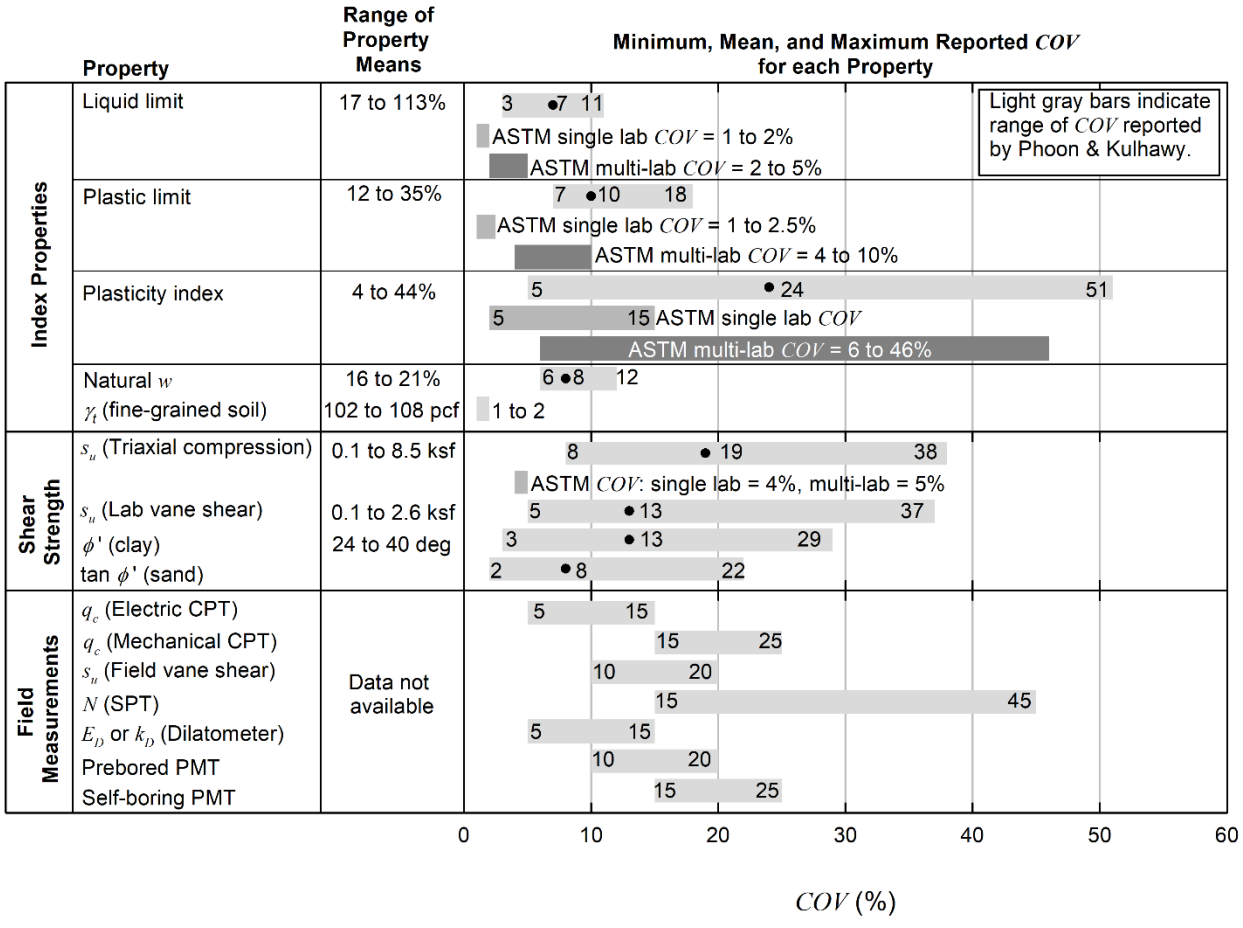

Figure 7-7 Typical Measurement COV (after Phoon and Kulhawy 1999a, ASTM D1586, ASTM D2216, ASTM D4318)

7-3.1.3 Transformation Uncertainty.

Phoon and Kulhawy (1999b) point out that the geotechnical parameters are often obtained by *transformation* from a more easily measurable property to that required for design through the use of empirical correlations,[43] such as those found in Chapter 8 of DM 7.1. Empirical correlations are based on observation and contain error, which adds an additional source of uncertainty into the assessment of geotechnical parameters.

When an empirical correlation is developed, transformation uncertainty is determined from the residual error between the supporting data and the empirical trend, which can either be expressed in terms of coefficient of variation or standard deviation. For example, Phoon and Kulhawy (1999b) provide examples of correlations for s_u from corrected vane shear tests (COV of 7.5 to 15%), from corrected tip resistance (COV of 29 to 35%), and from SPT (COV of 15%). Ching and Noorzad (2021) summarize the uncertainty in common empirical correlations for soil and rock properties.

7-3.1.4 Model Uncertainty.

The previous three sections dealt with uncertainties in the determination of geotechnical parameters. A related source of uncertainty is the selection of a shear strength model (e.g., linear vs. nonlinear) or a constitutive theory (e.g., Duncan-Chang vs. Cam Clay). None of these theories or models perfectly represent soil behavior, and each will cause uncertainty.

Uncertainty can also be introduced by the analytical or numerical approach selected to calculate design values. For example, consider the scenarios illustrated in Figure 7-8. The calculated bearing capacity will vary depending on which theory is used (i.e., lower bound, upper bound, etc.), and all of the theories contain empirical components. Similarly, the calculation of lateral earth pressure requires assumptions that lead to uncertainty in the calculated values.

Some calculation methods are much less certain than others. Estimates of settlement magnitude from consolidation calculations can be quite accurate, if the clay has low inherent variability and can be well-characterized. In contrast, estimates of sand compression from SPT blow counts will have much higher uncertainty. The greater uncertainty results from the empirical nature of the latter prediction method as well as the greater inherent variability of most sand deposits.

Unfortunately, little information is available on model uncertainty, especially for theoretical solutions. Where an analytical method is empirically based, the COV of the

[43] Empirical correlations are based on the statistical concept of correlation in which probability distributions of two or more random variables are dependent on each other. See Section 7-3.2.

model can be estimated from the errors between the observed data and the trend, similar to Phoon and Kulhawy's (1999b) approach for transformation uncertainty. Additional examples in which model uncertainty is considered can be found in McGuire and VandenBerge (2017).

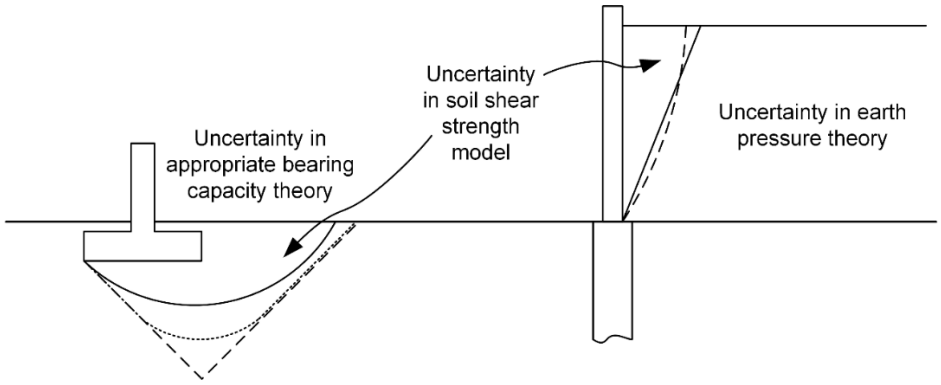

Figure 7-8 Model Uncertainty Examples

7-3.1.5 Combined Uncertainty Effects.

Figure 7-9 is a schematic illustration of how various sources of uncertainty combine to affect a geotechnical prediction. The example in the figure assumes that a soil layer with spatial variability is sampled at discrete locations. At these points, its properties may differ from the overall trend. Measurement of a desired property is made using sampling and/or testing, which introduces additional error. In many cases, the measured property must then be transformed into a useful engineering parameter.

Using a first-order approximation about the mean, the COV of the desired parameter can be estimated as

$$COV^2(\theta) = COV_w^2 + COV_e^2 + COV_t^2 \tag{7-5}$$

where:
θ = generic geotechnical parameter
COV_w = coefficient of variation of inherent variability,
COV_e = coefficient of variation of measurement error, and
COV_t = coefficient of variation of transformation.

One or more engineering parameters are used in an analytical model, which may have uncertainty of its own, to predict a desired outcome, such as settlement, bearing capacity, or factor of safety. The predicted outcome will be uncertain as depicted by the distribution at the bottom of Figure 7-9. The methods used to evaluate this uncertainty in engineering predictions are the subject of Section 7-4.2 on reliability analysis.

Figure 7-9 and Equation 7-5 are not intended to imply that the various sources of uncertainty in geotechnical parameters can easily be separated. This is especially true

for inherent variability and measurement error. Such separation may be necessary for rigorous consideration of uncertainty, particularly if the effects of correlation described in the next section are considered. However, for many applications and simplified reliability analyses, the selection of a combined COV for each parameter is appropriate.

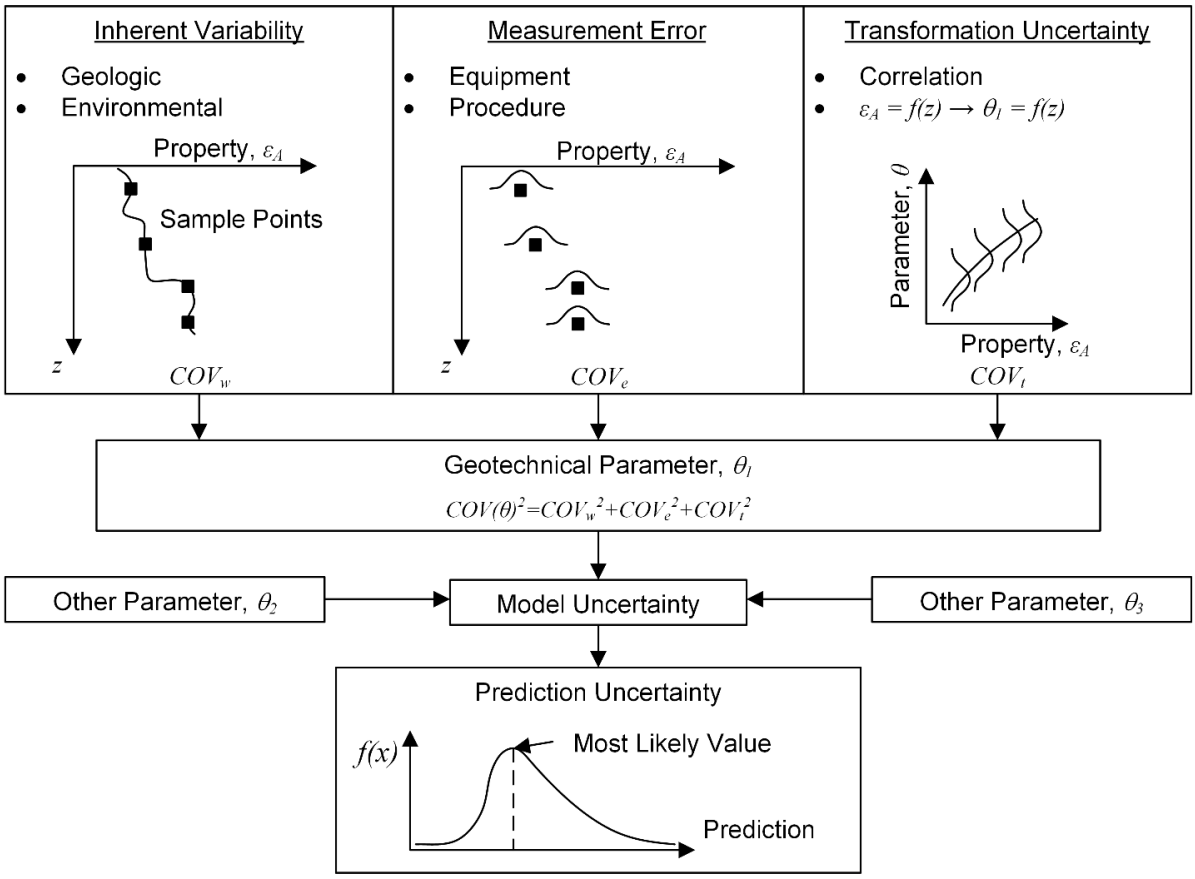

Figure 7-9 Combined Effects of Uncertainty on Geotechnical Design

Table 7-4 contains typical values of COV for a variety of geotechnical parameters. The values can be assumed to contain the combined effects of inherent, measurement, and transformation uncertainty. The values have been divided into categories for low, moderate, and high uncertainty, corresponding approximately to the lower, middle, and upper thirds of the reported COV values for each parameter. These values provide a rational means of accounting for the engineer's knowledge of site conditions, subsurface exploration techniques, and the use of transformations (if appropriate). For example, if a retaining wall is being planned at a site with an excellent site investigation and relatively uniform clay soils (i.e., low uncertainty), a COV of 25% would be appropriate for the undrained shear strength from laboratory tests. Continuing this example, the effective friction angle for the wall's sand backfill may be estimated based on the expected compaction, and a COV of 16% might be selected due to the high uncertainty associated with this estimate.

Table 7-4 Typical Combined COV for Common Geotechnical Parameters (after Phoon and Kulhawy 1999a,b; Sleep and Duncan 2014, FHWA 2001, Guan et al. 2001)

Property		Typical COV based on Uncertainty Level (%)		
		Low[A]	Moderate[B]	High[C]
Soil Index Properties	Unit weight	4	8	12
	Natural water content	10	15	25
	Liquid limit	10	15	25
	Plastic limit	10	15	25
	Void ratio (sand)	10	15	20
	Relative density (direct measurement)	15	20	30
	Relative density (from SPT)	50	60	70
Soil Compressibility, Hydraulic Conductivity, and Shear Strength	Compression index	25	35	45
	Recompression index	25	35	45
	Preconsolidation stress	15	20	30
	Overconsolidation ratio	10	20	30
	Coefficient of consolidation	40	50	60
	Coefficient of hydraulic conductivity (saturated)	75	80	85
	Coefficient of hydraulic conductivity (unsaturated)	150	180	210
	Effective stress friction angle (sand)	8	12	16
	Undrained shear strength (from laboratory tests)	25	40	50
	Undrained strength ratio (USR)	20	30	40
Field Measurements	SPT blow count (clay)	15	30	45
	SPT blow count (sand)	25	35	45
	CPT cone tip resistance (clay)	20	30	35
	CPT corrected cone tip resistance (clay)	5	10	15
	CPT cone tip resistance (sand)	25	40	55
	Dilatometer modulus (clay)	15	25	35
	Dilatometer modulus (sand)	30	50	70
	Dilatometer lateral earth pressure coefficient (clay)	15	30	40
	Dilatometer lateral earth pressure coefficient (sand)	20	45	70
	Vane shear test undrained shear strength	15	25	35
	Pressuremeter modulus (sand)	15	35	55
Rock Properties	Unit weight	1	5	10
	Porosity	25	50	75
	Point load index	15	35	55
	Unconfined compressive strength	15	35	55
	Intact modulus	20	35	50
	Rock mass modulus	30	55	80
	Compression wave velocity	5	15	25

COV was assumed to follow a normal distribution. The standard deviation of COV was estimated by the reported range and number of studies for each parameter (see Baecher and Christian 2003 Table 3.2). In order to limit the implied accuracy, values were rounded to regular intervals.

[A] Mean COV minus one standard deviation – use for well-characterized or relatively homogeneous site conditions

[B] Mean COV – use for typical site characterization and/or geologic variability

[C] Mean COV plus one standard deviation – use for limited characterization and/or highly variable soil conditions

7-3.2 Effects of Correlation on Uncertainty.

7-3.2.1 Correlation between Parameters.

Geotechnical parameters are often correlated with each other (i.e., covariance is non-zero – see Table 7-1), which means that the two parameters do not vary independently. For example, when c' and ϕ' are used to characterize shear strength, the values are negatively correlated. As c' increases, ϕ' decreases for a given soil and condition. The variation of undrained shear strength with depth is another example. Undrained strength is a function of effective stress, which depends on the soil unit weight. Thus, the undrained shear strength should be positively correlated to the unit weight.

Geotechnical applications of probability theory should account for correlation between parameters, if possible. The inclusion of correlation typically requires that additional terms be added to the calculation of the variance of the solution, which can substantially complicate the analysis.

7-3.2.2 Autocorrelation.

Within the ground, soil and rock properties vary spatially from point to point and/or with time at the same point. This is true even after removing the effects of geologic trends, such as layering or increasing stress with depth. *Autocorrelation* refers to the correlation of a soil or rock property with the same property at a different point in space or time (Baecher and Christian 2003). The amount of autocorrelation observed varies with the distance between the two observation points and the variability of the soil or rock. If the distance is zero, the two observation points are identical, and the correlation is perfect (r = 1). As the distance increases, the properties at the two points are no longer identical, and the correlation decreases (r approaches zero). The distance within which the property is significantly correlated with itself (perhaps $|r| \geq 0.1$) is referred to as the *correlation length* (Fenton and Griffiths 2008). Further discussion involves the topics of random field theory and geostatistics, which are beyond the scope of this manual.

Autocorrelation is sometimes presented in terms of the *scale of fluctuation* (δ_v for vertical and δ_h for horizontal) shown in Figure 7-5. The scale of fluctuation is the distance over which the soil properties are strongly correlated. Soils deposited in horizontal layers can have very different values of δ_v and δ_h. When δ_v is large, the soil properties are well-correlated and change less rapidly. As δ_v approaches zero, the properties become uncorrelated and can change rapidly. For small δ_v relative to the slip surface or structure passing through the soil, the uncertainty in the soil properties will tend to average out. A simplified method of considering the scale of fluctuation is found in Vanmarcke (1977). More rigorous consideration of fluctuation may require the use of the random finite element method (Fenton and Griffiths 2008).

7-3.3 Designing for Uncertainty.

Many different approaches have been taken in geotechnical engineering to address the uncertainties discussed in previous sections.

Design may implicitly account for uncertainty using a factor of safety. In this case, the design is approached in a *deterministic* manner, meaning that the calculations are based on a single value selected for each geotechnical parameter. Uncertainty is accounted for solely in the selection of a factor of safety, usually lumped into a single factor. The effects of uncertainty in the individual parameters or loads on the overall design cannot be determined. An alternative to this approach will be discussed further in Section 7-4.5, which describes load and resistance factor design.

In contrast, *stochastic* approaches explicitly consider the uncertainty associated with the design. In particular, reliability analysis provides an alternative to deterministic design that explicitly includes uncertainty as summarized in Section 7-4.2. Additional information about the probability distribution of the key geotechnical parameters must be determined or estimated to complete a reliability analysis. Duncan (2000) advocates for the use of reliability analysis alongside conventional design using factors of safety. The use of factor of safety provides continuity with past experience while the reliability analysis allows geotechnical engineers to more directly understand the impact of uncertainty on their designs. Reliability analysis is also used to inform estimates of probability for risk assessments.

Both the deterministic and stochastic approaches to geotechnical design seek to establish an appropriate level of conservatism that is in balance with direct costs (FHWA 1987). Many times, this is accomplished using specified factors of safety based on past experience.

Risk is the product of the probability of an adverse event multiplied by its consequence, which is often expressed in terms of fatalities or monetary cost. The cost of failure can be quantified and compared to the cost of designing a more conservative facility. In some cases, risk must be compared to either acceptable or tolerable levels. *Acceptable risk* can be defined as “a state of risk which stakeholders are willing to accept” while *tolerable risk* refers to a state of risk that society will tolerate because of the broader benefit (Timchenko et al. 2021). If risk is considered explicitly during design, the level of conservatism required in the design can be selected more rationally.

7-4 APPLICATIONS.

The purpose of this section is to help the engineer understand common uses of statistics and probability in geotechnical engineering and begin to use these methods. In particular, these sections should provide sufficient background to interpret reliability

analyses, risk assessments, and hazard analyses performed by others. In addition, the basis of LRFD is discussed and compared with ASD to elucidate LRFD.

7-4.1 Evaluation of Field and Laboratory Data.

Principles of statistics and probability can be used to both plan and analyze field and laboratory data. The following sections describe a few specific applications but are not a comprehensive list.

7-4.1.1 Selection of Geotechnical Parameters.

Geotechnical designs can be separated into three basic approaches with respect to the selection of parameters (i.e., c' and ϕ', s_u, k, γ, etc.). In the first approach, the design calculations are deterministic and based on a single estimate of each required parameter. Often, this approach implicitly recognizes uncertainty by the selection of test specimens or results that represent conservative conditions, especially when limited testing is performed. For example, specimens from the softest clay layers may be selected for the determination of compressibility. Another example is the *one-third rule*, which chooses a design parameter such that one-third of the data lies to the conservative side of the selected parameter (USACE 2001). Such practices introduce bias that may be appropriate for deterministic analysis.

The second approach is to use deterministic analysis for ranges of values for the important parameters. The ranges for each parameter are selected from the results of field or laboratory testing, or based on engineering judgment. This approach also implicitly recognizes uncertainty in the parameters but does not attempt to explicitly consider probability.

The third approach explicitly considers the probability distribution of the geotechnical parameters, likely for use in a reliability analysis (see Section 7-4.2). In this case, distribution statistics (usually the mean and standard deviation) of each parameter must be determined. In most cases, the type of distribution is also required for each parameter. For nearly all geotechnical projects, the sample sizes are small from a statistical viewpoint. Many parameters are selected based on the results of three or fewer tests (e.g., s_u from UU tests or c' and ϕ' from direct shear tests). In this case, the measured parameter(s) can be assumed to represent mean conditions unless correlations indicate the parameter(s) are unusually high or low. The COV for very small samples must be selected based on typical values (Table 7-4). As the sample size increases, improved estimates of the mean and standard deviation can be obtained directly from the data.

The standard deviation of a parameter can also be estimated using the so-called *n-sigma rule*. This method leverages the fact that 99.7% of all values fall within a range of three standard deviations above and below the mean for a normally distributed RV. The

highest conceivable value (HCV) and lowest conceivable value (LCV) of the variable should be separated by a distance of six standard deviations (i.e., n = 6), resulting in:

$$\sigma = \frac{HCV - LCV}{n} \quad \text{(7-6)}.$$

Because of a tendency to under- or overestimate the HCV and LCV, n is sometimes taken to be 3 or 4 in order to produce a conservatively high estimate of σ. An example of this approach is provided in Appendix B.

Three examples of geotechnical parameter selection are provided in Figure 7-10. In the first example, SPT blow counts are presented. For deterministic analyses using N as an input, an N of 21 might be selected or a range of 15 to 25 may be evaluated. Alternatively, a lognormal distribution has been fit to the N values, which could be used for a probabilistic analysis. The second example examines similar data for undrained shear strength. The drained strength data for the third example is presented in shear-normal stress space. The data is interpreted using a fixed adhesion (a') and stochastic ϕ'. For more information on fitting probability distributions to data, see Baecher and Christian (2003) or Ayyub and McCuen (2016).

7-4.2 Reliability Analysis.

Probabilistic principles can be applied to determine the reliability of a geotechnical design problem. *Reliability* is the probability that the design will perform in a satisfactory manner. This concept can also be stated in a negative sense as the *probability of unsatisfactory performance* (a.k.a., *probability of failure*), P_u. The reliability and the probability of unsatisfactory performance sum to unity.

In order to estimate reliability, a design problem is written in terms of a *limit state function*, $g(X)$, of random variables (X). Positive values of $g(X)$ correspond to satisfactory performance while negative values represent unsatisfactory performance or failure. Limit state functions are commonly written in terms of a safety margin or a safety factor as illustrated in Figure 7-11. The safety margin is the difference between the capacity and the demand, resulting in a negative value if demand exceeds capacity (Cornell 1969). For example, the predicted settlement for a foundation can be subtracted from the maximum allowable settlement. In the safety factor approach, the limiting safety factor of 1 is subtracted from the capacity divided by the demand (Rosenblueth and Esteva 1972). An example of this case would be foundation bearing capacity divided by the applied stress minus one.

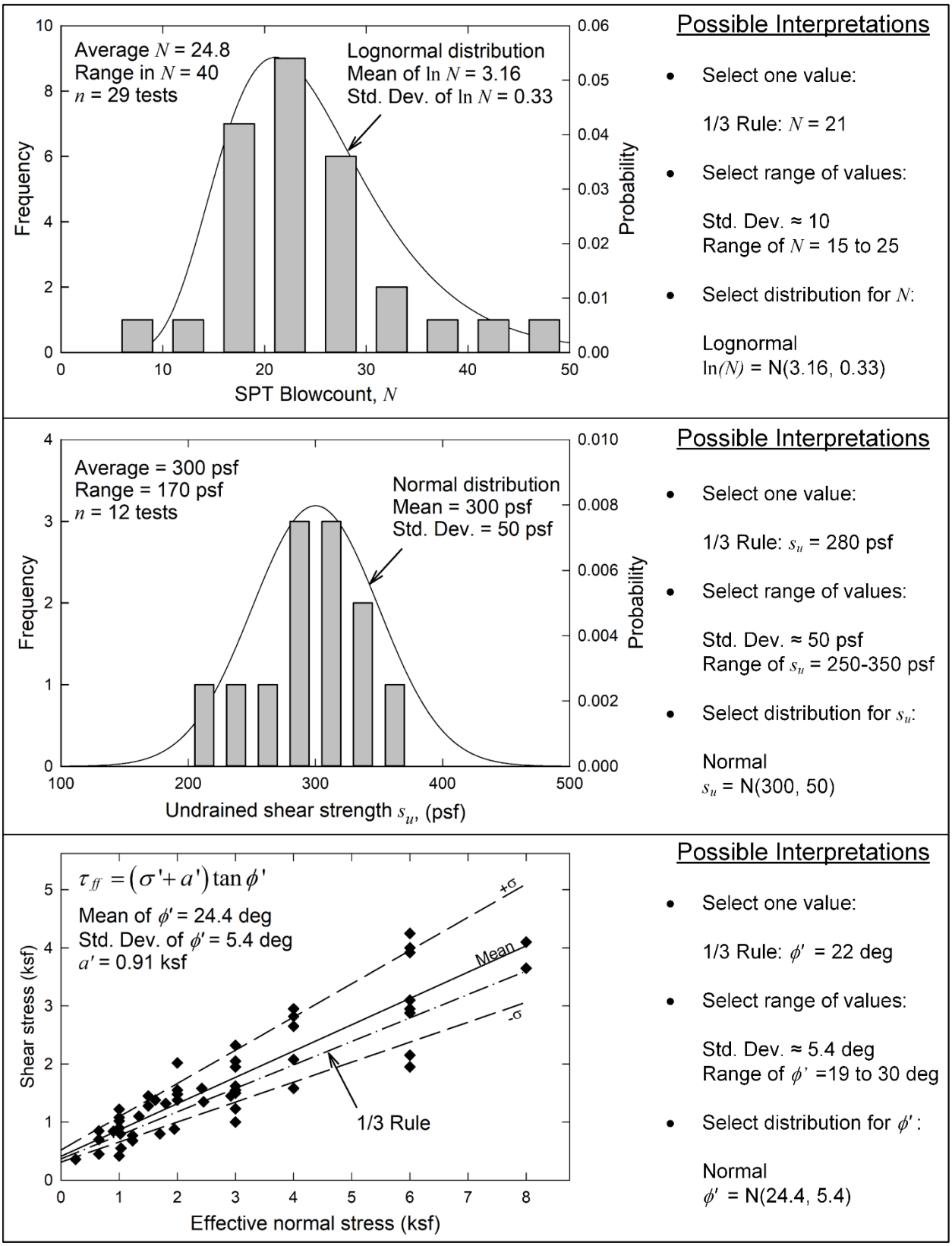

Figure 7-10 Parameter Selection Using Probabilistic Concepts

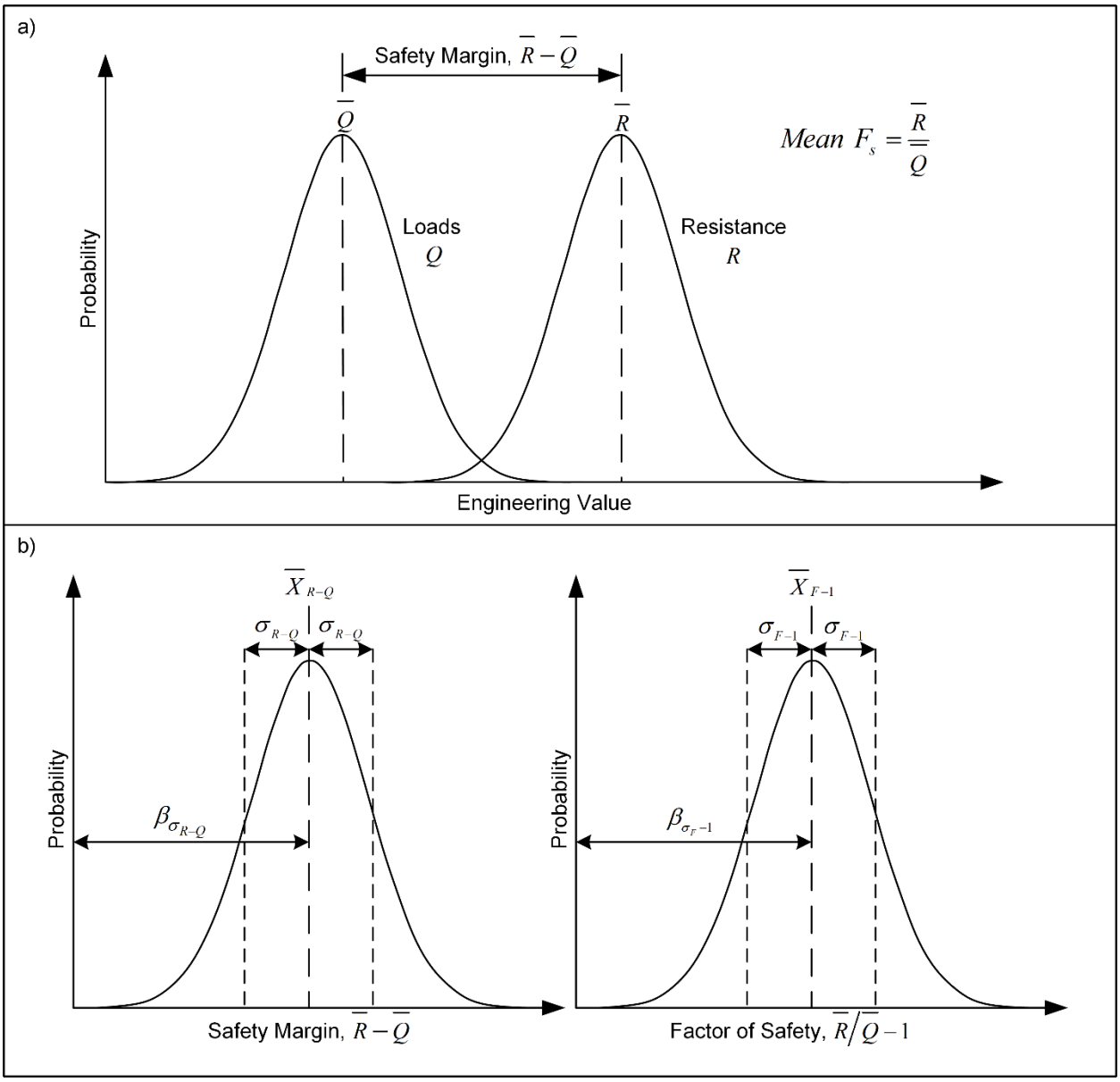

Figure 7-11 Example Distributions for (a) Load and Resistance and (b) Safety Margin and Factor of Safety Formulations

Once the design problem has been written as a limit state, the mean, $\mu_{g(X)}$, and standard deviation, $\sigma_{g(X)}$, of $g(X)$ must be determined. Differences in reliability analysis approaches lie mostly in the method and level of approximation involved in calculating these values. The results of limit state function will have a probability distribution that results from the distributions of the input random variables and their interactions within the limit state function. The level of difficulty associated with determining $\mu_{g(X)}$ and $\sigma_{g(X)}$ depends on the complexity of the design problem, the number of random variables, and probability distributions of those variables.

The *reliability index* (β) can be generically defined as the number of standard deviations that separate the mean design condition from a state of failure as shown in Figure 7-11 (Cornell 1969). If the problem is defined using a limit state function, then

$$\beta = \frac{\mu_{g(X)}}{\sigma_{g(X)}} \quad \text{(7-7).}$$

The value of β calculated for a specific problem will depend on the method used to determine the mean and standard deviation of $g(X)$. Transformations of the limit state function (e.g., use of logarithms) may also result in changes in the value of β. Thus, the reliability index can vary depending on how it is defined. Because of the uncertainty in the statistics of the input parameters, geotechnical reliability analyses produce values of β that are also uncertain (USACE 2020).

The reliability index provides a relative measure of the reliability of the solution but not the probability of unsatisfactory performance. The value of P_u can be estimated from β based on the distribution of the results of the limit state function. Usually the distribution of $g(X)$ is not known and must be assumed. The normal and lognormal distributions are common assumptions for the distribution of the results of $g(X)$.

Approximate methods are appropriate for application of reliability analysis to real-world problems. It is important to bear in mind the uncertainty involved in describing the probability distributions of geotechnical parameters, which will affect the calculated values of $\mu_{g(X)}$ and $\sigma_{g(X)}$. Four methods are considered in this section and summarized in Table 7-5: (1) first order, second-moment, including the so-called Taylor series approximation, (2) point estimate method, (3) Hasofer-Lind, and (4) Monte Carlo simulation. These methods can accommodate correlated random variables; however, only uncorrelated solutions are presented in this section. A detailed example of the four methods is provided in Appendix B.

7-4.2.1 First-Order, Second Moment Method.

The first-order, second moment (FOSM) method uses only the mean (μ_{Xi}) and variance (σ_{Xi}) of the random variables to define β. The mean of the limit state function is simply the function evaluated at the mean values of the parameters, or:

$$\mu_{g(X)} = g\left(\mu_{X_1}, \mu_{X_2}, ...\mu_{X_n}\right) \quad \text{(7-8)}$$

where:
n = number of random variables.

The variance of $g(X)$ for uncorrelated variables can be approximated by keeping only the first-order terms as:

$$Var\left(g(X)\right) = \left(\sigma_{g(X)}\right)^2 = \sum_{i=1}^{n}\left(\frac{\partial g\left(X\right)}{\partial X_i}\right)^2 \left(\sigma_{X_i}\right)^2 \tag{7-9}$$

where all the derivatives are evaluated at the mean values of the random variables.

Table 7-5 Reliability Analysis Methods

Method	Requirements	Advantages	Disadvantages
First-Order, Second Moment (FOSM)	• $g(X)$ must be explicit • $g(X)$ must be differentiable	• Requires only mean and standard deviation of the random variables, X_i, rather than full probability distribution	• Ignores higher order effects • Variant with respect to form of $g(X)$ • Requires differentiation • Must assume the probability distribution of $g(X)$ to determine P_u
Approx. Derivative Method of FOSM	• $g(X)$ can be evaluated at specific values of X_i • $g(X)$ must be evaluated $2n$ times	• Does not require an explicit function for $g(X)$ • Can be easily implemented in a spreadsheet	• Assumes linearity of the derivatives of $g(X)$ • Ignores higher order effects • Variant with respect to form of $g(X)$ • Must assume the probability distribution of $g(X)$ to determine P_u
Point Estimate (multiple RV)	• $g(X)$ can be evaluated at specific values of X_i • X_i must have symmetric distributions • $g(X)$ must be evaluated 2^n times	• Does not require an explicit function for $g(X)$ • Can be easily implemented in a spreadsheet • Often more accurate than FOSM and Taylor Series	• Large number of calculations required when the number (n) of RV is large • Less accurate for $g(X)$ that cause a large change in the distribution
Hasofer-Lind	• $g(X)$ must be explicit	• Calculates an invariant value of β with a geometric interpretation • Can be implemented in a spreadsheet (Low and Tang 1997) • Accommodates nonlinearity in $g(X)$	• Assumes linearity of the standardized $g(X)$ to determine P_u • Requires some programming experience or special software • Difficult for variables that are not normally or lognormally distributed
Monte Carlo Analysis	• $g(X)$ can be evaluated at specific values of X_i in a computer program • Random values of X_i based on probability distributions	• Full probability distribution can be accommodated for each variable • Provides direct estimates of $\mu_{g(X)}$ and $\sigma_{g(X)}$ • Provides direct estimate of P_u	• Large number of trials can be required to determine P_u for some problems • Requires programming experience or special software

The derivatives required for the FOSM method are not always easy to obtain. In addition, the limit state function for some problems cannot be written explicitly in terms of the random variables. For example, the limit state function for a slope stability analysis generally can be written only as $g(X) = F - 1$, where F is calculated by a numerical procedure. To alleviate this difficulty, the derivatives can be estimated using central differences about the mean (e.g., Duncan 2000, Wolff et al. 2004).[44]

Very small increments are typically used to estimate derivatives by central difference. However, in order to simplify the calculations and capture possible nonlinearity in $g(X)$, the increment can be set equal to the standard deviation of each random variable. Thus, for each random variable, $g(X)$ is evaluated at values of x_i that are one standard deviation (σ_{Xi}) above and below the mean (μ_{Xi}) with all other variables at their mean values. This results in a central difference (Δg_1) of:

$$\Delta g_1(X) = g\left(\mu_{X_1} + \sigma_{X_1}, \mu_{X_2} \ldots \mu_{X_n}\right) - g\left(\mu_{X_1} - \sigma_{X_1}, \mu_{X_2} \ldots \mu_{X_n}\right) \tag{7-10}$$

for the first random variable. A similar definition is used for the other variables. Using these central differences, the variance of $g(X)$ is estimated as:

$$\left(\sigma_{g(X)}\right)^2 = \sum_{i=1}^{n}\left(\frac{\Delta g_i(X)}{2}\right)^2 \tag{7-11.}$$

The mean value of $g(X)$ is evaluated using Equation 7.8. When $g(X)$ is defined using the safety factor format, a logarithmic distribution of the factor of safety is logical and the reliability index becomes:

$$\beta_{LN} = \frac{\mu_{\ln(g(X))}}{\sigma_{\ln(g(X))}} = \frac{\ln\left(\mu_{g(X)}\right) - 0.5\ln\left(1 + COV_g^2\right)}{\left(\ln\left(1 + COV_g^2\right)\right)^{0.5}} \tag{7-12}$$

where:
COV_g = coefficient of variation of the limit state function = $\sigma_{g(X)} / \mu_{g(X)}$.

7-4.2.2 Point Estimate Method.

The point estimate method was introduced by Rosenblueth (1975). According to Baecher and Christian (2003), this method is based on the premise that continuous random variables can be converted to equivalent discrete RV, usually with just two

[44] This method is sometimes referred to as the Taylor Series approach. However, the entire FOSM approach is based on a Taylor Series approximation. This method is distinguished by the numerical method used to determine the derivatives for Equation 7-9.

points. If those points and the associated probabilities (or weights) are chosen properly, the moments of the continuous distribution are maintained. These discrete RV are used to approximate the distribution of the limit state function.

While Rosenblueth (1975) proposed additional cases, the most common case used in geotechnical engineering allows $g(X)$ to be a function of n symmetric RV as illustrated for two RV in Figure 7-12. The limit state function is evaluated for 2^n cases with each RV either one standard deviation above or below the mean. The mean of $g(X)$ is calculated by:

$$\mu_{g(X)} \approx \sum_{i=1}^{2^n} P_i \cdot g(X)_i \tag{7-13}$$

where:
P_i = weighting factors (equal to 2^{-n} for uncorrelated RV) and
$g(X)_i$ = limit state function evaluated for each of i cases.

The variance of $g(X)$ can be found as:

$$\sigma^2_{g(X)} \approx \sum_{i=1}^{2^n} P_i \cdot \left(g(X)_i\right)^2 - \left(\sum_{i=1}^{2^n} P_i \cdot g(X)_i\right)^2 \tag{7-14}.$$

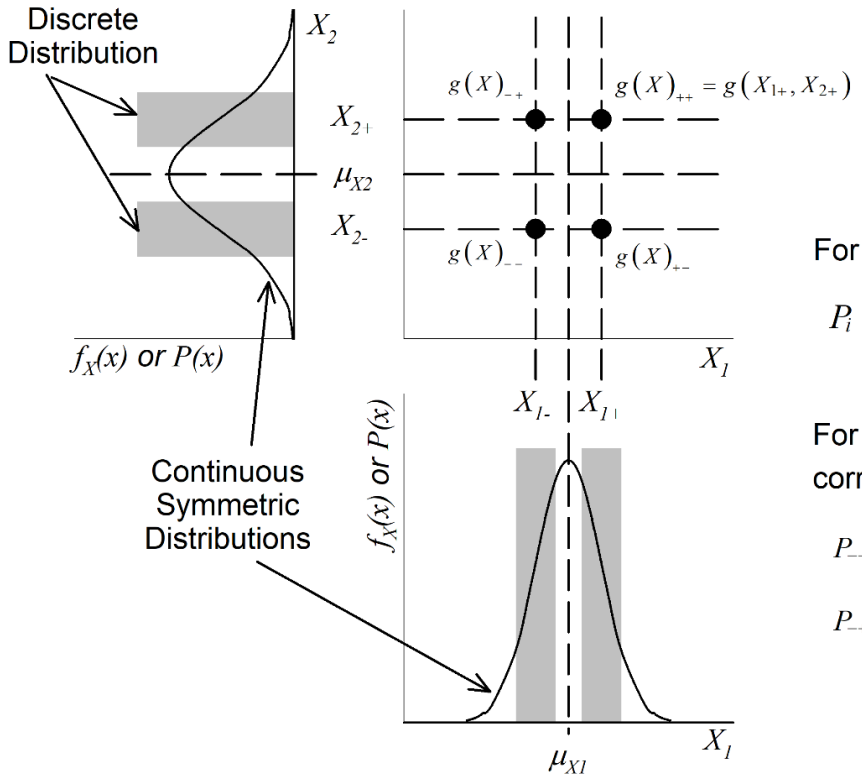

For uncorrelated X_1 and X_2 :

$$P_i = \frac{1}{4}$$

For X_1 and X_2 correlated with correlation coefficient, r_{12} :

$$P_{--} = P_{++} = \frac{1}{4}(1 + r_{12})$$

$$P_{-+} = P_{+-} = \frac{1}{4}(1 - r_{12})$$

Figure 7-12 Point Estimate Method for Two Random Variables (after Baecher and Christian 2003)

Figure 7-13 provides guidance for the combinations of plus or minus one standard deviation that make up each case for up to four RV. The cases are also illustrated in a branching format for eight cases required for three RV.

The point estimate method can accommodate correlation between the RV by changing the weighting factors. The equations for correlated P_i for two RV are shown in Figure 7-12 as an example. The method for determining weighting factors for additional correlated RV can be found in Baecher and Christian (2003) or Wolff et al. (2004).

The point estimate method cannot accurately approximate moments beyond the mean and variance (Baecher and Christian 2003). This is rarely a practical concern for reliability analysis. The method works best when the coefficients of variation of the random variables are relatively low. Inaccuracies have been shown to occur when $g(X)$ results in substantial change in the form of the probability distribution (i.e., normal to lognormal) and when $g(X)$ is highly nonlinear. Christian and Baecher (1999) provide additional guidance on the errors that may result for the point estimate method.

# Calcs	Case	# of RV (n) 1	2	3	4
2	1	-	-	-	-
	2	+	-	-	-
$2^2 = 4$	3	-	+	-	-
	4	+	+	-	-
$2^3 = 8$	5	-	-	+	-
	6	+	-	+	-
	7	-	+	+	-
	8	+	+	+	-
$2^4 = 16$	9	-	-	-	+
	10	+	-	-	+
	11	-	+	-	+
	12	+	+	-	+
	13	-	-	+	+
	14	+	-	+	+
	15	-	+	+	+
	16	+	+	+	+

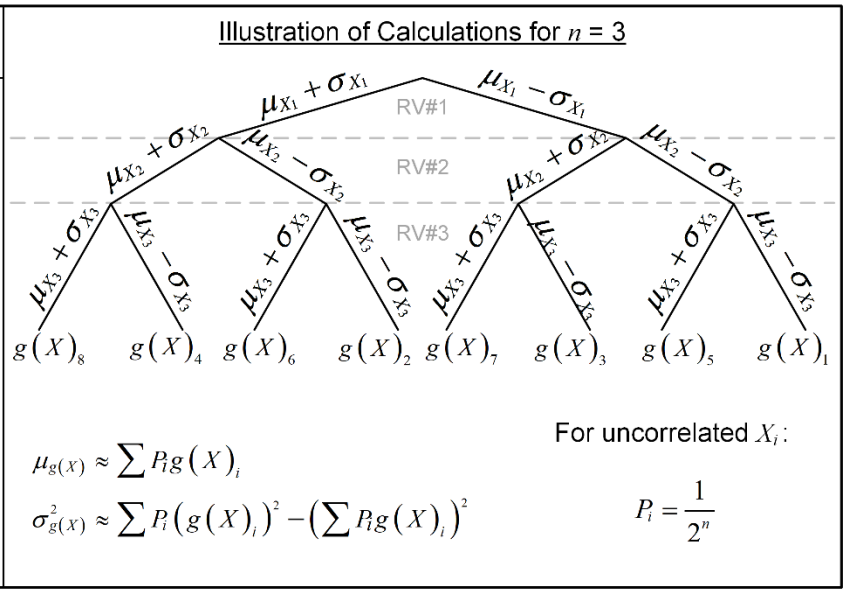

Figure 7-13 Guides for Application of the Point Estimate Method (after Harr 1987)

7-4.2.3 Hasofer-Lind Method.

The magnitude of the reliability index calculated by the first three methods can depend on how the limit state function is formulated. In other words, the safety margin and factor of safety definitions will result in different values of β. In order to overcome this limitation, Hasofer and Lind (1974) proposed a geometric interpretation of the reliability index. In their method, the value of β is defined as the shortest distance between the origin and the limit state function when all of the random variables are transformed into

standard normal space. The Hasofer-Lind approach can be used most easily when the random variables are normally or lognormally distributed both of which can be easily transformed into standard normal space. An equivalent tail approximation method is described in Ayyub and McCuen (2016) for non-normal variables.

The Hasofer-Lind method is illustrated for the case of two random variables in Figure 7-14. Each random variable is first transformed to an equivalent standard normal distribution (i.e., N(1,0)). The joint probability distribution for two uncorrelated variables is represented by circles centered on the origin in two-dimensions (Figure 7-14(b)). The point where the transformed limit state function comes closest to the origin corresponds to the *design point* for the analysis. This point can be found using a variety of numerical or iterative procedures. The distance between the design point and the origin is equal to β or the number of standard deviations separating the limit state function from the origin. The value of β is determined directly because the variables have been transformed to have a unit standard deviation.

The standard normal distribution is typically used to calculate P_u from β, which assumes that the limit state function is linear in the standard normal space. The potential error associated with this assumption is illustrated in Figure 7-14(c). The Hasofer-Lind method can also accommodate correlated random variables. The circles in Figure 7-14(b) become ellipses. A readily implementable spreadsheet solution to the Hasofer-Lind method is described by Low and Tang (1997), which includes the ability to consider correlated RV.

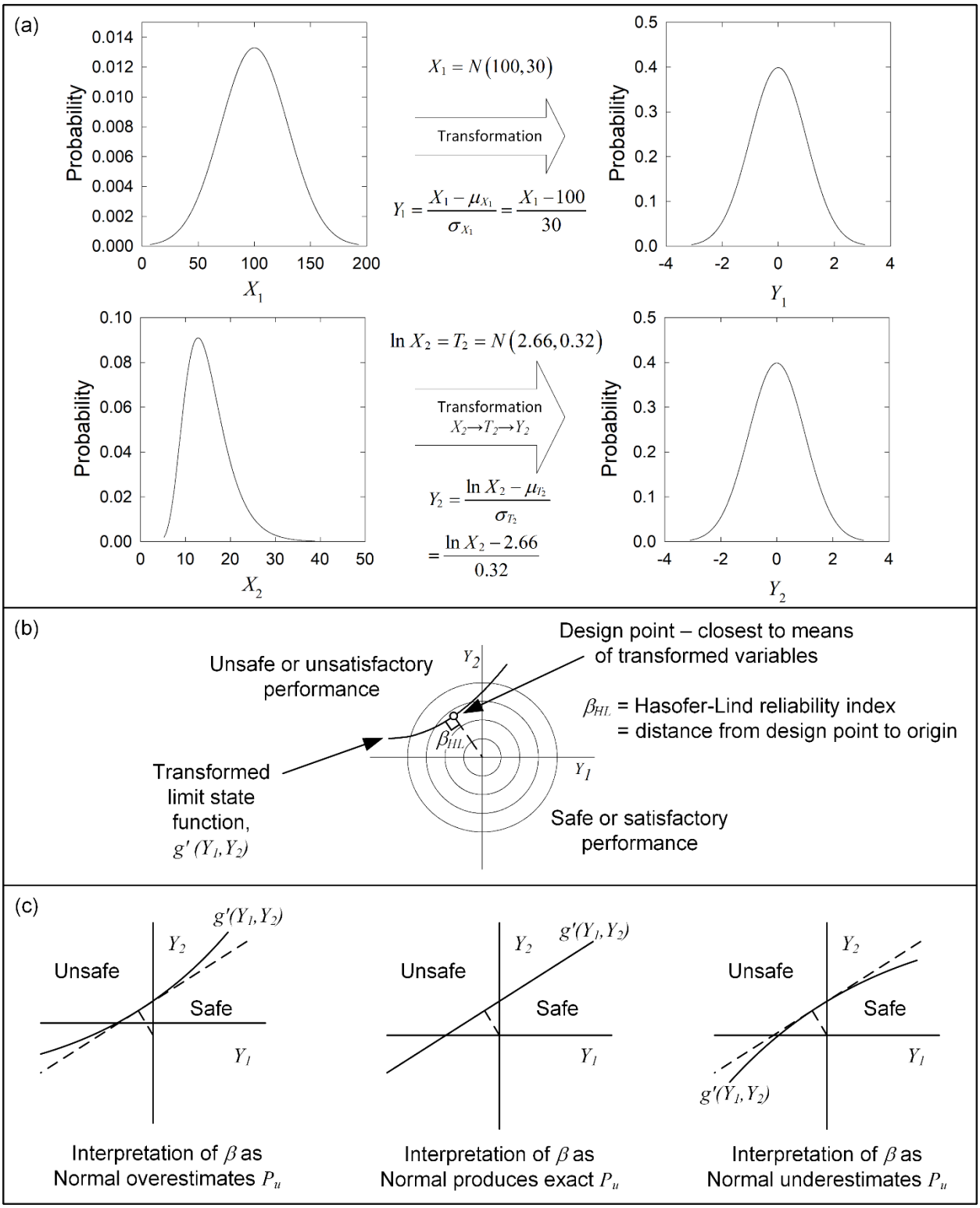

Figure 7-14 Hasofer-Lind Reliability Index Concept for Two Random Variables

7-4.2.4 Monte Carlo Simulation.

Monte Carlo simulation calculates the limit state function for a number of trials that is sufficiently large to define the probability of unsatisfactory performance. For each trial, Monte Carlo uses random number generation to select values from the probability distributions of each random variable in the design problem. The selected values are used to determine the value of $g(X)$ for that trial. If the value of $g(X)$ is negative, a failure is recorded. The number of failures divided by the total number of trials defines the probability of failure. The Monte Carlo process is repeated until the value of P_u remains stable as the number of trials increases.

Monte Carlo simulation can define the probability distribution of the limit state function. A value of $g(X)$ is generated for every trial, providing data to which a probability distribution can be fit. Limit state functions that are mostly addition and subtraction tend toward a normal distribution while those which use multiplication and division tend to be lognormally distributed.

The number of trials required for a Monte Carlo simulation depends on the problem being investigated and the information desired from the simulation. A common approach is to progressively increase the number of trials in the Monte Carlo simulation until the value of P_u is approximately constant. An example plot is provided in Figure 7-15.

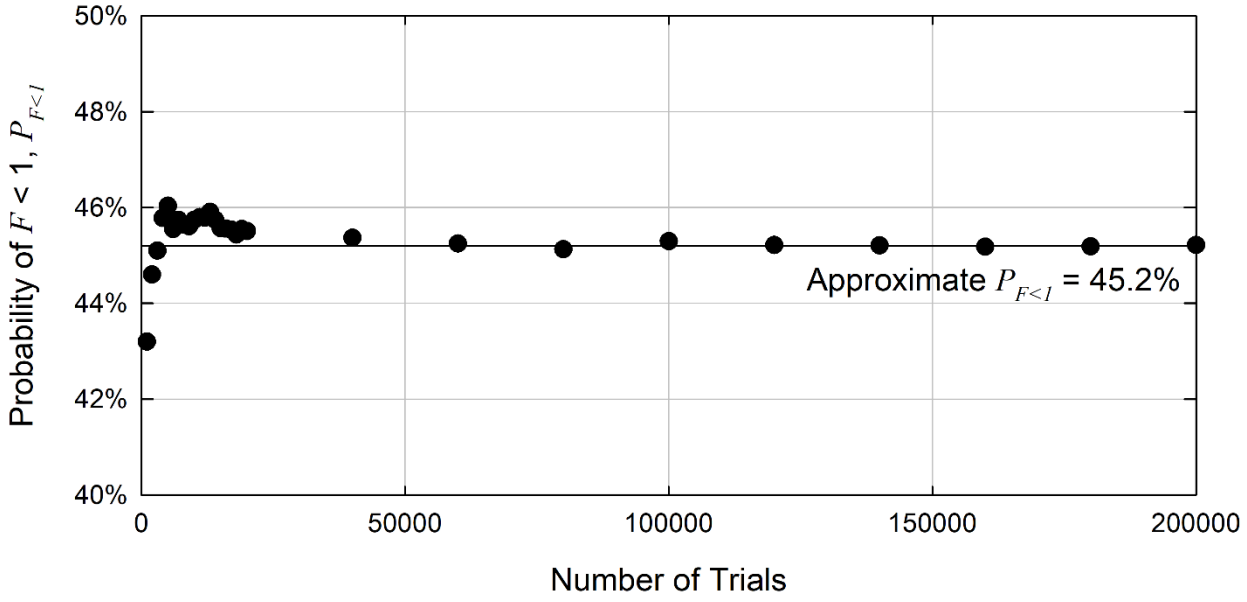

Figure 7-15 Convergence of Monte Carlo Simulation with Increasing Trials

The number of trials required to obtain simulated estimates of the mean and standard deviation can also be determined from Figure 7-16, based on the desired level of confidence and acceptable error in the estimates. If the acceptable error in the estimates of the mean and standard deviation is 10%, the required number of trials is in the range of 100 to 1000. In order to reduce the error to about 1%, the number of trials increases one-hundredfold to a range of 10,000 to 100,000. In order to estimate the probability of extreme events, the required number of trials is at least 100,000. In general, the number of trials should be sufficient so that the event of interest occurs many times (perhaps 10 to 100) in the simulation. For example, the simulation of a system with a reliability index of β = 4.26 (P_u = 0.0001) would require at least 10^6 trials.

The aforementioned requirements apply to simulations performed with random sampling implemented in a brute-force manner. In many cases, it may be necessary to reduce the number of trials in order to save computational effort as discussed in Baecher and Christian (2003). The *importance sampling* and *controlled variates* methods use a function that correlates well with the likely distribution of the solution. This concentrates the search in the area of interest. *Correlated sampling* is useful for comparing more than one design alternative. It recognizes that some random variables, such as those representing the soil conditions, can be used for assessment of all the design alternatives. *Stratified sampling* concentrates sampling in the regions that most affect the estimated variance. This approach can still lead to a large number of sampling points. The *Latin hypercube* method is a randomized approach that reduces the number of trials in a stratified simulation.

Monte Carlo methods rely on random number generators to simulate random variables. The quality of the simulation depends on the quality of the random numbers. Engineers should be aware of the random number generator used by their software and the limitations imposed. The use of more than one type of random number generator is encouraged (Baecher and Christian 2003).

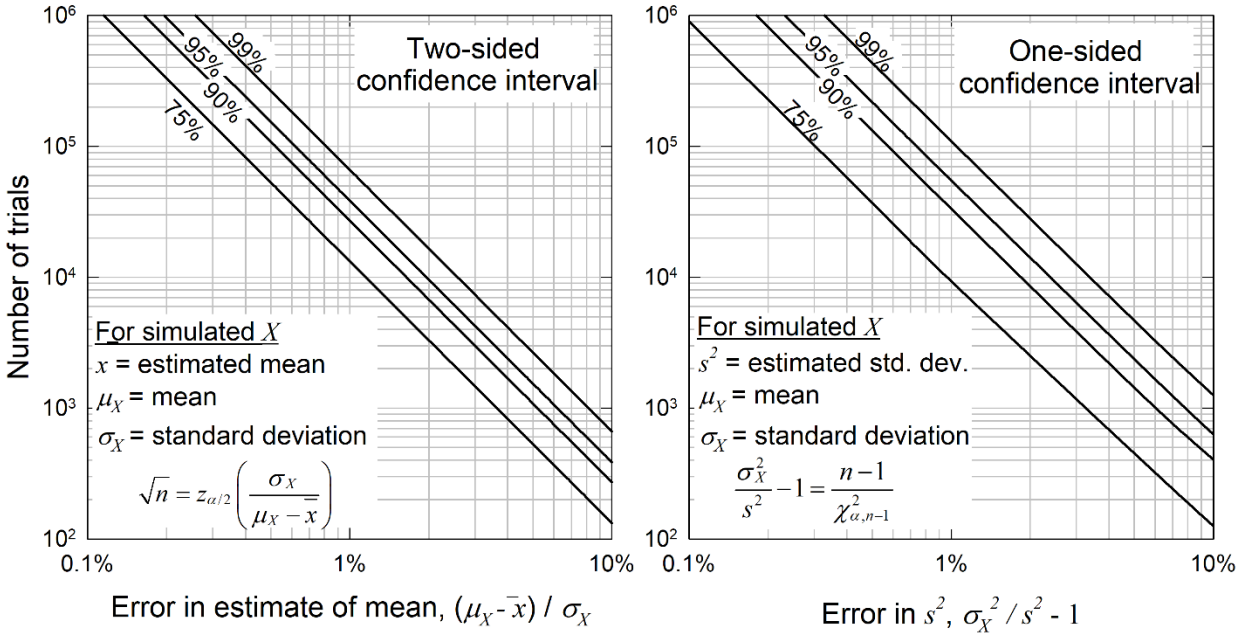

Figure 7-16 Monte Carlo Simulation Trial Number Requirements

7-4.2.5 Effect of Correlation on Reliability Analysis.

Correlation between parameters can either increase or decrease the reliability index. The influence of correlation depends on whether the correlation is negative or positive, and on the effect that each parameter has on the solution. An example of this is provided in Figure 7-17. If undrained shear strength is positively correlated to unit weight, the correlation will reduce the uncertainty in the factor of safety for an unsupported cut. This causes the reliability index to increase as a result of the inverse relationship between a driving force related to γ_t and a resistance (s_u). In contrast, the correlation will increase the uncertainty in the bearing capacity because both parameters (γ_t and s_u) are used to determine the resistance.

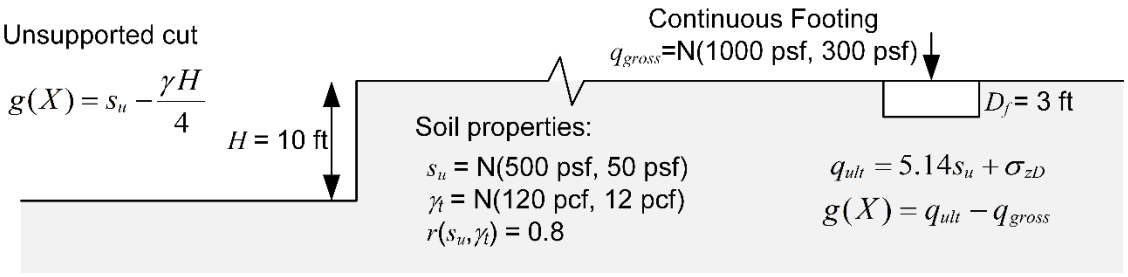

Use the First-Order, Second Moment Method (see Section 7.4.2.1) to find β.

Unsupported Cut (H is deterministic)

First, ignoring correlation between s_u and γ_t:

$$\sigma_{g(X)}^2 = \left(\frac{\partial g}{\partial \gamma_t}\right)^2 (\sigma_{\gamma_t})^2 + \left(\frac{\partial g}{\partial s_u}\right)^2 (\sigma_{s_u})^2$$

$$\sigma_{g(X)}^2 = \left(\frac{10\ ft}{4}\right)^2 (12\ pcf)^2 + (1)^2 (50\ psf)^2 = 3400\ psf^2$$

$$\mu_{g(X)} = 500 - \left(\frac{120\ pcf\,(10\ ft)}{4}\right)$$

$$\mu_{g(X)} = 200\ psf$$

$$\sigma_{g(X)} = 58.3\ psf$$

$$\beta = \frac{200}{58.3} = 3.43$$

Considering correlation between s_u and γ_t:

$$\sigma_{g(X)}^2 = 3400 + 2r(\gamma_t, s_u)\left(\frac{\partial g}{\partial \gamma_t}\right)\left(\frac{\partial g}{\partial s_u}\right)(\sigma_{\gamma_t})(\sigma_{s_u})$$

$$\sigma_{g(X)}^2 = 3400 - 2400$$

$$\sigma_{g(X)}^2 = 1000\ psf^2$$

$$\sigma_{g(X)} = 31.6\ psf$$

$$\beta = \frac{200}{31.6} = 6.33$$

Considering correlation increased β by about 85%.

Bearing Capacity (D_f is deterministic)

$$\sigma_{g(X)}^2 = \left(\frac{\partial g}{\partial \gamma_t}\right)^2 (\sigma_{\gamma_t})^2 + \left(\frac{\partial g}{\partial s_u}\right)^2 (\sigma_{s_u})^2 + \left(\frac{\partial g}{\partial q_{gross}}\right)^2 (\sigma_{q_{gross}})^2 + 2r(\gamma_t, s_u)\left(\frac{\partial g}{\partial \gamma_t}\right)\left(\frac{\partial g}{\partial s_u}\right)(\sigma_{\gamma_t})(\sigma_{s_u})$$

$$\sigma_{g(X)}^2 = 66049\ psf^2 + 11664\ psf^2 + 90000\ psf^2 + 14803\ psf^2$$

$$\mu_{g(X)} = 5.14(500\ psf) + (120\ pcf)(3\ ft) - 1000\ psf = 1930\ psf$$

Without correlation (first two terms): $\sigma_{g(X)}^2 = 167713\ psf^2$, $\sigma_{g(X)} = 409.5\ psf$, $\beta = \frac{1930}{409.5} = 4.71$

With correlation (all three terms): $\sigma_{g(X)}^2 = 182516\ psf^2$, $\sigma_{g(X)} = 427\ psf$, $\beta = \frac{1930}{427} = 4.52$

Considering correlation decreased β by about 4%.

Figure 7-17 Example of Correlation Effects on Geotechnical Analysis

7-4.2.6 Use of Reliability Analysis.

The utility of reliability analysis is the ability to understand and quantify the effects of uncertainty in the input parameters on the design. Reliability analysis can accompany traditional design and can also be incorporated in risk assessments. Duncan (2000) provides multiple examples of the application of reliability analysis to the design of foundations, retaining walls, and slopes.

Traditional deterministic design can be supplemented by reliability analysis. The reliability index and/or probability failure deepen the meaning of a particular factor of safety or other geotechnical calculation. For example, two shallow foundation designs may have factors of safety of 2.5 and 3, respectively. However, if the former design is based on more certain information, the respective reliability indices might be 4 and 3. Even if the estimates of β are approximate, the relative magnitude suggests that the first design is more reliable despite the lower factor of safety. The probability of failure can also be used to help individuals without geotechnical background understand the impact of changing the factor of safety or completing additional site characterization.

The probability of failure estimated from reliability analysis can also provide a useful input to larger scale risk assessments, which are discussed in the following section. The event trees used by these assessments have branches that can be filled using reliability analysis rather than relying solely on expert judgment.

7-4.3 Risk Assessment.

Risk assessment quantifies and describes the nature, likelihood, and magnitude of risk in a systematic, evidence-based manner. The performance of geotechnical structures and systems as a function of the applied loads is referred to as a *system response function*. For a given situation, risk assessment often involves determining the probabilities of unsatisfactory performance (e.g., failure, excessive settlement, etc.) over a time frame, as well as the consequences of those events. Sources of these probabilities include analytical reliability analyses, observations of past frequencies, and expert opinion (USACE 2020).

The combination of probability and consequences can be compared to specific criteria, such as F-N charts, or used for comparing multiple structures or systems. The example F-N chart in Figure 7-18 allows calculated risk to be compared to societal standards imposed by a regulatory agency (USACE 2014). In this case, the estimated probability and loss of life can be plotted, and subsequent action is based on the zone of the chart. Improvement plans are evaluated by assessing the resulting changes in probability and/or consequences (USACE 2020). Timchenko et al. (2021) have produced F-N charts in terms of both fatalities and cost, which compare geotechnical activities to other types of risk. Their study defined the low-risk threshold as either $10,000 per year (2020 US dollars) or 0.001 fatalities per year.

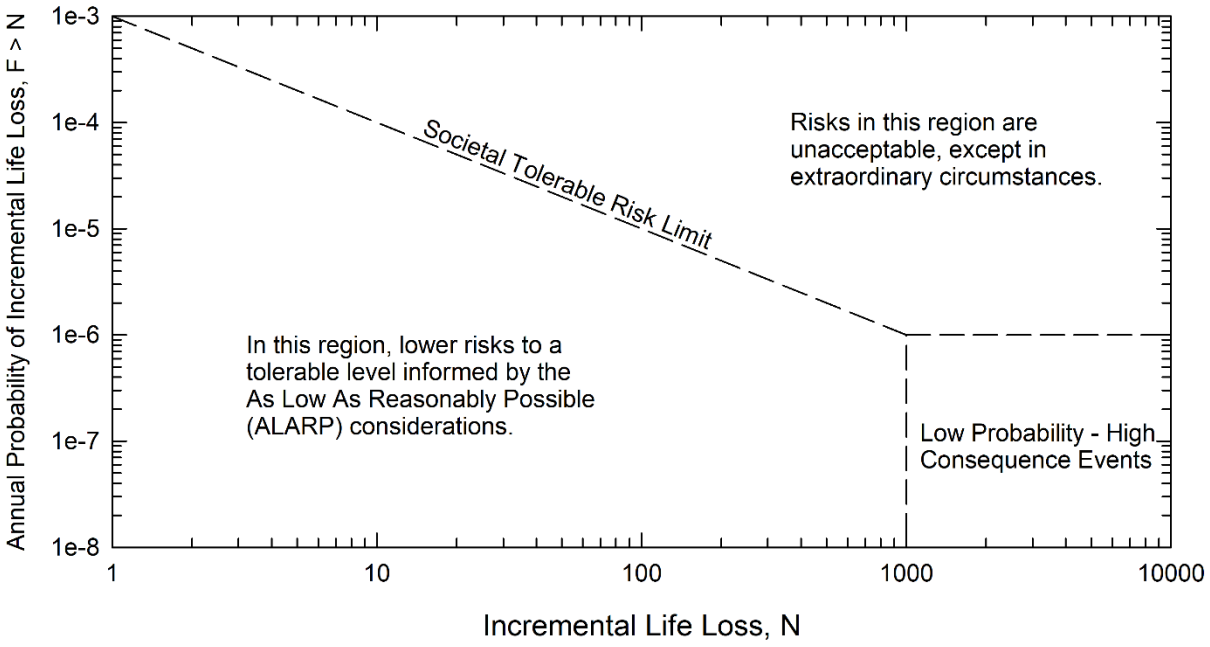

Figure 7-18 Example F-N Chart

Risk assessments require estimates of P_u over a defined time frame. The P_u calculated from reliability analysis typically starts with the assumption of a particular loading condition. Thus, the likelihood of the loading condition within the defined timeframe must be included. For example, levee stability following a flood may depend on the height of the flood. In this case, the time frequency can be incorporated by considering the return period of the particular flood level being analyzed.

Event trees, such as those shown in Figure 7-19, are another risk assessment tool, which help to evaluate complex chains of conditional probabilities. An event tree starts with an initiation event with a specified probability. At each intermediate node, the event tree will branch into two or more possible outcomes. At each node, the sum of the branch probabilities must equal 1.0. The final branches terminate at end nodes with a unique sequence of events or pathway. The probability for each pathway can be calculated by combining (i.e., multiplying) the probabilities for each branch. Fault trees are an alternate method used in risk assessment. Fault trees start from outcomes of interest and assess the events required to reach those outcomes (USACE 2020).

The *decision tree* is a similar risk assessment tool that combines probabilities with consequences in a graphical form (Baecher and Christian 2003). Decisions are made at some branches between options with different costs (or consequences). The other nodes represent possible events with associated probabilities and consequences.

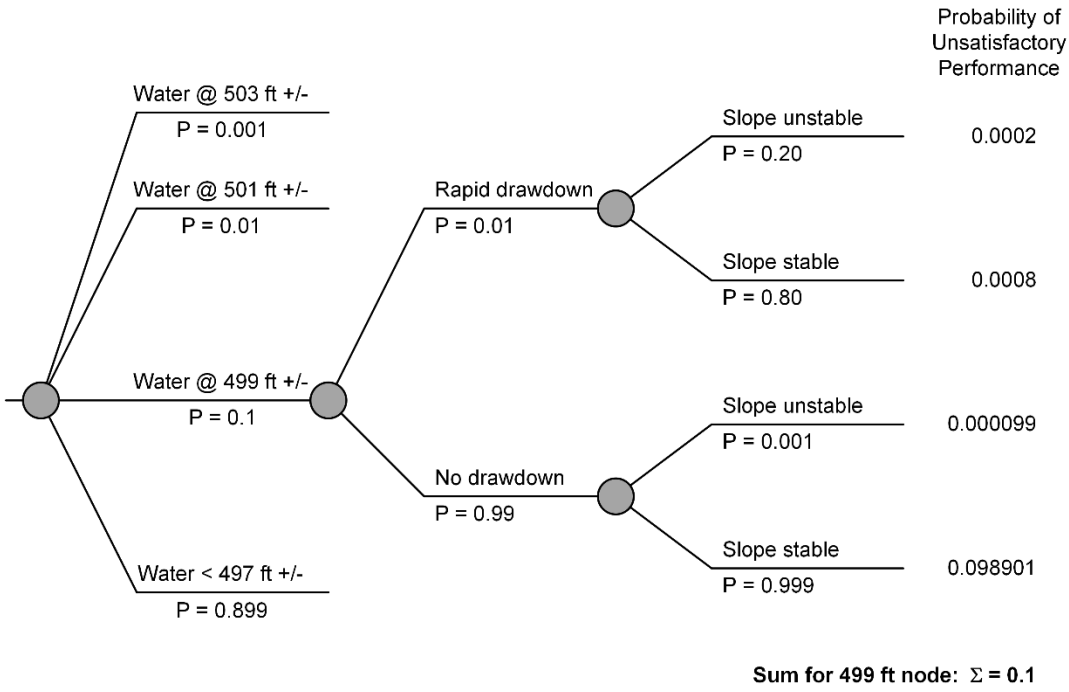

Figure 7-19 Example Event Tree (after USACE 2020)

An example decision tree for three pile testing methods is provided in Figure 7-20. In this example, a “normal” design is used if favorable soil conditions are predicted, while a more expensive modified design is used for unfavorable conditions. If a normal design is used for cases where soil conditions are actually poor, costly repair is required. For the values in this example, the higher uncertainty of the driving formula results in a higher risk. On the other hand, the increased cost of the static load testing exceeds the benefit of the decreased uncertainty about the soil conditions for this example.

7-4.4 Hazard Analysis and Return Periods.

In the context of civil engineering, a *hazard* is a condition that has the potential to cause damage to or loss to personnel, equipment, or property (DoD, 2021). All of these losses can limit the usefulness of a structure or system. A *hazard function* defines the probability that an event occurs (per time) assuming that the event has not occurred up to the given time. Many events related to geotechnical engineering, such as earthquakes and floods, are assumed to have a constant hazard function and are referred to as Poisson processes. An increasing hazard function implies that the likelihood of the event increases with time. A decreasing hazard function implies that the likelihood of the event decreases with time (USACE 2020).

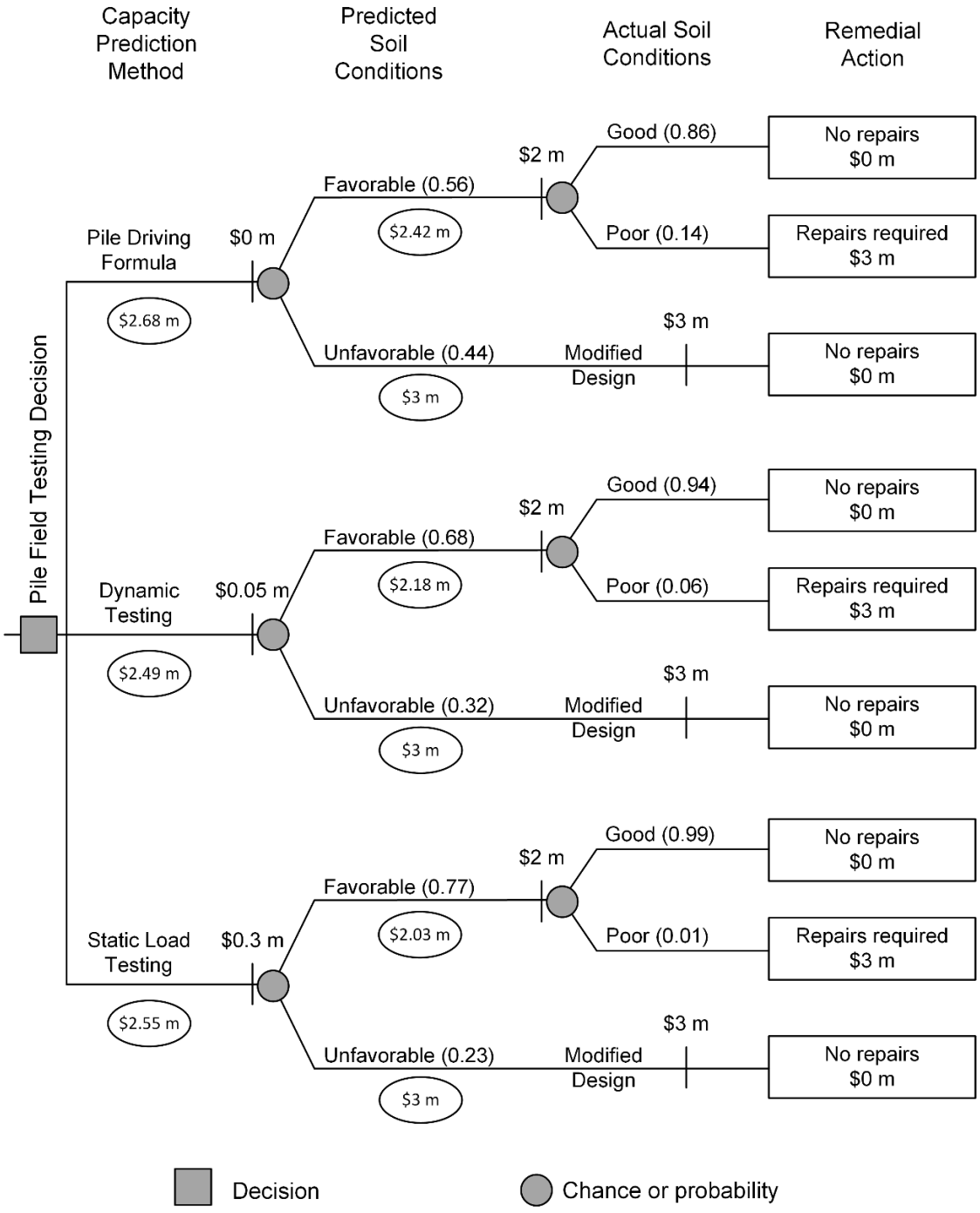

Underlying probabilities
Soil conditions: P(good) = 0.8, P(poor) = 0.2
Prediction:
Formula: P(correct) = 0.6, Dynamic: P(correct) = 0.8, Static: P(correct) = 0.95

Figure 7-20 Example Decision Tree (after Baecher and Christian 2003)

Many hazards are natural processes that create uncertainty in the loading applied to geotechnical structures. The *return period* or *mean recurrence interval* (R) for these events can be estimated based on historical data. The *rate of exceedance* (λ), which is an annual value if R is expressed in years, can be calculated as:

$$\lambda = \frac{1}{R} \quad \textbf{(7-15).}$$

The effect of hazards on engineering design is often characterized in terms of the loading parameters that result from the hazard. Databases of these engineering parameters, including those related to seismic and climatic hazards, can be accessed through government agencies and professional organizations, such as USGS, NOAA, and ASCE.[45] The databases provide values of R or λ for particular magnitudes of loading parameters, such as a level of peak ground acceleration, a 24-hour rainfall, or a wind speed, as illustrated in Figure 7-21(a) to (c). As the magnitude of the hazard increases, the annual probability of exceedance decreases (i.e., larger hazards are less common). This relationship is referred to as a *hazard curve*.

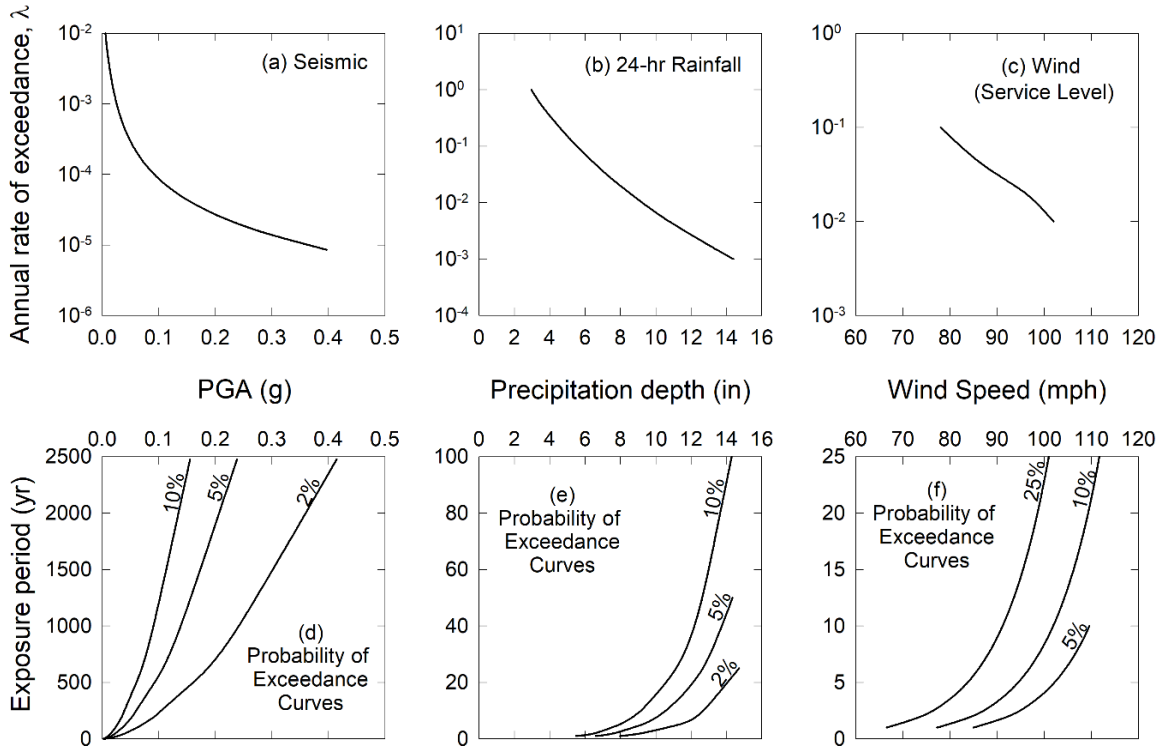

Figure 7-21 Example Hazards for an Eastern US Site – (a) to (c) Hazard Curves and (d) to (f) Probability of Exceedance Curves

[45] These resources have migrated primarily to the internet and are regularly updated. For this reason, specific links or citations have not been included herein.

In many cases, a particular value of the loading parameter is required in the design. Commonly, an *exposure period* (T_R) is selected, which is the length of time being considered in the design. A threshold probability of exceedance ($P(Y>y^*)$) is also selected. The value of $\lambda(y^*)$ which produces this probability can be found as:

$$\lambda\left(y^*\right) = -\frac{\ln\left(1 - P\left(Y > y^*\right)\right)}{T_R} \tag{7-16}$$

where:
Y = random variable representing loading parameter of interest and
y^* = value of Y that results in the desired probability of exceedance.

Once $\lambda(y^*)$ has been determined, the corresponding value of the loading parameter can be determined from the hazard curve. This process can be repeated for other exposure periods and probabilities of exceedance, allowing the loading parameter to be plotted against the exposure period as in Figure 7-21(d) to (f). For example, events with a probability of exceedance of 10% in 50 years have $\lambda(y^*)$ of 2.1×10^{-3} yr^{-1}, which corresponds to R of 475 years. Using the hazard curve, the 24-hour rainfall (Figure 7-21(b)) with this rate is about 12.6 inches.

In the case of seismic analysis, a hazard curve may represent the combined effects of multiple seismic sources and is developed using a process called *probabilistic seismic hazard analysis*. Each source will have a different distance or range of distances to the project site as well as different annual distribution of earthquake magnitude. These variations are used to predict the probability distribution of the desired loading parameters for each site. The effects from each site are combined to determine the probability that the loading parameter is greater than a given value. This information can be expressed as a hazard curve, similar to Figure 7-21(a).

7-4.5 Load and Resistance Factor Design (LRFD).

Load and resistance factor design (LRFD) is an application of reliability analysis, which separately factors both loads and resistances using probabilistically calibrated factors. LRFD uses the concept of limit states to define conditions in which a structure (used generically in this section) no longer performs its intended function. *Ultimate limit states* are those pertaining to collapse or safety. In geotechnical engineering, ultimate limit states are related to the shear strength of the soil, such as bearing capacity or slope stability. *Service limit states* are those pertaining to functionality or the ability of the structure to remain useful. Settlement criteria are a common geotechnical service limit state. Some LRFD codes, such as the AASHTO Bridge Design Code, define multiple types of ultimate and service limit states that must be considered in a particular design.

The ultimate limit state design equations and methodology for LRFD are compared in Table 7-6 to allowable stress design (ASD), multiple load and resistance factor design

(MRFD), and full reliability-based analysis. With the exception of full reliability analysis, all of the methods apply factors in some combination to the nominal loads (Q) and/or the nominal resistances (R). Progressing from ASD to MRFD, the factors are applied in greater specificity, which allows more flexibility to consider uncertainty but requires additional effort in both design and development of the appropriate factors.

Table 7-6 Comparison of Ultimate Limit State Design Methodologies (after Kulhawy 2017)

Method	Design Equation	Method for Calibrating Factors	Example
ASD	$Q_n \le \frac{R_n}{F}$	Appropriate F is selected by experience with similar calculation method and conditions. Uncertainty in both load and resistance is lumped into a single factor.	Common approach to many foundation and retaining wall designs.
LRFD	$\sum \gamma Q_n \le \varphi R_n$	Statistics of load and lumped resistance along with load factors are used to determine the φ required to achieve a particular value of β_t.	AASHTO (2020) driven pile design uses a single φ for static capacity analysis.
Multiple LRFD (MRFD)	$\sum \gamma_i Q_{n,i} \le \varphi_i R_{n,i}$	Statistics of loads and load factors are used to determine the resistance factors for various components of resistance that are required to achieve β_t. Different values of φ may be considered for different soil conditions or levels of uncertainty.	AASHTO (2020) drilled shaft design uses separate φ for side and tip resistance, recognizing differences in uncertainty associated with each.
Full Reliability Analysis	$\beta_{calc} > \beta_t$	The probability distributions for loads and resistances (or underlying geotechnical parameters) are determined directly. Methods from Section 7-4.2 are used to determine β_{calc}.	Design-specific methodology. Not codified.

Notation:
Q_n = nominal load (or stress), R_n = nominal resistance (or stress), F = factor of safety
γ = load factor, φ = resistance factor, β_{calc} = calculated reliability index, and β_t = target reliability index.

7-4.5.1 Components of LRFD.

The basic concept of LRFD is illustrated in Figure 7-22 in which the loads and resistances are shown along the same scale. The unfactored (nominal) loads are the lowest and plot at the left while the unfactored resistances are highest and on the right. These loads and resistances are those determined using the calculation approaches specified by the LRFD design code.

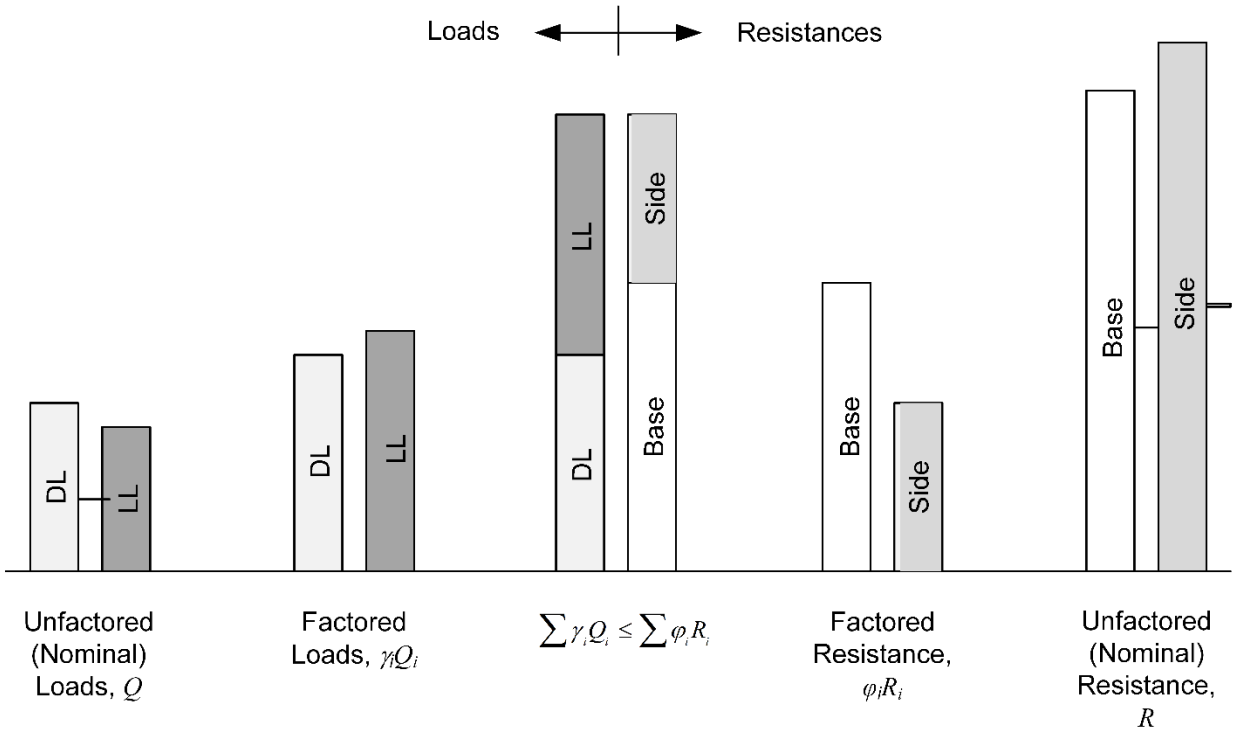

Figure 7-22 LRFD Concept (after FHWA 2001)

In order to account for uncertainty in load, the loads are multiplied by *load factors* (γ_i) that are greater than one to produce factored loads that are larger than the nominal values. Specific load factors are used for each type of load because of differences in the uncertainty associated with each type of load. Similarly, the resistances are multiplied by *resistance factors* (φ_i) that are less than one and produce lower factored resistances. The selection of appropriate values of γ_i and φ_i is the critical step in the development of an LRFD procedure or code.

The design equation for LRFD requires the sum of the factored loads to be less than or equal to the sum of the factored resistances, which is shown conceptually in the middle of Figure 7-22. This inequality is checked for each limit state that must be assessed for the structure or design. The details of the limit state will dictate the values of the loads, resistances, and factors. In other words, these values may change for each limit state considered.

7-4.5.2 LRFD Calibration.

The method used to determine the appropriate values for load and resistance factors is referred to as *calibration*. An engineer using LRFD does not perform this calibration but will benefit from understanding the general calibration process. Early efforts at calibration used direct fitting of the load factors (γ) and resistance factors (φ) to generate similar designs as those produced by ASD. An example of this approach is provided in

Table 7-7. While the direct fitting approach separates the uncertainty in load from the uncertainty in resistance, it is not based on reliability theory.

Table 7-7 Resistance Factors based on Fitting Directly to ASD rather than Reliability Theory (after FHWA 2001)

Factor of Safety	Resistance Factor, φ			
	$Q_D / Q_L = 1$	$Q_D / Q_L = 2$	$Q_D / Q_L = 3$	$Q_D / Q_L = 4$
1.5	1	0.94	0.92	0.90
2	0.75	0.71	0.69	0.68
2.5	0.60	0.57	0.55	0.54
3	0.50	0.47	0.46	0.45
3.5	0.43	0.40	0.39	0.39
4	0.38	0.35	0.34	0.34

Notes:
Load factors assumed to be: γ_D =1.25 and γ_L = 1.75.
Variables: Q_D = dead load, Q_L = dead load, γ_D = dead load factor, and γ_L = live load factor

Current LRFD codes, such as ACI, AISC, and AASHTO, are calibrated to achieve a consistent reliability across a broad range of design scenarios (Nowak 1995, Kulhawy 2017). The process used to develop LRFD codes starts with the selection of a set of representative structures. Statistical data is gathered for both load and resistance parameters, from which the cumulative distribution functions for load and resistance are defined. Reliability analysis is then completed, typically in a simplified form, to adjust γ and φ to result in a specific target value of β. Commonly, the load factors are first selected so that the factored load has a predetermined probability of exceedance (Nowak 1995). LRFD codes are periodically updated as new information and methods become available.

The calibration process uses the mean and coefficient of variation of the loads and resistances. The mean values of load and resistance may differ from the nominal values calculated by a particular design method. This difference is referred to as *bias*. For example, mean dead loads tend to be a few percentage points higher than the design values because structural members are slightly overbuilt. The calibration process uses bias factors (λ), which are the mean value divided by the nominal value, to incorporate this difference in the reliability analyses used for calibration.

The simplifications introduced in the LRFD calibration process produce designs that *on average* meet the target β. Improvements to the calibration can be made by using multiple load or resistance factors to separate sources of uncertainty. For example, many codes employ multiple resistance factors for loads, such as dead, live, seismic, and wind loads. In a few cases, codes may separate geotechnical resistance into multiple types of resistance, such as tip and side resistance for piles. Future

improvements to LRFD may include development of ranges of φ that depend on the expected variability of the site-specific resistance.

The calibration process is specific to each design methodology or model of resistance (e.g., Meyerhof bearing capacity for shallow foundations or the α method for deep foundations). For this reason, resistance factors are methodology specific, and careful attention must be given to selecting the appropriate φ for the design method used. The commentary section of the design codes often provides helpful information about the particular calibration process that was used (Kulhawy 2017).

7-4.5.3 Use of LRFD in Geotechnical Engineering.

The discussion herein is intended to provide the engineer with an understanding of the LRFD process and its basis in reliability analysis. Specific values of γ and φ are intentionally not included in this chapter, because they are code-dependent and can change as codes are updated. The most recent version of the appropriate code should be used. For example, the AASHTO LRFD Bridge Design Specifications apply LRFD to most of the design procedures covered in this manual. FHWA's Geotechnical Engineering Circulars on various foundation and retaining wall topics also provide excellent guidance on the application of LRFD.

Some types of geotechnical design have many different methods for determining resistance. LRFD facilitates the comparison of the reliability of these methods. An example is provided in the context of pile design in Figure 7-23. The generic resistance factors used in this example range from 0.1 to 0.9. The former represents a method that is very uncertain or unreliable. In contrast, the high value of 0.9 represents a method for predicting resistance with very low uncertainty. In this way, LRFD can be especially useful for deep foundations because of the large range of methods available for predicting the resistance.

To some extent, engineers can use differences in load factors to understand the uncertainty associated with loading. Larger load factors are typically associated with live loads, which have higher uncertainty. The load factors for extreme events may be close to 1.0. In this case, the lower load factor recognizes the small probability of occurrence associated with such events.

While LRFD can theoretically be used for any analysis involving load and resistance, some problems are poorly suited to this approach. This is especially true for cases, such as slope stability, where the primary load and the primary resistance are both functions of the soil's self-weight. If a load factor is applied to the soil unit weight, the stresses within the slope will change, which changes the shear strength (except for undrained analysis). A better alternative for slope stability is to complete reliability analyses using the methods described earlier in this chapter.

LRFD Pile Design Example

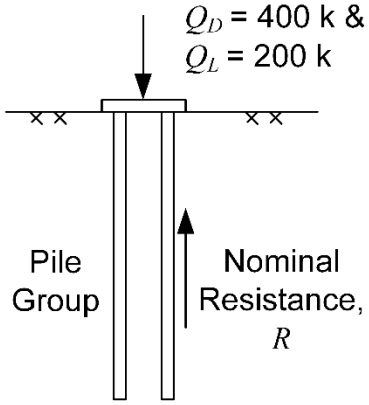

A pile group is being designed to resist a nominal dead load of 400 k and a nominal live load of 200 k. Load factors of γ_D = 1.25 and γ_L = 1.75 are determined. The factored load is calculated to be:

$$\sum \gamma_i Q_i = (1.25)(400\ k) + (1.75)(200\ k) = 850\ k$$

Preliminary Design with Static Capacity Analysis

A static capacity method is used to provide preliminary sizing for the piles. The method indicates a nominal group capacity of 2500 k. The resistance factor for the method is indicated to be 0.35. The factored resistance is:

$$\sum \varphi_i R_i = (0.35)(2500\ k) = 875\ k$$

The factored resistance is greater than the factored load so the preliminary design is satisfactory.

Dynamic Evaluation of Resistance

The engineer examines the available dynamic methods for determining pile resistance. The driving formula is disregarded as unreliable based on its low resistance factor (φ = 0.1). Dynamic testing is selected, which has a resistance factor of 0.65. Using dynamic testing, the group resistance is determined to be 2000 k. The factored resistance is calculated to be sufficient as:

$$\sum \varphi_i R_i = (0.65)(2000\ k) = 1350\ k$$

Static Load Testing

In order to further evaluate capacity, static load testing is completed, resulting in a group resistance of 2250 k. The resistance factor for this method is 0.9, indicating a factored resistance of:

$$\sum \varphi_i R_i = (0.9)(2250\ k) = 2025\ k$$

Based on this information, the pile group may be redesigned to more efficiently carry the factored load of 850 k.

Figure 7-23 LRFD Pile Design Example

7-5 NOTATION.

Variable	Definition
a, b	Limits of uniform distribution
a'	Tensile stress intercept of the Mohr Coulomb failure envelope
CF	Clay fraction
$cov(x,y)$	Covariance of variables x and y
COV_X	Coefficient of variation of x
$E(X)$	Expected value of a variable
E_D	Dilatometer modulus
E_i	Intact rock modulus
E_m	Rock mass modulus
F	Factor of safety
$g(X)$	Limit state function
GSI	Geological strength index
HCV	Highest conceivable value
I_{s50}	Point load index
k	Hydraulic conductivity
kD	Horizontal stress index from dilatometer
LCV	Lowest conceivable value
M_k	k^{th} moment about the mean
N, n	Number of items
N	Standard Penetration Test blow count
p	Probability of success in binomial trial
PI	Plasticity index
P_u	Probability of unsatisfactory performance
Q	Rock mass quality index
Q_n	Nominal load
q_c	Cone penetration resistance
q_t	Cone penetration resistance corrected for pore pressure effects

Variable	Definition
R	Return period
R_n	Nominal resistance
r_x	Range of a variable
r_{xy}	Sample correlation coefficient
RQD	Rock quality designation
RMR	Rock mass rating
s	Sample standard deviation
s^2	Sample variance
s_u	Undrained shear strength
t	Time
T_R	Exposure period
w	Water content
$\bar{x}$	Sample mean
x_{max}	Maximum value
x_{min}	Minimum value
x_P	Percentile value for which a fraction of the data, P, are smaller
z	Depth below the ground surface
β	Reliability index
δ_h, δ_v	Scale of fluctuation in the horizontal and vertical directions
φ	Resistance factor for LRFD
ϕ'	Effective stress friction angle
γ	Load factor for LRFD
γ_τ	Total unit weight
γ_δ	Dry unit weight
λ	Rate for Poisson and exponential distributions
μ	Population mean
σ	Population standard deviation
σ^2	Population variance

Variable	Definition
σ_{ci}	Unconfined compressive strength of rock

7-6 SUGGESTED READING.

Topic	Reference
Probability and statistics in civil engineering	Benjamin, J. R. and Cornell, C. A. 1970. *Probability, Statistics, and Decision for Civil Engineers*. Courier Corporation.
Probability and statistics in geotechnical engineering	Baecher, G. B. and Christian, J. T. 2005. *Reliability and statistics in geotechnical engineering*. John Wiley & Sons.
Methods of plotting data	Tukey, J. W. (1977). *Exploratory Data Analysis*. Addison-Wesley, Reading, MA.
Geotechnical risk analysis	Fenton, G. A. and Griffiths, D. V. 2008. Risk assessment in geotechnical engineering. New York: John Wiley & Sons.
Uncertainty of geotechnical parameters	Phoon, K. K. and Kulhawy, F. H. 1999. "Characterization of geotechnical variability." *Canadian Geotechnical Journal*, 36(4), 612-624.
	Phoon, K. K. and Kulhawy, F. H. 1999. "Evaluation of geotechnical property variability." *Canadian Geotechnical Journal*, 36(4), 625-639.
	ISSMGE-TC304. 2021. *State-of-the-Art Review of Inherent Variability and Uncertainty in Geotechnical Properties and Models*. Ed. Ching, J. and Schweckendiek, T., ISSMGE, 220 pp.
Application of reliability to geotechnical problems	Duncan, J. M. 2000. "Factors of safety and reliability in geotechnical engineering." *Journal of Geotechnical Engineering*, 126(4), 307-316.
Reliability and risk analysis of dams and levees	Wolff, T. F, Hassan, A., Khan, R., Ur-Rasul, I. and Miller, M. 2004. *Geotechnical Reliability of Dam and Levee Embankments, ERDC/GSL CR-04-1*, USACE, Washington D.C
	USBR and USACE. 2019. *Best Practices in Dam and Levee Safety Risk Analysis*. Risk Management Center, Denver, CO.
LRFD for shallow foundations	Paikowsky, S. G. 2010. *LRFD design and construction of shallow foundations for highway bridge structures (Vol. 651)*. Transportation Research Board.
LRFD for deep foundations	Paikowsky, S. G. 2004. *Load and resistance factor design (LRFD) for deep foundations (Vol. 507)*. Transportation Research Board.

APPENDIX A. REFERENCES

Aboshi, H., Kuwabara, M., and Mizuno, Y. 1991. “Present state of sand compaction pile in Japan." *Deep Foundation Improvements: Design, Construction, and Testing,* ASTM International, West Conshohocken, PA, 32-46.

Alwarawi, A. S., Leo, C. J., Liyanpathirana, D. S., and Sigdel, L. D. 2021. “A spreadsheet-based technique to calculate the passive pressure based on the log-spiral method,” *Computers and Geotechnics*, 130(3):103926.

American Concrete Institute (ACI). 2014. *Building Code Requirements for Structural Concrete, ACI 318-14*, ACI, Farmington Hills, MI.

American Association of State Highway and Transportation Officials (AASHTO). 2020. *LRFD Bridge Design Specifications*, 9th edition, AASHTO, Washington, DC.

AASHTO. 2021. *T272 Standard Method of Test for One-Point Method for Determining Maximum Dry Density and Optimum Moisture*. AASHTO.

American Concrete Institute (ACI). 2002. *Suggested Analysis and Design Procedures for Combined Footings and Mats, ACI 336.2R-88*, ACI.

American Petroleum Institute (API). 1993. *Recommended Practice for Planning, Designing, and Constructing Fixed Offshore Platforms – Load and Resistance Factor Design. API Recommended Practice 2A-LRFD (RP 2A-LRFD).* 1st Edition.

API. 2011. *Geotechnical and Foundation Design Considerations. ANSI/API Recommended Practice 2GEO.* American Petroleum Institute, Washington, DC.

American Society of Civil Engineers (ASCE). 2017. *Minimum design loads and associated criteria for buildings and other structures: ASCE/SEI 7-16.* ASCE, Reston, VA.

American Wood Preservers Institute (AWPI). 2002. *Timber Pile Design and Construction Manual*. Timber Piling Council, American Wood Preservers Institute, Birmingham, AL.

Anderson, D. G., Martin, G. R., Lam, I. P., and Wang, J. N. 2008. *Seismic Design and Analysis of Retaining Walls, Buried Structures, Slopes and Embankments, NCHRP Report 611*. Transportation Research Board, National Cooperative Highway Research Program, Washington, D.C.

Ang, A. H., and Tang, W. H. 1975. *Probability concepts in engineering planning and design, basic principles.* Vol. 1, John Wiley & Sons Inc.

Arellano, D. E. 2019. "Lightweight Fill Applications & Considerations." *50th Annual Southeastern Transportation Geotechnical Engineering Conference*, Chattanooga, TN.

Arulrajah, A., Disfani, M. M., Maghoolpilehrood, F., Horpibulsuk, S., Udonchai, A., Imteaz, M., and Du, Y. J. (2015). “Engineering and environmental properties of foamed recycled glass as a lightweight engineering material.” *Journal of Cleaner Production*, 94, 369-375.

Ashour, M., Norris, G., and Pilling, P. 1998. “Lateral loading of a pile in layered soil using the strain wedge model.” *Journal of Geotechnical and Geoenvironmental Engineering*, Vol. 124(4), 303-315.

ASTM International. 2021. A722/A722M-18 Standard Specification for High-Strength Steel Bars for Prestressed Concrete. West Conshohocken, PA; ASTM International.

ASTM International. 2018. D1586 Standard Test Method for Standard Penetration Test (SPT) and Split-Barrel Sampling of Soils. West Conshohocken, PA; ASTM International.

ASTM International. 2019. D2216 Standard Test Methods for Laboratory Determination of Water (Moisture) Content of Soil and Rock by Mass. West Conshohocken, PA; ASTM International.

ASTM International. 2017. D2487 Standard Practice for Classification of Soils for Engineering Purposes (Unified Soil Classification System).” West Conshohocken, PA; ASTM International.

ASTM International. 2018. D3385-18 Standard Test Method for Infiltration Rate of Soils in Field Using Double-Ring Infiltrometer. West Conshohocken, PA; ASTM International.

ASTM International. 2022. D4542-22 Standard Test Methods for Pore Water Extraction and Determination of the Soluble Salt Content of Soils by Refractometer. West Conshohocken, PA; ASTM International.

ASTM International. 2016. D4718/D4718M-15 Standard Practice for Correction of Unit Weight and Water Content for Soils Containing Oversize Particles. West Conshohocken, PA; ASTM International.

ASTM International. 2020. D4719-20 Standard Test Methods for Prebored Pressuremeter Testing in Soils. West Conshohocken, PA; ASTM International.

ASTM International. 2020. D5080-20 Standard Test Method for Rapid Determination of Percent Compaction. West Conshohocken, PA; ASTM International.

ASTM International. 2020. D5778-20 Standard Test Method for Electronic Friction Cone and Piezocone Penetration Testing of Soils. West Conshohocken, PA; ASTM International.

ASTM International. 2016. D6635-15 Standard Test Method for Performing the Flat Plate Dilatometer. West Conshohocken, PA; ASTM International.

ASTM International. 2023. D8167/D8167M-23 Standard Test Method for In-Place Bulk Density of Soil and Soil-Aggregate by a Low-Activity Nuclear Method (Shallow Depth). West Conshohocken, PA; ASTM International.

ASTM International. 2007. D1143-07 Standard Test Methods for Deep Foundation Elements Under Static Axial Compressive Load. West Conshohocken, PA; ASTM International.

ASTM International. 2007. D3689-07 Standard Test Methods for Deep Foundation Elements Under Static Axial Tensile Load. West Conshohocken, PA; ASTM International.

ASTM International. 2011. D3080/D3080M-11 Standard Test Method for Direct Shear Test of Soils Under Consolidated Drained Conditions. West Conshohocken, PA; ASTM International. (Withdrawn 2020)

ASTM International. 2012. D1557-12e1 Standard Test Methods for Laboratory Compaction Characteristics of Soil Using Modified Effort (56,000 ft-lbf/ft3 (2,700 kN-m/m3)). West Conshohocken, PA; ASTM International.

ASTM International. 2012. D698-12e2 Standard Test Methods for Laboratory Compaction Characteristics of Soil Using Standard Effort (12 400 ft-lbf/ft3 (600 kN-m/m3)). West Conshohocken, PA; ASTM International.

ASTM International. 2013. D6467-13e1 Standard Test Method for Torsional Ring Shear Test to Determine Drained Residual Shear Strength of Cohesive Soils. West Conshohocken, PA; ASTM International.

ASTM International. 2014. D4546-14e1 Standard Test Methods for One-Dimensional Swell or Collapse of Soils. West Conshohocken, PA; ASTM International.

ASTM International. 2015. D1556/D1556M-15e1 Standard Test Method for Density and Unit Weight of Soil in Place by Sand-Cone Method. West Conshohocken, PA; ASTM International.

ASTM International. 2015. D2167-15 Standard Test Method for Density and Unit Weight of Soil in Place by the Rubber Balloon Method. West Conshohocken, PA; ASTM International.

ASTM International. 2015. D2850-15 Standard Test Method for Unconsolidated-Undrained Triaxial Compression Test on Cohesive Soils. West Conshohocken, PA; ASTM International.

ASTM International. 2016. D1883-16 Standard Test Method for California Bearing Ratio (CBR) of Laboratory-Compacted Soils. West Conshohocken, PA; ASTM International.

ASTM International. 2016. D4644-16 Standard Test Method for Slake Durability of Shales and Other Similar Weak Rocks. West Conshohocken, PA; ASTM International.

ASTM International. 2016. D2166/D2166M-16 Standard Test Method for Unconfined Compressive Strength of Cohesive Soil. West Conshohocken, PA; ASTM International.

ASTM International. 2016. D4253-16e1 Standard Test Methods for Maximum Index Density and Unit Weight of Soils Using a Vibratory Table. West Conshohocken, PA; ASTM International.

ASTM International. 2016. D4254-16 Standard Test Methods for Minimum Index Density and Unit Weight of Soils and Calculation of Relative Density. West Conshohocken, PA; ASTM International.

ASTM International. 2016. 5084-16a Standard Test Methods for Measurement of Hydraulic Conductivity of Saturated Porous Materials Using a Flexible Wall Permeameter. West Conshohocken, PA; ASTM International.

ASTM International. 2017. D4318-17e1 Standard Test Methods for Liquid Limit, Plastic Limit, and Plasticity Index of Soils. West Conshohocken, PA; ASTM International.

ASTM International. 2017. D6913/D6913M-17 Standard Test Methods for Particle-Size Distribution (Gradation) of Soils Using Sieve Analysis. West Conshohocken, PA; ASTM International.

ASTM International. 2017. D7928-17 Standard Test Method for Particle-Size Distribution (Gradation) of Fine-Grained Soils Using the Sedimentation (Hydrometer) Analysis. West Conshohocken, PA; ASTM International.

ASTM International. 2017. D2937-17e2 Standard Test Method for Density of Soil in Place by the Drive-Cylinder Method. West Conshohocken, PA; ASTM International.

ASTM International. 2017. D6938-17a Standard Test Methods for In-Place Density and Water Content of Soil and Soil-Aggregate by Nuclear Methods (Shallow Depth). West Conshohocken, PA; ASTM International.

ASTM International. 2018. D4221-18 Standard Test Method for Dispersive Characteristics of Clay Soil by Double Hydrometer. West Conshohocken, PA; ASTM International.

ASTM International. 2018. D4944-18 Standard Test Method for Field Determination of Water (Moisture) Content of Soil by the Calcium Carbide Gas Pressure Tester. West Conshohocken, PA; ASTM International.

ASTM International. 2020. D2435/D2435M-11(2020) Standard Test Methods for One-Dimensional Consolidation Properties of Soils Using Incremental Loading. West Conshohocken, PA; ASTM International.

ASTM International. 2020. D4647/D4647M-13(2020) Standard Test Methods for Identification and Classification of Dispersive Clay Soils by the Pinhole Test. West Conshohocken, PA; ASTM International.

ASTM International. 2020. D4767-11(2020) Standard Test Method for Consolidated Undrained Triaxial Compression Test for Cohesive Soils. West Conshohocken, PA; ASTM International.

ASTM International. 2020. D6572-20 Standard Test Methods for Determining Dispersive Characteristics of Clayey Soils by the Crumb Test. West Conshohocken, PA; ASTM International.

ASTM International. 2020. D7181-20 Standard Test Method for Consolidated Drained Triaxial Compression Test for Soils. West Conshohocken, PA; ASTM International.

Aubeny, C. P. and Lytton, R. L. 2003. “Shallow Slides in Compacted High Plasticity Clay Slopes.” *Journal Geotechnical and Geoenvironmental Engineering*, 130(7), 717-727.

Ayyub, B. M. and McCuen , R. H. 2016. *Probability, Statistics, and Reliability for Engineers and Scientists*. CRC Press.

Azam, G. and Wang, M. C. 1991. “Bearing Capacity of Strip Footing Supported by Two-Layer c-phi Soils.” *Transportation Research Record*, 1331.

Baecher, G. B. and Christian, J. T. 2005. *Reliability and statistics in geotechnical engineering*. John Wiley & Sons.

Barden, L. and Sides, G. R. 1970. "Engineering behavior and structure of compacted clay," *Journal of the Soil Mechanics and Foundations Division*, 96(SM4), 1171-1200.

Barksdale, R. D. (1987). *State of the art for design and construction of sand compaction piles, Technical Report REMR-GT-4*, USACE Waterways Experiment Station, Vicksburg, MS.

Barton, N. and Kjærnsli, B. 1981. "Shear strength of rockfill." *Journal of the Geotechnical Engineering Division*, 107(7), 873-891.

Bay, J. A. 2003. "A summary of the research on pile driving vibrations." *Proceedings of the Pile Driving Contractors Association 7th Annual Winter Roundtable*, Atlanta, GA.

Bazett, D. J. and Foxall, R. G. 1972. "Control of Underwater Earthwork at Hugh Keenleyside (Arrow) Dam." *Underwater Soil Sampling, Testing, and Construction Control*, ASTM Special Technical Publication 501, ASTM International.

Benjamin, J. R. and Cornell, C. A. 1970. *Probability, Statistics, and Decision for Civil Engineers*. Courier Corporation.

Benson, C. H., and Trast, J. M. 1995. "Hydraulic Conductivity of Thirteen Compacted Clays." *Clays and Clay Minerals*, 43(6), 669–681.

Berezantzev, V. G., Khristoforov, V. S., and Golubkov, V. N. 1961. "Load bearing capacity and deformation of piled foundations." *Proc., 5th Int. Conf. Soil Mechanics and Foundation Engineering*, Paris, France.

Boscardin, M. D. and Cording, E. J. 1989. "Building Response to Excavation-Induced Settlement," *Journal of Geotechnical Engineering*, 115(1), 1-21.

Bowles, J. E. 1996. *Foundation Analysis and Design*, 5th Edition. McGraw-Hill Companies, Inc., New York, NY

Brandon, T. L., Duncan, J. M., and Gardner, W. S. 1990. "Hydrocompression Settlement of Deep Fills." *Journal of Geotechnical Engineering*, 116(10), 1536-1548.

Brandon, T. L.; Rose, A. T.; and Duncan, J. M. 2006. "Drained and Undrained Strength Interpretation of Low-Plasticity Silt," *Journal of Geotechnical and Geoenvironmental Engineering*, 132(2), 250-257.

Bray, J. D., Zekkos, D., and Merry, S. M. 2008. “Shear strength of municipal solid waste,” *Proc. International Symposium on Waste Mechanics*, ASCE, 44–75.

Bray, J. D., Zekkos, D., Kavazanjian, E., Athanasopoulos, G. A., and Riemer, M. F. 2009. “Shear strength of municipal solid waste,” *Journal of Geotechnical and Geoenvironmental Engineering*, 135(6), 709–722.

Breitenbach, A. J. 1993. “Rockfill placement and compaction guidelines.” *Geotechnical Testing Journal*, 16(1), 76-84.

Brettmann, T. and Duncan, J. M. 1996. “Computer application of CLM lateral load analysis to piles and drilled shafts.” *Journal of Geotechnical Engineering*, 122(6): 495-498.

Briaud, J.-L. 2008. “Case histories in soil and rock erosion: Woodrow Wilson Bridge, Brazos River Meander, Normandy Cliffs, and New Orleans Levees.” *Journal Geotechnical Geoenvironmental Engineering*, 134(10), 1425-1447.

Briaud, J.-L. 2013. *Geotechnical Engineering: Unsaturated and Saturated Soils*, Wiley, Hoboken, NJ.

Briaud, J.-L. and Tucker, L. 1984. “Piles in sand: a method including residual stresses.” *Journal of Geotechnical Engineering*, Vol. 10(11), 1666-1680.

Brinch Hansen, J. 1953. *Earth Pressure Calculations*, Danish Technical Press, Institution of Danish Civil Engineers, Copenhagen.

Brinch Hansen, J. 1957. “Foundations of structures – (a) General subjects and foundations other than piled foundations, General Report.” *Proc. of 4th Intl. Conf. Soil Mech. Found. Engr.*, Vol. II, 441-447.

Brinch Hansen, J. 1961. *A General Formula for Bearing Capacity, Bulletin No. 11*. Danish Geotechnical Institute, Copenhagen.

Brinch Hansen, J. 1970. *A Revised and Extended Formula for Bearing Capacity, Bulletin No. 28*. Danish Geotechnical Institute, Copenhagen.

Brinch Hansen, J. 1963. Discussion of “Hyperbolic stress-strain response: cohesive soils.” *Journal for Soil Mechanics and Foundation Engineering*, 89(SM4), 241-242.

Broms, B. B. 1964a. “Lateral resistance of piles in cohesive soils.” *Journal of the Soil Mechanics and Foundations Division*, 90(SM2), 27-63.

Broms, B. B. 1964b. “Lateral resistance of piles in cohesionless soils.” *Journal of the Soil Mechanics and Foundations Division*, 90(SM3), 123-156.

Broms, B. B. 1965. “Design of laterally loaded piles.” *Journal of the Soil Mechanics and Foundations Division*, 91(SM3), 79-99.

Broms, B. B. 1966. “Methods of calculating the ultimate bearing capacity of piles – a summary.” *Soils-Soils*, 5(18-19), 21-32.

Brooker, E. W. and Ireland, H. O. 1965. “Earth Pressure At-Rest Related to Stress History.” *Canadian Geotechnical Journal*, 11(1), 1-15.

Brown M. J. and Powell, J. J. M. 2013. “Comparison of Rapid Load Test Analysis Techniques in Clay Soils.” *Journal of Geotechnical and Geoenvironmental Engineering*, 139(1), 152-161.

Brown, A. C., Dellinger, G. F., El-Mohtar, C., Zornberg, J. G., and Gilbert, R. B. 2014. *Long-Term Performance of a Drilled Shaft Retaining Wall in Expansive Clay. Research Report FHWA/TX-13/0-6603-2*. Center for Transportation Research. University of Texas at Austin.

Brown, D. A. and Bollman, H. T. 1993. “Pile-Supported Bridge Foundations Designed for Impact Loading.” *Appended Document to the Proceedings of Design of Highway Bridges for Extreme Events*, Crystal City, VA, 265-281.

Brown, J. D. and Meyerhof, G. G. 1969. "Experimental study of bearing capacity in layered clays." *Proc. 7th ICSMFE*, Mexico City, Mexico.

Brown, P. P. 1963. Discussion of “Field Study of Cellular Cofferdams,” Transactions of ASCE, Paper No. 3426, Vol. 128, Part 1.

Brown, R. P. 2001. *Predicting the Ultimate Axial Resistance of Single Driven Piles*. PhD Dissertation, Department of Civil Engineering, The University of Texas at Austin, 168 pp.

Bryant, L., Mauldon, M., and Mitchell, J. K. 2003. *Geotechnical Problems with Pyritic Soil and Rock, CGPR #30*, Center for Geotechnical Practice and Research, Virginia Tech, Blacksburg, VA, 157 pp.

Burland, J. B. 1970. “Discussion, Session A.” *Proc. Conf. on In Situ Investigations in Soil and Rocks*, British Geotechnical Society, London, UK, 61-62.

Bursey, A.; Duncan, J. M.; and Smith, C. J. (2006). *A Review of Building Code Requirements and Engineering Practice for Expansive Soils, CGPR #39*, Center for Geotechnical Practice and Research, Virginia Tech, Blacksburg, VA, 30 pp.

Bustamante, M. and Gianesselli, L. 1982. “Pile bearing capacity prediction by means of static penetrometer CPT.” *Proc., 2nd European Symposium on Penetration Testing (ESOPT II)*, Vol. 2, 493-500.

Button, S. J. 1953. “The bearing capacity of footing on a two-layer cohesive subsoil.” *Proc. 3rd ICSMFE*, 1, 332-335.

Caicedo, B., Yamin, L., Giraldo, E., Coronado, O., and Soler, N. 2002. “Geomechanical properties of municipal solid waste in Dona Juana sanitary landfill.” *Proc. of the Fourth International Congress on Environmental Geotechnics*, Rio De Janeiro, Brazil, A.A. Balkema, Vol. 1, 177-182.

Caltrans. 2020. “Vertical Ground Anchors.” *Caltrans Geotechnical Manual*.

Canadian Geotechnical Society. 1978. “Excavations and Retaining Structures.” *Canadian Foundation Engineering Manual*, Part 4.

Caquot, A. and Kerisel, F. 1948. *Tables for the Calculation of Passive Pressure, Active Pressure and Bearing Capacity of Foundations*, Gauthier-Villars, Paris.

Carson, A. 1965. *Foundation Construction*, McGraw-Hill Book Co.

Castellanos, B. A. and Brandon, T. L. 2019. “Fully Softened Shear Strength: Application, Measurement, and Correlations.” *Proc. XVI Pan-American Conference on Soil Mechanics and Geotechnical Eng.*, Cancun, MX, 81–88.

Castellanos, B. A., Brandon, T. L., and VandenBerge, D. R. 2016. “Use of fully softened shear strength in slope stability analysis.” *Landslides*, 13(4), 697–709.

Caterpillar. 2000. *Handbook of Rippability*, 12th Edition, Caterpillar, Inc.

Cedergren, H. 1997. *Seepage, Drainage, and Flow Nets*, 3rd Ed., Wiley-Interscience, 496 pp.

Charles, J. A. and Soares, M. M. 1984. “The stability of slopes in soils with nonlinear failure envelopes.” *Canadian Geotechnical Journal*, 21(3), 397-406.

Chen, Y.-J. and Kulhawy, F. H. 1993. “Undrained strength interrelationships among CIUS, UU, and UC tests.” *J. Geotech. Geoenviron. Eng.*, 119(11): 1732-1750.

Chen, Y.-J. and Kulhawy, F. H. 2002. “Evaluation of drained axial capacity for drilled shafts.” *In Proc. Deep Foundations, Geotechnical Special Technical Publication 116*, 1200-2014, ASCE, Reston, VA.

Chen, Y.-J., Lin, S.-S., Chang, H-W., and Marcos, M. C. 2011. “Evaluation of side resistance capacity for drilled shafts.” *Journal of Marine Science and Technology*, Vol. 19(2), 210-221.

Cheng, Y. M. 2004. “Technical note, N_q factor for pile foundations by Berezantzev.” *Geotechnique*, 54(2), 149-150.

Cheng, Y. M. 2005. “Discussion, N_q factor for pile foundations by Berezantzev.” *Geotechnique*, 55(6), 493-494.

Chi, C.M. and Lin, Z.S. 2020. “The bearing capacity evaluations of a spread footing on single thick stratum or two-layered cohesive soils.” *Journal of Marine Science and Engineering*, 8(11), 853, 19 pp.

Chin, F.K., 1978. “Diagnosis of pile condition.” *Proc. 6th Southeast Asian Conference on Soil Engineering,* Bangkok, SEAGS Geotechnical Engineering, 9(2) 85-104.

Ching, J. and Noorzad, A. 2021. “Statistics for transformation uncertainties.” *State-of-the-art Review of Inherent Variability and Uncertainty*, ISSMGE, Technical Committee 304.

Christian, J. T. and Baecher, G. B. 1999. “Point-estimate method as numerical quadrature.” *J. of Geotechnical and Geoenvironmental Engineering*, 125(9), 779.

Clough, G. W. and Davidson. 1977. “Effects of Construction on Geotechnical Performance,” *Ninth International Conference on Soil Mechanics and Foundation Engineering*, Tokyo, Japan.

Clough, G. W. and O’Rourke, T. D. 1990. “Construction Induced Movements of In situ Walls.” *Proc. of Conf. on Design and Performance of Earth Retaining Structures, ASCE Geotech. Special Pub. No. 25*, Cornell University, Ithaca, NY, 439-470.

Clough, G. W., Smith, E. M., and Sweeney, B. P. 1989. “Movement Control of Excavation Support Systems by Iterative Design.” *Proc., Foundation Engineering: Current Principles and Practices*, Vol. 2. ASCE, 869-884.

Coduto, D. P., Kitch, W. A., and Yeung, M. 2016. *Foundation Design: Principles and Practices*, 3rd Edition, Pearson, New York, NY.

Coduto, D. P., Yeung, M. C. R., and Kitch, W. A. 2011. *Geotechnical Engineering: Principles and Practices*. Prentice Hall.

Coleman, D. M. and Arcement, B. J. 2002. “Evaluation of design methods for auger cast piles in mixed soil conditions.” *International Deep Foundations Congress*, Orlando, FL, ASCE, Reston, VA.

Cornell, C. A. 1969. “A probability-based structural code.” *Journal American Concrete Institute*, 66(12), 974-985.

Coulomb, C. A., 1776. “An Attempt to Apply the Rules of Maxima and Minima to Several Problems of Stability Related to Architecture,” *Mémoires de l’Académie Royale des Sciences*, Paris, France, 343-382.

Daniel, D. E. 1984. “Predicting hydraulic conductivity of clay liners.” *Journal of Geotechnical Engineering*, 110(2), 285-300.

Das, B. 2022. *Principles of Geotechnical Engineering*. 10th Edition, Cengage Learning, Inc., Boston, MA.

Davis, E. H. and Booker, J. R. 1973. “The effect of increasing strength with depth on the bearing capacity of clays.” *Geotechnique*, 23(4), 551-563.

Davis, F.J, 1953. “Quality control of earth embankments.” *Proc. of 3rd ICSMFE*.

Davisson, M. T. 1970. “Lateral load capacity of piles.” *In Proc., 49th Annual Meeting of the Highway Research Board*, Washington, DC, 104-112.

Davisson, M. T. and Robinson, K. E. 1965. “Bending and buckling of partially embedded piles.” *In Proc, 6th International Soil Mechanics and Foundation Engineering Conference*, Vol. 2, 243-246.

Davisson, M.T. 1972. “High Capacity Piles.” *In Proc. Soil Mechanics Lecture Series on Innovations in Foundation Construction*, American Society of Civil Engineers, ASCE, Illinois Section, Chicago, IL, 81-112.

Decker, J. B., Rollins, K. M., Ellaworth, J. C., 2008. “Corrosion rate evaluation and prediction for piles based on long-term field performance.” *J. Geotech. Geoenviron. Eng.*, 134(3), 341-351.

DeepEX. 2021. *Combined Sheet Pile Walls Software*, Deep Excavation LLC, New York, NY.

Deere, D. U. and Deere, D. W. 1989. *Rock Quality Designation (RQD) After Twenty Years*, U. S. Army Corps of Engineers, Waterways Experiment Station, Vicksburg, MS.

Deere, D. U. and Patton, F. D. 1971. “Slope Stability in Residual Soils”. *Proc., Fourth Pan American Conference on Soil Mechanics and Foundation Engineering*, San Juan, Puerto Rico, ASCE, Vol. 1, 87-1 70.

Deo. P., Wood, L. E., and Lovell, C.W. 1972. *Use of Shale in Embankments, Joint Highway Research Report 14*, Purdue Univ.

Department of Defense (DoD). 2021. *DOD Dictionary of Military and Associated Terms*. https://irp.fas.org/doddir/dod/dictionary.pdf.

DiBernardo, A. and Lovell, C. W. 1979. *The effect of laboratory compaction on the compressibility of compacted highly plastic clay: Interim Report, Publication FHWA/IN/JHRP-79/03*, Joint Highway Research Project, INDOT and Purdue Univ., West Lafayette, IN.

DiGioia, A. M. and Nuzzo, W. L. 1972. “Fly ash as structural fill.” *Journal of the Power Division*, 98(1), 77-92.

Dixon, N., Langer, U., Gotteland, P., 2008. “Classification and mechanical behavior relationships for municipal solid waste: study using synthetic waste.” *Journal of Geotechnical and Geoenvironmental Engineering*, 134(1), 79–90.

Doherty, P. and Gavin, K. 2011. “The shaft capacity of displacement piles in clay: a state of the art review.” *Geotech. Geol. Eng.*, Springer, DOI 10.1007/s10706-010-9389-2.

Dubbe, D. D., Usmen, M. A., and Moulton, L. K. 1984. “Expansive Pyritic Shales.” *Transportation Research Board 36*, Washington D.C.

Duncan, J. M. 2000. “Factors of safety and reliability in geotechnical engineering.” *Journal of Geotechnical Engineering*, 126(4), 307-316.

Duncan, J. M. and Buchignani, A. 1976. *An engineering manual for slope stability studies*, University of California, Berkeley, Department of Civil Engineering.

Duncan, J. M. and Buchignani, A. L. 1987. *An Engineering Manual for Settlement Studies, Report #2*, Center for Geotechnical Practice and Research, Virginia Tech, Blacksburg, VA.

Duncan, J. M. and Bursey, A. 2006. *Settlement of Valley Fills, CGPR #41*, Center for Geotechnical Practice and Research, Virginia Tech, Blacksburg, VA.

Duncan, J. M., Brandon, T. L., and VandenBerge, D. R. 2011. *Report of Workshop on Shear Strength for Stability of Slopes in Highly Plastic Clays, CGPR #67*, Center for Geotechnical Practice and Research, Virginia Tech, Blacksburg, VA.

Duncan, J. M., Evans, L. T., and Ooi, P. S. K. 1994. “Lateral load analysis of single piles and drilled shafts.” *Journal of Geotechnical Engineering*, 120(5), 1018-1033.

Duncan, J. M., Williams, G. W., Sehn, A. L., and Seed, R. B. 1991. “Estimation of Earth Pressures due to Compaction,” *Journal of Geotechnical Engineering*, 117(12), 1833-1847.

Duncan, J. M., Williams, G. W., Sehn, A. L., and Seed, R. B. 1991. Closure to “Estimation of Earth Pressures due to Compaction,” *Journal of Geotechnical Engineering*, 117(12), 1172-1177.

Duncan, J. M., Wright, S. G., and Brandon, T. L. 2014. *Soil Strength and Slope Stability*, 2nd ed. Wiley, Hoboken, NJ.

Ebeling, R. M. and Morrison, E.E. 1992. “The Seismic Design of Waterfront Retaining Structures,” *US Army Technical Report ITL-92-11, US Navy Technical Report NCEL TR-939*, USACE Waterways Experiment Station, Vicksburg, MS.

Eden, W. J. and Kuboto, J. K. 1962. “Some Observations on the Measurement of Sensitivity of Clays,” *Proceedings of the American Society for Testing and Materials*, Vol. 61, 1239-1249.

Edil, T. B. and Wang, X. 2000. “Shear Strength and Ko of Peats and Organic Soils,” *Geotechnics of High Water Content Materials, ASTM STP 1374*, T. B. Edil and P. J. Fox, Eds., ASTM, West Conshohocken, PA, 209-225.

Eid, H.T., Stark, T.D., Douglas, W.D., and Sherry, P.E. 2000. “Municipal solid waste slope failure waste and foundation properties,” *Journal of Geotechnical and Geoenvironmental Engineering*, 126(5), 397-407.

Eslami, A., and Fellenius, B. H. 1997. “Pile Capacity by Direct CPT and CPTu Methods Applied to 102 Case Histories.” *Canadian Geotechnical Journal*, 34(6), 880-898.

European Committee for Standardization. 1999. *Execution of Special Geotechnical Work - Sheet-pile Walls,* Standard EN 12063.

Evans, L. T. Jr. and Duncan, J. M. 1982. *Simplified Analysis of Laterally Loaded Piles. Report No. UCB/GT/82-04*, University of California, Berkeley, CA.

Fellenius, B. H. 1988. “Unified design of piles and pile groups.” *Transportation Research Record 1169*, 75-82.

Fellenius, B. H. 2021. “Basics of Foundation Design, Electronic Edition.” Accessed May 1, 2021. http://www.fellenius.net.

Fenton, G. A. and Griffiths, D. V. 2008. *Risk Assessment in Geotechnical Engineering*. New York: John Wiley & Sons.

Federal Highway Administration (FHWA). 1978a. *Design and Construction of Compacted Shale Embankments*. Offices of Research and Development, Washington, D.C.

FHWA. 1978b. *Guidelines For Cone Penetration Test, Performance, and Design, FHWA-TS-78-209*. U.S. Department of Transportation, Federal Highway Administration, Washington, D.C., 145 pp.

FHWA. 1978c. *Lateral Support Systems and Underpinning, Volume I: Design And Construction*, https://rosap.ntl.bts.gov/view/dot/14528.

FHWA. 1984. *Handbook on Design of Piles and Drilled Shafts Under Lateral Load, FHWA-IP-84-11*. U.S. Department of Transportation, Federal Highway Administration, Office of Implementation, Washington, D.C.

FHWA. 1986. *Behavior of Piles and Pile Groups Under Lateral Load, FHWA-RD-85-106*. U.S. Department of Transportation, Federal Highway Administration, Office of Engineering and Highway Operations Research and Development, Washington, D.C

FHWA. 1991. *Rock Blasting and Overbreak Control, FHWA-HI-92-001*. National Highway Institute, McLean, VA.

FHWA. 1993. *SPILE: A Microcomputer Program for Determining Ultimate Vertical Static Pile Capacity. FHWA-SA-92-044*. U.S. Department of Transportation, Federal Highway Administration, Washington, DC.

FHWA. 1999a. *Drilled Shafts: Construction Procedures and Design Methods. FHWA-IF-99-025.* U.S. Department of Transportation, Federal Highway Administration, Washington, DC.

FHWA. 1999b. *Ground Anchors and Anchored Systems. Geotechnical Engineering Circular No. 4. Publication FHWA-IF-99-015.* Federal Highway Administration, Washington, D.C.

FHWA. 2000. *Soils and Foundations Workshop Reference Manual, FHWA HI-00-045.* U.S. Department of Transportation, National Highway Institute, Federal Highway Administration, Washington, DC.

FHWA. 2001a. *Load and Resistance Factor Design (LRFD) for Highway Bridge Superstructures – Reference Manual*. Arlington, VA.

FHWA. 2001b. *Mechanically Stabilized Earth Walls and Reinforced Soil Slopes Design and Construction Guidelines, NHI-00-043.* National Highway Institute, Office of Bridge Technology.

FHWA. 2002a. E*valuation of Soil and Rock Properties, Geotechnical Engineering Circular No. 5, FHWA-IF-02-034)*. Federal Highway Administration. Office of Bridge Technology.

FHWA. 2002b. *Soils and Foundations Workshop Reference Manual, 2nd Edition, FHWA HI-88-009.* U.S. Department of Transportation, National Highway Institute, Federal Highway Administration, Washington, DC.

FHWA. 2005. *Micropile Design and Construction. Reference Manual for NHI Course 132078: FHWA-NHI-05-039*. U.S. Department of Transportation, Federal Highway Administration, Washington, DC.

FHWA. 2007. *Design and Construction of Continuous Flight Auger Piles, Geotechnical Engineering Circular No. 8, FHWA-HIF-07-03*, U.S. Department of Transportation, Federal Highway Administration, Washington, DC.

FHWA. 2008. *Earth Retaining Structures, FHWA NHI-07-071*. U.S. Department of Transportation, Federal Highway Administration, Washington, DC.

FHWA. 2009a. *Bridge Scour and Stream Instability Countermeasures: Experience, Selection, and Design Guidance, 3th Edition, Volumes 1 and 2. Hydraulic Engineering Circular No. 23, FHWA-HIF-09-111 and FHWA-HIF-09-112*, U.S. Department of Transportation, Federal Highway Administration, Washington, DC.

FHWA. 2009b. *Design and Construction of Mechanically Stabilized Earth Walls and Reinforced Soil Slopes – Volumes I and II, FHWA-NHI-10-024 and FHWA-NHI-10-025*, National Highway Institute, Washington, D.C.

FHWA. 2012a. *Evaluating Scour at Bridges, 5th Edition. Hydraulic Engineering Circular No. 18, FHWA-HIF-12-003*, U.S. Department of Transportation, Federal Highway Administration, Washington, DC.

FHWA. 2012b. *Stream Stability at Highway Structures, 4th Edition. Hydraulic Engineering Circular No. 20, FHWA-HIF-12-004*, U.S. Department of Transportation, Federal Highway Administration, Washington, DC.

FHWA. 2015. *Soil Nail Walls Reference Manual, FHWA NHI-14-007*. U.S. Department of Transportation, Federal Highway Administration, Washington, DC.

FHWA. 2016. *Design and Construction of Driven Pile Foundations. Geotechnical Engineering Circular No. 12, FHWA-NHI-16-009*, U.S. Department of Transportation, Federal Highway Administration, Washington, DC.

FHWA. 2017a. *Geotechnical Site Characterization, Geotechnical Engineering Circular No. 5*. U.S. Department of Transportation - Federal Highway Administration, Washington, DC.

FHWA. 2017b. *Ground Modification Methods Reference Manual – Volumes I and II, Geotechnical Engineering Circular No. 13, FHWA-NHI-16-009*, U.S. Department of Transportation, Federal Highway Administration, Washington, DC.

FHWA. 2018a. *Drilled Shafts: Construction Procedures and Design Methods, Geotechnical Engineering Circular No. 10, FHWA-NHI-18-024*, U.S. Department of Transportation, Federal Highway Administration, Washington, DC.

FHWA. 2018b. *Design, Analysis, and Testing of Laterally Loaded Deep Foundations that Support Transportation Facilities, Geotechnical Engineering Circular No. 9, FHWA-HIF-18-031*, U.S. Department of Transportation, Federal Highway Administration, Washington, DC.

FHWA. 2021. *Tech Brief: Scour considerations within AASHTO LRFD Design Specifications, FHWA-HIF-19-060*, U.S. Department of Transportation, Federal Highway Administration, Washington, DC.

Filz, G. M. 1992. *An experimental and analytic study of earth loads on rigid retaining walls*. Dissertation submitted in partial fulfillment for the degree of Doctor of Philosophy, Department of Civil Engineering, Virginia Tech, 345 pp.

Franklin, A. J. 1981. “A shale rating system and tentative applications to shale performance.” *Shales and Swelling Soils, Transportation Research Record 790*, National Research Council, Washington, D.C. 2-12.

Frossard, E. Hu, W., Dano, C., and Hicher, P.Y. 2012. “Rockfill shear strength evaluation: a rational method based on size effects.” *Géotechnique*, 2012, 62(5), 415-427.

Gabr, M.A. and Valero, S.N. 1995. “Geotechnical properties of municipal solid waste.” *Geotechnical Testing Journal*, ASTM 18 (2), 241–251.

Gabr, M.A., Hossain, M.S., Barlaz, M.A., 2007. “Shear strength parameters of municipal solid waste with leachate recirculation.” *Journal of Geotechnical and Geoenvironmental Engineering*, 133(4), 478–884.

Garcia-Bengochea, I., 1978. *The relation between permeability and pore size distribution of compacted clayey silts, Publ. JHRP-78-4*. Joint Highway Research Project, INDOT and Purdue Univ., West Lafayette, IN.

Giroud, J.-P. 1972. "Settlement of rectangular foundation on soil layer." *Journal of the Soil Mechanics and Foundations Division*, 98(SM1), 149-154.

Gould, J. P., 1954. *Compression Characteristics of Rolled Fill Materials in Earth Dams, TM 648*, U.S. Department of Interior Bureau of Reclamation, Denver, CO.

Gray, H. 1958. “Contribution to the Analysis of Seepage Effects in Backfills,” *Geotechnique*, 8(4), 166-170.

Greenfield, M. and Filz, G. M. 2009. *Downdrag and Drag Load on Piles, CGPR #56*, Center for Geotechnical Practice and Research, Virginia Tech, Blacksburg, VA.

Gregory, G. H. 1993. *Effect of Geogrid Reinforcement on Seepage Through Earth-Fill Dam Cores*. Masters Thesis, South Dakota School of Mines, Rapid City SD.

Gregory, G. H. 2006. *Shear Strength, Creep and Stability of Fiber-Reinforced Soil Slopes*. Dissertation submitted in partial fulfillment for the degree of Doctor of Philosophy, Oklahoma State Univ., Oklahoma City, OK.

Griffiths, D. V. 1999. “Computation of bearing capacity on layered soils.” *Proc. 4th Intl. Conf. Numer. Methods Geomech.*, Edmonton.

Griffiths, D. V. 1982. “Computation of bearing capacity factors using finite elements.” *Geotechnique*, 32(3), 195-202.

Grisolia, M. and Napoleoni, Q., 1996. “Geotechnical characterization of municipal solid waste: choice of design parameters.” *Proc. of the Second International Congress on Environmental Geotechnics*, Osaka, Japan, A.A. Balkema, Vol. 2, 641–646.

Grisolia, M., Napoleoni, Q., and Tangredi, G., 1995. “The use of triaxial tests for the mechanical characterization of municipal solid waste.” *Proc. of the Sardinia ‘95, Fifth International Landfill Symposium*, Vol. 2, Cagliari, Italy, 761–767.

GRL Engineers. 2013. “CAPWAP Models, Procedures, Parameters, Performance.” Presentation materials from PDCA Professors’ Driven Pile Institute (PDPI) meeting, Utah State University, Logan, UT.

Guan, Z., Ching, Y.-C., Wang, Y., Aladejare, A., Zhang, D. and Ching, J. 2021. “Site-specific statistics for geotechnical properties.” *State-of-the-art Review of Inherent Variability and Uncertainty*, ISSMGE, Technical Committee 304.

Harr, M.E. 1987. *Reliability-Based Design in Civil Engineering*. McGraw-Hill, New York.

Hasofer, A. M. and Lind, N. C. 1974. “Exact and invariant second-moment code format.” *Journal of the Engineering Mechanics Division*, 100(1), 111-121.

Hassouna, M.E. and Shenouda, W. K., 1970. "Filling and compaction of sand by deep vibrators and vibrorollers in the High Aswan Dam." *Proc. 10th International Congress on Large Dams*, Montreal, Vol. V, 411-432.

Hatami, K., Gregory, G. H., and Garland, G. S. 2018. *Guidelines for the Use of Fiber Reinforced Soil (FRS) in Highway Construction*. Southern Plains Transportation Center, Univ. of Oklahoma, Norman, OK.

Hetenyi, M. 1948. *Beams on Elastic Foundation*, Univ. of Michigan. Ann Arbor.

Hilf, J. W. 1956. *A rapid method of construction control for embankments of cohesive soil, Engrg. Monograph*, US Bureau of Reclamation, Denver, Colo.,(26), 1-29.

Hilf, J. W. 1991. “Compacted fill.” *Foundation Engineering Handbook*, 2nd Edition, Ed. H.-Y. Fang, Springer Nature, 249-316.

Hoek, E. and Bray, J. 1981. *Rock Slope Engineering*. 3rd Ed., Institute of Mining and Metallurgy, London, UK.

Hoek, E., Carranza-Torres, C., and Corkum, B. 2002. “Hoek-Brown failure criterion – 2002 Edition.” *Proc. North American Rock Mechanics Society Meeting*, Toronto, Canada.

Hoek, E., Wood D. and Shah S. 1992. “A modified Hoek–Brown Criterion for Jointed Rock Masses.” *Proc. Rock Characterization, Symp. Int. Soc. Rock Mech.: Eurock ’92*. J. A. Hudson Ed., Brit. Geotech. Soc., London, 209–214.

Hogentogler, C. A. 1936. “Essentials of soil compaction,” *Proc. of the Highway Research Board, 16th Annual Meeting*, Washington, D. C., R. W. Crum Ed., 309-316.

Holscher, P., Brassinga, H., Brown, M., Middendorp, P., Profittlich, M., and Tol, F. 2012. *Rapid Load Testing on Piles – Interpretation Guidelines*, CRC Press/ Baalkema, Leiden, 104 pp.

Holtz, R. D. 1989. “Treatment of problem foundations for highway embankments.” NCHRP Synthesis No. 147, Transportation Research Board, National Research Council, Washington, D.C., 72 pp.

Holtz, R. D., Kovacs, W. D., and Sheahan, T. C. 2011. *An Introduction to Geotechnical Engineering*, 2nd Ed. Prentice Hall, Upper Saddle River, NJ, 853 pp.

Hough, B. K. 1959. “Compressibility as the basis for soil bearing value.” *Journal for Soil Mechanics and Foundation Division*, 85(4), 11-40.

Houston, S. L., Houston, W. N., Zapata, C. E., and Lawrence, C. 2001. “Geotechnical engineering practice for collapsible soils.” *Unsaturated soil concepts and their application in geotechnical practice*, 333-355.

Huber, K. A., 1997. *Design of Shale Embankments*. Virginia Highway Research Council, Virginia Department of Transportation.

Hughes, S.A. 2001. “Scour and scour protection.” *Coastal Infrastructure Design, Construction and Maintenance Training: Chapter 4 - Design of Maritime Structures*, USACE, Vicksburg, MS.

Ingold, T. S. 1979. “Retaining Wall Performance During Backfilling,” Journal of the Geotechnical Engineering Division, ASCE, Vol. 105, GT5, 1979.

International Code Council (ICC). 2015. 2015 International Building Code. Accessed November 17, 2022. codes.iccsafe.org/content/IBC2015P4

International Society for Rock Mechanics (ISRM). 1978. "Suggested Methods for the Quantitative Description of Discontinuities in Rock Masses," *International Journal of Rock Mechanics*, 15, 319-368.

Jaky, J. 1944. “The Coefficient of Earth Pressure at Rest,” *Journal of the Society of Hungarian Architects and Engineers*, Vol. 7, pp. 355 – 358.

Jamiolkowski, M., Ladd, C. C., Germaine, J. T., and Lancellotta, R. 1985. “New developments in field and laboratory testing of soils.” *Proc. 11th Int. Conf. on Soil Mechanics and Foundation Engineering*, 1, 57-154.

Jardine, R. J., Standing, J. R., Jardine, F. M. , Bond, A. J., and Parker, E. 2001. “A competition to assess the reliability of pile prediction methods.” *Proc. 15th Intl. Conf. Soil Mech. Found. Engr.,* Istanbul, Turkey.

Jennings, J.K. and Knight, K. 1975. “The additional settlement of foundation due to collapse of sandy subsoils on wetting.” *Proc. 4th Intl. Conf. Soil Mech. Found. Engr.*

Jessberger, H. L. and Kockel, R., 1993. “Determination and assessment of the mechanical properties of waste materials.” *Proc. Sardinia ‘93, Fourth International Landfill Symposium*, S. Margherita di Pula, Cagliari, Italy, 1383–1392.

Johnson, J. M. and Lovell, C. W. 1979. *The effect of laboratory compaction on the shear behavior of a highly plastic clay after saturation and consolidation : interim report, Publication FHWA/IN/JHRP-79/07*, Joint Highway Research Project, INDOT and Purdue University, West Lafayette, Indiana.

Johnson, S. J.,, Compton, J. R., and Ling, S. C. 1972. “Control for underwater construction.” *Underwater Soil Sampling, Testing, and Construction Control, ASTM STP 501*, ASTM, Philadelphia, PA.

Justason, M.D. 1997. *Report of Load Testing at the Taipei Municipal Incinerator Expansion Project*, Taipei City, Taiwan.

Kavazanjian, E. 2001. “Mechanical properties of municipal solid waste.” *Proc. Sardinia 2001, Eighth International Waste Management and Landfill Symposium*, S. Margherita di Pula, Cagliari, Italy, V.3, 415–424.

Keller Moretrench American Corporation. 1954. *General Instructions for the Installation and Operation of Pumps and Wellpoint Systems.* Rockaway, NJ.

Kerisel, J. and Absi, E. 1990. *Active and passive earth pressure tables*. Balkema, Rotterdam, The Netherlands.

Kim, S. G., Duncan, J. M., and Rojiani, K. B. 1991. *Engineering Manual for Walls and Abutments*, Virginia Tech Civil Engineering Report, Blacksburg, VA.

Kitazume, M. 2005. *The sand compaction pile method*. CRC Press.

Konya, C., and Walter, E.J. 2006. *Rock Blasting and Overbreak Control*, 4th Edition, Montville, OH: Intercontinental Development Corporation, Inc.

Kraft, L. M., Ray, R. P., and Kagawa, T. 1981. “Theoretical t-z curves.” *Journal of the Geotechnical Division*, ASCE, Reston, VA.

Kramer, S. L. 1996. *Geotechnical Earthquake Engineering*. Prentice-Hall, 653 pp.

Kulhawy, F. H. 2017. “Foundation engineering, geotechnical uncertainty, and reliability-based design.” *Geotechnical Safety and Reliability*, 174-184.

Kulhawy, F. H. and Trautmann, C. H. 1996. “Estimation of in-situ test uncertainty.” *Uncertainty in the geologic environment: From theory to practice*, ASCE, 269-286.

Kulhawy, F. H., Duncan, J. M., and Seed, H. B. 1969. *Finite Element Analyses of Stresses and Movements in Embankments During Construction, Report No. TE 69-4*, Office of Research Services, University of California Berkeley.

Kulhawy, F.H. and Mayne, P.W. 1990. *Manual on Estimating Soil Properties for Foundation Design, Report EL-6800*, Electric Power Research Institute, Palo Alto, CA.

Kulhawy, F.H., Prakoso, W. A., and Akbas, S. O. 2005. “Evaluation of capacity of rock foundation sockets.” *Proc. Alaska Rocks, 40th U. S. Symposium on Rock Mechanics: Rock Mechanics for Energy, Mineral and Infrastructure Development in the Northern Regions*, American Rock Mechanics Association.

Lacroix, Y., Esrig, M. I., and Luschem, U. 1970. “Design, Construction and Performance of Cellular Cofferdams,” *Lateral Stresses in the Ground and Design of Earth Retaining Structures*, ASCE, Cornell University, 1970.

Lacy, H. S. and Gould, J. P. 1985. “Settlement from pile driving in sands.” *Vibration Problems in Geotechnical Engineering*, Special Technical Publication, ASCE, Reston, VA.

Lade, P.V. 2010. “The mechanics of surficial failure in soil slopes.” *Engineering Geology*, 114(1-2), 57-64.

Landva, A. O. and La Rochelle, P. 1983. “Compressibility and Shear Characteristics of Radforth Peats,” *Testing of Peats and Organic Soils*, ASTM STP 820, P. M. Jarrett, Ed., ASTM, 157-191.

Landva, A. O., Korpijaakko, E. O., and Pheeney, P. E. 1983. “Geotechnical Classification of Peats and Organic Soils,” *Testing of Peats and Organic Soils*, ASTM STP 820, P. M. Jarrett, Ed., ASTM, 37-51.

Lee, D.M. 1992. *The angles of friction of granular fills.* PhD dissertation, Univ. of Cambridge.

Lee, L. T. 2001. "Geotechnical properties and sediment characterization for dredged material models," *DOER Technical Notes Collection (ERDC TN-DOER-N13)*, U.S. Army Engineer Research and Development Center, Vicksburg, Mississippi. www.wes.army.mil/el/dots/doer/

Leps, T. M. 1970. “Review of shearing strength of rockfill.” *Journal of the Soil Mechanics and Foundations Division*, 96(4), 1159-1170.

Low, B. K. and Tang, W. H. 1997. “Efficient reliability evaluation using spreadsheet.” *Journal of Engineering Mechanics*, 123(7), 749-752.

Maitland, J. K. 1977. *Behavior of Cellular Bulkheads in Deep Sands*. Ph. D. Dissertation submitted at Oregon State University, Corvallis, Oregon.

Maitland, J. K. and Schroeder, W. L. 1979. “Model study of circular sheetpile cells.” *Journal of the Geotechnical Engineering Division*, 105(7), 805-821.

Mana, A. I. and Clough, G. W. 1981. "Prediction of movements for braced cuts in clay." *Journal of the Geotechnical Engineering Division*, 107(6), 759-777.

Mansur, C. and Kaufman, R. 1961. "Dewatering." *Foundation Engineering*, Ed. Leonards, McGraw Hill, 514 pp.

Marchetti, S. 2006. "Origin of the flat dilatometer." *Proc. 2nd International Conf. the Flat Dilatometer*, Washington, DC, 2-5).

Marinos, P. and Hoek, E. 2000. "GSI: A Geological Friendly Tool for Rock Mass Strength Estimation." *Proc. GeoEng 2000, Intl. Conf. Geot. Geol. Engr.*, Melbourne, 1422-1446.

Marsal, R. J. 1967. "Large scale testing of rockfill materials." *Journal of the Soil Mechanics and Foundations Division*, 93(2), 27-43.

Marschi, N. D., Chan, C. K., and Seed, H. B. 1972. "Evaluation of properties of rockfill materials." *Journal of the Soil Mechanics and Foundations Division*, 98(1), 95-114.

Martin, R. E. 2001. "Foundations in Weathering Profiles from Igneous and Metamorphic Rocks." *ASCE Geo-Institute Specialty Conference*, Virginia Tech, VA.

Martin, R.E. 1977. "Estimating Foundation Settlements in Residual Soils." *Journal of Geotechnical Engineering Division*, 103(GT3), 197-212.

Martin, R.E. 1987. "Settlement of Residual Soils.", *Proc. Foundations and Excavations in Decomposed Rock of the Piedmont Province*, ASCE, 1-14.

Masad, E., Taha, R., Ho, C., and Papagiannakis, T. 1996. "Engineering properties of tire/soil mixtures as a lightweight fill." *Geotechnical Testing Journal*, 19, 297-304.

Matlock, H. 1970. "Correlations for design of laterally loaded piles in soft clay." *Proc. Offshore Technology Conference*, Vol. 1, Houston, TX.

Matsuzawa, H., Ishibashi, I., and Kawamura, M. 1985. "Dynamic soil and water pressures of submerged soils." *Journal of Geotechnical Engineering*, 111(10), 1161-1176.

Mayne, P. W. 1985. "A review of undrained strength in direct simple shear." *Soils and Foundations*, 25(3), 64-72.

Mayne, P. W. and Kulhawy, F. H. 1982. "K_0 – OCR Relationships in Soil," *Journal of the Geotechnical Division*, 108(60, 851 – 872.

Mays, T. W. 2015. *Design Guide for Pile Caps*, Concrete Reinforcing Steel Institute, Schaumburg, Il.

Mazurkiewicz, B.K. 1980. *Design and Construction of Dry Docks*. Trans Tech Publications, Rockport, MA.

McCarthy, D. F. 2007. *Essentials of Soil Mechanics and Foundations: Basic Geotechnics*. Prentice Hall.

McCook, D. K. and Shanklin, D. W. 2000. “NRCS experience with field density test methods including the sand-cone, nuclear gage, rubber balloon, drive-cylinder, and clod test.” *Constructing and Controlling Compaction of Earth Fills*, ASTM Special Technical Publication 1384, 72-92.

McGregor, J. and Duncan, J.M. 1998. *Performance and Use of the Standard Penetration Test in Geotechnical Engineering Practice, CGPR #12*. Center for Geotechnial Practice and Research, Virginia Tech, Blacksburg, VA.

McGuire, M. P. and VandenBerge, D. R. (2017). “Interpretation of shear strength uncertainty and reliability analyses of slopes.” *Landslides*, 14(6), 2059-2072.

McVay, M.C., Kuo, C.L., and Guisinger, A.L., 2003. *Calibrating Resistance Factor in the Load and Resistance Factor Design of Statnamic Loading Test*. Project No. 4910450482312, Final Report, University of Florida, 129 pp.

Menard L. 1955. Travail personnel sur le pressiometre, Ecole nationale des ponts et chaussees, Paris.

Merifield, R. S., Sloan, S. W., and Yu, H. S. 1999. “Rigorous plasticity solutions for the bearing capacity of two-layered clays.” *Geotechnique*, 49(4), 471-490.

Meyerhof, G. G. 1951. “The ultimate bearing capacity of foudations.” *Geotechnique*, 2(4), 301-332.

Meyerhof, G. G. 1953. “Some recent foundation research and its application to design.” *The Structural Engineer*, 31(6), 151-167.

Meyerhof, G. G. 1957. “The ultimate bearing capacity of foundations on slopes.” *Proc. 4th Intl. Conf. Soil Mech. Found. Engr.*, Vol. 1, 384-386.

Meyerhof, G. G. 1963. “Some recent research on the bearing capacity of foundations.” *Canadian Geotechnical Journal*, 1(1), 16-26.

Meyerhof, G. G. 1974. “Ultimate bearing capacity of footings on sand layer overlying clay.” *Canadian Geotechnical Journal*, 11(2), 223-229.

Meyerhof, G. G. 1976. “Bearing capacity and settlement of pile foundations.” *Journal of the Geotechnical Engineering Division*, 102(GT3), 197- 228.

Meyerhof, G. G. and Hanna, A. M. 1978. “Ultimate bearing capacity of foundations on layered soils under inclined load.” *Canadian Geotechnical Journal*, 15(4), 565-572.

Middendorp, P., Bermingham, P. and Kuiper, B. 1992. “Statnamic load testing of foundation piles.” *Proc. 4th Intl. Conf. Appl. Stresswave Theory to Piles*, Balkema Publishers, A.A., The Hague, The Netherlands, 581-588.

Milovic, D. M. 1965. "Comparison between the calculated and experimental values of the ultimate bearing capacity." *Proc. 6th ICSMFE*, Montreal, 142-144.

Mitchell, J. K. and Soga, K. 2005. *Fundamentals of soil behavior*. John Wiley & Sons, New York, NY.

Mitchell, J. K., Hooper, D. R., and Campenella, R. G. (1965). “Permeability of compacted clay.” *Journal of the Soil Mechanics and Foundations Division*, 91(4), 41-65.

Mokwa, R. L. and Duncan, J. M. 2001a. “Experimental evaluation of lateral-load resistance of pile caps.” *Journal of Geotechnical and Geoenvironmental Engineering*, 127(2), 185-192.

Mokwa, R. L. and Duncan, J. M. 2001b, “Laterally Loaded Pile Groups and p-y Multipliers,” *Proc. Geo-Institute Conference 2001: A Geo-Odyssey, Geotechnical Special Publication Number 113*, ASCE.

Mononobe, N and Matsuo, H. (1929). “On the Determination of Earth Pressures during Earthquakes,” *Proc. World Engineering Congress*, 9 pp.

Muhs, D.R. 2013. “Loess and its Geomorphic, Stratigraphic, and Paleoclimatic Significance in the Quaternary.” *Treatise on Geomorphology, Vol 11, Aeolian Geomorphology.* Ed.: Shroder, J. F., Lancaster, N., Sherman, D.J., and Baas, A.C.W., San Diego: Academic Press, 149-183.

Mullins, G., Lewis, C., and Justason, M. 2002. “Advancements in Statnamic Data Regression Techniques.” *Proc. Deep Foundations 2002: An International Perspective on Theory, Design, Construction, and Performance*, *GSP No.116*, ASCE, Vol. 2, 915-930.

Narin, W. A. and Mitchell, J. K. 1994. “Soil improvement by blasting.” *Journal of Explosive Engineering*, 12(3), 34-41.

Natural Resource Conservation Service (NRCS). 2022. "Chapter 4 Engineering Classification of Rock Materials." *Part 631 Geology National Engineering Handbook*.

NCHRP (National Cooperative Highway Research Program). 2018. *Manual on Subsurface Investigations, Publication No. CRP Project 21-20*. Transportation Research Board, National Academies of Science Engineering, and Medicine, Washington, DC.

NCHRP. 1991. *Manuals for the Design of Bridge Foundations, Report 343*. Transportation Research Board, National Academies Press, Washington, DC.

NCHRP. 1997a. *Design and Construction Guidelines for Downdrag on uncoated and Bitumen-Coated Piles, Report 393*. Transportation Research Board, National Academies Press, Washington, DC.

NCHRP. 1997b. *Dynamic Effects of Pile Installations on Adjacent Structures, NCHRP Synthesis 253*, Transportation Research Board, Washington, DC.

NCHRP. 2006. *Innovative Load Testing Systems, NCHRP 21-08*. Transportation Research Program, Washington, D.C., 148 pp.

NCHRP. 2010. *Intelligent Soil Compaction Systems, Report 676*. Transportation Research Board, National Academies of Science Engineering, and Medicine, Washington, D.C.

NCHRP. 2015. *Current Practices for Design and Load Testing of Large Diameter Open-End Driven Pipe Piles, NCHRP Report 20-05, Topic 45-05*. Transportation Research Board, Washington, DC.

NeSmith, W. M. 2002. “Static capacity analysis of augered, pressure-injected displacement piles.” *Proc. Deep Foundations: An International Perspective on Theory, Design and Performance*, ASCE, Reston, VA.

Noorany, I. and Stanley, J. V. 1994. “Settlement of compacted fills caused by wetting.” *Proc. Vertical and Horizontal Deformations of Foundations and Embankments*, 1516-1530.

Noorany, I., Gardner, W. S., Corley, D. J., and Brown, J. L. 2000. “Variability in field density tests.” *Constructing and Controlling Compaction of Earth Fills*, ASTM Special Technical Publication 1384, 58-71.

Nordlund, R. L. 1963. “Bearing capacity of piles in cohesionless soils.” *Journal of the Soil Mechanics and Foundations Division*, 89(SM3), 1-35.

Nordlund, R. L. 1979. “Point bearing and shaft friction of piles in sand.” *Proc. 5th Annual Fundamentals of Deep Foundation Design*, St. Louis, MO.

Norris, G. M. 1986. “Theoretically based BEF laterally loaded pile analysis.” *Proc. 3rd Intl. Conf. Num. Methods in Offshore Piling*, Paris, France.

Norrish, N. I. and Wyllie, D. C. 1996. “Chapter 15, Rock Slope Stability Analysis.” *Special Report Number: 247. Landslides: Investigation and Mitigation*, TRB, 391-425.

Nowak, A. S. 1995. “Calibration of LRFD bridge code.” *Journal of Structural Engineering*, 121(8), 1245-1251.

O’Rourke, T. D. 1981. “Ground Movements Caused by Braced Excavations,” *Journal of the Geotechnical Engineering Division*, 107(GT9), 1159-1178.

Occupational Safety and Health Administration (OSHA). 2020. *CFR Part 1926, Subpart P, Excavations, with Appendices A - F*. https://www.osha.gov/laws-regs/regulations/standardnumber/1926/1926SubpartP.

Ohio Department of Transportation (ODOT). 2010. *Supplement 1015 Compaction Testing of Unbound Materials*. https://www.dot.state.oh.us/Divisions/ConstructionMgt/OnlineDocs/2013MOP/Supplements/S_1015.htm.

Okabe, S. 1926. “General theory on earth pressure and seismic stability of retaining wall.” *J. of Japan Soci. of Civil Engineers*, 10(6), 1277-1323.

Olson, R. E. 1963, "Effective Stress Theory of Soil Compaction", *Journal of the Soil Mechanics and Foundations Division*, 89(SM2), 27-45.

Olson, S. M. 2002. *Liquefaction Analysis of Level and Sloping Ground Using Field Case Histories and Penetration Resistance*. Ph.D. Thesis, University of Illinois at Urbana-Champaign, IL.

Oriard, L. L. 1987. “Resolution of Some Common Problems in Highway Blasting,” *Transportation Research Record, Issue Number 1119*, Washington, D.C., 119-125.

OSHA. 2020. "Section V: Chapter 2 Excavations: Hazard Recognition in Trenching and Shoring." *OSHA Technical Manual*. https://www.osha.gov/otm/section-5-construction-operations/chapter-2.

Ostadan, F. 2005. “Seismic Soil Pressure for Building Walls – an Updated Approach,” *Journal of Soil Dynamics and Earthquake Engineering*, 25, 785-793

Ovesen, N. K. 1962. *Cellular Cofferdams Calculation Method and Model Tests*, *Bulletin 14*, Danish Geotechnical Institute, Copenhagen.

Pandey, R. K. and Tiwari, R. P. 2015. “Physical Characterizations and Geotechnical Properties for Municipal Solid Waste,” *IOSR Journal of Mechanical and Civil Engineering*, 12(1), 15-21.

Pastore, E. I. 1995. “Weathering Profiles.” Proc. Conference on Soil Mechanics and Foundation Engineering, 363-364.

Pastore, E.L., 1995. “Weathering profiles.” *Proc. Panamerican Conference on Soil Mechanics and Foundation Engineering*, ISSMFE, Vol. 1, 353-364.

Peck, R. B. 1969. “Deep excavations and tunneling in soft ground, State-of-the-art report,” *7th International Conference on Soil Mechanics and Foundation Engineering*, Mexico City, Mexico, State-of-the-Art Volume, 225-290.

Perko, H. A. 2009. *Helical Piles: A Practical Guide to Design and Installation*. Wiley, Hoboken, NJ.

Perloff, W. H. and Baron, W. 1976. *Soil Mechanics Principles and Applications*, Ronald Press Co., New York.

Phoon, K. K. and Kulhawy, F. H. 1999a. “Characterization of geotechnical variability.” *Canadian Geotechnical Journal*, 36(4), 612-624.

Phoon, K. K. and Kulhawy, F. H. 1999b. “Evaluation of geotechnical property variability.” *Canadian Geotechnical Journal*, 36(4), 625-639.

Porter, O. 1943. “Foundations for flexible pavements.” *Proc. of 22nd Annual Meeting of the Highway Research Board*, Highway Research Board, 100-143.

Portland Cement Association (PCA). 1952. "Concrete Crib Retaining Walls." *Concrete Information No. St. 46*, Chicago, IL.

PCA. 1992. *PCA Soil Primer*. Skokie, IL.

Post-Tensioning Institute (PTI). 1996. *Recommendations for Prestressed Rock and Soil Anchors*, 3rd ed., Phoenix, Arizona.

Poulos, H.G. 1989. “Pile behaviour – theory and application.” *Geotechnique*, 39(3): 365-415.

Prandtl, L. 1920. “Über die Härte plastischer Körper.” Nachr. Ges. Wiss. Goettingen, Math.-Phys. Kl., 74-85.

Proctor, R. R. (1933). "Fundamental Principles of Soil Compaction," *Engineering News-Record*, 111(9), 245-248.

Randolph, M. F. and Murphy, B. S. 1985. "Shaft capacity of driven piles in clay. *Proc. 17th Annual Offshore Technology Conference*, Houston, TX.

Rankine, W. J. M. 1857. "On the Stability of Loose Earth," *Transactions of Royal Society*, London, England, Vol. 147, Part 1, 9-27.

Rausche, F. and Goble, G.G. 1979. "Determination of pile damage by top measurements." *Behavior of Deep Foundations. American Society for Testing and Materials, ASTM STP 670*, R. Lundgren, Editor, 500-506.

Rausche, F. and Webster, S. 2007. "Behavior of cylinder piles during pile installation." *Proc. Geo-Denver: Contemporary Issues in Deep Foundations, Geotechnical Special Technical Publication 158*, ASCE, Reston, VA.

Reddy, K. R., Hettiarachchi, H., Gangathulasi, J., and Bogner, J. 2011, "Geotechnical Properties of Municipal Solid Waste at Different Phases of Biodegredation," *Waste Management,* 31, 2275–2286.

Reddy, K.R., Hettiarachchi, H., Gangathulasi, J., Bogner, J., and Lagier, T. 2009. "Geotechnical properties of synthetic municipal solid waste," *International Journal of Geotechnical Engineering*, 3(3), 429–438.

Reese, L. C. and Matlock, H. 1956. "Non-dimensional solutions for laterally loaded piles with soil modulus assumed proportional to depth." Proc. *8th Texas Conf. Soil Mech. Found. Engr*. Association of Drilled Shaft Contractors, Dallas, TX.

Reese, L. C. and O'Neil, M. W. 1989. "New design method for dilled shafts from common soil and rock tests." *Proc. Foundation Engineering: Current Principles and Practices, Geotech. Special Tech. Publ. 22*, ASCE, Reston, VA, 1026-1039.

Reese, L. C., Wang, S. T., Isenhower, W. M., Arrellaga, J. A., and Hendrix, J. 2004. *LPILE Plus Version 5 Technical Manual*. Ensoft, Austin, TX.

Richards, R. J. and D. Elms. 1979. "Seismic Behavior of Gravity Retaining Walls," *Journal of the Geotechnical Engineering Division*, 105(GT4), 449-464.

Richart, F. E., and Schmertmann, F. 1957. "The effects of seepage on the stability of sea walls." *Coastal Engineering Procedings*, 6, 48.

Robertson, P. K. 2009. "Interpretation of cone penetration tests—a unified approach." *Canadian Geotechnical Journal*, 46(11), 1337-1355.

Robinette, M. D. and Duncan, J. M. 2005. *Pile Group 2.0 – A Spreadsheet for Laterally Loaded Pile Groups*, *CGPR #33*. Center for Geotechnical Practice and Research, Virginia Tech, Blacksburg, VA.

Rollins, K. M. and Rogers, G. W. 1994. "Mitigation measures for small structures on collapsible alluvial soils." *Journal of Geotechnical Engineering*, 120(9), 1533-1553.

Rollins, K. M., Clayton, R. J., Mikesell, R. C., and Blaise, B. C. 2005. "Drilled shaft side friction in gravelly soils." *J. Geotech. Geoenviron. Eng.*, 13(8), 987-1003.

Romanoff, M. 1962. "Corrosion of steel pilings in soils." *Journal of Research of the National Bureau of Standards – C. Engineering and Instrumentation*, Vol.66C(3), 223-244.

Rosenblueth, E. 1975. "Point estimates for probability moments." *Proc. of the National Academy of Sciences*, 72(10), 3812-3814.

Rosenblueth, E. and Esteva, L. 1972. "Reliability analysis for some Mexican codes." *American Concrete Institute*, Detroit.

Rosenqvist, I. T. 1953. "Considerations on the Sensitivity of Norwegian Quick-Clays," *Geotechnique*, 3, 195-200.

Rowe, P. W., Stroyer, Browzin, and Tschebotarioff. 1952. "Anchored Sheet Pile Walls," *Proc. Institution of Civil Engineers*, 1(1), 27-70.

Rowe, R. K. and H. H. Armitage. 1987a. *"*Theoretical solutions for axial deformation of drilled shafts in rock.*"* *Canadian Geotechnical Journal*, 24, 114-125.

Rowe, R. K. and H. H. Armitage. 1987b. "A design method for drilled piers in soft rock." *Canadian Geotechnical Journal*, 24, 126-142.

Salgado, R. 2006. "The role of analysis in pile design." *Modern Trends in Geomechanics, Springer Proc. Physics*, Vol. 106, 521-540.

Salgado, R. 2008. *The Engineering of Foundations*. McGraw Hill, New York, NY.

Satyanarayana, B. and Garg, R. K. 1980. "Bearing capacity of footings on layered c-ϕ soils." *Journal of the Geotechnical Engineering Division*, 106(7), 819-824.

Schmertmann, J. H. 1970. "Static Cone to Compute Static Settlement Over Sand," *Journal of the Soil Mechanics and Foundations Division*, 96(SM3), 1011-1043.

Schmertmann, J. H. 1989. “Density tests above zero air voids line.” *Journal of GeotechnicalEngineering*, 115(7), 1003-1018.

Schmertmann, J. H., Hartman, J. P., and Brown, P. R. 1978. “Improved strain influence factor diagrams,” *Journal of Geotechnical Engineering Division*, 104(GT8), 1131-1135.

Schroeder, W. L. and Maitland, J. K. 1979. "Cellular bulkheads and cofferdams." *Journal of Geotechnical Engineering Division*, 105(7), 823-837.

Schroeder, W. L., Marker, D. K., and Khuayjarernpanishk, T. 1977. "Performance of a cellular wharf." *Journal of Geotechnical Engineering Division*, 103(GT3), 153-168.

Seed, H. B. and R. V. Whitman. 1970. “Design of Earth Retaining Structures for Dynamic Loads.” *Proc. ASCE/SEI Specialty Conference on Lateral Stresses in the Ground and Design of Earth-Retaining Structures*, 103-147.

Seed, H. B., Mitchell, J. K., and Chan, C. K. 1960. “The strength of compacted cohesive soils.” *Research conference on the strength of cohesive materials*, ASCE, Boulder, CO, 877-964.

Seelye, E. E. 1956. *Foundations: Design and Practice*, John Wiley & Sons, Inc., New York.

Sehn, A. E. 1990. *Experimental Study of Earth Pressures on Retaining Structures.* Dissertation submitted in partial fulfillment for the degree of Doctor of Philosophy, Department of Civil Engineering, Virginia Tech, 347 pp.

Sellmeijer, J. B., Cools, J. P. A. E., Decker, J. and Post, W. J. 1995. “Hydraulic Resistance of Steel Sheet Pile Joints.” *Journal of Geotechnical Engineering*. 121(2), 105-110.

Sherard, J. L. 1953. *Influence of Soil Properties and Construction Methods on the Performance of Homogenous Earth Dams*, *TM-645*, United States Bureau of Reclamation.

Sherard, J. L. 1986. “Hydraulic fracturing in embankment dams.” *Journal of Geotechnical Engineering*, 112(10), 905-927.

Siegel, T.C., Lamb, R., Dasenbrock, D., and Axtell, P.J. 2013. “Alternative design approach for drag load and downdrag with the LRFD framework.” *Proc. 38th Annual Conference on Deep Foundations*, Phoenix, AZ, 23-39.

Siegel, T.C., Lamb, R., Dasenbrock, D., Axtell, P. J. 2014. “Neutral plane method for drag force of deep foundations and the AASHTO LRFD Bridge Design Specifications.” *Proc. Univ. of Minnesota Annual Geotechnical Conference*.

Skempton, A. W. 1942. “An investigation of the bearing capacity of a soft clay soil.” *J. Inst. Civil Eng.*,18, 307.

Skempton, A. W. 1964. “Long-term Stability of Clay Slopes.” *Géotechnique*, 14(2), 77–102.

Skempton, A. W. 1970. “First-time Slides in Overconsolidated Clays,” *Géotechnique*, 20(3), 320-324.

Skempton, A. W. 1977. “Slope Stability of Cuttings in Brown London Clay.” *9th Intl. Conf. Soil Mech. Geotech. Engr*. Tokyo, Japan, 261-270.

Skempton, A. W. and Golder, H. Q. 1948. “Practical examples of the ϕ= 0 analysis of stability of clays.” *Proc. 2nd Intl. Conf. Soil Mech. Found. Engr.*, Vol. 2, 63-70.

Sleep, M., Duncan, J. M., Hickerson, H., and Ritter, K. 2009. *Geotechnical Considerations for Organic Soils and Peat, CGPR #58*, Center for Geotechnical Practice and Research, Virginia Tech, Blacksburg, VA, 25 pp.

Sleep, M.D. and Duncan, J.M. 2014. *Manual for Geotechnical Engineering Reliability Calculations (2nd edition), CGPR #76*. Center for Geotechnical Practice and Research, Virginia Tech, Blacksburg, VA.

Smith, E. A. L. 1960. “Pile driving analysis by the wave equation.” *Journal of the Soil Mechanics and Foundations Division*, 86(4), 35-61.

Soleimanbeigi, A. and Edil, T. B. 2015. “Compressibility of recycled materials for use as highway embankment fill.” *Journal of Geotechnical and Geoenvironmental Engineering*, 141(5), 04015011.

Soleimanbeigi, A., Edil, T. B., and Benson, C. H. 2014. “Engineering properties of recycled materials for use as embankment fill.” *Geo-Congress 2014: Geo-characterization and Modeling for Sustainability*, 3645-3657.

Sotelo, M. J., Mazari, M., Garibay, J., and Nazarian, S. 2014. “Variability of moisture content measurement devices on subgrade soils.” *Geo-Congress 2014: Geo-characterization and Modeling for Sustainability*, 1425-1432.

Sowers, G. F. 1977. Closure to “Failures in Limestones in Humid Subtropics.” *Journal of the Geotechnical Engineering Division*, 103(GT7), 807-813.

Sowers, G. F. 1979. *Introductory Soil Mechanics and Foundations: Geotechnical Engineering*. Macmillan & Co, New York, New York.

Sowers, G.F. 1963. “Engineering Properties of Residual Soil Derived from Igneous and Metamorphic Rocks.” *Proc. Second Pan American Conference on Soil Mechanics and Foundation Engineering*, Brazil, Vol. 1, 39-61.

Stagg, K. G. and Zienkiewicz, O. C. 1968. *Rock Mechanics in Engineering Practice*. John Wiley & Sons, New York, 442 pp.

Szypcio, Z. and Dołżyk, K. 2006. “The bearing capacity of layered subsoil.” *Studia Geotechnica et Mechanica*, 28(1), 45-60.

Terzaghi, K. 1943. *Theoretical Soil Mechanics*. John Wiley and Sons, Inc., New York, NY.

Terzaghi, K. 1944. “Ends and Means in Soil Mechanics." *Engineering Journal of Canada*, Vol. 27, 608.

Terzaghi, K. 1945. "Stability and Stiffness of Cellular Cofferdams," *American Society of Civil Engineers, Transactions*, Vol 110, Paper No. 2253, 1083-1202.

Terzaghi, K. 1954. “Anchored Bulkheads,” *American Society of Civil Engineers, Transactions*, Vol. 119, Paper No. 2720, 1243-1280.

Terzaghi, K. and Peck, R. B. 1967. *Soil Mechanics in Engineering Practice*, 2nd Ed. Wiley and Sons, Inc., New York, NY.

Terzaghi, K., Peck, R. B., and Mesri, G. 1996, *Soil Mechanics in Engineering Practice*, 3rd Ed. John Wiley & Sons, Inc., New York.

Timchenko, A., Shidlovskaya, A. and Briaud, J.-L. 2021. “Tolerable risk chart.” *Proc. of 20th Intl. Conf. Soil Mech. Geotech. Engr*.

Tinjum, J. M., Benson, C. H., and Blotz, L. R. 1997. “Soil-water characteristic curves for compacted clays.” *Journal of Geotechnical and Geoenvironmental Engineering*, 123(11), 1060-1069.

Tomlinson, M. J. 1994. *Pile Design and Construction Practice*, 4th Ed. E & FN Spon, London, England.

Transportation Research Board (TRB). 1990. *Guide to Earthwork Construction, State of the Art Report 8*, National Research Council, Washington, D.C.

Troxler Labs. 2019. *Troxler Model 3430 and 3440 Moisture Density Gauges*. Research Triangle Park, NC.

Tschebotarioff, G.P. 1973. *Foundations, Retaining and Earth Structures*, 2nd Ed., McGraw-Hill, New York.

Tsiambaos, G. and Saroglou, H. (2010). "Excavatability Assessment of Rock Masses Using the Geological Strength Index (GSI)." *Bulletin of Engineering Geology and the Environment*, 69(1), 13-27.

Turnbull, W. J. and Foster, C. R. 1956. "Stabilization of materials by compaction." *Journal of the Soil Mechanics and Foundations Division*, 82(2), 1-23.

Unified Facilities Criteria (UFC). 2004. *Dewatering and Ground Control, UFS 3-220-05*. US Department of Defense, Washington, DC.

UFC. 2012. *General Criteria for Waterfront Construction, UFC 4-151-10*, US Department of Defense, Washington, DC.

UFC. 2021. *Geotechnical Engineering With Change 1, UFC 3-220-01*, US Department of Defense, Washington, DC.

UFC. 2022. *Soil mechanics (DM 7.1), UFC 3-220-10*, US Department of Defense, Washington, DC.

United States Army Corps of Engineers (USACE). 1960. "Appendix B, The Unified Soil Classification System." *Characteristics of Soil Groups Pertaining to Roads and Airfields. Technical Memorandum 3-357*. Waterways Experiment Station, Vicksburg, MS.

USACE. 1980. *Civil Works Construction Specifications for Wire Mesh Gabions, Slope and Channel Protection, CE 02541*, Department of the Army, Washington, DC, 17 pp.

USACE. 1983a. *Dewatering and Groundwater Control, TM 5/818-5/AFM 88-5.* Department of the Army, Washington, DC.

USACE. 1983b. *Procedures for Foundation Design of Buildings and Other Structures (Except Hydraulic Structures), TM 5/818-1/AFM 88-3*. Department of the Army, Washington, DC.

USACE. 1989. *Design of Sheet Pile Cellular Structures, Cofferdams, and Retaining Structures, EM 1110-2-2503*, Department of the Army, CECW-EP, 186 pp.

USACE. 1991. *Design of Pile Foundations. Engineer Manual: EM 1110-2-2906*, Department of the Army, Washington, DC.

USACE. 1994a. *Design of Sheet Pile Walls, EM 1110-2-2504*. Department of the Army, CECW-EP, 75 pp.

USACE. 1994b. *Test Quarries and Test Fills, EM 1110-2-2301*. Department of the Army, Washington, D.C.

USACE. 1995a. *Construction Control for Earth and Rock-Fill Dams, EM 1110-2-1911*. Department of the Army, Washington, D.C.

USACE. 1995b. *Design of Coastal Revetments, Seawalls, and Bulkheads, EM 1110-2-1614.* Department of the Army, CECW-EH-D, 110 pp.

USACE. 2001. *Geotechnical Investigations, EM 1110-1-1804.* Department of the Army, Washington, D.C.

USACE. 2004. *General Design and Construction Considerations for Earth and Rock-Fill Dams, EM 1110-2-2300*. Department of the Army, Washington, D.C.

USACE. 2012. *LPILE Method for Evaluating Bending Moments in Batter Piles Due to Ground Settlement for Pile-Supported Floodwalls in New Orleans and Vicinity. Report W912P8-07-D-0062*, US Army Corps of Engineers, Washington, DC.

USACE. 2014. *Safety of Dams – Policy and Procedures, EM 1110-2-1156*, Department of the Army, Washington, D.C.

USACE. 2020. *Geotechnical System Response Curves for Risk Assessments, ETL 1110-2-588*, Department of the Army, Washington, D.C.

United States Department of Agriculture (USDA). 2010. *Wood Handbook: Wood as an Engineering Material*, *General Technical Report: FPL-GTR-190*, Forest Products Laboratory, Madison, WS.

United States Steel (USS). 1984. *Steel Sheet Piling Design Manual*. Updated and reprinted by the US Dept. of Transportation/FHWA, 135 pp.

United States Bureau of Mines (USBM). 1971. *Blasting Vibrations and Their Effect on Structures*. United States Department of the Interior.

United States Bureau of Reclamation (USBR). 1960. *Petrographic and Engineering Properties of Loess, Engineering Monograph No. 28.*

USBR. 1987. *Design of Small Dams*. 3rd Edition, United States Department of the Interior.

USBR. 1988. *Bureau Case History of Loess Cut Slopes in Nebraska, GR-88-3*. United States Department of the Interior.

USBR. 1992. *Characteristics and Problems of Collapsible Soils.* United States Department of the Interior.

USBR. 1998. *Earth Manual, Part 1*. 3rd Ed., Earth Sciences and Research Laboratory, Technical Service Center, Denver, CO., 348 pp.

USBR. 2012. "Chapter 10: Embankment Construction." *Design Standards No. 13 Embankment Dams*, Technical Service Center.

USBR and USACE. 2019. *Best Practices in Dam and Levee Safety Risk Analysis*. Risk Management Center, Denver, CO.

VandenBerge, D. R., Castellanos, B. A., and McGuire, M. P. 2018. "Comparison and Use of Failure Envelopes for Slope Stability," *Geotechnical and Geological Engineering*, https://doi.org/ 10.1007/s10706-018-0742-1.

VandenBerge, D. R., Duncan, J. M., and Brandon, T. L. 2015. *Consolidated-Undrained Strength of Compacted Clay, CGPR #83*, Center for Geotechnical Practice and Research, Virginia Tech, Blacksburg, VA, 128 pp.

VandenBerge, D. R., Duncan, J. M., and Brandon, T. L. 2017. "Practical considerations for measuring the shear strength of compacted clay," *Proc. GeoFrontiers 2017*.

VandenBerge, D. R., Esser, A. J., and Bumpas, K. 2015. "An overview of sustainability applied to earth structures," *Proc. IFCEE 2015*, 2707-2716

VandenBerge, D. R., McGuire, M. P., and Castellanos, B. A. 2018. *Linear and Nonlinear Effective Stress Shear Strength Envelopes from Triaxial Test Data*, Center for Geotechnical Practice and Research, Virginia Tech, Blacksburg, VA, 57 pp.

VandenBerge, D. R., McGuire, M. P., and Castellanos, B. A. 2020. "Effective Stress Failure Envelope Forms and Parameter Variability." *Geo-Congress 2020: Modeling, Geomaterials, and Site Characterization*, ASCE, Reston, VA, 236-246.

VandenBerge, D. R.; Brandon, T. L.; and Wielputz, M. P. 2017. "Highly organic fill for levee stability berms," *Geotechnical Testing Journal*, ASTM, 38(3), 1-13.

Vanmarcke, E. H. 1977. “Probabilistic modeling of soil profiles.” *Journal of the Geotechnical Engineering Division*, 103(11), 1227-1246.

Vaughan, P. R. 1985. “Mechanical and Hydraulic Properties of In-Situ Residual Soils.” *General Report, Session 2, First International Conference on Geomechanics in Tropical, Lateritic and Saprolitic Soil*, Brasilia, 231–263.

Vesić, A. S. 1973. “Analysis of ultimate loads of shallow foundations.” *Journal of the Soil Mechanics and Foundations Division*, 99(1), 45-73.

Vesic, A. S. 1975. “Bearing capacity of shallow foundations.” *Foundation Engineering Handbook.* Ed. Winterkorn and Fang), Van Nostrand Reinhold, New York, NY, 121-147.

Vesic, A. S. 1977. *Design of Pile Foundation, Synthesis of Highway Practice No. 42*. National Cooperative Highway Research Program, Transportation Research Board, Washington, DC.

Vilar, O. and Carvalho, M. 2004. “Mechanical properties of municipal solid waste.” *ASTM Journal of Testing and Evaluation*, 32(6), 1–12.

Wan, C. F. and Fell, R. 2004. “Investigation of rate of erosion of soils in embankment dams.” *Journal of Geotechnical and Geoenvironmental Engineering*, 130(4), 373-380.

Weaver T.J. and Rollins, K.M. 2010. “Reduction factor for the unloading point method at clay sites.” *Journal of Geotechnical and Geoenvironmental Engineering*, 136(4), 643-646.

Wesley, L.D. 2009. “Behavior and Geotechnical Properties of Residual Soils and Allophane Clays,” *Works and Projects*, 6, 5-10.

Wesley, L.D. 2010. *Geotechnical Engineering in Residual Soils*. John Wiley, New York, NY.

Whitman, R. V. 1970. “Hydraulic fills to support structural loads.” *Journal of the Soil Mechanics and Foundations Division*, ASCE, 96(1), 23-47.

Whitman, R. V. 1991. “Seismic design of earth retaining structures.” *Proc. Second International Conference on Recent Advances in Geotechnical Earthquake Engineering and Soil Dynamics*, St. Louis, Missouri.

Wiles, T. T. 1988. *A Shale Durability Rating System Based on Shear strength.* Masters thesis, Univ. of Missouri-Rolla, Rolla, MO.

Wiss, J. F. 1981. “Construction vibrations: state-of-the-art.” *Journal of the Geotechnical Engineering Division*, 107(2), 167-181, ASCE, Reston, VA.

Wolff, T. F, Hassan, A., Khan, R., Ur-Rasul, I. and Miller, M. 2004. *Geotechnical Reliability of Dam and Levee Embankments, ERDC/GSL CR-04-1*, USACE, Washington D.C.

Wolosick, J. R. and Scott, R. F. 2012. “Design and applications for anchored earth retention systems.” Proc. ADSC IFCEE Geo-Construction Conference, San Antonion, TX, 55-75.

Wong, K. S. and Goh, A. T. C. 2002. “Basal heave stability for wide excavations.” *Geotechnical Aspects of Underground Construction in Soft Ground*. Kastner, Emeriault, Dias, and Guilloux, Eds., Specifique, Lyon.

Wood, J. H. 1973. *Earthquake-Induced Soil Pressures on Structures, Report EERL 73-05*. California Institute of Technology, Pasadena, CA.

Wyllie, D. C. 1999. *Foundations on Rock*, 2nd Ed., E & FN Spon, London, UK.

Wyllie, D. C. 2017. *Rock Slope Engineering: Civil Applications*, 5th Edition, CRC Press; New York, NY.

Wyllie, D. and Norrish, N. 1996. “Chapter 18 – Stabilization of rock slopes.” *Landslides: Investigation and Mitigation, Transportation Research Board Special Report Number 247*. National Research Council, Washington, D.C.

Xanthakos, P. P., Abramson, L. W., and Bruce, D. A. 1994. *Ground Control and Improvement*, Wiley.

Zelada, G. A. and Stephenson, R. W. 2000. “Design methods for auger CIP piles in compression.” *Proc. New Technological and Design Developments in Deep, Foundations, Geotechnical Special Publication 100*, 418-432, ASCE, Reston, VA.

Zhu, M. 2004. “Bearing capacity of strip footings on two-layer clay soil by finite element method.” *Proc. of ABAQUS Users' Conference*, Vol. 787.

Zola, S. P. and Boothe, P. M. 1960. “Design and construction of Navy's largest drydock.” *Journal of the Waterways and Harbors Division*, 86(1), 53-84.

This Page Intentionally Left Blank

APPENDIX B. VERIFICATION EXAMPLES

This appendix contains seven extended examples of the types of analyses presented in this manual, particularly from Chapters 4 to 7. The purpose of these examples is twofold. First, the examples provide the opportunity to present longer and more complete design calculations than is possible in the body of the manual. The second purpose is related to geotechnical software. Many designs are completed using software; however, the results can be difficult to verify. It is hoped that these examples will allow a user to verify their use of geotechnical software for relatively simple conditions prior to the application of such software to more complex design scenarios.

B-1 EXAMPLE 1 – CANTILEVER CUT WALL.

B-1.1 Description of the Problem.

A land development project requires a 15 ft vertical grade change in medium dense sandy soil. A reinforced concrete cantilever retaining wall has been selected to accomplish the grade change. A road will pass along the top of the wall that imposes a live load of 250 psf. The finished grade behind the wall will be approximately level and a drainage system will be incorporated behind the wall to avoid the development of water pressures acting on the wall. For frost considerations, the retaining wall must bear 3 ft below the final grade at the base of the wall.

B-1.2 Goals and Limitations of the Analysis.

The goal of this analysis is to size the geometry of the cantilever retaining wall for geotechnical stability considerations. Structural design of the wall and global stability analysis is outside the scope of this example. The geotechnical design of the wall will be approached using allowable stress design (ASD); however, the design checks can readily be applied within a Load and Resistance Factor Design (LRFD) framework. The analysis is approached using the following assumptions and performance requirements:

- The wall must have adequate resistance to overturning as evaluated by the eccentricity of the resultant force acting on the base of the wall. Since the wall is bearing on soil, the resultant force must be located within the middle third of the base of the wall.
- The wall must have a factor of safety against sliding on the foundation soil, F_{SL}, of at least 1.5.
- The wall must have a factor of safety against bearing capacity failure, F_{BC}, of at least 3.0.
- For structural considerations, the thickness of the top of the wall stem (t_2) is assumed to be equal to 1 ft, the thickness of the bottom of the wall stem (t_1) is assumed to be equal to 1.5 ft, and the thickness of the base of the wall (d) is

assumed to be equal to 2 ft. In this example, these thicknesses are considered to be appropriate for the type of concrete, grade of steel, steel area ratio, height of wall, and imposed forces.

- Passive resistance in front of the wall will be conservatively ignored in the stability calculations.
- For overturning and sliding checks, it is assumed that the traffic pressure does not act over the wall heel. For the check of bearing capacity, the traffic pressure is included. These assumptions increase the conservatism in the analyses.
- The lateral force imposed on the wall by the traffic pressure (P_{h1}) can be represented by an equivalent result force acting at half of the wall height, $0.5H$, as measured above the base of the wall.
- The horizontal component of the earth force (P_{h2}) is greater than zero. The vertical component of the earth force (P_v) is assumed toequal to zero. This is justified for translational wall movement by an assumption that an active wedge over the wall heel and the active wedge behind the wall heel move vertically together and therefore do not transfer shear force (Figure).
- The lateral earth force can be represented by an equivalent result force acting at one third of the wall height, $H/3$, as measured above the base of the wall.

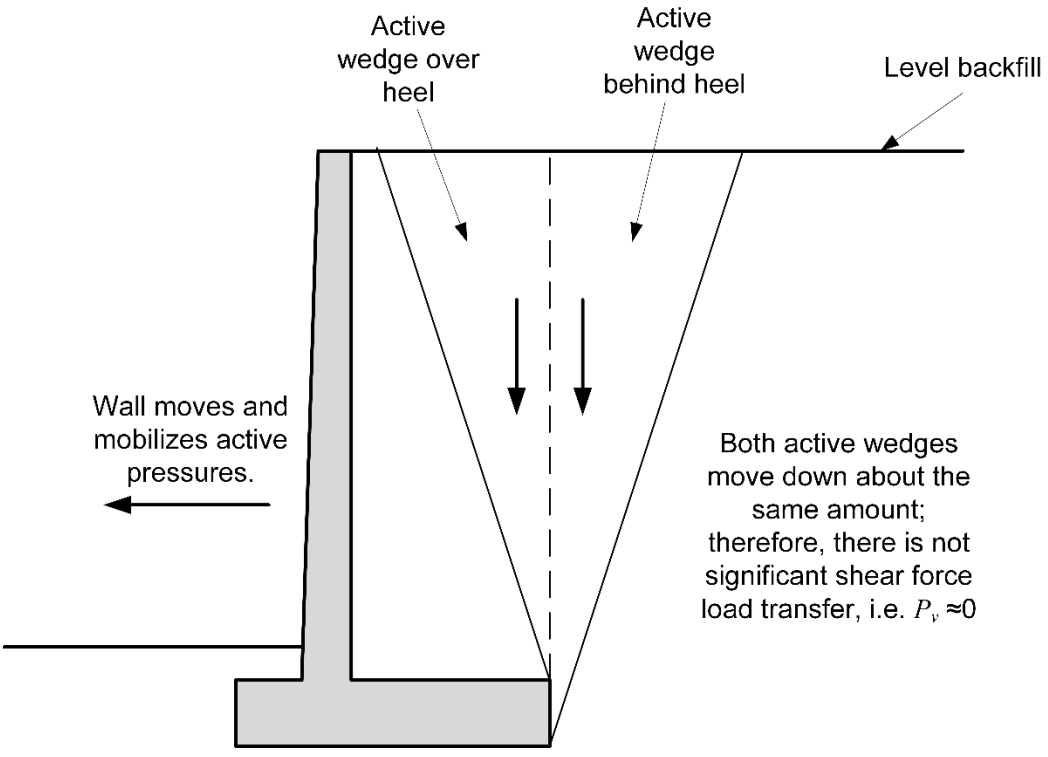

Figure B-1 Rationale for Assumption of No Vertical Earth Force

Based on these assumptions, the proposed cantilever retaining wall the geometry shown in Figure B-2. The unknown dimensions include: the width of the wall footing (B), the width of the heel (b_h), and the width of the toe (b_t). These dimensions will be determined by performing stability checks for overturning, sliding, and bearing capacity. These dimensions are related by:

$$B = b_t + t_1 + b_h .$$

If the width of the toe is assumed to be equal to 2 ft, the width of the footing becomes the only unknown since t_1 has been set equal to 1.5 ft for structural design reasons. The design process can be repeated using other assumptions regarding the wall geometry to determine which design makes the most efficient use of concrete.

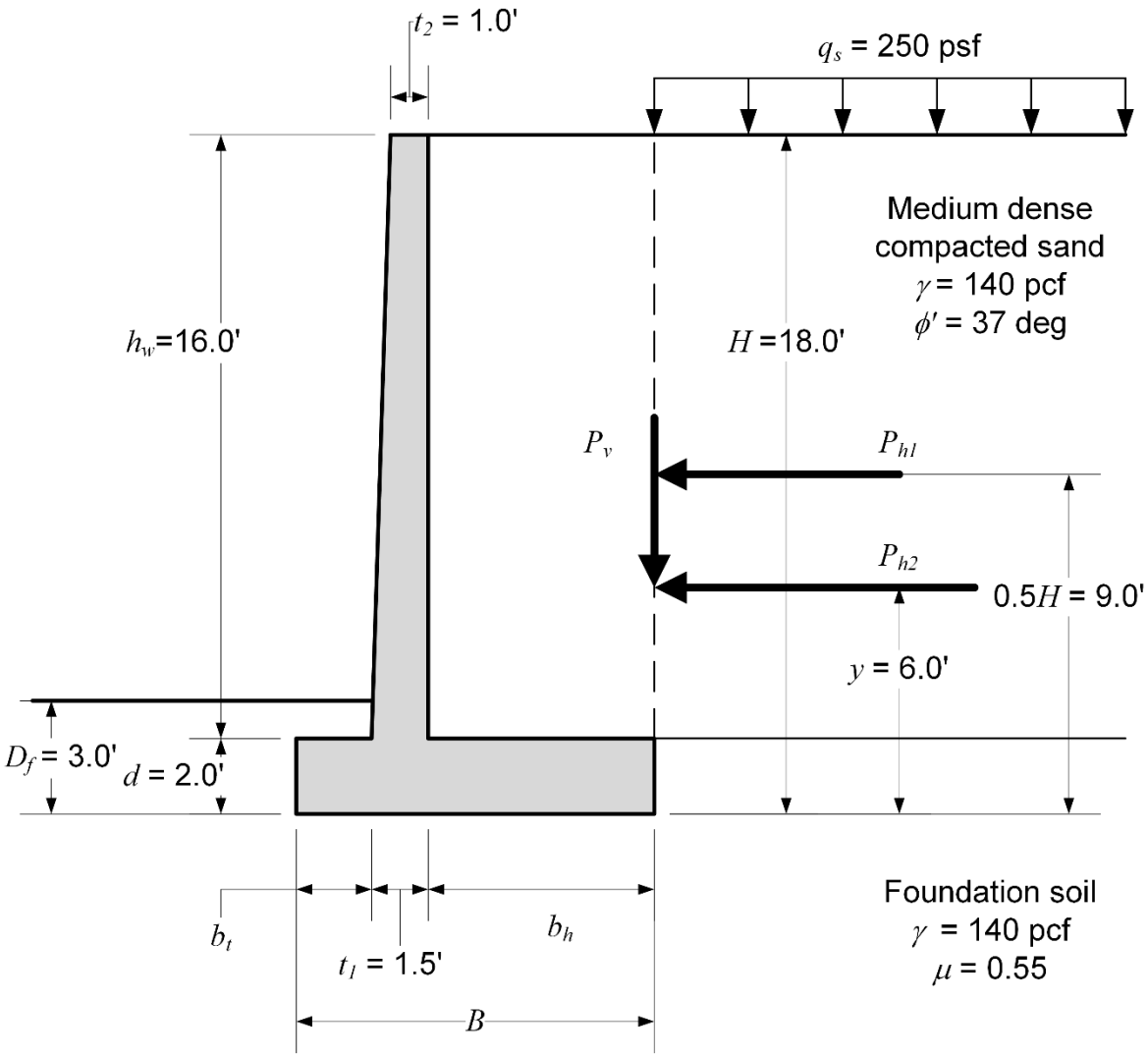

Figure B-2 Geometry of the Proposed Cantilever Retaining Wall

B-1.3 Evaluation of Forces and Moments.

The values of the lateral forces P_{h1} and P_{h2} depicted in Figure B-2 are determined assuming that the wall moves enough by sliding and/or rotation to mobilize the active condition. For the backfill having the properties given in Figure B-2, application of Rankine earth pressure theory produces a value for the active earth pressure coefficient equal to 0.25. It has already been assumed above that the vertical earth force, P_v, equals zero.

The backfill and a traffic pressure equal to 250 psf produce the following lateral forces per linear foot of wall:

$$P_{h1} = q_s K_A H = (250\,psf)(0.25)(18\,ft) = 1{,}125\,lb/ft$$

$$P_{h2} = 0.5 K_A \gamma H^2 = 0.5(0.25)(140\,pcf)(18\,ft)^2 = 5{,}670\,lb/ft$$

Assuming the unit weight of concrete is 150 pcf, the weight of the wall footing (W_f) per linear foot equals:

$$W_f = d \cdot \gamma_c \cdot B = (2\,ft)(150\,pcf)\,B = (300B)\,lb/ft$$

and the weight of the stem equals the sum of the weights of the uniform (W_{s1}) and tapered (W_{s2}) portions of the stem:

$$W_{s1} = t_2 \cdot h_w \cdot \gamma_c = (1\,ft)(16\,ft)(150\,pcf) = 2400\,lb/ft$$

$$W_{s2} = \frac{(t_1 - t_2)h_w}{2}\gamma_c = \frac{(1.5\,ft - 1\,ft)(16\,ft)}{2}(150\,pcf) = 600\,lb/ft\,.$$

The weight of the soil over the heel equals:

$$W_{bf} = h_w \cdot b_h \cdot \gamma = (16\,ft)(B - 3.5\,ft)(140\,pcf) = 2{,}240 \cdot (B - 3.5\,ft) = 2{,}240B - 4560\,(lb/ft)\,.$$

The weight of the soil over the toe equals:

$$W_{ff} = (D_f - d) \cdot b_t \cdot \gamma = (3\,ft - 2\,ft)(2\,ft)(140\,pcf) = 280\,lb/ft\,.$$

Vertical equilibrium requires that the vertical component of the reaction on the base of the wall (R) equals:

$$R = W_f + W_{s1} + W_{s2} + W_{bf} + W_{ff} + E_v = 2{,}540 \cdot B - 4560\ (lb/ft)\,.$$

Table B-1 summarizes these forces, their moment arms with respect to rotation about the toe of the wall, and moments. The moment arm of the reaction force (x_0) is defined in Figure B-3.

The primary task at this point in the design is the selection of B to meet the overturning, sliding, and bearing capacity criteria. Two approaches can be taken. The width can be selected by trial and error, realizing that B is typically 50 to 70% of H. It is also possible to derive equations that can be solved for B based on the design criteria. Both will be illustrated in this example.

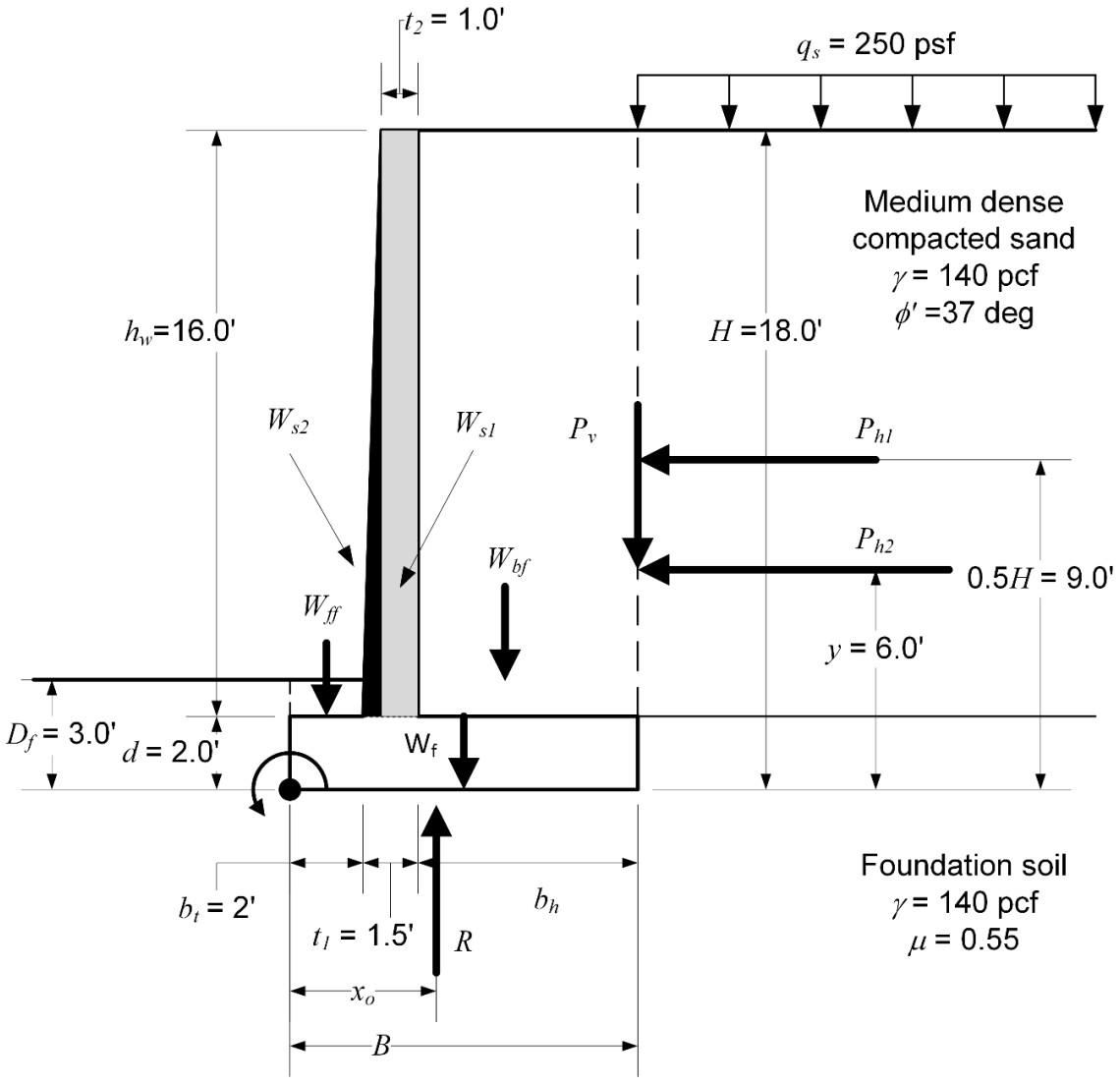

Figure B-3 Forces for Wall Stability Analysis

B-1.4 Overturning.

Using the forces and moments provided in Table B-1, the moment about the toe equals

$$\sum M_{toe} = 48985 - 1270 \cdot B^2 + 2540 \cdot B \cdot x_0 - 4560 \cdot x_0$$

The wall is acceptable with respect to overturning when R is located within the middle third of the base of the wall. The minimum value of x_0 from the toe that satisfies this requirement is equal to $B/3$. Substituting $B/3$ for x_0 enables the minimum width that satisfies the overturning requirement to be found by satisfying moment equilibrium:

$$\sum 0 = 48985 - 1520 \cdot B - 423.33 \cdot B^2$$

Solving this quadratic equation for B yields a minimum width equal to 9.11 ft.

Table B-1 Forces and Moments for Wall Stability Analysis

Force ID	Force (lb/ft)	Moment Arm Relative to the Wall Toe (ft)	Moment (ft-lb)
P_{h1}	1125	9	10125
P_{h2}	5670	6	34020
W_f	300(B)	-B/2	-150·B^2
W_{s1}	2,400	-(b_t+(t_1-t_2)+0.5t_2) = -3	-7200
W_{s2}	600	-(b_t+2(t_1-t_2)/3) = -2.33	-1400
W_{bf}	2240(B-3.5)	-(B+b_t+t_1)/2 = -(B+3.5)/2	-1120·(B^2-12.25)
W_{ff}	280	-b_t/2 = -1	-280
R	2540(B)-4,560	x_0	x_0·(2,540·B-4560)

B-1.5 Sliding

The sliding check is performed by comparing the mobilized horizontal shear load on the base of the wall (P_H) to the available shear resistance (T) as shown in Figure 4-27. In this case, the mobilized shear load equals:

$$P_H = P_{h1} + P_{h2} = 6795\, lb/ft$$

and the available resisting shear force equals:

$$T = R \cdot \tan\delta = \left(2540 \cdot B - 4560\right)\left(0.55\right) = 1397 \cdot B - 2508\ \left(lb/ft\right).$$

The factor of safety against sliding equals:

$$F_{SL} = \frac{T}{P_H} = \frac{1397 \cdot B - 2508}{6795} = 0.2056 \cdot B - 0.3691.$$

If F_{SL} is set equal to 1.5, this equation can be solved for B equal to 9.09.

B-1.6 Bearing capacity

Unlike the checks of overturning and sliding, it is conservative to include the surcharge over the heel of the wall, if this is possible to occur, in the bearing capacity check. The inclusion of the surcharge over the heel changes the forces W_{bf} and R.

The weight of the soil and the surcharge over the heel equals

$$W_{bf+q} = b_h \cdot \left(h_w \cdot \gamma + q_s\right) = \left(B - 3.5\,ft\right)\left[\left(16\,ft\right)\left(140\,pcf\right) + 250\,psf\right] = 2490\left(B - 3.5\,ft\right)\left(lb/ft\right)$$

The moment arm associated with W_{bf+q} is the same as W_{bf} and is equal to $-(B+3.5)/2$. The moment produced by W_{bf+q} is equal to $-1245(B^2-12.25)$.

The reaction on the base of the wall with the addition of the surcharge over the heel equals:

$$R = W_f + W_{s1} + W_{s2} + W_{bf+q} + W_{ff} + E_v = 2{,}790 \cdot B - 5435\ \left(lb/ft\right)$$

The moment produced by R is equal to $x_0 \cdot (2790 \cdot B - 5435)$.

Using the forces and moments provided in Table B-1, substituting W_{bf+q} and R that include the surcharge over the toe, the moment about the toe equals

$$\sum M_{toe} = 50{,}516 - 1395 \cdot B^2 + 2790 \cdot B \cdot x_0 - 5435 \cdot x_0$$

Moment equilibrium requires that

$$x_0 = \frac{1395 \cdot B^2 - 50{,}516}{2790 \cdot B - 5435}$$

where the value of x_0 will be found using bearing capacity theory.

The Meyerhof method was selected for the analysis of bearing capacity. The backfill loads cause the pressure on the base of the foundation to be eccentric and inclined. The uniform applied bearing pressure using the equivalent footing approach is:

$$q_{gross} = \frac{R}{2x_0} = \frac{2790 \cdot B - 5435}{2x_0}.$$

The load inclination can be found based on the normal and shear forces on the base,

$$\theta = \tan^{-1}\left(\frac{P_H}{R}\right) = \tan^{-1}\left(\frac{6795}{2790 \cdot B - 5435}\right)$$

For soil with a friction angle of 37 degrees, the Meyerhof bearing capacity factors are N_q = 42.92 and N_γ = 53.27. The inclination factors are found according to:

$$i_q = \left(1-\theta/90\right)^2 \text{ and } i_\gamma = \left(1-\theta/\phi'\right)^2$$

The bearing capacity for the foundation with the inclined load is found as:

$$q_{ult} = D_f \cdot \gamma \cdot N_q \cdot i_q + 0.5\left(2x_0\right) \cdot \gamma \cdot N_\gamma \cdot i_\gamma = \left(3\,ft\right)\left(140\,pcf\right)\left(42.92\right)i_q + x_0\left(140\,pcf\right)\left(53.27\right)i_\gamma .$$

Substituting known parameter values and dividing q_{ult} by F_{BC} of 3.0 gives the allowable bearing pressure:

$$q_{allow} = 6009 \cdot \left(1-\theta/90\right)^2 + 2486 \cdot x_0 \cdot \left(1-\theta/\phi'\right)^2$$

Setting q_{gross} equal to q_{allow} and solving for B results in:

$$B = 1.782x_0^2 \cdot \left(1-\theta/\phi'\right)^2 + 4.308x_0 \cdot \left(1-\theta/90\right)^2 + 1.948$$

Trial widths (B_{trial}) can be selected and used to calculate x_0 and θ. These can then be used to calculate B. An iterative process or spreadsheet can be used to the solution where B = B_{trial}. This solution technique results in B equal to 7.68 ft as shown in Table B-2 and in Figure B-4.

Table B-2 Implicit Solution for Footing Width with Desired F_{BC}

Assumed B_{trial} (ft)	Calculated based on B_{trial}		Resulting B_{calc} (ft)	Difference
	x_0 (ft)	θ (deg)		
7.50	1.805	23.686	6.920	-0.580
7.55	1.856	23.497	7.130	-0.420
7.60	1.906	23.312	7.343	-0.257
7.65	1.956	23.129	7.559	-0.091
7.70	2.006	22.949	7.779	0.079
7.75	2.055	22.771	8.002	0.252
7.80	2.104	22.596	8.228	0.428
7.85	2.153	22.424	8.458	0.608
7.90	2.201	22.254	8.691	0.791
7.95	2.248	22.086	8.927	0.977
8.00	2.296	21.921	9.167	1.167
Using Solver				
7.68	1.983	23.032	7.677	0.000

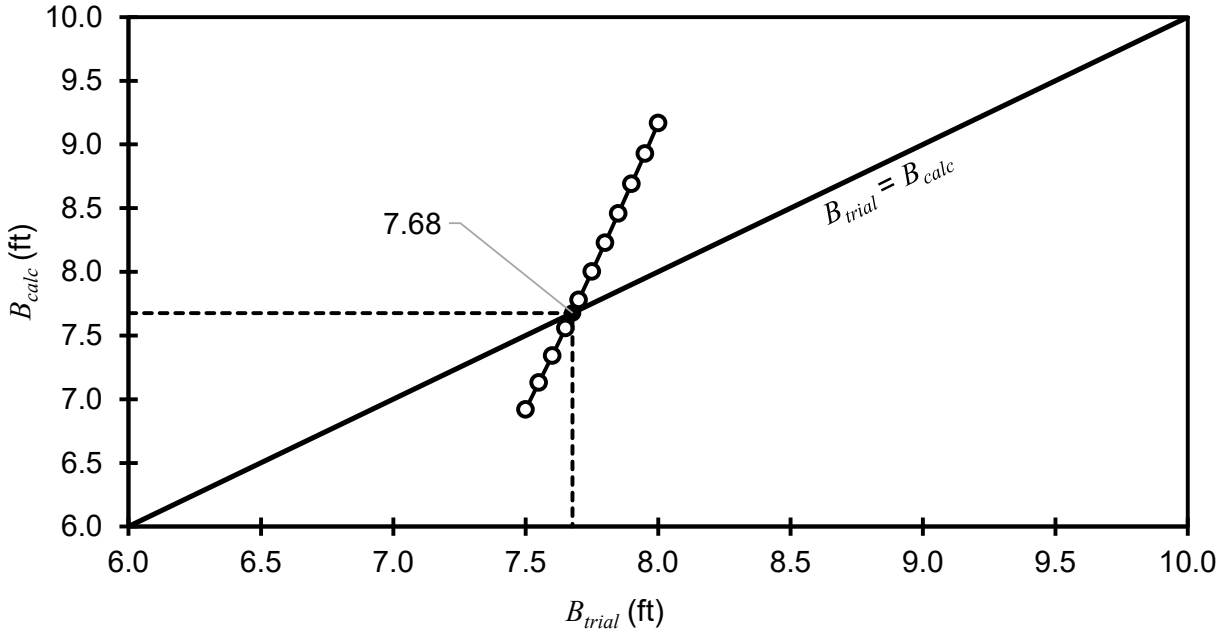

Figure B-4 Graphical Implicit Solution for Footing with Desired F_{BC}

B-1.7 Conclusions from the Analysis.

Table B-3 summarizes the minimum footing widths that meet the stability requirements with respect to overturning, sliding, and bearing capacity. This analysis shows that the footing width is controlled by overturning stability in this case.

Table B-3 Summary of Minimum Footing Widths Meeting Stability Requirements

Stability check	Required B (ft)
Overturning (x_0=B/3)	9.11
Sliding (F_{SL} = 1.5)	9.09
Bearing capacity (F_{BC} = 3)	7.68

Based on these stability checks, a design footing width equal to 9.5 feet is satisfactory.

Table B-4 provides the stability checks using the design value of B equal to 9.5 ft. Since the minimum required widths for overturning and sliding are close, both the overturning check and sliding checks are close to the minimum requirements for the design value of B. However, the design value of B is considerably greater than the minimum required value of 7.68 ft for bearing capacity, which gives the expected result of a factor of safety that significantly exceeds 3.0.

Table B-4 Summary of Stability Checks for Example 1

Stability check for B = 9.5 ft	Outcome
Overturning	$F_{SL} = 1.58 > 1.5$
Sliding	$x_0/B = 0.35 > 1/3$
Bearing capacity	$F_{BC} = 6.35 > 3$

B-1.8 Additional Comments on Overturning Factor of Safety.

Overturning resistance can also be checked using a factor of safety for overturning, F_{OT}, defined as the ratio of stabilizing moments to destabilizing moments about the toe of the wall. Referring to Table B-1, the absolute value of the moments having a negative sign according to the adopted sign convention are stabilizing moments that are located in the numerator of the factor of safety calculation. The moments in Table B-1 having a positive sign are destabilizing moments that are located in the denominator of the factor of safety calculation. Note that the moment from R is neglected in this calculation as:

$$F_{OT} = \frac{\text{Resisting moments}}{\text{Driving moments}} = \frac{1270 \cdot B^2 - 4840}{44145} = 2.49$$

For the design base width of 9.5 ft, F_{OT} is 2.49. It is instructive to consider how this factor of safety interacts with the design criterion requiring R to be in the middle third of the footing base. Recognizing that the resultant vertical force acting on the base of the wall is a destabilizing moment, the state of limit equilibrium corresponds to the resultant being located at the toe of the wall, i.e. x_0 = 0, as shown in Figure B-5.

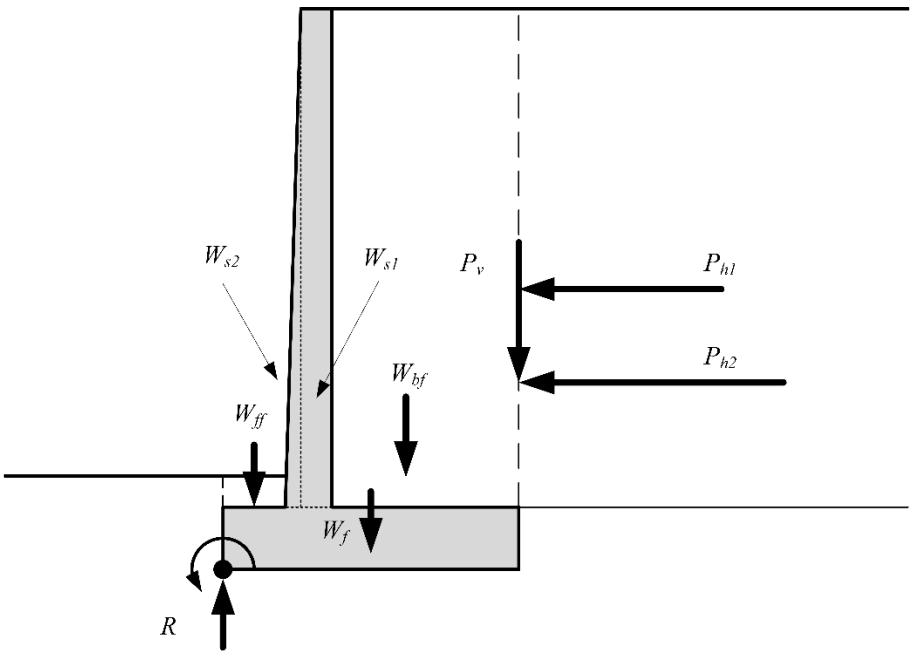

Figure B-5 Retaining Wall Conditions with F_{OT} = 1

For this condition with x_0 = 0 ft, the wall will have F_{OT} = 1. For this example, a footing having a width of 6.21 ft corresponds to F_{OT} = 1, which is found by solving:

$$\sum M_{toe} = 48{,}985 - 1270 \cdot B^2 + 2540 \cdot B \cdot x_0 - 4560 \cdot x_0 = 0$$
$$48{,}985 = 1270 \cdot B^2$$

The position of the reaction is related to F_{OT} according to

$$x_0 = a\left(\frac{W}{W + P_v}\right)\left(1 - \frac{1}{F_{OT}}\right) \quad \text{(xx)}$$

where W equals the sum of W_{ff}, W_f, W_{bf}, W_{s1}, and W_{s2} and a is the moment arm for W found by dividing the sum of the moments produced by wall and soil over the heel by the sum of the weights of the wall and soil over the heel. For the current example, E_v = 0 and a equals 5.61 resulting in:

$$x_0 = 5.61\left(1 - 1/2.49\right) = 3.36$$

For F_{OT} equal to 2.49, x_0 = 3.36 and x_0/B = 0.353.

B-2 EXAMPLE 2 – ANCHORED CUT WALL.

B-2.1 Description of the Problem.

An anchored bulkhead is needed for a land reclamation project that will provide a landside elevation that is 24 ft higher than the dredge line on the waterside (Figure B-6). The bulkhead will be anchored using a single row of anchors. The anchors will consist of horizontal steel tierods spaced every 6 ft and connected to a continuous concrete deadman located behind the bulkhead. The tierod elevation is established 1-ft above the water elevation so the tierod can be placed in the dry.

The site is sandy and dredged onsite soils will be used as fill. Due to tidal effects, the waterside water elevation is to be considered 2 ft below the landside water elevation. Figure B-6 provides relevant material properties, including the interface friction angle between the soil and sheetpile, δ.

During the service life of the project, industrial activities will impose ground pressures that can be modeled as a uniform surcharge equal to 500 psf.

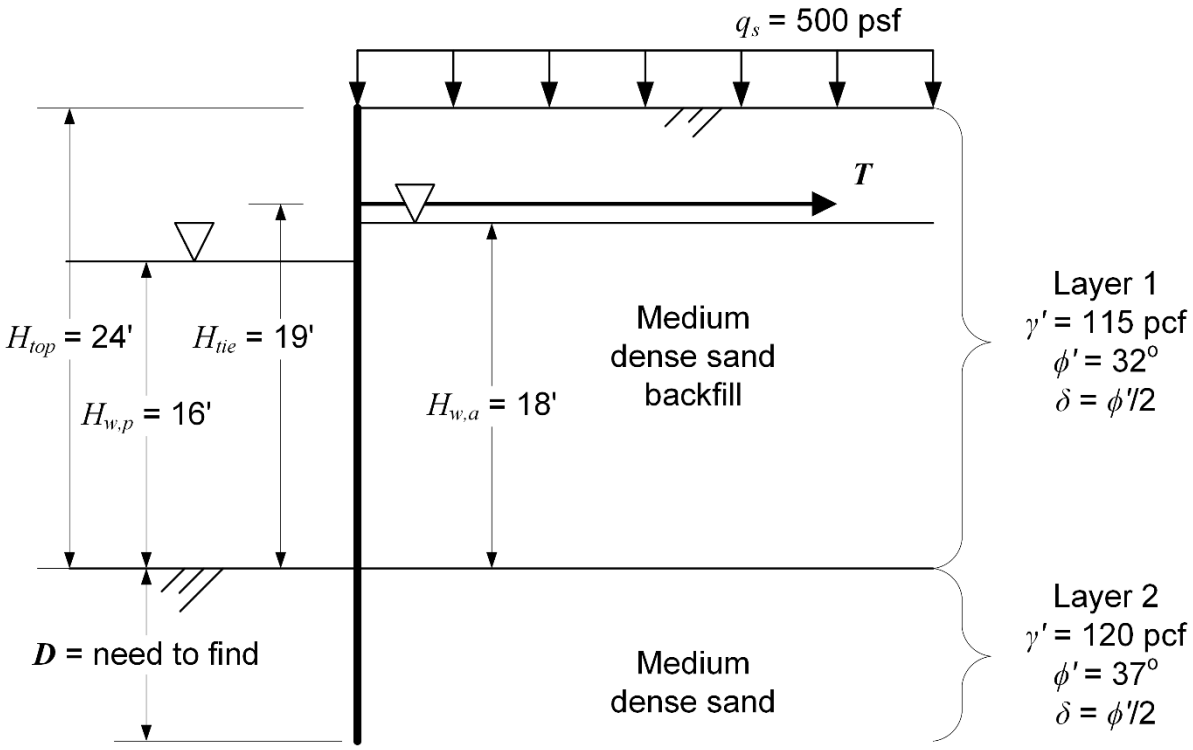

Figure B-6 Proposed Anchored Bulkhead in Sand

B-2.2 Goals and Limitations of the Analysis.

The goals of this analysis are to determine an appropriate steel sheetpile section, minimum embedment of the sheetpile, and size of the continuous anchor needed to provide adequate resistance. The Free Earth Support (FES) Method is applied to this example with the following assumptions and performance requirements:

- Allowable stress design will be applied using factored strengths for the evaluation of passive resistance of the embedded sheetpile and deadman anchor. A factor of safety equal to 2.0 is applied to determine the available resistance. This factor of safety accounts for typical uncertainty and variability with respect to soil properties as well the lateral displacements required to mobilize resistance.
- The sheetpile embedment determined by moment equilibrium calculations will be increased by 20% to account for the potential for scour and future dredging.
- Log spiral earth pressure theory is applied to estimate passive resistance while Rankine earth pressure theory is applied to estimate active pressures.
- This analysis ignores the reduction of the sheetpile section due to corrosion over the service life of the bulkhead.
- The selection of an acceptable tierod section, connections, turnbuckles, and wales are important design aspects that are not included in this example.

B-2.3 Calculation of Lateral Pressures and Forces.

Table B-5 summarizes the active and passive earth pressure coefficients used in the analysis. Because Rankine theory is used for active pressures and the ground surface behind the bulkhead is level, there is no vertical component to the active pressure. Therefore, the coefficient of horizontal active earth pressure ($K_{A,h}$) is equal to K_A. Because log spiral earth pressure theory is used for passive pressure and the interface friction angle is greater than zero, there is a vertical component to the passive pressure and the coefficient of horizontal passive earth pressure coefficient ($K_{P,h}$) must be found.

Table B-5 Earth Pressure Coefficients Used in the Design

Soil Layer	ϕ' (deg)	Rankine Active, K_A	Factored Friction Angles		Factored Passive Resistance
			ϕ'^* (deg)	δ^* (deg)	$K_{P,h}$
		$K_A = \frac{1-\sin\phi'}{1+\sin\phi'}$	$\phi'^* = \tan^{-1}\left(\frac{\tan\phi'}{F}\right)$	$\delta^* = \phi'^*\left(\frac{\delta}{\phi'}\right)$	$K_{P,h} = K_P\cos(\delta^*)$
1	32	0.31	17.4	8.7	2.1
2	37	0.25	20.6	10.3	2.4
Find log-spiral K_P using Equation 4-12: $\ln K_P = \ln\left(\frac{1+\sin\phi'^*}{1-\sin\phi'^*}\right)\left[1.443\left(\frac{\delta}{\phi'}\right)\sin\phi'^*+1\right]$					

Figure B-7 shows the distribution of earth pressures and net water pressure on both sides of the sheetpile. The pressures are divided into simple triangular and rectangular shapes to simplify the calculation of forces and moments. Table B-6 presents a summary of the pressure calculations. The vertical stresses listed in the table equal the incremental change in vertical effective stress at the top and bottom of the numbered shape that form the pressure distribution, $\Delta\sigma'_{v,top}$ and $\Delta\sigma'_{v,bot}$, respectively. The horizontal effective stresses at the top and bottom of each shape, $\Delta\sigma'_{h,top}$ and $\Delta\sigma'_{h,bot}$, respectively, are found by multiplying by the appropriate value of K_A or $K_{P,h}$.

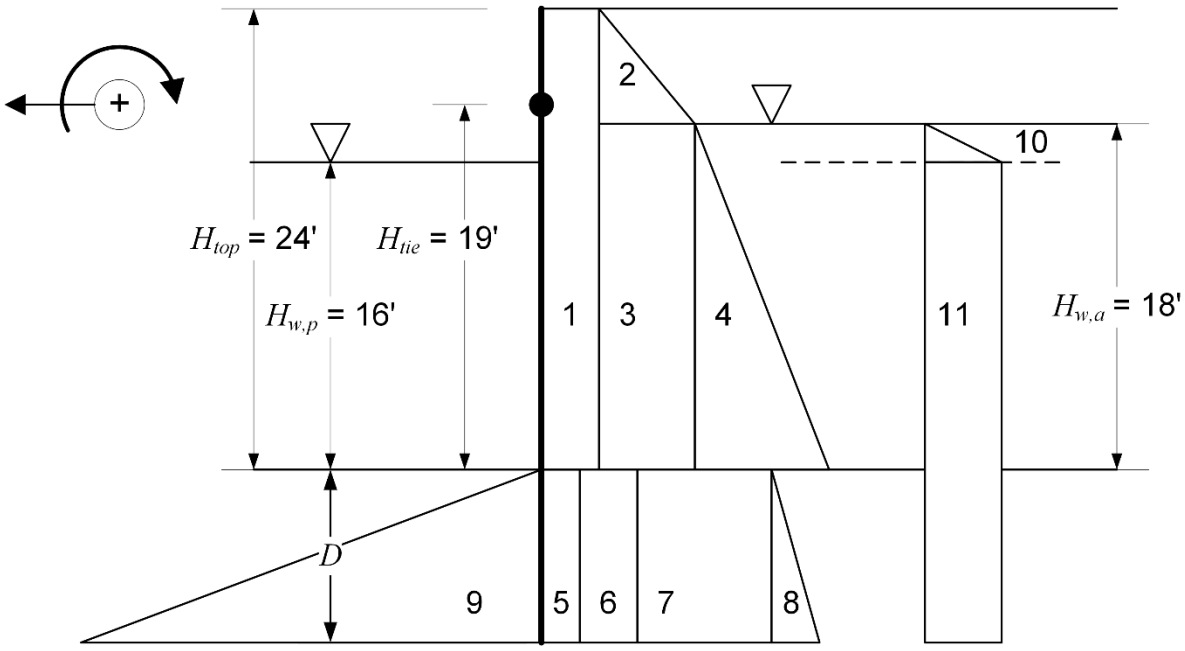

Figure B-7 Distribution of Earth and Water Pressures on the Sheetpile

Table B-6 Summary of Lateral Pressure and Force Calculations

Force ID	$\Delta\sigma'_{v,top}$ (psf)	$\Delta\sigma'_{v,bot}$ (psf)	K[A]	$\Delta\sigma'_{h,top}$ (psf)	$\Delta\sigma'_{h,bot}$ (psf)	h_{shape} (ft)	ΔP (lb/ft)
1	500	500	0.31	155	155	24	3720
2	0	690	0.31	0	214	6	642
3	690	690	0.31	214	214	18	3850
4	0	947	0.31	0	294	18	2642
5	500	500	0.25	125	125	D	$125 \cdot D$
6	690	690	0.25	172	172	D	$172 \cdot D$
7	947	947	0.25	237	237	D	$237 \cdot D$
8	0	$57.6(D)$	0.25	0	$14.4(D)$	D	$7.2 \cdot D^2$
9	0	$57.6(D)$	-2.4	0	$-138(D)$	D	$-69.1 \cdot D^2$
10	0	125	1	0	125	2	125
11	125	125	1	125	125	$16+D$	$125 \cdot (D+16)$

[A] The sign applied to K establishes the direction of the force as defined in Figure.

The lateral force due to each numbered shape that forms the lateral pressure distribution is found by:

$$\Delta P = \left(\frac{\Delta\sigma'_{h,top} + \Delta\sigma'_{h,bot}}{2} \right) \cdot h_{shape}$$

where:
h_{shape} = the height of each numbered shape.

B-2.4 Embedment of Sheet Pile and Tie Rod Force.

The embedment of the sheetpile is found by computing moment equilibrium about the elevation of the tierod. Referring to the numbered shapes in Figure B-7 and Table B-6, the elevation of the centroid of each component, y, relative to the dredge line is listed in Table B-7. Calculating the centroid as a separate step simplifies making changes to the tierod elevation in the design. The moment arm about the tierod elevation is equal to the difference between the elevation of the tierod and the elevation of the centroid for each component of the lateral force, i.e. H_t - y. The moment about the tierod elevation is found by multiplying the force listed in Table B-6 by the moment arm. The embedded depth of the sheetpile is found by summing moments and satisfying moment equilibrium. Calculations can be performed using an iterative guess and check technique or application of an implicit solving algorithm in a spreadsheet, e.g. Solver macro in MS Excel. Figure B-8 shows the sum of moments versus sheetpile embedment.

Table B-7 Summary of Moment Calculations

Force ID	Elevation of Centroid Relative to Dredge Line, y (ft)	Moment Arm at Tierod Elevation (ft)	Moment (ft-lbs)
1	H_{top} / 2 = 12	$H_t - y$ = 19-12 = 7	26,040
2	$H_{w,a}$ + (H_{top} - $H_{w,a}$) / 3 = 20	-1	-642
3	$H_{w,a}$ / 2 = 9	10	38,500
4	$H_{w,a}$ / 3 = 6	13	34,346
5	-D / 2	19+D / 2	125(D)(19+D/2)
6	-D / 2	19+D / 2	172(D)(19+D/2)
7	-D / 2	19+D / 2	237(D)(19+D/2)
8	-(2/3)D	19+(2/3) D	7.2(D^2)(19+(2/3)D)
9	-(2/3)D	19+(2/3) D	-69.1(D^2)(19+(2/3)D)
10	$H_{w,p}$ + ($H_{w,a}$ - $H_{w,3}$)/3 = 16.67	2.33	291
11	($H_{w,p}$ + D) / 2 - D =(16 + D) / 2 - D	19+D-(16+D)/2	125(D+16)(19+D-(16+D)/2)

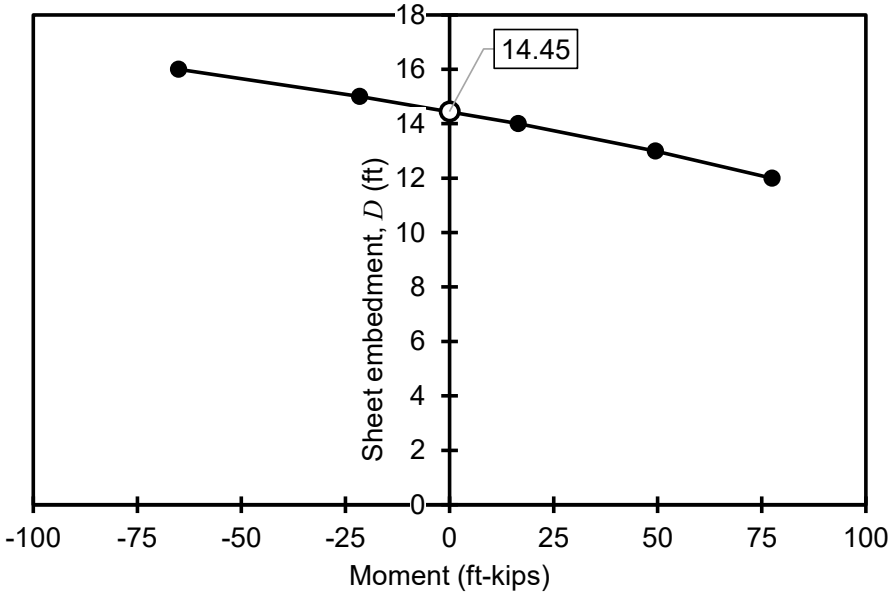

Figure B-8 Sum of Moments versus Trial Values of Sheet Pile Embedment

The calculated sheetpile embedment for this example equals 14.45 ft. This value will be used in subsequent calculation steps; however, a design value is found by increasing the embedment by 20% and rounding up to nearest whole foot. In this case, the design embedment is equal to 18 ft.

With the embedment of the sheetpile known, the magnitude of tierod force is found by satisfying horizontal force equilibrium. This calculation is performed using the embedment equal to 14.45 ft. For the sign convention defined in Figure B-7, the tierod force is equal to -9,568 lb/ft. This value will be used to design the sheeting and deadman in subsequent calculation steps. However, a value for designing the connection of the tierod to the sheetpile and deadman is found by increasing the tierod force by 20% and rounding up to nearest 100 lb/ft. In this case, the connections of the tierod to the sheetpile and deadman should be designed for 11,400 lb/ft. The tierod itself may be designed using the calculated value, with appropriate rounding, e.g. 9,600 lb/ft. For a tierod spacing of 6 ft, the tierod should be designed for a force equal to 58 kips, while the tierod connections should be designed for a force equal to 69 kips.

B-2.5 Selection of Sheet Pile Section.

This section provides the steps need to select an appropriate sheet pile section. The process involves identifying the location of the maximum moment, solving for the maximum moment, applying Rowe's moment reduction described in Section 4-7.2, and selecting a sheet with an adequate section modulus.

B-2.6 Location of Maximum Moment.

The elevation of the maximum moment above the dredge line is found by solving for the elevation of zero shear force. The location of zero shear force is found by integrating the pressure distribution in the direction of the dredge line starting from the top of the bulkhead. The shaded portion of Figure B-9 graphically shows the integration of the pressure distribution from the top of the bulkhead to the elevation of zero shear force, $h_{V=0}$ = 4.57 ft. Figure B-10 plots shear force against height above the dredge line.

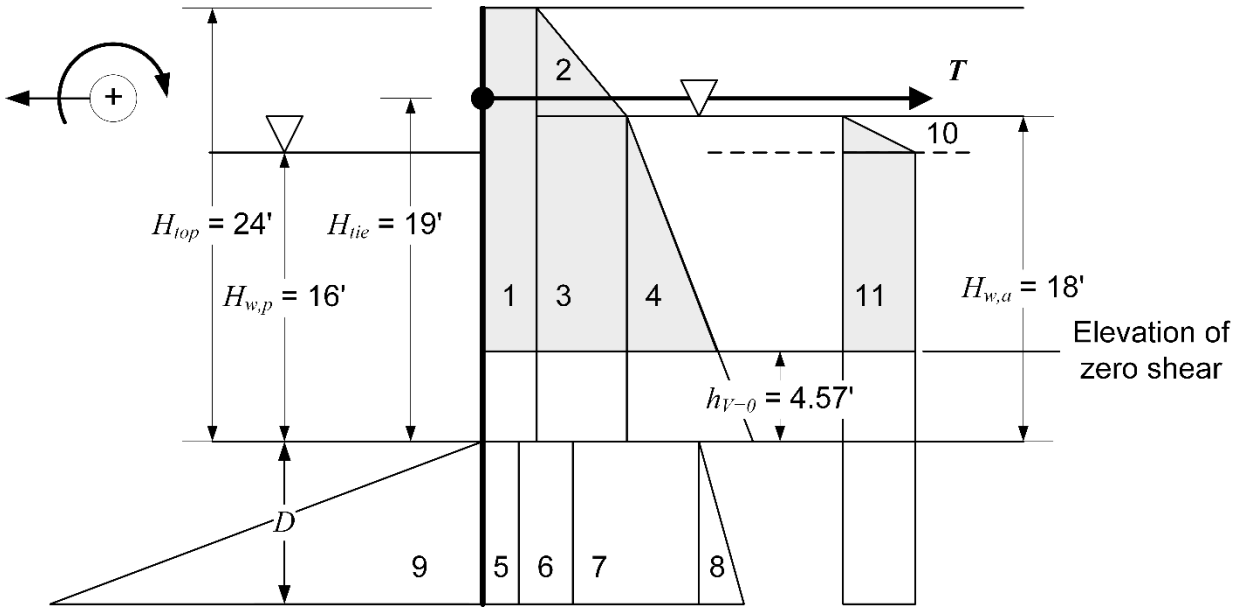

Figure B-9 Integration of Pressure Distribution to Locate Elevation of Zero Shear Force

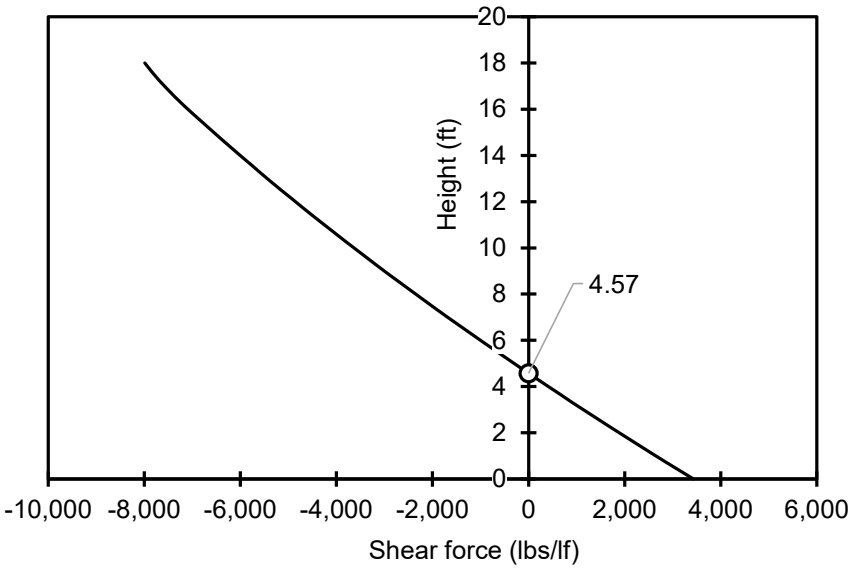

Figure B-10 Shear Force Versus Height Above the Dredge Line

The maximum bending moment in the sheetpile occurs at the elevation of zero shear, $h_{V=0}$, calculated in the previous section. Table B-8 summarizes the integrated loads to the elevation of zero shear as indicated by the shaded region in Figure B-9, the elevation of the centroid of each shaded area component, the moment arm relative to $h_{V=0}$, and the moment. The sum of the components of moment equals the maximum moment, M_{max}, equal to 63.4 ft-kips.

Table B-8 Calculation of the Maximum Bending Moment in the Sheet Pile

Force ID	Force (lb)	Elevation of Centroid Relative to Dredge Line, y (ft)	Moment Arm at $h_{V=0}$ (ft)	Moment (ft-lb)
Tierod	-9,568	19.0	-14.4	138,073
1	3,012	14.3	-9.7	-29,261
2	642	20.0	-15.4	-9,902
3	2,873	11.3	-6.7	-19,292
4	1,471	9.0	-4.5	-6,584
10	125	16.7	-12.1	-1,510
11	1,427	10.3	-5.7	-8,154
			Sum =	63,370

The steel sheetpile selected for the anchored bulkhead must have an elastic section modulus, S, that will keep the steel sufficiently below yield when subjected to the anticipated bending moment. Recall that the bending moment divided by the section modulus gives the bending stress. For this example, a PZ-22 section is selected for consideration. The PZ-22 section has the properties listed in Table B-9.

Table B-9 Properties of the PZ-22 Hot Rolled Steel Sheet Pile

Property	**Value**
Width of sheet	22 in.
Section modulus, S, per sheet	33.1 in^3
Section modulus, S, per foot	18.1 in^3
Moment of interia, I, per sheet	154.7 in^4
Moment of interia, I, per foot	84.4 in^4
Young's Modulus, E	29,000 ksi
Yield stress, f_s	38.5 ksi

Since the sheetpile is flexible and the soil is compressible, the maximum moment is expected to be less than the value calculated in the previous section. The method proposed by Rowe (1952) in Figure 4-36 reduces the maximum calculated moment to a value that is expected for the given stiffness of the steel section and soil. The reduction is based on the flexibility number, which is:

$$\rho = \frac{\left(H_{top} + D\right)^4}{E \cdot I} = \frac{\left[\left(\frac{12in}{1ft}\right)\left(24ft + 14.45ft\right)\right]^4}{\left(29,000ksi\right)\left(84.4in^4\right)} = 18.52\frac{in}{lb} \text{ per foot}$$

For medium dense sand, the moment reduction proposed by Rowe (1952) is given by

$$\frac{M_{design}}{M_{max}} = \frac{2.03}{\ln \rho} - 0.076 = \frac{2.03}{\ln\left(18.52\right)} - 0.076 = 0.62$$

Applying the moment reduction to the maximum moment calculated in the previous section yields a design moment equal to

$$M_{design} = M_{max}\left(\frac{M_{design}}{M_{max}}\right) = 63.4ft - k\left(0.62\right) = 39.3ft - k$$

The required section modulus per linear foot of bulkhead is equal to

$$S_{req} = \frac{M_{design}}{f_s} = \frac{39.3ft - k\left(12in/ft\right)}{38.5ksi} = 12.25in^3 \text{ per foot}$$

The PZ-22 sheetpile is an acceptable choice since the provided S equals 18.1 in^3/ft, which exceeds the required value of 12.25 in^3. A lighter-duty sheetpile section should be checked in cases where the section modulus of the candidate sheetpile significantly exceeds the required value. As stated above, this analysis ignores section loss due to corrosion over the service life of the bulkhead.

B-2.7 Design of Continuous Anchor.

Since this particular land reclamation project imposes no spatial constraints behind the bulkhead, the anchor can be placed far enough behind the bulkhead so that the active zone behind bulkhead does not interfere with the passive zone in front of the anchor. As shown in Figure B-11, the anchor should be placed at least 56 ft behind the sheetpile in order to have the potential to develop full resistance (see also Figure 4-39). Note that the inclinations of the active wedge and stable backslope are based on Layer 1 which has the lower friction angle. In Figure B-11, Construction Line 1 defines the active wedge behind the sheetpile, Construction Line 2 defines the inclination of a stable backslope, and Construction Line 3 defines the inclination of passive wedge in front of the anchor.

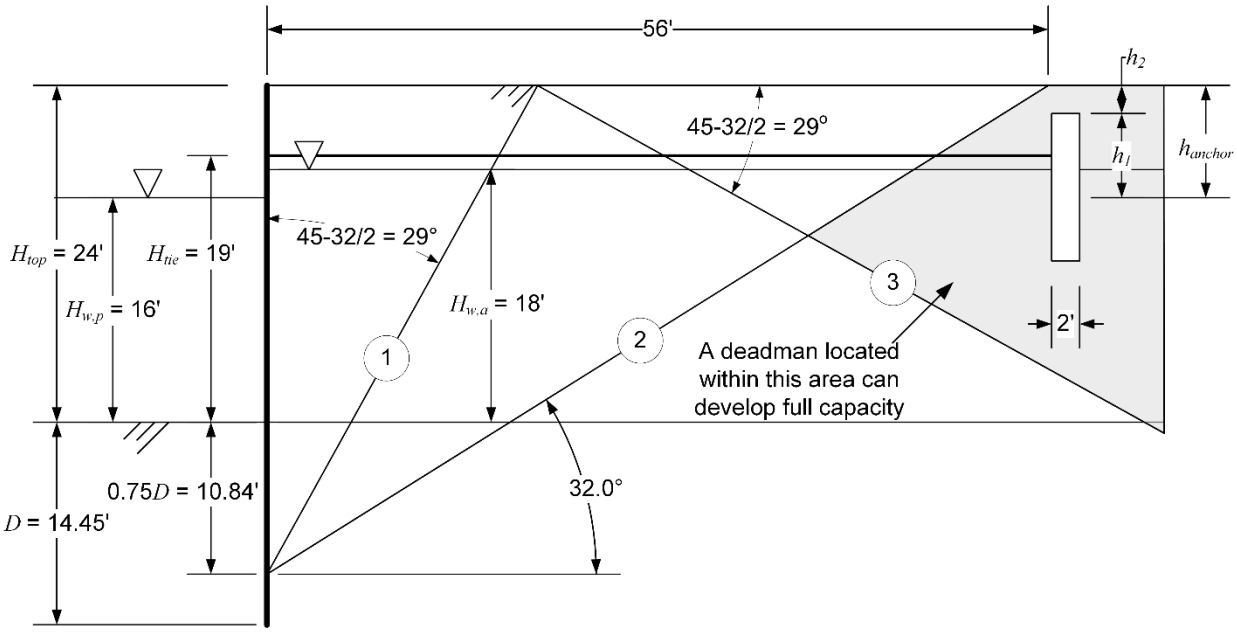

Figure B-11 Location of the Continuous Anchor

Since the deadman is embedded in Layer 1, the unfactored value of K_A of 0.31 (Table B-5) will be used to evaluate active pressure on the opposite side of the tierod force and the factored value of $K_{P,h}$ equal to 2.1 will be used to estimate passive resistance based on an applied factor of safety equal to 2.0 on the shear strength of the soil.

Assume that the anchor is 2 ft thick and made of reinforced concrete. In a complete design, this assumption would be checked as part of the structural design of the anchor. The mobilized vertical force due to interface friction between the anchor and soil is limited by the weight of the anchor. For the Layer 1 sand, the mobilized interface friction angle is limited according Duncan and Mokwa (2001) by:

$$\delta_{mob} = \min\begin{Bmatrix} (\delta/\phi')\cdot\phi'^{*} \\ \tan^{-1}(W_a/T) \end{Bmatrix} = \min\begin{Bmatrix} 8.7° \\ \tan^{-1}\left(\dfrac{(150\,pcf)(2\,ft)\cdot h_1}{9600\,lb/ft}\right) \end{Bmatrix}$$

where
W_a = weight of the concrete anchor per foot and
T = design tierod force per foot.

The minimum anchor height required to allow full mobilization of the factored interface friction is found by rearranging Equation (x)

$$\min h_1 = \frac{9600\,lb/ft}{(150\,pcf)(2\,ft)}\tan(8.7°) = 4.9\,ft$$

The calculations will proceed assuming that h_1 is greater than or equal to 4.9 ft and the embedment of the top of the anchor, h_2, equals 2 ft. With these dimensions, h_1 will be greater than (h_1 + h_2) and the anchor can be treated as extending to the ground surface (see Figure 4-40). These assumptions will be checked at the end of the design.

The net allowable resistance of the anchor, ignoring base sliding resistance, is estimated by the difference between the active and passive earth pressure coefficients, $K_{P,h} - K_{A,h}$, which in this case equals 1.79. Table B-10 summarizes the calculation of the net resistance of the anchor based on the sketch provided as Figure B-12.

Table B-10 Calculation of Net Allowable Anchor Resistance

Force ID	$\Delta\sigma'_{v,top}$ (psf)	$\Delta\sigma'_{v,bot}$ (psf)	$K_{p,h}$-$K_{a,h}$	$\Delta\sigma'_{h,top}$ (psf)	$\Delta\sigma'_{h,bot}$ (psf)	h_{shape} (ft)	ΔP (lb/ft)
12	0	690	1.79	0	1235	6	3705
13	690	690	1.79	1235	1235	h-6	1235(h - 6)
14	0	52.6(h - 6)	1.79	0	94.2(h - 6)	h-6	47.1(h - 6)^2

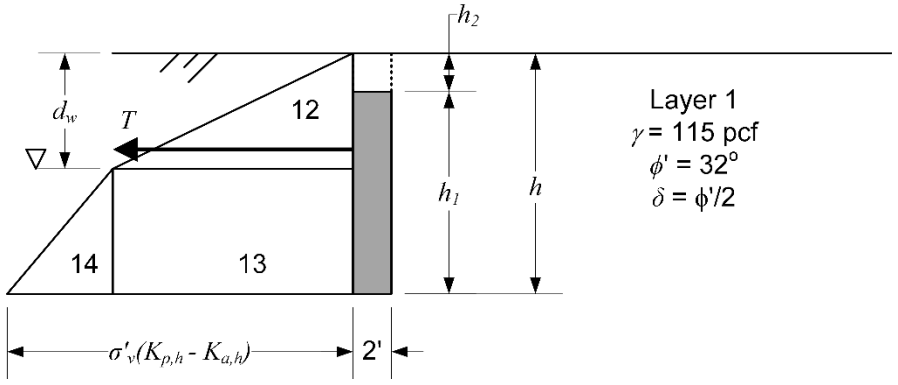

Figure B-12 Net Anchor Resistance to Counteract Tierod Force

The required height of the anchor can be found summing the horizontal forces:

$$\sum F_h = 0 = T - \sum \Delta P = 9600\frac{lb}{ft} - \left[3705\frac{lb}{ft} + (1235\,psf)(h - 6\,ft) + (47.1\,psf)(h - 6\,ft)^2 \right]$$

Solving, h equals 10.1 ft. The height of the anchor should be rounded to the nearest half foot for design, which is 10.5 ft in this case. Since h_1 exceeds h/2, it is acceptable to treat the anchor as extending to the ground surface. Since h_1 exceeds 4.9 ft, it is acceptable to assume that wall friction will be unimpeded by the weight of the anchor.

Table B-11 summarizes the design geometry of the anchor based on the analysis provided in this section.

Table B-11 Summary of Anchor Design

Dimension	Value
Total anchor depth, h	10.5 ft
Height of anchor block, h_1	8.5 ft
Depth of embedment, h_2	2 ft
Width	2 ft

The tierod connection is located 5 ft below the ground surface, which is 5.1 ft above the base of the anchor, using the unrounded depth. Ideally, the anchor should connect at the elevation of the net resultant resistance force. Table B-12 summarizes the calculation of the elevation of the resultant force relative to the base of the anchor. Based on this calculation, the tierod is located about 14 inches higher than the ideal location. Lowering the tierod elevation has implications on the design, including the embedment of the sheetpile. A final design should evaluate the advantages and disadvantages of revising the tierod elevation.

Table B-12 Calculation of the Elevation of the Resultant Force

Force ID	Force (lbs) for h = 10.1ft	Elevation of Resultant Relative to Anchor Base (ft)	Weighting by Force (Force) × (Resultant Elev.)
12	3705	10.1 – 4 = 7.1	3705(7.1) = 26,306
13	5064	(10.1-6)/2 = 2.0	10,128
14	792	(10.1-6)/3 = 1.4	1,109
$y_{resultant}$ = (26,306+10,128+1,109)/(3705+5064+792) = 3.93 ft			

B-2.8 Conclusions from the Analysis.

Table B-13 summarizes all of the design parameters determined in this example. Any changes to the problem require revisiting all calculated parameter values.

Table B-13 Summary of Anchored Bulkhead Design Example

Design Element	Design Parameter	Value
Sheet Pile	Sheetpile section	PZ-22
	Total length (H+D)	24+18 = 42 ft
	Embedment (D)	18 ft
	Position of tierod above pile tip	19+18 = 37 ft
Concrete Deadman Anchor	Depth to base of anchor, h	10.5 ft
	Height of anchor, h_1	8.5 ft
	Depth to top of anchor, h_2	2 ft
	Width of anchor	2 ft
Tierod	Spacing	6 ft
	Length	56 ft
	Force	58 kips
	Connection force	69 kips

B-3 EXAMPLE 3 – BEARING CAPACITY OF SHALLOW FOUNDATIONS.

B-3.1 Description of the Problem.

Three rows of footings are proposed for construction of a building on a site with medium to stiff consistency overconsolidated clay. The footings will be designed for the vertical loads indicated in Figure B-13. The design properties of the clay are provided in Table B-14. The depth to the bearing grade of the footings, D_f, is equal to 3 ft below the final ground surface for frost and shrink/swell considerations.

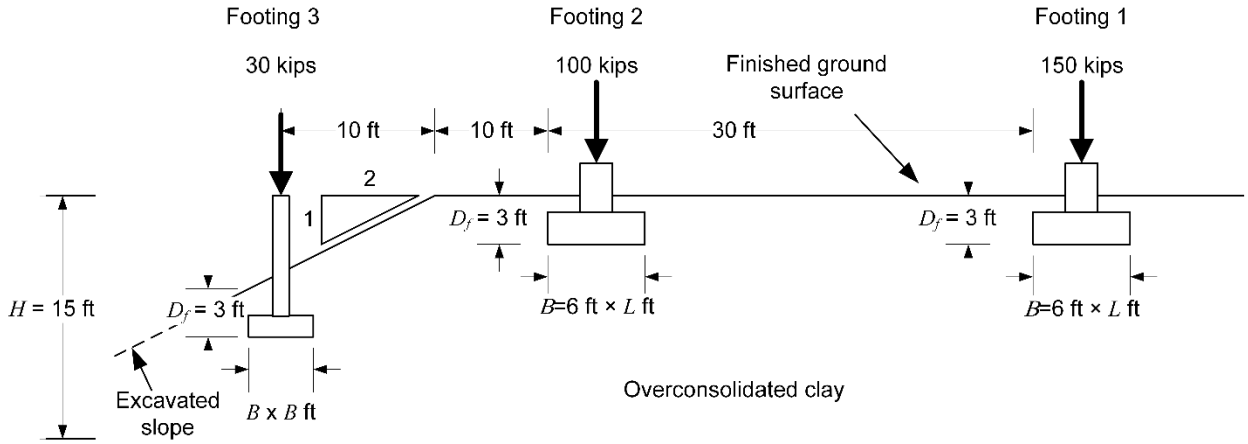

Figure B-13. Three Rows of Footings – Example 3

Table B-14 Design Properties of Overconsolidated Clay

Condition	Unit weight, γ (pcf)	Shear Strength Parameters
Short term (undrained)	115	ϕ = 0 deg, s_u = 1000 psf
Long Term (drained)		ϕ' = 30 deg, c' = 0 psf

B-3.2 Goals and Limitations of the Analysis.

Where applicable, the Meyerhof (1957, 1963) and Hansen (1970) methods will be used to evaluate the unknown dimensions of the three footings in order to have a factor of safety against bearing capacity failure, F_{BC}, of at least 2.5 for short-term and long-term conditions. It is assumed that the clay can be modeled as a saturated undrained soil in the short term and a drained soil in the long term that does not require correction for the presence of the water table. It is further assumed that the footings are spaced far enough away from each other that they can be treated as isolated footings. This example does not consider geotechnical design for settlement and structural design. Because the Footings 2 and 3 are on or near the 2H:1V slope, global stability analysis should also be performed as part of the overall footing design. For example, treating the slope in a long-term drained case as an infinite slope reveals that the slope is only marginally stable using the design strength parameter values.

$$F_{global} = \frac{\tan 30°}{0.5} = 1.15 .$$

The remainder of this example will consider the effects of the slope on bearing capacity. However, the controlling factor for this design is more likely the global stability of the slope itself.

B-3.3 Bearing Capacity Equations.

The generalized gross bearing capacity equation expressed using the notation found in Chapter 5 is as follows

$$q_{ult} = c \cdot N_c \cdot \psi_c + \sigma_{zD} \cdot N_q \cdot \psi_q + 0.5 \cdot B \cdot \gamma \cdot N_\gamma \cdot \psi_\gamma$$

where
N_c, N_q, N_γ = bearing capacity factors that are a function of friction angle,
c = the effective stess cohesion for drained conditions or s_u for undrained conditions,
σ_{zD} is the effective or total vertical stress at the bearing grade,
B = footing width,
γ = representative unit weight, and
ψ_c, ψ_q, ψ_γ = correction factors for the combined effect of complicating conditions.

Applying the desired minimum factor of safety and removing the self weight of the footing and overlying soil, ignoring the difference between the unit weight of concrete and soil, yields the allowable net bearing capacity

$$q_{net,all} = \frac{q_{ult}}{F_{BC}} - \sigma_{zD} .$$

Table B-15 presents the bearing capacity factors according to Meyerhof (1951) and Brinch Hansen (1970) as calculated from Figure 5-5 for short and long-term conditions.

Table B-15 Bearing Capacity Factors for the Example 3

Condition	Theory	N_c	N_q	N_γ
Short term (undrained) $\phi = 0°$	Meyerhof	5.14	1.00	0
	Brinch Hansen	5.14	1.00	0
Long term (drained) $\phi' = 30°$	Meyerhof	30.14	18.40	15.67
	Brinch Hansen	30.14	18.40	15.07

Because N_q equals 1.0 and N_γ equals zero for the undrained case, the net allowable bearing capacity equation reduces to

$$q_{all,net} = \frac{s_u N_c \psi_c}{F_{BC}} + \sigma_{zD}\left(\frac{\psi_q}{F_{BC}} - 1\right)$$

where
s_u is the undrained strength.

Because the shear strength of the clay in the drained condition is represented by a purely frictional material, i.e. c' = 0, the net allowable bearing capacity equation for drained conditions reduces to:

$$q_{all,net} = \sigma_{zD}\left(\frac{N_q \psi_q}{F_{BC}} - 1\right) + \frac{B \cdot \gamma \cdot N_\gamma \cdot \psi_\gamma}{2F_{BC}}.$$

When conditions do not match the assumptions used for the theoretical development of the bearing capacity equation, Meyerhof (1951) and Brinch Hansen (1970) use correction factors applied to the bearing capacity factors. In the current example, the relevant corrections are for footing shape, s_i, and depth, d_i, and ground inclination gi, where the subscript i is assigned characters c, q, or γ to denote which bearing capacity factor the correction is applied to. Recall from Section 5-3.3 that the correction factors are usually multiplied with the exception of the undrained case for Brinch Hansen's method.

The evaluation of the correction factors for each footing is presented in the subsections that follow. In the case of Footing 2, which is located close to the top of the slope, a special form of the bearing capacity equation presented in chart form by Meyerhof (1957) will be applied to account for the effects of the slope.

Applying known parameter values, the net allowable bearing pressure for undrained conditions for both Meyerhof and Brinch Hansen theories yields:

$$q_{all,net} = \frac{(1000\,psf)(5.14)\psi_c}{2.5} + (3\,ft)(115\,pcf)\left(\frac{\psi_q}{2.5} - 1\right) = 2056\psi_c + 138\psi_q - 345.$$

Applying known parameter values and a value of N_γ equal to 15.67, the net allowable bearing pressure for drained conditions according to Meyerhof (1951) yields:

$$q_{all,net} = (3\,ft)(115\,pcf)\left(\frac{18.4\psi_q}{2.5} - 1\right) + \frac{B(115\,pcf)(15.67)\cdot\psi_\gamma}{2(2.5)} = 2539\psi_q + 360B\cdot\psi_\gamma - 345$$

Using a value of N_γ equal to 15.07 according to Brinch Hansen (1970) gives:

$$q_{all,net} = (3ft)(115pcf)\left(\frac{18.4\psi_q}{2.5} - 1\right) + \frac{B(115pcf)(15.07)\cdot\psi_\gamma}{2(2.5)} = 2539\psi_q + 347B\cdot\psi_\gamma - 345.$$

These equations provide the basis for sizing footings 1, 2, and 3 with respect to bearing capacity. The design of Footing 1 is presented in Section B-3.4, the design of Footing 2 is presented in Section B-3.5, and the design of Footing 3 is presented in Section B-3.6. To illustrate a range of design approaches, the dimensions of Footing 1 will be determined by directly solving for B, while Footings 2 and 3 will use an iterative approach.

B-3.4 Footing 1 – Located Far from the Top of the Slope.

Footing 1 imposes a vertical design load, Q, equal to 150 kips that is distributed over the bearing area to produce the design bearing pressure,

$$q_{net} = \frac{Q}{B\cdot L} = \frac{150{,}000\,lb}{6\,ft\cdot L} = \frac{25000}{L} \text{ (psf).}$$

The design bearing pressure must not exceed the allowable bearing capacity, $q_{net} \le q_{all,net}$.

According to Meyerhof (1957), the bearing capacity of a footing is not affected by the inclination of the slope when it is located behind the top of the slope a distance of at least 2 to 6 times the width of the footing, depending on the inclination of the slope, the shear strength of the soil, and the embedment depth of the footing. Since Footing 1 is 6 ft wide and is located 40 ft from the top of the slope, which is 6.7 times the width of the footing, it can be assumed that the bearing capacity evaluation of Footing 1 does not need to consider the slope and the applicable bearing capacity corrections are limited to footing shape and depth. Table B-16 presents Meyerhof's (1951) corrections for shape and depth

Table B-16. Meyerhof Corrections for Footing Shape and Depth

Correction	Undrained, $\phi = 0$	Drained, $\phi' = 30°$, $K_P = 3$
Shape	$s_c = 1 + 0.2(B/L) = 1 + 0.2(6\text{ ft})/L = 1+1.2/L$ $s_q = 1$	$s_q = s_\gamma = 1 + 0.1(B/L)K_P$ $s_q = s_\gamma = 1 + 0.1(6\text{ ft}/L)(3) = 1 + 1.8/L$
Depth	$d_c = 1 + 0.2(D_f/B) = 1 + 0.2(3\text{ ft})/L = 1+0.6/L$ $d_q = 1$	$d_q = d_\gamma = 1 + 0.1(D_f/B)(K_P)^{0.5}$ $d_q = d_\gamma = 1 + 0.1(3\text{ft}/6\text{ ft})(3)^{0.5} = 1.087$
Combined	$\psi_c = [1 + 0.2(B/L)][1 + 0.2(D_f/B)]$ $\psi_c = [1+1.2/L][1+0.6/L]$ $\psi_q = 1$	$\psi_q = \psi_\gamma = [1 + 0.1(B/L)K_P][1 + 0.1(D_f/B)(K_P)^{0.5}]$ $\psi_q = \psi_\gamma = [1 + 1.8/L][1.087]$

Applying Meyerhof's corrections for footing shape and depth for undrained conditions results in:

$$q_{all,net} = 2056\psi_c + 138\psi_q - 345 = 2056\left(1+1.2/L\right)\left(1+0.6/L\right)+138\left(1\right)-345.$$

Setting the net bearing pressure equal to the net allowable and solving for L results in:

$$\begin{aligned} &q_{net} \le q_{all,net} \\ &\frac{25000}{L} \le 2056\left(1+1.2/L\right)\left(1+0.6/L\right)-207 \\ &L \ge 10.84\ ft \end{aligned}$$

This footing length produces a net bearing pressure of 2.31 ksf.

Applying Meyerhof's corrections for footing shape and depth for drained conditions results in:

$$\begin{aligned} q_{all,net} &= 2539\psi_q + 360B\cdot\psi_\gamma - 345 \\ q_{all,net} &= 2539\left(1+1.8/L\right)\left(1.087\right)+360(6\,ft)\left(1+1.8/L\right)\left(1.087\right)-345 \\ q_{all,net} &= 5108\left(1+1.8/L\right)-345 \end{aligned} \quad \text{(psf)}$$

Equating the net and net allowable bearing pressures:

$$\frac{25000}{L} \le 5108\left(1+1.8/L\right)-345 \ \rightarrow\ L \ge 3.32\ ft$$

This footing length produces a bearing pressure of 7.53 ksf. Since the required length is less than the width, the width of Footing 1 is oversized with respect to drained bearing capacity according to Meyerhof. If this case controlled the size of the footing, the calculations would need to be repeated with the lesser footing dimension assigned as the width.

Table B-17 presents Brinch Hansen's (1970) corrections for shape and depth.

Table B-17. Brinch Hansen Corrections for Footing Shape and Depth

Correction	Undrained, $\phi = 0$	Drained, $\phi' = 30°$, $K_P = 3$
Shape	$s_c = 1 + 0.2(B/L)$ $s_c = 1 + 0.2(6\text{ ft})/L = 1+1.2/L$	$s_q = 1 + \sin(\phi')(B/L) = 1+\sin(30)(6\text{ ft}/L) = 1+3/L$ $s_\gamma = 1 - 0.4(B/L) = 1 - 0.4(6\text{ ft}/L) = 1 - 2.4/L$
Depth	$d_c = 0.4(D_f/B) = 0.4(3\text{ ft})/L = 1.2/L$	$d_q = 1+2\cdot\tan(\phi')(1-\sin(\phi'))^2\cdot(D_f/B)$ $d_q = 1+2\cdot\tan(30)(1-\sin(30))^2\cdot(3\text{ ft}/6\text{ ft})=1.144$ $d_\gamma = 1$
Combined	$\psi_c = [1 + 0.2(B/L)]+0.4(D_f/B)$ $\psi_c = (1+1.2/L) + 1.2/L = 1+2.4/L$	$\psi_q = [1 + \sin(\phi')(B/L)][\ 1+2\cdot\tan(\phi')(1-\sin(\phi'))^2\cdot(D_f/B)]$ $\psi_q = (1+3/L)(1.144) = 1.144 + 3.43/L$ $\psi_\gamma = [1 - 0.4(B/L)][1] = 1 - 2.4/L$

Applying Brinch Hansen's corrections for footing shape and depth for undrained conditions results in:

$$q_{all,net} = 2056\psi_c + 138\psi_q - 345 = 2056\left(1 + 2.4/L\right) + 138\left(1\right) - 345 = 1849 + 4934/L$$

Setting the net bearing pressure equal to the net allowable and solving for L results in:

$$25000/L \le 1849 + 4934/L$$
$$L \ge 9.97\ ft$$

This footing length produces a bearing pressure of 2.51 ksf.

Applying Brinch Hansen's corrections for footing shape and depth for drained conditions results in:

$$q_{all,net} = 2539\psi_q + 347B \cdot \psi_\gamma - 345 = 2539\left(1.144 + 3.43/L\right) + 347\left(6\,ft\right)\left(1 - 2.4/L\right) - 345$$
$$q_{all,net} = 4642 - 3712/L$$

Equating the net and net allowable bearing pressures:

$$25000/L \le 4642 - 3712/L \ \rightarrow\ L \ge 4.58\,ft$$

The minimum footing length required to support the design load produces a bearing pressure of 5.46 ksf. As with the analysis using Meyerhof's bearing capacity theory, the required footing length is less than the width in this case, which indicates that the footing width is oversized with respect to drained bearing capacity. If this case controlled the sizing of the footing, the calculations would need to be repeated with the lesser footing dimension assigned as the width.

In summary, the minimum footing length is equal to 10.84 ft to achieve an F_{BC} of at least 2.5 as determined according to Meyerhof (1951) for the undrained case. For design with respect to bearing capacity, the footing should be sized with B equal to 6 ft and L equal to 11 ft.

B-3.5 Footing 2 – Located Close to the Top of the Slope.

Footing 2 is near the top of the slope and the effects on bearing capacity must be considered. Brinch Hansen's theory does not include a correction for a footing near the top of a slope. The method by Leshchinsky and Xie will be used.

Leshchinsky and Xie (2017) provided bearing capacity reduction factors for saturated undrained conditions. Their method requires that the following ratios be calculated:

$$\frac{\gamma H}{s_u} = \frac{\left(115\,pcf\right)\left(15\,ft\right)}{1000\,psf} = 1.725,\ \ \frac{B}{H} = \frac{6\,ft}{15\,ft} = 0.4,\ \ \frac{b}{B} = \frac{10\,ft}{6\,ft} = 1.7$$

Interpolation is required by selecting values from Table 5-9 as shown in Table B-18. The boldface values are interpolated.

Table B-18 Interpolation of Bearing Capacity Factors for Sloping Conditions

Bearing Capacity Reduction Factor, RC_{slope}						
b/B	$\gamma H/s_u = 0$			$\gamma H/s_u = 2$		
	$\beta = 0°$	$\beta = 26°$	$\beta = 30°$	$\beta = 0°$	$\beta = 26°$	$\beta = 30°$
1.25	1	---	0.94	1	---	0.92
1.7	**1**	**0.985**	**0.983**	**1**	**0.98**	**0.977**
1.88	1	---	1	1	---	1
Meyerhof Bearing Capacity Factor, $N_{\gamma,slope}$						
β (deg)	$D_f / B = 0$		$D_f / B = 0.5$		$D_f / B = 1$	
0	15		---		60	
26	**14.1**		**31.4**		**48.7**	
30	14		---		47	

Further interpolating for $\gamma H/s_u$ = 1.725 from Table B-18 yields RC_{slope} = 0.981. The ultimate and allowable bearing capacity are found as:

$$q_{ult} = 5.14 \cdot s_u \cdot RC_{slope} = 5.14\left(1000\,pcf\right)\left(0.981\right) = 5042\,psf$$

$$q_{all,net} = \frac{5042\,psf}{2.5} = 2017\,psf$$

The allowable bearing pressure can be considered a net value because the N_q term was neglected when q_{ult} was calculated. The required value of L can be found as:

$$q_{net,all} \geq q_{net}$$

$$2017\,psf \geq \frac{100000\,lb}{\left(6\,ft\right)L}$$

$$L \geq 8.26\,ft$$

For undrained conditions, the footing should be sized with a length of 8.5 ft.

For drained conditions with c' = 0, the chart solution by Meyerhof (1957) must be used. The following ratios are required:

$$b/B = 1.7$$

$$D_f/B = 3\,ft/6\,ft = 0.5$$

Values from Figure 5-8 are summarized in Table B-18. Interpolation for the 2H1V slope and embedment results in the boldface values in the table and $N_{\gamma,slope}$ = 31.4.

The ultimate and allowable bearing capacities for drained conditions are found as:

$$q_{ult} = 0.5 \cdot \gamma \cdot B \cdot N_{\gamma,slope} = 0.5(115\,pcf)(6\,ft)(31.4) = 10833\,psf$$

$$q_{all,net} = \frac{10833\,psf}{2.5} - (3\,ft)(115\,pcf) = 3988\,psf$$

As for Footing 1, the net allowable bearing pressure for drained conditions is higher than for undrained. Thus, the length of 8.5 ft obtained for undrained conditions should be used.

B-3.6 Footing 3 – Located on the Slope.

Footing 3 will be designed as a square footing for a bearing pressure equal to

$$q_{net} = \frac{Q}{B^2} = \frac{30000\,lb}{B^2} \text{ (psf).}$$

Footing 3 is located on the 2H:1V slope. Brinch Hansen (1970) provides correction for the effect of the slope on bearing capacity, which are implemented using simple equations. Footing 3 will be designed by selecting both B and iteratively changing B until the net bearing pressure is less than the allowable value. An initial guess of 2 ksf was selected to size Footing 3, which yields dimensions of:

$$B^2 \geq \frac{30000\,lb}{2000\,psf} = 15 \;\rightarrow\; B = 4\,ft\,.$$

Table B-19 presents Brinch Hansen's (1970) correction factors for both undrained and drained conditions. Applying Brinch Hansen's corrections for footing shape, depth, and ground inclination for undrained conditions and B = 4 ft results in:

$$q_{all,net} = \frac{5.14 s_u \cdot \psi_c + \sigma_{zD} N_q}{F_{BC}} - \sigma_{zD} = \frac{5.14(1000\,psf)(1.319)}{2.5} + (345\,psf)\left(\frac{1}{2.5} - 1\right) = 2505\,psf\,.$$

Table B-19 Corrections for Footing Shape, Depth, and Ground Inclination (Brinch Hansen 1970)

Correction	Undrained, $\phi = 0$	Drained, $\phi' = 30°$, $K_P = 3$
Shape	$s_c = 1 + 0.2(B/L)$ $s_c = 1 + 0.2(1) = 1.2$	$s_q = 1 + \sin(\phi')(B/L) = 1 + \sin(30)(1) = 1.5$ $s_\gamma = 1 - 0.4(B/L) = 1 - 0.4(1) = 0.6$
Depth	$d_c = 0.4(D_f/B) = 0.4(3\text{ ft})/4 = 0.3$	$d_q = 1 + 2\cdot\tan(\phi')(1-\sin(\phi'))^2\cdot(D_f/B)$ $d_q = 1 + 2\cdot\tan(30)(1-\sin(30))^2\cdot(3\text{ ft}/4\text{ ft}) = 1.217$ $d_\gamma = 1$
Ground	$g_c = \beta / 147 = 26.6/147 = 0.181$	$g_q = g_\gamma = [1-0.5\tan(\beta)]^2 = [1-0.5\tan(26.6)]^2 = 0.563$
Combined	$\psi_c = 1.2 + 0.3 - 0.181 = 1.319$	$\psi_q = (1.5)(1.217)(0.563) = 1.028$ $\psi_\gamma = (0.6)(1)(0.563) = 0.338$

The allowable net bearing pressure is greater than the net bearing pressure for B = 4 ft. A smaller size could be tried; however, drained conditions will be evaluated first. Applying Brinch Hansen's corrections for footing shape, depth, and ground inclinations for drained conditions and B = 4 ft results in:

$$q_{all,net} = \frac{\sigma_{zD} N_q \psi_q + 0.5 B \cdot \gamma \cdot N_\gamma \psi_\gamma}{F_{BC}} - \sigma_{zD}$$

$$q_{all,net} = \frac{(345)(18.4)(1.028) + 0.5(4\,ft)(115\,pcf)(15.07)(0.338)}{2.5} - (345\,psf) = 2734\,psf$$

The footing size of B = 4 ft is also acceptable for drained conditions, and a smaller size can be attempted. Table B-20 summarizes some of the calculations for other footing sizes. Footing 3 can be sized for B = 3.5 ft, which produces a bearing pressure of 2.45 ksf. This is higher than the bearing pressure for Footing 3 because the Leshchinsky and Xie method conservatively ignores shape factors and depth factors.

Table B-20 Iterative Sizing of Footing 3

B (ft)	q_{net} (psf)	Undrained		Drained			Acceptable?
		ψ_c	$q_{all,net}$ (psf)	ψ_q	ψ_γ	$q_{all,net}$ (psf)	
4	1875	1.319	2505	1.026	0.338	2729	Y
3.75	2133	1.339	2546	1.039	0.338	2731	Y
3.5	2449	1.362	2593	1.053	0.338	2737	Y
3.25	2840	1.388	2647	1.069	0.338	2749	N

B-3.7 Conclusions from the Analysis.

Table B-21 summarizes the bearing capacity analyses presented in this example. The sizing of Footings 1 and 2 with respect to bearing capacity was controlled by the short-term undrained case, which is expected for soil which gains strength by consolidation as drainage occurs. For Footing 3, the net allowable bearing pressure was approximately equivalent for both undrained and drained conditions.

Table B-21 Summary of Bearing Capacity Analyses – Example 3

Analysis	Footing 1 Far from Slope (Q=150 kips)	Footing 2 Near Top of Slope (Q=100 kips)	Footing 3 On Slope (Q=30 kips)
Short term, Meyerhof	6 ft × 11 ft, 2.27 ksf		
Short term, Brinch Hansen	6 ft × 10 ft, 2.50 ksf		3.5 ft × 3.5 ft, 2.45 ksf
Short term, Leshchinsky & Xie		6 ft × 8.5 ft, 1.96 ksf	
Long term, Meyerhof	6 ft × 3.5 ft, 7.14 ksf	6 ft × 4.25 ft, 3.92 ksf	
Long term, Brinch Hansen	6 ft × 4.75 ft, 5.26 ksf		3.5 ft × 3.5 ft, 2.45 ksf
Design	6 ft × 11 ft, 2.27 ksf	6 ft × 8.5 ft, 1.96 ksf	3.5 ft × 3.5 ft, 2.45 ksf

B-4 EXAMPLE 4 – MAT FOUNDATION DESIGN.

B-4.1 Description of the Problem.

A proposed 10-story building with underground parking is to be supported by a rectangular mat foundation having plan dimensions of 120 ft by 160 ft (Figure 1). The site is level with an exterior finished grade of El. 215 ft. The site conditions enable the bearing grade of the mat to be set at an elevation of El. 200 ft. In addition to providing space for parking, the excavation will reduce expected settlements since some of the weight of the new structure will be offset, or compensated, by the weight of the excavated material.

The subsurface exploration performed for the project indicates that the subsurface consists of the four strata listed in Table B-22. It is known that Stratum 4 continues for several hundred feet. The design groundwater elevation is El. 195 ft.

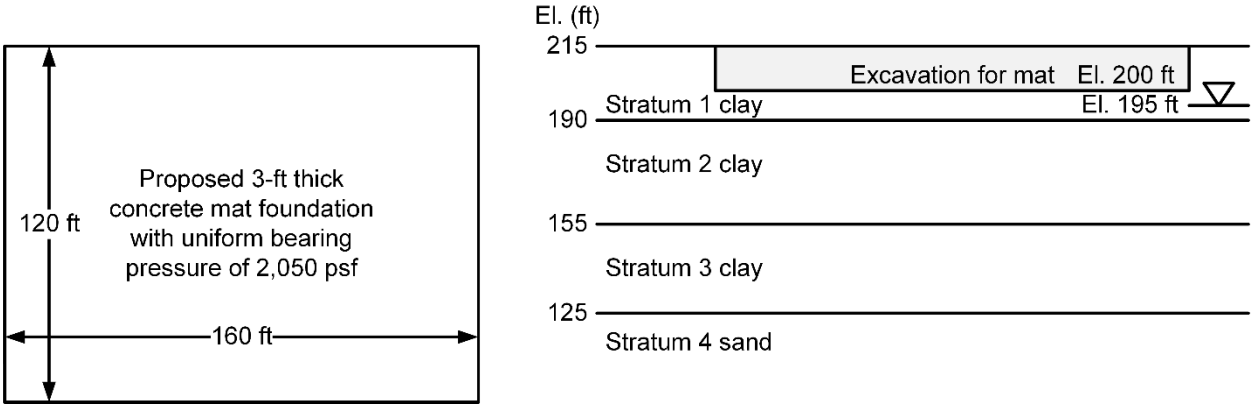

Figure B-14 Plan and Profile of Site

Table B-22 Subsurface Profile

Stratum	Description	Depth (ft)		Soil Properties			
		Top	Bottom	γ (pcf)	$C_{\varepsilon c}$	$C_{\varepsilon r}$	OCM (ksf)
1	Medium to stiff lean clay	0	25	110	0.07	0.007	2
2	Medium stiff lean clay	25	60	115	0.10	0.010	2
3	Very stiff lean clay	60	90	125	0.05	0.005	6
4	Dense fine to coarse sand	90	--				

The design of total unit weight (γ), modified compression index ($C_{\varepsilon c}$), modified recompression index ($C_{\varepsilon r}$), and overconsolidation margin (OCM) listed in Table B-22 are based on interpretation of in-situ and lab testing information as well as prior experience with the local geology. The OCM quantifies the preconsolidation and is equal to the difference between the preconsolidation stress and the current vertical effective stress

at any depth. The soil properties in Table B-22 reflect the soil prior to the excavation and foundation construction. Additionally, Atterberg limits testing suggests that the Strata 1-3 clays generally have plasticity index values less than 30.

The concrete mat foundation will be 3 ft thick and support a regular grid of columns on a 25 ft spacing. The columns will impose design loads of 1,000 kips each on the mat. Based on the self-weight of the mat and uniform distribution of the column load with each column's tributary area, the bearing pressure of the mat is equal to:

$$q_{net} = (3\,ft)(150\,pcf) + \frac{1000000\,lb}{(25\,ft)^2} = 2050\,psf\ .$$

The 15-ft deep excavation in Stratum 1 soil associated with accessing the bearing grade (El. 200 ft) from the ground surface (El. 215 ft) reduces the total vertical stress on the bearing grade by 1,650 psf. It is conservatively assumed that the excavation is left open long enough for the excess pore pressures generated by the excavation to fully dissipate and the effective vertical stresses in the ground to be reduced and be in equilibrium with the excavation prior to construction of the mat. The reduction in effective vertical stress due to the excavation causes the Stratum 1-3 clays to heave according to the swell ratio, which is assumed to be equal to the recompression ratio. It is further assumed that all settlement occurs after application of the full bearing pressure, i.e. no settlement occurs during construction. This assumption is conservative, particularly for immediate settlement, which occurs simultaneously with loading.

B-4.2 Goals and Limitations of the Analysis.

The first goal of this analysis is to estimate ultimate settlements of the mat foundation due to immediate elastic distortion under loading and time-dependent consolidation. The potential for secondary compression over the service life of the foundation is not considered in this analysis. Compression of the Strata 1-3 clays is considered while compression of the Stratum 4 sand is assumed to be small enough to ignore.

The second goal of the analysis is to estimate the modulus of subgrade reaction for the service loading condition based on the results of the settlement analysis.

The analysis is performed at the plan view location of the center of the mat. A full analysis of the mat foundation for geotechnical and structural design would likely involve evaluating settlement and the modulus of subgrade reaction at multiple locations.

B-4.3 Immediate Settlement.

Immediate settlement, s_i, of the compressible clay soils of Strata 1-3 is due to distortion, i.e. shape change rather than volume change, of the clay due to the finite loaded area of

the mat foundation. Immediate settlement calculations of this type are typically performed by approximating the soils that undergo distortion as a linear elastic material that experiences a uniform strain due to an applied uniform bearing pressure. The calculations require estimates of the Young's modulus, E_s, of the layers experiencing distortion as well as an estimate of the thickness of material that experiences the uniform strain. When multiple layers are present, a single composite estimate of Young's modulus can be estimated using the weighing method by layer thickness proposed by Bowles (1996). This approach does not weight layers by proximity to the bearing grade and soil profiles commonly become stiffer with depth, so care should be used when evaluating which layers to include in the calculation. The thickness of the soil experiencing the average strain is estimated by multiplying the width of the loaded area, B, by two influence factors, μ_0 and μ_1 (see Section 5-4.5).

Estimates of Young's modulus are almost always imprecise and often do not directly consider stress-strain nonlinearity. Since immediate settlement occurs with loading, the clay soils are best represented as being undrained. In this example, Young's modulus for undrained conditions is estimated using the correlation with undrained strength, OCR, and plasticity index proposed by Duncan and Buchignani (1987) as presented in Figure 8-51 of UFC 3-220-10 (UFC 2022). The Strata 1 to 3 clays generally have a plasticity index less than 30 and are slightly overconsolidated, so a ratio of Young's Modulus to undrained strength equal to 600 is a reasonable estimate. Because no direct measurements of shear strength are available, undrained strength is estimated using the correlation proposed by Jamiolkowski et al. (1985) using a fitting parameter, m, equal to 0.8. Expressing the effect of the OCR in terms of a constant value of OCM, yields:

$$s_u \approx 0.23 \cdot \sigma'_z \cdot OCR^{0.8} \approx 0.23 \cdot \sigma'_z \cdot \left(\frac{1 + OCM}{\sigma'_z} \right)^{0.8}$$

Combining the relationship among undrained strength, vertical effective stress, and OCM, with the ratio of undrained Young's modulus to undrained strength equal to 600 produces the following relationship:

$$E_{s,u} \approx 600 \cdot s_u \approx 138 \sigma'_z \cdot \left(\frac{1 + OCM}{\sigma'_z} \right)^{0.8}$$

Application of the relationship above with the vertical effective stress at the middle of each stratum prior to construction and the estimates of OCM given in Table B-22 produces the estimates of Young's Modulus provided in Table B-23. For Stratum 1, the vertical stress is evaluated at the midpoint between the bearing grade of the mat foundation and the bottom of the layer at a depth of 20 ft below the ground surface.

The weighed average modulus value is equal to:

$$E_{s,u} = \frac{(509ksf)(10\,ft)+(661ksf)(35\,ft)+(1281ksf)(30\,ft)}{75\,ft} = 889ksf$$

Table B-23 Calculated Vertical Stresses, *OCR*, and Modulus at Layer Midpoints

Stratum	σ'_z (ksf)	*OCM* (ksf)	*OCR*	$E_{s,u}$ (ksf)
1	2.20	2	1.9	509
2	3.27	2	1.6	661
3	4.89	6	2.2	1281

The values of influence factors, μ_0 and μ_1, are found using the charts found in Figure 5-29. Based on the geometric ratios and interpretation of the charts presented in Figure B-15, the values of the influence factors, μ_0 and μ_1, are taken to equal 0.97 and 0.2, respectively. Using the estimated value of Young's modulus, influence factors, and bearing pressure, the estimated immediate settlement of the mat is equal to:

$$s_i = \mu_0\mu_1 B\left(\frac{q}{E_{s,u}}\right) = (0.97)(0.2)(120\,ft)\left(\frac{2.05ksf}{889ksf}\right)\left(\frac{12in}{1\,ft}\right) = 0.64 \rightarrow \approx 0.7\,in.$$

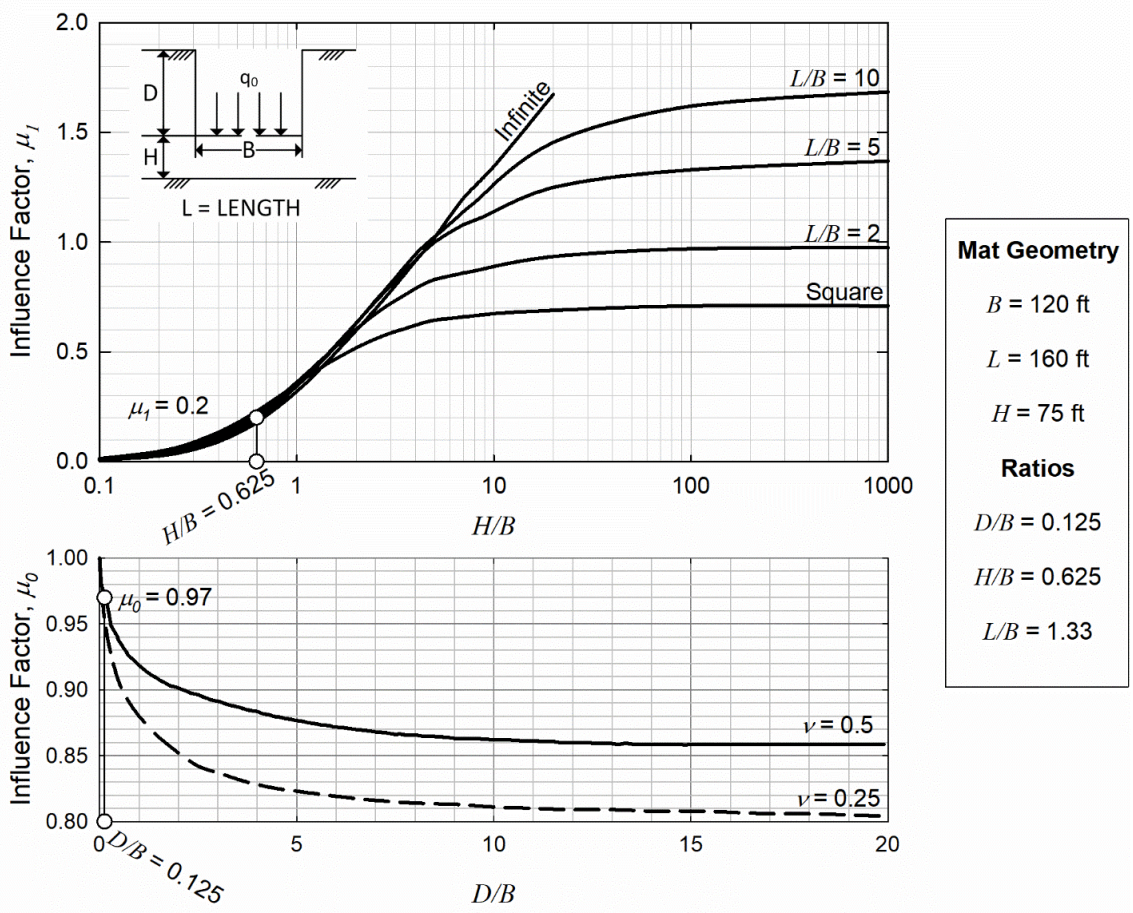

Figure B-15 Intepretation of Influence Factors for Elastic Settlement

B-4.4 Primary Consolidation.

Ultimate primary consolidation, s_c, of the compressible clay soils of Strata 1 to 3 is due to changes in effective stress from the foundation loading, incorporating the effects of the excavation on the stress history of the soils, i.e. preconsolidation stress. While commercial software and spreadsheet analysis of consolidation allow discretization of the compressible soils into a great number of thin layers, a relatively small number of layers having thickness that increases with depth from the bearing grade can produce results that closely match analyses using highly-discretized profiles. In this case ten sublayers are used as shown in Table B-24 along with the evaluation of the total and effective vertical stresses at the mid-depth of each layer prior to making the excavation for the foundation.

Table B-24 Evaluation of Initial Stresses Prior to Construction

Sublayer	Stratum	Top El. (ft)	Bottom El. (ft)	Thickness (ft)	Midpt. El. (ft)	γ_t (pcf)	At Mid-Depth		
							σ_{z0} (psf)	u (psf)	σ'_{z0} (psf)
Excavated		215	200	15	207.5	110	825	0	825
1	1	200	195	5	197.5	110	1925	0	1925
2	1	195	190	5	192.5	110	2475	156	2319
3	2	190	185	5	187.5	115	3038	468	2570
4	2	185	175	10	180.0	115	3900	936	2964
5	2	175	165	10	170.0	115	5050	1560	3490
6	2	165	155	10	160.0	115	6200	2184	4016
7	3	155	145	10	150.0	125	7400	2808	4592
8	3	145	135	10	140.0	125	8650	3432	5218
9	3	135	125	10	130.0	125	9900	4056	5844

Table B-25 presents values of preconsolidation stress for each layer (σ'_p) found by adding the OCM to the initial vertical effective stress from Table B-24. Changes in total vertical stress due to the excavation and foundation loading are estimated using Boussinesq elastic solutions for stress changes below the corner of a flexible rectangular-loaded area as presented in Table 4-2 in UFC 3-220-10 (UFC 2022). Stress changes due to the excavation are represented by $\Delta\sigma_{ze}$ and stress changes due to the foundation construction and loading are represented by $\Delta\sigma_{zl}$. The effective vertical stress after the excavation, σ'_{ze}, is the initial effective stress used in the strain calculations and the final effective stress, σ'_{zf}, is equal to the sum of σ'_{ze} and $\Delta\sigma_{zl}$.

Strain due to ultimate consolidation settlement is found according to:

$$\varepsilon_{z,ult} = C_{\varepsilon r} \log\left(\frac{\min\left(\sigma'_p, \sigma'_{zf}\right)}{\sigma'_{ze}}\right) + C_{\varepsilon c} \log\left(\frac{\max\left(\sigma'_p, \sigma'_{zf}\right)}{\sigma'_c}\right).$$

Table B-25 Evaluation of Preconsolidation Stress and Stress Changes

Sublayer	Stratum	*OCM* (psf)	σ'_c (psf)	$\Delta\sigma_{ze}$ (psf)	σ'_{ze} (psf)	$\Delta\sigma_{zl}$ (psf)	σ'_{zf} (psf)
1	1	2000	3925	-1650	275	2050	2325
2	1	2000	4319	-1648	671	2048	2719
3	2	2000	4570	-1642	927	2040	2968
4	2	2000	4964	-1621	1343	2013	3357
5	2	2000	5490	-1563	1927	1942	3869
6	2	2000	6016	-1476	2540	1834	4374
7	3	6000	10592	-1368	3224	1700	4924
8	3	6000	11218	-1251	3967	1555	5521
9	3	6000	11844	-1134	4710	1409	6119

Table B-26 summarizes the ultimate strain and compression, ΔH_{ult}, of each sublayer. The sum of the sublayer compressions equals the ultimate consolidation settlement, $\delta_{c,ult}$. In this case, the consolidation settlement is approximately 2.4 inches.

Table B-26 Strain and Compression Calculations

Sublayer	Stratum	$C_{\varepsilon c}$	$C_{\varepsilon r}$	$\varepsilon_{z,ult}$	Thickness (ft)	ΔH_{ult} (ft)
1	1	0.070	0.007	0.0065	5	0.032
2	1	0.070	0.007	0.0043	5	0.021
3	2	0.100	0.010	0.0051	5	0.025
4	2	0.100	0.010	0.0040	10	0.040
5	2	0.100	0.010	0.0030	10	0.030
6	2	0.100	0.010	0.0024	10	0.024
7	3	0.050	0.005	0.0009	10	0.009
8	3	0.050	0.005	0.0007	10	0.007
9	3	0.050	0.005	0.0006	10	0.006
					$\delta_{c,ult}$ = $\Sigma\Delta H$ (ft) =	0.195

B-4.5 Modulus of Subgrade Reaction.

The modulus of subgrade reaction is calculated for two conditions: 1) considering the immediate settlement response of the loaded mat foundation and 2) considering the additional time-dependent settlement from primary consolidation.

The modulus of subgrade reaction for the immediate response of the loaded mat foundation, k_s, is found by:

$$k_s = \frac{q}{s_i} = \frac{2.05 ksf}{0.7 in.}\left(\frac{1000 lb}{1 k}\right)\left(\frac{1 ft^2}{144 in^2}\right) = 20.3 pci .$$

Including the time-depending settlement from primary consolidation further reduces the modulus of subgrade reaction, k_{sc}. Using a value for s_i equal to 0.7 inches, a value for s_c equal to 2.4 inches, and a bearing pressure equal to 2.05 ksf (14.24 psi) produces:

$$k_{sc} = \frac{q}{s_i + s_c} = \frac{14.24 psi}{0.7 in + 2.4 in} = 4.6 pci .$$

B-4.6 Conclusions from the Analysis.

Settlement of the proposed mat foundation was calculated. The immediate and consolidiation settlements are summarized in Table B-27. The subgrade reaction moduli are also provided.

Table B-27 Summary of Estimated Settlements and Subgrade Reaction Moduli

Design Parameter	Value
Immediate settlement, s_i	0.7 inches
Consolidation settlement, s_c	2.4 inches
Immediate modulus of subgrade reaction, k_s	20.3 pci
Long-term modulus of subgrade reaction, k_{sc}	4.6 pci

B-5 EXAMPLE 5 – PILE GROUP CAPACITY AND SETTLEMENT.

B-5.1 Description of the Problem.

A bridge pier will be supported on concrete driven piles. The soil profile consists of normally consolidated soft clay overlying overconsolidated stiff clay as shown in Figure B-16. The proposed construction includes placement of 8 ft of new fill of broad lateral extent.

The bridge pier will require a foundation capable of supporting a permanent unfactored static axial compressive load acting on the pile cap equal to 1,500 kips and an

additional 600 kips due to transient vertical live loads. Lateral loads, uplift, and moments are not considered in this example.

Square precast prestressed concrete (PPC) piles having a 12-inch side length are selected for the project due to sourcing and transport considerations. The supplier produces piles up to a maximum length of 70 ft using 5,000 psi concrete that have a factored structural resistance in compression, P_r, equal to 200 kips. The piles will be installed in a square array with a center-to-center spacing of 3-ft and tied together in a 3.5-ft thick reinforced concrete cap. The weight of the cap and overlying soil should be added to the unfactored permanent loads considered in this analysis.

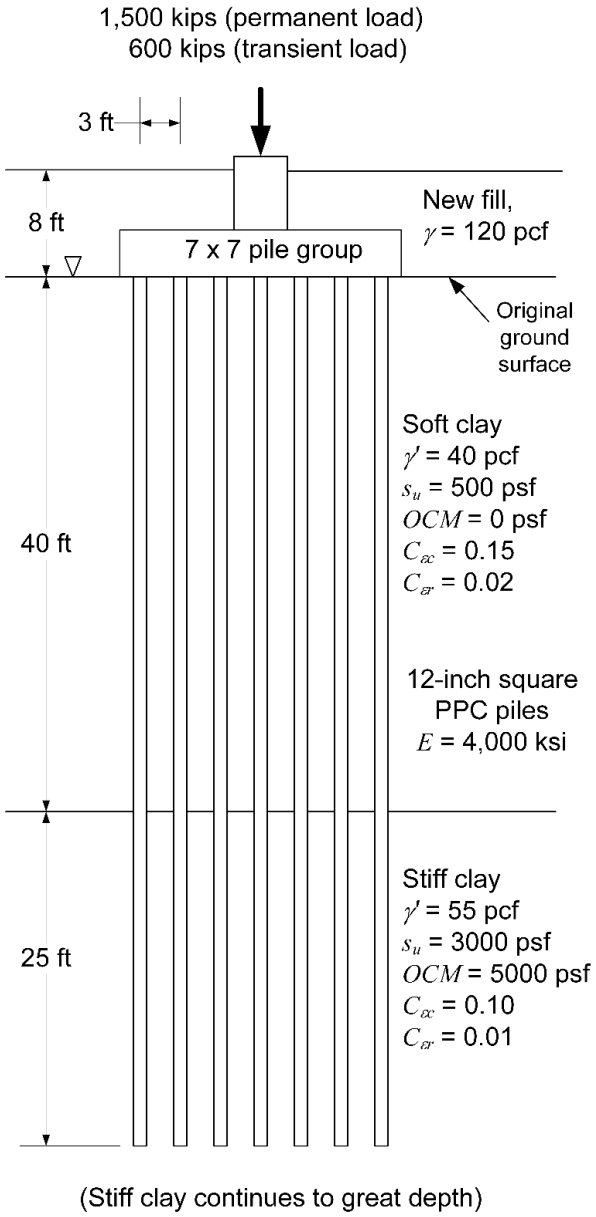

Figure B-16 Proposed Pile Group in Soft and Stiff Clay

B-5.2 Goals and Limitations of the Analysis.

The goal of this analysis is to check the proposed length and number of PPC piles against the geotechnical strength limit state and a serviceability limit with respect to settlement. The performance requirements as well as assumptions and simplifications are listed below:

- The geotechnical strength limit state is checked using load factors equal to 1.25 for permanent loads and 1.75 for transient loads. The geotechnical resistance for individual piles is estimated using the Alpha Method with a resistance factor equal to 0.35. Block failure of the group is checked using a resistance factor equal to 0.60.

- The structural strength limit state for the axial pile capacity is checked using load factors equal to 1.25 for permanent loads and 1.75 for transient loads

- The serviceability limit state with respect to settlement considers unfactored permanent loads only. Analysis results where 50% of the transient live loads are included in addition to the permanent loads are also presented. A limit on ultimate settlement of the pile cap equal to 3 inches is selected based on considerations for acceptable angular distortion and post construction settlement. Time rate of settlement analysis is not part of this example.

- Settlement analysis is limited to elastic shortening of the piles above the neutral plane and consolidation of clay soils below the neutral plane. Stress shielding and soil stiffening effects of the piles and cap are conservatively ignored.

The analysis will utilize the neutral plane method to evaluate the maximum load in the pile for the structural strength limit state check and to position the equivalent footing for the settlement analysis.

B-5.3 Trial Dimensions.

This example is performed for a square arrangement of 49 piles having a trial length below the pile cap equal to 65 ft. It is assumed that additional pile length to account for cutoff and embedment in the cap can be included within the 70 ft maximum length constraint. The cap is buried and will remain in contact with the ground.

For this arrangement, a cap width and length equal to 21 ft accommodates the piles with an allowance of 1 ft between the edge of the pile and the edge of the cap. The weight of the cap and overlying soil, $W_{cap+soil}$, is equal to:

$$W_{cap+soil} = (21ft)^2\left[(3.5ft)(0.15kcf)+(8ft-3.5ft)(0.12kcf)\right] = 470\,kips\ .$$

The permanent load from the superstructure acting on the pile cap plus the weight of the cap and the overlying soil equals the unfactored permanent load acting on the pile group:

$$Q_{g,d} = 1500\,kips + 470\,kips = 1976\,kips\,.$$

B-5.4 Geotechnical Strength Limit State Analysis.

For the trial dimensions described in Section 1-7.3, the pile group must resist a factored load equal to

$$Q'_g = (1.25)(1976\,kips) + (1.75)(600\,kips) = 3520\,kips\,.$$

Nominal shaft resistance for the soft and stiff clays is evaluated according to the Alpha method described in Section 6-5.4.2. As shown in Figure B-17, interpreted values of α for the soft and stiff clay, α_{soft} and α_{stiff}, are equal to 1.0 and 0.5, respectively. Fully-mobilized shaft friction per unit area for the soft and stiff clay, $f_{s,soft}$ and $f_{s,stiff}$ respectively, is equal to

$$f_{s,soft} = \alpha_{soft} \cdot s_{u,soft} = 1.0 \cdot (500\,psf) = \pm 500\,psf$$
$$f_{s,stiff} = \alpha_{stiff} \cdot s_{u,stiff} = 0.5 \cdot (3000\,psf) = \pm 1500\,psf$$

where the positive and negative signs indicate that shaft friction can be positive (shaft resistance) or negative (drag force), depending on the location of the neutral plane.

It possible that the soft clay will be dragged into a portion of the stiff clay and reduce shaft resistance. A length of pile equal to 10 times the width, in this case 10 ft, below top of the stiff clay is assigned a value of α according to Equation 6-9 in Section 6-5.4.2 based on guidance by Tomlinson (1980). For the current example,

$$f_{s,transition} = 0.28 \cdot s_{u,stiff} \left(\frac{s_{u,stiff}}{P_a} \right)^{-0.44} = 0.28(3000\,psf) \left(\frac{3000\,psf}{2116\,psf} \right)^{-0.44} = \pm 720\,psf\,.$$

Based on this approach, the load transfer per unit length of shaft, Δp, for the soft clay, stiff clay, and transition zone is equal to:

$$\Delta p_{soft} = 4 \cdot B \cdot f_{s,soft} = 4(1\,ft)(500\,psf) = \pm 2000\,lb/ft = \pm 2\,k/ft$$
$$\Delta p_{transition} = 4 \cdot B \cdot f_{s,transition} = 4(1\,ft)(720\,psf) = \pm 2900\,lb/ft = \pm 2.9\,k/ft$$
$$\Delta p_{stiff} = 4 \cdot B \cdot f_{s,stiff} = 4(1\,ft)(1500\,psf) = \pm 6000\,lb/ft = \pm 6\,k/ft$$

where B is the width of the square pile. For the sign convention adopted here, positive values of Δp indicate load transfer from the pile to the soil, i.e. resistance, and negative values of Δp indicate load transfer from the soil to the pile, i.e. drag force.

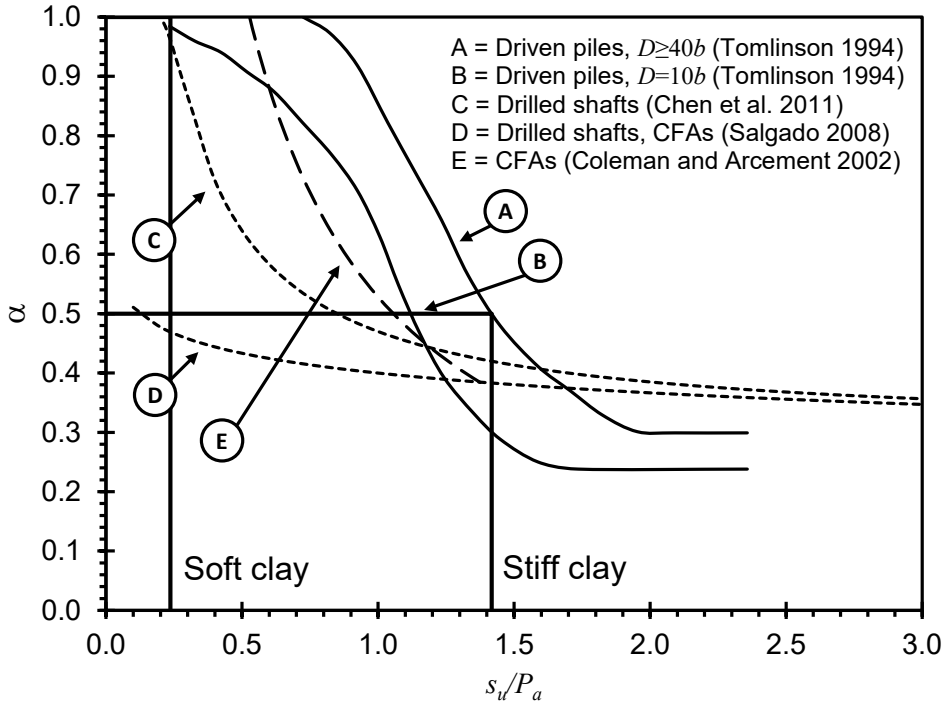

Figure B-17 Interpretation of Alpha Factor

For the total embedded length of the pile, the nominal shaft resistance equals:

$$R_s = (40\,ft)(2\,k/ft) + (10\,ft)(2.9\,k/ft) + (15\,ft)(6\,k/ft) = 199\,kips$$

and the nominal base resistance equals:

$$R_b = 9 \cdot s_u \cdot B^2 = 9 \cdot (3000\,psf) \cdot (1\,ft)^2 = 27000\,lb = 27\,kips$$

.

The total nominal pile resistance, R_n, is equal to 226 kips. Because the pile cap is in contact, the group efficiency factor (η_g) is equal to 1.0 (Table 6-26). The resistance factor is equal to 0.35, and the factored combined single pile capacity for is equal to

$$n(\eta_g R_{r,s}) = 49(1.0 \cdot 0.35 \cdot 226\,kips) = 3876\,kips\,.$$

Since the pile group includes more than 4 piles, a 20% reduction to the resistance factor is not needed. The resistance against block failure is checked according to

$$R_{n,gblock} = 2 \cdot L \cdot (B + Z) \cdot s_{u,1} + B \cdot Z \cdot s_{u,2} \cdot N_c$$

where L, B, and Z are the pile group dimensions provided in Figure 6-15 and N_c is the bearing capacity factor found by:

$$N_c = 5\left(1+0.2\frac{18\,ft}{18\,ft}\right)\left(1+0.2\frac{60\,ft}{18\,ft}\right) = 10 \rightarrow \text{Use maximum value of } N_c = 9$$

The weighted average shear strength along the sides of the block, $s_{u,1}$, is found by

$$s_{u,1} = \frac{s_{u,soft}L_{soft} + s_{u,stiff}L_{stiff}}{L_{soft} + L_{stiff}} = \frac{(0.5\,ksf)(40\,ft)+(3ksf)(20\,ft)}{60\,ft} = 1.33ksf$$

and the shear strength at the base of the block, $s_{u,2}$, is equal to 3 ksf.

Using these values, the nominal resistance again block failure is equal to

$$R_{n,gblock} = 2\cdot(60\,ft)\cdot(18\,ft+18\,ft)(1.33ksf)+(18\,ft)(18\,ft)(3ksf)(9) = 14494\,kips$$
$$R_{r,gblock} = 0.6(14494\,kips) = 8696\,kips$$

After applying a reduction factor equal to 0.6 for resistance to block failure, the combined single pile capacity is determined to control the capacity of the group:

$$R_{r,g} = \min\begin{cases} n(\eta_g R_{r,s}) = 3876\,kips \\ R_{r,gblock} = 8696\,kips \end{cases} = 3876\,kips$$

The geotechnical strength limit state is checked by comparing the factored resistance to the factored load acting on the pile group. The trial design is adequate with respect to the geotechnical strength limit state because the factored resistance is greater than or equal to the factored resistance:

$$3876\,kips = R_{r,g} \geq Q'_g = 3520\,kips\,.$$

B-5.5 Neutral Plane Analysis.

The unfactored permanent load and resistance curves for the trial design are shown in Figure B-18. The load curve was generated by computing the permanent load acting on the top of each pile and adding the accumulated drag force according to the due to negative skin friction according to

$$P_z = Q_d - \sum \Delta p_{soil}\cdot z_{soil}$$

where:
P_z = load in the pile as a function of depth,

Q_d = unfactored permanent load acting on top of a single pile,
Δp_{soil} = unit load transfer for each soil layer, and
z_{soil} = the depth below the top of each soil layer.

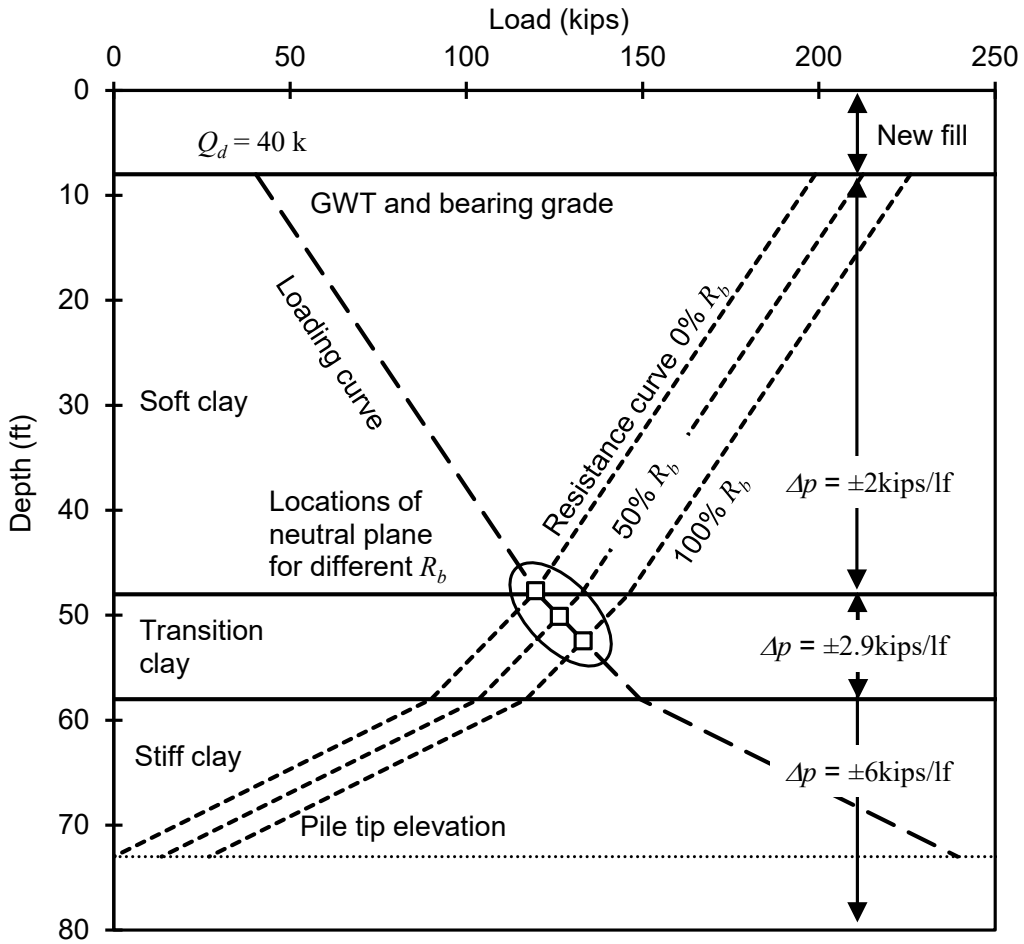

Figure B-18 Load and Resistance Curves

Based on the adopted sign convention, values of Δp_{soil} are negative. In this example, each pile is assumed to carry equal load; therefore, for 49 piles the load equals

$$Q_d = \frac{1976\,kips}{49} = 40\,kips\,.$$

The resistance curves shown in Figure B-18 were generated by computing the nominal single-pile geotechnical resistance and subtracting the accumulated resistance along the pile according to

$$R_z = R_n - \sum \Delta p_{soil} \cdot z_{soil}$$

where:
R_z = nominal geotechnical resistance as a function of depth.

Based on the adopted sign convention, values of Δp_{soil} are positive. To address uncertainty about the mobilization of base resistance, resistance curves are provided for 0%, 50%, and 100% mobilization of base resistance as recommended by Siegel et al. (2013).

The neutral plane is located at the intersection of the load curve with the resistance curve. The maximum load in the pile occurs at the neutral plane. It is apparent from Figure B-18 that mobilization of base resistance increases the depth of the neutral plane. The depth of the neutral plane is also increased by reducing the load applied to the top of the pile and increasing the penetration depth of the pile. As shown in Section 6-5.8.4, the estimated settlement increases as the position of the neutral plane moves closer to the top of the pile.

Table B-28 summarizes the key information used to generate and interpret the load and resistance curves for the trial pile design. The curves change with changes to the design, e.g. changes to the size, number, and/or length of piles.

Table B-28 Key Values for Load and Resistance Curves

Depth below ground surface, z (ft)	Loading curve values (kips)	Resistance curve values (kips), $R_b = 0\%$	Resistance curve values (kips), $R_b = 50\%$	Resistance curve values (kips), $R_b = 100\%$
8	40	199	213	226
48	120	119	133	146
58	149	90	104	117
73	239	0	14	27
Depth to neutral plane below ground surface, z_{np} (ft)		48	50	52
Max load in the pile, P_{max} (kips)		120	126	133

B-5.6 Structural Strength Limit State Analysis.

The factored structural resistance of the pile in compression, P_r, is equal to 200 kips as given in Section B-5.1. The factored resistance must be greater than or equal to the factored permanent load, including the largest drag force estimated by the neutral plane analysis in Section B-5.5. The check performed using Equation 6-80 in Section 6-7.4 shows that the trial design is acceptable with respect to the structural strength limit state:

$$1.25 \cdot Q_d + 1.1\left(Q_{np} - Q_d\right) \le P_r$$
$$1.25\left(40\,kips\right) + 1.1\left(133\,kips - 40\,kips\right) \le 200\,kips$$
$$152\,kips \le 200\,kips$$

B-5.7 Settlement Analysis.

Settlement of the pile cap is evaluated considering consolidation of the clay below the neutral plane and elastic compression of the piles above the neutral plane.

The ultimate consolidation settlement of the clay below the neutral plane is estimated using an equivalent footing located at the neutral plane. The vertical stress in the soil below the footing is increased due to the weight of the new fill and the unfactored permanent load shed from the piles to the ground. As stated in Section B-5.2, this analysis conservatively ignores the effects that piles can have on the ground which tend to stiffen the soil, i.e. decrease compressibility, and shield the soil within the pile group from increases in stress due to surface loads.

As demonstrated in Section B-5.2, the position of the neutral plane depends on many factors, including the degree to which base resistance is mobilized. The details of the settlement analysis assuming 50% mobilization of base resistance are presented here; however, settlements for 0% and 100% mobilization are also provided. Estimated settlement decreases as the assumed mobilization of base resistance increases.

For 50% mobilization of base resistance, the neutral plane is located 50 ft below the final ground surface. The equivalent footing positioned at the neutral plane has dimensions B and L equal to 18 ft based on the 7x7 square arrangement of piles on a 3-ft center-to-center spacing. Table 29 provides the boundaries, initial thickness, H_0, and average vertical effective stress ($\sigma'_{z,0}$) for ten compressible sublayers located below the footing. The boundaries for the sublayers were chosen to concentrate thin layers at the top of the profile where changes in stress are largest and to terminate the overall profile considered in the analysis at the depth where the stress change due to the equivalent footing falls below 10% of the initial vertical effective stress as recommended by FHWA (2016).

Table B-29 Delineation of Compressible Soil Profile and Initial Vertical Stress

Sublayer	z_{top} (ft)	H_0 (ft)	z_{bot} (ft)	z_{mid} (ft)	$\sigma'_{z,0}$ (psf)
1	50	1	51	50.5	1737.5
2	51	2	53	52	1820
3	53	2	55	54	1930
4	55	4	59	57	2095
5	59	4	63	61	2315
6	63	6	69	66	2590
7	69	6	75	72	2920
8	75	8	83	79	3305
9	83	8	91	87	3745
10	91	8	99	95	4185

The position of the neutral plane is below the bottom of the soft clay. Thus only the stiff clay is represented in the settlement analysis with properties given in Figure B-16. For each sublayer, Table B-30 presents the preconsolidation stress (σ'_c), stress change due to placement of the new fill ($\Delta\sigma_{z,fill}$), stress change due to the pile group loads ($\Delta\sigma_{z,piles}$), final effective stress ($\sigma'_{z,f}$), vertical strain ($\varepsilon_{z,ult}$), and compression (ΔH). Strain calculations are performed according to:

$$\varepsilon_{z,ult} = C_{\varepsilon r} \log\left(\frac{\min\left(\sigma'_p, \sigma'_{zf}\right)}{\sigma'_{z0}}\right) + C_{\varepsilon c} \log\left(\frac{\max\left(\sigma'_p, \sigma'_{zf}\right)}{\sigma'_p}\right).$$

Table B-30 Consolidation Settlement Calculations

Sublayer	σ'_c (psf)	$\Delta\sigma_{z,fill}$ (psf)	$\Delta\sigma_{z,piles}$ (psf)	σ'_{zf} (psf)	$\varepsilon_{z,ult}$	H_0 (ft)	ΔH (ft)
1	6737.5	960	5774	8471	0.0158	1	0.016
2	6820	960	4940	7720	0.0111	2	0.022
3	6930	960	4083	6973	0.0058	2	0.012
4	7095	960	3162	6217	0.0047	4	0.019
5	7315	960	2350	5625	0.0039	4	0.015
6	7590	960	1709	5259	0.0031	6	0.018
7	7920	960	1235	5115	0.0024	6	0.015
8	8305	960	895	5160	0.0019	8	0.015
9	8745	960	653	5358	0.0016	8	0.012
10	9185	960	498	5643	0.0013	8	0.010
						$\Sigma\Delta H$ =	0.15

The sum of the sublayer compressions provides the estimated magnitude of ultimate consolidation settlement, $\delta_{c,ult}$, equal to 0.15 ft (1.9 in).

The elastic compression of the piles above the neutral plane is due to the permanent load applied to the pile and the drag force. Elastic compression is evaluated by discretizing the pile into intervals of length that can be reasonably modeled by an average axial load, $P_{z,avg}$. The compression of each interval is estimated according to

$$\Delta L = \frac{P_{z,avg} \cdot L_0}{E \cdot A}$$

where:
L_0 = initial length of the interval of pile above the neutral plane,
E = Young's Modulus of the pile material, and
A = area of the pile cross section.

Table B-31 summaries the elastic compression calculations. The magnitude of elastic compression, δ_e, is estimated to equal 0.006 ft (0.1 in), which is an amount that is arguably smaller than what can be estimated using simple elastic methods.

Table B-31 Estimated Elastic Compression of the Piles above the Neutral Plane

Sublayer	z_{top} (ft)	L_0 (ft)	z_{bot} (ft)	z_{mid} (ft)	$P_{z,bot}$ (kips)	$P_{z,top}$ (kips)	$P_{z,avg}$ (kips)	ΔL (ft)
1	8	40	48	28	120	40	80	0.0056
2	48	2	50	49	126	120	123	0.0004

The total estimated settlement for the trial design, assuming 50% mobilization of base resistance is equal to 2.0 inches, which is below the limit of 3 inches. For the case of 0% base resistance, the settlement increases slightly to 2.1 inches and for the case of 100% base resistance, the estimated settlement remains equal to 2.0 inches. Therefore, the settlement is not significantly sensitive to the mobilization of base resistance for the conditions considered in the analysis.

B-5.8 Conclusions from Analysis.

Based on the analysis provided herein, a square arrangement of 49 piles having an embedded length of 65 ft below the bottom of the pile cap is satisfactory with respect to the geotechnical limit state (Section B-5.4), structural strength limit state (Section B-5.6), and serviceability limit state with respect to settlement (Section B-5.7).

However, if a portion of the transient live load is included in the neutral plane and settlement analysis, the depth of the neutral plane decreases. If the neutral plane is located within the soft clay, the estimated settlement can increase significantly. For example, for the case where 50% of the transient load is included in the neutral plane and settlement analysis, i.e. the unfactored load on each pile is 46.5 kips, and it is assumed that 0% of base resistance is mobilized, the neutral plane moves from the previously-estimated depth of 50 ft to a depth of 46 ft, which is 2 ft above the bottom of the normally-consolidated soft clay. The combination of the increased load on each pile and the shallower neutral plane, increases the estimated settlement from 2 inches to 4.8 inches, which exceeds the serviceability limit of 3 inches. The majority of the additional settlement is due to compression of the normally-consolidated soft clay below the neutral plane. However, if the stiffening effects of the piles are taken into account, for example by placing the equivalent footing at the bottom of the piles, the estimated settlement decreases from 4.8 inches to 1.9 inches.

Therefore, designers should carefully consider the characterization of subsurface conditions, the loads used, and assumptions made for this type of analysis. It is also important to consider the potential for stress overlap from nearby loads, e.g. adjacent pile caps.

B-6 EXAMPLE 6 – LATERAL LOAD ANALYSIS.

B-6.1 Description of the Problem.

For the pile-supported bridge pier considered in Example 5, evaluate the serviceability state limit with respect to lateral deflection of the pile cap due to an applied longitudinal shear load of 300 kips, i.e. a shear load parallel to the bridge span. The 300 kip load is comprised of a 100 kip permanent load and a 200 kip transient load. Transverse shear loads and applied moments are equal to zero in this example. Figure B-19 provides useful information for this example.

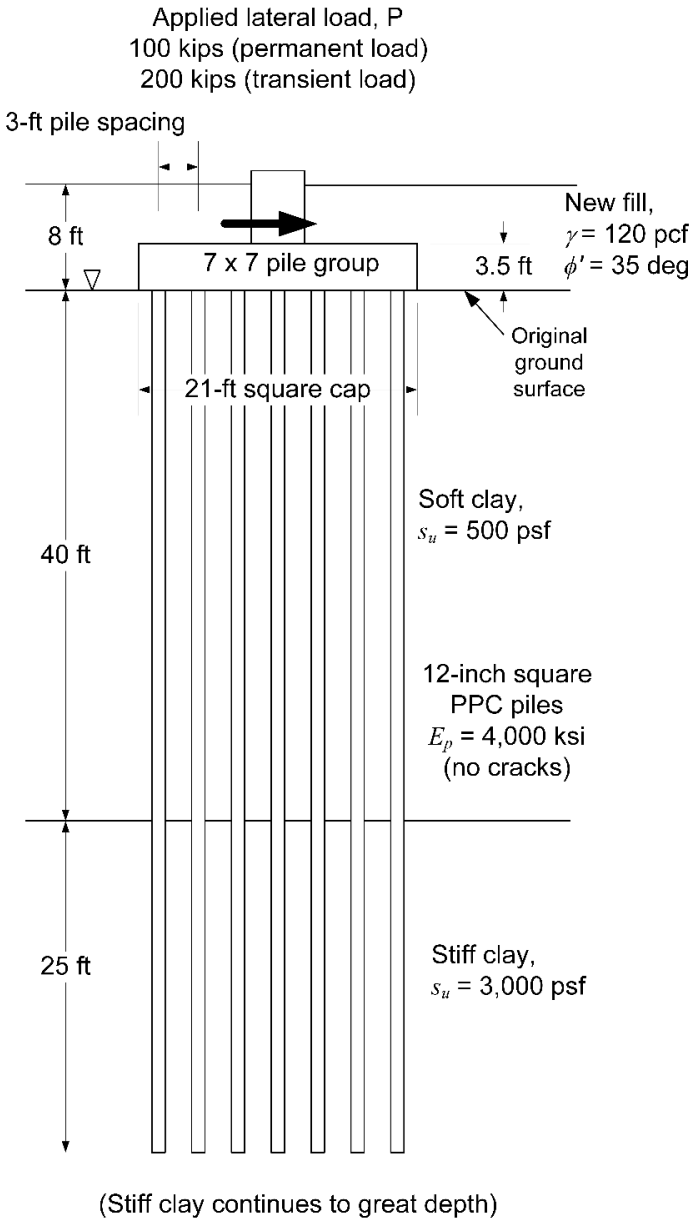

Figure B-19 Laterally Loaded Pile Group in Soft and Stiff Clay

B-6.2 Goals and Limitations of the Analysis.

The goal of this analysis is to determine whether the trial pile design analyzed in Example 6 satisfies the geotechnical strength limit state and serviceability limit state with respect to lateral deflection of the pile cap. The performance requirements as well as assumptions and simplifications are listed below:

- Both the geotechnical strength and service limit states only consider the application of shear load at the cap elevation, i.e. no moment is applied to the cap. The geotechnical resistance of the piles and pile cap are unfactored for both limit states. For the geotechnical strength limit state, the inverse of the resistance factor, equal to 0.8, is applied to the factored load, i.e. 1/0.8 = 1.25 (see Section 6-6.2.1).
- The geotechnical strength limit state is evaluated using load factors equal to 1.25 for permanent loads and 1.75 for transient loads. In actual design, factored load demands are typically determined using an iterative process of structural modeling and foundation response.
- The serviceability limit state with respect to lateral deflection is evaluated using unfactored loads. The limit on lateral deflection of the pile cap is equal to 0.5 inches based on consideration of negative impacts on the superstructure and alignment of the pier.
- The response of the pile group is modeled using the Characteristic Load Method (CLM) (Section 6-6.4.3) as adapted to pile groups (Section 6-6.5).
- The piles are modeled using a constant bending stiffness, i.e. nonlinear effects from concrete cracking are not considered. In this case, this assumption is deemed reasonable since the deflection limit is small. Furthermore, the effects of axial load on bending resistance and lateral deflection are not considered.
- The response of the pile cap is modeled using Rankine earth pressure theory and the simplified hyperbolic load-deflection relationship presented in Section 6-6.5.
- The piles are embedded a minimum of 12 inches into the pile cap; however, the degree of fixity is unknown.
- Scour and seismic considerations are not addressed in this example.

This analysis includes estimating the maximum bending moment developed in the piles for the serviceability limit state. This moment is not the value used to evaluate the structural strength limit state.

B-6.3 Characteristic Load Method Analysis

The CLM is suitable for modeling long piles in uniform ground. Since the pile length exceeds $18 \cdot b$ (18ft), the piles meet the minimum length requirement of the CLM. Since the upper $8 \cdot b$ (8ft) of the pile is in uniform soft clay, the ground conditions meet the uniform ground requirement of the CLM.

B-6.3.1 Calculation of p-Multiplier

Due to pile-soil-pile interaction, the softening of the p-y response of the ground is captured using a weighted average p-multiplier. There are 7 rows of piles aligned perpendicular to the applied lateral load. Table B-32 summarizes calculation of the weighted average p-multiplier as proposed by Mokwa (1999) using the equations in Table 6-38 for a normalized spacing, s/b, equal to 3.

Table B-32 Calculation of Weighted p-Multiplier

***p*-Multiplier**	**Equation and Result**
1st row	$p_m = 0.06(3) + 0.64 = 0.82$
2nd row	$p_m = 0.11(3) + 0.34 = 0.67$
3rd row	$p_m = 0.14(3) + 0.16 = 0.58$
4th – 7th rows	$p_m = 0.16(3) + 0.04 = 0.52$
Average: $p_m = (0.82 + 0.67 + 0.58 + 0.52 + 0.52 + 0.52 + 0.52) / 7 = 0.593$	

B-6.3.2 Calculation of the Characteristic Load and Moment.

The characteristic load and moment are calculated for the PPC pile in soft clay according to equations provided in Table 6-29 in Section 6-6.4.3. These equations require finding the ratio (R_I) of the moment of inertia of the pile section (I_p) to the moment of inertia of a solid circular section (I_{circ}). For an uncracked solid square section,

$$R_I = \frac{I_p}{I_{circ}} = \left(\frac{64}{\pi b^4}\right)\left(\frac{b^4}{12}\right) = 1.70$$

Applying the conditions considered in this example, the characteristic load equals:

$$P_c = 7.34(12\,in)^2\,(4000ksi)(1.70)\left(\frac{(500\,psf)(0.593)}{(4000\,ksi)(1.70)(144000\,psf/ksi)}\right)^{0.68} = 265\,kips$$

and the characteristic moment equals:

$$M_c = 3.86(12\,in)^3\,(4000ksi)(1.70)\left(\frac{(500\,psf)(0.593)}{(4000\,ksi)(1.70)(144000\,psf/ksi)}\right)^{0.46} = 45457\,in-kips\,.$$

B-6.3.3 Lateral Resistance of the Pile Cap.

The embedded pile cap is assumed to mobilize some amount of passive resistance on the leading face, full active pressure on the trailing face, and no shear resistance on the sides and base (Figure B-20). The resistance provided by the pier is also ignored.

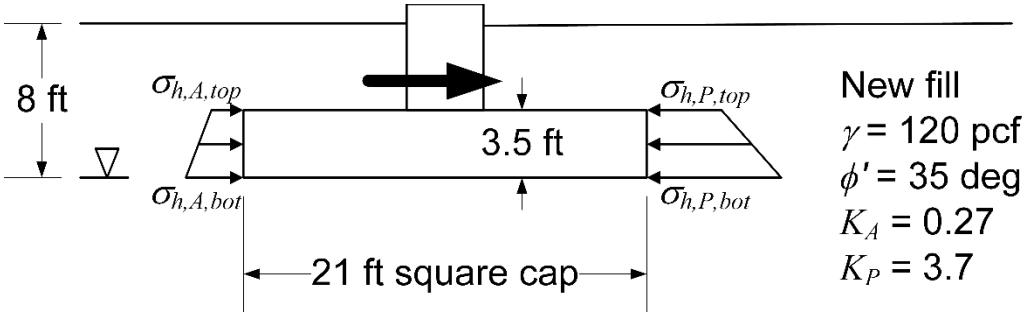

Figure B-20 Development of Active and Passive Pressures on Pile Cap

For the sand surrounding the pile cap having a friction angle of 35 degrees, the Rankine active and passive coefficients are equal to 0.27 and 3.7, respectively. As mentioned in Section 6-6.5, the use of Rankine earth pressure theory results in a conservative (in some cases excessively conservative) estimate of passive resistance. Table B-33 presents the fully-mobilized active and passive pressures and calculation of the active and passive earth forces.

Table B-33 Pile Cap Pressure Calculations

Calculation	Active side	Passive side
Pressure at top of cap	$\sigma'_{h,a,top}$ = 0.27(4.5 ft)(120 pcf) = 146 psf	$\sigma'_{h,p,top}$ = 1998 psf
Pressure at bottom of cap	$\sigma'_{h,a,bot}$ = 259 psf	$\sigma'_{h,p,bot}$ = 3552 psf
Fully-mobilized lateral earth force	P_a = 0.5(146+259 psf)(3.5 ft)(21 ft)(1 k/1000 lb) = 15 kips	P_p = 204 kips

Assuming that active resistance is fully mobilized by any pile cap deflection and passive resistance is mobilized according to the simplified hyperbolic relationship presented in Section 6-6.5, the resistance provided by the pile cap is equal to

$$P_{cap,mob} = \left[\max \left\{ 204\,kips \left(\frac{y_t}{0.85 y_t + 0.006\left(3.5\,ft\right)\left(12\,in/ft\right)} \right), 15\,kips \right\} \right] - 15\,kips$$

where:
y = average pile cap deflection in inches.

B-6.3.4 Lateral Deflection at the Geotechnical Strength Limit State.

Since the mobilization of cap resistance is a function of deflection, the geotechnical strength limit state is evaluated by incrementally increasing deflection up to a failure criterion defined by a deflection equal to 10% of the pile width. In this case, 1.2 inches of deflection defines the strength limit state. The lateral load at the deflection limit is P_{limit}. The trial design is acceptable if P_{limit} equals or exceeds the factored load multiplied by the inverse of the resistance factor, P'' or:

$$P_{limit} \le \frac{1}{\varphi} P_{factored} = P''$$

$$P'' = \left(\frac{1}{0.8}\right)\left[(1.25)(100\,kips) + (1.75)(200)\,kips\right]$$

A version of Equation 6-67 in Section 6-6.4.3 adapted to the pile group is used to estimate the lateral resistance provided by the piles as a function of deflection.

$$P_{t,group} = (49\ piles)\left(265\frac{kips}{pile}\right)\left(\frac{1}{a}\frac{y_t}{12\,in}\right)^{\frac{1}{n}}.$$

Values for the constants a and n are given in Table 6-31. For piles in clay, the constants a and n are equal to 50 and 1.822, respectively, for a free head condition and 14 and 1.846, respectively, for a fixed head condition.

The average deflection of the pile cap is assumed to equal the deflection at the top of the pile. The combined lateral resistance of the piles and cap, $P_{cap+piles}$, as a function of deflection is found by:

$$P_{cap+piles} = (49\ piles)\left(265\frac{kips}{pile}\right)\left(\frac{1}{a}\frac{y_t}{12\,in}\right)^{\frac{1}{n}} + \left[\max\left\{\begin{matrix}15\,kips \\ 204\,kips\left(\dfrac{y_t}{0.85y_t + 0.252}\right)\end{matrix}\right\}\right] - 15\,kips$$

A series of values of y_t can be assumed and the corresponding lateral resistance is calculated. Figure B-21 shows the development of lateral resistance as a function of deflection for the cases of 0% and 100% fixity. In both cases, the resistance at the failure criterion of 1.2 inches of deflection exceeds the maximum load, indicating that the trail design is acceptable with respect to the geotechnical strength limit state. While rotational restraint is not required to satisfy the geotechnical strength limit state in this example, it is apparent that rotational restraint contributes significantly to the overall lateral stiffness. If a free head condition is present, cap resistance is required to meet the deflection criteria.

B-6.3.5 Lateral Deflection at the Service Limit State.

Figure B-22 shows that the unfactored lateral load of 300 kips produces lateral deflections less than 0.5 inches, regardless of fixity. Cap resistance must be considered to meet this criterion for a free head condition.

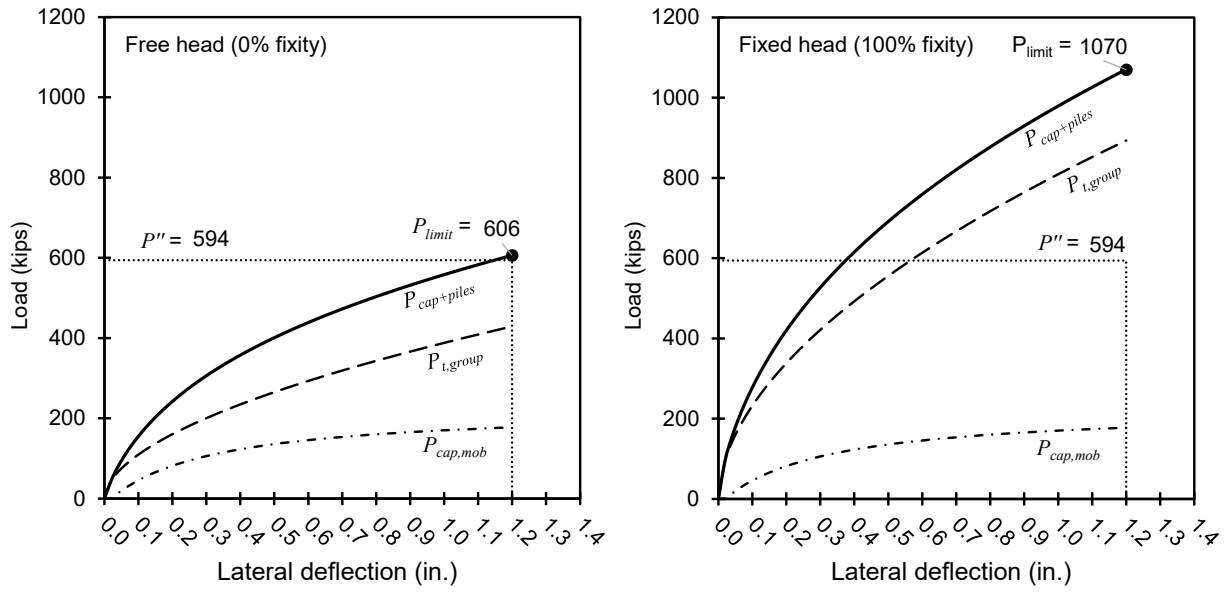

Figure B-21. Load-Deflection Relationship with Strength Limit State Check

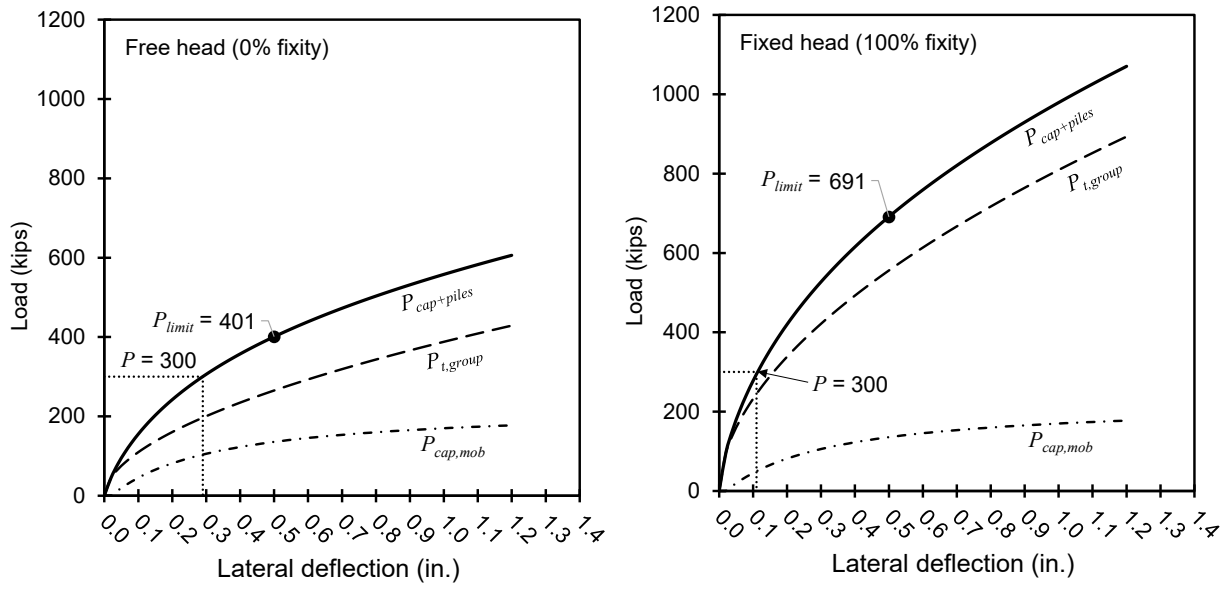

Figure B-22. Load-Deflection Relationship with Service Limit State Check

B-6.3.6 Calculation of Maximum Moment under Service Conditions.

The maximum moments in the piles at the service limit state are found using Equation 6-71 in Section 6-6.4.3. Use of a single weighted p-multiplier to account for group effects implicitly assumes that all piles in the group carry equal load. The maximum moments are corrected for group effects using the moment scaling factors provided in Section 6-6.5. This correction estimates the maximum moment in the corner piles of the lead row, which are expected to experience the highest moments in the pile group. For this example, the equation is:

$$M_{\max} \approx a \cdot M_c \left(\frac{P_t}{P_c} \right)^n \approx a\left(45457\, in-kip\right)\left(\frac{P_t}{265\, kips} \right)^n$$

where for piles in clay:
a = 0.855 for a free head and 0.782 for a fixed head and
n = 1.288 for a free head and 1.249 for a fixed head.

At the service limit state of 0.5 inch deflection, the resistance provided by the pile group is equal to 265 kips. Because the normalized pile spacing is equal to 3, a correction equal to 1.20 (see Section 6-6.5) is applied to estimate the maximum moment for the corner piles in the lead row. With these considerations, the maximum moment in the piles for a free head condition is equal to:

$$M_{\max,corner} = \left(\frac{1.2}{12\, in/ft} \right)\left(0.855\right)\left(45457\, in-kip\right)\left(\frac{259\, kips}{\left(265\, kips\,/\,pile\right)\left(49\, piles\right)} \right)^{1.288} = 26\, ft-kip$$

For fixed head conditions, similar calculations estimate a maximum moment equal to 69 ft-kips at the service limit state deflection of 0.5 inches.

Under service conditions, where an unfactored load of 300 kips is anticipated, the load-deflection relationships provided in Figures B-21 and B-22 can be interpreted to extract the portion of the resistance provided by the piles, $P_{t,group}$. Alternatively, the equation for $P_{cap+piles}$ can be solved for y_t corresponding to the unfactored load and that value of y_t can be used to find $P_{t,group}$. Table B-34 summarizes the values of y_t, $P_{t,group}$, and $M_{max,corner}$ for the applied unfactored load.

Table B-34 Deflection, Lateral Pile Load, and Maximum Moment due to Unfactored Loading

Parameter	Free head (0% fixity)	Fixed head (100% fixity)
y_t	0.29 in.	0.11 in.
$P_{t,group}$	197 kips	249 kips
$M_{max,corner}$	18 ft-kips	25 ft-kips

B-6.4 Conclusions from the Analysis.

Based on this analysis, the trial pile design satisfies the geotechnical strength limit state and the serviceability limit state with respect to lateral deflection. Given that the piles are embedded in the cap 1 ft, there is some amount of rotational restraint that can be justified in the design. Referring to Table B-34, the contribution of rotational restraint means that lateral deflection is expected to be less that 0.29 inches.

B-7 EXAMPLE 7 – RELIABILITY ANALYSIS OF A RETAINING WALL.

B-7.1 Description of the Problem.

A concrete, cantilever gravity retaining wall is being designed as shown in Figure B-23. The parameters shown in Table B-35 were assumed to be random variables with the properties provided. Note that the uncertainty in concrete unit weight is being used as a proxy for both the material variation and uncertainty in the structural dimensions. Any covariance between the parameters is being ignored.

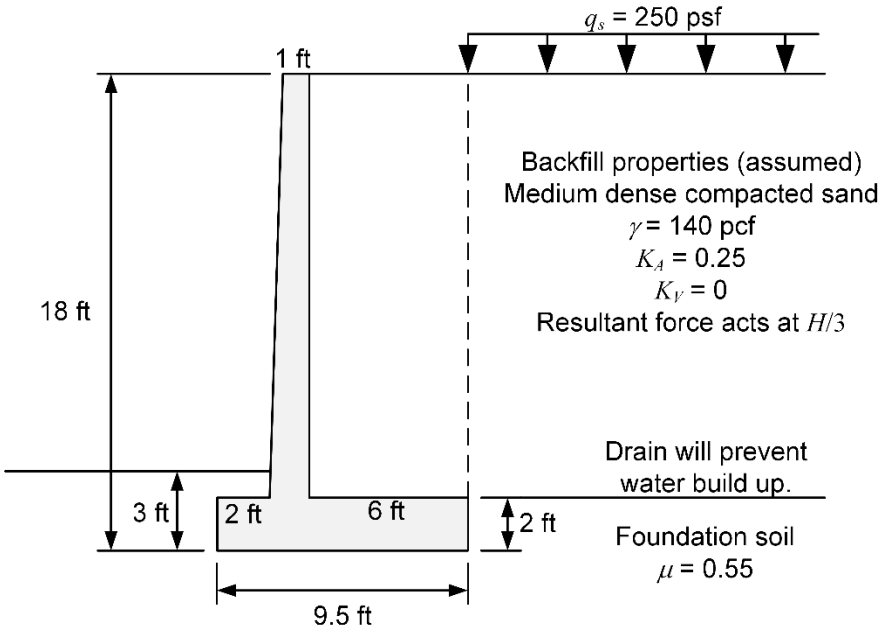

Figure B-23 Proposed Cantilever Retaining Wall

All four methods discussed in Chapter 7 will be used to evaluate the reliability of the wall design for overturning, sliding, bearing capacity, and settlement. Each section will focus on one of the methods and provide comparative results from the others.

Table B-35 Probabilistic Material Properties for Wall Design

Parameter or RV	Mean	Std. Dev.	COV	Comment
Backfill unit weight	140 pcf	16 pcf	11.4%	Table 7-4: Assumed value indicates high uncertainty
Backfill earth pressure coefficient	0.25	0.04	16%	Table 7-4: Assumed value indicates high uncertainty. Based on typical COV for friction angle.
Surcharge	250 psf	50 psf	20%	Judgment. Similar to load factor of 1.2.
Concrete unit weight	150 pcf	5 pcf	3.3%	High quality formwork and QA/QC will result in low uncertainty.
Base friction coefficient	0.55	0.07	13%	Table 7-4: Assumed value with moderate to high uncertainty. Based on typical COV for friction angle.
Wall height	18 ft	0.2 ft	1.1%	High quality construction will result in low uncertainty in wall dimensions.
All RV were assumed to be normally distributed.				

B-7.2 Overturning.

For overturning, a wall supported on soil must either meet a minimum factor of safety (F_{OT}) or the resultant must be within the middle one-third of the wall base. If the latter requirement is used, the entire base will be under compression, and the F_{OT} will typically far exceed 1.5. F_{OT} reaches unity as x_0 approaches zero, which means the limit state function can be defined as:

$$g(x) = x_0$$

where:
x_0 = horizontal distance of the resultant from the toe of the wall.

Using the mean values, the resultant is 3.35 ft from the toe, which is close to the middle one-third critierion. However, a positive value of the limit state function indicates a safe condition for overturning, even though values lower than $B/3$ indicate some loss of compression below the base. The approximate FOSM approach was used to evaluate overturning with the calculations summarized in Table B-36. Each of the five RV that affects overturning was systematically varied up or down one standard deviation. The difference in the limit state function for each pair of variation was divided by two and squared as an estimate of the variance from that variable. The square root of the sum of the individual variances gives an estimate of the standard deviation of the limit state function.

The reliability index is calculated as:

$$\beta_{x_0} = \frac{\mu_{x_0}}{\sigma_{x_0}} = \frac{3.35}{0.385} = 8.72 .$$

Table B-36 FOSM Approximation for Retaining Wall Example

Trial	γ_c (pcf)	γ_t (pcf)	q_s (psf)	K_a	H (ft)	x_N (ft)	$(\Delta g(x)/2)^2$
1	155	140	250	0.25	18	3.36	0.00002
2	145	140	250	0.25	18	3.35	
3	145	156	250	0.25	18	3.39	0.00207
4	145	124	250	0.25	18	3.30	
5	150	140	300	0.25	18	3.25	0.01071
6	150	140	200	0.25	18	3.46	
7	150	140	250	0.29	18	2.99	0.13026
8	150	140	250	0.21	18	3.71	
9	150	140	250	0.25	18.2	3.28	0.00482
10	150	140	250	0.25	17.8	3.42	
						Sum:	0.14788
						Estimated standard deviation of $g(x)$:	0.38456

•

The corresponding probability of overturning is (assuming a normal distribution for $g(x)$):

$$P_u = 1 - \Phi(8.72) = \text{Negligible}.$$

The P_u values are very small, indicating that an overturning failure is very unlikely for this case. The value of F_{OT} for the mean values is 2.49.

Table B-37 Summary of Probabilities of Unsatisfactory Overturning Resistance

Method	β_{x0}	P_u
FOSM by derivatives	6.45	6×10^{-11}
Approximte FOSM	8.72	Negligible
Point Estimate	8.69	Negligible
Hasofer Lind	7.41	6×10^{-14}
Monte Carlo (100,000 trials)	No failures encountered	
Calculations assume a normal distribution of x_0.		

B-7.3 Sliding.

The factor of safety against sliding at the mean values is 1.58. The reliability will be assessed by calculating the FOSM derivatives directly and using the Hasofer-Lind method. Sliding resistance depends on the weight and volume of the wall and backfill. The concrete volumes are $V_{c,base}$ = 19 ft^3/ft and $V_{c,stem}$ = 20 ft^3/ft. The soil volumes are V_{bf} = 96 ft^3/ft (backfill) and V_{ff} = 2 ft^3/ft (soil above toe).

The limit state function will be expressed as:

$$g(x) = F_{SL} - 1 = \frac{\gamma_c \mu \left(V_{c,base} + V_{c,stem}\right) + \gamma_t \mu \left(V_{bf} + V_{ff}\right)}{q_s K_a H + 0.5\gamma_t K_a H^3} - 1 = \frac{39\gamma_c \mu + 98\gamma_t \mu}{q_s K_a H + 0.5\gamma_t K_a H^3} - 1$$

Evaluating the first derivatives of *g(x)* with respect to each variable at the mean values:

$$\frac{\partial g}{\partial \gamma_c} = \frac{39\mu}{q_s K_a H + 0.5\gamma_t K_a H^2} = \frac{39(.55)}{(250\,psf)(0.25)(18\,ft) + 0.5(140\,pcf)(.25)(18)^2} = 3.157 \times 10^{-3}\, ft^3 / lb$$

$$\frac{\partial g}{\partial \gamma_t} = \frac{98\mu}{q_s K_a H + 0.5\gamma_t K_a H^2} = \frac{98(.55)}{(250\,psf)(0.25)(18\,ft) + 0.5(140\,pcf)(.25)(18)^2} = 7.932 \times 10^{-3}\, ft^3 / lb$$

$$\frac{\partial g}{\partial \mu} = \frac{39\gamma_c + 98\gamma_t}{q_s K_a H + 0.5\gamma_t K_a H^2} = \frac{(39)(150\,pcf) + (98)(140\,pcf)}{(250\,psf)(0.25)(18\,ft) + 0.5(140\,pcf)(.25)(18)^2} = 2.88$$

$$\frac{\partial g}{\partial q_s} = \frac{-(39\gamma_c + 98\gamma_t)\mu K_a H}{\left(q_s K_a H + 0.5\gamma_t K_a H^2\right)^2} = \frac{-\left((39)(150\,pcf) + (98)(140\,pcf)\right)(0.55)(0.25)(18)}{\left[(250\,psf)(0.25)(18\,ft) + 0.5(140\,pcf)(.25)(18)^2\right]^2} = -1.05 \times 10^3\, ft^2 / lb$$

$$\frac{\partial g}{\partial K_a} = \frac{-(39\gamma_c + 98\gamma_t)\mu}{\left(q_s H + 0.5\gamma_t H^2\right) K_a^2} = \frac{-\left((39)(150\,pcf) + (98)(140\,pcf)\right)(0.55)}{\left[(250\,psf)(18\,ft) + 0.5(140\,pcf)(18)^2\right](0.25)^2} = -6.336$$

$$\frac{\partial g}{\partial H} = \frac{-(39\gamma_c + 98\gamma_t)\mu\left(q_s K_a + \gamma_t K_a H\right)}{\left(q_s K_a H + 0.5\gamma_t K_a H^2\right)^2}$$

$$= \frac{-\left((39)(150\,pcf) + (98)(140\,pcf)\right)(0.55)\left((250)(0.25) + (140\,pcf)(0.25)(18\,ft)\right)}{\left((250\,psf)(0.25)(18\,ft) + 0.5(140\,pcf)(.25)(18)^2\right)^2} = -.1614\, ft^{-1}$$

The mean value of the limit state function is estimated by:

$$\mu_{g(x)} = F_{SL}\big|_{MV} - 1 = 1.58 - 1 = 0.58\,.$$

The estimated variance of the limit state function is:

$$\sigma_{g(x)}^2 \approx \left(\frac{\partial g}{\partial \gamma_c}\right)^2 \sigma_{\gamma_c}^2 + \left(\frac{\partial g}{\partial \gamma_t}\right)^2 \sigma_{\gamma_t}^2 + \left(\frac{\partial g}{\partial \mu}\right)^2 \sigma_{\mu}^2 + \left(\frac{\partial g}{\partial q_s}\right)^2 \sigma_{q_s}^2 + \left(\frac{\partial g}{\partial K_a}\right)^2 \sigma_{K_a}^2 + \left(\frac{\partial g}{\partial H}\right)^2 \sigma_H^2$$

$$\sigma_{g(x)}^2 \approx \left(3.076\times10^{-3}\, pcf^{-1}\right)^2 \left(5\, pcf\right)^2 + \left(7.892\times10^{-3}\, pcf^{-1}\right)^2 \left(16\, pcf\right)^2 + \left(2.88\right)^2 \left(0.07\right)^2$$

$$+\left(1.05\times10^{-3}\, psf^{-1}\right)^2 \left(50\, psf\right)^2 + \left(6.336\right)^2 \left(0.04\right)^2 + \left(0.1596\, ft^{-1}\right)^2 \left(0.2\, ft\right)^2$$

$$\sigma_{g(x)}^2 \approx 0.125$$

$$\sigma_{g(x)} \approx 0.354$$

The reliability index is:

$$\beta_{F_{SL}} = \frac{\mu_{g(x)}}{\sigma_{g(x)}} = \frac{1.58-1}{0.354} = 1.64\,.$$

Table B-38 Summary of Probabilities of Unsatisfactory Sliding Resistance

Method	β_F	P_u
FOSM – derivatives	1.64	5%
Taylor Series – approximate derivatives	1.67	4.7%
Point Estimate	1.84	3.3%
Hasofer Lind	2.22	1.3%
Monte Carlo (100,000 trials)	2.22	1.3%
Calculations assume a normal distribution of F_{SL}.		

B-7.4 Bearing Capacity.

For the analysis of bearing capacity, the Meyerhof method was selected. The backfill loads cause the pressure on the base of the foundation to be eccentric and inclined. The applied bearing pressure (q_{net}) using the equivalent footing approach is:

$$q_{net} = \frac{R}{2 \cdot x_0}$$

where:
R = vertical component of the load on the footing (including the surcharge) and
x_0 = horizontal distance of R from the toe of the wall.

Using the mean values of the parameters, R is 21,070 lb/ft and x_0 is 3.58 ft (different from the overturning analysis above because the surcharge has been included). The applied bearing pressure is 2945 psf.

The load inclination (θ) can be found based on the vertical reaction and the horizontal reaction (T):

$$\theta = \tan^{-1}\left(\frac{T}{R}\right)$$

The bearing capacity for the foundation with the inclined load is found as:

$$q_{ult} = \sigma_{zD} \cdot N_q \cdot i_q + 0.5 \cdot B' \cdot N_\gamma \cdot i_\gamma$$

where:
σ_{zD} = vertical stress at footing depth at toe = (3 ft)(140 pcf) = 420 psf,
B' = $2x_0$,
Nq and N_γ = Meyerhof bearing capacity factors = function of friction angle,
i_q = inclination factor = $(1 - \theta / 90)^2$, and
i_γ = inclination factor = $(1 - \theta / \phi')^2$.

Using the mean values, B' is 7.16 ft, N_q = 33, N_γ = 37, i_q = 0.64, and i_γ = 0.24. The resulting ultimate bearing capacity is 13338 psf. The calculated factor of safety for the mean values is 4.53.

The inclination factors and bearing capacity factors both have complex dependence on the random variables. A closed-form expression of the factor of safety will be cumbersome to manipulate, so the direct FOSM and Hasofer-Lind methods will not be considered for bearing capacity. Note that Filz and Navin (2006) present a simplified version of Hasofer-Lind that does not require a closed-form solution but for brevity is not presented here.

The approximate FOSM approach was performed first. The results are presented in Table B-39 for all six RV.

Table B-39 Approximate FOSM Analysis of Bearing Capacity

Variable	*F+*	*F-*	$(\Delta g(x)/2)^2$	Percentage of Variance
γ_t (pcf)	4.53	4.53	2.4 x 10-6	0%
γ_c (pcf)	4.65	4.38	0.017	0.4%
ϕ' (deg)	5.22	2.84	1.42	35%
q_s (psf)	6.73	4.78	0.948	23.4%
K_a	3.43	5.98	1.63	40.2%
H (ft)	4.33	4.73	0.390	1.0%
		Estimated Variance of F:	4.05	
		Estimated Standard Deviation of F:	2.01	
		Reliability Index (Assuming F is normally distributed):	1.75	
		Probability F < 1 (Assuming F is normally distributed):	4%	

The unit weights of the concrete and soil have very little effect on the variance as shown in the final column. For simplicity, these RV will be considered deterministic in the example of the Point Estimate method. For the four remaining RV, a total of $2^4 = 16$ cases must be analyzed for the Point Estimate method as demonstrated in the following table. If the factor of safety is assumed to be normally distributed, the reliability index is 1.48 and the probability of F < 1 is 6.9%.

Table B-40 Point Estimate Analysis of Bearing Capacity

Trial	ϕ' (deg)	q_s (psf)	K_A	H (ft)	q_{app} (psf)	q_{ult} (psf)	F_{BC}	P	$P \times F_{BC}$	$P \times (F_{BC})^2$
1	32	200	0.21	17.8	2590	10440	4.03	0.0625	0.252	1.016
2	38	200	0.21	17.8	2590	28089	10.85	0.0625	0.678	7.353
3	32	300	0.21	17.8	2723	10043	3.69	0.0625	0.231	0.850
4	38	300	0.21	17.8	2723	26975	9.91	0.0625	0.619	6.134
5	32	200	0.29	17.8	3071	7404	2.41	0.0625	0.151	0.363
6	38	200	0.29	17.8	3071	19507	6.35	0.0625	0.397	2.521
7	32	300	0.29	17.8	3284	7064	2.15	0.0625	0.134	0.289
8	38	300	0.29	17.8	3284	18479	5.63	0.0625	0.352	1.979
9	32	200	0.21	18.2	2660	10001	3.76	0.0625	0.235	0.883
10	38	200	0.21	18.2	2660	26844	10.09	0.0625	0.631	6.364
11	32	300	0.21	18.2	2802	9619	3.43	0.0625	0.215	0.737
12	38	300	0.21	18.2	2802	25763	9.20	0.0625	0.575	5.285
13	32	200	0.29	18.2	3211	7034	2.19	0.0625	0.137	0.300
14	38	200	0.29	18.2	3211	18382	5.73	0.0625	0.358	2.049
15	32	300	0.29	18.2	3445	6717	1.95	0.0625	0.122	0.238
16	38	300	0.29	18.2	3445	17414	5.05	0.0625	0.316	1.597
								Subtotals =	5.40	37.96
								Estimated mean =	5.40	
								Estimated variance = $37.96 - 5.40^2$ =	8.79	
								Estimated standard deviation =	2.96	

Monte Carlo simulation was performed in a spreadsheet for all six RV. The RAND() function generates a value on the interval (0,1) which can be treated as a cumulative probability.

Combined with the mean and standard deviation of each RV, random values of each RV were determined using the inverse normal function as:

$$x_i = \Phi^{-1}\left(RAND,\ \mu_x,\ \sigma_x\right) = NORMINV\left(RAND(),\ \mu_x,\ \sigma_x\right)$$

These values were placed in a spreadsheet row followed by all of the calculated moments, dimensions, forces, and bearing capacity factors. The values of q_{net} and q_{ult} are then calculated for each trial and the ratio is determined to find the factor of safety.

An additional column is added which records a "1" every time F < 1. The total number of trials for which F < 1 divided by the total number of trials is equal to the estimated probability of F < 1. For this particular case, the spreadsheet calculated 10,000 trials each time a value was changed. Ten sets of trials were completed resulting in 100,000 trials total. The combined probability of F < 1 was 0.57%, which is lower than predicted by the other methods when F is assumed to be normally distributed.

Table B-41 Monte Carlo Analysis of Bearing Capacity

Method	Normally Distributed F		Lognormally Distributed F	
	β	$P(F<1)$	β	$P(F<1)$
Approximate FOSM	1.75	4.0%	3.35	0.04%
Point Estimate	1.45	6.9%	3.03	0.12%
Monte Carlo	$P(F<1)$ = 0.57%			

In order to investigate this further, one set of 10,000 trials was divided into bins of factor of safety, and a histogram of the frequency was plotted in Figure B-24. The distribution of F is markedly skewed, and visually appears to be lognormal. This could be checked using statistical methods but has not bee completed here.

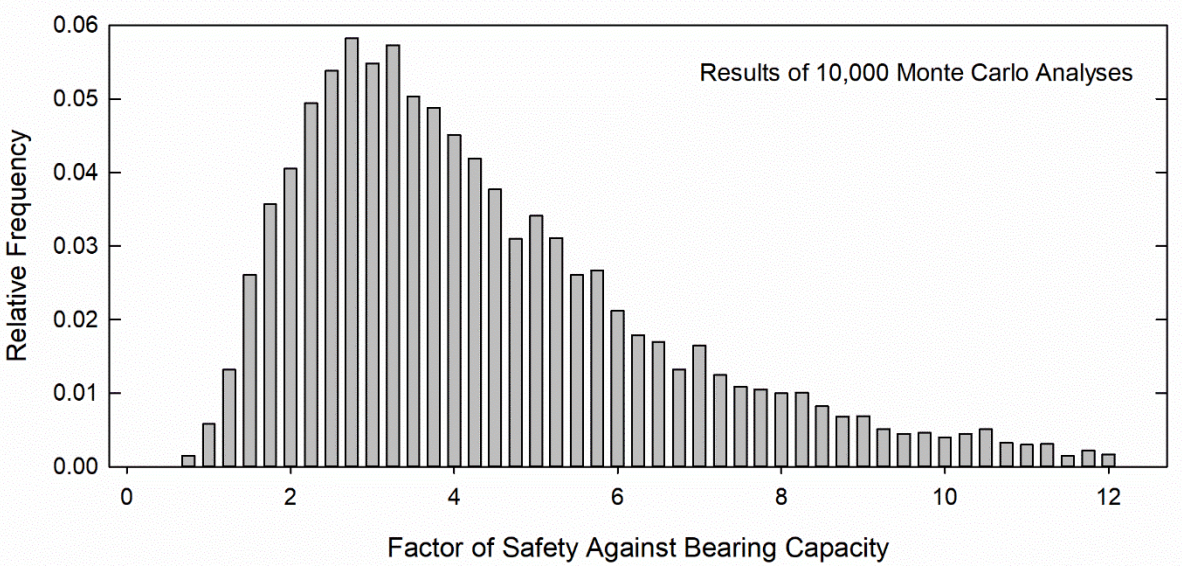

Figure B-24 Distribution of the Factor of Safety from a Subset of the Monte Carlo Analysis of Bearing Capacity

If the Taylor Series and Point Estimate methods are interpreted as lognormal, the probability of F < 1 becomes 0.04% and 0.12%, respectively, which is less than the value determined by Monte Carlo. This indicates that the actual distribution of F is something between normal and lognormal for this problem. This tendency results from

the fact that q_{net} and q_{ult} both have additive (tends toward normal) and multiplicative (tends toward lognormal) components.

In addition, the bearing capacity factors are highly non-linear, and the approximate FOSM and Point Estimate methods would only be expected to produce an approximate estimate of β.

B-7.5 Conclusions from Analysis.

The reliability analyses are for the retaining wall example are summarized in Table B-42. The probability of unsatisfactory performance for sliding is relatively high. To evaluate risk, an estimate of the cost of repair or the potential for loss of life would be required. The high value of P_u for sliding may indicate that the mean factor of safety of 1.58 is too low considering the large uncertainty in some of the input parameters. Another factor to consider for the probabilities in Table B-42 is the time scale. Probabilities and risk are often reported on an annual basis; however, none of the loading factors in this design include timing. Thus, the reported values can be taken as applying over the life of the structure rather than yearly probabilities.

Table B-42 Summary of Probabilistic Stability Checks for Wall Design

Failure Mode	Reliability Index	Probability of Unsatisfactory Performance	Comments / Observations
Overturning – resultant location	6 to 9	Negligible	F assumed to be normally distributed Close agreement between methods
Sliding factor of safety	1.6 to 2.2	5% to 1.3%	F assumed to be normally distributed Hasofer-Lind and Monte Carlo agreed. Other methods underestimate β.
Bearing capacity factor of safety	2.5 to 3	0.6%	Distribution of F appears to fall between normal and lognormal but closer to lognormal based on Monte Carlo simulation.

APPENDIX C. GLOSSARY

Active condition – Stress state in which the soil's shear strength is fully mobilized by lateral movement away from the soil mass, resulting in a corresponding reduction in lateral stress.

Adhesion – Undrained strength of the interface between the soil and a structural material, such as a wall or foundation.

Aeolian soil – Material transported and deposited by wind.

Aggregate columns – Cylindrical columns of gravel constructed in the ground to support loads and/or promote drainage. Borderline technology between ground improvement and deep foundation constructed by drilling a shaft in the ground and backfilling with aggregate.

Aleatory uncertainty – see natural variability.

Allowable bearing pressure – Highest bearing pressure that does not exceed the factored bearing capacity and produces estimated settlements below the design criteria. Often rounded down to a multiple of 500 or 1000 psf.

Alluvial soil – Material transported and deposited by a river or stream.

Alpha Method – Deep foundation static capacity analysis method which finds a coefficient, α, that can be multiplied by the undrained shear strength to determine the unit shaft resistance. The α coefficient accounts for differences in soil disturbance and adhesion caused by soil properties and pile geometry.

Angular distortion – Differential vertical movement between two points divided by distance separating the points.

Apparent earth pressure diagrams – Pressure diagrams semi-empirically drawn to encompass the earth pressures measured in excavations. Actual pressures are likely lower at many depths.

Asperity – Undulation or irregularity in rock fractures. Asperity angle is added to the frictional resistance of rock surfaces.

At-rest condition – Stress state resulting from loading under conditions of no lateral strain.

Autocorrelation – Correlation of a property with the same property at a different point in space or time.

Backward erosion piping (BEP) – Progressive erosion of soil into an internal void or pipe by seepage flow. BEP starts at the downstream or exit end of the flow path.

Basal heave – Tendency of the bottom of an excavation to move upward because of the weight of the soil adjacent to the excavation.

Batter pile – Driven pile installed at an angle to provide lateral as well as axial resistance.

Bearing surface – Interface between the base of a foundation and the underlying soil. The bearing surface is usually horizontal.

Bent – A intermediate support for bridge spans, consisting of the piles and cap.

Beta Method – Deep foundation static capacity analysis method which finds a coefficient, β, that can be multiplied by the vertical effective stress to determine the unit shaft resistance. The β coefficient combines the effects of the horizontal earth pressure coefficient and the interface friction between the soil and pile.

Bin wall – Wall constructed from corrugated steel panels that are bolted together and filled with coarse-grained soils.

Biogeotechnics – Practice of leveraging or mimicking natural biological processes to improve the engineering behavior of a soil.

Blast densification – Use of explosives to cause densification of coarse-grained deposits with little fines.

Blast furnace slag – By-product of iron production. Air-cooled slag is solidified under atmospheric conditions and is angular and vesicular. Expanded slag is solidified using water which increases cellular nature. Granulated slag is chilled quickly forming a glassy product.

Block (group) failure – Bearing failure of a group of deep foundation elements along the sides and at the base of the group.

Borrow – Source of material for an engineered fill.

Bottom heave – Upward movement of the base of an excavation caused by a high upward gradient that exceeds the critical gradient of the soil, a.k.a., a quick condition.

Box and whisker plot – A diagram depicting the mean, median, specified percentiles, and extreme values of a sample.

Box shoring – Timber trench support method that uses horizontal timbers to support the soil. Applicable in any soil. Only limited in depth by the structural strength and size of the timber.

Buckling – Failure mode for unbraced length of piles in compression. Primarily a concern for unsupported piles extending through air, voids, water, and/or liquefied soil.

Bulkhead – Waterfront structure used to allow a change in elevation and access to a body of water.

Bulk-Infill Grouting – Ground improvement technology that uses large quantities of cementitious grout to fill subsurface voids.

Bulking – In the context of earthwork, an increase in soil volume by excavation, transport, and compaction to a different dry unit weight than the borrow material.

Cantilever flexible wall – Flexible wall that relies solely on passive earth pressure for support rather than anchors or bracing.

Cantilever movement – Horizontal movement of the top of a deep excavation wall. Occurs prior to installation of support system

Case Method – Real time use of wave equation analysis and measurements of pile strain and acceleration during driving to estimate nominal pile resistance, hammer and drive system performance, driving stresses, and pile integrity.

Cellular cofferdams – Structures constructed from sheet piles driven in a variety of geometries and filled with soil. Cofferdams perform many purposes, such as creating dewatered construction areas, lock walls, retaining structures, mooring structures, and spillway weirs.

Cellular concrete – Manufactured, preformed foam mixed with cement slurry and pumped into place. Can be pervious.

Chemical grouting or injection – Ground improvement technology that uses grout with no suspended particles to bond soil particles and fill voids. Strengthens the soil and reduces hydraulic conductivity.

Chemical soil stabilization – Ground improvement technology that uses chemical admixtures to reduce plasticity, reduce water content, and/or chemically bound soil or aggregate particles. Admixtures are often lime, portland cement, fly ash, or byproducts.

Clay – Soil particles passing a No. 200 (75-µm) sieve that exhibit plasticity (putty-like properties) within a range of water contents, and considerable strength when air dried.

Clay-sized fraction – The portion of the soil which is finer than 0.002 mm. This is not a viable measure of the plasticity of the material or its characteristics as a clay.

Clearing – In the context of earthwork, the removal of vegetation, trash, debris, and topsoil from the ground surface.

Close (tight) shoring – Timber trench support method that uses continuous upright timbers to support the soil. Useful where seepage and cave-ins are expected.

Coarse-grained soil – Soil that contains more than 50% particles retained on a No. 200 (75 µm) sieve.

Coefficient of variation – Standard deviation of a variable divided by the mean value.

Cohesion intercept – Intercept of a linear failure envelope with the shear stress axis. Can be expressed in terms of either total or effective stress.

Cohesionless soils – Typically used as a synonym for coarse-grained soils. Also an official term in OSHA classification.

Cohesive soils – An overly simplistic term typically used to refer to clayey fine-grained soils because these soils cohere at low normal stress. Also an official term used by in OSHA classification.

Collapse index – Relative collapse from inundation at a stress of 4000 psf.

Collapse potential – Strain caused by wetting at any stress level.

Collapsible soil – Material characterized by a metastable structure that undergo an abrupt collapse when they are inundated. Exhibits large compressive volume change upon wetting.

Colluvial soil – Material transported and deposited by gravity, often found in the vicinity of slopes.

Column-supported embankments – Earth fill supported by a foundation reinforced with vertical elements. The base of the embankment may include a load transfer platform of geosynthetic reinforced soil and/or crushed stone.

Combined footing – Footing supporting more than one column load.

Compaction – Removal of air from soil by temporary application of a mechanical load, such as rolling, tamping, or vibration.

Compaction control – QA process coupled with in-depth testing and observation of the earthwork process appropriate to an owner’s representative.

Compaction grouting – Generally shallow ground improvement technology in which grout is pumped into the ground to displace and compact soil around the created grout bulb.

Compaction plane – Diagram that compares trends in compacted soil behavior that vary with dry unit weight and water content. The dry unit weight vs. water content relationship (a.k.a. compaction curve, Proctor curve, moisture density curve) is plotted on the compaction plane.

Compactive effort – Work performed on soil per unit volume during compaction.

Compensated foundation – Design method used to support heavy structures over compressible strata and reduce settlement. In this approach, the weight of the structure is balanced, completely or partially, by soil that is permanently excavated from the building footprint.

Competent person – Someone capable of identifying hazards or unsafe working conditions who also possesses authority to take corrective measures. See OSHA (2020) Paragraph 652(a)(1)(ii) for the legal definition of competent person.

Compression wave – Seismic wave in which the particles move longitudinally or in the same direction as the wave propagation.

Concentrated leak erosion – Erosion of soil particles at an interface in the soil at which a concentrated flow has developed.

Concrete diaphragm wall – retaining wall system constructed from overlapping concrete wall panels.

Continuous flight auger column – Deep foundation element constructed by inserting a continuous auger into the ground in one continuous operation, after which the hole is filled with grout or concrete under pressure. Reinforcing steel is pushed into the uncured concrete.

Continuous footing – Footing supporting two or more columns in a row or a wall. Continuous foundations are used under wall loads and when the distance between columns is sufficiently close that individual footings can be combined.

Controlled compacted fill – Use of a controlled compaction process to create a soil mass that is more rigid and uniform than most natural soils.

Correlation length – Distance in space or time within which a property is significantly correlated with itself.

Counterfort – Structural support member between the stem and base of a cast-in-place gravity retaining wall. The counterfort provides moment resistance to the stem without increasing the thickness of the entire stem.

Creep – Time-dependent deformation of a soil at a constant effective stress.

Crib wall – Wall constructed of timber or precast concrete beams. Interlocking precast concrete beams are available for rapid wall construction.

Critical height– Maximum height that a vertical excavation in clay soil will stand without support for short term conditions.

Cross-hole sonic logging – Integrity testing method that measures travel time of waves between a transmitter and a receiver in two access tubes embedded in the foundation. Typically used in drilled shafts. Only tests the portion of the foundation between the access tubes.

Cross-lot bracing – Structural element that supports an excavation by spanning between two sides of the excavation.

Cumulative density function – Function defining the probability that a continuous random variable is less than or equal to a particular value.

Cumulative distribution – Plot of the number of observations that are less than a particular value.

Cumulative mass function – Function defining the probability that a discrete random variable is less than or equal to a particular value.

Cut wall – Retaining structure that is inserted into the ground, followed by excavation to create the grade separation.

Dampproofing – Material applied to foundation walls that resists the passage of water under no hydrostatic pressure.

Deadman anchor – Buried discrete or continuous element that uses passive earth pressure to resist anchor forces.

Decision tree – Risk assessment tool that combines probabilities and consequences in graphical form. Decisions are made at each branch between options with different costs or consequences.

Deep and mass mixing – Ground improvement technology that creates strong, stiff elements or zones by mixing soil and cement with a mixing tool from the ground surface. Can extend to significant depth.

Deep dynamic compaction – Compaction of existing soil by dropping a large weight from substantial height. Useful for compacting existing deep coarse-grained fills or loose soils.

Deep foundation – Foundation with a depth to width ratio more than about five.

Deep inward movement – Horizontal movement of a laterally supported deep excavation that occurs near the base of the excavation. This type of movement may be associated with basal heave movement.

Deflocculation – Separation of clay particles caused by moving water or chemical reagents.

Degree of saturation – Ratio of the volume of water to the volume of voids, which is typically expressed as a percent.

Depth to fixity – Depth at which a laterally loaded pile experiences minimal rotation or translation. Can also refer to the unbraced pile length used in buckling calculations.

Desiccated – Fine-grained soil that has been dried, usually below the shrinkage limit, resulting in cracks.

Design point – In reliability analysis, the point on the limit state function that is most likely to occur based on the distributions of all the random variables. The design point defines the reliability of the design.

Deterministic – In the context of geotechnical calculations, the assumption that the input parameters take on a particular value or trend for each soil or rock unit, rather than being defined statistically.

Dewatering – Process where water is pumped from a foundation excavation or pumped from a pervious soil stratum with the purpose of lowering the water table. Allows construction below grade without water in the excavation.

Dip – In layered geologic material, the angle between the layering and the horizontal plane.

Discontinuity – Natural break in a rock mass, such as a joint, fault, or bedding plane.

Dispersive clays – Clays comprised of minerals that contain a high percentage of dissolved sodium in the pore water and are thus very susceptible to concentrated leak erosion.

Drag force – Vertical load transferred to pile by negative skin friction.

Drained – In the context of shear strength and soil mechanics, a condition in which all excess porewater pressures caused by changes in stress or boundary condition have dissipated by water flow and volume change. Does not imply that the soil is unsaturated.

Dredged soils – Excavated or pumped materials that are obtained from below a water surface, mainly from the maintenance of navigable waterways and harbors.

Drilled displacement piles – Deep foundation element similar to a continuous flight auger column but constructed with an auger that displaces the soil laterally as it is inserted.

Drilled shaft – Deep foundation element constructed by drilling a shaft in the ground, which is subsequently filled with reinforced concrete.

Drivability - Ability of a hammer and drive system to drive a pile efficiently without damaging the pile.

Driven pile – Preformed deep foundation element that is hammered or vibrated into the ground.

Driving stress – Axial stress in driven piles during the driving process.

Dry method – Drilled shaft construction that uses an open shaft without drilling slurry. The shaft will often be cased.

Dry of optimum – Compaction to a combination of water content and dry unit weight to the left of the line of optimums. Dry of optimum can also refer to compaction at a water content lower than the optimum water content for a particular energy.

Dry unit weight – Weight of solids per unit volume.

Dynamic formulae – Methods to estimate the capacity of a driven pile from the measured blow count or pile set. These formulae produce highly variable results.

Earth pressure coefficient – Nominally, the ratio of horizontal to vertical effective stress.

Earthwork – The process of changing the topography of the ground to accommodate construction and to provide drainage.

Eccentricity – A loading condition that results in an unbalanced foundation bearing pressure as a result of nonconcentric loading or applied moment.

Effective stress – Stress state that controls soil strength and compressibility. Effective stress found by subtracting the pore pressure from the total stress.

Effective stress analysis - Analysis of stability or deformation that uses effective stresses. Synonymous with drained analysis.

Electro-osmosis – Ground improvement technology that uses an electrical gradient to promote water flow in soil, particularly to promote consolidation.

Encapsulation – Method of protecting moisture sensitive soils from large fluctuations in moisture content, particularly below pavements. The soil can be fully or partially encapsulated.

End-of-construction – Design scenario for conditions immediately following the application of the full structural load. Fine-grained soils are typically assumed to be undrained in this condition.

End-result specifications – Specifications requiring that a particular threshold value or acceptable range be achieved for the parameter of interest, such as dry unit weight and water content for earth fill or concrete compressive strength for foundations.

Epistemic uncertainty – See knowledge uncertainty.

Equivalent fluid unit weight – Product of the soil unit weight and earth pressure coefficient. Used to calculate horizontal pressure with the same methodology as for hydrostatic fluids. The concept is commonly used by structural engineers.

Equivalent footing – In the context of shallow foundations, the reduced dimensions that define a bearing area for which the resultant soil reaction is centered (non-eccentric). In the context of deep foundations, the depth at which the foundation load is assumed to beginning shedding to the supporting soil or rock.

Event tree – Risk assessment tool used to evaluate complex chains of conditional probabilities starting at an initiation point with a specific probability. Branches extend at each intermediate node.

Expanded clay shale (ECS) – Synthetic, vitrified aggregate produced by heating clay or claystones. Often used as aggregate in lightweight concrete. Can degrade under steel-tracked equipment.

Expansive shale – Sedimentary rock composed of clay minerals that can swell when exposed to water.

Expected value – Summation of any function times the probability mass function (discrete) or probability density function (continuous) over the full range of the random variable. The expected value of a random variable is the mean.

Exposure period – Length of time being considered in a design.

External uncertainty – See natural variability.

Externally-supported – Retaining system that uses anchors or tiebacks within the soil that are external to the excavation.

Factor of safety – Ratio of capacity to demand, often expressed in terms of shear strength divided by shear stress or failure load divided by applied load.

Fault tree – Risk assessment tool that starts with outcomes and assesses events required to reach those outcomes.

Fiber reinforcement – Use of fibers mixed with soil to improve shear strength. The fiber materials include natural, fiberglass, and plastic.

Field test section – Full-scale field compaction test to determine the appropriate procedure for a particular combination of site conditions and fill material. May be used to develop a method specification. Can also refer to a test grouting program.

Fill preloading – Practice of using an earth fill to promote consolidation and strengthening of soil prior to construction of the final structure, a.k.a., surcharging.

Fill wall – Retaining structure for which the wall is constructed and subsequently backfilled, creating grade separation. Rigid walls and MSE walls classify as fill walls.

Filter cake – Bentonite that collects on the side of a drilled shaft from the bentonite slurry.

Fine-grained soil – Soil that contains 50% or more particles passing a No. 200 (75 µm) sieve.

Fissures – Cracks or joints in soil, typically clay, resulting from stress relief and passive failure caused by unloading.

Fixed earth support – Analysis method for flexible structures that assumes no movement of the tip of the wall. Less commonly used than free earth support.

Fixed head condition – Condition where full rotational restraint is applied to the top of a laterally loaded deep foundation element. The maximum moment occurs at the restraint at the top of the element.

Flexible foundation – Foundation system that does not meet the requirements for rigid foundations.

Flexible retaining structures – Primarily vertical structural elements that are inserted prior to excavation. Structures may be braced or anchored. See also cut walls.

Floating foundation – See compensated foundation.

F-N chart – Risk assessment diagram that plots the annual probability of a consequence (F) against the consequence (N). Usually has regions that define acceptable and unacceptable risks.

Foamed glass aggregate (FGA) – Synthetic aggregate produced by heating recycled glass. Closed and open cell FGA available.

Force polygon – A vector diagram of the forces on a free body, used to graphically evaluate equilibrium.

Free earth support – Analysis method for flexible structures which assumes tip deflection can occur. Tends to overpredict the bending moments in the structure. Techniques are available to correct the bending moment.

Free head condition – Condition where no rotational restraint is applied to the top of a laterally loaded deep foundation element. The maximum moment occurs below the top of the element.

Friction angle – Inclination of a linear failure envelope in shear stress versus normal stress space. Can be expressed in terms of either total or effective stress.

Full-displacement pile – Deep foundation element that compresses the surrounding soil during driving or drilling to allow for the volume of the pile, such as closed-end piles or piles that form plugs.

Fully softened shear strength – Drained shear strength condition used to account for the effects of weathering, stress relief, and progressive failure in moderate to high plasticity clays. Fully softened shear strength is empirically equal to the peak shear strength of the clay in a normally consolidated state.

Gabion – Compartmented, rectangular containers made of heavily galvanized steel or polyvinylchloride (PVC) coated wire. Filled with stone from 4 to 8 inches in size. Used for control of bank erosion and stabilization as well as earth retaining structures.

Gamma-gamma logging – Integrity testing method that uses a gamma ray detector to determine the unit weight of the concrete from a single access tube.

General shear failure – Bearing failure along a well-defined slip surface that extends below and beyond the edges of a footing. Typical of stiff saturated clays and relatively dense coarse-grained soils.

Geofoam – Blocks manufactured from expanded polystyrene (EPS) or extruded polystyrene (XPS), typically installed in large blocks.

Geologic Strength Index – Measure of rock strength based on the rock mass structure and the surface condition.

Geosynthetic – Polymer material used with soil or rock for a geotechnical purpose.

Geosynthetic reinforcement – Geosynthetic used to provide tensile resistance in geotechnical structures, often used in slopes, pavement subgrades, and behind walls.

Geotextile – Permeable geosynthetic made like a textile and used for separation, filtration, or reinforcement. Geotextiles can be made using both woven and nonwoven manufacturing processes.

Glacial till – An accumulation of debris, deposited beneath, at the side (lateral moraines), or at the lower limit of a glacier (terminal moraine). Material lowered to the ground surface in an irregular sheet by a melting glacier is known as a ground moraine. Also known as boulder clay.

Global stability – Equilibrium condition for retaining walls that considers slip surfaces that complete by-pass the wall structure and any reinforcing or anchors.

Granular – A common synonym for coarse-grained soils.

Gravel – Soil with more than 50% coarse-grained particles and more gravel than sand-sized particles.

Gravel-sized – Soil particle size between 4.75 mm and 75 mm (3 in.).

Grid foundation – Foundation system formed by intersecting continuous footings.

Gross bearing pressure – The total load applied to the foundation divided by the area of the bearing surface.

Ground anchor – Structural element used to transmit tensile force to soil or rock.

Ground improvement – Means of modifying the ground with the purpose of improving one or more properties, such as shear strength, compressibility, or hydraulic conductivity.

Grubbing – Removal of stumps, heavy root mats, and buried objects.

Hard driving – Pile driving to refusal on rock or very dense soil, or penetrating an obstruction.

Hazard – A condition that has the potential to cause damage to or loss to personnel, equipment, or property.

Hazard curve – Relationship between the rate of exceedance and the magnitude of the hazard.

Hazard function – The probability that an event occurs (per time) assuming that the event has not occurred up to the given time.

Helical piles – Deep foundation element with relatively low capacity consisting of a steel bar with circular steel bearing plates.

High-strain dynamic testing – Integrity testing method that employs wave equation analysis to detect pile length and defects. Typically used with driven piles.

Histogram – Bar graph with intervals on one axis that span the range of the plotted property. The total height of the bars equals the number of observations in the sample.

Hydraulic conductivity – Discharge velocity of water through a unit area under a unit hydraulic gradient. Can also be viewed as a coefficient of proportionality relating seepage velocity to hydraulic gradient. Often called permeability in geotechnical engineering practice.

Hydraulic fill – Fill placed using flowing water. Cannot be compacted during placement. Hydraulic fill tends to be weaker and more compressible than compacted fills.

Hydraulic shoring – Aluminum hydraulic cylinder braces and heavy plywood (Finform) sheets used to support excavations.

Hydrocompression – Compressive volume change that occurs as a result of wetting, which is particularly a concern in relatively thick compacted fills.

Hydrodynamic – Water pressure exerted by moving water, specifically by seismic excitation.

Hydrostatic – Water pressure exerted under conditions of no flow or movement.

In situ – Latin for “in the original position,” which refers to soil or rock that remains in place in the ground. Used with testing to refer to measurements that are made in the ground and do not require a soil sample to be obtained.

Integrity testing – Method used to detect and evaluate damage and/or defects in a deep foundation.

Intelligent compaction – Use of instrumented compaction equipment to provide a measure of the stiffness of the compacted soil during compaction. In order to fully implement, the equipment should automatically modify operation based on the stiffness measurements.

Interface friction angle – Arctangent of the coefficient of friction between the soil and a structural material, such as a wall or foundation.

Interlock – Connection between individual adjacent sheet piles.

Internal erosion – Movement of soil particles from within the soil structure by flowing water.

Internal uncertainty – See knowledge uncertainty.

Internally-supported – Retaining system that uses structural supports that are internal to the excavation.

Jet grouting – Grouting method that uses high pressure jets on the tooling to break apart the soil, followed by the insertion of cementitious grout.

Jet-eductor well – Dewatering system that uses a high-pressure nozzle to create a vacuum at the bottom of the well, which draws groundwater to the well.

Jetting – Pile driving aided by loosening sand and gravel soils with a high-pressure water nozzle on a probe.

Karst – Terrain usually formed from the dissolution of rocks such as limestone, dolomite, and gypsum. It normally contains an underground drainage system connected to sinkholes and caves.

Kneading compaction – Method of applying compactive effort that shears the soil using a roller with pads or feet that exert very high contact pressure. Usually used for fine-grained soils.

Knowledge uncertainty – Uncertainty that occurs from lack of knowledge, information, or understanding; a.k.a., epistemic or internal uncertainty.

Kurtosis – Fourth moment of a distribution about the mean.

Lacustrine soil – Material deposited within lakes by waves, currents, and organo-chemical processes. Deposits consist of unstratified organic clay or clay in central portions of the lake and typically grade to stratified silts and sands in peripheral zones.

Laterites – Residual soils rich in iron formed in hot and humid climates (tropical regions). The cementing action of iron oxides and hydrated aluminum oxides makes dry laterites extremely hard. The high content of iron oxide makes many laterites to be rusty-red in color. Laterites are usually developed after significant weathering of the parent rock.

Leads – Frame used to guide driven pile during driving. Leads can be either fixed or swinging.

Lightweight fill – Alternative fill materials with lower unit weights than natural mineral soils.

Limit state function – Mathematical expression that defines the boundary between satisfactory and unsatisfactory performance.

Line of optimums – Curve connecting the peaks of a series of compaction (a.k.a. Proctor or moisture density) curves for different compactive efforts.

Liquefaction – A variety of phenomena affecting saturated cohesionless soils, in which positive excess pore pressures approach the total normal stress, causing partial or complete loss of shear strength. Liquefaction phenomena are typically divided into two categories: flow liquefaction and cyclic mobility (liquefaction in place).

Load and resistance factor design – Method that applies probabilistically-calibrated factors separately to the pertinent loads and resistances. In general, the factored load must be lower than the factored resistance.

Load factor – Multiplicative factor used to increase the calculated or measured nominal demand to an acceptable level for design. Factor accounts for uncertainty in the method used to determine the demand.

Load transfer – Process by which resistance is mobilized along the shaft and at the base of a deep foundation by movement of the foundation element.

Local shear failure – Bearing failure where plastic shear failure below the foundation transitions to compression of the adjacent soil. Slip surfaces do not extend to the ground surface beyond the footing.

Loess – A wind deposited, calcareous, unstratified deposit of silt or sandy or clayey silt traversed by a network of vertical tubes formed by the decay of root fibers. Loess slopes have the ability to withstand vertical cuts.

Logarithmic spiral – In the context of soil mechanics, a spiral-shaped slip surface having a radius that increases exponentially based on the friction angle of the soil.

Long pile – Slender deep foundation that behaves as a flexible member with no base rotation or translation.

Low wall – Short retaining wall that may require less detailed design and defined as less than 12 feet in this manual.

Low-strain dynamic testing – Integrity testing methods that use relatively low energy, such as sonic echo and impulse response.

Mat foundation – Foundation in which the weight of the structure is distributed across the entire footprint of the structure. Typically supports columns in several rows in each direction. Foundation covers an area of at least 75 percent of the total structure area.

Maximum dry unit weight – Dry unit weight at the peak of a compaction (a.k.a. Proctor or moisture density) curve for a particular amount of compactive effort.

Maximum void ratio – Loosest state that the soil can sustain with a regular structure. Typically used for coarse-grained soils with little fines.

Mean recurrence interval – see return period.

Measurement value (MV) – Indicator used in the intelligent compaction process, such as soil stiffness, modulus, or roller vibration characteristics.

Mechanical subgrade stabilization – Improvement of unstable soils by drying and recompaction and/or mixing with stronger or more stable soil.

Mechanically stabilized earth wall (MSEW) – Reinforced soil mass with a face inclined at 70° or more. Usually has a facing element of precast blocks or wire baskets.

Method specifications – Requirement that the contractor use a particular process, such as fill placement, lift thickness, equipment type, equipment speed, water content, and number of passes in the context of earthwork.

Micropiles – Small diameter (≤ 12 inches) foundation elements that are bored and grouted. Many variations are possible with respect to casing, drilling technique, grout delivery, and grouting phases.

Minimum void ratio – Densest state that the soil can sustain with a regular structure. Typically used for coarse-grained soils with little fines.

Model uncertainty – Uncertainty associated with the theoretical or mathematical model used to idealize a scenario.

Modulus of subgrade reaction – Ratio of the bearing pressure to the corresponding settlement with units of force per cubic length.

Moment – In the context of probability, summation over the full range of the random variable of the probability mass function (discrete) or probability density function (continuous) multiplied by the distance from the origin or mean. Analogous to area moments from mechanics.

Moment reduction – Method for correcting the overconservative moment predicted by the free earth support method.

Municipal solid waste (MSW) – Common items that are used and thrown away from residential and commercial sources. Also called trash or garbage.

Natural variability – Variations that result from physical randomness. Describes variability at various locations at the same time or variations in time and space; a.k.a., aleatory or external uncertainty.

Negative skin friction – Load transferred from the soil to a deep foundation element when the soil moves down relative to the element from consolidation, secondary compression, or vibration-induced densification.

Net bearing pressure – Gross bearing pressure minus the existing vertical overburden pressure at the foundation bearing elevation.

Net pressure diagram – Plot of the calculated difference between the pressure on each side of a wall.

Neutral plane – The elevation along a deep foundation at which no relative displacement occurs between the foundation element and the soil. The maximum compressive load in the foundation occurs at the neutral plane.

Non-displacement pile – Deep foundation element constructed without displacing soil, such as a drilled shaft or micropile.

Nonplastic – Soil that moves immediately from a semi-solid to a liquid state as the water content increases. Exhibited by difficulty rolling a plastic limit thread or performing the liquid limit test.

Normally consolidated soil – Soil for which the current effective stress state is the highest stress experienced by that soil following deposition.

One-third rule – Methodology that selects design parameters such that one-third of the data lies to the conservative side of the selected parameters.

Optimum water content – Water content at the peak of a compaction (a.k.a. Proctor or moisture density) curve for a particular amount of compactive effort.

Overconsolidated soil – Soil that has been previously consolidated to a higher effective stress state than the current stress state. Possesses a relatively low void ratio for the current stress state.

Oversize – Large particles within a test volume that interfere with the preparation of the test specimen or the performance of the test. This interference does not mimic field conditions. In the context of compaction, the large particles prevent adequate compaction of the finer soil fraction in the mold.

Oversleeves – Steel tubes used to extend hydraulic shoring braces to increase trench width.

Overturning – Equilibrium condition for retaining walls that considers wall rotation about a point on the wall, typically the toe.

Parallel gradation – Soil sample for which the grain size distribution has been shifted to have 100% passing the largest allowable particle size but maintaining the shape of the distribution. Created to facilitate laboratory testing.

Passive condition – Stress state in which the soil's shear strength is fully mobilized by lateral movement toward the soil mass and a corresponding increase in lateral stress.

Peak particle velocity (PPV) – Highest velocity generated by blasting in the direction of the wave propagation.

Plasticity – Measure of a soil's ability to interact with water. High plasticity soils require a large change in water content to move from a solid state to a liquid state.

p-multiplier – Empirical coefficients used to reduce the force or reaction of particular piles in a pile group as a result of group interactions.

Population – In the context of statistics, the set of all possible outcomes for a particular situation.

Post grouting – Grout pumped to the base of a drilled shaft to premobilize base resistance by reducing the void ratio of the underlying soil or creating a grout bulb at the base.

Power function – Nonlinear failure envelope used to represent shear strength with two or more parameters.

Predrilling - Pile driving aid in which an auger is used to drill a pilot hole for the pile.

Prefabricated vertical drains – Drain with a rectangular cross-section and geotextile sleeve that is inserted into the ground to shorten the drainage path for consolidation.

Pressure slab and walls – Floor slab and exterior foundation walls that are designed to retain and resist permeation and pressure from an elevated water level adjacent to the structure.

Presumptive bearing pressure – Allowable bearing pressure selected without explicit calculation of bearing capacity and/or settlement.

Probability density function – The function equal to the derivative of the cumulative density function at each value of a continuous random variable.

Probability mass function – Discrete function defining the probability that a random variable is equal to particular value.

Proctor test – Standardized test method for determining the maximum dry unit weight and optimum water content for a particular soil. Two compactive efforts are standardized by ASTM – Standard and Modified.

Proof rolling – Systematic trafficking of the subgrade by a loaded dump truck or roller. The purpose is to find instability and inconsistency in the subgrade or fill.

Punching shear – Bearing failure dominated by compression of the soil below the footing and vertical shear along the sides of the footing.

Pushover analysis – Repeated lateral load calculations that determine lateral top of pile deflections for a range of specified loads or the loads required to cause a range of top of pile deflections.

p-y curve – Constitutive model for lateral loading that relates soil reaction or load (p) to deflection (y).

Pyritic shale – Sedimentary rock containing sulfur that can form pyrite when exposed to the atmosphere and water, commonly dark gray to black and Devonian in age.

Quality assurance (QA) – Control testing completed by an entity other than the contractor, often the owner’s representative.

Quality control (QC) – Control testing completed by the contractor.

Quick clay – Clay with a sensitivity greater than about eight.

Raker – Structural element that supports an excavation by transmitting load from the wall to the base of the excavation; a.k.a., raking braces.

Random variable – Variable that maps outcomes from a sample space to the real line.

Rapid drawdown – Design scenario for rapid lowering of water adjacent to a slope. Consolidated undrained shear strength is appropriate for this condition for soils with moderate to low hydraulic conductivity.

Rapid impact compaction – Method of compacting soil that drops a large weight many times per minute using an excavator as an alternative to deep dynamic compaction.

Rapid load test – Method to assess the capacity of a deep foundation that uses a dynamic load from a propellant or a dropped mass to load a foundation. The results must be interpreted to determine the failure load. Does not require reaction piles.

Rate of exceedance – Inverse of the return period in units of 1/time.

Record samples – In the context of earthwork, block or other intact samples of fill that can be used for laboratory characterization testing.

Reinforced soil slope – Reinforced soil mass with a face inclined flatter than 70°.

Relative compaction – Ratio of the compacted dry unit weight of a fill to a reference unit weight, typically the maximum dry unit weight for a particular compactive effort, such as Standard or Modified Proctor.

Relative density – Parameter used to quantify the density of a coarse-grained soil relative to the loosest and densest states. It is calculated as the ratio of the difference between the maximum void ratio and current void ratio to the difference between the maximum and minimum void ratios.

Relative water content – Algebraic difference between the compacted water content of a fill to a reference water content, typically the optimum water content for a particular compactive effort, such as Standard or Modified Proctor.

Relaxation – In the context of deep foundations, the reduction in pile resistance over time as negative driving-induced pore pressures dissipate.

Reliability – Probability that a design will perform in a satisfactory manner.

Reliability index – Number of standard deviations separating the mean value of a limit state function from the unsatisfactory condition.

Relieved slab and walls – Floor slab and exterior foundation walls that use a drainage system to relieve pressures from an elevated water level adjacent to the structure. Requires dampproofing.

Residual shear strength – The lowest drained shear strength of a soil that is achieved by shear displacement along a failure plane until particle alignment is achieved. This term is normally reserved for fine-grained soils. Residual conditions are often associated with slickensides forming on the failure plane.

Residual soils – Soil deposit formed by physical and chemical weathering of parent rocks in-place or from weathering of volcanic ash deposits.

Resistance factor – Multiplicative factor used to reduce the calculated or measured nominal capacity to an acceptable level for design. Accounts for uncertainty in the method used to determine the capacity.

Resultant – Reaction force acting on a structure or soil mass.

Return period – The mean amount of time between the return of a particular hazard; a.k.a., mean recurrence interval.

Rigid foundation – Foundation system for which the loads cause a ratio of differential to total settlement ratios less than or equal to 0.1.

Rippability – Ability to excavate rock directly using tracked equipment or an excavator. Rippability is dependent on the size of the equipment.

Riprap – Cobbles and boulders used as a slope protection to prevent scour. Size varies with classification.

Risk – Product of the probability of an adverse event multiplied by its consequence.

Risk assessment – Quantification and description of the nature, likelihood, and magnitude of risk in a systematic, evidence-based manner.

Rock fill – Fill containing at least 30% clean rock with a grain size greater than ¾-inch and containing less than 15% fines.

Running soils – Soils with no ability to hold a vertical face that will flow or cave into the excavation if unsupported, such as clean, dry coarse-grained soils. Seepage can cause running soil conditions.

Sample – In the context of statistics, a set of observations or measurements.

Sample space – See also population.

Sand – Soil with more than 50% coarse-grained particles and more sand-sized than gravel-sized particles.

Sand compaction piles – Columns of soil compacted in loose sand or soft clay using a driven installation pipe.

Sand-sized – Particle size between 0.075 mm and 4.75 mm.

Scale of fluctuation – Distance over which the soil properties are strongly correlated.

Scaled distance – Measure of the distance from a blasting charge to a structure that is corrected by the weight of the charge.

Scalped gradation – Soil sample for which all particles larger than a particular grain size have been removed to facilitate a particular laboratory testing method.

Scour – Loss of soil by erosion due to the drag force of moving water. Clear water scour occurs when the upstream bed material is not being actively transported and deposited. Live bed scour refers to a condition where the upstream bed material is transported and deposited to partially replenish eroded materials.

Secant pile wall – Retaining wall constructed from overlapping drilled shafts.

Sensitivity – Ratio of the peak undrained shear strength to the remolded undrained shear strength.

Service limit state – Design condition pertaining to the functionality or ability of the structure to remain useful.

Settlement – Downward movement of a structure.

Setup – In the context of deep foundations, the increase in pile resistance over time as driving-induced positive pore pressures dissipate.

Shallow foundation – Foundation with a depth to width (D/B) ratio less than about five, a.k.a., spread foundation, footing, or footer.

Shear strength – A measure of the shear stress sustained by a soil or rock at a state of shear failure. The shear stress on the failure plane and the maximum principal stress difference are two common measures of shear strength.

Shear wave – Seismic wave in which the particles move in the direction perpendicular to wave propagation.

Sheepsfoot roller – A type of kneading compactor with long tines or feet. Equipment replaced by tamping foot rollers in modern practice.

Sheet piling – Interlocking structural sections that are pushed or driven into the ground, often used for cut-type retaining walls. Cross-sectional shape varies based on usage. Most commonly steel but also available in plastic and timber.

Short pile – A deep foundation that can be considered rigid when laterally loaded. The rigid foundation element will rotate or translate at the base when loaded.

Shrinkage – In the context of earthwork, a reduction of soil volume by compaction to a higher dry unit weight than the borrow material.

Shrinkage factor – A factor multiplied by the final fill volume to account for shrinkage or bulking during the earthwork process.

Signal matching – Use of wave equation analysis along with strain gauges and accelerometers to estimate nominal pile resistance, hammer and drive system performance, driving stresses, and pile integrity.

Silt – Nonplastic or slightly plastic soil particles passing a No. 200 (75-μm) sieve that exhibit little or no strength when air dried. For classification of silty soils, refer to ASTM D2487.

Silt-sized – Soil particle size between 0.002 mm and 0.075 mm.

Simulation – Use of a complex, representative mathematical model to represent and calculate the performance of a design. Typically uses a numerical method such as finite element, finite difference, or Monte Carlo.

Skeleton shoring – Timber trench support method that uses discontinuous upright members and is applicable when running soils are not expected. Can be used to depths up to 20 feet.

Skew – Third moment of a distribution about the mean.

Sliding – Equilibrium condition for retaining wall and shallow foundations that considers movement parallel to the bearing surface.

Slurry cutoff wall – Subsurface barrier created by filling an excavated trench with a mixture of cement, bentonite, and/or soil. May be solely for seepage reduction or have structural components.

Soft driving – Pile driving through soft soil prior to reaching a competent bearing layer.

Soil nail (drilled) – Soil stabilization technique that drills and grouts a horizontal or inclined reinforcing elements in place. Soil nails are not prestressed or tension tested.

Soil nail (screw-in) – Soil stabilization technique that uses helical anchors as horizontal or inclined soil reinforcing elements. The anchors are installed by screwing into the ground. Soil nails are not prestressed or tension tested.

Soil nail (shoot in) – Soil stabilization technique that shoots a horizontal or inclined reinforcing elements into the soil. Depth of penetration and size of the nail are relatively limited; anchors are not grouted in place. Soil nails are not prestressed or tension tested.

Soldier pile and lagging – Retaining wall system with discrete vertical structural elements (soldier piles or soldier beams) and horizontal elements (lagging) that transfer load from the retained soil. Vertical elements are embedded deeper than the lagging to develop resistance to applied load. Most of the retained load arches to the piles.

Specific gravity of solids – Ratio of the density of the solids to the density of water.

Spudding – Practice of driving a heavy pile through an obstruction to make a hole for a production pile.

Static capacity analysis – Analytical method to estimate the axial capacity of a deep foundation element.

Static liquefaction – Behavioral condition in which soil liquefies as a result of an applied static shear stress in loose sands and non-plastic silts. Can occur when excavations are made in loose contractive sand deposits that were formed by sluicing or hydraulic fill.

Static load test – Method to assess the capacity and performance of a deep foundation in which a full-scale element is statically loaded after installation and the deformation is monitored. Results must be interpreted to determine the failure load. Requires reaction piles or anchors.

Stochastic – Random variation in time and space.

Sulfidic soil and rock – Geomaterials containing sulfur in various forms. Has the potential to be expansive when exposed to water and the atmosphere.

Surcharge – In the context of retaining wall or excavation design, a uniform pressure applied to the ground surface in many design calculations to represent live loading. In the context of earth fill or foundations, see Fill preloading.

Talus – A loose, colluvial deposit of rock debris located at the base of a cliff or mountain.

Tangent pile wall – Retaining wall constructed from adjacent but not overlapping drilled shafts. Due to the construction method, the wall may have gaps between the piles.

Telescopic shoring – Timber trench support method used for very deep trenches, which consists of nested trenches that decrease in width as the trench depth increases.

Thermal integrity profiling – Integrity testing method for drilled shafts that uses embedded temperature sensors to monitor the curing temperature of the concrete. Temperature patterns can be used to infer presence of defective concrete.

Tie back – Ground anchor installed through a retaining wall system to provide restraining force and/or moment. Tie backs are post-tensioned to reduce or eliminate the displacement required to develop capacity.

Timber shoring – A temporary structure made of wood used to support a trench.

Tire derived aggregate (TDA) – Lightweight construction material obtained by shredding or chipping scrap tires; a.k.a, tire shreds. The particle size usually ranges from 0.5 inches to 12 inches. TDA has been used in a wide range of projects, including lightweight embankment fill, landslide repair or stabilization, retaining wall backfill, roads, vibration mitigation, among others.

Top down method – Construction method where the retaining wall system is installed as the excavation progresses.

Total stress – Stress state that includes normal stresses from all sources, both soil contact forces and pore pressures.

Total stress analysis – Analysis of stability or deformation that only considers total stresses and represents shear strength in terms of total stress. Often synonymous with undrained analysis.

Total unit weight – Weight of solids plus liquids per unit volume.

Trench shield – A rigid prefabricated steel support system used in lieu of other types of shoring, which extends from the bottom of the excavation to the ground surface; a.k.a. trench box.

Two-thirds rule – Method in which a design parameter is selected such that one-third of the data lies to the conservative side of the selected parameter. Two thirds of the data falls on the other side of the selected value.

Ultimate bearing capacity – Gross bearing pressure that the soil or rock can withstand at the point of incipient plastic failure.

Ultimate limit state – Design condition pertaining to collapse.

Uncontrolled fill – Fill consisting of soil, rock, or other materials that are placed without control of material type, lift thickness, or compaction energy. The fill may contain industrial and domestic wastes, ash, slag, chemical wastes, building rubble, and refuse.

Underpinning – Installation of foundation elements below an existing structure that provides structural support when the bearing elevation of the existing foundations is higher than the bottom of an adjacent excavation.

Undrained – In the context of soil mechanics, a condition in which excess pore pressure caused by changes in stress or boundary condition is present. Commonly refers to the state immediately after loading where dissipation of excess pore pressures has not yet occurred.

Undrained shear strength – Strength measure of soil sheared without allowing excess pore pressures to dissipate. No volume change occurs during undrained shear of saturated specimens.

Unit base resistance – Deep foundation axial resistance at the base of the element per unit area.

Unit shaft resistance – Deep foundation axial resistance along the side of the element per unit area.

Vacuum preloading – Use of a vacuum to promote consolidation. The vacuum is applied within a sealed system to promote water flow to vertical drains.

Vibratory compaction – Method of applying compactive effort that uses a vibrating mass, which is usually used for coarse-grained soils.

Vibro-compaction – Densification of coarse-grained soils using a probe inserted into the ground and vibrated at different frequencies.

Vibro-concrete columns – Vertical elements created using a vibrating probe that penetrates the soil, delivers concrete to the base of the element, and expands the concrete through repeated penetration.

Void ratio – Ratio of the volume of voids to volume of solids.

Walk out – In the context of earthwork, the ability of tamping foot rollers to penetrate less and less into the fill as the fill becomes well-compacted.

Waste – The volume of soil lost in the earthwork process

Water content – Ratio of the weight of water to weight of solids, typically expressed as a percent. Can be expressed in terms of mass rather than weight.

Waterproofing – Material applied to foundation walls that resists the passage of water under hydrostatic pressure.

Wave equation analysis – Numerical approach that uses the characteristics of the pile, drive system, and hammer to evaluate nominal resistance and driveability, as well as hammer and drive system selection.

Wellpoint – Dewatering system that pumps water from the ground through a perforated well.

Wet method – Drilled shaft construction that uses a slurry mixture of water and bentonite or polymer to maintain shaft stability.

Wet of optimum – Compaction to a combination of water content and dry unit weight to the right of the line of optimums. Wet of optimum can also refer to compaction at a water content higher than the optimum water content for a particular energy.